CHROMOSPHERIC STRUCTURE OF THE K-TYPE COMPONENT OF ZETA AURIGAE

O. C. WILSON AND HELMUT A. ABT*
MOUNT WILSON AND PALOMAR OBSERVATORIES
CARNEGIE INSTITUTION OF WASHINGTON
CALIFORNIA INSTITUTE OF TECHNOLOGY
Received July 30, 1953

ABSTRACT

Spectrograms of 10 A/mm dispersion taken during the 1947–1948 eclipse have been measured for line intensities and for radial velocities, and the results are compared with those obtained previously for the 1939–1940 eclipse. Egress of 1947–1948 is found to be quite similar to ingress and egress of 1939–1940; ingress at the more recent eclipse differs, however, from the other three transits in the direction of a considerably slower gradient, particularly at the greater chromospheric heights. This effect is found from lines of all types. However, ingress of 1947–1948 is not distinguishable from the other transits in the values of any of the derived parameters: excitation temperature, turbulent velocity, or degree of ionization.

It is shown that the apparent rise of $\Delta\lambda_D$ with height found in 1939–1940 is really due to a systematic difference in this quantity between the neutral and ionized lines. Ions indicate slightly higher turbulent velocities than do neutral atoms. The excitation temperature increases with height at about the same rate as indicated by the earlier results.

Ionization in the chromosphere is studied in some detail, and Strömgren's theory of the penetration of ionizing radiation from the B star into the chromosphere of the K star is applied to the problem. The outcome is that it appears impossible to account for the spectroscopic phenomena on the basis of a smooth distribution of the chromospheric material. In fact, it is necessary to assume that the matter occurs in condensations of rather small size (thickness of the order of 10^3 km) and high density (log $n[H] = 13.8$) in order to keep the ionization at the required level and to avoid discordance with the solar abundance ratios. The model is in accord with all but one of the observed spectroscopic features, as well as with the recent interpretation of the photometric eclipse by Roach and Wood.

I. INTRODUCTION

In eclipsing binaries of which one component is a giant or supergiant star of large size and low surface temperature, while the other component possesses opposite characteristics, the eclipses of the small star by its companion offer an opportunity to determine the chromospheric structure of the large, cool star. At present, four systems of this type are known: Zeta Aurigae, 31 Cygni, 32 Cygni, and VV Cephei.[1] Zeta Aurigae has been known longer and investigated more completely than the others.

The period of Zeta Aurigae is about 972 days; hence favorable eclipses (in the sense that the star is observable throughout the night) occur every 8 years. The eclipse of December, 1939—January, 1940, was observed spectroscopically by one of the authors,[2] and more extensive observations were obtained of the 1947–1948 eclipse. In this paper the results of the more recent eclipse are derived and compared with those of the earlier one.

With a few exceptions noted in the text, the methods of measurement, reduction, and computation used in the earlier work have been employed for the more recent material. In fact, most of the spectrograms obtained in 1947–1948 were taken with the same

* Now at Yerkes Observatory, Williams Bay, Wisconsin.

[1] A semiquantitative comparison of the eclipse phenomena of these stars has recently been given by D. B. McLaughlin, *Pub. A.S.P.*, **64**, 173, 1952.

[2] O. C. Wilson, *Ap. J.*, **107**, 137, 1948.

equipment and on the same type of emulsion (Eastman 103-O) as were those of 1939–1940. For details, therefore, the reader is referred to the published report of the earlier eclipse.[2]

The principal advantage of the newer results lies in the greater range of atmospheric height covered in the 1947–1948 observations. A number of the spectrograms have been measured for the velocities, as well as the intensities, of the chromospheric lines, and these will be discussed in the appropriate place; also a few minor numerical errors discovered in the earlier work have been corrected. In the last half of the paper a chromospheric model is developed which is consistent with most of the spectroscopic observations.

II. OBSERVATIONS

For convenience, all the spectrograms utilized for both eclipses are listed in Table 1, which is self-explanatory except for the columns headed "Δt" and "Height." For these items we have arbitrarily adopted as zero points the times corresponding to what would be second and third contacts in a purely geometrical eclipse. These times have been obtained from Wood's epochs of minimum,[3] JD 2429637.10 and JD 2432553.67 for 1939 and 1947, respectively, and Pettit's[4] value for the duration of totality, 36.80 days. With Harper's elements,[5] modified only by the use of Wood's period of 972.16 days, and a mass ratio $M_K/M_B = 2.00$, the resulting conversion factor between time and height in the K star's atmosphere is 7.23×10^6 km/day and is the same for ingress and egress to within less than half a per cent. It should be noted that the heights given in Table 1 for the 1939–1940 spectrograms differ from those previously published because of the change in zero point.

III. SPECTROPHOTOMETRY

The same criteria of choice of lines for intensity measurement were applied to the 1947–1948 material as had been used previously.[2] Some lines of *Fe* II with unkown *f*-value have been measured on the plates of both eclipses, for reasons which will appear later; in other cases the *f*-values were taken from known sources.[6] Equivalent widths of the lines were determined as described previously,[2] and the logarithms of the equivalent widths of the metallic lines, reduced to a mean wave length of 3700 A, are given in Table 2.

Measures of equivalent width of *Ca* I, *Ca* II, and *H* lines are in Table 3, together with corresponding values of log N, which were read from theoretical curves of growth.[7] Values of $\Delta\lambda_D$ appropriate to the height were used for *Ca* I and *Ca* II, while a constant value of $\Delta\lambda_D = 0.15$ A was employed for all the *H* lines. For a few of the strongest *Ca* II lines it was necessary to free the chromospheric component from the effect of the normal K-spectrum line by means of Wilson's equation (3).[2] For convenience, revised values of log N for *Ca* I, *Ca* II, and *H* for the 1939–1940 eclipse are given in Table 4, with the heights corresponding to the usage of this paper. Table 4 thus replaces Wilson's Table 7.[2]

[3] *Ap. J.*, **114**, 505, 1951.

[4] *Pub. A.S.P.*, **60**, 102, 1948.

[5] *Dom. Ap. Obs. Victoria*, **3**, 151, 1924.

[6] *Fe* I: R. B. and A. S. King, *Ap. J.*, **87**, 24, 1938. *Ni* I: R. B. King, *Ap. J.*, **108**, 87, 1948. *Cr* I: A. J. Hill and R. B. King, *J. Opt. Soc. Amer.*, **41**, 315, 1951. *Ca* I, *Ca* II: P. Wellmann, *Veröff. Sternw. Berlin-Babelsberg*, **12**, Part IV, 56, 1939. *Ti* II: R. B. King, *Ap. J.*, **94**, 27, 1941. *H* I: D. H. Menzel and C. J. Pekeris, *M.N.*, **96**, 77, 1935. Miscellaneous solar values: H. H. Lane, *Harvard Ann.*, **105**, 69, 1937.

[7] As in n. 2, N in this paper indicates a total or integrated number of particles along a ray. The symbol n is restricted to number per cubic centimeter.

TABLE 1

SPECTROGRAMS, TIMES OF OBSERVATION, AND CALCULATED HEIGHTS

1947–1948 ECLIPSE

Plates (Coudé)	Date	P.S.T.*	JD 2432000+	Δt (Days)	Height (10^6 Km)
4992, 4994	Dec. 8	13:18	528.89	6.38	46.1
4995, 4996	Dec. 9	8:12	529.68	5.59	40.4
4999, 5000	Dec. 10	12:11	530.84	4.42	32.0
5001, 5002	Dec. 11	8:51	531.70	3.56	25.8
5004	Dec. 11	13:42	531.90	3.36	24.3
5006, 5008	Dec. 12	12:00	532.83	2.44	17.6
5010, 5011	Dec. 13	7:57	533.67	1.60	11.6
5014, 5015	Dec. 13	15:01	533.96	1.31	9.4
5019	Dec. 15	8:27	535.69	Totality	
5026	Dec. 22	9:00	542.71	Totality	
5028†	Dec. 22	13:22	542.89	Totality	
5059	Jan. 20	6:22	571.60	Totality	
5071	Jan. 22	7:52	573.66	1.60	11.5
5074	Jan. 23	6:01	574.58	2.52	18.2
5078	Jan. 24	6:14	575.59	3.53	25.5
5080	Jan. 24	13:14	575.88	3.82	27.6
5083	Jan. 26	11:11	577.80	5.74	41.5
5084	Jan. 27	9:01	578.71	6.64	48.0
5085	Jan. 28	5:51	579.58	7.51	54.3

* Time counted from noon of the day listed.

† Red-sensitive plate taken with the 114-inch camera.

1939–1940 ECLIPSE

Plate (Coudé)	Date	P.S.T.*	JD 2429000+	Δt (Days)	Height (10^6 Km)
2181, 2183	Dec. 16	11:38	614.82	3.88	28.0
2185, 2188	Dec. 17	11:36	615.82	2.88	20.8
2191, 2192, 2194	Dec. 18	9:23	616.72	1.98	14.3
2199	Dec. 19	9:53	617.74	0.96	6.9
2202	Dec. 19	12:55	617.87	Totality	
2205	Dec. 19	15:32	618.78	Totality	
2243	Jan. 26	9:11	655.74	Totality	
2245	Jan. 27	7:45	656.66	1.16	8.4
2248	Jan. 28	6:50	657.62	2.12	15.3
2252, 2253	Jan. 29	9:30	658.73	3.23	23.3
2254	Jan. 30	9:52	659.74	4.24	30.7
2255	Jan. 31	10:15	660.76	5.26	38.0

TABLE 2

Values of - Log W $\frac{3700}{\lambda}$

El. Mult. λ	Log gf	Ce 4992 4994	4995 4996	4999 5000	5001 5002	5004	5006 5008	5010 5011	5014 5015	5071	5074	5078	5080	5083	5084	5085
Fe I																
$a^5D-z^5P^o$																
3440.6	2.20						0.81	0.53		0.62	1.05	1.78				
3441.3	1.82						0.98	0.59		0.78						
3443.9	1.27															
3465.9	1.89					1.04	0.73	0.55	0.49	0.47	1.15	1.53	1.82			
3475.5	1.88						0.77	0.52	0.34							
3490.6	1.73								0.49	0.71		1.05				
$a^5P-z^3D^o$																
3521.3	2.42							0.82	0.52	1.30						
3526.2	2.14							0.76	0.54	1.03						
3565.4	3.14					0.98	0.81	0.64	0.53	0.67	1.45					
3570.1	3.35				0.73	0.72	0.68	0.54	0.41	0.59	0.79	1.56				
$a^5P-z^5D^o$																
3587.0	2.58				1.03	1.03	0.90	0.65	0.60	0.70	1.19					
3589.1	1.70							1.29	1.20							
3608.9	3.12				1.07	0.91	0.80	0.62	0.56	0.80	1.43					
3618.4	3.30				1.27	0.85	0.75	0.58	0.47	0.71	1.19					
3631.5	3.18			1.03	0.74	0.69	0.59	0.46	0.46	0.55	0.83	1.11	1.37			
3647.8	3.14					0.96	0.80	0.56	0.42	0.67						
$a^5D-z^5F^o$																
3649.5	0.43							1.23	1.28							
3679.9	1.78						0.99	0.60	0.63	0.75	1.48					
3683.0	0.89				0.88	0.87	0.77	0.68	0.69							
3705.6	1.98						0.90	0.64	0.51	0.56	1.62					

TABLE 2 (Cont'd)

El. Mult. λ	Log gf	Ce 4992 4994	4995 4996	4999 5000	5001 5002	5004	5006 5008	5010 5011	5014 5015	5071	5074	5078	5080	5083	5084	5085
3707.8	1.01							1.09	0.81							
3719.9	2.72				0.93	0.73	0.56	0.43	0.30	0.41	0.86	1.66				
3722.6	1.98					1.05	0.81	0.56	0.47	0.79						
3733.3	1.83						0.94	0.84	0.64	0.81	1.40					
3737.1	2.59				0.76	0.70	0.56	0.34	0.34	0.46	1.00	1.47	1.56			
3748.3	2.15				0.89	0.89	0.86	0.57	0.56	0.57	1.01	1.31	1.39			
$a^5F\text{-}y^5P^o$																
3687.5	2.63						1.05	0.80	0.60	0.96	1.17					
3709.2	2.78						1.02	0.71	0.56	0.83						
3727.6	2.76							0.57	0.50	0.66						
3734.9	3.67					0.56	0.43	0.36	0.38	0.59	0.84	1.31				
3743.3	2.59						1.12	0.75	0.63	1.00						
3749.5	3.50				0.75	0.59	0.56	0.35	0.34	0.55	0.83	1.14	1.31			
3758.2	3.33				0.96	0.78	0.71	0.53	0.57	0.57	1.17					
3763.8	3.10				1.06	0.93	0.82	0.51	0.59	0.67	1.22					
3767.2	2.93				1.13	1.09	0.95	0.65	0.54	0.67	1.08					
3787.9	2.52				1.32	1.29	1.18	0.81	0.72	1.01	1.27					
3795.0	2.61				1.27	1.07	1.10	0.70	0.60	0.96						
$a^5F\text{-}y^3D^o$																
3815.8	3.72				1.23	1.07	0.88	0.60	0.45	0.59	1.21					
3827.8	3.58				1.18	1.14	0.99	0.68	0.54	0.61	1.62					
3841.0	3.41				1.01	1.20	1.02	0.71	0.67	0.98						
3888.5	2.93															
3903.0	3.11					1.40		0.67	0.62	0.74						
$a^5F\text{-}y^5D^o$																
3820.4	3.49				0.93	0.81	0.63	0.47	0.42	0.50	0.87	1.24				
3825.9	3.28				1.04	0.97	0.78	0.51	0.46	0.47	1.03					
3834.2	3.06			1.60	1.14	1.02	0.91	0.54	0.59	0.64	1.11	1.45				
3840.4	2.78				1.07	1.07	0.88	0.65	0.57	0.77	1.32					
3850.0	2.53					1.35	1.18	0.92	0.83	1.04						
3865.5	2.44						1.40	0.97	0.71	0.91						
3872.5	2.46						1.03	0.88	0.76	1.08						

TABLE 2 (Cont'd)

3878.0	2.50			1.35	1.00	0.89	0.73	1.05	
3887.0	2.36			1.42	1.01	0.80	0.73	1.12	
3998.0	1.54						0.95		
3917.2	1.47					1.58	1.16		
3940.9	1.08					1.39	1.28		
a^5D-z^5D^o									
3824.4	1.94		1.29	1.39	1.10	0.70	0.62	0.69	1.25
3856.4	1.98			0.96	0.84	0.71	0.54	0.71	
3859.9	2.54		0.91	0.92	0.67	0.45	0.43	0.60	0.96
3878.6	1.84			1.19	0.97	0.68	0.53	0.77	1.40
3886.3	2.14			1.14	0.73	0.74	0.57	0.67	1.15
3895.7	1.58			1.09	1.00	0.83	0.65	0.92	
3899.7	1.74			1.29	1.00	0.80	0.58	0.94	
3906.5	1.15					0.96	0.78	1.04	
3920.3	1.54				1.20	0.80	0.62	0.97	
3922.9	1.70				1.02	0.72	0.65	0.84	
3927.9	1.71			1.39	1.08	0.73	0.58	0.95	
3930.3	1.79				1.05	0.73	0.56	0.88	
a^3F-y^3F^o									
4045.8	3.78		0.85	0.91	0.82	0.51	0.43	0.93	1.21
4063.6	3.54		1.20	0.90	0.93	0.62	0.50	1.15	
4071.8	3.43		1.21	1.09	0.80	0.61	0.52	1.10	1.20
Ni I									
a^3D-z^3F^o									
3414.8	6.90				1.05	0.60	0.51	0.87	1.61
3458.5	6.55				1.02	0.87	0.63	1.12	
3515.1	6.82		1.29	1.15	0.96	0.76	0.67	0.86	
a^3D-z^3D^o									
3446.3	6.70				1.18	0.78	0.67	0.92	
3472.5	6.24					0.98	0.74	1.29	
a^3D-z^3P^o									
3493.0	6.64					0.75	0.57	0.88	1.22
3524.5	6.95			0.97	0.84	0.59	0.45	0.63	1.24

TABLE 2 (Cont'd)

El. Mult. λ	Log gf	Ce 4992 4994	4995 4996	4999 5000	5001 5002	5004	5006 5008	5010 5011	5014 5015	5071	5074	5078	5080	5083	5084	5085
Mg I																
$3^3P^o-3^3D$																
3829.4	9.79				0.98	0.95	0.76	0.53	0.48	0.56	0.91	1.38				
3832.3	10.13			1.38	0.77	0.72	0.66	0.48	0.35	0.52	0.84	1.29	1.36			
3838.3	10.32			0.73	0.61	0.56	0.45	0.37	0.25	0.37	0.55	0.90	1.17			
Al I																
$3^2P^o-4^2S$																
3944.0								0.96	0.76	1.14						
3961.5							1.08	0.84	0.69	0.90						
Cr I																
$a^7S-y^7P^o$																
3578.7	7.02				0.96	0.78	0.68	0.52	0.32	0.54	0.83	1.47				
3593.5	6.98				0.80	0.68	0.65	0.47	0.37	0.52	0.99	1.55				
3605.3	6.82				0.99		0.71	0.49	0.36	0.66	1.32					
Ti II																
$b^4F-z^4F^o$																
3318.0	1.18		1.03	0.84	0.92		0.52	0.43	0.37	0.53	0.61	0.92				
3322.9	2.05	0.40	0.38	0.30	0.39		0.37	0.27	0.20	0.31	0.35	0.36		0.79	1.11	
3326.8	1.09			0.82	0.72		0.49	0.48	0.42	0.47	0.63	0.84	1.06			
3329.5	1.86	0.51	0.52	0.32	0.44		0.34	0.31	0.24	0.34	0.30	0.45	0.84	0.88	1.42	
3335.2	1.75	0.66	0.52	0.40	0.50		0.45	0.49	0.30	0.36	0.41	0.54	0.73	0.97	1.27	
3340.3	1.62	0.60	0.50	0.41	0.49		0.38	0.32	0.25	0.38	0.41	0.58		1.05		
3343.8	1.06			1.01	0.97		0.60	0.53	0.45	0.58	0.70	1.19	1.19	1.19		
3346.7	1.17			0.85	0.67		0.53	0.53	0.42	0.49	0.66	0.98	1.05			
$b^4P-z^4S^o$																
3332.1	2.85			0.83	0.72		0.55	0.50	0.45	0.50	0.69	0.92	1.19			

TABLE 2 (Cont'd)

$a^2F\text{-}z^2G^o$															
3341.8	2.13	0.39	0.32	0.28	0.33		0.33	0.30	0.20				0.82	0.85	1.20	
$a^4F\text{-}z^4G^o$																
3361.2	2.00									0.45		0.50	0.55	0.64	0.73	1.14
3372.8	2.30	0.27	0.26	0.21	0.36			0.17		0.16	0.30	0.35	0.43	0.54	0.75	
3380.3	1.56	0.56	0.44	0.35	0.37		0.33	0.28	0.15	0.22	0.37	0.52	0.83	1.16	1.40	
3383.8	2.23	0.34	0.26	0.20	0.27		0.32	0.24	0.19			0.41	0.50	0.55	0.77	1.38
3387.8	1.68	0.46	0.46	0.36	0.36		0.34	0.30	0.21	0.26	0.39	0.38	0.58	0.90		
3394.6	1.67	0.64	0.53	0.44	0.46		0.42	0.38	0.29	0.27	0.43	0.47	0.59	0.95	1.52	
3407.2	0.43						0.76	0.58	0.47	0.55	0.97	1.22				
3409.8	0.39						0.98	0.67	0.51	0.64	1.13					
$b^4F\text{-}z^4G^o$																
3444.3	1.43	0.72	0.73	0.65	0.57		0.49	0.43	0.31	0.40	0.49	0.75	0.78	1.45		
3461.5	1.34	0.76	0.81	0.56	0.60	0.47	0.45	0.36	0.34	0.40	0.50	0.73	0.91			
3477.2	1.29			0.66	0.61	0.58	0.39	0.37	0.31	0.38	0.49	0.82	0.95			
3489.8	0.41					1.03	1.05	0.79	0.44	0.73	1.12	1.65				
3491.1	1.12			0.83	0.71	0.40	0.48	0.44	0.47	0.42	0.54	0.87	1.11			
3500.3	0.35					0.93	0.89	0.73	0.64	1.02	1.54					
$b^2G\text{-}y^2G^o$																
3504.9	3.43				0.64	0.72	0.69	0.58	0.54	0.61	0.76	1.03				
3510.8	3.35					0.72	0.82	0.74	0.55	0.64	0.85	1.33				
$a^2F\text{-}z^4D^o$																
3561.6	0.96						1.37	0.83	0.79	1.19						
3573.7	1.11				1.02	1.04	1.02	0.66	0.53	0.83	1.04	1.57				
3596.1	1.19		1.09	0.80	0.71	0.80	0.71	0.62	0.52	0.54	0.85	1.09				
$a^2P\text{-}z^2S^o$																
3624.8	2.20					0.80	0.68	0.58	0.58	0.82	1.00	1.02	1.23			
3641.3	2.35				0.73	0.69	0.64		0.55	0.83	1.18					
$a^2F\text{-}z^2D^o$																
3685.2	2.52	0.48	0.32	0.44	0.34	0.23	0.40	0.22	0.31	0.38	0.32	0.40	0.59	0.68	0.99	
$a^2F\text{-}z^2F^o$																
3759.3	2.48	0.41	0.35	0.34	0.27	0.22	0.36	0.28	0.35			0.37	0.43	0.59	0.98	
3761.3	2.36	0.50	0.40	0.36	0.28	0.30	0.34	0.28	0.31	0.19	0.33	0.39	0.46	0.67	0.95	1.38

TABLE 2 (Cont'd)

El. Mult. λ	Log gf	Ce 4992 4994	4995 4996	4999 5000	5001 5002	5004	5006 5008	5010 5011	5014 5015	5071	5074	5078	5080	5083	5084	5085
$a^2G-z^2G^o$																
3900.5	2.42				0.78	0.74	0.57	0.56	0.50	0.53	0.73	0.87	1.17			
3913.5	2.38				0.88	0.88	0.57	0.54	0.48	0.56	0.71	0.90	1.27			
Cr II																
$a^4D-y^4P^o$																
3336.4	10.00						0.63	0.57	0.49	0.60	0.84	1.13				
3339.8	10.14	0.99		0.70	0.77		0.53	0.51	0.48	0.45	0.64	0.90		1.11		
3342.6	10.23	0.90	1.04	0.74	0.64		0.47	0.48	0.48	0.57	0.60	0.77	1.16	1.33		
3347.8	10.05			0.97	0.84		0.69	0.61	0.46	0.60	0.74	0.96	1.05			
3358.5	10.32	0.56	0.68	0.53	0.61		0.48	0.41	0.34	0.39	0.57	0.56	0.70	0.92	1.54	
3368.1	10.63	0.43	0.47	0.39	0.43		0.41	0.33	0.29	0.38	0.37	0.44	0.59	0.50	0.76	1.14
$a^4D-z^4P^o$																
3382.7	10.10	0.73	0.87	0.79	0.66		0.57	0.51	0.45	0.50	0.61	0.84	0.94	1.20		
3391.4	9.64							0.93	0.78	0.77	1.07					
3403.4	10.27	0.75	0.71	0.61	0.55		0.49	0.49	0.43	0.47	0.51	0.59	0.67	0.96	1.39	
3408.8	10.40	0.63	0.54	0.46	0.49		0.45	0.45	0.39	0.44	0.48	0.55	0.60	0.89	1.00	
3421.2	10.27	0.81	0.76	0.73	0.71		0.59	0.55	0.40	0.48	0.58	0.71	0.82	1.22	1.31	
3422.8	10.32	0.56	0.54	0.45	0.53		0.45	0.40	0.39	0.34	0.38	0.47	0.61	0.70	0.92	
3433.3	10.30	0.71	0.61	0.55	0.63		0.46	0.39	0.33	0.44	0.57	0.64	0.72			
$a^4D-z^6P^o$																
3495.4	9.06								0.95	1.09	1.35					
3511.8	8.96						1.18		0.92	1.04	1.25					
Sc II																
$a^3D-z^3P^o$																
3369.0	7.16						0.78	0.52	0.40	0.62	1.06					
3372.2	7.28						0.49	0.48		0.48	0.66	0.96	1.11			1.14

TABLE 2 (Cont'd)

$a^3D\text{-}z^3D^o$														
3558.5	6.87			1.08	0.82	0.75	0.63	0.52	0.48	0.64	0.93	1.18	1.26	
3567.7	6.78				1.09	0.85	0.74	0.69	0.63	0.71	0.94	1.54		
3572.5	7.21			1.02	0.61	0.57	0.56	0.51	0.42	0.43	0.65	1.01	1.12	
3576.3	7.11				0.78	0.71	0.61	0.56	0.44	0.55	0.79	1.30	1.47	
3580.9	7.31									0.59	0.94	1.46		
3590.5	6.58				1.22	1.19	0.99	0.73	0.62	0.75	1.27			
$a^3D\text{-}z^3F^o$														
3613.8	7.31			0.78	0.54	0.42	0.45	0.45	0.39	0.47	0.59	0.89	0.95	
3630.7	7.18			0.79	0.64	0.61	0.49	0.44	0.31	0.57	0.73	1.27	1.42	
3642.8	7.10			0.61	0.56	0.65	0.52	0.40	0.37	0.49	0.73	1.14	1.08	
3645.3	6.59				0.92	0.83	0.82	0.53	0.58	0.68	1.02			
3651.8	6.66				0.92	1.05	0.84	0.67	0.63	0.73	1.07			
Mn II														
$a^5D\text{-}z^5P^o$														
3442.0	9.70	0.66	0.55	0.44	0.50		0.42	0.40	0.31	0.33	0.40	0.52	0.60	1.00
3460.3	9.55	0.79	0.74	0.54	0.59		0.41	0.39	0.38	0.37	0.51	0.74	0.81	
3482.9	9.35			0.79	0.78	0.54	0.58	0.58	0.43	0.48	0.56	0.92	0.99	
3488.7	9.28			0.85	0.83	0.61	0.58	0.59	0.57	0.46	0.66	0.91	0.93	
3495.8	8.85					0.77	0.60	0.61	0.48	0.54	0.80	1.23	1.36	
3496.8	8.42						1.02	0.84	0.62	0.95				
3497.5	8.78					0.76	0.79	0.64	0.61	0.60	1.18			
V II														
$a^3F\text{-}z^5D^o$														
3517.3	7.78						0.96	0.89	0.80	0.93	1.24			
$a^3F\text{-}y^3D^o$														
3530.8	7.68						1.06	0.93	0.84	1.06				
3545.2	7.85						1.12	0.97	0.88	0.88	1.32			
3556.8	8.10			1.15	0.88	0.81	0.74	0.58	0.55	0.65	0.95	1.11	1.29	
Fe II														
$a^4D\text{-}z^6D^o$														
3255.9		0.88	0.57	0.47	0.50	0.46		0.37	0.31	0.36	0.48	0.57		0.81
3277.3		0.88	0.55	0.59	0.66			0.38	0.45	0.34	0.45	0.53		0.97

TABLE 2 (Cont'd)

El. Mult. λ	Log gf	Ce 4992 4994	4995 4996	4999 5000	5001 5002	5004	5006 5008	5010 5011	5014 5015	5071	5074	5078	5080	5083	5084	5085
														1.46		
3281.3		1.20	0.88	0.62	0.65	0.54		0.45	0.51	0.43	0.62	0.93			1.45	
3295.8		1.33	1.06	0.95	0.93	0.74	0.75	0.59	0.48	0.51	0.82	1.15				
3303.5			1.73		1.29	1.02	0.86	0.68	0.53	0.72	1.13	1.33				
3314.0				1.87		1.48	1.49	0.99	0.81	1.08						
$a^4P\text{-}z^4D^o$																
3166.7					1.02		0.96	0.90		0.76	1.53					
3170.3				1.00	0.91		0.64	0.76		0.62	0.94					
3186.7			0.49	0.38	0.40		0.40	0.38		0.31	0.40	0.53		1.02	1.01	
3192.9			0.66	0.55	0.57		0.45	0.45		0.32	0.53	0.77		0.87		
3193.8			0.55	0.42	0.48		0.51	0.45		0.38	0.53	0.58		0.83	1.12	
3210.4		0.55	0.40	0.26	0.39		0.35	0.40	0.19	0.30	0.42	0.39		0.78	1.09	
3213.3		0.31	0.36	0.25	0.35		0.34	0.32	0.30	0.24	0.33	0.42		0.48	0.73	0.84
$a^4P\text{-}z^4F^o$																
3183.1			0.69	0.56	0.55		0.41	0.43		0.40	0.58	0.60				
3185.3				1.17	1.09		0.78	0.65		0.60	0.98	1.12				
3196.1			0.65	0.52	0.46		0.37	0.44		0.36	0.55	0.66		0.85	1.42	
$b^4D\text{-}y^4F^o$																
3247.2								0.76	0.62							
$b^4D\text{-}x^4D^o$																
3177.5			1.30	0.99	1.13		0.93	0.73								
$c^2G\text{-}z^2F^o$																
3243.7				1.14	1.14			1.01	1.09							
3247.4								0.80	0.61							
$c^2D\text{-}y^2F^o$																
3179.5			1.08	0.96	0.99		0.93	0.58								

TABLE 3*

LOG W AND LOG N FOR *Ca* I, *Ca* II, AND H, 1947–1948

Line	4992, 94 46.1	4995, 96 40.4	4999, 00 32.0	5001, 02 25.8	5004 24.3	5006, 08 17.6	5010, 11 11.6	5014, 15 9.4	5071 11.5	5074 18.2	5078 25.5	5080 27.6	5083 41.5	5084 48.0
Ca II, K	− 0.03 15.3	− 0.03 15.3	0.00 15.5	0.02 16.1	0.04 16.3	0.01 16.4	0.33† 17.3	0.46† 17.6	− 0.11 15.7	− 0.12 15.6	− 0.16 14.7	− 0.28 13.8	− 0.30 13.4	− 0.43 13.0
Ca I, 4227	....	....	....	− 0.73 12.3	....	− 0.49 13.4	− 0.28 14.9	....	− 0.33 14.3	− 0.70 12.6	....	....	....	....
$H7$	− 0.31 15.6	− 0.25 15.9	− 0.24 16.0	− 0.25 15.9	− 0.24 16.0	− 0.24 16.0	− 0.21 16.2	− 0.32 15.5	− 0.35 15.4	− 0.32 15.5	− 0.33 15.4	− 0.35 15.4	− 0.47 14.9	− 0.71 14.1
$H8$	− 0.33 15.6	− 0.33 15.6	− 0.27 15.9	− 0.23 16.2	− 0.27 15.9	− 0.20 16.4	− 0.33 15.6	− 0.19 16.5	− 0.23 16.2	− 0.32 15.7	− 0.32 15.7	− 0.41 15.4	− 0.54 14.9	− 0.65 14.7
$H9$	− 0.40 15.6	− 0.40 15.6	− 0.38 15.7	− 0.32 15.9	− 0.27 16.1	− 0.34 15.8	− 0.28 16.1	− 0.38 15.7	− 0.38 15.7	− 0.41 15.6	− 0.40 15.6	− 0.46 15.4	− 0.78 14.6	− 1.04 14.2
$H10$	− 0.44 15.5	− 0.38 15.8	− 0.30 16.1	− 0.28 16.2	− 0.28 16.2	− 0.24 16.5	− 0.27 16.2	− 0.25 16.4	− 0.26 16.3	− 0.31 16.1	− 0.41 15.7	− 0.44 15.6	− 0.69 14.9	− 1.04 14.3
$H11$	− 0.50 15.5	− 0.51 15.4	− 0.47 15.5	− 0.46 15.5	− 0.37 15.9	− 0.36 15.9	− 0.32 16.1	− 0.29 16.2	− 0.38 15.9	− 0.41 15.8	− 0.53 15.3	− 0.63 15.1	− 0.70 14.9	− 1.03 14.5
$H12$	− 0.55 15.5	− 0.45 15.8	− 0.50 15.6	− 0.44 15.8	− 0.45 15.8	− 0.41 15.9	− 0.41 15.7	− 0.39 16.0	− 0.39 16.0	− 0.41 16.0	− 0.53 15.5	− 0.63 15.3	....	....

* Column headings are plate number, followed by heights in units of 10^6 km. Entries in table for each line are, above, log W in angstroms; below, log N. Entries marked † have been corrected for the effect of K-star line.

Curves of growth were constructed from the measured equivalent widths of the metallic lines as before, by plotting log $(w \times [3700/\lambda])$ against log $(gf \times [\lambda/3700])$, where w is the equivalent width in angstroms and g is the weight factor; and they were compared with curves calculated from the theoretical formulae. As far as possible, separate curves of growth were constructed at each atmospheric height for the lines of common excitation potential of each ion. For both *Fe* I and *Ti* II the measured lines covered a sufficient range of excitation potential to permit derivation of excitation temperatures.

IV. RESULTS

a) EVALUATION OF DOPPLER WIDTHS FROM CURVES OF GROWTH

For the 1939–1940 eclipse, neutral and ionized lines were plotted together in forming the observed curves of growth, and an increase of Doppler width with height was found.[2] Since neutral and ionized lines were plotted separately for the 1947–1948 eclipse, Doppler widths were estimated for both types of lines, as far as possible at each height. These estimates, obtained by fitting the observations to theoretical curves, were made independently by both authors, and in only two instances did they differ by more than

TABLE 4

LOG N AS FUNCTION OF HEIGHT FOR *H*, *Ca* I, *Ca* II
(Revised Values for 1939–1940 Eclipse)

Atom	Height × 10^{-6} Km								
	6.9	8.4*	14.3	15.3*	20.8	23.3*	28.0	30.7*	38.0*
H	15.5	15.8	15.6	15.9	15.3	15.7	15.2	15.4	15.6
Ca I	17.4	17.1	13.6	12.7	11.9	.....	.....	.....	.....
Ca II	18.6	18.0	16.4	16.2	15.5	15.9	14.5	14.4	14.0

* Egress.

0.02 A. Mean results are given in Table 5, together with corresponding turbulent velocities V_T and the data from the 1939–1940 eclipse on the revised height scale.

It is to be noted that the marked increase of $\Delta\lambda_D$ with height derived from the 1939–1940 data is not confirmed by the more recent material. Although there appears to be a slight tendency for the turbulent velocities of the ionized lines to increase upward, the most striking feature of Table 5 is the appearance of a systematic difference between the turbulent velocities for neutral and for ionized particles (Fig. 1). We can think of no observational deficiency to account for this difference, which, although small, appears so consistently that we are strongly inclined to believe in its reality. In fact, a difference of this kind between the neutral and ionized particle velocities is capable of accounting for the apparent rise of V_T with height, found in 1939–1940, for the following reason. The determination of $\Delta\lambda_D$ at this eclipse depended mostly upon the neutral lines at the lower heights and chiefly upon the ionized lines at the higher levels; hence an apparent increase of $\Delta\lambda_D$ with height is just what one would expect if the true situation is as given in Table 5. We feel that this consideration removes the inconsistency between the results for the two eclipses.

The explanation of the difference between the values of ionized and neutral $\Delta\lambda_D$ must be something like this: a ray through the chromosphere of Zeta Aurigae must penetrate regions of higher- and of lower-than-average ionization, and the mass motions in the regions of higher ionization must tend to be somewhat greater than in those of lower

ionization. A further important point contained in Table 5 is that there is no evidence for differences in turbulent velocity between ingress and egress.

Curves of growth were constructed also for the hydrogen lines from $H7$ to $H12$ for heights up to 48×10^6 km. All these curves yielded estimated values of $\Delta\lambda_D$ of approximately 0.14–0.16 A, with no evidence for a systematic variation with height. The expression for $\Delta\lambda_D$, including both thermal and mass motions, is

$$\Delta\lambda_D = \frac{\lambda}{c}\left(\frac{2kT}{m} + V_T^2\right)^{1/2}. \quad (1)$$

TABLE 5

DOPPLER WIDTHS AND TURBULENT VELOCITIES

1947–1948 ECLIPSE

HEIGHT (10^6 KM)	$\Delta\lambda_D$ (A)		V_T (KM/SEC)	
	Neut.	Ion.	Neut.	Ion.
9.4	0.10	0.13	8.1	10.5
11.5*	.10	.14	8.1	11.4
11.6	.10	.12	8.1	9.7
17.6	.09	.13	7.3	10.5
18.2*	.10	.14	8.1	11.4
24.3	0.10	.16	8.1	13.0
25.5*	.....	.15	.....	12.2
25.8	.....	.14	.....	11.4
27.6*	.....	.16	.....	13.0
32.0	.....	$\geq$ .16	.....	$\geq$13.0
40.4	.....	$\geq$ .16	.....	$\geq$13.0
41.5*	.....	$\geq$ .16	.....	$\geq$13.0
46.1	.....	$\geq$ .16	.....	$\geq$13.0
48.0*	.....	$\geq$0.16	.....	$\geq$13.0

* Egress.

1939–1940 ECLIPSE

Height (10^6 Km)	$\Delta\lambda_D$ (A) Neut.+Ion.	V_T (Km/Sec) Neut.+Ion.
6.9	0.08	6.4
8.4*	.08	6.4
14.3	.10	8.0
15.3*	.13	10.4
20.8	.13	10.4
23.3*	.15	12.1
28.0	0.16	12.9

* Egress.

For hydrogen at 4000° the first term alone yields a value $\Delta\lambda_D = 0.10$ A. If, in addition, there are mass motions corresponding to those given in Table 5 for the neutral particles, i.e., about 8 km/sec, the resulting combined $\Delta\lambda_D$ is 0.14 A. The observed $\Delta\lambda_D$ for hydrogen is therefore at least roughly consistent with the excitation temperatures and turbulent velocities deduced for the metals.

b) DOPPLER WIDTHS DURING TOTALITY

The mass motions derived from observations of the chromospheric lines are necessarily those motions approximately perpendicular to a line from the center of the star, and it would be of considerable interest to know how these motions compare with those in a radial direction. The radial motions can be obtained from direct observations of the star but will correspond to a considerably lower atmospheric level than do the transverse motions.

Several spectrograms of Zeta Aurigae were taken during totality with the 114-inch camera for the purpose of deriving the turbulent velocity in the reversing layer. The yellow-green region (dispersion 5.6 A/mm) was selected in order to minimize the effects of blends. Owing to instrumental difficulties, only one of these plates (Ce 5028) was satisfactory for the purpose. Equivalent widths of about sixty lines were measured in multiplets of *Fe* I, *Ti* I, *V* I, and *Ca* I in which the relative *f*-values are known from

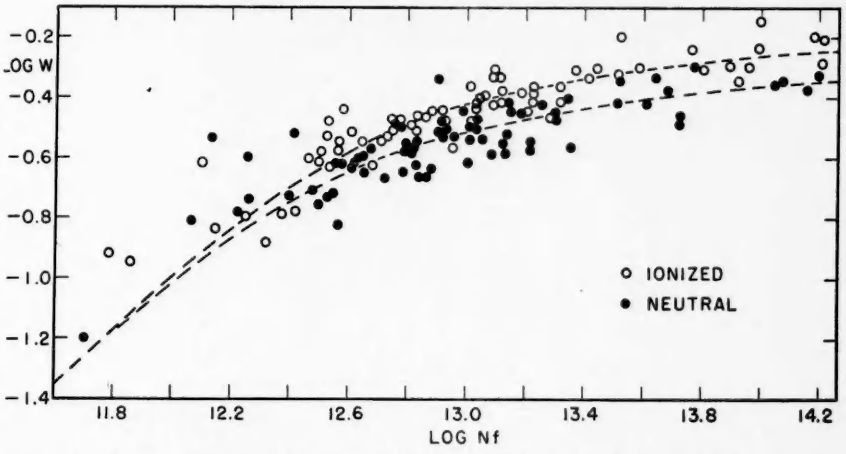

FIG. 1.—Curves of growth at height 9.4×10^6 km during ingress. The theoretical curves are for $\Delta\lambda_D = 0.13$ A (*upper*) and 0.10 A (*lower*).

laboratory data. The intensities were combined into a curve of growth in the usual way and yielded a $\Delta\lambda_D$ of 0.05 A, corresponding to $V_T = 2.3$ km/sec.

Unfortunately, the variation of V_T with height given in Table 5 is so uncertain (for the neutral lines there is no variation) that we do not believe it possible to extrapolate downward to the level of normal line formation. Apparently, judging from the results for the ionized lines, there is a tendency for V_T to increase slightly upward, and to this extent the disk lines and the chromospheric lines yield Doppler widths which differ in the correct sense. A numerical comparison, however, appears to lie beyond the proper use of the existing data, and we are unable to say whether the transverse and radial components of the mass motions are the same at a given height or not.

c) EXCITATION TEMPERATURES

Excitation temperatures have been determined both for *Fe* I and for *Ti* II, and the results are given in Table 6 and in Figure 2. The a^5 F and a^3 F states of *Fe* I, with excitation potentials of 0.86 and 1.48 volts, respectively, were compared with the ground state, a^5 D, and gave fairly accordant results. For *Ti* II only the a^2 F state at 0.57 volts

E.P. was far enough from the ground state, a^4F, and produced enough lines to yield reasonably good values.

In Figure 2 the *Fe* I excitation temperatures as determined at the 1939–1940 eclipse are included for comparison, and the agreement with the 1947–1948 values is fair. Taking all the data into account, there seems little doubt that T_{ex} does increase with height and at about the same rate as was indicated by the 1939–1940 data. Also, considering the scatter of the individual points, there are no certain differences in T_{ex} between ingress and egress.

From the plate (Ce 5028) taken during totality, a well-determined excitation temperature of 2880° was found from the lines of *V* I. This value is probably a little lower than the effective temperature of the star, which is generally considered to be about 3200°.[8]

TABLE 6

CHROMOSPHERIC EXCITATION TEMPERATURES IN ZETA AURIGAE

HEIGHT (10^8 KM)	*Fe* I			*Ti* II
	a^5F	a^3F	Mean	a^2F
9.4	4110	4540	4325	2790
11.5*	4200	5060	4630	2660
11.6	4380	4620	4500	3780
17.6	4290	4340	4315	3780
18.2*	4600	4750	4675	4950
24.3	5100	4930	5015	3800
25.5*	.....	.....	.....	4950
25.8	.....	.....	.....	7750
27.6*	.....	.....	.....	5410
32.0	.....	.....	.....	5410
41.5*	.....	.....	.....	7360
48.0*	.....	.....	.....	6520

* Egress.

d) NUMBERS OF ATOMS IN LINE OF SIGHT AND APPARENT GRADIENTS

The effective numbers of atoms in the line of sight at various heights were read for certain lines from the curves of growth. This material is given in Table 7, where corrections to the ground state by means of appropriate Boltzmann factors are included. Excitation temperatures for the corrections were read from the straight line of Figure 2. To get the numbers of atoms responsible for producing the lines listed in Table 7, it is necessary only to divide the entries by the *f*-values.

Mean values of apparent gradients, $\Delta \log N/\Delta h$, calculated from the values of $\log N$ show a large scatter, as is to be expected, since the derived values of $\log N$ do not form a smooth, monotonic progression. Data of this type are best shown graphically.

Figures 3, 4, and 5 show $\log N$ plotted against height for *Ca* I, *Ca* II, and *H* (first excited state) for both eclipses. Note that in all three diagrams ingress and egress of 1939–1940 agree approximately with egress 1947–1948, but that ingress 1947–1948 stands off in the direction of lower gradient and larger $\log N$ values.[9] Note also that for each particle all four sets of data show a strong tendency to converge to very similar

[8] P. Wellmann, *Mitt. Hamburger Sternwarte, Bergedorf*, No. 76, 1951.

[9] H. L. Welsh, *J.R.A.S. Canada*, **43**, 217, 1949, finds a similar result for *Ca* II alone.

values of log N at the lowest observed heights. Much the same behavior is exhibited by all the metallic lines. Typical of these are the curves for *Fe* I and *Mn* II shown in Figure 6.

In Figure 7 are shown the mean log Nf versus height-curves for ionized and neutral metals for the 1947–1948 eclipse. Two sets of curves have been drawn for the ions, one for low-excitation lines, the other for lines of higher excitation, since the shape of the curve seems to depend somewhat upon the degree of excitation. It is not certain, however, whether this difference is real, since in all these data the Boltzmann correction factors to the ground state are included and, as more highly excited levels are more sensitive to errors in Boltzmann corrections, the differences between the two curves for the ions might be attributable to this source.

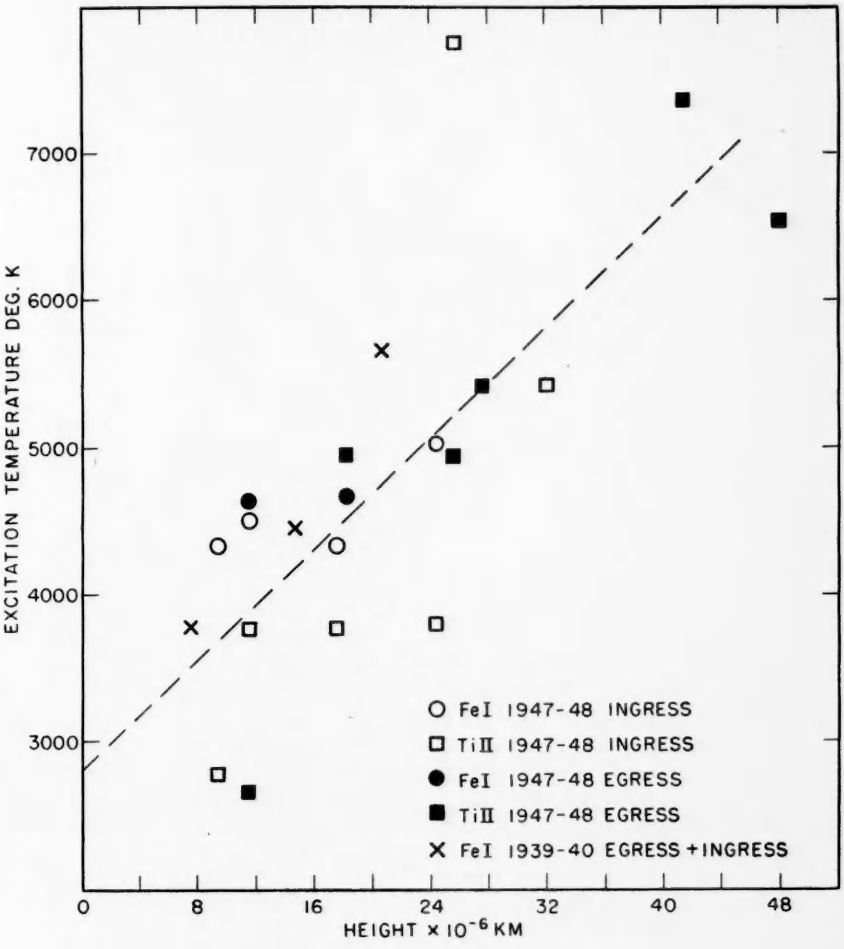

FIG. 2.—Dependence of excitation temperature on height

TABLE 7

VALUES OF LOG *Nf* CORRECTED TO GROUND STATE BY BOLTZMANN FACTOR

ATOMIC STATE	λ	E.P.	HEIGHT × 10^{-6} KM													
			9.4	11.5*	11.6	17.6	18.2*	24.3	25.5*	25.8	27.6*	32.0	40.4	41.5*	46.1	48.0*
Fe I a^5D	(3719.9)	0.00	13.77	13.22	13.42	12.94	12.39	12.58	12.05	12.36	11.75	.....	.....	.....	.....	.....
Fe I a^5F	(3709.2)	0.86	13.96	13.40	13.60	12.95	12.47	12.62	11.86	12.49	11.78	.....	.....	.....	.....	.....
Fe I a^3F	(3815.8)	1.48	15.17	14.72	14.74	14.24	13.47	13.54	13.23	13.40	.....	.....	.....	.....	.....	.....
Ni I a^3D	(3414.8)	0.02	12.95	12.25	12.60	12.13	11.26	11.90	.....	11.75	.....	.....	.....	.....	.....	.....
Mg I 3^3P	(3829.4)	2.70	17.40	16.45	16.48	15.41	15.03	14.74	13.98	14.57	13.72	.....	.....	.....	.....	.....
Cr I a^7S	(3578.7)	0.00	14.20	12.87	13.19	12.61	12.04	12.38	11.44	12.20	.....	.....	.....	.....	.....	.....
Ti II a^4F	(3387.8)	0.00	14.11	13.89	13.75	13.34	13.18	.....	12.81	12.99	12.34	12.92	12.70	12.01	12.55	11.62
Ti II b^4F	(3318.0)	0.11	13.46	12.98	13.03	12.85	12.70	12.83	12.23	12.43	12.02	12.35	12.09	11.49	12.02	11.02
Ti II a^2F	(3761.3)	0.57	14.58	14.30	14.46	13.95	13.97	13.91	13.51	13.98	13.07	13.64	13.43	12.74	13.14	12.32
Cr II a^4D	(3336.4)	2.41	16.06	15.77	15.70	15.22	15.04	.....	14.46	14.57	14.25	14.25	13.86	13.40	13.67	12.92
Sc II a^3D	(3369.0)	0.00	13.04	12.77	12.83	12.66	12.37	12.48	11.86	12.47	11.77	12.16	.....	.....	.....	.....
Mn II a^5D	(3442.0)	1.77	15.79	15.70	15.56	15.16	14.92	14.75	14.22	14.39	14.09	14.18	13.90	13.30	13.62	.....
V II a^3F	(3517.3)	1.07	13.66	13.53	13.54	13.17	12.89	12.95	12.57	12.85	12.34	12.51	.....	.....	.....	.....

* Egress.

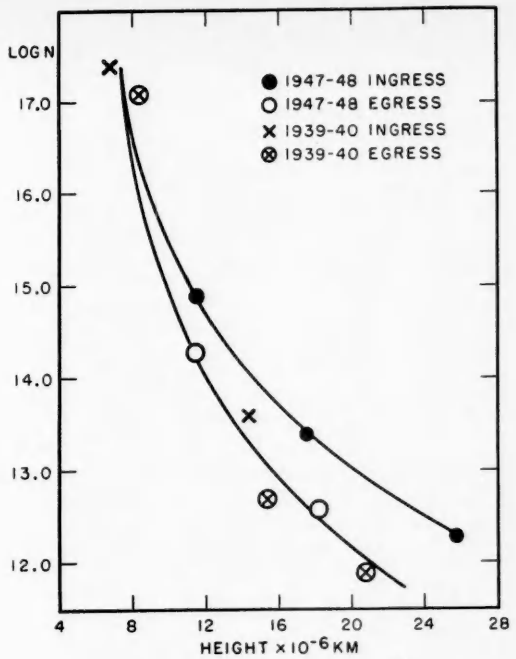

FIG. 3.—Log N versus height for *Ca* I

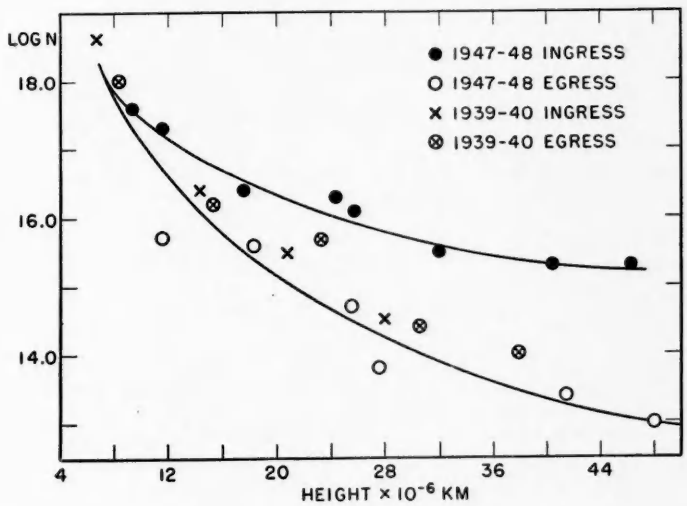

FIG. 4.—Log N versus height for *Ca* II

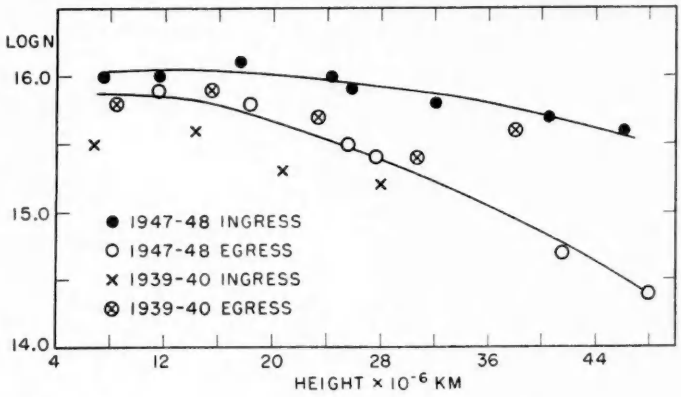

FIG. 5.—Log N versus height for first excited state of hydrogen

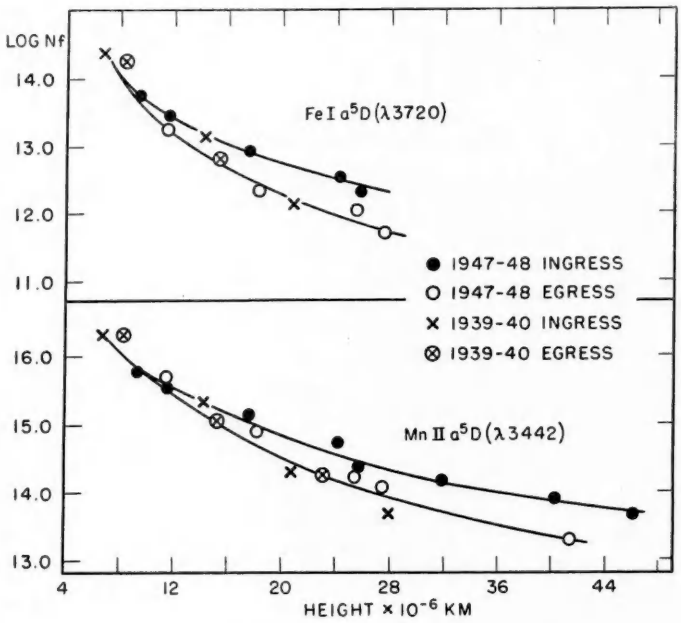

FIG. 6.—Log N versus height for *Fe* I and *Mn* II

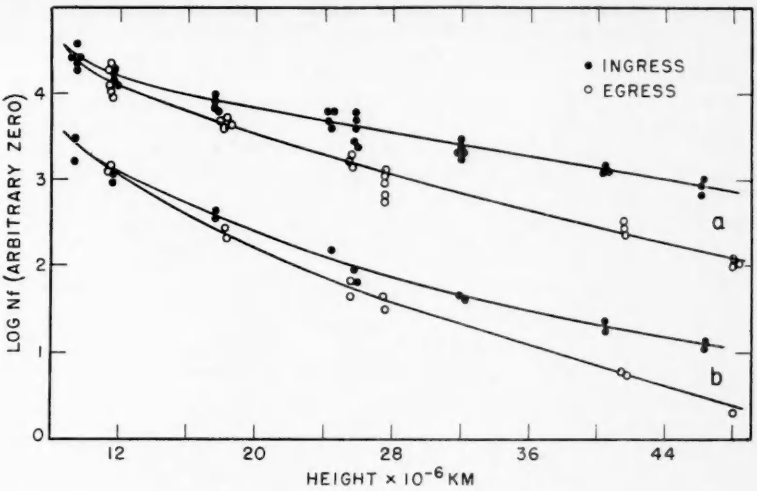

FIG. 7*a*.—Log *Nf* versus height for ionized metals, 1947–1948 eclipse. Curve *a*: *Ti* II, *Sc* II, *V* II. Curve *b*: *Cr* II and *Mn* II.

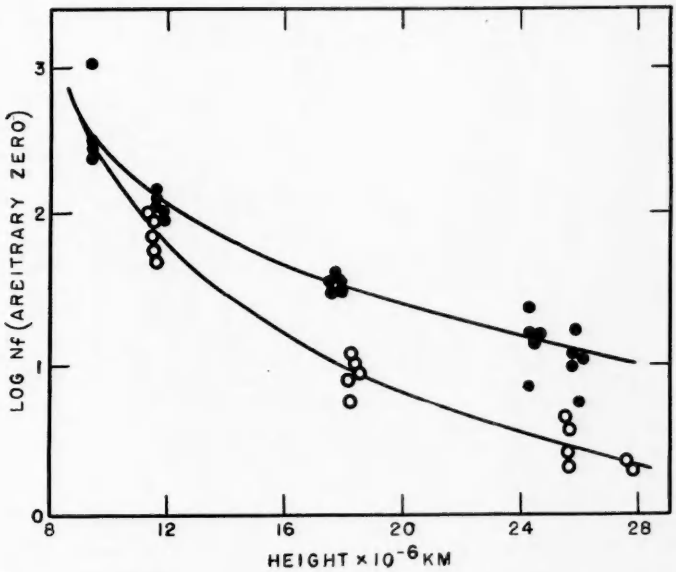

FIG. 7*b*.—Log *Nf* versus height for neutral metals, 1947–1948. Mean curves for *Fe* I, *Ni* I, *Cr* I

Values of log N for two stages of ionization of an element have hitherto been available only for calcium, and the *Ca* I and *Ca* II apparent gradients were found to be quite different in the earlier results.[2] This difference is confirmed by the more recent observations and is clearly evident by comparing Figures 3 and 4. Taking the ratio of $N(Ca\,II)$ to $N(Ca\,I)$ as a measure of the mean ionization of calcium along a ray, the very different apparent gradients for *Ca* I and *Ca* II indicate that the mean ionization of calcium varies rapidly with the height in the lower chromosphere. On the other hand, the approximate parallelism of the curves for other metallic ions and atoms does not show evidence of

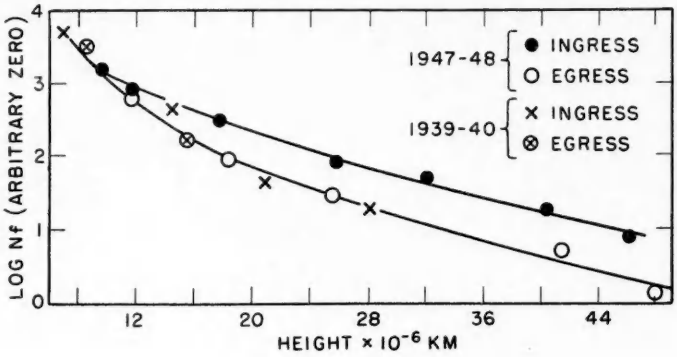

FIG. 8.—Log Nf versus height for *Fe* II

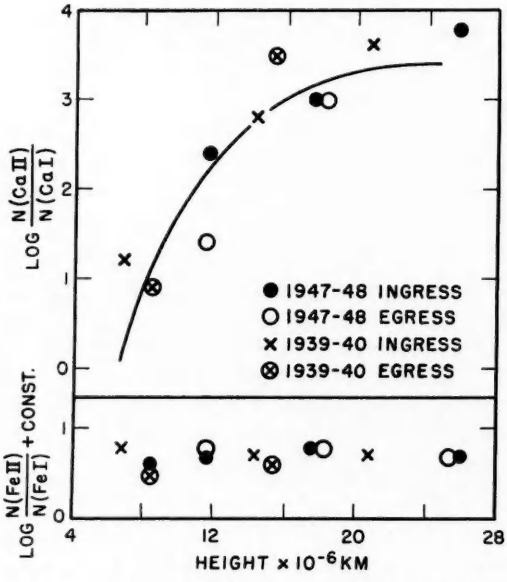

FIG. 9.—Mean ionization of *Ca* and *Fe* as function of height

much change in ionization with height, even though the atoms and ions compared are of different species.

Iron is the only element with enough lines in the spectrum from both the neutral and the singly ionized stage to permit a further study of mean ionization as a function of height. Intensities of about twenty-four lines of *Fe* II were measured on as many plates of both eclipses as possible. Unfortunately, no *f*-values are available for these lines, all of which lie in the region λλ 3167–3314, but they may be used to determine the rate of change with height of log N for *Fe* II. To do this, the log N for each line is read from the appropriate curve of growth. Then the values of $\Delta \log N$ for each line are obtained between successive heights, and the means of these quantities, corrected differentially for temperature differences, should represent fairly well the rate of change of log N with height for *Fe* II. The dependence of log N upon height for *Fe* II derived in this fashion is shown in Figure 8. Finally, comparison of these results with those for *Fe* I yields the height dependence of log $[N(Fe\ \text{II})/N(Fe\ \text{I})]$, apart from an additive, indeterminate, constant.

e) MEAN IONIZATION AS FUNCTION OF HEIGHT

The mean ionizations of *Ca* and of *Fe* as functions of height are shown in Figure 9. Such a gross difference in behavior can hardly be accounted for by errors of any kind and must be considered real. Since the apparent gradients of *Fe* I and *Fe* II are quite similar to those of the other metallic atoms and ions (apart from calcium), the proper conclusion would seem to be this: the mean ionization of the metals is not a function of height over a range in which the total number of atoms in the line of sight decreases by a factor of about 100. Calcium presents an outstanding exception to this rule, showing an increase in $N(\text{ion.})/N(\text{neut.})$ of more than 10^3 over the same range in height. It is noteworthy that in Figure 9 the ionizations of both calcium and iron during ingress 1947–1948 agree with those of the other atmospheric transits represented.

f) RADIAL VELOCITIES

Apart from studies of line intensity, measures of radial velocity of the chromospheric lines offer another line of attack on the problem of atmospheric structure. Most of the spectrograms used for photometric purposes at both eclipses have now been measured for radial velocity. Particularly for plates of the 1947–1948 eclipse, a special effort was made to answer two questions: First, are there, among the metallic lines (apart from *Ca* II), real differences in velocity between groups of strong lines as compared to groups of weak lines? Second, are there differences between lines of ions and of neutral atoms? Careful measurement of sizable groups of lines of the various kinds has shown that the answer to both questions is negative. Accordingly, all velocities of metallic lines, regardless of line strength and source of origin, have been lumped together in forming the mean values labeled "metals" in Table 8 and in Figures 10 and 11.

For the metallic lines the probable errors of the velocities are always considerably less than 1 km/sec. Except at the highest levels, these velocities depend upon measures of twenty or more selected lines. About eight hydrogen lines were measured on most plates, and for these also the probable errors are generally less than 1 km/sec. Since but two lines of *Ca* II are present, only an estimate of the accuracy may be made. On most plates the velocities of H and K agree to within about 2 km/sec, which may therefore be taken as a generous estimate of the probable error of the tabulated *Ca* II velocities. Hence we may conclude that all but the smallest differences shown in Figures 10 and 11 for the metals and for hydrogen almost certainly represent real velocity differences, while differences in *Ca* II velocity of as much as 3 or 4 km/sec are also probably real. At the highest observed levels, naturally, the number of available metallic lines falls off, and the probable error increases slightly.

With these estimates of accuracy in mind, some features of Figures 10 and 11 may be considered. The lines marked "Orbit" are calculated from Harper's elements[5] with the revised period of 972.16 days. The few measures in or close to totality fit the predicted velocity-curve fairly well, and there are not enough of them to show whether Harper's elements require further revision. The vertical lines marked "Eclipse" indicate the extent of the partial phases of the photometric eclipse.

TABLE 8

RADIAL VELOCITIES OF ZETA AURIGAE (KM/SEC)

1947–1948 ECLIPSE

Plates	JD 2432000+	Metals	*H*	*Ca* II
4992, 4994....	528.89	+11.9	+16.8	+11.8
4995, 4996....	529.68	16.0	16.7	14.9
4999, 5000....	530.84	17.0	17.9	15.8
5001, 5002....	531.70	14.2	13.3	18.1
5006, 5008....	532.83	18.8	19.1	23.7
5010, 5011....	533.67	18.8	16.1	25.6
5014, 5015....	533.96	16.7	16.9	19.3
5019*.....	535.69	15.2	.....	.....
5026*.....	542.71	17.9	.....	.....
5059*.....	571.60	23.8	.....	.....
5071.....	573.66	21.4	21.5	22.8
5074.....	574.58	21.5	21.0	19.0
5078.....	575.59	21.0	21.2	20.2
5080.....	575.88	17.8	19.3	18.0
5083.....	577.80	17.1	17.0	14.9
5084.....	578.71	20.4	18.6	17.4
5085.....	579.58	22.4	.....	20.3

*Totality.

1939–1940 ECLIPSE

Plates	JD 2429000+	Metals	*H*	*Ca* II
2183.....	614.82	+17.7	+15.5	+13.1
2188.....	615.82	14.1	17.1	12.1
2194.....	616.72	16.8	19.6	14.6
2202*.....	617.87	16.0	.....	.....
2205*.....	618.78	17.1	.....	.....
2243*.....	655.74	26.5	.....	.....
2245.....	656.66	24.8	.....	27.3
2248.....	657.62	26.1	26.3	28.4
2253.....	658.73	23.1	23.9	26.7
2254.....	659.74	22.4	18.9	21.8
2255.....	660.76	17.5	14.8	18.9

*Totality.

At both ingress and egress the general trend of the velocities is in the direction of a large deviation from the orbit immediately outside eclipse, followed by a return to, or at least toward, the orbital values. These deviations, therefore, cannot be due primarily to a rotation effect, although they are in the right sense if the star rotates in the direction of its orbital motion. Rather, they must be due to some kind of equatorial atmospheric current which exists in the lower chromospheric levels. This hypothetical current is by

no means constant, however. Note, for example, in Figure 10 the low *Ca* II velocities immediately preceding eclipse in 1939 as compared to the extremely high ones of about the same phase in 1947.[10] Another inconsistency is found in comparing the phases of maximum deviation at ingress with those at egress. At ingress the maximum deviations occur within about 1 day of first contact, while more than 4 days elapse after fourth contact before the maximum velocity deviations occur at egress. Moreover, except for *Ca* II, the egress deviations are about twice as large as those at ingress.

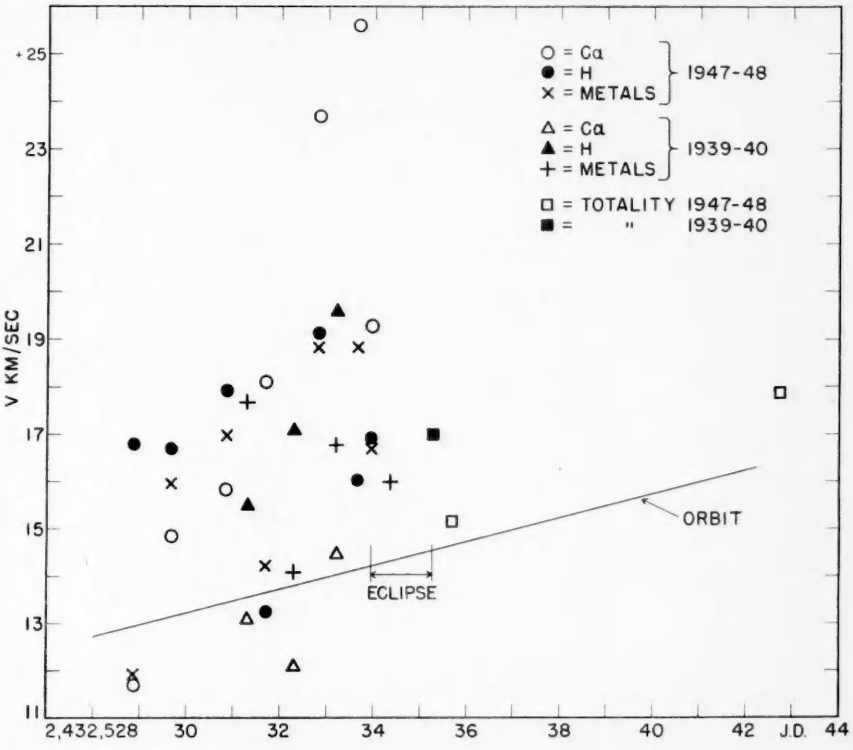

FIG. 10.—Radial velocities near ingress

Variations in velocity can be quite rapid. Note the two 1947 *Ca* II velocities nearest ingress. These are from plates taken only 7 hours apart, and the difference of about 6 km/sec is too large to be accidental.

In general, the hydrogen and metal velocities agree moderately well, with *Ca* II showing the most outstanding deviations, but always in the lower levels where the H and K lines are strong and almost square-sided. This behavior might be explained qualitatively as follows: Suppose that all the lines are really composite, made up of a number of overlapping components distributed in some manner about the mean wave length. Now, if the individual components of the H and K lines are themselves fairly strong,

[10] The JD scales of Figs. 10 and 11 are for the 1947–1948 eclipse. The points for 1939–40 were brought up to date by adding three periods of 972.16 days.

saturated lines, the accidental addition of such a component near one edge of the composite line can introduce an appreciable shift of the mean. If, however, the individual components of the metallic lines and, to a somewhat lesser extent, of the hydrogen lines are quite weak, the accidental addition of an off-center component will have a very much smaller effect on the mean.

That the foregoing explanation is probably correct is shown by careful comparator examination of K on plates 5011 and 5015. When the metallic lines are brought into

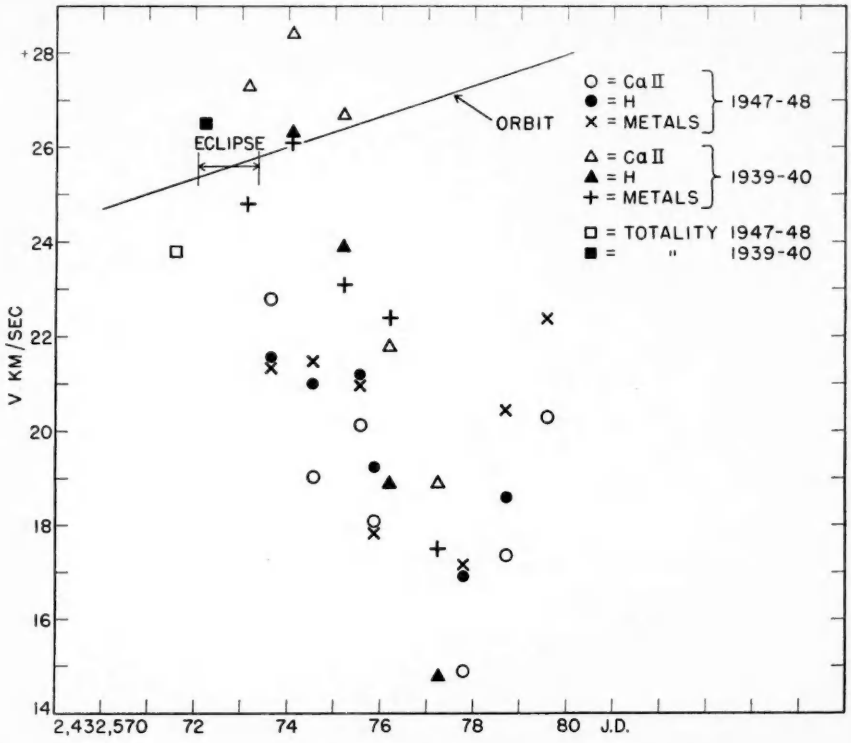

FIG. 11.—Radial velocities near egress

coincidence on these two plates, the violet edges of the two K lines also coincide, but the red side of K on 5015 has a slight redward extension not shared by the line on 5011. This effect, unfortunately too small to show on a reproduction, is qualitatively similar to those found recently in 31 Cygni,[11] where the K line has been observed to break up into distinct components. It is probable that much the same thing occurs in Zeta Aurigae but that the deviations of the components from the mean wave length are smaller in this star than in 31 Cygni.

Whatever the physical significance of the chromospheric radial velocities may be, variations in them do not seem to have much to do with chromospheric extension. Note that, except for the two large deviations of *Ca* II previously mentioned, the maximum

[11] A. McKellar, G. J. Odgers, L. H. Aller, and D. B. McLaughlin, *Nature*, **169**, 990, 1952.

deviations of the 1947–1948 ingress are only about half the deviations at egress. Yet the 1947–1948 ingress is the one transit of the four discussed here which differs from the others in the direction of greater chromospheric extension.

V. INTERPRETATION

a) SPECTROSCOPIC AND PHOTOMETRIC GRADIENTS

It is perfectly clear now that the chromospheres of stars like the K component of Zeta Aurigae are complex structures, far indeed from a state of simple hydrostatic equilibrium. A goodly portion of this complexity is no doubt inherent in the nature of the K star, but, in considering the problem as a whole, it must be remembered that the presence of the hot companion will introduce effects which would not be present, were the K star alone in space. The radiation of the companion, for instance, is likely to play a more or less complicated role in determining the physical state of at least the outer

TABLE 9

SPECTROSCOPIC LOGARITHMIC APPARENT GRADIENTS, $\Delta \ln N/\Delta h$, AT $h = 10 \times 10^6$ KM AND $h = 40 \times 10^6$ KM

ELEMENT	$\Delta \ln N/\Delta h$ (CM^{-1})			
	$h = 10 \times 10^6$ Km		$h = 40 \times 10^6$ Km	
	A*	B†	A*	B†
H‡	~ 0	~ 0	1.2×10^{-12}	0.5×10^{-12}
Ca I	12.7×10^{-12}	9.9×10^{-12}	.....	.....
Ca II	6.0×10^{-12}	3.9×10^{-12}	1.3×10^{-12}	0.6×10^{-12}
Fe I	4.4×10^{-12}	3.7×10^{-12}	.....	.....
Mn II	3.7×10^{-12}	2.8×10^{-12}	1.0×10^{-12}	0.6×10^{-12}
Fe II	4.2×10^{-12}	2.8×10^{-12}	1.2×10^{-12}	1.0×10^{-12}

* Ingress and egress, 1939–1940; egress, 1947–1948.
† Ingress, 1947–1948.
‡ Population of first excited level.

atmospheric layers of the K star. Thus a complete solution of the problems presented by the eclipse phenomena of Zeta Aurigae would doubtless necessitate a careful disentangling of the inherent properties of the chromosphere of the K star from those which are induced by the presence of the companion.

We must confess at the outset that a successful, comprehensive interpretation of the observations has eluded us. This lack of success is not too surprising in view of the fact that many aspects of the solar chromosphere, which is much more accessible to observation than that of Zeta Aurigae, still present unsolved problems. Nonetheless, in this section we wish to discuss some of the observed phenomena, even though the net result may be nothing more than a clarification of the difficulties encountered.

A comparison of the spectroscopic atmospheric gradients with those found from photometric measures is the first item for consideration. In Table 9 are given the logarithmic gradients, $\Delta \ln N/\Delta h$, for some representative particles for the heights 10×10^6 and 40×10^6 km. The lower of these two heights corresponds to a level in the chromosphere just outside the beginning or end of photometric eclipse, while the upper one is, of course, well away from all eclipse effects. The gradients were obtained by drawing the tangents to the curves of Figures 3, 4, 5, 6, and 8 at the heights specified and are given both for ingress 1947–1948 and for the mean of the other three transits.

While no high precision is claimed for the gradients of Table 9, there can be no doubt that the larger differences between the various entries are certainly real, as are also the differences between the columns labeled "A" and "B" at the two heights. The mean ratio, A/B, for $h = 10 \times 10^6$ km, is 1.4, while it is 1.9 for $h = 40 \times 10^6$ km, indicating that ingress 1947–1948 differs from the other transits increasingly with height.

Conversely, the curves of Figures 3–8 suggest that at the heights corresponding to photometric eclipse there is little or no difference in slope between ingress 1947–1948 and the other transits. This result is in agreement with the discussion of the photometric data by Roach and Wood,[12] who find no difference in eclipse gradient between ingress and egress in 1947–1948, although the material bearing on this point is not extensive. The conclusion therefore seems justified that the phenomena which differentiate ingress 1947–1948 from the other transits are restricted to the upper chromospheric heights and do not have much effect in the lower levels corresponding to photometric eclipse. In fact, there is no evidence that any of the derivable parameters—T_{ex}, V_T, or degree of ionization—are different for the abnormal transit, which therefore seems to deviate from the normal ones only in the sense of a slower decrement of density in the upper chromospheric levels.

It would be highly desirable to derive reliable spectroscopic density gradients in the lower chromosphere for comparison with the gradients found from the photometric measures. Reference to Figures 3–8 and to Table 9 shows, however, that this is not a simple straightforward matter. In the first place, different particles show a considerable range in apparent gradient at a height of 10×10^6 km, which is already outside photometric eclipse; and the graphs suggest that these differences probably become even greater at still lower heights. Moreover, all the plots indicate curvature, i.e., nonconstant gradients, so that it is not possible to extrapolate from the outer regions down to the lower levels. Since both the neutral and the ionized metals (excluding *Ca* I and *Ca* II) have similar apparent gradients, it appears that the results for these particles are probably least affected by variable ionization or excitation, and most nearly represent the true rate of change with height of the quantity of matter along successive rays. If this assumption is permissible, then from Table 9 it follows that, for normal transits, in the range of heights corresponding to photometric eclipse,

$$\frac{\Delta \ln N}{\Delta h} > 4 \times 10^{-12} \text{ cm}^{-1}, \tag{2}$$

and the establishment of this inequality is all that can be derived from the spectroscopic data.

In their discussion of the photometric results, Roach and Wood[12] assume that the K-star atmosphere is characterized by a constant density gradient, $n = n_0 e^{-\alpha \Delta h}$, and that the principal source of light-loss in the partial phases is the line absorption of the chromosphere. On the basis of these assumptions they deduce that the parameter α has the value 5.1×10^{-12} cm^{-1}. Our inequality (2) is therefore consistent with this value for α; but a closer comparison does not appear feasible, since our curves for log N versus height are not accurately enough defined at heights below 10×10^6 km.

The steepest of the curves for log Nf versus height (Fig. 3) suggests that the gradient may attain a value such that there is a ratio of about 100:1 in the number of *Ca* I atoms in the line of sight at the inner and outer limbs of the B star. Since the resultant absorption line produced under these circumstances may depend in a complicated way upon the curve of growth, a numerical investigation of the influence of the finite size of the disk of the B star was made for these extreme conditions. Three cases were considered in which the values of log Nf at the inner and outer limbs were taken to be, respectively, 10^{19} and 10^{17}; 10^{18} and 10^{16}; 10^{17} and 10^{15}. The disk of the B star was then divided into

[12] *Ann. d'ap.*, **15**, 21, 1952.

ten segments of equal area, and the contour of the absorption line produced by each segment was calculated by means of the standard formulae, using in each case the value of Nf corresponding to the distance of the segment from the limb. The ten lines from the segments were then added together to form the resultant calculated line whose area was measured with a planimeter, and the corresponding log Nf was read from an appropriate curve of growth.

From the results of this procedure given in Table 10, it is clear that even with the rather extreme assumed gradient and for values of Nf extending from the flat part of

TABLE 10

EFFECT ON LOG Nf OF FINITE SIZE OF B STAR FOR RATIO OF 100:1 FROM INNER TO OUTER LIMB

Log Nf at Limbs	Log Nf at Center of Disk	Log Nf from Composite Line
19–17.....	18.00	18.18
18–16.....	17.00	17.18
17–15.....	16.00	16.18

the curve of growth well into the square-root portion, the effect of the finite size of the B-type star is small and does not produce errors in log Nf in excess of 0.2. For weaker lines the effect will be still less; and we conclude, therefore, that none of the apparent gradients in Figures 3–8 are appreciably influenced by the finite size of the B star.

b) IONIZATION IN THE CHROMOSPHERE

The preceding section on gradients remains seriously incomplete in one major aspect. Although it has been established that the observed apparent gradients are probably fairly reliable and that the major differences between them (Figs. 3–8) are real, no reasons for these differences have been adduced. There are only two ways of accounting for differences in apparent gradient, and these need not, of course, necessarily be mutually exclusive. The first is to suppose that the various particles comprising the chromospheric material do not all have the same density distribution with height. In view of the well-established turbulent nature of the chromosphere, however, one would naturally be predisposed to consider it well mixed throughout and would not look with favor upon a hypothesis requiring a variety of density distributions. The alternative is to ascribe the observed gradient differences to the influence of ionization or excitation or both. In this section we shall inquire briefly into these and related questions.

We cannot proceed at this point without making some simplifying assumptions. First, because the neutral and ionized metals (again excepting *Ca* I and *Ca* II) all have similar apparent gradients, we shall assume that these particles indicate the true chromospheric density gradients. Thus at the lower heights, within the range of photometric eclipse, we shall adopt a value of $\alpha = 5 \times 10^{-12}$ cm^{-1}, while in discussions of higher levels well outside photometric eclipse we shall use $\alpha = 1 \times 10^{-12}$ cm^{-1}. These values are suggested by the data for the "normal" eclipses (see Table 9), and α is the quantity which appears in the density-distribution equation

$$n = n_0 e^{-\alpha \Delta h} . \tag{3}$$

In calculations of ionization we shall use throughout, for all particles, the simplified expression,

$$\frac{n_i n_e}{n_0} = 10^{15.4 - \vartheta I} T_e^{1/2} W . \tag{4}$$

In equation (4) ϑ is $5040/T$, I is the ionization potential in volts, T_* is the temperature of the radiation falling on the matter, T_e is the local electron temperature, and W is the geometrical dilution factor for the radiation. In case the ionizing radiation is weakened by penetrating an optical thickness τ, a factor $e^{-\tau}$ may be applied to the right-hand side of equation (4).

It is first necessary to deduce approximate values of density, and at this point we immediately encounter a difficulty. Only for calcium, and even here only in the lower levels, do we have actual values of N for more than one stage of ionization.

Thus, taking the height 8×10^6 km as a representative "low" level, we find from Figures 3 and 4 $\log N = 16.3$ for *Ca* I and 17.8 for *Ca* II. We do not know what fraction, if any, of the calcium along this ray is doubly ionized. If we assume that none of it is in the form *Ca* III, then the total number of all calcium atoms and ions along the ray is given by $\log N\ (Ca) = 17.8$. In the sun the most recent revision of abundances by Greenstein[13] indicates a hydrogen-to-calcium ratio of $10^{5.6}$. Accordingly, if the same abundance ratio holds in Zeta Aurigae, the number of hydrogen atoms per square centimeter along the ray at height 8×10^6 km should be $\log N\ (H) = 23.4$. Along this ray the observed number in the second state is (Fig. 5) $\log N\ (H_2) = 15.9$; and comparison with the total number leads, by means of the Boltzmann factor, to a mean excitation temperature for hydrogen of 6800°. If any appreciable fraction of the hydrogen along the ray is ionized, an even higher excitation temperature would result. In any case, the mean excitation temperature for hydrogen cannot be so low as that for the metals, which is about 3500° for the ray in question (Fig. 2). For this temperature and with the observed $\log N\ (H_2)$, the total number of hydrogen atoms on the ray would be given by $\log N\ (H) = 30.6$. This number is so large that the chromosphere would be completely opaque at the height in question, because of Rayleigh scattering by neutral hydrogen atoms.[14] Incidentally, the extreme sensitivity of $\log N\ (H_2)$ to the excitation temperature provides the simplest explanation of the difference in shape between the apparent gradient-curve for hydrogen (Fig. 5) and those for the neutral and ionized metals. Only a modest drop in the mean excitation temperature for hydrogen in the lower levels is necessary to account for the flattening of this curve at the lower heights.

Hence, lacking any better procedure, we shall adopt for the ray at 8×10^6 km the values $\log N\ (H) = 23.4$ and $\log N\ (Ca) = 17.8$. These total numbers are related approximately to the central densities on the ray through the expression

$$n_c = N\left(\frac{a}{2\pi R}\right)^{1/2}. \tag{5}$$

With $a = 5 \times 10^{-12}$ cm^{-1} and $R = 1.4 \times 10^{13}$ cm, we find $\log n_c\ (H) = 10.8$ and $\log n_c(Ca) = 5.2$. These would be the numbers of particles per cubic centimeter at the center of the ray if the matter were distributed smoothly according to the density distribution $n = n_0 e^{-a\Delta h}$.

The solar hydrogen-to-iron ratio[13] is $10^{4.9}$, and, if this ratio also holds for Zeta Aurigae, the expected total number of iron atoms and ions along the ray at height 8×10^6 km would be $\log N(Fe) = 18.5$. From Figure 6 we see that the number of atoms active in producing λ 3720 of *Fe* I at the height 8×10^6 km is $\log N = 14.0$. The most recent determination of the absolute f-value for this line[15] is 0.043, from which we deduce that

[13] *Physics for the Engineer* (in press).

[14] See discussion of this point by B. Strömgren, in G. Kuiper, O. Struve, and B. Strömgren, *Ap. J.*, **86**, 570, 1937. Equation (50) of this paper gives the scattering coefficient for neutral hydrogen,

$$\sigma_H = 1 \times 10^{-27}\left(\frac{5000\,A}{\lambda}\right)^4.$$

[15] H. Kopfermann and G. Wessel, *Zs. f. Phys.*, **130**, 100, 1951.

the number of neutral iron atoms on the ray is log $N(Fe\,\text{I}) = 15.8$. Comparing the expected total number with the observed number of neutral iron atoms, we find that the mean ionization of iron must be fairly high, $N(Fe\,\text{II})/N(Fe\,\text{I}) \sim 500$. In contrast, the mean ionization of calcium at the same height is much lower; in fact, from Figure 9, it is about $N(Ca\,\text{II})/N(Ca\,\text{I}) = 10$, even though the ionization potentials of *Fe* and *Ca* are 7.86 and 6.09 volts, respectively.

In comparing the ionizations of iron and calcium in the lower chromosphere, all the evidence indicates that it is the ionization of calcium which is anomalous. Thus the lines of *Fe* II are, in general, fully as strong as those of *Fe* I, even though the *Fe* II lines arise from levels with excitation potentials between 1 and 2 volts. Again, the lines of *Ti* II (I.P. = 6.8 volts) are generally stronger than those of *Fe* I, and no lines of *Ti* I are observed. Since *Ti* is probably about one hundred times less abundant[13] than *Fe*, this observation would imply that the *Fe* I lines are produced by only a small fraction of the total number of iron atoms. Hence we must conclude that, at the lower chromospheric heights, the ionization of the metals, except for *Ca*, is nearly complete. Furthermore, because of the general parallelism of the neutral and ionized log N versus height–curves, plus the definite result from iron (Fig. 9), we also conclude that the ionization of the metals, again with the exception of calcium, does not change appreciably with height over the range to which the neutral particles may be followed.

Is it possible to account for the curious "collapse" of the calcium ionization in the lower chromospheric levels? Presumably, the calcium is ionized by the radiation of the B-type star, and one would therefore expect that a radical change in ionization could result only from some large screening effect at the wave length corresponding to the ionization potential. For *Ca* this wave length is about 2040 A, and there seem to be no unusually strong absorption features in this neighborhood to cut off the radiation of the B-type star. Moreover, other elements of about the same ionization potential might reasonably be expected to be influenced in the same manner. Unfortunately, *Al* (I.P. = 5.96 volts) is the only element for which such a comparison may be made. The resonance lines of *Al* I at λ 3691 and λ 3944 appear in fair strength in the lower chromospheric levels. Although their intensities were not measured, they have been carefully compared with neighboring *Fe* I lines of similar strength, with the result that there can be little, if any, difference in gradient between *Al* I and *Fe* I, whereas if *Al* behaved as *Ca* does, one would expect a much steeper gradient for the *Al* I resonance lines, in analogy with λ 4227 of *Ca* I. Hence we must conclude that the anomalous behavior of calcium is probably not due to effects which might work on any element of similar ionization potential but is caused by something peculiar to calcium itself. We shall return to this point later.

Figure 9 shows that the ionization of calcium rises with height and appears to approach a value of log $N(Ca\,\text{II})/N(Ca\,\text{I}) \sim 3.4$ in the higher chromospheric levels, corresponding to $N(Ca\,\text{II})/N(Ca\,\text{I}) \sim 2500$. If we assume that this degree of ionization corresponds to the constant ionization of the other metals, we may legitimately compare the calcium and iron ionizations in the higher levels by means of equation (4). From the latter we have

$$\frac{N(Fe\,\text{II})\,/\,N(Fe\,\text{I})}{N(Ca\,\text{II})\,/\,N(Ca\,\text{I})} = 10^{-\vartheta(I_{Fe}-I_{Ca})} = 10^{-8900/T}. \qquad (6)$$

The left-hand side of equation (6), from the preceding discussion, is 0.20; the right-hand side is 0.26 or 0.18 for $T = 15{,}000°$ and $12{,}000°$, respectively. A temperature of $12{,}700°$ for the ionizing radiation gives exact agreement; but this whole procedure is rather crude, and no great weight should be given to this particular value. However, the general consistency attained thus far may give a little confidence in some of the assumptions which have necessarily been made.

Finally, assuming our value for the ionization of iron, $N(Fe\ \text{II})/N(Fe\ \text{I}) \sim 500$, to be correct, we may derive an estimate for the mean electron density from equation (4). The dilution factor for the radiation of the B-type star is $W = 3 \times 10^{-6}$, and we take $T_e = 4000°$ and $T_* = 15{,}000°$. Then from equation (4) we find $n_e = 3.6 \times 10^{10}$, which is approximately equal to the central hydrogen density on the ray found earlier. The implication in this result is that the hydrogen is also fairly heavily ionized throughout, and, if so, it is not clear how there can be enough neutral hydrogen to account for the strong Balmer line absorption. Before accepting these results it is necessary to examine the penetration of the ionizing radiation into the chromosphere.

c) APPLICATIONS OF STRÖMGREN'S THEORY

In a discussion of ϵ Aurigae, B. Strömgren[14] has developed methods of dealing with the ionization produced in the atmosphere of a large, cool star by radiation from a small, hot companion. In this section we shall make use of Strömgren's analysis to see whether it will further our understanding of the chromospheric structure of Zeta Aurigae. The geometrical arrangement is sketched in Figure 12. Briefly, Strömgren shows that, along a given ray from the B-type star, hydrogen will be almost completely ionized up

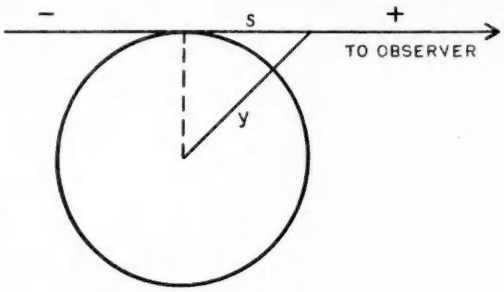

FIG. 12.—Geometry of Strömgren's analysis. The quantity t in the formulae is s/y

to a certain point. Then the ionization will drop very rapidly, owing to depletion of the ionizing quanta, to a value close to zero, which will persist along the remainder of the ray.

The position of the boundary, t_H, between the ionized and neutral zone (H II and H I regions) is given by

$$1 = \frac{a_H}{C_H}\,(n_e)^2 \left(\frac{\pi R}{a}\right)^{1/2} \tfrac{1}{2}\,[1 + \phi\,(t_H \sqrt{\,[aR]\,})\,]\,, \tag{7}$$

where a_H = continuous absorption coefficient of hydrogen at the Lyman limit = 6.3×10^{-18} cm^2; $C_H = 10^{15.4-\vartheta I}\, T_* T_e^{1/2} W$; R = radius of K-type star = 1.4×10^{13} cm; a = gradient = 5×10^{-12} cm^{-1} in the lower chromosphere, and ϕ is the probability integral,

$$\phi\,(x) = \frac{2}{\sqrt{\pi}} \int_0^x e^{-x^2} dx\,.$$

For $T_* = 15{,}000°$, $T_e = 4000°$, and $W = 3 \times 10^{-6}$, we find $C_H = 2.2 \times 10^{11}$.

To find, for any ray, the fraction of total hydrogen atoms contained within the ionized zone, Strömgren's equations may be slightly generalized. Thus the number of ions along the ray is given by

$$N_i = \int_{-\infty}^{t_H} n\,dt = n_e \left(\frac{\pi R}{2a}\right)^{1/2} [1 + \phi\,\{t_H \sqrt{\,(\tfrac{1}{2} aR)\,}\}]\,, \tag{8}$$

in which the value of t_H found from equation (7) is to be used, whereas the total number is given by

$$N_{\text{tot}} = \int_{-\infty}^{\infty} n\,dl = n_c \left(\frac{2\pi R}{a}\right)^{1/2}. \tag{9}$$

From equation (7), with the above values of the parameters and with $\log n_c = 10.8$ as found in the preceding section, we find $t_H(aR)^{1/2} = -3.21$. Then from equations (8) and (9) it follows that, for the ray at height 8×10^6 km, on the assumption of a smooth distribution of matter, only a small fraction of the hydrogen on the ray is ionized. In fact, we find $N_i/N_{\text{tot}} = 7 \times 10^{-4}$. In other words, the zone of highly ionized hydrogen extends inward only a short distance, and practically all the hydrogen on the ray is neutral, less than one-thousandth of it lying within the *H* II zone.

Returning to equation (7), that ray for which the ionization just extends through the atmosphere, the critical ray, is the one for which $t = +\infty$. Hence the central density on the critical ray is

$$(n_c)^2_{\text{crit}} = \frac{C}{a}\left(\frac{a}{\pi R}\right)^{1/2}. \tag{10}$$

For hydrogen, using the same numerical values as before, $(n_c)_{\text{crit}} \sim 10^8$. If we lump the metals together, taking the mean ionization potential to be 7.5 volts, the resulting central density on the critical ray is about 10^9. In making this last calculation, the continuous absorption coefficient for the average metal has been assumed equal to that of hydrogen, for want of more accurate information. The significance of the critical ray is that, for rays with lower central density than $(n_c)_{\text{crit}}$, the region of high ionization extends completely through the atmosphere; for rays with larger n_c, there is a nonionized region whose extent is given by equation (7).

The various values of $\log N$ and $\log n_c$ which have been deduced thus far on the assumption of a smooth density distribution are minimum values, since they are all based on the assumption of no *Ca* III along the ray under discussion at height 8×10^6 km. The minimum value of n_c for hydrogen, $\log n_c = 10.8$, is much larger than the critical central density, and, as we have seen, practically all the hydrogen on the ray should be neutral. The hydrogen-to-metal ratio is presumably of the order of 6000; thus $\log n_c$ for the metals would be about 7.0, which is much below the critical value for an ionization potential of 7.5 volts, namely, 9.0. Hence, along the ray in question, practically all the electrons must come from the metals, all of which should be highly ionized everywhere on the ray. We must next inquire how high the degree of metal ionization is. For this purpose we make use of iron, for which $\log n_c = 5.9$ if the solar abundance ratio of hydrogen to iron is applicable in Zeta Aurigae.

Let us suppose that about 10 per cent of the metal atoms are iron. Then $n_e = 10n(Fe)$, and we find from equation (4), for the center of the ray,

$$\left(\frac{n_i}{n_0}\right)_{Fe} = 10^{6.3}.$$

The ionization at the center of the ray should be a minimum, since the density there is maximum. Hence even the minimum calculated ionization of iron is greatly in excess of the mean value deduced from observation on the basis of no *Ca* III. Clearly, something is basically wrong, and there seem to be two ways out of the difficulty: either all our values of N and n are too small by a factor of about 10^4, or we must give up the smooth distribution altogether and assume that the chromospheric material occurs in condensations of sufficiently high density to yield a reasonable degree of ionization.

The first of these alternatives can be eliminated at once, in the following manner. Let us take for the central calcium density on the ray a value 10^4 times greater than was

found before, i.e., log $n_c(Ca) = 9.2$, and calculate the boundary between the *Ca* III and *Ca* II zones by means of equation (7). For this purpose we make use of the value of the continuous absorption coefficient of *Ca* II, $a_{Ca\ II} = 2.4 \times 10^{-19}$, computed by Bates and Massey.[16] The result is that the *Ca* III zone extends less than halfway along the ray; hence there should have been more than 10^3 as much calcium in the form *Ca* I and *Ca* II as was observed. This argument seems to dispose of the possibility of a smooth distribution with the density increased by 10^4.

d) CHROMOSPHERIC CONDENSATIONS

We are thus forced to give up the idea of a smooth distribution of chromospheric material and must consider a model in which the matter occurs in condensations of some kind. In order to attain some approximation to the nature of the condensations, we shall suppose them to be all alike as to size and density and, further, that the observed or deduced degrees of ionization are those which apply within each condensation.

If we now compare a ray which traverses a given amount of smoothly distributed hydrogen with a ray passing through the same total amount but in which the hydrogen is collected into condensations, we conclude as follows: the ray passing through the condensations will have suffered a larger depletion of ionizing radiation because a larger proportion of the hydrogen in the condensations is neutral, owing to their higher density. Hence, as in the smooth distribution, practically all the hydrogen on the 8×10^6-km ray should be neutral also in the nonsmooth distribution. This means that practically all the electrons in the condensations must come from single ionization of the metals.

We have seen that for $T_* = 12{,}700°$ the ionization of *Ca* and of *Fe* agrees in the higher levels. With this value of T_*, one finds from equation (4) that $n_e = 10^{10}$, in order to give the proper degrees of ionization for these elements. Hence $n(M) = 10^{10}$ also, where $n(M)$ is the number of metal atoms per cubic centimeter, and, with a hydrogen-to-metal ratio of 6000, $n(H) = 10^{13.8}$ cm^{-3}. The condensations have thus turned out to be surprisingly, even uncomfortably, dense. They must also be quite small, since, for a total number of hydrogen atoms $10^{23.4}$ per square centimeter and a condensation density of $10^{13.8}$ per cubic centimeter, only $10^{9.6}$ cm of the path can be occupied. In order that there may be enough condensations in the line of sight to account for the curve of growth, say, of the order of 10–100, it follows that the thickness of the condensations in the line of sight can be only a few hundred to a few thousand kilometers at most. The shape of the condensations cannot, of course, be specified. They might be thin sheets of large width compared to their thickness, or they might be thin, more or less round, filaments. In any event, their small thickness and high density are reminiscent of some of Menzel's descriptions of the structure of prominences and spicules in the solar chromosphere.[17]

e) RECONSIDERATION OF NUMBERS OF ATOMS

In the light of the results of the preceding section we must now retrace our steps to see whether our basic assumptions concerning numbers of atoms in the line of sight require modification. For the ray at height 8×10^6 km, it will be recalled that the observed value of log N for calcium, log $N(Ca) = 17.8$, led to the result that log $N(H) = 23.4$. Underlying this conclusion were the assumptions that (1) the solar abundance ratios hold also for Zeta Aurigae and (2) no large fraction of the calcium on the ray was in the form *Ca* III. We must now check this second assumption against the specifications of the condensations deduced above.

With $T_* = 12{,}700°$, $T_e = 4000°$, and log $n_e = 10$, equation (4) yields the result $n(Ca\ III)/n(Ca\ II) = 12.5$. In other words, over 90 per cent of the calcium in the con-

[16] *Proc. R. Soc. London, A*, 177, 281, 1941.

[17] D. H. Menzel, *Our Sun* (Philadelphia: Blakiston Co., 1949), chap. viii.

densations should exist as *Ca* III, and all the values of N based upon the observed value of log $N(Ca)$ should be increased by a corresponding factor. Such a change would be disastrous for the ionization computations. For instance, we should have $N(Fe\,\text{II})/N(Fe\,\text{I}) \sim 5000$ instead of 500, while $N(Ca\,\text{II})/N(Ca\,\text{I}) = 2500$ in the higher levels would remain as before, since it is an observed ratio. Before accepting this revision, let us consider the rather special circumstances surrounding the ionization of *Ca* II to *Ca* III.

The second ionization potentials of all the common metals except calcium exceed that of hydrogen. Hence, if the ray we are considering lies principally within the *H* I zone, all these metals except calcium are protected from second ionization by the radiation from the B-type star by the continuous absorption of hydrogen, which removes practically all the radiation lying above 13.54 volts. Since the second ionization potential of calcium is only 11.82 volts, it appears inevitable at first glance that most of the *Ca* II will be ionized to *Ca* III.

A second consequence of the neutrality of most of the hydrogen is, however, that the Lyman absorption lines will be tremendously strong over most of the ray, and we note that the principal *Ca* II absorption edge at 11.82 volts is only 19 A redward from Ly-β. Is it possible that the ionization of *Ca* II to *Ca* III is suppressed in the lower atmospheric levels by the presence of Ly-β?

The absorption coefficient in the wing of a line is given by[18]

$$k = 16.5 \times 10^{-26} \left(\frac{\lambda}{\Delta\lambda}\right)^2 f . \tag{11}$$

With $\lambda = 1029$ A, $\Delta\lambda = 19$ A, and $f = 7.9 \times 10^{-2}$, we find from equation (10) that $\tau = 3.84 \times 10^{-23} N$. Hence for log $N(H) = 23.4$ it follows that the opacity due to Ly-β is adequate to suppress the ionization of *Ca* II over about three-fourths of the light-path. When we consider that the numbers which have gone into this computation are fairly uncertain and that the opacity increases by a factor of nearly 2 by moving only 5 A shortward of the absorption edge of *Ca* II, it seems very probable that little *Ca* III will exist on the ray at height 8×10^6 km. If this argument is allowed, it follows that our estimates of $N(H)$ and $N(Fe)$ for this ray are essentially correct as given previously.

The foregoing discussion clarifies another puzzling observational point which has not hitherto been mentioned. Consider the curves of log N versus height in Figures 4 and 8. For the normal eclipses, between the heights 8×10^6 and 40×10^6 km, log N for *Ca* II decreases by 4.5, while the corresponding decrease for *Fe* II is only 2.9. This difference is not likely to mean that the relative abundances of calcium and iron change with height. It is, however, of the right order of magnitude to be accounted for if most of the calcium is in the form *Ca* II at the lower level and over 90 per cent of it exists as *Ca* III at the upper level, while the second ionizations of the other metals remain negligible. This last point requires investigation, since it might be supposed that eventually a height will be reached where the other metals would no longer be screened by the continuous absorption of hydrogen. With our specifications for the condensations, we find that this does not happen. From equation (4), with a hydrogen density of $10^{13.8}$, it follows that the ionization of hydrogen never exceeds about 5 per cent. Hence, without appreciable error, we may write, for the opacity at the Lyman limit,

$$\tau_{Ly} = L \times 10^{13.8} \times 6.3 \times 10^{-18} , \tag{12}$$

where L is the path length in centimeters. In order that τ_{Ly} may attain a value of 10, it follows that $L = 10^{4.4}$ cm. Thus less than 1 km of path length is required to provide virtually perfect screening against second ionization for metals such as iron. Hence in a condensation exposed to the full radiation of the B-type star, only a negligible fraction of the metals other than calcium will be doubly ionized.

[18] A. Unsöld, *Physik der Sternatmosphären* (Berlin: J. Springer, 1938), eq. (41.6).

f) CONTINUOUS ABSORPTION

The ray at height 8×10^6 km lies just within the range of heights included in the photometric eclipse, and we must next investigate the continuous opacity of the chromospheric material, since any model of the chromosphere must, of course, be consistent with the photometric results as well as with the spectroscopic observations. If the matter is in the form of condensations with neutral hydrogen and singly ionized metals, the only type of opacity which requires consideration is that due to negative hydrogen. Moreover, since we are assuming that all the condensations are alike, we need deal only with a uniform layer whose physical characteristics are the same as those of the condensations and whose thickness is such that the amount of matter per square centimeter is the same as that given by the spectroscopic observations. We therefore inquire into the continuous opacity of a layer in which there are $10^{13.8}$ neutral hydrogen atoms per cubic centimeter; $10^{23.4}$ neutral hydrogen atoms per square centimeter; and a hydrogen-to-metal ratio of 6000, with the metals all singly ionized, and therefore $n_e = 10^{10}$.

The ionization potential of H^- is 0.75 volt, and its ionization will therefore be governed by the radiation from the K-type star.[19] With a dilution factor $W = \frac{1}{2}$ for the K-type star, the Saha equation for negative hydrogen becomes

$$\frac{n_H n_e}{n_{H^-}} = 10^{15.7-\theta I} T^{3/2}, \tag{13}$$

where we have set $T = T_* = T_e = T_K$. Assuming the values $T_K = 3200°$, $n_H = 10^{13.8}$, and $n_e = 10^{10}$, we find from equation (13) that $n_{H^-} = 10^4$. Thus, since conditions are uniform in the layer under consideration, $N_{H^-} = N_H(n_{H^-}/n_H) = 10^{13.6}$, and this is the total number of negative hydrogen ions per square centimeter through the layer. At λ 4500 the absorption cross-section for H^- is approximately[20] 3×10^{-17} cm^2; therefore, the opacity at this wave length produced by H^- is only 1.2×10^{-3}.

We conclude that, according to the present chromospheric model for Zeta Aurigae, the major part of the photometric eclipse is, in fact, caused by line absorption, as suggested by Roach and Wood.[12] Only when the line of sight passes through about one hundred times as much material as at the 8×10^6-km level will the H^- opacity begin to play a role. For a gradient of 5×10^{-12} cm^{-1}, the amount of matter in the line of sight would be increased one hundred fold over that at 8×10^6 km at a height of -2×10^6 km, i.e., at a level below that corresponding to second and third contacts. Even making allowance for the uncertainty in our data and for the fact that the gradient may become appreciably steeper below the 8×10^6-km level, it would seem that H^- opacity is unlikely to play any role except possibly at the very end of partial phase, just prior to the onset of totality.

g) TURBULENCE AND EXCITATION TEMPERATURE

The observed difference in $\Delta\lambda_D$ between the neutral and ionized lines and the rise of excitation temperature with height require brief examination. Can these features be accounted for, even qualitatively, on the chromospheric model developed here? Let us consider these two items in the above order.

It is highly improbable that all the condensations have exactly the same density and hence exactly the same degree of metallic ionization. More likely, these parameters vary over some range, and the values we have deduced in the preceding sections are means of some kind. If, now, the less dense (and perhaps less massive?) condensations tend to

[19] It is easy to show that, for ionization processes requiring less than 3.7 volts, the ionization will be determined by the K-type star. Above this value the B-type star predominates.

[20] S. Chandrasekhar, *Ap. J.*, **102**, 395, 1945. The free-free opacity is negligible at λ 4500.

have somewhat more rapid motions than the denser ones, there should be a tendency for the ionized lines to yield a larger $\Delta\lambda_D$ than do the neutral lines. While this idea can hardly be considered as an explanation of the observed phenomenon, it is at least not unreasonable. Moreover, if the chromosphere were not discontinuous in nature and the neutral and ionized particles were thoroughly mixed, it is very difficult indeed to see how the observed difference in $\Delta\lambda_D$ could exist.

We have seen (Fig. 2) that the measured excitation temperature rises steadily with height, beginning at the lowest observed levels with values of the same order as the effective temperature of the K-type star. This fact suggests that perhaps the excitation temperature in the lower chromosphere is determined by the radiation of the K-type star but that the B-type star plays an increasingly important role in the higher levels.

We first consider the relative effectiveness of collisions and radiative processes in determining the populations of the various states of the metallic ions and atoms. The probability of an excitation by electron collision of a level E volts above the ground state is given approximately by the expression,[21]

$$p_c = 2n_e\sigma^2\left(\frac{2\pi kT}{m}\right)^{1/2} e^{-E/kT}, \tag{14}$$

in which n_e is electron density, σ^2 is the collisional cross-section, and T is the electron temperature. With $n_e = 10^{10}$, $\sigma^2 = 10^{-17}$, and $T = 4000°$, it follows that the probability of collisional excitation of a level of 1-volt energy is $p_c \sim 1$.

The probability of radiative excitation is computed from the usual formula,

$$p_r = B_{12}u_\nu ,$$

where B_{12} is the Einstein absorption coefficient, related to the f-value for the line concerned through the expression

$$B_{12} = \frac{\pi e^2}{mh\nu} f ,$$

and u_2 is the radiation density.

Assuming, now, that both stars radiate as black bodies, so that u_ν is given by the Planck function multiplied by the appropriate dilution factor and that the temperatures of the K-type and B-type stars are 3200° and 15,000°, respectively, one finds, for a line at λ 4000 A,

$$p_r = 3.3 \times 10^3 f \quad \text{for the radiation of the K-type star,}$$

$$p_r = 1.2 \times 10^2 f \quad \text{for the radiation of the B-type star.}$$

The f-values of the stronger metallic lines are of the order of 10^{-2}; hence there is some indication, though it is not decisive, that the excitation temperature of a condensation exposed to the full radiation of both stars would approximate that of the K-type rather than the B-type star. In the higher chromospheric levels there should be appreciable screening of the radiation of the K-type star by the underlying material, together with less screening of the radiation from the B-type star, and a corresponding tendency for the excitation temperature to be governed more by the B-type star and by the electron collisions. Since the velocity distribution of the electrons is determined by the higher temperature radiation, it might be expected that when they make a significant contribution to the excitation temperature, it, too, will be in the direction of higher values. There appears to be at least a possibility, therefore, that the variation of T_{ex} with height might be understandable somewhat along the lines of the foregoing discussion.

[21] O. Struve and K. Wurm, *Ap. J.*, **88**, 84, 1938.

h) SUMMARY AND CONCLUDING REMARKS

The picture of the chromosphere of Zeta Aurigae developed here is one of great discontinuity. A ray through the chromosphere passes mostly through empty (spectroscopically speaking) space and encounters here and there a condensation of matter of relatively small size and high density. Relative motion of the condensations will account for the shapes of the curves of growth, i.e., for the "turbulence"; and the size and density of the condensations explain the various ionizations required to bring the spectroscopic observations into agreement with the solar abundance ratios. Moreover, there is no conflict with the photometric observations or with their recent interpretation. Even the differences between abnormal chromospheric transits, such as ingress 1947–1948, and the normal ones receive a simple interpretation. An abnormal transit is simply one in which there are more than the average number of condensations in the line of sight, especially in the higher levels; but the condensations themselves are not observationally distinguishable from those present at other times. Taken as a whole, therefore, the analysis presented here appears fairly successful.

But there is one outstanding failure which we must regard as serious, namely, the fact that we cannot account for the "collapse" of the *Ca* II ionization in the lower chromospheric levels. Our entire analysis is based upon the idea that the degree of ionization in the chromosphere of the K-type star can be calculated by elementary means on the assumption of black-body radiation of the B-type star, with allowance, when necessary, for absorption features introduced by the chromosphere of the K-type star itself. That these simple considerations fail completely to explain the one ratio of ionized to neutral particles which we can observe directly is very unsatisfactory and gives no assurance that our other calculations can lead to useful results. Nevertheless, all the evidence indicates that the ionizations of the other metals do not vary with height, and we have been forced to regard this fact as the more fundamental datum to be explained.

We cannot get out of our difficulty by supposing that the rapid drop in the *Ca* II/*Ca* I ratio marks the height at which the boundary of the *Ca* II zone moves inward from $-\infty$ in the sense of Strömgren's theory. For Bates and Massey give $a = 2.5 \times 10^{-17}$ as the continuous absorption coefficient of *Ca* I; and, with this value for a and the observed number of *Ca* I atoms on the 8×10^6-km ray, $\log N(Ca\,\text{I}) = 16.3$, the total opacity over the entire path is only 0.5, far below what is needed for any appreciable effect on the ionization. Curiously, the *Ca* II/*Ca* I ratio at 8×10^6 km is about that to be expected if the ionization of *Ca* at this level is produced only by the radiation of the K-type star and if $n_e = 10^{10}$. But we are unable to account for the absence of the radiation from the B-type star and must, for the present, regard the behavior of the calcium ionization as an unexplained, and admittedly uncomfortable, phenomenon.

Finally, it must be emphasized that no attempt has been made here to give a *physical* explanation of the Zeta Aurigae chromosphere. Even if the existence of the condensations be accepted, we have no theory as to their origin or their persistence as discrete entities. These problems may very well be quite similar to those presented by many aspects of the solar chromosphere, to which, it seems, there are also no really satisfactory answers at the present time.

SPECTROSCOPIC OBSERVATIONS OF MIRA CETI, 1934–1952

ALFRED H. JOY
MOUNT WILSON AND PALOMAR OBSERVATORIES
CARNEGIE INSTITUTION OF WASHINGTON
CALIFORNIA INSTITUTE OF TECHNOLOGY
Received August 7, 1953

ABSTRACT

The use of coudé spectrograms with dispersions up to 2.3 A/mm permits a more critical study of the spectroscopic behavior of Mira Ceti than was possible with lower dispersions. Eighty-eight spectrograms were measured for velocity.

Absorption lines.—Radial velocities deduced from 70 selected lines, representing 16 cycles of the star's variation, indicate fluctuations from cycle to cycle in amounts comparable with the range within a single cycle. In each cycle, maximum velocity of recession usually occurred shortly after maximum light, but the observations near minimum light are too few to permit conclusions with regard to their application to the pulsation theory. Different elements yield slightly different velocities. The displacements of the *Fe* lines are correlated with the excitation potential.

Emission lines.—The intensity of the emission varies in different cycles, and the incidence of various lines of different elements and different multiplets is peculiar. In general, the velocities from the bright lines are more regular than those of the absorption lines. The velocities of recession of the metallic lines increase with phase, but the hydrogen velocities show approach until phase +65 days and then join the curve of the metals. With respect to the reversing layer, the velocities are always outward. Bright-line velocities are also correlated with excitation potential. Certain lines are greatly enhanced by fluorescent effects.

The visual companion.—Variations in the relative intensity of the spectrum of the visual companion indicate that the period of light-fluctuation may be about 12–14 years. The sharp reversal in the bright H and K lines shows a velocity of +52.3 km/sec, which may be the velocity of the star. No other absorption lines occur except the strong P Cygni absorption accompanying the hydrogen lines.

Discussion.—Velocity variations within the cycle are confirmed, but the evidence for volume pulsation of the whole star is open to question.

Since 1926, when an extended report[1] on low-dispersion spectroscopic observations of Mira Ceti was issued, many coudé spectrograms of the star have been obtained at Mount Wilson by P. W. Merrill, W. S. Adams, and A. H. Joy for various investigations and for recording the variations in different cycles. While these observations have not been systematic or exhaustive, the use of considerably higher dispersion makes possible a more precise examination of many details than has heretofore been possible. At the coudé spectrograph of the 100-inch telescope a dispersion of 10.3 A/mm was used to good advantage at all phases except near minimum light. At phases of greatest brightness the dispersion was, at times, increased to 2.9 A/mm. In 1950 a few spectrograms with dispersions of 2.3 and 9.1 A/mm were obtained by I. S. Bowen at the 200-inch Hale telescope. In addition, 117 spectrograms with dispersions of 36 and 75 A/mm, exposed at the 60- and 100-inch reflectors, were used for checking and comparison.

In Table 1 the coudé spectrograms measured for velocity are listed, together with the velocity results from absorption and emission lines. The number of lines used in determining the velocity from each plate appears in parentheses. The dispersion of the spectrograms is in the last column. The phases from maximum light, in the fourth column, are computed from the maxima of Table 2. The measurement has been shared by Miss Sylvia Burd. The mean systematic difference in our measures is less than 0.1 km/sec, and our accidental errors are nearly identical in amount. Because of the accuracy attained in

[1] A. H. Joy, *Mt. W. Contr.*, No. 311; *Ap. J.*, **63**, 281, 1926.

TABLE 1

VELOCITY OBSERVATIONS OF MIRA CETI

PLATE COUDÉ	DATE	JD 2400000+	PHASE FROM MAX. (DAYS)	VELOCITIES (KM/SEC)				DISP. (A/MM)
				Absorption	Neutral Bright	Bright $H\delta\gamma$	Bright *Fe* II	
885...	1935 Jan. 24	27827	+ 24	+67.1 (7)	+48.3 (6)	+48.6 (1)	+47.7 (1)	7.9
890...	Jan. 25	7828	+ 24	+63.4 (16)	+45.8 (9)	+42.4 (2)	+54.0 (2)	7.9
975...	1935 Dec. 6	8143	− 7	.....	+42.6 (1)	.....	.....	2.3
987...	Dec. 12	8180	+ 30	+57.2 (51)	+42.7 (3)	+40.8 (1)	.....	7.9
1208...	1936 Oct. 25	8467	− 14	.....	+45.0 (1)	.....	.....	3.1
1209...	Oct. 26	8468	− 13	+68.3 (20)	+45.2 (1)	.....	.....	7.9
1286...	Dec. 23	8526	+ 45	.....	+45.9 (6)	.....	+53.0 (1)	3.1
1287...	Dec. 23	8526	+ 45	+63.7 (20)	+46.4 (9)	.....	+50.5 (2)	2.5
1290...	Dec. 29	8532	+ 51	+62.4 (31)	+46.3 (17)	+47.2 (2)	+53.9 (3)	10.3
1298...	1937 Jan. 4	8538	+ 57	.....	+44.4 (6)	.....	+50.6 (1)	3.1
1315...	Jan. 31	8565	+ 84	.....	+43.5 (1)	+40.8 (1)	.....	3.1
1319...	Feb. 1	8566	+ 85	+59.7 (50)	+47.8 (11)	+46.9 (1)	+51.4 (1)	10.3
1472...	1937 Sept. 15	8792	− 38	+56.6 (11)	+43.7 (1)	.....	.....	20.0
1513...	Oct. 18	8825	− 5	+58.2 (30)	+43.1 (1)	+49.8 (1)	.....	10.3
1518...	Oct. 19	8826	− 4	.....	+45.7 (1)	+47.7 (1)	.....	10.3
1524...	Oct. 20	8827	− 3	.....	.....	+48.6 (1)	.....	10.3
1540...	Nov. 13	8851	+ 21	+57.9 (27)	+44.2 (2)	+46.3 (2)	.....	10.3
1774...	1938 Sept. 3	9145	− 14	.....	+45.1 (1)	.....	.....	3.1
1775...	Sept. 3	9145	− 14	.....	+44.6 (1)	.....	.....	3.1
1785...	Sept. 9	9151	− 8	+57.0 (37)	.....	+43.6 (1)	.....	10.3
1801...	Oct. 8	9180	+ 21	.....	+45.1 (3)	.....	+56.5 (2)	3.1
1843...	Dec. 3	9236	+ 77	+61.2 (10)	+51.0 (5)	.....	+61.0 (1)	10.3
1868...	Dec. 29	9262	+103	.....	+52.5 (1)	.....	.....	3.1
1870...	Dec. 30	9263	+104	+62.4 (25)	+52.6 (10)	+51.6 (1)	+57.8 (3)	10.3
2114...	1939 Sept. 4	9511	+ 30	.....	+49.3 (5)	.....	+55.8 (1)	2.9
2115...	Sept. 4	9511	+ 30	+64.4 (24)	+48.0 (7)	.....	+52.6 (1)	2.9
2118...	Sept. 21	9528	+ 47	.....	+48.8 (12)	.....	+56.9 (2)	2.9
2119...	Sept. 21	9528	+ 47	+63.5 (8)	+50.1 (11)	.....	+56.4 (2)	2.9
2120...	Sept. 21	9528	+ 47	.....	+49.2 (4)	.....	.....	2.9
2133...	Sept. 29	9536	+ 55	+63.2 (66)	+48.4 (15)	.....	+55.3 (3)	2.9
2140...	Oct. 21	9558	+ 77	.....	+50.1 (6)	.....	+56.0 (4)	2.9
2141...	Oct. 21	9558	+ 77	.....	+47.8 (10)	.....	+54.1 (3)	2.9
2173...	Nov. 29	9597	+116	.....	+51.0 (6)	.....	+53.6 (3)	2.9
2423...	1940 Sept. 22	9895	+ 75	+61.6 (11)	+50.2 (5)	.....	+54.6 (1)	2.9
2426...	Oct. 11	9914	+ 94	.....	+49.2 (10)	.....	+52.3 (3)	2.9
3216...	1943 Sept. 22	30990	+170	+53.2 (19)	+49.9 (9)	+45.2 (2)	+50.1 (3)	10.3
3279...	Nov. 12	1041	+221	.....	+53.4 (3)	.....	.....	10.3
3686...	1945 Jan. 1	1457	− 27	+59.9 (61)	.....	+50.2 (1)	.....	10.3
3695...	Jan. 3	1459	− 25	+60.3 (56)	.....	.....	.....	2.9
3703...	Jan. 26	1482	− 2	+61.9 (21)	.....	.....	.....	2.9

TABLE 1—*Continued*

Plate Coudé	Date	JD 2400000+	Phase from Max. (Days)	Velocities (Km/Sec)				Disp. (A/Mm)
				Absorption	Neutral Bright	Bright $H\delta\gamma$	Bright *Fe* II	
4042	1945 Oct. 25	301754	− 69	+57.5 (30)	+46.1 (2)	.....	.....	10.3
4047	Nov. 13	1773	− 50	+59.2 (39)	+43.5 (1)	.....	+53.0 (1)	10.3
4057	Nov. 20	1780	− 43	+57.9 (42)	+44.2 (1)	.....	+53.3 (1)	10.3
4077	Nov. 29	1789	− 34	+59.8 (43)	+43.8 (1)	.....	.....	10.3
4078	Dec. 11	1801	− 22	+58.1 (51)	+44.0 (1)	.....	+50.9 (1)	10.3
4079	Dec. 11	1801	− 22	+57.9 (22)	+44.2 (1)	.....	.....	10.3
4102	Dec. 23	1813	− 10	+57.3 (32)	+44.4 (3)	+46.7 (1)	+55.5 (1)	10.3
4103	Dec. 23	1813	− 10	+57.9 (59)	+43.2 (1)	+49.6 (2)	.....	10.3
4104	Dec. 23	1813	− 10	+58.5 (34)	+42.6 (1)	.....	.....	10.3
4108	Dec. 28	1818	− 5	+58.8 (40)	+45.8 (2)	+50.4 (2)	.....	10.3
4109	1946 Jan. 10	1831	+ 8	+59.8 (32)	+46.7 (3)	+47.1 (1)	+55.2 (2)	10.3
4127	Jan. 15	1836	+ 13	+59.0 (35)	+48.1 (2)	+47.7 (1)	+54.9 (2)	10.3
4138	Jan. 18	1839	+ 16	+58.7 (46)	+46.4 (3)	+46.0 (1)	+52.5 (2)	10.3
4141	Feb. 5	1857	+ 34	+60.1 (32)	+46.8 (3)	+49.3 (1)	+55.2 (3)	10.3
4170	Feb. 14	1866	+ 43	+59.9 (32)	+46.9 (5)	.....	+54.8 (3)	10.3
4180	Feb. 17	1869	+ 46	+60.5 (93)	+48.6 (3)	+49.4 (2)	+54.0 (3)	10.3
4457	1946 Oct. 11	2105	− 59	+61.8 (40)	+45.1 (1)	.....	+58.3 (1)	10.3
4464	Oct. 13	2107	− 57	+61.5 (33)	+43.6 (1)	.....	+56.3 (1)	10.3
4476	Nov. 8	2133	− 31	+62.3 (37)	+44.5 (1)	.....	.....	10.3
4502	Dec. 13	2168	+ 4	+61.7 (34)	+46.7 (5)	.....	+56.7 (2)	10.3
4547	1947 Jan. 11	2197	+ 33	+62.2 (34)	+48.4 (3)	.....	+55.6 (2)	10.3
4576	Feb. 5	2222	+ 58	+62.7 (34)	+49.9 (6)	.....	+55.7 (2)	10.3
4915	1947 Oct. 6	2465	− 15	+63.6 (31)	+46.2 (2)	.....	.....	10.3
4926	Oct. 23	2482	+ 2	+63.2 (35)	+48.3 (5)	.....	.....	10.3
4984	Dec. 2	2522	+ 42	+63.4 (32)	+48.1 (6)	.....	.....	10.3
5042	1948 Jan. 3	2554	+ 74	+62.4 (29)	+49.3 (7)	.....	+52.6 (3)	10.3
5056	Jan. 19	2570	+ 90	+62.2 (29)	+49.4 (16)	+50.8 (2)	+54.0 (3)	10.3
5306	1948 Aug. 23	2787	− 32	+59.6 (19)	+45.4 (1)	.....	.....	10.3
5307	Aug. 23	2787	− 32	+60.5 (22)	+45.7 (1)	.....	.....	10.3
5314	Sept. 11	2806	− 13	+60.9 (32)	.....	.....	.....	10.3
5319	Sept. 12	2807	− 12	+60.2 (29)	+44.0 (1)	.....	.....	10.3
5352	Oct. 13	2838	+ 19	+61.5 (29)	+47.0 (2)	.....	+58.1 (1)	10.3
5486	Dec. 11	2897	+ 78	+62.2 (19)	+51.1 (11)	.....	+55.1 (3)	10.3
5809	1949 Aug. 3	3132	− 21	+63.1 (26)	.....	.....	.....	10.3
5814	Aug. 4	3133	− 20	+62.7 (31)	+47.6 (1)	.....	.....	10.3
5925	Sept. 10	3170	+ 17	+63.8 (29)	+47.8 (3)	.....	.....	10.3
5981	Oct. 8	3198	+ 45	+63.3 (30)	+48.4 (5)	.....	+51.5 (1)	10.3
6028	Nov. 13	3234	+ 81	+62.5 (23)	+48.7 (11)	.....	+53.4 (2)	10.3
6088	1950 Jan. 5	3287	+134	+59.7 (15)	+51.7 (10)	+53.5 (1)	+53.7 (3)	10.3
6166	Feb. 23	3336	+183	.....	+48.9 (4)	.....	.....	10.3
6446	1950 Aug. 7	3501	+ 14	+61.5 (29)	.....	.....	.....	10.3
P 11	Sept. 23	3548	+ 61	+60.4 (78)	+46.6 (4)	.....	.....	2.3
P 17	Oct. 28	3583	+ 96	+62.6 (68)	+50.3 (3)	.....	.....	2.3
P 24	Nov. 17	3603	+116	+66.3 (36)	+54.5 (12)	.....	+58.0 (6)	9.1
P 36	Nov. 29	3615	+128	+59.0 (26)	+51.0 (14)	+51.5 (2)	+54.1 (3)	9.1
P 39	Dec. 22	3638	+151	+69.3 (34)	+50.3 (12)	+44.8 (2)	+53.2 (1)	9.1
7221	1951 Aug. 1	3860	+ 54	+62.9 (25)	.....	.....	.....	10.3
8516	1952 Nov. 28	4345	+194	+57.5 (43)	+51.6 (11)	.....	.....	10.3

the measures, a detailed study of the velocities in different cycles in the years 1935–1952 seems justified.

The dates of maximum light of Mira Ceti from observations by the American Association of Variable Star Observers are listed in Table 2. Maxima from 1926 to 1935 are from *The Story of Variable Stars* by Campbell and Jacchia; those of later date were compiled and courteously supplied by Recorders Leon Campbell and Margaret W. Mayall. The mean interval from maximum to minimum is 205 days. The major changes in the spectrum are illustrated in Figure 1, where spectrograms at phases −50, +17, and +134 days from maximum are reproduced.

TABLE 2

MAXIMA OF MIRA CETI

Date	Mag.	JD24+	Interval	Date	Mag.	JD24+	Interval
1926 Oct. 19	3.0	24808	319	1940 July 9	3.7	29820	339
1927 Sept. 26	4.1	5150	342	1941 June 18	3.6	30164	344
1928 Aug. 22	2.8	5481	331	1942 May 18	3.6	0498	334
1929 July 17	4.1	5810	329	1943 Apr. 5	3.1	0820	322
1930 June 22	3.5	6150	340	1944 Mar. 2	4.0	1152	332
1931 May 18	.....	6480	330	1945 Jan. 28	2.7	1484	332
1932 Apr. 18	.....	6816	336	1946 Jan. 2	4.0	1823	339
1933 Mar. 10	3.4	7142	326	1946 Dec. 9	4.3	2164	341
1934 Feb. 1	3.8	7470	328	1947 Oct. 21	3.1	2480	316
1934 Dec. 31	2.5	7803	333	1948 Sept. 24	3.4	2819	339
1935 Dec. 13	4.3	8150	347	1949 Aug. 24	2.8	3153	334
1936 Nov. 8	2.7	8481	331	1950 July 24	3.9	3487	334
1937 Oct. 23	4.7	8830	349	1951 June 8	3.3	3806	319
1938 Sept. 17	4.0	9159	329	1952 May 18	3.2	4151	345
1939 Aug. 5	2.9	9481	322				

VELOCITIES FROM ABSORPTION LINES

For measurement of the velocities from the absorption spectra, 70 atomic lines between λ 3770 and λ 4290 were selected, and the best of these lines on each plate were used. Some lines from other regions were included for comparison in the measures of a few plates. The lines chosen are free from troublesome blends and bright edges. With few exceptions, they have moderate intensities, and their excitation potentials are generally less than 1 volt. The results depend directly on laboratory wave lengths.

The average number of absorption lines measured is 33 per plate. With a dispersion of 10 A/mm, the average deviation of a single line from the mean is ±1.1 km/sec, corresponding to an internal probable error of 0.13 km/sec for the velocity determined from an average good plate. Eleven pairs of plates with dates differing by 5 days or less show a mean velocity difference of 0.6 km/sec. These deviations include errors in the published laboratory wave lengths, differences due to the systematic displacement of the lines of certain elements, and physical effects such as excitation potential, as well as variations in the comparison lines of the iron arc.

Radial velocities from measurement of the selected absorption lines were determined from 68 coudé spectrograms representing 16 cycles of the star's light-variation from 1935 to 1951. Only 3 cycles were unobserved. The coudé observations were necessarily limited to the brighter phases. In order to illustrate the velocity results in different cycles, the observed velocities were plotted (Fig. 2) against time for the 6 consecutive cycles from 1945 to 1950. Although this interval does not exhibit the extremes of which the star is capable, marked fluctuations are evident. The maximum light in this interval varied from magnitude 2.7 to 4.7, and the time intervening between maxima ranged between 316 and 349 days. The maximum velocity for a cycle varied between +60.5 km/sec in February, 1946, and +63.8 km/sec in September, 1949.

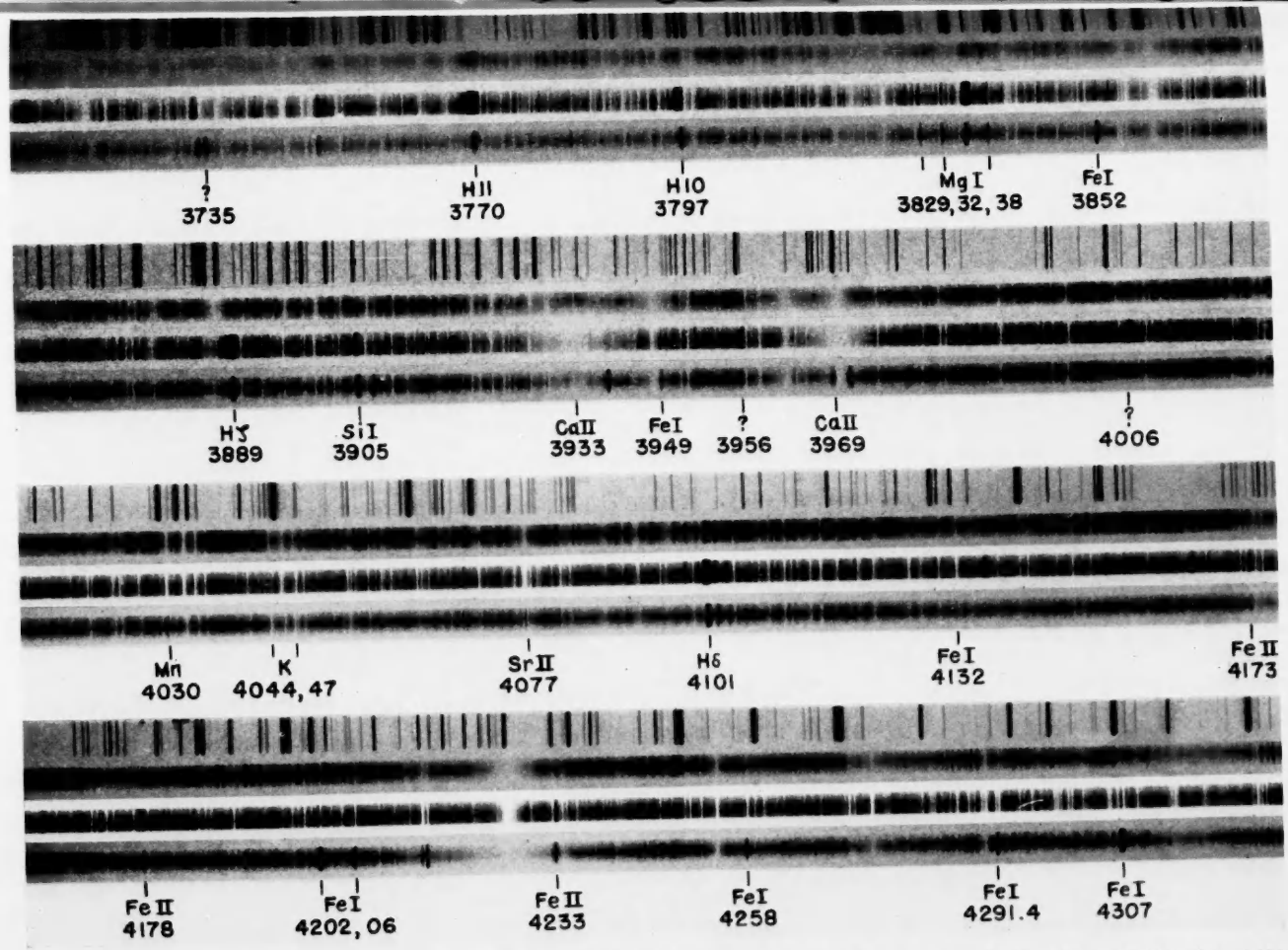

FIG. 1.—Spectra of Mira Ceti at widely different phases. *Above*, Ce 4047, phase −50 days; *center*, Ce 5925, phase +17 days; *below*, Ce 6088, phase +134 days. Spectrograms by P. W. Merrill.

In the whole 16-year interval of observation these extremes were: maximum light, 2.5–4.4 mag.; period, 311–355 days; maximum observed velocity, +57.2 in January, 1936, to +68.3 km/sec in the following cycle in October, 1936. While these extreme velocity maxima are based on few observations, the general accuracy of the measurements and the good quality of the plates indicates that these velocity variations are probably real.

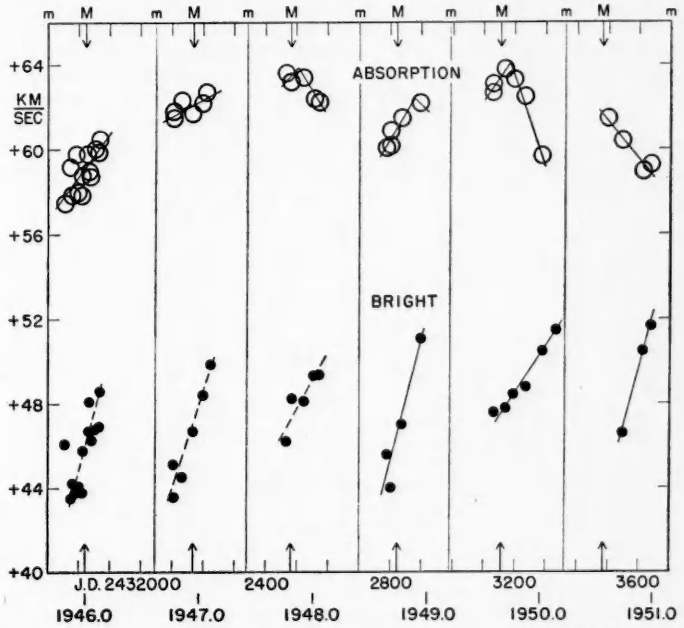

FIG. 2.—Radial velocities of Mira Ceti in six consecutive cycles, 1946–1950. Absorption above; emission below.

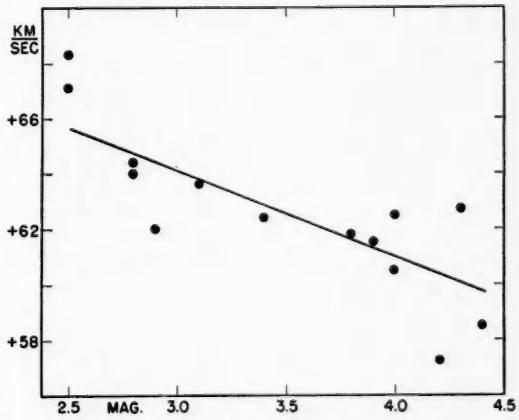

FIG. 3.—Plot showing correlation of maximum velocity with apparent magnitude in different cycles

The highest velocities attained in different cycles evidently vary by several kilometers per second. Usually greater positive velocities accompany maxima of greater brightness, as shown in Table 3 and Figure 3. The scatter is rather large for a direct physical relationship, but some connection between high velocity and high luminosity seems more than a coincidence. Possibly this correlation would be found to be more precise if complete velocity observations and more accurate magnitudes were available.

In each cycle having sufficient observations, a maximum value of the velocities observed occurs, on the average, 25 days after maximum light. Since the height of this maximum velocity changes from cycle to cycle and the time of its occurrence with respect to the observed epoch of maximum of light varies many days, the usual procedure of combining observations from different cycles according to phase, to form a characteristic mean curve, is justified only as a first approximation, showing the over-all composite movements of the star's atmosphere. A mean curve of this kind (Table 8, *a;* Fig. 4, *a*, *solid line*) representing the coudé observations may be compared with the low-dispersion-curve of 1926.

TABLE 3

MAGNITUDE AT MAXIMUM AND HIGHEST POSITIVE VELOCITY

Year	Magnitude at Maximum	Highest Velocity	Year	Magnitude at Maximum	Highest Velocity	Year	Magnitude at Maximum	Highest Velocity
1934.....	2.5	+67.1	1939.....	2.8	+64.4	1947.....	3.1	+63.6
1935.....	4.2	+57.2	1940.....	3.8	+61.8	1948.....	3.4	+62.4
1936.....	2.5	+68.3	1945.....	2.9	+62.0	1949.....	2.8	+64.0
1937.....	4.4	+58.5	1946.....	4.0	+60.5	1950.....	3.9	+61.5
1938.....	4.0	+62.5	1946.....	4.3	+62.7			

If, however, the velocities from different cycles are reduced to a standard maximum velocity and the phases to an average time lag of maximum velocity after maximum light, a mean curve which may have some significance may be plotted. A standard curve corrected in this arbitrary fashion was formed by reducing the velocities of each cycle to a standard maximum of +63.0 km/sec and by correcting the phases for each cycle by the number of days necessary to reduce the time of observed velocity maximum in the cycle to the average value of +25 days. In this adjusted mean curve (Fig. 4, *a*, *dashed line*) the velocities of recession reach a maximum at about 20 days after maximum light. In 112 days preceding its maximum the curve rises 2.2 km/sec, and after its maximum falls 4.0 km/sec in 116 days. The lack of observations does not permit the extension of the curve through minimum light.

Coudé observations of other long-period variables by P. W. Merrill[2, 3, 4, 5, 6] indicate that the velocities from the absorption lines are also subject to considerable irregularity. In different cycles these velocities are not precisely repeated. In 1943 R Aql showed no certain velocity variation between phases +5 and +70. In the same year R Leo had a definite velocity maximum at phase +50 days, rising 3.2 km/sec in 118 days and thereafter falling 0.8 km/sec in 30 days. In the next cycle in 1944 the rise was 1.0 km/sec

[2] *Mt. W. Contr.*, No. 713; *Ap. J.*, **102**, 347, 1945.

[3] *Mt. W. Contr.*, No. 720; *Ap. J.*, **103**, 275, 1946.

[4] *Mt. W. Contr.*, No. 717; *Ap. J.*, **103**, 6, 1946.

[5] *Mt. W. Contr.*, No. 730; *Ap. J.*, **105**, 360, 1947.

[6] *Mt. W. Contr.*, No. 735; *Ap. J.*, **106**, 274, 1947.

between phases −18 and +17 days, and the decline was 1.5 km/sec from +17 to +101 days. Measures of the postmaximum decrease in velocity for R Leo, R Hya, R And, and χ Cyg are summarized in Table 4.

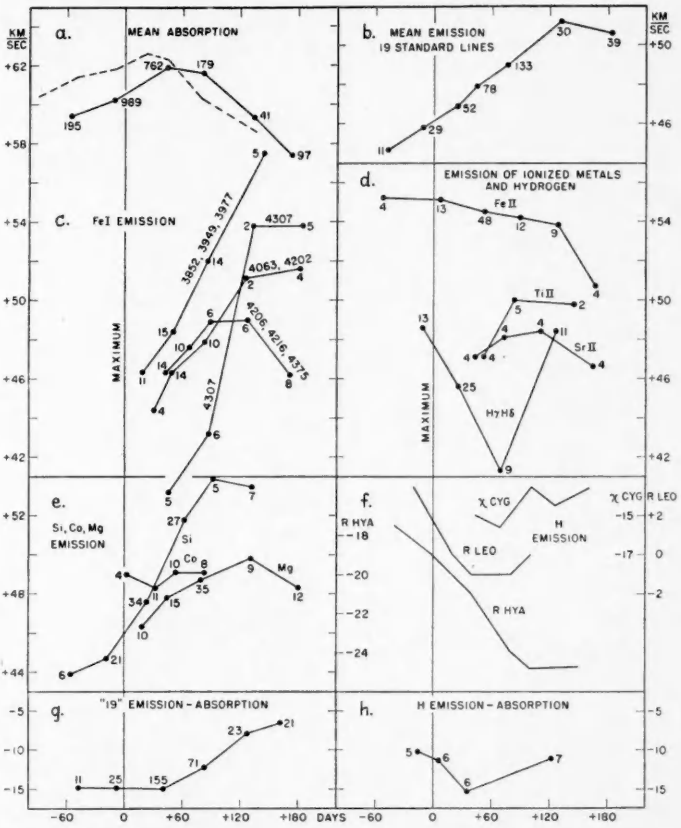

FIG. 4.—Mean velocities plotted according to phase from maximum light. *a*, Absorption lines; *b*, 19 standard emission lines (Table 9); *c*, groups of emission lines of different excitation potentials; *d*, emission lines of ionized metals and hydrogen; *e*, *Si*, *Co*, and *Mg* emission lines; *f*, hydrogen emission lines measured by P. W. Merrill; *g*, emission of 19 standard lines *minus* mean absorption velocities; *h*, hydrogen emission lines *minus* mean absorption velocities. The numerals represent the number of measures included in the means.

The premaximum behavior is not so regular. In 1944 the U Ori curve declined 0.9 km/sec between phases −38 and −3 days, and the velocities of R Hya fell continuously throughout the whole period of observation from phase −45 to +95 days, with a total range of 10.0 km/sec.

With allowance for considerable irregularity, we may conclude that the variation in the absorption velocities of several long-period variables resembles in some degree that of Mira. The velocity changes are small, but usually a maximum velocity occurs near the time of maximum light. In this respect the measures of higher precision agree with

the previous results obtained from low-dispersion spectrograms of Mira, but the total velocity range in any single cycle is probably smaller than that shown by the 1926 curve.

VELOCITIES FROM DIFFERENT ELEMENTS

The average residual from the mean for the lines of elements generally measured in Mira are collected in Table 5. Merrill's mean residuals for the same elements (not neces-

TABLE 4

POSTMAXIMUM VELOCITY DECLINE IN LONG-PERIOD VARIABLES (MERRILL) COMPARED WITH *o* CETI

Star	Year	Range of Velocity Decline (Km/Sec)	Phase (Days)
R Leo	1943	0.8	+49 to + 81
	1944	1.5	+17 to +101
R Hya	1943	7.4	+21 to +125
	1944	5.3	+38 to + 95
χ Cyg	1944	2.7	+70 to +162
R And	1944	2.8	+10 to +102
	1945	1.9	+27 to + 54
R Aql	1943	0.0	+ 5 to + 70
o Cet	1935–52	4.5	+45 to +174

TABLE 5

RELATIVE DISPLACEMENT OF ABSORPTION LINES OF DIFFERENT ELEMENTS

Element	Mira		7 Me Stars Mean Residual (Merrill) (Km/Sec)	Element	Mira		7 Me Stars Mean Residual (Merrill) (Km/Sec)
	No. Lines	Mean Residual (Km/Sec)			No. Lines	Mean Residual (Km/Sec)	
Sc	4	+0.10	+0.65	*Fe*	29	+0.26	+0.52
Ti	11	+ .33	− .60	*Co*	6	− .58	+ .08
V	10	− .41	− .28	*Ni*	3	+ .84	+ .22
Cr	4	−0.88	−0.70	*Sr* II	2	+0.33	(−0.4)

sarily the same lines) of seven other stars are entered for comparison. Except for *Ti*, the agreement is close. The deviation of velocities derived from different elements is doubtless real and may amount to nearly 1.5 km/sec. The reason for this difference is not evident.

ANOMALOUS RESIDUALS

The residuals from several lines are so large that the lines were omitted from the means. The ultimate potassium lines, λ 4044 and λ 4047, are displaced shortward with reference to the mean by 2.7 km/sec (10 plates) and 2.0 km/sec (7 plates), respectively. A similar displacement of even greater amount was found for these lines by Merrill in each of seven long-period variables. No emission components are involved.

The lines λ 3906.482 *Fe* (4), low E.P. 0.1, and λ 4045.815 *Fe* (43), E.P. 1.5, have much larger residuals than other lines of their multiplets. For λ 3906 the mean displacement is −2.8 km/sec (32 plates), and for λ 4045 it is +3.1 km/sec (34 plates). The measures are not affected by emission, which is extremely weak or absent in both lines in Mira. The mean displacement of seven other lines of multiplet (4) is −0.2 km/sec; that of four other lines of multiplet (43) is +0.4 km/sec. In Figure 5 the variation of the residuals of λ 4045 with phase is shown. For λ 3906 the change with phase is negligible.

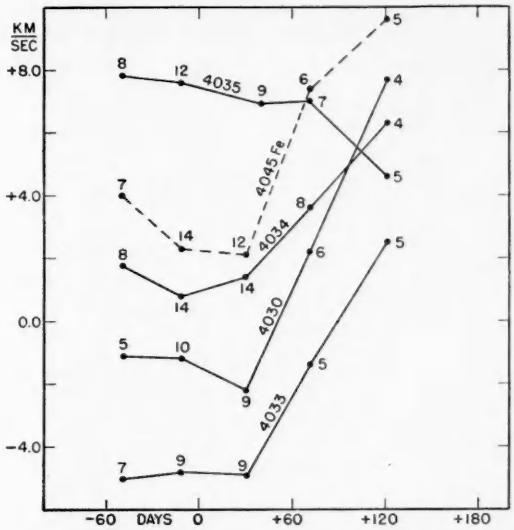

FIG. 5.—Residuals from the mean of absorption velocities of λ 4045 *Fe* and the *Mn* lines λλ 4030, 4033, 4034, and 4035. The numerals represent the number of measures included in the means.

TABLE 6

ANOMALOUS RESIDUALS OF λ 4045 *Fe* AND *Mn* ABSORPTION LINES

PHASE (DAYS)	λ 4045.815 *Fe*		λ 4030.755 *Mn*		λ 4033.073 *Mn*		λ 4034.490 *Mn*		λ 4035.728 *Mn*	
	No. Plates	Resid. (Km/Sec)	No. Plates	Resid. (Km/Sec)	No. Plates	Resid. (Km/Sec)	No. Plates	Resid. (Km/Sec)	No. Plates	Resid. (Km/Sec)
−49.....	7	+4.0	5	−1.1	7	−5.0	8	+1.8	8	+7.8
−11.....	14	+2.3	10	−1.2	9	−4.8	14	+0.8	12	+7.6
+31.....	12	+2.1	9	−2.2	9	−4.9	14	+1.4	9	+6.9
+72.....	6	+7.4	6	+2.2	5	−1.4	8	+3.6	7	+7.0
+122.....	5	+9.4	4	+7.7	5	+2.5	4	+6.3	5	+4.6

The manganese lines λλ 4030.755, 4033.073, and 4034.490 from the ground level of multiplet (2) and λ 4035.728 (5), E.P. 2.1, have anomalous displacements which necessitate their omission from mean velocities. The mean displacements of these four lines are −1.2 (24 plates), −4.5 (24 plates), +1.3 (36 plates), and +7.1 (28 plates) km/sec, respectively; but, as shown in Table 6 and Figure 5, the variation during the cycle of

light-change is large, indicating that these manganese atoms are peculiar. They tend to follow the motions of absorbing atoms of other elements near maximum light, but after phase +30 days their velocities of recession increase for at least 100 days. The problem is complicated by the presence of emission (see p. 51 and Fig. 6) on the shortward edge of λ 4030 and λ 4034; but the velocity changes do not seem to be well correlated with the strength of emission, and λ 4033 has similar velocity changes, although the emission is extremely weak or absent in this star. Contrary to the laboratory intensities, λ 4033 always appears stronger in absorption than λ 4030. The behavior of λ 4035.728 of multiplet (5) is most peculiar. It has a large longward displacement but does not share the velocity changes during the cycle shown by λ 4045 and the *Mn* lines of multiplet (2). Four other lines of multiplet (5) have normal displacements. Faint emission on the shortward edge appears for several days near phase +30 days and on both edges from minimum light until −50 days. It is hardly possible that the velocity measures are much affected by the emission, but an unidentified absorption line of slightly longer wave length may be present. At times, the line appears somewhat wide and hazy.

In addition to these lines of *K*, *Fe*, and *Mn*, the lines λλ 3875.075 *V*, 3906.482 *Fe*, 4113.518 *V*, and 4202.031 *Fe*, with mean residuals of +3.9, −2.8, +2.6, and +3.7 km/sec, respectively, were omitted from the means on account of their large discordances. The measures of the first three may be affected by blends and the last by emission on the shortward side having high intensity from phases +25 days until well after minimum light.

SHIFTS VARYING WITH EXCITATION POTENTIAL

In agreement with the results obtained by Adams[7] for *o* Ceti and of Merrill[2, 3, 4, 5, 6] for U Ori, R Ser, R Hya, R And, and χ Cyg, the present measures of Mira indicate that 17 dark lines having excitation potentials greater than 0.9 volts (mean E.P. 1.40 volts) have mean residuals of +1.12 km/sec with reference to 50 lines having low excitation potentials (mean E.P. 0.10 volts). For the absorption lines identified within the bright hydrogen lines of Mira, a larger range of excitation, 2.32 volts, was covered, giving a difference in velocity of +3.4 km/sec.[8] The five iron lines, λλ 3865.527, 3872.504, 4005.246, 4063.597, and 4071.740, of multiplets (20) and (43) were measured on many plates but show no variation of displacement with phase when compared with lines of low excitation potential. The line λ 4045.815 *Fe* (43), however, has extraordinary longward shifts at phases 60–120 days, as shown in Figure 5. These lines have excitation potentials ranging from 0.99 to 1.60 volts.

EMISSION LINES

The emission spectrum of Mira Ceti is conspicuous, especially at postmaximum phases, but the bright lines are less numerous and less intense[5, 6] than in R And and χ Cyg. Estimates of the approximate phases at which the bright lines of different elements become definitely visible, together with the times of maximum intensity and of disappearance, are in Table 7. Only the chief lines of the different multiplets are entered. The emission varies greatly in different cycles. Bright lines are stronger and more numerous in cycles of high maximum brightness (Fig. 7).

HYDROGEN

The Balmer lines of hydrogen are outstanding at all phases except for a few weeks near and shortly after minimum light. Their total width decreases from 70 km/sec at phase −50 days to 45 km/sec at +170 days. From the time of their appearance until phase about +110 days, the hydrogen emission lines are severely mutilated by the absorption

[7] *Mt. W. Contr.*, No. 638; *Ap. J.*, **93**, 19, 1941.

[8] A. H. Joy, *Mt. W. Contr.*, No. 737; *Ap. J.*, **106**, 288, 1947.

FIG. 6.—Series of spectra of Mira Ceti, λλ 3915–4078, at different phases, showing the strong lines of *Ca* II, *Al* I, and *Mn* I. Spectrograms by P. W. Merrill. *Top to bottom:* Ce 4057, phase −43 days; Ce 4103, phase −10 days; Ce 5981, phase +45 days; Ce 1319, phase +85 days; Ce 6088, phase +134 days; Ce 3216, phase +170 days.

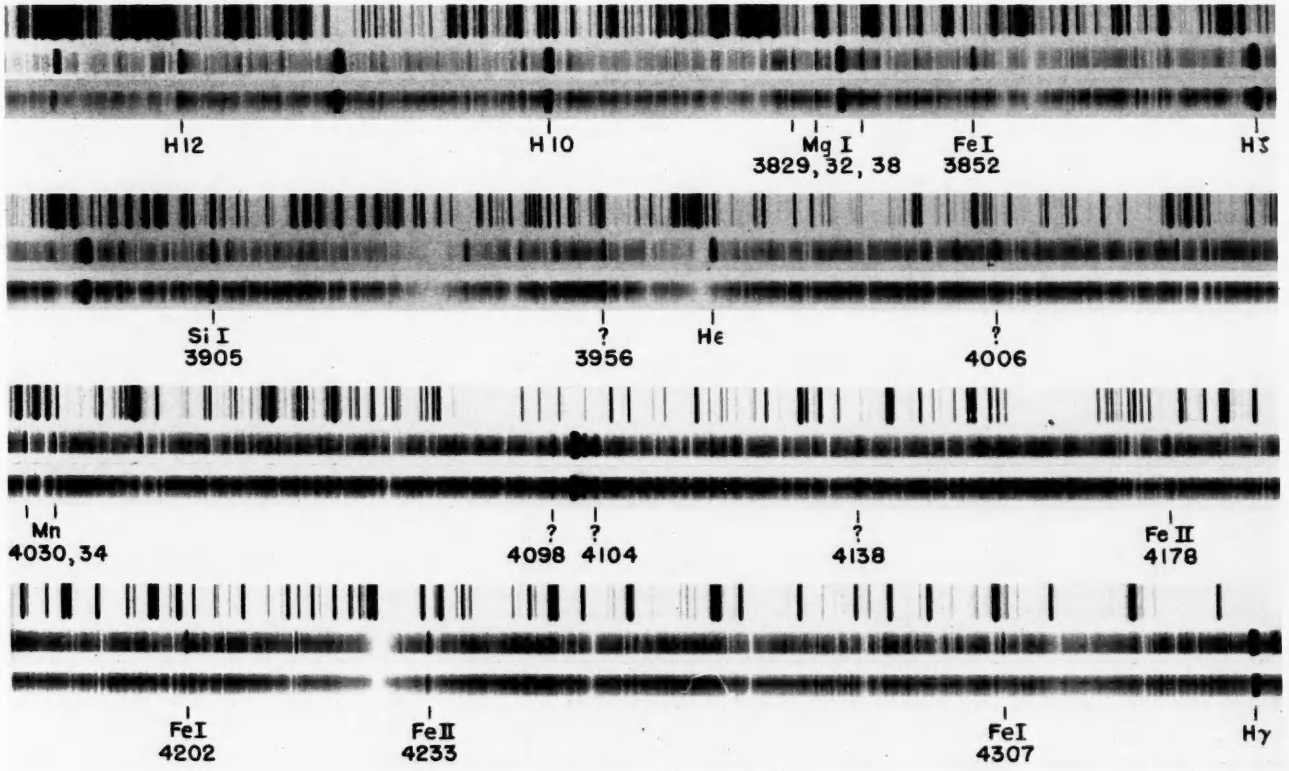

FIG. 7.—Spectra of Mira Ceti at the same phase after high and low maxima. The unidentified emission features at λλ 3956, 4906, 4998, 4104, and 4138 are marked. *Above*, Ce 1290, phase +51 days, maximum = 2.7 mag.; *below*, Ce 4180, phase +46 days, maximum = 4.0 mag. Spectrograms by P. W. Merrill.

of many lines of the reversing layer of the star.[7, 8, 9, 10] At later phases this absorption is no longer present, probably because of a relative uplift of the hydrogen sources, as Merrill has suggested, and the relative intensities of the Balmer lines take their laboratory values. The $H\beta$ and $H\gamma$ lines rise above the absorption of the titanium oxide bands. The absorption of $H\epsilon$ by H (*Ca* II) is noticeably reduced at phase +20 days and has little effect at phases greater than +50 days.

TABLE 7

OCCURRENCE OF CHIEF BRIGHT LINES

Element	Multiplet	Chief Line (λ)	Appearance Phase (Days)	Maximum		Disappearance Phase (Days)
				Phase (Days)	Int.	
Hγ	.....	4340	−65	0	Strong	+215
Hδ	.....	4101	−70	0	Strong	+190
Mg I	1	4571	+45	+180	15	+300
	3	3838	0	+ 80	2	+180
Si I	2	4102	−70	0	5	+200
	3	3905	−60	+ 80	4	+180
Sc I	8	3907	+30	+100	3	+180
Ti II	13	3759	+20	+ 80	1	+170
	14	3685	+10	+ 80	2	+170
Mn I	2	4030	0	+ 90	4	+210
	5	4035	−70	0	1	+ 45
Fe I	2	4375	−15	+130	5	+215
	3	4216	+10	+130	5	+210
	42	4307	0	+135	10	+260
	43	4063	+25	+ 70	2	+ 90
	72	3949	0	+ 80	3	+150
	73	3852	0	+ 80	8	+200
Fe II	3	3938	+33	+ 60	5	+160
	27	4233	−20	+ 50	5	+220
	28	4178	−70	+ 85	3	+200
Co I	28	4121	−10	+ 40	2	+100
	31	3995	−10	+ 40	2	+100
	32	3935	−40	0	2	+100
	32	3997	−10	+ 40	1	+100
Sr II	1	4077	+45	+ 80	2	+190
In I	1	4511	−70	+140	3	+190

If the hydrogen lines are strongly overexposed, fairly reliable velocity measures are possible at all phases. As Merrill has shown for other long-period variables, the velocity-curve of the hydrogen emission is quite different from that of the metallic lines. In order to determine the motions of the strata in which the hydrogen emission arises, the measurements of $H\gamma$ and $H\delta$ are the most useful because these lines are visible over the longest time interval and happen to be less severely affected by overlying absorption than do other hydrogen lines. Table 8, *d*, and Figure 4, *d* and *f*, indicate the course of the velocity variations of the $H\gamma$ and $H\delta$ emission sources in Mira Ceti (M6e) and, for com-

[9] C. D. Shane, *Lick Obs. Bull.*, **10**, 133, 1922.

[10] P. W. Merrill, *Pub. A.S.P.*, **57**, 178, 1945.

FIG. 7.—Spectra of Mira Ceti at the same phase after high and low maxima. The difference in emission features at Hγ, Hδ, and Ti are marked. *Above*, Ce 1290, phase +51 days, maximum = 2.7 mag.; *below*, Ce 4180, phase +46 days, maximum = 4.0 mag. Spectrograms by P. W. Merrill.

TABLE 8

SELECTED RADIAL VELOCITIES OF MIRA CETI

No. Lines	Mean Phase (Days)	Mean Velocity (Km/Sec)	No. Lines	Mean Phase (Days)	Mean Velocity (Km/Sec)
	a) Means of Absorption Lines by Phase			*b*) Means of 19 Metallic Emission Lines by Phase (Table 9)	
195	− 55	+59.4	11	− 47	+44.7
989	− 11	60.2	29	− 11	45.8
762	+ 45	61.9	52	+ 24	46.9
179	+ 82	61.6	78	+ 44	47.9
41	+134	59.3	133	+ 76	49.0
97	+174	57.4	30	+131	51.2
			39	+184	50.6
	c) Emission *Fe* I λλ 4206, 4216, 4375			*c*) Emission *Fe* I λ 4307	
14	+ 43	+46.3	5	+ 47	+40.2
10	68	47.6	6	84	43.2
6	90	48.9	2	134	53.8
6	129	49.0	5	185	53.8
8	173	46.2			
	c) Emission *Fe* I λ 4063, λ 4202			*c*) Emission *Fe* I λλ 3852, 3949, 3977	
4	+ 31	+44.4	11	+ 19	+46.3
14	49	46.3	15	51	48.4
10	84	47.9	14	87	52.0
2	126	51.1	5	146	57.5
4	183	51.6			
	d) Emission *Fe* II λλ 3938, 4173, 4178, 4233			*d*) Emission *Ti* II λ 3759, λ 3761	
4	− 52	+55.2	4	+ 52	+47.2
13	+ 7	55.1	5	84	50.0
48	+ 53	54.5	2	146	49.8
12	+ 90	54.2			
9	+129	53.8			
4	+167	50.7			
	d) Emission *Sr* II λ 4077, λ 4215			*d*) Emission *H* λ 4101, λ 4340	
4	+ 43	+47.1	13	− 10	+48.6
4	74	48.1	25	+ 26	45.6
4	110	48.4	9	+ 69	41.3
4	165	46.6	11	+127	48.4

TABLE 8—*Continued*

No. Lines	Mean Phase (Days)	Mean Velocity (Km/Sec)	No. Lines	Mean Phase (Days)	Mean Velocity (Km/Sec)
	e) Emission *Si* I λ 3905, λ 4102			*e*) Emission *Mg* I λλ 3829, 3832, 3838, 4571	
6	− 55	+43.9	10	+ 19	+46.3
21	− 18	44.7	15	46	47.8
34	+ 24	47.6	35	80	48.7
27	+ 63	51.8	9	132	49.8
5	+ 93	53.9	12	181	48.3
7	+133	53.5			
	e) Emission *Co* I λλ 3997, 4045, 4121			*e*) Emission *Sc* I λ 3907	
4	+ 3	+49.0	3	+ 45	+48.2
11	33	48.3	2	63	51.2
10	54	49.1	2	94	50.6
8	84	49.1	2	140	51.0

DISPLACEMENT OF EMISSION LINES

	g) "19 Bright"–Dark			*h*) Bright *H*–Dark	
11	− 48	−14.8	5	− 16	−10.1
25	− 7	14.9	6	+ 6	11.3
155	+ 41	15.0	6	+ 34	15.3
71	+ 83	12.2	7	+123	11.0
23	+134	7.9			
21	+163	6.6			

parison, in χ Cyg (M6e +S),[6] R Leo (M8e),[3] and R Hya (M6e),[4] from Merrill's measures of numerous hydrogen lines to *H*18. In these four stars we find that the hydrogen emission layers show increasing velocities of approach from their first manifestation at an epoch somewhat before maximum light until a time some 2 months after maximum, when the acceleration levels off or reverses its direction.

METALS

The lines of neutral *Mg* I, *Si* I, and *Fe* I are the most prominent of the many emission lines of metals occurring in Mira Ceti, and some of them are present at practically all phases of the star's variation. The emission is first seen on the shortward side of the absorption lines, and it is often difficult to determine the exact time when emission can first be distinguished. As the light decreases after maximum, the number of emission lines increases enormously, and lines of additional elements, such as *Sc* I, *V* I, *Cr* I, *Mn* I, *Co* I, *Ni* I, *In* I, *Ti* II, *Fe* II, and *Sr* II, emerge in considerable numbers. Lines of higher excitation potential, especially those of *Fe* I, are first seen. Later, the lines of lower excitation appear in great numbers.

FLUORESCENT EFFECTS

As described by Merrill for other long-period variables of type Me and for R And of type Se, the *Fe* I (42) lines λ 4202.031 and λ 4307.906 from the $z^3G_4^0$ level and *Fe* I (73) λ 3852.574 from the $w^5D_4^0$ level have by far the strongest emission in their respective multiplets. Their extraordinary intensity is well accounted for by excitation effects of *Mg* II λ 2795.53, as first suggested by Thackeray and Merrill.[11] They are seen in Mira Ceti from maximum until well after minimum light. Although it is fainter in the laboratory, λ 4202 appears first and is stronger than λ 4307 until phase +100 days, after which λ 4307 becomes more intense and endures for a longer time after minimum; λ 3852 also appears at maximum, but, although it reaches nearly the same intensity, it fades out somewhat earlier than the lines of multiplet (42). The *Zr* I singlets, λλ 4166.51, 4240.44, and 4242.61, observed by Merrill[12] in χ Cyg, show only a trace of emission in Mira.

In the only accessible multiplet of *In* the complete fluorescent mechanism is manifest. The line λ 4101.764, the shortward member of the doublet, has nearly the same wave length as *Hδ*. It is present in absorption[13] within the strong *Hδ* emission line until phase +130 days. The energy absorbed raises many of the *In* electrons to the $6^2S_{1/2}$ level, from which they are able to radiate λ 4511.310, the other member of the doublet. While this emission line never attains great intensity, it has a long lifetime, nearly coincident with that of *Hδ*. The *Sc* I line λ 3907.476 (8) from the $y^2F^0_{2\ 1/2}$ level is much strengthened in emission and is well seen between phases +30 and +180. The low-term line from the same level of this multiplet is λ 3933.381, which may be excited by emission of K (*Ca* II). The only visible emission in the K region is that of the broad displaced line which Merrill[3, 4, 5, 6] found to be of considerable strength in R Leo, R Hya, and R And and χ Cyg but which is weak in Mira. No evidence of an absorption line at K corresponding to λ 4101 of *In* I at *Hδ* is visible. The bright line λ 4372.3 was tentatively identified by Thackeray and Merrill[11] with the singlet *Ti* I (277) from the $v_1P_1^0$ level. It occurs in Mira between phases +75 and +220 days, with a maximum strength of about 5 at +130 days, but is not so strong as in χ Cyg, R Leo, and R And. Measurements indicate that the line is displaced longward on the basis of this identification by 4–5 km/sec; but if it is identified with the [*Fe* II] line λ 4372.43 (21F), the displacements agree with those found for *Fe* II. Much the same result was found by Merrill for R Leo and R Hyd. The line λ 4372 appears earlier and attains greater intensity than the other members of multiplet (21F). The identification remains uncertain. The bright line λ 4172.05 attributed by Merrill to *Ga* I is barely visible in Mira Ceti.

VELOCITIES FROM LINES OF METALS

Since the bright lines of metals are sharp and of moderate intensity, they can be measured with high accuracy. On spectrograms of the highest dispersion, between phases +50 and +100 days, the strong emission lines λλ 3852 *Fe* I, 3905 *Si* I, 4102 *Si* I, and 4307 *Fe* I are divided by a sharp absorption reversal. The separation of the emission components is about 0.2 A. Without exception, the emission lines are displaced shortward with respect to the absorption lines. When the emission first appears, the displacement of 15 km/sec is sufficient to separate the emission from the absorption lines, and the velocity measurements are not affected; but as the bright lines increase in strength, their displacements diminish (Table 8, *g*, and Fig. 4, *g*), and they encroach upon the absorption lines originating at a lower level. Thus the dark lines are apparently displaced longward. This effect is clearly shown (Fig. 4, *c*) in measures of the *Fe* I lines λ 4202 and λ 4307 of multiplet (42). Weaker absorption lines, such as λ 3852.574 *Fe* I (73), are completely covered by emission at later phases.

[11] *Pub. A.S.P.*, **48**, 331, 1936.

[12] *Ap. J.*, **106**, 283, 1947.

[13] P. W. Merrill, *Mt. W. Contr.*, No. 713; *Ap. J.*, **102**, 352, 1945; *Mt. W. Contr.*, No. 720; *Ap. J.*, **103**, 285, 1946; *Ap. J.*, **116**, 20, 1952; and A. H. Joy, *Mt. W. Contr.*, No. 737; *Ap.J.*, **106**, 292, 1947.

Although great numbers of bright lines of metals may usually be measured between maximum and minimum light, the most accurate determination of the changes in velocity of the emission strata of the star's atmosphere can be derived by limiting the measures to moderately strong lines which have a long lifetime covering as much as possible of the cycle of variation.

For this purpose the nineteen bright lines of Table 9 were chosen, and the mean velocities determined from such of these lines as were measured on each plate are shown in the sixth column of Table 1. The number of lines used is in parentheses. The resulting mean velocity-curve from the "19 standard emission lines" is found in Figure 4, *b* (Table 8, *b*), and the corresponding curves for each successive cycle between October, 1945, and December, 1950, are shown in the lower part of Figure 2. The curves of emission lines show less irregularity than those of absorption lines. As seen from the sun, the velocities of

TABLE 9

19 STANDARD BRIGHT LINES

Line	Element	Multiplet	Upper E.P. (Volts)	Line	Element	Multiplet	Upper E.P. (Volts)
4571.096	*Mg* I	1	2.7	4375.932	*Fe* I	2	2.8
3829.355		3	5.9	4206.702		3	3.0
3832.300		3	5.9	4216.186		3	2.9
3838.293		3	5.9	4202.031		42	4.4
				4307.906		42	4.4
4102.926	*Si* I	2	4.9	4063.597		43	4.6
3905.527		3	5.1	3949.954		72	5.3
				3977.743		72	5.3
3907.476	*Sc* I	8	3.2	3852.574		73	5.4
				4121.318	*Co* I	28	3.9
				4045.386		31	4.1
				3997.901		32	4.1

recession increase steadily from the time of the appearance of the lines, shortly before maximum, until their disappearance near minimum. The apparent change in the direction of the mean curve at +130 days results from combining different cycles which are not exactly alike.

In relation to the absorbing strata, the motions of the emission atmosphere are always outward. The difference in velocity is small at minimum light (Table 8, *g;* Fig. 4, *g*).

The mean velocity-curves for single lines and groups of similar lines of neutral atoms are plotted in Figure 4, *c* (Table 8, *c* and *e*), and those of ionized atoms in Figure 4, *d* (Table 8, *d*). The *Sr* II, *Ti* II, and *Fe* II emission lines show small velocity variations with phase, but, as for the absorption-line velocities, they vary with excitation potential (see accompanying tabulation). The *Fe* I bright lines also show velocities correlated with ex-

Element	Mean Upper E.P. (Volts)	Mean Velocity (Km/Sec)
Sr II	3.0	+47.5
Ti II	3.9	+48.9
Fe II	5.3	+54.3

citation potential, as Merrill[14, 15] has found in R Leo and in the variables T Cas, R LMi, W Hya, and T Cep. The lines λλ 3852.574 (73), 3949.954 (72), and 3977.743 (72) (Table 8, *c;* Fig. 4, *c*), with mean E.P. of 5.3 volts, give consistently higher positive velocities than do λλ 4063.597 (43), 4202.031 (42), and 4307.906 (42), with mean E.P. of 4.5 volts. The low-temperature lines λλ 4206.702 (3), 4216.186 (3), and 4375.932 (2), E.P. 2.9, have nearly the same velocities as λ 4063 and λ 4202 until phase +100 days, after which the velocities of the low-level lines fall rapidly. The mean difference between the high- and low-excitation groups is about 2.5 km/sec from phases +40 to +110 days and +13.3 km/sec from +110 to +170 days. The line λ 4307, for some unexplained reason, has a greater velocity range than λ 4202 of the same multiplet (42).

MAGNESIUM

At minimum light the ground-level intercombination line λ 4571.096 *Mg* I (1), $3^1S_0-3^3P^0_1$, reaches great intensity in emission, covering the absorption line completely. When its intensity is low, both before and after minimum light, it is seen on the shortward edge of the moderately strong absorption line. It usually appears at about +45 days and remains visible through minimum until about a month before the following maximum. The intensity varies in different cycles. At the minima of 1925, 1930, 1944, and 1946, λ 4571 was barely seen on low-dispersion plates and disappeared after minimum.

Except at the lowest temperatures, this line is weak in the laboratory because of its low transition probability; but, in the rarefied atmospheres of the Me and Se variables, its occurrence in great strength is generally permitted near the time of minimum light. The violet triplet of multiplet (3), λλ 3829.355, 3832.300, and 3838.293, with high excitation potential 5.92 volts, has a remarkably long lifetime with moderate intensity.

CALCIUM

The red triplet of *Ca* II, λλ 8498.018, 8542.089, and 8662.140, was observed in emission on five spectrograms taken near the bright maximum of December, 1936. The bright lines are superposed upon the wide absorption lines and appear fairly sharp, with intensities about 2, 3, and 4, respectively. The mean velocity from four plates with a dispersion of 20.7 A/mm is +45.6 km/sec. One plate by R. F. Sanford, taken on August 28, 1939, phase +23 days, gives a mean velocity of +49.1 km/sec for the three bright lines.

DISPLACED LINES OF *Al* I AND *Ca* II

Merrill found that wide emission lines on the shortward wings of the strong absorption lines λ 3944, λ 3961, *Al* I, and λ 3933, λ 3968, *Ca* II (K and H), occur in several M- and S-type variables. In the spectrum of Mira Ceti λ 3968 *Ca* II reaches considerable intensity, but λ 3933 and the lines of *Al* are wide and weak, with maximum intensity at about +140 days (Fig. 6). The bright *Ca* II lines become narrower with increasing phase, and their displacements (relative to the dark-line mean) become less, as shown in Table 10, in agreement with Merrill's measures in other stars in which they attain greater intensity. The mean displacement of K is about 9 km/sec greater than that of H. The broad lines are unsymmetrical, the longward wing being stronger, and measures are affected by the intensity of the exposure. A similar displaced emission line of λ 4226 *Ca* I appeared in September and October, 1943, but was not observed at other times.

SILICON

The singlets λ 3905 (2) and λ 4102 (3) of *Si* I are remarkably strong, and they are nearly as persistent in emission in Mira as are the hydrogen lines. Their high E.P. is 5.0

[14] *Ap. J.*, **116**, 337, 1952.

[15] *Ibid.*, p. 344.

volts. The line λ 4102 is much stronger than λ 3905. No other *Si* I lines fall in the region usually observed.

POTASSIUM

Although the ground-level lines λ 4044.145 and λ 4047.214 *K* I (3) become two or three times as strong in absorption as λ 4045.815 *Fe* I (43) at phases just preceding minimum light, no emission appears on any of our plates.

THE IRON GROUP: *Sc, Ti, V, Cr, Mn, Fe, Co, Ni*

The line λ 3907.476 *Sc* I (8) $a^2D-y^2F^0$ seems correctly identified, although it is the only strong bright line of this element. As suggested by Merrill,[6] the emission of K (*Ca* II) may be sufficient to excite electrons of λ 3933.381 *Sc* I, which has the same upper level

TABLE 10

DISPLACEMENT OF WIDE BRIGHT LINES OF *Al* I AND *Ca* II

Mean Phase (Days)	λ 3944, λ 3961 Mean Displacement (Km/Sec)	K and H Mean Displacement (Km/Sec)	Mean Phase (Days)	λ 3944, λ 3961 Mean Displacement (Km/Sec)	K and H Mean Displacement (Km/Sec)
+ 46	−47.9 (2)	−107.4 (1)	+158	.....	− 55.4 (1)
+ 80	−47.2 (2)	− 86.0 (3)	+170	.....	− 38.7 (2)
+134	.....	− 59.5 (3)			

(see p. 52). The wave length from 15 plates, assuming that it has the same velocity displacement as the "19 bright lines," agrees with the laboratory value within 0.01 A. The strong line of the multiplet, λ 3911.810, does not appear. The radial velocities from λ 3907 (Table 8, *e*) fall between those of *Mg* and *Si* but are too few to give certain information about the velocity-curve.

The emission of *Ti* I is surprisingly weak, but several lines of *Ti* II occur with low intensity. The identification of a strong bright line with the singlet λ 4372.383 *Ti* I (277), E.P. 5.30, as suggested by Thackeray and Merrill,[11] is not entirely convincing, largely because the measured wave length from six plates based on the velocity of the "19 bright lines" is too large by 0.181 A. The velocity changes resemble those of the *Fe* II lines.

Although the absorption lines of *V* are numerous, their identification in emission is uncertain. The line λ 3688.069 (29) is possibly present. The line measured reaches an intensity of 3, and its wave length referred to the "19 bright lines" is λ 3687.968. It is short-lived, showing between +20 and +120 days, with maximum intensity at about +50 days. The chief line of the multiplet, λ 3703.584, is blended with *H*16.

The great ground-level lines of *Cr* I (1) show no emission. The line λ 4325.073 (104) may be bright at times, but it is doubtful because of the band structure in that region. Other emission lines of *Cr* are weak and uncertain.

The ground-level *Mn* I (2) triplet is strong in absorption. The lines λ 4030.755 and λ 4034.490 have emission on their shortward edges from maximum to minimum, reaching considerable strength at +90 days. The general appearance of these lines varies greatly at different phases (Fig. 6). The line λ 4033.073 (2), the middle member of the triplet, is depressed in some stars observed by Merrill and shows very faint emission in Mira. In R And it is present in emission, and in χ Cyg it is stronger than λ 4034 and double. Merrill[6] suggests that energy from λ 4033 may be taken up in filling the upper level of λ 4172.05 *Ga* I, which is bright in several of the long-period variables. In Mira Ceti, however, λ 4172 is extremely weak. The *Mn* emission is peculiar. On account of asymmetry, the measurement of the lines is not of great precision.

Great numbers of lines of both neutral and ionized *Fe* atoms appear in emission. Multiplets (2), (3), (4), (20), (23), (24), (72), (73), (74), and (76), nearly all quintets, are represented more or less completely in the *Fe* I emission. The upper E.P. levels are from 2.8 to 5.5 volts. The stronger lines appear at maximum light, reach their maximum intensity about 100 days later, and disappear at minimum or soon after.

Several *Fe* II multiplets—(3), (27), (28), and (38)—are generally present. Except for the first, the levels are quartets with upper E.P. from 4.8 to 5.6 volts. The appearance of the combination multiplet (3) represented by λ 3914 and λ 3938 takes place after maximum, much like that of the neutral emission; but the other *Fe* II lines have a surprisingly long lifetime, covering all the star's period except a few weeks following minimum light.

The forbidden lines of *Fe* II (6F), (7F), and (21F) are definitely present in emission in the spectrum of Mira from phase +130 days until minimum in some cycles (Fig. 8, *a*). The spectrograms now available make it clear that the permitted and forbidden sharp lines of *Fe* II generally have their origin in the M-type star and not in the companion. Sharp bright lines of [*Fe* II] have also been identified by Merrill in the spectra of all other Me variables observed near minimum, but they have not been noted in S-, R-, or N-type variables. The relative intensities of these lines on Ce 3216 (September, 1943, phase +170 days), together with Merrill's intensities of the same lines at an advanced phase in χ Cyg (M6e + S), are in Table 11. They are evidently stronger at some minima than

TABLE 11

FORBIDDEN LINES OF *Fe* II

LINE	MULTIPLET	INTENSITY		LINE	MULTIPLET	INTENSITY	
		o Cet (+170 Days)	χ Cyg* (+162 Days)			o Cet (+170 Days)	χ Cyg* (+162 Days)
4243.97	21	3	3	4358.37	21	1	0.8
4276.83	21	.....	1	4359.34	7	2	3
4287.40	7	3	5	4413.78	7	2	2.5
4305.90	21	1	1.5	4416.27	6	2	3.5
4319.62	21	1	1	4452.11	7	1	1
4352.78	21	.....	0.8	4457.96	6	1	1

* P. W. Merrill, *Mt. W. Contr.*, No. 735; *Ap. J.*, **106**, 274, 1947.

at others. Observations between phases +130 and +240 days were made in 25 of the 39 cycles, 1918–1952, but [*Fe* II] lines were certainly present in only 11 cycles. The brightness of the star at these minima was about normal. The [*Fe* II] emission reached greatest strength at the normal minima of 1943 and 1945. Apparently, the intensity is somewhat independent of the sources of luminosity in the star and may originate in fluctuating streamers which can be observed only at minimum light. In R Leo, Merrill suggests[14] that [*Fe* II] may remain constant in intensity while the star varies in brightness.

Several faint bright lines of *Co* I in multiplets (28), (29), (31), (32), and (34) were identified. They appear about 10 days before maximum light and disappear at phase +100 days, with greatest intensity at +40 days. The *Ni* lines are not favorably placed for observation, but five low-excitation lines of multiplets (2), (30), and (33) have been found in emission.

STRONTIUM

The *Sr* II lines λ 4077 and λ 4215 appear in emission well after maximum light on the shortward edge of the absorption lines and last nearly until minimum, attaining only low intensities.

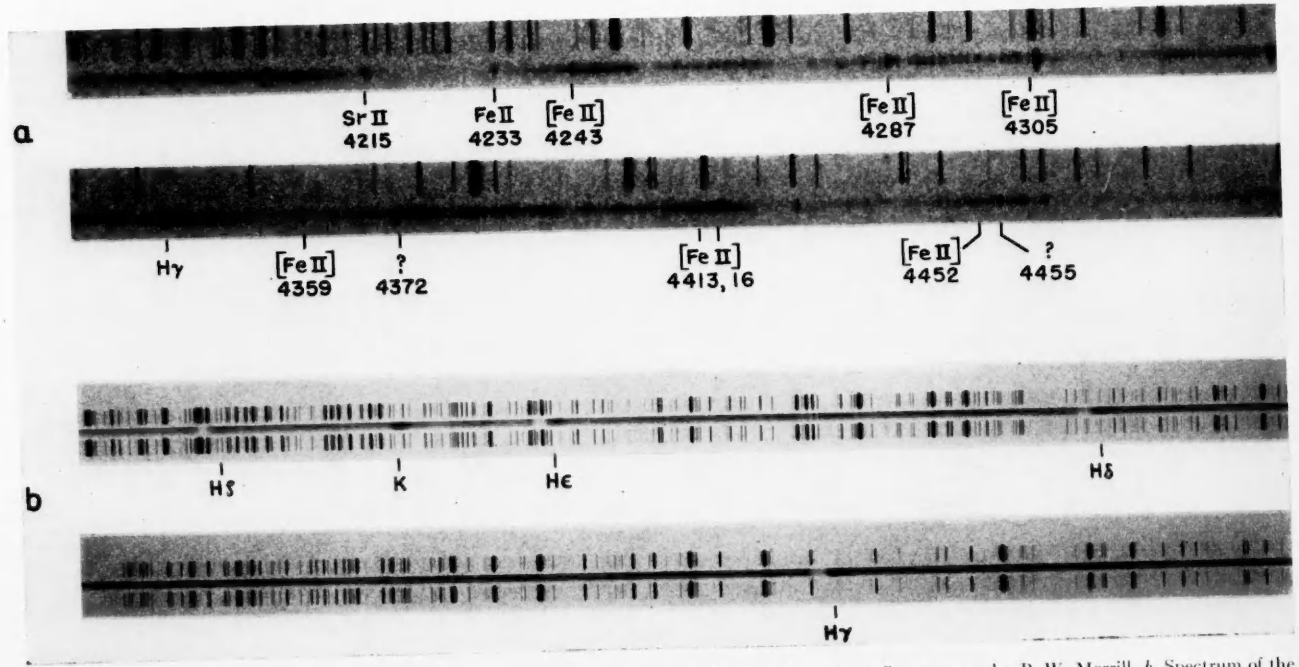

FIG. 8.—*a*, Spectrum of Mira Ceti, λλ 4175–4495, Ce 3216, phase +170 days, showing [*Fe* II] lines. Spectrogram by P. W. Merrill. *b*, Spectrum of the companion of Mira Ceti. Ce 8516, November 28, 1952. Spectrogram by O. C. Wilson.

INDIUM

The presence of the *In* I line λ 4511.310 in emission in moderate strength is well established. The bright line has the same long lifetime as *Hδ* (see p. 52).

UNIDENTIFIED LINES

The strong emission lines of Table 12 have no satisfactory identifications. The wave lengths have been corrected for the mean velocities of the chief neutral metallic bright lines of each plate. The table shows two groups of lines. The lines λλ 3735, 4372, and 4455 have similar behavior. They appear about 2 months after maximum and disappear at minimum, reaching maximum intensity at about phase +180 days. They are sharp and resemble the neutral metallic bright lines in appearance. For λ 3735.3 and λ 4455.3 the

TABLE 12

STRONG UNIDENTIFIED BRIGHT LINES

Wave Length	Plates Measured	Max. Strength		Possible Identifications and Remarks
		Phase	Int.	
3735.351	6	+180 days	5	λ 3735.325 *Fe* I (388)?
3956.082	9	+ 50	3	Wide, λ 3956.270 *Co* I (2)?
4006.772	7	+ 50	4	Wide
4098.940	9	+ 50	3	Wide
4104.455	8	+ 50	3	Wide
4138.483	5	+ 50	3	Wide
4372.564	7	+180	4	λ 4372.383 *Ti* I (277)?
4455.310	10	+180	3	λ 4455.321 *Ti* I (113)?

measured wave lengths suggest the identification of the last column. Unless their occurrence can be explained by fluorescence, these identifications seem unlikely because of their high excitation potentials. Lines of equal or greater strength in multiplets *Fe* I (388) and *Ti* I (113) do not appear in emission, although two other lines in the *Ti* I (113) multiplet have the same upper level as λ 4455.321. The velocity changes are similar to those of λ 4202 *Fe* I and λ 4307 *Fe* I. The identification of λ 4372 with *Ti* I (277) is doubtful on account of its wave length (see p. 52; also Thackeray, *Observatory*, **73**, 83, 1953).

All three of these prominent lines are stronger in Merrill's spectra of χ Cyg (M5e + S)[6] and R And (Se)[5] at phases 162 and 103 days, respectively, than in Mira Ceti. Their preference for S-type sources may be a clue to their final identification.

The five remaining lines of the table are quite different in appearance and behavior. They are wide (Fig. 7, Ce 1290) like the displaced lines of *Al* I and *Ca* II described by Merrill in other long-period variables. On account of their nebulous appearance, they are often assumed to be bright spaces between absorption lines. Their high intensity and their position with reference to adjacent absorption lines indicate that some other explanation is needed. No identification for any of the five is evident. They have a short lifetime of from −15 to +90 days, with a maximum intensity at about +45 days. On some of the spectrograms of highest dispersion they appear to be made up of two or more components. The measures of velocity are reasonably accordant, considering the character of the lines, and show no variations which can be definitely correlated with phase. Merrill[5] has measured λ 4098 and λ 4138 in R And but none of the five in χ Cyg.

THE VISUAL COMPANION

Observations by double-star observers show no certain change in distance or position angle of the two components of the visual pair greater than the errors of measurement,

except that in 1926 G. van Biesbroeck estimated that the distance had diminished and Aitken[16] made an uncertain measure of distance of 0".3 and position angle of 188°, when Mira was brighter than the sixth magnitude. This discordant observation deserves little weight, and Aitken[17] suggests that it may have been an illusion. Nevertheless, a consideration of the distance of the companion from the primary and the masses involved leads to the conclusion that the motion of the companion in its orbit must have been sufficient to make an easily measurable change in its position since its discovery in 1923.[18] Following this reasoning, P. P. Parenago[19] has computed a probable orbit assuming periastron in 1927.0. The elements are:

$P=14$ years	$e=0.7$	$\Omega=131°$
$a=0".50$	$i=85°$	$\omega=150°$

Our spectrograms are not timed to contribute evidence either in support of, or in contradiction to, this proposed orbit. It is possible that, with special care, spectrograms could be made which could be measured to find the displacement of the spectrum of the companion with reference to that of the M-type star, as was done at the time of the discovery of the companion, but such methods are subject to large errors on account of atmospheric

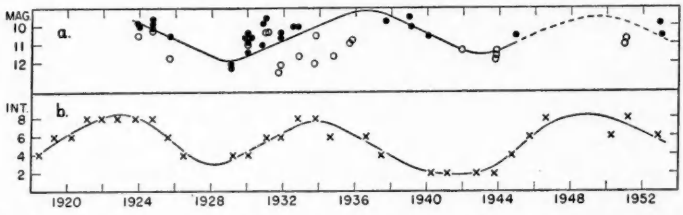

FIG. 9.—*a*, Visual estimates of the brightness of the companion of Mira Ceti by various double-star observers; *b*, estimates of the intensity of the spectrum of the companion from Mount Wilson spectrograms.

dispersion and poor seeing. Visual double-star measures are more dependable, but they must be made when the red star is close to minimum light in order to be trustworthy.

Estimates of the brightness of the companion before 1939 have been compiled by P. Baize.[20] These magnitudes, together with additional values by W. H. van den Bos[21] (1940–1945), P. Couteau[22] (1952–1953), and eight estimates (1935–1951) by van Biesbroeck, kindly supplied in advance of publication, are plotted in Figure 9, *a*. The 1953 point at 10.5 mag. is from a Δm estimate of 1.7 mag. made by G. H. Herbig with the 36-inch refractor of the Lick Observatory on January 31 and reported in a personal letter. The total brightness of the double star on that date was 8.6, according to the A.A.V.S.O. observers. The values of the brightness of the companion are computed from estimates of the total brightness and the difference in magnitude of the components. The consistency of the estimates is poor on account of the difference in color of the components. Van Biesbroeck's estimates (*circles*) are fainter than those of other observers. This lack of agreement may be, in part, due to instrumental differences. The curve indicates a real variation in brightness. Sudden changes have also been suspected by most observers. Systematic observations of this star are badly needed.

[16] *Pub. A.S.P.*, **38**, 334, 1926.

[17] *Ibid.*, **42**, 60, 1930.

[18] R. G. Aitken, *Ibid.*, **35**, 323, 1923.

[19] *Variable Stars*, **7**, 199, 1950.

[20] *Bull. Soc. astr. de France*, **53**, 360, 1939.

[21] *Union Obs. Circ.*, No. 108, p. 315, 1949.

[22] *J. des observateurs*, **36**, 46, 1953.

In comparison with the light-observations, the relative intensity of the spectrum of the companion at minimum light in successive cycles is shown in Table 13 and Figure 9, *b*. These estimates are subject to considerable uncertainty because the observations were made at different phases and the exact position of the star image on the spectrograph slit is not known. Poor seeing and atmospheric dispersion may have disturbing effects. Nevertheless, a variation in the intensity of the spectrum of the companion relative to that of the Me variable is clearly indicated. More than two complete cycles with periods of 12–15 years have been covered by observations. Maxima of intensity of the companion occur about 1922–1924, 1933–1935, and 1948–1950, with minima about 1927–1929 and 1941–1943. These extremes of intensity are corroborated to some extent by the light-curve, which has maxima about 1922–1924 and 1936–1937 and minima at 1927–1929 and 1942–1944. The minima of intensity correspond approximately to the times of periastron of Parenago's elements. The explanation of such a coincidence is difficult unless, as seen from the earth, absorbing matter between or surrounding the stars cuts down the light of the companion when it is near periastron.

TABLE 13

RELATIVE INTENSITY OF SPECTRUM OF THE COMPANION AT DIFFERENT MINIMA

Minimum	Int.	Minimum	Int.	Minimum	Int.
May, 1918	4	Jan., 1930	4	Jan., 1942	.....
Apr., 1919	6	Jan., 1931	6	Nov., 1942	2
Mar., 1920	6	Dec., 1931	6	Oct., 1943	2
Jan., 1921	8	Nov., 1932	8	Sept., 1944	4
Dec., 1921	8	Oct., 1933	8	Sept., 1945	6
Oct., 1922	8	Aug., 1934	6	July, 1946	8
Oct., 1923	8	Aug., 1935	.....	June, 1947	.....
Sept., 1924	8	July, 1936	6	May, 1948	.....
July, 1925	6	June, 1937	4	Mar., 1949	.....
June, 1926	4	May, 1938	.....	Mar., 1950	6
May, 1927	.....	Apr., 1939	.....	Feb., 1951	8
Apr., 1928	.....	Mar., 1940	2	Jan., 1952	.....
Mar., 1929	4	Feb., 1941	2	Dec., 1952	6

While there are changes in the wide bright hydrogen lines and the accompanying absorption from time to time, the fluctuations are probably slow and not related to the 332-day cycle. On most of the plates showing hydrogen emission lines the violet emission component is weak or entirely absent, but in the years 1921, 1923–1925, 1933–1934, and 1944–1946 it was seen in moderate strength, although the high intensity shown in Plate X*c* of *Contribution* No. 311[1] is not equaled on any other plate.

At the minima of 1924 and 1925 many fuzzy emission lines from the z^4D^0 multiplets of *Fe* II were seen, apparently in the spectrum of the companion; but these lines have not been found in other years. Sharp lines of *Fe* II and [*Fe* II], which are frequently seen near minimum light, doubtless have their source in the atmosphere of the M-type star.

The wide emission H and K lines of *Ca* II are cut by a narrow absorption line (Fig. 8, *b*). This line doubtless originates at a high level in the atmosphere of the companion and may indicate an expanding calcium shell. Probably it is not greatly affected by interstellar absorption. The velocities from measures of this line are given in the accompanying tabulation. Although the luminosity of the companion is certainly much fainter than that of stars of the main sequence, its spectrum resembles in many respects that of certain P Cygni stars of much higher luminosity. For example, the bright lines of hydrogen and their absorption components (Fig. 8, *b*) are much like those of BD+47°3487

(MWC 374) B3eq described by Swings and Struve[23] and by C. S. Beals.[24] For this star Beals estimates the absolute magnitude as -2.7 from the strength of the interstellar lines. The hydrogen series extends to *H*20 in emission and to *H*30 in absorption, while in the companion to Mira Ceti both bright and dark hydrogen lines are seen to *H*22 on O. C. Wilson's spectrogram Ce 8516, November 28, 1952. Both bright and dark lines are variable but on this plate are considerably wider than in BD+47°3487. The companion is peculiar, in that it has, except for the P Cygni components of the hydrogen lines and the narrow cores of H and K, no other absorption lines. Strong wide H and K, fuzzy *He* I, and perhaps sometimes wide *Fe* II lines appear in emission. The *He* I and *Fe* II lines are 5–6 A in width. These bright lines are apparently undisplaced and have no shortward absorption components such as are present in the *Fe* II lines of BD+47°3487.

Plate	Phase (Days)	Velocity (Km/Sec)	Plate	Phase (Days)	Velocity (Km/Sec)
P 24.....	+116	+52.0	Ce 8516...	+194	+52.7
P 36.....	+128	+52.4			
P 39.....	+151	+52.2	Mean...	.....	+52.3

DISCUSSION

As a result of a large observational effort with powerful equipment, considerable confidence in our knowledge of the superficial processes taking place in the atmospheres of Mira Ceti and other long-period variable stars has been secured. The origin of the disturbances and the fundamental causes of the rhythmic outbursts of these stars are still in the realm of speculation. Satisfactory explanations of a number of the activities have been proposed by Merrill in his reports on Me and Se stars.

McKellar and Odgers[25] find that the application of the notion[26] of a low-lying hydrogen convective zone with cyclic motions accounts for most of the observed phenomena. The high temperature of this stratum may supply the energy necessary for the emission lines.

In general, the results of the previous study with low-dispersion spectrograms are well confirmed. The more accurate recent observations of absorption lines indicate a smaller velocity range than that previously found, but a definite variation within each cycle seems certain. Maximum velocity of recession occurs near or shortly after maximum light. Preceding and following maximum, the positive velocities are less, but the observations near minimum are insufficient to complete the curve.

Explanations on the basis of general volume pulsation are open to question, but the rising and falling of strata at low levels are needed to account for the observed motions and to supply energy for the vast array of emission features. Further observations should be timed to contribute evidence concerning the possibility of explosive or shock effects, such as were found by R. F. Sanford[27] in W Vir. Adams[7] discovered widened and double lines of *Mn* I, *Cr* I, and *Sr* II in *o* Ceti on the high-dispersion spectrogram Ce 2133 at phase +55 days and attributed the effect to differential motions in the atmosphere of the star, as suggested by Lyman Spitzer, Jr.[28] The separation of 0.2 A between the components of the double lines is not sufficient to show on other plates. Recurrent turbulent effects might be difficult to distinguish from pulsation by velocity alone.

[23] *Ap. J.*, **91**, 577, 1940.

[24] *Pub. Dom. Ap. Obs. Victoria*, **9**, 88, 123, 1951.

[25] *Pub. A.S.P.*, **64**, 222, 1952.

[26] A. S. Eddington, *M.N.*, **101**, 177, 1941.

[27] *Ap. J.*, **116**, 331, 1953.

[28] *Ap. J.*, **90**, 494, 1939.

The difference between the displacement-curves of metallic (Fig. 4, *g*) and hydrogen (Fig. 4, *h*) emission lines relative to the absorption spectrum is interesting in this connection. The hydrogen source increases its velocity of ascent with respect to the reversing layer from phase −16 days until phase +40 days and then seems to subside, whereas the source of the emission of metals maintains a constant negative velocity difference of 15 km/sec from −50 days until +40 days, after which the curve follows that of the hydrogen displacements. The curve of emission velocities shown in *Contribution* No. 311 is evidently a composite of hydrogen and metal velocities.

An important result of the survey of the velocities from the absorption lines of Mira Ceti is the conclusion that the velocity maxima vary from cycle to cycle by an amount which is of the same order of magnitude as the variation within a single cycle. Since there is some indication that these variations are correlated with the luminosity and temperature at the maxima, it may be that the measured differences are not entirely due to velocity fluctuations.

This paper on Mira Ceti should be considered one of the series by P. W. Merrill on the spectra of the M- and S-type variables. He obtained nearly all the spectrograms with a dispersion of 10.2 A/mm, and his method of attack has been closely followed. The conclusions, for the most part, are the outcome of frequent discussions between us.

My thanks are also extended to W. S. Adams, I. S. Bowen, R. F. Sanford, and O. C. Wilson for spectrograms taken at critical phases and to Miss Sylvia Burd for much assistance in analyzing the extensive material, as well as for her contribution of precise measurements of the spectrograms.

AN ANALYSIS OF W VIRGINIS*

HELMUT A. ABT†
MOUNT WILSON AND PALOMAR OBSERVATORIES
CARNEGIE INSTITUTION OF WASHINGTON
CALIFORNIA INSTITUTE OF TECHNOLOGY
Received August 13, 1953

ABSTRACT

A study has been made of the population II cepheid, W Virginis, from high-dispersion spectra obtained by Sanford and Abt and from photoelectric colors and magnitudes obtained by Whitford and Code, Eggen, and Gordon and Kron. The radial velocity-curve by Sanford has been integrated for three different choices of a γ-velocity, each giving a total displacement of the order of 35×10^6 km. Layers of gas can be seen, one rising while the other is falling. Hydrogen emission lines are formed in the lower layer when it is first seen to rise. The light- and color-curves have been used to obtain relative radii. A comparison with displacements from the radial velocity-curve gives a maximum radius that is smaller than the total displacement of the atmosphere. Curves of growth were constructed for 17 of the plates. Excitation temperatures for *Fe* I and for lines of high excitation potential of *Mg* II show that when two layers are seen, their temperatures differ by 700°–1000°. Ionization temperatures calculated from the degree of ionization of *Fe* I and the continuous opacity agree with the effective temperatures from the colors and with the *Mg* II excitation temperatures. Relative to *Fe*, *Ba* and *Ca* have normal abundances, but the *Sr* and *Sc* abundances are small by factors of 5 and 3, respectively. Several lines of evidence indicate that the layers of gas are geometrically thin and transparent. A model of a shock wave traveling through an extended atmosphere was found to give too much material between the compressed regions following the shock fronts and too high temperatures. A model of shells of gas thrown off at maximum expansion of the photosphere explains the failure of Baade's method for finding the total radius. If these shells have to collide, they cannot be uniform but must consist of many condensations.

I. INTRODUCTION

There are certain obvious differences between the population I classical cepheids and the population II variables of the W Virginis class. The question arises as to whether these differences indicate fundamentally different mechanisms of pulsation. The purpose of this project is to study in detail a typical W Vir star, in order to analyze the kind of pulsatory motion involved and to provide a comparison with classical cepheids.

The W Vir stars occur in globular clusters and, in small numbers, in other parts of the Galaxy. They can be recognized by the following characteristics: (1) abnormal light-curve, having a shoulder on the decline after maximum light; (2) hydrogen emission lines at certain phases; (3) high radial velocity; (4) often a large galactic latitude; and (5) often a variable period. Other characteristics, such as the presence of double absorption lines at certain phases and spectral characteristics of a population II star, may be added in time. W Vir fulfils all requirements for membership in this class. It was chosen for study because of its relative brightness (P = 10.0 to 11.6).

II. PHOTOMETRIC DATA AND RESULTS

1. LIGHT- AND COLOR-CURVES

The photometric data show fluctuations that are larger than the observational errors and are probably intrinsic in the star. A photoelectric light-curve was obtained in 1948 by Gordon and Kron[1] at an effective wave length of about λ 5000. This light-curve, re-

* This project was completed in partial fulfilment of requirements for a doctoral thesis at the California Institute of Technology.

† Now at the Yerkes Observatory, Williams Bay, Wisconsin.

[1] *Ap. J.*, **109**, 177, 1949.

produced in Figure 1, clearly shows the shoulder on the decline after maximum light. At one light-maximum the photographic magnitude on the International System was 10.13.

Drs. A. E. Whitford and A. D. Code kindly consented to measure colors of W Vir with the 60-inch telescope on Mount Wilson in June and July, 1951. A refrigerated 1P21 photomultiplier was used with a 1-mm Schott BG12 filter and a 2-mm Schott GG7

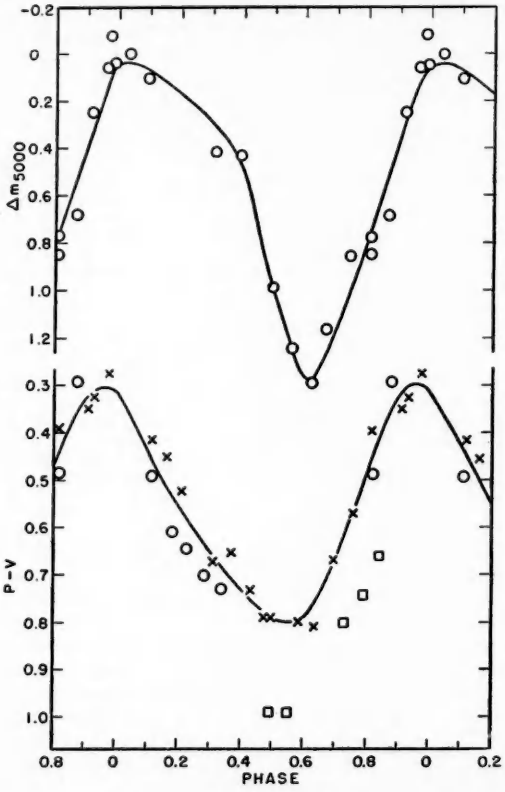

FIG. 1.—*Top:* light-curve at λ 5000 by Gordon and Kron; *bottom:* colors by Whitford and Code (*squares* for cycle 71, *circles* for cycle 72–73) and by Eggen (*crosses*). In drawing the curve the observations during cycle 71 were neglected.

filter, for blue and yellow magnitudes, respectively. A Corning 7380 glass filter was used in both cases to absorb UV light. The effective wave lengths are λ 4260 and λ 5280. No comparison stars were used, but stars 11 and 52 in Selected Area 57 (at 33° from W Vir) were generally used as extinction stars. Single measures on 12 nights during two cycles were obtained. Table 1 gives the times of observation, the phases computed from equation (3), and the photographic magnitudes and colors on the (***P***, ***V***) system.[2, 3] The colors are plotted in Figure 1.

[2] J. Stebbins, A. E. Whitford, and H. L. Johnson, *Ap. J.*, **112**, 469, 1950.

[3] H. L. Johnson and W. W. Morgan, *Ap. J.*, **114**, 526, 1951.

The color measures during the two cycles differ by 0.2 mag. at the phase of overlap. Since the estimated probable error is ± 0.02 mag., it is likely that either one or both cycles were abnormal. If these colors and magnitudes are used to obtain a light-curve at λ 5000 by means of a linear interpolation, it is found that the magnitudes during cycle 72–73 agree with those of Gordon and Kron (mean deviation, 0.06 mag.) but that those from cycle 71 are faint by an average of 0.30 mag. We have neglected the colors from cycle 71 when drawing a mean color-curve.

In advance of publication Dr. Olin Eggen has supplied photoelectric colors and magnitudes which he obtained with the 12-inch refractor at the Lick Observatory in 1949. The existence of these measures was unknown to the author until recently. The colors are plotted in Figure 1. Phases were computed with equation (3) and the colors were converted to the (*P*, *V*) system by applying Eggen's[4] correlation equations. The color-curves of Eggen and of Whitford and Code differ somewhat in range and shape.

In the absence of more complete information, I will arbitrarily adopt the following photometric data: (1) the light-curve at λ 5000 by Gordon and Kron, (2) a mean color-curve from measures by Whitford and Code during cycle 72–73 and by Eggen, and (3) a maximum photographic magnitude of 10.0.

TABLE 1

COLORS AND MAGNITUDES BY WHITFORD AND CODE

JD 2433000+	Cycle and Phase	*P*	*P*–*V*	JD 2433000+	Cycle and Phase	*P*	*P*–*V*
800.804.....	71.496	10.80	+0.99	824.670.....	72.878	10.34	+0.29
801.688.....	71.547	11.48	+ .99	828.681.....	73.110	10.14	+ .49
804.722.....	71.723	11.67	+ .80	829.765.....	73.173	10.13	+ .61
805.713.....	71.780	11.42	+ .74	830.700.....	73.227	10.23	+ .64
806.769.....	71.841	11.16	+ .66	831.683.....	73.284	10.46	+ .70
823.674.....	72.820	10.75	+0.48	832.690.....	73.342	10.43	+0.73

2. CONVERSION OF COLORS TO EFFECTIVE TEMPERATURES

We wish to apply Baade's[5] method to find the luminosity and radius of W Vir. The method consists in obtaining relative luminosities from the light-curve and bolometric corrections, effective temperatures from the colors, and hence relative radii from the luminosity laws. The relative radii are compared with the displacements derived from the radial velocity-curve. The total radius and absolute luminosity follow from this comparison. The best relation between colors and effective temperatures is probably that given by Stebbins and Whitford[6] in their six-color photometry of 238 stars. Our procedure will be to convert the colors to Stebbins and Whitford's $V - I$ system and then to temperatures. From their photometry of the North Polar Sequence we derive, by a least-squares solution, the relation

$$V - I = -1.58 \pm 0.16 + 2.744\,(P - V)\,. \qquad (1)$$

For a star of type F or G, like W Vir, it seems best to assume that Stebbins and Whitford's T_2 scale represents the color temperatures, T_c. This scale is based on Kuiper's solar color temperature of 6700° and spectral type dG2. Table 7 of Stebbins and Whitford's[6] paper then gives color temperatures as a function of $V - I$. In Table 2 of the present paper we give the smoothed color-curve, $P - V$, and the resultant T_c's.

Finally, we converted the T_c's to effective temperatures, T_e, by using Chandrasekhar

[4] *Ap. J.*, **114**, 144, 1951.

[5] *Mitt. Hamburg-Bergedorf*, Vol. **6**, No. 29, 1928.

[6] *Ap. J.*, **102**, 318, 1945.

and Münch's[7] theoretical relation. For $\theta_e = 5040/T_e < 0.8$, where the (θ_e, θ_e) relation depends on electron pressure, we made use of the electron pressures determined for W Vir (see Fig. 9). Values of T_e are also given in Table 2. From these we obtain spectral types, using Keenan and Morgan's[8] correlation. The over-all conversion from colors, $P - V$, to spectral types agrees with Eggen's[9] correlation to within one- or two-tenths of a spectral class.

TABLE 2

PHOTOMETRIC DATA AND RESULTS

Phase	$P-V$	T_c	T_e	Spectral Type	m_{5450}	B.C.	$L/L_{\min}$	$R/R_{\min}$
0.00.....	0.32	8210	6720	F3	9.63	−0.06	1.99	1.18
.05.....	.37	7770	6500	F4	9.65	− .09	2.01	1.27
.10.....	.43	7250	6220	F5	9.66	− .12	2.05	1.40
.15.....	.49	6810	5950	F6	9.65	− .16	2.15	1.56
.20.....	.55	6420	5680	F7	9.68	− .21	2.19	1.73
.25.....	.61	6120	5440	F7	9.69	− .22	2.19	1.89
.30.....	.66	5890	5220	F9	9.72	− .35	2.40	2.05
.35.....	.70	5720	5030	G0	9.77	− .41	2.42	2.32
.40.....	.74	5550	4840	G0	9.91	− .41	2.13	2.35
.45.....	.77	5440	4720	G1	10.14	− .47	1.82	2.29
.50.....	.79	5350	4640	G2	10.38	− .52	1.53	2.43
.55.....	.80	5330	4610	G2	10.62	− .52	1.22	1.96
.60.....	.80	5330	4610	G2	10.79	− .52	1.05	1.82
.65.....	.77	5440	4720	G1	10.79	− .47	1.00	1.69
.70.....	.67	5840	5160	F9	10.65	− .35	1.02	1.43
.75.....	.57	6320	5600	F7	10.52	− .22	1.02	1.21
.80.....	.48	6860	5980	F6	10.35	− .16	1.13	1.12
.85.....	.39	7580	6390	F4	10.19	− .09	1.22	1.02
.90.....	.32	8210	6720	F3	9.99	− .06	1.43	1.00
0.95.....	0.30	8420	6810	F3	9.91	−0.06	1.74	1.07

3. RELATIVE LUMINOSITIES AND RADII

Using a linear extrapolation, we can obtain magnitudes at λ 5450 from those at λ 5000 and the colors. Using the spectral types in Table 2 and Kuiper's[10] empirical bolometric corrections, we derived bolometric magnitudes. Table 2 also gives the light-curve at λ 5450, the bolometric corrections (B.C.), and luminosities relative to that at minimum luminosity.

The bolometric luminosity has a minimum at light-minimum, but maximum luminosity occurs at phase 0.33 after light-maximum, which is the phase of the shoulder on the photographic and visual light-curves.

The luminosity of a star is proportional to the area and T_e^4. Since we now have T_e as a function of phase and relative luminosities, we can find relative radii. These are given in Table 2, relative to the minimum radius, $R_{\min}$, which occurs just before maximum light. Maximum radius occurs at about phase 0.42. A comparison of relative radii with displacements will be made after the latter have been computed.

III. SPECTROSCOPIC DATA AND REDUCTIONS

1. OBSERVATIONS

Twenty-three coudé spectra of W Vir were obtained with the 100-inch telescope on Mount Wilson. The thirteen spectra taken by R. F. Sanford between January, 1948,

[7] *Ap. J.*, **104**, 446, 1946.

[8] *Astrophysics*, ed. J. A. Hynek (New York: McGraw-Hill Book Co., 1951), p. 20.

[9] *Ap. J.*, **113**, 663, 1951.

[10] *Ap. J.*, **88**, 429, 1938.

and April, 1950, and one taken by W. Buscombe were supplemented by nine spectra taken by the author near light-minima in the spring of 1951. The spectral range extended from $H\beta$ to the region of λλ 4200–3700, depending on the exposure of the plate. In addition, for six of the plates taken with the Wood grating before March, 1949, it was possible to obtain simultaneously the $H\alpha$ region. The dispersions were 10.3 A/mm in the blue region of the spectrum with both the Wood and the Babcock gratings and 20.3 A/mm in the red. Baked Eastman emulsions 103-O and II*a*-O were used in the blue and 103*a*-D and 103*a*-E in the red. Exposure times ranged from 2 to 7 hours. The projected slit width varied from 0.012 to 0.030 mm, while the spectrum width was 0.26 and 0.16 mm, respectively, with the earlier and later grating-collimator arrangements. Flanking the

TABLE 3

SPECTROGRAPHIC OBSERVATIONS

Plate No. Ce	JD 2430000+	Cycle and Phase	Phase Correction	Corrected Phase
5058	2571.008	0.283	+0.070	0.358
5092	2599.946	1.959	.....	.....
5110	2611.883	2.650	.....	.....
5187	2694.720	7.447	.....	.....
5216	2725.716	9.242	.....	.....
5556	2988.957	23.211	− .015	23.196
5616	3014.799	25.981	.000	25.981
5617	3015.843	26.042	.000	26.042
5618	3016.788	26.097	.000	26.097
5647	3049.753	28.005	.000	28.005
5651	3069.746	29.163	− .040	29.123
6207	3376.836	46.945	+ .095	47.040
6211	3377.854	47.004	+ .085	47.089
6889	3719.954	66.814	.....	.....
6947	3730.955	67.451	.....	.....
6965	3750.864	68.604	.....	.....
7010	3781.793	70.395	.....	.....
7013	3782.788	70.452	.....	.....
7017	3783.794	70.511	.....	.....
7080	3821.754	72.709	.....	.....
7085	3822.751	72.767	.....	.....
7091	3823.753	72.825	.....	.....
7102	3825.743	72.940	+0.090	73.030

spectra on the same plates were stepped-slit intensity calibrations with exposure times approaching those of the stellar spectra. No systematic differences were detected between the results from the spectra taken with the two different gratings or between those spectra taken by the two observers. The mid-exposure times for the spectrograms are given in Table 3.

2. PHASES

W Vir shows a long-term variation in period. Times of minima have been collected by Nielson.[11] Three recent epochs are obtained by fitting Joy's[12] radial velocity-curve to Sanford's,[13] and from the photoelectric observations. An ephemeris that fits the recent photoelectric observations exactly and the others fairly well is

$$\text{Minimum light: JD2432698.45} + 17.26944E\,. \qquad (2)$$

[11] *A.N.*, **262**, 422, 1937.
[12] *Ap. J.*, **86**, 363, 1937.
[13] *Ap. J.*, **116**, 331, 1952.

Residuals from the computed times of minima are plotted in Figure 2. The need for a higher-order term in equation (2) is apparent, but its nature is not yet clear. Since the present observations were all made in 3 years, this long-term variation is not large, and equation (2) is sufficiently accurate. Correcting to light-maximum and changing the epoch by seven periods, we obtain

$$\text{Maximum light: JD2432566.11} + 17.26944E\,. \tag{3}$$

Preliminary phases, computed with equation (3), are given in Table 3.

3. RADIAL VELOCITY-CURVE

Velocities for the absorption lines were measured and published by R. F. Sanford.[13] These are plotted in Figure 3. The interesting features of the curve are the presence of double lines and the discontinuity of the curve. The only measures added to Sanford's absorption velocities are those for the shortward components on plates Ce 7091 (phase,

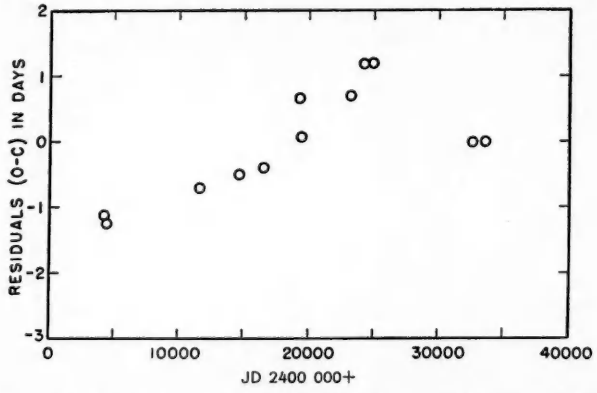

FIG. 2.—Residuals in the epochs of light-minima as computed from equation (2)

0.825; vel., −85.0 km/sec) and Ce 5616 (phase, 0.981; vel., −88.5 km/sec). Comparison of microphotometer tracings showed the presence of at least 13 shortward components on Ce 7091 and 41 on Ce 5616. Plate Ce 5092 (phase, 0.958) also showed a few shortward components, but no measurements were made on this plate. This means that all plates taken between phases 0.825 and 0.10 show double lines. The particular lines which are doubled depend on the excitation and ionization conditions in the two layers where they are formed and on the continuous opacity.

During the times that they exist, the hydrogen emission lines are much broader than the *H* absorption lines. The latter are displaced longward of the center of the emission lines, so the profile of some of the emission lines can be reconstructed with sufficient accuracy on the microphotometer tracings. Velocities for the emission lines during phases 0.65–0.825 agreed substantially with those published by Sanford;[13] they are plotted as squares in Figure 3. However, for later phases (0.94–0.10) the emission lines are weaker, and their profiles are distorted too greatly by the absorption lines to permit good velocity determinations.

Plate Ce 7091 has both strong, measurable emission lines and double metallic absorption lines. The average of Sanford's and my measures for the velocity of the emission lines is −86.5 km/sec, while the velocity of the shortward absorption lines (as measured on the microphotometer tracings) is -85.0 ± 5.1 km/sec. On the basis of this agreement

and the continuity of the measures of the emission and shortward absorption lines, we conclude that the emission and shortward absorption lines have the same velocities at all times when both are present and that they are formed at the same mean depth in the atmosphere. This allows us to extend the velocity-curve backward to phase 0.65 (see Fig. 3). We can then follow the motion of a layer of gas from minimum light until shortly after the second following light-maximum, or for 1.45*P*.

4. DISPLACEMENT-CURVES

By integrating the radial velocity-curve over time, we can find displacements of the atmosphere in kilometers as a function of phase. However, to do this we must first decide

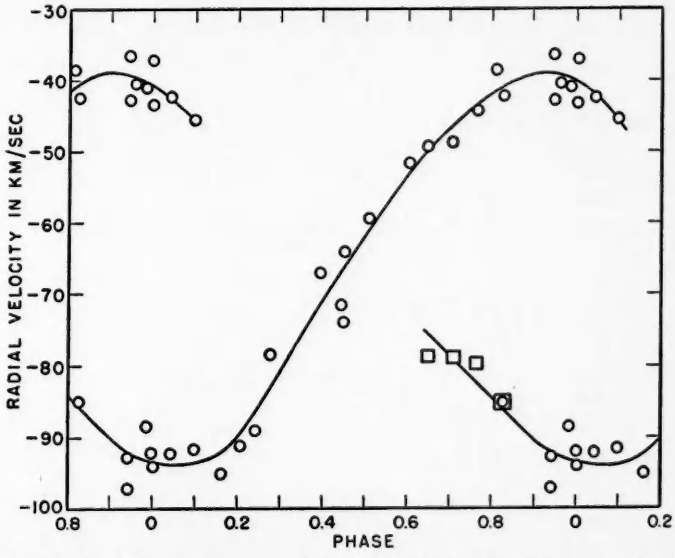

FIG. 3.—Radial-velocity measures, principally by Sanford. The circles represent absorption-line velocities and the squares hydrogen emission-line velocities. The lower part of the curve is drawn differently than by Sanford.

on the γ-velocity of the star. For a classical cepheid the radial velocity-curve is continuous and the γ-velocity can probably be taken as the mean velocity of the atmosphere. Since W Vir has a discontinuous velocity-curve, we obviously are not observing the motion of the same mass of gas during successive cycles. The velocity-curve may reflect predominantly inward or outward motion of the atmosphere. The atmosphere of the sun may provide an example of predominantly outward motion, since there is some evidence[14] for an outward motion of about 0.6 km/sec. On the other hand, the solar prominences appear to have a predominantly inward motion. A comparison of the mean velocities of W Vir stars in globular clusters given by Joy[15] with the velocities of the clusters given by Mayall[16] is of sufficient accuracy only to indicate that the mean and γ-velocities agree within 10 km/sec. Displacement-curves have therefore been calculated for three sample cases: (1) predominantly inward motion with a surface velocity of 9.1 km/sec, (2) sym-

[14] M. G. Adam, *M.N.*, **108**, 446, 1948.

[15] *Ap. J.*, **110**, 105, 1949.

[16] *Ap. J.*, **104**, 290, 1946.

metrical expansion and contraction, and (3) predominantly outward motion of 9.8 km/sec surface velocity.

For a limb-darkening coefficient of $\frac{3}{5}$, the surface velocity is $\frac{24}{17}$ times the radial velocity. The mean radial velocity integrated between phases 0.00 and 1.00 is -64.7 km/sec. This velocity is reached at phase 0.47. The above three examples of predominantly inward, symmetrical, and predominantly outward motion give maximum radii at phases 0.40, 0.47, and 0.55 for γ-velocities of -71.1, -64.7, and -57.7 km/sec, respectively. The displacement-curves are given in Figure 4.

The total displacements for the three cases in the order given above are 33.1, 34.6,

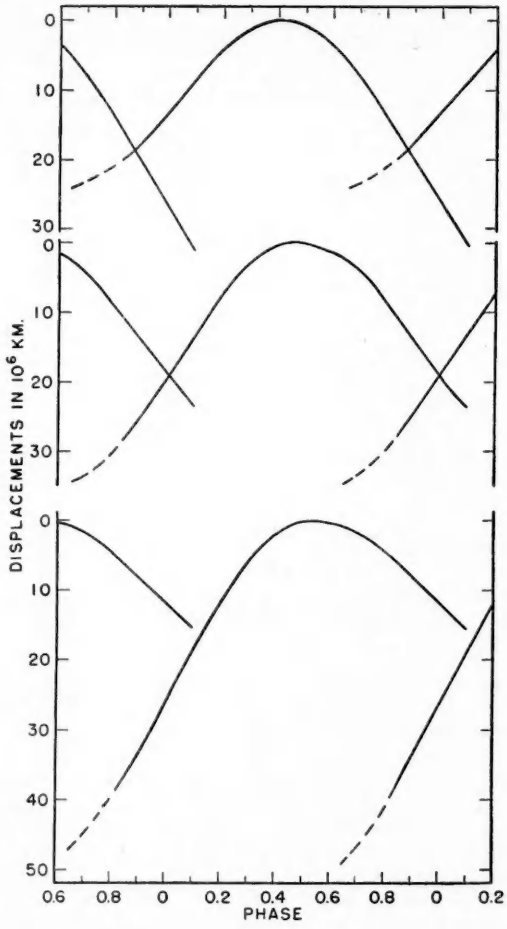

FIG. 4.—Displacements of the atmosphere from maximum radius for three types of expansion. *Top:* predominantly inward motion of 9.1 km/sec; *center:* symmetrical expansion and contraction; *bottom:* predominantly outward motion of 9.8 km/sec. Dashed lines represent displacements derived from emission-line velocities.

and 47.2×10^6 km. The largest total displacement reported for a classical cepheid is that of 24.3×10^6 km for l Carinae,[17] period 35.52 days.

The interesting feature of these curves is the overlap of cycles. There are times when a part of the atmosphere is rising while another part is falling. Whether we actually observe the collision of the two separate layers depends on the γ-velocity of the star. For the three γ-velocities selected, we find the collision phases to be 0.875, 0.00, and 0.13, respectively. We know that the collision phase cannot be earlier than 0.825, because, as will be shown in Section IV, 9, plate Ce 7091 taken at that phase showed the older layer to be above the new one. Therefore, the γ-velocity is not algebraically less than -73.5 km/sec.

The displacement-curves, particularly the one for symmetrical expansion and contraction, seem to indicate that the period of oscillation of the atmosphere is twice the period of light-variation and that the time between oscillation cycles is half the duration of one cycle. The curves indicate that perhaps the fundamental period is twice the period derived from the light-curve. The radial velocity-curve also suggests this; it is suggestive of a double-lined binary with a period $2P$. However, to double the periods of W Vir stars would not make them fit the characteristics of classical cepheids any better; the differences between their period-luminosity relations would be even larger, and the deviations from Code's[18] spectral-type limits as a function of period would also be larger.

5. COMPARISON OF RELATIVE RADII AND DISPLACEMENTS

We now have the material to apply Baade's method. In Figure 5 are plotted the relative radii from Table 2 and the displacement-curve which fits best, namely, the one for a small predominantly inward motion. The ordinates in Figure 5 have also been adjusted for a best fit. A comparison of ordinates then indicates a minimum radius of 15×10^6 km and a maximum radius of about 2.2 times this, or 33×10^6 km. These radii are smaller than the total displacement of the atmosphere, while one would expect the atmospheric displacement to be only a fraction of the total radius.

The method fails to give reasonable results for, perhaps, one or more of the following reasons: (1) the color-curve is not well enough determined, (2) the conversion from colors to effective temperatures may not be valid, or (3) the model of the star is such that the relative radii and displacements should not be compared. The intrinsic fluctuations in color as exhibited by the measures by Whitford and Code and the systematic differences between the colors of Whitford and Code and those of Eggen show that more extensive color measures are necessary. Neither of these color-curves individually gives better results. With Eggen's colors alone, the fit is better with the displacement-curve for symmetrical expansion and contraction.

Second, the bolometric corrections and the conversion from colors to temperatures were implicitly based on population I stars and may not apply to population II giants—particularly to such an extreme variable as W Vir. If the star has an extended atmosphere, the bolometric corrections[19] would be much larger and almost independent of temperature. Also, the surface velocities would be the same as the radial velocities. The presence of strong H emission lines suggests the existence of an excess of far UV radiation and a further distortion of the color-T_e relation.

Third, it may be that the regions of formation of the line spectra and the photosphere have different motions. For instance, the layers in which the absorption spectra are formed may be in the nature of shells which are often far above the photosphere and

[17] See, e.g., A. S. Eddington, *The Internal Constitution of the Stars* (Cambridge: At the University Press, 1926), p. 182. Published value corrected by $\frac{2}{1}\frac{4}{7}$.

[18] *Ap. J.*, **106**, 309, 1947.

[19] N. A. Kosirev, *M.N.*, **94**, 441, 1933.

transparent to the light from it. If we use the old Harvard period-luminosity relation[20] for classical cepheids and a mean $T_e = 5580°$, we obtain a mean radius of 28.8×10^6 km. Then we might propose the following model: At light-maximum the radius of the photosphere is 18×10^6 km and begins to expand. At about phase 0.4 or 0.5, when the photosphere has reached a radius of 40×10^6 km, it throws off a shell and then begins to contract. The transparent shell continues to move outward a total of 35×10^6 km in about one period before it begins to fall inward. Meanwhile, the photosphere has contracted, expanded again, and thrown off another shell. Hence the photosphere would pulsate be-

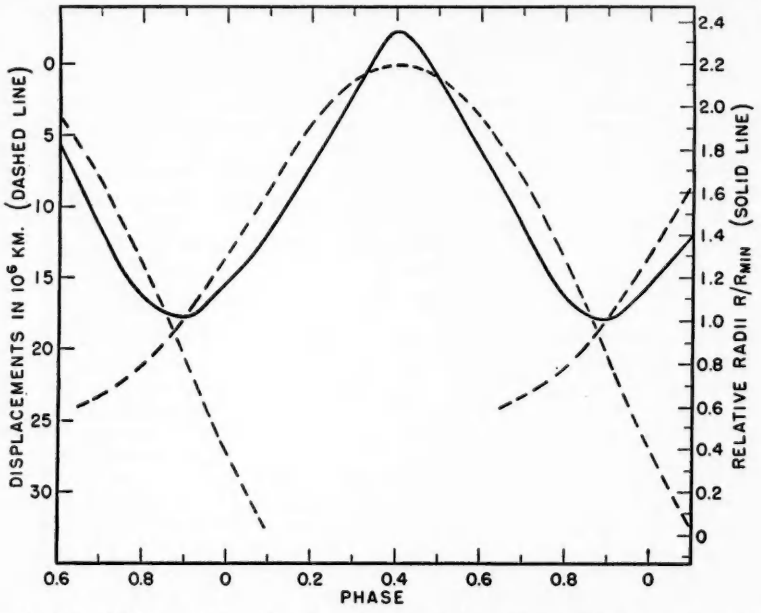

FIG. 5.—The solid line and the scale on the right give relative radii from the photometric data. The dashed line and the left-hand scale give displacements from the radial velocities for the sample case of predominantly inward motion.

tween radii of 18 and 40×10^6 km, while the shells would be thrown off at 40×10^6 km and rise to 75×10^6 km. This model will be discussed further after we have investigated the physical nature of the gas layers.

6. APPEARANCE OF THE ABSORPTION SPECTRUM

When they first appear just before maximum light, the shortward absorption lines are very weak but have the appearance of an F2 supergiant. The luminosity class at all phases is about *Ib*—certainly not II or III. The new group of lines quickly strengthens, while the longward components fade, until at phase 0.2 they have nearly reached their full strength. The spectral type becomes later until at minimum light (phase 0.62) the metallic lines indicate G6, although the G band is either absent or very weak. After minimum light the lines begin to fade, and the spectral type quickly returns to F2. Between phases 0.825 and 0.1, when both absorption components are present and weak,

[20] See, e.g., C. Payne-Gaposchkin, *Astrophysics*, ed. J. A. Hynek (New York: McGraw-Hill Book Co., Inc., 1951), p. 499.

both indicate a spectral type of F2, although there is a large difference in excitation temperature between the two spectra.

The *Ca* II K line shows an emission component in its core during some cycles from phase 0.00 to at least phase 0.20. There is a tendency for the emission to be present during odd cycles, as computed by equation (3), but not during even cycles. This is the only spectroscopic evidence for differences between successive cycles. The velocities of the emission lines are about the same as for the shortward absorption lines.

All measured parameters indicate fluctuations from cycle to cycle which become very troublesome when certain parameters vary rapidly with phase (e.g., the opacity varies by a factor of 100 in a quarter of a period). However, it appears, in general, that corrections to the computed phases that are based on one physical parameter will also apply to the others. We are particularly interested in the times of occurrence of double lines. The rapid variations in line strengths at these times afford a sensitive criterion of discordant cycles. Using the strengths of λ 4077 *Sr* II and λ 4554 *Ba* II, we determine the phase corrections that are listed in Table 3 for the spectra taken between phases 0.90 and 0.30. These corrections show no systematic variation over long time intervals. Spectra taken on successive nights (e.g., Ce 6207, 6211) show about the same corrections, but those taken during successive cycles (e.g., Ce 5647, 5651) do not necessarily show the same corrections. The corrected phases, which will be used in all further discussions of the spectra, do not distort any relationships but merely reduce scatter.

7. THE HYDROGEN LINES

The behavior of the hydrogen lines is complex and shows large variations from cycle to cycle. Neither the preliminary nor the corrected phases make all the *H*-line profiles fit into a well-ordered sequence. The smoothed intensity profiles in Figure 6 seem to represent the principal changes in $H\delta$. The sequence of changes is probably as follows: At minimum light there appear *H* emission lines, which increase in strength until about phase 0.75 and then gradually subside. The intensity gradient in the Balmer series is greater for the emission lines than for the absorption lines; for $H\alpha$ on plate Ce 5110 the intensity ratio of emission to absorption is 6.72 A/2.27 A = 2.96, while for $H\delta$ the ratio is 2.02 A/1.15 A = 1.76. For $H\beta$ emission on Ce 7091, the core corresponds to a velocity dispersion of 40 km/sec, while the wings are broader.

At maximum light, weak absorption wings appear. These are most prominent on Ce 7102 (see Fig. 6), where the ends reach to 9.5 A from the line center. The broad absorption wings have the same velocity as the shortward metallic lines and the *H* emission lines. By phase 0.1 the emission lines are entirely gone, leaving only broad absorption lines with well-defined wings. Hence it is likely that the broad, dish-shaped absorption wings present at light-maximum are the result of a superposition of a broad absorption line with prominent wings (as in an A-type star) upon a narrower emission line (as on Ce 7091).

As we progress toward minimum light, the *H* absorption lines become narrower and deeper, so that at minimum light they have become very narrow (half-width of 0.90 A). When the emission components appear at minimum light, the absorption lines remain as the sharp components which are displaced longward of the center of emission. Around maximum light, when the metallic lines are double, the sharp *H* absorption components correspond in velocity to the longward metallic lines, while the emission and broad absorption components correspond in velocity to the shortward metallic lines. At about phase 0.1 the sharp *H* absorption components disappear, along with the longward metallic lines.

8. LINE STRENGTHS AND *f*-VALUES

Equivalent widths were measured on microphotometer tracings of 17 of the coudé plates. The tracings, of magnification 100, covered the entire range from λ 3700 to

λ 4700 when the spectrum density permitted. Some tracings of the $H\alpha$ and $H\beta$ regions were also made. Intensity calibration-curves were constructed every 200 A from the stepped-slit calibration spectra. About four-fifths of the lines could be measured by representing them as single triangles or trapezoids on the density tracings; the remainder

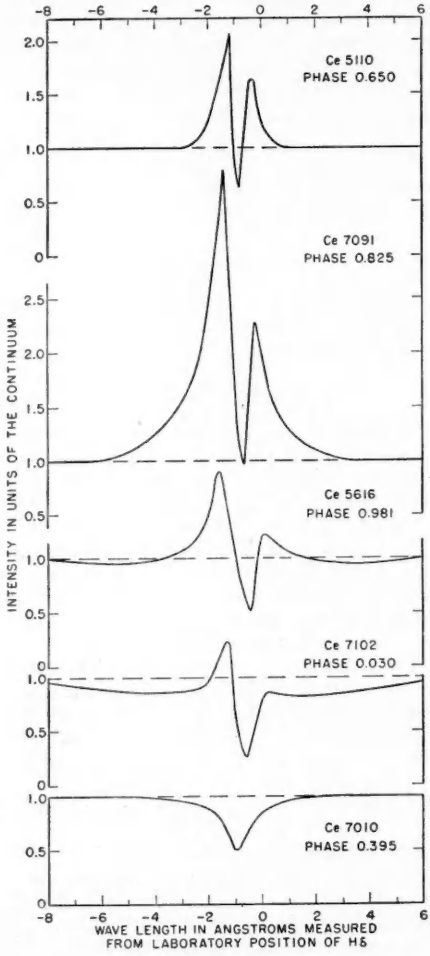

FIG. 6.—Sample $H\delta$ profiles

required stepwise numerical integrations. When double lines were present, they were sufficiently separated so that no serious problems of blending occurred. The equivalent widths are tabulated in Table 4.

Only *Fe* lines were used in constructing the principal curves of growth. Sources of *f*-values are as follows: (1) laboratory measures for *Fe* I by King and King[21] and by Car-

[21] *Ap. J.*, **87**, 24, 1938.

Values of -log W/λ

Plate Number, Corrected Phase, Components

Mult. No.	λ	log gfλ	5110 .650	7080 .709	7085 .766	7091 .825 1*	7091 .825 s*	5616 .981 1*	5616 .981 s*	5647 .006 1*	5647 .006 s*	7102 .030 1*	7102 .030 s*	6207 .041 1*	6207 .041 s*	5617 .044 1*	5617 .044 s*	6211 .094 1*	6211 .094 s*	5618 .099 1*	5618 .099 s*	5651 .123	5556 .198	5058 .358	7010 .401	7013 .458	7017 .516
Fe I																											
2	4347.24	- .53	4.79	5.19	5.48	5.21																5.23	5.17	4.77	4.95	5.07	5.05
	4375.93	+1.82	4.00	4.17	4.23	4.48	4.81		4.97				4.84		4.89				4.58		4.46	4.37	4.21	4.22	4.20	4.15	4.06
	4389.24	.34	4.32	4.51	5.17	5.42										5.31			5.53				4.61		4.36	4.75	4.45
	4427.31	1.87	4.00	4.02	4.13	4.59	5.07	5.21					4.67		4.67	5.61	5.04		4.42	5.07	4.49	4.34	4.21	4.17	4.07	4.11	4.06
	4489.74	.86	4.30		4.94	4.78										5.53						4.64	4.39	4.32	4.53	4.29	4.24
3	4199.97	.66	4.55	4.76	5.36	5.09									5.39	5.31			5.59			5.03	4.91	4.72	4.60	4.61	4.44
	4206.70	.99	4.23	4.39	4.54	4.86							5.11		5.31	4.92			4.94		4.69	4.49	4.34	4.24	4.48	4.31	4.21
	4216.19	1.51	4.08	4.11	4.35	4.79													4.60			4.32	4.21	4.05	3.92	4.12	4.14
3,41	4291.47	.74	4.20	4.16	4.61	5.03									5.41										4.26	4.34	
4	3824.44	2.97								4.00	4.27			4.47	3.94	4.04	4.22		3.99		4.10	3.95					
	3856.37	3.03								4.07	4.14				4.29	4.25				4.23	4.17	4.06					
	3859.91	3.61								3.99					4.08	4.32	4.52	4.71	4.05		4.24	4.11		3.81			
	3878.57	3.00								4.09					4.05	4.23	4.39		4.22	4.25		3.98					
	3886.28	3.26								4.00	4.47						4.57										
	3895.66	2.75								4.09	4.32				4.35	4.30	4.49		4.15		4.37	4.01		4.05			
	3899.71	2.87								4.05	4.40				4.27	4.19	4.35		4.06		4.42	4.18					
	3906.48	2.34													4.20				4.07		4.32						
	3920.26	2.73								4.20	4.44	4.84	4.41	4.74	4.21	4.33	4.60		4.27			4.19					3.71
	3922.91	2.84								4.28	4.52	4.75	4.37		4.23	4.40	4.56		4.14	4.36	4.22	4.27	4.10		3.78	3.81	
18	4100.74	2.10																							4.48		
	4139.93	1.44	4.55	4.54	4.97	4.85			5.24				5.62		5.34				5.16	5.71		4.69	4.52	4.55	4.57	4.50	4.45
19	4174.92	2.54	4.29	4.35		4.55									5.15		5.33		4.88		4.66	4.36	4.39		4.23	4.32	4.31
20	3820.43	4.55								3.99	4.37				4.01	4.08	4.47		4.18		4.17	3.94					
	3825.88	4.41								4.00	4.22				4.12	4.11	4.23				4.15	3.99					
	3840.44	4.01									4.59				4.39				4.13		4.22						
	3849.97	3.80								4.18	4.47				4.23	4.24	4.45				4.31	4.15					
	3865.53	3.67								4.28	4.38			4.82	4.37	4.46	4.50		4.13	4.61	4.24	4.17		4.00	3.91	3.82	
	3872.50	3.72																				4.13					
	3878.02	3.70													4.28				4.14		4.25	4.06		4.19		3.91	
	3887.05	3.50								4.36						4.57											
	3898.01	2.78						4.60	4.65						4.37			4.72	4.14		4.32	4.14		4.08	3.97	3.95	3.86
	3917.18	2.67											4.76						4.54		4.35	4.17	4.34	4.17	4.12	4.03	
21	3758.23	4.46																				4.03					
	3763.79	4.25								3.98	4.33																
	3767.19	4.15								4.11	4.26					4.21	4.46			4.03	4.21						
	3787.88	3.76								4.19	4.31				4.12	4.38	4.31		4.10	4.53	4.31	4.12					
	3795.00	3.84								4.08	4.38					4.39	4.38										
22	3786.68	2.62																	4.46			4.16					
	3790.09	3.06																	4.21	4.41	4.16						
	3812.96	3.56																	4.07			4.05					
	3814.53	2.43																				4.01					
	3850.82	3.12																	4.24			4.25		4.11	3.95	3.95	
38	4733.60	2.12																									4.53
39	4602.00	1.80			5.35																		5.39			4.75	4.72
	4602.94	3.01	4.41	4.66	4.69	5.07							4.90						4.96		5.02	4.40	4.44	4.43	4.26	4.35	4.38
	4632.91	2.35	4.87			5.15																5.06			4.54	4.60	4.46
41	4337.05	3.08						4.94											4.54			4.22		4.23	4.28	4.20	4.11
	4383.55	4.80	4.13	3.88	4.02	3.85	4.41	4.16	4.68				4.25		4.45	4.29	4.79		4.29		4.23	4.30	4.07		3.88	3.89	3.86
	4404.75	4.55	3.91	4.00	3.98	4.01	4.48	4.47	4.97			4.50	4.37	5.58	4.37	4.24	4.56	5.00	4.26	4.44	4.23	4.18	4.02	3.94	3.96	3.97	3.87
	4415.12	4.20	4.07	4.22	4.07	4.17	4.97	4.87	5.27			5.33	4.36		4.49		4.62		4.24		4.38	4.29	4.19	4.06	4.07	4.21	4.12
42	4147.67	2.83	4.18	4.36	4.70	4.59							5.13		5.17				4.63		4.84	4.38	4.34	4.32	4.29	4.30	4.24
	4202.03	4.06	4.13	4.03	4.06	4.14	4.58	4.46	4.78			5.31	4.37		4.48	4.72	4.43		4.17		4.08	4.19	3.97	3.95	3.92	4.09	3.92
	4250.79	4.03	4.22	4.07	4.14	4.19	4.90	4.73				5.32	4.36		4.53		4.64		4.26			4.29	4.19	4.10	4.12		4.08
	4271.76	4.46	3.94		4.04	4.01		4.37	4.84			4.70	4.26		4.65	4.52	4.44		4.20	4.31	4.03	4.29	4.10	3.98	3.93	3.92	3.89
	4325.76	4.68	4.07	3.95	4.04	3.86		4.38	4.86			4.73	4.32		4.35	4.47	4.47	5.40	4.33	4.32	4.19	4.21	4.14	4.00	3.99	3.92	3.90

Mult. No.	λ	log gfλ	5110 .650	7080 .709	7085 .766	7091 .825		5616 .981		5647 .006		7102 .030		6207 .041		5617 .044		6211 .094		5618 .099		5651 .123	5556 .198	5058 .358	7010 .401	7013 .458	7017 .516
						1*	s*	1*	s*	1*	s*	1*	s*	1*	s*	1*	s*	1*	s*	1*	s*						
Fe I																											
43	4005.25	4.18	4.10					4.44	4.55			4.55	4.27	4.79	4.34		4.28		4.14		4.33	4.09	4.02	3.85	3.86	3.76	3.94
	4043.81	4.87	3.92					4.25	4.58	4.20	4.38	4.33	4.03	4.88	4.11	4.26	4.36	4.90	4.06	4.28	4.21	3.98	3.88	3.74	3.70	3.64	3.80
	4063.60	4.64	3.95					4.31		4.22	4.47	4.81	4.20		4.25	4.32	4.54		4.02	4.73	4.34	4.12	4.01	3.92	3.79	3.75	3.83
	4071.74	4.68	4.00					4.31	4.63	4.19	4.48	4.99	4.30	4.97	4.36	4.28	4.63		4.15	4.60	4.37	4.18	4.10	4.01	3.92	3.90	3.87
	4132.06	4.24	4.12	3.98	4.16	4.20				4.40	4.71		4.53	4.93	4.51	4.47	4.59		4.18		4.32	4.24	4.14	4.01	4.05	4.06	3.98
	4143.87	4.21	4.19	3.99	4.18	4.22	4.68	4.59				4.99	4.59			4.50	4.41		4.18	5.23	4.26	4.24	4.08		4.16	4.00	3.92
45	3815.84	4.80								4.04	4.32			4.48	4.07			4.76	4.24			4.08		3.93			
	3827.82	4.58								4.19	4.39				4.15	4.22	4.23		4.22			4.03		3.87			
	3841.05	4.57								4.28					4.33				4.29	4.50							
	3902.95	4.32							4.65	4.08	4.29				4.30	4.28	4.39		4.05		4.22	4.13			3.89		
62	6430.85	2.65	4.54																								
68	4430.62	2.91										5.00										4.91	4.50		4.59	4.73	
	4442.34	3.96	4.29	4.72	4.62	5.12		5.47				4.69			4.68							4.72			4.54	4.43	4.51
	4447.72	3.95	4.37	4.56	4.64	4.72													4.93			4.74	4.45	4.30	4.32	4.46	4.47
	4494.57	4.13	4.58	4.63	4.53	5.03						4.89					4.97		4.82			4.46	4.32	4.36	4.33	4.35	4.43
	4528.62	4.59	4.12	4.32	4.26	4.57						4.49			4.63				4.30		4.54	4.21	4.15	4.23	4.21	4.23	4.16
71	4282.41	4.32	4.28		4.41	4.35	4.79	4.78	5.20			4.62			4.96				4.35		4.56	4.35		4.27	4.28	4.31	4.26
	4352.74	3.60	4.52	4.46	4.65	4.91													4.83			4.47		4.46	4.30	4.39	4.35
111	6421.35	2.39	4.49																								
116	4439.88	1.96	5.89	5.34		5.80						5.89										6.36			5.89	5.59	5.16
117,853	4047.31	1.76																									5.24
152	4187.04	4.67	4.29	4.39	4.44	4.46						4.46					4.51		4.35		4.54	4.35		4.17	4.42	4.25	4.21
	4187.80	5.25	4.32	4.33	4.38	4.33		4.72				4.44			4.53	4.93	4.70		4.29		4.48	4.35	4.20		4.20	4.16	4.26
	4191.44	4.60	4.44	4.29	4.50	4.73						4.61			4.54				4.37			4.36			4.26	4.39	4.37
	4210.35	4.32	4.42	4.48	4.66	4.80		5.25				4.79			4.81	5.33	4.61		4.51			4.64	4.31	4.33	4.34	4.38	4.40
	4222.22	4.25	4.29	4.60	4.69							4.91				5.21	4.87		4.57			4.68	4.36	4.33	4.36	4.45	4.42
	4233.61	4.56			4.49							5.56	4.37						4.55			4.43	4.25		4.24	4.28	
	4235.94	4.87	4.30	4.19	4.51	4.60		4.95	4.85								4.48		4.38		4.50	4.30	4.22	4.26	4.23	4.26	4.13
	4250.12	4.66	4.41	4.23	4.46	4.53	4.88		4.76				4.69			4.67	4.46		4.37			4.35	4.22	4.24	4.13	4.29	4.36
	4260.48	5.07	4.24	4.20	4.30	4.21	4.55	4.76	4.73			5.32	4.41		4.98	4.58			4.29	4.99	4.12	4.28	4.15	4.18	3.98	4.10	3.96
	4271.16	4.71	4.31		4.51	4.54		4.81	4.99			4.70	4.43		4.69		4.67		4.31		4.30	4.41	4.26	4.26	4.16	4.25	4.19
206	6475.02	2.06	5.47																								
218	4049.34	2.82	4.94					5.80												6.18			4.83	5.16	4.87	4.65	4.81
268	6546.24	2.36	5.17																								
342	6518.38	2.40	5.05																								
350	4476.02	4.60	4.31	4.54	5.06							4.64			4.83		5.01		4.68			4.69	4.41	4.35	4.44	4.46	4.47
352	4245.26	4.24	4.71	4.72	5.12	5.26			5.39			5.18			5.36	5.33	5.10		4.87		4.60	4.66	4.44	4.45	4.57	4.46	4.45
354	4107.50	4.25	4.55	4.58	5.18	4.79		5.07	5.24	5.12					4.68	4.93	4.98		4.51	5.42	4.71	4.54	4.34		4.27	4.42	4.30
	4156.80	4.37	4.36	4.47	4.38	4.66						4.84			4.91				4.63	5.11	4.67	4.41			4.31	4.31	4.27
	4175.64	4.31	4.53	4.62	5.00	4.98						4.84			4.91				4.59		4.74	4.57	4.33	4.34	4.35	4.48	4.46
355	4154.50	4.35		4.55	4.77	4.58						4.78										4.37				4.35	
	4184.89	4.26										4.94							4.62		4.65	4.57	4.46	4.40		4.58	4.43
	4203.99	4.71	4.52	4.80	4.74	5.36						4.80			4.95		4.99		4.70		4.49	4.58	4.29	4.19	4.45	4.34	4.36
	4213.65	3.80	4.85	5.15	5.33	5.29										5.52	4.81		5.02			4.80	4.69	4.64	4.82	4.94	4.61
357	4091.56	2.83			5.08																	5.39				4.88	5.02
	4114.45	3.72	4.77	4.85	5.50	5.21			5.30	5.42					4.90		4.99			5.34	4.80	4.99	4.58	4.46	4.63	4.60	4.45
	4132.90	4.10	4.55	4.58	5.05							4.81			5.08				4.65			4.64	4.32	4.32	4.51	4.35	4.44
359	4044.61	4.42						5.49	5.17	5.26		4.73			5.00	5.11	4.86		4.95	5.17	5.19	4.80	4.31	4.40	4.57	4.45	
	4062.45	4.13	4.39					4.73				4.85			4.89		4.81		4.72	5.37	5.07	4.68	4.62		4.44	4.54	4.31
	4079.85	3.70																				4.81					
409	4647.44	3.92																				4.97	4.60		4.93	4.67	4.57
	4661.97	2.57																				5.82				5.45	5.14
	4691.41	3.72																				4.77				4.68	
	4710.29	3.77																									4.80
415	4365.90	3.49				5.75																			5.55	5.63	

Mult. No.	λ	log gfλ	5110 .650	7080 .709	7085 .766	7091 .825		5616 .981		5647 .006		7102 .030		6207 .041		5617 .044		6211 .094		5618 .099		5651 .123	5556 .198	5058 .358	7010 .401	7013 .458	7017 .516
						1*	s*	1*	s*	1*	s*	1*	s*	1*	s*	1*	s*	1*	s*	1*	s*						
Fe I																											

| | | |

Mult. No.	λ	log gfλ	5110 .650	7080 .709	7085 .766	7091 .825		5616 .981		5647 .006		7102 .030		6207 .040		5617 .044		6211 .094		5618 .099		5651 .123	5556 .198	5058 .358	7010 .401	7013 .458	7017 .516
						1*	s*	1*	s*	1*	s*	1*	s*	1*	s*	1*	s*	1*	s*	1*	s*						
Fe I																											
828,848	4479.61	4.31																				5.46			5.34	4.85	
830	4388.41	4.63										5.22										5.07			5.04	4.68	
	4433.22	4.68			4.97	5.97		5.37				5.21										5.42		4.91	5.30	4.61	
	4485.68	4.16			5.24							5.04						5.40					5.16		5.59	5.12	
906	4246.09	4.67	5.82	5.10	5.82																						
973	4494.05	3.70																5.54				5.62		5.01	4.96	4.93	
976	4276.68	3.88	5.39			5.26																				4.97	
	4300.83	3.89																5.57				5.78		5.10	5.44	5.16	5.26
993	4264.74	3.58																									4.59
993,994	4265.26	3.93		5.58		5.80		5.78															5.74		5.92	6.04	
1042	4735.85	4.24																									
1068,821	4745.81	4.44																									5.00
																											4.85
Fe II																											
27	4128.73	3.84	4.90	4.47	4.99	5.18						4.84		4.87		5.01		4.96		4.82	4.74	4.44		4.53	4.54		
	4233.17	5.55			4.24	4.12		4.25	4.68			4.30		4.30		4.69		4.16		4.22	4.35	4.13		4.08	4.28		
	4303.17	5.02	4.38	4.50	4.43	4.43		4.55				4.37						4.42			4.50	4.22	4.15	4.26	4.24	4.23	
	4385.38	5.26	5.10	4.38	4.37	4.58			4.82			4.52		4.47				4.29	5.48	4.67	4.47	4.35	4.14	4.30	4.21	4.31	
	4416.82	4.94		4.60	4.41	4.47		4.54	5.13			4.55		4.59				4.39		4.44			4.34	4.40	4.32	4.25	
28	4178.85	5.03				4.56							4.85	4.34		4.89		4.27		4.31	4.29	4.23	4.15		4.22	4.19	
	4296.57	5.13	4.22		4.87	4.60		4.78	5.14			4.67			4.98	4.99		4.45	5.60	4.43	4.34	4.32	4.23	4.43	4.35	4.33	
	4369.40	3.94	4.88	4.72	4.90	4.85						5.05		5.07				4.82					4.49	4.64	4.63	4.50	
37	4472.92	4.60	4.54		5.00	5.34						4.74	5.62	4.82				4.92		4.72	4.68		4.29	4.48	4.58	4.45	
	4489.18	4.81	4.48	4.61	4.65	4.65		4.68	5.12			4.42		4.54	4.90	4.75		4.78		4.59	4.60		4.32	4.56	4.42	4.33	
	4491.40	4.84	4.68	4.66		5.03		4.85	5.45			4.61		4.48	4.92	4.73		4.49		4.55	4.39	4.43	4.29	4.55	4.33	4.45	
	4515.34	5.19	4.51	4.50	4.68	4.46	4.61	4.66	5.20			4.80	4.51	4.73	4.44			4.31		4.53	4.54	4.31	4.28	4.33	4.27	4.26	
	4520.22	5.11	4.31	4.53	4.66	4.52		4.64	5.11			4.73	4.55	4.81	4.41			4.36		4.71	4.43	4.36	4.30	4.28	4.30	4.31	
	4582.83	4.37	4.72	5.15	5.25								4.70		4.91			4.93			4.68	4.46	4.38	4.47	4.48	4.55	
	4666.75	4.29																			5.03			4.59	4.53		
38	4508.28	5.19	4.46	4.35	4.62	4.81		4.54	4.91			4.74	4.52	4.52	4.52	5.12	5.11	4.53		4.70	4.42	4.31	4.23	4.51	4.21	4.31	
	4522.63	5.81	4.15	4.21	4.26	4.27		4.65	4.89			4.59	4.38	4.73	4.43			4.29	4.84	4.46	4.26	4.13	4.10	4.17	4.17	4.15	
	4541.52	4.65	4.66	4.69	5.09	4.67									4.49			4.67	5.36	4.59	4.63	4.55	4.28	4.39	4.37	4.43	
	4576.33	4.53	4.49		5.27	4.81						4.74			4.69			4.74		4.59	4.73	4.45	4.26	4.48	4.49	4.47	
	4583.83	5.66	4.34	4.21	4.10	4.20		4.61	4.99			4.34	4.32	4.76	4.48			4.23	4.46	4.30	4.20		4.07	4.11	4.24	4.12	
	4620.51	4.17	4.84	4.82									4.99								4.93	4.51	4.40	4.83	4.64	4.66	
43	4731.44	4.39																								4.39	
Mg II																											
4	4481.2		4.30			4.28		4.41				4.10			5.04	4.37			4.50	4.38			4.11		4.28		
9	4427.99							5.72												5.36			5.02				
Ba II																											
1	4554.03		4.11	3.99	4.06	4.04	4.96	4.33	4.68		5.02	4.60		4.86				4.34	4.65	4.37	4.38	4.17	4.02	4.01	4.07	4.00	
Sr II																											
1	4077.71		3.99					4.25	4.48	4.08	4.39	4.16	4.24	4.58	4.24	4.12	4.27	4.39	4.03	4.28		4.07	3.97	3.71	3.75	3.73	3.76
	4215.52		4.01	3.96	3.96	3.95	4.63			4.16	4.54		4.40		4.46	4.12	4.41		4.31			4.22	4.11	3.99	3.84	3.89	3.90
Sc II																											
7	4246.83		4.32	4.08	4.19	4.23	5.04	4.32	5.09	4.29		4.77	4.72			4.57		4.54			4.63	4.33	4.21	4.26	4.32	4.28	
Ca I																											
2	4226.73		3.83	3.85	4.04	3.88				4.11	4.38	4.19		4.28				4.06			4.07	3.92	3.88	3.91	3.83	3.74	

ter;[22] (2) *Fe* I and *Fe* II values derived by Wright[23] from solar-line intensities and curves of growth based on the Kings' f-values; and (3) *Fe* I and *Fe* II values derived by Greenstein[24] from line strengths in the spectrum of τ Ursae Majoris. The relative weights assigned to these three sources in the order given are 3:1:1. The zero points of the three f-value scales are not the same. A comparison of f-values for lines common to two or more sources give the following zero-point corrections by least-squares solutions:

$$33\ Fe\ \text{I lines: } [\log \eta_0(\tau) + 0.91EP]_G - [\log gf\lambda]_K = +5.47 \pm 0.19\ ; \tag{4}$$

$$44\ Fe\ \text{I lines: } [\log \eta_0(\tau) + 0.91\ EP]_G - [\log X_f + 1.04\ EP]_W = +1.20 \pm 0.11\ ; \tag{5}$$

$$20\ Fe\ \text{II lines: } [\log \eta_0(\tau) + 0.91\ EP]_G - [\log X_f + 1.04\ EP]_W = +3.00 \pm 0.23\ . \tag{6}$$

The probable errors listed are those for a single line. All scales were corrected to Greenstein's zero point before averaging. Final averages are given in Table 4.

The first three columns of Table 4 give C. E. Moore's[25] multiplet numbers and wave lengths to two decimal places and the average log $gf\lambda$ values. The remainder of the table lists values of $-\log W/\lambda$, where W and λ are in the same units. The plate numbers and corrected phases are listed at the top of the columns. When double lines occur, the longward and shortward components are listed in separate columns.

IV. SPECTROPHOTOMETRIC RESULTS AND DISCUSSION

1. CURVES OF GROWTH; MILNE-EDDINGTON MODEL

The empirical curves of growth were first compared with curves calculated for integrated flux on the Milne-Eddington model by Wrubel.[26] The applicability of this model to W Vir will be discussed in Section IV, 10. Velocity dispersions, damping constants, excitation temperatures, and abundances were determined in the usual way. The results are given in Table 5, whose columns give (1) the plate number; (2) corrected phases; (3) the longward or shortward components; (4) the stage of ionization; (5) the damping constant parameter a; (6) $\log v/c$; (7) $\theta_{ex} = 5040/T_{ex}$ for *Fe* I, where T_{ex} is the excitation temperature; (8) the abundance ratio in W Vir compared to the sun; and (9) the number of lines used. Certain quantities in parentheses were assumed—principally the same damping constants, velocity dispersions, and excitation temperatures for *Fe* II as for *Fe* I.

The absolute f-values for *Fe* I were not used at this point because none are available for *Fe* II. In order to obtain the degree of ionization, we resorted to a comparison of line strengths with those in the solar spectrum. Curves of growth for the sun were constructed from Wright's[23] solar equivalent widths and the f-values listed in Table 4. The ratios of the resulting values of $\log \eta_0$ in W Vir to those in the solar spectrum are then given by

$$\log \frac{(\eta_0)_W}{(\eta_0)_\odot} = \log \frac{(N/\kappa)_W}{(N/\kappa)_\odot} + \log \frac{[vB(T_{ex})]_\odot}{[vB(T_{ex})]_W}\ , \tag{7}$$

where N is the number of ions per gram in a single stage of ionization and $B(T_{ex})$ is the corresponding partition function for the appropriate excitation temperature. With the measured velocity dispersions and partition functions calculated for the measured excitation temperatures, we obtained the values of $\log [(N/\kappa)_W/(N/\kappa)_\odot]$ for *Fe* I and *Fe* II that are listed in the eighth column of Table 5.

[22] *Phys. Rev.*, **76**, 962, 1949.

[23] *Pub. Dom. Ap. Obs. Victoria*, Vol. **8**, No. 1, 1948.

[24] *Ap. J.*, **107**, 151, 1948.

[25] *Contr. Princeton U. Obs.*, No. 20, 1945.

[26] *Ap. J.*, **109**, 66, 1949.

TABLE 5

RESULTS FROM CURVES OF GROWTH

Plate Ce	Phase	Comp.	Ion	log a	log v/c	θ_{ex}	log [(N/κ)/(N/κ)⊙]	No. of Lines
5110....	0.650	.....	*Fe* I	−1.8	−4.76	1.46	+0.39	90
		.....	*Fe* II	(−1.8)	−4.70	(1.46)	+1.48	17
7080....	.709	.....	*Fe* I	−1.8	−4.62	1.38	−0.14	63
		.....	*Fe* II	(−1.8)	(−4.62)	(1.38)	+0.84	16
7085....	.767	.....	*Fe* I	−1.8	−4.49	1.28	−0.99	75
		.....	*Fe* II	(−1.8)	(−4.49)	(1.28)	+0.24	17
7091....	.825	Long	*Fe* I	(−1.8)	−4.45	1.12	−1.45	66
		Long	*Fe* II	(−1.8)	(−4.45)	(1.12)	−0.25	18
		Short	*Fe* I	.....	.....	.....	.....	11
		Short	*Fe* II	.....	.....	.....	.....	1
5616....	.981	Long	*Fe* I	(−1.8)	−4.42	1.08	−2.48	33
		Long	*Fe* II	(−1.8)	(−4.42)	(1.08)	−0.38	11
		Short	*Fe* I	.....	.....	.....	.....	28
		Short	*Fe* II	(−1.8)	(−4.80)	(0.96)	−1.31 ±0.28	11
5647....	.005	Long	*Fe* I	(−1.8)	−4.49	1.11	−1.82	37
		Long	*Fe* II	.....	.....	.....	.....	0
		Short	*Fe* I	.....	.....	.....	.....	24
		Short	*Fe* II	.....	.....	.....	.....	0
7102....	.030	Long	*Fe* I	(−1.8)	−4.35	1.13	−2.97	16
		Long	*Fe* II	(−1.8)	−4.60	(1.13)	−0.42	9
		Short	*Fe* I	−1.8	−4.76	0.96	−1.78	70
		Short	*Fe* II	−1.8	−4.90	(0.96)	−0.01	18
6207....	.040	Long	*Fe* I	.....	.....	.....	.....	10
		Long	*Fe* II	(−1.8)	(−4.50)	(1.25)	−0.59 ±0.27	7
		Short	*Fe* I	(−1.8)	−4.66	1.09	−1.62	77
		Short	*Fe* II	(−1.8)	−4.80	(1.09)	+0.28	17
5617....	.042	Long	*Fe* I	(−1.8)	−4.40	1.10	−2.33	53
		Long	*Fe* II	(−1.8)	(−4.40)	(1.10)	−0.98	4
		Short	*Fe* I	(−1.8)	−4.80	0.94	−2.12	75
		Short	*Fe* II	(−1.8)	(−4.80)	(0.94)	−1.28	7
6211....	.089	Long	*Fe* I	.....	.....	.....	.....	6
		Long	*Fe* II	.....	.....	.....	.....	0
		Short	*Fe* I	(−1.8)	−4.64	1.05	−1.33	97
		Short	*Fe* II	(−1.8)	−4.58	(1.05)	+0.04	19
5618....	.097	Long	*Fe* I	(−2.2)	−4.40	1.36	−2.27	26
		Long	*Fe* II	(−2.2)	(−4.40)	(1.36)	−0.77	5
		Short	*Fe* I	−2.2	−4.78	1.07	−1.38	69
		Short	*Fe* II	(−2.2)	−4.86	(1.07)	+0.45	16
5651....	.123	.....	*Fe* I	−2.2	−4.80	1.25	−0.42	131
		.....	*Fe* II	−1.8	−4.80	(1.25)	+0.79	19
5556....	.196	.....	*Fe* I	−2.2	−4.74	1.22	−0.11	80
		.....	*Fe* II	−1.8	−4.86	(1.22)	+1.36	15
5058....	.358	.....	*Fe* I	−2.2	−4.68	1.18	−0.17	72
		.....	*Fe* II	−2.2	−4.86	(1.18)	+1.79	18
7010....	.395	.....	*Fe* I	−1.8	−4.78	1.29	−0.07	112
		.....	*Fe* II	−2.2	−4.84	(1.29)	+1.62	20
7013....	.452	.....	*Fe* I	−1.8	−4.70	1.28	−0.01	125
		.....	*Fe* II	−2.2	−4.80	(1.28)	+1.53	21
7017....	0.511	.....	*Fe* I	−2.2	−4.63	1.27	−0.07	112
		.....	*Fe* II	−1.8	−4.74	(1.27)	+1.26	19

2. VELOCITY DISPERSIONS

When the shortward components first appear, they indicate a Doppler width of about 4.8 km/sec (see Fig. 7), of which 4.6 km/sec are probably due to turbulent motion of some kind. The velocity dispersion increases during the expansion and subsequent contraction to a final maximum value of 12.3 km/sec.

3. DAMPING CONSTANTS

The damping constant parameters, log a, often could not be determined because of the lack of strong lines; they show no consistent variation with phase but are either

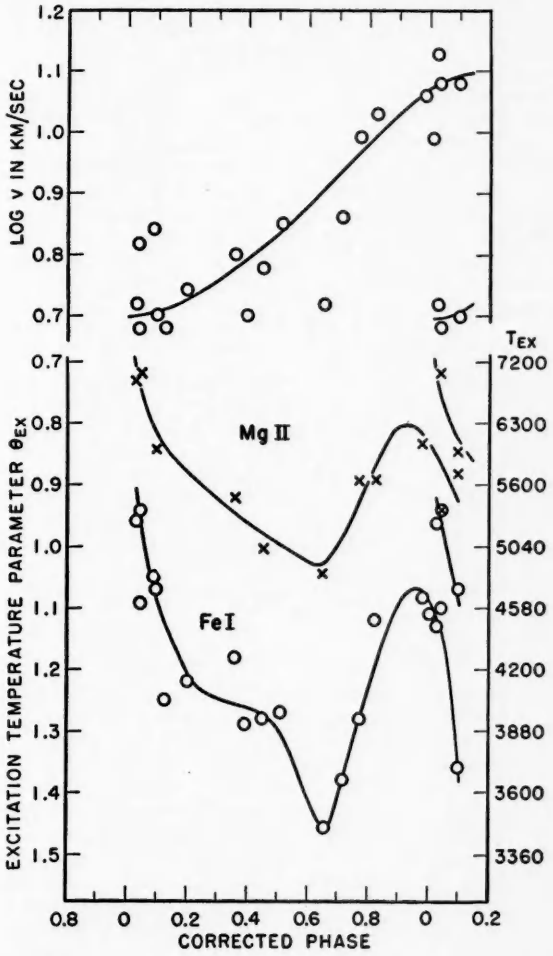

FIG. 7.—*Top:* Doppler velocity dispersions for *Fe* I; *center and bottom:* excitation temperatures for *Mg* II and *Fe* I. In all three cases, when both shortward and longward components on a plate yielded values, the shortward values were plotted on each side of the diagram.

-1.8 or -2.2. From the relation[24, 27]

$$\log \frac{\Gamma}{\gamma_{cl}} = \log a v - 2.62 , \tag{8}$$

we find that Γ/γ_{cl} varies from about 12 to 30 from the first to last appearance of the lines. These are large compared to values of 1–9 for F-type stars.[23, 24, 27]

4. EXCITATION TEMPERATURES FOR *Fe* I

The excitation temperatures for *Fe* I (see Fig. 7) are in phase with the light-variation. The plates taken between phases 0.02 and 0.10 and with temperature determinations for both components show a higher temperature for the shortward components by 700°–1000°. The evidence for a decline in temperature for the longward components after phase 0.00 is based mainly on plate Ce 5618 (phase 0.097), for which there is a very good temperature determination. Since we would expect the higher temperature layer to be lower in the atmosphere, the data suggest that possibly the upward- and downward-moving layers have not yet passed each other at phase 0.10.

The temperature-curve indicates that when a new layer first appears, its temperature is dropping rapidly from some very high value. This evidence is consistent with the model of predominantly inward motion in the atmosphere, i.e., when a new layer first rises, its temperature is so high that few strong lines of neutral and ionized atoms are produced. However, for this model the collision of layers occurs before phase 0.0, contradicting the evidence given in the last paragraph. The curve of excitation temperature does not solve the problem of the γ-velocity.

5. *Fe* ABUNDANCE AND THE DEGREE OF IONIZATION

Fe I and *Fe* II concentrations for W Vir relative to those in the sun are given in Table 5 and are plotted in Figure 8. These values are believed to be correct for phases of single lines (0.1–0.825), but at other times they probably include an error which cannot be removed at present. If absorption spectra from two layers are observed, we should consider the effect of the corresponding continuous opacities. Problems of this kind have been considered by Greenstein[28] and others. However, we cannot apply corrections to the line intensities until we know which layer is on the outside at each phase.

Dividing ordinates in Figure 8, we obtain the degree of ionization in W Vir compared to that in the sun. For an ionization temperature of 5300° and an electron pressure of 6.3 dynes/cm^2, we derive $\log N'/N = 1.07$ in the sun. The ionization of *Fe* in W Vir is in phase with the luminosities.

6. IONIZATION TEMPERATURES, PRESSURES, AND OPACITIES

The degree of ionization is essentially a function of the ionization temperature, T_{ion}, and the electron pressure, P_e. The continuous opacity also is a known function[7] of T_{ion} and P_e. We can obtain values of the continuous opacity from $\log [(N/\kappa)_W/(N/\kappa)_\odot]$, for *Fe* II and solve simultaneously for T_{ion} and P_e, if we make four assumptions. First, since the sources of opacity in W Vir and in the sun are probably the same, we will assume that the ratio of opacity in the blue to the mean opacity is the same in both stars. Second, we will have to assume a value for the hydrogen-to-metal ratio, A. There is some indication[29] that for high-velocity stars this ratio is larger than in the sun by a factor of 3. Unfortunately, we cannot obtain an explicit value for A from the data, so we shall calculate T_{ion} and P_e for both $A = A_\odot$ and $A = 3A_\odot$. Third, we shall assume that the ionization of *Fe* II is determined only by the local temperature and electron pressure and that there-

[27] J. L. Greenstein, *Ap. J.*, **113**, 205, 1951.

[28] *Ibid.*, **109**, 131, 1949.

[29] M. Schwarzschild, L. Spitzer, Jr., and R. Wildt, *Ap. J.*, **114**, 398, 1951.

fore the amount of *Fe* III is negligible. This would not be true with an excess of far UV radiation of 14-e.v. energy. One would not expect to find *Fe* III lines in the blue, even for a large *Fe* III abundance. As a fourth assumption we shall neglect the effects of the composite spectrum during the phases of double lines (0.825–0.1). With these four as-

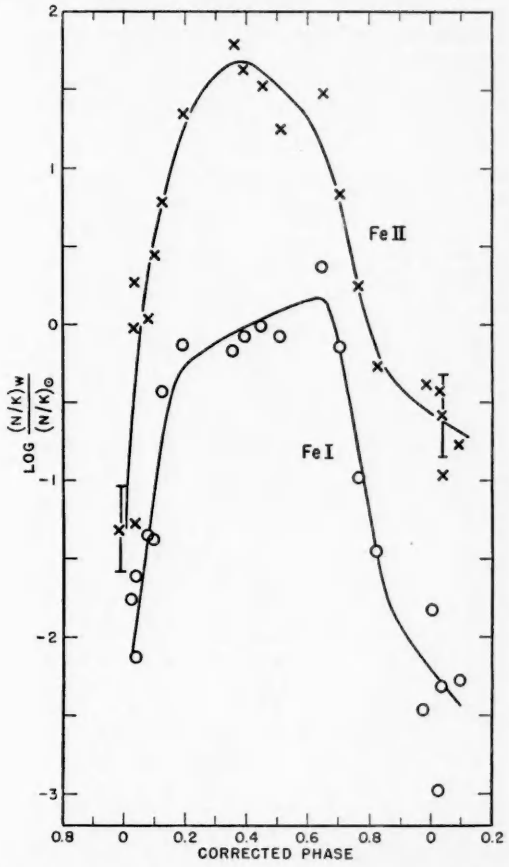

FIG. 8.—*Fe* I and *Fe* II abundances in W Vir as compared to those in the sun

sumptions, a graphical solution was made for θ_{ion} and P_e at each phase interval of 0.05. Table 6 gives the smoothed abundance-curve for *Fe* I, the degree of ionization of *Fe* I, and the resulting values of log $\bar{\kappa}$, θ_{ion}, and log P_e for $A = A_\odot$. For $A = 3\,A_\odot$ we find $\Delta \log \bar{\kappa} \approx -0.48$, $\Delta\theta \approx 0.06$, and $\Delta \log P_e \approx -0.6$. In the calculation we used $\log \bar{\kappa}_\odot = -0.53$. Figure 9 gives the curve of electron pressure and the curves for θ_{ion} for both values of A. Minimum electron pressure occurs at maximum expansion; the range in P_e is about a factor of 300.

Total gas pressures, P, can be evaluated from θ_{ion}, P_e, and A. Using B. Strömgren's[30]

[30] *Pub. Københavns Obs.*, No. 138, 1944.

tables of model atmospheres, we obtain for $A = A_\odot = 10^{3.8}$ the values given in Table 6. For $A = 3A_\odot \cong 10^{4.2}$, $\Delta \log P \approx -0.2$. Minimum pressure occurs at maximum luminosity, and maximum pressure occurs shortly after minimum luminosity.

7. EXCITATION TEMPERATURES FOR *Mg* II

The large difference between the ionization temperatures derived in the last section and excitation temperatures for *Fe* I lead us to wonder which represent the local temperatures in the gas layers and whether the four assumptions made in the last section are valid. Excitation temperatures for neutral atoms are notoriously low in the sun. It

TABLE 6

IONIZATION TEMPERATURES, PRESSURES, AND OPACITIES

PHASE	LOG $[(N/\kappa)/(N/\kappa)_\odot]$	LOG (N'/N)	$A = A_\odot$			
			log $\bar{\kappa}$	θ_{ion}	log P_e	log P
0.05	−1.74	2.35	−0.03	0.73	+1.51	3.77
0.10	−0.89	2.43	−0.94	.83	+0.55	3.31
0.15	−0.43	2.55	−1.50	.89	−0.13	2.81
0.20	−0.29	2.70	−1.79	.91	−0.45	2.47
0.25	−0.21	2.85	−2.01	.92	−0.71	2.11
0.30	−0.14	2.91	−2.14	.93	−0.85	1.97
0.35	−0.08	2.86	−2.15	.93	−0.83	2.11
0.40	0.00	2.74	−2.11	.94	−0.78	2.24
0.45	+0.07	2.61	−2.05	.95	−0.74	2.42
0.50	+0.13	2.47	−1.96	.95	−0.61	2.64
0.55	+0.19	2.34	−1.89	.96	−0.56	2.83
0.60	+0.23	2.20	−1.78	.965	−0.47	3.02
0.65	+0.20	2.07	−1.61	.96	−0.29	3.25
0.70	−0.09	2.07	−1.33	.92	+0.08	3.51
0.75	−0.80	2.17	−0.73	.825	+0.82	3.75
0.80	−1.30	2.28	−0.36	.775	+1.19	3.79
0.85	−1.60	2.40	−0.19	.75	+1.30	3.64
0.90	−1.83	2.52	−0.09	.72	+1.41	3.42
0.95	−2.03	2.63	0.00	.71	+1.43	3.32
1.00	−2.19	2.73	+0.06	.695	+1.46	3.17
1.05	−2.32	2.79	+0.14	.69	+1.47	3.12
1.10	−2.43	2.86	+0.21	0.665	+1.60	3.01

would be desirable to obtain excitation temperatures for an ionized atom. Excitation temperatures were computed for two lines (λ 4481, λ 4428) of *Mg* II that originate from nonmetastable levels of high potential (9 e.v.). To know the number of atoms in the ground state, an assumption had to be made about the abundance of *Mg* in W Vir. A comparison was made with α Persei F5 I*b*, for which Greenstein[24] has published equivalent widths. It was assumed that the *Mg*/*Fe* abundance ratio is the same in the two stars. For both stars it is calculated that almost all *Fe* and *Mg* are in the form *Fe* II and *Mg* II. From the apparent *Fe* II abundances in the two stars and from measures of velocity dispersions and excitation temperatures for *Fe* I, we can estimate the amount of *Mg* II in the ground state in W Vir. The success of the method depends on the fact that the excitation potentials of the states of *Mg* II are much larger than those of the excited states of *Fe* II (2–3 e.v.), so that only first-order corrections from excited to ground states of *Fe* II are necessary. For α Per we used θ_{ex} (*Mg* II) = θ_{ion} = 0.82. The resulting temperatures are given in Table 7 and are plotted in Figure 7.

The *Mg* II temperatures, like those of *Fe* I, show that during phases of double lines

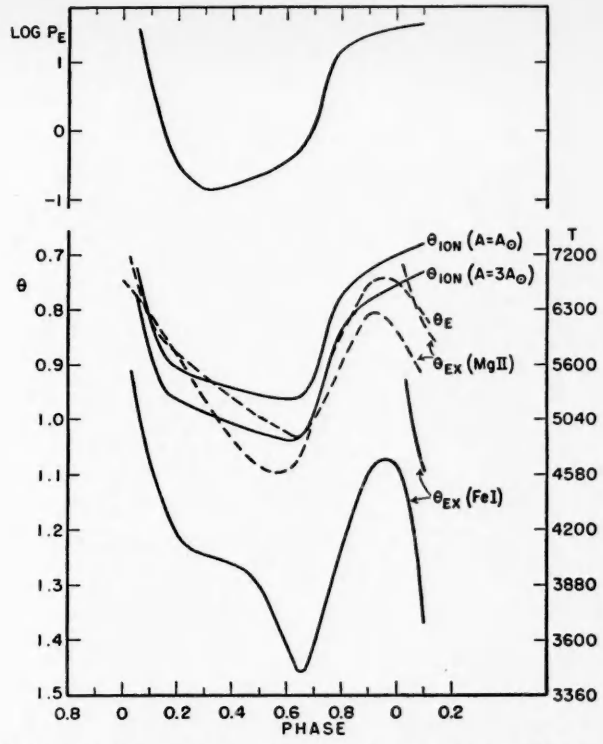

FIG. 9.—*Top:* electron pressures; *bottom:* ionization temperatures for two values of the hydrogen-to-metal ratio, effective temperatures, and excitation temperatures for *Mg* II and *Fe* I.

TABLE 7

EXCITATION TEMPERATURES FOR *Mg* II

PLATE CE	COMPONENT	PHASE	θ_{ex}		
			λ 4481 (8.82 e.v.)	λ 4428 (9.95 e.v.)	Mean
5058	.....	0.358	0.94	0.90	0.92
5110	.....	.650	1.04	.....	1.04
5616	Longward	.981	0.91	.79	0.85
5617	Longward	.042	0.94	.....	0.94
	Shortward	.042	.....	.72	0.72
5618	Longward	.097	0.88	.....	0.88
	Shortward	.097	0.87	.80	0.84
7013	.....	.452	1.00	.....	1.00
7085	.....	.767	0.99	0.79	0.89
7091	Longward	.825	0.89	.....	0.89
7102	Shortward	0.030	0.73	.....	0.73

the shortward components have temperatures that are about 700° higher than those for the longward components. However, the *Mg* II temperatures agree within the probable errors with the *Fe* ionization temperatures (see Fig. 9). This gives us some confidence in the latter but leaves the *Fe* I excitation temperatures unexplainably low.

8. COMPARISON WITH OTHER SUPERGIANTS

We may now compare the physical parameters for W Vir with those for normal, nonvariable supergiants. We find that log $\bar{\kappa}$, θ_{ion}, and log P_e take on their mean values (over phases 0.05–1.10) at phases 0.11 and 0.73. A comparison of W Vir at these phases with α Per[24] is made in Table 8. We see that the two stars are rather similar except that W Vir

TABLE 8

COMPARISON OF W VIRGINIS WITH α PERSEI AND α CARINAE

	α Per ($A\odot$)	W Vir (Mean of Phases 0.11 and 0.73)		α Car ($1.3A\odot$)	W Vir (Long. Comp. at Phase 1.00)	
		$A\odot$	$3A\odot$		$A\odot$	$3A\odot$
Spectrum	F5 I*b*	F7 I*b*		F0 I*b*	F2 I*b*	
θ_{ion}	0.82	0.86	0.92	0.69	0.695	0.755
log P_e	0.1	0.45	−0.30	1.0	1.5	0.9
log $\bar{\kappa}$	−1.4	−1.1	−1.6	−0.1	0.1	−0.4
log P	2.3	3.0	2.8	2.2	3.2	3.0
log v	5.80	5.81		5.54	6.05	
Γ/γ_{cl}	3.0	15		10	17	
θ_{ex}(*Fe* I)	0.98	1.24		1.03	1.10	

has a slightly lower effective temperature, a much larger damping constant, a larger total pressure, and a much lower excitation temperature for *Fe* I (by 1100°).

A comparison of W Vir at maximum light (longward components) with α Carinae[31] is also made in Table 8. For α Car, log $\bar{\kappa}$ was obtained from Chandrasekhar and Münch's[7] tables, and log P was obtained from Strömgren's[30] tables. We see that at maximum light W Vir is like a normal early F-type supergiant except for a larger Doppler width (although this is not so marked for the shortward components) and a larger pressure. This comparison indicates that perhaps our complete neglect of the effects of a composite spectrum near maximum light is not too serious.

The colors of W Vir indicate a spectral-type range of about F3–G2. Sanford classified the spectra on the Mount Wilson scale as F2–G6. However, the G band is either absent or very weak. The ionization temperatures, interpreted as effective temperatures, give ranges of F1–F9 ($A = A_\odot$) and F2–G1 ($A = 3A_\odot$). By using both Eggen's and Whitford and Code's color measures, we entirely eliminated any large discrepancy, previously reported,[32] between spectral types derived from the colors and from the absorption spectra. A classical cepheid of the same period would have a spectral-type range[18] of about F6–G8.

9. LOCATION OF THE REGION OF EMISSION

We shall investigate the location of the region of *H* emission by two methods. First, we shall consider the central intensities of the sharp *H* absorption lines. For example, *Hβ* on

[31] J. L. Greenstein, *Ap. J.*, **95**, 161, 1942.

[32] A. Abt, *A.J.*, **57**, 158, 1952.

plate Ce 7091 (phase 0.825) has a well-defined, broad emission component whose complete profile can be reconstructed. The sharp absorption component has a central intensity of 1.15 times that of the continuum outside the emission line. The reconstructed emission line has an intensity of 4.90 times the continuum at the position of the absorption line. If the emission line were formed above the absorption region, the absorption line would be filled in to a greater extent. If the emission line were formed below the absorption region, the actual central intensity of the absorption line is $1.15/4.90 = 0.23$, which is a reasonable value. Therefore, we conclude that—at least until phase 0.825—the *H* emission and shortward metallic absorption lines are formed below the region where the *H* absorption and longward metallic absorption lines are formed.

Second, we may study the strength of metallic absorption lines that fall within the wave-length range of the *H* emission lines. There are only a few cases in which both these lines are strong enough. For example, λ 4100.74, *Fe* I, lies within 1 A of *Hδ* on plate Ce 7080 (phase 0.709). The *Fe* line, with known *f*-value by King and King,[21] occurs at a point where the emission line would have a strength of 2.1 times that of the continuum. If the strength of the *Fe* line is measured in terms of the continuum outside the emission line, its equivalent width places it above the curve of growth by a factor of 1.9. If it is measured with the underlying emission line representing the continuum, the line falls on the curve of growth for *Fe* I. Hence we again conclude that the emission region lies below the absorption region. Only single lines are observed at phase 0.709.

10. THICKNESS OF THE GAS LAYERS

So far the picture presented is that of layers of gas which rise 35×10^6 km and fall. In this section we shall investigate the geometrical and optical thicknesses of these layers.

At minimum light we see two layers whose centers are about 30×10^6 km apart. Since the upper layer is partially transparent, its optical thickness is of the order of 1. From its known opacity of 10^{-2} cm^2/gm, as given in Table 6, and density from the perfect gas law of 3×10^{-9} gm/cm^3, we obtain a geometrical thickness, $\tau/\rho\bar{\kappa}$, of 0.3×10^6 km. We conclude that the layer thicknesses are of the order of 10^{-2} of their maximum separation.

Second, if the gas layers increased greatly in thickness while moving outward, the absorption lines would be broadened. Sample line-width measures for weak lines, corrected for instrumental broadening, are consistent with the velocity dispersions from curves of growth. If these entire velocity dispersions are interpreted as a dispersion in surface velocities, we find that during the expansion a thin layer would spread out to a thickness of 4.5×10^6 km, compared to a separation of layers of 35×10^6 km.

The optical thicknesses of these layers are given by the opacity per atom, $m_H\kappa$, times the total number of atoms, N/κ, in the layer. The opacity is given in Table 6, and the total abundance can be computed if we use R. B. King's[33] absolute *f*-value calibration for *Fe* I. It turns out that the optical thickness of the gas layer is about 0.06. It appears that these layers are geometrically thin and transparent and are, at times, very far above the photosphere. It seems advisable, therefore, to proceed with a Schuster-Schwarzschild model.

11. CURVES OF GROWTH ON A SCHUSTER-SCHWARZSCHILD MODEL AND ABUNDANCES

Curves of growth for W Vir were compared with theoretical ones by Menzel.[34] We used the equivalent widths in Table 4; the Doppler widths, damping constants, and *Fe* I excitation temperatures in Table 5; and the *Mg* II temperatures as ionization temperatures. Electron pressures were calculated from the *Mg* II temperatures and the degree of ionization in Table 6. For absolute *f*-values we found it desirable to increase those by

[33] *Ap. J.*, **95**, 78, 1942.

[34] *Ap. J.*, **84**, 462, 1936.

King[33] by a factor of 3.8 for the reason given below. The resulting *Fe* abundances in the gas layers are given in Table 9.

As a control, we obtained *Fe* abundances in α Per from Greenstein's[24, 27] equivalent widths, Doppler width, damping constant, and temperatures with the same *f*-values as for W Vir. We see from Table 9 that the *Fe* abundance in α Per is $10^{19.99}$, compared to

TABLE 9

NUMBER OF ATOMS ABOVE THE PHOTOSPHERE, LOG *NH*, IN W VIR

Phase	*Fe*	*Ba*	*Sr*	*Ca*	*Sc*
0.05	18.12	13.03	13.74	17.05	13.27
0.10	19.02	13.24	14.11	17.87	13.56
0.15	19.63	13.54	14.51	18.50	13.90
0.20	19.96	13.95	14.87	18.95	14.32
0.25	20.20	14.42	15.11	19.22	14.79
0.30	20.32	14.89	15.28	19.37	15.04
0.35	20.32	15.18	15.36	19.40	15.10
0.40	20.25	15.14	15.35	19.32	15.02
0.45	20.17	15.01	15.31	19.24	14.89
0.50	20.07	14.85	15.22	19.13	14.77
0.55	19.99	14.67	15.09	19.04	14.63
0.60	19.89	14.49	14.92	18.89	14.52
0.65	19.76	14.31	14.71	18.66	14.40
0.70	19.53	14.10	14.48	18.38	14.25
0.75	18.93	13.85	14.25	18.17	14.11
0.80	18.57	13.62	14.03	17.92	13.96
0.85	18.39	13.45	13.84	17.66	13.80
0.90	18.28	13.30	13.63	17.44	13.66
0.95	18.19	13.15	13.42	17.27	13.53
1.00	18.11	12.94	13.17	17.13	13.39
1.05	18.00	12.70	12.91	.....	13.26
1.10	17.89	12.47	12.64	.....	13.19
α Per	19.99	14.65	15.82	18.91	15.39

TABLE 10

ABUNDANCE RATIOS

	Meteorites (Urey)	α Per (Greenstein)	W Vir	Diff. α−*W*	Second I.P.
$\log N_{Fe}/N_{Ba}$	5.31	5.34	5.33±0.24	+0.01	9.96
$\log N_{Fe}/N_{Sr}$	4.22	4.17	4.89± .14	− .72	10.98
$\log N_{Fe}/N_{Ca}$	1.08	1.08	0.95± .09	+ .13	11.82
$\log N_{Fe}/N_{Sc}$	4.60	4.60 (assumed)	5.10±0.24	−0.50	12.8

$10^{19.14}$ for the two phases (0.11 and 0.73) when W Vir takes on mean physical characteristics.

Abundances for *Ba*, *Sr*, *Ca*, and *Sc* were obtained by using the known absolute *f*-values for λλ 4554 *Ba* II,[35] 4077 *Sr* II,[35] 4215 *Sr* II,[35] and 4226 *Ca* I,[36] and by assuming the same *Fe*/*Sc* abundance ratio ($10^{4.60}$) in α Per as in meteorites, as determined by Urey. This assumption yielded f_{abs} (4246 *Sc* II) = 0.56. The abundances in W Vir as a function of

[35] A. Unsöld, *Physik der Sternatmosphären* (Berlin: J. Springer, 1938), p. 234.

[36] P. Wellmann, *Veröff. d. Sternw. Berlin-Babelsberg*, Vol. 12, Part IV, 1939.

phase and in α Per are given in Table 9. The various abundance-curves for W Vir are similar in shape to that for *Fe* within their probable errors.

Abundance ratios, *Fe*/metal, for α Per and W Vir (now independent of phase) are given in Table 10. For comparison we give meteoric values by Urey. The good agreement in general between α Per and meteors was obtained by using 3.8 times King's absolute *f*-values. These corrected absolute *f*-values probably also give a better solar *Fe* abundance.[37] However, differences between W Vir and α Per are independent of any *f*-values used. It appears that, relative to *Fe*, *Ba* and *Ca* have normal abundances but *Sr* and *Sc* are underabundant by factors of 5 and 3, respectively. There is no relation between these abundance peculiarities and the second ionization potentials. This speaks against the existence of excessive UV radiation in the neighborhood of 10–13 e.v.

12. FURTHER EVIDENCE ON LAYER THICKNESSES

From the known *Fe* abundance, the ionization conditions, and an assumed $A = 10^{3.8}$, we can compute the number of electrons, N_eH, in the gas layers. The electrons come mostly from *H*. The electron density, N_e, is also equal to P_e/kT. Therefore, we can solve for the layer thicknesses, *H*, if we assume that the layers are homogeneous and contain no holes. These thicknesses vary from $10^{1.4}$ km at phase 0.05 to $10^{5.2}$ km at maximum expansion—once again indicating thin layers.

The optical thickness of the layers, computed with *Mg* II excitation temperatures, varies from 0.02 to 0.09 when only one layer is seen (phases 0.10–0.65) and varies from 0.001 to 0.02 when two layers are seen, one through another. It might be supposed that two layers are seen at certain phases and only one at others, because in the latter case the upper layer is not transparent. The computed optical thicknesses show the right kind of variation but are somewhat small to produce the desired effect. These optical thicknesses are directly proportional to the value of *A* adopted and inversely proportional to the absolute *f*-values for *Fe*.

V. PULSATION MODELS

1. SHOCK-WAVE MODEL

In a shock-wave model we would suppose that at an unknown depth below the photosphere a disturbance occurs which sends out a shock wave through an extended atmosphere. The layers of gas that we observe spectroscopically would be the compressed regions following the shock front. We can specify the temperature, total pressure, density, and velocity of flow of material in this compressed region. The Rankine-Hugoniot shock-wave equations should then give the physical conditions in the extended atmosphere ahead of the shock front.

Application of these equations[38] immediately revealed several serious difficulties with this model. First, a compression of a factor of only 4 or less could be expected. It turns out, then, that there would be 10^3 as much material in the extended atmosphere between compressed regions as in the compressed regions following the shock fronts. This material could hardly escape detection spectroscopically. Second, the large velocities of flow of material (of the order of 40 km/sec) are incompatible with the low temperatures (of the order of 6000°). One would expect temperatures of the order of 10^5 degrees if velocity changes of about 40 km/sec are involved.

2. SHELL MODEL

This is the model proposed in an earlier section (III, 5) of this paper. A photosphere expands periodically from about 18 to 40×10^6 km. At each expansion it throws off a shell which continues to rise for 35×10^6 km through a region relatively void of material

[37] D. H. Menzel and A. Unsöld, *Trans. I.A.U.*, **7**, 493, 1950.

[38] I am indebted to Dr. L. G. Henyey for a helpful discussion on this subject.

(compared to the amount of material in the shell). After expending its kinetic energy, the shell falls, meeting the next shell to rise. This model would explain the failure of Baade's method, although it must be realized that the shell's continuous opacity, which is nongray, somewhat alters the color of the photosphere, and therefore its computed radius changes. The temperatures of the detached shells could be maintained, since their outward velocities are three or four times their internal kinetic velocities.

The principal difficulty with this model lies in the impossibility of two homogeneous shells of these densities (10^{-5} to 10^{-10} gm/cm^3) passing through each other. In these shells the mean free path of an atom is of the order of a few centimeters. Two colliding shells would stop each other and would heat up to a temperature of the order of 10^5 degrees, since they meet with a difference in surface velocities of about 75 km/sec. The only solution is to suppose that the shells are not uniform but consist of many cloudlike condensations. The number and sizes of the condensations would have to be such as to make collisions improbable, since the spectral regions between double absorption lines are not observed to be filled in. Most of the *H* is not ionized, so we probably cannot suppose that the motions of the condensations are ordered by magnetic fields.

I wish to thank Dr. Jesse L. Greenstein for suggesting this problem, for starting me on the observations, and for valuable discussions during the whole of the project. I am grateful to Dr. Roscoe F. Sanford for loaning his W Vir spectra and providing his radial velocities in advance of publication. I am indebted to Drs. A. E. Whitford and A. D. Code for obtaining colors and magnitudes of W Vir for me and to Dr. O. J. Eggen for supplying his color and magnitude measures in advance of publication.

PHOTOMETRIC INVESTIGATION OF THE ECLIPSING BINARY UX URSAE MAJORIS*

H. L. JOHNSON,† BARBARA PERKINS, AND W. A. HILTNER
Yerkes and McDonald Observatories
Received November 27, 1953

ABSTRACT

Photoelectric observations of UX Ursae Majoris at three effective wave lengths on eleven nights are published and discussed. A "typical" light-curve appears to be one of a bright shoulder before principal minimum, a minimum with a depth of about 1.1 mag., a standstill on the ascending branch of the minimum, and after minimum a slow decrease in brightness to phase 0.7, when the light increases to the bright shoulder before minimum. No secondary minimum was detected. The light-curve does not repeat, however, with differences as great as 0.5 mag. in the ultraviolet. Fluctuations of a smaller scale of 0.2 mag. in the ultraviolet and half as great in the blue and yellow are often observed. These intrinsic variations in magnitude often have a period near 20 minutes. Fluctuations of much shorter duration are present but are not resolved. Data regarding changes in depth of minima are given. The presence of a mass of gas in and about the system is favored as a working hypothesis for the peculiarities of the "typical" light-curve and the intrinsic fluctuations. A geometrical analysis of the light-curve was not attempted.

INTRODUCTION

The eclipsing binary UX Ursae Majoris has a number of remarkable characteristics. First, it has the shortest known period (4^h43^m) among the eclipsing binary stars. Second, the duration of minimum is short, which, in addition to the short period, demands that the associated stars must be subdwarfs. Third, the integrated spectrum has been classified[1] as B3.

OBSERVATIONS

With the goal of obtaining additional data on this unique system, it was placed on the photometric observing program of the McDonald Observatory in 1948. Only a few preliminary observations were made in that year. One minimum was observed during the following season. No additional observations were made until May, 1951, when a long series at three effective wave lengths was obtained. The star was again observed the following season, during which three long runs were obtained. The observations were concluded with seven shorter runs in 1953.

Several photoelectric photometers were employed, all of which were attached to the 82-inch reflector of the McDonald Observatory. However, the instruments differed primarily in mechanical details, for all employed the same type of receiver (RCA 1P21 with refrigeration by solid CO_2 and without refrigeration) and filters. Three effective wave lengths were defined by three filter combinations—a Corning 3384 (yellow), a Corning 5030 plus Schott GG-13 (blue), and a Corning 9863 (ultraviolet). The output from one of several types of amplifiers was received by a Brown recording potentiometer driven at the rate of 30 inches per hour.

The observing procedure varied from night to night, and, since the weight of an individual published observation varied with the observing procedure, a detailed account is recorded below.

1951, May 19.—Three deflections of 25 seconds duration each for one color were obtained in the following order: Star plus sky, sky alone, star plus sky. These two deflections of the star, when compared with a comparison star, represent one observation in

* *Contributions from the McDonald Observatory, University of Texas*, No. 231.

† Now at the Lowell Observatory.

[1] Kuiper, *Pub. A.A.S.*, **10**, 206, 1941.

Tables 1–3. The other colors were observed in order and in like manner. A comparison star was observed at intervals of 30–60 minutes.

1952, March 5.—Deflections were obtained of 25 seconds duration each of the star plus sky for the three different filters and repeated for about twelve times. The sky for the three colors and the standard source were then observed. The above was then repeated. Extinction was determined by a second photometer on the 13-inch reflector. One deflection of 25 seconds represents one recorded observation in Tables 1–3.

1952, March 6.—The same procedure as for March 5, 1952, was followed, except that a comparison star was observed every 30–60 minutes with the same instrument.

1952, May 29.—Same as for March 6, 1952.

1953, May 22.—Same as for May 19, 1951.

1953, May 29.—Same as for May 19, 1951.

1953, June 3.—Same as for May 19, 1951.

1953, June 5.—Same as for May 19, 1951, except that the principal minimum was observed continuously in the blue only. At that time one 20-second exposure is recorded as one observation in Table 1.

1953, June 6.—Same as for June 5, 1953.

1953, June 7.—Same as for May 19, 1951.

1953, June 14.—Same as for March 6, 1952.

All observations were reduced to outside our atmosphere, but no attempt was made to correct the observations to identical magnitude systems. Only nights of photometric quality were used.

Tables 1–3 contain the 2775 observations for the blue, yellow, and ultraviolet, respectively. The difference between UX Ursae Majoris and a comparison star is recorded in the sense UX UMa − comparison, except for March 6, 1952, where UX UMa was compared with the standard source after the proper correction for extinction had been introduced. These observations, except for June 3, 1953, when only a few were obtained, are plotted in Figures 1–7. The yellow observations appear at the top of the figures, the blue in the center, and the ultraviolet at the bottom.

DISCUSSION OF THE OBSERVATIONS

The phases recorded in the second column of Tables 1–3 were computed from new light-elements as follows:

$$\text{Principal minimum} = \text{JD}2427341.2221 + 0.196671379E\,.$$

This formula, which differs by only one in the last place from that given by Krat,[2] was determined from the times of minima recorded in Table 4. Eleven minima were observed by us. For all except the 1951 observations, the times of minima are given separately for the three effective wave lengths. In addition, seven minima were kindly supplied by Dr. Linnell[3] and are included in the table. The 1953 observations were given great weight in determining the above elements. This is warranted by the small scatter of the individual observations. This small scatter may have resulted from the application of frequent time checks to the strip chart of the recorder. The observed *minus* the computed times of minima are plotted in Figure 8. The yellow and blue observations were combined to form one point on the diagram, and the ultraviolet observations are not considered. Although the evidence from Figure 8 is not at all overwhelming, there is some indication that the period of the system is increasing. The evidence rests heavily, however, upon the 1949 observations, and these observations show significantly more scatter than, for example, either the 1952 or the 1953 data. (One minimum for 1949 falls outside the chart and hence is neither plotted nor given any weight in the discussion.) Careful observations within five years should give definite evidence for a change in period of the order suggested by the present data, if such exists.

[2] *Poulkovo Circ.*, **30**, 11, 1939.

[3] Private communication.

TABLE 1

Photometric Observations of UX Ursae Majoris (Blue)

Julian Day 2430000+	Phase	Δ Mag	Julian Day 2430000+	Phase	Δ Mag	Julian Day 2430000+	Phase	Δ Mag
3785.6476	.4801	+2.402	4076.7013	.3787	+0.379	4076.8257	.0112	+1.139
3785.6504	.4943	+2.375	4076.7047	.3960	+0.367	4076.8267	.0163	+1.050
3785.6532	.5086	+2.424	4076.7092	.4189	+0.346	4076.8278	.0219	+0.914
3785.6605	.5457	+2.410	4076.7135	.4407	+0.362	4076.8287	.0265	+0.749
3785.6635	.5609	+2.447	4076.7181	.4641	+0.374	4076.8297	.0316	+0.629
3785.6665	.5762	+2.402	4076.7211	.4794	+0.370	4076.8306	.0362	+0.542
3785.6751	.6199	+2.420	4076.7242	.4951	+0.392	4076.8315	.0407	+0.528
3785.6781	.6352	+2.437	4076.7273	.5109	+0.373	4076.8326	.0463	+0.479
3785.6811	.6504	+2.453	4076.7301	.5251	+0.373	4076.8335	.0509	+0.460
3785.6880	.6855	+2.504	4076.7330	.5399	+0.373	4076.8342	.0544	+0.438
3785.6911	.7013	+2.416	4076.7360	.5551	+0.358	4076.8353	.0600	+0.440
3785.6942	.7170	+2.331	4076.7391	.5709	+0.342	4076.8362	.0646	+0.440
3785.7042	.7679	+2.390	4076.7426	.5887	+0.375	4076.8369	.0682	+0.432
3785.7071	.7826	+2.359	4076.7457	.6045	+0.422	4076.8386	.0768	+0.461
3785.7100	.7974	+2.356	4076.7489	.6207	+0.387	4076.8447	.1078	+0.344
3785.7172	.8340	+2.343	4076.7519	.6360	+0.380	4076.8490	.1297	+0.353
3785.7213	.8548	+2.263	4076.7552	.6528	+0.353	4076.8526	.1480	+0.349
3785.7251	.8742	+2.270	4076.7582	.6680	+0.343	4076.8567	.1689	+0.385
3785.7322	.9103	+2.263	4076.7614	.6843	+0.353	4076.8791	.2828	+0.407
3785.7354	.9265	+2.263	4076.7650	.7026	+0.328	4076.8839	.3072	+0.444
3785.7385	.9423	+2.361	4076.7685	.7204	+0.340	4076.8878	.3270	+0.394
3785.7458	.9794	+3.073	4076.7720	.7382	+0.301	4076.8930	.3534	+0.428
3785.7488	.9947	+3.246	4076.7755	.7560	+0.302	4076.8961	.3692	+0.384
3785.7518	.0099	+3.096	4076.7788	.7728	+0.296	4076.8989	.3834	+0.429
3785.7548	.0252	+2.682	4076.7823	.7906	+0.283	4076.8999	.3885	+0.445
3785.7580	.0414	+2.473	4076.7856	.8073	+0.233	4076.9009	.3936	+0.438
3785.7612	.0577	+2.385	4076.7891	.8251	+0.228	4076.9018	.3982	+0.435
3785.7680	.0923	+2.250	4076.7924	.8419	+0.232	4076.9027	.4028	+0.410
3785.7712	.1086	+2.256	4076.7958	.8592	+0.235	4076.9036	.4073	+0.425
3785.7800	.1533	+2.295	4076.7990	.8755	+0.214	4076.9045	.4119	+0.438
3785.7834	.1706	+2.317	4076.8021	.8912	+0.189	4076.9054	.4165	+0.405
3785.7868	.1879	+2.329	4076.8053	.9075	+0.199	4076.9075	.4272	+0.407
3785.7969	.2392	+2.331	4076.8083	.9228	+0.231	4076.9102	.4409	+0.424
3785.8010	.2601	+2.327	4076.8092	.9273	+0.229	4076.9111	.4455	+0.415
3785.8047	.2789	+2.311	4076.8101	.9319	+0.255	4076.9120	.4500	+0.422
3785.8163	.3379	+2.352	4076.8111	.9370	+0.254	4076.9129	.4546	+0.433
3785.8205	.3592	+2.361	4076.8122	.9426	+0.269	4076.9138	.4592	+0.435
3785.8244	.3791	+2.328	4076.8133	.9482	+0.315	4076.9147	.4638	+0.440
3785.8345	.4304	+2.360	4076.8144	.9538	+0.374	4076.9156	.4683	+0.442
3785.8380	.4482	+2.370	4076.8153	.9584	+0.405	4076.9165	.4729	+0.452
3785.8420	.4686	+2.374	4076.8163	.9634	+0.470	4076.9174	.4775	+0.452
3785.8510	.5143	+2.382	4076.8172	.9680	+0.584	4076.9182	.4816	+0.449
3785.8538	.5286	+2.374	4076.8181	.9726	+0.713	4076.9191	.4861	+0.436
3785.8568	.5438	+2.393	4076.8190	.9772	+0.858	4076.9204	.4928	+0.422
3785.8641	.5809	+2.379	4076.8199	.9817	+1.000	4076.9235	.5085	+0.431
3785.8673	.5972	+2.411	4076.8209	.9868	+1.101	4076.9243	.5126	+0.433
3785.8706	.6140	+2.428	4076.8219	.9919	+1.195	4076.9253	.5177	+0.417
3785.8791	.6572	+2.416	4076.8228	.9965	+1.234	4076.9261	.5217	+0.411
3785.8835	.6796	+2.418	4076.8238	.0016	+1.265	4076.9271	.5268	+0.406
4076.6977	.3604	+0.378	4076.8248	.0046	+1.211	4076.9281	.5319	+0.444

TABLE 1 (Cont'd)

Julian Day 2430000+	Phase	Δ Mag	Julian Day 2430000+	Phase	Δ Mag	Julian Day 2430000+	Phase	Δ Mag
4076.9290	.5365	+0.462	4077.0008	.9016	+0.226	4077.7877	.9027	+2.165
4076.9299	.5410	+0.470	4077.0017	.9061	+0.267	4077.7886	.9072	+2.167
4076.9312	.5477	+0.451	4077.0027	.9112	+0.286	4077.7894	.9113	+2.185
4076.9344	.5639	+0.471	4077.0038	.9168	+0.285	4077.7953	.9413	+2.157
4076.9353	.5685	+0.461	4077.0050	.9229	+0.301	4077.7962	.9459	+2.199
4076.9362	.5731	+0.428	4077.0080	.9382	+0.331	4077.7981	.9556	+2.283
4076.9372	.5782	+0.436	4077.0088	.9422	+0.347	4077.7990	.9601	+2.338
4076.9382	.5833	+0.410	4077.0098	.9473	+0.379	4077.7998	.9642	+2.398
4076.9392	.5883	+0.420	4077.0109	.9529	+0.450	4077.8006	.9683	+2.505
4076.9401	.5929	+0.428	4077.0136	.9666	+0.559	4077.8014	.9723	+2.615
4076.9411	.5980	+0.379	4077.0159	.9783	+0.921	4077.8023	.9769	+2.746
4076.9420	.6026	+0.384	4077.7237	.5773	+2.290	4077.8031	.9810	+2.855
4076.9431	.6082	+0.400	4077.7304	.6113	+2.282	4077.8040	.9856	+2.967
4076.9439	.6122	+0.424	4077.7327	.6230	+2.275	4077.8048	.9896	+3.047
4076.9451	.6183	+0.436	4077.7336	.6276	+2.265	4077.8056	.9937	+3.096
4076.9456	.6209	+0.479	4077.7344	.6317	+2.272	4077.8082	.0069	+3.096
4076.9483	.6346	+0.491	4077.7354	.6368	+2.282	4077.8090	.0110	+3.030
4076.9492	.6392	+0.482	4077.7363	.6413	+2.266	4077.8099	.0156	+2.965
4076.9501	.6438	+0.482	4077.7388	.6540	+2.271	4077.8107	.0196	+2.897
4076.9510	.6483	+0.486	4077.7397	.6586	+2.271	4077.8115	.0237	+2.756
4076.9520	.6534	+0.474	4077.7406	.6632	+2.280	4077.8124	.0283	+2.644
4076.9530	.6585	+0.431	4077.7415	.6678	+2.300	4077.8131	.0318	+2.565
4076.9540	.6636	+0.415	4077.7424	.6723	+2.303	4077.8140	.0364	+2.488
4076.9549	.6682	+0.429	4077.7433	.6769	+2.259	4077.8147	.0400	+2.434
4076.9559	.6732	+0.413	4077.7442	.6815	+2.269	4077.8155	.0440	+2.410
4076.9568	.6778	+0.377	4077.7466	.6937	+2.298	4077.8163	.0481	+2.386
4076.9577	.6824	+0.404	4077.7475	.6983	+2.296	4077.8172	.0527	+2.362
4076.9586	.6870	+0.430	4077.7484	.7028	+2.282	4077.8192	.0628	+2.347
4076.9598	.6931	+0.414	4077.7493	.7074	+2.251	4077.8201	.0674	+2.328
4076.9631	.7099	+0.423	4077.7502	.7120	+2.231	4077.8210	.0720	+2.306
4076.9640	.7144	+0.414	4077.7512	.7171	+2.236	4077.8219	.0766	+2.300
4076.9649	.7190	+0.386	4077.7522	.7222	+2.229	4077.8227	.0806	+2.290
4076.9658	.7236	+0.402	4077.7531	.7268	+2.226	4077.8235	.0847	+2.276
4076.9667	.7282	+0.368	4077.7540	.7313	+2.219	4077.8244	.0893	+2.265
4076.9678	.7338	+0.345	4077.7548	.7354	+2.216	4077.8252	.0934	+2.245
4076.9687	.7383	+0.352	4077.7572	.7476	+2.194	4077.8260	.0974	+2.255
4076.9699	.7444	+0.366	4077.7581	.7522	+2.202	4077.8269	.1020	+2.223
4076.9711	.7505	+0.389	4077.7590	.7567	+2.189	4077.8311	.1234	+2.233
4076.9733	.7617	+0.381	4077.7598	.7608	+2.198	4077.8332	.1340	+2.224
4076.9764	.7775	+0.316	4077.7607	.7654	+2.183	4077.8340	.1381	+2.232
4076.9773	.7821	+0.320	4077.7616	.7700	+2.168	4077.8351	.1437	+2.233
4076.9782	.7866	+0.328	4077.7624	.7740	+2.148	4077.8363	.1498	+2.245
4076.9790	.7907	+0.332	4077.7633	.7786	+2.130	4077.8374	.1554	+2.248
4076.9801	.7963	+0.323	4077.7643	.7837	+2.152	4077.8389	.1630	+2.260
4076.9810	.8009	+0.310	4077.7706	.8157	+2.206	4077.8403	.1701	+2.209
4076.9819	.8055	+0.305	4077.7717	.8213	+2.187	4077.8417	.1772	+2.267
4076.9831	.8116	+0.302	4077.7727	.8264	+2.189	4077.8447	.1925	+2.219
4076.9860	.8263	+0.300	4077.7735	.8305	+2.181	4077.8460	.1991	+2.217
4076.9869	.8309	+0.305	4077.7744	.8350	+2.169	4077.8472	.2052	+2.252
4076.9878	.8355	+0.289	4077.7768	.8472	+2.136	4077.8484	.2113	+2.289
4076.9888	.8405	+0.277	4077.7776	.8513	+2.101	4077.8496	.2174	+2.285
4076.9897	.8451	+0.270	4077.7784	.8554	+2.110	4077.8506	.2225	+2.253
4076.9906	.8497	+0.276	4077.7793	.8600	+2.101	4077.8517	.2281	+2.272
4076.9916	.8548	+0.256	4077.7802	.8645	+2.122	4077.8542	.2408	+2.221
4076.9926	.8599	+0.247	4077.7811	.8691	+2.122	4077.8551	.2454	+2.249
4076.9938	.8660	+0.258	4077.7820	.8737	+2.144	4077.8563	.2515	+2.252
4076.9969	.8817	+0.220	4077.7828	.8778	+2.158	4077.8574	.2571	+2.226
4076.9978	.8863	+0.248	4077.7836	.8818	+2.176	4077.8589	.2647	+2.263
4076.9988	.8914	+0.240	4077.7859	.8935	+2.171	4077.8601	.2708	+2.265
4076.9999	.8970	+0.235	4077.7868	.8981	+2.189	4077.8613	.2769	+2.258

TABLE 1 (Cont'd)

Julian Day 2430000+	Phase	Δ Mag	Julian Day 2430000+	Phase	Δ Mag	Julian Day 2430000+	Phase	Δ Mag
4077.8621	.2810	+2.257	4077.9387	.6705	+2.319	4078.0091	.0284	+2.611
4077.8690	.3161	+2.270	4077.9398	.6760	+2.300	4078.0110	.0381	+2.427
4077.8699	.3206	+2.258	4077.9408	.6811	+2.301	4078.0120	.0432	+2.427
4077.8708	.3252	+2.283	4077.9419	.6867	+2.311	4078.0128	.0472	+2.406
4077.8718	.3303	+2.277	4077.9440	.6974	+2.345	4078.0137	.0518	+2.386
4077.8727	.3349	+2.262	4077.9451	.7030	+2.327	4078.0157	.0620	+2.348
4077.8736	.3394	+2.237	4077.9462	.7086	+2.327	4161.6734	.4299	+2.427
4077.8747	.3450	+2.253	4077.9473	.7142	+2.310	4161.6763	.4446	+2.430
4077.8756	.3496	+2.244	4077.9484	.7198	+2.295	4161.6793	.4599	+2.437
4077.8765	.3542	+2.261	4077.9496	.7259	+2.285	4161.6817	.4721	+2.417
4077.8790	.3669	+2.283	4077.9505	.7305	+2.271	4161.6852	.4899	+2.457
4077.8801	.3725	+2.274	4077.9516	.7360	+2.251	4161.6877	.5026	+2.444
4077.8811	.3776	+2.232	4077.9578	.7676	+2.184	4161.6899	.5138	+2.444
4077.8820	.3822	+2.269	4077.9588	.7727	+2.183	4161.6926	.5275	+2.436
4077.8830	.3872	+2.273	4077.9599	.7782	+2.165	4161.6948	.5387	+2.434
4077.8840	.3923	+2.253	4077.9609	.7833	+2.147	4161.6970	.5499	+2.444
4077.8849	.3969	+2.264	4077.9619	.7884	+2.158	4161.6996	.5631	+2.456
4077.8857	.4010	+2.256	4077.9628	.7930	+2.181	4161.7019	.5748	+2.464
4077.8867	.4061	+2.250	4077.9647	.8027	+2.117	4161.7044	.5875	+2.448
4077.8877	.4111	+2.244	4077.9657	.8077	+2.099	4161.7068	.5997	+2.466
4077.8886	.4157	+2.256	4077.9667	.8128	+2.124	4161.7094	.6130	+2.464
4077.8895	.4203	+2.269	4077.9678	.8184	+2.179	4161.7119	.6257	+2.445
4077.8918	.4320	+2.291	4077.9689	.8240	+2.144	4161.7152	.6424	+2.511
4077.8927	.4366	+2.291	4077.9699	.8291	+2.163	4161.7171	.6521	+2.525
4077.8936	.4411	+2.273	4077.9710	.8347	+2.167	4161.7181	.6572	+2.524
4077.8945	.4457	+2.299	4077.9720	.8398	+2.130	4161.7192	.6628	+2.525
4077.8955	.4508	+2.269	4077.9730	.8449	+2.124	4161.7202	.6679	+2.523
4077.8965	.4559	+2.262	4077.9740	.8500	+2.118	4161.7213	.6735	+2.500
4077.8975	.4610	+2.292	4077.9750	.8550	+2.122	4161.7224	.6790	+2.507
4077.8984	.4656	+2.287	4077.9760	.8601	+2.112	4161.7234	.6841	+2.547
4077.8993	.4701	+2.278	4077.9783	.8718	+2.112	4161.7245	.6897	+2.550
4077.9016	.4818	+2.287	4077.9793	.8769	+2.093	4161.7250	.6923	+2.537
4077.9026	.4869	+2.321	4077.9801	.8810	+2.094	4161.7275	.7050	+2.473
4077.9035	.4915	+2.315	4077.9810	.8855	+2.095	4161.7288	.7116	+2.472
4077.9045	.4966	+2.321	4077.9821	.8911	+2.067	4161.7293	.7141	+2.496
4077.9055	.5016	+2.355	4077.9831	.8962	+2.076	4161.7317	.7263	+2.562
4077.9064	.5062	+2.338	4077.9840	.9008	+2.127	4161.7326	.7309	+2.554
4077.9074	.5113	+2.328	4077.9850	.9059	+2.135	4161.7339	.7375	+2.591
4077.9084	.5164	+2.341	4077.9868	.9150	+2.159	4161.7351	.7436	+2.569
4077.9093	.5210	+2.320	4077.9877	.9196	+2.131	4161.7364	.7502	+2.600
4077.9153	.5515	+2.266	4077.9887	.9247	+2.134	4161.7377	.7568	+2.534
4077.9164	.5571	+2.301	4077.9896	.9293	+2.140	4161.7389	.7630	+2.502
4077.9173	.5616	+2.293	4077.9905	.9338	+2.161	4161.7393	.7650	+2.512
4077.9183	.5667	+2.295	4077.9913	.9379	+2.155	4161.7425	.7812	+2.580
4077.9193	.5718	+2.310	4077.9933	.9481	+2.181	4161.7438	.7879	+2.538
4077.9204	.5774	+2.311	4077.9943	.9532	+2.241	4161.7451	.7945	+2.493
4077.9215	.5830	+2.300	4077.9952	.9577	+2.326	4161.7462	.8001	+2.515
4077.9224	.5876	+2.313	4077.9960	.9618	+2.380	4161.7476	.8072	+2.608
4077.9249	.6003	+2.327	4077.9969	.9664	+2.469	4161.7488	.8133	+2.507
4077.9258	.6049	+2.329	4077.9978	.9710	+2.575	4161.7500	.8194	+2.456
4077.9268	.6100	+2.313	4077.9987	.9755	+2.726	4161.7514	.8265	+2.412
4077.9278	.6150	+2.323	4077.9996	.9801	+2.883	4161.7518	.8285	+2.394
4077.9288	.6201	+2.320	4078.0006	.9852	+3.010	4161.7549	.8443	+2.362
4077.9298	.6252	+2.325	4078.9915	.9898	+3.097	4161.7560	.8499	+2.394
4077.9308	.6303	+2.347	4078.0025	.9949	+3.119	4161.7570	.8550	+2.367
4077.9319	.6359	+2.324	4078.0034	.9994	+3.145	4161.7582	.8611	+2.374
4077.9344	.6486	+2.360	4078.0043	.0040	+3.127	4161.7596	.8682	+2.372
4077.9356	.6547	+2.330	4078.0052	.0086	+3.075	4161.7607	.8738	+2.358
4077.9366	.6598	+2.304	4078.0073	.0193	+2.864	4161.7619	.8799	+2.396
4077.9376	.6649	+2.325	4078.0081	.0233	+2.733	4161.7623	.8819	+2.426

TABLE 1 (Cont'd)

Julian Day 2430000+	Phase	Δ Mag	Julian Day 2430000+	Phase	Δ Mag	Julian Day 2430000+	Phase	Δ Mag
4161.7658	.9048	+2.402	4161.8373	.2633	+2.336	4519.7302	.0141	+3.368
4161.7673	.9074	+2.392	4161.8387	.2704	+2.342	4519.7321	.0237	+3.060
4161.7685	.9134	+2.342	4161.8400	.2770	+2.321	4519.7342	.0344	+2.698
4161.7697	.9196	+2.324	4161.8412	.2831	+2.320	4519.7366	.0466	+2.604
4161.7708	.9252	+2.328	4161.8417	.2856	+2.319	4519.7389	.0583	+2.569
4161.7722	.9323	+2.348	4161.8445	.2999	+2.333	4519.7411	.0695	+2.533
4161.7734	.9384	+2.364	4161.8456	.3055	+2.327	4519.7436	.0822	+2.496
4161.7740	.9414	+2.359	4161.8468	.3116	+2.312	4519.7459	.0939	+2.457
4161.7768	.9557	+2.471	4161.8481	.3182	+2.337	4519.7483	.1061	+2.428
4161.7778	.9607	+2.542	4161.8495	.3253	+2.351	4519.7507	.1183	+2.418
4161.7786	.9648	+2.638	4161.8507	.3314	+2.332	4519.7568	.1493	+2.414
4161.7794	.9689	+2.749	4161.8519	.3375	+2.332	4519.7589	.1600	+2.415
4161.7803	.9734	+2.902	4161.8530	.3431	+2.338	4519.7610	.1707	+2.434
4161.7812	.9780	+3.063	4161.8536	.3462	+2.361	4519.7640	.1859	+2.468
4161.7820	.9821	+3.194	4161.8566	.3614	+2.410	4519.7661	.1966	+2.473
4161.7829	.9867	+3.295	4161.8581	.3690	+2.406	4519.7683	.2078	+2.479
4161.7840	.9923	+3.357	4161.8597	.3772	+2.401	4519.7704	.2185	+2.476
4161.7848	.9963	+3.402	4161.8609	.3833	+2.374	4519.7726	.2297	+2.455
4161.7858	.0014	+3.405	4161.8621	.3894	+2.395	4519.7747	.2404	+2.448
4161.7868	.0065	+3.310	4161.8633	.3955	+2.410	4526.6213	.0527	+2.591
4161.7877	.0111	+3.276	4161.8646	.4021	+2.417	4526.6236	.0644	+2.564
4161.7887	.0162	+3.146	4161.8650	.4041	+2.411	4526.6259	.0761	+2.557
4161.7898	.0218	+2.943	4519.6262	.4853	+2.479	4526.6281	.0873	+2.527
4161.7906	.0258	+2.776	4519.6290	.4995	+2.455	4526.6308	.1010	+2.466
4161.7918	.0319	+2.626	4519.6312	.5107	+2.487	4526.6333	.1137	+2.456
4161.7929	.0375	+2.563	4519.6337	.5234	+2.484	4526.6358	.1264	+2.461
4161.7939	.0426	+2.503	4519.6362	.5361	+2.455	4526.6382	.1386	+2.461
4161.7947	.0467	+2.502	4519.6388	.5493	+2.471	4526.6409	.1524	+2.467
4161.7951	.0487	+2.485	4519.6413	.5620	+2.484	4526.6435	.1656	+2.482
4161.7974	.0604	+2.462	4519.6438	.5748	+2.461	4526.6495	.1961	+2.475
4161.7986	.0665	+2.471	4519.6502	.6073	+2.486	4526.6518	.2078	+2.467
4161.7998	.0726	+2.459	4519.6527	.6200	+2.480	4526.6544	.2210	+2.447
4161.8016	.0818	+2.422	4519.6550	.6317	+2.472	4526.6565	.2317	+2.470
4161.8027	.0874	+2.380	4519.6573	.6434	+2.482	4526.6589	.2439	+2.466
4161.8039	.0934	+2.340	4519.6598	.6561	+2.449	4526.6614	.2566	+2.486
4161.8050	.0990	+2.335	4519.6625	.6698	+2.439	4526.6639	.2693	+2.492
4161.8063	.1056	+2.341	4519.6648	.6815	+2.451	4526.6695	.2978	+2.475
4161.8074	.1112	+2.311	4519.6676	.6958	+2.475	4526.6718	.3095	+2.475
4161.8078	.1133	+2.318	4519.6735	.7258	+2.414	4526.6744	.3227	+2.490
4161.8109	.1290	+2.276	4519.6761	.7390	+2.379	4526.6770	.3359	+2.489
4161.8123	.1362	+2.263	4519.6786	.7517	+2.394	4526.6796	.3492	+2.498
4161.8135	.1423	+2.262	4519.6812	.7649	+2.435	4526.6819	.3608	+2.498
4161.8148	.1489	+2.269	4519.6837	.7776	+2.429	4526.6842	.3726	+2.468
4161.8161	.1555	+2.311	4519.6860	.7893	+2.410	4526.6866	.3848	+2.483
4161.8172	.1611	+2.363	4519.6883	.8010	+2.401	4526.6889	.3964	+2.486
4161.8184	.1672	+2.380	4519.6903	.8112	+2.371	4526.6964	.4346	+2.490
4161.8197	.1738	+2.379	4519.6964	.8422	+2.350	4526.6988	.4468	+2.513
4161.8210	.1804	+2.368	4519.6990	.8554	+2.325	4526.7012	.4590	+2.510
4161.8215	.1829	+2.388	4519.7010	.8656	+2.350	4526.7036	.4712	+2.510
4161.8236	.1936	+2.306	4519.7037	.8793	+2.345	4526.7058	.4824	+2.519
4161.8248	.1997	+2.303	4519.7059	.8905	+2.345	4526.7083	.4951	+2.528
4161.8260	.2058	+2.299	4519.7081	.9017	+2.339	4526.7110	.5088	+2.487
4161.8273	.2124	+2.300	4519.7104	.9134	+2.355	4526.7135	.5215	+2.498
4161.8284	.2180	+2.316	4519.7160	.9419	+2.365	4526.7160	.5342	+2.503
4161.8298	.2251	+2.324	4519.7186	.9551	+2.514	4526.7183	.5459	+2.494
4161.8310	.2312	+2.322	4519.7204	.9642	+2.670	4526.7243	.5764	+2.468
4161.8321	.2355	+2.321	4519.7226	.9754	+2.981	4526.7268	.5892	+2.509
4161.8334	.2434	+2.318	4519.7244	.9846	+3.307	4526.7294	.6024	+2.476
4161.8347	.2501	+2.339	4519.7262	.9937	+3.501	4526.7317	.6141	+2.471
4161.8361	.2572	+2.313	4519.7282	.0039	+3.537	4526.7343	.6273	+2.466

TABLE 1 (Cont'd)

Julian Day 2430000+	Phase	Δ Mag	Julian Day 2430000+	Phase	Δ Mag	Julian Day 2430000+	Phase	Δ Mag
4526.7368	.6400	+2.470	4533.6912	.0005	+3.504	4534.6668	.9610	+2.630
4531.6263	.5012	+2.515	4533.6914	.0015	+3.492	4534.6670	.9621	+2.645
4531.6284	.5119	+2.488	4533.6916	.0025	+3.467	4534.6672	.9631	+2.664
4531.6307	.5236	+2.484	4533.6919	.0041	+3.461	4534.6675	.9646	+2.684
4531.6360	.5506	+2.430	4533.6921	.0051	+3.461	4534.6677	.9656	+2.715
4531.6383	.5623	+2.450	4533.6923	.0061	+3.450	4534.6679	.9666	+2.752
4531.6403	.5724	+2.453	4533.6928	.0086	+3.442	4534.6682	.9682	+2.764
4531.6452	.5973	+2.494	4533.6930	.0097	+3.416	4534.6684	.9692	+2.805
4531.6476	.6095	+2.506	4533.6933	.0112	+3.396	4534.6686	.9702	+2.848
4531.6498	.6207	+2.509	4533.6935	.0122	+3.364	4534.6689	.9717	+2.887
4531.6518	.6309	+2.488	4533.6937	.0132	+3.339	4534.6691	.9727	+2.946
4531.6589	.6670	+2.489	4533.6940	.0147	+3.309	4534.6693	.9738	+2.981
4531.6613	.6792	+2.510	4533.6942	.0158	+3.281	4534.6696	.9753	+3.046
4531.6636	.6909	+2.486	4533.6944	.0168	+3.254	4534.6698	.9763	+3.079
4531.6658	.7061	+2.485	4533.6946	.0178	+3.240	4534.6700	.9773	+3.126
4533.6260	.6690	+2.486	4533.6948	.0188	+3.198	4534.6703	.9788	+3.174
4533.6278	.6781	+2.480	4533.6950	.0198	+3.150	4534.6705	.9799	+3.205
4533.6300	.6893	+2.480	4533.6953	.0214	+3.126	4534.6710	.9824	+3.267
4533.6318	.6985	+2.462	4533.6957	.0234	+3.038	4534.6712	.9834	+3.297
4533.6338	.7086	+2.462	4533.6960	.0249	+3.005	4534.6714	.9844	+3.330
4533.6360	.7198	+2.442	4533.6962	.0259	+2.952	4534.6717	.9860	+3.360
4533.6379	.7295	+2.453	4533.6964	.0269	+2.921	4534.6719	.9870	+3.397
4533.6433	.7570	+2.416	4533.6967	.0285	+2.887	4534.6721	.9880	+3.443
4533.6450	.7656	+2.416	4533.6969	.0295	+2.854	4534.6724	.9895	+3.450
4533.6471	.7763	+2.388	4533.6971	.0305	+2.808	4534.6726	.9905	+3.474
4533.6494	.7880	+2.394	4533.6974	.0320	+2.790	4534.6728	.9916	+3.485
4533.6512	.7971	+2.383	4533.6976	.0330	+2.757	4534.6733	.9941	+3.521
4533.6531	.8068	+2.392	4533.7004	.0473	+2.662	4534.6735	.9951	+3.552
4533.6550	.8164	+2.412	4533.7017	.0539	+2.595	4534.6738	.9966	+3.549
4533.6566	.8246	+2.356	4533.7039	.0651	+2.534	4534.6740	.9977	+3.555
4533.6584	.8337	+2.369	4533.7087	.0895	+2.487	4534.6742	.9987	+3.555
4533.6603	.8434	+2.358	4533.7107	.0996	+2.448	4534.6745	.0002	+3.558
4533.6653	.8688	+2.342	4533.7129	.1108	+2.425	4534.6747	.0012	+3.563
4533.6672	.8785	+2.343	4533.7154	.1236	+2.429	4534.6749	.0022	+3.545
4533.6694	.8897	+2.350	4533.7204	.1490	+2.436	4534.6752	.0038	+3.551
4533.6714	.8998	+2.323	4533.7235	.1647	+2.458	4534.6754	.0048	+3.554
4533.6733	.9095	+2.377	4533.7264	.1795	+2.439	4534.6758	.0068	+3.519
4533.6754	.9202	+2.366	4533.7290	.1927	+2.456	4534.6761	.0083	+3.507
4533.6805	.9461	+2.454	4533.7319	.2074	+2.445	4534.6763	.0094	+3.499
4533.6825	.9563	+2.564	4533.7344	.2202	+2.454	4534.6765	.0104	+3.479
4533.6846	.9669	+2.733	4534.6232	.7394	+2.475	4534.6768	.0119	+3.452
4533.6863	.9756	+3.028	4534.6255	.7510	+2.466	4534.6770	.0129	+3.410
4533.6865	.9766	+3.077	4534.6273	.7602	+2.428	4534.6772	.0139	+3.393
4533.6867	.9776	+3.114	4534.6292	.7699	+2.440	4534.6774	.0149	+3.363
4533.6870	.9792	+3.161	4534.6312	.7800	+2.439	4534.6777	.0165	+3.322
4533.6872	.9802	+3.177	4534.6365	.8070	+2.407	4534.6779	.0175	+3.296
4533.6877	.9827	+3.261	4534.6382	.8156	+2.431	4534.6781	.0185	+3.257
4533.6879	.9837	+3.298	4534.6402	.8258	+2.411	4534.6786	.0210	+3.172
4533.6881	.9847	+3.338	4534.6421	.8355	+2.414	4534.6788	.0221	+3.122
4533.6884	.9863	+3.367	4534.6442	.8461	+2.392	4534.6790	.0231	+3.175
4533.6886	.9873	+3.387	4534.6464	.8573	+2.362	4534.6793	.0246	+3.020
4533.6888	.9883	+3.424	4534.6486	.8685	+2.367	4534.6795	.0256	+2.978
4533.6891	.9898	+3.447	4534.6505	.8782	+2.379	4534.6797	.0266	+2.939
4533.6893	.9908	+3.449	4534.6526	.8888	+2.404	4534.6800	.0282	+2.874
4533.6895	.9919	+3.482	4534.6546	.8990	+2.385	4534.6802	.0292	+2.841
4533.6900	.9944	+3.482	4534.6564	.9082	+2.389	4534.6804	.0302	+2.812
4533.6902	.9954	+3.502	4534.6583	.9178	+2.406	4534.6807	.0317	+2.791
4533.6905	.9969	+3.504	4534.6627	.9402	+2.428	4534.6809	.0327	+2.774
4533.6907	.9980	+3.504	4534.6652	.9529	+2.552	4534.6811	.0338	+2.755
4533.6909	.9990	+3.504	4534.6665	.9595	+2.624	4534.6814	.0353	+2.748

TABLE 1 (Cont'd)

Julian Day 2430000+	Phase	Δ Mag	Julian Day 2430000+	Phase	Δ Mag	Julian Day 2430000+	Phase	Δ Mag
4534.6816	.0363	+2.737	4535.7155	.2933	+2.462	4542.7173	.8948	+2.409
4534.6818	.0373	+2.712	4535.7173	.3024	+2.494	4542.7178	.8974	+2.390
4534.6821	.0388	+2.701	4535.7202	.3172	+2.470	4542.7185	.9009	+2.385
4534.6823	.0399	+2.688	4535.7224	.3284	+2.482	4542.7190	.9035	+2.396
4534.6825	.0409	+2.680	4535.7246	.3396	+2.489	4542.7195	.9060	+2.404
4534.6828	.0424	+2.674	4542.6350	.4764	+2.512	4542.7201	.9091	+2.388
4534.6830	.0434	+2.654	4542.6363	.4881	+2.520	4542.7207	.9121	+2.399
4534.6832	.0444	+2.646	4542.6396	.4998	+2.524	4542.7285	.9518	+2.572
4534.6837	.0470	+2.612	4542.6417	.5104	+2.532	4542.7304	.9614	+2.640
4534.6839	.0480	+2.612	4542.6439	.5216	+2.503	4542.7310	.9645	+2.700
4534.6842	.0495	+2.610	4542.6459	.5318	+2.534	4542.7317	.9681	+2.771
4534.6844	.0505	+2.605	4542.6511	.5582	+2.522	4542.7322	.9706	+2.842
4534.6846	.0516	+2.605	4542.6531	.5684	+2.522	4542.7327	.9732	+2.950
4534.6849	.0531	+2.592	4542.6551	.5786	+2.545	4542.7333	.9762	+3.056
4534.6851	.0541	+2.570	4542.6570	.5882	+2.533	4542.7339	.9792	+3.173
4534.6886	.0719	+2.568	4542.6591	.5989	+2.506	4542.7344	.9818	+3.270
4534.6933	.0958	+2.499	4542.6611	.6091	+2.515	4542.7350	.9848	+3.356
4534.6954	.1065	+2.487	4542.6631	.6193	+2.498	4542.7356	.9879	+3.397
4535.6464	.9420	+2.385	4542.6650	.6289	+2.529	4542.7361	.9904	+3.448
4535.6480	.9501	+2.440	4542.6699	.6538	+2.512	4542.7368	.9940	+3.502
4535.6497	.9588	+2.536	4542.6717	.6630	+2.475	4542.7373	.9965	+3.507
4535.6515	.9679	+2.690	4542.6737	.6732	+2.482	4542.7379	.9996	+3.515
4535.6532	.9766	+3.004	4542.6758	.6838	+2.481	4542.7385	.0026	+3.519
4535.6551	.9862	+3.253	4542.6779	.6945	+2.477	4542.7392	.0062	+3.490
4535.6569	.9954	+3.419	4542.6801	.7057	+2.463	4542.7397	.0087	+3.466
4535.6589	.0055	+3.419	4542.6866	.7388	+2.440	4542.7403	.0118	+3.403
4535.6608	.0152	+3.270	4542.6887	.7494	+2.444	4542.7410	.0154	+3.360
4535.6627	.0248	+2.934	4542.6906	.7591	+2.460	4542.7415	.0179	+3.268
4535.6648	.0355	+2.657	4542.6924	.7682	+2.445	4542.7422	.0214	+3.158
4535.6673	.0482	+2.564	4542.6944	.7784	+2.439	4542.7428	.0245	+3.068
4535.6697	.0604	+2.543	4542.6963	.7881	+2.440	4542.7434	.0276	+2.926
4535.6715	.0696	+2.508	4542.6984	.7987	+2.427	4542.7440	.0306	+2.837
4535.6736	.0802	+2.492	4542.7007	.8104	+2.416	4542.7445	.0332	+2.798
4535.6786	.1056	+2.399	4542.7026	.8201	+2.399	4542.7454	.0377	+2.721
4535.6805	.1153	+2.382	4542.7090	.8526	+2.376	4542.7459	.0403	+2.708
4535.6826	.1260	+2.395	4542.7110	.8628	+2.383	4542.7465	.0433	+2.696
4535.6849	.1377	+2.409	4542.7116	.8659	+2.407	4542.7471	.0464	+2.684
4535.6871	.1489	+2.403	4542.7122	.8689	+2.397	4542.7476	.0489	+2.655
4535.6892	.1596	+2.396	4542.7129	.8725	+2.374	4542.7483	.0525	+2.634
4535.6944	.1860	+2.406	4542.7135	.8755	+2.371	4542.7490	.0560	+2.630
4535.6963	.1956	+2.433	4542.7140	.8781	+2.358	4542.7495	.0586	+2.595
4535.7014	.2216	+2.433	4542.7145	.8806	+2.384	4542.7501	.0616	+2.573
4535.7038	.2338	+2.449	4542.7150	.8832	+2.374	4542.7507	.0647	+2.594
4535.7059	.2445	+2.462	4542.7157	.8867	+2.386	4542.7513	.0677	+2.574
4535.7077	.2536	+2.449	4542.7163	.8898	+2.391	4542.7518	.0703	+2.561
4535.7134	.2826	+2.475	4542.7168	.8923	+2.403	4542.7525	.0738	+2.573

TABLE 2

Photometric Observations of UX Ursae Majoris (Yellow)

Julian Day 2430000+	Phase	Δ Mag	Julian Day 2430000+	Phase	Δ Mag	Julian Day 2430000+	Phase	Δ Mag
3785.6485	.4847	+2.726	4076.7022	.3833	-0.270	4076.8260	.0128	+0.419
3785.6512	.4984	+2.731	4076.7059	.4021	-0.258	4076.8271	.0184	+0.353
3785.6541	.5131	+2.729	4076.7104	.4250	-0.322	4076.8281	.0234	+0.222
3785.6614	.5503	+2.750	4076.7147	.4468	-0.273	4076.8290	.0280	+0.100
3785.6645	.5660	+2.772	4076.7190	.4687	-0.269	4076.8299	.0326	+0.006
3785.6675	.5813	+2.727	4076.7219	.4834	-0.267	4076.8309	.0377	-0.062
3785.6761	.6250	+2.770	4076.7250	.4992	-0.255	4076.8318	.0422	-0.097
3785.6790	.6398	+2.779	4076.7281	.5150	-0.263	4076.8328	.0473	-0.135
3785.6821	.6555	+2.780	4076.7309	.5292	-0.277	4076.8338	.0524	-0.151
3785.6892	.6916	+2.835	4076.7338	.5440	-0.272	4076.8347	.0570	-0.160
3785.6922	.7069	+2.742	4076.7369	.5597	-0.301	4076.8356	.0616	-0.160
3785.6951	.7216	+2.684	4076.7400	.5755	-0.301	4076.8365	.0662	-0.177
3785.7052	.7730	+2.711	4076.7434	.5928	-0.254	4076.8372	.0697	-0.173
3785.7080	.7872	+2.724	4076.7465	.6085	-0.209	4076.8394	.0809	-0.172
3785.7111	.8030	+2.704	4076.7497	.6248	-0.268	4076.8458	.1134	-0.268
3785.7186	.8411	+2.689	4076.7528	.6406	-0.235	4076.8498	.1338	-0.281
3785.7224	.8604	+2.630	4076.7560	.6568	-0.266	4076.8538	.1541	-0.274
3785.7261	.8792	+2.659	4076.7591	.6726	-0.274	4076.8580	.1755	-0.272
3785.7331	.9148	+2.641	4076.7625	.6899	-0.266	4076.8805	.2899	-0.212
3785.7364	.9316	+2.675	4076.7660	.7077	-0.287	4076.8849	.3122	-0.233
3785.7395	.9474	+2.799	4076.7695	.7255	-0.271	4076.8887	.3316	-0.244
3785.7469	.9850	+3.455	4076.7730	.7433	-0.313	4076.8939	.3580	-0.219
3785.7497	.9992	+3.529	4076.7764	.7606	-0.303	4076.8968	.3728	-0.270
3785.7528	.0150	+3.316	4076.7798	.7778	-0.310	4076.8992	.3850	-0.247
3785.7558	.0302	+2.968	4076.7825	.7916	-0.344	4076.9004	.3911	-0.223
3785.7589	.0460	+2.829	4076.7866	.8124	-0.356	4076.9013	.3956	-0.216
3785.7620	.0616	+2.740	4076.7900	.8297	-0.363	4076.9020	.3992	-0.227
3785.7689	.0969	+2.615	4076.7934	.8470	-0.361	4076.9030	.4043	-0.242
3785.7721	.1131	+2.627	4076.7967	.8638	-0.370	4076.9039	.4088	-0.218
3785.7811	.1589	+2.654	4076.7999	.8800	-0.405	4076.9048	.4134	-0.245
3785.7843	.1752	+2.684	4076.8029	.8953	-0.402	4076.9057	.4180	-0.247
3785.7880	.1940	+2.675	4076.8062	.9121	-0.384	4076.9083	.4312	-0.233
3785.7982	.2458	+2.682	4076.8085	.9238	-0.371	4076.9105	.4424	-0.227
3785.8021	.2657	+2.692	4076.8095	.9289	-0.347	4076.9114	.4470	-0.243
3785.8065	.2880	+2.611	4076.8104	.9334	-0.334	4076.9123	.4516	-0.233
3785.8174	.3435	+2.701	4076.8114	.9385	-0.319	4076.9132	.4561	-0.238
3785.8216	.3648	+2.701	4076.8125	.9441	-0.281	4076.9141	.4607	-0.225
3785.8258	.3862	+2.665	4076.8137	.9502	-0.255	4076.9150	.4653	-0.209
3785.8355	.4355	+2.679	4076.8147	.9553	-0.196	4076.9159	.4699	-0.226
3785.8394	.4553	+2.710	4076.8156	.9599	-0.167	4076.9168	.4744	-0.225
3785.8432	.4746	+2.712	4076.8166	.9650	-0.078	4076.9177	.4790	-0.227
3785.8518	.5184	+2.702	4076.8175	.9695	+0.030	4076.9185	.4831	-0.216
3785.8547	.5331	+2.728	4076.8183	.9736	+0.147	4076.9195	.4882	-0.233
3785.8577	.5484	+2.739	4076.8193	.9787	+0.257	4076.9213	.4973	-0.241
3785.8650	.5855	+2.736	4076.8202	.9833	+0.379	4076.9237	.5095	-0.232
3785.8683	.6023	+2.720	4076.8212	.9884	+0.452	4076.9246	.5141	-0.243
3785.8716	.6190	+2.733	4076.8222	.9934	+0.510	4076.9255	.5187	-0.243
3785.8804	.6638	+2.734	4076.8231	.9980	+0.538	4076.9265	.5238	-0.262
3785.8846	.6852	+2.757	4076.8242	.0036	+0.538	4076.9274	.5283	-0.257
4076.6987	.3655	-0.277	4076.8251	.0082	+0.496	4076.9283	.5329	-0.216

TABLE 2 (Cont'd)

Julian Day 2430000+	Phase	Δ Mag	Julian Day 2430000+	Phase	Δ Mag	Julian Day 2430000+	Phase	Δ Mag
4076.9293	.5380	-0.210	4077.0021	.9082	-0.359	4077.7889	.9088	+2.572
4076.9302	.5426	-0.200	4077.0030	.9127	-0.342	4077.7897	.9128	+2.583
4076.9320	.5517	-0.227	4077.0041	.9183	-0.350	4077.7956	.9428	+2.589
4076.9347	.5655	-0.185	4077.0060	.9280	-0.305	4077.7966	.9479	+2.655
4076.9356	.5700	-0.229	4077.0082	.9392	-0.285	4077.7983	.9566	+2.719
4076.9365	.5746	-0.234	4077.0091	.9438	-0.264	4077.7992	.9611	+2.765
4076.9374	.5792	-0.241	4077.0100	.9483	-0.205	4077.8001	.9657	+2.856
4076.9385	.5848	-0.257	4077.0118	.9575	-0.152	4077.8009	.9698	+2.944
4076.9394	.5894	-0.251	4077.0143	.9702	+0.040	4077.8017	.9739	+3.050
4076.9404	.5944	-0.257	4077.0168	.9829	+0.357	4077.8025	.9779	+3.152
4076.9414	.5995	-0.295	4077.7247	.5823	+2.629	4077.8033	.9820	+3.227
4076.9424	.6046	-0.282	4077.7312	.6154	+2.651	4077.8042	.9866	+3.305
4076.9433	.6092	-0.265	4077.7330	.6245	+2.639	4077.8051	.9912	+3.377
4076.9442	.6138	-0.260	4077.7339	.6291	+2.623	4077.8059	.9953	+3.419
4076.9462	.6239	-0.190	4077.7348	.6337	+2.629	4077.8085	.0084	+3.395
4076.9485	.6356	-0.193	4077.7357	.6383	+2.645	4077.8092	.0120	+3.346
4076.9495	.6407	-0.207	4077.7366	.6428	+2.627	4077.8101	.0166	+3.304
4076.9504	.6453	-0.205	4077.7391	.6556	+2.636	4077.8110	.0212	+3.223
4076.9513	.6499	-0.200	4077.7399	.6596	+2.637	4077.8118	.0252	+3.109
4076.9523	.6550	-0.223	4077.7408	.6642	+2.659	4077.8126	.0293	+3.008
4076.9533	.6600	-0.23[illegible]	4077.7417	.6688	+2.654	4077.8133	.0328	+2.954
4076.9543	.6651	-0.260	4077.7426	.6734	+2.658	4077.8142	.0374	+2.893
4076.9552	.6697	-0.258	4077.7436	.6784	+2.637	4077.8150	.0415	+2.839
4076.9562	.6748	-0.274	4077.7445	.6830	+2.636	4077.8158	.0456	+2.811
4076.9571	.6794	-0.297	4077.7469	.6952	+2.662	4077.8166	.0496	+2.796
4076.9580	.6839	-0.257	4077.7478	.6998	+2.664	4077.8174	.0537	+2.793
4076.9590	.6890	-0.252	4077.7487	.7044	+2.622	4077.8195	.0644	+2.746
4076.9608	.6982	-0.262	4077.7497	.7095	+2.611	4077.8204	.0689	+2.727
4076.9633	.7109	-0.255	4077.7506	.7140	+2.607	4077.8213	.0735	+2.705
4076.9642	.7155	-0.254	4077.7515	.7186	+2.598	4077.8222	.0781	+2.706
4076.9652	.7205	-0.271	4077.7524	.7232	+2.598	4077.8230	.0822	+2.686
4076.9661	.7251	-0.291	4077.7534	.7283	+2.592	4077.8238	.0862	+2.674
4076.9671	.7302	-0.313	4077.7543	.7328	+2.597	4077.8247	.0908	+2.643
4076.9681	.7353	-0.322	4077.7552	.7374	+2.587	4077.8254	.0944	+2.657
4076.9690	.7399	-0.297	4077.7574	.7486	+2.574	4077.8263	.0989	+2.632
4076.9701	.7455	-0.291	4077.7584	.7537	+2.573	4077.8272	.1035	+2.582
4076.9715	.7526	-0.267	4077.7593	.7583	+2.572	4077.8314	.1249	+2.619
4076.9742	.7663	-0.293	4077.7601	.7623	+2.574	4077.8335	.1356	+2.629
4076.9766	.7785	-0.323	4077.7610	.7669	+2.574	4077.8343	.1396	+2.619
4076.9776	.7836	-0.323	4077.7618	.7710	+2.545	4077.8355	.1457	+2.632
4076.9784	.7877	-0.331	4077.7627	.7756	+2.544	4077.8366	.1513	+2.622
4076.9793	.7922	-0.313	4077.7637	.7806	+2.515	4077.8378	.1574	+2.651
4076.9803	.7973	-0.328	4077.7647	.7857	+2.534	4077.8393	.1600	+2.636
4076.9813	.8024	-0.340	4077.7709	.8172	+2.567	4077.8406	.1716	+2.597
4076.9822	.8070	-0.331	4077.7720	.8228	+2.565	4077.8421	.1793	+2.648
4076.9839	.8156	-0.359	4077.7730	.8279	+2.551	4077.8450	.1940	+2.607
4076.9863	.8278	-0.340	4077.7738	.8320	+2.567	4077.8463	.2006	+2.621
4076.9872	.8324	-0.360	4077.7747	.8366	+2.550	4077.8476	.2072	+2.645
4076.9881	.8370	-0.361	4077.7769	.8478	+2.525	4077.8488	.2134	+2.675
4076.9891	.8421	-0.374	4077.7779	.8528	+2.495	4077.8499	.2189	+2.666
4076.9901	.8472	-0.376	4077.7787	.8569	+2.511	4077.8509	.2240	+2.634
4076.9909	.8512	-0.376	4077.7796	.8615	+2.523	4077.8521	.2301	+2.660
4076.9919	.8563	-0.388	4077.7805	.8661	+2.523	4077.8546	.2428	+2.621
4076.9929	.8614	-0.389	4077.7814	.8706	+2.528	4077.8556	.2479	+2.641
4076.9945	.8695	-0.376	4077.7823	.8752	+2.553	4077.8568	.2540	+2.622
4076.9972	.8832	-0.391	4077.7831	.8793	+2.568	4077.8578	.2591	+2.621
4076.9981	.8878	-0.407	4077.7839	.8834	+2.576	4077.8592	.2662	+2.664
4076.9991	.8929	-0.403	4077.7862	.8950	+2.575	4077.8606	.2734	+2.637
4077.0002	.8985	-0.392	4077.7871	.8996	+2.576	4077.8617	.2789	+2.631
4077.0011	.9031	-0.405	4077.7880	.9042	+2.574	4077.8624	.2825	+2.633

TABLE 2 (Cont'd)

Julian Day 2430000+	Phase	Δ Mag	Julian Day 2430000+	Phase	Δ Mag	Julian Day 2430000+	Phase	Δ Mag
4077.8694	.3181	+2.644	4077.9401	.6776	+2.664	4078.0113	.0396	+2.960
4077.8702	.3222	+2.651	4077.9412	.6832	+2.658	4078.0123	.0447	+2.947
4077.8712	.3272	+2.666	4077.9422	.6882	+2.660	4078.0131	.0488	+2.801
4077.8721	.3318	+2.662	4077.9444	.6994	+2.697	4078.0140	.0533	+2.819
4077.8731	.3369	+2.618	4077.9454	.7045	+2.680	4078.0166	.0666	+2.697
4077.8739	.3410	+2.629	4077.9465	.7101	+2.670	4161.6742	.4340	+2.788
4077.8749	.3461	+2.631	4077.9476	.7157	+2.655	4161.6766	.4462	+2.807
4077.8758	.3506	+2.625	4077.9487	.7213	+2.643	4161.6799	.4630	+2.796
4077.8767	.3552	+2.653	4077.9499	.7274	+2.626	4161.6824	.4757	+2.772
4077.8793	.3684	+2.663	4077.9510	.7330	+2.627	4161.6860	.4940	+2.788
4077.8804	.3740	+2.634	4077.9519	.7375	+2.623	4161.6884	.5062	+2.782
4077.8814	.3791	+2.630	4077.9582	.7696	+2.567	4161.6906	.5174	+2.779
4077.8823	.3837	+2.650	4077.9592	.7747	+2.557	4161.6933	.5311	+2.790
4077.8833	.3888	+2.642	4077.9601	.7793	+2.545	4161.6955	.5423	+2.780
4077.8842	.3933	+2.635	4077.9612	.7849	+2.530	4161.6977	.5535	+2.794
4077.8852	.3984	+2.641	4077.9622	.7900	+2.536	4161.7004	.5672	+2.815
4077.8861	.4030	+2.619	4077.9631	.7945	+2.545	4161.7029	.5799	+2.814
4077.8870	.4076	+2.628	4077.9651	.8047	+2.490	4161.7051	.5911	+2.804
4077.8880	.4127	+2.611	4077.9660	.8093	+2.503	4161.7078	.6048	+2.811
4077.8889	.4172	+2.635	4077.9671	.8149	+2.527	4161.7102	.6170	+2.799
4077.8898	.4218	+2.631	4077.9681	.8200	+2.583	4161.7126	.6292	+2.833
4077.8920	.4330	+2.667	4077.9692	.8255	+2.531	4161.7158	.6455	+2.849
4077.8930	.4381	+2.653	4077.9703	.8311	+2.548	4161.7174	.6536	+2.858
4077.8939	.4427	+2.640	4077.9713	.8362	+2.553	4161.7183	.6582	+2.863
4077.8948	.4472	+2.656	4077.9723	.8413	+2.508	4161.7194	.6638	+2.861
4077.8959	.4528	+2.637	4077.9733	.8464	+2.530	4161.7205	.6694	+2.840
4077.8968	.4574	+2.645	4077.9743	.8515	+2.526	4161.7215	.6745	+2.838
4077.8977	.4620	+2.656	4077.9753	.8566	+2.524	4161.7226	.6801	+2.869
4077.8986	.4666	+2.648	4077.9763	.8616	+2.523	4161.7237	.6857	+2.892
4077.8996	.4716	+2.647	4077.9786	.8733	+2.505	4161.7253	.6938	+2.894
4077.9019	.4833	+2.658	4077.9796	.8784	+2.480	4161.7257	.6958	+2.877
4077.9029	.4884	+2.669	4077.9805	.8830	+2.490	4161.7278	.7065	+2.824
4077.9038	.4930	+2.682	4077.9813	.8871	+2.491	4161.7297	.7162	+2.759
4077.9048	.4981	+2.700	4077.9824	.8927	+2.473	4161.7300	.7177	+2.865
4077.9057	.5027	+2.700	4077.9835	.8982	+2.493	4161.7318	.7268	+2.895
4077.9068	.5083	+2.689	4077.9844	.9028	+2.522	4161.7329	.7324	+2.892
4077.9077	.5128	+2.685	4077.9853	.9074	+2.536	4161.7342	.7390	+2.925
4077.9086	.5174	+2.705	4077.9871	.9166	+2.569	4161.7354	.7452	+2.926
4077.9095	.5220	+2.687	4077.9881	.9216	+2.533	4161.7368	.7523	+2.916
4077.9155	.5525	+2.650	4077.9890	.9262	+2.546	4161.7381	.7589	+2.859
4077.9165	.5576	+2.643	4077.9899	.9256	+2.560	4161.7398	.7675	+2.867
4077.9176	.5632	+2.654	4077.9908	.9354	+2.583	4161.7402	.7696	+2.893
4077.9185	.5678	+2.641	4077.9916	.9394	+2.592	4161.7428	.7828	+2.919
4077.9195	.5728	+2.655	4077.9936	.9496	+2.630	4161.7441	.7894	+2.887
4077.9206	.5784	+2.674	4077.9946	.9547	+2.708	4161.7453	.7955	+2.855
4077.9217	.5840	+2.665	4077.9955	.9593	+2.774	4161.7466	.8021	+2.908
4077.9226	.5886	+2.649	4077.9964	.9638	+2.823	4161.7480	.8092	+2.924
4077.9252	.6018	+2.672	4077.9973	.9684	+2.905	4161.7492	.8153	+2.844
4077.9261	.6064	+2.671	4077.9981	.9725	+3.011	4161.7503	.8209	+2.824
4077.9272	.6120	+2.678	4077.9990	.9771	+3.122	4161.7523	.8311	+2.755
4077.9282	.6171	+2.676	4077.9999	.9816	+3.256	4161.7527	.8331	+2.753
4077.9292	.6222	+2.661	4078.0009	.9867	+3.348	4161.7552	.8458	+2.761
4077.9301	.6267	+2.690	4078.0018	.9913	+3.385	4161.7564	.8519	+2.784
4077.9311	.6318	+2.699	4078.0028	.9964	+3.425	4161.7573	.8565	+2.757
4077.9322	.6374	+2.676	4078.0037	.0010	+3.449	4161.7587	.8636	+2.760
4077.9348	.6506	+2.695	4078.0046	.0055	+3.410	4161.7600	.8702	+2.736
4077.9358	.6557	+2.669	4078.0056	.0106	+3.354	4161.7611	.8808	+2.752
4077.9369	.6613	+2.670	4078.0075	.0203	+3.189	4161.7627	.8840	+2.784
4077.9380	.6669	+2.668	4078.0084	.0249	+3.076	4161.7630	.8855	+2.791
4077.9390	.6720	+2.679	4078.0094	.0299	+2.989	4161.7661	.9012	+2.798

TABLE 2 (Cont'd)

Julian Day 2430000+	Phase	Δ Mag	Julian Day 2430000+	Phase	Δ Mag	Julian Day 2430000+	Phase	Δ Mag
4161.7677	.9094	+2.760	4161.8390	.2719	+2.712	4519.7327	.0268	+3.278
4161.7688	.9150	+2.741	4161.8403	.2785	+2.689	4519.7348	.0375	+3.052
4161.7700	.9211	+2.716	4161.8419	.2867	+2.700	4519.7373	.0502	+2.986
4161.7713	.9277	+2.734	4161.8424	.2892	+2.702	4519.7395	.0614	+2.925
4161.7727	.9348	+2.761	4161.8447	.3009	+2.694	4519.7416	.0720	+2.888
4161.7743	.9430	+2.785	4161.8460	.3075	+2.688	4519.7442	.0853	+2.849
4161.7749	.9460	+2.800	4161.8472	.3136	+2.680	4519.7465	.0970	+2.801
4161.7770	.9567	+2.920	4161.8484	.3197	+2.700	4519.7489	.1092	+2.776
4161.7780	.9618	+3.005	4161.8498	.3268	+2.726	4519.7515	.1224	+2.778
4161.7789	.9663	+3.076	4161.8510	.3329	+2.692	4519.7573	.1519	+2.755
4161.7797	.9704	+3.195	4161.8523	.3396	+2.710	4519.7596	.1636	+2.754
4161.7805	.9745	+3.303	4161.8531	.3436	+2.735	4519.7617	.1742	+2.791
4161.7814	.9790	+3.446	4161.8544	.3502	+2.734	4519.7645	.1885	+2.826
4161.7823	.9836	+3.535	4161.8572	.3645	+2.776	4519.7668	.2002	+2.806
4161.7832	.9882	+3.642	4161.8585	.3711	+2.771	4519.7688	.2104	+2.826
4161.7843	.9938	+3.652	4161.8601	.3792	+2.763	4519.7710	.2215	+2.826
4161.7850	.9974	+3.680	4161.8613	.3853	+2.758	4519.7731	.2322	+2.793
4161.7861	.0029	+3.680	4161.8624	.3909	+2.770	4519.7753	.2434	+2.792
4161.7870	.0075	+3.624	4161.8636	.3970	+2.791	4526.6220	.0563	+2.935
4161.7880	.0126	+3.584	4161.8653	.4056	+2.771	4526.6243	.0680	+2.915
4161.7890	.0177	+3.438	4161.8658	.4082	+2.794	4526.6265	.0792	+2.904
4161.7900	.0228	+3.278	4519.6271	.4898	+2.819	4526.6290	.0919	+2.821
4161.7907	.0263	+3.148	4519.6296	.5026	+2.805	4526.6315	.1046	+2.793
4161.7920	.0329	+3.016	4519.6320	.5148	+2.822	4526.6342	.1183	+2.785
4161.7932	.0390	+2.969	4519.6346	.5280	+2.822	4526.6365	.1300	+2.785
4161.7942	.0441	+2.926	4519.6371	.5407	+2.804	4526.6390	.1427	+2.804
4161.7956	.0512	+2.916	4519.6396	.5534	+2.799	4526.6417	.1564	+2.796
4161.7961	.0538	+2.899	4519.6421	.5661	+2.798	4526.6442	.1692	+2.811
4161.7977	.0619	+2.889	4519.6446	.5788	+2.792	4526.6502	.1997	+2.805
4161.7990	.0685	+2.866	4519.6509	.6109	+2.794	4526.6526	.2119	+2.796
4161.8002	.0746	+2.861	4519.6534	.6236	+2.808	4526.6550	.2241	+2.792
4161.8019	.0833	+2.822	4519.6558	.6358	+2.790	4526.6572	.2353	+2.796
4161.8031	.0894	+2.762	4519.6580	.6470	+2.798	4526.6598	.2485	+2.799
4161.8042	.0950	+2.743	4519.6605	.6597	+2.776	4526.6621	.2602	+2.811
4161.8053	.1006	+2.735	4519.6632	.6734	+2.765	4526.6642	.2708	+2.816
4161.8066	.1072	+2.722	4519.6657	.6861	+2.801	4526.6703	.3019	+2.793
4161.8083	.1158	+2.708	4519.6682	.6988	+2.796	4526.6727	.3141	+2.786
4161.8088	.1184	+2.688	4519.6742	.7293	+2.758	4526.6752	.3268	+2.800
4161.8114	.1316	+2.643	4519.6768	.7426	+2.710	4526.6778	.3400	+2.808
4161.8128	.1387	+2.647	4519.6795	.7563	+2.755	4526.6803	.3527	+2.820
4161.8139	.1443	+2.654	4519.6821	.7695	+2.773	4526.6825	.3629	+2.830
4161.8152	.1509	+2.665	4519.6845	.7817	+2.756	4526.6849	.3761	+2.797
4161.8164	.1570	+2.711	4519.6868	.7934	+2.763	4526.6873	.3883	+2.781
4161.8176	.1631	+2.748	4519.6887	.8031	+2.740	4526.6898	.4010	+2.801
4161.8187	.1687	+2.745	4519.6910	.8148	+2.715	4526.6972	.4386	+2.811
4161.8201	.1758	+2.755	4519.6971	.8458	+2.705	4526.6995	.4503	+2.817
4161.8219	.1850	+2.762	4519.6994	.8575	+2.707	4526.7018	.4620	+2.819
4161.8224	.1875	+2.753	4519.7018	.8697	+2.721	4526.7043	.4748	+2.820
4161.8240	.1956	+2.711	4519.7043	.8824	+2.724	4526.7066	.4864	+2.807
4161.8252	.2018	+2.706	4519.7067	.8946	+2.713	4526.7090	.4986	+2.793
4161.8263	.2074	+2.676	4519.7087	.9048	+2.715	4526.7118	.5129	+2.782
4161.8276	.2140	+2.701	4519.7110	.9164	+2.768	4526.7143	.5256	+2.796
4161.8288	.2201	+2.703	4519.7167	.9454	+2.794	4526.7167	.5378	+2.800
4161.8301	.2267	+2.717	4519.7192	.9582	+2.958	4526.7190	.5495	+2.779
4161.8312	.2323	+2.698	4519.7210	.9673	+3.096	4526.7251	.5805	+2.792
4161.8326	.2394	+2.697	4519.7230	.9775	+3.414	4526.7276	.5932	+2.773
4161.8339	.2460	+2.717	4519.7249	.9871	+3.646	4526.7301	.6059	+2.777
4161.8350	.2516	+2.707	4519.7268	.9968	+3.785	4526.7325	.6181	+2.762
4161.8365	.2592	+2.704	4519.7286	.0059	+3.764	4526.7351	.6314	+2.772
4161.8376	.2648	+2.714	4519.7307	.0166	+3.600	4526.7376	.6441	+2.783

TABLE 2 (Cont'd)

Julian Day 2430000+	Phase	Δ Mag	Julian Day 2430000+	Phase	Δ Mag	Julian Day 2430000+	Phase	Δ Mag
4531.6270	.5048	+2.807	4534.6407	.8283	+2.738	4542.6637	.6223	+2.815
4531.6291	.5155	+2.807	4534.6429	.8395	+2.727	4542.6657	.6325	+2.820
4531.6314	.5272	+2.788	4534.6449	.8497	+2.719	4542.6705	.6569	+2.791
4531.6366	.5536	+2.744	4534.6471	.8609	+2.696	4542.6724	.6665	+2.772
4531.6390	.5658	+2.757	4534.6491	.8710	+2.701	4542.6745	.6772	+2.777
4531.6409	.5755	+2.759	4534.6510	.8807	+2.712	4542.6765	.6974	+2.783
4531.6458	.6004	+2.793	4534.6532	.8919	+2.721	4542.6787	.6986	+2.763
4531.6481	.6121	+2.797	4534.6551	.9016	+2.695	4542.6806	.7082	+2.751
4531.6503	.6233	+2.783	4534.6569	.9107	+2.731	4542.6872	.7418	+2.722
4531.6525	.6345	+2.784	4534.6589	.9209	+2.746	4542.6894	.7530	+2.737
4531.6596	.6706	+2.772	4534.6633	.9432	+2.812	4542.6912	.7621	+2.759
4531.6621	.6833	+2.814	4534.6873	.0653	+2.900	4542.6932	.7723	+2.757
4531.6643	.6945	+2.773	4534.6892	.0749	+2.894	4542.6949	.7810	+2.727
4531.6664	.7051	+2.773	4534.6940	.0994	+2.826	4542.6969	.7911	+2.752
4533.5267	.6725	+2.767	4534.6958	.1085	+2.808	4542.6995	.8043	+2.718
4533.6287	.6827	+2.772	4535.6468	.9440	+2.762	4542.7013	.8135	+2.717
4533.6307	.6929	+2.768	4535.6484	.9522	+2.812	4542.7035	.8247	+2.723
4533.6325	.7020	+2.777	4535.6503	.9618	+2.931	4542.7096	.8557	+2.702
4533.6346	.7127	+2.756	4535.6520	.9704	+3.103	4542.7112	.8638	+2.719
4533.6367	.7234	+2.750	4535.6538	.9796	+3.377	4542.7118	.8669	+2.730
4533.6384	.7320	+2.750	4535.6556	.9888	+3.538	4542.7124	.8699	+2.721
4533.6438	.7595	+2.699	4535.6574	.9979	+3.651	4542.7131	.8735	+2.717
4533.6457	.7692	+2.717	4535.6595	.0085	+3.608	4542.7136	.8760	+2.707
4533.6478	.7798	+2.688	4535.6614	.0182	+3.438	4542.7142	.8791	+2.687
4533.6500	.7910	+2.706	4535.6634	.0284	+3.172	4542.7147	.8816	+2.717
4533.6520	.8012	+2.689	4535.6657	.0401	+2.980	4542.7152	.8842	+2.702
4533.6537	.8098	+2.720	4535.6679	.0512	+2.904	4542.7159	.8877	+2.719
4533.6556	.8195	+2.708	4535.6701	.0624	+2.862	4542.7164	.8903	+2.723
4533.6571	.8271	+2.677	4535.6721	.0726	+2.826	4542.7169	.8928	+2.734
4533.6590	.8368	+2.702	4535.6743	.0838	+2.816	4542.7174	.8954	+2.740
4533.6610	.8470	+2.676	4535.6791	.1082	+2.711	4542.7180	.8984	+2.724
4533.6659	.8719	+2.655	4535.6812	.1189	+2.708	4542.7187	.9020	+2.701
4533.6680	.8825	+2.695	4535.6833	.1296	+2.725	4542.7192	.9045	+2.721
4533.6700	.8927	+2.673	4535.6856	.1412	+2.743	4542.7197	.9070	+2.757
4533.6721	.9034	+2.681	4535.6878	.1524	+2.734	4542.7202	.9096	+2.744
4533.6738	.9120	+2.721	4535.6899	.1631	+2.736	4542.7306	.9625	+3.003
4533.6763	.9247	+2.721	4535.6949	.1885	+2.746	4542.7312	.9655	+3.049
4533.6812	.9497	+2.825	4535.6970	.1992	+2.757	4542.7318	.9686	+3.121
4533.6832	.9598	+2.952	4535.7021	.2251	+2.766	4542.7324	.9716	+3.177
4533.6852	.9700	+3.159	4535.7045	.2374	+2.771	4542.7329	.9742	+3.284
4533.6986	.0381	+3.046	4535.7063	.2465	+2.782	4542.7334	.9767	+3.381
4533.7024	.0574	+2.934	4535.7083	.2567	+2.761	4542.7340	.9798	+3.458
4533.7046	.0686	+2.884	4535.7140	.2856	+2.775	4542.7347	.9833	+3.523
4533.7093	.0925	+2.821	4535.7161	.2963	+2.783	4542.7351	.9854	+3.586
4533.7113	.1027	+2.789	4535.7183	.3075	+2.790	4542.7358	.9889	+3.618
4533.7134	.1134	+2.759	4535.7207	.3197	+2.800	4542.7363	.9914	+3.638
4533.7160	.1266	+2.765	4535.7231	.3319	+2.794	4542.7369	.9945	+3.671
4533.7214	.1541	+2.757	4535.7255	.3441	+2.787	4542.7375	.9976	+3.699
4533.7247	.1708	+2.760	4542.6359	.4810	+2.822	4542.7381	.0006	+3.685
4533.7273	.1841	+2.761	4542.6380	.4916	+2.824	4542.7386	.0032	+3.729
4533.7299	.1973	+2.777	4542.6403	.5033	+2.834	4542.7393	.0067	+3.705
4533.7326	.2110	+2.760	4542.6424	.5140	+2.817	4542.7399	.0098	+3.670
4533.7353	.2247	+2.772	4542.6446	.5252	+2.805	4542.7406	.0133	+3.649
4534.6237	.7419	+2.789	4542.6466	.5354	+2.831	4542.7411	.0159	+3.543
4534.6261	.7541	+2.758	4542.6518	.5618	+2.816	4542.7417	.0189	+3.506
4534.6278	.7627	+2.740	4542.6536	.5710	+2.816	4542.7424	.0225	+3.414
4534.6298	.7729	+2.742	4542.6557	.5816	+2.803	4542.7430	.0255	+3.312
4534.6319	.7836	+2.737	4542.6577	.5918	+2.805	4542.7436	.0286	+3.225
4534.6370	.8095	+2.731	4542.6596	.6015	+2.786	4542.7441	.0311	+3.149
4534.6388	.8187	+2.751	4542.6618	.6126	+2.803	4542.7448	.0347	+3.096

TABLE 2 (Cont'd)

Julian Day 2430000+	Phase	Δ Mag	Julian Day 2430000+	Phase	Δ Mag	Julian Day 2430000+	Phase	Δ Mag
4542.7456	.0387	+3.063	4542.7485	.0535	+2.984	4542.7509	.0657	+2.931
4542.7461	.0413	+3.044	4542.7492	.0570	+2.954	4542.7514	.0682	+2.898
4542.7467	.0443	+3.031	4542.7497	.0596	+2.931	4542.7521	.0718	+2.885
4542.7472	.0469	+3.019	4542.7503	.0626	+2.935	4542.7530	.0764	+2.923
4542.7479	.0504	+2.987						

TABLE 3

Photometric Observations of UX Ursae Majoris (Ultraviolet)

Julian Day 2430000+	Phase	Δ Mag	Julian Day 2430000+	Phase	Δ Mag	Julian Day 2430000+	Phase	Δ Mag
3785.6494	.4892	+1.690	3785.7851	.1792	+1.598	4076.7377	.5638	+0.230
3785.6521	.5030	+1.775	3785.7891	.1996	+1.554	4076.7409	.5800	+0.229
3785.6550	.5177	+1.774	3785.7995	.2524	+1.599	4076.7443	.5973	+0.389
3785.6623	.5548	+1.765	3785.8033	.2718	+1.628	4076.7474	.6131	+0.382
3785.6653	.5701	+1.740	3785.8077	.2941	+1.546	4076.7506	.6294	+0.313
3785.6685	.5864	+1.741	3785.8191	.3521	+1.655	4076.7537	.6451	+0.338
3785.6770	.6296	+1.794	3785.8231	.3724	+1.652	4076.7568	.6609	+0.318
3785.6799	.6443	+1.874	3785.8270	.3923	+1.591	4076.7600	.6772	+0.317
3785.6829	.6596	+1.823	3785.8368	.4421	+1.689	4076.7634	.6950	+0.297
3785.6900	.6957	+1.979	3785.8406	.4614	+1.738	4076.7670	.7128	+0.264
3785.6931	.7114	+1.715	3785.8444	.4808	+1.686	4076.7705	.7306	+0.234
3785.6959	.7257	+1.651	3785.8527	.5230	+1.691	4076.7739	.7478	+0.245
3785.7061	.7775	+1.828	3785.8556	.5377	+1.716	4076.7773	.7651	+0.245
3785 7090	.7923	+1.840	3785.8586	.5530	+1.725	4076.7808	.7829	+0.209
3785.7120	.8075	+1.798	3785.8659	.5901	+1.791	4076.7841	.7997	+0.136
3785.7199	.8477	+1.695	3785.8693	.6074	+1.791	4076.7875	.8170	+0.125
3785.7236	.8665	+1.714	3785.8726	.6241	+1.788	4076.7909	.8296	+0.120
3785.7270	.8838	+1.759	3785.8823	.6735	+1.807	4076.7943	.8516	+0.112
3785.7343	.9209	+1.748	3785.8856	.6902	+1.853	4076.7976	.8684	+0.074
3785.7374	.9367	+1.728	4076.6997	.3706	+0.306	4076.8007	.8841	+0.082
3785.7405	.9524	+1.839	4076.7030	.3873	+0.290	4076.8038	.8999	+0.107
3785.7478	.9896	+2.562	4076.7071	.4082	+0.315	4076.8071	.9166	+0.097
3785.7506	.0038	+2.477	4076.7116	.4311	+0.213	4076.8088	.9253	+0.129
3785.7537	.0196	+2.093	4076.7160	.4534	+0.342	4076.8098	.9304	+0.144
3785.7568	.0353	+1.764	4076.7197	.4723	+0.276	4076.8107	.9350	+0.130
3785.7600	.0516	+1.664	4076.7228	.4880	+0.303	4076.8117	.9400	+0.143
3785.7629	.0664	+1.581	4076.7259	.5038	+0.262	4076.8130	.9467	+0.182
3785.7699	.1019	+1.551	4076.7289	.5190	+0.305	4076.8140	.9517	+0.218
3785.7730	.1177	+1.573	4076.7317	.5333	+0.264	4076.8149	.9563	+0.231
3785.7821	.1640	+1.610	4076.7346	.5480	+0.335	4076.8159	.9614	+0.233

TABLE 3 (Cont'd)

Julian Day 2430000+	Phase	Δ Mag	Julian Day 2430000+	Phase	Δ Mag	Julian Day 2430000+	Phase	Δ Mag
4076.8169	.9665	+0.343	4076.9296	.5395	+0.368	4077.0023	.9092	+0.138
4076.8178	.9711	+0.482	4076.9306	.5446	+0.377	4077.0033	.9143	+0.233
4076.8187	.9756	+0.630	4076.9327	.5553	+0.347	4077.0043	.9194	+0.151
4076.8196	.9802	+0.766	4076.9350	.5670	+0.388	4077.0068	.9321	+0.263
4076.8205	.9848	+0.903	4076.9359	.5716	+0.328	4077.0084	.9402	+0.192
4076.8215	.9899	+0.969	4076.9368	.5761	+0.297	4077.0093	.9448	+0.208
4076.8225	.9950	+1.016	4076.9378	.5812	+0.269	4077.0103	.9499	+0.248
4076.8235	.0000	+1.058	4076.9387	.5858	+0.258	4077.0127	.9621	+0.324
4076.8244	.0046	+1.020	4076.9398	.5914	+0.282	4077.0151	.9743	+0.615
4076.8254	.0097	+0.927	4076.9408	.5965	+0.267	4077.0177	.9875	+0.994
4076.8263	.0143	+0.848	4076.9417	.6010	+0.207	4077.7256	.5869	+1.609
4076.8274	.0199	+0.757	4076.9426	.6056	+0.238	4077.7319	.6190	+1.622
4076.8283	.0244	+0.574	4076.9435	.6102	+0.297	4077.7333	.6261	+1.592
4076.8293	.0295	+0.415	4076.9444	.6148	+0.306	4077.7342	.6306	+1.598
4076.8302	.0341	+0.342	4076.9472	.6290	+0.415	4077.7351	.6352	+1.626
4076.8312	.0392	+0.317	4076.9488	.6372	+0.431	4077.7359	.6393	+1.627
4076.8321	.0438	+0.298	4076.9498	.6422	+0.420	4077.7369	.6444	+1.602
4076.8331	.0489	+0.328	4076.9507	.6468	+0.438	4077.7393	.6566	+1.623
4076.8341	.0539	+0.305	4076.9516	.6514	+0.424	4077.7395	.6576	+1.617
4076.8350	.0585	+0.295	4076.9526	.6565	+0.382	4077.7411	.6657	+1.657
4076.8359	.0631	+0.318	4076.9536	.6616	+0.342	4077.7420	.6703	+1.694
4076.8367	.0672	+0.297	4076.9546	.6666	+0.325	4077.7429	.6749	+1.653
4076.8375	.0712	+0.294	4076.9556	.6717	+0.302	4077.7438	.6795	+1.656
4076.8403	.0855	+0.315	4076.9565	.6763	+0.242	4077.7448	.6845	+1.653
4076.8469	.1190	+0.239	4076.9574	.6809	+0.223	4077.7472	.6968	+1.672
4076.8508	.1389	+0.196	4076.9583	.6855	+0.284	4077.7481	.7013	+1.668
4076.8549	.1597	+0.238	4076.9592	.6900	+0.297	4077.7490	.7059	+1.629
4076.8591	.1811	+0.202	4076.9618	.7032	+0.352	4077.7499	.7105	+1.604
4076.8820	.2975	+0.348	4076.9636	.7124	+0.373	4077.7508	.7150	+1.611
4076.8859	.3173	+0.226	4076.9645	.7170	+0.341	4077.7517	.7196	+1.600
4076.8897	.3466	+0.271	4076.9655	.7221	+0.340	4077.7527	.7247	+1.584
4076.8946	.3616	+0.306	4076.9664	.7266	+0.305	4077.7536	.7293	+1.571
4076.8978	.3778	+0.225	4076.9674	.7317	+0.254	4077.7545	.7339	+1.558
4076.8994	.3860	+0.347	4076.9683	.7363	+0.261	4077.7555	.7390	+1.526
4076.9006	.3921	+0.328	4076.9694	.7419	+0.280	4077.7577	.7501	+1.551
4076.9015	.3966	+0.331	4076.9705	.7475	+0.299	4077.7586	.7547	+1.530
4076.9023	.4007	+0.276	4076.9718	.7541	+0.307	4077.7595	.7593	+1.528
4076.9033	.4058	+0.273	4076.9752	.7714	+0.226	4077.7604	.7639	+1.512
4076.9041	.4099	+0.320	4076.9769	.7800	+0.163	4077.7612	.7679	+1.475
4076.9050	.4144	+0.272	4076.9778	.7846	+0.212	4077.7621	.7725	+1.438
4076.9059	.4190	+0.282	4076.9787	.7892	+0.200	4077.7630	.7771	+1.431
4076.9091	.4353	+0.278	4076.9796	.7938	+0.215	4077.7639	.7817	+1.420
4076.9107	.4434	+0.296	4076.9806	.7988	+0.181	4077.7650	.7872	+1.435
4076.9116	.4480	+0.279	4076.9815	.8034	+0.165	4077.7713	.8193	+1.439
4076.9125	.4526	+0.317	4076.9825	.8085	+0.158	4077.7723	.8244	+1.421
4076.9134	.4572	+0.315	4076.9848	.8202	+0.117	4077.7732	.8290	+1.449
4076.9144	.4622	+0.320	4076.9865	.8288	+0.163	4077.7741	.8335	+1.455
4076.9152	.4663	+0.344	4076.9875	.8339	+0.151	4077.7749	.8376	+1.450
4076.9161	.4709	+0.327	4076.9884	.8385	+0.136	4077.7773	.8498	+1.412
4076.9170	.4755	+0.327	4076.9894	.8436	+0.113	4077.7782	.8544	+1.366
4076.9179	.4800	+0.320	4076.9903	.8482	+0.134	4077.7790	.8584	+1.369
4076.9188	.4846	+0.331	4076.9912	.8527	+0.104	4077.7799	.8630	+1.419
4076.9198	.4897	+0.304	4076.9921	.8573	+0.083	4077.7807	.8671	+1.421
4076.9228	.5050	+0.313	4076.9932	.8629	+0.099	4077.7816	.8717	+1.460
4076.9240	.5110	+0.305	4076.9957	.8756	+0.132	4077.7825	.8762	+1.478
4076.9249	.5156	+0.285	4076.9975	.8848	+0.092	4077.7834	.8808	+1.510
4076.9258	.5202	+0.250	4076.9985	.8899	+0.094	4077.7841	.8844	+1.507
4076.9267	.5248	+0.238	4076.9994	.8944	+0.086	4077.7865	.8966	+1.496
4076.9277	.5299	+0.281	4077.0005	.9000	+0.059	4077.7874	.9012	+1.479
4076.9286	.5344	+0.352	4077.0014	.9046	+0.084	4077.7882	.9052	+1.496

TABLE 3 (Cont'd)

Julian Day 2430000+	Phase	Δ Mag	Julian Day 2430000+	Phase	Δ Mag	Julian Day 2430000+	Phase	Δ Mag
4077.7891	.9098	+1.518	4077.8696	.3191	+1.557	4077.9404	.6791	+1.649
4077.7900	.9144	+1.505	4077.8706	.3242	+1.566	4077.9415	.6847	+1.695
4077.7958	.9439	+1.480	4077.8715	.3288	+1.602	4077.9426	.6903	+1.710
4077.7968	.9490	+1.530	4077.8724	.3334	+1.590	4077.9447	.7010	+1.744
4077.7985	.9576	+1.586	4077.8733	.3379	+1.542	4077.9458	.7066	+1.749
4077.7994	.9622	+1.579	4077.8744	.3435	+1.561	4077.9469	.7122	+1.758
4077.8003	.9667	+1.663	4077.8752	.3476	+1.545	4077.9480	.7178	+1.726
4077.8011	.9708	+1.763	4077.8761	.3522	+1.574	4077.9491	.7233	+1.693
4077.8019	.9749	+1.910	4077.8771	.3572	+1.603	4077.9503	.7294	+1.662
4077.8028	.9794	+2.003	4077.8796	.3700	+1.571	4077.9512	.8340	+1.661
4077.8036	.9835	+2.133	4077.8807	.3756	+1.531	4077.9522	.7391	+1.608
4077.8044	.9876	+2.214	4077.8816	.3774	+1.560	4077.9584	.7706	+1.507
4077.8053	.9922	+2.295	4077.8827	.3857	+1.580	4077.9594	.7757	+1.488
4077.8061	.9962	+2.350	4077.8836	.3903	+1.533	4077.9605	.7813	+1.444
4077.8087	.0094	+2.243	4077.8845	.3949	+1.528	4077.9615	.7864	+1.442
4077.8095	.0135	+2.204	4077.8855	.4000	+1.528	4077.9625	.7915	+1.450
4077.8103	.0176	+2.133	4077.8864	.4045	+1.499	4077.9634	.7960	+1.456
4077.8112	.0222	+2.031	4077.8873	.4091	+1.527	4077.9653	.8057	+1.372
4077.8120	.0262	+1.892	4077.8882	.4137	+1.519	4077.9664	.8113	+1.421
4077.8128	.0303	+1.836	4077.8891	.4183	+1.553	4077.9674	.8164	+1.461
4077.8136	.0344	+1.745	4077.8900	.4228	+1.538	4077.9685	.8220	+1.470
4077.8144	.0384	+1.688	4077.8923	.4345	+1.603	4077.9695	.8271	+1.468
4077.8152	.0425	+1.657	4077.8933	.4396	+1.579	4077.9706	.8327	+1.510
4077.8160	.0466	+1.667	4077.8942	.4442	+1.584	4077.9716	.8377	+1.456
4077.8169	.0512	+1.640	4077.8952	.4493	+1.615	4077.9726	.8428	+1.414
4077.8177	.0552	+1.651	4077.8961	.4538	+1.562	4077.9735	.8474	+1.423
4077.8197	.0654	+1.601	4077.8970	.4584	+1.585	4077.9746	.8530	+1.416
4077.8207	.0705	+1.603	4077.8980	.4635	+1.612	4077.9756	.8581	+1.383
4077.8216	.0750	+1.586	4077.8990	.4686	+1.580	4077.9765	.8627	+1.414
4077.8224	.0791	+1.620	4077.8999	.4732	+1.597	4077.9788	.8744	+1.392
4077.8233	.0837	+1.595	4077.9023	.4854	+1.621	4077.9798	.8794	+1.349
4077.8241	.0876	+1.609	4077.9032	.4900	+1.683	4077.9807	.8840	+1.344
4077.8249	.0918	+1.548	4077.9041	.4945	+1.703	4077.9817	.8891	+1.355
4077.8257	.0959	+1.582	4077.9051	.4996	+1.725	4077.9826	.8937	+1.349
4077.8265	.1000	+1.579	4077.9061	.5047	+1.727	4077.9837	.8993	+1.390
4077.8274	.1045	+1.498	4077.9070	.5093	+1.684	4077.9847	.9044	+1.443
4077.8316	.1259	+1.537	4077.9080	.5144	+1.661	4077.9856	.9089	+1.447
4077.8337	.1366	+1.530	4077.9089	.5189	+1.665	4077.9874	.9181	+1.443
4077.8346	.1412	+1.528	4077.9098	.5235	+1.670	4077.9883	.9227	+1.379
4077.8358	.1472	+1.548	4077.9158	.5540	+1.586	4077.9893	.9277	+1.384
4077.8369	.1528	+1.556	4077.9168	.5591	+1.614	4077.9901	.9318	+1.419
4077.8383	.1600	+1.584	4077.9178	.5642	+1.617	4077.9910	.9364	+1.428
4077.8397	.1671	+1.537	4077.9189	.5698	+1.621	4077.9919	.9410	+1.420
4077.8411	.1742	+1.501	4077.9198	.5744	+1.653	4077.9939	.9511	+1.426
4077.8424	.1808	+1.569	4077.9210	.5805	+1.679	4077.9949	.9562	+1.559
4077.8453	.1956	+1.520	4077.9219	.5850	+1.672	4077.9958	.9608	+1.606
4077.8467	.2027	+1.547	4077.9229	.5901	+1.625	4077.9967	.9654	+1.675
4077.8479	.2088	+1.613	4077.9255	.6033	+1.664	4077.9975	.9694	+1.766
4077.8491	.2149	+1.671	4077.9265	.6084	+1.658	4077.9983	.9735	+1.893
4077.8501	.2200	+1.831	4077.9275	.6135	+1.672	4077.9992	.9781	+2.030
4077.8513	.2261	+1.567	4077.9285	.6186	+1.665	4078.0003	.9837	+2.201
4077.8524	.2316	+1.575	4077.9294	.6232	+1.675	4078.0012	.9882	+2.295
4077.8549	.2444	+1.525	4077.9304	.6283	+1.706	4078.0021	.9928	+2.329
4077.8560	.2500	+1.554	4077.9315	.6338	+1.675	4078.0031	.9979	+2.353
4077.8572	.2561	+1.524	4077.9325	.6389	+1.706	4078.0040	.0025	+2.336
4077.8583	.2616	+1.523	4077.9351	.6522	+1.708	4078.0049	.0071	+2.311
4077.8596	.2683	+1.578	4077.9362	.6578	+1.672	4078.0057	.0111	+2.203
4077.8609	.2749	+1.553	4077.9373	.6633	+1.685	4078.0078	.0218	+2.001
4077.8614	.2774	+1.529	4077.9383	.6684	+1.676	4078.0087	.0264	+1.890
4077.8627	.2840	+1.509	4077.9394	.6740	+1.684	4078.0097	.0315	+1.800

TABLE 3 (Cont'd)

Julian Day 2430000+	Phase	Δ Mag	Julian Day 2430000+	Phase	Δ Mag	Julian Day 2430000+	Phase	Δ Mag
4078.0116	.0411	+1.729	4161.7680	.9109	+1.779	4161.8394	.2740	+1.599
4078.0125	.0457	+1.728	4161.7691	.9165	+1.738	4161.8406	.2801	+1.585
4078.0134	.0503	+1.732	4161.7705	.9236	+1.698	4161.8428	.2912	+1.578
4078.0143	.0549	+1.708	4161.7717	.9297	+1.691	4161.8433	.2938	+1.579
4078.0174	.0706	+1.558	4161.7730	.9363	+1.702	4161.8451	.3029	+1.567
4161.6749	.4375	+1.709	4161.7752	.9475	+1.742	4161.8463	.3090	+1.584
4161.6781	.4538	+1.691	4161.7757	.9501	+1.778	4161.8476	.3156	+1.607
4161.6808	.4675	+1.707	4161.7774	.9587	+1.804	4161.8488	.3218	+1.631
4161.6831	.4792	+1.721	4161.7783	.9633	+1.901	4161.8502	.3289	+1.659
4161.6869	.4986	+1.757	4161.7791	.9674	+2.004	4161.8513	.3345	+1.588
4161.6891	.5097	+1.733	4161.7799	.9714	+2.162	4161.8526	.3411	+1.610
4161.6912	.5204	+1.692	4161.7808	.9760	+2.372	4161.8547	.3518	+1.688
4161.6940	.5346	+1.747	4161.7816	.9801	+2.511	4161.8554	.3553	+1.732
4161.6961	.5453	+1.732	4161.7826	.9852	+2.613	4161.8576	.3665	+1.733
4161.6984	.5570	+1.740	4161.7836	.9902	+2.725	4161.8588	.3726	+1.701
4161.7011	.5708	+1.752	4161.7845	.9948	+2.749	4161.8604	.3807	+1.667
4161.7036	.5835	+1.745	4161.7854	.9994	+2.784	4161.8616	.3868	+1.670
4161.7058	.5946	+1.765	4161.7864	.0045	+2.753	4161.8628	.3929	+1.715
4161.7085	.6084	+1.797	4161.7873	.0090	+2.655	4161.8640	.3990	+1.708
4161.7110	.6211	+1.756	4161.7883	.0141	+2.539	4161.8660	.4092	+1.725
4161.7134	.6333	+1.914	4161.7893	.0193	+2.262	4161.8666	.4123	+1.709
4161.7165	.6490	+1.855	4161.7903	.0243	+2.057	4519.6280	.4944	+1.763
4161.7176	.6546	+1.879	4161.7911	.0284	+1.899	4519.6303	.5061	+1.762
4161.7187	.6602	+1.886	4161.7925	.0355	+1.779	4519.6328	.5188	+1.748
4161.7197	.6653	+1.889	4161.7935	.0406	+1.736	4519.6353	.5316	+1.789
4161.7208	.6709	+1.844	4161.7944	.0452	+1.743	4519.6379	.5448	+1.750
4161.7219	.6765	+1.847	4161.7966	.0563	+1.772	4519.6404	.5575	+1.782
4161.7230	.6821	+1.941	4161.7970	.0584	+1.743	4519.6428	.5697	+1.788
4161.7241	.6877	+1.920	4161.7980	.0634	+1.751	4519.6453	.5824	+1.785
4161.7259	.6968	+1.915	4161.7993	.0701	+1.731	4519.6518	.6154	+1.741
4161.7264	.6994	+1.860	4161.8008	.0777	+1.763	4519.6541	.6271	+1.768
4161.7281	.7080	+1.849	4161.8022	.0848	+1.701	4519.6565	.6393	+1.758
4161.7304	.7197	+1.954	4161.8034	.0909	+1.639	4519.6587	.6505	+1.731
4161.7308	.7218	+1.954	4161.8044	.0960	+1.637	4519.6615	.6648	+1.749
4161.7322	.7289	+2.050	4161.8058	.1031	+1.650	4519.6640	.6775	+1.731
4161.7333	.7345	+2.072	4161.8069	.1087	+1.611	4519.6666	.6907	+1.813
4161.7346	.7411	+2.115	4161.8091	.1199	+1.562	4519.6691	.7034	+1.874
4161.7358	.7472	+2.159	4161.8096	.1224	+1.563	4519.6750	.7334	+1.656
4161.7372	.7543	+2.108	4161.8117	.1331	+1.511	4519.6776	.7466	+1.626
4161.7384	.7604	+2.055	4161.8131	.1402	+1.501	4519.6803	.7604	+1.729
4161.7406	.7716	+2.129	4161.8143	.1463	+1.507	4519.6828	.7731	+1.810
4161.7410	.7736	+2.148	4161.8156	.1529	+1.553	4519.6853	.7858	+1.782
4161.7431	.7843	+2.039	4161.8167	.1585	+1.602	4519.6873	.7960	+1.744
4161.7445	.7914	+2.027	4161.8180	.1651	+1.665	4519.6895	.8071	+1.643
4161.7458	.7980	+2.024	4161.8191	.1707	+1.646	4519.6917	.8183	+1.588
4161.7469	.8036	+2.147	4161.8205	.1779	+1.609	4519.6978	.8493	+1.565
4161.7483	.8107	+2.102	4161.8227	.1890	+1.604	4519.7002	.8615	+1.615
4161.7495	.8168	+1.978	4161.8232	.1916	+1.538	4519.7026	.8737	+1.596
4161.7508	.8235	+1.964	4161.8243	.1972	+1.538	4519.7050	.8860	+1.647
4161.7532	.8357	+1.719	4161.8256	.2038	+1.544	4519.7074	.8982	+1.625
4161.7536	.8377	+1.721	4161.8268	.2099	+1.500	4519.7096	.9093	+1.702
4161.7555	.8474	+1.871	4161.8279	.2155	+1.545	4519.7117	.9200	+1.766
4161.7567	.8535	+1.874	4161.8292	.2221	+1.538	4519.7176	.9500	+1.699
4161.7577	.8585	+1.784	4161.8306	.2292	+1.585	4519.7197	.9607	+1.831
4161.7592	.8662	+1.732	4161.8317	.2348	+1.559	4519.7217	.9709	+2.054
4161.7603	.8718	+1.708	4161.8329	.2409	+1.559	4519.7236	.9805	+2.437
4161.7615	.8779	+1.771	4161.8342	.2475	+1.596	4519.7255	.9902	+2.738
4161.7635	.8880	+1.869	4161.8354	.2536	+1.593	4519.7274	.9998	+2.820
4161.7639	.8901	+1.859	4161.8368	.2607	+1.600	4519.7292	.0090	+2.701
4161.7666	.9038	+1.888	4161.8380	.2668	+1.587	4519.7314	.0202	+2.414

TABLE 3 (Cont'd)

Julian Day 2430000+	Phase	Δ Mag	Julian Day 2430000+	Phase	Δ Mag	Julian Day 2430000+	Phase	Δ Mag
4519.7334	.0304	+1.982	4531.6277	.5084	+1.734	4534.6414	.8319	+1.826
4519.7356	.0415	+1.805	4531.6298	.5190	+1.746	4534.6435	.8426	+1.790
4519.7379	.0532	+1.836	4531.6320	.5302	+1.769	4534.6455	.8527	+1.721
4519.7402	.0649	+1.813	4531.6373	.5572	+1.734	4534.6478	.8644	+1.692
4519.7424	.0761	+1.739	4531.6396	.5689	+1.668	4534.6497	.8741	+1.749
4519.7451	.0898	+1.702	4531.6415	.5785	+1.729	4534.6516	.8838	+1.781
4519.7474	.1015	+1.710	4531.6467	.6050	+1.787	4534.6538	.8950	+1.759
4519.7498	.1137	+1.674	4531.6487	.6151	+1.767	4534.6557	.9046	+1.668
4519.7522	.1259	+1.678	4531.6510	.6268	+1.766	4534.6576	.9143	+1.687
4519.7580	.1554	+1.628	4531.6532	.6380	+1.767	4534.6594	.9234	+1.701
4519.7603	.1671	+1.659	4531.6604	.6746	+1.751	4534.6641	.9473	+1.719
4519.7632	.1819	+1.682	4531.6627	.6863	+1.790	4534.6879	.0683	+1.822
4519.7653	.1926	+1.723	4531.6648	.6970	+1.768	4534.6898	.0780	+1.822
4519.7675	.2037	+1.702	4531.6671	.7087	+1.774	4534.6945	.1019	+1.770
4519.7695	.2139	+1.688	4533.6273	.6756	+1.771	4534.6965	.1121	+1.734
4519.7716	.2246	+1.662	4533.6292	.6852	+1.814	4535.6473	.9466	+1.647
4519.7738	.2358	+1.651	4533.6313	.6959	+1.721	4535.6490	.9552	+1.717
4519.7760	.2470	+1.686	4533.6332	.7056	+1.772	4535.6508	.9644	+1.854
4526.6226	.0593	+1.795	4533.6353	.7163	+1.704	4535.6526	.9735	+2.111
4526.6250	.0715	+1.793	4533.6372	.7259	+1.721	4535.6543	.9822	+2.475
4526.6273	.0832	+1.793	4533.6391	.7356	+1.698	4535.6562	.9918	+2.688
4526.6297	.0954	+1.724	4533.6443	.7620	+1.737	4535.6581	.0015	+2.744
4526.6321	.1076	+1.718	4533.6464	.7727	+1.727	4535.6600	.0111	+2.606
4526.6349	.1219	+1.692	4533.6485	.7834	+1.656	4535.6620	.0212	+2.292
4526.6372	.1336	+1.670	4533.6505	.7936	+1.679	4535.6640	.0314	+1.967
4526.6397	.1463	+1.715	4533.6523	.8027	+1.701	4535.6664	.0436	+1.794
4526.6425	.1605	+1.694	4533.6542	.8124	+1.798	4535.6687	.0553	+1.769
4526.6449	.1727	+1.712	4533.6562	.8225	+1.683	4535.6707	.0655	+1.771
4526.6509	.2032	+1.687	4533.6576	.8297	+1.610	4535.6729	.0767	+1.756
4526.6534	.2159	+1.657	4533.6594	.8388	+1.636	4535.6749	.0868	+1.757
4526.6556	.2271	+1.687	4533.6617	.8505	+1.650	4535.6797	.1112	+1.656
4526.6579	.2388	+1.678	4533.6665	.8749	+1.599	4535.6817	.1214	+1.655
4526.6606	.2526	+1.707	4533.6686	.8856	+1.652	4535.6840	.1331	+1.668
4526.6628	.2637	+1.707	4533.6707	.8963	+1.597	4535.6863	.1448	+1.674
4526.6654	.2770	+1.724	4533.6726	.9059	+1.659	4535.6885	.1560	+1.643
4526.6710	.3054	+1.694	4533.6745	.9156	+1.669	4535.6906	.1667	+1.672
4526.6734	.3176	+1.718	4533.6768	.9273	+1.642	4535.6955	.1916	+1.677
4526.6760	.3308	+1.725	4533.6817	.9522	+1.727	4535.6977	.2028	+1.730
4526.6785	.3436	+1.715	4533.6839	.9634	+1.869	4535.7027	.2282	+1.688
4526.6810	.3563	+1.723	4533.6856	.9720	+2.132	4535.7050	.2399	+1.730
4526.6833	.3680	+1.702	4533.6994	.0422	+1.875	4535.7069	.2496	+1.703
4526.6867	.3853	+1.716	4533.7030	.0605	+1.820	4535.7089	.2597	+1.697
4526.6881	.3924	+1.702	4533.7051	.0712	+1.778	4535.7147	.2892	+1.705
4526.6904	.4041	+1.720	4533.7099	.0956	+1.742	4535.7167	.2994	+1.769
4526.6979	.4422	+1.758	4533.7119	.1058	+1.722	4535.7193	.3126	+1.727
4526.7002	.4539	+1.714	4533.7143	.1180	+1.737	4535.7214	.3233	+1.748
4526.7027	.4666	+1.759	4533.7167	.1302	+1.737	4535.7237	.3350	+1.716
4526.7050	.4783	+1.721	4533.7222	.1581	+1.706	4535.7263	.3482	+1.733
4526.7072	.4895	+1.767	4533.7256	.1754	+1.691	4542.6366	.4845	+1.799
4526.7098	.5027	+1.752	4533.7287	.1912	+1.690	4542.6388	.4957	+1.802
4526.7126	.5170	+1.739	4533.7306	.2008	+1.704	4542.6410	.5069	+1.822
4526.7150	.5292	+1.750	4533.7334	.2151	+1.697	4542.6430	.5170	+1.796
4526.7174	.5414	+1.691	4533.7358	.2273	+1.703	4542.6452	.5282	+1.826
4526.7199	.5541	+1.726	4534.6242	.7444	+1.849	4542.6473	.5389	+1.752
4526.7259	.5846	+1.773	4534.6266	.7566	+1.765	4542.6524	.5648	+1.791
4526.7284	.5973	+1.733	4534.6285	.7663	+1.750	4542.6543	.5743	+1.840
4526.7308	.6095	+1.756	4534.6305	.7765	+1.752	4542.6563	.5847	+1.829
4526.7332	.6217	+1.727	4534.6325	.7866	+1.755	4542.6584	.5954	+1.793
4526.7358	.6349	+1.706	4534.6375	.8121	+1.740	4542.6604	.6055	+1.780
4526.7385	.6486	+1.753	4534.6394	.8217	+1.788	4542.6625	.6162	+1.773

TABLE 3 (Cont'd)

Julian Day 2430000+	Phase	Δ Mag	Julian Day 2430000+	Phase	Δ Mag	Julian Day 2430000+	Phase	Δ Mag
4542.6643	.6254	+1.835	4542.7154	.8852	+1.663	4542.7389	.0047	+2.736
4542.6662	.6350	+1.829	4542.7161	.8887	+1.697	4542.7395	.0077	+2.722
4542.6710	.6594	+1.764	4542.7166	.8913	+1.712	4542.7401	.0108	+2.695
4542.6730	.6696	+1.743	4542.7171	.8938	+1.724	4542.7407	.0138	+2.566
4542.6751	.6803	+1.775	4542.7176	.8964	+1.713	4542.7414	.0174	+2.495
4542.6772	.6910	+1.785	4542.7181	.8989	+1.674	4542.7419	.0199	+2.429
4542.6793	.7016	+1.752	4542.7188	.9025	+1.658	4542.7426	.0235	+2.286
4542.6813	.7118	+1.747	4542.7194	.9055	+1.702	4542.7432	.0265	+2.153
4542.6877	.7443	+1.699	4542.7199	.9081	+1.697	4542.7438	.0296	+2.013
4542.6899	.7555	+1.737	4542.7204	.9106	+1.688	4542.7444	.0326	+1.966
4542.6919	.7657	+1.725	4542.7298	.9584	+1.820	4542.7450	.0357	+1.931
4542.6938	.7754	+1.707	4542.7308	.9635	+1.891	4542.7458	.0398	+1.902
4542.6956	.7845	+1.700	4542.7314	.9665	+1.939	4542.7463	.0423	+1.903
4542.6978	.7957	+1.720	4542.7319	.9691	+2.038	4542.7469	.0454	+1.931
4542.7001	.8074	+1.680	4542.7326	.9726	+2.112	4542.7475	.0484	+1.891
4542.7018	.8160	+1.685	4542.7331	.9752	+2.259	4542.7481	.0514	+1.960
4542.7043	.8287	+1.691	4542.7336	.9777	+2.387	4542.7488	.0550	+1.852
4542.7106	.8608	+1.631	4542.7342	.9808	+2.495	4542.7493	.0576	+1.828
4542.7115	.8654	+1.670	4542.7348	.9838	+2.560	4542.7500	.0611	+1.804
4542.7119	.8674	+1.695	4542.7354	.9869	+2.631	4542.7505	.0636	+1.805
4542.7125	.8704	+1.696	4542.7359	.9894	+2.658	4542.7511	.0667	+1.810
4542.7132	.8740	+1.666	4542.7365	.9925	+2.732	4542.7517	.0698	+1.789
4542.7138	.8770	+1.642	4542.7372	.9960	+2.768	4542.7522	.0723	+1.791
4542.7143	.8796	+1.664	4542.7376	.9981	+2.748	4542.7535	.0789	+1.839
4542.7149	.8826	+1.672	4542.7383	.0016	+2.771			

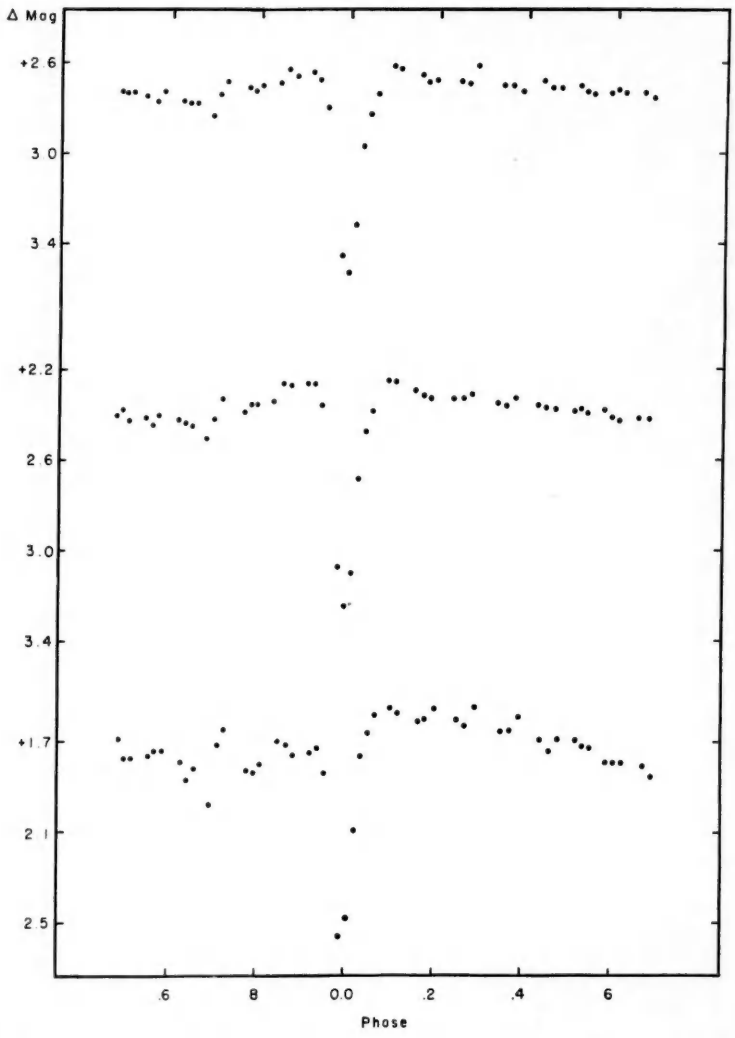

FIG. 1.—Light-curves of UX Ursae Majoris on May 19, 1953, for three effective wave lengths: yellow above, blue center, and ultraviolet below.

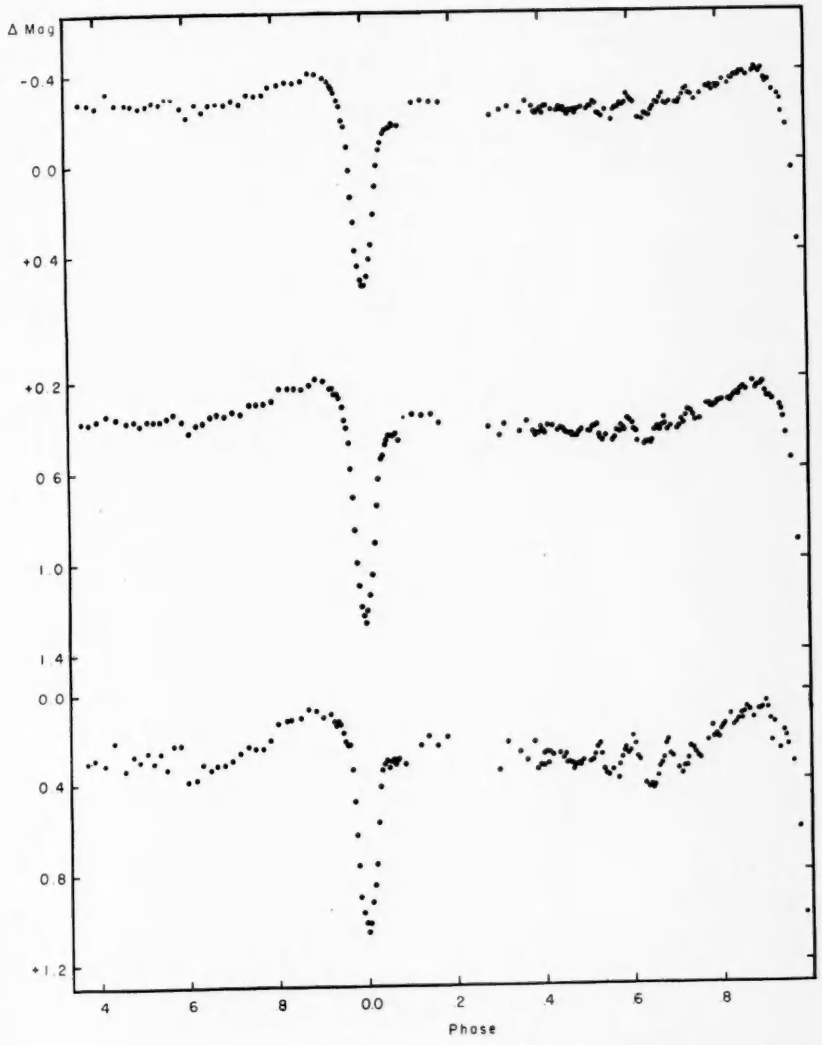

FIG. 2.—Light-curves of UX Ursae Majoris on March 5, 1952, for three effective wave lengths: yellow above, blue center, and ultraviolet below.

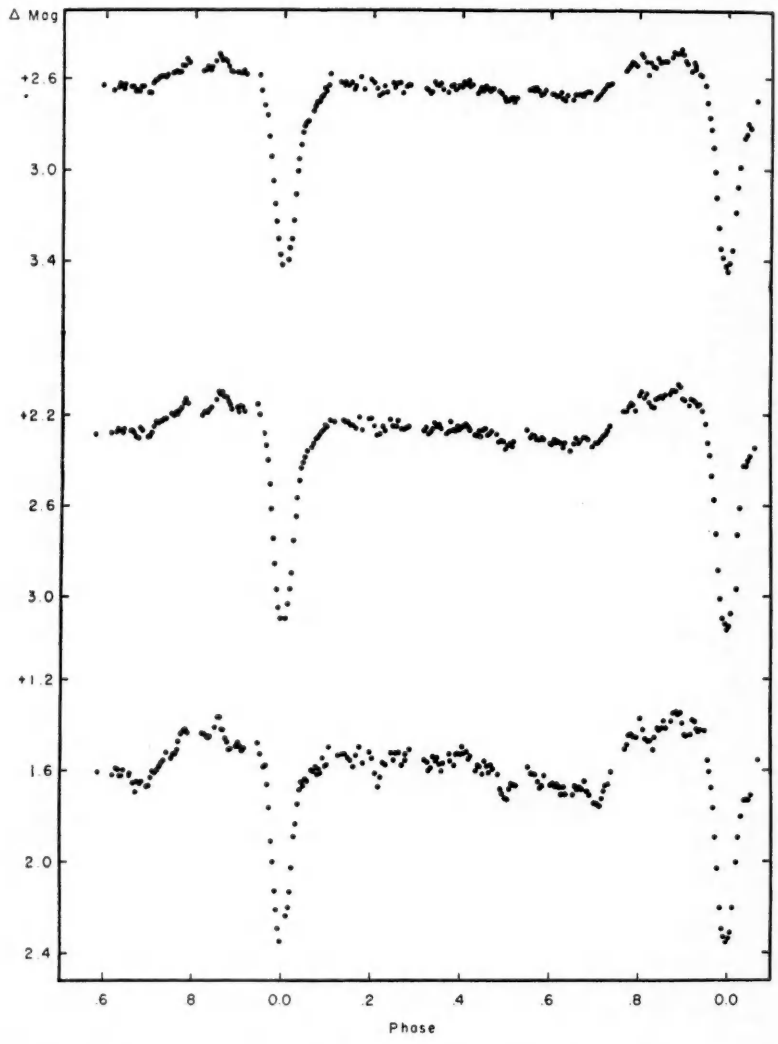

FIG. 3.—Light-curves of UX Ursae Majoris on March 6, 1952, for three effective wave lengths: yellow above, blue center, and ultraviolet below.

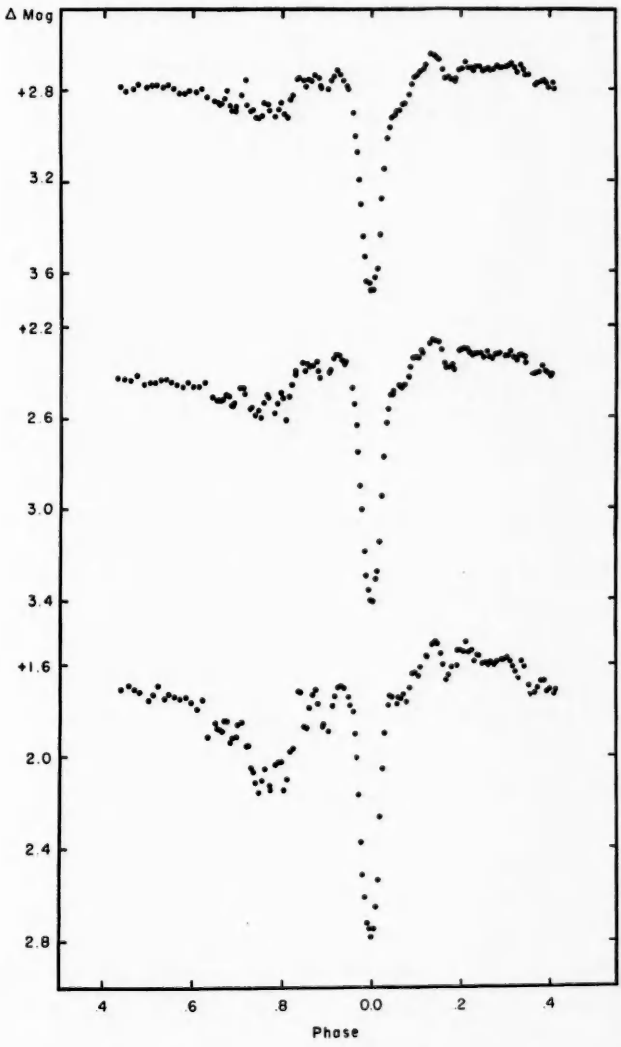

FIG. 4.—Light-curves of UX Ursae Majoris on May 29, 1952, for three effective wave lengths: yellow above, blue center, and ultraviolet below.

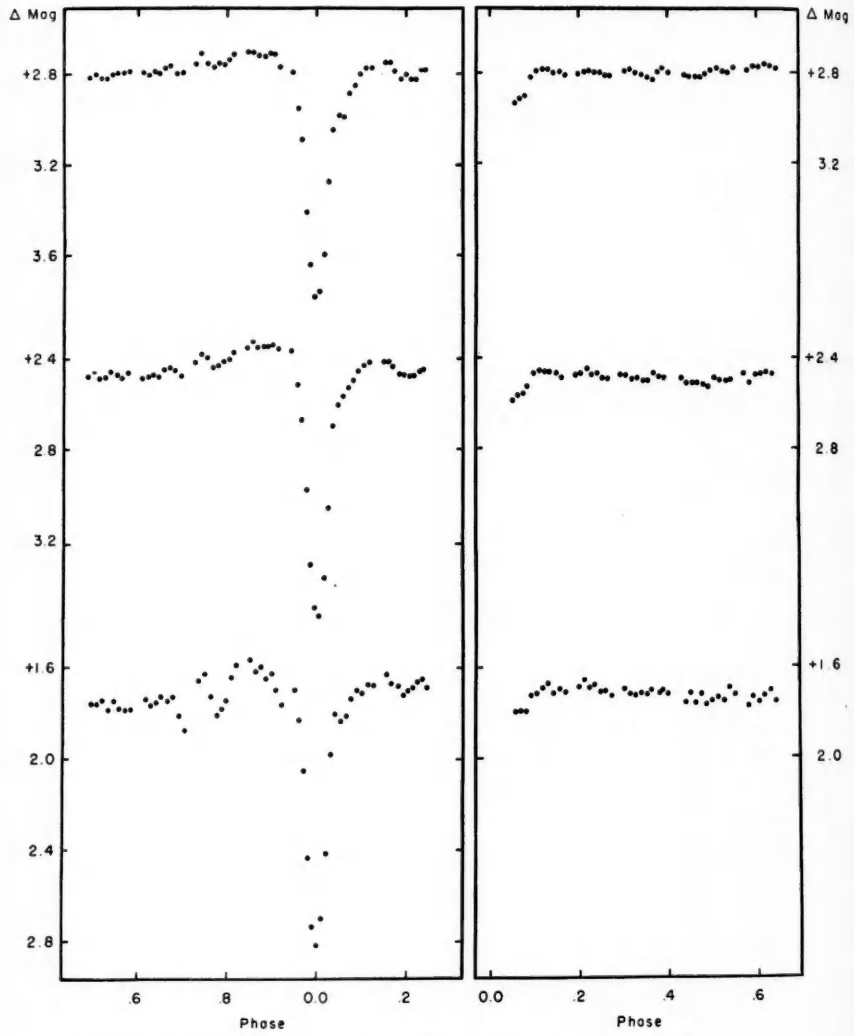

FIG. 5.—Light-curves of UX Ursae Majoris on May 22, 1953 (*left*), and May 29, 1953 (*right*), for three effective wave lengths: yellow above, blue center, and ultraviolet below.

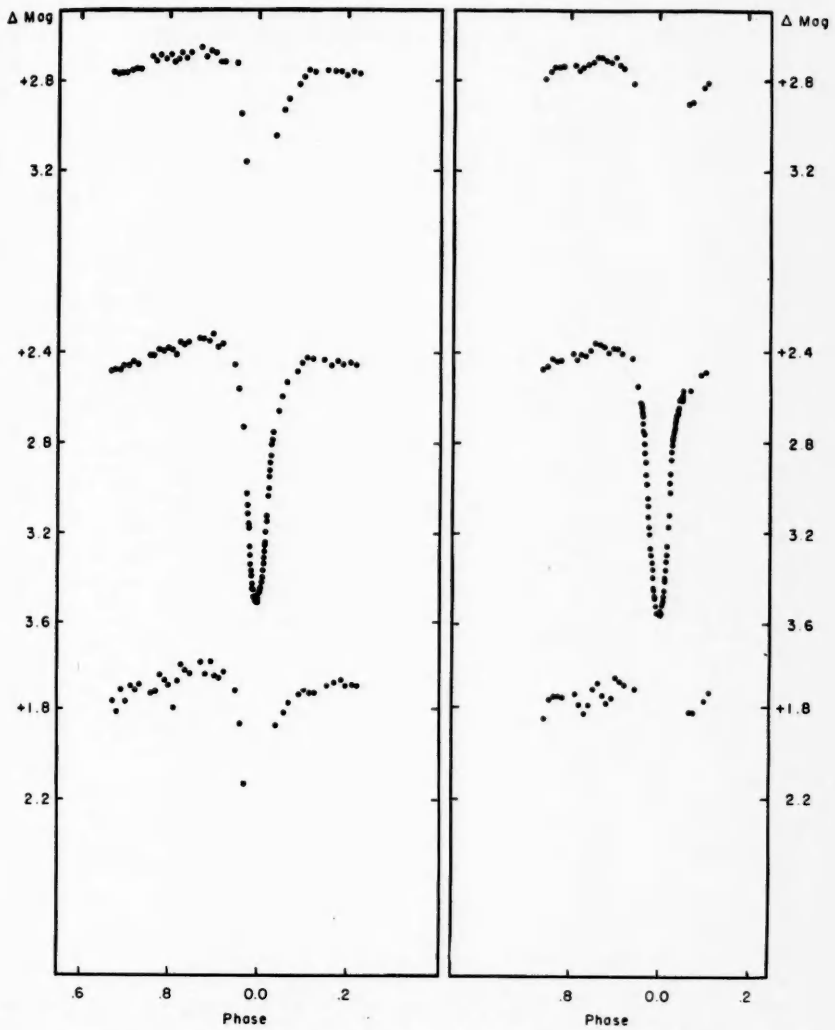

FIG. 6.—Light-curves of UX Ursae Majoris on June 5, 1953 (*left*), and June 6, 1953 (*right*), for three effective wave lengths: yellow above, blue center, and ultraviolet below.

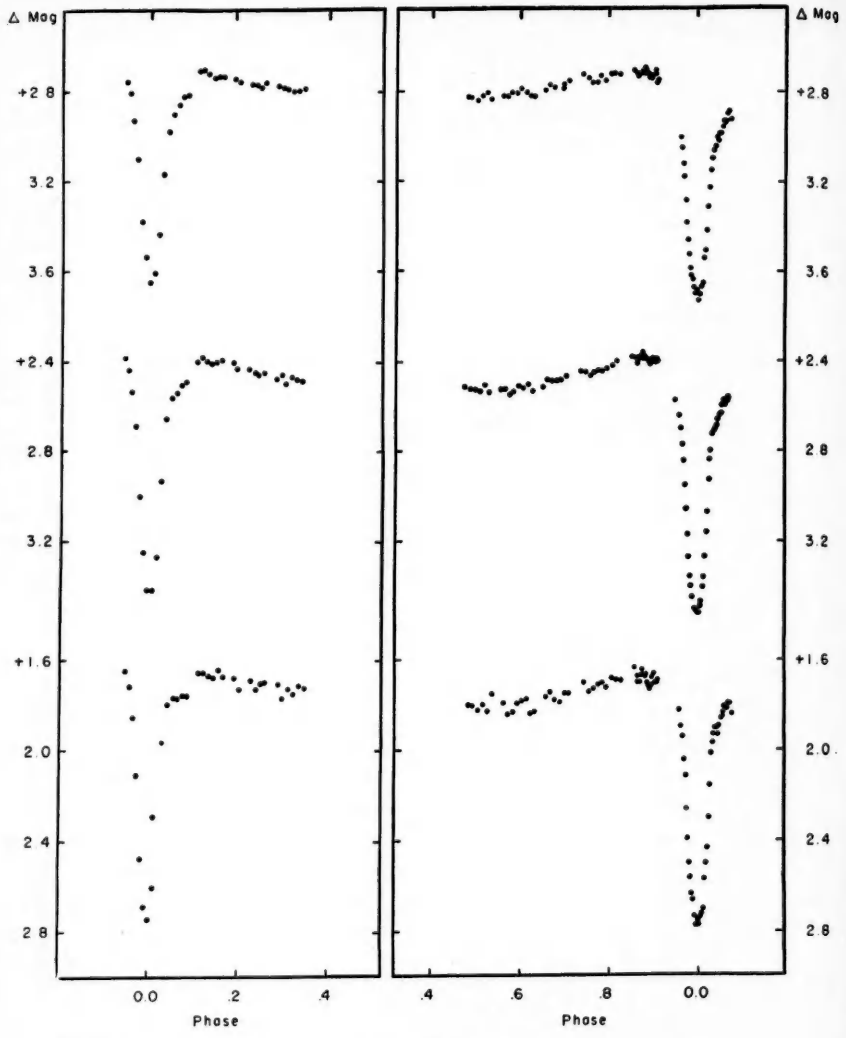

FIG. 7.—Light-curves of UX Ursae Majoris on June 7, 1953 (*left*), and June 14, 1953 (*right*), for three effective wave lengths: yellow above, blue center, and ultraviolet below.

TABLE 4

Observer	Color	Observed Time of Minimum	O−C
Zverev and Kukarkin		2427307.3949	+0.0003
Zverev and Kukarkin		27329.4219	+ .0001
Zverev and Kukarkin		27338.2728	+ .0008
Zverev and Kukarkin		27339.2562	+ .0008
Zverev and Kukarkin		27341.2221	.0000
Zverev and Kukarkin		27341.4195	+ .0007
Zverev and Kukarkin		27342.2052	− .0003
Zverev and Kukarkin		27356.5632	+ .0007
Zverev and Kukarkin		27482.4316	− .0006
Zverev and Kukarkin		27532.3873	+ .0006
Zverev and Kukarkin		27534.3537	+ .0003
Zverev and Kukarkin		27543.3996	− .0007
Zverev and Kukarkin		27566.4100	− .0008
Zverev and Kukarkin		27671.4335	+ .0002
Zverev and Kukarkin		27680.2828	− .0008
Zverev and Kukarkin		27722.5680	+ .0001
Zverev and Kukarkin		28013.4446	− .0003
Zverev and Kukarkin		28095.2601	− .0001
Zverev and Kukarkin		28248.4674	+ .0002
Zverev and Kukarkin		28252.3993	− .0013
Zverev and Kukarkin		28301.3714	− .0004
Lange		30960.171	− .001
Linnell		32971.7257	− .0013
Linnell		32971.9325	+ .0088
Linnell		33000.8331	− .0013
Hiltner		33003.7837	− .0007
Linnell		33004.7673	− .0005
Linnell		33011.6503	− .0010
Linnell		33011.8470	− .0010
Linnell		33066.7172	− .0021
Johnson, Perkins, and Hiltner		33785.7489	− .0009
Johnson, Perkins, and Hiltner	Blue	34076.82356	+ .00007
Johnson, Perkins, and Hiltner	Yellow	34076.82353	+ .00007
Johnson, Perkins, and Hiltner	Ultraviolet	34076.82334	− .00015
Johnson, Perkins, and Hiltner	Blue	34077.80703	+ .00018
Johnson, Perkins, and Hiltner	Yellow	34077.80712	+ .00027
Johnson, Perkins, and Hiltner	Ultraviolet	34077.80710	+ .00025
Johnson, Perkins, and Hiltner	Blue	34078.0032	− .0003
Johnson, Perkins, and Hiltner	Yellow	34078.0033	− .0002
Johnson, Perkins, and Hiltner	Ultraviolet	34078.0030	.0000
Johnson, Perkins, and Hiltner	Blue	34161.78516	− .00036
Johnson, Perkins, and Hiltner	Yellow	34161.78516	− .00036
Johnson, Perkins, and Hiltner	Ultraviolet	34161.78492	− .00060
Johnson, Perkins, and Hiltner	Blue	34519.72751	+ .00008
Johnson, Perkins, and Hiltner	Yellow	34519.72751	+ .00008
Johnson, Perkins, and Hiltner	Ultraviolet	34519.72535	− .00008
Johnson, Perkins, and Hiltner	Blue	34533.69105	− .00005
Johnson, Perkins, and Hiltner	Blue	34534.67446	.00000
Johnson, Perkins, and Hiltner	Blue	34535.65791	+ .00009
Johnson, Perkins, and Hiltner	Yellow	34535.65795	+ .00013
Johnson, Perkins, and Hiltner	Ultraviolet	34535.65773	− .00009
Johnson, Perkins, and Hiltner	Blue	34542.73803	+ .00004
Johnson, Perkins, and Hiltner	Yellow	34542.73811	+ .00012
Johnson, Perkins, and Hiltner	Ultraviolet	34542.73789	−0.00010

In discussing the times of minima, mention should be made of a comparison with wave length. When the ultraviolet data are compared with the yellow and blue, it is seen that the eclipse in the ultraviolet occurs, in the mean, 0.00019 days (16 seconds) earlier than the yellow and 0.00015 days earlier than the blue. The existence of this phenomenon appears to be well established but may have one of several interpretations of asymmetry in the system. The "occulting center" of the eclipsing star may be dependent on wave length, or the "radiating center" of the eclipsed star may not be superimposed for all wave lengths. Also, if the principal eclipse is not identically asymmetrical for all wave lengths, then a fictitious difference in times of minima may result from the observations, for the time of minimum is dependent upon the bisection of the minimum at various depths.

An examination of the individual light-curves of UX UMa readily reveals that a normal light-curve does not exist for this system. A comparison of, say, May 29, 1952, with, for example, any other curve shows differences as large as 0.5 mag. However, a more or less typical curve can be established. It consists of a principal minimum of about 1.1

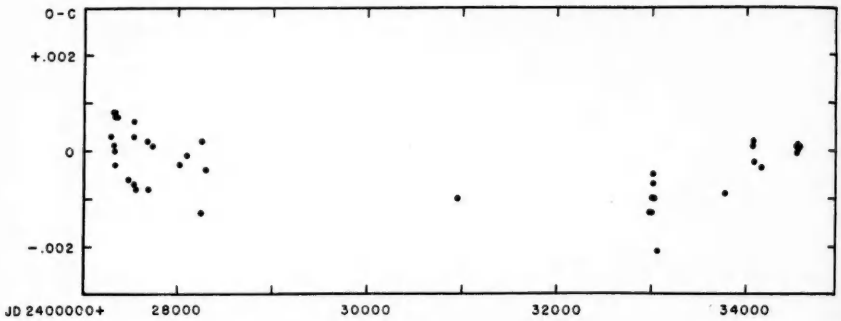

FIG. 8.—The observed times of principal minimum for UX Ursae Majoris. The O−C is in days

mag., a standstill on the ascending branch of the principal minimum, a gradual decrease in brightness from phase 0.1 to phase 0.7, when the system brightens to a maximum at phase 0.9. No secondary minimum has been observed.

The most persistent feature of the light-curve other than the principal minimum is the standstill observed by Linnell[4] on the ascending branch of this minimum. It is present to a greater or lesser degree on all the observed curves, with the possible exception of May 19, 1951. The standstill is most pronounced on the ultraviolet curves (see, e.g., June 7, 1953; March 5, 1952; etc.). It will be seen that all the abnormalities of the curves are emphasized in the ultraviolet.

The second most marked characteristic of the light-curves is the short-period fluctuations also first observed by Linnell.[5] In addition to fluctuations of very short period, not resolved by the present observations, one can observe variations in brightness that have a period of about 20 minutes. The light-curve of March 5, 1952, is a very good example. Their amplitudes are variable, with the ultraviolet always about twice that of either the blue or the yellow. Amplitudes as large as 0.4 mag. have been noted. These fluctuations may be observed at any phase but are seen most frequently between phases 0.4 and 0.8.

[4] *Harvard College Obs. Circ.*, No. 455.

[5] *Ibid.*; see also Merle F. Walker, *Pub. A.S.P.*, **65**, 206, 1953.

Of particular note are the observations of May 29, 1952. The light-curve for this night differs significantly from that of any other. In addition to the pronounced decrease in magnitude at phase 0.8 and maximum light, which occurs after principal minimum, the system as a whole is 0.4 mag. too faint. Variations in magnitude outside eclipse are more erratic and greater in amplitude than on any other night. To explain this decrease in over-all brightness and the large and erratic fluctuations, it may be necessary to introduce a veiling of the whole system by an irregular hydrogen "envelope."

One general feature of the light-curve of this star appears to confirm Struve's suggestion that at phase near 0.7 the hydrogen Balmer series is strong and that this strengthening of the Balmer lines is due to a "mass of gas at relatively low pressure on that hemisphere of the primary which is visible when this component is receding."[6] Also, the variation in the magnitude of the depression at this phase may well account for the variation

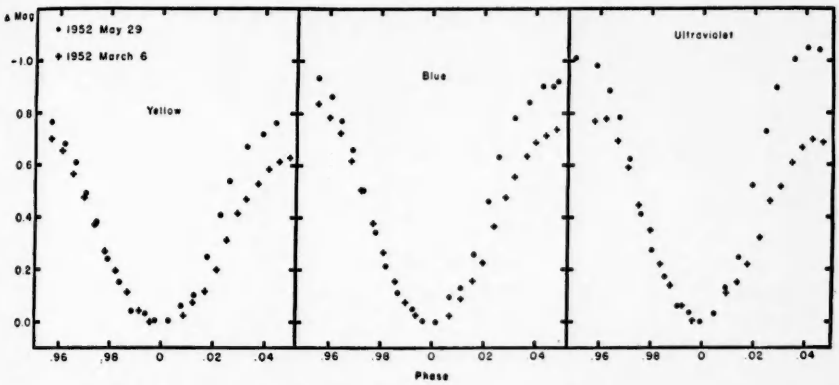

FIG. 9.—Principal minima of UX Ursae Majoris. Note the remarkable changes from one epoch to another.

in hydrogen absorption lines also observed by Struve, for it is seen that this depression is always more pronounced in the ultraviolet, which is a measure of the Balmer absorption.

Another significant feature of the light-curves is the variations in depth and shape of principal minimum. The variation in shape can be easily illustrated. In Figure 9 the minima of March 6 and May 29, 1952, are plotted. May 29 shows very little, if any, asymmetry, while that on March 6 is obvious. The changes in the depths of minimum are more difficult to establish, since a reliable magnitude reference point on the light-curve is not available. However, if maximum light, wherever it may occur, is used as a reference, the depths of minimum vary by 0.18 mag. in the yellow, 0.21 in the blue, and 0.30 in the ultraviolet. These changes in depth of minimum may represent a variation in the surface brightness of the primary star; but it is more probable that they represent a variation in the absorption of a mass of gas similar to that referred to above within the system which obliterates any significance of the adopted magnitude reference. It appears that, in general, the anomalies of the light-curve of UX UMa can best be interpreted in terms of absorption of radiation from the primary star rather than the existence of bright areas on the surface of the primary star.

[6] *Ap. J.*, **108**, 154, 1948.

ON NUCLEAR REACTIONS OCCURRING IN VERY HOT STARS. I. THE SYNTHESIS OF ELEMENTS FROM CARBON TO NICKEL

F. HOYLE*

MOUNT WILSON AND PALOMAR OBSERVATORIES
CARNEGIE INSTITUTION OF WASHINGTON
CALIFORNIA INSTITUTE OF TECHNOLOGY

Received December 22, 1953

ABSTRACT

The present paper aims to show that the abundances of the chemical elements over the portion of the periodic table from carbon to nickel are consistent with the view that the elements originate at the high temperatures that probably occur in the interiors of certain types of star. The argument takes its most definite form in the discussion of the synthesis of elements below sodium, where it seems that the abundances are in fairly close accord with the known properties of the various nuclei. For sodium and heavier elements sufficiently precise nuclear data are not available, and hence the argument becomes more qualitative than quantitative. Nevertheless, the general nature of the agreement between calculation and observation for these latter nuclei makes the discussion of them worth presenting.

The early parts of the paper are concerned with the relation to cosmogony of the theory of the origin of the elements.

I. INTRODUCTION

The purpose of the investigation of which this paper forms a part is to examine the changes of chemical composition that occur when material inside a star is heated to higher and higher temperatures. The heating of the material is due to the gravitational energy released by the shrinkage of the star. In this connection it may be noted that, so long as the shrinkage is not extremely rapid (i.e., not in a few hours, minutes, or seconds), the condition of hydrostatic equilibrium must be satisfied in a high degree of approximation. A generalized form of the virial theorem can then be established, requiring that the total gravitational potential—measured positively—must be equal to twice the total heat content of the star. Thus, since the gravitational potential of the star increases during shrinkage, the heat content (and hence the temperature) must increase correspondingly. The temperatures under consideration will lie considerably above the temperatures occurring in ordinary main-sequence stars and are to be thought of as temperatures attained in a collapsing sequence following the exhaustion of hydrogen in luminous stars.

Perhaps the best observational indication of the existence of collapsing stars comes from the faint blue stars present in the globular clusters and also in regions of the sky near the galactic pole. These stars are of type II.

Now supernovae of type I occur among the type II stars. Although it is not known with certainty where in a color-magnitude diagram the presupernova state lies, the balance of evidence would favor the view that it should be taken as among these same blue collapsing stars. That is to say, the same stars in which exceptional nuclear reactions occur at very high temperatures may well be the stars that by explosion come to scatter their materials into space. It is suggested that it is by this process that elements other than hydrogen and helium are built up and distributed in the universe. The present paper is, however, restricted to a discussion of elements in the periodic table ranging from carbon to nickel.

This suggestion derives some plausibility from the circumstance that the total quantity of material passing through the process can be seen to be roughly of the required

* Normally at St. John's College, Cambridge.

amount. Let us begin the argument with the globular-cluster stars. Recent observational evidence[1] indicates that the number of stars in active evolution in a typical globular cluster is of the order of 30,000. Moreover, the evidence suggests that the number of star deaths that have occurred in a globular cluster is probably also of the same order—the argument for this being that the observations require the number of star deaths in the *next* three billion years to be of the order of 30,000, and presumably the number that occurred during the *last* three billion years was of a similar order. Next, we may say that if the difference in luminosity between the type II population in M31, for example, and the luminosity of a typical globular cluster is due simply to a difference in the number of evolving stars in the two cases and not to some systematic difference between the stellar populations, the comparison requires the number of evolving stars in M31 to be of the order of 3×10^8, the number in our own Galaxy being by implication of a similar order. On this basis the total number of type II star deaths in M31, and in the Galaxy, must have been about 3×10^8. A last step would be to say that *if* each star death produced an explosion that distributed an average of 1 solar mass in space, then the total mass involved in the process would be of the order of $3 \times 10^8 \odot$. This mass, in the form of elements heavier than helium, is close to the amount that is required to explain their observed total abundance in the Galaxy.

Objection can be taken to the last step, however, on the grounds than 3×10^8 supernovae of type I is too great a number to have occurred in the history of even a large galaxy such as our own. Thus, even if we take the age of the Galaxy to be as high as 10^{10} years and even if the type I supernova rate is taken as an average of 1 per 300 years, the total number of supernovae of type I is still only about 3×10^7.

The explanation of this discrepancy is probably that the masses of the majority of dying stars are of the order of $1.2\odot$, whereas only a minority of stars with masses exceeding Chandrasekhar's limit (about $1.44\odot$ for stars without hydrogen) become supernovae. Thus most dying stars probably evolve without explosion, the evolution proceeding smoothly until the white-dwarf state is reached. This view is supported by the circumstance that, although 3×10^8 is too large a number for the supernovae that have occurred in the Galaxy, it is not too large for the number of stars that have evolved into white dwarfs.

These considerations suggest that the material provided by supernovae of type I should probably be placed at about $3 \times 10^7 \odot$, not at $3 \times 10^8 \odot$, and this reduced estimate is now too low by a factor of about 10. This may be taken as showing that supernovae of type I alone are not adequate to explain the total abundance of all elements heavier than helium. The supernovae of type I are indeed adequate to explain the total abundance of elements heavier than neon, but not that of the carbon, oxygen, and neon group, which exceeds the total abundance of heavier elements by a factor of about 10, this being just the order of the discrepancy revealed by the present discussion.

An attractive resolution of the difficulty would be to argue that the bulk of the lighter elements—carbon, oxygen, and neon—are produced in ejecting stars other than the supernovae, in particular, in the ejecting stars of population I.

It should be stressed at this stage, however, that the theory developed below is in no way dependent on the acceptance of such cosmogonic speculations. The theory deals with the nuclear processes that arise in stellar material at high temperatures (about 10^8 ° K), irrespective of the processes of evolution that cause such temperatures to arise. Nevertheless, discussions of the origin of the elements raise so many questions, both cosmogonic and cosmological, that some consideration of them, by way of introduction, does not seem out of place.

With this in mind, it is perhaps permissible to go on to a brief discussion of the particular cosmological framework into which the writer would seek to fit the present theory.

[1] I am indebted to A. R. Sandage and H. C. Arp for information concerning the results of their counts of stars in globular clusters.

This is outlined in Figure 1. The galaxies, which are taken as forming from an extragalactic cloud, are shown as consisting of interstellar gas (this is a nearly negligible component in the case of elliptical galaxies), ordinary noncollapsing stars, and collapsing stars. Heavy elements are generated and scattered into space by the latter, or by a proportion of them. The scattering process may lead either to the heavy elements being trapped inside interstellar gas or to their escaping entirely from the parent-galaxy into the extragalactic medium. In this connection it may be noted that the velocities of ejection from many exploding stars—the novae and supernovae in particular—considerably exceed the velocities of escape from the galaxies. Consequently, unless stopped by collisions with interstellar gas, the material ejected from such stars must move out into extragalactic space. Trapping of ejected material by interstellar gas may be taken as considerable in the spiral galaxies but not in the ellipticals.

The enrichment in this way of the heavy-element component of an extragalactic gas cloud means that even if the cloud were initially pure hydrogen, only the first galaxies formed could be of pure hydrogen. Subsequent galactic condensations must contain

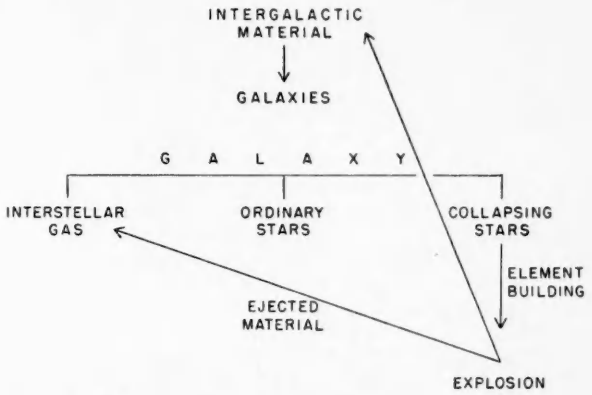

FIG. 1.—The general cosmological framework assumed for this discussion

heavy elements ejected from the "first" galaxies. Strictly speaking, the concept of "first" galaxies can be applied only in cosmologies that assign a finite age to the universe. In the steady-state theory of the universe, on the other hand, there are no "first" galaxies in the present sense, since, in this theory, the universe has an infinite past. Consequently, at all times the extragalactic material must contain heavy elements that were ejected from previously existing galaxies. Accordingly, all galaxies should possess heavy elements at the time of their birth.

An interesting estimate can be made on the basis of the steady-state cosmology. Let M be the total mass of the galaxies within a volume V, which is taken large enough to contain a reasonable average sample of the universe (say of dimensions 10^7 psc). As an order-of-magnitude estimate, we take M/V to be 10^{-29} gm/cm^3. Then, since in the steady-state cosmology[2] the mean space density of matter is 10^{-28} gm/cm^3, the mass of the uncondensed material in the volume V must be about $10M$. Now the extragalactic material is renewed (according to the theory) by continuous creation of new hydrogen in a time equal to one-third of Hubble's constant T, now estimated as 3.6×10^9 years, the

[2] A correction has to be applied to the numerical values given by Hoyle (1948), so as to take account of Baade's new distance scale.

older material being dispersed by expansion. Accordingly, effective enrichment with heavy elements must be regarded as confined to the time scale of order T.

Next, let the material condensed into galaxies produce in time T an amount $M\kappa$ ($\kappa \ll 1$) of heavy elements. Suppose, further, that, *on the average*, half these heavy elements are retained within their present galaxies and half are distributed within the extragalactic medium. Then the average concentration of heavy elements becomes $\kappa/2$ within the galaxies and $\kappa/20$ in the extragalactic medium. The latter concentration determines the heavy-element content of a galaxy at the time of its origin.

Consider now a galaxy, such as our own, that contains considerable quantities of interstellar material and hence must manage to trap an appreciable fraction—say a half—of the heavy elements that are produced within it. The initial heavy-element concentration at the time of formation of the galaxy would be about $\kappa/20$, as just indicated. This represents the heavy-element concentration of the first stars to form. After a time T, however, the heavy-element concentration rises to about $\kappa/2$, owing to the trapping process. Hence stars that form at a time of the order of T after the birth of the galaxy must contain about 10 times the heavy-element concentration of the oldest stars. This result would appear to be in good agreement with the difference of composition between stars of type I in the Galaxy and the oldest stars (probably represented among near-by stars by the subdwarfs). The present result is independent of κ and M but depends on the fraction of the material of the universe that is condensed into galaxies and on the assumption that half the heavy elements are, on the average, retained within their present galaxies.

II. PRELIMINARY DATA

Later calculations are dependent on certain theoretical data that will now be itemized.

1. The chemical composition of the material ejected from a hot star depends on the maximum temperature, τ, to which the material was heated during the collapsing phase of the star. To obtain theoretical estimates of the relative abundances of the elements, it is therefore necessary to specify a heating function whose nature will now be explained. Take an average over all the material ejected from a large number of stars, and write $H(\tau)d\tau$ for the fraction of the material heated prior to ejection to temperatures between τ and $\tau + d\tau$. Then the dependence of $H(\tau)$ on τ is a necessary datum of the theory. Unfortunately, this dependence cannot be specified from observation, although it might be said that for $\tau > 10^{8\,\circ}$ K, $H(\tau)$ probably decreases with increasing τ. In the sequel it will be assumed that

$$H(\tau) \propto \frac{1}{\tau^2}. \tag{1}$$

The calculated abundances are not particularly sensitive to the assumed form of $H(\tau)$. It should, however, be pointed out that form (1) is a somewhat favorable choice for the theory. That is to say, other choices for $H(\tau)$ might be made that would not turn out to give such good agreement between the theoretical and the observed abundances of the elements.

2. It will be assumed that there is no upper limit to τ, or, more precisely, that there is no upper limit less than $5 \times 10^{9\,\circ}$ K. The physical basis for this assumption rests on Chandrasekhar's limiting mass for degenerate configurations. When hydrogen is absent, a nonrotating star cannot be supported in hydrostatic equilibrium by degeneracy pressure alone when its mass is greater than about $1.44\odot$. This means that an unlimited degree of collapse occurs in such cases—unlimited, that is to say, when angular momentum and general relativity effects are ignored.

To understand this conclusion clearly, it is necessary to take account of several further points. The statement that hydrostatic equilibrium cannot be satisfied in hydrogen-poor, nonrotating stars with masses greater than $1.44\odot$ applies only when the internal temperature of the star is zero. At a finite internal temperature, equilibrium can be maintained. Now in actual stars there is always a finite internal temperature, and, except in

very unusual circumstances (which will form the background of the second paper of this series), this temperature is such as will maintain equilibrium in a high degree of approximation. Equilibrium can only be exact, however, if the energy escaping from the surface of the star is exactly balanced by a process of nuclear-energy generation in the interior. During certain periods in the history of the star this condition is satisfied, but it cannot be satisfied indefinitely, for the reason that there are no permanent sources of energy. Thus a finite internal temperature can, and usually does, prevent catastrophic shrinkage (in a few hours, minutes, or seconds), but it cannot prevent a slow steady collapse, except during finite periods of time when suitable nuclear sources of energy are available. The only way in which permanent equilibrium can be achieved is through degeneracy pressure at zero temperature, there being then no escape of radiation from the surface of the star; but even this is impossible in hydrogen-poor, nonrotating stars with masses greater than about $1.44\odot$. Hence the indefinite collapse of such stars.

These remarks refer only to nonrotating stars. Indefinite collapse cannot occur in rotating stars without highly flattened configurations arising, and such configurations are believed[3] to be rotationally unstable. Rotational instability causes material to be ejected from the star, as is required by the present theory. Now the moment of onset of the instability must depend on the initial angular momentum of the star. This may be taken as being variable from one star to another, thereby leading to a corresponding variability in the moment of onset of the instability. It is just this variability that introduces temperature differences between one exploding star and another, these temperature changes being contained in the heating function $H(\tau)$. A high value of τ, it may be noted, corresponds to a comparatively high degree of shrinkage and hence to an initially small angular momentum.

3. We shall also require the relation between the density ρ and the temperature T maintained during the collapse of a star. A star of mass $1.5\odot$, with uniform molecular weight $\frac{4}{3}$, built on the Cowling model, would satisfy the relations

$$\rho \sim 10^6 T^3, \qquad T \propto \frac{1}{r}, \tag{2}$$

at its center, where ρ is in grams per cubic centimeter, T is in units of $10^{9}\,^{\circ}$ K, and r is the radius. Relation (2) will be used throughout most of the subsequent work, on the basis that, first, the stars under consideration will be regarded as not differing much in mass from $1.5\odot$; second, the molecular weight in the absence of hydrogen can vary only from $\frac{4}{3}$ to about 2, in which range there is not an extensive change in the relationship of ρ to T; and, third, the Cowling model is probably fairly representative of the density distribution within collapsing stars, at any rate up to values of T of order $5 \times 10^{9}\,^{\circ}$ K. Moreover, in the Cowling model ρ/T^3 does not vary at all sensitively with distance from the center of the star, so that relation (2) can be used as a general approximation throughout the main mass of the star. In addition, most of the later calculations will be rather insensitive to the exact correspondence between ρ and T. In an exceptional case, however, where a sensitive dependence does indeed arise, we shall write $\rho = \alpha 10^6 T^3$ and shall consider different values of the parameter α separately.

III. NUCLEAR-PHYSICS REQUIREMENTS

Nuclear reaction rates when levels are widely spread.—In an assembly at kinetic temperature T the number of collisions per unit volume per unit time in which nuclei of

[3] Highly flattened rotating configurations are certainly rotationally unstable when the material is incompressible. Some doubt has been expressed as to whether the same conclusion also applies when, as in the stars, the material is compressible. In a recent lecture at the California Institute of Technology, I expressed the opinion that the unstable property is particularly likely to hold if a magnetic field happens to be present. This opinion is supported by the calculations of S. Chandrasekhar, who has kindly informed me that a rotating mass of gas tends to behave rather as an incompressible fluid when a strong magnetic field is present.

species 0 and 1 have a collision with kinetic energy, relative to their mass center, that lies between E and $E + dE$ is given by

$$\frac{4n_0n_1E\exp(-E/kT)}{(2\pi m)^{1/2}(kT)^{3/2}}\,dE, \tag{3}$$

where n_0, n_1 are the number densities of the two nuclear species under consideration, and $m = m_0m_1/(m_0 + m_1)$; m_0 and m_1 are the masses of the two species. The number of these collisions that result in the formation of a compound nucleus and in the subsequent emission of a particle i, which may be a material particle or a γ-ray, can be estimated by multiplying expression (3) by

$$\frac{\lambda^2}{4\pi}\,\frac{\omega\Gamma_s\Gamma_i}{(E_R-E)^2+\Gamma^2/4}, \tag{4}$$

where ω is a statistical-weight factor of the order of unity that depends on angular-momentum considerations; Γ_s is the width for elastic scattering; Γ_i is the width for the emission of the particle i; $\Gamma = \Sigma\Gamma_i$, the summation being over all particles that the compound nucleus is energetically capable of emitting; $\lambda = h/\sqrt{2Em}$, h being Planck's constant; and E_R is the energy level of the compound nucleus that is "nearest" to E. It is particularly to be noted that E_R is measured relative to the sum of the rest masses of nuclei 0 and 1 as the zero of energy, since E is the kinetic energy in the center-of-mass reference system.

Expression (4) is the Breit-Wigner one-level formula. It gives a good approximation when Γ is small compared to the separation of the energy levels of the compound nucleus and when E is sufficiently close to the one particular level E_R. When E falls fairly evenly between two levels, the use of expression (4), applied to one or the other of the two levels, may lead to an appreciable error (Teichmann 1950)—possibly by as much as a factor of 10.

The statistical-weight factor ω will be taken as equal to unity throughout the following work. This represents a further approximation in many cases, but the approximation is necessary, since ω is not known for many of the reactions of interest in the present paper.

Resonance contributions.—The yield, given by multiplying expressions (3) and (4), varies with E. In particular, the yield possesses a sharp maximum at $E = E_R$. The integral of the yield over this peak represents the resonance contribution (Gamow and Teller 1938) from the level E_R. A simple reduction leads to the following value of this contribution:

$$2.53\times10^{-13}n_0n_1\left(\frac{A_0+A_1}{A_0A_1}\right)^{3/2}\frac{\Gamma_s\Gamma_i}{T^{3/2}\Gamma}\qquad\exp\left(-\frac{E_R}{kT}\right), \tag{5}$$

where A_0 and A_1 are the atomic weights of the colliding species; T is now expressed in units of 10^9° K; Γ_s, Γ, Γ_i are in mev, and n_0 and n_1 are the numbers of nuclei per cubic centimeter.

There is a resonance contribution of the form (5) from each level, E_R, of the compound nucleus, such that E_R is appreciably greater than Γ, this being a necessary condition, since E—a kinetic energy—cannot be negative. For the sake of completeness it may be noted that in an unusual case where E_R differs from zero by an amount of order Γ, there is a partial resonance contribution, given by integrating over a portion of the resonance peak. It will be recalled, in this connection, that E_R is measured not relative to the ground state of the compound nucleus but relative to the sum of the rest masses of nuclei 0 and 1.

The width Γ_s may be represented as a product of a width "without barrier," G_s, and a Coulomb factor, P. Writing as a general function of E, we put

$$\Gamma_s = G_s P(E), \tag{6}$$

where

$$P(E) = E^{-1/2} \exp\left[\frac{8\pi e}{h}(2mZ_0Z_1R)^{1/2} - \frac{4\pi e^2 Z_0 Z_1}{h(2E/m)^{1/2}}\right], \tag{7}$$

Z_0e and Z_1e being the nuclear charges and R, the collision radius, taken in the following as $1.6 \times 10^{-13}(A_0 + A_1)^{1/3}$ cm.

In applications of expression (5), the energy E in equations (6) and (7) must be put equal to E_R. Also, in many applications of expression (5), $\Gamma_i = \Gamma_\gamma$, corresponding to the emission of a γ-ray, no other behavior of the compound nucleus being energetically allowed, except, of course, scattering back into the nuclei 0 and 1. Then Γ reduces to $\Gamma_s + \Gamma_\gamma$. In addition, in such applications Γ_s is considerably less than Γ_γ when P is small, in which case expression (5) takes the simplified form

$$2.53 \times 10^{-13} \frac{n_0 n_1}{T^{3/2}} \left(\frac{A_0 + A_1}{A_0 A_1}\right)^{3/2} G_s P(E_R) \exp\left(-\frac{E_R}{kT}\right), \tag{8}$$

where E_R and G_s are in mev, T is in units of 10^9° K, and kT is in mev.

The nonresonance contribution.—Although the yield possesses a sharp maximum at each resonance, the resonance contributions may still not be dominant. This arises in cases where all levels have E_R values that make the factor $P(E_R) \exp(-E_R/kT)$ in expression (5) extremely small. A nonresonance contribution must then be calculated.

To illustrate the method of calculation, consider the important case in which the emission of the particle i corresponds to the emission of a γ-ray. Then, for values of E between two resonance peaks, expression (4) can be replaced by

$$\frac{\lambda^2}{4\pi} \frac{\omega \Gamma_s \Gamma_\gamma}{(E_R - E)^2}. \tag{9}$$

The nonresonance contribution for the range E to $E + dE$ in the collisional energy spectrum is now given by multiplying expressions (3) and (9). Again, writing equation (6) for Γ_s, we see that the nonresonance contribution depends on E, according to the factor

$$\frac{P(E) \exp(-E/kT)}{(E_R - E)^2}. \tag{10}$$

In all nonresonance applications of present interest the factor $(E_R - E)^2$ varies slowly with E, in contrast with both $P(E)$ and $\exp(-E/kT)$.

Now the product of $\exp(-E/kT)$ with the exponential term in $P(E)$ possesses a strong maximum with respect to E at a value $E = E_0$, given by the equation

$$E_0^{3/2} = (2m)^{1/2} \pi^2 e^2 h^{-1} Z_0 Z_1 kT. \tag{11}$$

Relation (11) is often more usefully expressed in the form

$$E_0 = 0.123 \left(\frac{A_0 A_1 Z_0^2 Z_1^2 T^2}{A_0 + A_1}\right)^{1/3}, \tag{12}$$

where E_0 is now in mev and T is in units of 10^9° K.

In the neighborhood of E_0 the value of expression (10) is given to a good approximation by

$$P(E_0)(E_R - E_0)^{-2} \exp\left[-\frac{E_0}{kT} - \frac{3(E_0 - E)^2}{4E_0 kT}\right], \tag{13}$$

a quantity of the order of $(E_0 - E)^3$ being neglected in the exponent in the exponential term. The decline as E changes from E_0 is shown by the Gaussian exponential in expression (13). This may be expressed by saying that the nonresonance yield comes largely from the range of E near E_0. This is the well-known Gamow peak. Integration over the peak leads to

$$P(E_0)(E_R - E_0)^{-2}\left(\frac{4\pi E_0 kT}{3}\right)^{1/2} \exp\left(-\frac{E_0}{kT}\right). \tag{14}$$

This result, when multiplied by the factors not depending on E in the product of expressions (3) and (9), gives the nonresonance yield, which, after some reduction, gives a formula of the type first derived by Atkinson and Houtermanns (1929),

$$8.46 \times 10^{-15} n_0 n_1 \left(\frac{A_0 + A_1}{A_0 A_1}\right)^{4/3} \frac{(Z_0 Z_1)^{1/3} \Gamma_\gamma G_s}{T^{2/3}(E_R - E_0)^2} P(E_0) \exp\left(-\frac{E_0}{kT}\right), \tag{15}$$

the statistical-weight factor being again taken as unity.

In examples in which one of the nuclear species is an α-particle and the other is an α-particle nucleus (Be^8, C^{12}, O^{16}, Ne^{20}, Mg^{24}, . . .), we can write $A_0 = 2Z_0$, $A_1 = 2Z_1$, in which case, using equations (7) and (11), $E_0^{1/2} P(E_0) \exp(-E_0/kT)$ becomes simply the antilogarithm to the base 10 of the expression

$$\frac{Z_0 Z_1}{(Z_0 + Z_1)^{1/3}}\left(0.92 - \frac{2.34}{T^{1/3}}\right), \tag{16}$$

where T is again in units of 10^9 ° K.

Further remarks on the resonance contribution.—The discussion just given of the dependence of $P(E) \exp(-E/kT)$ on E shows that resonance effects must be particularly strong when an energy level, E_R, of the compound nucleus falls near the center, E_0, of the Gamow peak. In such cases, the resonance contribution may be written as

$$2.53 \times 10^{-13} \frac{n_0 n_1}{T^{3/2}}\left(\frac{A_0 + A_1}{A_0 A_1}\right)^{3/2} G_s P(E_0) \exp\left(-\frac{E_0}{kT}\right). \tag{17}$$

Nuclear reaction rates when levels are narrowly spaced.—In certain cases in which a compound nucleus is excited to very high energies (of the order of 16 mev above ground level), the total width Γ is of the order of 0.1 mev. This arises because the Coulomb-barrier factors for protons and α-particles emitted by the nucleus are now small, so that the proton width and the α-width become effectively the widths without barrier. Now a width of 0.1 mev is much greater than the separation of the levels at high energies of excitation. The Breit-Wigner one-level formula must then be abandoned, even as an approximation. In its place we use

$$\frac{\lambda^2}{4\pi}\frac{\Gamma_s \Gamma}{D^2}, \tag{18}$$

where D is the average level spacing (Blatt and Weisskopf). The width Γ_s still contains an important Coulomb-barrier term, however. Thus $\Gamma_s = G_s P(E)$, and, on multiplying expression (3) by expression (18), we again obtain an integral of $P(E) \exp(-E/$

kT) with respect to E. This is again just the integral over the Gamow peak. Accordingly, we obtain the following modified formula for the yield

$$8.46\times10^{-15}\left(\frac{A_0+A_1}{A_0A_1}\right)^{4/3}\frac{(Z_0Z_1)^{1/3}G_s\Gamma}{T^{2/3}D^2}P(E_0)\exp\left(-\frac{E_0}{kT}\right), \tag{19}$$

where E_0 is again given by equation (12).

Photodisintegration reaction rates.—Photodisintegration reactions, in which a nucleus, C, is disintegrated by γ-ray absorption into two nuclei, 0 and 1, are inverse to reactions already considered. Their rates can therefore be obtained by using the equation of thermodynamic balance for

$$C+\gamma\rightleftarrows 0+1\ , \tag{20}$$

together with results already obtained. We quote the well-known thermodynamic equation (possibly neglecting a weight factor of the order of unity) in the form

$$\log_{10}\left(\frac{n_C}{n_0n_1}\right)=-34.08-\tfrac{3}{2}\log_{10}T+\tfrac{3}{2}\log_{10}\left(\frac{A_0+A_1}{A_0A_1}\right)+\frac{5.04\chi}{T}, \tag{21}$$

where n_C is the number density of the nuclei C; χ is the smallest γ-ray energy, expressed in mev, that is required to disrupt the ground state of C; and T is once again in units of 10^9° K.

In addition, under conditions of detailed balancing we have the yield of nuclei C per unit volume per unit time equal to

$$n_C\times(\text{Probability of photodisintegration of nuclei } C \text{ per unit time}). \tag{22}$$

Combining formulae (21) and (22) gives

log (Probability of photodisintegration)

$$=34.08+(\tfrac{3}{2})\log T+(\tfrac{3}{2})\log\left(\frac{A_0A_1}{A_0+A_1}\right)-\frac{5.04\chi}{T}+\log\left(\frac{\text{Yield}}{n_0n_1}\right), \tag{23}$$

from which it is seen that a calculation of the yield rate implies a knowledge of the disintegration rate.

It is to be emphasized that equation (23) remains valid even when thermodynamic conditions do not in fact hold among the nuclei, provided always that the Planck distribution of radiation is maintained. It can readily be shown that under the conditions occurring inside hot stars electron–positive ion collisions maintain this latter requirement (Hoyle 1946).

IV. THE BUILDING OF CARBON, OXYGEN, AND NEON

It was pointed out some years ago by Bethe (1939) that effective element-building inside stars must proceed, in the absence of hydrogen, by triple α-particle collisions as a starting point:

$$3\alpha\rightarrow C^{12}+\gamma. \tag{24}$$

It is particularly to be noted that a serious difficulty, encountered by Gamow, Alpher, and Herman in their work on the origin of the elements, does not occur here. This difficulty arises only at the comparatively low density used by these authors, for reaction (24) cannot then be used to bridge the well-known gap caused by the instability of nuclei of atomic weight 5.

Recently Salpeter (1952) has developed these considerations and has suggested that the energy released in reaction (24) may have an important place in the theory of stellar

evolution and that the C^{12} so produced may provide a basis for explaining the excess carbon that is detected in the atmospheres of the R and N stars.

Now the release of energy by reaction (24) and by the further reactions

$$C^{12} + \alpha \rightarrow O^{16} + \gamma, \tag{25}$$

$$O^{16} + \alpha \rightarrow Ne^{20} + \gamma, \tag{26}$$

amounts to a total of about $Mc^2/1000$, where M is the mass of the star and c is the velocity of light. Thus the time scale for a collapse through the temperatures at which reactions (24), (25), and (26) occur must be of the order of $10^{-3}\ Mc^2/L$, where L is the luminosity of the star. For the stars under consideration, M/L may be taken as about 10^{-3} (for stars of $1.5\odot$ this would imply a bolometric magnitude of about -3, this being a reasonable value after effectively all the hydrogen has been exhausted). The time scale for collapse through the relevant temperatures is, accordingly, of the order of 10^{15} seconds. This result will be used in the following work. The conclusions reached are not at all sensitive to this particular value of the time scale.

It is convenient to replace reaction (24) by

$$\alpha + \alpha \rightleftarrows Be^8, \qquad Be^8 + \alpha \rightarrow C^{12} + \gamma. \tag{27}$$

This is a permissible step, since the lifetime of the unstable Be^8 is appreciably longer than the time required for a "nuclear" collision of two α-particles; that is, longer than the α-particle radius divided by the relative velocity. The merit of reaction (27) is that the number density n_4^8 of Be^8 nuclei is given in terms of the number density n_2^4 of α-particles by the equation of statistical equilibrium (Hoyle 1946),

$$\log n_4^8 = 2 \log n_2^4 - 34.53 - \tfrac{3}{2} \log T - \frac{0.464}{T}, \tag{28}$$

where the disintegration energy of Be^8 is taken as 0.092 mev, and T is in units of 10^9° K. We shall henceforth always use this unit for measuring T, unless otherwise stated.

The yield of C^{12} per cubic centimeter per second is given immediately by inserting $A_0 = 4$, $Z_0 = 2$, and $A_1 = 8$, $Z_1 = 4$, in the formulae of the previous section. The important energy level of the C^{12} nucleus in the present problem is one very recently identified by Dunbar, Pixley, Wenzel, and Whaling (1953). This level occurs at about 7.68 mev above ground level, which corresponds to a value of E_R of about 0.31 mev. (It will be recalled that E_R is measured relative to the sum of the masses of Be^8 and α-particle, this being about 7.37 mev above the ground level of C^{12}.) Assuming, as we shall do in this paper, that the $Be^8 + \alpha$ reaction through this level is not forbidden by strict selection rules, the resonance contribution from it quite overwhelms not only the nonresonance yield but also the resonance contributions from other levels.

The application of expression (8) gives, on eliminating n_4^8 by using equation (28),

$$1.71 \times 10^{-48}\, (n_2^4)^3 T^{-3} 10^{-0.464/T} G_s P(E_R) \exp\left(-\frac{E_R}{kT}\right), \tag{29}$$

where, for the moment, we retain the general form in terms of E_R.

Now it would be possible to put $E_R = 0.31$ mev in expression (29), to work out the yield of C^{12} over a time scale of 10^{15} seconds, and to show that for sufficiently high T the yield becomes comparable with $n_2^4/3$, thereby indicating that an appreciable fraction of the original helium has become built into carbon. It is not necessarily correct, however, to make the further step of arguing that a high concentration of C^{12} must then have been produced, for this assumes that the C^{12} so built up is not destroyed by other reactions.

It is plain that carbon will accumulate only if it is not destroyed by other reactions as fast as it is produced.

It can be shown that reaction (25) is the most effective in destroying C^{12}. Hence, to decide how far C^{12} accumulates, it is necessary to compare the rates of reactions (24) and (25). For the latter reaction the value of E_R of main interest is -0.05 mev, corresponding to a level at 7.10 mev above the ground state of O^{16}. This gives a nonresonance contribution

$$4.47 \times 10^{-15} n_6^{12} n_2^4 \frac{\Gamma_\gamma G_s}{T^{2/3} (E_R - E_0)^2} P(E_0) \exp\left(-\frac{E_0}{kT}\right), \tag{30}$$

where E_0 is given by equation (12), and $n_6^{12}$is the number density of C^{12} nuclei. There are resonance contributions to the yield of O^{16}, but these occur at such large positive values of E_R that, on account of the factor $\exp(-E_R/kT)$ in the resonance formula, these contributions are small compared with expression (30).

We now use expressions (29) and (30) in the construction of two differential equations. First, we write

$$\frac{dn_2^4}{dt} = -3A(n_2^4)^3 - Bn_2^4 n_6^{12}, \tag{31}$$

where A is the coefficient of $(n_2^4)^3$ in expression (29), and B is the coefficient of $n_2^4 n_6^{12}$ in expression (30). Equation (31) is approximate in that it neglects the removal of α-particles in reactions other than (24) and (25). We also have

$$\frac{dn_6^{12}}{dt} = A(n_2^4)^3 - Bn_2^4 n_6^{12}. \tag{32}$$

If f represents the fraction by mass of the material in the form of helium and g is the fraction in the form of C^{12}, then

$$\log n_2^4 = 23.18 + \log f + \log \rho, \qquad \log n_6^{12} = 22.70 + \log g + \log \rho.$$

After an elementary reduction it can be shown that, for changes at constant density, equations (31) and (32) lead to

$$\frac{dg}{df} = 3\frac{\kappa g/f^2 - 1}{\kappa g/f^2 + 3}, \tag{33}$$

where

$$\kappa = \frac{2.2 \times 10^{-24} B}{A\rho}. \tag{34}$$

Instead of expressing ρ in terms of T by means of the order-of-magnitude relation (2), we now obtain increased accuracy by writing

$$\rho = \alpha 10^6 T^3,$$

where α is a parameter of the order of unity that may vary from one sample of material to another. With this value of ρ, expression (34) for κ becomes (writing in the values of A and B)

$$\kappa = 5.7 \times 10^{3+0.464/T} T^{-2/3} \alpha^{-1} \frac{S}{J}, \tag{35}$$

where

$$S = \Gamma_\gamma G_s (E_R - E_0)^{-2} P(E_0) \exp\left(-\frac{E_0}{kT}\right),$$

all quantities in S being calculated for the $C^{12} + \alpha$ reaction, and

$$J = G_\alpha P(E_R) \exp\left(-\frac{E_R}{kT}\right), \tag{36}$$

all quantities in equation (36) being calculated for the $Be^8 + \alpha$ reaction.

Next we consider how g varies with f, subject to the following two approximations:

i) The temperature T and the total density ρ of the material remain constant as f decreases from 1 to 0.

ii) The removal of α-particles by reactions other than (24) and (25) is neglected.

With these approximations, κ remains constant as f changes. Hence the nature of the solutions of equation (33) can be seen by specifying various values of κ. In Figure 2 the variation of g with f is shown for four prescribed values of κ.

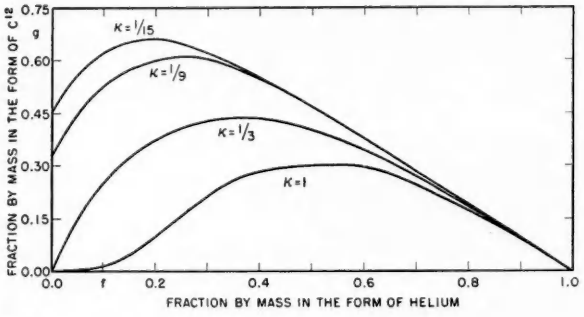

FIG. 2.—The formation of C^{12} from helium as a function of κ. The quantity f represents the fraction of the mass which is helium; g is the fraction which is C^{12}; the balance, $1-f-g$, is O^{16}.

The ratio of the mass of O^{16} produced to the mass of C^{12} produced may be estimated as

$$\left(\frac{\overline{1-g}}{g}\right)_{f=0}. \tag{37}$$

To agree with observed cosmic abundances, this ratio should take a value of about $\frac{2}{1}$, which would imply a value of κ not much greater than $\frac{1}{9}$. It is, however, to be emphasized that different samples of material may be expected to correspond to somewhat different values of κ. This arises because κ is proportional to α^{-1}, and α must vary from one sample to another. Accordingly, it is not a question of determining one unique value of κ, chosen so as to give the required ratio of oxygen to carbon. Rather, we should proceed in the following manner:

Suppose that $\alpha = 1$ for an average sample of material. If for $\alpha = 1$ we put $\kappa = \frac{1}{9}$, a typical sample of material would be built into a mixture with a C^{12} to O^{16} ratio of about $\frac{1}{2}$. On the other hand, in some exceptional samples α may well be as small as 0.3, in which case we have $\kappa = \frac{1}{3}$, and the material is then without C^{12}. Thus a variability of composition arises, C^{12} being produced in high abundance in some samples but not in others (a circumstance that may turn out to be of importance in relation to the carbon stars).

In accordance with these remarks, we see that astrophysical considerations suggest that we put $\kappa = \frac{1}{9}$ when $\alpha = 1$ in equation (35), thereby giving

$$J = 5.1 \times 10^{4+0.464/T} T^{-2/3} S. \tag{38}$$

The reaction widths being supposed given, equation (38) yields a relation between E_R and T, it being remembered that E_R represents the appropriate level in the C^{12} nucleus (E_R close to 0.31 mev). Hence equation (38) can be used to determine the temperature T at which these processes must take place if we are to obtain the required proportions of O^{16} and C^{12}.

But a second relation between E_R and T can be determined from the requirement that the time scale in which f is reduced to zero must correspond with the time of collapse of the star, which we have seen must be of the order of 10^{15} seconds. This enables us to make a strict test of the theory, since this second relation must yield the same value of T as that given by equation (38).

To carry out this test, we note that equation (31), after some reduction, can be written in the form

$$\frac{d(\log f)}{dt} = -0.040\,(\kappa g + 3f^2)\,\rho^2 T^{-3} 10^{-0.464/T} J\,, \tag{39}$$

again making the assumption that ρ and T remain constant.

Consider the application of equation (39) to the case $\kappa = \frac{1}{9}$. The main contribution to the time required for f to decrease effectively to zero comes from the late stages, when f is small compared to unity. The helium concentration then declines exponentially to zero, the characteristic time for the decline being close to

$$25\kappa^{-1} g_0^{-1} \rho^{-2} T^{-3} J^{-1} 10^{0.464/T}, \tag{40}$$

where g_0 is the value of g at $f = 0$. This characteristic time must be of the order of 10^{15} seconds. Putting $\kappa = \frac{1}{9}$ and $g_0 = 0.322$, we require

$$J = 7.0 \times 10^{-13} T^3 \rho^{-2} 10^{0.464/T}.$$

Remembering that the case $\kappa = \frac{1}{9}$ corresponds to $\alpha = 1$ in $\rho = \alpha 10^6 T^3$, this gives, on eliminating ρ,

$$J = 7.0 \times 10^{-25} T^{-3} 10^{0.464/T}. \tag{41}$$

Equation (41) gives the second determination of T (E_R supposed known).

It remains to test whether equations (38) and (41) do in fact give the same value of T (if they do not, we infer that the identification $\kappa = \frac{1}{9}$ with the case $\alpha = 1$ is in error and hence that the appropriate proportions of C^{12} and O^{16} are not produced). The test can be carried out in two ways. We could insert $E_R = 0.31$ mev in equations (38) and (41) and, making suitable estimates of the reaction widths, solve both equations for T. Or we can treat E_R as unknown and proceed to solve equations (38) and (41) for *both* E_R and T, the value of E_R so obtained being then compared with the value $E_R = 0.31$ mev, given by nuclear physics. Of these two procedures, the latter is preferable and will now be carried out.

When we put G_s for the $Be^8 + \alpha$ reaction equal to 0.1 mev, equation (41) gives

$$P(E_R) \exp\left(-\frac{E_R}{kT}\right) = 7.0 \times 10^{-24} T^{-3} 10^{0.464/T}, \tag{42}$$

and when we put $G_s/\sqrt{E_0} = 0.1$ mev, $\Gamma_\gamma = 10^{-6}$ mev, and $(E_R - E_0)^{-2} = 25$ mev^{-2} for the $C^{12} + \alpha$ reaction, equation (38) gives

$$P(E_R) \exp\left(-\frac{E_R}{kT}\right) = 1.3 T^{-2/3} 10^{0.464/T} \left(\text{antilogarithm of } 5.52 - \frac{14.04}{T^{1/3}}\right), \tag{43}$$

where expression (16) has been used to determine the value of $E_0^{1/2}P(E_0)\exp(-E_0/kT)$ for the $C^{12}+\alpha$ reaction. Solving equations (42) and (43) gives

$$T = 0.14, \qquad E_R = 0.33 \text{ mev.} \tag{44}$$

The agreement of this deduced value of E_R with the experimental value is highly satisfactory, thereby confirming our identification of $\kappa = \frac{1}{9}$ with the case $a = 1$ and hence giving the required relative concentrations of C^{12} and O^{16}.

An important step yet remains. Going back to expression (40), which determines the time scale required for the helium to become entirely used up, we must now consider cases where κ is greater than $1/9$ ($a < 1$). It transpires when we consider the cases $\kappa = \frac{1}{3}$ and $\kappa = 1$, for example, that the time scale diverges for small f. The time scale for the range of f from 1 to 0.15 is substantially the same as that calculated above, but as f approaches zero the time scale tends to infinity, since g tends to zero in these cases. This divergence is an outcome of the assumptions that were introduced into the calculations, particularly the assumption that reactions (24) and (25) are the only ones that contribute to the removal of α-particles. So long as either f is not too small or g does not become too small, this assumption is a good approximation, as it is in the case $\kappa = \frac{1}{9}$, considered above. But when both f and g become small, reactions (24) and (25) become unimportant compared with reaction (26), which converts O^{16} into Ne^{20} by α-particle addition. Thus, in the case $\kappa = \frac{1}{3}$, the last 10 per cent or so of the helium is consumed, not in the production of C^{12} and O^{16}, but in converting O^{16} into Ne^{20}. It should be noted that this does not mean that in such cases the amount of Ne^{20} produced is only 10 per cent of the amount of O^{16}, for the amount of Ne^{20} produced must have 5 times the mass of the helium that is used up in its production. Thus, if the helium so used up comprises 10 per cent of the total mass, the mass of the Ne^{20} produced must be of the order of 50 per cent of the total. That is to say, in the case $\kappa = \frac{1}{3}$ the Ne^{20} produced must have a total mass comparable with the mass of O^{16}. Accordingly, since we are regarding $\kappa = \frac{1}{3}$ as a not unusual case, it follows that Ne^{20} production must be roughly comparable with the production of O^{16}.

It should be added that the $O^{16}+\alpha$ reaction does not proceed with sufficient rapidity at $T = 0.14$. The temperature $T = 0.14$ still applies to the stages where f is reduced from unity down to about 0.1, but (in the case $\kappa = \frac{1}{3}$) not when f becomes so small that the production of C^{12} and O^{16} effectively ceases. Since energy is then no longer being released in any important degree by the nuclear reactions, the star must contract, and, as it does so, the temperature must rise until eventually the $O^{16}+\alpha$ reaction is speeded up sufficiently for the energy it provides to slow up the contraction of the star once again. The star then halts its collapse for a while until the helium concentration falls effectively to zero.

It is a straightforward calculation, of the type already considered above, to obtain the temperature at which the last of the helium becomes used up in the formation of Ne^{20}. The known levels in the Ne^{20} nucleus provide an important resonance corresponding to $E_R = 0.654$ mev, it being assumed that this resonance is not rendered ineffective by selection rules. Using this value for E_R, it turns out that the $O^{16}+\alpha$ reaction is adequately speeded up when T has risen to about 0.16. The criterion for deciding what constitutes an adequate speed is simply that the value of f must fall effectively to zero in a time of the order of 10^{15} seconds. It appears, therefore, that no large rise of temperature is required for neon production to set in.

To conclude the present section, we may sum up the main points considered above. Provided that α-particle resonance in a level in the C^{12} nucleus at about 7.7 mev above the ground state is not forbidden by selection rules, the theory is capable of giving roughly the astrophysical abundance ratios $\frac{1}{3} : 1 : 1$ for $C^{12} : O^{16} : Ne^{20}$. These abundances refer to samples of material where the relation between density and temperature is not much different from relation (2). In material of abnormally high density the produc-

tion of C^{12} would exceed oxygen and neon. In material of abnormally low density, on the other hand, the production of C^{12} would be negligible. Carbon and oxygen production occur at about $T = 1.4 \times 10^8$° K, and neon production at about $T = 1.6 \times 10^8$° K.

An implicit assumption is contained in the above remarks concerning neon production. It is assumed that the Ne^{20} is not destroyed by the reaction

$$Ne^{20} + \alpha \rightarrow Mg^{24} + \gamma \tag{45}$$

as soon as it is produced. In the absence of full information concerning the levels in the Mg^{24} nucleus, it is not possible to decide whether this assumption can be justified or not. It can, however, be said that at $T = 0.16$ the Ne^{20} is *not* destroyed by reaction (45) unless the Mg^{24} nucleus has a level giving an E_R value that is very close to the value making $P(E_R) \exp(-E_R/kT)$ a maximum, that is, close to the value of E_0 defined by equation (12). It will be assumed in the sequel that this is not the case. Later considerations contain an uncertainty on this account.

V. MINOR EFFECTS AMONG THE LIGHT ELEMENT GROUP

So far we have considered the nuclear reactions occurring in the temperature range around 0.14 as if the material were initially entirely pure helium. It is, of course, the case that the material must initially contain traces of other elements. From the present point of view the important trace elements are C^{13} and N^{14}.

The stars in question have masses of the order of, or greater than, $1.5\odot$. For such stars the energy production that occurred during the stage *before* the initial hydrogen content became exhausted would be through the carbon-nitrogen cycle, not through the proton-proton chain. Recent estimates[4] by Fowler would place the ratios $C^{12} : C^{13} : N^{14} : N^{15}$ occurring during this phase at about $1 : 0.25 : 10 : 0.004$, the temperature for the operation of the carbon-nitrogen cycle being taken as about 2×10^7° K. That is to say, the main trace element operating in the carbon-nitrogen cycle is N^{14}.

Now, with the heating of the material to temperatures in excess of $T = 0.1$, the presence of N^{14} leads to the reactions

$$N^{14} + \alpha \rightarrow F^{18} + \gamma\,, \tag{46}$$

$$F^{18} \rightarrow O^{18} + \beta^+\,, \tag{47}$$

$$O^{18} + \alpha \rightarrow Ne^{22} + \gamma\,, \tag{48}$$

it being noted that reactions such as $N^{14} + \alpha \rightarrow O^{17} + p$ do not occur in any appreciable intensity on account of energy requirements.

The next step is to estimate the concentrations of O^{18} and Ne^{22} that are built up by these reactions. In *normal* stellar material the ratio of hydrogen to N^{14} is about $\frac{10000}{1}$. It follows that when the hydrogen is converted into helium, the ratio He^4 to N^{14} is about $\frac{2500}{1}$. Thus, if the N^{14} were to become converted mainly into O^{18} and the He^4 were to become mainly converted into equal quantities of O^{16} and Ne^{20}, the ratio of O^{18} to O^{16} would be about $\frac{1}{30}$, which may be compared with the known terrestrial ratio of about $\frac{1}{500}$. Thus the present process is capable of providing considerably more O^{18} than is required. This result should not be regarded as a discrepancy, however, since it probably implies that most of the O^{18} produced by reactions (46) and (47) is converted to Ne^{22} by reaction (48). Thus the Ne^{22} to Ne^{20} ratio would then become about $\frac{1}{30}$, as compared with the observed terrestrial ratio of about $\frac{1}{10}$. In view of the order-of-magnitude character of the present argument, this may be taken as satisfactory agreement. We see that the

[4] Private communication. I am much indebted to Dr. Fowler for this information.

trace element N^{14} is capable of yielding approximately the required amounts of O^{18} and Ne^{22}.

The presence of the trace element C^{13} likewise leads to the reactions

$$C^{13} + \alpha \rightarrow O^{17} + \gamma\,, \tag{49}$$

$$O^{17} + \alpha \rightarrow Ne^{21} + \gamma\,. \tag{50}$$

Remembering that the C^{13} concentration is less than the N^{14} concentration by a factor of about 40, it follows that, since the N^{14} concentration led to ratios of the order of $\frac{1}{30}$, the O^{17} to O^{16} ratio given by reaction (49) is of the order of $\frac{1}{1200}$, as compared with a terrestrial value of $\frac{1}{4000}$. Again, it would seem that an appreciable fraction of the O^{17} produced by reaction (49) is destroyed by reaction (50), although not such a large fraction as in the case of O^{18}. The ratio of Ne^{21} to Ne^{20} given by reaction (50)is then about $\frac{1}{1200}$, as compared with the terrestrial value of $\frac{1}{300}$. This moderate discrepancy is, again, not very serious in an order-of-magnitude calculation. It is, in any case, mitigated by the considerations of a later section that provide an additional process for the formation of Ne^{21}.

It remains to be added that F^{19} is produced by the reaction

$$N^{15} + \alpha \rightarrow F^{19} + \gamma\,. \tag{51}$$

For a N^{15} to N^{14} ratio of $\frac{1}{4000}$, as indicated by present estimates for the carbon-nitrogen cycle, the F^{19} to O^{16} ratio would be about $1/10^5$. According to Urey (1952), the meteoritic abundance of fluorine yields a ratio of just this order. On the other hand, astrophysical estimates suggest a greater fluorine abundance. The discrepancy between the present value and the astrophysical requirements may possibly be due to the N^{15} to N^{14} ratio, as given by calculations on the carbon-nitrogen cycle, being too low. Thus, if we were to put the N^{15} to N^{14} ratio equal to the terrestrial value of about $\frac{1}{260}$, the F^{19} to O^{16} ratio would then become about $\frac{1}{8000}$.

VI. NOTABLE OMISSIONS AMONG THE LIGHT ELEMENTS

Among elements lighter than Ne^{22}, the nuclei C^{13}, N^{14}, and N^{15} are not synthesized by the processes described above. The view is here taken that these three nuclei owe their origin to the carbon-nitrogen cycle operating in normal stars, not in the very hot stars at present under consideration. The C^{12} that forms the basis of this cycle is indeed produced by the reactions already discussed. We have the scheme shown in the accompanying tabulation. The present suggestion is supported by the circumstance that it now seems

	C^{12}	C^{13}	N^{14}	N^{15}
Produced in very hot stars (per cent)	100	0	0	0
Produced after C^{12} has been put through the carbon-nitrogen cycle in ordinary stars with temperatures of order 2×10^{7}° K (approximate per cent)	9	2	89	0.022

possible to understand the wide variability of the C^{13} to C^{12} ratio that is found in different stars. The first sample in the accompanying table has a zero C^{13} content, such as seems to occur in hydrogen-poor stars.[5] The second sample has a ratio of 1/4.5, as in some giant

[5] I am indebted to W. P. Bidelman for a private communication on this point. See also Bidelman (1953).

stars, while a mixture of the two samples in equal proportions gives a ratio of about $\frac{1}{55}$—of the same order as the terrestrial value.

There remains, however, a serious discrepancy in the N^{15} to N^{14} ratio, which, at $\frac{1}{4000}$, is too low by a factor of more than 10 to explain the terrestrial ratio of $\frac{1}{260}$. It is possible that the above estimate of the N^{15} concentration stands in need of revision. This possibility may be related to the remarks of the previous section concerning the abundance of F^{19}.

VII. THE SYNTHESIS OF Na^{23}

The discussion has reached the point where an increase of temperature up to about 1.6×10^{8}° K causes the initial helium to be converted into elements lighter than Na^{23}. It must be stressed that considerations from this point become much more tentative. Not enough is known concerning the detailed properties of the nuclei to enable really reliable calculations of reaction rates to be made. Nevertheless, some progress toward a qualitative understanding of the further effects likely to arise at still higher temperatures can be made. With this limitation in mind, the present and following sections attempt in very brief outline to indicate what the main processes of element-building may be from sodium to nickel.

Any new reactions that arise as the temperature rises still further must come from either (i) collisions between the nuclei themselves or (ii) photodisintegration of the nuclei—protons, neutrons, or α-particles being released and then proceeding to contribute to further reactions. An analysis of the situation has shown that, with increasing T, the first important reaction to occur is probably of type i. It is

$$C^{12} + C^{12} \rightarrow Mg^{24}, \tag{52}$$

the Mg^{24} being excited to about 16 mev above ground level and decaying mainly by emitting an energetic proton or α-particle: thus

$$Mg^{24} \begin{cases} \rightarrow Ne^{20} + \alpha\,, \\ \rightarrow Na^{23} + p\,. \end{cases} \tag{53}$$

The temperature at which reactions (52) and (53) become important can be shown to be close to $T = 0.6$.

At first sight it might seem that Na^{23} is readily given by reaction (53), but this is not so, for the following reason: the protons released in the formation of Na^{23} quickly become attached to the heavy nuclei, and much the largest attachment probability is for

$$Na^{23} + p \rightarrow Ne^{20} + \alpha\,. \tag{54}$$

This is because attachment to other nuclei takes plase only through (p, γ) reactions, which are less probable than the exothermic reaction (54) by a factor of the order of 10^{5}. Thus the Na^{23} produced by reaction (53) is effectively wholly destroyed by reaction (54). The formation of Na^{23} would therefore appear to be confined to a less probable mode of decay of the highly excited Mg^{24} nuclei, namely, to the reaction

$$Mg^{24} \rightarrow Mg^{23} + n, \qquad Mg^{23} \rightarrow Na^{23} + \beta^{+}. \tag{55}$$

Reaction (55) is less probable than reaction (53) because the excited Mg^{24} nucleus formed in reaction (52) is energetically incapable of emitting a neutron unless the relative kinetic energy E of the colliding C^{12} nuclei exceeds the energy E_0 at the center of the Gamow peak by about 0.65 mev. For such an energy of collision, $P(E) \exp(-E/kT)$ is less than $P(E_0) \exp(-E_0/kT)$ by a factor close to 10. It appears, therefore, that reaction (55) is

less probable than reaction (53) by a factor of the order of 10—the neutron width for reaction (55) being taken as comparable with the proton and α-particle widths in reaction (53).

The Na^{23} produced by reaction (55) is not appreciably destroyed by neutron addition, since neutrons add with roughly equal probability to all nuclei present. Thus, since Na^{23} is present in low abundance compared with Ne^{20}, O^{16}, and C^{12}, most of the neutrons become attached to these latter nuclei. Attachment to O^{16} tends, however, to be impermanent because the photodisintegration

$$O^{17} + \gamma \rightarrow O^{16} + n$$

is already effective at the temperature at which reactions (52), (53), and (55) become important (the neutron binding in O^{17} is as low as 4.15 mev). Thus the neutrons produced in reaction (55) are mainly used up in the formation of Ne^{21}, either directly through the reaction

$$Ne^{20} + n \rightarrow Ne^{21} + \gamma$$

or indirectly through the reaction

$$C^{12} + n \rightarrow C^{13} + \gamma\,,$$

$$C^{12} + C^{13} \rightarrow Mg^{25} \rightarrow Ne^{21} + \alpha\,.$$

This mode of formation of Ne^{21} is of interest because the process discussed in a previous section was inadequate to explain the observed abundance of Ne^{21} by a factor of about 4. On the present basis the cosmic abundance of Ne^{21} should be closely comparable with the abundance of Na^{23}. Accepting the terrestrial value for the ratio Ne^{21}/Ne^{20}, this requirement would seem to be well satisfied. Thus

$$(Ne^{21}/Ne^{20})_{\text{terrestrial}} = 0.0030, \qquad (Na^{23}/Ne^{20})_{\text{astrophysical}} = 0.0045,$$

the astrophysical value being determined from the spectroscopic study of stellar atmospheres.[6]

The α-particles produced in reactions (53) and (54) are mainly absorbed by C^{12} in $C^{12} + \alpha \rightarrow O^{16} + \gamma$. This means that only about two-thirds of the C^{12} is effective in reaction (52), the remaining third being converted to O^{16} by α-particle addition. Accordingly, one Na^{23} nucleus is produced in the destruction of about 30 C^{12} nuclei (this assumes reaction [53] to be 10 times more probable than reaction [55]). Accepting a ratio of $\frac{1}{3}$ for C^{12}/O^{16}, this would imply a Na^{23} to O^{16} ratio of about $\frac{1}{90}$.

At first sight we might be inclined to accept this as an estimate of the average Na^{23} abundance in material ejected from stars, but this would be incorrect, since it would ignore the heating function, $H(\tau)$, defined in section II, 1, above. It will be recalled that, taking an average over the material ejected from a large number of stars, the fraction of material heated to temperatures in the range τ to $\tau + d\tau$, before ejection into space takes place, was written as $H(\tau)d\tau$. Thus, in obtaining the abundance ratio of two nuclear species, it is necessary to take into account the ratio of

$$\int_{\tau_f}^{\tau_d} H(\tau)\, d\tau \tag{56}$$

for the two nuclei. The lower limit, τ_f, in this integral represents the temperature of formation of the nuclear species, and τ_d is the temperature at which the species is effec-

[6] Cf., for example, Aller (1953).

tively destroyed (all heavy nuclei are destroyed by photodisintegration if τ is sufficiently high). In many cases τ_d is so much higher than τ_f that integral (56) may be approximated by

$$\int_{\tau_f}^{\infty} H(\tau)\, d\tau\,. \tag{57}$$

In the work of previous sections the nuclei whose abundances were compared were formed at such nearly equal temperatures, and τ_d was so large compared with τ_f, that integral (56) was effectively the same for all of them. Consequently, the present considerations could be ignored. They cannot be ignored, however, in comparing Na^{23} and O^{16}, for O^{16} is formed at about $\tau_f = 0.13$, whereas $\tau_f = 0.6$ is required for Na^{23}. When we put $H(\tau) \propto 1/\tau^2$, as indicated in section II, 1, the modification arising from integral (57) is a factor of 4.6, in the sense of a reduction of Na^{23} relative to O^{16}. The calculated abundance ratio of Na^{23} to O^{16} therefore becomes about $\frac{1}{400}$, as compared with a ratio of $\frac{1}{200}$ from astrophysical data (Aller 1953). In view of the approximations made above, this may be considered good agreement.

It may be added that in the calculation of the rate of occurrence of reactions (52) and (53), on which the temperature $T = 0.6$ (quoted above) was based, formula (19) was used. This is because the average spacing of the levels within the excited Mg^{24} nucleus is small compared with the total width Γ for decay. The width Γ_s in expression (19) corresponds to the width for the carbon-carbon collision (52). This contains an important Coulomb-barrier factor. The following values were used in making the estimate $T = 0.6$:

$$G_s = 0.1 \text{ mev}, \qquad \Gamma = 0.1 \text{ mev}, \qquad D = 0.01 \text{ mev},$$

while the time-scale criterion employed was that reactions (52) and (53) should be capable of destroying the C^{12} in 10^{15} seconds.

It may be wondered why the same time scale was used in the present case as in the synthesis of C^{12} from helium. The reason for this is that the reactions that lead to C^{12}, O^{16}, and Ne^{20} being built into heavier elements are exothermic and yield an amount of energy per unit mass of material that is of the same order as the energy released in the building of C^{12}. Hence we expect that the lifetime for the building of C^{12}, O^{16}, and Ne^{20} into such elements as Mg^{24}, Si^{28}, and S^{32} must also be of the order of 10^{15} seconds.

VIII. THE SYNTHESIS OF Mg^{24}

The next most important reaction is the photodisintegration of Ne^{20},

$$Ne^{20} + \gamma \rightarrow O^{16} + \alpha\,, \tag{58}$$

requiring a quantum with energy greater than 4.74 mev. The rate of this reaction may be calculated by using the method described in section 3. The quantity χ in equation (23) is now 4.74, and the yield from the inverse of reaction (58) is calculated for resonance in the neon level corresponding to $E_R = 0.654$ mev—it being assumed that this is not an entirely forbidden transition. Subject to this assumption, investigation of the photodisintegration process then shows that disruption becomes important when T rises to 0.8, the criterion of "importance" in the present sense being that an appreciable fraction the Ne^{20} is disintegrated in the time scale for the collapse of the star—namely, in about 10^{15} seconds. The α-particles produced in reaction (58) are rapidly absorbed at $T = 0.8$. The main source of absorption comes ultimately from

$$Ne^{20} + \alpha \rightarrow Mg^{24} + \gamma\,, \tag{59}$$

the Mg^{24} being highly stable against photodisintegration at $T = 0.8$. Thus the net effect of the photodisintegration of Ne^{20} is to produce Mg^{24} and O^{16}:

$$2Ne^{20} \rightarrow O^{16} + Mg^{24}.$$

The abundance of Mg^{24} can now be calculated relative to O^{16}. With an original Ne^{20} abundance comparable to that of O^{16}, the ratio of Mg^{24} to O^{16}, in the particular sample of material under consideration, is about $\frac{1}{3}$; but once again this does not give the required abundance ratio for the average of all material ejected from stars. The ratio of integral (56) for the two nuclei must once again be taken. Writing $\tau_f = 0.13$ for O^{16} and $\tau_f = 0.8$ for Mg^{24}, and quoting a result to be obtained in the next section—that τ_d is probably about 1.35 for both O^{16} and Mg^{24}—the required ratio becomes about 13.5 in the sense of a decrease of Mg^{24} relative to O^{16}. This leads to an Mg^{24} to O^{16} ratio of about $\frac{1}{40}$, as compared with an astrophysical value of about $\frac{1}{9}$. In view of the uncertainty concerning the form of $H(\tau)$, this may be considered a satisfactory agreement.

It may be noted in addition that, although Ne^{22} is stable against photodisintegration at these temperatures, a considerable proportion of Ne^{22} is nevertheless destroyed by the reaction

$$Ne^{22} + \alpha \rightarrow Mg^{25} + n, \qquad Mg^{24} + n \rightarrow Mg^{25} + \gamma\,.$$

On this basis the ratio Mg^{25}/Mg^{24} should be comparable with the ratio Ne^{22}/Ne^{20}. According to the composition of terrestrial material, this is indeed the case.

IX. ELEMENTS FROM ALUMINUM TO PHOSPHORUS

Of the nuclei so far built up, the most abundant are O^{16} and Mg^{24}. Of these, O^{16} is the less refractory. Calculation indicates that O^{16} undergoes photodisintegration,

$$O^{16} + \gamma \rightarrow C^{12} + \alpha\,, \tag{60}$$

at about $T = 1.35$, this result being based on the resonance effect of a level in O^{16} at 8.6 mev above ground level. The C^{12} so produced is mainly destroyed through the reaction

$$C^{12} + O^{16} \rightarrow Si^{28} \begin{cases} \rightarrow Mg^{24} + \alpha\,, \\ \rightarrow Si^{27} + n\,, \\ \rightarrow Mg^{26} + D\,. \end{cases} \tag{61}$$

Aluminum is then produced by the β-decay of Si^{27}. The disintegration of the Si^{28} in reaction (61) into $Al^{27} + p$ has been omitted for the reason that the protons so produced are removed by the reaction

$$Al^{27} + p \rightarrow Mg^{24} + \alpha\,,$$

this reaction, being exothermic, having a far higher probability than reactions of the (p, γ) type.

The situation is further complicated because at about the same temperature, $T = 1.35$, the following reaction becomes about equally effective in destroying the O^{16}:

$$O^{16} + O^{16} \rightarrow S^{32} \begin{cases} \rightarrow Si^{28} + \alpha\,, \\ \rightarrow P^{30} + D\,, \\ \rightarrow S^{31} + n\,. \end{cases} \tag{62}$$

The decay of S^{32} into $P^{31} + p$ has been omitted in reaction (62) for the reason that the reaction $P^{31} + p \rightarrow Si^{28} + \alpha$ reduces this case to a decay into $Si^{28} + \alpha$, exactly as in the case $Al^{27} + p$, discussed above.

If reactions (60) and (61) are more important than reaction (62), then approximately one α-particle is produced for every *two* O^{16} nuclei that are destroyed. Then, since the magnesium abundance is about one Mg^{24} nucleus for every *three* O^{16} nuclei, it follows that an excess of α-particles is made available, over and above the α-particles necessary to convert the magnesium entirely to silicon through the reaction

$$Mg^{24} + \alpha \rightarrow Si^{28} + \gamma\,. \tag{63}$$

It is to be noted that, so long as Mg^{24} remains available, reaction (63) is favored as compared with other (α, γ) reactions, such as

$$Si^{28} + \alpha \rightarrow S^{32} + \gamma\,,$$

by possessing a lower Coulomb barrier.

In contrast, if reaction (62) is more important than reactions (60) and (61), then the α-particles made available are fewer than in the case just discussed and may indeed be fewer than an average of one α-particle for every *three* O^{16} nuclei destroyed. Should this be so, there are insufficient α-particles to convert entirely the Mg^{24} into Si^{28} by reaction (63).

The discussion of the following section shows that the synthesis of the elements in the sulphur-calcium group is closely dependent on which of these two cases (an α-particle excess over Mg^{24} or vice versa) holds. To decide the matter, more precise nuclear data are required than are at present available.

From the point of view of the present section, however, the situation is substantially the same whichever alternative we adopt, for in both cases the amount of Si^{28} produced by reaction (63) gives an Si^{28} abundance comparable with that of Mg^{24}, as observation demands. In addition, reactions (61) and (62) provide for the origin of the nuclei Mg^{26}, Al^{27}, Si^{29}, Si^{30}, and P^{31}.

X. ELEMENTS FROM SULPHUR TO CALCIUM

The number of reactions that affect nuclei heavier than silicon increases so rapidly as T rises above 1.5 that it is difficult to obtain quantitative estimates for the abundances of such elements. For this reason, the present section will be concerned mainly with qualitative issues.

The procedure so far followed has an underlying feature that will now be explained. Thus far we have been following a set of nuclei (C^{12} to Si^{28}) that have, apart from local deviations, become increasingly stable as the atomic weight increased. The general effect of this increased stability toward magnesium and silicon has been to make both additive and disintegrative processes favor a progression along the sequence of atomic weights: if at a particular temperature a nucleus became unstable then we simply moved on to nuclei of higher atomic weight that were stable at the temperature in question. Consider the effect of the photodisintegration of Ne^{20}, for example.

Now the situation is entirely altered as soon as we come to consider nuclei from sulphur to calcium, for all these nuclei are considerably *less* stable than silicon. Consequently, it is pointless to attempt to explain the origin of these nuclei by increasing the temperature until silicon becomes unstable—at such temperatures all the nuclei in question would be extremely unstable against photodisintegration processes. What would then result would be an approximation to statistical equilibrium, and we shall see in the next section that the nuclei would then belong almost entirely to a group centered around Fe^{56}, not to the sulphur-calcium group.

It may be useful in this connection to give a table of the binding energies of the proton,

neutron, and α-particle for several nuclear species (see the accompanying tabulation). These binding energies give the χ-values for use in equation (23), which determines the effects of photodisintegration. It should be emphasized that the stability of a nucleus is

	Binding Energies in Mev															
	Mg^{26}	Al^{27}	Si^{28}	Si^{29}	Si^{30}	P^{31}	S^{32}	S^{33}	Cl^{35}	A^{36}	Cl^{37}	A^{38}	K^{39}	Ca^{40}	Ca^{42}	Ti^{46}
Proton	13.9	8.3	11.6	12.3	12.6	7.2	8.8	9.4	6.3	8.5	10.4	10.1	6.7	8.3	10.2	10.4
Neutron	11.1	13.8	17.0	8.5	10.6	12.4	14.5	8.7	12.7	14.7	10.3	11.7	13.1	15.7	11.3	13.3
α-Particle	10.4	10.1	10.0	11.1	10.7	9.6	6.9	7.0	6.8	6.4	8.2	7.0	7.5	7.3	6.6	7.7

decided by the most sensitive reaction: a nucleus that is unstable against proton removal, for example, cannot be classed as stable because it happens to be stable against α-particle removal or against neutron removal. Thus the stability of Cl^{35} against neutron removal does not make it a stable nucleus; on the contrary, it would seem rather markedly unstable to proton removal.

The above remarks pose a serious question as to the mode of origin of the nuclei in the sulphur-calcium group. The answer to the apparent dilemma would seem to be in the possibility of the existence of a moderate α-particle excess produced by the reactions that destroy O^{16}, an excess, that is to say, over and above the α-particles that are required for the conversion of Mg^{24} into Si^{28}. We saw in the previous section that the number of α-particles must be comparable with, and may indeed be somewhat greater than, the number of Mg^{24} nuclei. If this is so, then there is an excess of α-particles not used in the reaction $Mg^{24} + \alpha \rightarrow Si^{28} + \gamma$ and available for the reaction

$$Si^{28} + \alpha \rightarrow S^{32} + \gamma\,. \tag{64}$$

Thus an α-particle excess forces Si^{28} nuclei through into the sulphur-calcium group. Indeed, the extent of the α-particle excess would seem to determine the abundance of the latter group. A 33 per cent α-particle excess would give an abundance ratio, (sulphur-calcium group)/Si^{28}, of about $\frac{1}{2}$, which is in accordance with the astrophysical data.

When we come to consider individual nuclei within the sulphur-calcium group itself, once again the tendency is for increasing stability to go with increasing atomic weight. Thus Ca^{40} is more stable than either A^{36} or S^{32}, and A^{36} is probably slightly more stable than S^{32}, in spite of the fact that the α-binding in A^{36} is somewhat less than that in S^{32}. The reason for this is that the Coulomb barrier for the reaction

$$A^{36} + \gamma \rightarrow S^{32} + \alpha \tag{65}$$

is higher than that for the reaction

$$S^{32} + \gamma \rightarrow Si^{28} + \alpha\,. \tag{66}$$

This means that, although S^{32} is first formed by reaction (64), a temperature is eventually reached at which reaction (66) supplies α-particles that promote the inverse of reaction (65), namely,

$$S^{32} + \alpha \rightarrow A^{36} + \gamma\,. \tag{67}$$

At a slightly higher temperature, reaction (65) likewise provides α-particles that promote the reaction

$$A^{36} + \alpha \rightarrow Ca^{40} + \gamma, \tag{68}$$

the Ca^{40} so produced being stable at the temperature in question; it seems likely that Ca^{40} is stable up to about $T = 1.75$.

In addition to reactions (67) and (68), the reactions

$$P^{31} + \alpha \rightarrow Cl^{35} + \gamma\,, \tag{69}$$

$$Cl^{35} + \alpha \rightarrow K^{39} + \gamma\,, \tag{70}$$

occur with appreciable probability. It is accordingly possible to understand qualitatively how chlorine and potassium may originate. There is, however, a serious quantitative difficulty: it seems that both Cl^{35} and K^{39} must be highly unstable against proton removal by photodisintegration. Indeed, it is surprising that these nuclei can persist, even at $T = 1.35$, for the usual time scale of 10^{15} seconds. Yet, if they do not so persist, we should expect to find only extremely low abundances of these nuclei. While it is true that meteoritic data do indicate unusually low abundances for these nuclei, the abundances are not nearly so low as quantitative estimates might suggest. The resolution of the difficulty may turn out to lie in the fact that the energy-level diagrams of these two nuclei are somewhat unusual. It may be that the energy levels are peculiarly distributed, in the sense that there is no level at all close to the disintegration energies—that there is no level close to 6.3 mev above the ground level of Cl^{35} and no level close to 6.7 mev above ground level in K^{39}.

XI. STATISTICAL EQUILIBRIUM AND THE IRON PEAK

The present section encroaches on the topics to be discussed in the second paper of this series. Thus far we have regarded the collapse of the star as being brought about by the escape of radiation from its surface into space. However, as the temperature in the deep interior rises above $T = 2$, other effects come to control the collapse of the star. Thus, at about $T = 3$ the loss of energy through neutrinos escaping from the star—the Gamow urca process—becomes more effective than the escape of radiation in promoting the collapse of the star. At about $T = 5$, neutrino emission greatly dominates the collapse, producing an important shrinkage, not in the former time scale of 10^{15} seconds, but in a time of the order of a year. At temperatures above $T = 5$, nuclear reactions other than β-processes take over control of the shrinkage, at which stage the collapse occupies no more than a few seconds of time.

Thus the state of the star changes, as T rises above 2, from one of quasi-stability to one of severe instability. The division between the present paper and a future paper is made by the fact that we are here concerned with the discussion of the quasi-stable case, whereas future work will be concerned with the high-temperature states of dynamical instability. The two cases differ not only in the time scales to be applied to them but also in the relation between the density of material and its temperature. The relation used frequently in the above work, namely,

$$\rho = 10^6 T^3,$$

belongs to the quasi-stable case and cannot necessarily be applied under conditions of serious instability.

Now, although the behavior of stellar material at temperatures near $T = 5$ comes mainly under the terms of reference of the investigation of a later paper, there is one consideration relating to temperatures of this order that it is useful to discuss here, for the reason that it throws light on all the work of the present paper.

At temperatures near $T = 5$, in spite of the shortening of the time scale due to the rapid dynamical evolution of the star that then ensues, nuclear reactions occur so rapidly and in such profusion that an approximation to statistical equilibrium among them must of necessity be set up. Both associative and photodisintegrative processes happen very

quickly: the photodisintegration of the refractory nucleus Si^{28}, for example, takes less than a second at $T = 5$, as compared with more than 10^{15} seconds at $T = 2$.

The equations of statistical equilibrium are well known. The form in which they will now be used was arrived at in a former paper. Thus, we quote[7] the following equation,

$$\log n_A^Z - 34.08 - \tfrac{3}{2}\log T - \tfrac{3}{2}\log A = \frac{A}{A'}(\log n_{A'}^{Z'} - 34.08 - \tfrac{3}{2}\log T - \tfrac{3}{2}\log A') + \frac{5.04}{T} A\left(\frac{Q_A^Z}{A} - \frac{Q_{A'}^{Z'}}{A'}\right) + A\theta\left(\frac{Z}{A} - \frac{Z'}{A'}\right), \tag{71}$$

where logarithms are to the base 10; θ is the logarithm of the ratio of the density of free protons to the density of free neutrons; T is again in units of 10^9 ° K; Q_A^Z and $Q_{A'}^{Z'}$ represent the binding energies in mev of nuclei (A, Z) and (A', Z'), respectively; and n_A^Z and $n_{A'}^{Z'}$ are the number densities of these nuclei. For nuclei with experimentally determined binding energies, equation (71) serves to determine statistical abundance ratios when T, θ, and the total density are specified. In the accompanying tabulation the logarithms of abundance ratios, relative to Fe^{56}, are given for $T = 5.04$, $\theta = 2$, and $\log n_{56}^{26} = 28$—these values being chosen so as to be also consistent with statistical equilibrium between

ABUNDANCE RATIOS RELATIVE TO Fe^{56} (LOGARITHMS TO BASE 10)

	Nucleus											
	Ti^{48}	Cr^{52}	Fe^{54}	Mn^{55}	Fe^{57}	Fe^{58}	Ni^{58}	Co^{59}	Ni^{60}	Ni^{62}	Cu^{63}	Zn^{64}
Theoretical abundances	−3.3	−0.38	−0.47	−2.3	−2.3	−2.0	−1.5	−2.6	−0.67	−3.1	−4.8	−5.0
Meteoritic abundances	−2.6	−1.9	−1.2	−2.0	−1.6	−2.5	−1.8	−2.4	−1.4	−2.7	−3.4	−3.9
Adopted binding energy per nucleon (mev) (only differences affect the calculated abundances)	+8.702	+8.773	+8.737	+8.764	+8.769	+8.793	+8.733	+8.768	+8.785	+8.782	+8.741	+8.725

neutrons and protons (Hoyle 1948). A value of 492 mev was adopted for the binding energy of Fe^{56}.

These values provide a satisfactory explanation of the well-known sharp peak of abundances centered at Fe^{56}. Statistical balancing fails, however, to explain the abundances of elements in the far wings of the peak; the abundances are too low for elements lighter than titanium and for elements heavier than nickel. Taking different values for T and ρ (θ being determined by statistical considerations when T and ρ are given) does not alter this situation: a lowering of the temperature produces a *narrowing* of the peak (the abundances only being slightly altered by moderate variations of ρ). We may quote the result of a future paper that a significant increase of T above 5 is inapplicable to the building of these nuclei. The origin of elements from calcium to titanium and of elements heavier than nickel accordingly remains to be explained. Elements heavier than nickel will be considered in detail in a subsequent paper, but the elements from calcium to titanium will not receive consideration either in this or in the subsequent paper. The reason for this omission is that the members of the calcium-titanium group of nuclei probably originate at values of T only slightly above 2, before any useful approximation to statistical equilibrium is attained but at temperatures such that the reactions occurring are very numerous. Thus this group of nuclei probably belongs to an intermediate range of tem-

[7] Hoyle (1946, p. 375). The present eq. (71) is equivalent to eq. (50) of this former paper. It may be noted that a numerical difference arises in the coefficient that multiplies $(Q_A^Z/A - Q_{A'}^{Z'}/A')$, because Q_A^Z and $Q_{A'}^{Z'}$ are measured in mev in the present paper, as compared with the m.m.U. used in the former paper.

peratures in which it is extremely difficult to make quantitative estimates—where the reactions that occur are too numerous to be traced individually but where statistical equilibrium cannot be applied.

The present results put the work of earlier sections in a clearer light. We have seen that the general tendency with rising temperature has been for nuclei of increasing atomic weights to be synthesized. In this work we have been examining the details of a slow drift toward statistical equilibrium. If all additive and disintegrative reactions had taken place sufficiently rapidly at lower temperatures, the statistical distribution of nuclei centered around Fe^{56} would have been set up. The fact that this did not happen was due to the slowness of the reactions, but those reactions that did occur had the general effect of favoring the drift toward the iron peak.

Two further points must now be made concerning the abundances shown in the table on page 144. At temperature $T = 5$ an assumption used implicitly in previous sections cannot be safely made. Thus it has been assumed so far that the composition of material is not altered during the process that causes its ejection from the star. At temperatures at which nuclear reactions take place slowly, in a time of the order of 10^{15} seconds, for example, this is certainly valid, since the ejection presumably takes place in only a few seconds. At values of T near 5, however, many reactions also take place on a time scale of a few seconds. Accordingly, it is no longer valid to suppose that the composition remains unchanged during the expansion of the material. The freezing of the composition must then take place in a complex manner, and it does not follow that material with, say, the composition shown in the table on page 144 will necessarily reach a dispersed state without substantial changes taking place. Second, it is to be emphasized that the statistical equation (71) neglects the internal partition functions of the nuclei. Inclusion of the partition functions might well alter the calculated abundances by a factor of as much as 10. Furthermore, it may be added that the nucleus binding energies adopted above may be in error by a margin sufficient to alter the calculated abundances also by a factor 10.

Finally, we may note that, since Fe^{56} is the most abundant nucleus at $T = 5$, the absolute abundance of Fe^{56} must be roughly comparable with the abundance of Si^{28}, which, it will be recalled, was the most abundant nucleus at $T = 2$. This is in accordance with observation.

XII. CONCLUSIONS

It remains to collect in a table (see the accompanying tabulation) the main results deduced above (with the exception of the abundances of elements in the iron group, which have already been given in tabular form on p. 144). It is particularly stressed that

Results Deduced	Astrophysical Estimates	Terrestrial and/or Meteoritic Abundances
$C^{12}/O^{16} \doteq \frac{1}{3}$	$C^{12}/O^{16} = \frac{1}{3}$	
$O^{16}/Ne^{20} \doteq 1$	$O^{16}/Ne^{20} = 1$	
$O^{17}/O^{16} \leq \frac{1}{1200}$		$O^{17}/O^{16} = \frac{1}{4000}$
$O^{18}/O^{16} \leq \frac{1}{30}$		$O^{18}/O^{16} = \frac{1}{500}$
$Ne^{22}/Ne^{20} \doteq \frac{1}{30}$		$Ne^{22}/Ne^{20} = \frac{1}{10}$
$F^{19}/O^{16} \leq \frac{1}{8000}$	?	?
$Ne^{21}/Na^{23} \doteq 1$	$Na^{23}/Ne^{20} = 0.0045$	$Ne^{21}/Ne^{20} = 0.0030$
	$Ne^{21}/Na^{23} = \frac{2}{3}$	
$Na^{23}/O^{16} \doteq \frac{1}{400}$	$Na^{23}/O^{16} = \frac{1}{200}$	
$Mg^{24}/O^{16} \doteq \frac{1}{40}$	$Mg^{24}/O^{16} = \frac{1}{9}$	
$Ne^{22}/Ne^{20} \doteq Mg^{25}/Mg^{24}$		$Ne^{22}/Ne^{20} = Mg^{25}/Mg^{24}$
$Si^{28}/Mg^{24} \doteq \frac{2}{3}$	$Si^{28}/Mg^{24} \doteq \frac{1}{2}$	
$(S^{32}, A^{36}\ Ca^{40}) \doteq 0.5Si^{28}$	$(S^{32}, A^{36}, Ca^{40}) \doteq 0.5Si^{28}$	
$Si^{28} \doteq Fe^{56}$	$Si^{28} \doteq Fe^{56}$	$Si^{28} \doteq Fe^{56}$

the results given in the first column were obtained subject to certain assumptions and accordingly have not been demonstrated in a manner free from all doubt. Nevertheless, the number of assumptions made was much less than the number of results obtained.

The comparisons shown above can, in the view of the writer, be summed up in the statement that they provide considerable support for the belief that the elements from carbon to nickel have been synthesized by nuclear reactions occurring inside stars—albeit inside the special collapsed type of star that has been under consideration throughout the paper.

The writer is much indebted to Dr. W. A. Fowler and to Dr. J. L. Greenstein, both for valuable discussions concerning the subject matter of this paper and for help in its preparation.

REFERENCES

Aller, L. 1953, *Astrophysics* (New York: Ronald Press Co.), p. 327.
Atkinson, R. d'E., and Houtermanns, F. G. 1929, *Zs. f. Phys.*, **54**, 656.
Bethe, H. A. 1939, *Phys. Rev.*, **55**, 434.
Bidelman, W. P. 1953, *Ap. J.*, **117**, 25.
Blatt, J. M., and Weisskopf, V. F. 1952, *Theoretical Nuclear Physics* (New York: John Wiley & Sons), p. 386.
Dunbar, D. N. F.; Pixley, R. E.; Wenzel, W. A.; and Whaling, W. 1953, *Phys. Rev.*, **92**, 649.
Gamow, G., and Teller, E. 1938, *Phys. Rev.*, **53**, 608.
Hoyle, F. 1946, *M.N.*, **106**, 366.
Hoyle, F. 1948, *ibid.*, **108**, 372.
Salpeter, E. E. 1952, *Ap. J.*, **115**, 326.
Teichmann, T. 1950, *Phys. Rev.*, **77**, 506.
Urey, H. C. 1952, *Phys. Rev.*, **88**, 248.

ON THE DISSIPATION OF GAS AND VOLATILIZED ELEMENTS FROM PROTOPLANETS

HAROLD C. UREY
Institute for Nuclear Studies, University of Chicago
Received October 30, 1953; revised March 15, 1954

ABSTRACT

1. The chemical facts previously presented by Russell and Menzel relative to the loss of the inert gases and the retention of water by the earth and the evidence for the fractionation of the silicate and metallic phases in the terrestrial planets as presented previously by Urey are reviewed.

2. The evidence relative to the possible loss of elements from the meteorites and earth is reviewed, with the conclusion that there is no evidence for any important loss of elements less volatile than mercury from either of these classes of matter.

3. It is pointed out that the state of oxidation of iron and other elements in the meteorites and the earth shows that these classes of materials were not heated in contact with gases of cosmic composition. This conclusion has been presented previously.

4. It is shown that Eucken's model for the formation of the earth, namely, condensation of its substance in the presence of gases of cosmic composition at high temperatures, would result in the loss of certain elements from the earth, which is contrary to observation.

5. It is concluded that it is improbable that the maintenance of large objects within an Eucken gas sphere for long periods of time (10^8 years), as proposed by Kuiper, would result in their destruction and that the preservation of volatiles, such as mercury, arsenic, cadmium, and zinc, in approximately cosmic proportions would not have occurred.

6. Gases were lost from the protoplanets carrying the inert gases away from the forming earth before enough of the earth had accumulated to give a strong gravitational field. The planets accumulated from the satellite objects because of a loss of energy to a low-density gaseous mass surrounding the growing planet.

7. A possible evaporative process for the melting of silicates and nickel-iron with the high temperature produced by the sun is suggested. It is concluded that this is an improbable source of heat, though the possibility should be further investigated.

8. It is suggested as an approximate series of events that the solar nebula broke up into protoasteroidal-type masses; that the accumulation of asteroidal objects at low temperatures occurred within these; that subsequent heating occurred as the protoplanets were formed, producing melted silicates and nickel iron; and that the silicates were partially lost during collision processes during the latter part of this series of events. This mechanism is favored, though the evaporation at the surface of large objects during this approximate series of events may have contributed to the preferential loss of the silicate fraction.

9. The possibility that asteroidal-type objects existed in a dust cloud before its collision and capture by the sun is explored. It is concluded that there is no evidence for the existence of such bodies but that the possibility cannot be entirely excluded.

During recent years the writer (Urey 1951, 1952*b*) has put forward a suggested course of events for the early history of the solar system, based principally on chemical evidence. At the same time an effort has been made not to ignore physical and astronomical evidence in regard to this problem, and, in particular, an effort has been made to adjust the theory to Kuiper's (1951*a*, *b*) studies relative to the origin of the solar system. It has been postulated that the accumulation of substantial objects from dust occurred during a low-temperature period and that this accumulation was facilitated by the effects of condensed water and perhaps also ammonia. Following this, a high-temperature stage was assumed, during which reduced iron and iron carbide were produced at the surface of these bodies and silicates were evaporated from them, while some water and nitrogen were preserved in the interior. It was assumed that hydrogen, the inert gases, and most of the water, nitrogen, and methane were lost from the protoplanet during and at the end of this heating process, and, finally, after this these objects were accumulated into the earth and other planets. The successive stages were continuous, of course, and are divided only for purposes of presentation. This series of events was devised to account for the reten-

tion of water within the satellites[1] and for the varying density of the planets by the partial evaporation of the silicate phase, which may be assumed to have occurred in differing degrees in various terrestrial planets. In this paper this model will be reviewed in the light of additional evidence relative to other elements of different volatilities, in order to narrow, if possible, the conditions necessary for the retention and loss of elements from the meteorities, the earth, and the other terrestrial planets.

THE CHEMICAL FACTS

1. Russell and Menzel (1933) pointed out that neon has been lost from the earth to a much greater degree than have other elements of comparable cosmic abundance and atomic weight, namely, carbon as methane, nitrogen as the element or as ammonia, and oxygen as water. The neon has been reduced by a factor of about 10^7 relative to the surface water of the earth. Aston (1924) pointed out that all the inert gases are much rarer on earth than are the elements of similar atomic numbers. Evidently, these elements have been lost because of their inability to form chemical compounds, as suggested by Russell and Menzel. Brown (1952) and Suess (1949*b*) have discussed the details of the abundance of the inert gases, and Urey (1952*b*, chap. 4) has examined the chemical properties of carbon, nitrogen, and oxygen with a view to understanding how they were retained on the earth.[2] In fact, the outline of events given above was devised primarily to account for these facts. Table 1 summarizes some data relative to these facts. It is a revised version of a table published previously (Urey 1952*b*, p. 125).

2. The densities of the terrestrial planets vary from 3.31 for the moon to about 5.0 or greater for Mercury, estimated at zero pressure but not at ordinary temperatures. Values for these densities are given in Table 2, together with estimates of the amounts of metallic and silicate fractions necessary to account for the densities (Urey 1952*b*, p. 59). It seems impossible to account for all the difference in density on the basis of the formation of higher-density phases with increased pressure. It appears that a real separation of materials of different chemical composition is required, at least to some extent and for some planets. A fractionation of the metallic and silicate phases has occurred in the case of the chondritic meteorites, as shown by Urey and Craig (1953). The character of the fractionation is demonstrated by the relative abundances of the elements which they found for two groups of chondritic meteorites and which are given in Table 3. To a first approximation, the difference in concentration is between the siderophile and other elements. However, there is definite evidence that nickel and perhaps also cobalt are concentrated in the high-iron group more than the iron and that sulphur and calcium may also be concentrated in this group relative to silicon and other elements. If we assume that their low-iron group represents the primordial composition, then 42 per cent of the silicate fraction and 19 per cent of the iron were lost from that part of the parent-object which produced their high-iron group of meteorites, assuming that all the nickel was conserved. Other equally uncertain assumptions can be made, of course.

Estimates of the ratios of the initial masses of the nonvolatile materials of the protoplanets to those of the planets have been made on the assumption that the iron was quantitatively retained in the planets (Urey 1951, 1952*b*, p. 141). The calculation cannot be exact because the composition of the original cosmic matter is not known exactly, and the

[1] Previously these objects were called "planetesimals." G. K. Gilbert (1893) called them "moonlets." I prefer "satellites," since the Latin derivative is more easily internationalized.

[2] The discussion relative to the retention of carbon in the earth and meteorites neglected volatilities due to carbon monoxide, carbon dioxide, and acetylene and condensation as a solution of carbon in metallic iron, as well as the existence of nonstable carbon compounds. This subject is being restudied by the writer. It seems most probable that carbon was retained in the earth and meteorites through the accumulation at low temperature of carbon compounds such as those observed in the carbonaceous chondrites (see Mueller [1953] for a discussion of these objects; see also H. C. Urey, *Proceedings of the XIIIth International Congress of Pure and Applied Chemistry, Stockholm, 1953.*

composition of the mantle of the earth can only be guessed, since no samples are available. The process of removing silicates from the protoplanet can hardly have been such as to remove no elementary iron; but how much was removed is unknown. The conservation of elementary iron requires that

$$M_0 x_0 = M_r x_r + (M_0 - M_r)x\,,$$

where M_0 and M_r are the original and residual masses of the nonvolatile material of the protoplanet, i.e., silicate and metal phases; x_0 and x_r are the weight fraction of iron in the

TABLE 1*

Element	Cosmic Abundance ($Si = 10{,}000$)	Gram Atoms per Cm² on Earth's Surface	Depletion Relative to Water
H†	3.7×10^{8}	30,000	6.0×10^{-4}
He†	1.8×10^{7}	1.7×10^{-4}	7.1×10^{-11}
C	40,000	350	6.5×10^{-2}
N	80,000	54	5×10^{-3}
O	150,000 (total) 111,000 (H_2O)	15,000	1
Ne	166,000	6.5×10^{-4}	2.9×10^{-8}
S	2,510	23	6.8×10^{-2}
A	1,120	1.2×10^{-3}‡	8×10^{-6}
Kr	0.718	3.5×10^{-5}	3.6×10^{-4}
Xe	0.0665	2.8×10^{-6}	3.1×10^{-4}

* The cosmic abundances are those of Suess (1954). The depletion is calculated relative to surface water, i.e., it is the ratio of the surface abundance of the element to its cosmic abundance divided by this ratio for water. We do not know the abundances of these elements throughout the earth, and hence the depletions have only a comparative value for volatile substances. Suess (1949*b*) and Kuiper (1952*a*) have discussed the variation in the depletion of the inert gases. Kuiper concludes that the inert gases were lost before the earth acquired its present small size. Urey (1952*a*) has suggested that krypton and xenon may have been captured by the comets and returned to the earth.

† Suess's ratio of *H* to *He* is 7.2, while recent work shows that this ratio should be about 20–25 (Underhill 1951). We have used 20 for this ratio and lowered the abundance of *He*.

‡ This value includes only A^{36} and A^{38}, on the assumption that A^{40} has been produced from K^{40}.

TABLE 2*

CONSTANTS OF THE PLANETS

Planet	Mass (Earth = 1)	Radius (Earth = 1)	Mean Density	Mean Density at Zero Pressure	Per Cent Iron-Nickel Phase	Oblateness (ϵ)	$\epsilon MG/a^3\Omega^2$
Moon	0.012304	0.2728	3.34	3.31	0	.....	.....
Mercury	0.0543	{0.38 0.403	5.46 4.58	5.4 4.5	72 50	.....	.....
Venus	0.8136	0.961	5.06	4.4(?)	45	.....	.....
Earth	1	1	5.515	4.4	45	0.0033659	0.976
Mars	*0.1080	{0.520 0.523	4.24 4.17	4.02 3.95	30 27	.00520 0.00520	1.22 1.19

* This table differs slightly from a similar one in *The Planets*, p. 60 (Urey 1952*b*). Kuiper's (1952*a*) values of the radii of Mercury and Mars are included instead of the Russell, Dugan, and Stewart values. The 0.38 and 0.523 values for the radii of Mercury and Mars, respectively, are Kuiper's values, while the 0.403 value for Mercury is Rabe's (1929) average and the 0.520 value for Mars is Trumpler's (1927) result. The percentage of iron is calculated by assuming a density of silicate and iron of 3.3 and 7.23, respectively.

original and residual materials; and x is the weight fraction in the material removed. The value of x_0 from abundance tables such as those of Aller (1953), Urey (1952*c*), Urey and Craig (1953), or Suess (1949*a*, 1954) is about 22–28 per cent, and the lower value must be favored if silicates have been lost from the meteorites. The value of x_r is the mean percentage of iron in the earth and is about 31 per cent if there is no iron in the mantle, which is obviously not true. If the value is some 15 per cent by weight of the mantle, which seems likely, including both oxidized and metallic iron, the earth is about 41 per cent iron by weight. The value of x is unknown but cannot be zero. Using $x_0 = 0.22$, $x_r = 0.41$, and $x = 0$, we get

$$\frac{M_0}{M_E} = 1.9\,,$$

TABLE 3

ATOMIC ABUNDANCES OF THE ELEMENTS IN CHONDRITES
(Silicon = 10,000)

Element	Low Group	High Group	Difference (Per Cent)	Total Average
Oxygen	34,760	33,882	− 2.6	34,386
Sodium	509	490	− 3.8	500
Magnesium	9261	9444	+ 2.0	9335
Aluminum	778	769	− 1.2	774
Silicon	10,000	10,000	.....	10,000
Phosphorus	47	42	−12.6	45
Sulphur	1000	1100	+10.0	1041
Potassium	58	59	+ 1.1	58
Calcium	532	595	+12.0	558
Titanium	21	23	+ 8.8	22
Chromium	87	63	−37.9	76
Manganese	57	54	− 6.0	56
Iron	6084	8498	+39.7	7091
Cobalt	17	29	+68.6	23
Nickel	274	476	+73.3	360
Fe/Ni	22.17	17.87	−24.1	19.72
Fe/Ni (weight per cent)	22.07	17.01	−23.9	18.71

and, for ratio of initial silicate to final silicate,

$$\frac{M_0 \times 0.78}{M_E \times 0.59} = 2.5\,.$$

If x_0 is assumed to be 0.28, these numbers are 1.46 and 2.15, respectively. If x_0 is taken as 0.22 and x is taken as 0.10, which seems not at all unlikely to the writer, these numbers become 3.4 and 4.5. The calculation cannot be improved without more complete data. However, quite substantial amounts of the abundant difficultly volatile constituents, such as SiO_2, MgO, Al_2O_3, CaO, etc., and, of course, some Fe or FeO, must have been lost in order to produce the high density of the earth. Even more extensive loss from the planet Mercury, about the same from Venus, less from Mars, and little from the moon must have occurred if these variations in density are due to such loss. The model outlined in the introduction was devised to account for the variations in densities of the planets.

THE ABUNDANCES OF OTHER ELEMENTS

3. The preceding two observations relative to chemical fractionation have been previously presented, but it is of interest to consider possible fractionation of other ele-

ments, especially since it might be reasonably assumed that the retention of water and nitrogen could have resulted from some incidental process. For this purpose it would be most advantageous to have, on the one hand, a better knowledge of cosmic abundances and, on the other, far more accurate estimates of terrestrial and meteoritic abundances than we now have. It is not possible to specify precisely what the fractionation of elements during the formation of these bodies from primitive cosmic matter has been, but it is possible to observe that certain fractionations in a marked degree, which might be expected under specified conditions, have or have not occurred. The writer (1954) has shown that there is some evidence that the nonmetallic elements have been systematically lost from the meteorites; this could have occurred during the initial low-temperature stage, outlined in the introduction, through the volatility of carbon compounds. This possible fractionation is not important to the present discussion, though the outlined model of events provides a suitable condition for its occurrence.

The general trend of the abundances of the elements with atomic number is well established. The abundances of hydrogen and helium are very high; the curve falls to a minimum at lithium, beryllium, and boron and rises to a maximum at oxygen or neon, falls to a minimum at scandium and titanium, rises to a maximum at iron, and then falls slowly but steadily, with some irregularities.

Suess (1954, 1949*a*) has attempted to estimate the cosmic abundances of the elements, considering all the evidence available—astronomical, meteoritic, and terrestrial. This is an objective estimate, but the estimates are necessarily influenced by the observed meteoritic values. Obviously, we are not comparing independent values. Suess's argument is briefly as follows: meteoritic values indicate a regular trend of the abundances above copper, especially in the odd-mass elements; we assume that this is a true regularity of nature and interpolate abundances on this basis, using certain pairs of elements which stay together in nature, such as potassium and rubidium, and zirconium and hafnium, to estimate abundances from one part of the table to another. Thus "smoothed" values are obtained which are certainly not independent of the general trend of meteorite abundances. Yet these abundances should represent some process of synthesis of the elements which was surely independent of the differing chemical properties of neighboring elements in the periodic system; hence marked deviations from this smoothed curve may be correlated with differences in chemical properties, e.g., the almost complete absence of the inert gases for the earth may be correlated with very volatile properties. Moreover, the absence of such marked deviations is also significant.

We give Suess's estimated values for atomic abundances in column A of Table 4 for elements which are significant for the present study, that is, we omit the elements which have obviously been lost and the rare earths which have similar properties and abundances to those of lanthanum. In column B the abundances, as derived from the chondritic meteorites as given by Urey (1952*c*), and in the fourth column the ratios of the values of the second and third columns, B/A, are listed. Column C gives abundances in the earth's crust estimated from the data reviewed by Rankama and Sahama, with certain exceptions noted in the footnote to the table. The sixth column, C/A, gives the ratios of the values of the fifth and second columns. The sixth and seventh columns give the melting points and boiling points of the elements. Obviously, some of these are not applicable to cosmic conditions. The eighth column gives a chemical compound characteristic of the lithophile or chalcophile character of the element or is blank if the element has a siderophile character. The last two columns give the melting points and boiling points of the compound listed in the eighth column. If the boiling point is unknown, the melting point indicates a lower limit for the boiling point. These compounds may not be those which must be evaporated in order for the element to be lost, since reaction with hydrogen may produce more volatile compounds, e.g., SiO from SiO_2, Al_2O or AlH from Al_2O_3, etc. However, as will be shown later in the case of $MgSiO_3$, these high-boiling compounds are often very nonvolatile, and their boiling points may be taken as a qualitative estimate of their volatilities. In the meteorites the abundance of tungsten seems to be too high, prob-

TABLE 4*

ABUNDANCES AND PROPERTIES OF THE ELEMENTS AND SOME COMPOUNDS

ELEMENT	A SUESS'S ABUNDANCES	B METEORITIC ABUNDANCES	B/A	C TERRESTRIAL ABUNDANCES	C/A	ELEMENT		COMPOUND	TEMP. OF COMPOUND (° K)	
						M.P. (° K)	B.P. (° K)		M.P.	B.P.
3 *Li*	100	100	1	950	9.5	353	1599	Li_2SiO_3	1461	.....
4 *Be*	20	16	1	70	3.5	1556	(3040)	*BeO*	2823	(4173)
5 *B*	24	20	1	90	3.7	2313	(2823)	B_2O_3	723	1523
9 *F*	5000	300	0.06	3730	0.75	55.20	85.24	*NaF*	1268	1877
11 *Na*	46,200	51,000	1.10	125,000	0.27	371	1162	Na_2SiO_3	1362	.....
12 *Mg*	887,000	870,000	0.98	87,000	0.098	923	1393	*MgO*	3173	(3873)
13 *Al*	88,200	82,000	0.93	304,000	3.5	933	2600	Al_2O_3	2313	(2483)
14 *Si*	10^6	10^6	1	10^6	1	1683	2628†	SiO_2	1883	(2503)
15 *P*	9000	7500	0.83	3920	0.44	317.4	553	Fe_2P	1633	.....
16 *S*	251,000	98,000	0.39	1650	0.0066	392.0	717.76	*FeS*	(1466)	.....
17 *Cl*	2000	2100	1.05	570	0.28	172.16	239.10	*NaCl*	1081	1738
19 *K*	1800	3500	1.94	67,000	37.0	336.6	1030	K_2SiO_3	1249	.....
20 *Ca*	66,000	56,000	0.85	92,000	1.4	1123	(1473)	*CaO*	2873	(3123)
21 *Sc*	15	17	1.1	11	0.73	1673	4173	Sc_2O_3	.....	.....
22 *Ti*	2630	1800	0.68	9300	3.5	2085	.....	TiO_2	2108	(<3273)
23 *V*	150	150	1.0	420	2.8	2003	.....	V_2O_3	2250	.....
24 *Cr*	11,500	8200	0.71	780	0.068	2173	2933†	Cr_2O_3	2538	.....
25 *Mn*	8000	6800	0.85	2950	0.37	1517	2360	*MnO*	2053	.....
26 *Fe*	725,000	670,000	0.92	91,000	0.125	1808	3073	*FeS*	(1466)	.....
27 *Co*	3000	2900	1.0	69	0.023	1766	3373	*CoS*	1373	.....
28 *Ni*	38,000	39,000	1.0	170	0.0045	1728	3073	*NiS*	1070	.....
29 *Cu*	234	420	1.8	104	0.44	1356.2	2855	Cu_2S	1400	.....
30 *Zn*	841	180	0.21	78	0.093	692.7	1180	*ZnS*	.....	1455 (Sub.)
31 *Ga*	39.8	10	0.25	22	0.55	309.94	2300	*CaS*	1218	.....
32 *Ge*	158	110	0.70	5.6	0.035	1233	(2973)	.....	.....	.....
33 *As*	10	4.6	0.46	2.7	0.27	1090	883 (Sub.)	As_2S_2	580	838

* The terrestrial abundances are taken from the data reviewed by Rankama and Sahama, *Geochemistry* (Chicago: University of Chicago Press, 1950), except as follows: *Zn*, K. H. Wedepohl, *Geochim. et cosmochim. acta*, **3**, 93, 1953; *Cl*, P. K. Kuroda and E. B. Sandell, *Bull. Geol. Soc. Amer.*, **64**, 879, 1953; *As*, E. B. Sandell, private communication; *F*, S. Koritnig, *Geochim. et cosmochim. acta*, **1**, 89, 1951; *Br*, W. Behne, *Geochim. et cosmochim. acta*, **3**, 186, 1953; *Tl* and *In*, D. M. Shaw, *Geochim. et cosmochim. acta*, **2**, 118, 185, 1952.

The melting and boiling points are taken from *Selected Values of Chemical Thermodynamic Properties* (Circ. 500, Nat. Bur. Stand.), with the following exceptions: The temperatures in parentheses are from Lange's *Handbook of Chemistry* and are probably somewhat less reliable. Those marked with a dagger (†) are from the Landolt-Bornstein *Tabellen*. "(Sub.)" indicates sublimation at 1-atm. pressure. The boiling point of gallium is that given by P. Harteck, *Zs. f. phys. Chem.*, **134**, 21, 1928.

TABLE 4—*Continued*

parentheses are from Lange's *Handbook of Chemistry* and are probably somewhat less reliable. Those marked with a dagger (†) are from the Landolt-Börnstein *Tabellen*. "(Sub.)" indicates sublimation at 1-atm. pressure. The boiling point of gallium is that given by P. Harteck, *Zs. f. phys. Chem.*, **134**, 21, 1928.

TABLE 4—*Continued*

Element	A Suess's Abundances	B Meteoritic Abundances	B/A	C Terrestrial Abundances	C/A	Element		Compound	Temp. of Compound (° K)	
						M.P. (° K)	B.P. (° K)		M.P.	B.P.
34 *Se*	120	13	0.11	0.11	0.00096	490.6	958	*FeSe*		
35 *Br*	17.4	49	2.8	3.9	0.22	265.9	(331.9)	*NaBr*	1023	1665
37 *Rb*	11.5	15	1.3	370	32	312.0	952	Rb_2SiO_3		
38 *Sr*	72.5	41	0.57	350	4.8	1043	1657	*SrO*	2688	
39 *Y*	8.2	9.7	1.2	32	3.9	1773	4373	Y_2O_3	(2683)	(4573)
40 *Zr*	73.3	140	1.9	240	3.3	2125	(>3173)	ZrO_2	2950	
41 *Nb*	0.77	0.7	0.9	26	34	2760	(>3573)	Nb_2O_3	2045	
42 *Mo*	3.1	5.9	1.9	2.6	0.84	2883	(3973)			
44 *Ru*	1.32	2.1	1.6			2773	4383			
45 *Rh*	0.32	0.7	2.2	0.001	0.003	2233	4233			
46 *Pd*	1.1	1.3	1.2	0.009	0.007	1823	3833			
47 *Ag*	0.38	1.9	5.0	0.094	0.25	1234.0	2466	Ag_2S	1115	
48 *Cd*	1.36	2.2	1.6	0.13	0.096	594.1	1040	*CdS*		(1253)(Sub.)
49 *In*	0.18	0.27	1.5	0.097	0.54	430	2500	*InS*	965	
50 *Sn*	3.16	18	5.7	34	10.8	505.1	2600			
51 *Sb*	0.14	0.79	5.7	0.83	5.9	903.7	1713	Sb_4S_6	820	
52 *Te*	8.0	0.16	0.02	0.0014	0.0002	723	1360	*FeTe*		
53 *I*	1.41	1.5	1.1	0.24	0.17	386.8	(457.5)	*NaI*	935	1577
55 *Cs*	0.65	1.3	2.0	5.3	8.1	301.9	963	Cs_2O	763	
56 *Ba*	5.5	3.3	0.67	182	33	977	1911	*BaO*	2190	(2273±)
57 *La*	2.0	2.1	1.0	14.2	7.1	1153	(2073)	La_2O_3	2578	(4573)
72 *Hf*	0.69	1.4	2.0	2.5	3.6	2500	(>3473?)	HfO_2	3050	
73 *Ta*	0.25	0.26	1.0	1.2	4.8	3250	(>4373)	Ta_2O_5	2163	
74 *W*	1.26	13	10	0.82	0.65	3653	(6173)	WO_3	1743	
75 *Re*	0.096	0.07	0.73	0.0005	0.005	3420				
76 *Os*	1.00	0.97	1.0			2973	4673			
77 *Ir*	0.87	0.31	0.35	0.00049	0.0087	2716	4623			
78 *Pt*	1.62	1.5	0.92	0.0026	0.0016	2042.5	4283			
79 *Au*	0.16	0.21	1.3	0.0026	0.016	1336.16	2933			
80 *Hg*	0.031	<0.006	<0.2	0.039	1.2	234.29	629.73	*HgS*		(853)(Sub.)
81 *Tl*	0.028	0.11	3.9	0.64	23	576.8	1730	Tl_2O	573	773
82 *Pb*				8.0		600.6	2023			
83 *Bi*		0.14		0.1		544.2	1683	*BiS*	958	

ably because of analytical errors. Selenium and tellurium appear to be definitely lower by about a factor of 10 than one would expect by comparison with neighboring elements. Mercury was not found in the chondrites by the Noddacks (1931, 1934), but its presence (0.2 p.p.m.) has been reported in the Canyon Diablo troilite. It is nearly a missing element in the meteorites. The elements, from copper to selenium inclusive, seem to be consistently low in the meteorites, while those from silver to antimony are consistently high and tellurium is low.

It is possible to conclude that some of the more volatile elements are depleted by small factors. Suess's estimate for the cosmic abundance of mercury seems to be too low, in the writer's estimation. The abundance of selenium, tellurium, and mercury (?) seems to be low by a factor of about 10, and these seem to be outside analytical errors. All other depletions seem to be within analytical error and reasonable estimates of the uncertainties of Suess's values for cosmic abundances.

The decreased abundances of the siderophile elements, cobalt, nickel, germanium, ruthenium, rhodium, lead, rhenium, osmium, iridium, platinum, and gold, constitute the most prominent irregularity of the terrestrial data. Molybdenum, which is siderophile and chalcophile, and tin, which is siderophile, are not markedly depleted in the earth's surface. Among the chalcophile elements, only sulphur, selenium, tellurium, and cadmium show a marked decrease in abundances. Among the lithophile elements, potassium, rubidium, niobium, and barium are markedly concentrated, and aluminum, titanium, vanadium, strontium, zirconium, cesium, and hafnium are moderately concentrated at the earth's surface. Though uranium and thorium are not included in the table, they have been markedly concentrated in these surface regions also. All these are referred to silicon, which is itself concentrated at the earth's surface as compared to its concentration in the meteorites. These relationships are well known and have been interpreted as due to the loss of the metallic and iron sulfide phases to the earth's interior, and to the concentration of elements in the partial melting processes which have produced the basalts and other surface rocks of the earth.

Certain elements—chlorine, bromine, iodine, and boron—in addition to water, nitrogen, and carbon, are concentrated in the ocean, sedimentary rock, and atmosphere of the earth. Urey (1953) has shown that these are volatiles, namely, water, carbon as methane or carbon dioxide, nitrogen as ammonia or the element, or that they form compounds soluble in water. The latter owe their surface abundance to their solubility in the primitive oceans and to removal from the interior of the earth by water during geologic time. He found no evidence that these elements or any others had been removed from the igneous rocks by high-temperature volatilization processes. The high concentration of chlorine, bromine, iodine, and boron in the earth's surface will not be discussed in this paper, since it is believed that the solubility in water accounts for their increased surface abundances.

HIGH-TEMPERATURE VOLATILITIES OF SOME ELEMENTS

It is evident that the permanent gases, namely, hydrogen, the inert gases, methane, and nitrogen, have been almost completely lost from the earth and meteorites. Also the low-temperature volatiles, water and ammonia, have been largely lost. The model for the origin of the earth and planets previously presented by the writer was devised in order to retain some water, nitrogen, and carbon while the other gases were lost. In the following discussion the arguments will be based temporarily on other evidence.

First, we shall investigate the volatilities of certain elements in the presence of a cosmic mixture of gases at high temperatures. The following groups of elements will be considered first: iron, copper, zinc, gallium, germanium, arsenic, selenium; silver, cadmium, indium, tin, antimony, tellurium; mercury, thallium.

Iron exists in the earth and meteorites as the metal, its oxides and silicates, and its sulfide. At low temperatures, oxidized iron and its sulfide are the stable forms in the

presence of cosmic proportions of hydrogen, water, and hydrogen sulfide, but at higher temperatures only the metallic form is stable. These facts argue that the materials of the earth and meteorites were not condensed from a high-temperature gas in such a way that intimate contact between a finely divided solid and the gas was possible. The data on the oxides and sulfide were presented previously (Urey 1952*b*, p. 127). If the iron sulfide were all reduced, any chalcophile elements remaining as sulfides would be nearly in a pure state. Thermodynamic calculations for the reduction of ZnS, Cu_2S, CdS, Ag_2S, and HgS by hydrogen show that all these sulfides would be reduced in the presence of a cosmic mixture of gases at temperatures above 1500° K and, in fact, at somewhat lower temperatures as well. Since gallium, indium, and thallium exist in meteorites to a larger extent in the reduced state than do zinc, copper, cadmium, silver, and mercury, it can be expected that they would be reduced to metals also, though their thermodynamic properties are unknown. Germanium and tin are siderophile, and hence their sulfides and oxides are easily reduced. Data for arsenic and antimony are not available. However, we can conclude that most chalcophile elements would be reduced to the elements, which is definitely contrary to observation for the meteorites, as well as for the earth, so far as the limited surface regions of the earth indicate. Condensation of these objects from a high-temperature gas of cosmic composition would give a condensate of very much more highly reduced condition than we find in the meteorites and the earth.

In order to retain iron sulfide and the chalcophile elements and iron oxide in the oxidized form and, at the same time, have intimate contact between the condensed phases and the gas phase, it is necessary for the ratio of hydrogen to hydrogen sulfide and of hydrogen to water to be reduced. The amount of such reduction required can be estimated. Since the meteorites show that molten iron, iron sulfide, and oxidized iron have existed in contact with one another, we ask for a ratio of their gaseous compounds such that a gas phase could also have been in equilibrium with these liquid phases. A temperature of 2000° K would be appropriate for liquid iron, iron sulfide, and oxidized iron as silicate.

At 2000° K the fused nonvolatile materials would consist of silicate melt containing the oxides of silicon, magnesium, calcium, aluminum, and ferrous iron and the less abundant elements. Such melts are electrically conducting and hence are highly ionized. However, Taylor and Chipman (1942) have shown that the thermodynamic activity of FeO in slags is approximately equal to its mole fraction, quite independently of its molecular form. Hence we can consider the reaction

$$FeO + H_2 = Fe + H_2O\,,$$

whose equilibrium constant is

$$K = \frac{p_{H_2O}}{p_{H_2} X_{FeO}}\,.$$

The values for this constant have been measured up to the melting point of iron by Chipman and Marshall (1940). The values of log K at 1500° and 2000° K are -0.1 and -0.25, respectively. Using these values and the cosmic ratio of hydrogen to water, we find that the equilibrium values for X_{FeO} are 7.6×10^{-4} and 10^{-3} at these two temperatures. It is evident that iron would be reduced to the metallic state unless the ratio of hydrogen to water were reduced by about 10^3. The composition predicted by these calculations is about that of some of the achondritic meteorites, i.e., the bustites (Urey and Craig 1953, p. 66), which may have been subjected to such processes. Equilibrium constants for the reduction of $FeSiO_3$ and Fe_2SiO_4 by hydrogen can be calculated by making estimates for certain of the thermodynamic properties; the values so secured are in accord with the conclusions reached above. At lower temperatures the equilibrium constants for the reduction reactions show that iron should be oxidized in the presence of cosmic proportions

of hydrogen and water (Urey 1952*b*, p. 127). Experiments made in these laboratories by Dr. George Edwards on a melt of about cosmic composition and a mixture of 1000 parts of hydrogen to 1 of water have confirmed these conclusions relative to the extent of iron reduction.

Iron sulfide reacts with hydrogen according to the reaction

$$FeS + H_2(g) = Fe + H_2S(g), \qquad K_{2000} = 4 \times 10^{-2}.$$

Since the cosmic ratio of hydrogen (H_2) to sulfur is 7.4×10^4, it would be necessary to change this ratio by about 3000, for FeS to remain in the system. Some increased stability would result from its solubility in molten silicates. However, it would be largely reduced to iron if it were subjected to a cosmic mixture of gases in sufficiently finely divided form. We conclude that neither the meteorites generally nor the materials of the earth could have been subjected to the reducing action of cosmic gases except in the form of large objects and for not too long periods of time.

At 2000° K and with even a large fraction of the hydrogen removed relative to hydrogen sulfide, we still cannot expect Cu_2S, ZnS, As_2S_2, Ag_2S, CdS, and Sb_2S_3 to be stable, as observed in the meteorites, for at least some of these are volatile either as the elements or as sulfides, as seen from Table 4. Gallium, indium, and thallium could be distributed among the silicate, iron, and iron sulfide phases, and germanium and tin could be siderophile, as observed. Conclusions relative to selenium and tellurium are difficult because of the instabilities of H_2Se and H_2Te and the lack of data on $FeSe$ and $FeTe$. In particular, mercury, arsenic, cadmium, and zinc should be more volatile than germanium and tin and probably also gallium and indium. Hence separation of these elements in any condensing or evaporation process could be expected. Selenium and tellurium are also volatile.

The groups of elements copper, zinc, gallium, germanium, arsenic, selenium, bromine, and silver, cadmium, indium, tin, antimony, tellurium, and indium show considerable regularity in abundances with increasing atomic numbers; but, on the basis of volatility, it would be expected that zinc, arsenic, selenium, cadmium, and tellurium should all have been preferentially lost, and the degree of such preferential loss should be very great, say, compared to the loss of the inert gases, whereas only selenium and tellurium appear to have been moderately lost. It should be noted that the ratio of volatilities of two elements whose boiling points differ by a factor of 2 in absolute temperatures should have a ratio of vapor pressures of about 10^4 at the lower temperature. If these losses have occurred, then these more volatile elements must have a much higher cosmic abundance than Suess estimates, and nuclear processes which produced the elements must have favored these chemically volatile elements. This is an impossible assumption.

The earth contains a large amount of high-density substance, probably mostly metallic nickel-iron, with unknown amounts of iron sulfide. The proportion of iron, as interpreted by the present writer (Urey 1952*c*; Urey and Craig 1953), is higher than that of the meteorites, but it definitely is not completely reduced. The abundances of the more volatile chalcophile elements are more irregular than those of the meteorites, but there appears to be no evidence of extreme loss of the more volatile elements. The moderate depletion of these elements at the earth's surface can be ascribed to other geochemical and geophysical processes.

These considerations show that the composition of the meteorites and their parent-objects cannot be understood if their substance was exposed to gases of cosmic composition at the temperature of melting iron and above. The presence of massive iron bodies and silicate minerals in the meteorites shows that they were heated to such temperatures; hence we must conclude that any gases present were greatly depleted in hydrogen relative to cosmic proportions or that the materials were in such massive bodies that intimate contact with the gases during the period of heating was not possible, or that both

these conditions obtained. Some gravitational field must have been present for the observed separation of iron and silicate phases to have occurred. External heating of asteroidal-like bodies would be a satisfactory model for such processes. The similarities between the chemical composition of the earth's surface and that of the meteorites in the light of known processes which have formed the earth's crust are sufficient to justify similar conclusions relative to the processes which formed the earth.

The loss of elements as derived from the study of meteoritic and terrestrial abundances, compared to the cosmic values as derived from astronomical data, can be summarized as follows: The permanent gases have been lost almost completely and the low-temperature volatiles to a marked degree, but there has been no marked loss of any other elements relative to silicon. Yet the ratio of the low-density fraction, i.e., silicates, to the high-density one, i.e., metallic iron-nickel, varies distinctly in the terrestrial planets, indicating that one or the other of these two classes of matter has been lost in varying amounts or that both have been lost in varying relative amounts during the formation of the planets. Elementary abundances derived from astronomical data indicate that the silicate fraction was lost preferentially.

The great grooves on the moon and the evidence that these structures were formed at the terminal stage of the moon's formation indicate that large iron-nickel alloy masses were present in the solar system during the process of formation of the planets (Urey 1952*c*, pp. 30 ff.; Gilbert 1893).

INDICATED REQUIREMENTS OF A SATISFACTORY MODEL

These chemical characteristics of the substances of the terrestrial planets and the meteorites are explained by the model previously proposed. Objects some hundreds of kilometers in dimension accumulated at temperatures below 0° C, thus separating the permanent gases and some of the water from the nonvolatile fraction. Carbon compounds were condensed at the same time. All the elements less volatile than mercury were condensed in cosmic proportions. Subsequent external heating of these objects in the presence of gases of cosmic composition reduced the iron oxide and iron sulfide on the surfaces and produced molten iron and silicates, which separated in the gravitational field. Owing to limited access of the gases, complete reduction did not occur. This process provided the silicate minerals and the massive nickel-iron of the meteorites and the substantial iron objects which left their grooves on the moon (Urey 1952*b*, pp. 39 ff.). Partial separation of the silicate and iron fractions took place, and the silicate fraction was lost to a larger degree from the forming terrestrial planets. This occurred to a greater extent in the case of some planets than others, and a trend with distance from the sun in this respect is evident, with Mercury having the highest density and the meteorites the least.

EUCKEN'S MODEL FOR THE ORIGIN OF THE EARTH

Eucken (1944) developed a model for the formation of the earth, starting from an Emden gas sphere. He assumed an initial mass 200 times that of the present earth and hence no removal of nonvolatile elements but only the loss of hydrogen, the inert gases, and the low-temperature volatiles, since this is approximately the cosmic ratio of volatiles to nonvolatiles. He showed that iron should condense first in the interior, followed by silica and other oxides. He described a process by which condensed phases fell to the interior of the earth's protoplanet and evaporated, thus suggesting a very effective countercurrent distillation column effect. He made no effort to account for the variation of the densities of the planets by the differential loss of some elements. Obviously, the inert gases must have been lost.

Latimer (1950) has discussed the problem and has suggested that the core of the earth was formed by dust particles of metallic iron falling more rapidly through gas than did other particles composed of silicates, because of the greater density of the former. The

model requires that the gas be supported by pressure in the interior of the gas sphere, which can occur only because of high pressures and high temperatures in the interior. The model must be the same physically as that of Eucken, and thus both models can be considered simultaneously.

This model was not accepted by the writer because it provided no way for the loss of the very nonvolatile silicates and the simultaneous retention of water and other volatiles, of which only mercury was mentioned. It is well to consider these difficulties in greater detail. For the moment we shall assume that the retention of a small fraction of the water, nitrogen, and carbon was due to some incidental process and shall consider the loss or retention of other elements only.

At some radius within such a sphere, the temperature and pressure will be such that condensation of the various constituents will occur. Since the pressures and temperatures within such an Emden gas sphere are given in tables (Emden 1907, p. 79; Eddington 1930, chap. iv) and since the dependence of thermodynamic properties on pressure and temperature is a complicated one, particularly where phase transitions occur, the approximate conditions for condensation have been determined by trial. It was first found

TABLE 5*

$M = 6 \times 10^{30}$ g, $R = 6.37 \times 10^{11}$ Cm

Polytropic Index	Molecular Weight	r/R	Temperature (° K)	Pressure (Atm.)
2 (γ=1.67)	1.2	0	4881	11.2
		0.68	1545	0.63
		0.75	1145	0.30
2.5 (γ=1.4)	2.2	0	11,690	59
		0.74	1672	0.065
		0.83	966	0.0096

* Molecular weights are calculated by assuming a 20:1 ratio for *H* to *He* and assuming atomic hydrogen in one case and molecular hydrogen in the other and making allowance for some molecules of higher molecular weight.

that condensation of $MgSiO_3$ should occur in gas of cosmic composition when the hydrogen pressure was about 0.1 atm. and the temperature 1500° K, and it was found that polytropic gas spheres of index 2.0 or 2.5 provide a region which approximates these conditions. Pressures and temperatures change slowly within the gas sphere, and vapor pressures change rapidly with temperature; hence a substance will be vaporized at smaller radii than a critical value and will be nearly completely condensed at greater radii.

We assume that the original mass of the protoplanet was 10^3 times the mass of the earth and that at some time its radius was 10^3 times the present earth radius. This makes the escape velocity the same as its present value. It seems likely that this velocity must have been less than this for the higher-mass inert gases to escape according to the Eucken model. If the radius was larger, the temperatures and pressures were lower. However, no modification of our conclusions results from considerable changes in this model. Table 5 gives a few values of temperature and pressure for such a sphere.

Magnesium and silicon are the most abundant of the lithophile elements, and an estimate of the volatility of $MgSiO_3$ in gases of cosmic composition should be representative. Eucken considered this problem, as did the writer (Urey 1952*d*), but they underestimated the volatility of silicon as silicon monoxide. Silicon volatilizes as this gas rather than as *Si* gas. At higher pressures, SiH_4 is an important volatile constituent, though the data for the heat of formation of this gas are doubtful. Revised calculations require a considerable modification of the previous results but do not change the fundamental

conclusion that silicon is much more volatile than magnesium from silicates.[3] We shall make our calculations by using only SiO gas as the volatile constituent but shall remember that silicon is always more volatile than calculated. Koch (1954) has given the writer a revised value for the heat of formation of SiO, namely, -21.4 ± 0.6 kcal at 298°16 K, which is used in the following calculations, together with spectroscopic values for the entropy and heat capacity at higher temperatures. Calcium in calcium metasilicate is less easily reduced to the gaseous calcium than is magnesium in magnesium metasilicate. Aluminum as Al_2O is less volatile than magnesium as gaseous magnesium, and sodium is more volatile than magnesium (Urey 1952*d*). We estimate the volatility of $MgSiO_3$ from the reaction

$$MgSiO_3 + 2H_2(g) = Mg(g) + SiO(g) + 2H_2O\,.$$

The equilibrium constant for this reaction at 1500° K is $10^{-17.6}$, the standard heat content change is 246 kcal, and the standard entropy change is 83.2 cal per °K. This gives

$$\log K = -\frac{53800}{T} + 18.2 \tag{1}$$

for the value of K as a function of T. Then

$$K = \frac{p_{Mg}p_{SiO}p^2_{H_2O}}{p^2_{H_2}} = 10^{-17.6}. \tag{2}$$

Using 6×10^{-4} as the ratio of water to hydrogen (H_2) (see Table 1), we obtain

$$p_{Mg}p_{SiO} = 7 \times 10^{-12}\,.$$

Magnesium is less volatile than silicon; but here we wish to compare the volatilities of these two elements with others which are much more volatile than either. Hence we take the vapor pressures as equal and obtain

$$p_{Mg} = p_{SiO} = 2.6 \times 10^{-6} \text{ atm.}$$

Using the cosmic abundances of magnesium and silicon, the pressure of hydrogen is 0.048 atm. if complete evaporation exists. This calculation means that $MgSiO_3$ will just begin to condense from gas of cosmic composition when the temperature is as low as 1500° K and the pressure of the hydrogen in the cosmic gases becomes as high as 0.048 atm. The equation, above, for K shows that its value changes very rapidly with temperature, and hence considerable variation of the total pressure varies the temperature of condensation but slightly.

The vapor-pressure equation for iron is

$$\log p_{Fe} = -\frac{21677}{T} + 4.438 \times 10^{-4}T - 3.157 \times 10^{-7}T^2 + 7.5918\,, \tag{3}$$

and the vapor pressure at 1500° K is 4.5×10^{-7} atm. If the pressure of hydrogen is 0.1 atm., we calculate from the cosmic abundances of iron and molecular hydrogen that the partial pressure of iron would be 3.9×10^{-6} if it were all in the gas phase. Hence only 4.5/39, or 11.5 per cent, of the iron remains in the gas at the time the $MgSiO_3$ begins to

[3] The area of Fig. 1 in Urey (1952*d*) within which SiO_2 is stable would be decreased somewhat when SiO gas is included. Further revision may be reserved until better data are available.

condense. At higher temperatures and pressures the iron will condense even more readily relative to $MgSiO_3$, because of the difference in the numerical coefficients of the terms in $1/T$ of equations (1) and (3). This is in accord with Eucken's calculation, though, because of considerable uncertainties in the calculations for $MgSiO_3$, the conclusion is not a firm one. Eucken assumed that the core of the earth condensed first, followed by the silicate mantle.

Mercury has been reported in the troilite phase of the Canyon Diablo meteorite and exists as HgS in terrestrial sources. It is reduced according to the equation

$$HgS + H_2(g) = Hg(g) + H_2S(g) .$$

The value of the equilibrium constant[4] at 25° C is 4.8×10^{-9}. Since mercuric sulfide may form a solid solution in iron sulfide,

$$K = \frac{p_{Hg} p_{H_2S}}{x_{HgS} p_{H_2}} , \tag{4}$$

where x_{HgS} is the mole fraction and ideal-solution laws are assumed in the iron sulfide. About 0.1 of the iron is present in meteorites as FeS, and we will assume this value in making the present estimate. Using Suess's values, this means that 0.71 of the sulphur will be present as H_2S.

If y is the fraction of all the mercury in the iron sulfide phase, the mole fraction of HgS is

$$\frac{y A_{HgS}}{A_{Fe} + y A_{HgS}} \cong \frac{y A_{HgS}}{A_{Fe}} = \frac{y R_{HgS}}{0.1 R_{Fe}} \qquad (A_{HgS} \ll A_{Fe}) , \tag{5}$$

where the A's are atomic abundances and the R's the ratio of the abundances of the substance indicated by the subscript to the molecular hydrogen abundances. The pressure of Hg is evidently $(1 - y)R_{Hg}P_{H_2}$ and that of H_2S is $0.71\ R_S P_{H_2}$. Then

$$K = (1 - y) R_{Hg} R_S \frac{R_{Fe}}{y R_{HgS}} P_{H_2}^2 \times 0.071 ; \tag{6}$$

and, since $y \ll 1$,

$$y = \frac{R_S R_{Fe} P_{H_2}^2}{K} \times 0.071 . \tag{7}$$

Substituting numerical values and using P_{H_2} equal to 0.1 atm., we obtain 7.8×10^{-3} as a value for y. This shows that mercury would not condense as sulfide from cosmic gases in which the hydrogen pressure was 0.1 atm. at 25° C. This temperature would not be attained in the protoplanet except at much lower pressures, and hence much lower temperatures would be required in order to condense mercury at all. Mercury would adsorb to some extent on solid particles at ordinary terrestrial temperatures, and this may have condensed the element somewhat. Reactions between hydrogen and mercuric sulfide or between hydrogen sulfide and mercury are not rapid, and equilibrium probably would not have been attained; but it is not possible to produce a solid from a gas if the solid is not thermodynamically stable relative to the gas. Similar conclusions were reached previously, with similar calculations applied to elementary mercury dissolved in metallic iron or nickel (Urey 1952*b*, p. 131).

At 1500° K, iron sulfide and mercury sulfide would be reduced to the metals and hydro-

[4] This value, calculated from the sources previously cited, agrees with values calculated from W. D. Treadwell and F. Schaufelberger (1946) within a factor of 3, and this is regarded as a reasonable probable error for this quantity.

gen sulfide. The vapor pressure of pure mercury is 670 atm. at this temperature. If its solution in iron is ideal, the ratio of its pressure to its mole fraction in iron will be equal to this number. As before, we ask for the mole fraction of mercury in iron when all the iron is reduced and when the pressure of hydrogen is 0.1 atm. and hence the mercury pressure is 0.1 R_{Hg}. Proceeding as before but assuming all the iron to be in the metal phase, we have

$$y = \frac{R_{Fe}}{670} P_{H_2} = 5.1 \times 10^{-} \tag{8}$$

i.e., the mercury is depleted in the metallic iron to 5.1×10^{-9} of its cosmic value. If Eucken's argument that iron would condense out of the protoplanet is valid, it is also true that mercury definitely would not, and the conclusion is not in doubt because of the approximate nature of the calculation.

The vapor pressure of zinc and cadmium at 1500° K is 12 and 35 atm., respectively. Calculation similar to that for mercury gives 3.3×10^{-7} and 1.1×10^{-7} for the fraction of zinc and cadmium, respectively, dissolved in the iron at this temperature when the pressure of hydrogen is 0.1 atm. Data for arsenic are lacking, but it should be intermediate between mercury and the cadmium and zinc. The conclusion that these elements will concentrate in the gaseous phase is definite. It is also evident that large fractionation between these elements and the other less volatile elements—say antimony and thallium—and the even less volatile elements—gallium, germanium, indium, tin, silver, and copper—should occur, if iron separated from the silicates by the Eucken process.

Eucken assumed no loss of the silicate fraction from the protoplanet; and if these elements less volatile than the permanent gases were retained, they should be highly concentrated at the surface of the earth, which is not observed. If it is assumed that they were lost, then it would be remarkable if these elements with varying physical properties were partially lost from the earth's protoplanet and partially concentrated at its surface in such a way as to simulate the abundances of the less volatile neighboring elements of the periodic table, whose abundances at the earth's surface have been produced by very different processes.

Previous attempts have been made to estimate the relative volatilities of the more abundant constituents of the silicate phases. We do not have definite data for the activities of the constituents of a fused silicate mixture of cosmic composition. The elements magnesium, calcium, silicon, aluminum, and sodium are more volatile in the reduced or partially reduced state as *Mg*, *Ca*, *SiO*, Al_2O, and *Na*. In the cooler stellar sources the spectra of *MgH*, *CaH*, *AlH*, *AlO*, and *SiH* have been reported. From the spectroscopic data for these molecules, the first four can be excluded as important volatile constituents on the basis of statistical mechanical calculations of their thermodynamic properties. The data for *SiH* are inadequate for such calculations.

The relative volatilities can be compared by considering the eight reactions[5] given in

[5] The thermodynamic data used are those of Rossini *et al.* (1952) and Kelley (1949), together with the data of Brewer and Searcy (1951) for Al_2O. The heat of formation of *SiO*, 21.4 ± 0.6 kcal at 298.16° K, was supplied by Koch (1954), and the heat content at higher temperatures and entropy values was calculated from spectroscopic data. Our values for *SiO* are as follows:

T (° K)	298.16	1200	1500	2000
S (cal/degree)	50.53	61.59	63.54	66.09
$H^0 - H_0$ (kcal.)	2.08	9.41	12.03	16.46

Dr. G. J. F. MacDonald informs me that he is reconsidering the data on the silicates, but his selection of values does not change the present calculated values at these high temperatures in any important way. I am indebted to him for calling my attention to an error in the heat of formation of Mg_2SiO_4 in Rossini *et al.* (1952). Using Rossini's values for the heat of formation of SiO_2, the heat of formation of Mg_2SiO_4 is −5082 kcal instead of −488.2.

the accompanying tabulation. When the equilibrium constants of reactions such as 1 and 2 show that the reactions are strongly and consistently displaced toward one side—the

Reaction	log K_{1500}	log K_{2000}
1. $MgO+SiO(g)=Mg(g)+SiO_2$	−1.4	−1.6
2. $Mg_2SiO_4+SiO(g)=Mg(g)+3MgSiO_3$	−2.4	−2.9
3. $MgO+SiO_2=MgSiO_3$	+1.1	+0.8
4. $MgSiO_3+Ca(g)=Mg(g)+CaSiO_3$	+5.2	+4.1
5. $\frac{1}{2}Mg_2SiO_3+Ca(g)=Mg(g)+\frac{1}{2}Ca_2SiO_4$	+4.1	+3.1
6. $2MgO+Al_2O(g)=2Mg(g)+Al_2O_3$	+2.0	+1.6
7. $2Mg_2SiO_4+Al_2O(g)=2Mg(g)+Al_2O_3+MgSiO_3$	+0.3	+0.0
8. $Na_2SiO_3+Mg(g)=2Na(g)+MgSiO_3$	−1.8	−1.9

left in this case—it is evident that the silicon as *SiO* is more volatile than the magnesium. The first three reactions, assuming ideal-solution laws and that the molecular species as written in these equations are present in the solution, permit a calculation of the ratio of magnesium gas to *SiO* gas in equilibrium with a melt containing equal amounts of silicon and magnesium. This is found to be 130 at 2000° K. Since SiH_4 is present, the volatility of silicon would be even greater. The equilibrium constants of reactions 4 and 5 show that magnesium is about 10^4 times as volatile as calcium. The equilibrium constants of reactions 6 and 7 are unity or somewhat larger. If the partial pressures of *Mg* and Al_2O are low, namely, about 10^{-4} or 10^{-3} atm., corresponding to a hydrogen pressure of 1 or 10 atm., respectively, in cosmic gases, magnesium is more volatile than aluminum by a factor of about 10^4. The equilibrium constant of reaction 8 shows that sodium is more volatile than magnesium at sufficiently low pressures.[6] At pressures which we have estimated in the protoplanet, sodium is more volatile than magnesium, and the latter more volatile than aluminum by factors of 10^3 or 10^4. The eucrites and angrites of the achondritic meteorites have high concentrations of calcium and aluminum, as would be expected if they were partly the residue of an evaporation process (Urey and Craig 1953, p. 68).

The order of decreasing volatility indicated is thus silicon, sodium, magnesium, calcium, and aluminum, and the indicated differences are large. No separation of these elements in accordance with these estimated volatilities appears in the meteorite abundances, as compared to stellar abundances. The terrestrial data are more complicated again, but there appears to be no evidence for separation by differing volatilities in this case either.[7]

But the varying densities of the planets require a substantial loss of the silicate fraction such as $MgSiO_3$. If this occurred through evaporation and escape from the proto-

[6] Let x and y equal the fractions of *Na* and *Mg* in the gaseous phase, and then $(1-x)$ and $(1-y)$ are their fractions in the melt. The partial pressures p_{Na} and p_{Mg} are $xR_{Na}P_{H_2}$ and $yR_{Mg}P_{H_2}$; and the mole fractions of Na_2SiO_3 and $MgSiO_3$ in the melt are proportional to $(1-x)\frac{1}{2}R_{Na}$ and $(1-y)R_{Mg}$. Then

$$K=\frac{p_{Na}^2}{p_{Mg}}\frac{[MgSiO_3]}{[Na_2SiO_3]}=\frac{2x^2R_{Na}P_{H_2}}{(1-x)}\frac{(1-y)}{y}=10^{-1.9};$$

and

$$R_{Na}=\frac{500}{1.85\times10^8}.$$

When $P_{H_2}=1$ and y and $1-y$ equal $\frac{1}{2}$, then $1-x=4.3\times10^{-4}$. Other examples are easily calculated. At lower pressures of hydrogen, the difference in volatility is greater. The assumption of ideal-solution laws is a rough approximation, but nevertheless the qualitative conclusion is not in doubt.

[7] H. C. Urey (1952*d*) discussed this previously and came to similar conclusions.

planet, then it is very difficult to see how these more volatile elements were retained in roughly cosmic proportions while the much less volatile elements were lost. The distillation formula for a binary ideal solution is

$$\log \frac{x_1}{x_0} = \alpha \log \frac{y_1}{y_0}, \tag{9}$$

where x_0 and x^1 are the initial and final amounts of one constituent, y_0 and y_1 are these amounts for the other consituent, and α is the ratio of the vapor pressures of the pure constituents and is very great for the processes considered. With y_1/y_0 equal to 0.2–0.5 for the silicates, as indicated by the variation in the density of the planets, the volatile elements should be lost completely from the planets. Even great variations in the abundances of magnesium, calcium, aluminum, sodium, silicon, and many other elements of similar properties should be expected, even though ideal-solution laws would not be followed in such an evaporation process. Eucken did not consider the removal of these very nonvolatile substances from the protoplanet and surely would have understood the difficulty that this requirement makes in accepting his model.

Some kind of similar model must be applied to the other terrestrial planets and the asteroids. Mars apparently has no core, and hence the iron-rain hypothesis does not apply. The meteorites show no violent variations in abundances of the intermediate volatiles. In the case of the asteroids, straight fractional distillation uncomplicated by gravitational-field effects should have occurred. Equilibrium evaporation along the lines indicated is completely inconsistent with the approximately cosmic relative abundances of the elements in meteorites and the earth's surface. It seems doubtful whether any modification of Eucken's model could vitiate this conclusion.

The writer previously considered these questions and came to the same conclusion (Urey 1952*b*, chap. 4). Water and nitrogen are present on the earth with far less depletion relative to cosmic abundances than are the inert gases (Table 1) and have been greatly depleted relative to the less volatile elements; this was not regarded as due to some incidental process. There seems to be no reason for so explaining their presence, which makes the previous conclusion valid.

It is general chemical experience that it requires very carefully designed and elaborate apparatus and carefully controlled operation to produce large changes in relative proportions of substances, i.e., to secure the effects of many theoretical plates, by distillation processes. On the other hand, it is also chemical experience that it is very difficult to avoid the effect of at least the simple-process fractionation factor or somewhat more than this if any distillation or partial condensation process takes place. *On this basis we would conclude that no high-temperature volatilization process occurred at any time during the formation of the earth and meteorites.* If the special volatilization process proposed by the writer occurred, it must have been under the specific conditions proposed, and it is well to consider persistently alternative fractionation processes. If one feeds a piece of solid material into a high-temperature flame, complete volatilization can take place without any fractionation of the residue except in a transition region. Evaporation from the surface of an asteroidal object would fulfil this condition and provide for the separation and preservation of the metallic phase.

Eucken's model might well be satisfactory for the major planets. The countercurrent distillation is just the process needed to remove hydrogen, helium, and neon and also probably some of the methane, while the less volatile water and ammonia (and, of course, the even less volatile elements) were retained. In this way it is possible to account for the loss of the low-density hydrogen and helium from Uranus and Neptune.

KUIPER'S MODEL FOR THE FORMATION OF THE PLANETS

Kuiper (1951*b*) has developed a model for the formation of the planets. He first presents an exceedingly reasonably development for the solar-disk nebula and its breakup

into protoplanets, one for each planet; and he shows that the spacing can be reasonably accounted for if the protoplanets had masses several times as large as the mass of cosmic matter, which would include a mass of silicates and iron now in the terrestrial planets. He gives, for the values of log [M(protoplanet)/M(planet)], 3.18, 3.10, and 4.14 for Venus, the earth, and Mars, respectively, and shows that protoplanets containing these masses would be stable under the tidal action of the sun if their diameters were about equal to the differences in orbital radii of the successive planetary orbits. His formula is

$$\frac{M\,(PP)}{M_0} = f\beta^3 \left(\frac{\Delta}{a}\right)^3,$$

where $M(PP)$ is the mass of the protoplanet; f a correction factor due to flattening of the protoplanet; β a numerical factor about equal to unity; Δ the diameter of the protoplanet; and a the distance to the sun. He assigns 0.27, 0.38, and 0.63 A.U. as the diameters of the Venus, Earth, and Mars protoplanets, respectively. He is able to account for the spacing of the planetary orbits, the nearly circular shape of planetary orbits, and the generally eastward rotation of the planets. (The inclination of the axis of Uranus by 98° causes some difficulty.)

Kuiper describes the accumulation of the planets as essentially that given by Eucken during some 10^8 years, with the evaporation of gases from the protoplanets occurring because of the light and particle pressure from the sun. Condensation of the growing planet is assumed to take place in the center of the mass at very high temperatures. His development of the subject is a very nice one, and it is desirable to ask whether it is possible to modify this model in order to include the large objects postulated on the basis of the chemical evidence and without losing the explanations of the astronomical data for which the model was primarily designed. Kuiper's assumption is in disagreement with certain conclusions of the writer, for his process requires that the earth be formed in a very high-temperature state, while evidence has been presented which indicates a low temperature for the formation of the earth (Urey 1953*a*, *b*). However, all possibilities should be explored, and, in order to do this, it is necessary to consider the process of evaporation of these satellite objects.

It is difficult to understand how the volatilized silicates can leave the protoplanet. It is assumed that high temperatures are due to adiabatic compression of gases by their own gravitational attraction. These high temperatures must be maintained by the presence of the gases, and, at the same time, silicates must be volatilized and lost from the protoplanet. Silicon and magnesium and other elements would be volatilized in the deep interior of the protoplanet; but when they moved toward the surface, they would condense as oxides into dust particles, which must then be lost from the gravitational field of the protoplanet. Their molecular weights would be very high and molecular escape impossible. However, the process would be a very complicated one, and it is always reasonable to assume some unusual solar activity, which may have aided the process.

The rate of heating of a sphere or a semi-infinite solid as a function of radius, diffusivity, and time is well known (Carslaw and Jaeger 1947, p. 200). Using 0.005 for the diffusivity, a value suitable for igneous rocks, one finds that after 10^8 years the center of a sphere 100 km in radius will differ in temperature from the surface by 42 per cent of the initial difference. The value for a point 100 km below a plane surface is 92.5 per cent of the initial difference. Substantial heating of smaller objects would occur.

However, if the chemical differentiation discussed above is to be accounted for, reduction of oxidized iron and loss of silicates from the surface must occur, leaving an object with increased iron content. Figure 1 shows diagrams of the type of objects required. *A* shows the primitive object before differentiation; *B* shows an object which has been partially melted with iron on the surface, from which the silicate layer has evaporated, and with an unchanged interior of cosmic nonvolatile material; *C* illustrates an object

from which the silicate layer has not been completely evaporated. Such objects are not excluded, but extensive fractionation of the constituents of this layer might occur. These objects are all in unstable equilibrium and should rapidly become unsymmetrical, as shown in *D*, where the low-density cosmic interior material will extend above the molten iron layer. Objects of this latter type should certainly be formed if the heating time were even very much less than 10^8 years. Small objects may have been present, but they cannot have supplied the major fraction of terrestrial or meteoritic material, since fractionation of the elements would occur in such objects.

About 100 cm^3 of water per square centimeter per year are evaporated from the oceans of the earth. This takes place mostly in the tropics, where ocean temperatures are about 25° C and the vapor pressure of water equals 0.031 atm. (Sverdrup, Johnson, and Flem-

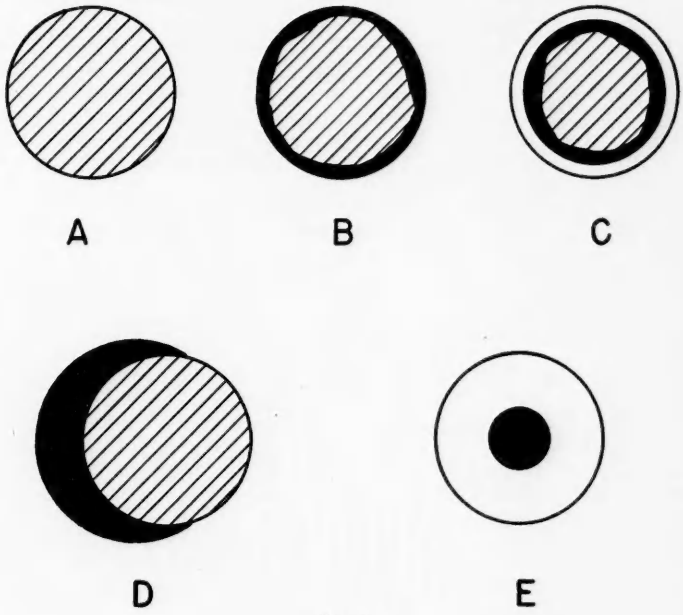

FIG. 1

ing 1946). The vapor pressure of $MgSiO_3$ from equations 1 and 2 is 0.07 atm. at 2000° K. Perhaps comparable rates of evaporation from the surface of an asteroidal body moving in a gas and from the ocean can be assumed. In this case a layer some 10^7 cm thick would be evaporated in 10^5 years, that is, much less than the time estimated by Kuiper.

But what can we reasonably postulate in regard to the properties of this primitive cosmic nonvolatile material? According to the postulates of the present writer, this must be finely divided, unconsolidated material, with its iron mostly oxidized, black in color because of the presence of iron sulfide, and containing some water and other volatiles. This description agrees with the general properties of the carbonaceous chondrites. They contain water and carbon compounds in appreciable amounts, which is in accord with the writer's general expectations for this primitive material. Since the time when they were formed from an accumulation of dust, they have never been heated to high temperatures. The writer has maintained that the moon resulted from this same accumulation process

and that it is an object consisting of nearly primitive cosmic composition (Urey 1952*b*, chap. 3). Urey and Craig (1953) argue that their low-iron group of chondritic meteorites represents more nearly the cosmic nonvolatile material. Recent estimates of astronomical abundances of iron (Aller 1953, p. 327) indicate a lower abundance of iron than that given by Goldschmidt and are in accord with the estimates of Urey and Craig and with the assumption that the moon is composed of material of similar composition. The density of the cosmic nonvolatile fraction with the iron completely oxidized to bivalent iron is about 3.45 at ordinary temperatures and would be considerably less at higher temperatures, say 1200° C, and hence could approximate the density of the material of the moon. Analyses of the iron and nickel contents of the carbonaceous chondrites do not seem to be very reliable (Urey and Craig 1953, p. 63), and preliminary analyses made recently at the University of Chicago on some of them indicate that careful repetition of these analyses would be most desirable.[8] These objects have many properties expected for the primitive cosmic matter postulated for the first accumulations discussed by the writer, though present evidence does not justify the conclusion that they are identical with such matter. Probably the amount of carbonaceous matter is too high, since in any heating process greater reduction of iron should result than is observed and great loss of volatiles might result, especially if those containing the higher amounts of carbon are considered to be average. Alternatively, something like the "amphoteric chondrites" might be samples of such primitive materials, and again it may be that no samples of such materials have survived.

If an object some hundreds of kilometers in radius, consisting of carbonaceous chondritic material, were heated on the surface to a high temperature in the presence of cosmic gases, vigorous degassing would occur, and any molten layer on the surface would be vigorously agitated. The molten iron would penetrate the relatively soft and unconsolidated material, and blocks of it would rise through the iron. It would seem that much more rapid heating and melting of the satellite objects would occur than is indicated by the calculations.

It is necessary to consider the possibility that complete melting took place in a rather short time, with the production of an object with a liquid iron core and completely molten exterior (see Fig. 1, *E*). This object would then evaporate at the surface; and if no convection occurred, no important fractionation of the silicate materials would have resulted. Higher surface temperatures would favor low convection. Even moderate winds due to movement of the satellite through the gas of the protoplanet might be of dominating importance in determining whether convection would occur on an object of low gravitational field. Such winds would be expected, since the gas of the protoplanet, in its rotation, would approximate a solid body to some extent, while solid objects would move in approximately Keplerian orbits. This argument should not apply to an asteroid if it was at the center of a mostly gaseous protoasteroid.[9]

It is possible to estimate the rapidity with which the surface must be renewed, if preferential evaporation of more volatile constituents from an evaporating liquid occurs. The rate of evaporation will be equal to the total thickness evaporated, Δ, divided by the total time, τ, namely, Δ/τ; and the time for effective diffusion is given by $t = l^2/2D$. We set dl/dt equal to Δ/τ, and thus

$$\frac{\Delta}{\tau} = \frac{D}{l}.$$

[8] The iron content for a number of them was found to be 22–23 per cent, in agreement with Urey and Craig's low group; but the iron-nickel ratio agreed with their high group. In another connection another analyst got different results. More careful and extensive analytical work is needed.

[9] As this was written, Dr. H. Craig discussed some results of his study of the meteorites with the writer. His arguments, which appear to be valid, indicate that a superficial silicate layer, as illustrated in Fig. 1, *C* and *E*, with no convection would fit the chemical evidence better than model *B* for the asteroids.

We estimate Δ/τ to be some 100 km in 10^5 years, which gives

$$\frac{\Delta}{\tau} = \frac{10^7}{3.16 \times 10^{12}} = 3.2 \times 10^{-6};$$

hence, with a value of D of about 10^{-5}, we get $l = 3.1$ cm as the thickness through which effective diffusion can be established. Thus mixing must occur within a time

$$\frac{l}{\Delta/\tau} = \frac{3.1}{3.2 \times 10^{-6}} = 1 \times 10^6 \text{ sec},$$

or about 10 days. If the times are much longer than 10^5 years, very slow convection would suffice for adequate mixing, and more rapid evaporation would require quite rapid convection.

Satellite objects some hundreds of kilometers in size were selected for consideration because of the estimated size, i.e., 100 km in radius, of the Imbrian planetesimal which collided with the moon (Urey 1952*b*, pp. 39 ff.) and because of the sizes of the asteroids. Smaller objects fell onto the moon, but it would appear that the largest contributions to the moon's substance, during its terminal stages at least, were made by these substantial objects. Also the writer has assumed that the moon itself is only one of the largest of these objects. Some different assumption relative to size might be made. Perhaps some objects such as the moon supplied the silicate fraction, with little silicate removed from the lunar-type objects and nearly all silicate from the smaller ones. But the evidence indicating that the moon was never completely molten must be explained, for complete melting of the moon in 10^8 years would appear to have been likely (Gilbert 1893; Urey 1952*b*, chap. 2). If no convection occurred in an object such as that depicted in Figure 1, *E*, the chemical requirements outlined above could be met. However, it seems unlikely that such completely stagnant behavior would obtain.

While the evaporation process was proceeding at these high temperatures, the earth must have accumulated from these satellite objects and hence must have been formed at a very high temperature. At least in the terminal stages of its formation, the intermediate-temperature volatiles should have been concentrated in the earth's atmosphere, for they could not have escaped from the earth's gravitational field. Since no increase in these volatiles exists in the earth's surface regions, it is improbable that this is the correct order of events.

It is difficult to introduce large objects in the Eucken model as used by Kuiper unless the time between the formation of the protoplanet and the dissipation of the gases from the protoplanet is much less than 10^8 years.

FIRST ALTERNATIVE PROCESS

Evaporation process for the separation of the silicate and metallic fractions.—From the preceding discussion it is easy to state the processes which would meet the chemical requirements most easily and directly. At some time, the protoplanets, while their masses were dispersed throughout a large volume, contained within their predominantly gaseous substance solid objects of substantial size, e.g., some hundreds of kilometers in radius. These contained the nonvolatile elements, i.e., elements as volatile as and less volatile than mercury, in cosmic proportions. The material resembled the carbonaceous chondrites in general structure and composition. At this time a high-temperature flash (or flashes) from the sun, of brief duration, occurred, which drove all the gases and finely divided solids from the protoplanets. The intensity of the flash was sufficient to raise the temperature at the asteroids sufficiently to produce melting and some vaporization of silicates. After this flash the sun cooled down to about its present rate of radiation, and the satellites of the terrestrial protoplanets accumulated into the present planets. The gases

were not lost completely from the major planets, and, except for their moons, the accumulation followed Eucken's model.

The writer has suggested that some residual gas dissipated the energy of the satellites and caused all of them except the moon of the earth and the two moons of Mars to fall into their primaries.[10]

But the question arises as to whether a young star such as we assume the sun to have been could have behaved in this way; current stellar theory for the main-sequence stars would answer this question in the negative. In fact, a nova behavior would be nearly ideal for the process outlined, but novae are produced by outbursts—in some cases at least, repeated outbursts—of small subdwarf stars with high surface temperatures. Such stars do not appear to represent a likely stage in the early history of the sun. A new sun with planets forming about it might be unstable because of a fall of objects into it incidental to the formation of the system. Also an investigation should be made of the possible instabilities of new stars as their deuterium and possibly also He^3 react in their early stages.[11] An instability which would result in a high emissivity, say 2×10^4 times that of the present sun, for a short time, say 10^3 or 10^4 years, would be ideal for the process considered. The absolute temperatures at the planets would then be: Mercury, 5300; Venus, 4000; earth, 3300; Mars, 2700; asteroids, 2000; Jupiter, 1450; Saturn, 1100; Uranus, 760; Neptune, 620; and Pluto, 530. Thus silicates of the moons of Jupiter and Saturn would not melt, and an insulating layer would protect their volatiles, water and methane, against complete loss, and yet melting and some volatilization would occur at the asteroids. The light-pressure would rapidly remove gas and dust from the terrestrial protoplanets, leaving the larger satellite objects to accumulate into the planets. Another source of energy for the evaporative process will be presented in the next section.

SECOND ALTERNATIVE PROCESS

Collision process for the separation of the silicate and metallic fractions.—If it is assumed that the accumulation of the protoplanets took place essentially as gaseous material within which nonvolatile dust was suspended, this dust could not become separated in a

[10] For supersonic velocities, the rate of loss of energy for an object in a circular orbit is

$$-\frac{dE}{dt} = (\pi r^2)\ (\rho v^2)\ v\,,$$

where πr^2 is the area, ρv^2 the back pressure on the object, ρ the density of the gaseous medium, which is assumed to be constant, and v the velocity of the object. The total energy in an inverse-square field is equal to the negative of the kinetic energy, and, substituting $E = -\frac{1}{3}\pi r^3 \rho_0 v^2$, where ρ_0 is the density of the object, we obtain

$$\tfrac{4}{3} r \frac{1}{v^2}\, dv = dt\,,$$

which gives

$$t - t_0 = \tfrac{4}{3} r \left(\frac{1}{v_0} - \frac{1}{v}\right).$$

The linear velocity of the moon is 10^5 cm sec^{-1} and that of an object in a circumsurface orbit about the earth is 7.9×10^5 cm sec^{-1}. Using the values of ρ_0 and r for the moon and $t - t_0$ equal to 1.5×10^{17} sec, i.e., the age of the solar system, gives ρ equal to 5×10^{-14}. It can be seen that rather low densities of gas would cause the satellites to accumulate into planets, and the formula shows that the larger and more dense objects would be captured last. The solution is very approximate in any case but is especially so because the linear velocity of the moon is less than the velocity of sound in hydrogen and the smoothed field of a self-gravitating star system is not an inverse-square field. Only the order of magnitude of the required gas density can be estimated in this way.

[11] G. Boato (1954) has shown that the deuterium-protium ratio in the carbonaceous chondritic meteorites is about the same as that for terrestrial hydrogen. The same conclusion is indicated by the studies of G. Edwards (1954) on the iron meteorites.

high degree from the gas. Fluctuation in densities in the nebula would supply gaseous masses which would coalesce into larger masses, but dust and gas would move together in such processes. Hence the protoplanet consisted of cosmic proportions of the gaseous and condensed materials, and the Eucken condensation process is necessary to form the planets and, because of the fractionation of the elements, as discussed in the preceding sections, leads to serious difficulties.

However, if the primary condensation process consisted of protoasteroidal-type bodies, i.e., objects accumulated at low temperatures some hundreds of kilometers in size and surrounded by gaseous envelopes, the accumulation of the protoplanets would be quite different. The collision of two such objects could result in a substantial separation of the gaseous and condensed phases, for the gas spheres would collide and rebound to some extent, while the condensed silicate spheres would usually move through the gaseous bodies without colliding and would become partially separated from the gas. Multiple collisions of this kind may have produced a protoplanet similar to a miniature globular-cluster type of object. The object could have contained some gas but not in cosmic proportion, while much of the gas and some dust of cosmic composition could have been dissipated from the solar system by the sun's radiation, without ever becoming a part of the protoplanets. This means that the protoplanets could not be as large as Kuiper assumed and yet be stable relative to the tidal forces of the sun. Yet if the masses were only 0.1 of his values, the extent of the protoplanets would be decreased by $10^{-1/3}$ or $1/2.15$, and hence substantial loss of gas would not vitiate his derivation of planetary spacings; for one can hardly be at all certain that "touching" of successive protoplanets was a necessary condition for determining such spacings.

In the collection process the condensed asteroidal bodies would be accumulated by the protoplanets, for the gaseous masses could be dispersed by the sun's radiation, but the condensed massive asteroidal bodies, if not captured at the first collisions, would collide again with the protoplanet. This is shown by Öpik's (1951) calculations on the capture of asteroids by Mars. He showed that the longest probable life of any of the asteroids known to be crossing the orbit of Mars is 3×10^{10} years. Since the protoplanets are assumed to have been some thousand and more times the linear dimensions of planets, the probability of collision will be some 10^6 or 10^7 times greater, and hence the collisions could have occurred within 10^3 or 10^4 years. (Parenthetically, this is just the order of the duration of the collisions which produced the surface of the moon, as estimated previously [Urey 1952*b*, p. 42]. The short duration of this bombardment of the moon is most striking, and perhaps there is some confirmation in the coincidence of these two estimates.)

The general picture is one of many collisions of many objects and recalls the conditions indicated by the structure of the chondritic meteorites. Urey and Craig (1953) have constructed a model process for the formation of these objects. Objects some hundreds of kilometers in radius accumulated at low temperatures, thus retaining the elements less volatile than mercury in cosmic proportions. Following this, a high-temperature stage occurred, during which silicates were melted and metallic iron was produced by reduction of iron oxides and sank as molten iron below the silicates. A low-temperature stage followed, during which the silicate crystallized, thus producing the crystalline minerals of the stony meteorites. Following this, smaller asteroidal bodies collided with such larger asteroids and produced the rubble-like material of the chondrites. The chondrules have long been recognized as objects which solidified as free droplets, of which some at least were once glass which crystallized slowly. It was assumed that partial volatilization of the silicate layer occurred during the high-temperature stage and that this proceeded to different extents in the case of different asteroids. It was assumed that two of these objects collided and that each supplied one group of meteorites, without great mixing of the substance of the two asteroids in the process.

Vaporization at high temperature was assumed as the process for changing the proportions of iron and silicate, because of the previous application of this idea by Urey to the

problems discussed in this paper. However, the escape velocity of an asteroid is small, namely,

$$v = \sqrt{G\tfrac{8}{3}\pi\rho r^2} = 1.4 \times 10^{-3} r \text{ cm sec}^{-1},$$

where G is the gravitational constant, ρ the density, and r the radius. Hence much of the collisional debris would be lost; and this might well be silicates rather than metallic iron, since the silicate layer may have been on the surface while the metal was not and since lower-density and smaller-sized objects are more easily accelerated in explosive processes. The bombardment recorded in the moon's surface is most suggestive of the postulated process.

It should be noted that objects with radii of some hundreds of kilometers are required to give gravitational fields of a few tens of dynes necessary for the separation of molten silicates and nickel-iron but that larger objects could hardly be broken up by collisions because of their large gravitational energies. Objects as large as the moon would probably be too large for this reason.

But now it is possible to apply this same process to the fractionation of the silicate and metallic-iron phases in the terrestrial planets, if we assume that asteroidal-type bodies were present as precursors of the protoplanets. Collisional debris of the type found in the chondritic meteorites, i.e., objects ~0.1–1.0 cm in diameter, would accompany the gas in collisions between protoasteroids and be lost with it, while the larger asteroidal-type bodies would become separated from the gas. In this way the silicates could be preferentially lost from the planets with less danger of the separation of the intermediate and high-temperature volatiles than would be true if volatilization were the mechanism of their removal.

The decreasing density of the planets with distance from the sun could be correlated with decreasing temperature, on the basis of the volatilization mechanism, but also with the probability of collision between condensed objects. A higher density of objects can be reasonably expected at smaller distances from the sun. The collisions reduced the solid objects to smaller sizes as the distances from the sun became less, and metallic iron was preferentially preserved because of its greater physical strength. Finally, at Mercury the proportion of metallic iron retained in the protoplanet was a maximum.

If the partial separation of the silicate and metal fractions occurred through mechanical means, that is, through collisions, no high temperatures were required beyond those necessary to produce melting of iron and silicate phases on the protoasteroidal bodies. The temperatures which could occur within gas masses of the magnitude of protoasteroids can be estimated from Emden's (1907) theory of gaseous spheres. Using his tables and formulae for $\gamma = C_p/C_v$ equal to 1.4 and a mean molecular weight of 2.2, we secure formulae for T_0, ρ_0, and P_0, that is, values for the temperature, density, and pressure at zero radius, in terms of the mass and radius. These equations are easily solved for R_0, ρ_0, and P_0 as functions of the mass and T_0, and reduce to

$$R = 1.236 \times 10^{-15} \frac{M}{T_0}, \qquad \rho_0 = 3.04 \times 10^{45} \frac{T_0^3}{M^2}, \qquad P_0 = 1.15 \times 10^{53} \frac{T_0^4}{M^2}. \quad (10)$$

Since the iron and silicate phases were melted in the iron and stone meteorites, these objects were subjected to temperatures greater than 1800° K. We use 2000° K as a reasonable value. Table 6 gives calculated values for asteroidal bodies of different radii whose masses are calculated, assuming a density of 3.5. The mass of the protoasteroid is secured by multiplying by 286, which is the ratio of the hydrogen and helium masses to the mass of silicates and iron in the meteorites. It is evident that the values of the radii, densities, and pressures secured are impossible for the asteroidal bodies, including the moon. If the hydrogen-to-silicon ratio is increased by a factor of 5, on the assumption that the cosmic ratio is in error by this factor, still no possible solution is secured, except possibly in the case of the moon. If the calculation is made for T_0 equal to 300° K, the

radii, densities, and pressures are changed by the factors 30/3, 27/8000, and 81/160,000, respectively. Still the values for the asteroidal bodies do not conform to physical possibilities. We conclude that the asteroidal bodies could not have been heated to high temperatures by the adiabatic compression of their gases in their own gravitational fields and, in fact, that their temperatures would be determined largely by external sources of heat. But Emden's gas spheres are assumed to be isolated, and the gas masses we are discussing were part of the solar nebula, whose temperature was about the same as that of a black body at the same distance from the sun. If fluctuations in pressure by factors of 100 or 1000 occurred in this mass, the adiabatic compressions would produce temperatures about sufficient to melt iron and silicates and partially volatilize them.

TABLE 6*

Radius of Solid Body (Km)	Mass of Solid Body (Gm)	Mass of Solid Body plus Gas (Gm)	T_0=2000° K		
			R (Calc.) (Cm)	ρ_0 (Calc.) (Gm Cm^{-3})	P_0 (Calc.) (Dynes Cm^{-2})
100	1.47×10^{22}	4.19×10^{24}	2.6×10^{6}	1.4×10^{6}	1.0×10^{17}
200	11.7×10^{22}	3.35×10^{25}	2.1×10^{7}	2.2×10^{4}	1.6×10^{15}
400	93.8×10^{22}	2.68×10^{26}	1.7×10^{8}	3.4×10^{2}	2.6×10^{13}
1734 (moon)	7.35×10^{25}	2.10×10^{28}	1.3×10^{10}	0.55	4.2×10^{9}

* The solution, when the temperature is assumed to be finite at the surface, is easily secured by setting the integration constant at eq. (55.2), p. 80, of Eddington (1930) equal to $[\gamma/(\gamma-1)](RT_s/\mu)$ instead of zero and following through the development of the following pages. The tables can be used as before, but u is not zero at the surface of the sphere. It is found that no important changes in calculated central temperatures and pressures result for the cases used here. For the moon, one consistent set of values is $T_0 = 2060$; $\rho_0 = 0.090$; $P = 7\times10^9$; $R = 8.2\times10^8$, with the temperature of the surface, T_s, taken as 300° K, and thus they are not significantly different from those of the table.

Jeans's formula for the gravitational instability of a gas mass gives, for the order of the dimensions of the stable bodies of gas which are formed,

$$\lambda^2 = \frac{\pi\gamma v^3}{3G\rho},$$

and, for the mass,

$$\rho\lambda^3 = \left(\frac{\pi\gamma}{3G}\right)^{3/2}\frac{v^3}{\rho^{1/2}},$$

where ρ is the density, γ the ratio of heat capacities at constant pressure and volume, G the gravitational constant, and v the velocity of the gas molecules. Taking v equal to 2×10^5 for molecular hydrogen at 300° K and $\rho = 10^{-6}$ gm cm^{-3}, the mass is 7.5×10^{29} gm. The nonvolatile fraction is about 2.6×10^{27}, or half the mass of the earth. Since the formula is only approximate and since only a fraction of the nonvolatiles would have accumulated into a solid object, this indicates that masses such as the asteroids, the Imbrian planetesimal, or even the moon could have been formed in the solar nebula.

The moon is not in isostatic equilibrium and hence can hardly be liquid in its interior. Heat generation and heat losses are such that it could never have been molten on the interior if it is not so now (Urey 1952*b*, p. 49). Hence objects even of this size did accumulate at low temperatures. The conclusions reached on chemical grounds in regard to the accumulations of asteroidal objects at low temperatures are substantiated by this physical evidence. We then assume that these objects were at times immersed in gases at higher pressures and became superficially heated, and at other times were not so immersed and their temperatures fell, permitting the formation of the crystalline silicates observed in the meteorites. At the high temperatures, evaporation of the silicates occurred. Collisions may have produced finely divided material, which moved with the gas and was dispersed with it. Evidence for this is found in the structure of the meteorites and the surface of the moon. In this way a separation of silicate and metallic fractions

and a preferential loss of the silicate fraction without the preferential loss of the more volatile elements of the silicate and iron sulfide phases may be understood.

THIRD ALTERNATIVE PROCESS

The solar nebular probably resulted from a collision of the sun when its radius was less than the orbital radius of Mercury with a gas cloud having a mass of about solar magnitude. Since stars are formed in groups and residual gas clouds exist in the region of such stars, e.g., the ζ Persei cluster (Blaauw 1952; Blaauw and Savendoff 1953), such a collision during the early history of the sun would seem to be probable or at least more probable than such an event for the sun at the present time. If the collision were head-on and hence symmetrical, the gas would be compressed as it enveloped the sun and would move on and partly escape. Since accelerations would be quite different in different parts, turbulence would occur, thermodynamically reversible compression would not take place, and hence part of the cloud would be retained about the sun. If substantial solid objects existed in this cloud before the collision, they would be captured, since they would move on initially hyperbolic orbits through the gas, lose some of their energy to the gas, and be captured in elliptical orbits. However, there would be no resultant angular momentum; hence this would not be a possible model. An unsymmetrical collision would be more probable. The gas-cloud collision would not be thermodynamically reversible at all, and much gas would be captured by the sun, and the gas and solid objects would rotate about the sun in one direction, giving the system its resultant angular momentum.

During such a collision the gas cloud would be heated by adiabatic compression of the gases in the sun's field and by the absorption of the sun's radiation by the gas and dust of the cloud. The first effect would be comparable to that expected for an Emden gas sphere of radius equal to the orbital radius of Pluto. At the terrestrial planets this would amount to higher than 10,000° K. However, the full effect would not develop within the time of the collision. The radiation from the present sun would increase the temperature of atomic hydrogen of mass equal to that of the sun only 0°.5 in one year. However, the mass of the cloud within a sphere of radius of, say, 3 A.U. would be only a small fraction of the total, and hence high temperatures from this source can be postulated. The solid objects would cross the gas stream at high velocities and be heated superficially during this process. All three of these sources of heat would decrease with increasing distance from the sun, and thus the decreasing density of the terrestrial planets with distance from the sun would be explained.

However, we have no evidence for the existence of solid objects of substantial size in dust clouds in space, and apparently there is no known possible method of detecting them. Also the accumulation of such objects could not occur in such quiescent dust clouds (Whipple 1946) as we now observe in interstellar space, for only larger masses of cloud would be gravitationally unstable, according to Jeans's formula, and the settling of dust would be very slow in small masses. Only if the process of formation of stars produced local high densities, could we expect such objects to be formed.

Struve (1954) has shown that the properties of certain subgiant stars that occur in eclipsing binary systems can be explained by just such a partial separation of hydrogen from the heavier elements in the one star as compared with the other as that postulated above. He also suggests a possible relation of the separation of elements in these stars to a similar process during the formation of the solar system.

CONCLUDING REMARKS

What is maintained in this paper is that the planetesimals previously postulated by the writer and presented in the opening paragraph of this paper are a necessary part of the process of formation of the terrestrial planets. Extensive chemical evidence is reviewed which supports this view. Three alternative physical processes for the formation and dissipation of the solar nebula are discussed. Chemical experiments to confirm the thermodynamic calculations would be highly desirable.

I am indebted to Professor W. F. Libby for reading and constructively criticizing this manuscript and its arguments at several stages of its preparation, and to A. D. MacLean for checking the thermodynamic calculations.

REFERENCES

Aller, L. 1953, *Astrophysics* (New York: Ronald Press), p. 327.
Aston, F. W. 1924, *Nature*, **114**, 786.
Behne, W. 1953, *Geochim. et cosmochim. acta*, **3**, 186.
Blaauw, A. 1952, *B.A.N.*, **11**, 405, 414.
Blaauw, A., and Savendoff, M. P. 1953, *B.A.N.*, **12**, 69.
Boato, G. 1954, *Phys. Rev.*, **93**, 640.
Brewer, L., and Searcy, A. W. 1951, *J. Amer. Chem. Soc.*, **73**, 5308.
Brown, H. S. 1952, *The Atmospheres of the Earth and Planets*, ed. G. P. Kuiper (Chicago: University of Chicago Press), chap. 9.
Carslaw, H. C., and Jaeger, J. C. 1947, *Conduction in Solids* (London: Clarendon Press).
Chipman, J., and Marshall, S. 1940, *J. Amer. Chem. Soc.*, **62**, 299.
Eddington, A. 1930, *The Internal Constitution of the Stars* (Cambridge: At the University Press).
Edwards, G. 1954, unpublished data.
Emden, R. 1907, *Gaskugeln* (Berlin: B. G. Teubner).
Eucken, A. 1944, *Nachr. Akad. Wiss., Göttingen, math.-phys. Kl.*, Heft 1.
Gilbert, G. K. 1893, *Bull. Phil. Soc. Washington*, **12**, 241.
Harteck, P. 1892, *Zs. f. phys. Chem.*, **134**, 21.
Kelley, K. K. 1949, *Contributions to the Data of Theoretical Metallurgy* (U.S. Bur. of Mines Bull. 476).
Koch, M. 1954, private communication.
Koritnig, F. S. 1951, *Geochim. et cosmochim. acta*, **1**, 89.
Kuiper, G. P. 1951*a*, *Astrophysics*, ed. J. A. Hynek (New York: McGraw-Hill Book Co.), chap. 8.
Kuiper, G. P. 1951*b*, *Proc. Nat. Acad. Sci.*, **37**, 383.
Kuiper, G. P. 1952*a*, *The Atmospheres of the Earth and Planets* (Chicago: University of Chicago Press).
Kuroda, P. K., and Sandell, E. B. 1953, *Bull. Geol. Soc. Amer.*, **64**, 879.
Latimer, W. M. 1950, *Science*, **112**, 101.
Mueller, G. 1953, *Geochim. et cosmochim. acta*, **4**, 1.
Noddack, I., and Noddack, W. 1931, *Zs. f. phys. Chem., A*, **154**, 207.
Noddack, I., and Noddack, W. 1934, *Svensk Kem. Tid.*, **46**, 173.
Öpik, E. J. 1951, *Proc. Roy. Irish Acad.*, **54**, 165.
Rabe, W. 1929, *A.N.*, **234**, 153.
Rossini, F. D.; Wagman, D. D.; Evans, W. H.; Levine, S.; and Jaffe, I. 1952, *Selected Values of Chemical Thermodynamic Properties* (Circ. 500, Nat. Bur. of Standards).
Russell, H. N., and Menzel, D. H. 1933, *Proc. Nat. Acad. Sci.*, **19**, 997.
Sandell, E. B. 1954, private communication.
Shaw, D. M. 1952, *Geochim. et cosmochim. acta*, **2**, 118, 185.
Struve, O. 1954, *Les Processus nucléaires dans les astres* (extrait des *Mémoires in 8° de la Soc. Roy. des Sciences de Liège*, 4th ser., Vol. **14**, Fasc. 1), p. 236.
Suess, H. E. 1949*a*, *Experientia*, **5**, 226.
Suess, H. E. 1949*b*, *J. Geol.*, **51**, 600.
Suess, H. E. 1954, unpublished.
Sverdrup, H. V.; Johnson, M. W.; and Fleming, R. H. 1946, *The Oceans* (New York: Prentice-Hall), p. 120.
Taylor, C. R., and Chipman, J. 1942, *Trans. Amer. Inst. Min. Met. Eng.* (Tech. Pub.).
Treadwell, W. D., and Schaufelberger, F. 1946, *Helvet. chim. acta*, **29**, 1936.
Trumpler, R. J. 1927, *Lick Obs. Bull.*, **13**, 19.
Underhill, Ann. 1951, *Canadian J. Phys.*, **29**, 447.
Urey, H. C. 1951, *Geochim. et cosmochim. acta*, **1**, 239.
Urey, H. C. 1952*a*, *L. Farkas Memorial Volume* (Nat. Res. Council of Israel), pp. 10 and 11.
Urey, H. C. 1952*b*, *The Planets* (New Haven: Yale University Press).
Urey, H. C. 1952*c*, *Phys. Rev.*, **88**, 248.
Urey, H. C. 1952*d*, *Geochim. et cosmochim. acta*, **2**, 263.
Urey, H. C. 1953*a*, *Proc. Roy. Soc. London, A*, **219**, 281.
Urey, H. C. 1953*b*, *Proc. Nat. Acad. Sci.*, **39**, 933.
Urey, H. C. 1954, *Les Processus nucléaires dans les astres* (extrait des *Mémoires in 8° de la Soc. Roy. des Sciences de Liège*, 4th ser., Vol. **14**, Fasc. 1), p. 481.
Urey, H. C., and Craig, H. 1953, *Geochim. et cosmochim. acta*, **4**, 36.
Wedepohl, K. H. 1953, *Geochim. et cosmochim. acta*, **3**, 93.
Whipple, F. L. 1946, *Ap. J.*, **104**, 1.

CATALOGUE AND BIBLIOGRAPHY OF EMISSION-LINE STARS OF TYPES LATER THAN B

Prepared at the Yerkes Observatory, Williams Bay, Wisconsin, and the Lick Observatory, Mount Hamilton, California

WILLIAM P. BIDELMAN

Lick Observatory, University of California

ABSTRACT

This catalogue enumerates the known middle- and late-type emission-line stars and provides a comprehensive bibliography of the spectroscopic observations of these objects. A total of 1114 stars whose spectra show bright hydrogen lines is included, grouped into eleven separate tables to permit similar objects to be listed together. An additional 426 stars whose spectra show bright lines of ionized calcium are also included. The bibliography gives references to all spectroscopic observations of the stars having bright hydrogen lines, but only references pertaining specifically to observations of the emission lines in the case of the Ca II emission stars. In all, 903 references are listed. An extensive set of remarks accompanies the catalogue, giving supplementary or previously unpublished data concerning the objects included.

INTRODUCTION

Emission-line stars have become in recent years the subject of much astrophysical research. The presence of bright lines in the spectrum of a star is a widely recognized indication that unusual and little-understood phenomena are occurring in the stellar atmosphere. The diversity of stellar spectra that show emission lines is very great, and our knowledge of these peculiar stars has grown rapidly within the last few years. An enumeration of the early-type emission-line stars known is contained in Merrill and Burwell's extremely useful Catalogue and Bibliography of Stars of Classes B and A Whose Spectra Have Bright Hydrogen Lines (1933, 1943, 1949); the present work provides a similar listing of the emission-line stars of later type.

Most of the stars contained in the present catalogue are of spectral classes F and later, but a number of A-type stars which are members of binary systems or which are involved in nebulosity are included. Early A-type supergiants and A-type shell stars are not included. The present bibliography, like that of Merrill and Burwell, contains only references to spectroscopic observations. Values of radial velocity and proper motion are not given; these may be found for many of the stars in Wilson's General Catalogue of Stellar Radial Velocities (1953). References to the light-variations of the variable stars are given in the special bibliographies of this subject (Prager 1934, 1936, 1941; Schneller 1952), as well as in the General Catalogue of Variable Stars (Kukarkin and Parenago 1948) and its supplements.

In view of the great variety of intermediate and late-type stars whose spectra show emission lines, it was considered of value to group similar objects to the extent that present data allow. Two main groups are immediately evident: one comprises those stars whose spectra have bright hydrogen lines, and the other those whose spectra have only bright H and K lines of ionized calcium. Most of the stars of the former group are var-

iable in light and spectroscopically peculiar, but many of the members of the latter group are apparently quite normal. In fact, it may be surmised that the number of objects known to show Ca II emission in their spectrum could be extended indefinitely by suitable observations with high-dispersion spectrographs. Hence it appears that a listing of these stars does not have the same significance as one of the stars whose spectra have emission lines of hydrogen. As a consequence of this fact, while all stars known to show Ca II emission are contained in the catalogue, the references given for these are only those relating specifically to the emission lines, while in the case of the stars known to show hydrogen emission, all spectroscopic observations are included.

Further subdivisions of each of the two main groups have been made: the complete catalogue of emission-line stars is presented in a series of fifteen separate tables, eleven containing stars with hydrogen emission and the remaining four containing the Ca II emission stars. A series of notes which customarily refer to unpublished data follows each table. In addition to data on position, magnitude, spectral type, etc., each tabular entry is accompanied by a series of numbers which refer to items in the general list of references, which contains 903 entries. The arrangement of the list of references is similar to that adopted by Merrill and Burwell. The following table gives a summary of the contents of the various parts of the catalogue, together with explanatory notes:

CONTENTS OF THE VARIOUS TABLES COMPRISING THE CATALOGUE

No. of Table	Type of Object Included	No. of Stars
	Part I. Hydrogen Emission Stars	
1. . . .	Variables of the o Ceti Class	685
2. . . .	Long-Period Variables of Small Range, Semiregular and Irregular Variables of Spectral Types M, S, and C	109
3. . . .	Variables of Unknown Type of Variation	16
4. . . .	Intrinsic Variables of Spectral Types F, G, and K	49
5. . . .	Stars with Combination Spectra	23
6. . . .	Variables of the U Geminorum Type	9
7. . . .	Emission-Line Stars Associated with Nebulosity	74
8. . . .	M-Type Dwarf Stars with Hydrogen Emission	67
9. . . .	Binaries with Hydrogen Emission	35
10. . . .	Binaries of the VV Cephei Type	8
11. . . .	Miscellaneous Emission-Line Stars	39
	Total	1114
	Part II. Ca II Emission Stars	
12. . . .	Spectroscopic Binaries with Ca II Emission	72
13. . . .	Giant, Subgiant, and Supergiant Stars with Ca II Emission	116
14. . . .	Dwarf Stars with Ca II Emission	222
15. . . .	Cepheid Variables with Ca II Emission	16
	Total	426
	Grand total	1540

EXPLANATORY NOTES

General.--The notation used throughout the catalogue is largely standard or is evident from the references cited. Under the heading "Designation" are given the serial numbers

of stars in the Henry Draper Catalogue and its Extensions, in the B.D. and the Co.D., in the Astrographic Catalogue, and in Cincinnati Publications, Vol. 20. A "K" number for an unnamed variable refers to the Catalogue of Stars Suspected of Variability (Kukarkin, Parenago, Efremov, and Kholopov 1951). Visual magnitudes are given unless the values are underlined, in which case they are photographic or photoelectric determinations. The spectral types given are taken from a variety of sources, in many cases not specifically referred to. This is especially true in the case of Tables 12-15. In general, the spectral type and luminosity class on the system of the Yerkes Spectral Atlas (Morgan, Keenan, and Kellman 1943), as revised, has been given whenever available, but many classifications are taken from various publications of the Mount Wilson Observatory. Most of the other sources from which spectral types have been taken but to which no reference is otherwise made are listed below.

LIST OF REFERENCES FOR SPECTRAL TYPE

M. W. Mayall and M. H. Baker, Harvard Circ., No. 436, 1940.

P. C. Keenan, Ap. J., 95, 461, 1942.

A. N. Vyssotsky, Ap. J., 97, 381, 1943.

A. N. Vyssotsky, E. M. Janssen, W. J. Miller, and M. E. Walther, Ap. J., 104, 234, 1946.

A. D. Code, Ap. J., 106, 309, 1947.

W. W. Morgan and N. G. Roman, Ap. J., 112, 362, 1950.

N. G. Roman, Ap. J., 112, 554, 1950.

P. C. Keenan and W. W. Morgan, in Astrophysics, ed. J. A. Hynek (New York: McGraw-Hill Book Co., Inc., 1951), chap. 1.

W. P. Bidelman, Ap. J., 113, 304, 1951.

A. N. Vyssotsky and B. A. Mateer, Ap. J., 116, 117, 1952.

N. G. Roman, Ap. J., 116, 122, 1952.

H. L. Johnson and W. W. Morgan, Ap. J., 117, 313, 1953.

R. E. Wilson, General Catalogue of Stellar Radial Velocities ("Publications of the Carnegie Institution of Washington," No. 601 [Washington, 1953]).

Tables 1, 2, and 3.--These tables contain "normal" intrinsic variables of types M, S, and C. The decision on whether a variable star should be included in Table 1 or in Table 2 was made entirely on the basis of the classifications of variable-star light-curves given in the General Catalogue of Variable Stars (Kukarkin and Parenago 1948) and its first six annual supplements. The variables listed in Table 1 have light-ranges of more than 2 1/2 mag., while those in Table 2 have smaller light-ranges or show light-variations of an unusual type. If available, the spectral type near or at maximum light is given, but in many cases the types refer to phases well below maximum light. The classifications given for the carbon stars are on the system set up by Keenan and Morgan (1941), if available; otherwise, the designation "Ce" has been used. A few of the cooler carbon stars have been given approximate types by reference to data given by Sanford (1944). These types appear in parentheses in the tables. Presumably, all the stars included in Table 3 actually belong in either Table 1 or Table 2, but sufficient data on their light-curves are not available.

Table 4.--This group contains largely RV Tauri stars and abnormal cepheid variables, including a number of stars in globular clusters; most of the spectral types are taken from the work of Joy at Mount Wilson Observatory.

Table 5.--Stars with combination spectra are those whose spectra show simultaneously very high-excitation emission lines and low-temperature absorption features, but which cannot be considered certain binaries. Some or all may, however, be so. A number of these stars show nova-like light-variations.

Table 6.--This table lists only those U Geminorum variables which appear to show an absorption spectrum of type later than B. Several other stars of this class have been found to show a continuous spectrum characteristic of still higher temperature.

Table 7.--This table contains those stars which appear to be intimately associated with nebulosity, a group whose characteristics were first systematically studied by Joy (1945). In order to insure homogeneity, only those stars have been included which have been observed with slit spectrographs. Consequently, the very large number of H α-emission objects found by Haro in the region of the Orion Nebula (1953) and elsewhere have not been included, nor have the many recent similar discoveries of Herbig (1954) and Weston (1953), though most of these stars are undoubtedly similar to those in the table.

Table 8.--Several of these dMe stars, the so-called "flare stars," have been found to be variable in light, and a few are also variable in spectrum.

Tables 9 and 10.--These tables contain those binary stars whose spectra have bright hydrogen lines which do not fall into one of the other groups. A number of the A-type binaries listed in Table 9 are also included in the work of Merrill and Burwell, in which case a reference is made to this fact. Table 10 contains a selected group of supergiant binary systems whose spectra also show, in addition to bright hydrogen lines, emission lines of [Fe II]. Of the stars of this type, only VV Cephei is known to be an eclipsing variable.

Table 11.--A number of emission-line stars that do not appear to belong to any of the other groups on the basis of present information are placed in this table. All, with the possible exception of R CrB, show hydrogen emission and, in many cases, other unusual spectroscopic characteristics as well.

Tables 12, 13, and 14.--Most of the stars contained in these tables were included in the list of all stars known to show Ca II emission lines published by Joy and Wilson (1949). Probably all late-type giant stars show some emission (usually self-reversed) at H and K, and most dwarf stars of types later than G5 do also. However, there are surprising variations in intensity between different stars of the same spectral class. The Ca II emission lines are probably stronger in binaries than in single stars. In the list of binaries, Table 12, the spectral type of the component which shows the Ca II emission is underlined. The letter (H), (U), or (C) following the spectral type of certain stars indicates membership in the Hyades, Ursa Major, or Coma Berenices clusters, respectively.

Table 15.--Ca II emission is observed in the spectra of these cepheid variables during only a fairly small part of the cycle, generally during the rise to maximum light and near that phase. The presence of emission at H and K appears to be a common characteristic of classical cepheids, although the structure of the emission differs greatly from that of normal supergiant stars, in that the emission in the case of the cepheids shows a large violet displacement. In addition to the stars listed in Table 15, the carbon cepheid RU Cam has also been found to show bright Ca II, but this object is included in Table 4, since bright hydrogen lines also appear in its spectrum.

The writer is grateful to a number of astronomers who have assisted him by communicating unpublished data and by supplementing information already published. He is especially indebted in this connection to Drs. A. H. Joy, P. W. Merrill, and R. F. Sanford, of the Mount Wilson Observatory; to Dr. G. H. Herbig, of the Lick Observatory; and to Dr. E. R. Dyer, Jr., of the Leander McCormick Observatory. A grant from the Office of Naval Research, which is herewith gratefully acknowledged, made it possible for the writer to visit the offices of the Mount Wilson and Palomar Observatories and to inspect those observatories' spectrograms of a great number of emission-line stars, which were made available to him through the kindness of the director, Dr. I. S. Bowen.

The writer also wishes to express his gratitude to Drs. S. Chandrasekhar, W. W. Morgan, and B. Strömgren, of the Yerkes Observatory, who encouraged him to prepare this catalogue and who made observational facilities available to him. And, finally, though most of the work in the preparation of this catalogue was done at the Yerkes Observatory, the writer is also grateful to Dr. C. D. Shane, director of the Lick Observatory, who has enabled him to bring the work to completion.

REFERENCES

Haro, G. 1953, Ap. J., 117, 73.

Herbig, G. H. 1954, Pub. A.S.P., 66, 19.

Joy, A. H. 1945, Ap. J., 102, 168.

Joy, A. H., and Wilson, R. E. 1949, Ap. J., 109, 231.

Keenan, P. C., and Morgan, W. W. 1941, Ap. J., 94, 501.

Kukarkin, B. W., and Parenago, P. P. 1948, Moscow: Akademiia Nauk, S.S.S.R.

Kukarkin, B. W.; Parenago, P. P.; Efremov, Yu. I.; and Kholopov, P. N. 1951, Moscow: Akademiia Nauk, S.S.S.R.

Merrill, P. W., and Burwell, C. G. 1933, Ap. J., 78, 87.

-----. 1943, ibid., 98, 153.

-----. 1949, ibid., 110, 387.

Morgan, W. W.; Keenan, P. C.; and Kellman, E. 1943, An Atlas of Stellar Spectra (Chicago: University of Chicago Press).

Prager, R. 1934 and 1936, Geschichte und Literatur des Lichtwechsels der veränderlichen Sterne, Vols. 1 and 2 (Berlin: Dummler).

Prager, R. 1941, Harvard Ann., Vol. 111.

Sanford, R. F. 1944, Ap. J., 99, 145.

Schneller, H. 1952, Geschichte und Literatur des Lichtwechsels der veränderlichen Sterne, Vol. 3 (Berlin: Akademie Verlag).

Weston, E. B. 1953, A.J., 58, 48.

Wilson, R. E. 1953, "Carnegie Institution of Washington Publications," No. 601 (Washington, D.C.).

TABLE 1

VARIABLES OF THE o CETI CLASS

Cat. No.	Name	Desig-nation	R.A. 1900 h m	Dec. 1900	l	b	Magnitude	Period (Days)	Spec-tral Type	References
1.	SY Scl		0 2.5	-26° 2'	11°	-81°	12.4-<16.3	411	M6e	696
2.	V Scl	409	0 3.6	-39 47	300	-76	9.4- 14.5	296	M4e	612,614,698
3.	SS Cas	499	0 4.4	51 1	84	-11	8.8- 13.2	141	M4e	451,612,614,709,742
4.	S Scl	1115	0 10.3	-32 36	323	-82	6.3- 13.4	366	M6e	311,384,447,451,612,614, 765
5.	X And	1167	0 10.9	46 27	85	-15	8.1- 15.1	346	Se	150,195,381,384,391,451, 612,614,708
6.	BB And		0 12.5	44 36	85	-17	13.0-<15.5	290	Se	220,525
7.*	AP Cep		0 16.0	75 54	88	+14	12.6-<16	125	Me	
8.	T And	1795	0 17.2	26 26	84	-35	7.3- 14.2	280	M4e	384,447,451,609,612,614
9.	T Cas	1845	0 17.8	55 14	87	- 7	6.7- 12.7	445	M8e	77,355,384,398,428,447, 451,537,591,612,614,742, 752
10.	S Tuc	1925	0 18.4	-62 14	274	-56	9.7-<15	240	M3e	359,612,614
11.	R And	1967	0 18.8	38 1	85	-24	5.0- 15.3	409	Se	77,195,254,286,381,384, 391,428,451,508,521,535, 536,566,586,596,602,612, 614,642,741,752,851,901
12.	S Cet	1987	0 19.0	- 9 53	74	-71	7.0- 14.7	321	M3e	384,451,612,614,648
13.	NGC 104-1		0 19.7	-72 40	272	-45	11.3-<16.0	212	Me	842
14.	NGC 104-2		0 19.8	-72 41	272	-45	11.6- 15.3	203	Me	842
15.	NGC 104-3		0 20.8	-72 37	272	-45	11.4- 16.1	192	Me	842
16.	YZ And		0 22.0	30 21	85	-31	11.0-<15.5	208	M5e	245
17.	T Phe	2725	0 25.6	-46 58	277	-71	8.7- 14.6	281	M5e	612,614,702
18.	TU And	2890	0 27.1	25 29	86	-36	7.8- 13.1	316	M4e	245,612,614,741
19.	Y Cep	3344	0 31.3	79 48	90	+18	8.3- 16.0	333	M5e	451,612,614,656
20.	U Cas	4350	0 40.8	47 42	90	-14	7.6- 16.0	278	Se	195,381,384,391,451,586, 612,614,649,752
21.	RW And	4489	0 41.9	32 8	90	-30	7.7- 15.4	431	M5e	451,612,614
22.	V And	4779	0 44.7	35 6	91	-27	8.3- 15.2	258	M2e	384,451,612,614,654,741
23.	RR And	4895	0 45.9	33 50	91	-28	8.4- 15.5	329	Se	228,451,612,614,710,741
24.	RV Cas	5016	0 47.1	46 52	91	-15	7.4- 16.0	331	M7e	451,612,614
25.	W Cas	5235	0 49.0	58 1	91	- 4	7.8- 12.5	406	Ce	99,195,362,391,451,612, 614,709,726,742,752
26.	TZ Tuc		0 49.3	-70 25	269	-48	9.8- 15.8	229	M0e	696
27.	U Tuc	5774	0 54.2	-75 32	269	-42	8.5- 15.2	262	M3e	612,614,704,781
28.	W Psc		0 54.4	27 24	94	-34	11.4- 14.8	189	M2e	614,741
29.	Z Cet	6592	1 1.6	- 2 1	102	-64	8.4- 14.2	184	M2e	451,612,614
30.	HV Cas		1 5.1	53 10	94	- 9	12.9- 17.2	517	Ce	219,476
31.	X Psc	7160	1 6.7	21 41	98	-40	8.5-<14	353	M6e	451,614,726,741
32.	U Scl	-30°375	1 6.8	-30 39	206	-84	9.0- 15.1	334	M5e	690
33.	RS Hyi		1 8.0	-77 22	268	-41	10.0- 16.0	216	M3e	696
34.	U And	7482	1 9.8	40 11	96	-21	9.0- 15.0	348	M6e	451,612,614,652,741
35.	RS Phe		1 9.8	-57 16	262	-60	10.6-<12.8	239	M2e	696
36.	VZ Cas	+55°275	1 10.3	55 52	94	- 6	9.3- 13.5	170	M0e	245
37.	UZ And	7540	1 10.4	41 13	96	-20	9.0- 15.2	314	M7e	451,612,614,712
38.	S Cas	7769	1 12.3	72 5	92	+10	6.2- 15.3	610	Se	195,381,384,391,612,614, 647,752
39.	S Psc	7773	1 12.3	8 24	103	-53	8.2- 15.4	406	M7e	612,614,648
40.	W Phe	8166	1 15.9	-56 27	260	-61	8.8- 16	332	M5e	612,614,720
41.	TX And		1 16.2	38 10	98	-23	10.4- 13.8	234	M1e	688,741

TABLE 1—Continued

Cat. No.	Name	Designation	R.A. 1900 h m	Dec. 1900	l	b	Magnitude	Period (Days)	Spectral Type	References
42.*	U Psc	+12°170a	1 17.7	12°21'	104°	-49°	9.3- 14.7	173	M4e	
43.	RX Psc		1 20.2	20 52	102	-40	8.8- 14.6	280	M1e	688,741
44.*	RZ Per		1 23.6	50 20	97	-11	8.6- 14.0	354	Se	451,742
45.	R Psc	9203	1 25.5	2 22	112	-58	7.0- 14.8	344	M4e	77,384,451,612,614,649, 740,752,892
46.	SX And		1 27.6	46 00	99	-15	8.7-<13	335	M6e	245,451,612
47.	RY Hyi	CPD-75° 103	1 32.4	-75 45	266	-42	11.0- 15.5	319	M5e	696
48.	RU And		1 32.8	38 10	101	-23	9.5- 14.5	237	M5e	465
49.	Y And	10112	1 33.8	38 50	101	-22	8.1- 14.5	220	M3e	384,451,612,614,708,741
50.	X Cas	+58°334a	1 49.8	58 46	99	- 2	8.4- 13.2	425	Ce	179,314,362,426,476,752, 819
51.	T Tri		1 50.9	33 32	106	-26	10.0-<14	322	M8e	225
52.	U Per	12025	1 52.9	54 20	101	- 6	7.5- 11.7	318	M6e	384,445,447,451,612,614, 742,752,856
53.	S Ari	12701	1 59.3	12 3	118	-46	9.1- 15.7	295	M4e	451,612,614,709,740
54.	Z Tri		2 2.1	27 28	111	-31	11.2- 14.8	218	M2e	245,741
55.	Y Eri	13009	2 2.2	-57 37	250	-57	10.7- 13.5	303	M7e	612,614,709
56.	AG Cep		2 8.8	78 19	95	+17	11 -<16	446	M10e	245
57.	R Ari	13913	2 10.4	24 36	115	-33	7.2- 13.7	187	M3e	77,149,384,451,612,614, 647,741
58.	W And	14028	2 11.2	43 50	107	-15	6.5- 14.3	397	M8e	77,384,451,537,609,612, 614,742,892
59.	RY Cet		2 11.4	-20 59	166	-68	10.5-<13.5	374	M5e	688
60.*	o Cet	14386	2 14.3	- 3 26	137	-57	2.0- 10.1	331	M6e	5,6,18,21,22,27,52,54, 55,56,77,78,105,106,112, 117,118,125,128,129,131, 148,156,174,205,206,208, 240,361,366,367,368,385, 388,398,402,409,414,444, 455,471,482,513,516,536, 537,542,578,584,586,596, 611,612,614,642,679,684, 730,732,738,740,752,753, 757,762,770,783,787,789, 790,794,796,802,804,817, 818,821,823,824,825,831, 832,835,846,853,858,859, 901,902
61.	R Cet	15105	2 20.9	- 0 38	136	-54	7.2- 14	167	M4e	384,451,609,612,614,740, 752,892
62.	S Tri		2 21.4	32 17	114	-25	8.7-<12.4	248	M2e	688,741
63.	RR Per	15186	2 21.7	50 49	106	- 8	7.9- 14.7	391	M6e	451,612,614,657,742
64.	S Hor	15280	2 22.4	-60 1	249	-54	9.7-<12.7	338	M6e	612,614,699
65.	R For	-26°892	2 24.8	-26 33	183	-67	8.1- 13.0	387	Ce	214,476
66.	K 229		2 28.0	-65 33	253	-49	12 - 13		M5e	696
67.	U Cet	15971	2 28.9	-13 35	156	-61	6.7- 13.0	235	M3e	384,451,612,614,642
68.	R Tri	16210	2 31.0	33 50	115	-23	5.4- 12.0	266	M4e	384,447,451,537,612,614, 741,752,856
69.	RS Hor		2 33.4	-63 1	250	-50	9.8-<15.0	203	M3e	696
70.	HV 11094		2 42.0	-36 41	206	-63			Me	696
71.	R Hor	18242	2 50.5	-50 18	231	-57	6.3- 15	401	M7e	352,384,451,612,614,765
72.	T Hor	18949	2 57.7	-51 2	231	-55	9.2- 15	218	M4e	612,614
73.	U Ari	19737	3 5.5	14 25	134	-35	6.4- 15.2	370	M5e	308,451,612,614,684
74.	TW Per	278549	3 13.7	32 47	124	-19	11 -<13.5	336	M2e	688
75.	X Cet	20646	3 14.4	- 1 26	151	-45	7.9- 13.0	177	M2e	451,612,614,740

TABLE 1—Continued

Cat. No.	Name	Designation	R.A. 1900 h m	Dec. 1900	l	b	Magnitude	Period (Days)	Spectral Type	References
76.	R Per	21567	3 23.7	35°20'	124°	-16°	7.7- 14.7	210	M3e	384,451,612,614,647,752
77.	RT Hor		3 26.2	-56 19	236	-49	10.0-<14.0	335	M5e	696
78.	RT Eri	22228	3 29.6	-16 30	173	-49	8.5- 12.9	371	M7e	614,725
79.	X Men		3 34.8	-76 47	259	-37	11.4-<15.0	380	M3e	696
80.	RX Per	279135	3 44.9	32 44	129	-15	9.0-<13	422	M3e	688
81.	U Eri	24220	3 46.2	-25 16	187	-49	9.9- 16.5	275	M4e	451,612,614
82.	U Hor	24607	3 49.6	-46 8	219	-49	7.8-<15.1	349	M6e	612,614,714
83.	T Eri	24754	3 51.0	-24 20	186	-47	7.1- 12.6	252	M4e	384,451,609,612,614
84.	AK Tau	+20°688	3 56.9	20 46	140	-22	11.8- 15.8	243	M1e	225,741
85.	SS Dor		4 3.6	-55 8	231	-45	11 - 15.8		M5e	696
86.	W Eri	26601	4 7.3	-25 24	189	-44	9.6- 14.5	376	M7e	384,451,612,614,703
87.	HV 11095		4 8.8	-80 7	261	-34			M5e	696
88.	RS Eri		4 13.5	-18 45	181	-41	10.1-<12.8	296	Me	688
89.*	EV Tau		4 18.0	6 21	155	-27	12 -<16		M8e	
90.	R Tau	28309	4 22.8	9 56	153	-24	7.4- 15.0	324	M5e	384,451,612,614,642,752
91.	S Tau	+9°586	4 23.7	9 44	153	-24	8.7- 15.6	373	M7e	451
92.	WY Cam		4 23.9	78 56	100	+21	11.4-<15.1	406	Se	225,228,742
93.	HV 11096		4 26.5	-54 50	230	-42			M0e	696
94.	T Cam	29147	4 30.4	65 57	111	+14	6.4- 14.4	373	Se	195,315,381,384,391,451, 612,614,647,709,742,819
95.	R Ret	29383	4 32.5	-63 14	241	-39	8.5- 14.6	277	M4e	451,609,612,614,765
96.	X Cam	29384	4 32.8	74 55	104	+19	7.3- 13.8	143	M3e	384,451,612,614,709,742
97.	RX Tau	29411	4 32.8	8 8	156	-23	9.1- 14.5	337	M7e	451,612,614,708
98.	R Cae	29844	4 37.0	-38 26	208	-40	8.6- 16.0	392	M6e	612,614,855
99.	T Dor	30642	4 44.3	-59 58	236	-38	10.5-<14	168	M3e	614
100.	EP Ori		4 45.7	2 58	163	-23	11 -<14	364	M10e	245
101.*	V Tau	30868	4 46.3	17 22	150	-15	8.5- 14.7	170	M2e	451,612,614,650,752
102.	AU Aur		4 46.6	49 43	125	+ 5	13.0- 15.8	400	Ce	191,426,476
103.	R Ori	31798	4 53.6	7 59	160	-19	8.5- 13.4	379	Ce	99,195,381,391,451,612, 614,708,709
104.	R Lep	31996	4 55.0	-14 57	182	-30	5.5- 10.7	436	$C7_4e$	61,157,163,179,237,265, 355,426,454,476,554,614, 752,761,767,848,901
105.	T Lep	32803	5 0.6	-22 2	190	-31	7.5- 13.0	367	M7e	359,384,451,612,614,752
106.	V Ori	+3°766	5 0.8	3 58	164	-20	8.4- 14.5	268	M3e	384,451,609,612
107.	S Pic	33894	5 8.3	-48 38	222	-35	9.3- 16	428	M7e	359,612,614
108.*	R Aur	34019	5 9.2	53 28	124	+10	6.6- 13.8	458	M7e	77,384,445,451,612,614, 642,742,752
109.	U Dor	271044	5 9.6	-64 26	241	-35	9.2-<15	393	M7e	614,729
110.	T Pic	34448	5 12.3	-47 2	220	-35	9.2- 15	200	Me	612,614,704
111.	T Col	34897	5 15.6	-33 49	204	-32	6.6- 12.6	225	M4e	384,451,612,614,698,765
112.	AC Aur		5 19.3	50 2	128	+ 9	10.7- 14.8	311	M5e	451,614
113.	W Aur	281118	5 20.1	36 49	139	+ 2	8.4- 15.0	274	M3e	451,612,614
114.	S Ori	36090	5 24.1	- 4 46	175	-19	7.5- 13.5	416	M7e	357,451,612,614,740,752
115.	RU Aur		5 33.3	37 35	140	+ 5	9.0-<14.0	467	M8e	451,741
116.	SZ Aur	37645	5 35.0	38 53	139	+ 6	10.5-<14.1	453	M6e	612,614,741
117.	U Aur	37724	5 35.6	31 59	145	+ 2	7.4- 15.5	408	M7e	451,609,612,614,752
118.	S Col	-31°2732	5 43.2	-31 44	204	-26	8.4- 14.1	325	M6e	451
119.	R Col	39324	5 46.7	-29 14	202	-24	8.2- 14	327	M3e	356,451,612,614
120.	V Cam	39741	5 49.4	74 30	107	+24	8.0- 16	519	M6e	612,614,708,709,742

TABLE 1—Continued

Cat. No.	Name	Desig-nation	R.A. 1900 h m	Dec. 1900 ° ′	l	b	Magnitude	Period (Days)	Spec-tral Type	References
121.	U Ori	39816	5 49.9	20°10′	156°	- 1°	5.2- 12.9	373	M8e	205,384,398,424,428,445, 451,490,535,612,614,642, 741,752,851,892,901
122.	AZ Aur		5 54.2	39 40	140	+ 9	10.5- 15.5	420	(C8e)	191,197,426,476
123.	R Oct	40857	5 56.4	-86 26	266	-29	8.0- 14.3	406	M6e	352,451,612,614,765
124.	YY Aur		5 57.0	42 1	138	+11	11.2- 17	336	M5e	225
125.	RR Ori	250795	5 57.3	16 23	161	- 1	10 -<13	252	M5e	741
126.	X Aur	42212	6 4.4	50 15	131	+16	7.9- 13.5	163	M3e	384,451,612,614,709,742
127.	RR Aur	42311	6 4.9	43 11	138	+13	9.0- 15	308	M3e	451,612,614,707
128.	RW Pup	-50°2092	6 6.7	-50 11	225	-26	9.6-<14.2	332	M3e	696
129.	HV 11097		6 11.2	-68 59	246	-29			M1e	696
130.	K 739		6 16.5	-61 52	238	-27	11.5-<13		M3e	696
131.	V Aur	44388	6 16.5	47 45	134	+17	8.1- 13.0	353	Ce	191,426,476,612,614,752
132.	V Mon	44639	6 17.7	- 2 9	179	- 6	6.0- 14.0	334	M5e	77,384,451,612,614,643, 708,740,752
133.	ZZ Gem	44653	6 17.8	25 5	155	+ 7	11.9- 15.8	320	Ce	476,612,752
134.	RT Cam	45968	6 25.6	64 10	118	+23	10.8-<13.0	366	M6e	612,614,742
135.*	AL Aur		6 26.8	31 40	150	+12	10.9-<15.2	389	M7e	741
136.	U Lyn		6 31.8	59 57	123	+23	8.8- 15.0	438	M8e	451
137.	SY Mon	292010	6 32.5	- 1 18	180	- 2	9.6-<13.5	422	M6e	614,740
138.	AA Aur	47523	6 34.0	44 15	139	+18	11 - 16	269	M3e	614,724
139.	S Lyn	47929	6 35.9	58 0	125	+23	8.4- 15.1	301	M7e	451,612,614,710,742
140.	RV Pup	48675	6 39.4	-42 16	219	-19	9.7- 13.0	188	M1e	612,614
141.	X Gem	48912	6 40.7	30 23	153	+14	7.5- 13.9	264	M5e	384,451,612,614,709,741
142.	CL Mon		6 50.2	6 31	175	+ 5	11.0-<16.0	493	Ce	61,191,476
143.	Y Mon	51189	6 51.3	11 22	171	+ 8	8.3- 11.4	230	M4e	451,612,614
144.	R Lyn	51610	6 53.0	55 28	128	+25	6.5- 14.8	379	Se	77,195,381,391,451,526, 612,614,642,742,752,901, 902
145.	T Vol	52905	6 57.8	-66 59	245	-24	9.7-<13.9	176	M4e	612,614,715
146.	ET Aur		7 0.3	37 11	148	+20	11.6-<15.0	204	M2e	225
147.	R Gem	53791	7 1.3	22 52	162	+15	5.9- 14.1	370	Se	1,99,150,195,381,384,391, 398,424,451,526,527,586, 612,614,655,741,752,892, 901
148.*	V CMi	53847	7 1.5	9 2	174	+ 9	8.0- 15.0	366	M6e	451,612,614,698,740
149.	RS Mon		7 2.2	5 8	178	+ 7	9.4-<12.7	264	M3e	696
150.	R CMi	54300	7 3.2	10 11	174	+10	7.0- 11.8	338	Ce	99,195,381,384,391,451, 526,612,614,649,739,752
151.	VX Gem	55284	7 7.1	14 46	170	+13	10.8-<14.9	377	(C8e)	157,386,426,476,614,724, 752
152.*	R Vol	-72°378	7 7.4	-72 51	251	-25	8.8- 13.8	445	Ce	612
153.	WZ Gem		7 10.4	26 10	159	+18	10.5-<15	332	M3e	614
154.	RR Mon	56567	7 12.4	1 16	183	+ 8	8.0- 15.0	393	M6e	451,612,614,657,740
155.	V Gem	57770	7 17.6	13 18	172	+14	7.5- 14.5	275	M4e	384,451,612,614,709
156.	XX Gem		7 19.7	33 33	153	+23	9.5- 13	382	M10e	225
157.	TT Mon		7 20.8	- 5 39	190	+ 6	8.4- 13.2	324	M5e	690
158.	RX Mon	59334	7 24.4	- 4 4	189	+ 8	10 -<13.5	343	M5e	612,614,740
159.	S CMi	59950	7 27.3	8 32	178	+14	6.9- 13.4	332	M7e	384,451,612,614,644,684, 740,752
160.	Z Pup	60218	7 28.3	-20 27	204	+ 1	7.4- 14.7	512	M6e	384,451,612,614
161.	T CMi	+12°1594a	7 28.4	11 57	175	+16	8.9- 15.0	319	M5e	451,612

TABLE 1—Continued

Cat. No.	Name	Designation	R.A. 1900 h m	Dec. 1900	l	b	Magnitude	Period (Days)	Spectral Type	References
162.	S Vol	-73°371	7 31.5	-73°10'	252°	-23°	8.5- 13.7	396	M4e	696
163.	HV 11100		7 32.5	-59 45	239	-18			M2e	696
164.	U CMi	61789	7 35.9	8 37	179	+16	8.0- 13.6	411	M4e	451,612,614,752
165.	S Gem	62045	7 37.0	23 41	164	+23	7.8- 15.0	293	M5e	355,451,595,612,614
166.	SS Pup	63195	7 42.5	-26 6	210	0	12.5- 16	391	Me	614,724
167.	W Pup	63218	7 42.6	-41 57	224	- 8	7.9- 12.8	121	M3e	451,609,612,614
168.	T Gem	63334	7 43.3	23 59	165	+24	7.6- 15.0	288	Se	195,355,381,384,391,451, 612,614,752,901
169.	AE CMi		7 47.8	1 25	187	+16	12.3-<15		M2e	346
170.*	VX CMi		7 48.8	1 59	186	+16	11.8-<16.4	273	Me	
171.	V Cha		7 50.7	-77 46	257	-24	12 -<14		M5e	696
172.	BP Gem		7 53.3	20 55	169	+25	11.5-<12.5	224	M2e	225,741
173.*	BC Mon		7 54.0	- 4 14	193	+14	11 -<13	293	M3e	
174.	AF CMi		7 54.5	0 47	188	+17	12 -<14		M7e	346
175.	BD Mon		7 56.1	- 5 21	194	+14	10.3-<12.4	366	Se	244,245
176.	U Pup	65940	7 56.2	-12 34	200	+10	8.4- 14.7	316	M6e	357,451,612,614,752
177.	RR Cnc		8 5.1	23 27	167	+29	11.6- 15	298	M3e	273
178.	DP Pup		8 6.1	-15 2	204	+11	11.5-<16		M8e	225
179.*	RT Lyn		8 8.3	37 58	151	+33	10.5-<13	396	M6e	
180.	R Cnc	69243	8 11.0	12 2	180	+26	6.1- 11.9	361	M7e	384,451,612,614,643,740, 752
181.	RY Hya	70072	8 14.9	3 5	189	+22	8.4- 11.6	529	Ce	179,362,426,476,612,752
182.*	V Cnc	70276	8 16.0	17 36	174	+29	6.8- 13.8	272	Se	195,381,384,391,451,526, 612,614,646,752
183.	T Lyn	+33°1686	8 16.4	33 50	156	+34	9.0- 13.3	420	$C6_3e$	191,197,426,454,476,614
184.	X Lyn	+35°1821	8 19.1	35 44	154	+35	9.5- 16	321	M5e	614
185.	R Cha	71793	8 24.0	-76 2	257	-21	8.5- 15.5	335	M6e	612,614,705
186.	U Cnc	72863	8 30.0	19 14	174	+33	8.4- 15.3	305	M2e	384,451,612,614,650,741
187.	X UMa	73507	8 33.6	50 29	136	+39	8.8-<14.7	248	M4e	384,451,612,614,708,709
188.	KK Car		8 33.9	-59 37	243	-11	12 - 15		M5ep	696
189.	S Hya	76011	8 48.3	3 27	193	+30	7.2- 14.0	256	M4e	77,384,451,612,614,642, 752
190.	T Hya	76400	8 50.8	- 8 46	205	+24	6.8- 13.4	289	M3e	77,384,451,612,614,647, 752
191.*	TU Hya	AC-1° 1480-126	8 53.2	- 0 27	198	+29	10.5- 15.8	278	M5e	740
192.	S Pyx	78000	9 0.7	-24 41	220	+15	8.3- 13.1	207	M3e	451,609,612,614
193.	W Cnc	78585	9 4.0	25 39	170	+42	7.4- 14.6	392	M7e	451,609,612,614,741
194.*	WX Hya		9 8.7	-13 59	212	+24	9.1-<12.5	234	M3e	
195.	RW Vel	80837	9 16.9	-49 6	240	+ 1	8.9-<13.1	452	M7e	612,614
196.	RW Car	81055	9 18.1	-68 20	253	-13	8.6- 15.0	316	M4e	612,614,705
197.	RZ Hya		9 19.9	- 6 22	208	+31	9.2-<12.5	336	M4e	273
198.	RS Vel	81432	9 20.4	-48 26	239	+ 1	9.1-<12.6	410	M7e	612,614,706
199.	Y Vel	-51°3858	9 25.7	-51 45	242	0	9.7- 16	446	Me	612
200.*	R Car	82901	9 29.7	-62 21	250	- 8	5.6- 11.1	309	M5e	306,451,608,612,614,765
201.	X Hya	83048	9 30.7	-14 15	216	+28	7.2- 13.5	302	M7e	451,612,614,649
202.	Y Dra	83114	9 31.1	78 18	101	+36	7.8- 15.0	326	M5e	451,612,614,709,742
203.	UU Vel	298563	9 32.2	-53 37	244	- 1	11.7-<16	409	M2e	614
204.	R LMi	84346	9 39.6	34 58	158	+51	6.0- 13.3	372	M8e	77,205,384,428,451,584, 591,612,614,709,741,752, 783
205.	RR Hya	84474	9 40.4	-23 34	225	+23	9.9- 16.0	342	M4e	451,612,614

TABLE 1—Continued

Cat. No.	Name	Designation	R.A. 1900 h m	Dec. 1900	l	b	Magnitude	Period (Days)	Spectral Type	References
206.	R Leo	84748	9 42.2	11°54′	192°	+46°	4.4- 11.6	313	M8e	77,172,205,254,286,302, 377,384,385,398,414,424, 428,445,451,497,513,521, 536,537,586,590,596,612, 614,642,740,752,851,901
207.	HV 11101		9 42.6	-67 28	254	-11			Me	696
208.	CM Car		9 45.6	-66 59	254	-10	11.5-<14	335	M2e	696
209.	S LMi	85597	9 47.8	35 24	157	+53	7.7- 14.3	234	M4e	451,610,612,614,741
210.	Z Vel	298731	9 49.4	-53 42	246	0	9.6- 16	425	Me	614
211.	V Leo	86608	9 54.5	21 44	180	+52	7.9- 14.0	273	M5e	357,384,451,612,614,741
212.	RV Car	307482	9 55.6	-63 25	253	- 7	9.4-<14.0	365	M6e	614
213.	S Car	88366	10 6.2	-61 4	252	- 4	6.9- 11.0	149	K5e	158,353,451,608,612,614, 618,667,765
214.	SU Car	88918	10 10.2	-60 23	252	- 4	10 - 17.5	231	Me	612,614
215.	Z Car	88946	10 10.5	-58 22	251	- 2	9.6- 15.1	383	M6e	357,612,614
216.	W Vel	299011	10 11.5	-53 59	249	+ 2	9.5- 15	393	M7e	614
217.	V Ant		10 16.7	-34 18	239	+19	9.2-<12.5	303	M7e	614
218.*	CZ Hya	-24°9072	10 22.6	-25 3	235	+27	9.7-<14	456	Ce	
219.	S Sex	91637	10 29.8	0 10	216	+48	8.6- 14	263	M3e	451,612,614,740
220.	RZ Car	92090	10 32.8	-70 12	260	-11	8.8-<15.0	273	M4e	612,614,706
221.	UX Vel		10 36.2	-54 12	252	+ 4	10 -<17	226	M0e	696
222.	R UMa	92763	10 37.6	69 18	105	+45	6.2- 13.6	301	M4e	77,384,447,451,612,614, 642,752
223.	WX Vel	299399	10 44.8	-53 39	253	+ 5	11.4- 14.2	412	M5e	614,659
224.	WW Vel	CPD-48° 3567	10 46.1	-48 9	251	+10	10.8- 14	187	M5e	614,727
225.	RS Hya	94103	10 46.6	-28 6	242	+28	10.1- 16	335	M6e	612,614
226.	W Leo	94362	10 48.3	14 15	202	+61	8.7- 15.0	386	M7e	451,612,614,709
227.	VX UMa		10 48.3	72 25	101	+43	11.7-<14.5	215	M6e	225,742
228.	S Leo	+6°2412a	11 5.7	6 0	220	+59	9.1- 14.5	189	M3e	451
229.	U Crt		11 7.7	- 6 45	234	+49	9.5-<13	169	M0e	225
230.*	Y Crt	-24°9682	11 15.5	-24 22	247	+34	10.2-<15.0	158	M3e	
231.	RS Cen	98678	11 16.1	-61 20	260	- 1	9.2- 15	164	M2e	612,614,699
232.	RU UMa	101605	11 36.4	39 2	136	+73	8.5- 14.0	253	M3e	451,612,614
233.	VV Cen	309078	11 41.7	-61 20	263	0	10.2-<14.0	199	M3e	690
234.	X Cen	102681	11 44.2	-41 12	259	+20	7.0- 13.9	314	M6e	451,609,612,614,765
235.	W Cen	103513	11 50.0	-58 42	264	+ 3	8.6- 15.5	201	M3e	609,612,614
236.	AL Cru	309295	11 51.7	-61 55	264	0	11.1-<13	328	M4e	690
237.	SV Vir		11 55.3	- 9 39	252	+51	9.3-<12.5	296	M4e	273
238.	R Com	+19°2527	11 59.1	19 20	221	+77	7.3- 14.6	362	M5e	384,451,612,614,656,741
239.	SU Vir	104959	12 0.1	12 55	236	+72	8.4- 14.5	210	M3e	451,612,614,713
240.	T Vir	106430	12 9.5	- 5 29	256	+56	8.2- 14.8	339	M6e	451,612,614,708,752
241.	R Crv	107199	12 14.5	-18 42	262	+43	5.9- 14.4	317	M5e	77,384,451,612,614,642, 752
242.	ST Cru	-59°4250	12 20.3	-59 27	267	+ 2	10.7- 13.7	440	M6e	614,661
243.*	T CVn	108833	12 25.3	32 3	127	+85	8.6- 12.8	290	M6e	612,614,709,741
244.	U Cru	109090	12 26.8	-57 2	268	+ 5	10.3- 14	351	M4e	612,614,701
245.	U Cen	109231	12 28.0	-54 6	268	+ 8	9.3- 15	220	M3e	357,612,614
246.*	Y Vir		12 28.7	- 3 52	265	+58	8.8- 14.7	218	M2e	245,451,609,612,740
247.	YY Cen		12 30.2	-54 1	269	+ 8	12.5-<14.3		M5e	696

TABLE 1—Continued

Cat. No.	Name	Desig-nation	R.A. 1900	Dec. 1900	l	b	Magnitude	Period (Days)	Spec-tral Type	References
248.	T UMa	109729	12h31m.8	60° 2'	92°	+58°	6.4- 13.5	257	M4e	77,149,384,445,447,451, 537,612,614,642,742,752
249.	RV Dra		12 33.2	66 7	91	+52	8.4- 14.2	207	M1e	273
250.	R Vir	109914	12 33.4	7 32	265	+69	6.2- 12.6	146	M4e	77,384,395,447,451,612, 614,642,684,740,752
251.	RS UMa	110064	12 34.4	59 2	91	+59	8.2- 14.8	260	M4e	451,612,614,709,742
252.	FI Hya	-25°9367	12 34.6	-26 8	269	+36	10.9- 15.0		M4e	262
253.*	V Crv		12 35.3	-17 6	268	+45	11 -<15	194	M2e	
254.	S UMa	110813	12 39.6	61 38	90	+56	7.1- 12.9	226	Se	77,99,150,195,381,384, 391,398,447,451,526,527, 586,612,614,642,742,752
255.	RU Vir	111166	12 42.2	4 42	271	+67	8.0- 14.2	437	Ce	426,476,612,614,716
256.	U CVn	111223	12 42.5	38 55	87	+79	9.9-<12.5	348	M7e	384,451,612,614,718,741
257.	U Vir	111691	12 46.0	6 6	274	+68	7.3- 14.0	207	M4e	355,384,445,447,451,612, 614,642,740,752
258.	V Cru	112319	12 50.6	-57 22	271	+ 5	10.4- 13.4	377	Ce	612,614,653,706,716
259.*	BZ Vir		12 55.4	-17 6	275	+45	9.5-<13	151	M5e	
260.	SW Hya	113344	12 57.9	-28 34	275	+33	9.7-<14	219	M2e	614,724
261.	RV Vir		13 2.7	-12 38	278	+49	10.0-<15.0	269	M5e	451
262.	U Oct	115486	13 12.3	-83 42	271	-22	8.9- 15.5	302	M4e	614,725
263.	VY Vir		13 13.3	- 4 9	285	+57	10.5- 14.7	279	M3ep	740
264.	TT Cen	-60°4608	13 13.3	-60 16	274	+ 1	11.5- 16.5	462	Me	712
265.	U Mus		13 18.3	-64 8	274	- 2	10.5-<14.0	356	M6e	614,696,711
266.	OS Cen		13 21.2	-58 50	275	+ 3	11.0- 15.4	433	M6e	696
267.	RR UMa		13 22.4	62 54	82	+54	8.6- 14.2	231	M4e	451,612,710,712
268.	V Vir	117045	13 22.6	- 2 39	290	+58	8.2- 14.6	250	M5e	384,451,609,612,614,752
269.*	R Hya	117287	13 24.3	-22 46	283	+38	3.5- 10.9	387	M7e	77,172,205,305,377,384, 398,414,424,445,451,493, 585,586,611,612,614,752, 851,901
270.	S Vir	117833	13 27.8	- 6 41	290	+53	6.0- 13.0	377	M7e	384,451,612,614,642,752
271.	T UMi	118556	13 32.6	73 56	85	+44	8.4- 14.7	316	M5e	451,612,614,710
272.	OW Cen		13 35.0	-61 50	276	- 1	12.0-<18	290	M4e	690
273.	T Cen	119090	13 36.0	-33 6	283	+27	5.2- 10.0	91	M0e	313,384,451,612,614,734, 759,765,766
274.	AN Cen		13 42.1	-37 38	283	+23	11.5-<14	333	Me	614,727
275.	RT CVn		13 44.3	34 11	28	+75	12.0-<14	254	M5e	451
276.	R CVn	120499	13 44.7	40 2	46	+72	6.1- 12.8	328	M6e	77,384,445,451,612,614, 648,741,752
277.	RX Cen	CPD -36° 6158	13 45.5	-36 27	284	+24	8.6-<15.0	327	M5e	451
278.	T Aps	-77°622	13 46.1	-77 18	274	-16	8.4- 14.8	261	M3e	614
279.	HY Cen		13 50.2	-56 26	280	+ 4	12.4-<16.0	311	Me	696
280.	TW Cen	121714	13 52.0	-30 34	288	+29	8.9-<12.6	269	M4e	612,614,718
281.	Z Boo	123304	14 1.6	13 58	328	+66	8.4- 15.0	281	M5e	451,612,614,703,708,741
282.	Z Vir	-12°3983	14 5.0	-12 50	300	+44	9.1- 15.0	307	M5e	451
283.	RU Hya	-28° 10490	14 5.8	-28 25	292	+30	7.6- 14.5	334	M6e	451
284.*	R Cen	124601	14 9.4	-59 27	281	+ 1	7.7- 12.0	559	M4e	451,609,612,614,765
285.	U UMi	125556	14 15.1	67 15	76	+48	7.6- 13.0	327	M6e	384,445,447,451,612,614, 657
286.	S Boo	126289	14 19.5	54 16	62	+58	7.2- 14.0	271	M4e	357,384,451,612,614

TABLE 1—Continued

Cat. No.	Name	Desig-nation	R.A. 1900 h m	Dec. 1900	l	b	Magnitude	Period (Days)	Spec-tral Type	References
287.	RS Vir	126753	14 22.3	5° 8'	321°	+57°	7.3- 14.3	352	M6e	352,384,451,612,614
288.	HV 11102		14 22.7	-62 40	281	- 3			Me	696
289.	R Cam	127226	14 25.1	84 17	87	+33	6.8- 14.4	270	Se	195,381,384,391,451,526, 612,614,642,742,752
290.	V Boo	127335	14 25.7	39 18	34	+65	6.4- 11.5	259	M6e	77,355,384,445,451,612, 614,741,752
291.	TU Cen	127773	14 28.1	-31 15	295	+25	10.6- 14.5	294	M4e	612,614,712
292.	R Boo	128609	14 32.8	27 10	5	+65	5.9- 13.1	223	M4e	77,384,451,537,612,614, 642,741,752
293.	V Lib	-17°4142	14 34.8	-17 14	305	+37	8.5- 15.0	256	M5e	451
294.	RR Boo		14 43.2	39 44	33	+62	8.0- 12.8	194	M3e	451,614,741
295.	RY Cen	130471	14 43.4	-42 6	293	+14	10.5- 16.4	328	M5e	612,614,707
296.*	S Lup	131169	14 46.7	-46 12	292	+10	10.7- 15	341	Se	313,612,614
297.	HV 11103		14 46.9	-33 18	298	+22			Me	696
298.	Y Lup	132125	14 52.3	-54 33	288	+ 3	8.1- 15.2	403	M7e	612,614,712
299.	AO Cen	-41°9373	14 54.3	-42 6	295	+13	10.6-<12.5	189	M2e	614,727
300.	AP Cen	-33°10231	14 55.0	-34 5	299	+20	10.4-<13.5	357	M5e	696
301.	HV 11104		14 55.2	-39 21	297	+16			M3e	696
302.*	RT Lib	133710	15 0.8	-18 21	310	+32	7.8-<14.0	252	M4pe	451,612,614
303.	TT Lib		15 3.4	-15 7	313	+35	10.9- 16	278	M3e	614,727
304.	T Lib	-19°4041	15 5.0	-19 38	310	+31	9.2- 15.5	237	M4e	451
305.	Y Lib	134739	15 6.4	- 5 38	322	+41	7.5- 14.2	274	M5e	384,451,612,614,649
306.	RT Boo		15 13.4	36 44	25	+57	10.8- 14.0	274	M8e	225
307.	S Lib	136458	15 15.6	-20 2	312	+29	7.7- 13.5	193	M2e	149,384,451,595,612,614, 646,752
308.	S Ser	136695	15 17.0	14 40	348	+51	7.6- 14.2	367	M5e	384,451,612,614,643,741, 752
309.*	RW Lib	136734	15 17.2	-23 43	310	+26	10.4-<14.0	203	M3e	195,381,391,451,526,595, 612,614,715
310.	S CrB	136753	15 17.3	31 44	16	+56	5.8- 13.9	361	M7e	77,384,451,537,612,614, 642,741,752
311.*	RS Lib	136986	15 18.5	-23 33	311	+26	6.5- 13.0	218	M7e	352,384,451,612,614
312.	WX Ser		15 23.3	19 55	357	+52	12 -<16	425	M8e	245,273
313.	WW Ser		15 27.4	3 59	337	+44	11.4-<15.8	369	M8e	245
314.	RU Lib	138547	15 27.7	-14 59	319	+31	7.2- 14.3	317	M5e	384,451,609,612,614
315.*	R Nor	138743	15 28.8	-49 10	296	+ 4	8.5- 14.0	488	M3e	612,614
316.	TU Lib	-23°12396	15 29.5	-23 37	313	+24	11.4- 14.5	287	M3e	614,727
317.	X Lib	-20°4275	15 30.4	-20 49	315	+26	9.4- 14.5	165	M3e	451
318.	S UMi	139492	15 33.4	78 58	81	+36	7.5- 13.0	324	M7e	451,609,612,614,710,742
319.	U Lib	-20°4305	15 36.2	-20 52	316	+25	8.9- 15.0	226	M3e	451,609,612
320.	T Nor	140041	15 36.3	-54 40	294	- 1	7.2- 13.1	243	M4e	451,612,614,708,765
321.*	BG Ser		15 38.4	- 1 24	333	+38	11.0- 15	143?	M6e	740
322.	RX Lup	·329889	15 39.4	-47 45	298	+ 4	10 -<14	237	M3e	614,727
323.	Z Lib		15 40.7	-20 49	317	+25	10.4-<14.0	299	M3e	690
324.	X CrB	141678	15 45.1	36 33	25	+50	8.0- 14.5	240	M6e	451,595,612,614,710,741
325.	V CrB	141826	15 45.9	39 52	30	+50	6.8- 12.4	358	$C6_3e$	7,163,179,237,362,426, 454,476,554,610,612,614, 752,800,848,860,901
326.	R Ser	141850	15 46.1	15 26	354	+45	5.6- 14.0	357	M7e	77,370,377,384,385,398, 428,447,451,490,535,537, 612,614,651,741,752
327.	R Lib	-15°4208	15 47.9	-15 56	322	+27	9.5- 15.1	242	M5e	451

TABLE 1—Continued

Cat. No.	Name	Desig-nation	R.A. 1900 h m	Dec. 1900	l	b	Magnitude	Period (Days)	Spec-tral Type	References
328.	RR Lib	142641	15 50.6	-18° 1'	321°	+25°	8.0- 14.8	277	M4e	384,451,609,612,614
329.	Z CrB	142927	15 52.1	29 32	14	+48	8.9- 15.5	250	M4e	451,612,614,712,741
330.*	BC Ser		15 55.9	2 28	340	+37	10 -<14	238	M3e	740
331.	RR Lup		15 58.6	-34 6	310	+12	11.0-<14.1	184	M3e	688
332.	RZ Sco	144018	15 58.6	-23 50	318	+19	8.0- 13.0	160	M4e	451,595,612,614,657
333.	Z Sco	144311	16 0.1	-21 28	320	+21	8.9- 13.8	355	M6e	451,614,725
334.	R Her	144622	16 1.7	18 38	0	+43	7.3- 15.8	322	M6e	384,451,612,614,643
335.	U Ser	144782	16 2.5	10 12	350	+39	7.6- 14.0	238	M3e	384,451,612,614,703,740
336.*	X Sco	-21°4283	16 2.6	-21 16	320	+21	9.6- 14.4	200	M2e	
337.*	VZ Aps		16 4.3	-73 47	283	-17	8.2- 17.5	377	M5e	326
338.	SS Nor	-59°6051	16 4.9	-59 31	293	- 7	12.2-<16	291	Me	673
339.	RU Her	145459	16 6.0	25 20	9	+44	6.9- 14.3	483	M7e	384,451,612,614,651,741
340.	RU Nor	145905	16 8.3	-44 32	304	+ 3	11.2-<13.5	393	M7e	614,725
341.	KR Sco		16 8.5	-32 8	313	+12	11.6- 14.4	357	M3e	687
342.	R Sco	-22°4140	16 11.7	-22 42	321	+18	9.5- 15.5	223	M3e	451
343.	S Sco	-22°4141	16 11.7	-22 39	321	+18	9.3- 14.8	177	M3e	451
344.	WCrB	146560	16 11.8	38 3	27	+45	7.6- 13.4	238	M4e	384,451,612,614,710
345.	W Oph	-7°4267	16 16.0	- 7 28	334	+27	9.2- 14.6	331	M6e	214,451
346.	WW Aps		16 19.0	-74 46	283	-19	9.0- 16.8	267	Me	326
347.	WW Sco		16 21.0	-31 5	316	+11	12 -<16	431	M6e	690
348.	V Oph	148182	16 21.2	-12 12	331	+23	6.9- 10.8	298	$C7_4e$	179,237,426,454,476,554, 612,614,646,752
349.	U Her	148206	16 21.4	19 7	3	+39	6.2- 13.3	406	M7e	77,384,428,451,537,612, 614,642,741,752
350.	T Oph	-15°4338	16 28.0	-15 55	329	+19	8.8-<14	365	M6e	451
351.	SS Her	+7°3199	16 28.0	7 4	350	+32	7.6- 13.2	107	M3e	451,614
352.	RU TrA	149221	16 28.1	-68 20	289	-15	9.8-<13	326	M4e	614,725
353.	X Ara	149234	16 28.3	-55 12	299	- 6	9.0- 14.5	176	M5e	612,614,715
354.	S Oph	-16°4307	16 28.5	-16 57	328	+19	8.2- 14.7	233	M5e	451
355.	Y Ara	149554	16 30.4	-59 36	296	-10	9.8-<13.0	241	M2e	612,614,715
356.*	W Her	149749	16 31.7	37 33	27	+41	7.3- 14.5	280	M3e	77,384,451,612,614,643, 752
357.	R Dra	149880	16 32.4	66 58	65	+38	6.3- 13.9	245	M5e	149,384,445,451,537,612, 614,642,742,752
358.	AS Her		16 34.3	14 16	359	+34	9.9- 15.3	268	M2e	614,674,741
359.	UV Her	151204	16 40.9	12 19	357	+32	8.3- 13.5	341	M6e	451,612,614,740
360.	TV Ara		16 41.6	-53 28	301	- 7	12 -<15	367	M3e	614,666
361.	RR Oph	151592	16 43.2	-19 17	328	+15	7.8-<14.8	294	M4e	451,609,612,614
362.	AE Sco		16 43.9	-28 17	321	+ 9	12.2- 16.4	174	M0e	696
363.	Z TrA	151896	16 45.1	-65 2	292	-14	9.8-<12.5	151	M3e	614,727
364.	Z Ara	152064	16 46.0	-56 6	300	- 9	10 - 13.5	289	M3e	612,614,715
365.	S Her	152276	16 47.3	15 7	1	+32	5.9- 13.6	307	M5e	77,384,451,612,614,643 741,752
366.	RS Sco	152476	16 48.4	-44 56	309	- 2	6.0- 12.7	320	M6e	447,451,612,614,765,855
367.	SZ Sco	152666	16 49.6	-39 28	313	+ 1	11.1-<13.0	321	M6e	614,715
368.	RR Sco	152783	16 50.3	-30 25	320	+ 6	5.0- 12.2	279	M6e	311,358,384,447,451,612, 614,765
369.	AI Her		16 51.1	49 7	42	+38	10.5-<14	405	M6e	273
370.*	SS Oph	153167	16 52.6	- 2 36	344	+22	8.0- 13.6	180	M2e	384,451,612,614,740
371.	RV Her	+31°2949a	16 56.7	31 22	20	+35	9.0- 15.5	205	M2e	451

TABLE 1—Continued

Cat. No.	Name	Desig-nation	R.A. 1900 h m	Dec. 1900	l	b	Magnitude	Period (Days)	Spec-tral Type	References
372.	RT Sco	153858	16 56.8	-36°47'	316°	+ 2°	7.3-<14.5	448	M6e	354,451,612,614
373.*	SY Her	+22°3048	16 57.3	22 37	10	+32	9.5- 14.0	117	M1e	273
374.	WZ Dra		16 57.6	52 29	46	+37	10.5- 15.5	400	M6e	325,451
375.*	UX Oph	-11°4288	16 59.4	-12 4	337	+16	9.4-<13.5	117	M4e	
376.	TU Sco	154566	17 1.1	-31 42	321	+ 4	10.0- 14	375	M6e	612,614,718
377.	R Oph	154721	17 2.0	-15 58	334	+13	6.2- 14.4	302	M5e	77,384,451,612,614,642, 752
378.	BG Her		17 5.1	18 48	7	+29	9.1-<12	345	M3e	273
379.	RT Her	155481	17 6.8	27 11	16	+32	8.5- 15.5	298	M5e	451,612,614,712
380.	RWSco	155734	17 8.3	-33 19	320	+ 2	9.1-<14.0	389	M5e	609,612,614
381.	Z Oph	156801	17 14.5	1 37	351	+20	7.5- 13.5	349	M2e	77,311,384,451,612,614, 740
382.	BL Sco	157288	17 17.2	-38 46	317	- 3	11.0- 17.0	396	M5e	614,725
383.	RS Her	157330	17 17.5	23 1	13	+28	7.2- 13.4	219	M5e	384,451,612,614,651,741
384.	SW Sco	157436	17 18.1	-43 44	313	- 6	10.8- 14	261	M4e	612,614,705
385.	RU Ara	CPD -60° 6831	17 20.0	-60 49	299	-15	10.2-<12	252	M5e	612,614,665
386.	RR Ara	157768	17 20.1	-49 49	308	- 9	10.7-<13.2	206	M3e	612,614,718
387.	VW Oph		17 22.5	4 19	355	+19	10.5- 14	283	M5e	245
388.	S Oct	158413	17 24.0	-86 46	273	-27	8.8- 15.4	259	M4e	352,612,614
389.	UZ Her		17 26.0	18 0	8	+24	9.3- 12	264	M5e	245,741
390.	RU Oph	+9° 3414	17 28.1	9 30	0	+20	8.6- 14.3	202	M3e	451
391.	SY Dra	159854	17 32.1	54 2	48	+32	11.5-<14	392	M7e	612,614,715
392.	FX Sco	324100	17 35.1	-39 12	318	- 6	12.0- 16.4	264	M1e	690
393.	RU Sco	160496	17 35.2	-43 42	315	- 8	7.8- 13.5	366	M7e	359,612,614,699
394.	RZ Ara	161416	17 40.3	-52 37	307	-14	11 -<14	300	M3e	614,725
395.	W Pav	161567	17 41.1	-62 22	298	-18	9.4- 16	283	M4e	612,614,703
396.	SV Sco	161652	17 41.6	-35 40	322	- 5	8.5- 13.5	256	M3e	612,614
397.	SY Pav		17 43.4	-57 50	303	-16	11.3-<14.3	194	M1e	687
398.	SU Her	162198	17 44.8	22 34	15	+22	10.5- 13.0	334	M6e	612,614
399.	V764 Sgr		17 45.5	-23 5	333	0	13.0-<17.0	267	Me	696
400.	U Ara	162398	17 45.7	-51 39	308	-14	9.2- 15.4	225	M3e	612,614,703
401.	GH Sco		17 45.8	-43 37	316	-10	10.5-<12.5	277	Me	680
402.	V407 Sco	320767	17 45.8	-35 2	323	- 6	12.8-<16.5	396	Me	696
403.*	SY Sco	320846	17 47.2	-34 23	324	- 6	10.5-<13.0	235	Me	696
404.	V Ara	162729	17 47.3	-48 17	312	-13	10.9-<14.0	377	M6e	612,614,705
405.	V438 Sco	324669	17 50.5	-37 28	321	- 8	11.5- 16.2	392	M3e	
406.	VV Sgr		17 51.1	-19 19	337	+ 1	10.5-<14	400	Me	696
407.	SV Oph		17 51.4	3 24	357	+12	9.4- 13	217	M2e	614
408.	KS Sco		17 51.6	-42 23	317	-10	11.4-<16.3	429	M2e	687
409.	RT Oph		17 51.9	11 11	4	+16	9.0- 15.5	427	M7e	245,451
410.	KM CrA		17 52.1	-39 29	320	- 9	12.0-<16.5	241	Me	696
411.	AF CrA	324785	17 54.7	-37 11	322	- 8	12.0-<16.5	467	M5e	696
412.*	T Dra	+58°1772a	17 54.9	58 14	54	+29	7.2- 13.9	423	(C8e)	185,314,426,476
413.	RY Her	164307	17 55.4	19 29	13	+19	8.2- 14.2	221	M4e	384,451,612,614,709,741
414.*	WY Her		17 55.9	23 36	17	+20	11 - 15.5	376	M5e	741
415.	V Dra	+54°1927a	17 56.3	54 53	50	+29	8.8- 15.4	278	M4e	451
416.	HV 11105		17 56.3	-41 54	318	-11			Me	696

TABLE 1—Continued

Cat. No.	Name	Desig-nation	R.A. 1900 h m	Dec. 1900	l	b	Magnitude	Period (Days)	Spec-tral Type	References
417.	TT Ara	164523	17 56.4	-47°14'	313°	-13°	11.0-<14	175	M6e	614,727
418.	MQ CrA	324876	17 56.6	-39 52	320	-10	13.5-<16.5	204	Me	696
419.	IY CrA		17 58.1	-43 34	317	-12	13.0-<15.7		Me	690
420.	RR CrA	165065	17 59.0	-38 15	322	-10	9.8-<14.0	280	M3e	612,614,718
421.	GR CrA	324932	18 1.9	-37 38	322	-10	12.7-<16.5	220	Me	696
422.	R Pav	165961	18 3.3	-63 38	298	-21	8.2- 15	230	M3e	355,612,614
423.	T Her	166382	18 5.3	31 0	25	+21	6.8- 14.2	165	M3e	77,149,384,445,451,537, 612,614,642,741,892
424.	W Dra	166407	18 5.5	65 57	63	+29	8.7- 15.0	262	M3e	451,612,614,657
425.	TV Her		18 11.0	31 47	26	+20	9.0- 15.0	304	M4e	451,614
426.	W Lyr	167740	18 11.5	36 38	31	+22	7.2- 13.1	196	M4e	77,149,384,451,595,612, 614,708,741,892
427.	RY Oph	167766	18 11.6	3 40	0	+ 8	7.2- 14.4	151	M5e	384,451,612,614,656
428.	TX Lyr		18 13.2	40 40	35	+23	10.4-<13	223	M2e	245
429.*	BC Oph		18 13.3	6 54	3	+ 9	10.0- 15.3	307	M7e	
430.	BR Sgr	319274	18 13.7	-32 15	328	- 9	11 -<15	303	M4e	614,663
431.	HI Lyr		18 13.7	46 25	41	+24	12.5-<14.5	185	M0e	245
432.	RY CrA		18 14.6	-44 57	317	-15	12.1-<14	195	M4e	614,727
433.*	TV Lyr		18 17.8	30 25	25	+18	10.0- 13.9	263	M4e	741
434.*	RU Dra		18 18.0	59 30	56	+27	9.4-<13.6	297	M5e	742
435.	RX CrA	169343	18 19.2	-44 20	318	-16	10.6-<15	286	M3e	614,725
436.	RY Tel	169409	18 19.3	-50 54	311	-18	11 -<15	239	M3e	614,725
437.	DG Her	348639	18 19.9	18 21	14	+13	11.1-<13.5	295	M5e	225,688
438.	RV Sgr	169831	18 21.3	-33 23	328	-11	7.2- 14.7	318	M5e	451,612,614,698,708
439.	AK Sgr	170034	18 22.3	-16 50	343	- 4	10.5-<14	420	M5e	612,614,700,720
440.	SV Her		18 22.3	24 58	21	+15	8.9- 15.0	239	M5e	451
441.	Z CrA	170334	18 23.8	-45 2	317	-17	11.0-<12.9	303	M6e	612,614,705
442.	T Ser	+6°3805a	18 23.9	6 14	4	+ 6	8.8- 15.5	342	M7e	451
443.	V910 Sgr	-34° 12893	18 25.4	-34 46	327	-13	10.6- 14.7	376	Me	688
444.	IM Sgr		18 25.9	-25 18	336	- 9	12.1-<17	283	Me	689
445.	BI Oph		18 26.3	6 56	5	+ 6	11.6- 15.9	204	M3e	614
446.	V911 Sgr	171059	18 27.5	-32 26	330	-12	12.5- 15		M4e	614,727
447.*	NGC 6656-14		18 30.6	-23 52	338	- 9	13.8-<15.5	200	M3.5e	539
448.	SV Dra		18 31.1	49 18	45	+22	8.0- 14.6	258	M6e	245,451
449.	BK Oph		18 31.2	7 36	6	+ 5	12.3- 16.8	376	M6e	614
450.	V444 Sgr		18 32.5	-33 53	329	-14	11.9- 16.2	210	Me	688
451.	RZ Her	172008	18 32.7	25 58	23	+13	8.8- 15.5	328	M5e	451,612,614,657
452.	V742 Sgr		18 32.9	-36 54	326	-15	11.5- 17		M1e	690
453.*	X Oph	172171	18 33.6	8 45	7	+ 5	5.9- 9.2	335	M6e	77,353,377,383,384,451, 612,614,740,752,901
454.	MO Sgr		18 34.0	-28 40	334	-12	12.5- 17.0	297	Me	696
455.	U CrA	172301	18 34.3	-37 56	325	-16	9.9- 14.3	148	M2e	612,614,619,699
456.	YY CrA		18 34.5	-37 8	326	-15	10.8- 16.0	126	Me	690
457.	AE Her	342906	18 39.0	22 54	20	+11	10.4- 15	247	M5e	384,451,614,729
458.*	RS Dra	+74°788	18 40.2	74 14	72	+27	8.3- 12.4	280	M5e	451,742
459.	RY Lyr		18 41.3	34 34	31	+15	9.1- 15.7	327	M6e	451,614
460.	BH Tel		18 42.0	-50 0	314	-21	11.8- 17	210	M0e	696
461.	RW Lyr	173798	18 42.1	43 32	40	+19	9.2- 15.6	504	M7e	612,614,708
462.	CN CrA		18 44.4	-41 22	322	-19	11.4-<14.5	214	M1e	687

TABLE 1—Continued

Cat. No.	Name	Designation	R.A. 1900 h m	Dec. 1900	l	b	Magnitude	Period (Days)	Spectral Type	References
463.*	ST Sct		18 45.9	-13° 3'	349°	- 7°	11.5-<15.0	219	M4e	
464.*	SV Sct		18 48.0	-14 19	348	- 8	12.0- 15.4	310	Se	560
465.	SV Tel	-49° 12412	18 48.6	-49 36	314	-22	10.2-<13.2	226	M4e	614,727
466.	OX Sgr		18 48.8	-25 40	338	-13	12.8-<15.6	348	M2e	678
467.	TU Dra		18 48.9	48 48	46	+19	10.0-<13.3	344	M4e	273
468.	RX Lyr		18 50.4	32 42	30	+13	10.8- 16.0	250	Me	754
469.	UX CrA		18 50.7	-37 56	326	-19	10.9-<17.0	348	Me	688
470.	BU Sgr	CPD -22° 7287	18 52.0	-22 42	341	-13	12 -<16	313	M3e	696
471.*	AK Aql		18 55.1	- 7 4	355	- 7	10.8-<17.0	297	M6e	
472.	ST Sgr	176592	18 55.9	-12 54	350	- 9	7.3-<15.0	395	Se	451,612,614,705
473.	Z Lyr	+34°3382a	18 56.0	34 49	33	+13	9.2- 15.0	288	M5e	451,741
474.	RT Lyr	+37°3309a	18 57.8	37 23	36	+13	9.3- 15.6	251	M5e	245,451,612
475.	VY Aql		18 58.0	- 7 18	356	- 7	11 -<16	334	M5e	225
476.*	WZ Lyr		18 59.4	47 4	45	+17	11 - 15	378	M9e	
477.	U Tel	177666	19 0.5	-49 4	316	-24	10.6-<13.0	445	M7e	612,614,705,718
478.	RU Tel	177692	19 0.6	-48 24	316	-24	10.1- 15	271	M4e	612,614,718
479.	AG Sgr	177868	19 1.3	-29 1	336	-17	10.0-<14.0	359	M5e	612,614,657
480.	R Aql	177940	19 1.5	8 5	10	- 1	6.2- 12.1	300	M7e	384,428,445,451,490,537, 612,614,643,740,752
481.	RZ CrA	177951	19 1.5	-42 31	322	-22	9.9-<13.5	460:	M6e	614,727
482.*	AB Lyr		19 3.3	33 34	32	+11	11 - 15	217	M4e	
483.	V Lyr	178876	19 5.2	29 30	29	+ 8	8.5- 15.7	374	M7e	451,612,614,651
484.	TY Lyr	337648	19 5.8	27 55	28	+ 8	9.0- 13	332	M8e	245
485.*	ST Lyr		19 6.7	43 27	42	+14	10.6-<14	300	M4e	597,742
486.	TW Sgr	179451	19 7.5	-21 44	343	-16	9.1-<13.5	221	M2e	612,614,717
487.	TX Sgr	179631	19 8.2	-17 36	347	-14	10 -<14	242	M3e	612,614,717
488.	RX Sgr	179769	19 8.7	-18 59	346	-15	9.0- 14.0	334	M5e	451,612,614,698
489.	RU Lyr	+41°3264a	19 9.1	41 8	40	+13	9.4- 15.5	370	M8e	451
490.	S Lyr	+25°3752a	19 9.1	25 50	26	+ 6	9.0- 15.5	441	Me	612,812
491.	RS Lyr	+33°3371a	19 9.3	33 15	33	+ 9	9.9- 15.5	301	M5e	451,612
492.	U Dra	180050	19 9.9	67 7	65	+23	9.0- 14.7	315	M6e	451,612,614,710,742
493.*	W Aql		19 10.0	- 7 13	357	-10	10.4- 17	489	Se	451,614,777
494.	SS Lyr	180162	19 10.4	46 49	45	+15	8.4- 13	349	M5e	597,612,614
495.	T Sgr	180196	19 10.5	-17 9	348	-15	7.0- 13.0	392	Se	195,381,384,391,451,586, 612,614,646,717
496.	R Sgr	180275	19 10.8	-19 29	346	-16	6.6- 13.3	269	M5e	384,451,609,612,614,752
497.	TY Sgr	180491	19 11.6	-24 7	342	-18	9.2-<15.0	325	M3e	612,614,715
498.	V1158 Sgr		19 13.3	-41 3	325	-24	11 - 14		M2e	690
499.	SW Sgr	180958	19 13.4	-31 54	334	-21	9.5-<14.5	290	M5e	612,614,707
500.	S Sgr	181005	19 13.6	-19 12	346	-16	9.1- 15.0	231	M4e	451,612,614
501.	Z Sgr	181060	19 13.8	-21 7	345	-17	8.1-<15	450	M5e	451,612,614,708,717
502.*	ER Aql		19 14.1	3 13	7	- 6	11.8- 16.3	338	Me	
503.	HN Lyr		19 14.2	42 38	42	+13	10.5-<14	406	M4e	273,633
504.	CY Aql		19 14.3	0 20	4	- 7	11.0-<15	351	M8e	245
505.	W Sge	181332	19 15.1	17 1	19	0	8.8- 13.2	279	M4e	451,612,614,710,741
506.	ER Lyr		19 16.5	40 4	40	+11	12 - 15.5	190	M5e	245
507.*	U Lyr	+37°3418a	19 16.6	37 41	37	+10	7.9- 12.4	456	Ce	185,191,426,476,814
508.	HO Lyr		19 16.9	41 30	41	+12	11.4- 14.0	100	M2e	225

TABLE 1—Continued

Cat. No.	Name	Designation	R.A. 1900 h m	Dec. 1900	l	b	Magnitude	Period (Days)	Spectral Type	References
509.	UU Sgr		19 17.8	-39°27'	327°	-24°	10.5-<14	268	Me	612
510.	TT Sgr	182480	19 19.7	-20 18	346	-18	10.5- 16.1	332	M4e	612,614,715,717
511.	SW Tel	182610	19 20.4	-46 4	320	-27	11.0- 14	230	M4e	614,727
512.	AN Sgr	182794	19 21.2	-18 43	348	-17	9.7- 15.0	338	M5e	612,614,720
513.	ET Sgr		19 21.4	-15 2	351	-16	12.8-<15	221	Me	696
514.	HV 11107		19 23.4	-50 36	315	-28			M0e	696
515.	YZ Dra		19 24.9	71 29	70	+23	11 -<15.5	348	M8e	245
516.	DD Cyg	+34°3588	19 27.8	34 30	36	+ 7	10.5-<13	148	M0e	682
517.*	TY Cyg	184524	19 29.8	28 7	30	+ 3	8.5- 15	350	M6e	612,614
518.	BM Sgr	184989	19 31.9	-36 36	331	-26	10.5-<13	403	M3e	614,725
519.	EZ Sgr		19 32.2	-14 22	353	-18	12.0- 16	249	Me	696
520.	Z Tel	185111	19 32.4	-45 48	321	-28	10.4-<13.2	230	M4e	612,614
521.	RT Aql	185293	19 33.3	11 30	16	- 6	6.7- 14.4	326	M7e	77,384,451,612,614,651, 740
522.	R Cyg	185456	19 34.1	49 58	50	+13	5.9- 14.6	426	Se	77,98,99,132,150,195, 381,384,391,392,398,428, 451,526,586,610,612,614, 643,710,742,752,788,826, 827
523.	BO Sgr	185558	19 34.5	-44 50	322	-29	12.5-<15.0	290	M5e	614,727
524.	RV Aql	185821	19 35.9	9 42	15	- 8	8.1- 15.0	219	M3e	451,609,612,614,740
525.	V984 Sgr		19 37.0	-21 38	346	-22	11 -<15	1030/n	M0e	690
526.	TV Sgr	186087	19 37.3	-42 5	325	-28	10.0-<13.5	266	M6e	612,614
527.	T Pav	186484	19 39.5	-72 1	290	-31	8.8- 15	244	M4e	447,451,612,614,698,765
528.*	V369 Cyg		19 39.6	54 26	55	+14	9.8- 14.1	104	M4e	
529.	V1167 Sgr		19 39.6	-26 50	341	-24	11.5- 14.8		M0e	696
530.*	YZ Vul		19 40.0	27 32	31	+ 1	10.7- 17.3	376	M5e	741
531.*	ZZ Dra		19 40.5	67 32	67	+20	11 -<15.5	275	M7e	
532.	RT Cyg	186686	19 40.8	48 32	49	+11	6.2- 13.0	190	M2e	14,77,149,234,384,451, 595,612,614,742,752,854
533.	W Tel	187113	19 43.0	-50 16	316	-31	9.6-<12.6	304	M5e	612,614,705
534.	TU Cyg	187159	19 43.3	48 50	50	+11	8.1- 14.8	219	M4e	451,612,614,710,742
535.*	XY Cyg		19 45.3	41 23	43	+ 7	11 -<15	298	Se	
536.	X Aql	187757	19 46.5	4 13	12	-13	8.2- 15.0	348	M6e	311,451,612,614
537.	χ Cyg	187796	19 46.7	32 40	36	+ 2	2.3- 14.3	407	Se	68,77,111,164,167,195, 302,318,364,377,384,398, 424,428,445,451,515,526, 535,536,537,570,586,612, 614,642,752,851,901
538.*	V553 Aql		19 46.9	2 33	10	-13	10.9-<16	213	M3e	
539.*	NT Cyg		19 47.6	38 45	41	+ 5	14.0-<16.0	390	M7e	
540.*	NW Cyg		19 48.5	38 39	41	+ 5	14.1-<16.5	338	M6e	
541.	RZ Aql		19 49.1	9 24	17	-10	12.1-<14.5	337	M5e	614
542.*	BS Cyg		19 49.3	53 26	54	+13	11.0-<16	431	Ce	273,560
543.	RR Sgr	188378	19 49.7	-29 27	339	-27	5.5- 14.0	335	M5e	352,451,612,614
544.*	CU Cyg		19 50.1	55 4	56	+13	9.5- 14.1	215	M6e	
545.*	PP Cyg		19 51.8	39 11	42	+ 5	13.2-<16.0	296	M7e	
546.	RU Sgr	188813	19 51.8	-42 7	326	-31	6.3- 14.0	241	M4e	307,451,612,614
547.	RR Aql	188915	19 52.4	- 2 9	7	-17	8.4- 14.0	394	M6e	315,451,612,614,709
548.*	PX Cyg		19 53.1	37 22	41	+ 4	14.0-<17.0	309	M5e	329,537
549.	RS Aql	189191	19 53.7	- 8 9	1	-20	8.6-<15.0	413	M7e	245,451,609,612,614
550.*	CM Cyg		19 55.9	51 49	53	+11	10.5-<14.7	253	Se	742

TABLE 1—Continued

Cat. No.	Name	Designation	R.A. 1900 h m	Dec. 1900	l	b	Magnitude	Period (Days)	Spectral Type	References
551.*	V338 Cyg		19 56.5	38°42'	42°	+ 4°	13.1-<16.3	321	M5e	329
552.*	V341 Cyg		19 57.4	38 38	42	+ 4	14.0-<16.5	351	M6e	329
553.	RR Pav	189993	19 57.7	-63 42	300	-33	11.0-<14	240	M4e	612,614,718
554.	Z Cyg	190163	19 58.6	49 46	52	+10	7.0- 14.7	264	M5e	149,384,451,595,609,612, 614,710,742,752,892
555.	SY Aql	190970	20 2.4	12 40	21	-12	8.5- 15.5	356	M5e	451,612,614,710,740
556.	S Cyg	+57°2134	20 3.4	57 42	59	+13	8.8- 16.8	323	Se	195,384,391,451
557.*	R Cap	-14°5663	20 5.7	-14 34	356	-25	8.7- 14.0	346	Ce	103
558.	R Tel	192016	20 7.6	-47 16	320	-35	8.4- 16	461	M5e	359,612,614
559.	TV Aql	192082	20 7.9	6 0	16	-16	9.2-<14	240	M4e	614
560.	RU Aql	192081	20 8.0	12 42	22	-13	7.9- 14.5	274	M5e	451,612,614,740
561.	W Cap	-22°5373	20 8.6	-22 17	349	-29	10.2-<14	208	M5e	451
562.	SU Pav		20 9.3	-60 22	304	-35	9.6-<14	245	M4e	614,668
563.	WZ Aql	192407	20 9.7	4 29	15	-17	9.3-<12.5	319	M5e	614,726,740
564.	Z Aql	-6°5419	20 9.8	- 6 27	5	-23	8.5- 14.2	129	M3e	384,451,612
565.	R Del	192502	20 10.1	8 47	19	-15	7.1- 13.9	285	M5e	384,451,612,614,646,740
566.	RT Sgr	192702	20 11.1	-39 25	329	-34	7.2- 15	306	M6e	451,612,614,855
567.	X Tel	192725	20 11.2	-52 55	313	-36	10.4- 14.0	310	M5e	612,614,705
568.	SX Cyg	192788	20 11.5	30 46	38	- 3	8.0- 15.2	412	M7e	451,612,614,655,741
569.	SZ Cep	193028	20 12.9	76 53	77	+22	11.1-<15	327	Se	614,725,742
570.	BQ Tel		20 13.2	-56 31	309	-36	10.0-<14.5	290	M5e	696
571.	AU Cyg	193345	20 14.7	34 5	41	- 2	10.0- 15.3	436	M6e	612,614,710,741
572.	WX Cyg	193368	20 14.8	37 8	43	0	8.6- 13.5	408	(C8e)	163,179,362,426,476,553, 610,612,614,752
573.*	CN Cyg		20 15.9	59 29	62	+13	7.3- 14.0	198	M5e	
574.	U Cyg	193680	20 16.5	47 35	52	+ 6	6.1- 12.2	462	$C7_2e$	50,163,179,197,210,222, 237,265,292,426,454,476, 553,554,587,612,614,643, 658,752,761,763,767,892
575.	U Mic	194814	20 22.6	-40 45	328	-37	9.1- 15	333	M6e	612,614,703
576.	KZ Cyg		20 23.8	40 45	47	+ 1	11.6-<15.5	392	M8e	225
577.*	RU Cap	-22°14788	20 26.7	-22 2	351	-33	9.1- 15.0	347	Me	612
578.	HV 11108		20 27.3	-24 1	348	-34			M5e	696
579.	Z Del	195763	20 28.1	17 7	29	-14	8.2- 15.5	304	Se	195,391,451,586,612,614, 741
580.	ST Cyg	196070	20 29.9	54 37	59	+ 8	8.8- 14.3	334	M6e	451,612,614
581.	BD Vul		20 33.0	26 8	37	-10	9.3- 12.7	430	Ce	476
582.	R Mic	196717	20 34.0	-29 9	343	-37	9.8- 15	139	M4e	313,451,612,614
583.*	TX Cap		20 34.9	-17 25	357	-33	10.9-<14.5	130	M4e	
584.	FF Cyg		20 35.1	37 32	46	- 3	8.3- 14.2	324	M4e	688,741
585.	Y Del		20 36.9	11 31	25	-19	8.7- 16	466	M8e	225
586.	V Cyg	+47°3167a	20 38.1	47 47	54	+ 3	6.8- 13.8	420	$C7_4e$	185,191,362,426,476,752, 848
587.*	S Del	197420	20 38.5	16 44	30	-16	8.2- 12.7	277	M6e	451,612,614,709,741,752
588.	DR Cyg		20 39.9	37 48	47	- 4	9.3-<15.5	314	M3e	688
589.	T Del	197772	20 40.7	16 2	30	-17	8.2- 15.3	332	M4e	451,612,614,649
590.	W Aqr		20 41.2	- 4 27	11	-29	7.0- 15.0	380	M7e	245,451,612,614,740,857
591.	BR Del		20 41.6	4 1	19	-24	10 -<12.5	670	M8e	225
592.	V Del	198136	20 43.2	18 58	32	-16	8.1- 17.3	536	M6e	451,614,857
593.	T Aqr	198373	20 44.7	- 5 31	10	-30	8.4- 16	202	M3e	384,445,451,537,612,614, 644,752

TABLE 1—Continued

Cat. No.	Name	Designation	R.A. 1900 h m	Dec. 1900	l	b	Magnitude	Period (Days)	Spectral Type	References
594.	U Pav	198735	20 47.2	-63° 5'	300°	-39°	8.6-<12	290	M4e	612,614,698
595.*	RX Vul		20 48.6	23 0	36	-14	11 - 15	457	M9e	
596.	S Ind	199003	20 49.0	-54 42	310	-41	7.4-<14.0	401	M6e	359,612,614
597.	X Del	199170	20 50.3	17 16	32	-18	8.0- 14.8	280	M4e	384,451,609,612,614,741
598.	UX Cyg	199252	20 50.9	30 2	42	-10	7.2- 14.5	560	M6e	451,612,614,708,741
599.*	AT Cyg		20 53.1	32 50	44	- 9	11 -<15	263	M5e	
600.	VW Aqr		20 55.7	- 1 55	16	-31	10.0-<13.6	417	Me	688
601.	RR Cap	200128	20 56.4	-27 29	347	-41	9.2- 16	278	M5e	451,612,614
602.	T Oct	200286	20 57.5	-82 30	277	-32	8.4- 13.6	218	M2e	359,612,614
603.	V523 Cyg		20 58.0	34 55	47	- 8	11.8-<15	372	M7e	741,750
604.	DI Cyg		20 58.3	30 32	44	-11	11.8-<15.5	352	M2e	245
605.	X Mic	200460	20 58.4	-33 40	339	-43	9.8-<14.3	240	M4e	612,614,720
606.	R Vul	200687	20 59.9	23 26	38	-16	7.0- 13.6	137	M4e	77,384,451,612,614,646, 752
607.	GQ Cyg		21 0.1	33 19	46	-10	11.1-<15	332	M5e	225
608.	RV Aqr		21 0.7	- 0 37	18	-31	8.7-<13.6	454	Ce	214,476
609.	TW Cyg	+28°3986a	21 1.7	29 0	43	-13	8.8- 14.8	341	M10e	245
610.	V Cap	201015	21 1.8	-24 19	351	-41	8.6- 14.4	275	M5e	451,609,612,614
611.	X Cep	201305	21 3.7	82 40	84	+24	8.7- 17.2	534	M5e	451,610,612,614
612.	TZ Peg	201417	21 4.3	15 38	33	-22	10.1-<14.0	214	M3e	612,614,720
613.	Z Cap	358906	21 5.0	-16 35	1	-39	8.7- 15.0	181	M3e	451,614,665
614.	WX Vul		21 5.1	26 16	42	-15	11 -<14	281	M5e	245
615.*	X UMi		21 5.5	87 54	88	+27	12.5- 18.4	343	Me	
616.	RS Aqr	-4°5381	21 5.7	- 4 26	15	-34	9.1- 14.5	215	Me	688
617.	T Cep	202012	21 8.2	68 5	72	+14	5.2- 11.2	388	M7e	77,337,384,385,398,451, 591,612,614,642,742,752
618.	R Equ	202051	21 8.4	12 23	31	-25	8.5- 15.0	261	M3e	384,451,612,614,710,740
619.	AS Peg		21 8.4	18 32	36	-21	11.0- 15	330	M2e	245,741
620.	RR Aqr	202306	21 9.8	- 3 19	16	-34	8.6- 14.8	182	M2e	149,384,451,612,614,710
621.	X Peg	+13°4676a	21 16.3	14 2	34	-25	8.8- 14.8	201	M4e	245,451,609,612,614
622.	T Cap	203349	21 16.5	-15 35	4	-42	10.2- 15.7	269	M3e	451,612,614,648
623.	W Mic	203370	21 16.6	-42 24	327	-47	10.3-<13.5	199	M4e	612,614,718
624.	V Mic	203495	21 17.5	-41 8	329	-47	9.4-<13.5	382	M6e	612,614,707
625.	SW Peg		21 17.9	21 34	40	-20	8.0- 14	396	M4e	688
626.	RW Aqr	+0°4716	21 18.0	0 25	22	-34	8.7- 13.6	140	M2e	614,740
627.	S Mic	204045	21 20.8	-30 17	344	-47	9.9- 16	212	M3e	451,609,612,614
628.	TV Peg		21 22.1	16 9	36	-25	9 -<14	247	M0e	688
629.	X Ind	204438	21 23.5	-54 24	309	-46	9.0-<13	227	M4e	612,614,718
630.	AP Peg		21 24.5	17 44	38	-24	10.5-<14	320	M5e	245,741
631.*	GS Cyg		21 25.4	30 7	48	-16	12 -<16	390	M6e	245,741
632.	UU Peg		21 26.2	10 43	33	-29	11.1-<14	456	M7e	614,740
633.	S Cep	206362	21 36.5	78 10	81	+19	7.1- 13.2	485	$C7_4e$	11,61,179,362,426,454, 476,614,752,848
634.	Y Ind	206458	21 37.1	-53 11	310	-48	9.8-<13	304	M6e	612,614,718
635.	RR Peg	206890	21 40.0	24 33	46	-22	8.5- 14.3	264	M5e	451,612,614,708
636.	TU Peg	+12°4678	21 40.2	12 14	37	-31	8.2- 13.8	322	Me	688
637.	BN Cyg		21 41.0	46 1	61	- 6	11.9- 17.5	174	M4e	333,742
638.	R Gru	207192	21 42.1	-47 23	318	-51	8.7- 16.9	332	M5e	359,612,614
639.*	WY Cyg		21 44.8	43 47	60	- 8	7.6- 14.9	304	M6e	333
640.	RW Ind		21 50.3	-69 41	288	-42	9.6-<13.4	150±	M2e	696

TABLE 1—Continued

Cat. No.	Name	Desig-nation	R.A. 1900 h m	Dec. 1900	l	b	Magnitude	Period (Days)	Spec-tral Type	References
641.	V Peg	209127	21 56.0	5°38'	34°	-38°	7.8- 14.8	303	M5e	451,609,612,614
642.	S PsA	209400	21 58.0	-28 32	349	-54	9.4-<13.0	273	M3e	609,612,614
643.*	RT Peg	209641	21 59.8	34 38	56	-17	9.4- 14.4	215	M4e	451,612,614,712,741
644.*	RZ Peg	209890	22 1.5	33 1	56	-18	8.0- 13.6	440	(C9e)	426,476,612,614,710
645.	T Peg	210251	22 4.0	12 3	41	-35	8.4- 15.0	374	M6e	384,451,612,614,710,740
646.	Y Peg	210662	22 6.8	13 52	43	-34	9.7- 15.5	207	M3e	451,612,614
647.	RS Peg	210749	22 7.4	14 4	44	-34	8.8- 14.5	413	M6e	384,451,612,614,710,741
648.	DH Lac		22 8.1	38 56	60	-14	11.2- 15	286	M5e	245
649.	R PsA	211493	22 12.3	-30 6	347	-58	9.2- 14.7	293	M3e	355,612,614
650.	X Aqr	211610	22 13.1	-21 24	3	-56	9.7- 15.9	311	M4e	359,451,612,614
651.	SS Aqr	-15°6193	22 14.5	-14 54	14	-54	8.6- 13.2	208	M2e	614
652.	UU Tuc		22 15.5	-61 23	295	-49	10.4- 13.6	335	M4e	696
653.	RT Aqr	212243	22 17.7	-22 34	1	-57	8.8- 13.1	245	M6e	384,451,612,614,705
654.	T Gru	212537	22 19.8	-38 4	332	-59	9.3- 13.0	137	M0e	451,612,614,698
655.	S Gru	212539	22 19.9	-48 56	312	-56	7.3- 15.8	401	M5e	451,612,614,698,765
656.	RV Peg	212678	22 21.0	29 58	58	-23	9.0- 14.5	387	M6e	319,451,612,614
657.	S Lac	213191	22 24.6	39 48	64	-15	7.3- 13.9	240	M5e	351,384,451,612,614,741
658.	R Ind	213797	22 28.9	-67 48	287	-46	8.0- 14.8	216	M2e	612,614
659.	SS Peg	213837	22 29.2	24 3	56	-29	8.0-<13.0	417	M7e	451,612,614,741
660.	T Tuc	214575	22 34.0	-62 4	292	-50	9.3- 15.5	250	M2e	612,614
661.*	R Lac	215254	22 38.8	41 51	67	-15	7.8- 15.4	300	M5e	384,451,612,614,649
662.*	SX Peg		22 45.5	17 22	55	-37	8.4- 13.4	306	Se	103,741
663.	S Aqr	216907	22 51.8	-20 53	10	-64	9.3- 15.6	279	M4e	384,451,612,614,645
664.	RW Peg	217949	22 59.2	14 46	57	-41	8.9- 15.0	209	M3e	451,612,614
665.	R Peg	218292	23 1.6	10 0	54	-45	6.9- 13.5	378	M7e	451,612,614,648,740,752, 892
666.	V Cas	218997	23 7.4	59 9	78	- 1	6.7- 13.4	229	M6e	317,384,451,537,612,614, 648,742
667.	UX Aqr		23 8.2	-15 52	25	<66	10.8-<15.7	320	M4e	688
668.	W Peg	219946	23 14.9	25 44	67	-33	7.3- 14.0	343	M7e	77,316,384,451,612,614, 651,741
669.	S Peg	220033	23 15.5	8 22	58	-48	7.2- 13.8	319	M6e	77,384,451,612,614,644, 752,892
670.*	RY Cep	+78°830	23 18.0	78 25	86	+17	9.4- 13.6	149	M0e	742
671.	RU Phe	-48°14512	23 22.7	-48 0	302	-65	10.8-<12.9	289	M1e	690
672.	V Phe	221433	23 27.0	-46 32	303	-67	8.9- 14.2	257	M4e	612,614,657
673.	LS Cas		23 33.2	55 30	81	- 5	14.5-<16		Ce	560
674.	Z Cas	222914	23 39.7	56 2	82	- 5	8.5- 15.4	495	M7e	451,612,614,710,742
675.	DU Peg		23 46.7	29 12	76	-31	12 -<15	161	M5e	245
676.	RR Cas	+52°3559a	23 50.8	53 10	83	- 8	9.5- 14.5	300	M5e	451,742
677.	R Phe	224269	23 51.3	-50 21	289	-66	9.2- 15	267	M3e	357,451,612,614,765
678.	R Tuc	224379	23 52.2	-65 56	278	-51	8.7- 15.2	286	M5e	352,612,614
679.	V Cet	224442	23 52.8	- 9 31	57	-68	8.6- 14.7	260	M3e	384,451,612,614
680.	R Cas	224490	23 53.3	50 50	83	-10	4.8- 13.6	431	M7e	77,384,398,428,445,451, 490,537,612,614,642,742, 752
681.	Z Peg	224709	23 55.0	25 20	77	-36	7.9- 13.5	324	M7e	451,612,614,656,705,741
682.	W Cet	224960	23 57.0	-15 14	50	-74	9.2- 16	352	Se	451,612,614,708,777
683.	IW Cas		23 57.6	48 10	83	-13	11.5-<14.7	384	Se	220
684.	Y Cas	225082	23 58.2	55 7	84	- 6	8.7- 14.8	415	M7e	451,612,614,703
685.	SV And	225192	23 59.2	39 33	82	-22	7.7- 14.0	316	M7e	384,451,595,612,614,741

NOTES TO TABLE 1

7. AP Cep. Emission at H γ and H δ was found by Schwassmann, Bergedorfer Spektral-Durchmusterung, 1, 21, 1935.

42. U Psc. Strong H α emission is present on a Yerkes spectrogram taken on September 17, 1950, m_v = 11.2.

44. RZ Per. Mount Wilson spectrograms show no TiO bands and only very weak ZrO bands. Ba II λ 4554 is strong.

60. o Cet. This star is the primary of ADS 1778, a physical pair. The faint companion is an extraordinary emission object of early type.

89. EV Tau. The spectral type, due to Vyssotsky, is quoted in the Fourth Supplement to the General Catalogue of Variable Stars.

101. V Tau. On the Mount Wilson spectrogram taken on December 15, 1929, H β emission is exceptionally strong, and the type is M0e.

108. R Aur. The Sr II lines are very strong on the Mount Wilson spectrogram taken on September 19, 1935.

135. AL Aur. Emission H δ was found by Schwassmann, Bergedorfer Spektral-Durchmusterung, 3, 102, 1947.

148. V CMi. On the Mount Wilson spectrogram taken on October 25, 1937, the Sr II lines are very strong.

152. R Vol. This object is assumed to be a carbon star because of its very large color index (over 6 mag.), determined by S. Gaposchkin, Harvard Ann., 115, 106, 1947.

170. VX CMi. The spectral type is taken from the General Catalogue of Variable Stars.

173. BC Mon. Weak H α emission is present on a Yerkes spectrogram taken on December 24, 1951, m_v = 9.5.

179. RT Lyn. The spectral type is from a McDonald spectrogram taken on April 9, 1951, m_v = 9.5.

182. V Cnc. This star is the primary of ADS 6763. The faint, 10" distant companion may be optical.

191. TU Hya. The spectral type is from a Yerkes spectrogram taken on February 28, 1951, m_v = 10.5. Weak H α emission is present.

194. WX Hya. The spectral type is from a McDonald spectrogram taken on April 9, 1951, m_v = 9.5. Ca I λ 4227 is very narrow, H β emission moderately strong.

200. R Car. Finsen has found a twelfth-magnitude companion at a distance of 2", Union Obs. Circ., 3, 99, 1929.

218. CZ Hya. Very strong H α emission is present on a spectrogram taken at Yerkes on December 27, 1952, m_v = 9.8.

230. Y Crt. On spectrograms taken and measured by Joy at Mount Wilson the spectral type varies from M3e to M5e; the radial velocity is +220 km/sec.

243. T CVn. The spectral type is from a McDonald spectrogram taken on April 2, 1951, m_v = 9.5.

246. Y Vir. The type M2e is assigned to this star by both the McCormick and the Dearborn observers, though Merrill's catalogue gives M(5)e.

253. V Crv. Strong H α emission is present on a Yerkes spectrogram taken on February 17, 1953, m_v = 10.3.

259. BZ Vir. The spectral type is from a McDonald spectrogram taken on April 2, 1951, m_v = 10.5.

269. R Hya. This star is the primary of ADS 8920, which appears to be a common proper-motion pair.

284. R Cen. This star has an abnormal light-curve, each cycle containing two minima. It fits the period-spectrum relation only if the half-period, rather than the whole period, is used. A twelfth-magnitude star is 28" distant.

296. S Lup. The star X Lupi is 13" distant.

302. RT Lib. The extraordinary strength of absorption bands of AlO in the spectrum of this star at one maximum, as reported by Merrill, marks it as a most peculiar object. It should be further observed.

309. RW Lib. Though previously considered an S-type star, this object does not appear to belong to that class.

311. RS Lib. In view of the relatively short period of this star, the spectral type, as observed at Harvard and at Mount Wilson, seems rather late.

315. R Nor. Light-curve similar to that of R Centauri. See note concerning that star, No. 284. Rossiter has found a faint companion, 6" distant, Mem. R.A.S., 65, 27, 1933.

321. BG Ser. A Yerkes spectrogram taken on April 14, 1953, m_V = 9.5, shows emission H δ much stronger than H γ, and also shows postmaximum emissions of Fe I and Mg I. The type on this plate is about M8e. Presumably the elements of the light-curve are in error.

330. BC Ser. On a McDonald spectrogram taken on April 5, 1951, m_V = 10.0, the spectral type is M5e.

336. X Sco. The spectral type is from a McDonald spectrogram taken on April 15, 1951, m_V = 10.6.

337. VZ Aps. The type M5e is given by F. Becker in Potsdam Pub., Vol. 27, Part 1, 1931.

356. W Her. This star is the primary of ADS 10121. The faint, 6" distant companion may be optical.

370. SS Oph. The type given is that determined at Harvard, rather than the somewhat later type given in Merrill's catalogue.

373. SY Her. The spectral type is from a Yerkes spectrogram taken on June 14, 1950, m_V = 8.5.

375. UX Oph. Weak H α emission is present on a Yerkes spectrogram taken on May 19, 1950, m_V = 9.8.

403. SY Sco. The spectral type is confirmed by one Mount Wilson spectrogram.

412. T Dra. The 14" distant companion has been shown by Sanford to be optical, Pub. A.S.P., 53, 291, 1941.

414. WY Her. On a McDonald spectrogram taken on April 8, 1951, m_V = 10.2, the spectral type is M7e.

429. BC Oph. The spectral type is from a McDonald spectrogram taken on August 3, 1953, m_V = 10.8.

433. TV Lyr. The spectral type is from a McDonald spectrogram taken on April 13, 1951, m_V = 10.5.

434. RU Dra. The type M5e is from a McDonald spectrogram taken on September 20, 1951, m_V = 9.4. Ca I λ 4227 is narrow, and emission H β is fairly strong. The considerably earlier Dearborn classification may not refer to the same star.

447. NGC 6656-14. This star is not a cluster member.

453. X Oph. This star is the primary of ADS 11524, a physical pair.

458. RS Dra. On the Mount Wilson spectrograms, taken on October 5, 1939, the emission lines are weak. This fact is perhaps related to the peculiarities of the light-curve of this star.

463. ST Sct. Moderately strong H α emission is present on a Yerkes spectrogram taken on June 12, 1950, m_V = 10.5.

464. SV Sct. Mount Wilson spectrograms show bright H α and H β and very little, if any, absorption due to TiO. On a McDonald spectrogram taken on August 9, 1953, m_V = 12.0, the Sr I resonance line, λ 4607, is very intense, and all oxide bands are very weak.

471. AK Aql. The spectral type is from a McDonald spectrogram taken on September 21, 1951, m_V = 10.0.

476. WZ Lyr. The spectral type is from a McDonald spectrogram taken on April 13, 1951, m_V = 11.5.

482. AB Lyr. Moderately strong Hα emission is present on a Yerkes spectrogram taken on March 25, 1950, m_v = 10.0.

485. ST Lyr. The spectral type is from a McDonald spectrogram taken on September 20, 1951, m_v = 9.9.

493. W Aql. Mount Wilson spectrograms show that the TiO bands are very weak in the spectrum of this object.

502. ER Aql. The spectral type is taken from the General Catalogue of Variable Stars.

507. U Lyr. A faint companion, distant 9", has been measured by Espin and Milburn, M.N. 92, 216, 1932.

517. TY Cyg. The spectral type is from a McDonald spectrogram taken on September 26, 1951, m_v = 9.4.

528. V369 Cyg. Moderately strong Hα emission is present on a Yerkes spectrogram taken on April 20, 1950, m_v = 9.5.

530. YZ Vul. The spectral type is from a McDonald spectrogram taken on September 26, 1951, m_v = 10.5.

531. ZZ Dra. Weak Hα emission is present on a Yerkes spectrogram taken on June 1, 1950, m_v = 9.7.

535. XY Cyg. A Mount Wilson spectrogram taken on July 8, 1941, by Sanford and measured by him shows bright Hα, Hβ, and Hγ; the velocity given by Hα is -20 km/sec. TiO absorption is very weak or absent, but weak ZrO bands are probably present. The spectral type is uncertain.

538. V553 Aql. The spectral type is from a McDonald spectrogram taken on August 9, 1953, m_v = 11.3.

539. NT Cyg. The spectral type, due to Merrill, is from a Mount Wilson spectrogram taken by Humason.

540. NW Cyg. The spectral type, due to Merrill, is from a Mount Wilson spectrogram taken by Humason.

542. BS Cyg. Mount Wilson spectrograms show that the C_2 bands are weak and that Ba II λ4554 is strong in the spectrum of this star.

544. CU Cyg. The spectral type is from a McDonald spectrogram taken on September 20, 1951, m_v = 10.2.

545. PP Cyg. The spectral type, due to Merrill, is from a Mount Wilson spectrogram taken by Humason.

548. PX Cyg. The spectral type, due to Merrill, is from Mount Wilson spectrograms taken by Humason and Joy.

550. CM Cyg. A McDonald spectrogram taken on August 13, 1953, m_v = 12.0, shows bright Hβ and Hγ; ZrO bands are present, as is Sr I λ4607. TiO bands appear to be absent.

551. V338 Cyg. The spectral type, due to Merrill, is from Mount Wilson spectrograms taken by Humason.

552. V341 Cyg. The spectral type, due to Merrill, is from a Mount Wilson spectrogram taken by Humason.

557. R Cap. Very strong Hα emission is present on a Yerkes spectrogram taken on July 14, 1950, m_v = 10.1.

573. CN Cyg. The spectral type is from Yerkes spectrograms taken on March 17, 1953, m_v = 8.5, and April 14, 1953, m_v = 8.7.

577. RU Cap. This star is the primary of ADS 13958, d = 1".5.

583. TX Cap. Strong Hα emission is present on a Yerkes spectrogram taken on October 11, 1950, m_v = 10.2.

587. S Del. On a Mount Wilson spectrogram taken on June 30, 1937, near maximum light, the emission lines are quite weak. The lines of Sr II are very intense.

595. RX Vul. The type M9e is from a McDonald spectrogram taken on September 21, 1951, m_v = 10.5. The emission lines of hydrogen are very weak on this plate, and several postmaximum emission lines appear.

599. AT Cyg. The spectral type is from a McDonald spectrogram taken on September 20, 1951, m_v = 10.5.

615. X UMi. The type Me was determined at the Warner and Swasey Observatory, according to Harris.

631. GS Cyg. The spectral type given is the average of the McCormick and Dearborn classifications.

639. WY Cyg. Moderately strong H α emission is present on a Yerkes spectrogram taken on September 17, 1950, m_v = 8.5.

643. RT Peg. Hartwig, in A.N., 164, 129, 1904, measured a companion to this star at 16" distance.

644. RZ Peg. Some Mount Wilson spectrograms show strong bands of CaCl in the spectrum of this star. RY Pegasi, now considered unvariable, is about 20" distant.

661. R Lac. This star is the primary of ADS 16217. The faint, 6" companion may be optical.

662. SX Peg. Very strong H α emission is present on a Yerkes spectrogram taken on October 31, 1950, m_v = 8.5. There is very little TiO absorption in the spectrum of this star.

670. RY Cep. The spectral type is from Yerkes spectrograms taken on August 18, 1952, m_v = 8.6, and June 23, 1953, m_v = 9.2.

TABLE 2

LONG-PERIOD VARIABLES OF SMALL RANGE, SEMIREGULAR, AND IRREGULAR VARIABLES OF TYPES M, S, AND C

Cat. No.	Name	Desig-nation	R.A. 1900	Dec. 1900	l	b	Magnitude	Type of Vari-ation	Period (Days)	Spec-tral Type	References
1.*	SW Scl	151	$0^h\ 1^m.1$	-33°22'	325°	-80°	10.3- 11.7	LP	144	M2e	133,420,581
2.	TT Peg	+26°4746	0 1.3	26 32	79	-35	9.3- 11.2	LP	153	M3e	465,614,741
3.	T Cet	1760	0 16.7	-20 37	53	-81	6.6- 7.7	SR	157	M5e II	465,609,614,752
4.	RW Psc	+21°188	1 18.8	21 20	102	-40	11.2- 12.4	SR	154	M0e	465,688,741
5.*	RV And	+48°616	2 4.6	48 28	104	-11	8.3- 11.5	SR	167	M3e	312,465,614,742
6.*	S Per	14528	2 15.7	58 8	102	- 2	7.2- 12.2	SR		M3e Ia	509,609,612,614,742,752
7.	Y Ari	16643	2 35.0	30 46	117	-25	10.2- 11.4	LP	267	M5e	614,720,741
8.	T Ari	17446	2 42.8	17 6	127	-36	7.4- 11.1	LP	314	M6e	473,612,614,656,741,752
9.	Y Per	21280	3 20.9	43 50	118	- 9	8.2- 10.9	LP	251	Ce	179,314,426,476,609,612, 614,709
10.*	RU Per	275376	3 23.9	39 19	121	-13	10.0- 12.0	SR?	310	M4e	465,614,741
11.	U Cam	22611	3 33.2	62 20	109	+ 7	7.7- 8.7	SR	411	C64e	362,426,476,609,612,752, 761,767,848
12.	RY Ret	24408	3 47.9	-57 39	236	-46	11.0- 12.2	LP	237	M3e	696
13.	SY Per	+50°961	4 9.0	50 23	120	+ 1	10.3- 12.6	LP	474	Ce	191,426,476,819
14.	R Pic	30551	4 43.5	-49 26	223	-39	8.3- 11.9	SR	168	M1e	158,359,447,451,612,614, 765
15.	GP Ori	+15°726	4 57.1	15 11	154	-14	11.8- 13.6	LP?		Se	273,563,739,848,902
16.	DH Ori	290428	5 21.1	- 0 22	171	-18	9.4- 11.7	SR	165	M0e	65,245,740
17.	S Cam	36972	5 30.2	68 44	112	+20	7.6- 11.4	SR	326	Ce	179,426,476,612,614,649, 752,767
18.	Y Tau	38307	5 39.7	20 39	155	- 3	6.8- 9.2	SR	241	C74e	426,476,609,612,752,761, 767,848
19.	BQ Ori	39983	5 51.1	22 50	154	+ 1	6.9- 8.9	SR	126	M5e III	316,461,465,614,726,741
20.	RS Aur	+46°1089	5 56.3	46 18	134	+13	11.1- 12.4	LP	171	M4e	451,614,742
21.*	FU Mon	44544	6 17.2	3 28	174	- 3	11.6- 12.7	SR	310	Se	191,563,739,752
22.	X Mon	51478	6 52.4	- 8 56	189	- 1	6.8- 10.4	LP	156	M3e	149,384,451,595,612,614, 703
23.	L_2 Pup	56096	7 10.5	-44 28	223	-14	3.4- 6.2	LP	140	M5e	77,303,384,447,451,608, 612,614,642,684,765,770, 786
24.*	VY CMa	58061	7 18.8	-25 34	207	- 4	8.8- 9.3	I?		cM3e	151,465
25.	VX Aur	+41°1660	7 21.6	41 10	145	+25	9.1- 12.4	SR?	326	M4e	614,742
26.	Y Gem	+20°1875	7 35.3	20 40	167	+21	10.4- 11.1	SR	142	M6e	465,614,741,752
27.	RT Hya	71887	8 24.7	- 5 59	198	+20	8.7- 10.7	SR	254	M6e	384,451,612,614,657,703
28.	W Pyx	-17°2578	8 32.3	-17 38	210	+15	10.8- 12.5	LP	166	M5e	225
29.*	RS Cnc	78712	9 4.6	31 22	162	+44	5.5- 7.0	SR	253	M6e	51,82,461,614,741,752
30.	TW Leo		9 19.3	30 25	164	+46	12.9-<14	LP	309	Me	327
31.	W Sex	85319	9 45.9	- 1 34	208	+39	10.3- 12.3	SR		Ce	360,426,476,612
32.	SZ Vel	-44°5914	9 46.2	-44 11	240	+ 8	9.4- 10.9	SR	150:	M5e	620
33.*	U LMi		9 48.6	36 34	155	+53	9.8- 12.8	SR	272	M6e	741
34.	RY Leo	+14°2194	9 58.9	14 28	191	+50	9.0- 11.7	SR	155	M2e	465,614,741
35.	VZ Vel	298126	10 24.2	-50 40	249	+ 6	10.4- 12.5	LP	317	M6e	614,727
36.	RT Vel	91110	10 26.0	-46 12	247	+10	10.5-<12	LP	141	M7e	612,614,715
37.	X Oct	91620	10 29.5	-83 50	266	-23	8.7- 12.7	LP	205	M3e	614
38.	V Hya	-20°3283	10 46.8	-20 43	238	+34	6.0- 12.5	SR	532	C75e	7,426,454,476,554,752
39.	RU Vel	94507	10 49.4	-52 40	253	+ 6	10.6- 12.5	SR?	125	M3e	612,614,715
40.	CI Vel		10 56.7	-53 52	255	+ 5	11.0- 13.5	LP	142	M0e	696

TABLE 2—Continued

Cat. No.	Name	Desig-nation	R.A. 1900 h m	Dec. 1900	l	b	Magnitude	Type of Vari-ation	Period (Days)	Spec-tral Type	References
41.	V491 Cen		11 30.3	-56°57'	261°	+ 4°	11.3- 12.5	LP	202	Me	696
42.	S Crt	103154	11 47.6	- 7 2	248	+53	10.7- 12.3	SR	155	M6e	465,612,614,710
43.	AD Cen	307252	11 48.2	-58 45	263	+ 3	9.8- 11.4	SR	62:	M0e	614
44.	Z UMa	103681	11 51.3	58 26	102	+58	6.6- 9.1	SR	198	M5eIII	314,384,447,451,461,612, 614,706,742
45.	RY UMa	107397	12 15.7	61 52	95	+56	7.0- 8.0	SR	311	M3eIII	461,465,614,742
46.	SS Vir	108105	12 20.1	1 19	259	+63	9.9- 13.3	SR	354	$C6_3e$	272,362,426,454,476,609, 612,614,752,767,848
47.	V CVn	115898	13 15.1	46 3	71	+71	7.0- 8.2	LP	196	M5e	430,451,614,742
48.	W Hya	120285	13 43.4	-27 52	287	+32	7.0- 9.9	LP	386	M8e	304,384,398,424,451,591, 612,614,856,901
49.	VX Cen	120460	13 44.4	-59 55	278	+ 1	9.5- 12.8	SR	308	M4e	614,656,725
50.	SX Boo		13 51.3	14 38	325	+69	12.0- 14.2	LP	153	M0e	225
51.*	AO Vir	+4°2853	14 16.8	4 22	319	+57	10.2- 12.3	LP	256	M2e	273,740
52.*	RX Boo	126327	14 19.7	26 10	1	+68	6.9- 9.1	SR	78	M7e	465,609,614,741,752
53.	RV Boo	129004	14 35.1	32 58	19	+65	7.5- 8.8	SR	140	M5e	465,612,614,682,718,741, 752
54.	U Boo	+18°2952a	14 49.7	18 6	349	+59	9.4- 13.3	LP	186	M4e	451,741
55.	Y Ser	135205	15 8.8	- 1 31	327	+44	10.0- 11.4	SR	433	M4e	465,614,740
56.	X Her	144205	15 59.6	47 31	41	+47	6.3- 7.4	SR	100	M6e	32,384,465,609,610,612, 742,752
57.	RR Her	144578	16 1.5	50 46	45	+46	7.8- 9.5	LP	241	$C7_2e$	314,426,454,476,554,609, 612,614,819
58.	R UMi	149683	16 31.3	72 30	72	+36	8.7- 10.7	LP	325	M7e	465,609,614,752
59.	TX Dra	150077	16 33.6	60 40	57	+39	6.8- 8.1	SR	79	M4e	314,465,614,742
60.	MU Her	AC+43°699 -55	16 33.8	42 57	34	+41	11.9- 13.2	LP	192	M2e	245,742
61.	AH Sco	155161	17 4.8	-32 12	321	+ 3	8.1- 12.0	LP	714	M3e	612,614
62.*	V447 Oph		17 7.2	8 27	357	+24	9.5- 13.5	I?		M6e	
63.*	V438 Oph	+11°3139	17 10.0	11 11	0	+25	9.3- 11.6	SR	154	M7e	273,740
64.	UW Her	156163	17 10.9	36 29	27	+33	7.5- 8.6	SR	81	M4e	317,465,614,741
65.	V776 Oph		17 28.3	11 23	2	+21	13.3- 15.5	LP	200	M0e	225
66.	VX Sgr	165674	18 2.0	-22 14	336	- 2	10.9-<12.7	SR	686+	M3e	614
67.	TU Lyr	168829	18 16.7	31 43	27	+19	11.1- 12.3	I		M6e	315,612,614,708,741
68.	T Tel	169324	18 19.0	-49 43	313	-18	11.3-<12.7	LP	256	M4e	612,614,705
69.	RW Tel	172605	18 36.0	-45 53	317	-19	9.4- 11.8	SR	127	M5e	614,719
70.	K 4666		19 21.7	44 17	44	+12	13.7-<15.0	LP		Se	597
71.	V374 Aql		19 25.1	- 1 2	4	-10	11.9- 15.5	RW		Ce	476,740
72.	AF Cyg	184008	19 27.2	45 56	46	+12	7.4- 9.4	SR	94	M5e	37,465,612,614,685,718, 742,752
73.	BG Cyg		19 34.9	28 17	31	+ 2	9.4- 12.5	LP	292	M7e	245,741
74.*	TT Cyg	186047	19 37.1	32 23	35	+ 4	7.4- 8.7	SR	119	$C6_4e$	7,362,426,476,609,612, 614,752,848,901
75.	NO Aql	+4°4212	19 40.2	4 39	11	-11	11.0- 12.7	SR	74	M3e	465
76.	S Pav	187835	19 46.8	-59 27	305	-32	8.6- 11.2	LP	387	M7e	313,451,612,614,765
77.	W Vul	191652	20 5.9	25 59	33	- 5	8.3- 10.2	LP	234	M4e	312,465,614,741
78.	S Aql	+15°4078	20 7.0	15 19	24	-11	8.4- 12.2	LP	146	M3e	451,752
79.	RS Cyg	192443	20 9.8	38 26	44	+ 2	6.7- 9.7	SR	416	$C8_2e$	179,197,362,426,454,476, 612,614,648,752,761,763, 767,792,848,860
80.*	T Mic	194676	20 21.8	-28 35	343	-34	7.7- 9.6	SR	347	M6e	273,612,614,698
81.	KN Aql	195275	20 25.2	1 32	14	-22	9.4- 10.9	SR	139	M5e	465,740

TABLE 2—Continued

Cat. No.	Name	Desig-nation	R.A. 1900 h m	Dec. 1900	l	b	Magnitude	Type of Vari-ation	Period (Days)	Spec-tral Type	References
82.	RU Vul	196792	20 34.5	22°54'	34°	-12°	8.5- 11.5	LP	156	M3e	451,612,614,741
83.	V Aqr	197942	20 41.8	2 4	17	-25	9.6- 10.4	SR	121	M6e	384,451,612,614,649, 740
84.	AM Peg	+11°4494	21 5.4	12 3	30	-24	9.0- 11.0	LP	137	M1e	614,740
85.	W Ind	201866	21 7.2	-53 26	311	-44	9.4- 11.5	SR	199	M4e	612,614,718
86.	RZ Aqr		21 17.8	- 7 32	13	-38	11.0-<12.5	LP	399	M3e	696
87.	W Cyg	205730	21 32.2	44 56	59	- 5	5.0- 7.6	SR	131, 120	M4e	32,37,51,77,78,82,384, 451,609,614,742,752, 755
88.	AB Cyg	205733	21 32.3	31 39	50	-15	7.4- 8.5	SR	520	M4e III	465,614,741
89.*	RU Cyg	206483	21 37.3	53 52	65	+ 1	6.9- 10.2	SR	470	M7e	609,612,614,657,742, 752
90.	RV Cyg	206750	21 39.1	37 34	55	-12	10.9- 12.0	SR	400+	$C6_4e$	362,426,454,476,612, 752,761,767
91.*	μ Cep	206936	21 40.4	58 19	68	+ 4	3.6- 5.1	SR		M2e Ia	30,32,33,37,389,420, 485,494,566,607,742, 752,758,770,810,876, 879,902
92.	V Oct	209512	21 58.8	-75 16	282	-39	11.6-<13.0	SR?	289	M6e	612,614,715
93.	TX Peg	211647	22 13.4	13 6	44	-36	9.3- 10.6	SR	120	M5e	465,614,740
94.	UV Tuc		22 31.2	-65 29	289	-47	11.7-<13.4	LP	310	M4e	696
95.	ST Peg	216026	22 44.3	26 50	61	-29	8.8- 9.9	SR	136	M6e	465,614,741,752
96.	BI Peg	+17°4841	22 52.9	17 29	57	-38	9.9- 11.2	SR	500	M6e	465,741
97.	TV And	+41°4651	22 53.5	42 12	70	-16	8.4- 11.0	SR	114	M4e	451,465,614,742
98.*	UY Cas		22 57.8	57 6	76	- 2	9.8- 12.0	SR	103	M3e	465
99.	AK Peg	+10°4870	22 58.2	10 49	54	-44	8.9- 10.8	LP	195	M3e	225,614,740
100.	EK Peg		23 3.0	28 47	66	-29	12.7-<14.7	LP?		M5e	245
101.	TY And	219346	23 10.0	40 15	72	-19	7.9- 10.3	SR	135	M4e	314,465,612,614,718, 741
102.	AN Cep	+82°715	23 16.3	82 28	87	+21	9.6- 12.2	SR	243	M8e	616
103.	RU Aqr	220515	23 19.2	-17 52	24	-69	9.0- 10.3	SR	69	M5e	465,614,705
104.	BG And	+42°4690	23 26.2	42 43	76	-17	11.3- 13.3	LP		Se	228,742
105.	SU Peg		23 32.0	32 9	74	-28	9.2- 11.5	LP	198	M3e	614
106.	ST And	222241	23 33.8	35 13	75	-25	8.3- 11.6	LP	337	Ce	179,426,476,612,710
107.	Z Aqr	223737	23 47.1	-16 25	41	-73	9.5- 12.0	LP	137	M2e	451,612,614,698
108.	S Phe	224583	23 53.9	-57 8	282	-60	8.6- 10.1	SR	141	M5e	359,447,451,612,614, 765
109.*	WZ Cas	224855	23 56.2	59 48	85	- 2	9.2- 11.0	SR	188	$C9_1e$	57,211,362,426,454, 476,532,551,553,563, 612,752,763,767,771, 792,848,860,861,884, 890,902

NOTES TO TABLE 2

1. SW Scl. On a McDonald spectrogram taken on December 4, 1949, the spectrum resembles to a considerable extent that of the M2 Ib star 119 Tauri, except for the hydrogen lines.

5. RV And. The Mount Wilson spectrogram taken on September 2, 1930, shows bright H β, H γ, and H δ.

6. S Per. A McDonald spectrogram taken on November 29, 1949, m_v = 9.5, is of type M5, with no emission present. Several Mount Wilson spectrograms also fail to show emission lines, although one, taken on October 5, 1947, by Miller, shows bright H γ and H δ.

10. RU Per. The Sr II lines are strong on the Mount Wilson spectrograms.

21. FU Mon. H β emission occurs on a spectrogram taken at McDonald on December 23, 1949. The absorption line of Sr I, λ 4607, is strong.

24. VY CMa. This star is the primary of ADS 6033, a remarkable nebulous multiple system. On spectrograms taken at Mount Wilson by Joy and at McDonald by Herbig its spectrum resembles that of an M-type supergiant star of luminosity class Ia or Iab, aside from the bright hydrogen lines. According to van den Bos, the close companion of the primary star is also red in color, B.A.N., 3, 263, 1927.

29. RS Cnc. Although the Sr II lines are very strong in the spectrum of this star, it is probably not a supergiant. It may be related to the objects of type S.

33. U LMi. Bright H γ and H δ appear on a McDonald spectrogram taken on December 22, 1949, m_v = 10.0.

51. AO Vir. A companion 5" distant was discovered by Sanford. This star is of spectral type G2 and has the same radial velocity as the primary star.

52. RX Boo. Hydrogen and Si I emission lines appear on David Dunlap spectrograms taken on April 12, 1949, May 2, 1951, and May 15, 1951, according to Heard.

62. V447 Oph. Herbig at Lick has found H β, H γ, and H δ to be strong emission lines on plates taken on March 26, 1946, and June 16, 1951; no emission appears on a plate taken on August 8, 1949.

63. V438 Oph. The emission lines are quite weak on the Mount Wilson spectrogram of this star.

74. TT Cyg. H α is probably faintly bright on one Mount Wilson spectrogram.

80. T Mic. The emission lines are very weak on the Mount Wilson spectrogram of this star.

89. RU Cyg. This star is the primary of ADS 15220, a triple star. It is not known whether this is a physical system or not.

91. μ Cep. This star is the primary of ADS 15271, but the two faint companions may be optical. Mount Wilson spectrograms taken on July 11 and July 13, 1930, by Joy and Adams, give a type of M0 and show bright H δ, in agreement with McLaughlin's published observations.

98. UY Cas. On Mount Wilson spectrograms the spectrum resembles that of a Mira-type variable in the strength of the bright lines.

109. WZ Cas. HD 224869 is 58" distant from this variable. This may be a common proper-motion pair.

TABLE 3

VARIABLES OF UNKNOWN TYPE OF VARIATION

Cat. No.	Name	Designation	R.A. 1900 h m	Dec. 1900	l	b	Magnitude	Spectral Type	References
1.		-60°171	0 52.3	-60°13'	267°	-58°	10.7- 11.2	M2e	697
2.	K 366		3 51.2	-55 13	232	-46	14.5- 16.5	M2e	696
3.	K 557		5 18.0	-73 52	252	-32	12.5- 15	Me	696
4.	K 656		5 35.5	-55 44	231	-32	11.0-<13.5	M3e	696
5.	K 1061		7 25.7	-61 39	240	-19	12.5- 14	M5e	696
6.	K 1205		7 58.8	-55 22	237	-13	13.8-<18	M0e	696
7.	K 2657	330673	16 16.6	-49 5	302	- 1	12.5-<15.5	M1e	
8.	CO Oph		16 48.9	-25 43	324	+10	13.6- 15.5	Me	696
9.	K 2899		16 56.1	-32 34	319	+ 4	13.6- 15.8	Ce	219,476
10.	K 3772		18 2.0	-34 2	326	- 8	15.6- 18	Me	696
11.	K 4021		18 14.6	-31 12	329	- 9	13.0- 15.5	Me	696
12.	K 4029	317421	18 14.9	-30 28	330	- 9	12.3- 13.7	Me	689
13.	K 4301		18 36.2	-39 1	324	-17	12.5-<14.5	M3e	690
14.	K 4468		18 53.3	-44 58	319	-22	12 -<13	Me	328
15.			19 16.6	43 34	43	+13	11.7- 14.2	M8e:	597
16.	K 4708		19 27.9	-23 3	344	-21	11 -<16	M3e	696

TABLE 4

INTRINSIC VARIABLES OF TYPES F, G, AND K

Cat. No.	Name	Designation	R.A. 1900 h m	Dec. 1900	l	b	Magnitude	Type of Variation	Period (Days)	Spectral Type	References
1.	TZ Cep		0 19.4	73°21'	88°	+11°	9.0- 11.0	SR	83	G6-K2e(M2)	577
2.	TX Per		2 41.8	36 33	116	-19	11.1- 13.7	SR	76	G5e-K2(M3)	577,688,889
3.	WW Tau	+29°662	3 55.5	29 58	133	-16	9.1- 11.9	SR	125±	G4e-K2(M3)	577,614,741
4.	RV Tau	283868	4 41.0	26 0	143	-11	9.8- 13.3	RV	79	G4e-K1(M1)	565,577,617,733,741
5.	Z Aur	+53°979	5 53.6	53 18	127	+16	8.9- 11.9	SR	137	G0e-G6e(M1)	577,614,742
6.*	AG Aur	AC+48°218-218	6 20.1	47 5	135	+17	10.0- 13.1	SR	96	G2e-K0(M3)	192,565,577,614,742,776
7.*	RU Cam	56167	7 10.9	69 51	113	+29	9.0- 10.4	Cep	22.0	$C0_1$-$C3_2e$	12,120,169,334,394,454,691,692,722,726,848
8.	U Mon	59693	7 26.0	- 9 34	194	+ 5	6.1- 8.1	RV	92	F8e-K2(M2)	51,406,420,565,577,617,681,731,774,835
9.	AB Leo	+20°2337	9 27.7	20 18	179	+46	10.3- 12.0	SR	103	F5e-G3e	577,694,741
10.	W LMi	AC+27°26462	10 39.2	26 34	176	+63	10.5- 13.5	SR	117	G2e-K2e(M3)	577,741
11.	SV UMa	237929	10 40.4	55 34	120	+55	9.0- 10.3	SR	76	G2e-G8(M4)	461,565,577,833
12.*	RU Cen	105578	12 4.2	-44 52	263	+17	9.3- 10.5	RV	65	Fpe	731
13.	W Vir	116802	13 20.9	- 2 52	289	+58	9.9- 11.2	Cep	17.3	cFe	107,154,159,276,293,431,589,612,646,773,865
14.	NGC 5272-95		13 37.4	28 53	7	+77	13.7- 14.4	SR	103	G4e-M2e	15,506,539
15.	NGC 5272-154		13 37.6	28 53	7	+77	12.9- 14.0	Cep	15.3	F5-G3e	41,443,539
16.	UW Lib	-16°3882	14 25.4	-16 22	303	+39	10.0- 11.0	RV	85	G2e-K0(M3)	59,577
17.	NGC 5904-42		15 13.4	2 25	332	+45	11.2- 12.2	RV	25.7	F4-G3e	539
18.	NGC 5904-84		15 13.5	2 26	332	+45	11.5- 12.6	RV	26.5	F5e-G5	539
19.*	RX Lib		15 36.2	-20 27	316	+26	11.6- 13.7	Cep	25.0		431
20.	U Lup	-29°12172	15 54.5	-29 38	313	+16	10.8- 13.2	SR	87	G2-K0e(M2)	577,888
21.	SX Her	144921	16 3.3	25 11	9	+45	9.0- 11.1	SR	103	G3e-K0(M3)	20,141,403,565,577,661,764,835
22.	NGC 6093-1		16 10.9	-22 43	321	+18	13.1- 14.5	Cep	16.0	F6e-G0e	539
23.	NGC 6218-1		16 42.0	- 1 48	343	+25	11.9- 13.2	Cep	15.5	F8-G5e	539
24.	TT Oph	+3°3281	16 44.6	3 48	349	+27	9.8- 11.7	RV	61	G2e-K0	16,565,577,612,617,774
25.	NGC 6254-2		16 51.9	- 3 55	343	+22	11.9- 13.7	Cep	18.8	F5e-G2	539
26.	TX Oph		16 59.1	5 7	352	+25	9.8- 12.1	RV?	138?	F5e-G6e	565,577,617,733,775
27.	UZ Oph	+7°3348	17 17.1	7 1	356	+22	10.5- 13.1	RV	87	G2e-G8(M2)	565,577,617,733
28.	NGC 6402-7		17 32.5	- 3 13	349	+13	14.9- 16.2	Cep	13.6	F5-G2e	539
29.	QT CrA	325013	18 2.2	-40 13	320	-11	11.5- 12.5	Cep	79	Fe-K	612,619
30.*	AC Her	170756	18 26.0	21 48	18	+13	7.1- 9.4	RV	75	F1-K4e	51,293,401,536,565,577,617,675,728,733,835,867
31.	NGC 6656-5		18 30.1	-24 1	338	- 9	12.0- 12.8	SR		G0-G6e	539
32.	NGC 6656-8		18 30.3	-24 1	338	- 9	12.0- 12.7	SR	67±	G2-G5e	539
33.	R Sct	173819	18 42.1	- 5 49	355	- 3	6.3- 8.6	RV	144	G5e-K2(M3)	23,32,37,44,51,80,147,565,577,612,614,617,725,733,752,755
34.*	V377 Sgr		18 42.2	-20 14	342	-10	13.7- 15.0	Cep	16.2	cFe	431
35.*	V383 Sgr		18 44.7	-32 22	331	-15	13.1- 14.4	Cep	16.4		
36.	AR Sgr	-23°14922	18 53.6	-23 51	340	-14	9.6- 11.5	RV	88	F5e-G6	577,612,617
37.	NGC 6779-6		19 12.7	30 1	30	+ 7	13.1- 14.8	RV	90	F6-G4e	539

TABLE 4—Continued

Cat. No.	Name	Designation	R.A. 1900 h m	Dec. 1900	l	b	Magnitude	Type of Variation	Period (Days)	Spectral Type	References
38.	AV Cyg		19 16.8	29°19'	30°	+ 6°	11.0- 12.9	SR	88	G0e-G6	577,617,682
39.	DY Aql	-11°5117	19 41.0	-11 12	357	-19	10.2- 12.9	RV	131	G5e-K0(M3)	577
40.	KK Aql	353685	19 43.3	14 19	20	- 7	10.9- 12.9	SR	89	G2e-G6(M2)	577
41.*	V336 Cyg		19 56.3	38 30	42	+ 4	15.1- 16.6	Cep	15.8		
42.*	TW Cap	-14°5679	20 8.9	-14 8	357	-26	10.3- 11.8	Cep	28.6	F8e	
43.*	V Vul	340667	20 32.3	26 15	37	- 9	9.0- 11.0	RV	76	G4e-K3(M2)	51,154,376,413, 449,565,577,617, 774,779,801,902
44.*	VX Cyg	+39°4379	20 53.6	39 48	50	- 4	10.7- 12.3	Cep	20.1	cF5e-cK	431,612,615,691
45.	V360 Cyg		21 6.4	30 16	45	-13	10.8- 13.3	RV	70	F5-G0e	565,577
46.	NGC 7089-1		21 28.3	- 1 15	22	-37	13.2- 14.8	Cep	15.6	F8-G2e	539
47.	NGC 7089-5		21 28.3	- 1 16	22	-37	13.2- 14.9	Cep	17.6	F6-G0e	539
48.	NGC 7089-11		21 28.4	- 1 16	22	-37	12.5- 13.7	RV	67	F5-G3e	539
49.*	WY And	+46°4128	23 36.6	47 2	79	-14	9.5- 10.6	SR	109	G2e-K2(M3)	192,565,577,742

NOTES TO TABLE 4

6. AG Aur. On a spectrogram taken at Mount Wilson by Sanford on December 15, 1943, the H α emission line is double, with a strong central reversal. The total width of the emission is about 2.7 A; the violet component is about twice as strong as the red. On this plate the velocity of the absorption line at H α is +197 km/sec, and that of the other absorption lines present is +185 km/sec.

7. RU Cam. Miss D. Jehoulet has found Ca II emission lines to be present on spectrograms taken at McDonald.

12. RU Cen. A McDonald spectrogram taken on April 17, 1951, $m_v = 9.2$, shows emission H β, H γ, and H δ and very strong Sr II absorption lines. Otherwise the spectrum appears greatly veiled.

19. RX Lib. Bright H β and H γ were discovered by Joy on a Mount Wilson spectrogram taken on May 16, 1932. Several other plates show no emission.

30. AC Her. Sanford has found broad and violet-displaced Ca II emission lines in this star on a Mount Wilson spectrogram taken on July 26, 1947.

34. V377 Sgr. On the Mount Wilson spectrograms, taken by Joy, the spectrum of this star is rather similar to that of W Virginis.

35. V383 Sgr. Hydrogen emission lines are present on two Mount Wilson spectrograms of this star.

41. V336 Cyg. Joy has found bright hydrogen lines on one Mount Wilson spectrogram. Three other plates show no emission.

42. TW Cap. Bright hydrogen lines have been recently found in the spectrum of this cepheid variable by Joy at Mount Wilson. The type F8 is due to F. Becker, Potsdam Pub., Vol. 28, Part 2, 1938.

43. V Vul. Very weak hydrogen emission has been detected by Joy on Mount Wilson spectrograms.

44. VX Cyg. H α appears in emission on a Mount Wilson spectrogram taken by Sanford on May 4, 1947, near maximum light. Plates taken at McDonald show that at maximum light the spectrum resembles that of the F5 Iab supergiant star 44 Cygni, while at minimum light it is similar to that of a K-type supergiant. The bands of C_2 do not appear on the McDonald spectrograms.

49. WY And. On a Mount Wilson spectrogram taken by Sanford on November 10, 1943, the H α emission line is symmetrically divided by a strong absorption line. The total width of the emission is about 2.4 A. On this plate the velocity of the H α absorption line is -194 km/sec and that of the other absorption lines present is -198 km/sec.

TABLE 5

STARS WITH COMBINATION SPECTRA

Cat. No.	Name	Designation	R.A. 1900	Dec. 1900	l	b	Magnitude	Period (Days)	Spectral Type	References
1.	AX Per	AC+54° 2255 -440	h m 1 30.0	53°45'	97°	- 8°	10.8- 12.5	675	gM3ep	181,404,405,440,452, 456,462,470,501,536, 742,845
2.*	BX Mon	MHα 61-12	7 20.4	- 3 24	188	+ 7	10.0- 13.0	1379	Mep	560,690
3.	RX Pup	69190	8 10.7	-41 24	226	- 3	11.1- 14.1		pec.	452,612,613,614,702, 723
4.	SY Mus	100336	11 27.6	-64 52	262	- 4	11.3- 12.3	621	Mep	579,724
5.	RW Hya	117970	13 28.8	-24 52	283	+36	9.8- 11.1	370	gMep	181,405,452,462,474, 557,612,614,718,780, 845,901
6.	T CrB	143454	15 55.3	26 12	9	+47	2.0- 11		gM3ep	8,9,10,63,76,133,134, 145,182,201,202,207, 224,246,247,250,251, 252,257,258,267,274, 310,317,335,437,452, 462,470,498,503,518, 533,601,605,613,634, 635,747,748,749,752, 774,837,845,864,869, 872,875,893,894
7.		+67°922	16 1.0	67 4	67	+41	9.4		Gep	227,230,243,603,742
8.	HK Sco	MHα 71-6	16 48.3	-30 14	320	+ 7	13.1- 15.8	700±	pec.	450,560
9.	CL Sco	MHα 71-5	16 48.7	-30 29	320	+ 7	11.2- 13.9		pec.	469,560
10.	V455 Sco	MHα 71-15	17 0.8	-33 57	319	+ 3	12.8-<16.5		pec.	560
11.	RS Oph	162214	17 44.8	- 6 41	348	+ 9	5.3- 11.5		pec.	79,171,187,188,190, 194,264,288,330,331, 332,343,344,345,412, 419,437,491,503,601, 613,622,623,624,625, 706,805
12.		F 6-7	17 59.6	-20 21	337	- 1	11		Mep	560
13.	V1148 Sgr		18 2.9	-26 0	333	- 4	8 -<16		pec.	94
14.	Y CrA	166813	18 7.2	-42 52	318	-13	12.0- 12.9		pec.	612,613,683,705
15.	YY Her	MHα 352-34	18 10.3	20 57	16	+16	11.1-<13.2		M2ep	281,560
16.*	FN Sgr		18 48.0	-19 7	344	-11	9 - 14		pec.	281,560
17.	CM Aql		18 58.4	- 3 12	359	- 6	14.4- 16.5		pec.	669
18.	BF Cyg		19 20.0	29 29	31	+ 6	9.3- 13.4	754	pec.	296,409,471,474,536, 542,557
19.		MHα 80-5	19 41.4	18 22	23	- 4	11		pec.	560
20.	CI Cyg		19 46.5	35 26	39	+ 4	10.8- 13.0	855	gM4ep	181,296,404,405,440, 536,557,662,741
21.*	V407 Cyg	MHα 289-90	20 58.7	45 23	55	- 1	13.3-<16.5		Mep	560
22.*	AG Peg	207757	21 46.2	12 10	38	-32	6.9- 7.6		Bep+M	67,75,409,471,474,536, 542,568,575,736,740, 883,902
23.	Z And	221650	23 28.8	48 16	78	-12	8.0- 12.4	694	gMep	36,66,72,183,204,296, 350,392,440,446,452, 456,462,466,470,474, 477,484,505,522,536, 557,605,613,632,705, 721,736,830,834,843, 845,877,883

NOTES TO TABLE 5

2. BX Mon. A McDonald spectrogram taken on April 8, 1951, m_v = 11.0, shows strong and rather broad emission at H β, H γ, and H δ and an absorption spectrum of type M4. This star is under investigation at the Mount Wilson Observatory.

16. FN Sgr. According to Herbig, a late-type continuum is probably present in the spectrum of this star at minimum light.

21. V407 Cyg. A low-dispersion spectrogram taken by Herbig at Lick on October 10, 1952, shows strong TiO bands and emission H δ.

22. AG Peg. Babcock has found that the bright lines in the spectrum of this star give evidence of a variable magnetic field, M.N., 113, 357, 1953.

TABLE 6

VARIABLES OF THE U GEMINORUM TYPE

Cat. No.	Name	Designation	R.A. 1900 h m	Dec. 1900	l	b	Magnitude	Period (Days)	Spectral Type	References
1.	RX And		0 59.0	40°46'	94°	-21°	10.3- 13.6	14	Ae?	48,209,469,536
2.	U Gem	64511	7 49.2	22 16	167	+25	8.8- 13.8	103	Ge?	48,209,469,536,612
3.	SU UMa		8 3.7	62 54	121	+34	11.1- 14.5	16	Fe?	48,209,469
4.	Z Cam	AC+73° 3544	8 14.0	73 26	108	+33	10.2- 13.4	20	dG5e?	48,209,469,536
5.	AH Her	AC+26° 39763	16 40.0	25 26	12	+37	10.9- 14.7	20	Ge?	469
6.	UU Aql		19 51.9	- 9 35	0	-20	11.0- 16.8	56	Ge?	469
7.*	AE Aqr		20 35.0	- 1 14	13	-26	10.8- 12.0		dG8ep	231,327,536
8.*	SS Cyg	206697	21 38.8	43 8	58	- 8	8.2- 12.1	50	dGep	18,48,231,333,338,469,536, 612,686
9.	RU Peg		22 9.1	12 12	43	-36	10.0- 13.1	70	dG3ep	209,231,469,536

NOTES TO TABLE 6

7. AE Aqr. The unusual light-variation of this star is discussed by Henize in A.J., 54, 89, 1949.

8. SS Cyg. Late-type absorption lines are visible on a number of Mount Wilson spectrograms taken near or at minimum light and are also well seen on a recent McDonald plate. They are not, however, invariably present at minimum light, according to Joy.

TABLE 7

EMISSION-LINE STARS ASSOCIATED WITH NEBULOSITY

Cat. No.	Name	Designation	R.A. 1900 h m	Dec. 1900	l	b	Magnitude	Spectral Type	References
1.	CW Tau	MH α 259-3	4 8.1	27°56'	136°	-15°	13.6-<15.6	dK5e	536,543
2.	CX Tau	MH α 259-22	4 8.7	26 33	137	-16	14.5- 15.3	dM1.5e	536,543
3.		MH α 259-23	4 8.7	26 31	137	-16	15.1- 15.4	dM2.5e	536,543
4.	CY Tau	MH α 259-5	4 11.4	28 6	137	-14	13.4- 15.0	dM2e	536,543
5.	CZ Tau	MH α 259-6(n)	4 12.3	28 2	137	-14	15.8- 17.3	dM2e	266,536,543
6.	DD Tau	MH α 259-6(s)	4 12.3	28 2	137	-14	14.5- 15.5	dK6e	266,536,543
7.	BP Tau	281934	4 13.0	28 52	136	-14	12.3- 13.3	dK5e	536,543
8.*	RY Tau	283571	4 15.7	28 12	137	-14	8.8- 11.2	dF8e-dG2e	261,880,489,536,612,852
9.	DE Tau	MH α 259-8	4 15.7	27 41	138	-14	13.8- 14.8	dM1e	536,543
10.*	T Tau	284419	4 16.2	19 18	144	-20	9.6- 13.5	dG5e	115,116,126,198,253,259, 270,373,380,392,489,536, 546,612,752,769,811,815, 816,820,822,852
11.	DF Tau	AC+25°12159	4 20.9	25 29	140	-14	11.9- 13.8	dM0e	536,543
12.	DG Tau	AC+25°12210	4 21.0	25 53	140	-14	11.8- 14.9	dGe	536,543
13.	DH Tau	MH α 259-9(np)	4 23.5	26 20	140	-14	14 - 15	dM0e	536,543,852
14.	DI Tau	MH α 259-9(sf)	4 23.6	26 20	140	-14	14 - 15	dM0.5e	536,543,852
15.	UX Tau	285846	4 24.2	18 0	147	-19	10.7- 13.4	dG5e	261,489,536,688,852
16.*			4 24.2	18 0	147	-19	13	dM2e	489,536
17.	DK Tau	AC+26°10585	4 24.6	25 48	140	-14	12.4- 14.9	dM0e	536,543
18.	XZ Tau		4 25.9	18 1	147	-19	11 - 14	dGe	489,536
19.*			4 25.9	18 1	147	-19	15	dMe	
20.	UZ Tau		4 26.6	25 40	141	-14	11.7- 14.9	dGe-dM2e	218,223,489,536
21.*			4 26.6	25 40	141	-14	13.3	dM3e	218,489,536
22.*		AC+18°1515-162	4 26.7	17 19	147	-19	13.4- 14.0	dK6e	536,543,560
23.	DL Tau	MH α 259-13	4 27.6	25 8	141	-14	13.5- 14.8	dGe	536,543
24.	CI Tau	MH α 259-20	4 27.9	22 37	143	-15	13.8- 15.2	dGe	536,543
25.	DM Tau	MH α 257-6	4 28.0	17 57	147	-18	14.5- 15.2	dK5e	536,543
26.	AA Tau	MH α 259-17	4 28.9	24 16	142	-14	13.1- 16.1	dM0e	536,543
27.	DN Tau	AC+25°12308	4 29.4	24 3	142	-14	13.2- 14.0	dK6e	536,543
28.	DO Tau	MH α 259-15	4 32.4	25 59	141	-12	13.7- 15.5	dGe	536,543
29.	DP Tau	MH α 259-19	4 36.5	25 4	143	-12	13.7- 15.4	dM0e	536,543
30.		MH α 259-24	4 36.9	25 9	143	-12	16.6	dK5e	536,543
31.	DQ Tau	MH α 257-7	4 41.1	16 49	150	-16	14.0- 15.0	dM0e	536,543
32.	DR Tau	MH α 257-8	4 41.3	16 48	150	-16	13.4- 14.7	dK5e	536,543
33.	DS Tau	AC+30°7943	4 41.5	29 14	140	- 9	12.1- 13.6	dK4e	536,543
34.*	UY Aur		4 45.4	30 37	140	- 7	11.6- 14.0	dG5e	184,489,536
35.	GM Aur	MH α 259-1	4 48.8	30 12	140	- 7	13.1- 13.9	dK5e	536,543
36.*	SU Aur	282624	4 49.6	30 24	140	- 7	9.3- 10.1	gGe	154,376,393,852
37.	RW Aur	240764	5 1.4	30 16	142	- 5	9.0- 12.0	dG5e	239,248,270,489,536
38.*			5 1.4	30 16	142	- 5	11.5	dM0e	489,536
39.	CO Ori	+11°809	5 22.1	11 20	161	-11	10.0- 13.0	gGe	469,536
40.	GW Ori	244138	5 23.5	11 47	160	-11	10.8- 11.5	dK3e	536,543
41.		AC+12°1799-321	5 23.8	11 46	160	-11	13.0	dK3e	536,543
42.*		MH α 265-5	5 23.9	12 50	159	-10	15.2- 16.6	dM0e	536,543
43.	GX Ori	MH α 265-6	5 24.4	12 9	160	-10	14.1- 15.2	dK3e	536,543
44.		MH α 265-9	5 25.3	12 6	160	-10	15.2- 15.7	dK4e	536,543
45.	HI Ori	MH α 265-16	5 25.8	12 5	160	-10	13.2- 15.5	dK0e	536,543

TABLE 7—Continued

Cat. No.	Name	Designation	R.A. 1900 h m	Dec. 1900	l	b	Magnitude	Spectral Type	References
46.	HK Ori	AC+12°1789-22	5 25.9	12° 5′	160°	-10°	11.4- 12.5	A4ep	471,543
47.	EZ Ori	Brun 224	5 29.4	- 5 9	176	-18	12.3- 13.7	Ge V	547
48.	IX Ori	Brun 340	5 29.8	- 5 27	177	-18	13.4- 15.1	?e	547,600
49.	YZ Ori	Brun 422	5 30.0	- 5 8	176	-18	15.1- 15.8	?e	97,547,600
50.	KR Ori	Brun 467	5 30.1	- 5 27	177	-18	13.5- 14.9	K0e	547
51.	V356 Ori	Brun 522	5 30.2	- 5 34	177	-18	14.0- 14.6	dK1e	547
52.	AN Ori	Brun 831	5 30.8	- 5 32	177	-18	12.3- 13.5	K1e IV	256,536,547
53.*	T Ori	-5°1329	5 30.9	- 5 32	177	-18	9.6- 13.5	A3e	97,256,542,600
54.	AZ Ori	Brun 982	5 31.4	- 5 16	177	-18	13.0- 15.6	dK4e	547
55.	V380 Ori	-6°1253	5 31.6	- 6 47	178	-18	9.7- 10.3	dAe	248,496,524,536,543,600,903
56.	BF Ori	-6°1259	5 32.3	- 6 39	178	-18	9.8- 13.4	gA5e	97,600,852
57.*	RR Tau	+26°887a	5 33.3	26 19	149	- 1	10.2- 14.2	gA2e	560
58.*	FU Ori		5 39.9	9 2	165	- 9	9.7- 16	gFp	336,347,348,349,573,628,852,897,900
59.	R Mon	+8°1427	6 33.7	8 50	171	+ 3	10 - 14	Fpe	24,47,92,203,372,374,380,392,489,524,536,743,745,760,903
60.	RU Lup	142560	15 50.1	-37 32	307	+11	9.7- 13.4	dGe	217,489,536,725
61.	EX Lup	325367	15 56.3	-40 2	306	+ 8	11.4- 13.4	?e	85,95,281
62.	V852 Oph	S,R 22	16 19.4	-24 16	321	+16	14.5- 15	Ae:	90,93,534
63.		S,R 4	16 19.9	-24 6	321	+16	13	dK5e	90,93,534,536,560
64.		S,R 12	16 21.2	-24 27	321	+15	13.5	dMe	90,93,534,536
65.		-24°12689	16 21.6	-24 7	321	+15	12.5	dK2e	90,93,534,536,560
66.		S,R 10	16 21.8	-24 9	321	+15	15	dKe:	90,93,534,536
67.	V853 Oph	S,R 13	16 22.7	-24 13	321	+15	12.5- 14.0	dKe	90,93,534,536
68.*	S CrA		18 54.4	-37 5	327	-19	10.8- 12.6	dGe	489,536,751
69.	R CrA	-37°13027	18 55.1	-37 6	327	-19	10.0- 13.6	Fpe	261,380,392,489,523,743,744,746,751,828,829,903
70.*	T CrA		18 55.2	-37 6	327	-19	11.7- 13.8	F0eα	489
71.*	VV CrA		18 56.4	-37 21	327	-20	13.0-<17.0	?e	
72.*	V536 Aql		19 34.2	10 17	16	- 7	12.6- 15.2	dKe	
73.	DI Cep	MHα 47-30	22 52.1	58 8	76	- 1	11.9- 13.5	dK3e	536,543,560
74.*	BM And		23 32.8	47 51	78	-13	12.7-<14.4	Ge	

NOTES TO TABLE 7

8. RY Tau. On a Mount Wilson spectrogram taken on September 29, 1947, Sanford has found that the total width of the Hα emission in this star is 11.6 Å. This emission consists of two parts separated by a strong violet-displaced reversal. The intensity of the longward emission is about six times that of the shortward emission; the radial velocity of the Hα absorption line is -78 km/sec.

10. T Tau. Herbig has recently discussed this star and its associated nebulosities in Leaflet No. 293 published by the Astronomical Society of the Pacific, September, 1953.

16. Anon. This star is 5".7 distant from UX Tauri.

19. Anon. This star, discovered by Herbig, is 23" from XZ Tauri in position angle 273°. The magnitude and spectral type are due to Herbig.

21. Anon. This star precedes UZ Tauri by 3".7.

22. AC +18° 1515-162. This star is MHα 257-2 and is probably also MHα 334-3.

34. UY Aur. A twelfth-magnitude companion is 0".8 distant from this star.

36. SU Aur. Herbig suspects weak emission at Hα and Hβ on spectrograms taken at Mount Wilson and Lick.

38. Anon. This star is 1".2 distant from RW Aurigae.

42. MHα 265-5. Another star of equal visual magnitude follows this star by 20".

53. T Ori. This variable was apparently first classified by Trumpler, who assigned to it a type of A0: (Pub. A.S.P., 43, 255, 1931).

57. RR Tau. The type gA2e is due to Herbig, who finds its hydrogen lines similar to those of stars of luminosity classes II or III.

58. FU Ori. Hydrogen emission has not been observed in the spectrum of this extraordinary variable star.

68. S CrA. A somewhat fainter star is 1" distant, noted by Joy, Pub. A.S.P., 56, 123, 1944.

70. T CrA. Emission Hα has been found by Herbig in the spectrum of this object.

71. VV CrA. Bright lines are present on Lick spectrograms taken by Herbig.

72. V536 Aql. The spectral type is due to Herbig.

74. BM And. Herbig has found strong Hα emission in the spectrum of this star.

TABLE 8

M-TYPE DWARF STARS WITH HYDROGEN EMISSION

Cat. No.	Name	Designation	R.A. 1900 h m	Dec. 1900	l	b	Magnitude	Spectral Type	References
1.*	ADS 246(B)	+43°44(B)	0 12.7	43°27'	85°	-18°	11.0	dM4e	146,389,420,434,457,504, 536
2.		+34°106	0 37.3	35 0	89	-27	10.0	dM0e	499,536
3.		+70°68	0 55.3	71 9	91	+ 9	9.9	dM3.5e	457,504,536
4.*	Wolf 47		0 57.0	61 50	92	0	13.7	dM3pe	441
5.	LPM 63		1 7.5	-17 32	123	-78	11.6	dM5e	504,536
6.	L 726-8(p)		1 34.0	-18 29	145	-74	12.5	dM5.5e	275,536,538,639
7.*	UV Cet		1 34.0	-18 28	145	-74	6.8- 12.4	dM5.5e	275,536,538,639
8.	Ross 15		1 52.5	58 1	99	- 3	12.1	dM4e	441,457,536
9.*	ADS 2894(B)	-1°565(B)	3 52.4	- 1 27	159	-37	11.3	dM3e	232,233,457,504,536
10.	o^2 Eri(C)	-7°781(B)	4 10.7	- 7 49	168	-36	11.1	dM4.5e	135,136,215,389,420,457, 504,536
11.*	Wolf 1539		4 46.7	6 19	160	-22	11.8	dM4e	441,536
12.		AC+2°2283-259	4 54.4	1 36	165	-22	10.0	dM1e	499,531,536,740
13.*	Ross 42		5 26.7	9 45	162	-11	11.4	dM4e	441,504,536
14.*	V371 Ori		5 28.6	1 53	170	-15	11.0- 12.9	dM3e	347
15.	Ross 614	CC 390	6 24.3	- 2 44	181	- 5	11.3	dM4.5e	215,457,504,536,631
16.*	Ross 986		7 3.3	38 43	146	+21	12.0	dM5e	441,492,504,536
17.*		+36°1638(A)	7 25.4	36 26	150	+25	10.8	dM3.5e	441,457,472,504,536,741
18.		+36°1638(B)	7 25.4	36 27	150	+25	12.2	dM4.5e	441,457,504,536
19.*	YY Gem	+32°1582	7 28.2	32 6	155	+24	8.6- 9.2	dM1e	101,127,215,280,291,389, 390,420,434,536,562,582, 604,772
20.*	YZ CMi		7 39.4	3 48	184	+15	11.8- 13.2	dM4.5e	241,441,504,536
21.*		+33°1646(A)	8 2.6	33 6	156	+31	9.6	dM0e	588
22.*		+33°1646(B)	8 2.6	33 6	156	+31	10.2- 11	dMe	
23.*		AC+22°214-129	10 8.7	21 37	182	+55	9.5	dM0e	499
24.*	AD Leo	+20°2465	10 14.2	20 22	185	+56	10.2- 10.6	dM4e	101,142,213,215,382,389, 420,434,435,457,536,552, 741
25.	L 1113-55		10 30.9	5 38	210	+52	12.2	dM4e	441,504,536
26.*	Wolf 359	CC 600	10 51.6	7 36	213	+57	13.5	dM6e	166,215,435,457,504,536
27.*	WX UMa	+44°2051(B)	11 0.5	44 2	135	+64	14.2- 16.0	dM5.5e	215,457,458,504,536,629
28.*	ADS 8242(sp)	+48°1958(sp)	11 31.9	48 1	119	+66	10.3	dM0e	588,742
29.*	Wolf 424	CC 716	12 28.4	9 34	261	+71	12.0	dM5.5e	215,435,457,504,536
30.*		+36°2322(A)	12 53.0	35 46	71	+82	10.7	dM0e	588,741
31.*		+36°2322(B)	12 53.0	35 46	71	+82	15:	dM4e	
32.*	Wolf 461	CC 754	12 55.6	6 13	280	+68	13.2	dM5e	441,457,504,536
33.		+13°2618	12 55.9	12 54	285	+74	9.9	dM2e	457,472,499,504,536,740
34.*		AC+18°1204-96(A)	13 28.1	17 16	318	+75	11.0	dM4e	499,504,536
35.*		AC+18°1204-96(B)	13 28.1	17 16	318	+75	11.5	dM4.5e	499,504,536
36.	Ross 845	CC 837	14 7.8	-11 33	301	+45	13.5	dM5.5e	441,504,536
37.*	V645 Cen		14 22.9	-62 15	282	- 3	12.4- 13.4	dMe	806,842
38.*		+16°2708	14 49.7	16 30	346	+58	10.5	dM0e	499,741
39.*	L 1130-30(A)		16 1.6	8 38	348	+39	12.0	dM3e	504,536
40.		+55°1823	16 14.9	55 32	51	+43	10.1	dM1.5e	478,499,504,536,742
41.*		152751	16 50.1	- 8 9	339	+20	9.2	dM3e	114,142,215,382,389,420, 435,457,504,536
42.*	Ross 867		17 16.1	26 36	16	+30	13.4	dM5e	441,504,536

TABLE 8—Continued

Cat. No.	Name	Designation	R.A. 1900 h m	Dec. 1900	l	b	Magnitude	Spectral Type	References
43.	Ross 868		17 16.1	26 36	16	+30	11.2	dM4e	441,504,536,741
44.	F 1-41		18 7.4	-16°12'	342°	- 1°	12.5	dM1e	536
45.*		234677	18 31.6	51 39	48	+23	8.3	dM1e	478,536,552,671
46.*	V1216 Sgr	CC 1108	18 43.6	-23 57	339	-12	10.1- 10.5	dM4.5e	215,457,504,536
47.*		AC+8°142-393	18 50.7	8 17	9	+ 2	9.8	dM2e	499;740
48.	ADS 12882(B)	+3°4138(B)	19 41.0	4 0	11	-11	11.4	dM2e	236,504,536
49.*	Wolf 1130	CC 1191	20 2.7	54 10	56	+11	12.2	dM3e	146,504,536
50.		196982(A)	20 35.6	-32 47	339	-38	10.9	dM4.5e	171,215,457,504,536,672
51.*		196982(B)	20 35.6	-32 47	339	-38	11.1	dM4.5e	171,215,457,504,536,672
52.		197481	20 39.0	-31 42	340	-38	8.7	dM2e	171,215,457,504,536
53.	Wolf 1084	CC 1227	20 40.5	54 57	60	+ 7	15.3	dM5e	215,441,504,536
54.*		AC+39°1214-608	20 56.2	39 41	50	- 5	10.3	dM3e	146,161,215,396,420,457, 499,536,670,741
55.*	Wolf 922	CC 1288	21 25.9	-10 14	11	-41	11.5	dM4.5e	457,504,536
56.	Wolf 1561(A)		22 12.1	- 9 18	21	-51	13.5	dM4.5e	441,504,536
57.*	Wolf 1561(B)		22 12.1	- 9 18	21	-51	14.5	dM5e	441,504,536
58.*	DO Cep	+56°2783(B)	22 24.4	57 12	72	0	9.8- 11.3	dM4.5e	170,215,457,504,536
59.	LPM 837		22 33.0	-15 53	16	-58	12.3	dM5.5e	215,457,504,536
60.*		214479	22 33.3	-21 8	6	-60	9.3	dM2e	588
61.*		-21°6267(B)	22 33.3	-21 8	6	-60	10.2- 11.0	dM4.5e	
62.*	EV Lac	+43°4305	22 42.6	43 49	69	-13	9.5- 11.5	dM4.5e	215,389,396,420,457,504, 536,742
63.		AC+31°70565	22 47.2	31 13	64	-25	11.2	dM3.5e	226,504,536
64.		+19°5116(A)	23 26.7	19 23	67	-39	10.3	dM4e	216,467,468,504,536,741
65.*		+19°5116(B)	23 26.7	19 23	67	-39	12.8	dM5.5e	467,468,504,536
66.*	Ross 248	CC 1445	23 37.0	43 39	78	-17	13.6- 13.7	dM5.5e	457,504,536
67.*		+1°4774	23 44.0	1 52	63	-57	9.1	dM2e	113,142,389,420,457,468, 740

NOTES TO TABLE 8

1. ADS 246(B). Joy has found that bright hydrogen lines appear on only one of a number of Mount Wilson spectrograms.

4. Wolf 47. The type dM3pe is from a McDonald spectrogram taken on September 19, 1951, on which the emission lines are extremely strong and the absorption spectrum much veiled. Johnson and Morgan have reported that this star flared during photoelectric observations, Ap. J., 117, 313, 1953.

7. UV Cet. This flare star is the following component of L 726-8, a binary of 1".5 separation.

9. ADS 2894(B). This star is a spectroscopic binary.

11. Wolf 1539. On the Mount Wilson spectrogram of this star all emission lines are weak.

13. Ross 42. This star is a spectroscopic binary.

14. V371 Ori. The type dM3e is due to Herbig, who has found bright hydrogen and Ca II lines on Lick spectrograms. The light-variation of this star has recently been discussed by Miss Hoffleit, Harvard Bull., 921, 5, 1952.

16. Ross 986. This star is a spectroscopic binary.

17. +36°1638(A). This star is a spectroscopic binary. The Mount Wilson spectrograms show that the hydrogen emission lines are rather weak.

19. YY Gem. This is the only known dMe eclipsing binary.

20. YZ CMi. Joy has found the helium line λ 4471 to be bright at times in the spectrum of this flare star. Both the hydrogen and the helium emission lines are variable in intensity.

NOTES TO TABLE 8—Continued

21. +33°1646(A). The emission lines were discovered by Dyer on a spectrogram taken at Mount Wilson.

22. +33°1646(B). Bright hydrogen and Ca II lines were discovered by Dyer, who suspects the variability of this star.

23. AC +22°214-129. The emission lines were discovered by Dyer on a spectrogram taken at Mount Wilson.

24. AD Leo. Herbig has found bright Hα and He I λ 5876, as well as emission cores, in the Na I lines on Mount Wilson spectrograms of this flare star.

26. Wolf 359. The emission lines are very strong in the spectrum of this star, which Sandig has observed to vary in light, A.N., 280, 39, 1951.

27. WX UMa. This object is a flare star.

28. ADS 8242 (sp). The type dM0e is due to Dyer.

29. Wolf 424. This object is a visual binary with equally bright components and 1" separation.

30. +36°2322(A). The emission lines were found by Dyer.

31. +36°2322(B). Very strong bright hydrogen and Ca II lines are present on Mount Wilson spectrograms taken by Dyer. This star is about 10" from its primary.

32. Wolf 461. This star is a spectroscopic binary.

34. AC +18°1204-96(A). On the Mount Wilson spectrograms, the hydrogen emission lines are very weak.

35. AC +18°1204-96(B). This star is 2".9 distant from its primary.

37. V645 Cen. This object is Proxima Centauri, a flare star whose light-variation has been discussed by Shapley in Pub. N.A.S., 37, 15, 1951. The emission lines in its spectrum were first noted at the Córdoba Observatory.

38. +16°2708. The bright lines in the spectrum of this star were found by Dyer on a spectrogram taken at Mount Wilson.

39. L 1130-30(A). The emission lines are very weak in the spectrum of this star, which is a spectroscopic binary. A fainter star is 2" distant.

41. HD 152751. This is a very close and exceedingly short-period visual binary.

42. Ross 867. Sandig has observed a variation in the light of this star, A.N., 280, 39, 1951.

45. HD 234677. A spectroscopic flare of this star has recently been reported by Popper, Pub. A.S.P., 65, 278, 1953.

46. V1216 Sgr. The light of this star has been found to vary by Kron, J.R.A.S. Canada, 47, 24, 1953.

47. AC +8°142-393. The emission lines were found by Dyer.

49. Wolf 1130. A light-variation of this star has been observed by Sandig, A.N., 280, 39, 1951. A large variation in radial velocity has been found by Joy.

51. HD 196982(B). This star is 3" distant from its primary.

54. AC +39°1214-608. A twelfth-magnitude companion is 1" distant.

55. Wolf 922. The bright hydrogen lines are very weak on the Mount Wilson spectrograms.

57. Wolf 1561(B). This star is 8" distant from its primary.

58. DO Cep. Van de Kamp and Miss Lippincott have reported a flare of this star, Pub. A.S.P., 63, 141, 1951.

60. HD 214479. Bright lines were found in the spectrum of this star by Dyer.

61. -21°6267(B). This star is about 8" distant from its primary. Very strong hydrogen and Ca II emission lines are present on spectrograms taken at Mount Wilson by Dyer.

62. EV Lac. A flare of this star has been observed at the Allegheny Observatory, Sky and Telescope, 13, 54, 1953.

65. +19°5116(B). This star is 3".5 distant from its primary.

66. Ross 248. Kron has found a small light-variation with a period of approximately 120 days, A.J., 55, 69, 1950. The hydrogen emission lines are quite weak on the Mount Wilson spectrograms of this star.

67. +1°4774. Very weak bright hydrogen lines are present on a Mount Wilson spectrogram of this star.

TABLE 9

BINARIES WITH HYDROGEN EMISSION

Cat. No.	Name	Designation	R.A. 1900 h m	Dec. 1900	l	b	Magnitude	Period (Days)	Spectral Type	References
1.	SX Cas	232121	0 5.5	54°20'	85°	- 7°	9.5- 10.7	36.6	cA6e+gG6	471,542
2.	BM Cas	+63°110	0 48.6	63 32	91	+ 2	9.1- 9.6	197	A5e Ia	269,340,560
3.*		17306	2 41.6	53 44	107	- 4	7.8		composite	560,583
4.	RX Cas	+67°244	2 58.8	67 11	103	+ 9	8.8- 9.5	32.3	gG3+gA5e	479,542
5.	RW Tau	25487	3 57.8	27 51	135	-17	8.0- 12.3	2.8	gB9e+sgK0	471,542,544
6.	RW Per	276247	4 13.3	42 4	127	- 4	9.9- 12.0	13.2	A5e+gG0	542
7.*		30353	4 41.8	43 6	129	0	7.7		Ape α	290,542,555
8.	RS Cep		4 48.6	80 6	100	+23	10.2- 11.9	12.4	A5e+G	542
9.	ε Aur	31964	4 54.8	43 40	130	+ 2	3.7- 4.5	9883	A8e Ia	17,25,26,28,29,31, 42,60,64,83,91,102, 177,263,285,287, 300,320,322,363, 375,376,397,400, 407,408,410,415, 416,418,420,425, 427,433,452,481, 545,571,574,607, 612,621,676,677, 756,770,784,797, 803,810,850,866, 871,876,883,885, 886,891,898,902
10.		242257	5 11.2	33 56	140	- 1	10.3		peculiar	471,542,580,736, 883
11.*		37453	5 33.6	30 2	146	+ 1	8.2		composite	221,559
12.	DN Ori	40632	5 55.0	10 13	166	- 5	9.8- 10.9	13.0	A2e+gF5	512,542
13.*		43246	6 10.1	28 54	151	+ 7	7.3	23.2	composite	436,560,849
14.*	HR 2577	50820	6 49.7	- 1 38	183	+ 1	6.2		composite	542,552
15.	RY Gem	58713	7 21.7	15 52	170	+16	8.5- 11.3	9.3	A2e+K2	542,881
16.*	HR 2859	59067-8	7 23.2	-11 21	195	+ 4	5.9		composite	404,552,725
17.		59771	7 26.4	-18 2	201	+ 1	9.1		cFe	221,580
18.	3 Pup	62623	7 39.8	-28 43	212	- 1	4.1	138	A3ep II	13,69,471,542
19.	UX Mon	65607	7 54.4	- 7 14	195	+13	8.7- 9.7	5.9	A7e+G2	84,507,514,550, 768,870
20.	XY Pup	67862	8 4.8	-11 42	201	+13	9.2- 11.4	13.8	A3e α	88
21.*	S Vel	82829	9 29.5	-44 46	238	+ 5	8.0- 10.5	5.9	dA5e+gK5	612
22.	TT Hya	97528	11 8.3	-25 55	246	+32	7.5- 9.3	7.0	A3e+G5	542
23.	W Ser	166126	18 4.1	-15 34	342	0	8.9- 10.5	14.2	cG2e	119,154,168,295, 300,301,376,392, 483,536,612
24.*		166612-3	18 6.3	-28 16	331	- 6	7.4		composite	560,725
25.	RY Sct	169515	18 19.9	-12 45	346	- 2	9.4- 9.9	11.1	Bep	74,409,471,542
26.	RZ Oph	+7°3832	18 40.9	7 7	6	+ 3	10.0- 10.9	262	F3e Ib+cK5	16,154,221,420,502, 768,899
27.	U Sge	181182	19 14.4	19 26	21	+ 2	6.4- 9.0	3.4	B9e+gG2	18,173,284,365,399, 429,576,612,795, 836,840
28.	υ Sgr	181615-6	19 16.0	-16 9	350	-15	4.3- 4.4	138	Ape α	96,104,409,471,542, 548,862
29.	SW Cyg	191240	20 3.8	46 1	49	+ 7	9.3- 11.9	4.6	A2e+K0	542
30.*	KU Cyg AC	+48°1759-217	20 9.6	47 5	51	+ 7	11.4- 14.3	38.4	Fpe+gK5	269
31.	VW Cyg	228545	20 11.4	34 12	40	- 1	9.7- 12.4	8.4	A3e+G5	542
32.	W Del	352682	20 33.1	17 56	30	-15	9.4- 12.8	4.8	A0e+G5	542
33.*	V367 Cyg	198287-8	20 44.2	38 55	48	- 3	7.7- 8.2	18.6	F2pe	152,178,279,404, 411,726

TABLE 9—Continued

Cat. No.	Name	Designation	R.A. 1900 h m	Dec. 1900	l	b	Magnitude	Period (Days)	Spectral Type	References
34.	AQ Peg	+12°4653	21 32.5	13° 2'	36°	-29°	10.0- 12.7	5.5	A2e+G5	542
35.*		207739	21 46.1	43 29	60	- 8	8.5		composite	221

NOTES TO TABLE 9

3. HD 17306. On spectrograms taken at McDonald and Mount Wilson, the spectral type of the component of later type appears to be about K3 Iab, while the other component has strong hydrogen lines.

7. HD 30353. The radial-velocity variation of this peculiar star is under investigation at the David Dunlap Observatory.

11. HD 37453. The spectral type of the brighter component is about F5 II, while that of the fainter is earlier. A variation in radial velocity is probable, since two Lick spectrograms taken on December 23, 1928, and October 17, 1930, give +58 and +54 km/sec, respectively, in contrast to the Mount Wilson velocity of +22 km/sec from a plate taken on March 7, 1941.

13. HD 43246. On a Yerkes spectrogram the type of the component of later type is estimated at F5 III, with considerable uncertainty; the other component is of earlier spectral class.

14. HR 2577. McDonald spectrograms taken by Mrs. E. M. Burbidge indicate that one component is a high-luminosity K-type star, while the other is of type B.

16. HR 2859. This is the close binary ADS 6104; the composite spectrum observed is probably due to the visual pair. The spectral type of the brighter star is quite uncertain but near G8 Ib-II, while that of the fainter is B.

21. S Vel. This interesting system is discussed by Sahade, Ap. J., 116, 35, 1952.

24. HD 166612-3. Mount Wilson and McDonald spectrograms indicate that one component is of spectral type F or G, while the other is of type B.

30. KU Cyg. The spectrum of the primary star, though resembling to a considerable extent that of a very luminous F-type supergiant, shows evidence of dilution of radiation and hence probably is actually that of a shell.

33. V367 Cyg. The observed spectrum of this eclipsing system appears to be that of a shell. This star is the primary of ADS 14314, separation 2".3 and Δ m 7 mag.; but the brighter star itself has been found to be a very close double by Aitken, Lick Obs. Bull., 18, 109, 1937.

35. HD 207739. On a McDonald spectrogram the spectrum of the component of later type is veiled but is probably of type F8 II, while the other component appears to be a B-type star.

TABLE 10

BINARIES OF THE VV CEPHEI TYPE

Cat. No.	Name	Designation	R.A. 1900 h m	Dec. 1900	l	b	Magnitude	Spectral Type	References
1.*	KN Cas	+61°8	0 4.4	62° 7'	86°	0°	10.5- 11.1	M1ep Ib+B	100,314,387,389,404, 420,742
2.*	WY Gem	42474	6 5.9	23 14	156	+4	9.5- 9.7	M2ep Iab+B	138,143,229,238,389, 392,404,420,440,448, 833,878
3.*	HR 2902	60414-5	7 29.2	-14 18	198	+4	5.1	M2ep Iab+B	70,160,268,392,440, 448,581,737,752,770
4.	WY Vel	81137	9 18.7	-52 8	242	-1	8.8- 10.2	Mep	664
5.		-61°3575	12 38.5	-61 23	270	+1	11.0	Mep	579
6.*	HR 8164	203338-9	21 16.5	58 12	66	+6	5.8	M1ep Ib+B	371,392,402,440,725, 742
7.*	VV Cep	208816	21 53.8	63 9	72	+7	6.6- 7.4	M2ep Ia	35,40,42,43,45,53,81, 133,140,143,189,199, 294,389,392,402,404, 417,420,459,461,475, 484,486,510,572,611, 626,627,735,742,752, 770,791,847,863,879
8.*	W Cep	214369	22 32.6	57 54	74	0	8.8- 9.8	K0ep Ia	18,137,392,404,440, 752

NOTES TO TABLE 10

1. KN Cas. The spectral type is from a McDonald spectrogram taken on December 14, 1949.
2. WY Gem. The spectral type is from a McDonald spectrogram taken on November 29, 1949. Babcock has discovered that this star has a general magnetic field, M.N., 113, 357, 1953.
3. HR 2902. The spectral type is from a McDonald spectrogram taken on November 29, 1949. This star is a spectroscopic binary. A general magnetic field is present according to Babcock, M.N., 113, 357, 1953.
6. HR 8164. The spectral type is from a McDonald spectrogram taken on December 5, 1949. McLaughlin writes: "No certain changes have occurred in this spectrum over the interval 1933 to 1952. H β is suspected of having weak emission borders. A plate taken December 6, 1949, shows H α as a sharp absorption line with definite narrow equal emission edges." This star is the primary of ADS 14864, separation 5"; the faint companion is a normal B-type star, as shown by a spectrogram taken at Lick by L. W. Ross.
7. VV Cep. The spectral type of this eclipsing variable is from a McDonald spectrogram taken on December 5, 1949. Babcock has found evidence of a variable general magnetic field, M.N., 113, 357, 1953.
8. W Cep. The spectral type is from a McDonald spectrogram taken on November 30, 1949. The rapid variations in the intensity of the H α emission line reported by Merrill, Humason, and Burwell, Ap. J., 76, 156, 1932, should be further investigated.

TABLE 11

MISCELLANEOUS EMISSION-LINE STARS

Cat. No.	Name	Designation	R.A. 1900 h m	Dec. 1900	l	b	Magnitude	Spectral Type	References
1.		4174	0 39.1	40° 8'	90°	-22°	7.5	Mep	278,283,741
2.	MH α 58-26		3 54.5	53 47	116	+ 2	10	Fpe	560
3.*	UV Aur	34842	5 15.3	32 25	142	- 1	9.8- 11.1	(C8ep)	50,162,235,237,265, 277,476,554,612,630, 720,752
4.		-59°1105	5 37.1	-59 8	235	-32	9.6- 10.1	F5pe	697
5.*	17 Lep	41511	6 0.5	-16 29	190	-16	5.0	Aeq+M2	471,542,605,736,770, 883
6.			6 22.0	- 7 49	185	- 8		M5e	245
7.	AX Mon	45910	6 25.2	5 56	173	0	6.6- 6.8	Beq+gM2	339,409,471,542,594, 605,736,883
8.	ZZ CMi	+9°1633	7 18.8	9 5	176	+13	10.7- 11.8	gM6ep	260,740
9.*		-30°5135	7 45.2	-30 53	215	- 2	9.2	F2e Iab	221,404
10.	MSB 32		7 52.7	- 0 24	189	+16	9.6	Ce	191,476
11.	MSB 57		9 9.0	-22 59	220	+18	9.0	Ce	219,476
12.		-57°3057	10 7.5	-57 18	251	- 1	10.0	Mep	579
13.*	η Car	93308	10 41.2	-59 10	255	- 1	-0.8- 7.9	pec.	110,409,471,542,556, 736,786,793,844,883
14.*	HR 4352	97534	11 8.3	-59 46	259	0	4.7	F0e Ia	608,676,770
15.*	K 2011	115921	13 15.1	-61 3	274	+ 1	10.5- 11.3	pec.	703,799
16.		117555	13 26.0	24 44	345	+79	8.0	gG5e	271,536
17.	R CrB	141527	15 44.5	28 28	12	+50	5.8-≥14	Fpep	34,38,153,186,193,310, 317,321,365,422,432, 439,536,540,599,611, 752,798,874
18.*		-27°11363	16 54.4	-27 29	323	+ 8	9.7	dK0e	560,696
19.	RT Ser		17 34.3	-11 53	342	+ 8	10.6-<16	pec.	16,73,409,471
20.*		160529	17 35.3	-33 27	323	- 3	6.7	A3e Ia	409,471,542,552,736, 883
21.*	ι^1 Sco	161471	17 40.6	-40 5	318	- 7	3.1	F2e Ia	420,608,676,738,770, 810,841
22.*	89 Her	163506	17 51.4	26 4	19	+22	5.5	F2e Ia	420,427,552,770,810, 871,873
23.			17 55.1	-33 15	326	- 7		Mep	255
24.*		319139	18 7.6	-32 50	327	- 9	9.7	dK5e	560,689
25.		172450	18 35.2	9 53	8	+ 6	8.0	M5e	245,740
26.		-26°13521	18 43.8	-26 31	337	-13	9.5	Fe	560
27.		+ 0°4080	18 56.4	0 29	2	- 3	9.5	Ge	560,569
28.	MH α 215-33		19 19.0	24 16	26	+ 3	10	Ce or Se	560
29.			19 32.2	29 19	32	+ 3		Mep	255
30.*		186058	19 37.1	-40 40	326	-28	9.3	pec.	612,700
31.*		338970	19 46.9	26 53	31	- 1	9.4	Ape α	560
32.	RR Tel		19 56.3	-56 0	309	-33	7.0- 16.5	pec.	573,640,641,695,842
33.	Lee 153		22 40.0	17 36	54	-36	9	Ce	476,741
34.	MH α 73-59		22 53.6	58 15	76	- 1	10.5	?e	560
35.		-62°1425	22 53.9	-62 8	290	-52	11.3- 11.6	F5e	697
36.		+73°1031	23 17.0	73 42	84	+13	9.5	Ke	560
37.	R Aqr	222800	23 38.6	-15 50	37	-71	6.7- 11.6	M7ep	19,39,122,123,124,130, 139,144,165,196,341, 342,379,384,392,421, 428,440,445,456,471, 474,500,564,612,614, 642,736,752,845,883, 901

TABLE 11—Continued

Cat. No.	Name	Designation	R.A. 1900 h m	Dec. 1900	l	b	Magnitude	Spectral Type	References
38.*	ρCas	224014	23 49.4	56°57'	83°	- 4°	4.1-6.2	Fvep Ia	86,87,108,109,121,323, 324,371,375,376,420, 427,432,438,517,528, 607,636,637,638,693, 705,742,752,770,778, 785,810,838,839,843, 871,876,880,902
39.	MSB 75		23 54.0	56 25	84	- 5	10.2	Ce	219,476

NOTES TO TABLE 11

3. UV Aur. This peculiar carbon star is the primary of ADS 3934, a probable physical pair. The companion is an AO star.

5. 17 Lep. The bands of TiO were discovered in the spectrum of this shell star by Slettebak, Ap. J., 112, 559, 1950. Other peculiarities of the star have been discussed by Struve, Pub. A.S.P., 63, 82, 1951.

9. -30°5135. The spectral type is from a McDonald spectrogram taken on April 2, 1951.

13. η Car. Gaviola has recently discussed the spectrum of this extraordinary variable star, Ap. J., 118, 234, 1953.

14. HR 4352. The spectral type was determined from a spectrogram taken at the Santiago station of the Lick Observatory. No emission appears on the Chile plates.

15. K 2011. This star may be a binary of the VV Cephei type.

18. -27°11363. The spectral type is due to Herbig, from spectrograms taken at Lick. Emission lines of hydrogen and Ca II are present and appear to vary in strength.

20. HD 160529. The type A3e Ia is from a McDonald spectrogram taken on April 25, 1948. While the spectrum is not that of a normal supergiant, this star is undoubtedly of very high luminosity.

21. ι^1Sco. No emission appears on spectrograms taken at the Santiago station of the Lick Observatory.

22. 89 Her. A weak variable central emission has been found at Hβ by Herbig on 11 A/mm spectrograms taken at Lick.

24. HD 319139. A McDonald spectrogram taken on April 15, 1951, shows moderately strong emission lines of hydrogen and Ca II.

30. HD 186058. It is not certain that this object should be included in the catalogue.

31. HD 338970. On a McDonald spectrogram taken on April 12, 1951, the spectrum is rather similar to that of ε Aurigae, except that Mg II λ 4481 is weaker than in the spectrum of that star. The observed spectrum may thus be that of a shell.

38. ρ Cas. The light-variation of this extraordinary star has been discussed by Hassenstein, A.N., 253, 457, 1934, and more recently by Gaposchkin, Harvard Bull., 919, 18, 1949.

TABLE 12

SPECTROSCOPIC BINARIES WITH CA II EMISSION

Cat. No.	Name	Designation	R.A. 1900 h m	Dec. 1900	l	b	Magnitude		Period (Days)	Spectral Type	References
1.	ADS 48(A)	38(A)	0 0.4	45°16'	83°	-16°	9.4			dK6	504,536
2.	ADS 246(A)	1326	0 12.7	43 27	85	-18	8.1			M1 V	504,536
3.	ζ And	4502	0 42.0	23 43	91	-38	5.1-	5.2	17.8	K1 II	290,536,549
4.*		+61°195	0 56.3	61 48	92	0	9.5			dM2	458,536
5.	δ Tri	13974	2 10.9	33 46	111	-25	5.1		9.9	G0 V	536
6.*		+47°612	2 15.7	47 24	106	-12	9.4			dM1.5	536
7.		21242	3 20.5	28 23	128	-22	6.5			dG5	807
8.	5 Tau	21754	3 25.4	12 36	140	-33	4.3		960	K0 II-III	536
9.*	HR 1176	23838	3 43.1	44 40	121	- 6	5.8			gG5	536
10.*		+16°516	3 44.7	16 57	141	-27	9.2			dK0	536
11.	μ Per	26630	4 7.6	48 9	122	- 1	4.3		283	G0 Ib	536
12.*		27149	4 12.2	18 0	145	-21	7.5			dG3(H)	536
13.*	58 Per	29094-5	4 29.8	41 4	130	- 3	4.5		10470	G8 II+B	
14.	RZ Eri	30050	4 39.0	-10 52	176	-32	8.0-	9.7	39.3	A5m+sgG8	487,536
15.*		283882	4 43.1	24 38	144	-11	9.1			dK2(H)	536
16.*	ζ Aur	32068-9	4 55.5	40 56	133	+ 1	5.0-	5.6	972	K4 II+B7 V	423
17.*	α Aur	34029	5 9.3	45 54	130	+ 6	0.2		104	G5+F6	2,71,180,536,598, 782
18.	η Gem	42995	6 8.8	22 32	157	+ 4	3.1-	3.9	2983	M3 III	180,536
19.*	SV Cam	44982	6 19.8	82 21	99	+27	9.8-	10.5	0.6	dG3	
20.	SS Cam		7 4.2	73 30	109	+28	10.1-	10.7	4.8	G1+F5	519
21.	AR Mon	57364	7 15.9	- 5 4	189	+ 5	10.1-	10.9	21.2	K0 II	480,536
22.	σ Gem	62044	7 37.1	29 8	159	+25	4.3		19.6	K1 III	180,369,536
23.*	81 Gem	62721	7 40.3	18 45	170	+22	5.0			K5 III	536
24.*	FG Hya	+3°1979	8 21.8	3 49	189	+24	10.8-	11.2	0.3	G	
25.	RU Cnc	+24°1959	8 31.6	23 55	169	+35	9.9-	11.5	10.2	dF9+dG9	488
26.	RZ Cnc	73343	8 32.9	32 9	159	+37	9.2-	10.8	21.6	gK2+gK5	249
27.*	ε Hya	74874	8 41.5	6 47	189	+30	3.5		5492	gG8	
28.	W UMa	83950	9 36.7	56 24	126	+47	8.3-	9.1	0.3	dG0+dG0	561
29.*		86590	9 54.4	25 2	175	+53	7.9			dG5	536
30.	λ Hya	88284	10 5.7	-11 52	222	+35	3.8		1586	K0 III	536
31.*	HR 4006	88639	10 8.2	27 38	171	+57	6.1			gG2	536
32.*	μ UMa	89758	10 16.4	42 0	145	+58	3.2		230	M0 III	536
33.	ξ UMa(A)	98231	11 12.9	32 6	162	+71	4.4		669	G0 V	290,536
34.	RW UMa	+52°1579	11 35.4	52 33	112	+63	9.9-	10.9	7.3	dF9+dG9	62,488
35.	HR 4665	106677	12 11.0	73 7	93	+45	6.6			K0	807
36.*		108102	12 20.1	26 4	202	+85	8.6			F8+ V(C)	
37.*		+25°2511	12 24.6	25 3	220	+85	10.4			G8: V(C)	
38.	RW Com		12 28.0	27 16	194	+87	11.3-	12.0	0.2	G2+G2	558
39.	RS CVn	114519	13 6.0	36 28	59	+80	8.0-	9.3	4.8	F4n+dG8	519,536
40.	4 UMi	124547	14 9.2	78 1	84	+39	5.0		575	K3 III	536
41.*	RV Lib	128171	14 30.3	-17 36	304	+37	9.8-	10.5	10.7	G5	
42.	RR UMi	132813	14 56.0	66 20	71	+46	6.2-	6.5	750	gM5	536
43.	SS Boo	+39°2849	15 9.8	38 56	29	+57	10.0-	10.5	7.6	dG5+dG8	242,488,495,536
44.*	UZ Lib	-8°3999	15 27.0	- 8 12	324	+36	10.3-	11.1		Kp	
45.*	TW Dra	139319	15 32.4	64 14	65	+45	7.8-	9.5	2.8	A6+sgK2	
46.	β Her	148856	16 25.9	21 42	6	+39	2.8		411	G8 III	536
47.*		150409	16 35.8	49 4	42	+41	6.7			gM4	536

TABLE 12—Continued

Cat. No.	Name	Designation	R.A. 1900 h m	Dec. 1900	l	b	Magnitude	Period (Days)	Spectral Type	References
48.	WW Dra	150708	16 37.7	60°54'	57°	+39°	8.8- 10.0	4.6	sgG2+sgK0	212,453,536
49.	ϵ UMi	153751	16 56.2	82 12	82	+31	5.0- 5.1	39.5	G5 III	882
50.	Z Her	163930	17 53.6	15 9	8	+17	7.2- 7.7	4.0	F2+F2	519
51.	AW Her	+18°3678	18 21.3	18 14	14	+12	9.5- 10.9	8.8	K2+G4	519
52.*	β Sct	173764	18 41.9	- 4 51	356	- 3	4.5	834	G5 II	
53.*		175742	18 51.7	23 26	22	+ 8	8.4		dK1	536
54.*		178450	19 3.6	30 5	29	+ 9	8.1		dG6	536
55.	HR 7275	179094	19 6.1	52 16	50	+18	5.9	28.6	sgK0	536,808
56.	26 Aql	181391	19 15.2	- 5 36	359	-10	5.1	267	G8 III-IV	593
57.	HR 7428	184398-9	19 29.1	55 31	55	+16	6.5	109	K2 II-III+A	549
58.	δ Sge	187076-7	19 42.9	18 17	24	- 4	3.8	3710	M2 Ib-II+A	49,297,460,536
59.*	31 α^1Cyg	192577-8	20 10.5	46 26	50	+ 6	4.9- 5.3	3803	K2 II+B3 V	536
60.*	32 α^2Cyg	192909-10	20 12.4	47 24	51	+ 6	5.2- 5.4	1141	K3 Ib-II+B	536,606
61.	47 Cyg	196093-4	20 30.0	34 54	43	- 4	4.8		K2 Ib+B	536
62.*	ϵ Cyg	197989	20 42.2	33 36	44	- 7	2.6		K0 III	180,536
63.	RT Lac	209318	21 57.5	43 24	61	- 9	8.8- 9.6	5.1	sgG9+sgK1	58,519,536
64.		209813	22 1.0	46 45	64	- 7	6.5	24.4	sgK0	809
65.*	AR Lac	210334	22 4.6	45 15	63	- 9	7.3- 8.2	2.0	sgG5+sgK0	289,519,529,536, 567,768
66.*	5 Lac	213310-1	22 25.4	47 12	68	- 9	4.6		M0 Ib-II+A	49,536
67.*	HR 8575	213389	22 26.0	48 51	69	- 8	6.5	17.8	sgK1	
68.*	η Peg	215182	22 38.3	29 42	61	-25	3.1	818	G2 II-III	
69.*		216899	22 51.8	16 2	56	-39	8.7		dM2.5	458,536
70.	RT And	+52°3383a	23 6.7	52 29	76	- 7	9.0- 10.1	0.6	dG0+dK1	280
71.*	λ And	222107	23 32.7	45 55	78	-15	5.0- 5.3	20.5	G8 III-IV	89,180,290,536, 549,868
72.*		224085	23 49.9	28 6	77	-33	7.3	6.7	K0 V	378,536

NOTES TO TABLE 12

4. +61°195. The radial velocity of this star is variable, according to Joy and Mitchell, Ap. J., 108, 234, 1948.

6. +47°612. The radial velocity of this star is variable, according to Joy and Mitchell, Ap. J., 108, 234, 1948.

9. HR 1176. The variable radial velocity of this star was found by Young, Pub. David Dunlap Obs., 1, 69, 1939.

10. +16°516. This star has a very large range in radial velocity, found by Wilson, Ap. J., 107, 119, 1948.

12. HD 27149. This star is a probable spectroscopic binary, according to Wilson, Ap. J., 107, 119, 1948.

13. 58 Per. McLaughlin writes: "K absorption is always bordered by narrow emission components, whose outer edges are about 2 A apart. These components vary slowly in relative intensity. In 1938 they were about equal. Since then they have passed through stages of R>V, R=V, R<V, and finally in 1951 they were again equal." New orbital elements of this system have recently been determined by Sanford, Ap. J., 118, 35, 1953.

NOTES TO TABLE 12—Continued

15. HD 283882. Wilson has found this star to be a double-lined spectroscopic binary, Ap. J., 107, 119, 1948.

16. ζ Aur. The spectral type given is that determined by Wellmann, A.N., 279, 257, 1951. A bright line of Si I, λ 3906, has been reported by Christie and Wilson, Ap. J., 81, 426, 1935.

17. α Aur. The combined spectral type is given by Morgan as G2 II-III in the Yerkes Spectral Atlas. Struve has recently published a general account of the peculiarities of this binary, Sky and Telescope, 10, 135, 1951.

19. SV Cam. Spectroscopic observations of this star are reported by Hiltner in Ap. J., 118, 262, 1953.

23. 81 Gem. A radial-velocity variation of 12 km/sec has been found from Lick spectrograms, Pub. Lick Obs., Vol. 16, 1928.

24. FG Hya. Moderately strong Ca II emission lines appear on a McDonald spectrogram taken by Mrs. E. M. Burbidge. This object has been found to be an eclipsing variable by H. J. Smith of Yale.

27. ε Hya. Weak central emission lines of Ca II were found by Herbig at Lick. The spectrum of this close visual binary (which has also been followed spectroscopically) is to some extent composite; the type given is an estimate of that of the primary star.

29. HD 86590. The variable radial velocity of this star was discovered by Wilson and Joy, Ap. J., 111, 221, 1950.

31. HR 4006. This star was found to show variable velocity by Albitzky and Shajn, Pub. Pulkovo Obs., Vol. 43, 1933.

32. μ UMa. An orbit for this spectroscopic binary has been recently determined at Lick by Miss B. A. Turner and E. S. Jackson.

36. HD 108102. Weak Ca II emission lines are present on a McDonald spectrogram of this star. According to Weaver, this object is a double-lined binary, Ap. J., 116, 612, 1952. The spectral type is due to Weaver.

37. +25°2511. Apparently double Ca II emission lines appear on a McDonald spectrogram of this star, which was found to be a spectroscopic binary by Trumpler, Lick Obs. Bull., 18, 167, 1938. The spectral type is due to Weaver, Ap. J., 116, 612, 1952.

41. RV Lib. Bright lines of ionized calcium are present on Mount Wilson spectrograms taken by Joy.

44. UZ Lib. Mrs. E. M. Burbidge has discovered very strong Ca II emission lines in the spectrum of this star on spectrograms taken at McDonald.

45. TW Dra. Bright lines of Ca II were found by Miss Roman on Yerkes spectrograms of the secondary component. The spectral type is due to Wyse, Lick Obs. Bull., 17, 37, 1934.

47. HD 150409. The variable radial velocity of this star was found by Wilson and Joy, Ap. J., 111, 221, 1950.

52. β Sct. Weak double emission lines of Ca II are present on Mount Wilson spectrograms. The violet emission component is stronger than the red component.

53. HD 175742. The radial velocity of this star is variable, according to Wilson and Joy, Ap. J., 111, 221, 1950.

54. HD 178450. The radial velocity of this star is variable, according to Wilson and Joy, Ap. J., 111, 221, 1950.

59. 31 Cyg^1. A study of this binary has recently been published by Larsson-Leander, Stockholm Ann., Vol. 17, No. 5, 1953. This object has recently been named V695 Cygni.

60. 32 Cyg^2. This eclipsing star has been the object of a recent study by Wright, Pub. Dom. Ap. Obs. Victoria, 9, 189, 1952. McLaughlin writes: "The possibility of intrinsic variations of the Ca II emission is suggested by the fact that, during the total phase of eclipse, in 1949, November, the red component greatly exceeded the violet."

62. ε Cyg. The variable radial velocity of this star was found on Lick spectrograms,

NOTES TO TABLE 12—Continued

Pub. Lick Obs., Vol. 16, 1928.

65. AR Lac. The unusual light-variation of this eclipsing binary has been discussed by Kron, Pub. A.S.P., 59, 261, 1947.

66. 5 Lac. The variable radial velocity of this star was discovered by Hynek, Ap. J., 88, 201, 1938.

67. HR 8575. Ca II emission lines were found by Miss Roman and Miss Northcott on spectrograms taken at the David Dunlap Observatory.

68. η Peg. Weak double Ca II emission lines are present on a Mount Wilson spectrogram taken by Sanford.

69. HD 216899. The radial velocity of this star was found to be variable by Joy, Ap. J., 105, 96, 1947.

71. λ And. Miss Roman has found that the CN band in the spectrum of this star is abnormally weak, Ap. J., 116, 122, 1952.

72. HD 224085. A new orbit for this spectroscopic binary has recently been determined by Halliday, J.R.A.S. Canada, 46, 103, 1952.

TABLE 13

GIANT, SUBGIANT, AND SUPERGIANT STARS WITH CA II EMISSION

Cat. No.	Name	Designation	R.A. 1900 h m	Dec. 1900	l	b	Magnitude	Spectral Type	References
1.*	ι Cet	1522	0 14.3	- 9°23'	71°	-69°	3.8	K2 III	
2.*	δ And	3627	0 34.0	30 19	88	-32	3.5	K3 III	180,536
3.	α Cas	3712	0 34.8	55 59	89	- 6	2.5	K0 II-III	180,536
4.	β Cet	4128	0 38.6	-18 32	88	-81	2.2	K0 III	180,290,536
5.	36 And	5286	0 49.6	23 5	93	-39	5.6	sgK1	536
6.*	η Cet	6805	1 3.6	-10 43	109	-72	3.6	K2 III	
7.	β And	6860	1 4.1	35 5	96	-27	2.4	M0 III	176,180,536
8.	51 And	9927	1 31.9	48 7	99	-13	3.8	K3 III	536
9.*	γ And(A)	12533	1 57.8	41 51	105	-18	2.3	K2 III	
10.	α Ari	12929	2 1.5	22 59	113	-35	2.2	K2 III	2,180,536
11.	HR 748	16028	2 29.5	36 52	113	-20	5.9	gK4	536
12.	14 Per	16901	2 37.6	43 52	111	-13	5.6	G0 Ib	536
13.	η Per	17506	2 43.4	55 29	107	- 2	3.9	K3 Ib	180,536
14.	RZ Ari	18191	2 50.2	17 56	128	-34	7.3- 7.7	gM6	536
15.*	η Eri	18322	2 51.5	- 9 18	155	-54	4.0	K1 III-IV	
16.*	α Cet	18884	2 57.1	3 42	142	-44	2.8	M2 III	180,536
17.	ρ Per	19058	2 58.8	38 27	118	-16	3.2- 3.8	M4 II-III	536
18.*	HR 978	20277	3 10.5	31 49	124	-20	6.0	sgG8	
19.	δ Eri	23249	3 38.5	-10 6	166	-45	3.7	K0 IV	180,536
20.*	25 Eri	23413	3 39.8	- 0 37	159	-35	5.8	gK5	
21.*	δ Tau	27697	4 17.2	17 18	146	-21	3.9	K0 III	
22.	θ^1 Tau	28307	4 22.9	15 44	148	-21	4.0	K0 III	536
23.	α Tau	29139	4 30.2	16 18	149	-19	1.1	K5 III	175,180,290,369,536
24.	ι Aur	31398	4 50.5	33 0	138	- 5	2.9	K3 II	536
25.	π^6 Ori	31767	4 53.4	1 34	165	-23	4.7	K2 II	536
26.*	CI Ori	36167	5 24.6	- 1 10	172	-17	5.0	K5 III	
27.*	α Ori	39801	5 49.8	7 23	168	- 8	0.4- 1.3	M2 Iab	3,180,301,536,896
28.	π Aur	40239	5 52.5	45 56	134	+12	4.6	M3 II	536
29.	μ Gem	44478	6 16.9	22 34	157	+ 6	3.2	M3 III	180,536
30.	25 Gem	47731	6 35.0	28 17	154	+12	6.5	G5 Ib	536
31.	ϵ Gem	48329	6 37.8	25 14	157	+11	3.2	G8 Ib	3,176,180,290,536
32.	ω Gem	52497	6 56.3	24 21	160	+15	5.2	G5 II	536
33.		55178	7 6.8	59 56	124	+27	7.3	gG6	536
34.	β Gem	62509	7 39.2	28 16	160	+25	1.2	K0 III	2,180,536
35.	11 Pup	65228	7 52.6	-22 37	208	+ 4	4.4	F8 II	536
36.	ζ Mon	65594	8 3.6	- 2 42	193	+17	4.4	G2 Ib	536
37.	β Cnc	69267	8 11.1	9 30	182	+24	3.8	K4 III	536
38.	31 Lyn	70272	8 16.0	43 31	145	+36	4.4	K5 III	536
39.	HR 3459	74395	8 38.8	- 6 52	201	+22	4.7	G2 Ib	536
40.	σ^1 UMa	77800	8 59.6	67 16	114	+39	5.3	K5 III	536
41.	α Lyn	80493	9 15.0	34 49	158	+46	3.3	M0 III	536
42.	α Hya	81797	9 22.7	- 8 14	210	+30	2.2	K3 III	536
43.	HR 3751	81817	9 22.9	81 46	97	+33	4.6	K3 III	536
44.	ϵ Leo	84441	9 40.2	24 14	175	+50	3.1	G0 II	536
45.*	γ Leo(A)	89484	10 14.5	20 21	185	+56	2.6	K0 III	536
46.	HR 4156	91880	10 31.4	-15 50	231	+36	6.2	gM1	536
47.	37 LMi	92125	10 33.1	32 30	163	+62	4.8	G2 II	536

TABLE 13—Continued

Cat. No.	Name	Designation	R.A. 1900 h m	Dec. 1900	l	b	Magnitude	Spectral Type	References
48.	46 LMi	94264	10 47.7	34°45'	157°	+65°	3.9	K1 III	536
49.	VY Leo	94705	10 50.8	6 43	214	+57	7.3- 7.6	gM5	536
50.	HR 4280	95212	10 54.5	46 4	132	+62	5.7	gK5	536
51.	HR 4333	96813	11 3.8	36 51	150	+68	6.0	gM3.5	536
52.*	ψ UMa	96833	11 4.0	45 2	132	+64	3.2	K1 III	
53.*		97918	11 10.7	-12 3	239	+44	6.7	gM4	
54.	χ UMa	102224	11 40.8	48 20	115	+67	3.8	K0 III	536
55.	3 CVn	107274	12 14.9	49 32	101	+68	5.6	gM1	536
56.	β Crv	109379	12 29.1	-22 51	267	+39	2.8	G5 II	536
57.	33 Vir	111028	12 41.3	10 6	271	+72	5.9	sgK1	536
58.	δ Vir	112300	12 50.6	3 56	276	+66	3.7	gM3	536
59.	ϵ Vir	113226	12 57.2	11 30	285	+73	3.0	G9 III	536
60.	41 Com	113996	13 2.4	28 10	3	+85	4.9	K5 III	536
61.	HR 5091	117566	13 26.1	79 10	87	+39	5.9	gG4	536
62.	HR 5219	120933	13 47.4	34 56	30	+74	5.0	gM2	536
63.*	α Boo	124897	14 11.1	19 42	343	+68	0.2	K2 III	175,180,200,369,536,895
64.	ρ Boo	127665	14 27.5	30 49	13	+66	3.8	K3 III	536
65.	5 UMi	127700	14 27.7	76 8	82	+40	4.4	K4 III	536
66.	ϵ Boo(A)	129989	14 40.6	27 30	6	+63	2.7	gK0	180,536
67.	β UMi	131873	14 51.0	74 34	79	+41	2.2	K4 III	2,536
68.*		133254	14 58.4	32 4	16	+60	6.8	gM4	
69.	ν^1 Boo	138481	15 27.3	41 10	32	+54	5.2	K5 III	536
70.	α Ser	140573	15 39.3	6 44	342	+43	2.8	K2 III	180,536
71.	δ CrB	141714	15 45.4	26 22	9	+49	4.7	G5 III-IV	536
72.*	δ Oph	146051	16 9.1	- 3 26	337	+31	3.0	M1 III	180,536
73.*	α Sco(A)	148478-9(A)	16 23.3	-26 13	320	+14	0.9- 1.8	M1 Ib	175,180,520,536
74.	30 Her	148783	16 25.4	42 6	33	+43	4.6- 6.0	gM6	536
75.		149198	16 28.1	67 16	66	+38	6.7	gM3	536
76.	η Her	150997	16 39.5	39 7	29	+40	3.6	G8 III-IV	290,536
77.*	α Her(A)	156014	17 10.1	14 30	3	+26	3.0- 4.0	M5 II	175,180,520,536
78.		156074	17 10.4	42 15	34	+34	7.7	$C1_2$	553
79.	π Her	156283	17 11.6	36 55	28	+33	3.4	K3 II	536
80.	β Dra	159181	17 28.2	52 23	46	+33	3.0	G2 II	4,180,290,536
81.		159968	17 32.4	27 39	19	+26	6.6	gM4	536
82.*		160538	17 35.4	74 17	72	+31	7.1	K0 III	
83.*	β Oph	161096	17 38.5	4 37	357	+16	2.9	K2 III	
84.*	ξ Her	163993	17 53.9	29 16	22	+23	3.8	K0 III	
85.	γ Dra	164058	17 54.3	51 30	46	+28	2.4	K5 III	2,180,536
86.*	109 Her	169414	18 19.4	21 43	17	+14	3.9	K2 III	
87.	R Lyr	175865	18 52.3	43 49	41	+17	4.0- 5.0	gM5	536
88.*	ϵ Aql	176411	18 55.1	14 56	15	+ 4	4.2	K2 III	536
89.	HR 7191	176668	18 56.3	62 16	60	+23	6.4	gK6	536
90.	HR 7237	177808	19 1.2	31 36	31	+10	5.8	gK5	536
91.*	α Vul	183439	19 24.5	24 28	27	+ 2	4.6	gM1	
92.*	γ Aql	186791	19 41.5	10 22	17	- 8	2.8	K3 II	180,536
93.	γ Sge	189319	19 54.3	19 13	26	- 6	3.7	K5 III	536
94.	α^1 Cap	192876	20 12.1	-12 49	359	-26	4.6	G3 Ib	536
95.*	α^2 Cap	192947	20 12.5	-12 51	359	-26	3.8	G9 III	
96.	θ Del	196725	20 34.0	12 58	26	-18	6.1	K3 Ib	536

TABLE 13—Continued

Cat. No.	Name	Designation	R.A. 1900 h m	Dec. 1900	l	b	Magnitude	Spectral Type	References
97.	η Cep	198149	20 43.3	61° 27'	65°	+11°	3.6	K0 IV	536
98.*		199178	20 50.4	44 0	53	- 1	7.6	gG8	
99.		199251	20 50.9	33 22	45	- 8	7.4	gM3	536
100.	ξ Cyg	200905	21 1.3	43 32	54	- 3	3.9	K5 Ib	180,536,606
101.*	ζ Cyg	202109	21 8.7	29 49	45	-13	3.4	G8 II	
102.*	HR 8165	203344	21 16.5	23 26	41	-19	5.8	gG8	
103.*	ζ Cap	204075	21 21.0	-22 51	355	-45	3.9	Gp	290,536
104.	β Aqr	204867	21 26.3	- 6 1	16	-39	3.1	G0 Ib	536
105.*	ρ Cyg	205435	21 30.2	45 9	59	- 5	4.2	G8 III	536
106.	ϵ Peg	206778	21 39.3	9 25	34	-32	2.5	K2 Ib	4,176,180,536
107.	9 Peg	206859	21 39.8	16 53	40	-27	4.5	G5 Ib	536
108.	α Aqr	209750	22 0.6	- 0 48	29	-43	3.2	G2 Ib	536
109.	ζ Cep	210745	22 7.4	57 42	71	+ 1	3.6	K1 Ib	180,536
110.	HR 8517	212047	22 16.4	26 26	54	-26	6.5	gM4	536
111.*		215953	22 43.8	49 3	71	- 9	7.2	gM4	
112.	λ Aqr	216386	22 47.4	- 8 7	31	-57	3.8	gM2	536
113.*	β Peg	217906	22 58.9	27 32	64	-29	2.6	M2 II-III	176,180,511,536
114.*	56 Peg	218356	23 2.2	24 56	64	-32	5.0	K0p II	463,536
115.	γ Cep	222404	23 35.2	77 4	86	+16	3.4	K1 IV	180,536
116.		224186	23 50.8	14 41	73	-46	6.6	gM3.5	536

NOTES TO TABLE 13

1. ι Cet. Double Ca II emission lines were found by Schopp and Schwarzschild on spectrograms taken at Mount Wilson.
2. δ And. The radial velocity of this star is probably variable, Pub. Lick Obs., Vol. 16, 1928.
6. η Cet. Double Ca II emission lines were found by Schopp and Schwarzschild on spectrograms taken at Mount Wilson.
9. γ And(A). Moderately strong bright double Ca II lines appear on spectrograms taken at Mount Wilson by Schopp and Schwarzschild.
15. η Eri. Double Ca II emission lines were found by Schopp and Schwarzschild on spectrograms taken at Mount Wilson.
16. α Cet. This star also shows weak H ϵ emission on Mount Wilson spectrograms, according to O. C. Wilson.
18. HR 978. Bright lines of Ca II are present on Mount Wilson spectrograms.
20. 25 Eri. Weak double Ca II emission lines appear on spectrograms taken at Palomar by O. C. Wilson.
21. δ Tau. Bright lines of Ca II are present on Mount Wilson spectrograms.
26. CI Ori. Ca II emission lines appear on a McDonald spectrogram taken by Keenan.
27. α Ori. A McDonald spectrogram, measured by W. S. Fitch, shows several Fe II emission lines in the region of the spectrum below 3300 A. These lines are weaker than those found by Herzberg in the spectra of α Herculis and α Scorpii, Ap. J., 107, 94, 1948.
45. γ Leo(A). CN is abnormally weak in the spectrum of this star, as noted in the Yerkes Spectral Atlas.
52. ψ UMa. Double emission lines of Ca II are present on Mount Wilson spectrograms.

NOTES TO TABLE 13—Continued

53. HD 97918. Ca II emission lines appear on Mount Wilson spectrograms of this star.

63. α Boo. CN is abnormally weak in the spectrum of this star, as noted in the Yerkes Spectral Atlas. According to O. C. Wilson, H ε is present in emission, Pub. A.S.P., 50, 245, 1938.

68. HD 133254. Bright lines of Ca II are present on Mount Wilson spectrograms.

72. δ Oph. This star also shows weak H ε emission on Mount Wilson spectrograms, according to O. C. Wilson.

73. α Sco(A). Ultraviolet emission lines of Fe II were discovered by Herzberg, Ap. J., 107, 94, 1948.

77. α Her(A). Ultraviolet emission lines of Fe II were discovered by Herzberg, Ap. J., 107, 94, 1948.

82. HD 160538. Strong bright lines of Ca II are present on a Yerkes spectrogram of this star taken by Miss Roman.

83. β Oph. Double Ca II emission lines were found by Schopp and Schwarzschild on spectrograms taken at Mount Wilson.

84. ξ Her. A weak central emission in H and K was found by Herbig on spectrograms taken at Lick.

86. 109 Her. Weak emission lines of Ca II were found by Schopp and Schwarzschild on spectrograms taken at Mount Wilson.

88. ε Aql. The radial velocity of this star may be variable, as announced by Küstner, A.N., 198, 409, 1914.

91. α Vul. Double Ca II emission lines appear on spectrograms taken at Palomar by O. C. Wilson.

92. γ Aql. According to O. C. Wilson, H ε is also in emission on spectrograms taken at Mount Wilson.

95. α^2 Cap. Weak double Ca II emission lines were found by Schopp and Schwarzschild on spectrograms taken at Mount Wilson.

98. HD 199178. Herbig has found moderately strong emission lines of Ca II on Lick spectrograms of this star.

101. ζ Cyg. Ca II emission lines are present on a Mount Wilson spectrogram.

102. HR 8165. Weak double Ca II emission lines appear on a spectrogram taken at Palomar by O. C. Wilson.

103. ζ Cap. The spectroscopic peculiarities of this star have been briefly discussed by Garstang, Pub. A.S.P., 64, 227, 1952.

105. ρ Cyg. Miss Roman has found that the CN band in the spectrum of this star is abnormally weak, Ap. J., 116, 122, 1952.

111. HD 215953. Weak Ca II emission lines are present on a Mount Wilson spectrogram.

113. β Peg. A McDonald spectrogram shows several emission lines due to Fe II in the region of the spectrum below 3300 A. These lines are somewhat weaker than those found by Herzberg in the spectra of α Herculis and α Scorpii, Ap. J., 107, 94, 1948.

114. 56 Peg. Miss Roman has noted that the hydrogen lines are too weak for the strength of Sr II and CN in the spectrum of this star, Ap. J., 116, 122, 1952. According to Herbig, the small variations in radial velocity are not due to orbital motion.

TABLE 14

DWARF STARS WITH CA II EMISSION

Cat. No.	Name	Designation	R.A. 1900 h m	Dec. 1900	l	b	Magnitude	Spectral Type	References
1.	ADS 48(B)	38(B)	0 0.4	45°16'	83°	-16°	9.4	dM0	536
2.	HR 8	166	0 1.4	28 28	80	-33	6.2	dK0	536
3.	ADS 433(A)	+66°34(A)	0 26.3	66 41	89	+ 5	10.4	dM2.5	536
4.		3765	0 35.3	39 40	89	-22	7.5	dK5	536
5.#		4967	0 46.5	-23 27	108	-85	8.5	dM0	
6.	Wolf 44	CC 65	0 55.1	60 50	92	- 1	10.8	dM2.5	536
7.		5996	0 56.2	68 42	91	+ 7	8.1	dG7	536
8.	26 Cet(B)	+0°174(B)	0 58.7	0 50	100	-61	9.0	dG8	536
9.	Wolf 91	CC 131	1 46.7	17 27	112	-42	10.5	dM0	536
10.		11507	1 48.0	-22 55	165	-74	8.9	dM1.5	536
11.	ADS 1613	12376	1 56.2	36 14	107	-23	8.0	dG5	536
12.	ADS 1752(A)	14082	2 11.6	28 17	113	-30	6.6	dF6	536
13.	ADS 1752(B)	+28°382(B)	2 11.6	28 17	113	-30	7.6	dG0	536
14.		AC+49°2493-285	2 18.6	49 21	106	-10	11.2	dM0	536
15.		15285	2 22.5	3 59	132	-50	8.6	dM1.5	536
16.		16157	2 30.6	-44 13	224	-63	8.6	dK6	887
17.	θ Per(B)	+48°746(B)	2 37.4	48 48	109	- 9	10.0	dM2.5	536
18.	Ross 556	CC 180	2 38.4	25 6	121	-30	10.5	dM3	536
19.*		17382	2 42.2	26 40	121	-28	8.2	dK0	
20.	HR 857	17925	2 47.7	-13 11	160	-57	6.1	dK0	536
21.		+29°503	2 51.8	29 16	121	-25	9.2	dK0	536
22.#		AC+45°130-216	3 2.8	45 21	115	-10	10.2	dM0	
23.	Wolf 1325	275122	3 11.6	37 53	120	-15	10.0	dM1.5	536
24.	κ Cet	20630	3 14.1	3 0	146	-42	5.0	G5 V	536
25.		+6°525	3 19.2	6 40	144	-38	10.0	dM0	536
26.*		21663	3 24.7	19 46	134	-28	7.9	dG5	
27.		+23°465	3 26.9	23 21	132	-25	9.0	dG8(H)	536
28.	ϵ Eri	22049	3 28.2	- 9 48	164	-47	3.8	K2 V	180,536
29.		+20°598	3 31.7	21 0	135	-26	9.0	dK0(H)	536
30.		278968	3 38.0	34 39	127	-15	10.7	dM0	536
31.		+27°555	3 38.3	27 53	131	-20	9.0	dG2	536
32.#		23453	3 40.2	25 56	133	-21	9.5	dM0	
33.	ADS 2768	23524	3 40.9	51 44	116	- 1	8.4	dG6	536
34.		283066	3 45.1	23 36	135	-22	10.5	dK6(H)	536
35.	Ross 23	CC 271	3 49.1	53 17	116	+ 1	10.5	dM1.5	536
36.*		283104	3 50.6	27 1	134	-18	9.1	dK0	
37.	ADS 2894(A)	24916	3 52.4	- 1 27	159	-37	8.6	dK5	472,536
38.		+19°641	3 54.8	20 6	140	-23	8.6	dG6(H)	536
39.	HR 1279(B)	+14°657(B)	4 2.0	14 54	145	-25	8.8	dK0	536
40.		26736	4 8.6	23 20	140	-18	8.0	dG7(H)	536
41.		26756	4 8.8	14 22	147	-24	8.4	dG8(H)	536
42.		284253	4 10.6	21 40	141	-19	9.0	dG9(H)	536
43.	o^2 Eri(A)	26965	4 10.7	- 7 49	168	-36	4.5	dK0	536
44.		283518	4 12.3	28 13	137	-14	9.5	dK5	536,543
45.	Hub. No. 4		4 12.6	28 5	137	-14	12.5	dK3	536,543
46.		27250	4 13.1	19 40	143	-20	8.4	dK0(H)	536
47.		27282	4 13.4	17 17	145	-21	8.3	dG8(H)	536

TABLE 14—Continued

Cat. No.	Name	Designation	R.A. 1900 h m	Dec. 1900	l	b	Magnitude	Spectral Type	References
48.		27685	4 17.0	16°34'	147°	-21°	7.8	dG2(H)	536
49.		27732	4 17.5	21 9	143	-18	8.7	dG4(H)	536
50.*		285749	4 17.7	15 32	147	-22	10.5	dK6(H)	
51.*		27771	4 17.9	14 26	148	-22	9.0	dG9(H)	
52.		285720	4 18.5	17 47	146	-20	9.8	dK6(H)	536
53.		27836	4 18.5	14 32	148	-22	7.6	dG0(H)	536
54.		285742	4 19.3	16 45	147	-21	10.4	dK4(H)	536
55.		27990	4 20.0	17 48	146	-20	9.0	dK0(H)	536
56.		28068	4 20.7	16 37	147	-20	8.2	dG2(H)	536
57.		285828	4 21.7	14 0	149	-22	10.4	dK5(H)	536
58.		28258	4 22.4	13 38	150	-22	8.8	dK0(H)	536
59.		28291	4 22.7	19 31	145	-18	8.4	dG7(H)	536
60.		28343	4 23.1	21 41	143	-17	9.0	dM1	536
61.		283704	4 23.4	26 28	140	-14	9.0	dG8(H)	536
62.		285773	4 23.7	17 40	147	-19	8.9	dK0(H)	536
63.		285805	4 23.8	16 2	148	-20	10.3	dK5(H)	536
64.		28462	4 24.2	16 26	148	-20	9.0	dK0(H)	536
65.		28545	4 24.9	15 31	149	-20	8.8	dG8(H)	536
66.		28977	4 28.8	15 37	149	-20	9.5	dK0(H)	536
67.		29159	4 30.4	15 28	150	-19	9.2	dG8(H)	536
68.		284574	4 34.0	23 6	144	-14	9.2	dG8(H)	536
69.		29608	4 34.7	16 20	150	-18	9.4	dK3(H)	536
70.		29713	4 35.7	69 54	108	+17	8.8	dK0	536
71.	Ross 33	285968	4 37.0	18 47	148	-16	9.8	dM2.5	536
72.		284787	4 42.7	20 56	147	-14	8.9	dK0	536
73.		30505	4 43.2	18 27	149	-15	8.8	dK1	536
74.		30572	4 43.7	23 14	145	-12	8.6	dG4	536
75.		30676	4 44.6	17 2	150	-16	7.2	dF8(H)	536
76.		30712	4 44.9	14 55	152	-17	8.2	dG5(H)	536
77.		30957	4 46.9	64 15	113	+14	8.6	dK0	536
78.#		+49°1280	4 49.4	49 48	125	+ 5	9.4	dM2	
79.		32347	4 57.4	13 35	155	-15	9.3	dK0(H)	536
80.		35171	5 17.8	17 14	155	- 9	8.2	dK5	536
81.*	111 Tau	35296	5 18.6	17 17	155	- 9	5.1	F8 V	
82.		36395	5 26.4	- 3 42	175	-18	8.0	dM2	458
83.*	HR 1925	37394	5 33.2	53 26	126	+13	6.4	dK0	
84.		+62°780	5 36.3	62 15	118	+18	9.2	dK5	536
85.#		AC+72°3130	5 55.4	72 11	109	+23	10.0	dM0	
86.		41593	6 1.0	15 34	162	- 1	7.6	dK0	536
87.		42581	6 6.4	-21 49	196	-17	8.2	dM2.5	472
88.*		45088	6 20.3	18 49	161	+ 5	6.9	dK3	
89.		+12°1343	6 49.2	12 18	170	+ 8	10.4	dM1	536
90.#		266611	6 50.6	30 54	153	+16	9.5	dM0	
91.#		52284	6 55.5	16 2	167	+11	10.0	dK8	
92.		+27°1311	6 59.5	27 37	157	+17	10.7	dM0	536
93.		53532	7 0.3	22 50	162	+15	8.1	dG5	536
94.		56168	7 10.9	67 51	115	+29	8.6	dK1	536
95.		61606	7 35.0	- 3 21	190	+10	7.2	dK3	536
96.#		+14°1802	7 54.7	14 5	176	+23	10.3	dK8	

TABLE 14—Continued

Cat. No.	Name	Designation	R.A. 1900 h m	Dec. 1900	l	b	Magnitude	Spectral Type	References
97.#		AC+33°213-242	7 56.7	33°53'	155°	+30°	10.4	dM0	
98.		+14°1876	8 15.3	14 23	178	+28	10.5	dM0.5	536
99.		+22°1921	8 17.6	22 11	170	+31	9.5	dM0	536
100.	HR 3625	78366	9 2.7	34 18	158	+44	6.0	dG0	536
101.#		AC+27°23636	9 3.2	27 51	167	+43	10.3	dM0	
102.		80768	9 16.5	76 22	103	+36	9.1	dK5	536
103.#		+40°2208	9 21.3	39 57	150	+48	10.0	dK8	
104.	11 LMi	82885	9 29.7	36 16	156	+49	5.5	G8 IV-V	290
105.#		+23°2121	9 31.6	23 9	175	+47	9.2	dK8	
106.#		+23°2124	9 32.3	22 58	176	+48	9.8	dK8	
107.*	Ross 85	CC 540	9 35.8	13 40	189	+45	10	dM2.5	
108.#		+33°1931	9 53.9	33 34	161	+54	10.8	dM0	
109.#		+3°2316	10 1.7	3 28	206	+45	10	dM0	
110.		+75°403	10 1.7	75 37	102	+39	9.3	dK6	536
111.		88230	10 5.2	49 57	132	+53	6.8	dK5	536
112.		+56°1458	10 24.1	56 30	121	+53	8.7	K7 V	472
113.#		+57°1274	10 25.5	57 39	119	+52	10.3	dM0	
114.#	ADS 7915(A)	+39°2376(A)	10 39.6	39 2	148	+63	8.5	dM2	
115.#		95650	10 57.3	22 30	188	+66	9.9	dM2	
116.		95735	10 57.9	36 38	152	+67	7.5	M2 V	536
117.		+44°2051(A)	11 0.5	44 2	135	+64	8.7	dM2	536
118.#		+19°2427	11 6.4	19 32	196	+67	10.5	dK8	
119.#		AC+40°477-39	11 19.5	40 32	138	+69	9.5	dM0	
120.	57 UMa(B)	+40°2433(B)	11 23.7	39 53	138	+70	8.2	dG5	536
121.#		+63°965	11 25.5	63 41	103	+52	9.9	dM0	
122.#		+23°2359	11 26.6	23 14	192	+73	10.3	dM0	
123.#		+40°2442	11 31.3	39 48	136	+72	10.2	dM0	
124.#	ADS 8242(nf)	+48°1958(nf)	11 31.9	48 1	119	+66	10.5	dM0	
125.	61 UMa	101501	11 35.8	34 46	150	+75	5.5	G8 V	290
126.#		+36°2219	11 45.9	35 49	142	+76	10.3	dM2	
127.#		+29°2228	11 49.7	29 18	170	+79	10.8	dM0	
128.#	Ross 917		12 12.7	47 10	104	+70	11.5	dM	
129.#		+1°2684	12 15.3	1 8	257	+62	10.0	dM0	
130.		107596	12 16.9	42 42	106	+75	9.1	dM0	536
131.#		+28°2110	12 17.5	28 12	176	+85	10.8	dM0	
132.	ADS 8553(B)	108421(B)	12 22.2	27 35	185	+86	8.7	dK6	536
133.		109011	12 26.5	55 40	94	+62	8.1	K2 V(U)	541
134.#			12 30.4	34 38	107	+83	10.3	dM0	
135.		110010	12 34.1	79 46	90	+38	7.0	dG2	536
136.		110463	12 37.2	56 17	91	+62	8.4	K3 V(U)	536,541
137.		110833	12 39.8	52 19	90	+66	7.0	dK0	536
138.#		+32°2274	12 42.5	31 45	82	+86	9.7	dM0	
139.		AC+66°3955	12 45.1	66 40	89	+51	10.5	dM3	458
140.		111631	12 45.6	- 0 13	273	+62	8.5	M0.5 V	472
141.		115043	13 9.5	57 14	82	+60	6.7	G1 V(U)	536
142.*	ADS 8841(B)	+17°2611(B)	13 11.9	17 33	307	+77	10.2	dM2	
143.#		AC+37°30242	13 13.5	36 52	54	+79	10.5	dM2	
144.	ADS 8862	115953	13 15.4	48 18	74	+69	8.8	dM2	536
145.#		+39°2643	13 20.7	39 27	56	+76	9.5	dK8	

TABLE 14–Continued

Cat. No.	Name	Designation	R.A. 1900 h m	Dec. 1900	l	b	Magnitude	Spectral Type	References
146.#		118100	13 29.6	- 7°50'	290°	+52°	9.3	dK8	
147.#		+36°2393	13 32.9	36 14	40	+76	8.7	dM2	
148.#		+39°2675	13 39.0	39 45	48	+73	9.0	dK8	
149.		119850	13 40.7	15 26	321	+71	8.6	dM2.5	536
150.#		AC+16°799-62	13 57.0	15 59	330	+69	10.0	dM2	
151.#		AC+14°1105-9	13 57.5	14 13	327	+67	10.0	dM0	
152.	ADS 9090(N)	+47°2112(N)	13 58.5	46 49	56	+66	9.9	dM3	536
153.	ADS 9090(S)	+47°2112(S)	13 58.5	46 49	56	+66	9.9	dM3	536
154.#		+81°465	14 8.4	81 5	86	+36	10.3	dM0	
155.		129333	14 36.9	64 43	72	+49	7.4	dG0	536
156.#		+20°3009	14 37.9	19 55	350	+62	10.2	dM0	
157.	ξ Boo(A)	131156	14 46.8	19 31	351	+60	4.8	G8 V	290,536
158.	ξ Boo(B)	+19°2870(B)	14 46.8	19 31	351	+60	6.8	dK5	536
159.*	ADS 9507(nf)	134066(nf)	15 2.8	9 37	338	+52	7.4	dG5	
160.		134319	15 4.1	64 26	68	+47	8.3	dG5	536
161.#		+40°2881	15 21.1	39 59	31	+55	9.9	dK8	
162.		+44°2555	16 10.3	44 42	37	+45	9.3	dK5	536
163.*	12 Oph	149661	16 31.1	- 2 7	342	+27	5.9	dG9	
164.		+68°901	16 56.6	68 10	66	+35	9.5	dG4	536
165.		154734	17 2.1	6 56	355	+25	9.1	dK3	536
166.		+7°3307	17 2.1	6 56	355	+25	9.3	dK2	536
167.	36 Oph(A)	155885-6(A)	17 9.2	-26 27	326	+ 5	5.3	dK2	536
168.#		+5°3409	17 25.5	5 38	356	+19	9.5	dM1	
169.#	ADS 10675(s)	+23°3151(s)	17 33.6	23 1	14	+25	10.4	dM	
170.#		AC+61°26806	17 34.2	61 54	58	+32	10.3	dM2	
171.	μ Her(BC)	+27°2888(BC)	17 42.5	27 47	20	+24	9.8	dM3.5	536
172.		+46°2361	17 43.0	46 53	40	+29	10.3	dM1.5	536
173.		+4°3562	17 53.5	4 29	359	+12	9.5	dK5	536
174.*	70 Oph(A)	165341	18 0.4	2 31	358	+10	4.3	K0 V	180,290,536
175.	70 Oph(B)	+2°3482(B)	18 0.4	2 31	358	+10	6.0	dK6	180,290,536
176.		167605	18 10.9	69 40	67	+29	9.1	dK0	536
177.		168442	18 14.6	- 1 58	355	+ 5	10.4	dM0	536
178.		172393	18 34.9	42 35	39	+19	8.7	dK0	536
179.	Ross 160	229793	18 47.5	16 29	15	+ 6	10.5	dM1.5	536
180.#		AC+75°7157	19 0.6	75 10	74	+26	10.1	dM0	
181.		180617	19 12.0	5 1	8	- 5	9.1	dM3	536
182.		189087	19 53.2	29 33	34	- 1	8.2	dG7	536
183.		190007	19 57.8	3 2	12	-16	7.8	dK4	536
184.#		351151	19 58.5	19 49	27	- 7	10.2	dM0	
185.	27 Cyg	191026	20 2.6	35 42	41	+ 1	5.5	dG3	536
186.#		+77°767	20 14.2	77 24	77	+22	10.7	dK8	
187.		196794	20 34.5	9 43	23	-20	8.9	dK1	536
188.		+56°2471	20 39.0	57 4	61	+ 9	10.3	dM0	536
189.		+19°4499	20 39.8	19 24	32	-15	10.5	dM1.5	536
190.*		199305	20 51.3	61 49	66	+11	8.5	dM2	
191.		199803	20 54.4	0 40	18	-29	8.7	dG4	536
192.*	61 Cyg(A)	201091	21 2.4	38 15	50	- 6	5.6	K5 V	155,180,536
193.	61 Cyg(B)	201092	21 2.4	38 15	50	- 6	6.3	K7 V	180,536
194.#		-5°5480	21 3.6	- 4 50	14	-34	9.4	dK8	
195.	Ross 775	CC 1285	21 24.8	17 12	38	-25	10.4	dM4	536

TABLE 14—Continued

Cat. No.	Name	Designation	R.A. 1900 h m	Dec. 1900	l	b	Magnitude	Spectral Type	References
196.		204734	21 25.7	63°57'	70°	+10°	9.0	dK0	536
197.#		+27°4120	21 33.5	27 16	47	-19	10.0	dM2	
198.*	ADS 15186(E)	206225	21 35.6	41 16	57	- 9	8.7	dG7	
199.	HR 8314	206860	21 39.7	14 19	38	-29	6.1	dG0	536
200.		208313	21 50.4	31 52	53	-18	7.6	dK0	536
201.		209290	21 57.1	0 56	30	-41	9.2	dK6	458,536
202.#		AC+7°166-62	22 5.7	7 27	38	-39	11.0	dM0	
203.	Ross 271	AC+18°1937-307	22 6.6	17 55	46	-31	10.3	dM2.5	536
204.		+30°4633	22 7.6	31 5	56	-21	10.0	dM0	536
205.#		AC+27°66379	22 9.9	27 22	54	-24	10.4	dM0	
206.		+21°4747	22 20.1	22 3	52	-30	9.1	dM0	536
207.	ADS 16145(p)	214615(p)	22 34.3	-13 8	20	-57	8.8	dK0	536
208.	ADS 16145(f)	214615(f)	22 34.3	-13 8	20	-57	8.8	dK0	536
209.	Ross 223	AC+44°955-266	22 41.3	44 51	69	-12	10.5	dK6	536
210.		AC+24°44-11	22 43.7	24 13	59	-31	10.9	dM0	536
211.		216133	22 45.1	- 7 38	31	-56	10.2	dM1	536
212.		+30°4824	22 47.3	31 12	64	-25	9.4	dK5	536
213.*	HR 8721	216803	22 50.8	-32 6	343	-66	6.5	dK5	
214.#		217379	22 55.1	-26 51	357	-67	9.6	dM0	
215.		+65°1846	23 0.5	66 14	80	+ 6	9.9	dM1	536
216.		220140	23 16.2	78 27	86	+17	7.7	dK0	536
217.		+57°2735	23 20.0	57 19	79	- 3	10.2	dM2	536
218.		221503	23 27.6	-17 23	29	-70	8.6	dK5	478,536
219.		+0°5017	23 29.9	1 3	57	-56	9.5	dM0.5	536
220.#		-13°6464	23 43.2	-13 33	45	-70	9.6	dK8	
221.#		+28°4660	23 48.1	28 28	77	-32	9.8	dM0	
222.	ADS 48(F)	+44°4548	23 59.9	45 14	83	-16	9.9	dM2	536

NOTES TO TABLE 14

The symbol # after the catalogue number indicates that Ca II emission lines were found by Dyer on spectrograms taken by him at Mount Wilson.

19. HD 17382. Ca II emission lines appear on Mount Wilson spectrograms.

26. HD 21663. Weak Ca II emission lines appear on Mount Wilson spectrograms.

36. HD 283104. Ca II emission lines are present on Mount Wilson spectrograms.

50. HD 285749. Ca II emission lines are present on Mount Wilson spectrograms.

51. HD 27771. Ca II emission lines appear on Mount Wilson spectrograms.

81. 111 Tau. A Mount Wilson spectrogram shows bright Ca II lines.

83. HR 1925. Emission lines of Ca II appear on a spectrogram taken at Lick by W. H. Wehlau.

88. HD 45088. Ca II emission lines appear on a spectrogram taken at Lick by W. H. Wehlau.

107. Ross 85. Moderately strong emission lines of Ca II are present on Mount Wilson spectrograms.

142. ADS 8841(B). Mount Wilson spectrograms show moderately strong emission lines of Ca II.

159. ADS 9507 (nf). Bright Ca II lines appear on Mount Wilson spectrograms.

NOTES TO TABLE 14—Continued

163. 12 Oph. Weak Ca II emission lines are present on a Lick spectrogram taken by W. H. Wehlau.

174. 70 Oph(A). This star appears to be slightly variable in radial velocity, according to Berman, Lick Obs. Bull., 16, 24, 1932.

190. HD 199305. Moderately strong Ca II emission lines are present on Mount Wilson spectrograms.

192. 61 Cyg(A). The Ca II emission lines show very weak and narrow central reversals on a Mount Wilson spectrogram taken by Adams.

198. ADS 15186(E). Bright Ca II lines appear on Mount Wilson spectrograms.

213. HR 8721. On a Lick spectrogram taken by W. H. Wehlau, moderately strong emission appears at H and K.

TABLE 15

CEPHEID VARIABLES WITH CA II EMISSION

Cat. No.	Name	Designation	R.A. 1900 h m	Dec. 1900	l	b	Magnitude	Period (Days)	Spectral Type	References
1.*	β Dor	37350	5 32.8	-62° 33'	239°	-32°	4.5- 5.7	9.8	F2-F9	
2.*	T Mon	44990	6 19.8	7 8	171	- 1	6.3- 7.8	27.0	F7 Iab-K1 Iab	536
3.*	W Gem	46595	6 29.2	15 24	165	+ 5	6.7- 7.3	7.9	F6-G5	
4.	ζ Gem	52973	6 58.2	20 43	163	+13	4.3- 5.1	10.2	F7 Ib-G3 Ib	46,536
5.	X Sgr	161592	17 41.3	-27 48	329	- 1	5.0- 6.1	7.0	F5-G9	298
6.	W Sgr	164975	17 58.6	-29 35	329	- 5	5.0- 6.4	7.6	F2-G6	298
7.	Y Sgr	168608	18 15.5	-18 54	340	- 4	5.8- 6.9	5.8	F6-G5	298
8.	U Sgr	170764	18 26.0	-19 12	341	- 6	6.9- 8.0	6.7	F7-G5	298
9.*	YZ Sgr	174089	18 43.7	-16 50	345	- 9	7.6- 8.6	9.6	G0-G7	
10.	TT Aql	178359	19 3.2	1 8	4	- 5	7.2- 8.9	13.8	F8-K0	298
11.	U Aql	183344	19 24.0	- 7 15	359	-13	6.7- 7.8	7.0	G0-G6	298
12.*	SV Vul	187921	19 47.4	27 12	32	- 1	7.6- 9.5	45.1	F7 Ia-K0	
13.	η Aql	187929	19 47.4	0 45	9	-14	3.9- 5.1	7.2	F6 Ib-G4 Ib	282,298,536, 592
14.	S Sge	188727	19 51.5	16 22	23	- 7	5.7- 6.9	8.4	F6 Ib-G5 Ib	592
15.	X Cyg	197572	20 39.5	35 14	45	- 5	6.4- 8.1	16.4	F7 Ib-G8 Ib	530,536
16.	δ Cep	213306	22 25.4	57 54	73	0	3.9- 5.0	5.4	F5 Ib-G2 Ib	298

NOTES TO TABLE 15

1. β Dor. Emission lines of Ca II have recently been found in the spectrum of this star by Gratton, Ap. J., 118, 570, 1953.

2. T Mon. Sanford states: "T Mon shows an emission component of H and K near maximum light. This lies to the violet of a deep rather narrow central absorption core."

3. W Gem. Violet-displaced Ca II emission lines have been found in the spectrum of this cepheid by R. P. Kraft at Lick.

9. YZ Sgr. Violet-displaced Ca II emission lines have been found in the spectrum of this star by R. P. Kraft at Lick.

12. SV Vul. Ca II emission lines have been found in the spectrum of this long-period cepheid by Sanford, who states: "SV Vulpeculae shows an emission component of H and K near light maximum. This lies to the violet of a deep rather narrow central absorption core."

LIST OF REFERENCES

General Catalogues

Henry Draper Catalogue, Harvard Ann., 91-99, 1918-1924.

Henry Draper Extension, Harvard Ann., 100, 112, 1925-1949.

General Catalogue of Stellar Radial Velocities, by R. E. Wilson ("Publications of the Carnegie Institution of Washington," No. 601 [Washington, 1953]).

Fifth Catalogue of Spectroscopic Binary Stars, by J. H. Moore and F. J. Neubauer, Lick Obs. Bull., 20, 1, 1948 (No. 521).

Académie des Sciences, Comptes Rendus

1. Secchi, P. Résultats fournis par l'analyse spectrale de la lumière d'Uranus, de l'étoile R des Gémeaux, et des taches solaires. 68, 761, 1869.
2. Deslandres, H., and Burson, V. Reconnaissance d'étoiles qui ont les mêmes raies brillantes de l'atmosphère que le Soleil. 172, 405, 1921.
3. _____. Reconnaissance de la couche supérieure dans quelques étoiles et comparaison avec le Soleil. 172, 729, 1921.
4. _____. Propriétés des étoiles qui ont les mêmes radiations et les mêmes couches de la chromosphère que le Soleil. 175, 121, 1922.
5. Grouiller, H. Le Spectre de Mira Ceti dans le violet et le proche ultraviolet. 214, 211, 1942.
6. _____. Bandes moléculaires dans le violet et le proche ultraviolet dans le spectre de Mira Ceti. 214, 256, 1942.
7. Daudin, A., and Fehrenbach, C. L'Isotope C^{13} du carbone dans les étoiles de class R et N. 222, 1083, 1946 (Haute-Provence Pub., Vol. 1, Ser. B, No. 2).
8. Bloch, M.; Dufay, J.; Fehrenbach, C.; and Tcheng, M. Les Raies brillantes de la couronne solaire dans le spectre de nova T Coronae Borealis. 223, 72, 1946 (Haute-Provence Pub., Vol. 1, Ser. B, No. 3).
9. Bloch, M.; Fenrenbach, C.; and Tcheng, M. Le Spectre continu de nova T Coronae Borealis en 1946. 223, 196, 1946 (Haute-Provence Pub., Vol. 1, Ser. B, No. 4).
10. Bloch, M. Le Spectre de nova T Coronae Borealis en février 1947. 224, 802, 1947 (Haute-Provence Pub., Vol. 1, Ser. B, No. 5).
11. Bouigue, R., and Fehrenbach, C. Sur le spectre des étoiles carbonées. 229, 1207, 1949 (Haute-Provence Pub., Vol. 1, Ser. B, No. 26).
12. Jehoulet, D. RU Cam. Céphéide probable de type II. 236, 663, 1953.

Académie Royale de Belgique, Bulletins

13. Crespin, D., and Swensson, J. W. Le Spectre ultraviolet de l'étoile supergéante 3 Puppis. Ser. 5, 38, 376, 1952 ("Liège 8° Coll.," No. 343).

American Astronomical Society, Publications

14. Frost, E. B. Observations of Radial Velocities. 1, 243, 1905 (Science, 23, 449, 1906).
15. Sanford, R. F. Spectrum of Bailey's Variable Star No. 95 in the Globular Cluster M3. 4, 47, 1918 (Pop. Astr., 27, 99, 1919).
16. Adams, W. S., and Joy, A. H. The Spectra of Some Variable Stars. 4, 138, 1920 (Pop. Astr., 28, 513, 1920).
17. Frost, E. B. On Some "Irreconcilables" among Stellar Radial Velocities. 4, 217, 1920 (Pop. Astr., 29, 158, 1921).

18. Adams. W. S., and Joy, A. H. Spectroscopic Notes on Some Variable Stars. 4, 305, 1921 (Pop. Astr., 30, 102, 1922).

19. Lampland, C. O. The Discovery of Faint Nebular Structure around R Aquarii. 4, 319, 1921 (Pop. Astr., 30, 162, 1922).

20. Jordan, M. F. The Variable Star SX Herculis. 4, 362, 1922 (Pop. Astr., 30, 615, 1922).

21. Joy, A. H. The Spectrum of o Ceti at Minimum. 5, 14, 1922 (Pop. Astr., 31, 237, 1923).

22. _____. Radial Velocity Measurements of the Spectrum of o Ceti. 5, 64, 1923 (Pop. Astr., 31, 645, 1923).

23. Curtiss, R. H. Changes in the Magnitude and Spectrum of R Scuti. 5, 143, 1923 (Pop. Astr., 32, 220, 1924).

24. Lampland, C. O. The Variable Nebula NGC 2261. 5, 390, 1926 (Pop. Astr., 34, 621, 1926).

25. Elvey, C. T. Contours of Some Lines in the Spectrum of 7 ε Aurigae. 6, 226, 1928 (Pop. Astr., 37, 265, 1929).

26. McLaughlin, D. B. Note on the Light and Velocity Curves of Epsilon Aurigae. 6, 271, 1929 (Pop. Astr., 38, 29, 1930).

27. Cannon, A. J. Omicron Ceti: Photographic Light Curve and Spectroscopic Notes. 6, 338, 1929 (Pop. Astr., 38, 401, 1930).

28. Struve, O., and Elvey, C. T. Note on the Spectrum of 7 ε Aurigae. 6, 349, 1929 (Pop. Astr., 38, 411, 1930).

29. McLaughlin, D. B. The Eclipse of Epsilon Aurigae. 6, 368, 1930 (Pop. Astr., 38, 601, 1930).

30. _____. Note on the Spectrum of Mu Cephei. 6, 369, 1930 (Pop. Astr., 39, 14, 1931).

31. Struve, O., and Elvey, C. T. Note on the Spectrum of 7 Epsilon Aurigae. 6, 376, 1930 (Pop. Astr., 39, 21, 1931).

32. McLaughlin, D. B. Spectroscopic Notes on Semi-regular Variables. 7, 94, 1931.

33. _____. The Velocity and Light Curves of Mu Cephei and Eta Geminorum. 7, 178, 1932.

34. Berman, L. The Spectrum of R Coronae Borealis. 7, 212, 1933.

35. Harper, W. E., and Christie, W. H. Note on the Variable VV Cephei. 8, 9, 1933.

36. Hogg, F. S. Recent Variations in the Spectrum of Z Andromedae. 8, 14, 1933.

37. McLaughlin, D. B. Notes on Light Curves and Spectra of Irregular Variable Stars. 8, 15, 1933.

38. Berman, L. The Spectrum Analysis of the Hot Carbon Star, R Coronae Borealis. 8, 107, 1934.

39. Merrill, P. W. Spectral Peculiarities of R Aquarii. 8, 119, 1934.

40. Gaposchkin, S. The Eclipsing Star VV Cephei. 9, 39, 1937.

41. Joy, A. H. Spectrographic Observations of Barnard's Variable Star in Messier 3. 9, 45, 1937.

42. McLaughlin, D. B. Extensive Stellar Atmospheres. 9, 50, 1937.

43. Goedicke, V. A. Recent Spectrographic Observations of VV Cephei. 9, 122, 1937.

44. McLaughlin, D. B. The Velocity Curves of R Scuti. 9, 126, 1937.

45. Goedicke, V. A. The Structure of the Atmosphere of VV Cephei. 9, 154, 1938.

46. Adams, W. S., and Joy, A. H. The Behavior of the Calcium H and K Lines in the Spectrum of ζ Geminorum. 9, 254, 1939.

47. Lampland, C. O. Hubble's Variable Nebula, NGC 2261, during the Interval 1918-1939. 9, 264, 1939.

48. Elvey, C. T., and Babcock, H. W. The Spectrum of Z Camelopardalis and of Other U Geminorum-Type Variables. 10, 51, 1940.

49. Hynek, J. A. Three New Emission Line Stars. 10, 56, 1940.

50. Sanford, R. F. Spectral Changes in U Cygni and UV Aurigae between Minimum and Maximum. 10, 114, 1941.

51. McLaughlin, D. B. The Semi-regular Variable Stars. 10, 116, 1941.

52. Scott, R. M. The Pulsation Theory for Long-Period Variables. 10, 144, 1941.

53. Goedicke, V. A. Atmospheric Velocities in VV Cephei. 10, 162, 1941.

54. Hall, J. S. Spectrophotometric Observations of o Ceti near Minimum Light in the Infrared Region of the Spectrum. 10, 163, 1941.

55. Scott, R. M. The Spectrophotometry of Mira Ceti. 10, 172, 1941.

56. _____. The Behavior of Hε in Mira Ceti. 10, 234, 1941.

57. McKellar, A., and Stillwell, W. H. The λ 6708 Li I Line in the Spectra of the Red Carbon Stars. 10, 254, 1942.

58. Popper, D. M. Remark concerning RT Lacertae. 10, 292, 1942.

American Philosophical Society, Proceedings

59. Payne-Gaposchkin, C. Variable Stars: A Plan of Study. 81, 189, 1939 (Harvard Repr., No. 170).

Annales d'Astrophysique

60. Barbier, D., and Chalonge, D. Etude du rayonnement continu de quelques étoiles entre 3100 et 4600 Å. IV. 4, 30, 1941.

61. Fehrenbach, C. Le Spectre de l'étoile rouge J 2001. 8, 26, 1945 (Haute-Provence Pub., Vol. 1, Ser. A, No. 5).

62. Struve, O. Emission Lines of Ca II in Eclipsing Binaries. 9, 1, 1946.

63. Bloch, M.; Dufay, J.; Fehrenbach, C.; and Tcheng, M. Étude préliminaire du spectre de nova T Coronae Borealis en 1946. 9, 157, 1946 (C.R., 223, 134, 1946; Haute-Provence Pub., Vol. 1, Ser. A, No. 10).

64. Barbier, D.; Chalonge, D.; and Canavaggia, R. Étude du rayonnement continu de quelques étoiles entre 3100 et 4600 Å. V. 10, 195, 1947 (Inst. d'Astrophysique Contr., Ser. B, No. 16).

65. Fehrenbach, C. Le Spectre de l'étoile variable DH Orionis. 11, 223, 1948.

66. Tcheng, M. Le Spectre de Z Andromedae. 12, 264, 1949 (C.R., 229, 348, 1949; Haute-Provence Pub., Vol. 1, Ser. A, No. 24).

67. _____. Le Spectre de AG Pegasi. 13, 51, 1950 (Haute-Provence Pub., Vol. 1, Ser. A, No. 25).

68. _____. Le Spectre de Khi Cygni, peu avant le maximum d'éclat de 1948. 13, 57, 1950 (C.R., 229, 1301, 1949; Haute-Provence Pub., Vol. 1, Ser. A, No. 18).

69. Swings, P. Le Spectre de l'étoile supergéante 1 Puppis de classe cA2ep. 13, 114, 1950 ("Liège 4° Coll.," No. 22).

70. _____. The Shell Spectrum of BD-14°1971 (PGC 1985) in 1947. 13, 134, 1950 ("Liège 4° Coll.," No. 23).

71. Struve, O. The Emission Lines of Ca II in the Spectrum of Capella. 14, 245, 1951.

72. Bloch, M., and Tcheng, M. Mesures spectrophotométriques de Z Andromedae. 14, 266, 1951 (Haute-Provence Pub., Vol. 2, No. 27).

73. Grandjean, J. Le Spectre de nova RT Serpentis 1909 en 1950. 15, 7, 1952 ("Liège 4° Coll.," No. 33).

74. Tcheng, M., and Bloch, M. Le Spectre de RY Scuti. 15, 12, 1952 (Haute-Provence Pub., Vol. 2, No. 36).

75. _____ Le Spectre de AG Pegasi. 15, 104, 1952 (C.R., 234, 810, 1952; Haute-Provence Pub., Vol. 2, No. 38).

76. Bloch, M., and Tcheng, M. Spectrophotométrie de T Coronae Borealis de 1946 à 1952. 16, 73, 1953.

Ann Arbor, University of Michigan, Publications

77. Merrill, P. W. Spectroscopic Observations of Stars of Class Md. 2, 45, 1916.

78. Rufus, W. C. Typical Stellar Spectra. 3, 257, 1923.

79. McLaughlin, D. B. A Note on the Spectrum of Nova Ophiuchi No. 3 (RS Ophiuchi). 5, 119, 1934.

80. _____. A Spectrographic Study of R Scuti. 7, 57, 1938.

81. Goedicke, V. A Study of the Spectrum of VV Cephei. 8, 1, 1939.

82. McLaughlin, D. B. Spectrographic Studies of Two Semi-regular Variable Stars: W Cygni and RS Cancri. 8, 107, 1941.

Astronomical Journal

83. McLaughlin, D. B. Note on the Relation of Light and Velocity Curves of Variable Stars. 40, 16, 1929.

84. Gaposchkin, S. UX Monocerotis, an Eclipsing System with Thick Atmosphere. 52, 42, 1946.

85. McLaughlin, D. B. The Nova-like Variable Star HV 11976. 52, 109, 1946.

86. Payne-Gaposchkin, C.; Gaposchkin, S.; and Mayall, M. The Variations of ρ Cassiopeiae. 52, 123, 1947.

87. Popper, D. M. The Spectrum of ρ Cassiopeiae. 52, 129, 1947.

88. Hiltner, W. A. Remark concerning XY Puppis. 53, 158, 1948.

89. Gratton, L. The Radial Velocity of λ Andromedae from the Ca II Emission Lines. 54, 38, 1948.

90. Struve, O., and Rudkjøbing, M. Stellar Spectra in the Region of the Obscuring Clouds of Ophiuchus and Scorpius. 54, 51, 1948.

91. Wright, K. O., and van Dien, E. The Spectrum of ϵ Aurigae, 1946-1948. 54, 53, 1948.

92. Lampland, C. O., and Ashbrook, J. The Nebular Variable R Monocerotis. 54, 91, 1949.

93. Haro, G. Faint Spectra Showing Hα in Emission in the Obscuring Clouds of Ophiuchus and Scorpius and in a Region in Sagittarius. 54, 188, 1949.

94. Mayall, M. W. Six Novae, One with a Late-Type Spectrum. 54, 191, 1949.

95. Herbig, G. H. Remark concerning EX Lupi. 54, 228, 1949.

96. Greenstein, J. L. The Spectrum of ν Sagittarii. 55, 72, 1950.

97. Haro, G. Faint Stars with Strong Emission in and around the Orion Nebula. 55, 72, 1950.

98. Keenan, P. C. Bands in the Photographic Infrared Spectra of S-Type Stars. 55, 74, 1950.

99. _____. Temperature Classification of the S-Type Stars. 55, 172, 1950.

100. Bidelman, W. P. Remark concerning KN Cassiopeiae. 55, 213, 1951.

101. Wildt, R. New Emission Lines in M Dwarfs. 56, 51, 1951.

102. Struve, O. Recent Progress in Stellar Spectroscopy. 56, 114, 1951.

103. Bidelman, W. P. Remarks concerning SX Pegasi and R Capricorni. 56, 177, 1951.

104. _____. Remarks concerning υ Sagittarii. 56, 179, 1951.

105. Buscombe, W., and Merrill, P. W. Variation of Intensities of Atomic Absorption Lines in the Spectrum of Mira Ceti. 57, 8, 1952.

106. Joy, A. H. Recent Radial Velocity Measures of Mira. 57, 16, 1952.

107. Abt, A. An Analysis of W Virginis. 57, 158, 1952.

108. Bidelman, W. P. Remark concerning ρ Cassiopeiae. 57, 203, 1952.

109. Beardsley, W. R. The Spectrum of ρ Cassiopeiae. 58, 34, 1953.

Astronomical Journal of the Soviet Union

110. Parenago, P. On the System of Eta Carinae. 14, 339, 1937.

Astronomical Society of Japan, Publications

111. Fujita, Y. Spectrophotometry of Chi Cygni. 4, 81, 1952 (Tokyo Repr., No. 100).

Astronomical Society of South Africa, Monthly Notes

112. Feast, M. W. The Spectrum of Mira Ceti during the Minimum of 1952-1953. 12, 55, 1953.

Astronomical Society of the Pacific, Publications

113. Adams, W. S., and Pease, F. G. The Spectra of Ten Stars of Very Low Luminosity. 26, 258, 1914.

114. Adams, W. S. Three Stars with Bright Hydrogen Lines. 26, 260, 1914.

115. Adams, W. S., and Pease, F. G. The Spectrum of T Tauri. 27, 132, 1915.

116. Curtis, H. D. Note on Hind's Variable Nebula. 27, 242, 1915.

117. Adams, W. S., and Joy, A. H. Note on the Spectrum of o Ceti. 29, 112, 1917.

118. _____. Note on the Identification of Certain Bright Lines in the Spectrum of o Ceti. 30, 193, 1918.

119. _____. Spectroscopic Notes. 30, 306, 1918.

120. Joy, A. H. The Spectrum of RU Camelopardalis. 31, 180, 1919.

121. Adams, W. S., and Joy, A. H. Eighteen Stars with Spectra Similar to Those of the Cepheid Variables. 31, 184, 1919.

122. Merrill, P. W. A Variable Star with a Peculiar Spectrum. 31, 305, 1919.

123. Wright, W. H. Comments on the Occurrence of Nebular Lines in the Spectrum of R Aquarii. 31, 309, 1919.

124. Moore, J. H. The Nebular Line 3869 in R Aquarii. 31, 309, 1919.

125. Shane, C. D. The H α Line in o Ceti. 31, 318, 1919.

126. Sanford, R. F. The Spectrum of T Tauri. 32, 59, 1920.

127. Adams, W. S., and Joy, A. H. The Spectrum of the Companion to Castor and of W. B. 16^h906. 32, 158, 1920.

128. _____. Changes in the Spectrum of Omicron Ceti. 32, 163, 1920.

129. Shane, C. D. Observations of the Spectrum of o Ceti in 1919. 32, 234, 1920.

130. Merrill, P. W. The Spectrum of R Aquarii at Minimum Brightness. 32, 247, 1920.

131. Adams, W. S., and Joy, A. H. The Spectrum of o Ceti near Minimum of Light. 33, 107, 1921.

132. Merrill, P. W. Note on the Spectrum of R Cygni. 33, 206, 1921.

133. Adams, W. S., and Joy, A. H. The Spectra of Three M-Type Stars with Bright Lines. 33, 263, 1921.

134. Lundmark, K. The Spectrum of Nova T Coronae. 33, 271, 1921.

135. Leonard, F. C. Note on the Spectrum of Component C in the Triple System o^2 Eridani. 33, 272, 1921.

136. _____. Second Note on the Spectrum of o^2 Eridani C. 33, 323, 1921.

137. Humason, M. L. Discovery of Bright Hydrogen Lines in the Spectrum of the Variable Star W Cephei. 34, 58, 1922.

138. _____. An M-Type Star Whose Spectrum Contains Bright Lines. 34, 133, 1922.

139. Merrill, P. W. The Nebular Line λ 4658 in Stellar Spectra. 34, 134, 1922.

140. Campbell, W. W. Stars Whose Radial Velocities Vary. 34, 167, 1922.

141. Luyten, W. J. Note on the Variable Star V24 = SX Herculis. 34, 171, 1922.

142. Adams, W. S., and Joy, A. H. A List of Dwarf M-Type Stars. 34, 174, 1922.

143. Adams, W. S.; Joy, A. H.; and Humason, M. L. The Wavelengths of Certain Bright Lines in the Spectra of Some M-Type Stars. 34, 175, 1922.

144. Lampland, C. O. Observations of the Faint Nebular Structure around R Aquarii. 34, 218, 1922.

145. Lundmark, K. Proper Motion and Hypothetical Parallax of Nova T Coronae 1866. 34, 225, 1922.

146. Luyten, W. J. A List of New and Suspected Dwarfs of Class M. 34, 342, 1922 (Lick Obs. Bull., 11, 127, 1924).

147. Joy, A. H. Spectroscopic Observations of R Scuti. 34, 349, 1922.

148. Adams, W. S., and Joy, A. H. The Identification of Certain Low Temperature Lines in the Spectrum of o Ceti. 35, 168, 1923.

149. Merrill, P. W. Long-Period Variables Having High Radial Velocities. 35, 171, 1923.

150. _____. Zirconium Bands in Stellar Spectra of Class S. 35, 217, 1923.

151. Perrine, C. D. Spectroscopic Notes on Southern Clusters, Nebulae, and Red Stars. 35, 229, 1923.

152. Merrill, P. W. Two Stars of Class F Having the $H\alpha$ Bright Line. 35, 263, 1923.

153. Joy, A. H., and Humason, M. L. The Spectrum of R Coronae at Minimum. 35, 325, 1923.

154. Adams, W. S.; Joy, A. H.; and Sanford, R. F. Ninety-seven Stars with Variable Velocity. 36, 137, 1924.

155. Adams, W. S., and Joy, A. H. The H and K Lines in the Spectrum of 61^1 Cygni. 36, 142, 1924.

156. Joy, A. H. The Spectrum of the Close Companion to o Ceti. 36, 290, 1924.

157. Sanford, R. F. Notes on Stars of Spectral Classes R, N, and S. 36, 351, 1924.

158. Allen, L. B. Two Red Variable Stars with High Velocities. 37, 94, 1925.

159. Joy, A. H. The Spectrum and Radial Velocity of W Virginis. 37, 156, 1925.

160. Adams, W. S.; Joy, A. H.; and Humason, M. L. An Additional Star of the W Cephei Type of Spectrum. 37, 161, 1925.

161. Adams, W. S., and Joy, A. H. A List of Stars with Radial Velocities Exceeding 50 Km/Sec. 38, 121, 1926.

162. Merrill, P. W. Note on the Spectrum of UV Aurigae. 38, 175, 1926.

163. Sanford, R. F. Two Bands in Spectra of Class N. 38, 177, 1926.

164. Merrill, P. W. S-Type Features in the Spectrum of χ Cygni. 38, 329, 1927.

165. _____. Changes in the Spectrum of R. Aquarii. 39, 48, 1927.

166. van Maanen, A.; Brown, J. A.; and Humason, M. L. A Star of Extremely Low Luminosity. 39, 173, 1927.

167. Merrill, P. W., and Humason, M. L. Note on Very Cool Stars. 39, 198, 1927.

168. Joy, A. H. The Spectrum and Velocity Curve on W Serpentis. 39, 234, 1927.

169. Sanford, R. F. On the Radial Velocity and Spectrum of the Variable Star RU Camelopardalis. 39, 235, 1927.

170. Leonard, F. C. The Spectrum of the Fainter Component of Krüger 60. 39, 362, 1927.

171. Adams, W. S.; Humason, M. L.; and Joy, A. H. Observations of Faint Spectra. 39, 365, 1927.

172. Merrill, P. W. Notes on the Spectra of Long-Period Variable Stars. 40, 268, 1928.

173. Joy, A. H. Spectroscopic Observations of U Sagittae during Eclipse. 40, 268, 1928.

174. Baxandall, F. E. Absorption Bands of Scandium Oxide in the Spectrum of o Ceti. 41, 168, 1929.

175. Adams, W. S., and Joy, A. H. Bright H and K Lines in the Spectra of Some Giant Stars. 41, 311, 1929.

176. _____. Note on Bright H and K Lines in the Spectra of Some Giant Stars. 41, 372, 1929.

177. Adams, W. S., and Sanford, R. F. Note on the Spectrum of ϵ Aurigae. 42, 203, 1930.

178. Humason, M. L., and Christie, W. H. Note on Two F-Type Stars with Bright Lines. 42, 252, 1930.

179. Sanford, R. F. Note on the Difference in Radial Velocity from Emission and Absorption Lines for Stars of Spectral Classes R and N. 42, 287, 1930.

180. Adams, W. S., and Joy, A. H. Giant and Dwarf Stars with Bright H and K Lines. 43, 407, 1931.

181. Merrill, P. W., and Humason, M. L. A Bright Line of Ionized Helium, λ 4686, in Three Stellar Spectra with Titanium Bands. 44, 56, 1932.

182. Berman, L. The Spectrum and Temperature of T Coronae (Nova 1866). 44, 318, 1932.

183. Hogg, F. S. On the Presence of Titanium Oxide Bands in the Spectrum of Z Andromedae. 44, 328, 1932.

184. Joy, A. H. Notes on the Spectra of Certain Variable Stars. 44, 385, 1932.

185. Sanford, R. F. Seven Stars of Spectral Class N with Emission Lines of Hydrogen. 45, 44, 1933.

186. Berman, L. Note on the Radial Velocity of R Coronae Borealis. 45, 55, 1933.

187. Adams, W. S., and Joy, A. H. The Spectrum of RS Ophiuchi (Nova Ophiuchi No. 3). 45, 249, 1933.

188. Wright, W. H., and Neubauer, F. J. Notes on the Spectrum of Nova Ophiuchi No. 3. 45, 252, 1933.

189. Christie, W. H. Note on the Variable Velocity of VV Cephei (Boss 5650). 45, 258, 1933.

190. Adams, W. S., and Joy, A. H. Coronal Lines in the Spectrum of RS Ophiuchi. 45, 301, 1933.

191. Merrill, P. W.; Sanford, R. F.; and Burwell, C. G. Additional Stars of Classes N and S. 45, 306, 1933.

192. Joy, A. H. Intersteller Lines Observed in Spectra of Stars of Late Type. 46, 51, 1934.

193. Berman, L. Abnormal Abundance of Carbon in the Atmosphere of R Coronae and Its Effect upon the Light Variation. 46, 60, 1934.

194. Adams, W. S., and Joy, A. H. The Present Spectrum of RS Ophiuchi. 46, 223, 1934.

195. Davis, D. N. The Spectral Sequence in Stars of Class S. 46, 267, 1934.

196. Merrill, P. W. Forbidden Lines in the Spectrum of R Aquarii. 46, 296, 1934.

197. Sanford, R. F. Class N Stars with Exceptional Sodium Lines. 47, 101, 1935.

198. Lampland, C. O. Hind's Variable Nebula (NGC 1555). 48, 318, 1936.

199. Christie, W. H. Note on the Spectrum of VV Cephei. 50, 52, 1938.

200. Wilson, O. C. H ϵ Emission in the Spectrum of Arcturus. 50, 245, 1938.

201. Joy, A. H. Recent Spectral Changes in T Coronae. 50, 300, 1938.

202. Minkowski, R. Note on the Spectrum of T Coronae. 51, 54, 1939.

203. Slipher, V. M. The Spectrum of the Variable Nebula NGC 2261. 51, 115, 1939.

204. Struve, O., and Elvey, C. T. The Spectrum of Z Andromedae. 51, 297, 1939.

205. Merrill, P. W. Notes on Bands in the Visual Region of the Spectra of Long-Period Variable Stars. 51, 356, 1939.

206. Swings, P. New Emission Lines in Mira Ceti. 52, 143, 1940.

207. Swings, P.; Elvey, C. T.; and Struve, O. The Spectrum of T Coronae. 52, 199, 1940.

208. Davis, D. N. The ScO Band at λ 4858 in o Ceti. 52, 207, 1940.

209. Joy, A. H. Spectroscopic Observations of SS Cygni Variables. 52, 324, 1940.

210. Sanford, R. F. Ca_2 Bands in the Spectrum of U Cygni. 52, 325, 1940.

211. McKellar, A. Intense λ 6708 Resonance Doublet of Li I in the Spectrum of WZ Cassiopeiae. 52, 407, 1940.

212. Joy, A. H. Radial Velocities and Absolute Dimensions of the Eclipsing Variable WW Draconis. 53, 230, 1941.

213. Swings, P., and Struve, O. On the Emission Lines in the Spectrum of BD+20°2465. 53, 244, 1941.

214. Sanford, R. F. Spectral Classification of Five Red Variables. 53, 290, 1941.

215. Joy, A. H., and Humason, M. L. Dwarf Stars with Emission Lines of Hydrogen and Calcium. 53, 296, 1941.

216. Wirtanen, C. A. A New dMe Double Star. 53, 340, 1941.

217. Merrill, P. W. The Spectrum of RU Lupi. 53, 342, 1941.

218. Joy, A. H. The "Nova-like" Variable UZ Tauri. 54, 33, 1942.

219. Merrill, P. W.; Sanford, R. F.; and Burwell, C. G. Additional Stars of Classes N and S. Second List. 54, 107, 1942.

220. Vyssotsky, A. N. Seven New S-Type Stars. 54, 153, 1942.

221. Merrill, P. W. Five Bright-Line Stars of Class F. 54, 155, 1942.

222. Sanford, R. F. Evidence of Chlorine in U Cygni. 54, 158, 1942.

223. Joy, A. H. The Spectrum of UZ Tauri in 1942. 55, 38, 1943.

224. Minkowski, R. Nova T Coronae Borealis. 55, 101, 1943.

225. Vyssotsky, A. N. Spectral Classification of 25 Red Variables. 55, 198, 1943.

226. Joy, A. H. A New Dwarf Me Star near BD+30°4824. 55, 242, 1943.

227. Janssen, E. M., and Vyssotsky, A. N. A Peculiar Emission-Line Object. 55, 244, 1943.

228. _____ Seven New S-Type Stars. 55, 245, 1943.

229. Swings, P. Forbidden Lines of Ionized Nickel in the Spectra of Bright-Line Stars. 55, 276, 1943.

230. Wilson, R. E. The Spectrum of BD+67°922. 55, 282, 1943.

231. Joy, A. H. AE Aquarii: An SS Cygni Variable and Spectroscopic Binary. 55, 283, 1943.

232. Leonard, F. C. The Spectra of the Double Star β543= ADS 2894. 56, 38, 1944.

233. _____. Second Note on the Spectra of the Double Star β543. 56, 85, 1944.

234. Pettit, M. S. The Long-Period Variable Star RT Cygni. 56, 107, 1944.

235. Sanford, R. F. Emission Lines in the Spectrum of UV Aurigae. 56, 122, 1944.

236. Leonard, F. C. The Spectrum of the Double Star β468= ADS 12882. 56, 202, 1944.

237. Sanford, R. F. Velocity Changes in Long-Period Variables of Spectral Class Ne. 56, 237, 1944.

238. Swings, P. Forbidden Lines of Cr II, Ni II, and Fe II. 56, 242, 1944.

239. Herbig, G. H. Emission Lines of Fe I in RW Aurigae. 57, 166, 1945.

240. Merrill, P. W. Level of Hydrogen Emission in the Atmospheres of Me Variable Stars. 57, 178, 1945.

241. van Maanen, A. Variable Star with Faint Absolute Magnitude. 57, 216, 1945.

242. Sanford, R. F. Bright H and K in the Spectrum of SS Boötis. 57, 217, 1945.

243. Wilson, R. E. The Spectrum of BD+67°922. 57, 309, 1945.

244. Vyssotsky, A. N., and Miller, W. J. Five New S Stars. 58, 53, 1946.

245. Vyssotsky, A. N. Spectral Classification of 40 Red Variables. Second List. 58, 53, 1946.

246. Sanford, R. F. The Spectrum of T Coronae Borealis, Feb. 10-22, 1946. 58, 156, 1946.

247. McLaughlin, D. B. The Spectrum of T Coronae Borealis in 1946 and 1866. 58, 159, 1946.

248. Herbig, G. H. A Possible T Tauri Variable in the Diffuse Nebula NGC 1999. 58, 163, 1946.

249. Hiltner, W. A. Ca II Emission in RZ Cancri. 58, 166, 1946.

250. Herbig, G. H., and Neubauer, F. J. The Spectrum of T Coronae Borealis at the 1946 Maximum. 58, 196, 1946.

251. Salanave, L. E. The Spectrum of T Coronae Borealis. 58, 238, 1946.

252. Sanford, R. F. Velocities for the System of Nova T Coronae Borealis. 58, 240, 1946.

253. Thackeray, A. D. The Bright Lines Fe 4063, 4132 in T Tauri Variables and in the Solar Chromosphere. 58, 301, 1946.

254. Merrill, P. W. Level of Iron Emission in the Atmospheres of Me Variable Stars. 58, 304, 1946.

255. Minkowski, R. New Emission Nebulae. 58, 305, 1946.

256. Greenstein, J. L., and Struve, O. Spectra of Variable Stars in the Orion Nebula. 58, 366, 1946.

257. McLaughlin, D. B. Some Anomalies in the Behavior of λ 4686 He II in the Spectra of Novae. 59, 81, 1947.

258. Sanford, R. F. Changes in the Spectrum and Velocity of Nova T Coronae Borealis. 59, 87, 1947.

259. _____. High-Dispersion Spectrogram of T Tauri. 59, 134, 1947.

260. _____. The Spectrum of BD+9°1633. 59, 136, 1947.

261. Greenstein, J. L., and Aller, L. H. Spectra of Stars in Diffuse Nebulae. 59, 139, 1947.

262. Greenstein, J. L.; Bidelman, W. P.; and Popper, D. M. Variable 27 in the Globular Cluster Messier 68. 59, 143, 1947.

263. Wright, K. O. Curves of Growth for Epsilon Aurigae. 59, 171, 1947.

264. Sanford, R. F. The Spectrum of RS Ophiuchi with High Dispersion. 59, 331, 1947.

265. _____. Lanthanum in Variable Stars of Class N. 59, 333, 1947.

266. Struve, O., and Swings, P. An Unusual Stellar Species. 60, 61, 1948.

267. Deutsch, A. J. Notes on the Spectrum of T Coronae Borealis. 60, 120, 1948.

268. McLaughlin, D. B. Changes in the Spectrum of Boss 1985. 60, 200, 1948.

269. Popper, D. M. Spectra of Long-Period Eclipsing Binaries. 60, 248, 1948.

270. Herbig, G. H. The Irregular Variable RW Aurigae and Related Objects. 60, 256, 1948.

271. Merrill, P. W. A Rapidly Rotating G-Type Star. 60, 382, 1948.

272. McKellar, A. The 4,0 Isotopic $C^{13}N$ Band of the Red CN System in Spectra of Classes R and N. 61, 34, 1949.

273. Sanford, R. F. Spectral Types and Radial Velocities of 21 Red Stars. 61, 43, 1949 (Mt. W. and P. Repr., No. 1).

274. McLaughlin, D. B. The "Transition" Stage of Novae. 61, 74, 1949.

275. Joy, A. H., and Humason, M. L. Observations of the Faint Dwarf Star L 726-8. 61, 133, 1949 (Mt. W. and P. Repr., No. 4).

276. Sanford, R. F. Double Absorption Lines in the Spectrum of W Virginis. 61, 135, 1949 (Mt. W. and P. Repr., No. 4).

277. _____. Phases for Emission Lines in the Spectrum of UV Aurigae. 61, 261, 1949 (Mt. W. and P. Repr., No. 13).

278. Wilson, R. E. The Spectrum of HD 4174. 62, 14, 1950 (Mt. W. and P. Repr., No. 19).

279. Sanford, R. F. Velocity Variation from λ 4481 of Mg II in V367 Cygni. 62, 21, 1950 (Mt. W. and P. Repr., No. 19).

280. Kron, G. E. Emission-Line Variability in Dwarf Stars. 62, 141, 1950.

281. Herbig, G. H. The Spectra of Five Irregular Variable Stars. 62, 211, 1950.

282. Jacobsen, T. S. Note on the H and K Lines of Ca II in Eta Aquilae. 62, 269, 1950.

283. Babcock, H. W. Magnetic Field of a Late-Type Star, HD 4174. 62, 277, 1950 (Mt. W. and P. Repr., No. 37).

284. McNamara, D. H. The Spectrum of U Sagittae at Minimum Light. 63, 38, 1951.

285. Struve, O. Notes on Stellar Spectra. 63, 138, 1951 (Berkeley Repr., No. 10).

286. Buscombe, W., and Merrill, P. W. Relative Intensities of Lines of Various Metals in Spectra of Classes Me and Se. 63, 235, 1951 (Mt. W. and P. Repr., No. 56).

287. Poveda, A. Systematic Displacements of Absorption Lines in ε Aurigae. 63, 254, 1951.

288. Merrill, P. W., and Bowen, I. S. The Spectrum of RS Ophiuchi in May 1951. 63, 255, 1951 (Mt. W. and P. Repr., No. 56).

289. Struve, O. Notes on Stellar Spectra. II. 64, 20, 1952 (Berkeley Repr., No. 15).

290. Greenstein, J. L. Some Emission-Line G-Type Stars. 64, 71, 1952.

291. Struve, O. Notes on Stellar Spectra. III. 64, 117, 1952 (Berkeley Repr., No. 19).

292. Bidelman, W. P. The Ultraviolet Spectrum of U Cygni. 64, 133, 1952.

293. Sanford, R. F. The Widening or Doubling of Lines in the Spectra of Variable Stars. 64, 135, 1952.

294. McLaughlin, D. B. The Atmospheric Eclipses of Four Supergiant Binary Systems. 64, 173, 1952.

295. Struve, O. Notes on Stellar Spectra. IV. 64, 180, 1952 (Berkeley Repr., No. 20).

296. Aller, L. H. Nova-like Variables with Combination Spectra. 64, 228, 1952.

297. McLaughlin, D. B.; Weston, E. B.; and Chadwick, M. A. Note on the Orbit of δ Sagittae. 64, 300, 1952.

298. Herbig, G. H. Emission Lines of Ca II in Classical Cepheid Variables. 64, 302, 1952.

299. Jacobsen, T. S. Radial-Velocity Curves of η Aquilae from the H and K Lines of Ca II. 64, 308, 1952.

300. Struve, O. Notes on Stellar Spectra. 65, 81, 1953 (Berkeley Repr., No. 40).

301. _____. Notes on Stellar Spectra. 65, 185, 1953 (Berkeley Repr., No. 48).

302. Merrill, P. W., and Lowen, L. The Gallium Line Lambda 4172 in Spectra of Long-Period Variable Stars. 65, 221, 1953.

Astronomische Nachrichten

303. Pickering, E. C. List of Peculiar Stars. 99, 375, 1881.

304. _____. Stars with Peculiar Spectra, Discovered at the Astronomical Observatory of Harvard College. 101, 73, 1881.

305. Pickering, E. C. Southern Stars Having Peculiar Spectra. 123, 95, 1889.

306. Fleming, W. P. Stars Having Peculiar Spectra. 125, 155, 1890.

307. _____. Stars Having Peculiar Spectra. 128, 11, 1891.

308. Pickering, E. C. A New Variable Star in Aries. 131, 61, 1892.

309. Espin, T. E. Stars with Remarkable Spectra. 133, 43, 1893.

310. _____. Stars with Remarkable Spectra. 134, 123, 1893.

311. Pickering, E. C. New Variable Stars in Sculptor, Scorpius, Ophiuchus, and Aquila. 135, 161, 1894.

312. Espin, T. E. Stars with Remarkable Spectra. 135, 265, 1894.

313. Fleming, W. P. Stars Having Peculiar Spectra. 137, 71, 1894.

314. Espin, T. E. Stars with Remarkable Spectra. 137, 369, 1895.

315. _____. Stars with Remarkable Spectra. 140, 241, 1896.

316. _____. Stars with Remarkable Spectra. 149, 129, 1899.

317. _____. Stars with Remarkable Spectra. 152, 135, 1900.

318. Eberhard, G. Über die Bewegung von χ Cygni im Visionsradius. 157, 341, 1902.

319. Pickering, E. C. Variabilis oder Nova 159.1904 Pegasi. 166, 173, 1904.

320. Ludendorff, H. Über die Radialbewegung von ε Aurigae. 171, 49, 1906.

321. _____. Untersuchungen über die Spektren der Sterne R Coronae Borealis, 12 Canum Venaticorum und 72 Ophiuchi. 173, 1, 1906.

322. _____. Bearbeitung der Schmidtschen Beobachtungen der Veränderlichen ε Aurigae. 192, 389, 1912.

323. Küstner, F. Radialgeschwindigkeiten von 227 Sternen des Spektraltypus F bis M beobachtet 1908 bis 1913 am Bonner 30 cm-Refraktor. 198, 409, 1914.

324. Guthnick, P. Weitere Ergebnisse photoelektrischer Messungen. 199, 177, 1914.

325. Schwassmann, A., and Wachmann, A. A. Var. WZ (247.1928) Draconis. 234, 411, 1929.

326. Becker, F. Zwei neue Me-Spektren. 235, 85, 1929.

327. Wachmann, A. A. Neue Veränderliche. 242, 381, 1931.

328. Becker, F. 1.1932 Coronae Australis. 245, 119, 1932.

329. Guthnick, P., and Prager, R. Benennung von veränderlichen Sternen. 249, 253, 1933.

330. Müller, R. RS=Nova 3 Ophiuchi. 249, 403, 1933.

331. _____. RS=Nova 3 Ophiuchi. 250, 143, 1933.

332. _____. RS=Nova 3 Ophiuchi. 250, 175, 1933.

333. Wachmann, A. A. Photographische Beobachtungen von Veränderlichen auf dem Kapteyn-Eichfeld 41. 255, 341, 1935.

334. Nielsen, A. V. RU Camelopardalis. 260, 377, 1936.

335. Hachenberg, O., and Wellmann, P. Ein Spektrum der Nova T Coronae Borealis. 266, 375, 1938.

336. Wellmann, P., and Hachenberg, O. Die Verfärbung des Veränderlichen 1.1939 Orionis. 268, 213, 1939.

337. Noll, H. H. Spektralphotometrische Untersuchungen des langperiodisch veränderlichen Sterns T Cephei. 268, 293, 1939.

338. Hinderer, F. Spektralphotometrische Untersuchungen über den Veränderlichen SS Cygni. 277, 193, 1949.

339. Miczaika, G. R. Spektrographische Beobachtungen von Be- und Ae-Sternen. III. 279, 19, 1950.

340. Beyer, M. Die Lichtwechsel des langperiodischen β Lyrae-Sterns BM Cassiopeiae. 280, 267, 1952.

Astronomische Nachrichten, Beobachtungs-Zirkulare

341. Guthnick, P.; Bernewitz, E.; and Pavel, F. R Aquarii. 1, 26, 1919.
342. Guthnick, P. R Aquarii. 1, 33, 1919.
343. Brück, H., and Müller, R. Spectrum of RS Ophiuchi. 15, 54, 1933.
344. Wachmann, A. A. Spectrum of RS Ophiuchi. 15, 55, 1933.
345. Gerasimovič, B. P. Spectrum of RS Ophiuchi. 15, 62, 1933.
346. Wachmann, A. A. Drei neue veränderliche Sterne. 21, 7, 1939.
347. _____. Ein neuer Veränderlicher mit ungewöhnlichem Spektrum. 21, 25, 1939.
348. Dieckvoss, W. 1.1939 Orionis (Wachmann). 21, 30, 1939.
349. Struve, O. 1.1939 Orionis. 21, 60, 1939.
350. Wellmann, P. Das Spektrum von Z Andromedae. 21, 105, 1939.

Astronomy and Astrophysics

351. Fleming, W. P. Stars Having Peculiar Spectra. New Variable Star in Lacerta, DM+39°4851. 11, 27, 1892 (A.N., 128, 121, 1891).
352. _____. Stars Having Peculiar Spectra. 11, 765, 1892 (A.N., 130, 125, 1892).
353. Pickering, E. C. Peculiar Stellar Spectra. 11, 945, 1892.
354. Fleming, W. P. Stars Having Peculiar Spectra. 12, 170, 1893.
355. _____. Stars Having Peculiar Spectra. 12, 546, 1893.
356. _____. Stars Having Peculiar Spectra. 12, 810, 1893.
357. _____. Stars Having Peculiar Spectra. 13, 501, 1894.

Astrophysical Journal

358. Pickering, E. C. Discovery of Variable Stars from Their Photographic Spectra. 1, 27, 1895.
359. Fleming, W. P. Stars Having Peculiar Spectra. 1, 411, 1895 (A.N., 138, 175, 1895).
360. _____. Stars Having Peculiar Spectra. 2, 354, 1895.
361. Campbell, W. W. Notes on the Spectrum of o Ceti. 9, 31, 1899.
362. Dunér, N. C. On the Spectra of Stars of Class IIIb. 9, 119, 1899.
363. Vogel, H. C. ϵ Aurigae, a Spectroscopic Binary. 17, 243, 1903.
364. Eberhard, G. On the Spectrum and Radial Velocity of χ Cygni. 18, 198, 1903.
365. Frost, E. B. Spectrographic Observations of Certain Variable Stars. 22, 213, 1905.
366. Slipher, V. M. Preliminary Note on the Spectrum of o Ceti. 25, 66, 1907.
367. _____. The Spectrum of Mira Ceti. 25, 235, 1907.
368. Cortie, A. L. The Variability in Light of Mira Ceti and the Temperature of Sun-Spots. 26, 123, 1907.
369. Eberhard, G., and Schwarzschild, K. On the Reversal of the Calcium Lines H and K in Stellar Spectra. 38, 292, 1913.
370. Merrill, P. W. The Radial Velocities of Stars of Class Md. 41, 247, 1915.
371. Adams, W. S. The Radial Velocities of Five Hundred Stars. 42, 172, 1915 (Mt. W. Contr., No. 105).
372. Hubble, E. P. The Variable Nebula NGC 2261. 44, 190, 1916.
373. Pease, F. G. Hind's Variable Nebula NGC 1555. 45, 89, 1917 (Mt. W. Contr., No. 127).

374. Hubble, E. P. Recent Changes in the Variable Nebula NGC 2261. 45, 351, 1917.

375. Adams, W. S., and Joy, A. H. The Luminosities and Parallaxes of Five Hundred Stars. 46, 313, 1917 (Mt. W. Contr., No. 142).

376. Adams, W. S.; Joy, A. H.; Strömberg, G.; and Burwell, C. G. The Parallaxes of 1646 Stars Derived by the Spectroscopic Method. 53, 13, 1921 (Mt. W. Contr., No. 199).

377. Merrill, P. W. Characteristic Behavior of the Bright Lines in Stellar Spectra of Class Md. 53, 185, 1921 (Mt. W. Contr., No. 200).

378. Sanford, R. F. The Orbits of Seven Spectroscopic Binaries. 53, 201, 1921 (Mt. W. Contr., No. 201).

379. Merrill, P. W. Observations of the Nebular Lines in the Spectrum of the Long-Period Variable Star R Aquarii. 53, 375, 1921 (Mt. W. Contr., No. 206).

380. Hubble, E. P. A General Study of Diffuse Galactic Nebulae. 56, 162, 1922 (Mt. W. Contr., No. 241).

381. Merrill, P. W. Stellar Spectra of Class S. 56, 457, 1922 (Mt. W. Contr., No. 252).

382. Adams, W. S., and Joy, A. H. The Radial Velocities of 3013 Stars. 57, 149, 1923 (Mt. W. Contr., No. 258).

383. Merrill, P. W. Spectroscopic Observations of Both Components of the Variable Double Star X Ophiuchi. 57, 251, 1923 (Mt. W. Contr., No. 261).

384. _____. The Radial Velocities of Long-Period Variable Stars. 58, 215, 1923 (Mt. W. Contr., No. 264).

385. Frost, E. B., and Lowater, F. Spectrographic Observations of Mira Ceti, R Leonis, T Cephei, and R Serpentis. 58, 265, 1923.

386. Sanford, R. F. Radial Velocities of Stars of Spectral Class R. 59, 339, 1924 (Mt. W. Contr., No. 276).

387. Merrill, P. W.; Humason, M. L.; and Burwell, C. G. Discovery and Observations of Stars of Class Be. 61, 389, 1925 (Mt. W. Contr., No. 294).

388. Joy, A. H. A Spectrographic Study of Mira Ceti. 63, 281, 1926 (Mt. W. Contr., No. 311).

389. Adams, W. S.; Joy, A. H.; and Humason, M. L. The Absolute Magnitudes and Parallaxes of 410 Stars of Type M. 64, 225, 1926 (Mt. W. Contr., No. 319).

390. Joy, A. H., and Sanford, R. F. The Dwarf Companion to Castor as a Spectroscopic Binary and Eclipsing Variable. 64, 250, 1926 (Mt. W. Contr., No. 320).

391. Merrill, P. W. Stellar Spectra of Class S. II. Changes in Spectra of Long-Period Variable Stars. 65, 23, 1927 (Mt. W. Contr., No. 325).

392. _____. Stars Whose Spectra Have Bright Iron Lines. 65, 286, 1927 (Mt. W. Contr., No. 334).

393. Russell, H. N. On the Relations between Period, Luminosity, and Spectrum among Cepheids. 66, 122, 1927 (Mt. W. Contr., No. 339).

394. Sanford, R. F. The Spectrum and Radial-Velocity Variation of RU Camelopardalis. 68, 408, 1928 (Mt. W. Contr., No. 372).

395. Merrill, P. W., and Joy, A. H. Spectroscopic Observations of R Virginis. 69, 379, 1929 (Mt. W. Contr., No. 382).

396. Adams, W. S.; Joy, A. H.; Sanford, R. F.; and Strömberg, G. The Radial Velocities of 741 Stars. 70, 207, 1929 (Mt. W. Contr., No. 387).

397. Struve, O., and Elvey, C. T. Preliminary Results of Spectrographic Observations of 7 ϵ Aurigae. 71, 136, 1930.

398. Merrill, P. W., and Burwell, C. G. Behavior of Bright Lines in the Spectra of Several Long-Period Variable Stars. 71, 285, 1930 (Mt. W. Contr., No. 399).

399. Joy, A. H. A Spectrographic Study of U Sagittae. 71, 336, 1930 (Mt. W. Contr., No. 401).

400. Elvey, C. T., and Struve, O. A Study of Stellar Hydrogen Lines and Their Relation to the Stark Effect. 72, 277, 1930.

401. Sanford, R. F. The Spectrum and Radial Velocity of AC Herculis. 73, 364, 1931 (Mt. W. Contr., No. 424).

402. Merrill, P. W. A Plane-Grating Spectrograph for the Red and Infrared Regions of Stellar Spectra. 74, 188, 1931 (Mt. W. Contr., No. 432).

403. Joy, A. H. Spectroscopic Observations of SX Herculis. 75, 127, 1932 (Mt. W. Contr., No. 443).

404. Merrill, P. W.; Humason, M. L.; and Burwell, C. G. Discovery and Observations of Stars of Class Be: Second Paper. 76, 156, 1932 (Mt. W. Contr., No. 456).

405. Merrill, P. W. Four Stars Whose Spectra Have Bright Helium Lines. 77, 44, 1933 (Mt. W. Contr., No. 460).

406. Sanford, R. F. On the Spectrum and Radial Velocity of U Monocerotis. 77, 120, 1933 (Mt. W. Contr., No. 465).

407. Morgan, W. W. Some Effects of Changes in Stellar Temperatures and Absolute Magnitudes. 77, 291, 1933.

408. Hynek, J. A. Note on the Spectra of 17 Leporis and 7 ϵ Aurigae. 78, 54, 1933.

409. Merrill, P. W., and Burwell, C. G. Catalogue and Bibliography of Stars of Classes B and A Whose Spectra Have Bright Hydrogen Lines. 78, 87, 1933 (Mt. W. Contr., No. 471).

410. Morgan, W. W. On the Relative Intensities of Certain Lines of Ti II in the Spectra of Three F-Type Stars. 78, 158, 1933.

411. Christie, W. H. Preliminary Report on the Investigation of the System of HD 198287-8. 78, 200, 1933 (Mt. W. Contr., No. 475).

412. Westgate, C. Note Concerning the Spectrum of Nova Ophiuchi No. 3 (RS Ophiuchi). 78, 372, 1933.

413. Sanford, R. F. The Radial-Velocity Variations of V Ursae Minoris, R Sagittae, and V Vulpeculae. 79, 77, 1934 (Mt. W. Contr., No. 481).

414. Merrill, P. W. Photography of the Near Infrared Region of Stellar Spectra. 79, 183, 1934 (Mt. W. Contr., No. 486).

415. McLaughlin, D. B. Some Spectroscopic Phenomena of the Eclipse of ϵ Aurigae. 79, 235, 1934.

416. Elvey, C. T. The Intensities of Some Multiplets of Fe II and Ti II in Stellar Spectra. 79, 263, 1934.

417. McLaughlin, D. B. The Variable Spectrum of VV Cephei. 79, 380, 1934.

418. Struve, O., and Elvey, C. T. The Intensities of Stellar Absorption Lines. 79, 409, 1934.

419. Wilson, O. C., and Williams, E. G. Spectrophotometry of RS Ophiuchi (Nova Ophiuchi No. 3). 80, 344, 1934 (Mt. W. Contr., No. 501).

420. Adams, W. S.; Joy, A. H.; Humason, M. L.; and Brayton, A. M. The Spectroscopic Absolute Magnitudes and Parallaxes of 4179 Stars. 81, 187, 1935 (Mt. W. Contr., No. 511).

421. Merrill, P. W. The Spectrum of R Aquarii, 1919-1934. 81, 312, 1935 (Mt. W. Contr., No. 513).

422. Berman, L. The Spectrum Analysis of the Hot Carbon Star, R Coronae Borealis. 81, 369, 1935.

423. Christie, W. H., and Wilson, O. C. ζ Aurigae: The Structure of a Stellar Atmosphere. 81, 426, 1935 (Mt. W. Contr., No. 519).

424. Thackeray, A. D. The Emission Line λ 4511 in Late-Type Variables. 81, 467, 1935 (Mt. W. Contr., No. 517).

425. McLaughlin, D. B. Variable Hα Emission in ϵ Aurigae. 82, 95, 1935.

426. Sanford, R. F. The Radial Velocities of the Stars of Spectral Classes R and N. 82, 202, 1935 (Mt. W. Contr., No. 525).

427. Hynek, J. A. A Quantitative Study of Certain Phases of F-Type Spectra. 82, 338, 1935 (Perkins Contr., No. 1).

428. Merrill, P. W. Notes on the Spectra of Several Long-Period Variable Stars at Various Phases of Their Light-Curves. 83, 272, 1936 (Mt. W. Contr., No. 539).

429. Luyten, W. J. A Rediscussion of the Orbits of Seventy-seven Spectroscopic Binaries. 84, 85, 1936 (Minn. Pub., 2, 53, 1936).

430. Joy, A. H., and Merrill, P. W. Spectroscopic Observations of V Canum Venaticorum. 85, 9, 1937 (Mt. W. Contr., No. 559).

431. Joy, A. H. Radial Velocities of Cepheid Variable Stars. 86, 363, 1937 (Mt. W. Contr., No. 578).

432. Rense, W. A., and Hynek, J. A. Photometry of the G Band in Representative Stellar Spectra. 86, 460, 1937 (Perkins Contr., No. 8).

433. Kuiper, G. P.; Struve, O.; and Strömgren, B. The Interpretation of ε Aurigae. 86, 570, 1937.

434. Morgan, W. W. On the Spectral Types and Luminosities of the M Dwarfs. 87, 589, 1938.

435. Kuiper, G. P. Notes on Proper-Motion Stars. 87, 592, 1938.

436. Christie, W. H., and Wilson, O. C. The Radial Velocities of 600 Stars and Measures of 69 Spectroscopic Binaries. 88, 34, 1938 (Mt. W. Contr., No. 593).

437. Humason, M. L. The Present Spectral Characteristics of Sixteen Old Novae. 88, 228, 1938 (Mt. W. Contr., No. 596).

438. Burwell, C. G. Lines of Ionized Barium in Stellar Spectra. 88, 278, 1938 (Mt. W. Contr., No. 598).

439. O'Keefe, J. A. Remarks on Loreta's Hypothesis concerning R Coronae Borealis. 90, 294, 1939.

440. Swings, P., and Struve, O. Spectrographic Observations of Peculiar Stars. 91, 546, 1940 (McDonald Contr., No. 22).

441. Kuiper, G. P. Notes on Proper-Motion Stars. 92, 126, 1940 (McDonald Contr., No. 23).

442. Swings, P., and Struve, O. The Nebular Spectra of Two Slow Novae: DQ Herculis and RT Serpentis. 92, 295, 1940 (McDonald Contr., No. 25).

443. Joy, A. H. Spectroscopic Observations of Barnard's Variable in Messier 3. 92, 396, 1940 (Mt. W. Contr., No. 637).

444. Adams, W. S. Some Results with the Coudé Spectrograph of the Mount Wilson Observatory. 93, 11, 1941 (Mt. W. Contr., No. 638).

445. Merrill, P. W. Ultraviolet Emission Lines in the Spectra of Me Variables. 93, 40, 1941 (Mt. W. Contr., No. 642).

446. Swings, P., and Struve, O. The Evolution of a Peculiar Stellar Spectrum: Z Andromedae. 93, 356, 1941 (McDonald Contr., No. 31).

447. Merrill, P. W. Displacements of Lines in the Spectra of Long-Period Variables. 93, 380, 1941 (Mt. W. Contr., No. 644).

448. Swings, P., and Struve, O. The Emission Lines in the Spectra of B 1985 and WY Geminorum. 93, 455, 1941 (McDonald Contr., No. 34).

449. McLaughlin, D. B. The Characteristic Velocity-Curves of RV Tauri Variables. 94, 94, 1941.

450. Elvey, C. T. Note on the Spectrum of HK Scorpii. 94, 140, 1941.

451. Merrill, P. W. The Radial Velocities of Long-Period Variable Stars. Second Paper. 94, 171, 1941 (Mt. W. Contr., No. 649).

452. Swings, P., and Struve, O. Spectrographic Observations of Peculiar Stars. II. 94, 291, 1941 (McDonald Contr., No. 37).

453. Joy, A. H. A Spectrographic Study of the Eclipsing Variable Star, WW Draconis. 94, 407, 1941 (Mt. W. Contr., No. 654).

454. Keenan, P. C., and Morgan, W. W. The Classification of the Red Carbon Stars. 94, 501, 1941.

455. Scott, R. M. The Pulsation Theory of Long-Period Variables. 95, 58, 1942 (Harvard Repr., No. 235).

456. Swings, P., and Struve, O. Spectrographic Observations of Peculiar Stars. III. 95, 152, 1942 (McDonald Contr., No. 42).

457. Kuiper, G. P. The Nearest Stars. 95, 201, 1942 (McDonald Contr., No. 44).

458. Popper, D. M. Radial Velocities of Proper-Motion Stars. 95, 307, 1942 (McDonald Contr., No. 47).

459. Goedicke, V. Atmospheric Velocities in VV Cephei. 95, 319, 1942.

460. Hynek, J. A. Note on the Spectrum of δ Sagittae. 95, 324, 1942.

461. Keenan, P. C. Luminosities of the M-Type Variables of Small Range. 95, 461, 1942 (McDonald Contr., No. 48).

462. Swings, P., and Struve, O. Spectrographic Observations of Peculiar Stars. IV. 96, 254, 1942 (McDonald Contr., No. 56).

463. Keenan, P. C., and Greenstein, J. L. Ca II Emission in 56 Pegasi. 96, 309, 1942 (McDonald Contr., No. 53).

464. Kuiper, G. P. Notes on Proper-Motion Stars. IV. 96, 315, 1942 (McDonald Contr., No. 58).

465. Joy, A. H. A Survey of the Spectra and Radial Velocities of the Less Regular M-Type Variable Stars. 96, 344, 1942 (Mt. W. Contr., No. 668).

466. Swings, P., and Struve, O. Spectrographic Observations of Peculiar Stars. V. 97, 194, 1943 (McDonald Contr., No. 64).

467. Kuiper, G. P. Notes on Proper-Motion Stars. V. 97, 275, 1943 (McDonald Contr., No. 67).

468. Vyssotsky, A. N. Dwarf M Stars Found Spectrophotometrically. First List. 97, 381, 1943.

469. Elvey, C. T., and Babcock, H. W. The Spectra of U Geminorum Type Variable Stars. 97, 412, 1943 (McDonald Contr., No. 69).

470. Swings, P., and Struve, O. Spectrographic Observations of Peculiar Stars. VI. 98, 91, 1943 (McDonald Contr., No. 72).

471. Merrill, P. W., and Burwell, C. G. Supplement to the Mount Wilson Catalogue and Bibliography of Stars of Classes B and A Whose Spectra Have Bright Hydrogen Lines. 98, 153, 1943 (Mt. W. Contr., No. 682).

472. Popper, D. M. Radial Velocities of Proper-Motion Stars. II. 98, 209, 1943 (McDonald Contr., No. 74).

473. Joy, A. H., and Merrill, P. W. Spectroscopic Observations of T Arietis. 98, 331, 1943 (Mt. W. Contr., No. 686).

474. Merrill, P. W. Spectroscopic Observations of AX Persei, RW Hydrae, CI Cygni, and Z Andromedae. 99, 15, 1944 (Mt. W. Contr., No. 688).

475. Struve, O. The Ultraviolet Spectrum of VV Cephei. 99, 70, 1944 (McDonald Contr., No. 79).

476. Sanford, R. F. Radial Velocities of 383 Stars of Spectral Classes R and N. 99, 145, 1944 (Mt. W. Contr., No. 689).

477. Struve, O. Notes on Stellar Spectra. 99, 205, 1944 (McDonald Contr., No. 81).

478. Münch, G. Radial Velocities of Proper-Motion Stars. 99, 271, 1944 (McDonald Contr., No. 89).

479. Gaposchkin, S. The Eclipsing System RX Cassiopeiae. 100, 230, 1944 (Harvard Repr., No. 265).

480. Sahade, J., and Cesco, C. U. The Spectroscopic Orbit of AR Monocerotis. 100, 374, 1944 (McDonald Contr., No. 98).

481. Payne-Gaposchkin, C., and Gaposchkin, S. Eclipses of Stars with Thick Atmospheres. 101, 56, 1945 (Harvard Repr., No. 270).

482. Scott, R. M. Spectrophotometry of Mira Ceti. 101, 71, 1945 (Harvard Repr., No. 269).

483. Bauer, C. A. The Spectrum of W Serpentis. 101, 208, 1945 (McDonald Contr., No. 102).

484. Swings, P., and Struve, O. Spectrographic Observations of Peculiar Stars. VII. 101, 224, 1945 (McDonald Contr., No. 103).

485. Keenan, P. C., and Hynek, J. A. The Use of Infrared Spectra for the Determination of Absolute Magnitudes. 101, 265, 1945 (Perkins Contr., No. 22).

486. Hynek, J. A., and Keenan, P. C. The Presence of Strong Lines of O I in the Infrared Spectrum of VV Cephei. 101, 270, 1945 (Perkins Contr., No. 23).

487. Cesco, C. U., and Sahade, J. The Spectroscopic Orbit of RZ Eridani. 101, 370, 1945 (McDonald Contr., No. 109).

488. Struve, O. Spectrographic Observations of Thirteen Eclipsing Variables. 102, 74, 1945 (McDonald Contr., No. 110).

489. Joy, A. H. T Tauri Variable Stars. 102, 168, 1945 (Mt. W. Contr., No. 709).

490. Merrill, P. W. Measurements in the Spectra of U Orionis, R Serpentis, R Aquilae, and R Cassiopeiae. 102, 347, 1945 (Mt. W. Contr., No. 713).

491. Joy, A. H., and Swings, P. Identification of the Postmaximum Lines in the Spectrum of Nova (RS) Ophiuchi. 102, 353, 1945 (Mt. W. Contr., No. 714).

492. Luyten, W. J. Radial Velocities and Spectral Classes for Some Stars of Large Proper Motion. 102, 382, 1945.

493. Merrill, P. W. Measurements in the Spectrum of R Hydrae. 103, 6, 1946 (Mt. W. Contr., No. 717).

494. McLaughlin, D. B. Spectrographic Observations of μ Cephei. 103, 35, 1946.

495. Sanford, R. F. Orbital Elements of the Algol Variable SS Boötis. 103, 114, 1946 (Mt. W. Contr., No. 719).

496. Morgan, W. W., and Sharpless, S. An Interesting Emission-Line Star near the Orion Nebula. 103, 249, 1946.

497. Merrill, P. W. Atomic Lines in the Spectrum of R Leonis. 103, 275, 1946 (Mt. W. Contr., No. 720).

498. Payne-Gaposchkin, C., and Wright, F. W. The Photographic Light-Curve of T Coronae Borealis. 104, 75, 1946 (Harvard Repr., No. 282).

499. Vyssotsky, A. N.; Janssen, E. M.; Miller, W. J.; and Walther, M. E. Dwarf M Stars Found Spectrophotometrically. Second List. 104, 234, 1946.

500. Payne-Gaposchkin, C., and Boyd, C. The Light-Curves of R Aquarii. 104, 357, 1946 (Harvard Repr., No. 287).

501. Payne-Gaposchkin, C. The Light-Curves of Z Andromedae and AX Persei. 104, 362, 1946 (Harvard Repr., No. 288).

502. Hiltner, W. A. Spectrographic Observations of RY Persei and RZ Ophiuchi. 104, 396, 1946 (McDonald Contr., No. 129).

503. Bowen, I. S., and Swings, P. The Relative Intensities of the Coronal and Other Forbidden Lines. 105, 92, 1947 (Mt. W. Contr., No. 725).

504. Joy, A. H. Radial Velocities and Spectral Types of 181 Dwarf Stars. 105, 96, 1947 (Mt. W. Contr., No. 726).

505. Merrill, P. W. The Spectrum of Z Andromedae in August, 1946. 105, 120, 1947 (Mt. W. Contr., No. 728).

506. Popper, D. M. Spectral Types of Stars in the Globular Clusters Messier 3 and Messier 13. 105, 204, 1947 (McDonald Contr., No. 131).

507. Gaposchkin, S. The Eclipsing System UX Monocerotis. 105, 258, 1947 (Harvard Repr., No. 293).

508. Merrill, P. W. Atomic Lines in the Spectrum of R Andromedae. 105, 360, 1947 (Mt. W. Contr., No. 730).

509. Bidelman, W. P. The M-Type Supergiant Members of the Double Cluster in Perseus. 105, 492, 1947 (McDonald Contr., No. 134).

510. Keenan, P. C., and Hynek, J. A. Changes in the Infrared Spectrum of VV Cephei. 105, 500, 1947.

511. Davis, D. N. The Spectrum of β Pegasi. 106, 28, 1947 (Mt. W. Contr., No. 733).

512. Struve, O. Spectrographic Observations of Eight Eclipsing Binaries. 106, 92, 1947 (McDonald Contr., No. 137).

513. Kuiper, G. P.; Wilson, W.; and Cashman, R. J. An Infrared Stellar Spectrometer. 106, 243, 1947 (McDonald Contr., No. 139).

514. Struve, O. The Spectrum of the Eclipsing Binary UX Monocerotis. 106, 255, 1947 (McDonald Contr., No. 138).

515. Merrill, P. W. The Postmaximum Spectrum of χ Cygni. 106, 274, 1947 (Mt. W. Contr., No. 735).

516. Joy, A. H. The Absorption Lines within the Hydrogen Emission of Mira Ceti. 106, 288, 1947 (Mt. W. Contr., No. 737).

517. Keenan, P. C. The Infrared Spectrum of $\bar{\rho}$ Cassiopeiae in 1946. 106, 295, 1947 (Perkins Contr., No. 24).

518. Morgan, W. W., and Deutsch, A. J. The Spectrum of T Coronae Borealis at Its 1946 Outburst. 106, 362, 1947.

519. Hiltner, W. A. Eclipsing Binaries with Ca II Emission. 106, 481, 1947 (McDonald Contr., No. 141).

520. Herzberg, G. Fe II Emission Lines in α Herculis and α Scorpii. 107, 94, 1948 (McDonald Contr., No. 143).

521. Merrill, P. W. Wave Lengths of Atomic Absorption Lines in the Spectra of Long-Period Variable Stars. 107, 303, 1948 (Mt. W. Contr., No. 743).

522. _____. The Spectrum of Z Andromedae in 1946 and 1947. 107, 317, 1948 (Mt. W. Contr., No. 744).

523. Whitney, W. T., and Weston, E. B. A Polarigraphic Study of the Reflection Nebula NGC 6729. 107, 371, 1948.

524. Greenstein, J. L. Stars in Diffuse Nebulae. 107, 375, 1948 (McDonald Contr., No. 148).

525. Nassau, J. J., and van Albada, G. B. A Faint S-Type Star in the Clear Region in Cygnus. 107, 418, 1948.

526. _____. A New Band in the Infrared Spectra of S-Type Stars. 107, 418, 1948.

527. Keenan, P. C. On the Occurrence of Lanthanum Oxide in S-Type Stars. 107, 420, 1948 (Perkins Contr., No. 25).

528. Greenstein, J. L. Rapid Variations in the Spectrum of Rho Cassiopeiae. 108, 78, 1948 (McDonald Contr., No. 151).

529. Struve, O. An Attempt To Detect Polarization in the Ca II Emission Lines of AR Lacertae. 108, 155, 1948.

530. Van Hoof, A. Emission Lines of Ca II in X Cygni. 108, 160, 1948.

531. Joy, A. H., and Mitchell, S. A. Spectroscopic Observations of 90 Stars. 108, 234, 1948 (Mt. W. Contr., No. 747).

532. McKellar, A. The Far Violet Region in the Spectra of the Cool Carbon Stars. 108, 453, 1948 (Dom. Ap. Obs. Contr., No. 15).

533. Sanford, R. F. High-Dispersion Spectrograms of T Coronae Borealis. 109, 81, 1949 (Mt. W. Contr., No. 756).

534. Struve, O., and Rudkjøbing, M. Stellar Spectra with Emission Lines in the Obscuring Clouds of Ophiuchus and Scorpius. 109, 92, 1949 (McDonald Contr., No. 158).

535. Herbig, G. H. Identification of a Molecular Band at λ 3682 in the Spectra of Late-Type Stars. 109, 109, 1949 (Mt. W. Contr., No. 754).

536. Joy, A. H., and Wilson, R. E. Stars Whose Spectra Have Bright H and K Lines of Calcium. 109, 231, 1949 (Mt. W. Contr., No. 758).

537. Nassau, J. J.; van Albada, G. B.; and Keenan, P. C. New Bands in the Photographic Infrared Spectra of Long-Period Variables. 109, 333, 1949 (W. and S. Repr., No. 36).

538. Luyten, W. J. A New Star of Large Proper Motion (L 726-8). 109, 532, 1949 (Minn. Pub., Vol. 2, No. 13, 1949).

539. Joy, A. H. Spectra of the Brighter Variables in Globular Clusters. 110, 105, 1949 (Mt. W. and P. Repr., No. 5).

540. Herbig, G. H. The Spectrum of R Coronae Borealis at the 1948-1949 Minimum. 110, 143, 1949 (McDonald Contr., No. 174).

541. Roman, N. G. The Ursa Major Group. 110, 205, 1949.

542. Merrill, P. W., and Burwell, C. G. Second Supplement to the Mount Wilson Catalogue and Bibliography of Stars of Classes B and A Whose Spectra Have Bright Hydrogen Lines. 110, 387, 1949 (Mt. W. and P. Repr., No. 8).

543. Joy, A. H. Bright-Line Stars among the Taurus Dark Clouds. 110, 424, 1949 (Mt. W. and P. Repr., No. 12).

544. Hiltner, W. A., and Hardie, R. H. The Spectrum of RW Tauri. 110, 438, 1949 (McDonald Contr., No. 180).

545. Keenan, P. C., and Hynek, J. A. Neutral Oxygen in Stellar Atmospheres. 111, 1, 1950 (Perkins Contr., No. 26).

546. Herbig, G. H. The Spectrum of the Nebulosity Surrounding T Tauri. 111, 11, 1950 (McDonald Contr., No. 181).

547. _____. Spectra of Variable Stars in the Orion Nebula. 111, 15, 1950 (McDonald Contr., No. 183).

548. Greenstein, J. L. The Variability of the Spectrum of Upsilon Sagittarii. 111, 20, 1950 (Mt. W. and P. Repr., No. 11).

549. Gratton, L. Ca II Emission in Lambda and Zeta Andromedae. 111, 31, 1950 (McDonald Contr., No. 185).

550. Sahade, J. Spectrographic Observations of the Eclipsing Variable UX Monocerotis at Bosque Alegre. 111, 194, 1950 (Cordoba Tir. Ap., No. 38).

551. Nassau, J. J., and Colacevich, A. Note on the Spectral Classification of Carbon Stars in the Infrared. 111, 199, 1950.

552. Wilson, R. E., and Joy, A. H. Radial Velocities of 2111 Stars. 111, 221, 1950 (Mt. W. and P. Repr., No. 18).

553. Sanford, R. F. An Atlas of Spectra of Six Stars of Classes R and N. 111, 262, 1950 (Mt. W. and P. Repr., No. 14).

554. _____. Variations in Velocity and Spectrum of Eight N-Type Long-Period Variable Stars. 111, 270, 1950 (Mt. W. and P. Repr., No. 17).

555. Bidelman, W. P. The Peculiar Star HD 30353. 111, 333, 1950 (McDonald Contr., No. 184).

556. Gaviola, E. Eta Carina. I. The Nebulosity. 111, 408, 1950 (Cordoba Tir. Ap., No. 40).

557. Merrill, P. W. Measurements in the Combination Spectra of RW Hydrae, BF Cygni, and CI Cygni. 111, 484, 1950 (Mt. W. and P. Repr., No. 22).

558. Struve, O. Bright Lines of Ca II in the Spectrum of RW Comae Berenices. 111, 658, 1950.

559. Moore, J. H., and Paddock, G. F. Radial Velocities, Spectral Types, and Luminosity Classes of 820 Stars. 112, 48, 1950 (Lick Obs. Contr., Ser. II, No. 28).

560. Merrill, P. W., and Burwell, C. G. Additional Stars Whose Spectra Have a Bright H α Line. 112, 72, 1950 (Mt. W. and P. Repr., No. 24).

561. Struve, O., and Horak, H. G. Spectrographic Observations of W Ursae Majoris. 112, 178, 1950 (McDonald Contr., No. 191).

562. Struve, O.; Herbig, G.; and Horak, H. The Spectrum of YY Geminorum (Castor C). 112, 216, 1950.

563. Bidelman, W. P. The Spectrum of GP Orionis. 112, 219, 1950.

564. Merrill, P. W. The Spectrum of R Aquarii, 1936-1949. 112, 514, 1950 (Mt. W. and P. Repr., No. 27).

565. Rosino, L. The Spectra of Variables of the RV Tauri and Yellow Semiregular Types. 113, 60, 1951.

566. Aller, L. H., and Keenan, P. C. The Spectra of R Andromedae (Maximum) and Mu Cephei between 7400 and 8800 A. 113, 72, 1951 (Perkins Contr., No. 27).

567. Sanford, R. F. The Spectra and Orbits of AR Lacertae. 113, 299, 1951 (Mt. W. and P. Repr., No. 31).

568. Merrill, P. W. The Spectrum of BD + 11°4673 during the Years 1942-1950. 113, 605, 1951 (Mt. W. and P. Repr., No. 36).

569. Miller, W. C., and Merrill, P. W. Spectroscopic Observations of Be Stars. 113, 624, 1951 (Mt. W. and P. Repr., No. 41).

570. Fujita, Y. Absorption Lines and Bands in the Spectrum of Chi Cygni. 113, 626, 1951.

571. Struve, O. Circumstellar Lines of Ca II in the Spectrum of Epsilon Aurigae. 113, 699, 1951.

572. McLaughlin, D. B. The Spectral Changes of VV Cephei outside Eclipse. 114, 47, 1951.

573. Henize, K. G., and McLaughlin, D. B. A Note on the Spectrum of RR Telescopii. 114, 163, 1951.

574. Huang, S. On the Variation of Turbulent Velocities in Stellar and Solar Atmospheres. 114, 287, 1951.

575. Merrill, P. W. Displaced Helium Lines in the Spectrum of BD+11°4673. 114, 338, 1951 (Mt. W. and P. Repr., No. 48).

576. McNamara, D. H. The Eclipsing Binary U Sagittae. 114, 513, 1951 (Berkeley Repr., No. 13).

577. Joy, A. H. The Semiregular Variable Stars of the RV Tauri and Related Classes. 115, 25, 1952.

578. Keenan, P. C., and Schroeder, L. W. An Infrared System of Bands of VO in M-Type Stars. 115, 82, 1952 (Perkins Contr., No. 32).

579. Henize, K. G. Six Peculiar Hα-Emission Stars. 115, 133, 1952.

580. Merrill, P. W. Two F-Type Stars with Expanding Hydrogen Atmospheres. 115, 154, 1952.

581. Wilson, R. E., and Joy, A. H. Radial Velocities of 360 Stars. 115, 157, 1952.

582. Kron, G. E. A Photoelectric Study of the Dwarf M Eclipsing Variable YY Geminorum. 115, 301, 1952 (Lick Obs. Contr., Ser. II, No. 40).

583. Nassau, J. J., and Morgan, W. W. A Finding List of F Stars of High Luminosity. 115, 475, 1952 (W. and S. Repr., No. 46).

584. Bowen, I. S. The Spectrographic Equipment of the 200-Inch Hale Telescope. 116, 1, 1952.

585. Merrill, P. W. The Postminimum Spectrum of R Hydrae. 116, 18, 1952 (Mt. W. and P. Repr., No. 68).

586. _____. Spectroscopic Observations of Stars of Class S. 116, 21, 1952.

587. Fujita, Y. The Spectrum of U Cygni (Minimum) in the Visual and Infrared Regions. 116, 46, 1952.

588. Vyssotsky, A. N., and Mateer, B. A. Dwarf M Stars Found Spectrophotometrically. Third List. 116, 117, 1952.

589. Sanford, R. F. The Spectrum and Radial Velocities of W Virginis. 116, 331, 1952.

590. Merrill, P. W. The Preminimum Spectrum of R Leonis. 116, 337, 1952 (Mt. W. and P. Repr., No. 72).

591. _____. Measurements in the Spectra of Four Long-Period Variable Stars of Class Me. 116, 344, 1952.

592. Herbig, G. H. The Cepheid Variable S Sagittae. II. The Emission Lines. 116, 369, 1952 (Lick Obs. Contr., Ser. II, No. 42).

593. Franklin, K. L. The Spectroscopic Orbit of 26 Aquilae. 116, 383, 1952 (Lick Obs. Contr., Ser. II, No. 43).

594. Merrill, P. W. The Low-Temperature Spectrum of HD 45910. 116, 498, 1952.

595. _____. Spectrograms of Ten High-Velocity Me Variable Stars. 116, 523, 1952.

596. Buscombe, W., and Merrill, P. W. Intensities of Atomic Absorption Lines in the Spectra of Long-Period Variable Stars. 116, 525, 1952.

597. MacRae, D. A. Stellar Spectra and Colors in Cygnus at Galactic Latitude + 14°. 116, 592, 1952.

598. Struve, O., and Kung, S. M. The F-Type Component of Capella. 117, 1, 1953 (Berkeley Repr., No. 36).

599. Bidelman, W. P. The Spectra of Certain Stars Whose Atmospheres May Be Deficient in Hydrogen. 117, 25, 1953 (McDonald Contr., No. 215).

600. Haro, G. Hα Emission Stars and Peculiar Objects in the Region of the Orion Nebula. 117, 73, 1953.

601. McLaughlin, D. B. The Spectra of Novae near Minimum. 117, 279, 1953.

602. Bidelman, W. P. Lines of the Rare-Earth Elements in the Spectrum of R Andromedae. 117, 377, 1953.

603. Roman, N. G. The Spectrum of BD+67°922. 117, 467, 1953 (McDonald Contr., No. 221).

604. Struve, O., and Ebbighausen, E. G. The Spectroscopic Orbit of YY Geminorum (Castor C). 117, 468, 1953.

605. Merrill, P. W., and Lowen, A. L. Intercomparison of Shell Spectra. 118, 18, 1953.

Bulletin Astronomique

606. Tremblot, R. Contribution à l'étude des étoiles à spectre composite. 11, 377, 1938.

Cambridge, Massachusetts, Harvard College Observatory, Annals

607. Maury, A. C. Spectra of Bright Stars. 28, 1, 1897.

608. Cannon, A. J. Spectra of Bright Southern Stars. 28, 129, 1901.

609. _____. A Provisional Catalogue of Variable Stars. 48, 91, 1903.

610. _____. Second Catalogue of Variable Stars. 55, 1, 1907.

611. _____. Classification of 1,477 Stars by Means of Their Photographic Spectra. 56, 65, 1912.

612. Fleming, W. P. Stars Having Peculiar Spectra. 56, 165, 1912.

613. Cannon, A. J. Spectra Having Bright Lines. 76, 19, 1916.

614. Townley, S.; Cannon, A. J.; and Campbell, L. Harvard Catalogue of Long-Period Variable Stars. 79, 159, 1928.

615. Robinson, L. V. The Light-Curves of Cepheid Variables. 90, 27, 1933.

616. Prager, R. History and Bibliography of the Light Variations of Variable Stars. 111, 1, 1941.

617. Payne-Gaposchkin, C.; Brenton, V. K.; and Gaposchkin, S. The Variables of RV Tauri Type. 113, 1, 1943.

618. Payne-Gaposchkin, C. Variable Stars in Milton Field 49. 115, 87, 1947.
619. _____. Variable Stars in Milton Field 43. 115, 137, 1950.
620. Gaposchkin, S. Variable Stars in Milton Field 38. 115, 197, 1950.

Cambridge, Massachusetts, Harvard College Observatory,
Announcement Cards

621. McLaughlin, D. B. ϵ Aurigae. No. 63, 1928.
622. _____. Nova Ophiuchi No. 3, No. 276, 1933.
623. Struve, O. Nova Ophiuchi No. 3. No. 278, 1933.
624. _____. Nova Ophiuchi No. 3. No. 280, 1933.
625. Adams, W. S., and Joy, A. H. Coronal Lines in RS Ophiuchi Spectrum. No. 281, 1933.
626. McLaughlin, D. B. VV Cephei. No. 397, 1936.
627. Christie, W. H. VV Cephei. No. 427, 1937.
628. Keenan, P. C. Wachmann's Peculiar Variable. No. 472, 1939.
629. Humason, M. L. Companion of Lalande 21258. No. 486, 1939.
630. Sanford, R. F. Spectrum of UV Aurigae. No. 545, 1940.
631. Vyssotsky, A. N. New Dwarf Me Star. No. 550, 1940.
632. Struve, O., and Swings, P. Z Andromedae. No. 598, 1941.
633. Miller, W. J. Star with Emission Bands. No. 711, 1945.
634. Sahade, J. Nova T Coronae Borealis. No. 713, 1945.
635. Deutsch, A. J.; Morgan, W. W.; and Münch, G. T Coronae Borealis. No. 738, 1946.
636. Popper, D. M. Rho Cassiopeiae. No. 752, 1946.
637. Popper, D. M., and Bidelman, W. P. Rho Cassiopeiae. No. 816, 1947.
638. Greenstein, J. L. Rho Cassiopeiae. No. 860, 1947.
639. Luyten, W. J. Near-by Red Dwarf Double Star. No. 990, 1949.
640. Paraskevopoulos, J. S. RR Telescopii. No. 1019, 1949.
641. _____. RR Telescopii. No. 1020, 1949.

Cambridge, Massachusetts, Harvard College Observatory,
Annual Reports

642. 45th Annual Report, 1890.
643. 46th Annual Report, 1891.
644. 47th Annual Report, 1892.
645. 48th Annual Report, 1893.
646. 49th Annual Report, 1894.
647. 50th Annual Report, 1895.
648. 51st Annual Report, 1896.
649. 52d Annual Report, 1897.
650. 53d Annual Report, 1898.
651. 54th Annual Report, 1899.
652. 56th Annual Report, 1901.
653. 57th Annual Report, 1902.
654. 61st Annual Report, 1906.

655. 62d Annual Report, 1908.

656. 63d Annual Report, 1909.

657. 64th Annual Report, 1910.

Cambridge, Massachusetts, Harvard College Observatory, Bulletins

658. Cannon, A. J. Spectrum of U Cygni. No. 701, 1919.

659. _____. New Variable Star of Long Period, 104453. No. 771, 1922.

660. _____. New Long Period Variable. No. 774, 1922.

661. Shapley, H. Star with Variable Bright Lines. No. 774, 1922.

662. Cannon, A. J. Star Resembling RS Ophiuchi. No. 778, 1922.

663. _____. Five New Variable Stars. No. 781, 1923.

664. _____. New Variable with Remarkable Spectrum and Light Curve. No. 783, 1923.

665. _____. RU Arae and Z Capricorni. No. 787, 1923.

666. _____. New Variable Star in Ara. No. 796, 1923.

667. _____. Spectrum of S Carinae. No. 798, 1924.

668. Shapley, H. New Variable Star in Pavo, H.V. 3740. No. 803, 1924.

669. Harwood, M. New Variable Resembling a Nova. No. 826, 1925.

670. Luyten, W. J. Dwarf Star with Variable Bright Lines. No. 830, 1925.

671. _____. Spectra of Faint Proper Motion Stars. No. 834, 1926.

672. _____. Proper Motion Star with Variable Bright Lines. No. 835, 1926.

673. Cannon, A. J. Peculiar Spectra. No. 837, 1926.

674. Shapley, H. New Long Period Variable Star. No. 842, 11, 1927.

675. Waterfield, W. F. H. Light Curve and Period of AC Herculis. No. 845, 11, 1927.

676. Davidovich, P. Transition of Absorption into Emission in Stellar Spectra. No. 846, 5, 1927.

677. Payne, C. H. A Photometric Analysis of the Spectrum of ϵ Aurigae. No. 855, 7, 1928.

678. Woods, I. E. Forty New Variable Stars in Sagittarius. No. 855, 22, 1928.

679. Hogg, F. S. Contours of Calcium Lines in Late Type Stars. No. 859, 4, 1928.

680. Cannon, A. J. Three New Variable Stars. No. 861, 5, 1928.

681. Shapley, H., and Payne, C. H. The c-Characteristic and the Brightness of Cepheid Variables. No. 872, 5, 1930.

682. Cannon, A. J., and Walton, M. L. Spectra of Cepheids of the International Program. No. 874, 19, 1930.

683. Payne, C. H. Classification of the O Stars. No. 878, 1, 1930.

684. Hughes, E. M. Ionization of Calcium in the Atmospheres of Long Period Variable Stars. No. 882, 23, 1931.

685. O'Connell, D. J. K. An Investigation of the Semiregular Variable AF Cygni. No. 888, 1, 1932.

686. Gerasimovič, B. P., and Payne, C. H. On the Colors of SS Cygni Variables. No. 889, 3, 1932.

687. Cannon, A. J. Five New Variable Stars. No. 891, 9, 1933.

688. _____. Spectra of Ninety-four Variable Stars. No. 897, 12, 1934.

689. Cannon, A. J., and Mayall, M. W. New Peculiar Spectra. No. 908, 20, 1938.

690. Mayall, M. W., and Cannon, A. J. New Peculiar Spectra. No. 913, 7, 1940.

691. Payne-Gaposchkin, C. A Photographic Study of RU Camelopardalis. No. 915, 10, 1941.

692. Mayall, M. W. Spectral Curves of RU Camelopardalis. No. 915, 14, 1941.

693. Payne-Gaposchkin, C., and Mayall, M. W. The Variations of ρ Cassiopeiae. No. 918, 11, 1946.

694. Hoffleit, D. A New RV Tauri Star, BD+20°2337 (HV 11092). No. 919, 11, 1949.

695. Mayall, M. W. Recent Variations of RR Telescopii. No. 919, 15, 1949.

696. _____. New Peculiar Spectra. No. 920, 32, 1951.

697. Hoffleit, D. Three Possible Variable-Emission Spectra. No. 920, 45, 1951.

Cambridge, Massachusetts, Harvard College Observatory,

Circulars

698. Pickering, E. C. New Variable Stars. No. 6, 1896 (A.N., 140, 173, 1896; Ap. J., 3, 296, 1896).

699. _____. Ten New Variable Stars. No. 7, 1896 (A.N., 141, 33, 1896; Ap. J., 4, 138, 1896).

700. _____. Stars Having Peculiar Spectra. No. 9, 1896 (A.N., 141, 169, 1896; Ap. J., 4, 142, 1896).

701. _____. Stars Having Peculiar Spectra. New Variable Stars in Crux and Cygnus. No. 12, 1896 (A.N., 142, 87, 1896; Ap. J., 4, 369, 1896).

702. _____. Stars Having Peculiar Spectra. No. 17, 1897 (A.N., 143, 227, 1897; Ap. J., 5, 350, 1897).

703. _____. New Variable Stars. No. 24, 1898 (A.N., 146, 113, 1898; Ap. J., 7, 208, 1898).

704. _____. Stars Having Peculiar Spectra. No. 32, 1898 (A.N., 147, 247, 1898; Ap. J., 8, 116, 1898).

705. _____. Sixty-four New Variable Stars. No. 54, 1901 (A.N., 154, 423, 1901; Ap. J., 13, 226, 1901).

706. _____. Stars Having Peculiar Spectra. No. 76, 1904 (A.N., 165, 187, 1904; Ap. J., 19, 287, 1904).

707. _____. Six New Variable Stars. No. 80, 1904 (A.N., 166, 39, 1904).

708. _____. Stars Having Peculiar Spectra. No. 92, 1904 (A.N., 167, 181, 1905; Ap. J., 21, 292, 1905).

709. _____. Stars Having Peculiar Spectra. No. 98, 1905 (A.N., 168, 303, 1905; Ap. J., 22, 87, 1905).

710. _____. Stars Having Peculiar Spectra. 13 New Variable Stars. No. 111, 1906 (A.N., 171, 139, 1906; Ap. J., 23, 257, 1906).

711. _____. Thirty-one New Variable Stars. No. 120, 1906 (A.N., 173, 263, 1906).

712. _____. Stars Having Peculiar Spectra. 18 New Variable Stars. No. 124, 1907 (A.N., 174, 101, 1907).

713. _____. Stars Having Peculiar Spectra. 15 New Variable Stars. No. 132, 1907 (A.N., 176, 257, 1907; Ap. J., 27, 80, 1907).

714. _____. 28 New Variable Stars in Harvard Map, Nos. 30 and 33. No. 142, 1908 (A.N., 179, 159, 1908).

715. _____. Stars Having Peculiar Spectra. 28 New Variable Stars. No. 143, 1908 (A.N., 179, 191, 1908).

716. _____. A Sixth Type of Stellar Spectra. No. 145, 1908 (A.N., 179, 379, 1909).

717. _____. Group of Red Stars in the Constellation Sagittarius. No. 149, 1909 (A.N., 181, 21, 1909).

718. _____. Stars Having Peculiar Spectra. 38 New Variable Stars. No. 158, 1910 (A.N., 185, 251, 1910).

719. Pickering, E. C. 22 New Variable Stars in Harvard Map, No. 52. No. 162, 1910 (A.N., 186, 317, 1910).

720. _____. Stars Having Peculiar Spectra. 31 New Variable Stars. No. 167, 1911 (A.N., 190, 107, 1911).

721. _____. The Variable Star, 232848, Z Andromedae. No. 168, 1911 (A.N., 191, 57, 1912).

722. _____. Stars Having Peculiar Spectra. No. 178, 1913.

723. _____. The Variable Star, 081041, −41°3911, H.V. 3372. No. 182, 1914.

724. _____. Stars Having Peculiar Spectra. No. 184, 1914 (A.N., 207, 213, 1918).

725. Cannon, A. J. Stars Having Peculiar Spectra. 13 New Variable Stars. No. 196, 1916 (A.N., 207, 213, 1918).

726. _____. Stars Having Peculiar Spectra. Six New Variable Stars. No. 221, 1920, (A.N., 211, 191, 1920).

727. _____. Stars Having Peculiar Spectra. 16 New Variable Stars. No. 224, 1921.

728. Bailey, S. I. Fifty-one New Variable Stars. No. 225, 1921.

729. Cannon, A. J., Stars Having Peculiar Spectra. Eight New Variable Stars. No. 231, 1922.

730. Payne, C. H., and Hogg, F. S. Photometry of the Spectrum of Mira Ceti at the Maximum of 1926-27. No. 308, 1927.

731. Shapley, H., and Walton, M. L. Investigations of Cepheid Variables. No. 313, 1927.

732. Payne, C. H., and Hogg, F. S. On the Pressures in the Atmospheres of Stars. No. 334, 1928.

733. Gerasimovič, B. P. Investigations of Semiregular Variables. No. 341, 1929.

734. Morse, A. H. A Study of the Variable Star T Centauri. No. 358, 1931.

735. Gaposchkin, S. The Variable Star VV Cephei as an Eclipsing System. No. 421, 1937.

Canadian Journal of Research

736. Beals, C. S., and Hatcher, R. D. The Photoelectric Temperatures of the P Cygni Stars. 26A, 149, 1948 (Dom. Obs. Contr., Vol. 2, No. 1, 1948).

Cape Observatory, Annals

737. Lunt, J. The Radial Velocities of 120 Southern Stars, Observed at the Cape. Vol. 10, Part 5, 1921.

738. Jones, H. S. Radial Velocity Determinations. Vol. 10, Part 8, 1928.

Evanston, Dearborn Observatory, Annals

739. Baldwin, R. B., and Hamlin, D. W. Two Peculiar Red Stars. Vol. 4, Part 15, 1940.

740. Lee, O. J.; Baldwin, R. B.; and Hamlin, D. W. Titanium Oxide Stars in Zones −4.5° to +13.5°. Vol. 5, Part 1A, 1943.

741. Lee, O. J., and Bartlett, T. J. Titanium Oxide Stars in Zones +13.5° to +40.5°. Vol. 5, Part 1B, 1944.

742. Lee, O. J.; Gore, G. D.; and Bartlett, T. J. Titanium Oxide Stars in Zones +40.5° to +90°. Vol. 5, Part 1C, 1947.

Flagstaff, Lowell Observatory, Bulletins

743. Slipher, V. M. A New Type of Nebular Spectrum. 3, 63, 1918 (Pub. A.A.S., 4, 50, 1918; Pop. Astr., 27, 149, 1919).

Helwan Observatory, Bulletins

744. Knox-Shaw, H. Preliminary Note on the Variable Nebula (NGC 6729) in Corona Australis. 1, 141, 1915.

745. _____. Hubble's Variable Nebula, NGC 2261. 1, 178, 1920.

746. _____. The Variable Nebula (NGC 6729) in Corona Australis and the Stars in Its Neighborhood. 1, 182, 1920.

I.A.U. Circulaires

747. Brahde, R. T Coronae Borealis. No. 1034, 1946.

748. Bloch, M., and Tcheng, M. T Coronae Borealis. No. 1036, 1946.

749. Dufay, J. T Coronae Borealis. No. 1039, 1946.

750. Elvius, T. Star in Cygnus. No. 1236, 1949.

Johannesburg, Transvaal Observatory, Circulars

751. Innes, R. T. A. Region around S Coronae Austrinae. No. 5, 1910.

Kiel Observatory, Publications

752. Krüger, F. Catalog der farbigen Sterne. 8, 1, 1893.

Mount Hamilton, Lick Observatory, Bulletins

753. Stebbins, J. The Spectrum of Omicron Ceti. 2, 78, 1903 (Ap. J., 18, 341, 1903; Pub. A.S.P., 15, 187, 1903).

754. Perrine, C. D. Observations of 10,1903 Lyrae. 2, 124, 1903.

755. Curtiss, R. H. On the Spectra of R Scuti and W Cygni. 3, 41, 1904 (Ap. J., 20, 232, 1904).

756. Campbell, W. W., and Curtis, H. D. On the Radial Velocities of Polaris, η Piscium, ϵ Aurigae, and β Orionis. 3, 86, 1905.

757. Wright, W. H. Notes on an Attempt To Detect Polarization in the Bright H γ Line in the Spectrum of o Ceti. 6, 60, 1910.

758. Campbell, W. W. Two Stars Whose Radial Velocities Are Variable. 7, 102, 1912.

759. Paddock, G. F. The Radial Velocities of Eleven Southern Light-Variables. 9, 68, 1917.

760. Meyer, W. F. A Study of Certain Nebulae for Evidences of Polarization Effects. 10, 68, 1920.

761. Shane, C. D. The Spectra of Certain Class N Stars. 10, 79, 1920.

762. _____. The Spectrum of o Ceti in 1919. 10, 131, 1922.

763. Moore, J. H. Radial Velocities of Twenty-five Stars of Secchi's Fourth Type. 10, 160, 1922.

764. Luyten, W. J. A Study of the Variable Star SX Herculis. 11, 124, 1924.

765. Allen, L. B. The Radial Velocities of Twenty Southern Variable Stars of Class Me. 12, 71, 1925 (Pub. A.S.P., 37, 323, 1925).

766. _____. A Study of the Changes in the Spectrum of T Centauri. 12, 73, 1925 (Pub. A.S.P., 37, 325, 1925).

767. Shane, C. D. The Spectra of the Carbon Stars. 13, 123, 1928.

768. Wyse, A. B. A Study of the Spectra of Eclipsing Binaries. 17, 37, 1934.

Mount Hamilton, Lick Observatory, Publications

769. Burnham, S. W. Observations of Nebulae with the 36-Inch Refractor of the Lick Observatory. 2, 168, 1894.

770. Campbell, W. W., and Moore, J. H. Radial Velocities of Stars Brighter than Visual Magnitude 5.51 as Determined at Mount Hamilton and Santiago. Vol. 16, 1928.

Mount Kanobili, Abastumani Astrophysical Observatory, Bulletins

771. Shajn, G. A. The Occurrence of Carbon Isotopes in the Spectra of N-Type Stars. 6, 1, 1942.

Mount Wilson Observatory, Annual Reports

772. Remark concerning the Faint Companion of Castor. 1916, p. 251.

773. Remark concerning W Virginis. 1921, p. 269.

774. Remarks concerning T CrB, U Mon, V Vul, and TT Oph. 1922, p. 234.

775. Remark concerning TX Ophiuchi. 1926-1927, p. 121.

776. Remark concerning AG Aurigae. 1927-1928, p. 136.

777. Remarks concerning W Aquilae and W Ceti. 1927-1928, p. 138.

National Academy of Sciences, Proceedings

778. Adams, W. S., and Joy, A. H. Some Spectral Characteristics of Cepheid Variables. 4, 129, 1918 (Mt. W. Comm., No. 53).

779. _____. The Relationship of Spectral Type to Period among Variable Stars. 13, 391, 1927 (Mt. W. Comm., No. 100).

780. Swings, P., and Struve, O. The Spectrum of RW Hydrae. 26, 458, 1940.

781. Shapley, H., and Nail, V. M. Supergiant Red Variable Stars in the Small Cloud. 37, 138, 1951 (Harvard Repr., No. 346).

782. Struve, O. The Spectrum of Capella. 37, 327, 1951.

National Bureau of Standards, Bulletins

783. Merrill, P. W. Application of Dicyanin to the Photography of Stellar Spectra. 14, 487, 1919.

Nature

784. Struve, O., and Elvey, C. T. Stellar Absorption Lines. 125, 308, 1930.

785. Thackeray, A. D. Spectrum of ρ Cassiopeiae. 160, 370, 1947.

Observatory

786. Clerke, A. M. Southern Star Spectra. 11, 429, 1888.

787. _____. The Spectrum of Mira Ceti. 22, 152, 1899.

788. _____. Changes in Stellar Spectra. 29, 164, 1906.

789. Baxandall, F. E. The Bright Lines in the Spectrum of o Ceti. 46, 82, 1923.

790. _____. The Bright Lines in the Spectrum of o Ceti. 46, 226, 1923.

791. Goedicke, V. A. The Eclipsing Binary VV Cephei. 62, 197, 1939.

792. McKellar, A. The λ 6708 Resonance Line of Li I in the Spectrum of the N-Type Variable Star WZ Cassiopeiae. 64, 4, 1941.

793. Thackeray, A. D. Nebulosity Surrounding Eta Carinae. 69, 31, 1949.

Ottawa, Dominion Observatory, Publications

794. Harper, W. E. Radial Velocities of 30 Stars. 4, 331, 1919.

Pittsburgh, Allegheny Observatory, Publications

795. Fowler, M. The Orbit of U Sagittae. 3, 11, 1912.

Popular Astronomy

796. Wilson, H. C. The Spectrum of Mira (o Ceti). 3, 390, 1896.

797. McLaughlin, D. B. The Eclipsing Variable Epsilon Aurigae. 36, 569, 1928.

Potsdam Observatory, Publications

798. Ludendorff, H. Der veränderliche Stern R Coronae Borealis. Vol. 19, Part 2, 1908.

799. Becker, F. Spektral-Durchmusterung der Kapteyn-Eichfelder des Südhimmels. Vol. 27, Part 2, 1930.

Poulkovo Observatory, Circulars

800. Shajn, G. A. The Large Velocity of V CrB and the Character of Hydrogen Lines in Its Spectrum. 10, 12, 1934.

801. Ilinič, A. A. Note on Radial Velocities of RV Tauri Variables. 15, 40, 1935.

Preussischen Akademie der Wissenschaften, Sitzungsberichte

802. Vogel, H. C. Über das Spektrum von Mira Ceti. 1896, p. 395.

803. Ludendorff, H. Über die Radialgeschwindigkeit von ε Aurigae. 1924, p. 49.

Reale Accademia Lincei, Rendiconti

804. Armellini, G. Sopra la teoria delle variabili della famiglia di Mira Ceti. Ser. 6, 13, 313, 1931.

805. Colacevich, A. Osservazioni spettroscopiche della stella variabile RS Ophiuchi. Ser. 6, 18, 307, 1933.

Revista Astronomica

806. Gaviola, E. Remark concerning Proxima Centauri. 18, 243, 1946 (Cordoba Tir. Ap., No. 12).

Richmond Hill, David Dunlap Observatory, Publications

807. Young, R. K. The Radial Velocities of 500 Stars. 1, 69, 1939.

808. _____. The Radial Velocities of 681 Stars. 1, 309, 1945.

809. Northcott, R. J. The Orbits of the Spectroscopic Binaries, HD 99967, HD 181144, HD 209813, and HD 213389. 1, 367, 1947.

Royal Astronomical Society, Memoirs

810. Rimmer, W. B. The Luminosities and Parallaxes of 525 Stars, Types F0 to Mb. 64, 1, 1925.

Royal Astronomical Society, Monthly Notices

811. Burnham, S. W. Note on Hind's Variable Nebula in Taurus. 51, 94, 1890.

812. Espin, T. E. Two New Variable Stars. 54, 100, 1893.

813. _____. Note on the Spectra of Certain Red Stars. 54, 100, 1893.

814. _____. A New Variable Star of Type IV. 54, 442, 1894.

815. Barnard, E. E. On the Variable Nebulae of Hind (N.G.C. 1555) and Struve (N.G.C. 1554) in Taurus, and on the Nebulous Condition of the Variable Star T Tauri. 55, 442, 1895.

816. Barnard, E. E. Invisibility of Hind's Variable Nebula (N.G.C. 1555). 56, 66, 1895.

817. McClean, F. Photographic Stellar Spectra of the Variable Star β Lyrae, and also of Types III and IV. 57, 6, 1896.

818. Sidgreaves, W. The Spectrum of o Ceti as Photographed at Stonyhurst College Observatory. 58, 344, 1898.

819. Espin, T. E. Revised Catalogue of the Stars of the IV Type. 58, 443, 1898.

820. Barnard, E. E. Observations of Hind's Nebula in Taurus (N.G.C. 1555) Made with the 40-Inch Refractor of the Yerkes Observatory. 59, 372, 1899.

821. Sidgreaves, W. Notes on the Spectra of γ Cassiopeiae and o Ceti. 59, 505, 1899.

822. Keeler, J. E. Photographic Observations of Hind's Variable Nebula in Taurus, Made with the Crossley Reflector of the Lick Observatory. 60, 424, 1900.

823. Sidgreaves, W. The Spectrum of Mira Ceti in Dec. 1906, as Photographed at Stonyhurst College Observatory. 67, 534, 1907.

824. Cortie, A. L. Note on the Visual Spectrum of Mira Ceti in December, 1906. 67, 537, 1907.

825. Fowler, A. Spectroscopic Comparison of o Ceti with Titanium Oxide. 69, 508, 1909.

826. Espin, T. E. The Spectrum of R Cygni. 72, 546, 1912.

827. Wright, W. H. The Spectrum of R Cygni. 72, 548, 1912.

828. Reynolds, J. H. The Variable Nebula in Corona Australis (N.G.C. 6729). 76, 645, 1916.

829. Knox-Shaw, H. Note on the Variable Nebula in Corona Australis. 76, 646, 1916.

830. Espin, T. E. Z Andromedae. 79, 149, 1918.

831. Lockyer, W. J. S. Spectroscopic and Magnitude Observations of o (Mira) Ceti, 1924. 84, 558, 1924.

832. Baxandall, F. E. On the Presence of Radiation Bands of Aluminum Oxide in the Spectrum of Mira Ceti at the Maximum of 1924 February. 88, 679, 1928.

833. Redman, R. O. Note on Three Variable Stars: (i) SV Ursae Majoris, (ii) V Ursae Minoris, (iii) WY Geminorum. 92, 116, 1931.

834. Payne, C. H. An Interpretation of Absorption and Emission Lines in Early Type Spectra. 92, 368, 1932 (Harvard Repr., No. 75).

835. Getting, I. A. The Characteristic Curves of Some Variable Stars. 95, 139, 1934.

836. Redman, R. O. Center to Limb Variation in Fraunhofer Line Intensity over the Disc of the Primary Star of U Cephei and of U Sagittae. 96, 488, 1936.

837. Gregory, C. C. L., and Peachey, E. M. The Spectrum of T Coronae Borealis on 1946 February 11. 106, 135, 1946 (Observatory, 66, 241, 1946).

838. Tai, W. S., and Thackeray, A. D. The Spectrum of ρ Cassiopeiae in 1939. 108, 271, 1948.

839. Thackeray, A. D. The Spectrum of ρ Cassiopeiae 1946-1947. 108, 276, 1948.

840. Struve, O. Spectroscopic Binaries. 109, 487, 1949.

841. Gascoigne, S. C. B. Relative Gradients for 166 Southern Stars. 110, 15, 1950.

842. Thackeray, A. D. Five Southern Stars with Emission-Line Spectra. 110, 45, 1950 (Radcliffe Comm., No. 15).

843. Johnson, M. Adjustments within Shells and Asymmetric Ejecta from Z And, ζ Aur, β Lyr, ρ Cas, and γ Cas. 110, 84, 1950.

844. Thackeray, A. D. Some Southern Stars Involved in Nebulosity. 110, 524, 1950 (Radcliffe Comm., No. 18).

845. Johnson, M. Delays in Fluorescence Applicable to the Blue-red Binaries T CrB, Z And, R Aqr, AX Per, α Sco, and RW Hya. 111, 490, 1951.

Royal Astronomical Society of Canada, Journal

846. Plaskett, J. S. The Spectrum of Mira Ceti. 1, 45, 1907.

847. Harper, W. E. Spectroscopic Notes. 28, 172, 1934.

848. McKellar, A., and Stilwell, W. H. The Resonance Lines of Li I and Na I in Spectra of the Red Carbon Stars. 38, 237, 1944.

849. Petrie, R. M. The Orbits and Dimensions of the Components of the Spectroscopic Binary HD 43246. 42, 140, 1948 (Dom. Ap. Obs. Contr., No. 9; A.J., 52, 128, 1947).

850. Wright, K. O., and Van Dien, E. The Spectrum of Epsilon Aurigae, 1946-1948. 43, 15, 1949 (Dom. Ap. Obs. Contr., No. 17).

851. Merrill, P. W. Emission Lines in the Spectra of Long-Period Variable Stars. 46, 181, 1952 (Dom. Ap. Obs. Contr., No. 27, Part 2).

852. Herbig, G. H. Emission-Line Stars in Galactic Nebulosities. 46, 222, 1952 (Dom. Ap. Obs. Contr., No. 27, Part 3).

Royal Society of London, Proceedings

853. Fowler, A. The Spectra of Antarian Stars in Relation to the Fluted Spectrum of Titanium. 73, 219, 1904 (M.N., 64, appendix, p. 16, 1904).

Sidereal Messenger

854. Pickering, E. C. New Variable Stars in Cygnus. 9, 232, 1890 (A.N., 124, 271, 1890).

855. Fleming, W. P. Stars Having Peculiar Spectra. 9, 379, 1890 (A.N., 124, 175, 1890; 125, 361, 1890; 125, 365, 1890).

856. _____. Stars Having Peculiar Spectra. 10, 7, 1891 (A.N., 126, 117, 1890; 126, 163, 1891).

857. _____. Stars Having Peculiar Spectra. 10, 106, 1891 (A.N., 127, 5, 1891).

Simeis, Crimea Astrophysical Observatory, Publications

858. Shajn, G. A. Emission Lines of H, Fe II, and Fe I in the Spectra of Long-Period Variable Stars. 1, Part 1, 5, 1947 (Astr. News Letter, No. 49).

859. Shajn, P. F. A Systematic Shift of Certain Spectral Lines in the Spectrum of o Ceti. 1, Part 1, 116, 1947 (Astr. News Letter, No. 49).

860. Gaze, V. F., and Shajn, G. A. An Investigation of the Spectra of the Carbon Stars. 2, 51, 1948 (Astr. News Letter, No. 44).

861. Shajn, G. A., and Gaze, V. F. Bands of the Heavy Cyanogen Molecule in the Spectra of the Carbon Stars (Violet System $^2\Sigma - {}^2\Sigma$). 2, 131, 1948 (Astr. News Letter, No. 44).

862. Shajn, G. A., and Shajn, P. F. The Differential Systematic Displacements of Lines in the Spectra of White Supergiants. 4, 49, 1949 (Astr. News Letter, No. 44).

Sky and Telescope

863. Goedicke, V. The Story of VV Cephei. 2, No. 12, 3, 1943.

864. McLaughlin, D. B. The Spectrum of T Cor Bor. 5, No. 6, 7, 1946.

865. Struve, O. Variable Stars and Stellar Evolution. I. 9, 131, 1950.

866. _____. The Coming Eclipse of Epsilon Aurigae. 12, 99, 1953.

Società Astronomica Italiana, Memorie

867. Colacevich, A., and Masani, A. Osservazioni spettrofotometriche della variabile AC Herculis. 13, 331, 1940.

868. Gratton, L. Breve notizia sullo spettro di λ Andromedae. 16, 267, 1944 (Merate Contr., No. 17, 1944).

869. Gratton, L., and Krüger, E. C. Lo spettro della Nova T Coronae Borealis nell' esplosione del Febbraio 1946. 20, 197, 1949 (Merate Contr., No. 28, 1949).

870. Kranjc, A. Atmosfere intermedie fra binarie strette. 22, 131, 1951.

Stockholm Observatory, Annals

871. Iwanowska, W. The Spectrophotometric Criteria of the Pseudo-cepheids in Low Dispersion. Vol. 12, No. 5, 1936.

872. Brahde, R. A Spectrophotometric Investigation of Nova T Coronae Borealis 1946. Vol. 15, No. 7, 1949.

Stockholm Observatory, Meddelanden

873. Öhman, Y., and Iwanowska, W. Note on the Continuous Hydrogen Absorption of cF Stars. No. 21, 1935.

The Telescope

874. Morgan, W. W. Some Uses of Spectral Classification. 8, 77, 1941.

Variable Stars

875. Erpylev, N. P. An Investigation of the Spectrum of the Nova T Coronae Borealis. 7, 273, 1950 (Astr. News Letter, No. 61).

Victoria, Dominion Astrophysical Observatory, Publications

876. Young, R. K., and Harper, W. E. The Absolute Magnitudes and Parallaxes of 1105 Stars. 3, 1, 1924.

877. Plaskett, H. H. The Composite Stellar and Nebular Spectrum of Z Andromedae. 4, 119, 1928.

878. Redman, R. O. The Galactic Rotation Effect in Some Late Type Stars (Second Paper). 6, 27, 1931.

879. Harper, W. E. The Radial Velocities of 477 Stars. 6, 149, 1934.

880. Pannekoek, A. Line Intensities in Spectra of Advanced Type. 8, 141, 1950.

881. McKellar, A. Spectrographic Observations of the Eclipsing Binaries DI Herculis and RY Geminorum. 8, 235, 1950.

882. Climenhaga, J. L.; McKellar, A.; and Petrie, R. M. Spectrographic Observations of Epsilon Ursae Minoris. 8, 401, 1951 (A.J., 56, 36, 1951).

883. Beals, C. S. The Spectra of the P Cygni Stars. 9, 1, 1951.

Williams Bay, Yerkes Observatory, Publications

884. Hale, G. E.; Ellerman, F.; and Parkhurst, J. A. The Spectra of Stars of Secchi's Fourth Type. 2, 251, 1903.

885. Frost, E. B.; Struve, O.; and Elvey, C. T. A Study of the Spectrum of 7 ε Aurigae. 7, 81, 1932.

886. Morgan, W. W. A Descriptive Study of the Spectra of the A-Type Stars. 7, 133, 1935.

Zeitschrift für Astrophysik

887. Becker, F. Helle Calciumlinien in Sternspektren. 1, 208, 1930.

888. Brück, H. Spektralaufnahmen von Exnovae und veränderlichen Sternen. 4, 70, 1932.

889. _____. Spektralaufnahmen schwacher veränderlicher Sterne. 4, 399, 1932.

890. Wurm, K. Zur Intensität der C_2- und CN-Banden in den Spektren der R- und N-Sterne. 5, 260, 1932.

891. Günther, S. Die Absorption der Balmerlinien in Sternspektren. 7, 106, 1933 (Göttingen Veröff., No. 36).

892. Shajn, G. A. Über die Emissionslinien des Wasserstoffs in den Spektren langperiodischer Veränderlicher. 10, 73, 1935.

893. Hachenberg, O., and Wellmann, P. Das Spektrum und die Lichtkurve der Nova T Coronae Borealis 1866 während ihres Maximums Juli 1938. 17, 246, 1939.

894. Wellmann, P. Das zusammengesetzte Spektrum von T Coronae Borealis. 19, 16, 1939.

895. _____. Die doppelte Umkehr der Linien H und K im Spektrum von α Boötis. 19, 236, 1940.

896. _____. Die doppelte Umkehr der Ca II-Linien im Spektrum von α Orionis. 20, 214, 1940.

897. Walter, K. Über Polarisation im Nebel um FU Orionis. 20, 256, 1941 (Potsdam Mitt., No. 10).

898. Günther, S. Die Wasserstoffabsorption in Sternspektren. 22, 185, 1943.

899. Lohmann, W. Das Problem RZ Ophiuchi. 27, 161, 1950.

900. Wellmann, P. Veränderungen im Spektrum von FU Orionis. 29, 154, 1951.

Separate Publications

901. Merrill, P. W. Spectra of Long-Period Variable Stars. ("Astrophysical Monographs.") Chicago: University of Chicago Press, 1940.

902. Morgan, W. W.; Keenan, P. C.; and Kellman, E. An Atlas of Stellar Spectra. ("Astrophysical Monographs.") Chicago: University of Chicago Press, 1943.

903. Greenstein, J. L. Stars in Diffuse Nebulae. ("Centennial Symposia," "Harvard Monographs," No. 7.) Cambridge: Harvard University Press, 1948.

THE INDEX OF CLUMPINESS OF THE DISTRIBUTION OF IMAGES OF GALAXIES*

JERZY NEYMAN AND ELIZABETH L. SCOTT
Statistical Laboratory
AND
C. D. SHANE
Lick Observatory, University of California
Received February 8, 1954

ABSTRACT

The subject of study is the index K of clumpiness of the distribution of images of galaxies on a photographic plate. Its definition, referring to counts of galaxies in areas ω on the photographic plate, is suggested by that of a related characteristic $k(z, n)$ studied by Zwicky. With reference to the recent theory of the distribution of galaxies in space, the dependence of K upon the physical characteristics of this distribution (the frequency of clusters, the variation in the number of galaxies per cluster, the compactness of clusters) and upon observational factors (size and shape of regions ω in which counts are made and limiting apparent magnitude of plate) is studied. The theoretical conclusions regarding the dependence of K on the size and shape of ω are found to contradict the conclusions implied by an alternative theory of Chandrasekhar-Münch-Limber. Empirical values of K obtained from counts of images of galaxies on Lick Observatory plates appear to agree with the theory of the authors. Also the same empirical values of K appear to agree qualitatively with those found by Zwicky. However, at least within the range of limiting magnitudes investigated, in order to explain the shape of the empirical curves, there is no necessity for the hypothesis of extragalactic absorbing clouds.

I. INTRODUCTION

In a recent paper by F. Zwicky (1953) the opinion is expressed that "a decision for or against the concept of the expanding universe is not possible on the basis of nebular counts" and that the solution of the problem may be expected from methods "which belong to the realm of dimensionless morphology." The latter consist in the study of the structure of the distribution of images of galaxies on photographic plates. The particular methods illustrated by Zwicky are (*a*) the study of the variance of counts of images of galaxies in small areas on a photographic plate and (*b*) the study of the number $N_\gamma d\gamma$ of clusters of galaxies with their angular dimensions between γ and $\gamma + d\gamma$.

While the present authors would not insist that the classical methods are inapplicable for the decision as to whether or not the universe is expanding, they agree that the methods of "dimensionless morphology" or, more simply, the methods of the morphology of the distribution of images of galaxies throw a new light on the problem and may be quite helpful. It is with this possibility in mind that two of the authors developed a general theory of the spatial distribution of galaxies based on the assumption of stationarity of the universe and on the assumption that galaxies occur only in smaller or larger clusters. The paper in question (Neyman and Scott 1952) will be referred to as "Paper I." In a later paper (Paper II), by the present authors (1953), this general theory was specialized by postulating particular forms of several relevant functions. This specialization of the general theory was then confronted with counts of galaxies made at the Lick Observatory. The comparison showed a general agreement between theory and observation and led to tentative estimates of the density of cluster centers in space, of the average number of galaxies per cluster, and of the average dimensions of a cluster. In the third paper (Scott, Shane, and Swanson 1954) of the series ("Paper III"), it was shown that the visual appearance of a "synthetic" photographic plate, obtained by means of a

* All computations for this paper were performed at the Statistical Laboratory, University of California, with the partial support of the Office of Naval Research. Counts of galaxies were made at the Lick Observatory by C. D. Shane and C. A. Wirtanen. This paper is a joint publication of the Statistical Laboratory and of the Lick Observatory (*Contributions from the Lick Observatory*, Ser. II, No. 55).

large-scale sampling experiment conforming exactly with the assumptions of the theory, is very similar to that of an actual plate. The only difference noticed between the two is concerned with the small-scale clumpiness of images of galaxies. This clumpiness is somewhat more intense on the actual than on the synthetic plate.

When discussing the relevance of counts of clusters classified according to the angular values of their diameters, Zwicky points out some of the difficulties involved and, in particular, that a small group of galaxies may be mistaken for a cluster. In this connection it may be interesting to mention that, although the distribution of images of galaxies on the synthetic plate in Paper III was derived solely from the superposition of randomly distributed clusters, these clusters are entirely unidentifiable on the synthetic plate. On the other hand, the synthetic plate presents many local condensations of images of galaxies that might be taken for clusters. For a number of such instances a check was performed, and it was found invariably that the condensations are composed of galaxies belonging to several different clusters, one behind another.[1] Although this difficulty may depend on the particular structure of clusters used in the sampling experiment, which may be found unrealistic, the authors feel that the statistics of clusters of galaxies compiled on the basis of numbers N_γ are likely to require quite important corrections. In order to evaluate these corrections, it is necessary to establish empirically the relative frequencies of correct and mistaken identifications of clusters and also the distribution of errors in estimating the visual diameter of a cluster. In this connection the method of synthetic photographic plates may be useful.

The purpose of the present paper is to connect some of the discussions of Zwicky with the theory of Paper I. Specifically, we are concerned with the question as to whether or not the shape of a graph of an empirical quantity $k(z, n)$, studied by Zwicky, can be taken as an argument in favor of his hypothesis of intergalactic absorbing clouds.

II. INDEX OF CLUMPINESS OF THE DISTRIBUTION OF IMAGES OF GALAXIES ON A PHOTOGRAPHIC PLATE

Consider a large solid angle, Ω, divided into a substantial number z of equal parts of size $\omega = \Omega/z$. Let n denote the total number of galaxies brighter than a fixed limiting magnitude, all located in Ω, and let n_i be their number within the ith partial solid angle ω. In the paper under discussion (1953) and also in an earlier paper (1952) Zwicky considers the sample variance S_1^2 of the numbers n_i defined by

$$S_1^2 = \sum_{i=1}^{z} \frac{(n_i - n/z)^2}{z}. \tag{1}$$

This quantity is compared with another, S_0^2, meant to represent the variance of the n_i on the assumption that the n galaxies counted in Ω are uniformly and independently distributed among the z partial solid angles ω, so that

$$S_0^2 = \frac{n(1 - 1/z)}{z}. \tag{2}$$

Actually, Zwicky considers the quotient[2] denoted by $k(z, n) = S_1/S_0$. In the paper (1953) under discussion he produces Figure 2 with three curves marked *I*, *II*, and *III* that represent the expected dependence of $k(z, n)$ on n when the value of z is kept constant.

[1] The authors are indebted to Dr. N. U. Mayall for the suggestion that this result may be helpful in explaining the large velocity dispersion in some groups and apparent clusters.

[2] It will be noticed that $k^2(z, n)$ is proportional to the so-called "index of dispersion" introduced by Lexis for the study of a certain problem of stability of probabilities of certain demographic events, such as probabilities of deaths, probabilities that a child to be born will be a male, etc. The theory of the index of dispersion was first given by L. von Bortkiewicz (*Skandinavisk Aktuarietidskrift*, **1**, 1, 1918). However, the developments in the following pages refer to an entirely different problem and have no connection with the problem of Bortkiewicz.

The first of the curves is more or less level and corresponds to the hypothesis that the galaxies are distributed in space uniformly and independently from one another and that intergalactic space contains no absorbing material. The second curve corresponds to Zwicky's expectation of the effect of clustering of galaxies in the absence of intergalactic clouds. This curve begins with $k(z, n) = 1$ at $n = 0$, then climbs up to about $k(z, n) = 7$ and thereafter declines to unity. The third curve, described as representing schematically the actual empirical findings, climbs steadily over the whole range of values of n. Zwicky's interpretation of the shape of the schematically represented empirical curve *III* is that it is evidence of the existence of intergalactic absorbing clouds.

The purpose of this paper is to present certain theoretical considerations that are based on the theory of the spatial distribution of galaxies presented in Paper I and to show that, at least over a range of limiting magnitudes, in order to explain the shape of Zwicky's curve *III* there is no necessity of making any assumptions regarding the existence of intergalactic absorbing clouds. This result is obtained from a study of the quotient K, related to, but different from, $k(z, n)$, described as the index of clumpiness of the distribution of images of galaxies on a photographic plate. This index appears to have a certain advantage over the quotient $k(z, n)$.

The point is that $k(z, n)$ as defined by Zwicky depends on n, the total number of images of galaxies within the solid angle Ω, and it is subject to random variation. Also the quotient $k(z, n)$ depends on the numbers n_i of images of galaxies in the partial solid angles ω_i. These numbers n_i are also random variables. As a result, the value of $k(z, n)$ itself is subject to random variation, which brings about a certain waviness of the three curves in Zwicky's graphs. Naturally, the presence of random fluctuations may occasionally lead to a confusion as to what is a real characteristic of a phenomenon and what is due to chance.

Instead of depending on random variables, the index of clumpiness K depends on several factors involved in the spatial distribution of galaxies and also on the size and shape of the region ω on the photographic plate in which the images of galaxies are counted and on the limiting apparent magnitude. The quantity K is defined as the quotient $K = \sigma_1/\sigma_0$ of two sure (that is, nonrandom) numbers σ_1 and σ_0. The first of these is the square root of the true variance of the random number of galaxies in ω brighter than a fixed limiting apparent magnitude, computed on the assumption of no interstellar or intergalactic absorbing clouds and on the assumption that the galaxies are clustered. The second quantity is the square root of the variance of the same number of galaxies in ω, computed on the same assumption of absence of absorbing clouds and on the assumption that the galaxies are distributed in space singly, independently from one another, and with statistical uniformity. In other words, σ_1 and σ_0 are, so to speak, the theoretical values of S_1 and S_0, respectively. The operational interpretation of these theoretical values is as follows: if S_1^2 and S_0^2 are computed for many different but equal solid angles Ω in randomly selected directions, always with the same substantial number z of parts, then the average values of the S_1^2 and S_0^2 so obtained will be approximately equal to σ_1^2 and σ_0^2.

Zwicky's discussions of $k(z, n)$ are concerned with the behavior of this quantity when z and n are changed. In order to establish the relation between questions of this kind and those studied in the present paper, we notice that an increase in z means a decrease in the size of the solid angle ω within which galaxies are counted. Thus the study given below of the dependence of the index of clumpiness K on the size (and shape) of ω will constitute an analogon of Zwicky's studies of $k(z, n)$ when z is either increased or decreased.

Proceeding further, we notice that the argument n in $k(z, n)$ cannot be changed at will but depends on the chance that a solid angle Ω will contain a larger or smaller number n of galaxies brighter than the limiting apparent magnitude of the plate. In order to obtain an analogon to the discussion of Zwicky of $k(z, n)$ when n is changed, we notice that the angles Ω of a given size will *generally* contain more bright galaxies (sufficiently bright to be visible on the photographic plate) either (i) when the average density of

galaxies per unit volume in space is increased or (ii) when the limiting apparent magnitude of the plate is augmented, or both.[3] We notice also that the increase (i) may result from the appropriate change of two different elements in the contemplated scheme of the spatial distribution of galaxies. Specifically, an increase in the average density of galaxies per unit of volume may be the result of either (*a*) an increase in the average number, say λ, of clusters per unit volume or (*b*) an increase in the average number, say ν_1, of galaxies per cluster, or both.

Thus, in order to obtain an analogon of Zwicky's study of $k(z, n)$ in relation to changes in n while z is fixed, we shall study the dependence of K on the average density λ of clusters per unit volume in space, on the general properties of the distribution of the number ν of galaxies per cluster, and on the limiting apparent magnitude of the plates used. For this purpose we shall need some of the general results obtained in Paper I.

III. BASIC ASSUMPTIONS AND SOME RESULTS OF THE THEORY OF CLUSTERING OF GALAXIES

The theory of the spatial distribution of galaxies developed in Paper I is based on the following five postulates.

(i) Galaxies occur only in clusters.

Remark.—As stated in postulate (iii), the number ν of galaxies in a cluster is contemplated as a random variable with an arbitrary distribution that includes the possibility that ν is identically equal to unity. It follows that the above first postulate does not involve any limitation but, rather, serves to define a particular point of view, which introduces the concept of a cluster as an element in the general spatial distribution of galaxies.

(ii) To every region R in space there corresponds a random variable $\gamma(R)$, depending only on the volume V of R and representing the number of cluster centers falling within R. If $R_1, R_2, \ldots, R_n, \ldots$, are nonoverlapping regions in space, then the corresponding variables $\gamma(R_1), \gamma(R_2), \ldots, \gamma(R_n), \ldots$, are completely independent. If R_1 is a region of finite positive volume known to contain exactly n cluster centers, say $C_1, C_2, \ldots, C_n$, and if R_1^* is an arbitrary part of R_1, then the probability that R_1^* will contain any particular group of these cluster centers, say $C_{a_1}, C_{a_2}, \ldots, C_{a_m}$, with $m < n$, depends only on m and n and on the volumes of R_1 and R_1^*.

The distribution of clusters satisfying the foregoing conditions was called "quasi-uniform." It was shown that, without loss of generality, it may be assumed that each $\gamma(R)$ is a Poisson random variable with probability-generating function,

$$G_\gamma(t \mid V) = E\{t^{\gamma(R)}\} = e^{-\lambda V(1-t)}, \tag{3}$$

where, as before, V stands for the volume of R and λ stands for the average number of cluster centers per unit volume.

(iii) The number ν of galaxies per cluster is a random variable with an unspecified probability-generating function $G_\nu(t)$.

(iv) Given the co-ordinates u, v, w of the center of a cluster (these co-ordinates are measured from a rectangular system of axes with origin at the observer), the positions of galaxies forming this cluster are random. More specifically, it is assumed that these galaxies are distributed in space independently of one another, and so that the triplet of co-ordinates X, Y, Z of any one of them has a continuous probability density $f(\eta)$ depending only upon the argument

$$\eta = \{(x-u)^2 + (y-v)^2 + (z-w)^2\}^{1/2}, \tag{4}$$

[3] Dr. Zwicky confirms that in drawing his curves *I*, *II*, and *III* he assumed that the increase in n is brought about either by an increase in the angle ω or by an increase in the limiting apparent magnitude of the plate. Moreover, it is his understanding that the effects of these two methods of increasing n are not the same (private communication, November 4, 1953).

where x, y, z stand for the particular values of X, Y, Z. The function of $f(\eta)$ is left unspecified.

Remark.—Postulate (iv) in this form coincides with that in Paper I. However, the following developments depend only on the assumption that f is a continuous function of the differences $x - u$, $y - v$, and $z - w$.

(v) Given the position (x, y, z) of a galaxy, with its distance from the observer

$$\xi = \{x^2 + y^2 + z^2\}^{1/2}, \tag{5}$$

and given a number m^*, there exists the probability $\theta(\xi, m^*)$ that the apparent magnitude of the galaxy in question will be brighter than the specified number m^*. This probability, depending on the luminosity function of the galaxies and on the relation between the apparent magnitude, the absolute magnitude, the distance, and the dimming due to reddening, is left unspecified. In addition, it is postulated that the absolute magnitudes of galaxies are mutually independent and that the corresponding apparent magnitudes depend on distance only.

It will be seen that the five postulates do not mention anything that may include the extinction of light from galaxies either by interstellar or by intergalactic absorbing material. In fact, the conditional independence of apparent magnitudes of galaxies, given their distances, postulated in (v), eliminates the possibility of a cloud obscuring two or more galaxies simultaneously. It follows that the theory in question is applicable only in regions in space, if any, where the obscuration by light-absorbing clouds can be neglected.

The evaluation of both σ_1 and σ_0, needed to compute K, the index of clumpiness, will be based on these five postulates. In order to obtain σ_1, no change in the postulates is needed. On the other hand, in order to obtain σ_0, it will be sufficient to assume that for each cluster the number ν of galaxies is exactly equal to unity. This assumption would mean that $G_\nu(t) \equiv t$.

The main result of Paper I concerns two random variables, N_1 and N_2, representing the numbers of galaxies within two arbitrary solid angles, say ω_1 and ω_2, overlapping or not, in which galaxies are counted up to the limiting apparent magnitudes m_1^* and m_2^*, respectively. This result gives the probability-generating function $G_{N_1, N_2}(t_1, t_2)$ of N_1 and N_2, expressed in terms of the unspecified parameter λ and in terms of the unspecified functions $G_\nu(t)$, $f(\eta)$, and $\theta(\xi, m_i^*)$. Unless explicitly stated, in the following discussions no restriction will be placed on these three functions except that their nature must insure the convergence of integrals (6) and (9), below, with $m + n = 1$. This restriction is needed in order to insure that the theory under consideration conforms with the empirical fact that the number of galaxies with their apparent magnitude brighter than a a fixed number m^* is finite.

In the present study, we shall need the expression for $G_{N_1, N_2}(t_1, t_2)$ for the particular case where $m_1^* = m_2^* = m^*$ (say) and where the two solid angles ω_1 and ω_2 do not overlap. In this case we have, say,

$$\begin{aligned} H(t_1, t_2) &= \log G_{N_1, N_2}(t_1 t_2) \\ &= -\lambda \int_{-\infty}^{+\infty}\!\!\int\!\!\int \{1 - G_\nu[1 - p_1(1 - t_1) - p_2(1 - t_2)]\}\, du\, dv\, dw, \end{aligned} \tag{6}$$

where p_1 and p_2 are functions of u, v, w, depending on the solid angles ω_1 and ω_2,

$$p_i = \int_{\omega_i}\!\!\int\!\!\int \theta(\xi, m^*)\, f(\eta)\, dx\, dy\, dz. \tag{7}$$

It is seen, for $i = 1, 2$, that p_i represents the probability that a galaxy belonging to a cluster centered at (u, v, w) will be included within the solid angle ω_i and that its apparent magnitude will be brighter than m^*.

We shall notice at once that, if the number ν of galaxies is always unity for all clusters, so that $G_\nu(T) \equiv T$, then formula (6) reduces to, say,

$$H^*(t_1, t_2) = -\lambda\{(1 - t_1)R_{10} + (1 - t_2)R_{01}\}, \tag{8}$$

where, generally,

$$R_{m,n} = \int_{-\infty}^{+\infty}\int\int p_1^m p_2^n du\, dv\, dw. \tag{9}$$

It is seen from equation (8) that, in case $\nu \equiv 1$, the numbers N_1 and N_2 of galaxies in ω_1 and ω_2, with their brightness exceeding the limiting magnitude of the plate, are independent Poisson variables, with expected values

$$E(N_1) = \lambda R_{10}, \qquad E(N_2) = \lambda R_{01}. \tag{10}$$

As is well known, the variance of a Poisson variable is equal to the expectation of this same variable. Thus the quantities (10) also represent the variances of N_1 and N_2, respectively, computed on the assumption that $\nu \equiv 1$ and, therefore, that the galaxies are not clustered.

We need formula (6) in order to compute the expectations $E(N_i)$ of N_i, for $i = 1, 2$, as well as their variances,

$$\sigma^2_{N_i} = E\,[N_i - E\,(N_i)\,]^2, \tag{11}$$

and their correlation, say,

$$\rho\,(\omega_1, \omega_2) = \frac{E\{\,[N_1 - E\,(N_1)\,][N_2 - E\,(N_2)\,]\,\}}{\sigma_{N_1}\sigma_{N_2}}. \tag{12}$$

All these quantities are obtainable by differentiating $H(t_1, t_2)$ with respect to appropriate arguments and then substituting $t_1 = t_2 = 1$. Using the symbols ν_1 and ν_2 to represent the first two moments of the random variable ν, so that

$$\nu_1 = E\,(\nu) = \frac{dG_\nu}{dT}, \tag{13}$$

$$\nu_2 = E\,(\nu^2) = \frac{d^2G_\nu}{dT^2} + \frac{dG_\nu}{dT}, \tag{14}$$

we have from (6), say,

$$\bar{N}_1 = E\,(N_1) = \frac{\partial H}{\partial t_1} = \lambda\nu_1 R_{10}, \tag{15}$$

$$\bar{N}_2 = E\,(N_2) = \frac{\partial H}{\partial t_2} = \lambda\nu_1 R_{01}, \tag{16}$$

$$\sigma^2_{N_1} = \frac{\partial^2 H}{\partial t_1^2} + \frac{\partial H}{\partial t_1} = \lambda\,(\nu_2 - \nu_1)\,R_{20} + \bar{N}_1, \tag{17}$$

$$\sigma^2_{N_2} = \frac{\partial^2 H}{\partial t_2^2} + \frac{\partial H}{\partial t_2} = \lambda\,(\nu_2 - \nu_1)\,R_{02} + \bar{N}_2, \tag{18}$$

and

$$\sigma_{N_1}\sigma_{N_2}\rho(\omega_1, \omega_2) = \frac{\partial^2 H}{\partial t_1 \partial t_2} = \lambda(\nu_2 - \nu_1) R_{11}, \tag{19}$$

where it should be understood that all the derivatives are evaluated at $t_1 = t_2 = 1$. It follows that

$$\rho(\omega_1, \omega_2) = \frac{(\nu_2 - \nu_1) R_{11}}{\{[(\nu_2 - \nu_1) R_{20} + \nu_1 R_{10}][(\nu_2 - \nu_1) R_{02} + \nu_1 R_{01}]\}^{1/2}}. \tag{20}$$

Upon examining formulae (9) and (7) it will be seen that, irrespective of the form of the unspecified functions $\theta(\xi, m^*)$ and $f(\eta)$, the integrals $R_{m,n}$ cannot be negative. It follows that the correlation coefficient $\rho(\omega_1, \omega_2)$ cannot be negative. In fact, if the two solid angles ω_1 and ω_2 are not too far apart, it is safe to assume that $\rho(\omega_1, \omega_2)$ is positive. On the other hand, by the Schwartz inequality,

$$R_{11} \leqq (R_{20} R_{02})^{1/2}. \tag{21}$$

Combining this result with formula (20), we have

$$0 \leqq \rho(\omega_1, \omega_2) \leqq \left(\left[1 + \frac{\nu_1 R_{10}}{(\nu_2 - \nu_1) R_{20}}\right]\left[1 + \frac{\nu_1 R_{01}}{(\nu_2 - \nu_1) R_{02}}\right]\right)^{-1/2} < 1. \tag{22}$$

It is interesting to point out that the correlation (20) between counts of galaxies in two arbitrary nonoverlapping solid angles ω_1 and ω_2 does not depend upon λ, which, it will be remembered, is the average density of cluster centers per unit volume. On the other hand, $\rho(\omega_1, \omega_2)$ does depend on the variability of the number ν of galaxies from one cluster to another and, of course, on ω_1, ω_2 and on the functions $f(\eta)$ and $\theta(\xi, m^*)$.

In the following we shall need formulae (10), (15) through (18), (20), and (22).

IV. ANALYSIS OF THE INDEX OF CLUMPINESS K BASED ON THE THEORY OF CLUSTERING OF GALAXIES

In order to compute the index of clumpiness K, using the theory of Paper I, we shall consider a single solid angle ω (later specialized as a rectangle with angular dimension $2a_1 \times 2a_2$), the number N of galaxies brighter than a limiting apparent magnitude m^* this solid angle contains, and two hypothetical situations as follows. In the first we shall assume that there is no clustering in the strict sense of the word and that the galaxies are distributed in space singly and independently of one another. As we have seen before, this amounts to assuming $\nu \equiv 1$ for all "clusters." Let λ^* denote the average number of galaxies per unit volume. Then formulae (10) give the variance of N that we shall denote by σ_0^2. We have

$$\sigma_0^2 = \lambda^* R_{10}. \tag{23}$$

In the second situation we shall assume the presence of clustering, so that ν is not identically equal to unity for all clusters, but shall not make any other assumption regarding the distribution of this quantity, except that its first two moments exist. However, we shall assume that the density λ of cluster centers and the average number ν_1 of galaxies per cluster are so adjusted that the expectation of N is exactly the same as in the first situation. This assumption requires that λ^* be equal to $\lambda\nu_1$. The variance, say σ_1^2, of N corresponding to this second situation is given by formula (17), namely,

$$\sigma_1^2 = (\nu_2 - \nu_1) R_{20} + \lambda\nu_1 R_{10}. \tag{24}$$

Dividing (24) by (23), with $\lambda^* = \lambda\nu_1$, we obtain the expression for the square of the index of clumpiness,

$$K^2 = 1 + \frac{\nu_2 - \nu_1}{\nu_1}\frac{R_{20}}{R_{10}} = 1 + (c-1)\frac{R_{20}}{R_{10}}, \tag{25}$$

where $c = \nu_2/\nu_1$.

We shall now study the dependence of the quantity K on the various factors involved in the spatial distribution of galaxies and on observational factors, such as the size and shape of the solid angle ω and the limiting apparent magnitude m^* of the plate. Although the various conclusions reached are very simple, for convenience of reference they are listed as separate theorems.

The first interesting circumstance that attracts attention is that (25) does not involve λ, the average number of cluster centers per unit volume. Thus we have

THEOREM 1.—*The index of clumpiness of the distribution of images of galaxies is independent of the density* λ *of cluster centers in space.*

The second circumstance that we shall note is that K depends on the variation from one cluster to another of the number ν of galaxies per cluster. More specifically, we have the following result:

THEOREM 2.—*The index of clumpiness* K *is an increasing function of the ratio* $c = \nu_2/\nu_1$ *of the first two moments of the distribution of* ν, *but does not depend on any other property of this distribution. The minimum value of* K *is unity and is reached only when* $\nu \equiv 1$, *that is to say, when the galaxies are not clustered.*

The last conclusion of Theorem 2 is due to the fact that, of necessity, ν can take on only nonnegative integer values and, therefore,

$$\nu_2 - \nu_1 = \sum_{j=1}^{\infty} (j^2 - j) P\{\nu = j\} = 2P\{\nu = 2\} + 6P\{\nu = 3\} + \ldots \geqq 0 . \tag{26}$$

Thus the minimum value of $\nu_2 - \nu_1$ is zero and is reached only when $P\{\nu > 1\} = 0$.

In order to investigate the dependence of K on the size and shape of the solid angle ω in which the galaxies are counted, we shall consider separately two cases: first, when ω is small, with its area tending to zero, and, second, when it is increased by regular steps. The first of these two cases corresponds to Zwicky's $z \to \infty$. Also we shall specialize ω to be of rectangular shape with dimensions $2\alpha_1 \times 2\alpha_2$.

Referring to (25), we see that the subject of our interest is the quotient R_{20}/R_{10} and, in particular, its behavior when either α_1 or α_2 or both tend to zero. Up to the present, the system of co-ordinates considered was arbitrary. Now it will be convenient to assume that the X-axis is the axis of symmetry of ω and that the two other co-ordinate axes are parallel to the planes limiting ω. Introducing a system of polar co-ordinates ξ, ϕ, and ψ, and using the fact that the integral of $f(\eta)$ with respect to u, v, w taken over the whole space must be equal to unity, we find the value of R_{10} to be

$$R_{10} = 4\alpha_2 \sin \alpha_1 \int_0^{\infty} \xi^2 \theta(\xi, m^*)\, d\xi . \tag{27}$$

In order to evaluate R_{20}, we first write

$$R_{20} = \int_{-\infty}^{+\infty}\int\int p_1^2 du\, dv\, dw = \int_{-\infty}^{+\infty}\int\int p_1 \times p_1 du\, dv\, dw \tag{28}$$

and treat the two factors p_1 in the integrand as two separate integrals of type (7), both taken over ω. In one of these integrals the variables of integration are denoted by x_1,

y_1, z_1 and in the other by x_2, y_2, z_2. Each of these triplets is now transformed into polar co-ordinates. Inverting the order of integration, we find

$$R_{20} = \int_{-a_1}^{+a_1} d\phi_1 \int_{-a_1}^{+a_1} d\phi_2 \int_{-a_2}^{+a_2} d\psi_1 \int_{-a_2}^{+a_2} F(\phi_1, \phi_2, \psi_1, \psi_2)\, d\psi_2 , \tag{29}$$

where

$$\begin{aligned} F(\phi_1, \phi, \psi_1, \psi_2) &= \cos\phi_1 \cos\phi_2 \int_0^\infty \xi_1^2 \theta(\xi_1, m^*) \\ &\times \int_0^\infty \xi_2^2 \theta(\xi_2, m^*) \left[\iiint_{-\infty}^{+\infty} f(\eta_1)\, f(\eta_2)\, du\, dv\, dw \right] d\xi_2 d\xi_1 . \end{aligned} \tag{30}$$

Here, of course,

$$\begin{aligned} \xi_i^2 &= x_i^2 + y_i^2 + z_i^2 , \\ \eta_i^2 &= (x_i - u)^2 + (y_i - v)^2 + (z_i - w)^2 , \\ x_i &= \xi_i \cos\phi_i \cos\psi_i , \\ y_i &= \xi_i \cos\phi_i \sin\psi_i , \\ z_i &= \xi_i \sin\phi_i , \end{aligned} \tag{31}$$

for $i = 1, 2$. It will be noticed that, on the assumption of continuity of $f(\eta)$, function (30) must be bounded. Thus formula (29) implies that, as either a_1 or a_2 or both tend to zero, the order of magnitude of R_{20} is that of $a_1^2 a_2^2$. With reference to (27) and (25), we now have:

THEOREM 3.—*If the probability density of* $f(\eta)$ *governing the internal structure of clusters is continuous, then, whenever the solid angle* ω *in which galaxies are counted tends to zero, the index of clumpiness* K *converges to unity.*

This result is in agreement with the corresponding conclusion of Zwicky regarding $k(z, n)$ when $z \to \infty$.

Remark added July 4, 1954.—The remarks of the referee raised a theoretical question which may be interesting to other readers of the paper. This question is whether or not distributions are at all possible such that, with the decrease in the size of the solid angle ω, the corresponding value of K tends to a limit greater than unity. The answer to this question is in the affirmative. In fact, relevant examples are provided by the quasi-uniform distributions considered in Paper I. To take the simplest case, it will be seen that, if for every ω the distribution of $N(\omega)$ had the probability-generating function

$$G_{N(\omega)}(t) = \exp\{\lambda\omega[\alpha t + (1 - \alpha)t^2 - 1]\} ,$$

where $\lambda > 0$ and $0 < \alpha < 1$, then the corresponding value of K^2 would have the constant value

$$K^2 = 1 + 2\,\frac{1 - \alpha}{2 - \alpha} > 1 ,$$

independent of ω.

In order to investigate the second case, where the dimensions of ω are increased, we shall assume that this increase affects only one of its dimensions, for example, $2a_2$, which is simply multiplied by increasing integers, 2, 3, 4, . . . , s, etc. It will then be obvious that, *mutatis mutandis*, the conclusions reached will apply to other cases. For every positive integer s, let $W(s)$ denote a rectangular solid angle with dimensions $2a_1 \times 2sa_2$. This solid angle $W(s)$ may be considered as the union of s nonoverlapping solid angles all in one row, which we shall denote by $\omega_1, \omega_2, \ldots, \omega_s$. Denote by $N(s)$ the total num-

ber of galaxies brighter than the apparent limiting magnitude m^*, all located in $W(s)$, and by n_i the number of those in ω_i, $i = 1, 2, \ldots, s$. Naturally,

$$N(s) = \sum_{i=1}^{s} n_i . \tag{32}$$

In order to compute the value of K, say $K(s)$, corresponding to $W(s)$, it will be sufficient to compute the variance of $N(s)$ on the two alternative hypotheses, one that $\nu \equiv 1$ and, therefore, the galaxies do not cluster, and the other that the galaxies are clustered in an arbitrary manner. Let $\sigma_0^2(s)$ and $\sigma_1^2(s)$ be the variances of $N(s)$ so obtained.

As already stated, the assumption of no clustering implies that all the s variables $n_1, n_2, \ldots, n_s$ are completely independent. It follows that

$$\sigma_0^2(s) = s\lambda\nu_1 R_{10} = s\sigma_0^2(1) , \tag{33}$$

where R_{10} is given by (27). As to $\sigma_1^2(s)$, it is obtained from the familiar formula,

$$\sigma_1^2(s) = \sum_{i=1}^{s} \sigma_{n_i}^2 + 2\sum_{i=1}^{s-1}\sum_{j=i+1}^{s} \rho_{ij}\sigma_{n_i}\sigma_{n_j} , \tag{34}$$

where $\sigma_{n_i}^2$ stands for the variance of n_i and ρ_{ij} for the correlation coefficient between n_i and n_j. Since all the component solid angles ω_i are of the same size and shape, it follows that all the $\sigma_{n_i}^2$ have the same value $\sigma_1^2(1)$ obtainable from (24), with R_{20} represented by (29) and R_{10} by (27). Thus

$$\sigma_1^2(s) = \sigma_1^2(1)\left[s + 2\sum_{i=1}^{s-1}\sum_{j=i+1}^{s} \rho_{ij}\right] . \tag{35}$$

Reference to formula (20) shows that all the correlations $\rho_{i,\,i+1}$ have the same value, which we may denote by $\rho(1)$; that all the correlations $\rho_{i,\,i+2}$ have the same value, which we may denote by $\rho(2)$; etc. Thus (35) can be written as

$$\begin{aligned}\sigma_1^2(s) &= \sigma_1^2(1)[s + 2(s-1)\rho(1) + 2(s-2)\rho(2) + \ldots + 2\rho(s-1)] \\ &= \sigma_1^2(1)\left[s + 2\sum_{i=1}^{s-1}(s-i)\rho(i)\right] .\end{aligned} \tag{36}$$

Dividing (36) by (33), we obtain the value of $K^2(s)$ sought:

$$K^2(s) = K^2(1)\left[1 + \frac{2}{s}\sum_{i=1}^{s-1}(s-i)\rho(i)\right] . \tag{37}$$

Similarly,

$$K^2(s+1) = K^2(1)\left[1 + \frac{2}{s+1}\sum_{i=1}^{s}(s+1-i)\rho(i)\right] . \tag{38}$$

In order to investigate the behavior of $K(s)$ when s is increased, we take the difference

$$\begin{aligned}K^2(s+1) - K^2(s) &= \frac{2}{s(s+1)} K^2(1)\left\{ s\rho(s) \right. \\ &\qquad \left. + \sum_{i=1}^{s-1}[s(s+1-i) - (s+1)(s-i)]\rho(i)\right\} \\ &= \frac{2}{s(s+1)} K^2(1)\sum_{i=1}^{s} i\rho(i) .\end{aligned} \tag{39}$$

Since $\rho \geqq 0$, it follows that $K(s)$ is a monotone nondecreasing function of s. As we have seen, the values of the correlations $\rho(i)$ depend on $c = \nu_2/\nu_1$ and on the functions $f(\eta)$ and $\theta(\xi, m^*)$ that we left unspecified. However, according to formula (22), there is an upper bound on the value of $\rho(i)$. Since in the present case all the component solid angles ω_i are of the same dimensions, we have

$$0 < \rho(i) < \left[1 + \frac{\nu_1 R_{10}}{(\nu_2 - \nu_1) R_{20}}\right]^{-1} = \frac{K^2(1) - 1}{K^2(1)}, \tag{40}$$

as is easily found by reference to (25). Substituting the upper bound (40) for each $\rho(i)$ in (39), we find that

$$0 \leqq K^2(s+1) - K^2(s) < K^2(1) - 1. \tag{41}$$

These general findings may now be summarized in the following:

THEOREM 4.—*The square of the index of clumpiness,* $K^2(s)$, *corresponding to a rectangular solid angle* $2\alpha_1 \times 2s\alpha_2$ *is a nondecreasing function of* s. *The rate of increase in* $K^2(s)$ *corresponding to a unit increase in* s *is less than* $K^2(1) - 1$.

This theorem applies to arbitrary ν_1, ν_2, $f(\eta)$, and $\theta(\xi, m^*)$. However, the empirical study of the Lick Observatory data and also of counts of one 48-inch Schmidt plate, made by A. G. Wilson,[4] indicates that, in actual fact, the correlations $\rho(i)$ decrease rapidly when i increases. In fact, if $\alpha_1 = \alpha_2$ does not exceed the arc of 30 minutes, $\rho(i)$ may be taken as zero for all $i > 8$. In these conditions, formula (39) can be written as

$$K^2(s+1) - K^2(s) = \frac{2}{s(s+1)} K^2(1) \sum_{i=1}^{s_0} i\rho(i), \tag{42}$$

where s_0 is the limit beyond which the value of $\rho(i)$ is negligible. It is seen that (42) indicates a rate of increase in $K^2(s)$ that rapidly decreases as s becomes larger.

It is now clear that, if both dimensions of the regular solid angle ω in which the galaxies are counted are increased simultaneously, then the corresponding index of clumpiness will also grow. In fact, since the correlation between the counts in two solid angles is large when these solid angles are near each other and small when they are distant, the increase in K corresponding to a given increase in $4\alpha_1\alpha_2$, the area of ω, will be faster when this area is increased by increasing both α_1 and α_2 rather than by increasing only one of these numbers.

Theorem 4 is particularly relevant from the point of view of the discussion of Zwicky's curve *II* in Figure 2 of his paper (1953). The dependence of K on the area of the rectangle ω on the photographic plate may be represented graphically. In this case we would measure the area of ω on the axis of abscissae and K on the axis of ordinates. In accordance with Theorem 4, the resulting curve would rise monotonically at a decreasing rate. In order to bring this result into correspondence with Zwicky's curve *II*, we notice that, instead of measuring the area of ω on the axis of the abscissae, we may as well measure on it the expected number $E[N(\omega)]$ of images of galaxies to be found in this area. In this fashion a curve will be obtained that represents a perfect analogon of Zwicky's curve of $k(z, n)$ plotted against n, when z is kept constant but the solid angle Ω is increased. Theorem 4 asserts, then, that in the absence of intergalactic and interstellar absorbing clouds, and irrespective of what the luminosity function of the galaxies may be, irrespective of what the structure of the clusters may be, and irrespective of the variability of the number of galaxies per cluster, the curve K will be monotone increasing, without any maximum. From the point of view of the theory of clustering of Paper I, this result appears to be an indication that the general shape of curve *III* (monotone increasing),

[4] The authors are indebted to Dr. A. G. Wilson for letting them use his counts in advance of publication.

that Zwicky obtained empirically, cannot be taken as an argument in favor of the existence of intergalactic absorbing clouds.

In the previous paragraphs we have contemplated the possibility that the increase in Zwicky's n is obtained by increasing the solid angle ω in which the galaxies are counted. The case where the increase in n is brought about by an increase in the limiting apparent magnitude m^* of the plates remains to be considered. Unfortunately, the complexity of dependence of the quotient R_{20}/R_{10} on m^* prevented the authors from obtaining a conclusion that is valid for all unspecified functions $f(\eta)$ and $\theta(\xi, m^*)$ intervening in this quotient. Later we study the problem numerically with relation to the specialization of these functions adopted in Paper II.

V. NUMERICAL ILLUSTRATIONS

In this section we give a few graphs and numerical tables illustrating the dependence of K, the index of clumpiness, (i) upon various characteristics of the spatial distribution of galaxies and (ii) upon several observational factors, namely, on the size and shape of the solid angle ω in which galaxies are counted and on the limiting apparent magnitude of the plate. Naturally, the curves falling under the heading (i) must be theoretical and cannot have an empirical counterpart: for example, we cannot arrange that the actual number of galaxies per cluster be doubled and observe the effect. Thus the curves in question are intended to clarify the consequences of the various details in the adopted model of the spatial distribution of galaxies but are not subject to empirical verification. As to the illustrations falling under the heading (ii), they all can be, and for the most part actually are, obtained both from theory and from observations. The latter are based on counts of galaxies on the plates taken at the Lick Observatory. Essentially, the material used is that described in detail in Paper II. It consists of counts of galaxies in $1^\circ \times 1^\circ$ squares on plates covering a region near the north galactic pole described in Paper II as the "area used." However, as was the case in Paper II, particular emphasis is placed on data referring to the "upper right quadrant," which is closest to the galactic pole and is expected to be the least affected by interstellar clouds. In addition to the foregoing material, a relatively small amount of new data is used. These are counts of galaxies in $10' \times 10'$ squares in 16 Lick Observatory plates. The purpose in using these additional counts is to illustrate the effect on K of the size of the solid angle ω in which the galaxies are counted, when all the other factors are kept constant. For this reason, the 16 plates had to be specially selected. As is well known, in spite of all the care and all the precautions taken with a given observational setup, the limiting apparent magnitude does vary somewhat from one plate to the next, and this variation affects the counts. Another factor that may affect the counts is the individual counting the galaxies. With this in mind, the 16 plates used were all those in the upper right quadrant that satisfy the two principles: (i) all the plates were counted by C. D. Shane, and (ii) all plates have their limiting magnitude correction[5] between 0.90 and 1.11.

Still another precaution was taken to keep the limiting magnitude approximately constant. As explained in Paper III, the analysis of the Lick Observatory plates shows a systematic east-west change in the limiting apparent magnitude as well as an off-axis change. In order to avoid these effects, only the 504 central $10' \times 10'$ squares in each plate were used for the computations. Specifically, the areas eliminated from computations were, on each plate: the 1° marginal strips at north, south, and east edges and the $1^\circ 30'$ marginal strip on the west edge. The remaining rectangle, $3^\circ 30'$ east-west by 4° north-south, contained the 504 cells that were used.

All the empirical results given later were obtained by applying the corrections for general galactic absorption and for "errors of counting," as explained in Paper II. Specifically, the second-error model was used.

[5] The details of this correction are to be found in a forthcoming paper by C. D. Shane and C. A. Wirtanen.

Contrary to the general character of the discussions in the preceding section, all the results of the present section refer to particular specializations adopted and particular estimates obtained in Paper II, using the data of the Lick Observatory. However, the authors wish to make it clear that they do not insist on either the particular specializations or the estimates. They are used tentatively for illustrative purposes.

The function $f(\eta)$ adopted is the symmetrical normal probability density with an unspecified standard deviation σ, treated as an adjustable parameter,

$$f(\eta) = (\sigma\,[2\pi]^{1/2})^{-3} \exp\left\{-\frac{\eta^2}{2\sigma^2}\right\}. \tag{43}$$

It may be useful to remind the reader heuristically of the significance of the parameter σ. This number has the property that 90 per cent of all galaxies belonging to a cluster can be expected to lie within a distance of 2.5 σ from the cluster's center.

The function adopted to represent $\theta(\xi, m^*)$ is

$$\theta(\xi, m^*) = \sigma_M^{-1}\Phi\left(\frac{m^* - M_0 + 5 - 5\log_{10}\xi - 5.19\times 10^{-9}\xi}{\sigma_M}\right), \tag{44}$$

where $\Phi(x)$ is the normal integral,

$$\Phi(x) = (2\pi)^{-1/2}\int_{-\infty}^{x} \exp\left\{-\frac{t^2}{2}\right\} dt. \tag{45}$$

Here $m^* - M_0$ is an adjustable parameter and is the difference between the limiting magnitude of the plate and the mean absolute magnitude of the galaxies. The parameter σ_M, the standard deviation of the absolute magnitudes, is also adjustable. The coefficient 5.19×10^{-9}, providing the dimming with distance due to reddening, is considered as known from the observations of Hubble and Humason (Hubble 1936*a*, *b*).

We begin by illustrating how the dependence of K upon the area of ω changes as we change the hypotheses specializing the several factors in the spatial distribution of galaxies. In the four panels of Figure 1 the quantity measured on the axis of the abscissae is the same s, the area in square degrees of a rectangle ω on the photographic plate in which the galaxies are counted. The dimensions of this rectangle are $1^\circ \times s^\circ$. On the axis of ordinates we measure the corresponding value of the index of clumpiness. All the curves in Figure 1 are based on the theory of Papers I and II and correspond to different sets of estimates of the constants involved. It will be seen that all these curves have approximately the same shape. At $s = 0$ the value of K is always unity. Then the curve go up, first fast and then slower and slower. However, the rate of increase in K depends on the properties of the spatial distribution of galaxies. *Ceteris paribus*, the larger the ratio $c = \nu_2/\nu_1$ or the larger $m^* - M_0$, the larger the value of K. On the other hand, an increase in either σ_M or σ depresses the value of K.

If the galaxies were all of the same absolute magnitude, so that $\sigma_M = 0$, then the value of K would increase the fastest with increasing area s, other factors being fixed. In order to explain this effect intuitively, we refer to Figure 2 of Paper II (p. 101). This figure illustrates that clusters having galaxies visible on the photographic plate must, on the average, be closer to the observer in order to be visible in the case $\sigma_M = 0$ than in the case $\sigma_M > 0$. Thus, when σ_M is substantial, that is, with a substantial variation in the absolute magnitude of galaxies, the photographic plate will, on the average, record galaxies from more clusters, and more of the distant clusters, than if σ_M were zero. Further, the plate will record only one or two galaxies from each of the many extremely distant clusters. Since the cluster centers are supposed to be uniformly distributed in space, the final effect must consist in decreasing the clumpiness of the distribution of images of galaxies as σ_M increases.

The effect illustrated in the lower right panel of Figure 1 is, of course, very intuitive.

The smaller the value of σ, the more concentrated are the clusters; and this must contribute to an increase in the clumpiness of the distribution of images of galaxies on the photographic plate.

As mentioned, in Figure 1 the independent variable, of which K is a function, is a controllable observational factor, namely, s = area of a rectangle $1^\circ \times s^\circ$ in which the

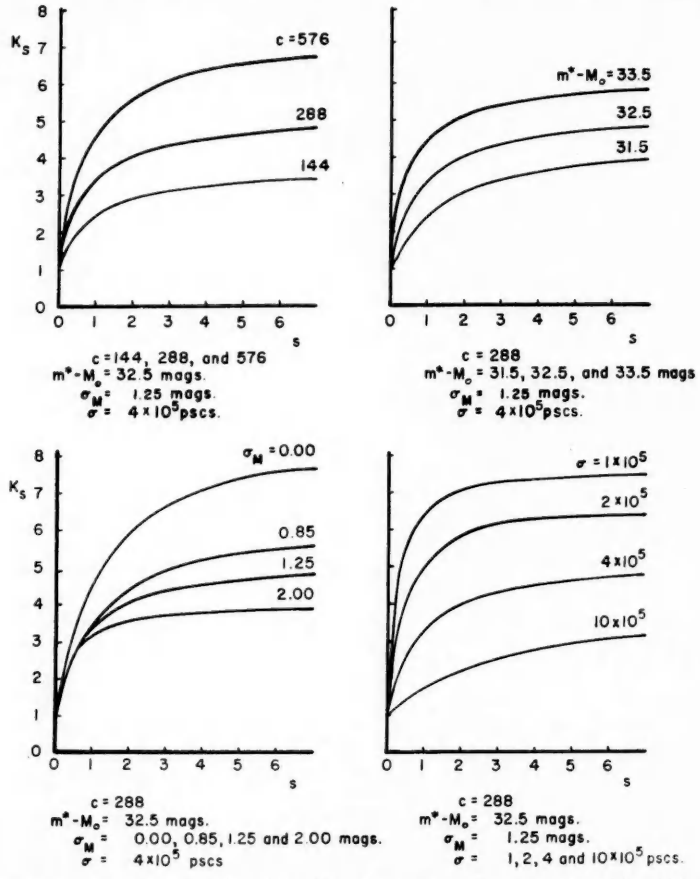

FIG. 1.—Dependence of index of clumpiness K on the area s of a rectangle $1^\circ \times s^\circ$ in which galaxies are counted, in relation to various hypotheses regarding the spatial distribution of galaxies.

galaxies are counted. It is now interesting to replot the same curves against another independent variable, namely, $\bar{N}$ = the expected number of galaxies within the rectangle $1^\circ \times s^\circ$ counted up to the limiting apparent magnitude m^*. According to formula (15), this $\bar{N} = \lambda\nu_1 R_{10}$, where $\lambda\nu_1$ is the density of galaxies per cubic parsec. Figure 2 shows the dependence of the integral R_{10} on the two constants $m^* - M_0$ and σ_M. The ordinate scale at the right-hand edge of Figure 2 provides the dependence of $\bar{N}$ on the same two constants $m^* - M_0$ and σ_M when $\lambda\nu_1$ is assumed to be 2×10^{-17} galaxies per cubic parsec.

The curves in Figure 1 were replotted to represent the dependence of K on the expected number $\bar{N}$ of galaxies counted within a rectangle $1° \times s°$. The resulting curves, which may be considered analogous to those studied by Zwicky (1953), are given in Figure 3. In interpreting these curves it is *important to remember that the increase in* $\bar{N}$ measured on the axis of the abscissae *is achieved by increasing the area of the rectangle* ω *in which the galaxies are counted.* Later we produce other graphs, also representing the dependence of K on $\bar{N}$. However, these graphs are very different from the ones in Figure 3, because the increase in $\bar{N}$ is produced by varying not the area of ω but either the limiting

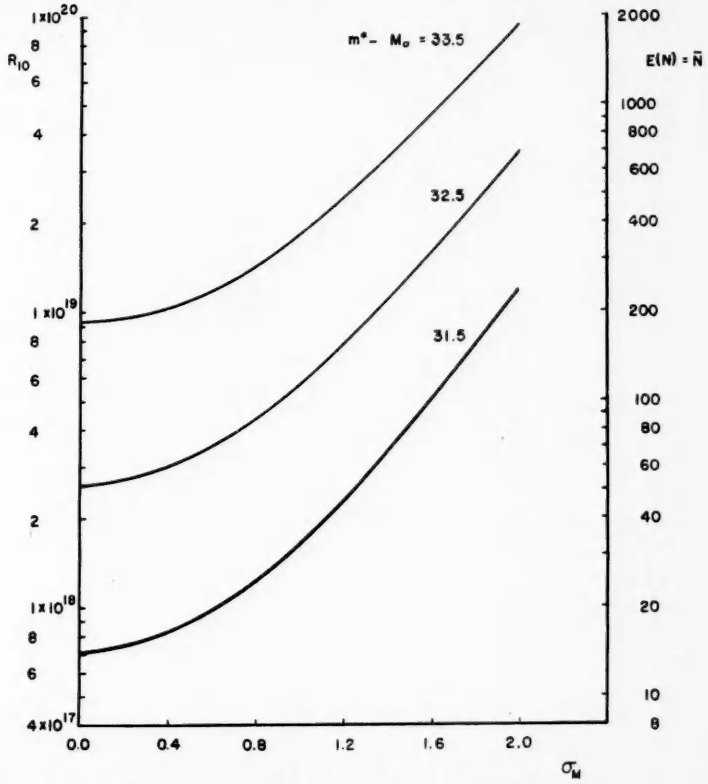

FIG. 2.—Dependence of expected number $\bar{N}$ of galaxies per $1° \times 1°$ on $m^* - M_0$ and on σ_M

apparent magnitude of the plate or the dispersion σ_M of the absolute magnitude of the galaxies. As mentioned, the purpose of all these graphs is to obtain results that are analogous to those of Zwicky. However, it is not suggested that $\bar{N}$ is the most appropriate independent variable against which to plot K.

Figure 4 exhibits plots of K against varying $\bar{N}$, where this variation is achieved by changing the limiting magnitude of the plate. More strictly, because of the particular structure of formula (44), this variation is achieved by varying the difference $m^* - M_0$ between the limiting magnitude m^* and the mean absolute magnitude M_0 of the galaxies.

Thus the curves of Figure 4 can be interpreted in several ways. There are two groups of curves shown, both computed on the same hypotheses except that for one group $\sigma = 10^5$ parsecs, while for the other group $\sigma = 4 \times 10^5$ parsecs. The curves belonging to the same group refer to different areas of rectangles $1^\circ \times s^\circ$ in which the galaxies are counted. It is remarkable that, although the curves belonging to a given group are different, they are so close together that it would probably be impossible to distinguish them empirically. In other words, other things being equal, the dependence of K on the expected number $\bar{N}$ of galaxies within a solid angle ω, when changes in $\bar{N}$ are produced by changes in the limiting magnitude of the plate, is not very sensitive to moderate changes in the area of ω. This somewhat curious circumstance may be very useful in

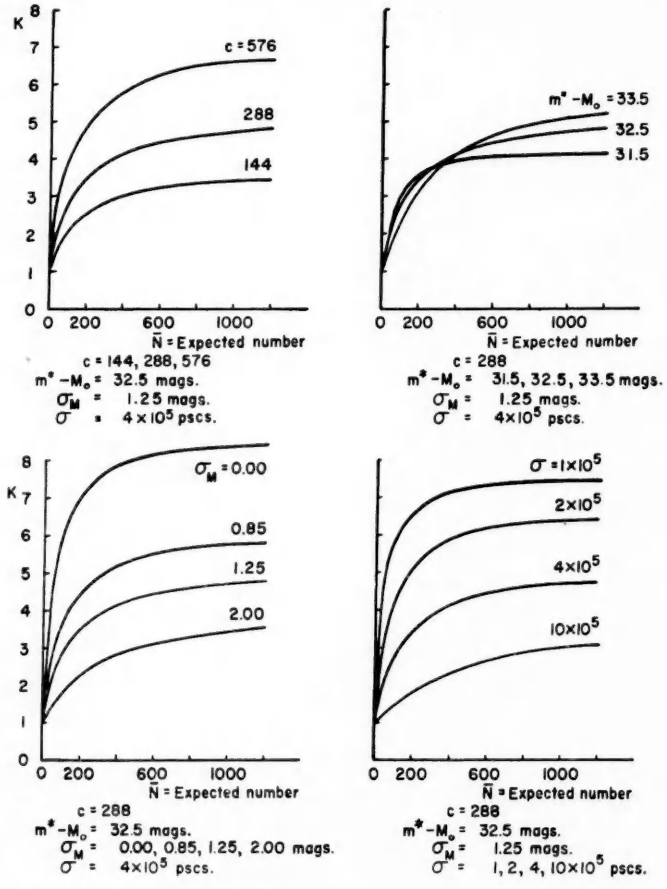

FIG. 3.—Dependence of index of clumpiness K on the expected number $\bar{N}$ of images of galaxies in a rectangle $1^\circ \times s^\circ$ in which galaxies are counted, in relation to various hypotheses regarding the spatial distribution of galaxies. The increase in $\bar{N}$ is effected by increasing the length s° of the rectangle.

dealing with counts of galaxies made at different observatories referring to slightly different areas of ω. This property applies to the index of clumpiness K but, unfortunately, not to other relevant statistics, such as, for example, serial quasi-correlations (see Papers I and II). For this reason, it will be most desirable if the units of area (presumably squares) ω, in which images of galaxies are counted, could be standardized. For example, it may be agreed that the dimension of ω always be integer multiples of 1 minute of arc.

The curves in Figure 4 are the last of those computed for the purpose of comparison with the curves contemplated by Zwicky. Here again we see that an increase in $\bar{N}$ is invariably accompanied by an increase in K, which qualitatively agrees with Zwicky's curve *III*. Thus, in the range considered, when an increase in $\bar{N}$ is produced by an increase in the limiting magnitude of the plate, the shape of curve *III* does not require for its explanation any hypothesis about the presence of extragalactic absorbing clouds.

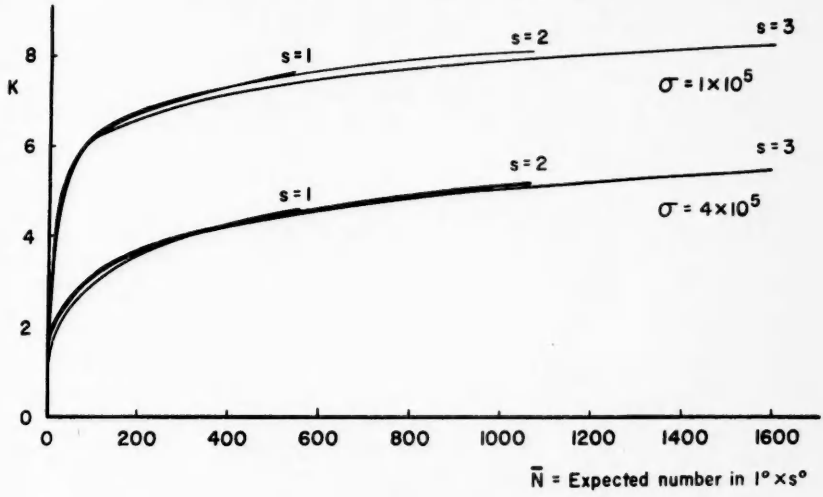

FIG. 4.—Dependence of index of clumpiness K on the expected number $\bar{N}$ of images of galaxies in a rectangle $1^\circ \times s^\circ$. The increase in $\bar{N}$ is effected by increasing the limiting magnitude m^* of the plate.

While formulating this conclusion, we wish to emphasize its limitations. Unlike the conclusions of the preceding section, the present conclusion is not general and applies to the particular range of limiting magnitude m^* or, more strictly, to the particular range of the difference $m^* - M_0$, namely, $31.5 \leqq m^* - M_0 \leqq 34.5$ mag., that was covered by the computations. Also, the conclusion applies only to the general framework of Paper II and to the particular sizes and shapes of the solid angle ω for which the computations were performed. Therefore, it is not impossible that, for other angles and/or for larger values of $m^* - M_0$, the curves will decline and approach Zwicky's curve *II*. Nevertheless, the curves actually drawn in Figure 4 do indicate that, under the conditions specified, Zwicky's curve *III* is consistent with the total absence of extragalactic absorbing clouds.

Figure 5 illustrates still another dependence of K on the expected number $\bar{N}$ of galaxies visible in an area ω on the photographic plate. Here the change in $\bar{N}$ is supposed to be produced by a change in σ_M, the standard deviation of the absolute magnitude of the galaxies. As will be noticed from Figure 2, *ceteris paribus*, the expectation $\bar{N}$ is an increas-

ing function of σ_M. Thus the least value of $\bar{N}$ is obtained when $\sigma_M = 0$. This minimum value of $\bar{N}$ is positive and depends on the area s. Thus the three curves in Figure 5, corresponding to $s = 1$, 2, and 3, begin at three different values of $\bar{N}$ and then extend to the right indefinitely. The fact that $\bar{N}$ increases indefinitely with increasing σ_M corresponds to the circumstance that, if σ_M could be made to grow without limit while all other factors (including $m^* - M_0$) were held constant and if equation (44) still applied, then the photographic plate would have a chance to record galaxies from clusters located at greater and greater distances, the number of these clusters increasing without limit.

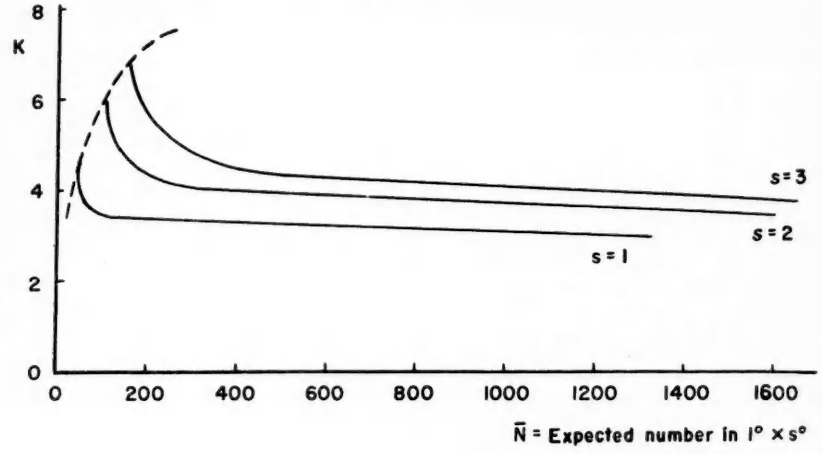

FIG. 5.—Dependence of index of clumpiness K on the expected number $\bar{N}$ of images of galaxies in a rectangle $1° \times s°$. The increase in $\bar{N}$ is effected by increasing σ_M, the dispersion in luminosity of the galaxies.

TABLE 1

DEPENDENCE OF K^2 ON THE SHAPE OF ω

($c = 288$; $\sigma_M = 0.85$; $m^* - M_0 = 32.5$; $\sigma = 4 \times 10^5$)

$2a_1 \times 2a_2$	K^2	$2a_1 \times 2a_2$	K^2	$2a_1 \times 2a_2$	K^2
$5' \times 80'$	1.96	$10' \times 40'$	1.98	$20' \times 20'$	2.00

As already mentioned when discussing Figure 1, as σ_M increases, the index of clumpiness decreases. Thus all the curves in Figure 5 are monotone decreasing.

Our last purely theoretical illustration refers to the dependence of K on the shape of the region ω when this region is small. The extent of this dependence is interesting, because, as was shown in the preceding section, if the structure of clusters is determined by a continuous probability density $f(\eta)$, then the values of K corresponding to small solid angles ω must be close to unity.

Table 1, based on the specialized model of Paper II, illustrates the changes in K^2 due to changes in the shape of ω when its area is equal to 400 square minutes.

As mentioned above, all the empirical illustrations in this paper are based on the data of the Lick Observatory and therefore do not include the dependence of K on the limit-

ing magnitude of the plate.[6] Figure 6 exhibits four series of symbols, one above the other. These symbols represent the empirical values of K plotted against the area s of a rectangle $1° \times s°$. The four series of values of K correspond to four "quadrants" of the "area used," as described in Paper II. The continuous curve represents the theoretical values of K computed upon the theory of Papers I and II.

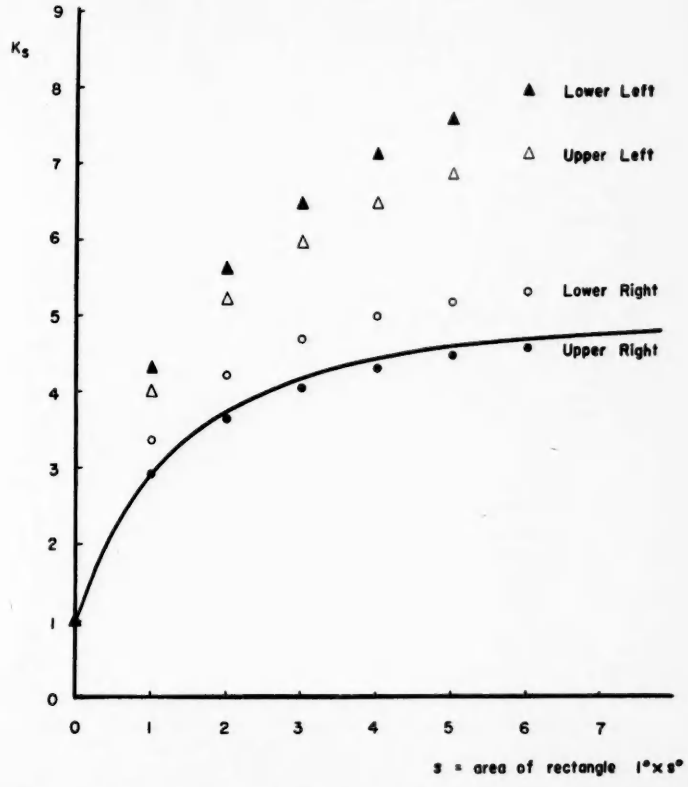

FIG. 6.—Empirical (Lick Observatory data) values of K, the index of clumpiness, plotted against the area of a rectangle $1° \times s°$ in which the images of galaxies were counted. Continuous curve represents theory using "best-fitting" parameters for the upper right quadrant.

[6] There are two main difficulties in using data from other sources in which the limiting magnitude of the plate is different. One difficulty has already been mentioned. It depends on the fact that counts of galaxies made in different institutions refer to widely different solid angles ω. Thus, for example, in a set of data made available to the authors the original counts are made in squares $5'36'' \times 5'36''$. The second and more important difficulty is presented by the uncertainty as to the so-called "errors in counting" galaxies. As explained in detail in Paper II, this term covers not only the unavoidable mistakes in identification of galaxies and oversights but also the variation in the limiting magnitude from one plate to another and from one spot on the same plate to the next. Experience shows that these "errors" are by no means negligible and that corrections for them are imperative. However, the nature of these corrections depends on the machinery of errors, which vary from one observer to another, and reliable corrections may be deduced only as a result of a study of repeated counts referring to the same area in the sky made on different plates. Thus far, the authors have been able to analyze only one substantial set of data of this

As explained in Paper II, the estimates[7] of the various parameters involved in the model depend strongly on the luminosity function of the galaxies, that is, on $m^* - M_0$ and σ_M. Since the values of these two parameters are uncertain, twelve different combinations of, so to speak, trial values were used in Paper II, in order to obtain the corresponding estimates of the parameters involved in the model of the spatial distribution of galaxies. All these computations were performed for the upper right quadrant.

When preparing data for Figure 6 in the present paper, it was intended to use all the twelve systems of trial values of $m^* - M_0$ and σ_M combined with the corresponding estimates of parameters involved in the model, in order to produce an equal number of theoretical curves that could be compared with the lowest series of symbols. It was hoped that this comparison would help in the choice among the twelve systems of trial values of $m^* - M_0$ and σ_M. Unfortunately, these hopes were frustrated. Because of the general property of formula (25) representing K^2, all the twelve curves had to pass through the point ($s = 0$, $K = 1$). Furthermore, the process of fitting the estimates of the parameters involved in the model forced all the curves to pass through the empirical point corresponding to $s = 1$. Therefore, the curves could diverge only for $s = 2, 3, \ldots$. When the computations were completed, it was found that the twelve values of K corresponding to the same s were so close that they could not be distinguished on the graph. Therefore, the unique theoretical curve exhibited in Figure 6 is, in reality, a superposition of twelve curves, each corresponding to a different system of trial values of $m^* - M_0$ and σ_M and the corresponding estimates of the parameters involved in the model.

As was mentioned in Paper II, the problem of the choice among the alternative trial values of $m^* - M_0$ and σ_M is not an easy one. However, the study of the quasi-correlations permitted us to eliminate the extreme value of $\sigma_M = 0$ and indicated that $\sigma_M = 0.85$ is probably too small. The present experience shows that no progress in this direction can be expected from the study of K. The authors' hopes are connected with the possibility of studying the quasi-correlations between counts in the same solid angles ω made to varying limiting magnitudes.

Figure 6 exhibits several interesting features. One is that all four series of symbols are remarkably regular. The second is that the coinciding theoretical curves for the first quadrant are in excellent agreement with the empirical data. The third is that the series corresponding to different quadrants deviate from one another in a clear-cut, systematic manner.

The first two striking regularities are easily explained by referring to the method of computing the successive values of $K(s)$ of each series and to formula (37). It must be remembered that in any one series the ordinates $K(s)$ were computed by making repeated use of the same data, namely, the counts in the quadrant to which the series refers. Thus the several points of the series do not represent *independent* measurements. In order to obtain an idea as to the character of the dependence involved, we refer to formula (37). As already mentioned, the correlations $\rho(i)$ involved in this formula decrease rapidly with increasing i. It follows that, when s is increased, the corresponding values of $K(s)$ are pretty much determined by the value of $K(1)$ and by the values of the first few $\rho(i)$.

---

kind, namely, the counts in several thousand $1^\circ \times 1^\circ$ squares in overlapping plates of the Lick Observatory collection. In addition, an analysis of a somewhat smaller number of recounts in $10' \times 10'$ was performed in connection with the present paper. The difficulties mentioned affect the present study of the index of clumpiness. They affect also, even to a much stronger degree, the possibility of the study of the correlation between counts in the same solid angles ω, that is, in the same $1^\circ \times 1^\circ$ squares, made on different plates, with different limiting magnitudes.

[7] When computing the theoretical values of K, an error in the computation of the parameter c was discovered. The fourth column of Table 2, p. 118 of Paper II, *should read* 91, 90, 89; 222, 218, 201; 395, 336, 267; 942, 801, 686. The bounds on the estimates of λ and of ν_1 described in the next section will be affected, these estimates still being very uncertain.

Primarily this applies to the theoretical $K(s)$. However, the same conclusion applies approximately to the values obtained empirically, *provided that the computations leading to these values are so conducted as to insure the sameness of* $K(1)$ *and of* $\rho(1), \rho(2), \ldots$. If the consecutive $K(s)$ are computed using the data from a fixed area, this latter condition is obviously satisfied. Thus the regularity of the symbols of each series and also the agreement between the theoretical curves and the empirical results corresponding to the upper right quadrant are consequences of the dependence indicated and should not be surprising.

In order to explain the divergence between the values of $K(s)$ referring to the four quadrants, we offer two hypotheses. One is that the four quadrants are likely to be affected by irregular (as contrasted with general) interstellar absorption to an unequal degree. As discussed in Paper II, the quadrant least affected by interstellar absorption seems to be the upper right quadrant, which was used to obtain the estimates of all the constants involved in the model. Next follow the lower right, the upper left, and, finally, the lower left quadrant. The latter appears to reflect a very substantial effect of interstellar absorption.

It must be clear that irregular interstellar absorption, of a random character, will increase the clumpiness of the distribution of galaxies by increasing both $K(1)$ and the $\rho(i)$. Thus it is not surprising that the empirical values of $K(s)$ corresponding to the lower left quadrant are so much above all the others. However, the influence of irregular interstellar absorption alone does not seem sufficient to explain the differences between the empirical $K(s)$ for the remaining three quadrants. In fact, as noted in Paper II, after applying the corrections for errors of counting and for general galactic absorption, the quasi-correlations computed for the two right quadrants were found to have practically the same values. This would seem to indicate that these two quadrants are affected by irregular galactic absorption to approximately the same degree.

The explanation of the differences among the values of the $K(s)$ in the two right quadrants and in the upper left quadrant is suggested by formula (25) and by the graphs in the upper left-hand panel of Figure 1. Both indicate that $K(s)$ increases rapidly with an increase in the value of $c = \nu_2/\nu_1$. Although the area covered by each of the quadrants is substantial, it would be plainly unrealistic to suppose that it is large enough for all the variations from one cluster to the next to average out entirely. Consequently, the value of c corresponding to clusters within one quadrant need not be the same as that corresponding to another. The actual situations prevailing in the three quadrants considered may be appraised by inspecting Figure 5 of Paper II, which gives the contour map of number of galaxies per square degree in the whole area covered by the Lick plates. It will be seen that the upper right quadrant is fairly rich in galaxies but does not include any outstanding accumulations. On the other hand, the lower right and the upper left quadrants, while about equally rich in galaxies in general, exhibit several very dense accumulations. Therefore, if the formulae leading to an estimate of c were applied to either one of these quadrants (the lower right and the upper left), it is safe to predict that the estimates obtained would have been much larger than that for the upper right quadrant. This conclusion is quite intuitive if one keeps in mind that the definition of c is

$$c = \frac{\text{Average of second powers of numbers } \nu \text{ of galaxies per cluster}}{\text{Average of first powers of numbers } \nu \text{ of galaxies per cluster}}.$$

Our final illustration refers to the dependence of $K(s)$ on the shape of the region ω in the photographic plate in which the images of galaxies are counted. This illustration is also empirical and is based on the Lick Observatory data, referring to the upper right quadrant. The lower curve or, rather, the lower sequence of symbols in Figure 7 is the same as the lower sequence of symbols in Figure 6. It corresponds to a sequence

of rectangles $1° \times s°$ in the upper right quadrant. The upper sequence of symbols was obtained from the same data but refers to square regions ω. The smallest of these is of angular dimensions $10' \times 10'$. Then follow the squares $1° \times 1°$, $2° \times 2°$, $3° \times 3°$, and $4° \times 4°$. The value of K is plotted against the area of ω.

It is seen that, as predicted by the theory, with a fixed area of ω, the values of K are larger for squares than for the corresponding rectangles.

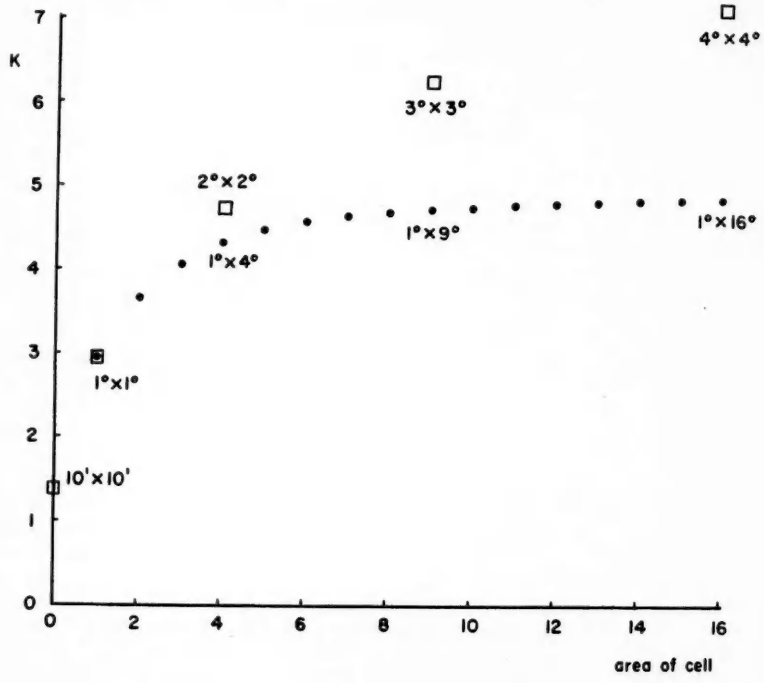

FIG. 7.—Empirical (Lick Observatory data) values of K, the index of clumpiness, plotted against the area of the cell in which the images of galaxies were counted. Dots correspond to rectangular cells $1° \times s°$. Squares correspond to square cells. Note effect on K of shape of cell.

VI. COMPARISON WITH THE THEORY OF CHANDRASEKHAR-MÜNCH-LIMBER

It is interesting that the empirical results exhibited in Figure 7 contradict certain formulae of an alternative theory of the spatial distribution of galaxies due to Chandrasekhar and Münch (1952) and to Limber (1953). Theoretically, formulae (38) and (40) of Limber, modeled upon analogous formulae (37) and (38) of Chandrasekhar and Münch, contain an inconsistency. Specifically, the discussions of Section IV of the present paper indicate that Limber's formula (40) cannot be true for any bona fide distribution of images of galaxies (nor can formula [14] or [26] or [31] in Limber's alternative cases). If we remember that the number $N(\omega)$ of galaxies counted within an area ω

on the photographic plate is necessarily a nonnegative integer and then refer to our formula (26), we see that the expectation of the square of such a number must always be greater than, or equal to, the expectation of the first power,

$$\overline{N^2(\omega)} - \overline{N(\omega)} \geqq 0 . \tag{46}$$

This must be true, irrespective of the size of ω. However, it is violated by Limber's formulae (38) and (40) whenever ω is small.

Limber's formulae (38) and (40), as written, imply that the variance of the counts of images of galaxies in a region ω on a photographic plate is independent of the shape of the region and that it is proportional to the square of the area of ω. A further conclusion is (i) that K must be independent of the shape of ω and (ii) that it must be proportional to the square root of the area of ω. This last implies that $K(\omega)$ would tend to zero as the area of ω tends to zero. On the other hand, if $\overline{N(\omega)}$ tends to zero as the area of ω tends to zero, then formula (46) above shows that the variance of $\overline{N(\omega)}$ cannot decrease faster than $\overline{N(\omega)}$. Thus, for small values of ω, the values of K cannot be less than unity.

We now note that both conclusions (i) and (ii) are contradicted by the empirical results of Figure 7. As to conclusion (i), it may perhaps be said that the formulae of the Chandrasekhar-Münch-Limber theory are only approximate and do not apply to solid angles with an area of 4 square degrees or larger. In fact, the three authors limit their considerations to *small* solid angles ω. However, contradiction (ii) seems to persist even if the application of the formulae is limited to rather small regions ω.

In his introduction, Limber emphasizes that the Lick Observatory data may be suitable material for an analysis using his formulae. Since the Lick Observatory data that were available at the time represented counts in $1^\circ \times 1^\circ$, it is reasonable to presume that Limber's formulae were expected to hold good for solid angles ω up to at least $1^\circ \times 1^\circ$ in size.

It is obvious that adjusting the constants involved in the Chandrasekhar-Münch-Limber theory so as to fit the Lick Observatory counts in $1^\circ \times 1^\circ$ squares would force the curve of K to pass through the empirical point in Figure 7 corresponding to $s = 1$. The corresponding value of K is $K(1) = 2.94$. Because of the proportionality of K to the square root of the area, Limber's value of K corresponding to the $10' \times 10'$ square would be one-sixth as large, that is, $K(\frac{1}{36}) = 0.49$. On the other hand, the empirical value obtained from the Lick Observatory counts in $10' \times 10'$ cells is 1.46—a clear disagreement.

VII. CONCLUSION

1. The authors agree with Zwicky that the study of what he calls the "dimensionless morphology" of the distribution of images of galaxies on a photographic plate is a fruitful source of information regarding the distribution of galaxies in space. Studies of this kind are particularly interesting if conducted with reference to some mathematical theory of the spatial distribution of galaxies that is specific enough to predict what the behavior of a given statistic should be under specified observational conditions.

2. Starting with Zwicky's statistic $k(z, n)$, an index K of clumpiness of the distribution of images of galaxies on the photographic plate was defined, and the theory of spatial distribution of galaxies (Papers I and II) was used, in order to deduce the dependence of K upon the various characteristics of the spatial distribution of galaxies and on several controllable characteristics of the observational setup. Here K appears as an idealization of $k(z, n)$, in the sense that, if the value of $k(z, n)$ could be calculated by using an infinity of observations, the result of such calculation would coincide with K.

3. In the absence of extragalactic absorption, the assumption that galaxies are

clustered in space necessarily implies that the index of clumpiness K is a monotone increasing function of the size of the region ω on the photographic plate in which images of galaxies are counted. This conclusion is general and applies irrespective of the luminosity function of the galaxies and irrespective of the structure of the clusters.

With reference to Zwicky's index $k(z, n)$, the foregoing result indicates that, if the variation of n, the total number of galaxies in a region $\Omega = z\omega$, is brought about by a change in the size of Ω while z is fixed, then Zwicky's curve *III* does not require for its explanation any additional hypothesis, such as, for example, postulating the existence of extragalactic absorbing clouds.

A similar conclusion was obtained for the case where the increase in n is brought about by an increase in the limiting magnitude of the plate. However, in this case, the conclusion is not general but applies to the specialized model of Paper II and to a particular range of limiting magnitude.

4. It was shown that, under the assumption that galaxies are clustered in space and in the absence of extragalactic absorbing clouds, the index of clumpiness K must depend on the shape as well as on the size of region ω on the photographic plate in which the images of galaxies are counted. For a fixed area of ω, the value of K must be larger when ω is a square than when it is elongated.

5. Under any theory of the spatial distribution of galaxies in which the number $N(\omega)$ of images of galaxies in a region ω on a photographic plate is treated as a bona fide integer number, the value of K cannot be less than unity. Under the theory of Paper I, the value of K must tend toward unity as the size of the area ω is decreased to zero. On the other hand, the formulae of the alternative theory by Chandrasekhar-Münch-Limber imply that the value of K should be proportional to the square root of the area of ω, at least when this area is small. Thus their theory implies that K may be less than unity, provided that the area of ω is sufficiently small. Also, at least for small ω, the value of K should be independent of the shape of ω. The empirical values of K computed from the Lick Observatory data appear to conform with the theory of Papers I and II but not with that of Chandrasekhar-Münch-Limber.

6. The empirical study of the index of clumpiness (and also certain other similar studies) would be most interesting if it could be made with observations to varying limiting magnitudes, that is, for data collected with different telescopes. Unfortunately, work of this kind is difficult for seemingly trivial reasons. One of them is that the several observational programs are not co-ordinated. Thus, for example, even though a given region in the sky may be covered by two or more observational programs, it is currently impossible (except by recounting) to obtain the numbers of images of galaxies on plates taken at two different observatories, counted in the same $1^\circ \times 1^\circ$ areas in the sky. The authors are of the opinion that much of future research would be considerably simplified if it were possible to agree on a sufficiently dense lattice of cells in the sky, perhaps $5' \times 5'$ or so, in which the counts in all future surveys would be made.

Another circumstance that makes it difficult to work simultaneously on counts of galaxies made in different observatories is the uncertainty about the errors of counting, which include the variation in the limiting magnitude from one point on the plate to another and from one plate to the next. As yet, no satisfactory theory of these errors is available, but the need of such a theory is already strongly felt and, as research progresses, is likely to become quite acute. One may hope that eventually the theory will be devised. However, whatever the theory, it is safe to say that its applications to counts made in different observatories will require different constants, and such constants can be evaluated only by using counts and recounts made at the observatory concerned. Thus it appears desirable, at least in systematic surveys, to adopt some sort of routine that would accumulate systematically a certain amount of duplicate counts of images of galaxies in the same unit areas of the sky made on independently taken plates. To be

useful, such duplicate counts must be prepared by the same routine procedure and concurrently with the collection of the main body of data.

One possible routine procedure providing gradual accumulation of the data for studying the errors in counting, concurrent with the general progress of the survey, consists in arranging that any two neighboring plates have a certain area of overlap. Because of the deterioration in the quality of the images at the edge of the plate, one may also contemplate an alternative routine. This would consist in taking, at reasonable intervals, additional plates, perhaps centered so as to have equal overlap with four neighboring plates that constitute the main body of the data collected.

The authors wish to thank Mrs. Jeanne Lovasich and Mrs. Marija Vasilevskis for their help in the computations involved in this paper.

REFERENCES

Chandrasekhar, S., and Münch, G. 1952, *Ap. J.*, **115**, 103.
Hubble, E. 1936*a*, *Mt. W. Contr.*, No. 549; *Ap. J.*, **84**, 270.
———. 1936*b*, *Mt. W. Contr.*, No. 557; *Ap. J.*, **84**, 517.
Limber, N. 1953, *Ap. J.*, **117**, 134.
Neyman, J., and Scott, E. L. 1952, *Ap. J.*, **116**, 144.
Neyman, J., Scott, E. L., and Shane, C. D. 1953, *Ap. J.*, **117**, 92.
Scott, E. L., Shane, C. D., and Swanson, M. D. 1954, *Ap. J.*, **119**, 91.
Zwicky, F. 1952, *Pub. A.S.P.*, **64**, 247.
———. 1953, *Helvet. phys. acta*, **26**, 241.

THE SPECTRUM OF THE *CN* MOLECULE

A. E. Douglas and P. M. Routly*

Division of Physics, National Research Council, Ottawa, Canada

Received September 10, 1954

ABSTRACT

In the spectrum of a discharge through *He* mixed with a trace of C_2N_2, four new band systems of *CN* have been found. These four band systems arise from three new electronic states, here designated as the $H^2\Pi_r$, $F^2\Delta_r$, and $D^2\Pi_i$ states. The $H^2\Pi-B^2\Sigma$, $F^2\Delta-A^2\Pi$, $D^2\Pi-A^2\Pi$, and $D^2\Pi-X^2\Sigma$ band systems have been observed, and the rotational fine structures of bands of each system have been analyzed. The $v = 0$ levels of the H, F, and D states are 60,938.7, 59,682.8, and 53,955.0 cm^{-1}, respectively, above the $v = 0$ level of the ground electronic state. The B_0 values of the H, F, and D states are 1.520, 1.374, and 1.155 cm^{-1}, respectively. The red ($A^2\Pi-X^2\Sigma$) and the violet ($B^2\Sigma-X^2\Sigma$) band systems have been extended by the discovery of a number of new bands of high vibrational quantum number. The rotational lines of the 0–1 sequence of the violet system have been measured. The problem of the dissociation energy of *CN* is discussed, and it is shown that the observed spectrum tends to support the high value (8.2 ev), but no definite conclusion can be reached.

INTRODUCTION

The spectrum of the *CN* molecule is readily excited in an arc or discharge tube, and two band systems of the molecule have been known for many years. The $A^2\Pi-X^2\Sigma$ system, known as the "red system," extends from the near infrared into the visible. Various workers have measured parts of this system, but the most complete and accurate set of measurements is given by Jenkins, Roots, and Mulliken (1932). The $B^2\Sigma-X^2\Sigma$ system of bands, known as the "violet system," extends from the visible into the near-ultraviolet. The first analysis of the violet system was given by Jevons (1926), and this analysis was later extended by Jenkins (1928). Little has been added to our knowledge of the spectrum of *CN* during the last twenty years.

In the course of a search for the spectrum of the CN^+ molecule, a large number of previously unknown bands were observed. Eleven of these new bands have already been described and are attributed to CN^+ (Douglas and Routly 1954). Of the remaining new bands, the majority can be assigned to four new band systems of neutral *CN* and to extensions of the known red and violet systems. The new *CN* band system arises from three new electronic states, here designated as the $H^2\Pi$, $F^2\Delta$, and $D^2\Pi$ states. The present paper gives an account of these new data on *CN*.

EXPERIMENTAL

The experimental method used to excite and photograph the bands of *CN* has been described previously (Douglas and Routly 1954). Here it is sufficient to state that the bands were excited in a hollow cathode discharge tube through which helium containing a trace of C_2N_2 was pumped and that the spectrum of the discharge was photographed from 8500 to 1900 A with a 21-foot concave grating spectrograph.

It appears that all bands occurring in the spectrum of the discharge from 8500 to 4000 A belong to either the *CN* red or the *CN* violet system. Some of the bands found in this region are new members of the red system. Between 4500 and 2500 A, bands of the violet system, including a number not previously observed, appeared with considerable intensity. Also, in the 4000–1900 A region many bands were found which did not belong to any known system. As mentioned above, eleven of these new bands have been attributed to CN^+. Twenty-two more have been shown to belong to four new band systems of *CN*.

* National Research Laboratories postdoctorate fellow. Present address: Pomona College, Claremont, California.

A number of new bands remain, some of them weak or overlapped, which are as yet unidentified.

ANALYSES OF THE BANDS

a) THE $H^2\Pi - B^2\Sigma$ BAND SYSTEM

On a single plate, taken when the ratio of C_2N_2 to *He* in the discharge tube was large, two moderately intense red-shaded bands appeared with their strongest heads at 3025.6 and 2842.9 A. On later plates taken with a much lower proportion of C_2N_2 in the gas mixture entering the discharge tube, the bands appeared only very weakly. The bands are quite similar in appearance to the familiar red bands of *CN*. It was therefore assumed that these bands also arose from a $^2\Pi - ^2\Sigma$ transition, and subsequent analyses did indeed prove this to be so. Unfortunately, the iron-arc comparison spectrum on the plate is defective, and the absolute wave numbers of the lines might be in error by as much as 0.20 cm^{-1}. The wave numbers of the lines of the two bands are given in Table 1.

The analyses of the bands presented no difficulty. It has been found that the combination differences $\Delta_2F(J)$ of the lower states of the new bands are identical within experimental error with the known combination differences of the $v = 0$ and $v = 1$ vibrational levels of the $B^2\Sigma$ state. Also, the difference between the two band origins is 2123.47 cm^{-1}, which agrees within the error of measurement with the value 2123.55 cm^{-1} for $\Delta G(\frac{1}{2})$ of the $B^2\Sigma$ state. Therefore, we consider it definitely established that the lower state of the new bands is the $B^2\Sigma$ state. Since the lower state has been established as a $^2\Sigma$ state and since the bands each have two subbands with strong Q branches, it follows that the common upper state is a $^2\Pi$ state.

To determine whether the $^2\Pi$ state is regular or inverted, one must determine which of the two subbands has lines originating from a $J = \frac{1}{2}$ level. No lines arising from the $J = \frac{1}{2}$ level have been observed in any of the subbands because of the intrinsic weakness of such lines and because of a perturbation which will be discussed below. The Q_2 branch does, however, end abruptly at the line originating on the $J = 1\frac{1}{2}$ level, and the intensity of the last-observed line is such that one should see the line originating from the $J = \frac{1}{2}$ level if such a level exists. If the $J = \frac{1}{2}$ line of the Q_2 branch is missing, then the $^2\Pi$ state must be a regular state. This observed abrupt termination of the Q_2 branch is the only evidence we have regarding the relative positions of the $^2\Pi_{1/2}$ and $^2\Pi_{3/2}$ components of the H state, but it does seem fairly good evidence that the $^2\Pi_{3/2}$ component is the higher one.

The bands we have photographed are not sufficiently strong or free from overlapping to allow very accurate measurements. Therefore, no attempt has been made to improve the constants of the B state, which are already known from the violet bands. Also, since it is known that the spin splitting of the rotational levels of the B state is very small, we have neglected it and used only the N numbering of the lower-state levels. Only one upper-state vibrational level has been observed, and it is therefore not possible to determine the vibrational constants of this new state. There remains the determination of the rotational constants of the upper state, but even this is somewhat difficult because of a perturbation in the $^2\Pi_{1/2}$ component.

The perturbation in the $^2\Pi_{1/2}$ component is observed only in the P and R branches and not in the Q branch. In the P and R branches, lines originating in rotational levels of high J value can readily be identified, but lines originating from levels with J less than $5\frac{1}{2}$ have not been identified. Many lines, probably belonging to the P and R branches, are observed near the origin, but their assignment is uncertain.

Since the perturbation affects only the P and R branches and not the Q branch, the perturbing state must be a Σ state (Herzberg 1950, p. 288). A short extrapolation of the vibration levels of the $B^2\Sigma$ state shows that it is most unlikely that the levels of this state can cause the perturbation. It is therefore probable that the perturbation is caused by some Σ state that has not yet been observed.

The method of determining the constants of a $^2\Pi$ state from a $^2\Pi - ^2\Sigma$ transition has

TABLE 1

WAVE NUMBERS OF THE LINES OF THE $H^2\Pi - B^2\Sigma$ BANDS

N	$P_1(N)$	$Q_1(N)$	$R_1(N)$	$P_2(N)$	$Q_2(N)$	$R_2(N)$	$R_{21}(N)$
	0–0 Band, ν_0 = 35,140.84 Cm^{-1}						
0							
1		35,118.41				35,165.09	35,172.97
2		17.71			35,157.27	65.09	76.09
3		16.03			53.36	64.33	78.44
4		13.42			48.59	62.76	79.94
5		10.03		35,129.20	43.09	60.42	80.72
6		05.67		19.76	36.92	57.27	
7		00.43			29.88	53.36	
8		093.97	35,123.63	098.57	22.00	48.59	
9	35,060.89	86.77	19.03	86.77	13.42	43.09	
10	49.34	78.61	13.42	74.17	03.78	36.53	
11	36.77	69.53	07.16	60.89	093.54	29.20	
12	23.47	59.54	099.90	46.59	82.34	21.15	
13	09.34	48.59	92.19	31.47	70.37	12.30	
14	34,994.33	36.77		15.60	57.50	02.49	
15	78.68	24.28		34,998.76	43.86		
16	61.65			81.22	29.20		
17	43.74			62.68	13.82		
18				43.74			
19							
	0–1 Band, ν_0=33,017.37 Cm^{-1}						
0							33,045.53
1		32,994.87				33,041.66	49.47
2		94.26			33,033.90	41.66	52.68
3		92.73			30.11	41.08	55.13
4		90.39			25.57	39.67	56.85
5		87.11		33,006.24	20.33	37.50	57.88
6	32,967.23	82.96	33,007.54	32,997.27	14.32	34.60	57.88
7	59.06	77.90	05.16	87.11	07.54	30.96	57.41
8	49.73	71.98	01.67	76.51	32,999.99	26.48	56.03
9	39.24	65.10	32,997.27	65.10	91.67	21.25	53.91
10	28.08	57.38	92.23	52.95	82.61	15.25	51.11
11	16.03	48.73	86.32	39.91	72.68	08.45	47.28
12	03.15	39.24	79.61	26.26	62.11	00.90	
13	89.53	28.84		11.69	50.62		
14		17.57			38.35		
15		05.43			25.18		
16		892.40					
17		78.39					
18							
19							

been given by Jenkins, Roots, and Mulliken (1932) and will not be discussed here. In the new bands the perturbations prevent us from making use of the P and R branches of the $^2\Pi_{1/2}$ subband. Therefore, we have determined the $B' - B''$ values from the Q branches by the relationship[1]

$$Q_2(N) + Q_1(N-1) = 2(B' - B'')N^2 - 2B' + 2\nu_0 . \quad (1)$$

Since B'' is known to be 1.958 and 1.938 cm^{-1} for the $v = 0$ and $v = 1$ states, respectively, the values of B' and ν_0 can be determined. The result is somewhat inaccurate because the Λ doubling is neglected, but the error is quite small.

The spin coupling constant can be found from the relationship

$$Q_2(N) - Q_1(N-1) + 2B''N = \sqrt{(4B'_v N^2 + A^2 - 4AB'_v)} . \quad (2)$$

Since B'' and B'_v are known, A can be determined from the observed Q lines. The constants of the observed vibrational level of the new $H^2\Pi$ state are as follows:

$$B = 1.581, \quad A = 49.57, \quad T_0 = 60{,}938.68 \text{ cm}^{-1} .$$

The two bands have their origins at 35,140.84 and 33,017.37 cm^{-1}.

b) THE $F^2\Delta_r - A^2\Pi_i$ BAND SYSTEM

In the ultraviolet part of the spectrum a progression of five red-shaded bands was found. The bands consist of two subbands and show a number of heads, but in each band two heads separated by 110 cm^{-1} are the most obvious. The band heads of shortest wave length in the bands of the progression are at 2047.9, 2123.6, 2204.9, 2291.4, and 2383.5 A. The 2204.9 A band is shown in Figure 1, *a*.

The analysis of the new bands proved to be quite straightforward. The wave-number differences between successive members of the progression agreed with the values of the vibrational quanta of the $A^2\Pi$ state given by Jenkins, Roots, and Mulliken (1932). Thus all the bands arise from a single vibrational level of the upper state (here assumed to be the $v = 0$ level), and the lower state is the $A^2\Pi$ state. The separation of the two subbands within each band is 110 cm^{-1}, that is, about twice the doublet separation in the $A^2\Pi$ state. It therefore follows that the upper state must have a large doublet separation and cannot be a Σ state. Furthermore, since each of the subbands has a strong Q branch, it follows that the bands cannot be $\Pi - \Pi$ bands but must be $\Delta - \Pi$ bands. A detailed rotational analysis has confirmed this assignment.

The rotational fine structures of the 0–2 and 0–3 bands have been analyzed. The wave numbers of the lines are given in Table 2. Because the constants of the $A^2\Pi$ state are well known from the analysis of the red CN bands and all the new bands arise from the same vibrational level, it did not seem profitable to analyze additional bands.

Analysis has shown that the subbands in the bands of the new system correspond to $F^2\Delta_{5/2} - A^2\Pi_{3/2}$ and $F^2\Delta_{3/2} - A^2\Pi_{1/2}$ transitions, in accordance with the selection rule for case *a* coupling, that the spin component along the internuclear axis must not change, i.e., $\Delta\Sigma = 0$. The subband terminating on the $A^2\Pi_{1/2}$ component lies 110 cm^{-1} to the red of the subband terminating on the $A^2\Pi_{3/2}$ component. Since the A state of CN is known to be inverted, with the $A^2\Pi_{1/2}$ component about 50 cm^{-1} above the $A^2\Pi_{3/2}$ component, it follows that the new $F^2\Delta$ state is regular and has a doublet separation of approximately 60 cm^{-1}.

The fact that the transition is between a regular and an inverted state leads to some peculiarities in the spectrum. For low J values, in both the upper and lower states, Hund's case *a* coupling applies. The F_1 component of the $^2\Delta$ state combines with the F_2

[1] The quantum number N was previously designated by the letter K.

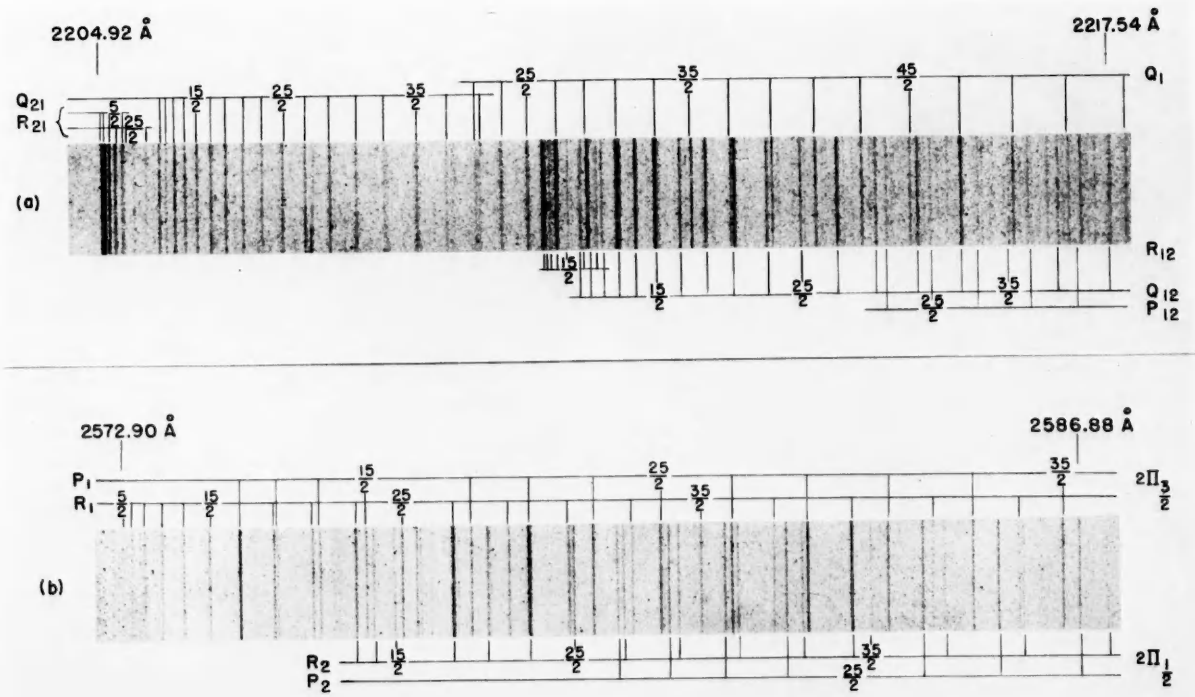

FIG. 1.—*a:* the 0–3 band of the $F^2\Delta - A^2\Pi$ system; *b:* the 1–4 band of the $D^2\Pi - A^2\Pi$ system

TABLE 2

WAVE NUMBERS OF THE LINES OF THE $F^2\Delta - A^2\Pi$ SYSTEM

J	0–2 Band							0–3 Band					
	$Q_1(J)$	$P_{21}(J)$	$Q_{21}(J)$	$R_{21}(J)$	$P_{12}(J)$	$Q_{12}(J)$	$R_{12}(J)$	$Q_1(J)$	$Q_{21}(J)$	$R_{21}(J)$	$P_{12}(J)$	$Q_{12}(J)$	$R_{12}(J)$
½							46,960.57						
1½				47,070.16		46,955.37	62.03			45,334.02		45,220.04	45,225.70
2½			47,062.46	72.23	46,947.32	53.45	62.86			35.70		17.13	26.56
3½			60.99	73.58	41.57	50.85	62.86		45,324.59	37.16		14.62	26.56
4½			59.04	74.53	36.28	47.32	62.03		22.88	38.21		11.35	26.56
5½			56.65	75.02	28.51	43.13	60.57		20.60	38.99		07.26	24.70
6½	46,998.97		53.82	75.02	20.89	38.22	58.41		18.04	38.99		02.52	22.80
7½	94.36	47,029.41	50.61	74.53	12.59	32.56	55.37		15.00	38.99		197.39	20.04
8½	89.65	22.91	46.85	73.58	03.41	26.15	51.69		11.51	38.21		91.08	16.58
9½	84.18	15.88	42.53	72.23	893.52	19.17	47.32		07.63	37.16		84.30	12.74
10½	78.31	08.36	37.84	70.16	83.25	11.25	42.14	45,243.48	03.25	35.70		76.93	
11½	71.22	00.41	32.73	67.79	71.80	02.75	36.28	36.96	298.41	33.50	45,137.98	68.65	
12½	64.08	46,991.91	26.98	64.83	59.94	893.52	29.50	30.33	93.16	30.81	26.56	60.00	
13½	56.38		20.76	61.37	47.27	83.25	22.47	22.80	87.48	28.02	14.44	50.52	
14½	47.96		14.04		34.06	72.92	14.70	15.11	81.06	24.59	01.69	40.61	
15½	38.99		06.88		20.12	61.72		06.55	74.35	20.60	088.33	29.90	
16½	29.50		46,998.97		05.50	49.86		197.39	67.16		74.22	18.74	
17½	19.17		90.67		790.26	37.27		88.00	58.82			06.67	
18½	08.56		81.38		74.22	24.02		77.89	51.02			093.98	
19½	896.57		72.48		57.03	10.12		67.24	42.40			80.89	
20½	85.14		62.03		40.39	795.73		56.04				67.27	
21½	71.80		51.69		22.44	80.43		44.16				52.72	
22½	59.94		40.62		03.31	64.68		31.71				37.78	
23½	45.71		28.51			47.82		18.74					
24½	31.56		16.86					05.39					
25½	16.37		03.85					091.25					
26½	799.81		890.59					76.62					
27½	84.68							61.22					
28½	68.03							45.59					
29½	47.82												
30½	32.53												
31½	13.91												
32½	694.93												

component of the $^2\Pi$ state to give the $^2\Delta_{3/2}-{}^2\Pi_{1/2}$ subband. Thus the P_{12}, Q_{12}, and R_{12} branches are strong. Similarly, the P_{21}, Q_{21}, and R_{21} branches form the $^2\Delta_{5/2}-{}^2\Pi_{3/2}$ subbands. For all these branches the transitions are such that the change in J is not equal to the change in N. For high J values the coupling in both states approaches case *b*, and N becomes a good quantum number and Σ a poor quantum number. For case *b* coupling the selection rule $\Delta J = \Delta N$ applies, and the rule $\Delta\Sigma = 0$ does not apply. Hence for high J values the P_1, Q_1, R_1, P_2, Q_2, and R_2 branches, for which $\Delta J = \Delta N$, should be the strong ones. Such a change in the relative intensities of the branches as we go from low to high J is indeed observed in the Q branches. For low J values the Q_{21} and Q_{12} branches are the strong ones, but for high J values the Q_1 branch becomes the strongest. Because of overlapping, it has not been possible to pick out the Q_2 branch, although some lines of the branch are visible.

The analysis of the F—A bands proved to be quite straightforward. The large doublet splitting of both the upper and lower states makes it possible to analyze each of the subbands independently and to determine the effective B values, B^*, of each component. The Λ doubling of both states is small and cannot be observed. Since the bands have Q_{12}, Q_{21}, and Q_1 branches, it is possible to determine directly the spin splitting in both the upper and the lower state. The observed constants are listed in Table 3.

TABLE 3

CONSTANTS OF THE $F^2\Delta$–$A^2\Pi$ BANDS (CM^{-1})

Band	ν_0	$B'^*_{+1/2}$	$B'^*_{-1/2}$	$B''^*_{+1/2}$	$B''^*_{-1/2}$	A'	A''
0–2.....	47,015.98	1.409	1.340	1.630	1.718	28.82	−52.79
0–3.....	45,279.34	1.4055	1.3430	1.6040	1.7060	28.77	−52.56

c) THE $D^2\Pi_i-A^2\Pi_i$ BAND SYSTEM

A weak but extensive system of red-shaded *CN* bands was found in the region from 2200 to 3000 A. The 1–4 band at 2575 A, shown in Figure 1, *b*, is a typical member of the new system. The bands have an open structure, and the band heads are not obvious. Each band has four strong branches, two P and two R branches. Since no Q branches are observed, the bands must arise from a transition in which $\Delta\Lambda = 0$. By comparing the lower-state rotational and vibrational constants of the new bands with the known constants of the $A^2\Pi$ state, it was established that the lower state is the $A^2\Pi$ state of *CN*. It therefore follows that the new upper state is a $^2\Pi$ state. The wave numbers of the lines in all the bands that have been measured are given in Table 4.

No difficulties were encountered in analyzing the bands. Each band consists of two subbands, each with one P and one R branch. These two subbands can be designated as the $^2\Pi_{3/2}-{}^2\Pi_{3/2}$ and the $^2\Pi_{1/2}-{}^2\Pi_{1/2}$ subbands. The constants of the lower state are already known from the work of Jenkins, Roots, and Mulliken (1932). The B values of the upper state can be found from the average value of $\Delta_2F'(J)$ of the two subbands, since, by the Hill–Van Vleck formulae, we have

$$\Delta_2F'(J) \text{ (average)} = 4B(J + \tfrac{1}{2}) - 8D(J + \tfrac{1}{2})^3 . \qquad (3)$$

The band origins were readily found in the usual way by plotting the sum $R_1(J - 1) + P_1(J) + R_2(J - 1) + P_2(J)$ against J^2 and finding the intercept on the axis at $J^2 = 0$. It is only in the determination of the spin coupling constant A that some difficulty was encountered.

In order to determine the spin coupling constant from the new bands alone, it would

TABLE 4

WAVE NUMBERS OF THE LINES OF THE $D^2\Pi - A^2\Pi$ BANDS

J	2-4 Band $\nu_0 = 39,797.47$ Cm^{-1}				3-3 Band $\nu_0 = 42,460.27$ Cm^{-1}				0-7 Band $\nu_0 = 32,861.01$ Cm^{-1}				0-6 Band $\nu_0 = 34,495.15$ Cm^{-1}				1-4 Band $\nu_0 = 38,827.52$ Cm^{-1}			
	$P_1(J)$	$R_1(J)$	$P_2(J)$	$R_2(J)$	$P_1(J)$	$R_1(J)$	$P_2(J)$	$R_2(J)$	$P_1(J)$	$R_1(J)$	$P_2(J)$	$R_2(J)$	$P_1(J)$	$R_1(J)$	$P_2(J)$	$R_2(J)$	$P_2(J)$	$R_1(J)$	$P_2(J)$	$R_2(J)$
$\frac{1}{2}$										32,889.53										
$1\frac{1}{2}$		39,825.84								87.79										
$2\frac{1}{2}$	24.78	22.78	39,763.12	39,778.55						87.47	32,827.27			34,510.90						
$3\frac{1}{2}$	39,806.76	57.91	57.91	77.94	42,469.36					86.21	22.61	32,843.06		04.94						
$4\frac{1}{2}$	799.33	19.80	51.38	76.25	61.78	42,481.98	42,420.03	42,437.92	32,871.11	85.24	16.93	42.35		497.35						
$5\frac{1}{2}$	90.92	15.84	44.18	73.37	53.13	77.73	05.85	34.68	64.21	84.95	10.51	40.57		90.17						
$6\frac{1}{2}$	81.73	10.94	35.77	69.50	43.43	72.42	13.37	30.63	58.50	78.60	03.16	37.67		81.32						
$7\frac{1}{2}$	71.29	05.15	26.22	64.54	32.68	66.11	87.20	24.94	48.92	73.80	794.82	34.04		71.99						
$8\frac{1}{2}$	59.97	798.34	15.64	58.42	20.82	58.73	76.02	18.36	38.86	68.11	85.64	29.50		61.75						
$9\frac{1}{2}$	47.66	90.62	04.02	51.35	08.10	50.53	63.74	10.57	27.80	61.87	75.46	23.90		50.69						
$10\frac{1}{2}$	34.48	81.73	691.28	43.02	394.28	41.06	50.47	01.65	16.97	54.78	64.46	17.57		39.63						
$11\frac{1}{2}$	20.28	72.14	77.48	33.71	79.53	30.63	36.03	391.62	06.22		52.51	10.51		28.33						
$12\frac{1}{2}$	05.14	61.46	62.61	23.46	63.74	19.33	20.34	80.35	793.72		39.65	01.94		15.65						
$13\frac{1}{2}$	659.02	49.84	46.66	11.82	46.65	06.79	03.60	68.16	79.75		25.94	792.84		01.99						
$14\frac{1}{2}$	71.92	37.03	29.66	699.38	28.85	393.40	285.77	54.59	66.49	28.86	11.32	81.75		397.45						
$15\frac{1}{2}$	53.83	23.46	11.62	85.63	09.97	78.86	66.70	40.01	51.61		695.76	71.67		92.94						
$16\frac{1}{2}$	634.83	708.97	592.50	671.02	289.86	362.74	246.62		35.94			59.91		85.53						
$17\frac{1}{2}$	14.70	693.31	72.32	55.31	68.82		25.43		02.07					46.72						
$18\frac{1}{2}$	593.69	76.79	51.11	38.53	46.62				683.73		62.03			30.74						
$19\frac{1}{2}$	71.63	59.12	28.81	20.84	23.63									11.91						
$20\frac{1}{2}$	48.62	40.58		01.88										292.53						
$21\frac{1}{2}$	24.65	20.84												71.24						
$22\frac{1}{2}$														50.41						
$23\frac{1}{2}$														27.91						
$24\frac{1}{2}$														04.82						
$25\frac{1}{2}$														180.79						
$26\frac{1}{2}$																				

be necessary to find lines corresponding to $D^2\Pi_{1/2}-A^2\Pi_{3/2}$ or $D^2\Pi_{3/2}-A^2\Pi_{1/2}$ transitions. No such lines were found. It is possible, however, to obtain A if the measurements of Jenkins, Roots, and Mulliken of the $A^2\Pi-X^2\Sigma$ bands are combined with the measurements of the new bands. For example, from their measurements of the 6–2 band, it is possible to determine quite accurately the positions of all the rotational energy levels of the $v = 6$ vibrational level of the $A^2\Pi$ state. From these energy levels and the P and R lines of the 0–6 band of the new system, it is possible to determine all the rotational levels of the $v = 0$ vibrational level of the $D^2\Pi$ state and hence to find the doublet splitting of the levels.

The doublet splittings thus determined for the $v = 0$ level are shown in Table 5. The

TABLE 5

SPIN DOUBLET SPLITTING OF THE ROTATIONAL LEVELS OF THE $D^2\Pi$ STATE (CM^{-1})

N	Determined from the $D^2\Pi-A^2\Pi$ System	Determined from the $D^2\Pi-X^2\Sigma$ System	N	Determined from the $D^2\Pi-A^2\Pi$ System	Determined from the $D^2\Pi-X^2\Sigma$ System
3	1.15	1.32	7	0.59	0.70
4	1.06	1.08	8	.44	.59
5	0.98	0.91	9	.48	.53
6	0.85	0.76	10	0.43	0.50

second set of values shown in the same table has been determined from the $D^2\Pi-X^2\Sigma$ system, which will be discussed later. The splitting is small, and the $^2\Pi$ state approaches close to case b coupling. By fitting the observed splitting to the Hill–Van Vleck formulae, one obtains $A = 7.64$ or $A = -3.03$ cm^{-1}. It is found, however, that for a given N the rotational level with the lower J value has the higher energy. Therefore, the state is an inverted one, and the correct value of A is -3.03 cm^{-1}. It is somewhat surprising that the new bands which result from a transition between an upper state having case b coupling and a lower state having case a coupling should have only four branches in each band.

Table 6 is a Deslandres table of the bands observed in the new $D^2\Pi_i-A^2\Pi_i$ system.

TABLE 6

WAVE NUMBERS OF THE BAND ORIGINS OF THE $D^2\Pi-A^2\Pi$ SYSTEM

v'	v''					
	2	3	4	5	6	7
0	.....	.....	.....	.....	34,495.15	32,861.00
1	.....	(40,538.54)*	38,827.52	(37,142.01)*	.....	.....
2	.....	(41,508.49)*	39,797.47	.....	.....	.....
3	(44,196.71)*	42,460.26	.....	.....	.....	.....

* Calculated band origins; observed but not measured.

Band origins marked with an asterisk were not measured. While the lower-state vibrational numbering was readily obtained from the known ΔG values of the A state, the numbering in the upper state is not certain. The lowest vibrational level observed in the upper state gives rise to two strong bands with origins at 32,861 and 34,495 cm^{-1}. The

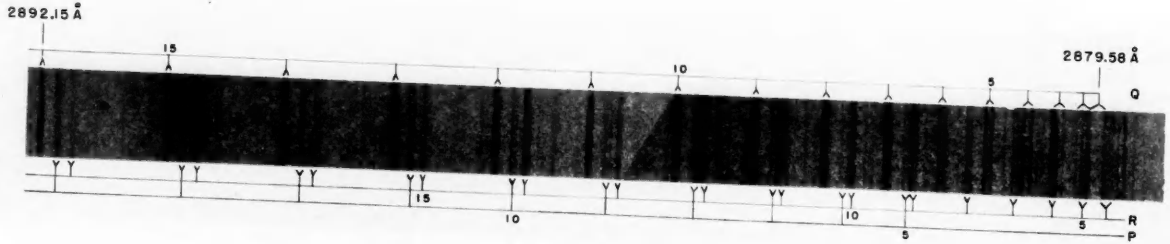

FIG. 2.—The 0–9 band of the $D^2\Pi - X^2\Sigma$ system

spectral region to the red of these two bands is heavily masked by other strong band systems, and it is therefore possible that bands originating from lower vibrational levels of the D state do exist but were not detected. However, the intensities of the bands originating from the lowest observed vibrational level and the distribution of observed bands within the Deslandres table are such that it is considered unlikely that the upper-state vibrational numbering given in Table 6 can be in error by more than one unit.

The constants of the five bands that have been measured are given in Table 7. The B values of the lower $^2\Pi$ state agree well with those measured or predicted from the red CN bands. The upper state appears to be well behaved, suffering from no vibrational or rotational perturbations. The analysis leads to the following constants:

TABLE 7

CONSTANTS OF THE $D^2\Pi - A^2\Pi$ BANDS (CM^{-1})

Band	ν_0	D'	B'	$B''_{+1/2}$	$B''_{1/2}$
0–6	34,495.15	7×10^6	1.155	1.558	1.647
0–7	32,861.00	.....	1.155	1.544	1.630
1–4	38,827.52	6×10^6	1.141	1.592	1.686
2–4	39,797.47	10×10^6	1.129	1.591	1.688
3–3	42,460.26	.....	1.115	1.608	1.699

$$\nu_{00} = 44{,}836.97\ \text{cm}^{-1}, \quad \omega_0 = 995.93\ \text{cm}^{-1}, \quad \omega_0 x_0 = 8.78\ \text{cm}^{-1},$$

$$B_0 = 1.155\ \text{cm}^{-1}, \quad \alpha = 0.013\ \text{cm}^{-1}.$$

d) THE $D^2\Pi_i - X^2\Sigma$ BAND SYSTEM

The fourth new band system observed in CN arises from the transition $D^2\Pi - X^2\Sigma$. The most prominent feature in each band of this system is the Q branch, which consists of a series of narrow doublets whose separation increases toward the band head. The P and R branches consist of similar doublets, but they are considerably weaker than the Q branch. Because the difference between the B values of the upper state and those of the lower state is large, the band heads are not prominent. The 0–10, 0–9, 0–8, 0–7, 0–6, 0–5, and 1–8 bands have been observed, but only the 0–9 and 0–10 bands have been measured. The wave numbers of the rotational lines of these two bands are given in Table 8. Figure 2 shows the 0–9 band at 2880 A.

The analysis of the bands leaves no doubt as to the correct assignment of the measured bands. The upper-state combination differences agree with the upper-state combination differences obtained from the $D^2\Pi - A^2\Pi$ bands, and the lower-state combination differences agree with those given by Jenkins for the $v = 9$ and $v = 10$ levels of the $X^2\Sigma$ state. The constants of the two bands are given in Table 9. The constants have been determined from the mean value of the doublets.

Though the bands give no new information about the rotational constants, they do give a more direct measure of the doublet splitting of the D state than can be obtained otherwise. The observed separations of the doublets of the Q branch are the sums (or differences) of the doublet separations in the X and D states. It is known that the doublet separation in the X state is very small and can be completely neglected for low values of N. Therefore, the observed doublet separation gives us directly the doublet separation in the D state. It is the mean values of the doublet separations taken from the two bands that are listed in Table 5.

TABLE 8

WAVE NUMBERS OF THE LINES OF THE $D^2\Pi - X^2\Sigma$ BANDS

K	0–9 BAND $\nu_0 = 34{,}718.34$ CM^{-1}			0–10 BAND $\nu_0 = 36{,}522.48$ CM^{-1}		
	$P(N)$	$Q(N)$	$R(N)$	$P(N)$	$Q(N)$	$R(N)$
0						
1		34,718.27 15.93				
2		15.93 14.23			36,519.47 18.25	36,526.76 23.74
3		12.28 11.00			16.25 14.87	25.34 22.90
4		07.74 06.63	34,719.61 18.27	36,501.95 01.16	11.45 10.39	19.47 18.25
5	34,690.66 89.56	02.63 01.12	15.93 14.99	493.91 93.29	05.65 04.73	14.87 13.49
6	80.55	695.21 94.43	11.00	84.74 84.03	498.63 97.88	08.94 07.86
7	71.26 70.47	87.38 86.66	05.77 05.19	74.21 73.64	90.49 89.80	01.95 01.16
8	659.32	678.34 77.77	699.10 98.56	462.66 62.12	481.23 80.61	493.91 93.29
9	47.51 46.95	68.26 67.72	91.33 90.66	49.99 49.44	70.79 70.26	84.74 84.03
10	34.06 33.49	57.08 56.58	82.37 81.93	36.10 35.59	59.21 58.71	74.21 73.64
11	19.34 18.88	44.80 44.26	72.45 71.94	21.06 20.61	46.55 46.02	62.66 62.12
12	03.64 03.19	31.33 30.87	61.34 60.83	04.86 04.46	32.65 32.20	49.99 49.44
13	586.84 86.34	16.83 16.39	49.05 48.61	387.33	17.65 17.22	36.10 35.59
14	68.86 68.46	01.11 00.72	35.73 35.21	68.83	01.47 01.04	21.06 20.61
15	49.76 49.32	584.34 83.92	21.12 20.78	49.18	383.92	04.86 04.46
16	529.39	566.46 66.10	605.63 05.19	328.51	365.46	387.33
17		47.41 47.08	588.54	06.51	45.87	68.83
18		27.27 26.89	70.88	283.36	25.07	49.18
19			51.98	59.37	03.18	28.51
20					280.06	06.51
21					55.71	283.36
22						59.37

e) UNIDENTIFIED BANDS

There are a number of bands on the plates which have not been identified. Some of these bands which appear to arise from singlet states of CN^+ have already been described (Douglas and Routly 1954). There are, however, a number of weak bands in the ultraviolet which are quite complex and may be due to *CN*. One of the isolated bands near 3060 A which occurs under the same experimental conditions as the H−B system has been analyzed. This band is very similar in appearance to the D → X bands, and it seems certain that the band arises from a $^2\Pi-{}^2\Sigma$ transition. The analysis shows that the lower-state combination differences $\Delta_2F(N)$ of the new band are the same as those of the $v = 1$ level of the $B^2\Sigma$ state, and it was at first thought that the new band belonged to a D−B system. The upper state of the new band (assuming that the lower state is the B state) lies 6671 cm^{-1} above the $v = 0$ level of the D state. This energy would correspond to a vibrational level of the D state with a quantum number v of about 7. The B value of the new state is, however, considerably larger than the value that one might expect for the $v = 7$ level of the D state. Also, the doublet splitting of the new state appears even

TABLE 9

CONSTANTS OF THE $D^2\Pi-X^2\Sigma$ BANDS (CM^{-1})

Band	ν_0	A'	B'	B''
0–9.....	36,522.48	−3.03	1.154	1.732
0–10.....	34,718.34	−3.03	1.154	1.713

smaller than that of the D state. Therefore, it is probable that the 3060 A band arises from still another new electronic state.

The wave numbers of the lines of the new band are given in Table 10. The analysis gave the following constants:

$$B' = 1.085\ cm^{-1},\quad B'' = 1.941\ cm^{-1},\quad \nu_0 = 32{,}702.60\ cm^{-1}.$$

It is not possible to determine the coupling constant A, but it is certainly very small.

Two other quite strong red-shaded bands, with their strongest heads at 2078.8 and 2161.0 A, appear on our plates and may be due to *CN*. Also, there is a considerable number of unidentified bands between 1950 and 2050 A. It appears that an investigation of the spectrum of the source used in this work in the vacuum ultraviolet region would show a large number of new bands.

f) THE VIOLET BAND SYSTEM, $B^2\Sigma-X^2\Sigma$

The most familiar band system of *CN* is the $B^2\Sigma-X^2\Sigma$ system, which extends from the visible into the near ultraviolet. The bands of this system of low vibrational numbering have been measured by Uhler and Patterson (1915), Kayser and Runge (1910), and Heurlinger (1918), and these measurements have been reviewed by Jevons (1926). A few measurements have been made more recently by Jenkins and Wooldridge (1938). Though the early measurements of the 0–0 band by Uhler and Patterson agree very well with the more recent measurements of Jenkins and Wooldridge, there is considerable disagreement between the various measurements for the other bands. Furthermore, none of the sets of measurements is very extensive, and at the present time there exists no complete and accurate set of vibrational and rotational constants for the low vibrational levels of the B and X states of *CN*. The best values for the rotational and vibrational constants of the lower state are those obtained from measurements of the red $A^2\Pi-X^2\Sigma$ bands of

CN by Jenkins, Roots, and Mulliken (1932). No equally good values of the constants of the B state are known.

For the vibrational level with v' and v'' between 8 and 15 the measurement of Jenkins (1928) provides an excellent set of constants. Up to the present, no bands have been found with either v' or v'' greater than 15, and it has been suggested that the absence of higher vibrational quanta may be caused by a predissociation occurring above this point.

The source used in the present work was found to give the B−X bands with high intensity. It was found that all the bands which had been identified previously (except some of the bands found in an arc source by Feast [1949]) were present, and, in addition, some new bands with v' and v'' greater than 15 were found. The 16–13, 19–15, 18–17, 18–18, and 19–18 bands and a rather weak 14–10 band have been measured, and, in order to obtain better constants for the low vibrational levels, the bands of the 0–1 sequence

TABLE 10

WAVE NUMBERS OF THE LINES OF THE 3060 A BAND

N	*P(N)*	*Q(N)*	*R(N)*
1	.....	32,700.39	.....
2	.....	696.20	.....
3	.....	692.49 92.08	.....
4	.....	85.69 85.34	32,696.92 96.20
5	.....	77.30 76.83	90.40 89.85
6	32,654.22 53.56	67.00 66.61	82.29 81.81
7	39.99 39.56	55.11 54.65	72.44 72.07
8	24.23 23.65	41.46 41.02	60.92 60.59
9	06.36	26.11 25.64	47.65 47.39
10	87.30 86.90	09.02 08.54	32.61
11	66.35 65.97	590.23 89.83	15.85
12	43.72 43.40	69.81 69.35	97.61
13	19.42 19.12	47.68 47.23	77.72
14	93.48 93.14	23.88 23.43	56.00
15	.....	498.41 97.92	32.73
16	.....	42.31 41.76	....

have been measured up to the 5–6 band. A number of new bands with vibrational quantum numbers v' and v'' between 9 and 15 are present on the plates, but they add nothing to the accurate constants obtained by Jenkins and therefore have not been measured.

The wave numbers of the bands of the 0–1 sequence are given in Table 11. The wave numbers of the bands of high vibrational quantum number are given in Table 12. In Table 13 the band origins and the B values of all the accurately measured violet bands of *CN* are given. In Table 13 the vibrational quanta are shown along the bottom and the right of the table; those values that are not known from direct measurement but are obtained by interpolating between known values are given in parentheses.

The vibrational quanta of the ground electronic state can be represented by the equation:

$$\Delta G(v + \tfrac{1}{2}) = 2042.39 - 26.228v - 0.02728v^2 . \quad (4)$$

The vibrational quanta of the B state cannot be represented by any simple equation. Figure 3 shows a graph of the vibrational quanta $\Delta G(v + \frac{1}{2})$ plotted against the quantum number v for the $B^2\Sigma$ state. In this graph a linear dependence of $\Delta G(v + \frac{1}{2})$ upon v has

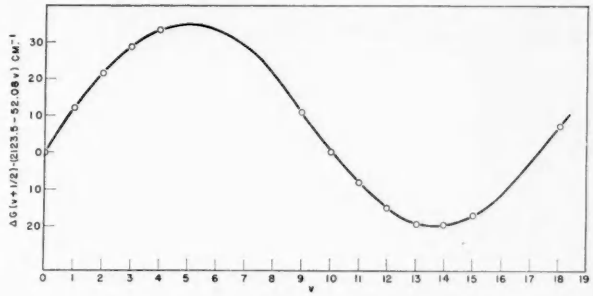

FIG. 3.—A graph of the vibrational quanta $\Delta G(v + \frac{1}{2})$ of the $B^2\Sigma$ state plotted against the quantum number v. A linear dependence of $\Delta G(v + \frac{1}{2})$ upon v has been subtracted from the observed $\Delta G(v + \frac{1}{2})$ values to enlarge the scale of the graph.

already been subtracted from the observed $\Delta G(v + \frac{1}{2})$ values in order to enlarge the scale of the graph. The irregular shape of this graph shows that it requires an equation in high powers of v to represent the $\Delta G(v + \frac{1}{2})$ values, and it appears that there is no accurate method of extrapolating the curve to obtain vibrational quanta beyond those that have been observed.

The B values of the vibrational levels of the $X^2\Sigma$ state can be represented within the experimental error of the measurements by the equation

$$B_v = 1.8903 - 0.01722v - 4.73 \times 10^{-5}v^2 . \quad (5)$$

For the $B^2\Sigma$ state the B values cannot be represented by such a simple equation, since the values of B_v, when plotted against v, follow a curve somewhat like the corresponding $\Delta G(v + \frac{1}{2})$ curve.

A search was made for bands arising from still higher vibrational levels, but none were found. The strong bands from the low and intermediate vibrational levels fall in the same spectral region as the weaker bands from the high levels, and it may be this overlapping rather than the actual absence of the bands that limits a further extension of the Deslandres table.

The constants of the low vibrational levels of the $X^2\Sigma$ and particularly the $B^2\Sigma$ state

TABLE 11

Wave Numbers of the Lines of the 0–1 Sequence of the $B^2\Sigma - X^2\Sigma$ Bands

N	0–1 Band $\nu_0 = 23{,}755.48$ Cm^{-1}		1–2 Band $\nu_0 = 23{,}862.93$ Cm^{-1}		2–3 Band $\nu_0 = 23{,}956.57$ Cm^{-1}		3–4 Band $\nu_0 = 24{,}034.20$ Cm^{-1}		4–5 Band $\nu_0 = 24{,}093.21$ Cm^{-1}		5–6 Band $\nu_0 = 24{,}130.88$ Cm^{-1}	
	$P(N)$	$R(N)$	$P(N)$	$R(N)$	$P(N)$	$R(N)$	$P(N)$	$R(N)$	$P(N)$	$R(N)$	$P(N)$	$R(N)$
0	.....	23,759.39	.....	23,866.81	.....	23,960.41	.....	24,037.99	.....	.....	.....	24,134.44
1	23,751.72	63.48	23,859.21	70.84	23,952.89	64.40	.....	41.95	.....	24,101.11	.....	38.32
2	48.15	67.73	55.67	75.04	49.37	68.53	24,027.04	45.99	24,086.18	04.85	24,123.77	42.27
3	44.73	72.18	52.28	79.41	46.00	72.84	23.71	50.26	82.81	08.98	20.47	46.37
4	41.52	76.76	49.05	83.95	42.81	77.29	20.52	54.57	79.59	13.26	17.28	50.52
5	38.47	81.52	46.01	88.65	39.73	81.89	17.44	59.13	76.53	17.68	14.21	54.81
6	35.55	86.38	43.11	93.49	36.84	86.63	14.52	63.76	73.61	22.22	11.25	59.19
7	32.83	91.58	40.40	98.50	34.11	91.54	11.77	68.59	70.80	26.86	08.38	63.64
8	30.22	96.85	37.85	903.69	31.52	96.63	09.15	73.21 73.61	68.14	31.43	05.67	68.13
9	27.92	802.29	35.44	09.03	29.09	24,001.85	06.69	78.50 78.75	65.59	36.55	02.98	72.15
10	25.70	07.89	33.16	14.57	26.83	07.23	04.42	83.73 83.94	63.19	41.69	00.31	77.62
11	23.66	13.65	31.14	20.19	24.71	12.77	04.26	89.11 89.34	60.95	46.87	097.72	82.40
12	21.78	19.64	29.23	26.02	22.75	18.45	00.25 00.03	94.61 94.86	58.83	52.16	95.64	.....
13	20.09	25.72	27.51	31.91 32.06	20.94	24.30	23,998.36 98.14	100.31 00.56	56.87	57.58	93.02	.....
14	18.55	31.83	25.97	38.07 38.21	19.32	30.20 30.37	.....	06.01 06.36	55.06	63.36	.....	.....
15	17.18	38.35 38.54	24.50	44.37 44.52	17.83	36.35 36.51	95.07 94.83	12.04 12.33	53.37 53.12	69.08	.....	.....
16	15.87	44.96 45.15	23.33 23.16	50.82 51.02	16.49	42.62 42.84	93.62 93.38	18.14 18.43	51.78 51.57	.....	.....	.....
17	15.02	51.74 51.94	22.26 22.06	57.43 57.66	15.32	49.04 49.28	92.33 92.07	24.40 24.68	.....	.....	.....	.....
18	14.19	58.71 58.87	21.35 21.16	.....	14.44 14.19	55.63 55.83	91.18 90.91	30.25 30.55	49.04 48.77	.....	.....	.....
19	13.50	65.79 65.99	20.63 20.41	71.16 71.40	13.50 13.34	.....	90.19 89.90	.....	47.79 47.51	.....	.....	.....
20	12.98	73.04 73.27	.....	78.27 78.48	12.79 12.64	.....	89.33 89.05	.....	46.78 46.31	.....	.....	.....
21	12.57	80.51 80.73	.....	85.51 85.74	.....	.....	88.60 88.31	.....	45.99 45.63	.....	.....	.....
22	.....	88.13 88.34	.....	.....	.....	.....	.....	.....	45.07 44.75	.....	.....	.....
23	.....	95.91 96.10	.....	.....	.....	.....	.....	.....	44.41 44.14	.....	.....	.....
24	.....	.....	.....	.....	.....	.....	.....	.....	43.90 43.49	.....	.....	.....

TABLE 12

Wave Numbers of the Lines of New $B^2\Sigma - X^2\Sigma$ Bands of CN

24 ..... { 43.90 / 43.49

TABLE 12

WAVE NUMBERS OF THE LINES OF NEW $B^2\Sigma - X^2\Sigma$ BANDS OF *CN*

N	16–13 Band ν_0=29,175.78 Cm^{-1}		18–17 Band ν_0=25,063.04 Cm^{-1}		18–18 Band ν_0=23,474.42 Cm^{-1}		19–15 Band ν_0=29,515.15 Cm^{-1}		19–18 Band ν_0=24,667.57 Cm^{-1}		14–10 Band ν_0=31,728.77 Cm^{-1}	
	P(*N*)	*R*(*N*)	*P*(*N*)	*R*(*N*)	*P*(*N*)	*R*(*N*)	*P*(*N*)	*R*(*N*)	*P*(*N*)	*R*(*N*)	*P*(*N*)	*R*(*N*)
0	.....	29,178.83	.....	25,065.97	.....	23,477.31	.....	29,518.01	.....	24,670.22	.....	31,731.99
1	29,172.37	81.47	25,059.82	68.46	23,471.28	79.89	29,511.90	20.41	24,664.45	72.91	.....	34.81
2	68.82	83.79	56.40	70.79	67.87	82.25	08.17	22.32	61.00	75.10	31,721.53	37.27
3	64.82	85.81	52.65	72.86	64.21	84.35	04.04	23.84	57.25	76.98	17.55	39.45
4	60.58	87.56	48.59	74.50	60.32	86.19	499.46	24.99	53.17	78.52	13.20	41.35
5	55.96	88.96	44.23	75.04	56.14	87.76	94.55	25.61	48.77	79.63	08.59	43.16
6	51.05	89.98	39.59	77.00	51.72	89.03	89.19	25.61	44.05	80.39	03.59	44.26
7	45.79	90.52	34.63	77.79	47.03	90.11	83.38	25.61	39.01	81.09	98.36	45.01
8	40.24	91.15	29.39	78.31	42.08	90.90	77.14	24.99	{ 33.55 / 33.73 }	81.34	92.94	45.61
9	34.35	91.15	23.84	78.31	36.87	91.40	70.42	23.84	{ 27.86 / 28.04 }	81.09	87.28	.....
10	28.17	91.15	17.99	78.31	31.40	91.69	63.33	22.32	{ 21.85 / 22.06 }	80.69	80.97	.....
11	21.61	90.52	11.85	77.79	25.67	91.69	55.82	20.41	{ 15.54 / 15.75 }	80.18	.....	.....
12	.....	89.54	05.39	77.00	19.68	91.40	47.79	18.01	{ 08.92 / 09.11 }	79.13	.....	.....
13	.....	88.30	24,998.64	76.12	13.41	90.90	39.36	15.20	{ 01.95 / 02.14 }	77.76	.....	.....
14	.....	86.77	91.60	74.84	{ 06.84 / 06.96 }	90.11	30.51	11.90	{ 594.67 / 94.86 }	76.08	.....	.....
15	.....	84.84	{ 84.15 / 84.31 }	73.08	{ 400.17 / 399.97 }	89.03	21.20	08.17	87.15	74.12	.....	.....
16	.....	82.61	{ 76.47 / 76.65 }	71.10	{ 92.93 / 93.13 }	87.76 / 87.47	11.47	04.04	79.22	71.73	.....	.....
17	.....	80.02	{ 68.44 / 68.71 }	.....	85.57 / 85.81	86.19 / 85.90	01.34	499.46	70.95	69.01	.....	.....
18	.....	{ 76.89 / 77.19 }	60.14 / 60.43	.....	77.84 / 78.16	84.35 / 83.93	390.68	94.32	62.35	65.95	.....	.....
19	.....	{ 73.61 / 73.99 }	51.49 / 51.84	.....	70.12 / 70.37	81.65 / 82.25	79.66	88.77	53.40	62.62	.....	.....
20	.....	{ 69.99 / 70.38 }	42.50 / 42.89	.....	61.73 / 62.13	79.43 / 79.89	68.12	82.77	44.14	.....	.....	.....
21	.....	{ 65.90 / 66.36 }	33.11 / 33.62	.....	53.18 / 53.63	.....	.....	76.33	34.54	.....	.....	.....
22	.....	{ 61.47 / 62.01 }	23.39 / 23.96	.....	44.25 / 44.83	.....	.....	69.27	24.58	.....	.....	.....
23	.....	{ 56.60 / 57.24 }	.....	.....	.....	.....	.....	62.00	14.29	.....	.....	.....
24	.....	.....	.....	.....	.....	.....	.....	54.16	.....	.....	.....	.....
25	.....	.....	.....	.....	.....	.....	.....	45.70	.....	.....	.....	.....

TABLE 13

Band Origins and B Values of the Violet Band System

v'	v''									
	0	1	2	3	4	5	6	7	8	9
0	25,797.84* $B'=1.962$ $B''=1.891$	23,755.48† 1.958 1.873	21,739.30‡							
1		25,879.00* 1.942 1.875	23,862.93† 1.938 1.856							
2				23,956.57† 1.916 1.838						
3					24,034.20† 1.894 1.820					
4						24,093.21†§ 1.870 1.804				
5							24,130.88†§ 1.849 1.786			
6										
7										
8										
9									27,642.10‖ 1.7278 1.7496	
10										27,476.94‖ 1.6968 1.7325
11										29,079.70‖ 1.6630 1.7318
12										
13										
14										
15										
16										
17										
18										
19										
$\Delta G''(v+\frac{1}{2})$	2042.43#	2016.06#	1989.80#	1963.38#	1937.01#	(1910.61)	(1884.10)	(1857.52)	(1830.88)	1804.25

* Uhler and Patterson 1915.
† Present work.
‡ Jenkins and Wooldridge 1938.
§ These values are less reliable than other band origins.
‖ Jenkins 1928.
Jenkins, Roots, and Mulliken 1932.

TABLE 13—*Continued*

v''									$\Delta G'(v+\frac{1}{2})$
10	11	12	13	14	15	16	17	18	
									2123.55
									2083.44
									2041.01
									1996.02
									(1948.25)
									(1897.7)
									(1844.6)
									(1787.3)
									(1728.0)
25,672.69‖ 1.6964 1.7137									1665.72
27,275.45‖ 1.6624 1.7141	25,498.07‖ 1.6631 1.6945								1602.76
28,817.87‖ 1.6292 1.7147	27,040.49‖ 1.6281 1.6941	25,287.98‖ 1.6281 1.6768							1542.42
	28,524.07‖ 1.5969 1.6943		25,048.63‖ 1.5956 1.6591						1483.58
31,728.77†				24,778.89‖ 1.5629 1.6427					1427.32
					24,483.85‖ 1.5307 1.6226				1374.90
			29,175.78† 1.500 1.661						1324.93
									(1279.4)
							25,063.04† 1.585	23,474.40† 1.438 1.566	(1235.8)
					29,515.15† 1.409 1.622			24,667.57† 1.404 1.563	1193.17
1777.38	1752.51	1722.93	1697.05	(1669.94)	(1642.91)	(1615.84)	1588.63		

† Present work. ‖ Jenkins 1928.

are still not so accurately known as might be desired. The 4–5 and particularly the 5–6 bands that we have measured are badly overlapped, and the measurements cannot be considered satisfactory. A measurement of the 0–0 and the 0–2 sequences from high-dispersion plates would considerably improve the constants given here.

g) THE RED BAND SYSTEM, $A^2\Pi - X^2\Sigma$

The red bands of *CN* have been known for many years and have been measured by many observers. Jenkins, Roots, and Mulliken (1932) have given an accurate and extensive set of measurements of band heads, together with a detailed analysis of a number of bands. Except for the fact that Herzberg and Phillips (1948) have shown that the vibrational numbering of the upper state must be increased by one unit, these measurements are still the most reliable now available. From these measurements the positions of the vibrational levels of the A state are known up to $v = 12$, and a detailed rotational analysis has been given for the levels with $v' = 5$, 6, 7, 8, and 9.

The red band system appeared very strongly on our plates, and it was found that a number of new bands were present. By measuring a number of lines leading up to the

TABLE 14

HEADS OF NEW BANDS OF THE $A^2\Pi_i - X^2\Sigma$ (RED) SYSTEM (CM^{-1})

	Band						
	12–4	14–6	15–7	16–7	15–8	16–8	17–8
R_2 head...	20,894.62	19,978.92	19,521.57	20,921.78	17,664.13	19,064.38	20,437.85

	Band					
	17–9	18–9	17–10	10–10	18–11	19–11
R_2 head...	18,607.31	19,954.15	16,803.19	18,150.27	16,372.87	17,692.69

R_2 head and hence establishing accurately the position of these heads, the system has been extended up to $v' = 19$, and, in addition, the rotational structure of the 15–8 band has been analyzed. The wave numbers of the R_2 band heads are listed in Table 14, and the wave numbers of the lines of the 15–8 band are given in Table 15.

From the new measurements, together with those of Jenkins, Roots, and Mulliken, it is possible to determine the vibrational quanta of the A state up to $\Delta G(18\frac{1}{2})$. The values are given in Table 16. The band-head measurements were corrected for the distance between the head and the origin of the $^2\Pi_{1/2}$ component, and the $\Delta G(v)$ values given are really the values for this component only. The values for the $^2\Pi_{3/2}$ component would only be slightly different from those given here. The $\Delta G(v)$ values can be represented by the equation

$$\Delta G(v + \tfrac{1}{2}) = 1787.10 - 25.25v - 0.037v^2 . \qquad (6)$$

The values of $\Delta G(v + \frac{1}{2})$ calculated from this equation are also given in Table 16.

The rotational analysis of the 15–8 band gives the following constants:

$$B^*_{+1/2} = 1.4042 \text{ cm}^{-1}, \quad B^*_{-1/2} = 1.4779 \text{ cm}^{-1}, \quad B' = 1.4406 \text{ cm}^{-1}, \quad A' = -50.66 \text{ cm}^{-1},$$

$$B'' = 1.7498 \text{ cm}^{-1}.$$

Using the above value of B', together with those given by Jenkins, Roots, and Mulliken (1932) and by Parker (1932), it is possible to determine an expression giving the B values as a function of the vibrational quantum number. It is found that for the $A^2\Pi$ state within the experimental error the B values are given by the equation

$$B_v = 1.7080 - 0.01720v - 4.14 \times 10^{-5}v^2 . \quad (7)$$

TABLE 15

WAVE NUMBERS OF THE LINES OF THE 15–8 BAND OF THE RED SYSTEM

N	$P_1(N)$	$Q_1(N)$	$R_1(N)$	$P_2(N)$	$Q_2(N)$	$R_2(N)$
0	.....	.....	17,613.57	.....	.....	.....
1	.....	.....	17.01	.....	.....	.....
2	17,603.21	17,610.05	19.87	17,652.06	17,656.76	17,664.13
3	599.58	09.37	21.99	46.28	53.66	64.13
4	95.39	07.99	23.57	.....	50.00	63.38
5	90.52	05.93	24.21	32.58	45.84	62.14
6	84.92	03.21	24.21	24.91	41.11	60.37
7	78.69	599.78	23.57	16.63	35.79	58.04
8	71.79	95.67	22.35	07.99	29.96	55.12
9	64.17	90.93	20.43	598.59	23.57	51.67
10	55.91	85.45	17.75	88.70	16.63	47.64
11	46.94	79.35	14.45	78.26	09.10	43.07
12	37.35	72.57	10.48	67.25	01.01	37.89
13	27.07	65.12	05.93	55.67	592.36	32.13
14	16.11	57.04	00.57	43.53	83.13	25.81
15	04.54	48.29	594.65	30.81	73.32	18.93
16	492.27	38.91	88.06	17.52	62.94	11.42
17	79.39	28.86	80.81	03.66	51.97	.....
18	.....	18.19	72.98	489.20	40.41	.....
19	.....	06.86	64.60	.....	28.29	.....
20	.....	494.89	55.25	.....	15.57	.....

TABLE 16

OBSERVED AND CALCULATED VALUES OF $\Delta G(v+\frac{1}{2})$ FOR THE $A^2\Pi$ STATE (CM^{-1})

v	$\Delta G(v+\frac{1}{2})_{obs}$	$\Delta G(v+\frac{1}{2})_{calc}$	v	$\Delta G(v+\frac{1}{2})_{obs}$	$\Delta G(v+\frac{1}{2})_{calc}$
0	.....	1787.10	10	1530.86	1530.90
1		1761.81	11	1505.26	1504.87
2	6894.81	1736.45	12	2929.51	1478.77
3		1711.01	13		1452.60
4		1685.51	14	1426.79	1426.35
5	1659.69	1659.92	15	1400.43	1400.03
6	1634.22	1634.27	16	1373.67	1373.63
7	1606.87	1608.54	17	1347.15	1347.16
8	1583.35	1582.73	18	1320.02	1320.61
9	1556.87	1556.85			

DISCUSSION

One of our main interests in the spectrum of *CN* arose from the possibility of determining the dissociation energy from the spectrum. This was attempted by Schmid, Gerö, and Zemplén (1938), but there seem to be no firm grounds for the conclusion they reach. We have examined our new data to see if they lead to any conclusion regarding the dissociation energy, but, as will be shown below, no definite conclusion is possible.

The dissociation energy of the *CN* molecule can be calculated from the dissociation energy of nitrogen and the heat of sublimation of carbon, together with the heat of formation of *CN* from solid carbon and nitrogen. The work of Brewer, Templeton, and Jenkins (1951) and of Long (1949) has established the heat of formation of *CN* to be 4.07 ev. If the value of $D(N_2)$ is taken to be 9.76 ev (Douglas 1952), then values of 7.39, 6.13, and 5.42 ev for the heat of sublimation of carbon (Gaydon 1953) will yield 8.2 ev (66,000 cm^{-1}), 6.9 ev (56,000 cm^{-1}), and 6.2 ev (50,000 cm^{-1}), respectively, for $D(CN)$. The spectrum has been examined to see whether it is possible to decide which of these values is correct.

The present work gives four independent sets of data which offer some hope of yielding the dissociation energy of *CN*. From the observed vibrational levels of the X, B, and A states it is possible to estimate the dissociation limit of each state by a Birge-Sponer extrapolation. Also, it may be possible to locate indirectly the positions of high vibrational levels of the A state by means of the perturbations that these levels cause in the observed levels of the B state. From the dissociation limit, knowing the atomic states of the dissociation products at each limit, four values of $D(CN)$ may be obtained. There seems no doubt that the X and the A states dissociate into atoms in the ground state, and therefore the dissociation limit of these two states is equal to $D(CN)$. The B state cannot dissociate into the ground state of the *C* and *N* atoms and probably dissociates into $C(^3P)$ and $N(^2D)$, thereby placing the dissociation limit of the B state 19,000 cm^{-1} above $D(CN)$. Therefore, if the dissociation limit of any one of the X, the A, and the B states could be established, the dissociation energy of *CN* would follow directly.

The vibrational levels of the ground state $X^2\Sigma$ have been observed up to $v = 18$, which lies 32,700 cm^{-1} above the $v = 0$ level. If the expression for the energies of the vibrational levels given in equation (4) is used to determine the dissociation limit, it is found to be at 77,650 cm^{-1}.

The last observed band of the red system arises from the $v = 19$ vibrational level of the A state. This level lies 38,670 cm^{-1} above the $v = 0$ level of the X state. If the vibrational levels of the A state are extrapolated to their dissociation limit, according to equation (6), the limit is found to be at 69,500 cm^{-1}.

The vibrational levels of the $B^2\Sigma$ state can be observed up to $v = 19$. The last observed level lies at 57,380 cm^{-1} above the $v = 0$ level of the ground state. As has been discussed earlier, it is not possible to extrapolate the series of vibrational levels with any accuracy, since they do not follow a simple equation. It would, however, be somewhat surprising if the convergence limit were below 70,000 cm^{-1}, and a value near 80,000 appears more likely. This dissociation limit of the B state corresponds to a dissociation energy of *CN* which is most likely over 51,000 cm^{-1} and probably nearer to 61,000 cm^{-1}.

The plots of $\Delta G(v + \frac{1}{2})$ against $v + \frac{1}{2}$ for each of the X, A, and B states are shown in Figure 4. The observed values are extrapolated in two ways corresponding to the two dissociation energies of 66,000 and 56,000 cm^{-1}. In each case it is possible, by assuming a sudden change in curvature, to obtain a dissociation energy as low as 56,000 cm^{-1} and perhaps as low as 50,000 cm^{-1}. However, the value 66,000 cm^{-1} appears more probable in all three extrapolations. Thus we can say that the present data favor the high value of 8.20 ev for the dissociation energy of *CN*, but the lower values cannot be ruled out.

Schmid, Gerö, and Zemplén (1938) have attempted to determine the positions of vibrational levels of the A state, beyond those that can be observed directly, by means of the observed perturbations that these levels cause in the B state. They have given no detailed information, and it is difficult to determine how they interpreted the perturbations. Perhaps the most important point that they have made is that the perturbation of the $v = 14$ level of the B state is caused by the $v = 29$ level of the A state. If this is true, it follows at once that the convergence limit of the A state is above 56,000 cm^{-1}. There is no doubt that the $v = 14$ level of the B state is severely perturbed. There is,

however, at the present time no convincing evidence that this perturbation is caused by the A state and still less evidence that it is the $v = 29$ level that is responsible. We have attempted to obtain such evidence from a study of the 14–12 band of the violet system, but we have been unable to obtain a sufficiently detailed analysis to establish the nature of the perturbing state. Thus the interpretation given by Schmid, Gerö, and Zemplén (1938), though not unreasonable, stands without proof. It does not seem possible at the present time to obtain a decisive answer to the problem of the dissociation energy of *CN* from a study of the perturbations in the B state.

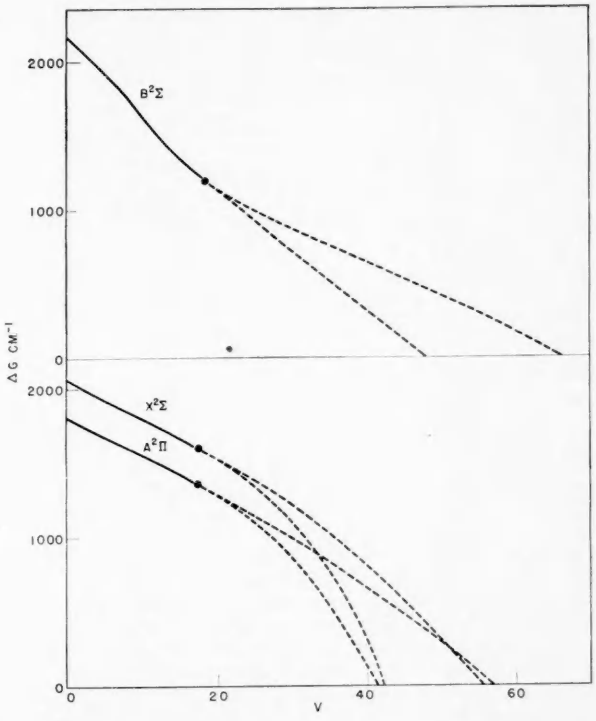

FIG. 4.—Birge-Sponer extrapolations of the observed vibrational quanta of the X, A, and B states. For each state the curves have been extrapolated to give dissociation energies of 66,000 and 56,000 cm^{-1}.

The constants of the six known electronic states of *CN* are given in Table 17. It is worth noting that, whereas the three lower electronic states of *CN* have analogues in each of the molecules of the isoelectronic series *BO*, CO^+ and N_2^+, the three higher states of *CN* are unknown for the other molecules.

It is interesting to inquire what electron configurations of *CN* give rise to the six known states. Since the absence of the B—A transition in the observed spectrum of *CN* seems to show that there still remains sufficient symmetry in the molecule for the *g* and *u* symbols to have some meaning, it appears reasonable to use the same notation for the

CN orbitals as is used for the isoelectronic molecule N_2^+. The following are the electron configuration and the resulting doublet states that may be important for *CN*:

$$KK(\sigma_g 2s)^2(\sigma_u 2s)^2(\pi_u 2p)^4(\sigma_g 2p); \quad X\Sigma_g^+,$$

$$KK(\sigma_g 2s)^2(\sigma_u 2s)^2(\pi_u 2p)^3(\sigma_g 2p)^2; \quad A\Pi_u,$$

$$KK(\sigma_g 2s)^2(\sigma_u 2s)(\pi_u 2p)^4(\sigma_g 2p)^2; \quad B\Sigma_u^+,$$

$$KK(\sigma_g 2s)^2(\sigma_u 2s)^2(\pi_u 2p)^4(\pi_g 2p); \quad \Pi_g,$$

$$KK(\sigma_g 2s)^2(\sigma_u 2s)^2(\pi_u 2p)^3(\sigma_g 2p)(\pi_g 2p); \quad \Sigma_u^+(2);^* \Sigma_u^-(2), \Delta_u(2),$$

$$KK(\sigma_g 2s)^2(\sigma_u 2s)(\pi_u 2p)^4(\sigma_g 2p)(\pi_g 2p); \quad \Pi_u(2).$$

* The (2) indicates that two such states exist.

It has long been assumed and it seems certain that the first three electron configurations give rise to the first three electronic states as indicated. It is not unreasonable to consider that each of the next three electron configurations gives rise to one of the new electronic states. The F state is almost certainly one of the Δ states arising from the fifth configuration. If one assumes that the D state is the Π_g state of the fourth configuration, then the

TABLE 17

CONSTANTS OF THE ELECTRONIC STATES OF *CN* (CM^{-1})

State	T_0	ω_0	$\omega_0\chi_0$	B_0	α	A
$H^2\Pi_r$	60,938.72	.....	.....	1.520	.....	+49.6
$F^2\Delta_r$	59,682.80	.....	.....	1.374	.....	+28.8
$D^2\Pi_i$	53,954.99	995.93	8.78	1.155	0.013	− 3.0
$B^2\Sigma^+$	25,797.84	2143.7	20.2	1.962	.023	.....
$A^2\Pi_i$	9118.02	1799.72	12.61	1.7165	.01716	−52.2
$X^2\Sigma^+$	.....	2055.50	13.114	1.8903	0.01722	.....

D−A transition involves a double electron jump. The D−X transition is, however, forbidden to the extent that the *g* and *u* symbols have a meaning for *CN*, and it is not unreasonable that the D−X and the D−A transition probabilities should be of the same order of magnitude. It is not obvious, however, why this electron configuration should give rise to an inverted Π state with a small *B* value, as is observed for the D state. If one assumes that the H state is one of the Π states arising from the last configuration listed above, then the observed H−B transition is a forbidden one, in so far as the *g* and *u* symbols have meaning. The H−X transition, which might be expected to have a much higher transition probability, would give its strongest bands in the vacuum ultraviolet and has not been observed.

It is to be expected that future work with *CN* will lead to the discovery of additional electronic states. Indeed, the large number of unidentified bands that we have found near 2000 A indicates that an extension of the present work into the vacuum ultraviolet region would show new band systems. On the other hand, it is not at all obvious how one must proceed in order to obtain spectra of *CN* from which the dissociation energy can be derived. It appears that it will be quite difficult to obtain a sufficient extension of the red or violet systems to establish a dissociation limit. Also, it is not at all certain that a sufficient number of perturbations of the B state can be found and analyzed to establish the positions of the high vibrational levels and hence the dissociation limit of the A state. Possibly a somewhat more hopeful approach to the problem would be to study the absorption spectrum of *CN* in the vacuum ultraviolet. It is possible that in this region the

spectrum might show some predissociated bands or a progression of bands leading up to a dissociation limit.

We wish to thank Dr. G. Herzberg for many helpful discussions and to thank Mrs. Ruth Innes for assisting in the calculations.

REFERENCES

Brewer, L., Templeton, L. K., and Jenkins, F. A. 1951, *J. Amer. Chem. Soc.*, **73**, 1462.
Douglas, A. E. 1952, *Canadian J. Phys.*, **30**, 302.
Douglas, A. E., and Routly, P. M. 1954, *Ap. J.*, **119**, 303.
Feast, M. W. 1949, *Proc. Phys. Soc. London, A*, **62**, 121.
Gaydon, A. G. 1953, *Dissociation Energies and Spectra of Diatomic Molecules* (2d ed.; London: Chapman & Hall, Ltd.).
Herzberg, G. 1950, *Spectra of Diatomic Molecules* (2d ed.; New York: D. Van Nostrand Co.).
Herzberg, G., and Phillips, J. G. 1948, *Ap. J.*, **108**, 163.
Heurlinger. 1918, dissertation, University of Lund.
Jenkins, F. A. 1928, *Phys. Rev.*, **31**, 539.
Jenkins, F. A., Roots, Y. K., and Mulliken, R. S. 1932, *Phys. Rev.*, **39**, 16.
Jenkins, F. A., and Wooldridge, D. E. 1938, *Phys. Rev.*, **53**, 137.
Jevons, W. 1926, *Proc. Roy. Soc. London, A*, **112**, 407.
Kayser, H., and Runge, C. 1910, *Handbuch der Spectroscopie* (Leipzig: Hirzel), **5**, 229.
Long, L. H. 1949, *Proc. Roy. Soc. London, A*, **198**, 62.
Parker, A. E. 1932, *Phys. Rev.*, **41**, 274.
Schmid, R., Gerö, L., and Zemplén, J. 1938, *Proc. Phys. Soc. London*, **50**, 283.
Uhler, H. S., and Patterson, R. A. 1915, *Ap. J.*, **42**, 434.

NUMERICAL INTEGRATIONS FOR THE STELLAR INTERIOR

R. HÄRM AND M. SCHWARZSCHILD*
Princeton University Observatory
Received November 3, 1954

ABSTRACT

Fifteen families of integrations for the stellar interior are tabulated.

I. INTRODUCTION

During the last three years a number of solutions of the differential equations for the stellar interior have been obtained by numerical integration at the Princeton Observatory. The integrations were performed in each case with a specific problem in mind. The problems in question each involved not just one particular stellar model but rather whole families of models, and, correspondingly, the solutions are not individual eigen solutions but rather families of solutions characterized by one or more parameters. Owing to this more general nature of the integrations, they can be—and have already been—applied to a variety of problems beyond their original purpose. It is for this reason that they are now being published.

It seems not unlikely that in the future much of the numerical work in the theory of the stellar interior will be done on large electronic computers. It may well be that the computers will be coded to derive the eigen solution for a specific problem *ab initio* without reference to any previous computations. But even in this case, experience seems to indicate that it will be necessary to orient one's self regarding the physical processes likely to be encountered, the ranges covered by the variables, and the general behavior of the solutions before such a problem can be efficiently put on a large computer. It is felt that for purposes of such orientation the integrations published here may be sufficiently general and thus may continue to be useful.

Of the fifteen families of integrations which are included in the present tabulation, the first thirteen were computed at this Observatory with desk calculators, the fourteenth was obtained by G. W. Wares at the Yerkes Observatory, and the last, large family was integrated with the electronic computer of the Institute for Advanced Study. None of the tabulated integrations covers an entire star from the center to the surface. Rather, each family covers only a region, either the envelope or an intermediate zone or the core. Hence, by combining various integrations, complete stellar models can be constructed.

In these integrations radiation pressure has generally been neglected (except in Family 2), degeneracy has been ignored (except in Family 14), the chemical composition has been taken as constant throughout the region covered (except in Families 8 and 9), radiative equilibrium has been applied (except in Families 13, 14, and 15), and no energy sources have been included (except in Families 3, 10, 11, and 12).

The integrations were performed in terms of logarithmic variables, since these have a great practical advantage because of the structure of the differential equations here in question. Thus the dependent variable is

$$y = \log x = \log\left(\frac{r}{r_0}\right) \quad \text{or} \quad z = \log\left(\frac{1}{x} - 1\right) = \log\left(\frac{r_0 - r}{r}\right),$$

* This research was supported in part by funds of the Eugene Higgins Trust allocated to Princeton University.

where y is generally used for cores and intermediate zones and z for envelopes, and the dependent variables are

$$\psi = \log q = \log\left(\frac{M_r}{M_{r_0}}\right), \qquad \tau = \log t = \log\left(\frac{T}{T_0}\right),$$

$$\lambda = \log p = \log\left(\frac{P}{P_0}\right), \qquad \phi = \log f = \log\left(\frac{L_r}{L_{r_0}}\right).$$

The quantities designated by a zero subscript are free constants which may be chosen partly so as to eliminate the constants in some or all of the differential equations and partly so as to normalize the starting values.

The main characteristics of the 15 families of integrations are given in the accompanying table.

Family	Region	Opacity	Remarks
1	Envelope	Kramers' opacity	.....
2	Envelope	Kramers' opacity + electron scattering	With radiative pressure
3	Envelope	Modified Kramers' opacity	Proton-proton source
4	Envelope extension	Electron scattering	Attached to Family 1
5	Intermediate zone	Kramers' opacity	Attached to convective core
6	Intermediate zone	Electron scattering	Attached to convective core
7	Intermediate zone	Modified Kramers' opacity	Attached to convective core
8	Intermediate zone	Kramers' opacity	Variable composition
9	Intermediate zone	Kramers' opacity	Variable composition
10	Radiative core	Modified Kramers' opacity	Proton-proton source
11	Contracting core	Modified Kramers' opacity	Gravitation energy source
12	Contracting core	Electron scattering	Gravitation energy source
13	Intermediate zone	.....	Isothermal, nondegenerate
14	Exhausted core	.....	Isothermal, partially degenerate
15	Convective envelope	.....	Adiabatic

The following references contain tables of integrations for the stellar interior published in the past: envelopes with Kramers' opacity, Strömgren (1931); envelopes with modified Kramers' opacity, Williamson and Duff (1948), Richardson and Schwarzschild (1948), and Epstein (1950); intermediate zones attached to a convective core, with modified Kramers' opacity, Li Hen and Schwarzschild (1949); convective core (polytrope $n = 1.5$), Comrie (1932); completely degenerate cores, Chandrasekhar (1938); isothermal nondegenerate core, Wares and Chandrasekhar (1949). This list of references is not complete and essentially contains those published integrations which have already been used in connection with the integration families here tabulated.

II. EQUATIONS AND CONDITIONS

Here are listed for each family of integrations the differential equations and initial conditions used. The reference at the start of each family gives the paper in which the corresponding integrations were first used.

Family 1.—Oke and Schwarzschild (1952). Envelopes. Kramers' opacity. No energy source.

Differential equations:

$$\log\left(-\frac{d\psi}{dz}\right) = -\psi - \tau + \lambda + 4y + z\,, \tag{1}$$

$$\log\left(+\frac{d\tau}{dz}\right) = -9.5\tau + 2\lambda + z + \log C\,, \tag{2}$$

$$\log\left(+\frac{d\lambda}{dz}\right) = +\psi - \tau + z\,. \tag{3}$$

Initial conditions:

$$q = 1\,, \quad t = 0\,, \quad p = 0 \quad \text{at} \quad x = 1\,.$$

Starting values near surface:

$$q = 1\,, \quad t = \frac{1}{4.25}\left(\frac{1}{x} - 1\right), \quad p = (4.25\,C)^{-1/2} t^{4.25}\,. \tag{4}$$

Parameter:

log C listed in Table 1.

TABLE 1

CONSTANTS FOR FAMILY 1

Int.	log C	Int.	log C	Int.	log C	Int.	log C
1.1.....	−1.0	1.5.....	−4.0	1.9.....	−5.5	1.13.....	−5.9
1.2.....	−2.0	1.5	−4.5	1.10.....	−5.6	1.14.....	−6.0
1.3.....	−3.0	1.7.....	−5.0	1.11.....	−5.7	1.15.....	−6.5
1.4.....	−3.5	1.8.....	−5.25	1.12.....	−5.8	1.16.....	−7.0

Family 2.—Envelopes. No energy source. Kramers' opacity plus electron scattering (δ = total opacity divided by Kramers' opacity). Radiation pressure included (β = gas pressure divided by total pressure).

Differential equations:

$$\log\left(-\frac{d\psi}{dz}\right) = -\psi - \tau + \lambda + 4y + z + \log\beta\,, \tag{5}$$

$$\log\left(+\frac{d\tau}{dz}\right) = -9.5\tau + 2\lambda + z + 2\log\beta + \log\delta + \log C\,, \tag{6}$$

$$\log\left(+\frac{d\lambda}{dz}\right) = +\psi - \tau + z + \log\beta\,, \tag{7}$$

with

$$\log(1-\beta) = +4\tau - \lambda + \log B \tag{8}$$

and

$$\log(\delta - 1) = +0.5\tau + \log(1-\beta) - \log\beta + \log A\,. \tag{9}$$

Initial conditions:

$$q = 1\,, \quad t = 0\,, \quad p = 0 \quad \text{at} \quad x = 1\,.$$

Starting values near surface (based on $\delta \propto t^{\epsilon}$ and $\beta \propto t^{\zeta}$ near surface):

$$q = 1\,, \qquad t = \frac{2\,(1-\zeta)}{8.5-\epsilon-\zeta}\,\beta\left(\frac{1}{x}-1\right), \qquad p = \left(\frac{8.5-\epsilon-\zeta}{2}\,\delta\beta C\right)^{-1/2} t^{4.25} \tag{10}$$

with β, δ, ϵ, ζ solved from

$$(1-\beta)^2 = B^2C\left(\frac{8.5-\epsilon-\zeta}{2}\right)^{3/2}(1-\zeta)^{-1/2}\beta^{1/2}\left(\frac{1}{x}-1\right)^{-1/2} + AB^2C\,\frac{8.5-\epsilon-\zeta}{2}\,(1-\beta)\,,$$

$$\delta = 1 + A\,(1-\beta)\left[\frac{1}{\beta}\,\frac{2\,(1-\zeta)}{8.5-\epsilon-\zeta}\left(\frac{1}{x}-1\right)\right]^{1/2}, \tag{11}$$

$$\zeta = \frac{1}{2}\,\frac{1-\beta}{1+\beta\delta} \qquad \text{and} \qquad \epsilon = \frac{\beta}{2}\,\frac{\delta-1}{1+\beta\delta}\,.$$

Parameters:
$\log A$, $\log B$, $\log C$, listed in Table 2.

TABLE 2

CONSTANTS FOR FAMILY 2

Int.	log A	log B	log C	Int.	log A	log B	log C
2.1.....	+1.5	0.0	−3.0	2.3.....	0.0	+1.0	−5.0
2.2.....	+1.5	+1.0	−5.0	2.4.....	+1.5	+2.0	−7.0

Family 3.—Osterbrock (1953). Envelopes. Modified Kramers' opacity ($\kappa \propto \rho^{0.5}T^{-3.5}$). Energy source from proton-proton reaction ($\epsilon \propto \rho T^{4.5}$).

Differential equations:

Equations (1) and (3),

$$\log\left(+\frac{d\tau}{dz}\right) = -9.0\tau + 1.5\lambda + \phi + z + \log C\,, \tag{12}$$

$$\log\left(-\frac{d\phi}{dz}\right) = +2.5\tau + 2\lambda - \phi + 4y + z + \log D\,. \tag{13}$$

Initial conditions:

$$q = 1\,, \qquad t = 0\,, \qquad p = 0\,, \qquad f = 1 \qquad \text{at} \qquad x = 1\,.$$

Starting values near surface:

$$q = 1\,, \qquad t = \frac{3}{16}\left(\frac{1}{x}-1\right), \qquad p = (\tfrac{16}{3}C)^{-2/3}t^{16/3}\,, \qquad f = 1\,. \tag{14}$$

Parameters:

For integration 3.1: $\log C = -4.6453\,,$ $\log D = -3.1556;$

For integration 3.2: $\log C = -4.7\,,$ $\log D = -3.07\,.$

Family 4.—Sandage and Schwarzschild (1952). Envelope extensions, attached to Family 1. Electron scattering. No energy source.

Differential equations:

Equations (1) and (3),

$$\log\left(+\frac{d\tau}{dz}\right) = -5\tau + \lambda + z + \log C_{\mathrm{El}}\,. \tag{15}$$

Initial conditions:

q, t, and p continuous at x_s (or z_s), where the envelope with Kramers' opacity (Family 1) is terminated and the extension with electron scattering (this family) is started; an integration of this family is therefore characterized by two parameters, log C, indicating the envelope to which it is attached, and z_s, indicating the point on the envelope at which it is attached. The parameter in equation (15) is then fixed by

$$C_{\mathrm{El}} = p_s t_s^{-4.5} C\,, \tag{16}$$

which follows from the condition of continuity of the opacity (or of $d\tau/dz$) at z_s.

Starting values:

Read from Family 1 according to log C and z_s values.

Parameters:

log C, z_s, log C_{El} listed in Table 3.

TABLE 3

CONSTANTS FOR FAMILY 4

Int.	log C_{Kr}	z_s	log C_{El}	Int.	log C_{Kr}	z_s	log C_{El}
4.1	−2.0	+1.0	−1.4150	4.19	−4.5	−0.2	−2.3578
4.2	−2.0	+1.8	−1.6340	4.20	−4.5	+0.6	−2.6003
4.3	−2.0	+2.6	−1.8564	4.21	−4.5	+1.4	−2.9322
4.4	−2.0	+3.4	−2.0773	4.22	−4.5	+2.2	−3.1583
4.5	−3.0	+0.2	−1.7086	4.23	−5.0	−0.6	−2.5072
4.6	−3.0	+1.0	−1.9312	4.24	−5.0	+0.2	−2.7217
4.7	−3.0	+1.8	−2.1770	4.25	−5.0	+1.0	−3.0848
4.8	−3.0	+2.6	−2.4090	4.26	−5.0	+1.8	−3.3698
4.9	−3.5	−0.2	−1.8573	4.27	−5.25	0.0	−2.7885
4.10	−3.5	+0.6	−2.0713	4.28	−5.25	+0.8	−3.1404
4.11	−3.5	+1.4	−2.3333	4.29	−5.25	+1.6	−3.4903
4.12	−3.5	+2.2	−2.5799				
4.13	−3.5	+3.0	−2.7972	4.30	−5.5	+0.6	−3.1809
				4.31	−5.5	+1.4	−3.6181
4.14	−4.0	−0.6	−2.0071				
4.15	−4.0	+0.2	−2.2118	4.32	−5.7	+0.44	−3.2076
4.16	−4.0	+1.0	−2.4762	4.33	−5.7	+1.24	−3.7165
4.17	−4.0	+1.8	−2.7557				
4.18	−4.0	+2.6	−2.9719				

Family 5.—Oke and Schwarzschild (1952). Intermediate zones, attached to convective core. Kramers' opacity. No energy source.

Differential equations:

$$\log\left(+\frac{d\psi}{dy}\right) = -\psi - \tau + \lambda + 3y\,, \tag{17}$$

$$\log\left(-\frac{d\tau}{dy}\right) = -9.5\tau + 2\lambda - y\,, \tag{18}$$

$$\log\left(-\frac{d\lambda}{dy}\right) = +\psi - \tau - y\,. \tag{19}$$

Initial conditions:

U, V, and $(n+1)$ continuous at x_1 (or ξ_1 in terms of Emden's independent variable), where the convective core (Comrie 1932) is terminated and the intermediate zone (this family) is started. Furthermore, $x_1 = 1$.

Starting values:

$$\begin{aligned} y_1 &= 0\,, \\ \psi_1 &= \frac{2}{5.5}\log U_1 + \frac{6.5}{5.5}\log V_1 + \frac{1}{5.5}\log(n+1)_1\,, \\ \tau_1 &= \frac{2}{5.5}\log U_1 + \frac{1}{5.5}\log V_1 + \frac{1}{5.5}\log(n+1)_1\,, \\ \lambda_1 &= \frac{9.5}{5.5}\log U_1 + \frac{7.5}{5.5}\log V_1 + \frac{2}{5.5}\log(n+1)_1\,, \end{aligned} \tag{20}$$

with U_1 and V_1 read from the convective core at ξ_1, and $(n+1)_1 = 2.5$. Integration 5.5 is not started directly at the convective core but farther out, by interpolation between neighboring integrations.

Parameter:

ξ_1 listed in Table 4.

TABLE 4

CONSTANTS FOR FAMILIES 5, 6, AND 7

Int.	ξ_1	Int.	ξ_1	Int.	ξ_1
5.1	1.194	6.1	1.30	7.1	1.12012
5.2	1.193	6.2	1.55	7.2	1.120093
5.3	1.19250	6.3	1.565		
5.4	1.19232	6.4	1.570		
5.5	1.192309	6.5	1.575		
5.6	1.192304	6.6	1.580		
5.7	1.19200	6.7	1.585		
5.8	1.188				

Family 6.—Hoyle and Schwarzschild (1955). Intermediate zones, attached to convective core. Electron scattering. No energy source.

Differential equations:

Equations (17) and (19),

$$\log\left(-\frac{d\tau}{dy}\right) = -5\tau + \lambda - y\,. \tag{21}$$

Initial conditions:
As for Family 5.

Starting values:

$$\begin{aligned} y_1 &= 0\,, \\ \psi_1 &= \tfrac{1}{3}\log U_1 + \log V_1 + \tfrac{1}{3}\log(n+1)_1\,, \\ \tau_1 &= \tfrac{1}{3}\log U_1 + \tfrac{1}{3}\log(n+1)_1\,, \\ \lambda_1 &= \tfrac{5}{3}\log U_1 + \log V_1 + \tfrac{2}{3}\log(n+1)_1\,, \end{aligned} \tag{22}$$

with U_1 and V_1 read from the convective core at ξ_1 and $(n+1)_1 = 2.5$.

Parameter:
ξ_1 listed in Table 4.

Family 7.—Oke and Schwarzschild (1952). Intermediate zones, attached to convective core. Modified Kramers' opacity ($\kappa \propto \rho^{0.75}T^{-3.5}$). No energy source.

Differential equations:

Equations (17) and (19),

$$\log\left(-\frac{d\tau}{dy}\right) = -9.25\tau + 1.75\lambda - y\,. \tag{23}$$

Initial conditions:
As for Family 5.

Starting values:
By interpolation between neighboring integrations of this family which have already been published (Li Hen and Schwarzschild 1949) and of which the present integrations are an extension.

Parameter:
ξ_1 listed in Table 4.

Family 8.—Härm and Schwarzschild (1955). Intermediate zones with variable composition (mean molecular weight $\propto q^{-\nu}$, coefficient of opacity $\propto q^{+0.7\nu}$), attached to convective core. Kramers' opacity. No energy source.

Differential equations:

$$\log\left(+\frac{d\psi}{dy}\right) = -(1+\nu)\psi - \tau + \lambda + 3y\,, \tag{24}$$

$$\log\left(-\frac{d\tau}{dy}\right) = -1.3\nu\psi - 9.5\tau + 2\lambda - y\,, \tag{25}$$

$$\log\left(-\frac{d\lambda}{dy}\right) = +(1-\nu)\psi - \tau - y\,. \tag{26}$$

Initial conditions:
As for Family 5.

Starting values:

$$y_1 = 0\,,$$

$$\psi_1 = \frac{1}{5.5 - 8.2\nu}\,[2\,\log U_1 + 6.5\,\log V_1 + \log\,(n+1)_1]\,,$$

$$\tau_1 = \frac{1-\nu}{5.5 - 8.2\nu}\left[2\,\log U_1 + \frac{1+1.7\nu}{1-\nu}\,\log V_1 + \log\,(n+1)_1\right], \tag{27}$$

$$\lambda_1 = \frac{1}{5.5 - 8.2\nu}\,[\,(9.5 - 8.2\nu)\,\log U_1 + (7.5 + 8.2\nu)\,\log V_1 + 2\,\log\,(n+1)_1]\,,$$

with U_1 and V_1 read from the convective core at ξ_1, and $(n+1)_1 = 2.5$. Integration 8.7 is a backward integration as described in Section III.

Parameters:

ν and ξ_1 listed in Table 5.

TABLE 5

CONSTANTS FOR FAMILY 8

Int.	ν	ξ_1	Int.	ν	ξ_1
8.1.....	1.0	1.40	8.5.....	0.4	1.294490
8.2.....	1.0	1.43	8.6.....	0.4	1.294495
8.3.....	0.5	1.318	8.7.....	0.38	1.2895943
8.4.....	0.5	1.319			

Family 9.—Härm and Schwarzschild (1955). Intermediate zones with variable composition (mean molecular weight $\propto q^{-\nu}$, coefficient of opacity $\propto q^{+0.7\nu}$), attached to isothermal core. Kramers' opacity. No energy sources.

Differential equations:

Equations (24), (25), and (26).

Initial conditions:

U_1 and V_1 continuous at x_1 (or ξ_1 in terms of Emden's independent variable), where the isothermal core (Wares and Chandrasekhar 1949) is terminated and the intermediate zone (this family) is started. The choice of $(n+1)_1$ is arbitrary, corresponding to a shell source of arbitrary strength at the interface. Furthermore, $x_1 = 1$.

Starting values:

Equations (27), with U_1 and V_1 read from the isothermal core at ξ_1. Integrations 9.3–9.6 are backward integrations, as described in Section III.

Parameters:

ν, ξ_1, and $(n+1)_1$ listed in Table 6.

TABLE 6

CONSTANTS FOR FAMILY 9

Int.	ν	ξ_1	$(n+1)_1$	Int.	ν	ξ_1	$(n+1)_1$
9.1.....	1.0	9.0	3.402	9.4.....	0.49	9.0	3.511750422238
9.2.....	1.0	9.0	3.404	9.5.....	0.50	25.0	3.4882655
9.3.....	0.50	9.0	3.509650329	9.6.....	0.42	25.0	3.5059384945

Family 10.—Osterbrock (1953). Radiative cores. Modified Kramers' opacity ($\kappa \propto \rho^{0.5}T^{-3.5}$). Energy source from proton-proton reaction ($\epsilon \propto \rho T^{4.5}$).

Differential equations:

Equations (17) and (19),

$$\log\left(-\frac{d\tau}{dy}\right) = -9.0\tau + 1.5\lambda + \phi - y\,, \tag{28}$$

$$\log\left(+\frac{d\phi}{dy}\right) = +2.5\tau + 2\lambda - \phi + 3y\,. \tag{29}$$

Initial conditions:

$$q = 0\,, \quad t = 1\,, \quad f = 0 \quad \text{at} \quad x = 0\,.$$

Starting values near center:

$$\begin{aligned} q &= \tfrac{1}{3}p_c x^3 - \tfrac{1}{30}p_c^2(1 - p_c^{2.5})\,x^5 + \tfrac{1}{2520}p_c^3(8 - 31.5p_c^{2.5} + 42.5p_c^5)\,x^7\,, \\ t &= 1 - \tfrac{1}{6}p_c^{3.5}x^2 + \tfrac{1}{360}p_c^{4.5}(13.5 - 32.5p_c^{2.5})\,x^4\,, \\ p &= p_c - \tfrac{1}{6}p_c^2 x^2 + \tfrac{1}{45}p_c^3(1 - p_c^{2.5})\,x^4\,, \\ f &= \tfrac{1}{3}p_c^2 x^3 - \tfrac{1}{30}p_c^3(2 + 2.5p_c^{2.5})\,x^5 + \tfrac{1}{2520}p_c^4(26 + 67.75p_c^{2.5} - 62.5p_c^5)\,x^7\,. \end{aligned} \tag{30}$$

Only integrations 10.1, 10.2, 10.7, and 10.15 are directly started near the center with these values. All other integrations are started, successively, farther out, by interpolation between neighboring integrations.

Parameter:

$(n+1)_c = p_c^{-2.5}$ listed in Table 7.

TABLE 7

CONSTANTS FOR FAMILY 10

Int.	$(n+1)_c$	Int.	$(n+1)_c$	Int.	$(n+1)_c$
10.1	3.00	10.6	3.1376	10.11	3.140425
10.2	3.10	10.7	3.14	10.12	3.14043
10.3	3.1133	10.8	3.1403	10.13	3.1405
10.4	3.126666	10.9	3.14036	10.14	3.1415
10.5	3.134	10.10	3.14041	10.15	3.20

Family 11.—Sandage and Schwarzschild (1952). Contracting cores. Modified Kramers' opacity ($\kappa \propto \rho^{0.75}T^{-3.5}$). Gravitational energy source (ϵ = Const., i.e., $L_r \propto M_r$).

Differential equations:

Equations (17) and (19),

$$\log\left(-\frac{d\tau}{dy}\right) = \psi - 9.25\tau + 1.75\lambda - y + \log C\,. \tag{31}$$

Initial conditions:

$$q = 0 \qquad t = 1\,, \quad p = 1 \quad \text{at} \quad x = 0\,.$$

Starting values near center:

$$q = \tfrac{1}{3}x^3 - \tfrac{1}{30}(1-C)\,x^5 + \tfrac{1}{2520}(8 - 29.75C + 54.25C^2)\,x^7,$$

$$t = 1 - \tfrac{1}{6}Cx^2 + \tfrac{1}{360}C(11.75 - 44.25C)\,x^4, \tag{32}$$

$$p = 1 - \tfrac{1}{6}x^2 + \tfrac{1}{45}(1-C)\,x^4.$$

Only integrations 11.1, 11.2, and 11.8 are directly started near the center with these values. All other integrations are started, successively, farther out, by interpolation between neighboring integrations.

Parameter:
C listed in Table 8.

TABLE 8

CONSTANTS FOR FAMILY 11

Int.	C	Int.	C	Int.	C
11.1	0.175	11.5	0.212117569	11.9	0.21212120848
11.2	0.2109	11.6	0.2121208478	11.10	0.2121210907
11.3	0.21175695	11.7	0.2121211757		
11.4	0.212084786	11.8	0.21212121		

Family 12.—Sandage and Schwarzschild (1952). Contracting cores. Electron scattering. Gravitational energy source (ϵ = Const., i.e., $L_r \propto M_r$).

Differential equations:

Equations (17) and (19),

$$\log\left(-\frac{d\tau}{dy}\right) = +\psi - 5\tau + \lambda - y + \log C. \tag{33}$$

Initial conditions:

$$q = 0, \quad t = 1, \quad p = 1 \quad \text{at} \quad x = 0.$$

Starting values near center:

$$q = \tfrac{1}{3}x^3 - \tfrac{1}{30}(1-C)\,x^5 + \tfrac{1}{2520}(8 - 26C + 33C^2)\,x^7,$$

$$t = 1 - \tfrac{1}{6}Cx^2 + \tfrac{1}{360}C(8 - 23C)\,x^4, \tag{34}$$

$$p = 1 - \tfrac{1}{6}x^2 + \tfrac{1}{45}(1-C)\,x^4.$$

Only integrations 12.1, 12.2, and 12.9 are directly started near the center with these values. All other integrations are started, successively, farther out, by interpolation between neighboring integrations.

Parameter:
C listed in Table 9.

TABLE 9

CONSTANTS FOR FAMILY 12

Int.	C	Int.	C	Int.	C
12.1	0.20	12.4	0.248702	12.7	0.2498945
12.2	0.23	12.5	0.2495673	12.8	0.2499472
12.3	0.245872	12.6	0.2497879	12.9	0.25

Family 13.—Intermediate zones. Isothermal.

Differential equations:
Equations (17) and (19) with $\tau = \text{Const.}$

Initial conditions:

$$x = 1\,, \qquad q = 1 \qquad \text{at} \qquad U = 1\,.$$

Starting values:

$$y_1 = 0\,, \qquad \psi_1 = 0\,, \qquad \lambda_1 = \tau\,.$$

Integrations 13.1–13.5 are integrated forward and backward from the starting point at $U = 1$. They are tabulated, however, in order of continuously increasing x.

Parameter:
τ listed in Table 10.

TABLE 10

CONSTANTS FOR FAMILY 13

Int.	τ	Int.	τ	Int.	τ
13.1	−0.5	13.4	−0.8	13.7	−1.1
13.2	−0.6	13.5	−0.9	13.8	−1.2
13.3	−0.7	13.6	−1.0	13.9	−1.3

Family 14.—Wares (1944). Partially degenerate cores. Isothermal.

Differential equations, etc.:
See Wares (1944), particularly his equations (4) and (39).

Homology invariants:

$$U = F_{1/2}(\psi)\,\xi\left(-\frac{d\psi}{d\xi}\right)^{-1}, \qquad V = \tfrac{3}{2}F_{1/2}(\psi)\,F_{3/2}^{-1}(\psi)\,\xi\left(-\frac{d\psi}{d\xi}\right). \tag{35}$$

Initial conditions:

$$\psi = \psi_0\,, \qquad \frac{d\psi}{d\xi} = 0 \qquad \text{at} \qquad \xi = 0\,.$$

Starting values near center:

$$\psi = \psi_0 - \tfrac{1}{6}F_{1/2}(\psi_0)\,\xi^2 + \ldots\,. \tag{36}$$

Parameter:
ψ_0 listed in first line of tabulation of each integration.

Family 15.—Osterbrock (1953). Envelopes. Adiabatic.

Differential equations:
Equations (17) and (19), with τ given by

$$\lambda = 2.5\tau + \log E\,. \tag{37}$$

Initial conditions:

$$q = 1\,, \quad t = 0\,, \quad p = 0 \quad \text{at} \quad x = 1\,.$$

Starting values near surface:

$$q = 1\,, \quad t = \frac{1}{2.5}\left(\frac{1}{x} - 1\right), \quad p = Et^{2.5}\,. \tag{38}$$

Parameter:
E listed in Table 11.

TABLE 11

CONSTANTS FOR FAMILY 15

Int.	E	Int.	E	Int.	E	Int.	E
15.01	0.1	15.11	5.0	15.21	15.0	15.31	34.0
15.02	0.2	15.12	6.0	15.22	16.0	15.32	36.0
15.03	0.3	15.13	7.0	15.23	18.0	15.33	38.0
15.04	0.5	15.14	8.0	15.24	20.0	15.34	40.0
15.05	0.75	15.15	9.0	15.25	22.0	15.35	42.0
15.06	1.0	15.16	10.0	15.26	24.0	15.36	44.0
15.07	1.5	15.17	11.0	15.27	26.0	15.37	46.0
15.08	2.0	15.18	12.0	15.28	28.0		
15.09	3.0	15.19	13.0	15.29	30.0		
15.10	4.0	15.20	14.0	15.30	32.0		

III. NUMERICAL METHODS

The first thirteen integration families were obtained with the use of desk calculators. The integration scheme used is given by

$$g(z+\Delta) = g(z) + \Delta \cdot g'(z) + \tfrac{1}{2}{}^{1}D(z+\tfrac{1}{2}\Delta) - \tfrac{1}{12}{}^{2}D(z) - \tfrac{1}{24}{}^{3}D(z-\tfrac{1}{2}\Delta)\,.$$

Here g stands for any of the dependent variables and g' stands for its derivative as given by the differential equations. The D's stand for the successive differences of $\Delta \cdot g'$. The last three terms in this equation are initially obtained at every step from a forward guess. This guess is checked by computing $\Delta \cdot g'(z+\Delta)$ with the help of the differential equation from the value of $g(z+\Delta)$ obtained from the foregoing equation. Then the necessary D-values can be computed. If they do not check with the guessed values within two units of the last digit, the cycle is repeated. With some experience, the forward guessing can be done sufficiently accurately so that repetition of the cycle is necessary in perhaps only one-third of the steps. The whole procedure of one integration step has, of course, to be done simultaneously for all the dependent variables.

For these thirteen families the step length, Δ, was chosen so that the fourth difference had no influence on the integration formula and so that forward guessing of the lower differences was reasonably easy. All integration steps executed are reproduced in the following tabulations. The integrations were performed with one more digit than is given in the tabulations. The integrations of Families 1–13 are approximately equivalent to the work of one man during one year.

The last family of integrations was obtained with the electronic computer of the Institute for Advanced Study. The integration scheme here used is given by

$$g^*(z+\Delta) = g(z) + \Delta \cdot g'(z),$$

$$g(z+\Delta) = g(z) + \Delta \cdot \tfrac{1}{2}[g'(z) + g^{*\prime}(z+\Delta)].$$

Here g^*, given by the first formula, represents a preliminary value which is used only to obtain the $g^{*\prime}$-value needed in the second formula. Only every fifth step was read out of the computer. Correspondingly, the actual step values used are five times smaller than those appearing in the present tabulation. The computer carried approximately ten decimals in all the dependent variables.

Inward integrations of the differential equations for the stellar interior show a comfortable stability, while outward integrations show a well-known instability. A family of outward integrations characterized by one parameter will generally have only a very narrow range in the parameter for which integrations can be carried outward over long distances with the polytropic index behaving properly. At one end of this range the corresponding integrations will show, after some distance, a strong drop in the polytropic index, with consequent convective instability, while on the other end of the range the corresponding integrations show, after some distance, a rapid increase in the polytropic index, approaching isothermal conditions. This instability is particularly strong when Kramers' opacity, with its high temperature sensitivity, is used. An example of this instability is shown by the intermediate zones represented in Figure 1 of Li Hen and Schwarzschild (1949). If long outward integrations with radiative equilibrium are needed, it is not practicable to proceed directly, since a very large number of digits would have to be carried in the first portion of such an integration in order to retain any accuracy in the last portion of the integration. However, such integrations can be obtained by the following scheme without increasing the necessary labor too seriously. Three (or more) integrations corresponding to three values of the parameter are started at the initial conditions in the usual way and are carried forward until the two outer ones show indications that the polytropic index is commencing rapid changes toward small and large values, respectively. Here the three integrations are terminated, and three new integrations, corresponding to three new parameter values, are started by interpolation between the terminal values of the original three integrations. The parameter values for the new integrations are so chosen as to straddle that value which appears to give the best-behaved polytropic index. Then the three new integrations are carried forward, and the whole procedure is repeated as often as necessary. By such successive interpolations, parameter values are obtained with very many digits. This large number of digits indicates only the accuracy relative to the parameter values of neighboring solutions but not the absolute accuracy, which is, of course, much lower.

If such a particular problem involves a terminal condition, the solution fulfilling this terminal condition can be obtained by interpolating between the last three integrations. To obtain the complete run of such a final solution without a large amount of interpolation between the successive sets of three integrations, one may once more cover the entire range by a backward integration from the terminal point to the initial point—which, at the same time, is a thorough check of the entire computation.

IV. ACKNOWLEDGMENTS

Two-thirds of the integrations of the first 13 families were performed by the first author, and the remainder by G. Field, Miss E. Gertlein, B. Oke, D. Osterbrock, I. Rabinowitz, Mrs. M. Reeves, A. Sandage, and Mrs. E. V. Tershune.

Family 14 had been integrated by G. Wares, at the Yerkes Observatory, in 1944 but

had not been published then. It is now published here by arrangement with Dr. S. Chandrasekhar.

The large Family 15 was integrated with the electronic computer of the Institute for Advanced Study. The form in which the equations were used in the machine integration was suggested by Dr. J. von Neumann, the basic coding was laid out by Dr. H. Goldstein, while Mrs. H. Selberg performed the final coding and supervised the actual computations.

Family 15 was printed, directly from punched cards, at the Watson Scientific Computing Laboratory by the permission of Dr. W. Eckert, with Miss R. Jones arranging and guiding the work.

The work at this Observatory was sponsored in part by the Office of Naval Research under Contract No. N9onr-86500, Authority No. NR 010-019/4-5-49. The work at the Institute for Advanced Study was sponsored by the Office of Naval Research under Contract No. N-7-ONR-388, Task Order I, and the Ordnance Corps of the United States Army under Contract No. DA-36-034-ORD-1023-RD.

We acknowledge with sincere gratitude the valuable help that we have received in this work from all those mentioned above.

V. TABULATION OF INTEGRATIONS

In the following tabulation each integration is characterized by a number which consists of the family number in front of the decimal point and the individual integration number after the decimal point. The column headings have the following meanings:

(1) $y = \log x$,

(2) $z = \log\left(\frac{1}{x} - 1\right)$,

(3) $+\psi = +\log q$,

(4) $-\psi = -\log q$,

(5) $\tau = \log t$,

(6) $\lambda = \log p$,

(7) $U = +\frac{d\psi}{dy}$,

(8) $V = -\frac{d\lambda}{dy}$,

(9) $n + 1 = \frac{d\lambda}{d\tau}$,

(10) β,

(11) δ,

(12) $\phi = \log f$,

(13) $W = \frac{d\phi}{dy}$,

(14) ξ,

(15) ψ,

(16) $F_{1/2}(\psi)$,

(17) $-\xi^2 \frac{d\psi}{d\xi}$,

(18) $\frac{2}{3}F_{3/2}(\psi)$.

REFERENCES

Chandrasekhar, S. 1938, *Stellar Structure* (Chicago: University of Chicago Press).
Comrie, L. J. 1932, *Brit. A. Adv. Sci., Math. Tables*, Vol. **2.**
Epstein, I. 1950, *Ap. J.*, **112**, 6.
Härm, R., and Schwarzschild, M. 1955, *Ap. J.*, Vol. **121** (in press).
Hoyle, F., and Schwarzschild, M. 1955 (in preparation).
Li Hen, and Schwarzschild, M. 1949, *M.N.*, **109**, 632.
Oke, J. B., and Schwarzschild, M. 1952, *Ap. J.*, **116**, 317.
Osterbrock, D. E. 1953, *Ap. J.*, **118**, 529.
Richardson, R. S., and Schwarzschild, M. 1948, *Ap. J.*, **108**, 373.
Sandage, A. R., and Schwarzschild, M. 1952, *Ap. J.*, **116**, 463.
Strömgren, B. 1931, *Zs. f. Ap.*, **2**, 345.
Wares, G. W. 1944, *Ap. J.*, **100**, 158.
Wares, G. W., and Chandrasekhar, S. 1949, *Ap. J.*, **109**, 551.
Williamson, R. E., and Duff, G. F. D. 1948, *M.N.*, **109**, 46.

1.1

(2)	(4)	(5)	(5)	(7)	(8)	(9)
-1.00	+0.0000	-1.62839	- 6.7348	0.000	46.750	4.250
-0.95	+0.0000	-1.57839	- 6.5224	0.000	42.128	4.250
-0.90	+0.0000	-1.52839	- 6.3098	0.000	38.009	4.250
-0.85	+0.0000	-1.47839	- 6.0974	0.000	34.338	4.250
-0.80	+0.0000	-1.42839	- 5.8848	0.000	31.066	4.250
-0.75	+0.0000	-1.37839	- 5.6724	0.000	28.149	4.250
-0.70	+0.0000	-1.32839	- 5.4598	0.000	25.551	4.250
-0.65	+0.0000	-1.27839	- 5.2474	0.000	23.234	4.250
-0.60	+0.0000	-1.22839	- 5.0348	0.000	21.170	4.250
-0.55	+0.0000	-1.17839	- 4.8224	0.000	19.330	4.250
-0.50	+0.0000	-1.12839	- 4.6098	0.000	17.690	4.250
-0.45	+0.0000	-1.07839	- 4.3974	0.000	16.228	4.250
-0.40	+0.0000	-1.02839	- 4.1848	0.000	14.926	4.250
-0.35	+0.0000	-0.97839	- 3.9724	0.001	13.765	4.250
-0.30	+0.0000	-0.92839	- 3.7598	0.001	12.729	4.250
-0.25	+0.0000	-0.87839	- 3.5474	0.001	11.807	4.250
-0.20	+0.0000	-0.82839	- 3.3348	0.001	10.985	4.250
-0.15	+0.0001	-0.77840	- 3.1224	0.001	10.252	4.250
-0.10	+0.0001	-0.72840	- 2.9099	0.001	9.599	4.250
-0.05	+0.0001	-0.67841	- 2.6975	0.001	9.016	4.250
0.00	+0.0001	-0.62841	- 2.4850	0.002	8.498	4.250
+0.05	+0.0002	-0.57842	- 2.2726	0.002	8.035	4.250
+0.10	+0.0003	-0.52844	- 2.0602	0.003	7.622	4.249
+0.15	+0.0003	-0.47846	- 1.8478	0.003	7.254	4.249
+0.20	+0.0004	-0.42848	- 1.6354	0.004	6.926	4.249
+0.25	+0.0006	-0.37852	- 1.4231	0.004	6.633	4.249
+0.30	+0.0007	-0.32856	- 1.2108	0.005	6.372	4.249
+0.35	+0.0009	-0.27861	- 0.9986	0.005	6.139	4.248
+0.40	+0.0011	-0.22867	- 0.7865	0.006	5.931	4.248
+0.45	+0.0013	-0.17875	- 0.5744	0.007	5.745	4.248
+0.50	+0.0016	-0.12884	- 0.3625	0.008	5.579	4.247
+0.55	+0.0020	-0.07896	- 0.1506	0.009	5.430	4.247
+0.60	+0.0023	-0.02909	+ 0.0612	0.010	5.298	4.246
+0.65	+0.0028	+0.02075	+ 0.2728	0.011	5.179	4.246
+0.70	+0.0032	+0.07056	+ 0.4843	0.012	5.072	4.245
+0.75	+0.0038	+0.12035	+ 0.6957	0.013	4.977	4.245
+0.80	+0.0043	+0.17011	+ 0.9069	0.014	4.892	4.245
+0.85	+0.0050	+0.21983	+ 1.1179	0.015	4.815	4.244
+0.90	+0.0057	+0.26952	+ 1.3288	0.016	4.746	4.243
+0.95	+0.0064	+0.31917	+ 1.5394	0.017	4.684	4.243
+1.00	+0.0072	+0.36878	+ 1.7499	0.018	4.628	4.242
+1.05	+0.0081	+0.41834	+ 1.9602	0.019	4.578	4.242
+1.10	+0.0090	+0.46787	+ 2.1702	0.021	4.532	4.241
+1.15	+0.0100	+0.51735	+ 2.3800	0.022	4.491	4.240
+1.20	+0.0110	+0.56678	+ 2.5896	0.023	4.454	4.240
+1.25	+0.0121	+0.61616	+ 2.7990	0.024	4.421	4.239
+1.30	+0.0133	+0.66550	+ 3.0081	0.025	4.390	4.239
+1.35	+0.0145	+0.71479	+ 3.2170	0.026	4.362	4.238
+1.40	+0.0157	+0.76403	+ 3.4257	0.027	4.337	4.238
+1.45	+0.0170	+0.81322	+ 3.6341	0.028	4.314	4.237
+1.50	+0.0184	+0.86236	+ 3.8423	0.029	4.293	4.236
+1.55	+0.0198	+0.91145	+ 4.0503	0.030	4.274	4.236
+1.60	+0.0213	+0.96048	+ 4.2580	0.031	4.256	4.235
+1.65	+0.0228	+1.00947	+ 4.4654	0.032	4.240	4.235
+1.70	+0.0244	+1.05840	+ 4.6726	0.033	4.225	4.234
+1.75	+0.0260	+1.10729	+ 4.8796	0.034	4.211	4.234
+1.80	+0.0277	+1.15612	+ 5.0864	0.035	4.198	4.233
+1.85	+0.0294	+1.20491	+ 5.2928	0.035	4.186	4.233
+1.90	+0.0312	+1.25364	+ 5.4991	0.036	4.175	4.232
+1.95	+0.0330	+1.30232	+ 5.7051	0.037	4.164	4.232
+2.00	+0.0349	+1.35095	+ 5.9109	0.038	4.154	4.231
+2.10	+0.0387	+1.44807	+ 6.3217	0.040	4.136	4.230
+2.20	+0.0428	+1.54493	+ 6.7317	0.042	4.120	4.229
+2.30	+0.0470	+1.64171	+ 7.1407	0.044	4.106	4.228
+2.40	+0.0515	+1.73824	+ 7.5488	0.045	4.093	4.227
+2.50	+0.0609	+1.83458	+ 7.9560	0.047	4.080	4.226
+2.60	+0.0608	+1.93074	+ 8.3623	0.049	4.069	4.225
+2.70	+0.0658	+2.02671	+ 8.7677	0.051	4.058	4.224
+2.80	+0.0710	+2.12249	+ 9.1723	0.052	4.048	4.223
+2.90	+0.0763	+2.21810	+ 9.5760	0.054	4.038	4.222
+3.00	+0.0818	+2.31352	+ 9.9789	0.056	4.029	4.221
+3.10	+0.0874	+2.40878	+10.3809	0.057	4.019	4.220
+3.20	+0.0932	+2.50385	+10.7821	0.059	4.011	4.219
+3.30	+0.0992	+2.59876	+11.1825	0.061	4.002	4.219
+3.40	+0.1053	+2.69349	+11.5821	0.062	3.994	4.218
+3.50	+0.1116	+2.78806	+11.9810	0.064	3.985	4.217
+3.60	+0.1180	+2.88246	+12.3790	0.065	3.977	4.216
+3.70	+0.1246	+2.97670	+12.7763	0.068	3.969	4.215
+3.80	+0.1314	+3.07078	+13.1728	0.068	3.962	4.214
+3.90	+0.1383	+3.16470	+13.5685	0.070	3.954	4.213

1.1 (CONT.)

(2)	(4)	(5)	(6)	(7)	(8)	(9)
+4.00	+0.1453	+3.25847	+13.9636	0.071	3.947	4.213
+4.10	+0.1524	+3.35208	+14.3579	0.072	3.940	4.212
+4.20	+0.1597	+3.44556	+14.7516	0.073	3.934	4.211
+4.30	+0.1671	+3.53889	+15.1446	0.075	3.927	4.210
+4.40	+0.1746	+3.63208	+15.5369	0.076	3.920	4.210
+4.50	+0.1822	+3.72514	+15.9286	0.077	3.914	4.209
+4.60	+0.1900	+3.81806	+16.3197	0.078	3.908	4.208
+4.70	+0.1978	+3.91087	+16.7103	0.079	3.902	4.208
+4.80	+0.2058	+4.00355	+17.1002	0.080	3.897	4.207
+4.90	+0.2138	+4.09611	+17.4896	0.081	3.891	4.207
+5.00	+0.2219	+4.18856	+17.8785	0.082	3.886	4.206
+5.10	+0.2301	+4.28091	+18.2669	0.082	3.881	4.206
+5.20	+0.2384	+4.37314	+18.6548	0.083	3.877	4.205
+5.30	+0.2468	+4.46528	+19.0422	0.084	3.872	4.205
+5.40	+0.2552	+4.55733	+19.4292	0.085	3.868	4.204
+5.50	+0.2637	+4.64929	+19.8158	0.085	3.864	4.204
+5.60	+0.2722	+4.74116	+20.2020	0.086	3.861	4.204
+5.70	+0.2808	+4.83296	+20.5879	0.086	3.857	4.203
+5.80	+0.2894	+4.92469	+20.9734	0.087	3.854	4.203
+5.90	+0.2981	+5.01635	+21.3586	0.087	3.850	4.203
+6.00	+0.3069	+5.10794	+21.7436	0.088	3.848	4.202
+6.10	+0.3157	+5.19947	+22.1282	0.088	3.845	4.202
+6.20	+0.3245	+5.29094	+22.5126	0.088	3.842	4.202
+6.30	+0.3333	+5.38236	+22.8967	0.089	3.840	4.202
+6.40	+0.3422	+5.47373	+23.2806	0.089	3.838	4.201
+6.50	+0.3511	+5.56505	+23.6642	0.089	3.836	4.201
+6.60	+0.3600	+5.65634	+24.0477	0.089	3.834	4.201
+6.70	+0.3690	+5.74758	+24.4310	0.090	3.832	4.201
+6.80	+0.3779	+5.83878	+24.8142	0.090	3.831	4.201
+6.90	+0.3869	+5.92996	+25.1972	0.090	3.829	4.201
+7.00	+0.3959	+6.02110	+25.5801	0.090	3.828	4.201
+7.10	+0.4050	+6.11222	+25.9628	0.090	3.827	4.201
+7.20	+0.4140	+6.20331	+26.3454	0.090	3.826	4.200
+7.30	+0.4230	+6.29438	+26.7280	0.091	3.825	4.200
+7.40	+0.4321	+6.38542	+27.1104	0.091	3.824	4.200
+7.50	+0.4411	+6.47645	+27.4927	0.091	3.823	4.200

1.2

(2)	(4)	(5)	(6)	(7)	(8)	(9)
-1.05	+0.0000	-1.67839	- 6.4474	0.000	51.936	4.250
-1.00	+0.0000	-1.62839	- 6.2348	0.000	46.750	4.250
-0.95	+0.0000	-1.57839	- 6.0224	0.000	42.128	4.250
-0.90	+0.0000	-1.52839	- 5.8098	0.000	38.009	4.250
-0.85	+0.0000	-1.47839	- 5.5974	0.000	34.338	4.250
-0.80	+0.0000	-1.42839	- 5.3848	0.000	31.066	4.250
-0.75	+0.0000	-1.37839	- 5.1724	0.000	28.149	4.250
-0.70	+0.0000	-1.32839	- 4.9598	0.000	25.551	4.250
-0.65	+0.0000	-1.27839	- 4.7474	0.000	23.234	4.250
-0.60	+0.0000	-1.22839	- 4.5348	0.000	21.170	4.250
-0.55	+0.0000	-1.17839	- 4.3224	0.000	19.330	4.250
-0.50	+0.0000	-1.12839	- 4.1098	0.001	17.690	4.250
-0.45	+0.0000	-1.07839	- 3.8974	0.001	16.228	4.250
-0.40	+0.0000	-1.02839	- 3.6848	0.001	14.925	4.250
-0.35	+0.0000	-0.97839	- 3.4724	0.001	13.764	4.250
-0.30	+0.0000	-0.92839	- 3.2599	0.001	12.729	4.250
-0.25	+0.0000	-0.87840	- 3.0474	0.002	11.806	4.250
-0.20	+0.0001	-0.82840	- 2.8350	0.002	10.983	4.250
-0.15	+0.0002	-0.77841	- 2.6225	0.003	10.250	4.250
-0.10	+0.0002	-0.72843	- 2.4101	0.004	9.596	4.249
-0.05	+0.0003	-0.67844	- 2.1977	0.005	9.013	4.249
-0.00	+0.0004	-0.62847	- 1.9854	0.006	8.493	4.249
+0.05	+0.0006	-0.57850	- 1.7731	0.007	8.029	4.249
+0.10	+0.0008	-0.52855	- 1.5608	0.008	7.614	4.248
+0.15	+0.0011	-0.47861	- 1.3487	0.010	7.245	4.248
+0.20	+0.0014	-0.42869	- 1.1367	0.011	6.914	4.247
+0.25	+0.0018	-0.37880	-0.9248	0.013	6.619	4.246
+0.30	+0.0023	-0.32893	- 0.7130	0.015	6.355	4.246
+0.35	+0.0028	-0.27909	- 0.5015	0.018	6.119	4.245
+0.40	+0.0035	-0.22929	- 0.2901	0.020	5.907	4.244
+0.45	+0.0043	-0.17954	- 0.0790	0.023	5.717	4.243
+0.50	+0.0052	-0.12984	+ 0.1318	0.026	5.546	4.242
+0.55	+0.0062	-0.08020	+ 0.3424	0.028	5.393	4.240
+0.60	+0.0074	-0.03062	+ 0.5525	0.032	5.254	4.239
+0.65	+0.0088	+0.01888	+ 0.7623	0.035	5.130	4.237
+0.70	+0.0102	+0.06830	+ 0.9717	0.038	5.017	4.236
+0.75	+0.0119	+0.11762	+ 1.1806	0.041	4.916	4.234
+0.80	+0.0137	+0.16686	+ 1.3890	0.044	4.823	4.233
+0.85	+0.0157	+0.21598	+ 1.5969	0.047	4.739	4.231
+0.90	+0.0179	+0.26500	+ 1.8042	0.050	4.663	4.229

1.2 (CONT.)

(2)	(4)	(5)	(6)	(7)	(8)	(9)
+0.95	+0.0202	+0.31391	+ 2.0110	0.054	4.593	4.227
+1.00	+0.0227	+0.36270	+ 2.2172	0.057	4.529	4.225
+1.05	+0.0253	+0.41136	+ 2.4228	0.060	4.471	4.224
+1.10	+0.0281	+0.45989	+ 2.6277	0.063	4.417	4.222
+1.15	+0.0311	+0.50829	+ 2.8320	0.065	4.368	4.220
+1.20	+0.0342	+0.55656	+ 3.0357	0.068	4.323	4.219
+1.25	+0.0375	+0.60468	+ 3.2386	0.071	4.281	4.217
+1.30	+0.0409	+0.65267	+ 3.4410	0.073	4.242	4.215
+1.35	+0.0445	+0.70053	+ 3.6426	0.076	4.207	4.214
+1.40	+0.0482	+0.74824	+ 3.8437	0.078	4.174	4.212
+1.45	+0.0520	+0.79582	+ 4.0440	0.080	4.143	4.211
+1.50	+0.0560	+0.84326	+ 4.2438	0.082	4.114	4.209
+1.55	+0.0600	+0.89056	+ 4.4428	0.084	4.088	4.208
+1.60	+0.0642	+0.93774	+ 4.6413	0.086	4.063	4.207
+1.65	+0.0684	+0.98479	+ 4.8392	0.088	4.040	4.206
+1.70	+0.0728	+1.03171	+ 5.0365	0.090	4.019	4.204
+1.75	+0.0772	+1.07850	+ 5.2333	0.091	3.999	4.203
+1.80	+0.0817	+1.12519	+ 5.4294	0.092	3.981	4.202
+1.85	+0.0863	+1.17175	+ 5.6251	0.094	3.963	4.201
+1.90	+0.0909	+1.21821	+ 5.8203	0.095	3.947	4.200
+1.95	+0.0956	+1.26455	+ 6.0149	0.096	3.932	4.200
+2.00	+0.1004	+1.31080	+ 6.2091	0.097	3.918	4.199
+2.10	+0.1101	+1.40300	+ 6.5962	0.098	3.893	4.198
+2.20	+0.1200	+1.49486	+ 6.9817	0.100	3.872	4.196
+2.30	+0.1299	+1.58640	+ 7.3658	0.101	3.853	4.196
+2.40	+0.1400	+1.67765	+ 7.7486	0.101	3.838	4.195
+2.50	+0.1501	+1.76866	+ 8.1304	0.102	3.825	4.194
+2.60	+0.1603	+1.85946	+ 8.5112	0.102	3.814	4.194
+2.70	+0.1705	+1.95008	+ 8.8913	0.102	3.805	4.194
+2.80	+0.1806	+2.04055	+ 9.2707	0.102	3.797	4.194
+2.90	+0.1908	+2.13090	+ 9.6496	0.102	3.792	4.194
+3.00	+0.2010	+2.22115	+10.0281	0.102	3.787	4.194
+3.10	+0.2111	+2.31133	+10.4063	0.101	3.784	4.194
+3.20	+0.2212	+2.40145	+10.7843	0.101	3.781	4.194
+3.30	+0.2312	+2.49154	+11.1621	0.100	3.780	4.194
+3.40	+0.2412	+2.58160	+11.5399	0.100	3.779	4.195
+3.50	+0.2511	+2.67166	+11.9176	0.099	3.779	4.195
+3.60	+0.2610	+2.76172	+12.2954	0.099	3.779	4.195
+3.70	+0.2708	+2.85179	+12.6733	0.098	3.780	4.195
+3.80	+0.2806	+2.94187	+13.0512	0.098	3.781	4.196
+3.90	+0.2904	+3.03197	+13.4293	0.097	3.782	4.196
+4.00	+0.3001	+3.12211	+13.8075	0.097	3.783	4.196
+4.10	+0.3097	+3.21228	+14.1859	0.096	3.785	4.196
+4.20	+0.3193	+3.30248	+14.5644	0.096	3.786	4.197
+4.30	+0.3289	+3.39271	+14.9431	0.095	3.788	4.197
+4.40	+0.3384	+3.48299	+15.3220	0.095	3.790	4.197
+4.50	+0.3478	+3.57330	+15.7011	0.095	3.792	4.198
+4.60	+0.3573	+3.66366	+16.0804	0.094	3.794	4.198
+4.70	+0.3667	+3.75405	+16.4599	0.094	3.796	4.198
+4.80	+0.3760	+3.84449	+16.8395	0.094	3.797	4.198
+4.90	+0.3854	+3.93495	+17.2193	0.093	3.799	4.198
+5.00	+0.3947	+4.02545	+17.5993	0.093	3.800	4.199
+5.10	+0.4040	+4.11599	+17.9794	0.093	3.802	4.199
+5.20	+0.4133	+4.20655	+18.3596	0.092	3.803	4.199
+5.30	+0.4225	+4.29715	+18.7400	0.092	3.805	4.199
+5.40	+0.4317	+4.38778	+19.1206	0.092	3.806	4.199
+5.50	+0.4410	+4.47843	+19.5013	0.092	3.807	4.199

1.3

(2)	(4)	(5)	(6)	(7)	(8)	(9)
-1.00	+0.0000	-1.62839	- 5.7348	0.000	46.750	4.250
-0.95	+0.0000	-1.57839	- 5.5224	0.000	42.128	4.250
-0.90	+0.0000	-1.52839	- 5.3099	0.000	38.009	4.250
-0.85	+0.0000	-1.47839	- 5.0974	0.000	34.338	4.250
-0.80	+0.0000	-1.42839	- 4.8849	0.000	31.066	4.250
-0.75	+0.0000	-1.37839	- 4.6724	0.000	28.149	4.250
-0.70	+0.0000	-1.32840	- 4.4599	0.000	25.550	4.250
-0.65	+0.0000	-1.27840	- 4.2474	0.001	23.234	4.250
-0.60	+0.0000	-1.22840	- 4.0349	0.001	21.170	4.250
-0.55	+0.0000	-1.17840	- 3.8224	0.001	19.329	4.250
-0.50	+0.0000	-1.12841	- 3.6099	0.002	17.689	4.250
-0.45	+0.0001	-1.07841	- 3.3975	0.002	16.227	4.250
-0.40	+0.0001	-1.02841	- 3.1850	0.003	14.923	4.250
-0.35	+0.0002	-0.97842	- 2.9725	0.003	13.761	4.249
-0.30	+0.0002	-0.92843	- 2.7601	0.004	12.725	4.249

1.3 (CONT.)

(2)	(4)	(5)	(6)	(7)	(8)	(9)
-0.25	+0.0003	-0.87845	- 2.5477	0.006	11.801	4.249
-0.20	+0.0004	-0.82847	- 2.3354	0.007	10.977	4.249
-0.15	+0.0006	-0.77850	- 2.1231	0.009	10.242	4.249
-0.10	+0.0008	-0.72855	- 1.9108	0.011	9.586	4.248
-0.05	+0.0011	-0.67861	- 1.6987	0.014	9.001	4.247
0.00	+0.0015	-0.62869	- 1.4867	0.017	8.477	4.246
+0.05	+0.0020	-0.57880	- 1.2749	0.021	8.009	4.246
+0.10	+0.0026	-0.52895	- 1.0632	0.026	7.590	4.244
+0.15	+0.0034	-0.47914	- 0.8518	0.030	7.215	4.243
+0.20	+0.0044	-0.42938	- 0.6408	0.036	6.878	4.241
+0.25	+0.0056	-0.37971	- 0.4302	0.042	6.575	4.239
+0.30	+0.0071	-0.33011	- 0.2200	0.049	6.301	4.236
+0.35	+0.0089	-0.28062	- 0.0104	0.056	6.055	4.234
+0.40	+0.0110	-0.23126	+ 0.1985	0.064	5.832	4.230
+0.45	+0.0134	-0.18202	+ 0.4067	0.072	5.630	4.227
+0.50	+0.0163	-0.13296	+ 0.6140	0.080	5.445	4.223
+0.55	+0.0196	-0.08407	+ 0.8203	0.089	5.276	4.219
+0.60	+0.0233	-0.03539	+ 1.0256	0.098	5.122	4.214
+0.65	+0.0274	+0.01306	+ 1.2297	0.107	4.980	4.210
+0.70	+0.0321	+0.06126	+ 1.4325	0.117	4.849	4.205
+0.75	+0.0372	+0.10920	+ 1.6339	0.126	4.728	4.200
+0.80	+0.0427	+0.15685	+ 1.8339	0.134	4.616	4.194
+0.85	+0.0488	+0.20420	+ 2.0324	0.143	4.512	4.189
+0.90	+0.0552	+0.25123	+ 2.2293	0.151	4.416	4.184
+0.95	+0.0622	+0.29793	+ 2.4246	0.159	4.326	4.179
+1.00	+0.0695	+0.34430	+ 2.6182	0.166	4.242	4.174
+1.05	+0.0772	+0.39032	+ 2.8102	0.172	4.164	4.169
+1.10	+0.0853	+0.43600	+ 3.0006	0.178	4.092	4.165
+1.15	+0.0937	+0.48134	+ 3.1893	0.183	4.024	4.160
+1.20	+0.1023	+0.52634	+ 3.3764	0.187	3.962	4.156
+1.25	+0.1113	+0.57101	+ 3.5620	0.191	3.904	4.153
+1.30	+0.1204	+0.61535	+ 3.7460	0.194	3.850	4.150
+1.35	+0.1297	+0.65937	+ 3.9287	0.196	3.801	4.146
+1.40	+0.1391	+0.70310	+ 4.1099	0.197	3.756	4.144
+1.45	+0.1487	+0.74655	+ 4.2899	0.198	3.715	4.142
+1.50	+0.1582	+0.78972	+ 4.4687	0.198	3.678	4.140
+1.55	+0.1678	+0.83265	+ 4.6464	0.197	3.644	4.139
+1.60	+0.1774	+0.87536	+ 4.8231	0.196	3.614	4.138
+1.65	+0.1870	+0.91785	+ 4.9990	0.195	3.588	4.138
+1.70	+0.1964	+0.96016	+ 5.1741	0.193	3.564	4.138
+1.75	+0.2058	+1.00231	+ 5.3485	0.190	3.544	4.138
+1.80	+0.2151	+1.04432	+ 5.5224	0.187	3.527	4.139
+1.85	+0.2243	+1.08620	+ 5.6957	0.184	3.512	4.140
+1.90	+0.2333	+1.12799	+ 5.8688	0.181	3.501	4.141
+1.95	+0.2421	+1.16969	+ 6.0415	0.178	3.492	4.143
+2.00	+0.2508	+1.21134	+ 6.2140	0.174	3.484	4.144
+2.05	+0.2594	+1.25295	+ 6.3865	0.170	3.480	4.146
+2.10	+0.2677	+1.29453	+ 6.5590	0.167	3.477	4.148
+2.15	+0.2759	+1.33611	+ 6.7315	0.163	3.476	4.150
+2.20	+0.2839	+1.37770	+ 6.9041	0.159	3.476	4.152
+2.25	+0.2917	+1.41932	+ 7.0770	0.156	3.478	4.154
+2.30	+0.2994	+1.46097	+ 7.2501	0.152	3.482	4.156
+2.35	+0.3068	+1.50267	+ 7.4235	0.148	3.487	4.159
+2.40	+0.3142	+1.54444	+ 7.5972	0.145	3.492	4.161
+2.45	+0.3213	+1.58628	+ 7.7713	0.142	3.499	4.163
+2.50	+0.3283	+1.62820	+ 7.9459	0.139	3.506	4.165
+2.55	+0.3351	+1.67021	+ 8.1209	0.136	3.515	4.167
+2.60	+0.3418	+1.71231	+ 8.2964	0.132	3.523	4.169
+2.65	+0.3484	+1.75451	+ 8.4724	0.130	3.533	4.171
+2.70	+0.3548	+1.79682	+ 8.6489	0.127	3.541	4.173
+2.75	+0.3610	+1.83923	+ 8.8259	0.125	3.552	4.174
+2.80	+0.3672	+1.88176	+ 9.0035	0.122	3.562	4.176
+2.85	+0.3732	+1.92439	+ 9.1816	0.120	3.572	4.178
+2.90	+0.3792	+1.96714	+ 9.3602	0.118	3.583	4.179
+2.95	+0.3850	+2.01001	+ 9.5394	0.116	3.593	4.181
+3.00	+0.3907	+2.05299	+ 9.7191	0.114	3.603	4.182
+3.05	+0.3964	+2.09608	+ 9.8994	0.112	3.614	4.182
+3.10	+0.4019	+2.13928	+10.0802	0.110	3.624	4.185
+3.15	+0.4074	+2.18260	+10.2615	0.108	3.634	4.186
+3.20	+0.4127	+2.22602	+10.4433	0.107	3.643	4.187

1.3 (CONT.)

(2)	(4)	(5)	(6)	(7)	(8)	(9)
+3.25	+0.4180	+2.26956	+10.6256	0.105	3.653	4.188
+3.30	+0.4233	+2.31319	+10.8084	0.104	3.662	4.189
+3.35	+0.4285	+2.35693	+10.9916	0.103	3.671	4.190
+3.40	+0.4336	+2.40077	+11.1753	0.102	3.680	4.191
+3.45	+0.4386	+2.44470	+11.3594	0.101	3.688	4.192
+3.50	+0.4436	+2.48872	+11.5440	0.100	3.696	4.193
+3.55	+0.4486	+2.53283	+11.7290	0.099	3.704	4.193
+3.60	+0.4535	+2.57703	+11.9143	0.098	3.712	4.194
+3.65	+0.4584	+2.62131	+12.1000	0.097	3.719	4.194
+3.70	+0.4632	+2.66566	+12.2861	0.096	3.726	4.195
+3.75	+0.4680	+2.71010	+12.4725	0.096	3.732	4.196
+3.80	+0.4728	+2.75460	+12.6592	0.095	3.739	4.196
+3.85	+0.4775	+2.79918	+12.8463	0.094	3.744	4.197
+3.90	+0.4822	+2.84381	+13.0336	0.094	3.750	4.197
+3.95	+0.4869	+2.88851	+13.2213	0.093	3.756	4.198
+4.00	+0.4915	+2.93327	+13.4092	0.093	3.761	4.198

1.4

(2)	(4)	(5)	(6)	(7)	(8)	(9)
-1.00	+0.0000	-1.62839	- 5.4848	0.000	46.750	4.250
-0.95	+0.0000	-1.57839	- 5.2724	0.000	42.128	4.250
-0.90	+0.0000	-1.52839	- 5.0598	0.000	38.009	4.250
-0.85	+0.0000	-1.47839	- 4.8474	0.000	34.338	4.250
-0.80	+0.0000	-1.42839	- 4.6348	0.000	31.066	4.250
-0.75	+0.0000	-1.37839	- 4.4224	0.000	28.149	4.250
-0.70	+0.0000	-1.32839	- 4.2098	0.001	25.551	4.250
-0.65	+0.0000	-1.27839	- 3.9974	0.001	23.234	4.250
-0.60	+0.0000	-1.22839	- 3.7848	0.001	21.170	4.250
-0.55	+0.0000	-1.17839	- 3.5724	0.002	19.329	4.250
-0.50	+0.0000	-1.12839	- 3.3599	0.002	17.688	4.250
-0.45	+0.0001	-1.07840	- 3.1474	0.003	16.226	4.250
-0.40	+0.0001	-1.02840	- 2.9349	0.004	14.921	4.250
-0.35	+0.0002	-0.97841	- 2.7225	0.006	13.759	4.250
-0.30	+0.0003	-0.92843	- 2.5101	0.008	12.722	4.249
-0.25	+0.0005	-0.87846	- 2.2978	0.010	11.797	4.249
-0.20	+0.0007	-0.82849	- 2.0855	0.013	10.971	4.248
-0.15	+0.0010	-0.77855	- 1.8734	0.016	10.234	4.247
-0.10	+0.0014	-0.72862	- 1.6614	0.020	9.575	4.246
-0.05	+0.0019	-0.67873	- 1.4495	0.025	8.986	4.245
0.00	+0.0026	-0.62888	- 1.2379	0.031	8.459	4.244
+0.05	+0.0035	-0.57908	- 1.0266	0.038	7.986	4.242
+0.10	+0.0046	-0.52934	- 0.8157	0.045	7.562	4.240
+0.15	+0.0060	-0.47968	- 0.6052	0.054	7.180	4.237
+0.20	+0.0078	-0.43012	- 0.3953	0.064	6.836	4.234
+0.25	+0.0099	-0.38069	- 0.1861	0.075	6.524	4.230
+0.30	+0.0126	-0.33141	+ 0.0223	0.086	6.241	4.226
+0.35	+0.0157	-0.28232	+ 0.2296	0.099	5.984	4.221
+0.40	+0.0194	-0.23343	+ 0.4358	0.113	5.748	4.215
+0.45	+0.0238	-0.18478	+ 0.6407	0.127	5.532	4.209
+0.50	+0.0288	-0.13642	+ 0.8441	0.142	5.332	4.202
+0.55	+0.0346	-0.08838	+ 1.0458	0.157	5.148	4.194
+0.60	+0.0411	-0.04069	+ 1.2456	0.172	4.977	4.186
+0.65	+0.0483	+0.00662	+ 1.4435	0.187	4.817	4.178
+0.70	+0.0563	+0.05351	+ 1.6392	0.202	4.668	4.170
+0.75	+0.0651	+0.09995	+ 1.8326	0.216	4.529	4.161
+0.80	+0.0747	+0.14592	+ 2.0237	0.229	4.399	4.152
+0.85	+0.0849	+0.19139	+ 2.2123	0.242	4.276	4.143
+0.90	+0.0958	+0.23636	+ 2.3984	0.253	4.162	4.134
+0.95	+0.1074	+0.28080	+ 2.5819	0.263	4.055	4.126
+1.00	+0.1195	+0.32472	+ 2.7630	0.272	3.955	4.118
+1.05	+0.1320	+0.36812	+ 2.9415	0.278	3.863	4.111
+1.10	+0.1450	+0.41101	+ 3.1177	0.283	3.778	4.104
+1.15	+0.1582	+0.45340	+ 3.2915	0.286	3.699	4.098
+1.20	+0.1717	+0.49531	+ 3.4632	0.288	3.627	4.093
+1.25	+0.1853	+0.53676	+ 3.6327	0.288	3.562	4.089
+1.30	+0.1990	+0.57778	+ 3.8004	0.287	3.503	4.086
+1.35	+0.2126	+0.61841	+ 3.9664	0.284	3.451	4.084
+1.40	+0.2262	+0.65868	+ 4.1308	0.280	3.405	4.083
+1.45	+0.2396	+0.69862	+ 4.2939	0.275	3.365	4.082
+1.50	+0.2527	+0.73828	+ 4.4558	0.269	3.330	4.083
+1.55	+0.2656	+0.77770	+ 4.6168	0.262	3.302	4.085
+1.60	+0.2782	+0.81691	+ 4.7770	0.255	3.278	4.088
+1.65	+0.2905	+0.85595	+ 4.9367	0.247	3.260	4.091
+1.70	+0.3024	+0.89487	+ 5.0959	0.239	3.246	4.094

1.4 (CONT.)

(2)	(4)	(5)	(6)	(7)	(8)	(9)
+1.75	+0.3139	+0.93370	+ 5.2550	0.230	3.237	4.098
+1.80	+0.3250	+0.97248	+ 5.4140	0.222	3.231	4.103
+1.85	+0.3357	+1.01124	+ 5.5731	0.213	3.230	4.108
+1.90	+0.3460	+1.05002	+ 5.7325	0.205	3.231	4.113
+1.95	+0.3560	+1.08885	+ 5.8923	0.197	3.236	4.118
+2.00	+0.3655	+1.12775	+ 6.0526	0.190	3.244	4.123
+2.05	+0.3747	+1.16676	+ 6.2135	0.182	3.254	4.128
+2.10	+0.3836	+1.20588	+ 6.3751	0.175	3.266	4.133
+2.15	+0.3921	+1.24516	+ 6.5375	0.168	3.280	4.138
+2.20	+0.4002	+1.28460	+ 6.7008	0.162	3.295	4.142
+2.25	+0.4081	+1.32422	+ 6.8650	0.156	3.312	4.147
+2.30	+0.4157	+1.36402	+ 7.0302	0.150	3.330	4.151
+2.35	+0.4230	+1.40404	+ 7.1963	0.144	3.348	4.155
+2.40	+0.4301	+1.44426	+ 7.3635	0.139	3.368	4.159
+2.45	+0.4369	+1.48469	+ 7.5318	0.135	3.388	4.163
+2.50	+0.4436	+1.52535	+ 7.7011	0.130	3.408	4.166
+2.55	+0.4500	+1.56624	+ 7.8715	0.126	3.428	4.169
+2.60	+0.4562	+1.60734	+ 8.0430	0.122	3.448	4.172
+2.65	+0.4622	+1.64868	+ 8.2155	0.119	3.468	4.175
+2.70	+0.4680	+1.69023	+ 8.3890	0.116	3.488	4.178
+2.75	+0.4738	+1.73201	+ 8.5636	0.113	3.508	4.180
+2.80	+0.4794	+1.77400	+ 8.7391	0.110	3.526	4.182
+2.85	+0.4848	+1.81620	+ 8.9157	0.108	3.545	4.184
+2.90	+0.4901	+1.85861	+ 9.0931	0.106	3.563	4.186
+2.95	+0.4953	+1.90121	+ 9.2715	0.103	3.580	4.188
+3.00	+0.5004	+1.94401	+ 9.4508	0.101	3.597	4.189
+3.05	+0.5055	+1.98700	+ 9.6309	0.100	3.613	4.191
+3.10	+0.5104	+2.03016	+ 9.8118	0.098	3.629	4.192
+3.15	+0.5153	+2.07350	+ 9.9935	0.096	3.644	4.193
+3.20	+0.5200	+2.11700	+10.1759	0.095	3.658	4.194
+3.25	+0.5248	+2.16065	+10.3590	0.094	3.671	4.195
+3.30	+0.5294	+2.20446	+10.5428	0.093	3.684	4.196
+3.35	+0.5340	+2.24840	+10.7272	0.092	3.696	4.197
+3.40	+0.5386	+2.29248	+10.9122	0.091	3.708	4.198
+3.45	+0.5431	+2.33669	+11.0978	0.090	3.718	4.198
+3.50	+0.5476	+2.38101	+11.2839	0.089	3.727	4.199
+3.55	+0.5520	+2.42545	+11.4706	0.088	3.738	4.200
+3.60	+0.5564	+2.47000	+11.6576	0.088	3.747	4.200
+3.65	+0.5608	+2.51464	+11.8451	0.087	3.755	4.201
+3.70	+0.5652	+2.55937	+12.0330	0.087	3.763	4.201
+3.75	+0.5695	+2.60419	+12.2213	0.086	3.770	4.202
+3.80	+0.5738	+2.64909	+12.4100	0.086	3.777	4.202
+3.85	+0.5781	+2.69406	+12.5990	0.086	3.784	4.202
+3.90	+0.5824	+2.73911	+12.7883	0.085	3.790	4.202
+3.95	+0.5866	+2.78422	+12.9779	0.085	3.795	4.203
+4.00	+0.5909	+2.82940	+13.1677	0.085	3.800	4.203

1.5

(2)	(4)	(5)	(6)	(7)	(8)	(9)
-1.00	+0.0000	-1.62839	- 5.2348	0.000	46.750	4.250
-0.95	+0.0000	-1.57839	- 5.0224	0.000	42.128	4.250
-0.90	+0.0000	-1.52839	- 4.8098	0.000	38.009	4.250
-0.85	+0.0000	-1.47839	- 4.5974	0.000	34.338	4.250
-0.80	+0.0000	-1.42839	- 4.3848	0.000	31.066	4.250
-0.75	+0.0000	-1.37839	- 4.1724	0.001	28.149	4.250
-0.70	+0.0000	-1.32839	- 3.9598	0.001	25.550	4.250
-0.65	+0.0000	-1.27839	- 3.7474	0.002	23.233	4.250
-0.60	+0.0000	-1.22839	- 3.5349	0.003	21.168	4.250
-0.55	+0.0001	-1.17839	- 3.3224	0.004	19.326	4.250
-0.50	+0.0001	-1.12840	- 3.1099	0.004	17.685	4.250
-0.45	+0.0002	-1.07841	- 2.8975	0.006	16.221	4.249
-0.40	+0.0003	-1.02843	- 2.6851	0.008	14.916	4.249
-0.35	+0.0004	-0.97846	- 2.4728	0.010	13.752	4.249
-0.30	+0.0006	-0.92849	- 2.2605	0.014	12.714	4.248
-0.25	+0.0009	-0.87854	- 2.0483	0.018	11.786	4.247
-0.20	+0.0013	-0.82861	- 1.8363	0.023	10.958	4.247
-0.15	+0.0018	-0.77872	- 1.6244	0.029	10.218	4.245
-0.10	+0.0025	-0.72885	- 1.4128	0.036	9.555	4.244
-0.05	+0.0034	-0.67905	- 1.2014	0.044	8.961	4.242
0.00	+0.0046	-0.62931	- 0.9905	0.055	8.427	4.239
+0.05	+0.0062	-0.57966	- 0.7801	0.067	7.947	4.236
+0.10	+0.0082	-0.53012	- 0.5704	0.081	7.513	4.232
+0.15	+0.0107	-0.48073	- 0.3615	0.096	7.120	4.227
+0.20	+0.0139	-0.43152	- 0.1536	0.114	6.762	4.221

1.5 (CONT.)

(2)	(4)	(5)	(6)	(7)	(8)	(9)
+0.25	+0.0177	-0.38252	+ 0.0531	0.132	6.436	4.214
+0.30	+0.0224	-0.33379	+ 0.2582	0.153	6.136	4.206
+0.35	+0.0279	-0.28538	+ 0.4617	0.175	5.859	4.198
+0.40	+0.0345	-0.23733	+ 0.6631	0.199	5.602	4.187
+0.45	+0.0422	-0.18970	+ 0.8623	0.223	5.363	4.176
+0.50	+0.0510	-0.14256	+ 1.0589	0.248	5.139	4.164
+0.55	+0.0610	-0.09595	+ 1.2527	0.273	4.929	4.150
+0.60	+0.0723	-0.04993	+ 1.4433	0.298	4.731	4.136
+0.65	+0.0848	-0.00455	+ 1.6307	0.321	4.544	4.122
+0.70	+0.0985	+0.04014	+ 1.8146	0.344	4.368	4.107
+0.75	+0.1134	+0.08412	+ 1.9949	0.364	4.203	4.091
+0.80	+0.1294	+0.12735	+ 2.1714	0.382	4.047	4.076
+0.85	+0.1463	+0.16982	+ 2.3442	0.397	3.901	4.062
+0.90	+0.1641	+0.21152	+ 2.5133	0.409	3.766	4.047
+0.95	+0.1826	+0.25246	+ 2.6787	0.417	3.640	4.035
+1.00	+0.2016	+0.29265	+ 2.8407	0.422	3.525	4.024
+1.05	+0.2209	+0.33212	+ 2.9993	0.424	3.420	4.014
+1.10	+0.2404	+0.37091	+ 3.1548	0.421	3.326	4.006
+1.15	+0.2599	+0.40905	+ 3.3075	0.416	3.242	4.000
+1.20	+0.2792	+0.44661	+ 3.4576	0.408	3.168	3.996
+1.25	+0.2982	+0.48363	+ 3.6056	0.397	3.104	3.995
+1.30	+0.3168	+0.52019	+ 3.7516	0.384	3.050	3.996
+1.35	+0.3348	+0.55634	+ 3.8961	0.369	3.005	3.999
+1.40	+0.3521	+0.59216	+ 4.0394	0.354	2.970	4.003
+1.45	+0.3687	+0.62770	+ 4.1818	0.337	2.942	4.010
+1.50	+0.3846	+0.66305	+ 4.3237	0.320	2.923	4.017
+1.55	+0.3997	+0.69826	+ 4.4653	0.302	2.911	4.026
+1.60	+0.4140	+0.73340	+ 4.6069	0.285	2.906	4.036
+1.65	+0.4275	+0.76852	+ 4.7489	0.269	2.908	4.047
+1.70	+0.4403	+0.80369	+ 4.8914	0.252	2.915	4.058
+1.75	+0.4523	+0.83896	+ 5.0347	0.237	2.928	4.068
+1.80	+0.4636	+0.87438	+ 5.1790	0.223	2.943	4.079
+1.85	+0.4742	+0.91000	+ 5.3245	0.209	2.964	4.090
+1.90	+0.4842	+0.94585	+ 5.4713	0.196	2.988	4.100
+1.95	+0.4937	+0.98197	+ 5.6196	0.185	3.014	4.110
+2.00	+0.5026	+1.01839	+ 5.7695	0.174	3.044	4.119
+2.05	+0.5109	+1.05513	+ 5.9210	0.164	3.074	4.128
+2.10	+0.5188	+1.09222	+ 6.0742	0.155	3.107	4.136
+2.15	+0.5263	+1.12967	+ 6.2293	0.147	3.141	4.143
+2.20	+0.5334	+1.16750	+ 6.3861	0.139	3.175	4.150
+2.25	+0.5402	+1.20571	+ 6.5448	0.132	3.210	4.156
+2.30	+0.5466	+1.24431	+ 6.7054	0.126	3.245	4.162
+2.35	+0.5527	+1.28330	+ 6.8677	0.120	3.280	4.167
+2.40	+0.5586	+1.32267	+ 7.0319	0.115	3.314	4.172
+2.45	+0.5643	+1.36244	+ 7.1978	0.111	3.348	4.176
+2.50	+0.5697	+1.40258	+ 7.3656	0.107	3.381	4.179
+2.55	+0.5749	+1.44309	+ 7.5349	0.103	3.414	4.183
+2.60	+0.5800	+1.48396	+ 7.7059	0.100	3.444	4.186
+2.65	+0.5849	+1.52517	+ 7.8785	0.097	3.475	4.189
+2.70	+0.5896	+1.56673	+ 8.0526	0.094	3.504	4.191
+2.75	+0.5942	+1.60860	+ 8.2282	0.092	3.531	4.193
+2.80	+0.5988	+1.65078	+ 8.4051	0.089	3.557	4.195
+2.85	+0.6032	+1.69326	+ 8.5833	0.087	3.582	4.197
+2.90	+0.6075	+1.73602	+ 8.7628	0.086	3.606	4.198
+2.95	+0.6117	+1.77904	+ 8.9434	0.084	3.628	4.200
+3.00	+0.6159	+1.82231	+ 9.1252	0.083	3.649	4.201
+3.05	+0.6200	+1.86582	+ 9.3080	0.082	3.669	4.202
+3.10	+0.6240	+1.90954	+ 9.4918	0.080	3.688	4.203
+3.15	+0.6280	+1.95348	+ 9.6764	0.079	3.705	4.204
+3.20	+0.6320	+1.99761	+ 9.8620	0.079	3.721	4.205
+3.25	+0.6359	+2.04192	+10.0483	0.078	3.736	4.205
+3.30	+0.6398	+2.08640	+10.2354	0.077	3.750	4.206
+3.35	+0.6436	+2.13103	+10.4231	0.077	3.763	4.207
+3.40	+0.6475	+2.17581	+10.6115	0.076	3.775	4.207
+3.45	+0.6513	+2.22072	+10.8004	0.076	3.786	4.207
+3.50	+0.6550	+2.26576	+10.9899	0.076	3.796	4.208
+3.55	+0.6588	+2.31090	+11.1799	0.075	3.805	4.208
+3.60	+0.6626	+2.35616	+11.3703	0.075	3.814	4.208
+3.65	+0.6664	+2.40151	+11.5612	0.075	3.822	4.208
+3.70	+0.6701	+2.44694	+11.7524	0.075	3.829	4.208
+3.75	+0.6738	+2.49246	+11.9439	0.075	3.835	4.209
+3.80	+0.6776	+2.53804	+12.1358	0.075	3.841	4.209
+3.85	+0.6814	+2.58370	+12.3279	0.075	3.846	4.209
+3.90	+0.6851	+2.62941	+12.5203	0.075	3.851	4.209
+3.95	+0.6889	+2.67517	+12.7130	0.075	3.855	4.209
+4.00	+0.6926	+2.72098	+12.9058	0.075	3.859	4.209

1.6

(2)	(4)	(5)	(6)	(7)	(8)	(9)
-1.00	+0.0000	-1.62839	- 4.9848	0.000	46.750	4.250
-0.95	+0.0000	-1.57839	- 4.7724	0.000	42.128	4.250
-0.90	+0.0000	-1.52839	- 4.5598	0.000	38.009	4.250
-0.85	+0.0000	-1.47839	- 4.3474	0.000	34.338	4.250
-0.80	+0.0000	-1.42839	- 4.1348	0.001	31.066	4.250
-0.75	+0.0000	-1.37839	- 3.9224	0.001	28.148	4.250
-0.70	+0.0000	-1.32839	- 3.7099	0.002	25.548	4.250
-0.65	+0.0001	-1.27839	- 3.4974	0.003	23.231	4.250
-0.60	+0.0001	-1.22840	- 3.2849	0.005	21.166	4.250
-0.55	+0.0002	-1.17841	- 3.0725	0.006	19.323	4.249
-0.50	+0.0002	-1.12842	- 2.8601	0.008	17.681	4.249
-0.45	+0.0004	-1.07844	- 2.6477	0.011	16.217	4.249
-0.40	+0.0005	-1.02847	- 2.4354	0.014	14.910	4.248
-0.35	+0.0008	-0.97851	- 2.2231	0.019	13.744	4.248
-0.30	+0.0011	-0.92857	- 2.0110	0.025	12.703	4.247
-0.25	+0.0016	-0.87866	- 1.7990	0.032	11.772	4.246
-0.20	+0.0023	-0.82878	- 1.5873	0.040	10.938	4.244
-0.15	+0.0032	-0.77895	- 1.3759	0.051	10.192	4.242
-0.10	+0.0044	-0.72919	- 1.1649	0.064	9.521	4.239
-0.05	+0.0061	-0.67953	- 0.9545	0.080	8.917	4.235
0.00	+0.0082	-0.62999	- 0.7448	0.098	8.372	4.231
+0.05	+0.0110	-0.58060	- 0.5360	0.119	7.877	4.225
+0.10	+0.0146	-0.53142	- 0.3284	0.143	7.426	4.218
+0.15	+0.0190	-0.48250	- 0.1222	0.170	7.013	4.209
+0.20	+0.0246	-0.43388	+ 0.0821	0.201	6.633	4.198
+0.25	+0.0314	-0.38565	+ 0.2844	0.234	6.281	4.186
+0.30	+0.0397	-0.33788	+ 0.4840	0.270	5.952	4.172
+0.35	+0.0495	-0.29065	+ 0.6807	0.309	5.643	4.155
+0.40	+0.0610	-0.24404	+ 0.8740	0.349	5.352	4.137
+0.45	+0.0745	-0.19815	+ 1.0634	0.389	5.076	4.117
+0.50	+0.0898	-0.15305	+ 1.2485	0.430	4.815	4.095
+0.55	+0.1072	-0.10883	+ 1.4291	0.469	4.566	4.070
+0.60	+0.1264	-0.06557	+ 1.6046	0.506	4.330	4.046
+0.65	+0.1476	-0.02331	+ 1.7750	0.540	4.106	4.019
+0.70	+0.1705	+0.01789	+ 1.9401	0.570	3.896	3.993
+0.75	+0.1950	+0.05802	+ 2.0998	0.594	3.699	3.967
+0.80	+0.2209	+0.09705	+ 2.2542	0.611	3.515	3.942
+0.85	+0.2477	+0.13500	+ 2.4034	0.622	3.347	3.919
+0.90	+0.2753	+0.17191	+ 2.5476	0.626	3.194	3.898
+0.95	+0.3032	+0.20780	+ 2.6871	0.622	3.056	3.880
+1.00	+0.3311	+0.24275	+ 2.8225	0.612	2.934	3.866
+1.05	+0.3587	+0.27682	+ 2.9540	0.595	2.828	3.857
+1.10	+0.3857	+0.31011	+ 3.0823	0.573	2.738	3.851
+1.15	+0.4118	+0.34271	+ 3.2078	0.547	2.662	3.851
+1.20	+0.4367	+0.37470	+ 3.3311	0.517	2.601	3.855
+1.25	+0.4603	+0.40621	+ 3.4527	0.485	2.554	3.864
+1.30	+0.4826	+0.43732	+ 3.5731	0.452	2.520	3.877
+1.35	+0.5033	+0.46814	+ 3.6928	0.418	2.497	3.892
+1.40	+0.5226	+0.49877	+ 3.8123	0.385	2.487	3.912
+1.45	+0.5403	+0.52931	+ 3.9321	0.353	2.486	3.932
+1.50	+0.5567	+0.55986	+ 4.0525	0.323	2.495	3.954
+1.55	+0.5716	+0.59050	+ 4.1740	0.294	2.511	3.977
+1.60	+0.5853	+0.62131	+ 4.2969	0.268	2.536	3.999
+1.65	+0.5978	+0.65238	+ 4.4215	0.244	2.567	4.021
+1.70	+0.6093	+0.68377	+ 4.5481	0.223	2.604	4.042
+1.75	+0.6197	+0.71554	+ 4.6768	0.203	2.645	4.062
+1.80	+0.6293	+0.74776	+ 4.8080	0.186	2.691	4.081
+1.85	+0.6380	+0.78046	+ 4.9417	0.170	2.739	4.097
+1.90	+0.6461	+0.81370	+ 5.0782	0.156	2.790	4.112
+1.95	+0.6535	+0.84749	+ 5.2173	0.144	2.844	4.126
+2.00	+0.6603	+0.88186	+ 5.3594	0.133	2.898	4.138
+2.05	+0.6667	+0.91684	+ 5.5043	0.124	2.953	4.148
+2.10	+0.6726	+0.95243	+ 5.6521	0.115	3.009	4.158
+2.15	+0.6782	+0.98864	+ 5.8028	0.108	3.064	4.166
+2.20	+0.6834	+1.02546	+ 5.9563	0.101	3.118	4.173
+2.25	+0.6883	+1.06289	+ 6.1126	0.096	3.172	4.179
+2.30	+0.6929	+1.10093	+ 6.2717	0.091	3.224	4.184
+2.35	+0.6973	+1.13954	+ 6.4334	0.086	3.274	4.189
+2.40	+0.7015	+1.17873	+ 6.5976	0.082	3.323	4.193
+2.45	+0.7055	+1.21847	+ 6.7643	0.079	3.370	4.196
+2.50	+0.7093	+1.25874	+ 6.9333	0.076	3.414	4.200
+2.55	+0.7131	+1.29950	+ 7.1046	0.073	3.457	4.202
+2.60	+0.7166	+1.34075	+ 7.2780	0.071	3.497	4.205
+2.65	+0.7201	+1.38245	+ 7.4534	0.069	3.535	4.207
+2.70	+0.7235	+1.42459	+ 7.6307	0.067	3.571	4.208
+2.75	+0.7268	+1.46712	+ 7.8097	0.066	3.604	4.210
+2.80	+0.7301	+1.51004	+ 7.9904	0.064	3.635	4.211
+2.85	+0.7333	+1.55330	+ 8.1726	0.063	3.665	4.212
+2.90	+0.7364	+1.59690	+ 8.3563	0.062	3.692	4.213
+2.95	+0.7395	+1.64080	+ 8.5413	0.062	3.717	4.214

1.6 (CONT.)

(2)	(4)	(5)	(6)	(7)	(8)	(9)
+3.00	+0.7426	+1.68499	+ 8.7275	0.061	3.740	4.215
+3.05	+0.7456	+1.72944	+ 8.9149	0.060	3.762	4.216
+3.10	+0.7486	+1.77414	+ 9.1033	0.060	3.781	4.216
+3.15	+0.7516	+1.81905	+ 9.2927	0.059	3.799	4.217
+3.20	+0.7545	+1.86417	+ 9.4830	0.059	3.816	4.217
+3.25	+0.7575	+1.90947	+ 9.6740	0.059	3.831	4.217
+3.30	+0.7604	+1.95495	+ 9.8658	0.059	3.844	4.218
+3.35	+0.7634	+2.00058	+10.0582	0.059	3.857	4.217
+3.40	+0.7663	+2.04635	+10.2513	0.059	3.868	4.218
+3.45	+0.7693	+2.09225	+10.4449	0.059	3.878	4.218
+3.50	+0.7722	+2.13826	+10.6390	0.059	3.887	4.218
+3.55	+0.7752	+2.18438	+10.8335	0.059	3.896	4.218
+3.60	+0.7782	+2.23059	+11.0284	0.060	3.902	4.218
+3.65	+0.7812	+2.27687	+11.2236	0.060	3.909	4.218
+3.70	+0.7842	+2.32324	+11.4191	0.060	3.914	4.217
+3.75	+0.7872	+2.36966	+11.6150	0.061	3.919	4.217
+3.80	+0.7902	+2.41615	+11.8110	0.061	3.924	4.218
+3.85	+0.7933	+2.46268	+12.0072	0.061	3.927	4.217
+3.90	+0.7964	+2.50926	+12.2036	0.062	3.930	4.217
+3.95	+0.7995	+2.55587	+12.4002	0.062	3.933	4.217
+4.00	+0.8026	+2.60251	+12.5969	0.063	3.935	4.217
+4.05	+0.8057	+2.64918	+12.7937	0.063	3.937	4.216
+4.10	+0.8089	+2.69586	+12.9905	0.064	3.938	4.216
+4.15	+0.8121	+2.74257	+13.1874	0.064	3.939	4.216
+4.20	+0.8153	+2.78928	+13.3844	0.065	3.940	4.216
+4.25	+0.8186	+2.83600	+13.5813	0.065	3.940	4.215

1.7

(2)	(4)	(5)	(6)	(7)	(8)	(9)
-1.00	+0.0000	-1.62839	- 4.7348	0.000	46.750	4.250
-0.95	+0.0000	-1.57839	- 4.5224	0.000	42.128	4.250
-0.90	+0.0000	-1.52839	- 4.3098	0.002	38.009	4.250
-0.85	+0.0000	-1.47839	- 4.0974	0.002	34.338	4.250
-0.80	+0.0000	-1.42839	- 3.8848	0.003	31.064	4.250
-0.75	+0.0000	-1.37839	- 3.6724	0.003	28.147	4.250
-0.70	+0.0001	-1.32839	- 3.4599	0.005	25.547	4.250
-0.65	+0.0001	-1.27840	- 3.2474	0.006	23.229	4.250
-0.60	+0.0002	-1.22841	- 3.0350	0.008	21.162	4.249
-0.55	+0.0003	-1.17842	- 2.8226	0.011	19.319	4.249
-0.50	+0.0004	-1.12844	- 2.6102	0.014	17.675	4.249
-0.45	+0.0006	-1.07848	- 2.3980	0.019	16.208	4.248
-0.40	+0.0009	-1.02853	- 2.1858	0.025	14.898	4.247
-0.35	+0.0014	-0.97860	- 1.9738	0.034	13.728	4.246
-0.30	+0.0020	-0.92871	- 1.7619	0.044	12.681	4.244
-0.25	+0.0029	-0.87887	- 1.5504	0.056	11.743	4.242
-0.20	+0.0040	-0.82909	- 1.3393	0.072	10.902	4.240
-0.15	+0.0057	-0.77940	- 1.1287	0.091	10.143	4.235
-0.10	+0.0079	-0.72983	- 0.9189	0.114	9.459	4.231
-0.05	+0.0108	-0.68043	- 0.7101	0.142	8.839	4.224
0.00	+0.0146	-0.63124	- 0.5025	0.174	8.273	4.215
+0.05	+0.0196	-0.58233	- 0.2966	0.211	7.754	4.205
+0.10	+0.0259	-0.53377	- 0.0927	0.254	7.274	4.192
+0.15	+0.0338	-0.48566	+ 0.1086	0.303	6.828	4.176
+0.20	+0.0437	-0.43809	+ 0.3069	0.356	6.410	4.157
+0.25	+0.0558	-0.39117	+ 0.5014	0.414	6.014	4.135
+0.30	+0.0703	-0.34503	+ 0.6916	0.476	5.638	4.109
+0.35	+0.0876	-0.29980	+ 0.8768	0.541	5.280	4.079
+0.40	+0.1077	-0.25560	+ 1.0564	0.607	4.936	4.045
+0.45	+0.1310	-0.21256	+ 1.2297	0.672	4.607	4.008
+0.50	+0.1574	-0.17078	+ 1.3963	0.735	4.293	3.967
+0.55	+0.1868	-0.13036	+ 1.5557	0.793	3.994	3.923
+0.60	+0.2192	-0.09138	+ 1.7078	0.844	3.712	3.877
+0.65	+0.2541	-0.05387	+ 1.8524	0.885	3.447	3.831
+0.70	+0.2913	-0.01785	+ 1.9895	0.916	3.203	3.784
+0.75	+0.3303	+0.01670	+ 2.1195	0.933	2.979	3.739
+0.80	+0.3703	+0.04982	+ 2.2426	0.936	2.778	3.698
+0.85	+0.4108	+0.08158	+ 2.3595	0.926	2.600	3.662
+0.90	+0.4512	+0.11208	+ 2.4707	0.902	2.445	3.632
+0.95	+0.4908	+0.14141	+ 2.5768	0.866	2.312	3.610
+1.00	+0.5289	+0.16970	+ 2.6788	0.820	2.202	3.597
+1.05	+0.5652	+0.19710	+ 2.7773	0.766	2.113	3.594
+1.10	+0.5991	+0.22372	+ 2.8730	0.706	2.044	3.601
+1.15	+0.6305	+0.24971	+ 2.9668	0.643	1.993	3.617
+1.20	+0.6592	+0.27522	+ 3.0594	0.580	1.960	3.642
+1.25	+0.6851	+0.30037	+ 3.1514	0.519	1.942	3.675
+1.30	+0.7083	+0.32530	+ 3.2435	0.460	1.939	3.713
+1.35	+0.7289	+0.35014	+ 3.3363	0.406	1.950	3.756
+1.40	+0.7472	+0.37502	+ 3.4303	0.356	1.971	3.802
+1.45	+0.7632	+0.40006	+ 3.5260	0.312	2.004	3.848

1.7 (CONT.)

(2)	(4)	(5)	(6)	(7)	(8)	(9)
+1.50	+0.7773	+0.42536	+ 3.6240	0.273	2.046	3.893
+1.55	+0.7897	+0.45103	+ 3.7245	0.238	2.096	3.936
+1.60	+0.8006	+0.47717	+ 3.8279	0.208	2.153	3.977
+1.65	+0.8101	+0.50386	+ 3.9346	0.183	2.216	4.014
+1.70	+0.8185	+0.53120	+ 4.0448	0.161	2.285	4.047
+1.75	+0.8259	+0.55924	+ 4.1587	0.142	2.358	4.076
+1.80	+0.8325	+0.58804	+ 4.2764	0.126	2.434	4.102
+1.85	+0.8384	+0.61766	+ 4.3983	0.112	2.512	4.123
+1.90	+0.8436	+0.64813	+ 4.5242	0.101	2.592	4.141
+1.95	+0.8484	+0.67949	+ 4.6543	0.091	2.673	4.156
+2.00	+0.8526	+0.71174	+ 4.7885	0.082	2.754	4.169
+2.05	+0.8566	+0.74489	+ 4.9269	0.075	2.834	4.180
+2.10	+0.8601	+0.77894	+ 5.0694	0.069	2.913	4.189
+2.15	+0.8634	+0.81389	+ 5.2159	0.064	2.991	4.196
+2.20	+0.8665	+0.84971	+ 5.3663	0.060	3.066	4.201
+2.25	+0.8694	+0.88639	+ 5.5205	0.056	3.138	4.206
+2.30	+0.8720	+0.92389	+ 5.6784	0.052	3.208	4.210
+2.35	+0.8747	+0.96219	+ 5.8396	0.050	3.274	4.213
+2.40	+0.8771	+1.00124	+ 6.0042	0.047	3.337	4.216
+2.45	+0.8794	+1.04101	+ 6.1720	0.045	3.397	4.219
+2.50	+0.8816	+1.08146	+ 6.3427	0.044	3.454	4.220
+2.55	+0.8838	+1.12256	+ 6.5162	0.042	3.507	4.223
+2.60	+0.8858	+1.16426	+ 6.6923	0.041	3.556	4.224
+2.65	+0.8878	+1.20653	+ 6.8709	0.040	3.603	4.226
+2.70	+0.8898	+1.24932	+ 7.0517	0.039	3.645	4.226
+2.75	+0.8917	+1.29260	+ 7.2347	0.038	3.685	4.227
+2.80	+0.8936	+1.33633	+ 7.4195	0.038	3.722	4.228
+2.85	+0.8955	+1.38048	+ 7.6062	0.037	3.756	4.229
+2.90	+0.8973	+1.42501	+ 7.7945	0.037	3.786	4.229
+2.95	+0.8991	+1.46989	+ 7.9843	0.036	3.815	4.229
+3.00	+0.9009	+1.51509	+ 8.1755	0.036	3.841	4.230
+3.05	+0.9028	+1.56059	+ 8.3680	0.036	3.864	4.230
+3.10	+0.9046	+1.60635	+ 8.5615	0.036	3.886	4.230
+3.15	+0.9064	+1.65236	+ 8.7562	0.036	3.905	4.230
+3.20	+0.9082	+1.69858	+ 8.9517	0.036	3.922	4.230
+3.25	+0.9100	+1.74500	+ 9.1481	0.036	3.938	4.230
+3.30	+0.9118	+1.79160	+ 9.3452	0.037	3.952	4.230
+3.35	+0.9137	+1.83837	+ 9.5430	0.037	3.964	4.230
+3.40	+0.9155	+1.88527	+ 9.7411	0.037	3.976	4.230
+3.45	+0.9174	+1.93230	+ 9.9404	0.038	3.985	4.230
+3.50	+0.9193	+1.97945	+10.1398	0.038	3.994	4.230
+3.55	+0.9212	+2.02669	+10.3397	0.038	4.002	4.230
+3.60	+0.9231	+2.07402	+10.5399	0.039	4.008	4.230
+3.65	+0.9251	+2.12143	+10.7404	0.039	4.014	4.230
+3.70	+0.9270	+2.16891	+10.9412	0.040	4.019	4.229
+3.75	+0.9290	+2.21644	+11.1422	0.040	4.024	4.229
+3.80	+0.9311	+2.26403	+11.3435	0.041	4.027	4.229
+3.85	+0.9331	+2.31165	+11.5449	0.041	4.030	4.229
+3.90	+0.9352	+2.35931	+11.7464	0.042	4.032	4.228
+3.95	+0.9373	+2.40700	+11.9480	0.042	4.034	4.228
+4.00	+0.9394	+2.45471	+12.1498	0.043	4.035	4.228
+4.05	+0.9416	+2.50244	+12.3515	0.044	4.036	4.227
+4.10	+0.9438	+2.55018	+12.5534	0.044	4.037	4.227
+4.15	+0.9461	+2.59793	+12.7552	0.045	4.037	4.227
+4.20	+0.9483	+2.64568	+12.9570	0.046	4.037	4.226
+4.25	+0.9506	+2.69344	+13.1588	0.046	4.036	4.226

1.8

(2)	(4)	(5)	(6)	(7)	(8)	(9)
-1.05	+0.0000	-1.67839	-4.8224	0.000	51.936	4.250
-1.00	+0.0000	-1.62839	-4.6098	0.000	46.750	4.250
-0.95	+0.0000	-1.57839	-4.3974	0.002	42.128	4.250
-0.90	+0.0000	-1.52839	-4.1848	0.002	38.009	4.250
-0.85	+0.0000	-1.47839	-3.9724	0.002	34.336	4.250
-0.80	+0.0000	-1.42839	-3.7599	0.003	31.063	4.250
-0.75	+0.0001	-1.37839	-3.5474	0.004	28.145	4.250
-0.70	+0.0001	-1.32840	-3.3349	0.006	25.545	4.250
-0.65	+0.0002	-1.27841	-3.1225	0.008	23.226	4.249
-0.60	+0.0003	-1.22842	-2.9101	0.011	21.159	4.249
-0.55	+0.0004	-1.17844	-2.6977	0.015	19.314	4.249
-0.50	+0.0006	-1.12847	-2.4854	0.019	17.670	4.248
-0.45	+0.0009	-1.07852	-2.2732	0.026	16.201	4.248
-0.40	+0.0013	-1.02856	-2.0611	0.034	14.888	4.246
-0.35	+0.0019	-0.97869	-1.8493	0.045	13.715	4.245

1.8 (CONT.)

(2)	(4)	(5)	(6)	(7)	(8)	(9)
-0.30	+0.0027	-0.92883	-1.6377	0.058	12.665	4.243
-0.25	+0.0038	-0.87904	-1.4265	0.075	11.722	4.240
-0.20	+0.0054	-0.82934	-1.2159	0.096	10.873	4.236
-0.15	+0.0076	-0.77975	-1.0059	0.122	10.107	4.231
-0.10	+0.0105	-0.73033	-0.7970	0.152	9.412	4.224
-0.05	+0.0144	-0.68112	-0.5894	0.189	8.780	4.215
0.00	+0.0195	-0.63220	-0.3834	0.232	8.198	4.204
+0.05	+0.0261	-0.58364	-0.1796	0.282	7.661	4.190
+0.10	+0.0345	-0.53555	+0.0215	0.339	7.161	4.172
+0.15	+0.0451	-0.48804	+0.2192	0.403	6.690	4.151
+0.20	+0.0582	-0.44124	+0.4129	0.473	6.244	4.125
+0.25	+0.0743	-0.39529	+0.6018	0.550	5.818	4.095
+0.30	+0.0935	-0.35034	+0.7851	0.630	5.410	4.059
+0.35	+0.1164	-0.30655	+0.9619	0.714	5.018	4.019
+0.40	+0.1430	-0.26407	+1.1317	0.798	4.641	3.972
+0.45	+0.1735	-0.22302	+1.2937	0.880	4.280	3.921
+0.50	+0.2079	-0.18354	+1.4474	0.975	3.935	3.865
+0.55	+0.2461	-0.14569	+1.5926	1.025	3.609	3.805
+0.60	+0.2878	-0.10955	+1.7290	1.082	3.304	3.742
+0.65	+0.3324	-0.07511	+1.8568	1.125	3.023	3.678
+0.70	+0.3795	-0.04238	+1.9761	1.151	2.767	3.615
+0.75	+0.4281	-0.01129	+2.0876	1.158	2.537	3.555
+0.80	+0.4775	-0.01824	+2.1917	1.146	2.334	3.500
+0.85	+0.5268	-0.04632	+2.2893	1.116	2.159	3.454
+0.90	+0.5750	-0.07307	+2.3812	1.068	2.011	3.417
+0.95	+0.6214	-0.09864	+2.4683	1.006	1.889	3.393
+1.00	+0.6652	-0.12318	+2.5513	0.931	1.791	3.382
+1.05	+0.7059	-0.14683	+2.6314	0.850	1.715	3.384
+1.10	+0.7431	-0.16976	+2.7091	0.764	1.661	3.401
+1.15	+0.7766	-0.19212	+2.7855	0.677	1.625	3.431
+1.20	+0.8064	-0.21405	+2.8612	0.594	1.608	3.474
+1.25	+0.8325	-0.23570	+2.9369	0.519	1.615	3.525
+1.30	+0.8553	-0.25721	+3.0133	0.444	1.617	3.583
+1.35	+0.8750	-0.27872	+3.0911	0.380	1.642	3.648
+1.40	+0.8918	-0.30034	+3.1707	0.325	1.678	3.713
+1.45	+0.9063	-0.32222	+3.2526	0.276	1.724	3.778
+1.50	+0.9186	-0.34446	+3.3374	0.235	1.780	3.842
+1.55	+0.9292	-0.36717	+3.4253	0.200	1.844	3.901
+1.60	+0.9382	-0.39046	+3.5166	0.171	1.915	3.955
+1.65	+0.9459	-0.41443	+3.6122	0.146	1.992	4.003
+1.70	+0.9525	-0.43917	+3.7117	0.126	2.074	4.054
+0.75	+0.9583	-0.46474	+3.8156	0.109	2.161	4.080
+1.80	+0.9633	-0.49122	+3.9241	0.094	2.251	4.110
+1.85	+0.9676	-0.51866	+4.0373	0.083	2.343	4.135
+1.90	+0.9714	-0.54711	+4.1552	0.073	2.437	4.155
+1.95	+0.9748	-0.57660	+4.2780	0.065	2.532	4.171
+2.00	+0.9779	-0.60713	+4.4056	0.058	2.626	4.184
+2.05	+0.9806	-0.63873	+4.5380	0.052	2.720	4.195
+2.10	+0.9831	-0.67139	+4.6751	0.048	2.812	4.203
+2.15	+0.9853	-0.70510	+4.8169	0.044	2.902	4.210
+2.20	+0.9874	-0.73983	+4.9632	0.040	2.989	4.215
+2.25	+0.9893	-0.77556	+5.1139	0.037	3.073	4.219
+2.30	+0.9911	-0.81225	+5.2687	0.035	3.154	4.223
+2.35	+0.9928	-0.84986	+5.4276	0.033	3.231	4.225
+2.40	+0.9944	-0.88836	+5.5903	0.031	3.304	4.227
+2.45	+0.9959	-0.92769	+5.7566	0.030	3.373	4.229
+2.50	+0.9973	-0.96781	+5.9263	0.028	3.438	4.231
+2.55	+0.9987	-1.00867	+6.0992	0.027	3.498	4.232
+2.60	+1.0000	-1.05022	+6.2751	0.026	3.555	4.233
+2.65	+1.0013	-1.09242	+6.4538	0.026	3.608	4.234
+2.70	+1.0026	-1.13523	+ 6.6350	0.025	3.656	4.235
+2.75	+1.0038	-1.17858	+ 6.8186	0.025	3.701	4.235
+2.80	+1.0051	-1.22245	+ 7.0044	0.024	3.743	4.236
+2.85	+1.0063	-1.26679	+ 7.1922	0.024	3.781	4.236
+2.90	+1.0074	-1.31156	+ 7.3819	0.024	3.815	4.237
+2.95	+1.0086	-1.35672	+ 7.5732	0.024	3.847	4.237
+3.00	+1.0098	-1.40225	+ 7.7661	0.024	3.876	4.237
+3.05	+1.0110	-1.44810	+ 7.9604	0.024	3.926	4.237
+3.10	+1.0122	-1.49425	+ 8.1559	0.024	3.926	4.237
+3.15	+1.0134	-1.54067	+ 8.3526	0.024	3.947	4.237
+3.20	+1.0145	-1.58733	+ 8.5504	0.024	3.966	4.237
+3.25	+1.0157	-1.63422	+ 8.7490	0.024	3.984	4.237
+3.30	+1.0169	-1.68129	+ 8.9485	0.024	3.999	4.237
+3.35	+1.0182	-1.72855	+ 9.1487	0.024	4.013	4.237
+3.40	+1.0194	-1.77596	+ 9.3496	0.025	4.026	4.237
+3.45	+1.0206	-1.82352	+ 9.5511	0.025	4.037	4.237
+3.50	+1.0218	-1.87120	+ 9.7531	0.025	4.046	4.237
+3.55	+1.0231	-1.91899	+ 9.9556	0.026	4.055	4.237
+3.60	+1.0244	-1.96688	+10.1585	0.026	4.063	4.263
+3.65	+1.0257	-2.01486	+10.3618	0.026	4.069	4.236

1.8 (CONT.)

(2)	(4)	(5)	(6)	(7)	(8)	(9)
+3.70	+1.0271	-2.06291	+10.5654	0.027	4.075	4.236
+3.75	+1.0284	-2.11103	+10.7692	0.027	4.080	4.236
+3.80	+1.0298	-2.15920	+10.9732	0.028	4.084	4.236
+3.85	+1.0312	-2.20742	+11.1775	0.028	4.087	4.236
+3.90	+1.0326	-2.25569	+11.3819	0.029	4.090	4.236
+3.95	+1.0341	-2.30398	+11.5865	0.029	4.093	4.235
+4.00	+1.0355	-2.35231	+11.7911	0.030	4.095	4.235
+4.05	+1.0370	-2.40066	+11.9959	0.030	4.096	4.235
+4.10	+1.0386	-2.44902	+12.2007	0.031	4.097	4.234
+4.15	+1.0401	-2.49740	+12.4055	0.031	4.097	4.234
+4.20	+1.0417	-2.54579	+12.6104	0.032	4.097	4.234
+4.25	+1.0434	-2.59418	+12.8152	0.033	4.097	4.234

1.9

(2)	(4)	(5)	(6)	(7)	(8)	(9)
-1.00	+0.0000	-1.62839	- 4.4848	0.000	46.750	4.250
-0.95	+0.0000	-1.57839	- 4.2724	0.002	42.128	4.250
-0.90	+0.0000	-1.52839	- 4.0598	0.002	38.009	4.250
-0.85	+0.0000	-1.47839	- 3.8474	0.003	34.336	4.250
-0.80	+0.0000	-1.42839	- 3.6349	0.004	31.063	4.250
-0.75	+0.0001	-1.37839	- 3.4224	0.005	28.145	4.250
-0.70	+0.0001	-1.32840	- 3.2099	0.007	25.544	4.250
-0.65	+0.0002	-1.27841	- 2.9975	0.011	23.224	4.249
-0.60	+0.0003	-1.22842	- 2.7851	0.014	21.156	4.249
-0.55	+0.0005	-1.17845	- 2.5728	0.019	19.310	4.248
-0.50	+0.0008	-1.12849	- 2.3605	0.024	17.663	4.248
-0.45	+0.0011	-1.07855	- 2.1484	0.034	16.192	4.247
-0.40	+0.0017	-1.02864	- 1.9365	0.046	14.877	4.245
-0.35	+0.0024	-0.97877	- 1.7248	0.060	13.699	4.243
-0.30	+0.0035	-0.92896	- 1.5136	0.077	12.643	4.240
-0.25	+0.0051	-0.87924	- 1.3028	0.100	11.693	4.236
-0.20	+0.0072	-0.82963	- 1.0928	0.128	10.836	4.231
-0.15	+0.0101	-0.78018	- 0.8837	0.162	10.059	4.224
-0.10	+0.0140	-0.73094	- 0.6759	0.203	9.351	4.215
-0.05	+0.0192	-0.68200	- 0.4699	0.252	8.701	4.203
0.00	+0.0260	-0.63343	- 0.2661	0.309	8.100	4.188
+0.05	+0.0348	-0.58534	- 0.0651	0.376	7.539	4.169
+0.10	+0.0460	-0.53786	+ 0.1323	0.452	7.011	4.146
+0.15	+0.0601	-0.49114	+ 0.3253	0.536	6.509	4.117
+0.20	+0.0775	-0.44534	+ 0.5131	0.629	6.029	4.082
+0.25	+0.0988	-0.40064	+ 0.6947	0.729	5.567	4.040
+0.30	+0.1243	-0.35722	+ 0.8691	0.834	5.121	3.992
+0.35	+0.1545	-0.31524	+ 1.0355	0.942	4.690	3.935
+0.40	+0.1895	-0.27490	+ 1.1930	1.049	4.275	3.871
+0.45	+0.2295	-0.23631	+ 1.3410	1.151	3.879	3.800
+0.50	+0.2744	-0.19959	+ 1.4792	1.245	3.503	3.721
+0.55	+0.3240	-0.16480	+ 1.6072	1.326	3.152	3.637
+0.60	+0.3777	-0.13198	+ 1.7252	1.390	2.829	3.550
+0.65	+0.4348	-0.10109	+ 1.8334	1.432	2.535	3.460
+0.70	+0.4944	-0.07208	+ 1.9325	1.452	2.274	3.372
+0.75	+0.5554	-0.04484	+ 2.0232	1.446	2.044	3.288
+0.80	+0.6168	-0.01926	+ 2.1064	1.415	1.847	3.212
+0.85	+0.6772	+0.00483	+ 2.1830	1.359	1.680	3.147
+0.90	+0.7355	+0.02758	+ 2.2540	1.280	1.543	3.097
+0.95	+0.7906	+0.04914	+ 2.3204	1.184	1.434	3.064
+1.00	+0.8417	+0.06969	+ 2.3832	1.074	1.349	3.050
+1.05	+0.8880	+0.08940	+ 2.4433	0.957	1.287	3.056
+1.10	+0.9294	+0.10841	+ 2.5016	0.838	1.246	3.082
+1.15	+0.9657	+0.12689	+ 2.5590	0.722	1.222	3.125
+1.20	+0.9969	+0.14497	+ 2.6160	0.614	1.215	3.187
+1.25	+1.0236	+0.16281	+ 2.6735	0.516	1.223	3.261
+1.30	+1.0460	+0.18052	+ 2.7320	0.430	1.244	3.346
+1.35	+1.0647	+0.19825	+ 2.7921	0.356	1.276	3.438
+1.40	+1.0802	+0.21611	+ 2.8544	0.293	1.320	3.532
+1.45	+1.0931	+0.23423	+ 2.9192	0.241	1.373	3.626
+1.50	+1.1037	+0.25273	+ 2.9871	0.198	1.436	3.717
+1.55	+1.1124	+0.27171	+ 3.0585	0.163	1.506	3.802
+1.60	+1.1197	+0.29129	+ 3.1338	0.135	1.584	3.880
+1.65	+1.1257	+0.31158	+ 3.2132	0.112	1.669	3.948
+1.70	+1.1307	+0.33267	+ 3.2971	0.093	1.759	4.007
+1.75	+1.1349	+0.35464	+ 3.3857	0.078	1.854	4.057
+1.80	+1.1384	+0.37760	+ 3.4793	0.066	1.953	4.097
+1.85	+1.1414	+0.40160	+ 3.5781	0.056	2.056	4.130
+1.90	+1.1440	+0.42671	+ 3.6821	0.048	2.161	4.157
+1.95	+1.1462	+0.45297	+ 3.7916	0.042	2.268	4.177

1.9 (CONT.)

(2)	(4)	(5)	(6)	(7)	(8)	(9)
+2.00	+1.1481	0.48042	+ 3.9065	0.036	2.376	4.193
+2.05	+1.1498	0.50907	+ 4.0268	0.032	2.483	4.205
+2.10	+1.1513	0.53895	+ 4.1526	0.028	2.589	4.214
+2.15	+1.1527	0.57004	+ 4.2837	0.026	2.694	4.220
+2.20	+1.1539	0.60233	+ 4.4200	0.023	2.796	4.225
+2.25	+1.1550	0.63579	+ 4.5615	0.021	2.895	4.229
+2.30	+1.1560	0.67039	+ 4.7079	0.019	2.991	4.233
+2.35	+1.1569	0.70609	+ 4.8590	0.018	3.083	4.235
+2.40	+1.1577	0.74285	+ 5.0147	0.017	3.171	4.237
+2.45	+1.1586	0.78061	+ 5.1748	0.016	3.254	4.238
+2.50	+1.1593	0.81933	+ 5.3389	0.015	3.332	4.239
+2.55	+1.1600	0.85895	+ 5.5068	0.014	3.406	4.240
+2.60	+1.1607	0.89942	+ 5.6784	0.014	3.475	4.241
+2.65	+1.1614	0.94067	+ 5.8534	0.013	3.539	4.241
+2.70	+1.1621	0.98266	+ 6.0315	0.013	3.599	4.242
+2.75	+1.1627	1.02532	+ 6.2125	0.012	3.654	4.242
+2.80	+1.1633	1.06862	+ 6.3962	0.012	3.705	4.243
+2.85	+1.1639	1.11249	+ 6.5823	0.012	3.752	4.243
+2.90	+1.1645	1.15690	+ 6.7707	0.012	3.794	4.243
+2.95	+1.1651	1.20179	+ 6.9612	0.012	3.834	4.243
+3.00	+1.1657	1.24713	+ 7.1536	0.012	3.869	4.243
+3.05	+1.1663	1.29287	+ 7.3477	0.012	3.902	4.244
+3.10	+1.1669	1.33898	+ 7.5433	0.012	3.931	4.244
+3.15	+1.1675	1.38542	+ 7.7404	0.012	3.958	4.244
+3.20	+1.1680	1.43216	+ 7.9388	0.012	3.982	4.244
+3.25	+1.1686	1.47917	+ 8.1383	0.012	4.003	4.244
+3.30	+1.1692	1.52643	+ 8.3388	0.012	4.023	4.244
+3.35	+1.1698	1.57392	+ 8.5404	0.012	4.041	4.244
+3.40	+1.1704	1.62160	+ 8.7427	0.012	4.056	4.244
+3.45	+1.1711	1.66946	+ 8.9458	0.012	4.070	4.244
+3.50	+1.1717	1.71748	+ 9.1496	0.013	4.083	4.244
+3.55	+1.1723	1.76564	+ 9.3539	0.013	4.094	4.243
+3.60	+1.1730	1.81392	+ 9.5588	0.013	4.104	4.243
+3.65	+1.1737	1.86232	+ 9.7642	0.014	4.112	4.243
+3.70	+1.1743	1.91082	+ 9.9700	0.014	4.120	4.243
+3.75	+1.1750	1.95940	+10.1761	0.014	4.127	4.243
+3.80	+1.1757	2.00806	+10.3826	0.014	4.133	4.243
+3.85	+1.1764	2.05679	+10.5893	0.014	4.138	4.243
+3.90	+1.1772	2.10558	+10.7963	0.015	4.143	4.242
+3.95	+1.1779	2.15442	+11.0035	0.015	4.147	4.242
+4.00	+1.1787	2.20331	+11.2109	0.015	4.150	4.242
+4.05	+1.1795	2.25224	+11.4185	0.016	4.153	4.242
+4.10	+1.1802	2.30119	+11.6262	0.016	4.155	4.242
+4.15	+1.1811	2.35018	+11.8340	0.016	4.157	4.242
+4.20	+1.1819	2.39919	+12.0418	0.017	4.159	4.242
+4.25	+1.1827	2.44821	+12.2498	0.017	4.160	4.241

1.10

(2)	(4)	(5)	(6)	(7)	(8)	(9)
-1.00	+0.0000	-1.62839	-4.4349	0.002	46.750	4.250
-0.95	+0.0000	-1.57839	-4.2224	0.002	42.128	4.250
-0.90	+0.0000	-1.52839	-4.0099	0.002	38.007	4.250
-0.85	+0.0000	-1.47839	-3.7974	0.003	34.336	4.250
-0.80	+0.0001	-1.42839	-3.5849	0.004	31.061	4.250
-0.75	+0.0001	-1.37840	-3.3724	0.007	28.144	4.250
-0.70	+0.0002	-1.32841	-3.1600	0.009	25.542	4.249
-0.65	+0.0003	-1.27842	-2.9476	0.012	23.221	4.249
-0.60	+0.0004	-1.22844	-2.7352	0.016	21.153	4.249
-0.55	+0.0006	-1.17848	-2.5229	0.022	19.307	4.248
-0.50	+0.0009	-1.12852	-2.3107	0.029	17.658	4.247
-0.45	+0.0013	-1.07859	-2.0987	0.038	16.186	4.246
-0.40	+0.0019	-1.02870	-1.8869	0.051	14.870	4.245
-0.35	+0.0028	-0.97885	-1.6753	0.067	13.691	4.242
-0.30	+0.0040	-0.92906	-1.4642	0.087	12.632	4.239
-0.25	+0.0057	-0.87938	-1.2536	0.112	11.679	4.235
-0.20	+0.0081	-0.82982	-1.0439	0.143	10.818	4.229
-0.15	+0.0114	-0.78044	-0.8353	0.181	10.036	4.221
-0.10	+0.0157	-0.73130	-0.6281	0.228	9.321	4.211
-0.05	+0.0216	-0.68247	-0.4228	0.283	8.662	4.197
0.00	+0.0293	-0.63408	-0.2201	0.347	8.050	4.180
+0.05	+0.0392	-0.58623	-0.0206	0.421	7.478	4.159
+0.10	+0.0518	-0.53906	+0.1750	0.506	6.938	4.132
+0.15	+0.0676	-0.49272	+0.3658	0.601	6.421	4.100
+0.20	+0.0871	-0.44741	+0.5507	0.705	5.926	4.061
+0.25	+0.1109	-0.40331	+0.7287	0.816	5.447	4.013
+0.30	+0.1395	-0.36060	+0.8990	0.933	4.984	3.958
+0.35	+0.1732	-0.31948	+1.0604	1.052	4.536	3.894
+0.40	+0.2123	-0.28012	+1.2123	1.170	4.106	3.821
+0.45	+0.2568	-0.24265	+1.3539	1.282	3.696	3.740

1.10 (CONT.)

(2)	(4)	(5)	(6)	(7)	(8)	(9)
+0.50	+0.3068	-0.20719	+1.4850	1.384	3.310	3.649
+0.55	+0.3618	-0.17376	+1.6054	1.470	2.950	3.552
+0.60	+0.4212	-0.14239	+1.7153	1.538	2.621	3.451
+0.65	+0.4843	-0.11303	+1.8151	1.582	2.325	3.347
+0.70	+0.5501	-0.08560	+1.9055	1.600	2.063	3.245
+0.75	+0.6173	-0.05999	+1.9874	1.590	1.836	3.148
+0.80	+0.6847	-0.03604	+2.0617	1.551	1.642	3.059
+0.85	+0.7508	-0.01361	+2.1294	1.485	1.480	2.983
+0.90	+0.8144	+0.00748	+2.1917	1.393	1.348	2.923
+0.95	+0.8742	+0.02740	+2.2495	1.281	1.243	2.883
+1.00	+0.9293	+0.04632	+2.3038	1.155	1.164	2.863
+1.05	+0.9790	+0.06440	+2.3555	1.021	1.106	2.866
+1.10	+1.0230	+0.08180	+2.4056	0.885	1.068	2.892
+1.15	+1.0611	+0.09865	+2.4547	0.755	1.047	2.938
+1.20	+1.0936	+0.11512	+2.5036	0.634	1.042	3.005
+1.25	+1.1209	+0.13132	+2.5529	0.526	1.051	3.087
+1.30	+1.1436	+0.14739	+2.6032	0.432	1.072	3.182
+1.35	+1.1623	+0.16345	+2.6552	0.352	1.105	3.286
+1.40	+1.1775	+0.17961	+2.7092	0.286	1.148	3.395
+1.45	+1.1900	+0.19600	+2.7657	0.231	1.200	3.505
+1.50	+1.2001	+0.21272	+2.8252	0.187	1.261	3.611
+1.55	+1.2082	+0.22988	+2.8881	0.151	1.330	3.712
+1.60	+1.2149	+0.24760	+2.9547	0.123	1.407	3.805
+1.65	+1.2203	+0.26598	+3.0254	0.100	1.490	3.888
+1.70	+1.2248	+0.28513	+3.1006	0.082	1.580	3.960
+1.75	+1.2284	+0.30514	+3.1804	0.068	1.675	4.021
+1.80	+1.2315	+0.32609	+3.2653	0.056	1.775	4.072
+1.85	+1.2340	+0.34808	+3.3553	0.047	1.879	4.113
+1.90	+1.2361	+0.37117	+3.4506	0.040	1.987	4.145
+1.95	+1.2379	+0.39543	+3.5515	0.034	2.096	4.171
+2.00	+1.2395	+0.42089	+3.6580	0.029	2.208	4.189
+2.05	+1.2408	+0.44761	+3.7701	0.025	2.319	4.204
+2.10	+1.2420	+0.47559	+3.8879	0.022	2.431	4.215
+2.15	+1.2431	+0.50484	+4.0113	0.020	2.542	4.222
+2.20	+1.2440	+0.53537	+4.1403	0.017	2.651	4.228

1.11

(2)	(4)	(5)	(6)	(7)	(8)	(9)
-1.00	+0.0000	-1.62839	-4.3849	0.002	46.750	4.250
-0.95	+0.0000	-1.57839	-4.1724	0.002	42.128	4.250
-0.90	+0.0000	-1.52839	-3.9599	0.002	38.007	4.250
-0.85	+0.0000	-1.47839	-3.7474	0.003	34.336	4.250
-0.80	+0.0001	-1.42839	-3.5349	0.004	31.061	4.250
-0.75	+0.0001	-1.37840	-3.3224	0.007	28.144	4.250
-0.70	+0.0002	-1.32841	-3.1100	0.010	25.542	4.249
-0.65	+0.0003	-1.27842	-2.8976	0.013	23.222	4.249
-0.60	+0.0004	-1.22844	-2.6852	0.018	21.153	4.249
-0.55	+0.0006	-1.17847	-2.4729	0.025	19.305	4.248
-0.50	+0.0010	-1.12852	-2.2608	0.032	17.656	4.247
-0.45	+0.0014	-1.07860	-2.0488	0.044	16.182	4.246
-0.40	+0.0021	-1.02872	-1.8370	0.057	14.864	4.244
-0.35	+0.0031	-0.97889	-1.6256	0.075	13.682	4.241
-0.30	+0.0045	-0.92913	-1.4146	0.098	12.620	4.238
-0.25	+0.0065	-0.87947	-1.2043	0.126	11.664	4.233
-0.20	+0.0091	-0.82997	-0.9949	0.161	10.798	4.226
-0.15	+0.0127	-0.78066	-0.7867	0.204	10.010	4.218
-0.10	+0.0176	-0.73162	-0.5801	0.256	9.288	4.206
-0.05	+0.0242	-0.68294	-0.3757	0.317	8.620	4.191
0.00	+0.0327	-0.63473	-0.1741	0.389	7.999	4.172
+0.05	+0.0438	-0.58712	+0.0240	0.473	7.414	4.148
+0.10	+0.0579	-0.54026	+0.2176	0.568	6.859	4.118
+0.15	+0.0756	-0.49434	+0.4059	0.674	6.327	4.080
+0.20	+0.0975	-0.44955	+0.5877	0.789	5.814	4.036
+0.25	+0.1242	-0.40609	+0.7620	0.914	5.317	3.982
+0.30	+0.1562	-0.36416	+0.9276	1.044	4.835	3.919
+0.35	+0.1939	-0.32396	+1.0837	1.176	4.370	3.846
+0.40	+0.2375	-0.28567	+1.2295	1.306	3.923	3.762
+0.45	+0.2873	-0.24940	+1.3642	1.430	3.499	3.668

1.11 (CONT.)

(2)	(4)	(5)	(6)	(7)	(8)	(9)
+0.50	+0.3430	-0.21526	+1.4877	1.541	03.102	3.564
+0.55	+0.4042	-0.18328	+1.5999	1.636	02.735	3.452
+0.60	+0.4704	-0.15344	+1.7012	1.710	02.401	3.334
+0.65	+0.5405	-0.12569	+1.7921	1.758	02.103	3.214
+0.70	+0.6136	-0.09992	+1.8733	1.777	01.842	3.093
+0.75	+0.6882	-0.07599	+1.9460	1.766	01.617	2.978
+0.80	+0.7630	-0.05375	+2.0110	1.722	01.428	2.872
+0.85	+0.8364	-0.03302	+2.0696	1.648	01.271	2.779
+0.90	+0.9069	-0.01362	+2.1227	1.544	01.143	2.703
+0.95	+0.9731	+0.00461	+2.1715	1.417	01.043	2.650
+1.00	+1.0340	+0.02185	+2.2168	1.273	00.967	2.619
+1.05	+1.0886	+0.03825	+2.2597	1.119	00.912	2.613
+1.10	+1.1366	+0.05396	+2.3008	0.963	00.876	2.632
+1.15	+1.1779	+0.06913	+2.3411	0.814	00.856	2.676
+1.20	+1.2128	+0.08389	+2.3810	0.677	00.851	2.743
+1.25	+1.2418	+0.09835	+2.4213	0.554	00.858	2.829
+1.30	+1.2655	+0.11265	+2.4625	0.448	00.877	2.932
+1.35	+1.2847	+0.12689	+2.5050	0.360	00.907	3.046
+1.40	+1.3001	+0.14117	+2.5494	0.287	00.946	3.170
+1.45	+1.3125	+0.15561	+2.5961	0.228	00.993	3.296
+1.50	+1.3223	+0.17030	+2.6455	0.181	01.049	3.423
+1.55	+1.3302	+0.18536	+2.6979	0.143	01.113	3.544
+1.60	+1.3364	+0.20088	+2.7538	0.114	01.184	3.660
+1.65	+1.3414	+0.21697	+2.8136	0.091	01.262	3.764
+1.70	+1.3454	+0.23372	+2.8774	0.073	01.347	3.858
+1.75	+1.3486	+0.25124	+2.9458	0.059	01.438	3.939
+1.80	+1.3512	+0.26962	+3.0189	0.048	01.535	4.008
+1.85	+1.3534	+0.28896	+3.0969	0.039	01.636	4.064
+1.90	+1.3551	+0.30934	+3.1802	0.032	01.742	4.110
+1.95	+1.3566	+0.33084	+3.2690	0.027	01.851	4.146
+2.00	+1.3578	+0.35352	+3.3633	0.023	01.963	4.173
+2.05	+1.3588	+0.37744	+3.4634	0.019	02.078	4.194
+2.10	+1.3597	+0.40264	+3.5693	0.017	02.193	4.209
+2.15	+1.3605	+0.42915	+3.6810	0.014	02.309	4.219
+2.20	+1.3611	+0.45699	+3.7986	0.012	02.424	4.227

1.12

(2)	(4)	(5)	(6)	(7)	(8)	(9)
-1.05	+0.0000	-1.67839	- 4.5474	0.000	51.936	4.250
-1.00	+0.0000	-1.62839	- 4.3349	0.002	46.750	4.250
-0.95	+0.0000	-1.57839	- 4.1224	0.002	42.128	4.250
-0.90	+0.0000	-1.52839	- 3.9099	0.004	38.007	4.250
-0.85	+0.0000	-1.47839	- 3.6974	0.005	34.334	4.250
-0.80	+0.0001	-1.42840	- 3.4849	0.006	31.061	4.250
-0.75	+0.0001	-1.37840	- 3.2724	0.008	28.143	4.250
-0.70	+0.0002	-1.32841	- 3.0600	0.011	25.540	4.249
-0.65	+0.0003	-1.27843	- 2.8476	0.014	23.219	4.249
-0.60	+0.0005	-1.22845	- 2.6353	0.020	21.149	4.248
-0.55	+0.0007	-1.17849	- 2.4230	0.027	19.301	4.248
-0.50	+0.0011	-1.12855	- 2.2109	0.037	17.651	4.247
-0.45	+0.0017	-1.07864	- 1.9990	0.048	16.176	4.245
-0.40	+0.0024	-1.02877	- 1.7873	0.064	14.856	4.243
-0.35	+0.0035	-0.97895	- 1.5760	0.084	13.671	4.240
-0.30	+0.0051	-0.92923	- 1.3653	0.110	12.606	4.236
-0.25	+0.0072	-0.87962	- 1.1552	0.141	11.645	4.231
-0.20	+0.0102	-0.83018	- 0.9462	0.180	10.774	4.223
-0.15	+0.0143	-0.78096	- 0.7385	0.229	09.979	4.213
-0.10	+0.0198	-0.73204	- 0.5327	0.287	09.249	4.201
-0.05	+0.0272	-0.68352	- 0.3293	0.356	08.573	4.184
0.00	+0.0368	-0.63552	- 0.1290	0.437	07.939	4.162
+0.05	+0.0492	-0.58820	+ 0.0673	0.530	07.341	4.135
+0.10	+0.0650	-0.54171	+ 0.2588	0.637	06.770	4.101
+0.15	+0.0849	-0.49626	+ 0.4442	0.755	06.221	4.060
+0.20	+0.1095	-0.45206	+ 0.6226	0.885	05.689	4.008
+0.25	+0.1393	-0.40931	+ 0.7926	1.023	05.173	3.947
+0.30	+0.1751	-0.36824	+ 0.9533	1.168	04.673	3.875
+0.35	+0.2173	-0.32904	+ 1.1036	1.314	04.190	3.790
+0.40	+0.2660	-0.29189	+ 1.2427	1.459	03.727	3.694
+0.45	+0.3216	-0.25691	+ 1.3701	1.595	03.290	3.586
+0.50	+0.3837	-0.22418	+ 1.4855	1.719	02.883	3.466
+0.55	+0.4520	-0.19371	+ 1.5892	1.825	02.509	3.335
+0.60	+0.5258	-0.16547	+ 1.6815	1.909	02.173	3.198
+0.65	+0.6042	-0.13937	+ 1.7631	1.965	01.875	3.055
+0.70	+0.6859	-0.11528	+ 1.8349	1.991	01.616	2.913
+0.75	+0.7697	-0.09306	+ 1.8981	1.984	01.395	2.773
+0.80	+0.8539	-0.07253	+ 1.9537	1.943	01.209	2.644
+0.85	+0.9368	-0.05351	+ 2.0029	1.867	01.057	2.527
+0.90	+1.0169	-0.03582	+ 2.0467	1.758	00.934	2.428

1.13

(2)	(4)	(5)	(6)	(7)	(8)	(9)
-1.05	+0.0000	-1.67839	-4.4974	0.000	51.936	4.250
-1.00	+0.0000	-1.62839	-4.2848	0.002	46.750	4.250
-0.95	+0.0000	-1.57839	-4.0724	0.002	42.128	4.250
-0.90	+0.0000	-1.52839	-3.8598	0.004	38.007	4.250
-0.85	+0.0000	-1.47839	-3.6474	0.005	34.334	4.250
-0.80	+0.0000	-1.42839	-3.4349	0.006	31.189	4.250
-0.75	+0.0001	-1.37840	-3.2224	0.009	28.142	4.250
-0.70	+0.0002	-1.32841	-3.0100	0.012	25.539	4.249
-0.65	+0.0003	-1.27843	-2.7976	0.016	23.218	4.249
-0.60	+0.0005	-1.22846	-2.5853	0.023	21.147	4.248
-0.55	+0.0008	-1.17850	-2.3731	0.030	19.299	4.248
-0.50	+0.0012	-1.12857	-2.1610	0.041	17.647	4.246
-0.45	+0.0018	-1.07866	-1.9492	0.054	16.170	4.245
-0.40	+0.0027	-1.02881	-1.7376	0.072	14.848	4.243
-0.35	+0.0039	-0.97902	-1.5264	0.095	13.661	4.239
-0.30	+0.0057	-0.92933	-1.3159	0.123	12.592	4.235
-0.25	+0.0081	-0.87976	-1.1061	0.158	11.626	4.228
-0.20	+0.0115	-0.83038	-0.8975	0.203	10.749	4.220
-0.15	+0.0161	-0.78126	-0.6905	0.257	9.946	4.209
-0.10	+0.0222	-0.73247	-0.4855	0.322	9.207	4.194
-0.05	+0.0305	-0.68413	-0.2831	0.399	8.519	4.176
-0.00	+0.0413	-0.63637	-0.0843	0.490	7.873	4.151
+0.05	+0.0552	-0.58936	+0.1102	0.595	7.259	4.120
+0.10	+0.0730	-0.54327	+0.2992	0.714	6.671	4.081
+0.15	+0.0953	-0.49834	+0.4816	0.847	6.103	4.034
+0.20	+0.1228	-0.45477	+0.6561	0.992	5.551	3.976
+0.25	+0.1563	-0.41280	+0.8216	1.146	5.015	3.906
+0.30	+0.1964	-0.37266	+0.9768	1.308	4.495	3.827
+0.35	+0.2435	-0.33455	+1.1207	1.471	3.994	3.727
+0.40	+0.2981	-0.29864	+1.2526	1.632	3.516	3.616
+0.45	+0.3603	-0.26503	+1.3721	1.785	3.066	3.490
+0.50	+0.4298	-0.23379	+1.4790	1.926	2.650	3.350
+0.55	+0.5064	-0.20491	+1.5736	2.048	2.272	3.197
+0.60	+0.5894	-0.17832	+1.6565	2.149	1.933	3.034
+0.65	+0.6778	-0.15393	+1.7284	2.223	1.636	2.864
+0.70	+0.7706	-0.13158	+1.7905	2.268	1.380	2.691
+0.75	+0.8664	-0.11110	+1.8439	2.281	1.164	2.520
+0.80	+0.9637	-0.09232	+1.8897	2.260	0.983	2.356

1.14

(2)	(4)	(5)	(6)	(7)	(8)	(9)
-1.00	+0.0000	-1.62839	-4.2348	0.002	46.750	4.250
-0.95	+0.0000	-1.57839	-4.0224	0.002	42.128	4.250
-0.90	+0.0000	-1.52839	-3.8098	0.004	38.009	4.250
-0.85	+0.0000	-1.47839	-3.5974	0.005	34.336	4.250
-0.80	+0.0001	-1.42839	-3.3849	0.007	31.061	4.250
-0.75	+0.0001	-1.37840	-3.1724	0.009	28.142	4.250
-0.70	+0.0002	-1.32841	-2.9600	0.013	25.538	4.249
-0.65	+0.0003	-1.27842	-2.7476	0.018	23.218	4.249
-0.60	+0.0006	-1.22845	-2.5353	0.025	21.146	4.248
-0.55	+0.0009	-1.17850	-2.3231	0.034	19.296	4.247
-0.50	+0.0013	-1.12857	-2.1111	0.046	17.644	4.246
-0.45	+0.0020	-1.07867	-1.8992	0.061	16.165	4.244
-0.40	+0.0029	-1.02882	-1.6877	0.081	14.840	4.242
-0.35	+0.0043	-0.97906	-1.4767	0.106	13.649	4.238
-0.30	+0.0063	-0.92939	-1.2664	0.138	12.576	4.233
-0.25	+0.0090	-0.87988	-1.0570	0.178	11.605	4.226
-0.20	+0.0128	-0.83057	-0.8488	0.227	10.721	4.216
-0.15	+0.0179	-0.78154	-0.6424	0.288	9.910	4.204
-0.10	+0.0249	-0.73289	-0.4382	0.361	9.160	4.188
-0.05	+0.0341	-0.68475	-0.2371	0.448	8.460	4.166
0.00	+0.0462	-0.63725	-0.0398	0.550	7.800	4.139
+0.05	+0.0619	-0.59058	+0.1525	0.668	7.169	4.104
+0.10	+0.0818	-0.54494	+0.3388	0.801	6.562	4.060
+0.15	+0.1068	-0.50058	+0.5178	0.950	5.974	4.006
+0.20	+0.1377	-0.45772	+0.6881	1.112	5.401	3.940
+0.25	+0.1752	-0.41661	+0.8485	1.286	4.843	3.860
+0.30	+0.2202	-0.37748	+0.9977	1.466	4.303	3.765
+0.35	+0.2731	-0.34054	+1.1348	1.649	3.783	3.654
+0.40	+0.3343	-0.30594	+1.2590	1.831	3.290	3.524
+0.45	+0.4040	-0.27379	+1.3701	2.006	2.829	3.377
+0.50	+0.4823	-0.24411	+1.4680	2.170	2.405	3.212
+0.55	+0.5687	-0.21687	+1.5532	2.319	2.023	3.030
+0.60	+0.6630	-0.19200	+1.6262	2.450	1.684	2.836
+0.65	+0.7643	-0.16935	+1.6882	2.562	1.389	2.629
+0.70	+0.8721	-0.14877	+1.7401	2.654	1.137	2.416

1.14 (CONT.)

(2)	(4)	(5)	(6)	(7)	(8)	(9)
+0.75	+0.9853	−0.13006	+1.7833	2.726	0.924	2.200
+0.80	+1.1032	−0.11304	+1.8190	2.777	0.748	1.986
+0.85	+1.2247	−0.09750	+1.8483	2.808	0.603	1.778
+0.90	+1.3488	−0.08328	+1.8722	2.817	0.485	1.581
+0.95	+1.4745	−0.07020	+1.8916	2.804	0.391	1.398
+1.00	+1.6006	−0.05811	+1.9075	2.767	0.315	1.232
+1.05	+1.7256	−0.04687	+1.9205	2.703	0.256	1.084
+1.10	+1.8482	−0.03637	+1.9312	2.607	0.210	0.956
+1.15	+1.9665	−0.02651	+1.9401	2.477	0.174	0.847
+1.20	+2.0789	−0.01720	+1.9476	2.312	0.146	0.759
+1.25	+2.1834	−0.00836	+1.9540	2.111	0.125	0.688
+1.30	+2.2782	+0.00009	+1.9595	1.879	0.110	0.637
+1.35	+2.3619	+0.00819	+1.9645	1.627	0.100	0.600
+1.40	+2.4337	+0.01600	+1.9691	1.368	0.093	0.581
+1.45	+2.4936	+0.02356	+1.9735	1.117	0.089	0.575
+1.50	+2.5420	+0.03091	+1.9777	0.888	0.087	0.583
+1.55	+2.5801	+0.03809	+1.9820	0.688	0.088	0.602
+1.60	+2.6094	+0.04512	+1.9863	0.523	0.090	0.633
+1.65	+2.6316	+0.05203	+1.9908	0.390	0.095	0.675
+1.70	+2.6481	+0.05884	+1.9956	0.288	0.100	0.726
+1.75	+2.6602	+0.06559	+2.0007	0.210	0.108	0.787
+1.80	+2.6690	+0.07228	+2.0062	0.152	0.116	0.856
+1.85	+2.6754	+0.07895	+2.0122	0.110	0.126	0.936
+1.90	+2.6800	+0.08560	+2.0187	0.079	0.138	1.023
+1.95	+2.6834	+0.09226	+2.0258	0.057	0.151	1.120
+2.00	+2.6857	+0.09895	+2.0336	0.040	0.166	1.225
+2.05	+2.6874	+0.10567	+2.0422	0.029	0.182	1.337
+2.10	+2.6886	+0.11246	+2.0517	0.021	0.201	1.458
+2.15	+2.6895	+0.11933	+2.0622	0.015	0.221	1.587
+2.20	+2.6902	+0.12629	+2.0737	0.011	0.243	1.721
+2.25	+2.6906	+0.13338	+2.0864	0.008	0.268	1.863
+2.30	+2.6909	+0.14061	+2.1004	0.006	0.296	2.011

1.15

(2)	(4)	(5)	(6)	(7)	(8)	(9)
-1.00	+0.0000	-1.62839	-3.9848	0.003	46.750	4.250
-0.95	+0.0000	-1.57839	-3.7724	0.004	42.126	4.250
-0.90	+0.0000	-1.52839	-3.5599	0.007	38.005	4.250
-0.85	+0.0001	-1.47839	-3.3474	0.010	34.330	4.250
-0.80	+0.0002	-1.42840	-3.1350	0.013	31.054	4.249
-0.75	+0.0003	-1.37842	-2.9226	0.017	28.134	4.249
-0.70	+0.0004	-1.32844	-2.7102	0.024	25.528	4.249
-0.65	+0.0007	-1.27849	-2.4980	0.033	23.202	4.248
-0.60	+0.0011	-1.22853	-2.2858	0.045	21.125	4.247
-0.55	+0.0016	-1.17862	-2.0739	0.061	19.268	4.245
-0.50	+0.0024	-1.12875	-1.8622	0.082	17.606	4.243
-0.45	+0.0036	-1.07894	-1.6510	0.108	16.114	4.240
-0.40	+0.0054	-1.02922	-1.4403	0.144	14.771	4.235
-0.35	+0.0078	-0.97964	-1.2305	0.188	13.558	4.228
-0.30	+0.0113	-0.93024	-1.0218	0.246	12.457	4.220
-0.25	+0.0162	-0.88111	-0.8148	0.317	11.448	4.207
-0.20	+0.0229	-0.83233	-0.6100	0.405	10.517	4.190
-0.15	+0.0321	-0.78405	-0.4082	0.513	9.649	4.167
-0.10	+0.0444	-0.73643	-0.2104	0.644	8.819	4.137
-0.05	+0.0609	-0.68966	-0.0178	0.799	8.045	4.098
0.00	+0.0824	-0.64400	+0.1682	0.981	7.288	4.047
+0.05	+0.1103	-0.59972	+0.3460	1.191	6.548	3.981
+0.10	+0.1459	-0.55713	+0.5139	1.429	5.823	3.897
+0.15	+0.1905	-0.51656	+0.6700	1.697	5.112	3.791
+0.20	+0.2457	-0.47830	+0.8126	1.992	4.416	3.660
+0.25	+0.3132	-0.44266	+0.9403	2.317	3.743	3.496
+0.30	+0.3946	-0.40983	+1.0520	2.674	3.102	3.295
+0.35	+0.4921	-0.37998	+1.1469	3.074	2.502	3.051

1.16

(2)	(4)	(5)	(6)	(7)	(8)	(9)
-1.00	+0.0000	-1.62839	-3.7348	0.007	46.748	4.250
-0.95	+0.0000	-1.57839	-3.5224	0.008	42.124	4.250
-0.90	+0.0001	-1.52839	-3.3099	0.011	38.000	4.249
-0.85	+0.0002	-1.47840	-3.0975	0.016	34.325	4.249
-0.80	+0.0003	-1.42842	-2.8851	0.022	31.045	4.249
-0.75	+0.0005	-1.37844	-2.6728	0.030	28.122	4.248
-0.70	+0.0008	-1.32848	-2.4605	0.043	25.510	4.247
-0.65	+0.0012	-1.27855	-2.2484	0.059	23.177	4.246
-0.60	+0.0019	-1.22865	-2.0366	0.080	21.090	4.244
-0.55	+0.0029	-1.17880	-1.8251	0.108	19.220	4.242
-0.50	+0.0044	-1.12903	-1.6141	0.145	17.539	4.237
-0.45	+0.0065	-1.07937	-1.4038	0.193	16.025	4.232
-0.40	+0.0095	-1.02987	-1.1945	0.256	14.652	4.223
-0.35	+0.0139	-0.98061	-0.9868	0.336	13.400	4.212
-0.30	+0.0201	-0.93167	-0.7810	0.438	12.247	4.195
-0.25	+0.0288	-0.88320	-0.5782	0.566	11.174	4.173
-0.20	+0.0408	-0.83535	-0.3792	0.724	10.163	4.142
-0.15	+0.0572	-0.78835	-0.1855	0.917	9.198	4.101
-0.10	+0.0793	-0.74248	+0.0014	1.152	8.262	4.044
-0.05	+0.1088	-0.69804	+0.1796	1.432	7.346	3.970
0.00	+0.1475	-0.65541	+0.3468	1.764	6.441	3.871
+0.05	+0.1978	-0.61499	+0.5008	2.155	5.546	3.742
+0.10	+0.2624	-0.57718	+0.6393	2.613	4.663	3.572
+0.15	+0.3447	-0.54235	+0.7601	3.160	3.803	3.350
+0.20	+0.4493	-0.51081	+0.8615	3.839	2.978	3.061

2.1

(2)	(4)	(5)	(6)	(10)	(11)	(7)	(8)	(9)
-1.30	+0.0000	-2.07162	-7.7008	0.7404	2.0212	0.000	91.684	4.148
-1.25	+0.0000	-2.01887	-7.4820	0.7450	2.0592	0.000	82.186	4.148
-1.20	+0.0000	-1.96613	-7.2633	0.7495	2.0988	0.000	73.704	4.147
-1.15	+0.0000	-1.91339	-7.0446	0.7539	2.1403	0.000	66.134	4.146
-1.10	+0.0000	-1.86066	-6.8261	0.7582	2.1838	0.000	59.382	4.145
-1.05	+0.0000	-1.80795	-6.6076	0.7624	2.2293	0.000	53.361	4.143
-1.00	+0.0000	-1.75527	-6.3894	0.7665	2.2770	0.000	47.991	4.142
-0.95	+0.0000	-1.70262	-6.1714	0.7704	2.3270	0.000	43.205	4.140
-0.90	+0.0000	-1.64999	-5.9536	0.7743	2.3794	0.000	38.939	4.138
-0.85	+0.0000	-1.59741	-5.7360	0.7780	2.4344	0.000	35.138	4.137
-0.80	+0.0000	-1.54486	-5.5187	0.7816	2.4921	0.000	31.750	4.135
-0.75	+0.0000	-1.49236	-5.3016	0.7851	2.5527	0.000	28.734	4.133
-0.70	+0.0000	-1.43990	-5.0849	0.7885	2.6161	0.000	26.046	4.131
-0.65	+0.0000	-1.38749	-4.8684	0.7918	2.6829	0.000	23.652	4.129
-0.60	+0.0000	-1.33513	-4.6522	0.7950	2.7529	0.000	21.519	4.127
-0.55	+0.0000	-1.28282	-4.4364	0.7981	2.8265	0.000	19.621	4.125
-0.50	+0.0000	-1.23056	-4.2208	0.8011	2.9038	0.000	17.930	4.123
-0.45	+0.0000	-1.17835	-4.0056	0.8040	2.9850	0.001	16.424	4.121
-0.40	+0.0000	-1.12619	-3.7907	0.8068	3.0705	0.001	15.084	4.119
-0.35	+0.0000	-1.07408	-3.5761	0.8095	3.1604	0.001	13.890	4.117
-0.30	+0.0000	-1.02203	-3.3619	0.8122	3.2549	0.001	12.825	4.114
-0.25	+0.0001	-0.97002	-3.1480	0.8147	3.3544	0.002	11.878	4.112
-0.20	+0.0001	-0.91806	-2.9344	0.8171	3.4591	0.002	11.033	4.110
-0.15	+0.0001	-0.86616	-2.7211	0.8195	3.5695	0.002	10.281	4.107
-0.10	+0.0002	-0.81431	-2.5082	0.8218	3.6857	0.003	9.611	4.105
-0.05	+0.0003	-0.76252	-2.2957	0.8240	3.8083	0.003	9.013	4.102
0.00	+0.0004	-0.71077	-2.0835	0.8261	3.9375	0.004	8.481	4.100
+0.05	+0.0005	-0.65908	-1.8716	0.8281	4.0737	0.005	8.006	4.097
+0.10	+0.0006	-0.60745	-1.6601	0.8300	4.2175	0.006	7.582	4.094
+0.15	+0.0008	-0.55587	-1.4490	0.8319	4.3694	0.008	7.204	4.091
+0.20	+0.0011	-0.50435	-1.2384	0.8337	4.5299	0.009	6.866	4.088
+0.25	+0.0014	-0.45290	-1.0281	0.8354	4.6995	0.010	6.564	4.085
+0.30	+0.0017	-0.40150	-0.8182	0.8370	4.8790	0.012	6.294	4.082
+0.35	+0.0022	-0.35018	-0.6088	0.8385	5.0689	0.014	6.052	4.078
+0.40	+0.0027	-0.29893	-0.3999	0.8400	5.2701	0.015	5.835	4.075
+0.45	+0.0033	-0.24776	-0.1915	0.8414	5.4832	0.017	5.641	4.071
+0.50	+0.0040	-0.19666	+0.0164	0.8426	5.7091	0.019	5.466	4.067
+0.55	+0.0048	-0.14566	+0.2238	0.8438	5.9486	0.021	5.309	4.063
+0.60	+0.0056	-0.09474	+0.4306	0.8450	6.2029	0.023	5.167	4.059
+0.65	+0.0066	-0.04392	+0.6368	0.8460	6.4726	0.025	5.040	4.055
+0.70	+0.0077	+0.00680	+0.8424	0.8470	6.7592	0.027	4.925	4.051
+0.75	+0.0089	+0.05741	+1.0473	0.8478	7.0635	0.029	4.821	4.047
+0.80	+0.0102	+0.10792	+1.2516	0.8486	7.3869	0.031	4.726	4.043
+0.85	+0.0116	+0.15832	+1.4553	0.8493	7.7308	0.033	4.641	4.039
+0.90	+0.0130	+0.20860	+1.6583	0.8500	8.0962	0.034	4.563	4.035
+0.95	+0.0146	+0.25876	+1.8606	0.8506	8.4846	0.036	4.493	4.031
+1.00	+0.0163	+0.30881	+2.0622	0.8510	8.8975	0.038	4.429	4.027
+1.05	+0.0180	+0.35874	+2.2632	0.8515	9.3365	0.039	4.370	4.023
+1.10	+0.0199	+0.40855	+2.4634	0.8518	9.8036	0.040	4.317	4.019
+1.15	+0.0218	+0.45823	+2.6631	0.8521	10.3000	0.042	4.268	4.016
+1.20	+0.0237	+0.50780	+2.8620	0.8524	10.8278	0.042	4.223	4.012
+1.25	+0.0258	+0.55725	+3.0603	0.8525	11.3894	0.044	4.183	4.009
+1.30	+0.0278	+0.60659	+3.2580	0.8527	11.9863	0.044	4.145	4.005
+1.35	+0.0300	+0.65581	+3.4551	0.8527	12.6210	0.045	4.112	4.002
+1.40	+0.0321	+0.70493	+3.6516	0.8527	13.2954	0.046	4.080	3.999
+1.45	+0.0343	+0.75393	+3.8475	0.8527	14.0127	0.046	4.052	3.997
+1.50	+0.0366	+0.80284	+4.0429	0.8526	14.7751	0.046	4.026	3.994
+1.55	+0.0388	+0.85164	+4.2378	0.8525	15.5844	0.047	4.002	3.992
+1.60	+0.0411	+0.90035	+4.4322	0.8524	16.4452	0.047	3.980	3.989
+1.65	+0.0434	+0.94898	+4.6261	0.8522	17.3604	0.047	3.960	3.987
+1.70	+0.0457	+0.99752	+4.8196	0.8519	18.3329	0.047	3.942	3.985
+1.75	+0.0480	+1.04597	+5.0126	0.8516	19.3655	0.047	3.926	3.983
+1.80	+0.0503	+1.09435	+5.2053	0.8514	20.4621	0.047	3.911	3.981
+1.85	+0.0526	+1.14266	+5.3976	0.8510	21.6275	0.047	3.897	3.980
+1.90	+0.0549	+1.19091	+5.5896	0.8507	22.8645	0.046	3.885	3.978

2.2

(2)	(4)	(5)	(6)	(10)	(11)	(7)	(8)	(9)
-1.30	+0.0000	-2.07162	-6.7008	0.7404	2.0212	0.000	91.684	4.148
-1.25	+0.0000	-2.01887	-6.4820	0.7450	2.0591	0.000	82.186	4.148
-1.20	+0.0000	-1.96613	-6.2633	0.7495	2.0987	0.000	73.707	4.147
-1.15	+0.0000	-1.91339	-6.0446	0.7539	2.1403	0.000	66.134	4.146
-1.10	+0.0000	-1.86066	-5.8260	0.7582	2.1838	0.000	59.382	4.144
-1.05	+0.0000	-1.80795	-5.6076	0.7624	2.2293	0.000	53.363	4.143
-1.00	+0.0000	-1.75527	-5.3894	0.7665	2.2770	0.000	47.993	4.142
-0.95	+0.0000	-1.70261	-5.1714	0.7704	2.3270	0.000	43.205	4.140
-0.90	+0.0000	-1.64998	-4.9535	0.7743	2.3796	0.000	38.937	4.138
-0.85	+0.0000	-1.59740	-4.7360	0.7780	2.4344	0.000	35.136	4.137
-0.80	+0.0000	-1.54486	-4.5186	0.7816	2.4921	0.000	31.751	4.135
-0.75	+0.0000	-1.49236	-4.3016	0.7851	2.5526	0.001	28.732	4.133
-0.70	+0.0000	-1.43990	-4.0848	0.7885	2.6161	0.001	26.045	4.131
-0.65	+0.0000	-1.38749	-3.8684	0.7918	2.6828	0.001	23.651	4.129
-0.60	+0.0000	-1.33513	-3.6522	0.7950	2.7530	0.002	21.518	4.127
-0.55	+0.0001	-1.28282	-3.4364	0.7981	2.8266	0.003	19.618	4.125
-0.50	+0.0001	-1.23056	-3.2209	0.8011	2.9040	0.003	17.926	4.123
-0.45	+0.0002	-1.17836	-3.0057	0.8040	2.9854	0.004	16.419	4.121
-0.40	+0.0002	-1.12621	-2.7909	0.8068	3.0709	0.006	15.076	4.118
-0.35	+0.0003	-1.07412	-2.5764	0.8095	3.1611	0.008	13.879	4.116
-0.30	+0.0005	-1.02209	-2.3624	0.8121	3.2562	0.011	12.812	4.113
-0.25	+0.0007	-0.97013	-2.1487	0.8146	3.3562	0.014	11.862	4.110
-0.20	+0.0010	-0.91823	-1.9355	0.8170	3.4617	0.018	11.012	4.107
-0.15	+0.0014	-0.86640	-1.7227	0.8192	3.5735	0.023	10.253	4.103
-0.10	+0.0020	-0.81465	-1.5105	0.8214	3.6916	0.029	9.575	4.099
-0.05	+0.0027	-0.76300	-1.2989	0.8234	3.8168	0.036	8.968	4.095
0.00	+0.0037	-0.71145	-1.0879	0.8254	3.9495	0.044	8.423	4.089
+0.05	+0.0049	-0.66002	-0.8778	0.8272	4.0909	0.053	7.933	4.083
+0.10	+0.0065	-0.60873	-0.6685	0.8288	4.2417	0.064	7.492	4.077
+0.15	+0.0085	-0.55761	-0.4603	0.8302	4.4028	0.076	7.093	4.069
+0.20	+0.0109	-0.50668	-0.2533	0.8315	4.5755	0.088	6.731	4.060
+0.25	+0.0139	-0.45598	-0.0477	0.8326	4.7610	0.103	6.401	4.050
+0.30	+0.0175	-0.40553	+0.1564	0.8335	4.9615	0.118	6.100	4.039
+0.35	+0.0218	-0.35538	+0.3586	0.8341	5.1780	0.134	5.823	4.026
+0.40	+0.0268	-0.30557	+0.5588	0.8345	5.4129	0.150	5.569	4.012
+0.45	+0.0325	-0.25613	+0.7568	0.8346	5.6678	0.166	5.333	3.998
+0.50	+0.0391	-0.20712	+0.9524	0.8344	5.9454	0.183	5.114	3.982
+0.55	+0.0464	-0.15858	+1.1453	0.8339	6.2484	0.198	4.910	3.965
+0.60	+0.0545	-0.11053	+1.3354	0.8331	6.5789	0.214	4.721	3.948
+0.65	+0.0634	-0.06302	+1.5225	0.8320	6.9401	0.227	4.544	3.930
+0.70	+0.0730	-0.01607	+1.7066	0.8305	7.3350	0.239	4.379	3.912
+0.75	+0.0833	+0.03030	+1.8876	0.8288	7.7660	0.249	4.226	3.894
+0.80	+0.0941	+0.07606	+2.0654	0.8267	8.2366	0.256	4.084	3.877
+0.85	+0.1054	+0.12122	+2.2401	0.8243	8.7495	0.262	3.952	3.860
+0.90	+0.1170	+0.16577	+2.4117	0.8216	9.3087	0.265	3.831	3.845
+0.95	+0.1289	+0.20972	+2.5804	0.8187	9.9158	0.266	3.721	3.832
+1.00	+0.1409	+0.25310	+2.7464	0.8155	10.5750	0.264	3.621	3.819

2.3

(2)	(4)	(5)	(6)	(10)	(7)	(8)	(9)
-1.30	+0.0000	-2.04022	-6.4382	0.8106	0.000	93.386	4.224
-1.25	+0.0000	-1.98746	-6.2154	0.8157	0.000	83.707	4.224
-1.20	+0.0000	-1.93472	-5.9926	0.8207	0.000	75.068	4.225
-1.15	+0.0000	-1.88201	-5.7698	0.8255	0.000	67.366	4.225
-1.10	+0.0000	-1.82932	-5.5472	0.8302	0.000	60.494	4.226
-1.05	+0.0000	-1.77668	-5.3247	0.8348	0.000	54.368	4.227
-1.00	+0.0000	-1.72407	-5.1023	0.8393	0.000	48.908	4.228
-0.95	+0.0000	-1.67151	-4.8801	0.8437	0.000	44.041	4.228
-0.90	+0.0000	-1.61899	-4.6580	0.8479	0.000	39.704	4.229
-0.85	+0.0000	-1.56652	-4.4361	0.8521	0.000	35.842	4.230
-0.80	+0.0000	-1.51411	-4.2144	0.8561	0.001	32.400	4.230
-0.75	+0.0000	-1.46174	-3.9929	0.8601	0.001	29.334	4.231
-0.70	+0.0000	-1.40942	-3.7715	0.8639	0.002	26.601	4.231
-0.65	+0.0000	-1.35716	-3.5504	0.8676	0.003	24.166	4.232
-0.60	+0.0001	-1.30496	-3.3295	0.8713	0.004	21.996	4.232
-0.55	+0.0001	-1.25282	-3.1088	0.8748	0.005	20.064	4.232
-0.50	+0.0002	-1.20073	-2.8883	0.8783	0.008	18.344	4.233
-0.45	+0.0003	-1.14870	-2.6681	0.8816	0.011	16.808	4.233
-0.40	+0.0005	-1.09674	-2.4481	0.8849	0.015	15.439	4.233
-0.35	+0.0008	-1.04484	-2.2285	0.8880	0.019	14.219	4.233
-0.30	+0.0011	-0.99302	-2.0091	0.8911	0.025	13.130	4.232
-0.25	+0.0016	-0.94127	-1.7901	0.8941	0.033	12.156	4.231
-0.20	+0.0024	-0.88962	-1.5716	0.8969	0.043	11.284	4.230
-0.15	+0.0033	-0.83808	-1.3536	0.8997	0.055	10.503	4.228
-0.10	+0.0047	-0.78667	-1.1363	0.9024	0.070	9.800	4.226
-0.05	+0.0065	-0.73541	-0.9198	0.9049	0.089	9.168	4.222

2.3 (CONT.)

(2)	(4)	(5)	(6)	(10)	(7)	(8)	(9)
0.00	+0.0089	-0.68435	-0.7044	0.9073	0.110	8.595	4.217
+0.05	+0.0121	-0.63352	-0.4902	0.9096	0.136	8.074	4.211
+0.10	+0.0162	-0.58300	-0.2776	0.9118	0.166	7.597	4.203
+0.15	+0.0214	-0.53283	-0.0669	0.9138	0.200	7.158	4.194
+0.20	+0.0279	-0.48309	+0.1414	0.9156	0.238	6.750	4.181
+0.25	+0.0360	-0.43388	+0.3468	0.9173	0.281	6.369	4.167
+0.30	+0.0460	-0.38529	+0.5489	0.9187	0.327	6.013	4.150
+0.35	+0.0579	-0.33744	+0.7470	0.9200	0.376	5.672	4.131
+0.40	+0.0720	-0.29042	+0.9407	0.9210	0.427	5.348	4.108
+0.45	+0.0885	-0.24436	+1.1294	0.9218	0.480	5.040	4.083
+0.50	+0.1075	-0.19936	+1.3125	0.9224	0.532	4.744	4.055
+0.55	+0.1290	-0.15552	+1.4897	0.9227	0.583	4.461	4.025
+0.60	+0.1529	-0.11292	+1.6605	0.9228	0.630	4.192	3.993
+0.65	+0.1792	-0.07163	+1.8246	0.9226	0.672	3.936	3.960
+0.70	+0.2077	-0.03169	+1.9821	0.9222	0.707	3.696	3.926
+0.75	+0.2381	+0.00687	+2.1328	0.9215	0.733	3.473	3.892
+0.80	+0.2698	+0.04407	+2.2770	0.9207	0.750	3.266	3.860
+0.85	+0.3028	+0.07994	+2.4149	0.9197	0.757	3.075	3.831
+0.90	+0.3360	+0.11452	+2.5470	0.9185	0.753	2.911	3.805
+0.95	+0.3694	+0.14791	+2.6736	0.9172	0.740	2.763	3.785
+1.00	+0.4024	+0.18019	+2.7956	0.9158	0.717	2.634	3.769

2.4

(2)	(4)	(5)	(6)	(10)	(11)	(7)	(8)	(9)
-1.30	+0.0000	-2.07162	-5.7008	0.7404	2.0212	0.000	91.684	4.148
-1.25	+0.0000	-2.01887	-5.4820	0.7450	2.0591	0.000	82.186	4.148
-1.20	+0.0000	-1.96613	-5.2633	0.7495	2.0989	0.000	73.704	4.147
-1.15	+0.0000	-1.91339	-5.0446	0.7539	2.1404	0.000	66.134	4.146
-1.10	+0.0000	-1.86066	-4.8261	0.7582	2.1838	0.000	59.382	4.144
-1.05	+0.0000	-1.80796	-4.6076	0.7624	2.2293	0.000	53.358	4.143
-1.00	+0.0000	-1.75527	-4.3894	0.7665	2.2770	0.002	47.991	4.142
-0.95	+0.0000	-1.70262	-4.1714	0.7704	2.3271	0.002	43.203	4.140
-0.90	+0.0000	-1.64999	-3.9536	0.7743	2.3795	0.002	38.935	4.138
-0.85	+0.0000	-1.59741	-3.7360	0.7780	2.4345	0.003	35.133	4.136
-0.80	+0.0001	-1.54487	-3.5188	0.7816	2.4922	0.006	31.744	4.135
-0.75	+0.0001	-1.49238	-3.3018	0.7851	2.5529	0.008	28.724	4.133
-0.70	+0.0002	-1.43994	-3.0851	0.7885	2.6166	0.011	26.034	4.131
-0.65	+0.0003	-1.38754	-2.8687	0.7918	2.6835	0.014	23.635	4.128
-0.60	+0.0005	-1.33521	-2.6528	0.7949	2.7539	0.019	21.497	4.126
-0.55	+0.0007	-1.28294	-2.4372	0.7980	2.8279	0.026	19.591	4.123
-0.50	+0.0011	-1.23074	-2.2220	0.8009	2.9061	0.036	17.889	4.120
-0.45	+0.0016	-1.17862	-2.0074	0.8037	2.9886	0.048	16.368	4.116
-0.40	+0.0024	-1.12659	-1.7934	0.8063	3.0760	0.064	15.007	4.111
-0.35	+0.0034	-1.07468	-1.5802	0.8088	3.1690	0.084	13.786	4.105
-0.30	+0.0050	-1.02291	-1.3678	0.8111	3.2680	0.110	12.689	4.098
-0.25	+0.0072	-0.97132	-1.1566	0.8132	3.3742	0.142	11.698	4.088
-0.20	+0.0102	-0.91994	-0.9469	0.8150	3.4889	0.181	10.799	4.076
-0.15	+0.0143	-0.86886	-0.7390	0.8165	3.6135	0.228	9.977	4.061
-0.10	+0.0198	-0.81814	-0.5335	0.8176	3.7503	0.285	9.222	4.042
-0.05	+0.0270	-0.76788	-0.3310	0.8182	3.9020	0.352	8.521	4.017
0.00	+0.0365	-0.71821	-0.1323	0.8183	4.0718	0.429	7.864	3.986
+0.05	+0.0486	-0.66928	+0.0619	0.8176	4.2645	0.515	7.243	3.948
+0.10	+0.0639	-0.62125	+0.2504	0.8161	4.4855	0.610	6.652	3.901
+0.15	+0.0928	-0.57430	+0.4322	0.8136	4.7411	0.712	6.086	3.845
+0.20	+0.1057	-0.52863	+0.6064	0.8098	5.0401	0.816	5.543	3.779
+0.25	+0.1329	-0.48442	+0.7718	0.8048	5.3917	0.919	5.023	3.703
+0.30	+0.1646	-0.44185	+0.9276	0.7982	5.8076	1.016	4.527	3.617
+0.35	+0.2005	-0.40108	+1.0732	0.7899	6.3010	1.100	4.060	3.523
+0.40	+0.2404	-0.36222	+1.2082	0.7798	6.8864	1.164	3.625	3.423
+0.45	+0.2835	-0.32534	+1.3325	0.7677	7.5802	1.205	3.227	3.320
+0.50	+0.3290	-0.29046	+1.4466	0.7536	8.3995	1.217	2.871	3.218
+0.55	+0.3756	-0.25755	+1.5509	0.7376	9.3624	1.197	2.557	3.121
+0.60	+0.4220	-0.22653	+1.6463	0.7197	10.4868	1.148	2.286	3.034

3.1

(2)	(3)	(5)	(6)	(12)	(7)	(8)	(13)	(9)
−0.675	−0.0000	−1.40200	−4.8651	−0.0000	0.000	30.568	0.000	5.333
−0.650	−0.0000	−1.37700	−4.7318	−0.0000	0.000	29.156	0.000	5.333
−0.625	−0.0000	−1.35200	−4.5985	−0.0000	0.000	27.823	0.000	5.333
−0.600	−0.0000	−1.32700	−4.4651	−0.0000	0.000	26.565	0.000	5.333
−0.575	−0.0000	−1.30200	−4.3318	−0.0000	0.000	25.378	0.000	5.333
−0.550	−0.0000	−1.27700	−4.1985	−0.0000	0.001	24.256	0.000	5.333
−0.525	−0.0000	−1.25200	−4.0651	−0.0000	0.001	23.197	0.000	5.333
−0.500	−0.0000	−1.22700	−3.9318	−0.0000	0.001	22.198	0.000	5.333
−0.475	−0.0000	−1.20200	−3.7985	−0.0000	0.001	21.254	0.000	5.333
−0.450	−0.0000	−1.17700	−3.6651	−0.0000	0.001	20.363	0.000	5.333
−0.425	−0.0000	−1.15200	−3.5318	−0.0000	0.002	19.522	0.000	5.333
−0.400	−0.0000	−1.12700	−3.3985	−0.0000	0.002	18.728	0.000	5.333
−0.375	−0.0001	−1.10200	−3.2652	−0.0000	0.002	17.978	0.000	5.333
−0.350	−0.0001	−1.07700	−3.1319	−0.0000	0.003	17.270	0.000	5.333
−0.325	−0.0001	−1.05201	−2.9986	−0.0000	0.004	16.602	0.000	5.333
−0.300	−0.0002	−1.02701	−2.8653	−0.0000	0.004	15.970	0.000	5.333
−0.275	−0.0002	−1.00202	−2.7320	−0.0000	0.005	15.373	0.000	5.333
−0.250	−0.0002	−0.97702	−2.5987	−0.0000	0.006	14.810	0.000	5.332
−0.225	−0.0003	−0.95203	−2.4654	−0.0000	0.008	14.278	0.000	5.332
−0.200	−0.0004	−0.92704	−2.3322	−0.0000	0.009	13.775	0.000	5.332
−0.175	−0.0005	−0.90206	−2.1990	−0.0000	0.011	13.300	0.000	5.331
−0.150	−0.0006	−0.87707	−2.0658	−0.0000	0.013	12.851	0.000	5.331
−0.125	−0.0008	−0.85210	−1.9326	−0.0000	0.016	12.427	0.000	5.330
−0.100	−0.0010	−0.82712	−1.7995	−0.0000	0.018	12.025	0.000	5.329
−0.075	−0.0012	−0.80215	−1.6665	−0.0000	0.022	11.645	0.000	5.329
−0.050	−0.0014	−0.77719	−1.5335	−0.0000	0.026	11.285	0.000	5.328
−0.025	−0.0018	−0.75225	−1.4006	−0.0000	0.031	10.944	0.000	5.326
0.000	−0.0022	−0.72731	−1.2678	−0.0000	0.036	10.620	0.000	5.325
+0.025	−0.0027	−0.70238	−1.1351	−0.0000	0.042	10.313	0.000	5.323
+0.050	−0.0033	−0.67748	−1.0026	−0.0000	0.050	10.021	0.000	5.321
+0.075	−0.0040	−0.65260	−0.8702	−0.0000	0.058	9.743	0.000	5.319
+0.100	−0.0049	−0.62774	−0.7380	−0.0000	0.068	9.478	0.000	5.315
+0.125	−0.0060	−0.60291	−0.6061	−0.0000	0.079	9.225	0.000	5.312
+0.150	−0.0072	−0.57811	−0.4744	−0.0000	0.092	8.983	0.000	5.307
+0.175	−0.0087	−0.55336	−0.3431	−0.0000	0.106	8.750	0.000	5.302
+0.200	−0.0104	−0.52866	−0.2122	−0.0000	0.123	8.525	0.000	5.296
+0.225	−0.0124	−0.50402	−0.0818	−0.0000	0.142	8.308	0.000	5.290
+0.250	−0.0149	−0.47944	+0.0481	−0.0000	0.163	8.098	0.000	5.282
+0.275	−0.0177	−0.45495	+0.1773	−0.0000	0.186	7.893	0.000	5.273
+0.300	−0.0210	−0.43056	+0.3058	−0.0000	0.213	7.692	0.000	5.262
+0.325	−0.0248	−0.40627	+0.4335	−0.0000	0.242	7.494	0.000	5.250
+0.350	−0.0292	−0.38211	+0.5601	−0.0000	0.276	7.299	0.000	5.236
+0.375	−0.0343	−0.35810	+0.6857	−0.0000	0.312	7.105	0.000	5.220
+0.400	−0.0402	−0.33425	+0.8100	−0.0000	0.353	6.911	0.000	5.202
+0.425	−0.0470	−0.31059	+0.9328	−0.0000	0.398	6.717	0.000	5.181
+0.450	−0.0547	−0.28714	+1.0540	−0.0000	0.447	6.521	0.001	5.158
+0.475	−0.0635	−0.26394	+1.1734	−0.0000	0.500	6.323	0.001	5.131
+0.500	−0.0735	−0.24100	+1.2907	−0.0000	0.559	6.121	0.001	5.102
+0.525	−0.0848	−0.21837	+1.4058	−0.0000	0.622	5.916	0.002	5.068
+0.550	−0.0975	−0.19607	+1.5185	−0.0001	0.689	5.707	0.003	5.031
+0.575	−0.1117	−0.17413	+1.6284	−0.0001	0.762	5.494	0.004	4.990
+0.600	−0.1276	−0.15260	+1.7354	−0.0002	0.839	5.276	0.007	4.945

3.2

(2)	(3)	(5)	(6)	(12)	(7)	(8)	(13)	(9)
−0.675	−0.0000	−1.40200	−4.8287	−0.0000	0.000	30.568	0.000	5.333
−0.650	−0.0000	−1.37700	−4.6953	−0.0000	0.000	29.156	0.000	5.333
−0.625	−0.0000	−1.35200	−4.5620	−0.0000	0.000	27.823	0.000	5.333
−0.600	−0.0000	−1.32700	−4.4287	−0.0000	0.000	26.565	0.000	5.333
−0.575	−0.0000	−1.30200	−4.2953	−0.0000	0.001	25.378	0.000	5.333
−0.550	−0.0000	−1.27700	−4.1620	−0.0000	0.001	24.256	0.000	5.333
−0.525	−0.0000	−1.25200	−4.0287	−0.0000	0.001	23.197	0.000	5.333
−0.500	−0.0000	−1.22700	−3.8953	−0.0000	0.001	22.198	0.000	5.333
−0.475	−0.0000	−1.20200	−3.7620	−0.0000	0.001	21.254	0.000	5.333
−0.450	−0.0000	−1.17700	−3.6287	−0.0000	0.001	20.363	0.000	5.333
−0.425	−0.0000	−1.15200	−3.4953	−0.0000	0.002	19.522	0.000	5.333
−0.400	−0.0000	−1.12700	−3.3620	−0.0000	0.002	18.728	0.000	5.333
−0.375	−0.0001	−1.10200	−3.2287	−0.0000	0.003	17.978	0.000	5.333
−0.350	−0.0001	−1.07701	−3.0954	−0.0000	0.003	17.270	0.000	5.333
−0.325	−0.0001	−1.05201	−2.9621	−0.0000	0.004	16.602	0.000	5.333
−0.300	−0.0002	−1.02702	−2.8288	−0.0000	0.005	15.970	0.000	5.333
−0.275	−0.0002	−1.00202	−2.6955	−0.0000	0.006	15.373	0.000	5.332
−0.250	−0.0002	−0.97703	−2.5622	−0.0000	0.007	14.810	0.000	5.332
−0.225	−0.0003	−0.95203	−2.4290	−0.0000	0.008	14.278	0.000	5.332
−0.200	−0.0004	−0.92705	−2.2957	−0.0000	0.010	13.774	0.000	5.331

3.2 (CONT.)

(2)	(3)	(5)	(6)	(12)	(7)	(8)	(13)	(9)
−0.175	−0.0005	−0.90206	−2.1626	−0.0000	0.012	13.299	0.000	5.331
−0.150	−0.0006	−0.87708	−2.0294	−0.0000	0.014	12.850	0.000	5.331
−0.125	−0.0008	−0.85210	−1.8962	−0.0000	0.017	12.425	0.000	5.330
−0.100	−0.0010	−0.82714	−1.7632	−0.0000	0.020	12.023	0.000	5.330
−0.075	−0.0013	−0.80217	−1.6301	−0.0000	0.024	11.643	0.000	5.329
−0.050	−0.0016	−0.77721	−1.4972	−0.0000	0.028	11.282	0.000	5.327
−0.025	−0.0019	−0.75226	−1.3643	−0.0000	0.033	10.941	0.000	5.325
−0.000	−0.0024	−0.72733	−1.2315	−0.0000	0.039	10.616	0.000	5.324
+0.025	−0.0029	−0.70241	−1.0989	−0.0000	0.046	10.308	0.000	5.322
+0.050	−0.0036	−0.67752	−0.9664	−0.0000	0.054	10.015	0.000	5.320
+0.075	−0.0044	−0.65264	−0.8341	−0.0000	0.064	9.737	0.000	5.317
+0.100	−0.0053	−0.62779	−0.7020	−0.0000	0.074	9.470	0.000	5.314
+0.125	−0.0064	−0.60298	−0.5702	−0.0000	0.086	9.216	0.000	5.310
+0.150	−0.0078	−0.57820	−0.4387	−0.0000	0.100	8.972	0.000	5.305
+0.175	−0.0094	−0.55347	−0.3076	−0.0000	0.116	8.737	0.000	5.300
+0.200	−0.0113	−0.52880	−0.1769	−0.0000	0.134	8.511	0.000	5.293
+0.225	−0.0135	−0.50419	−0.0467	−0.0000	0.154	8.291	0.000	5.286
+0.250	−0.0161	−0.47965	+0.0828	−0.0000	0.177	8.078	0.000	5.277
+0.275	−0.0192	−0.45520	+0.2118	−0.0000	0.202	7.869	0.000	5.267
+0.300	−0.0228	−0.43086	+0.3398	−0.0000	0.231	7.665	0.000	5.255
+0.325	−0.0269	−0.40663	+0.4670	−0.0000	0.264	7.464	0.000	5.242
+0.350	−0.0317	−0.38254	+0.5931	−0.0000	0.299	7.264	0.000	5.227
+0.375	−0.0373	−0.35861	+0.7180	−0.0000	0.339	7.065	0.000	5.210
+0.400	−0.0437	−0.33486	+0.8415	−0.0000	0.383	6.866	0.000	5.190
+0.425	−0.0510	−0.31131	+0.9635	−0.0000	0.432	6.666	0.000	5.168
+0.450	−0.0594	−0.28799	+1.0837	−0.0000	0.485	6.464	0.000	5.142
+0.475	−0.0689	−0.26493	+1.2019	−0.0000	0.542	6.258	0.001	5.114
+0.500	−0.0798	−0.24216	+1.3180	−0.0000	0.605	6.050	0.001	5.081
+0.525	−0.0920	−0.21971	+1.4317	−0.0000	0.673	5.837	0.002	5.045
+0.550	−0.1057	−0.19762	+1.5427	−0.0001	0.746	5.620	0.004	5.005
+0.575	−0.1211	−0.17592	+1.6508	−0.0001	0.823	5.399	0.006	4.960
+0.600	−0.1382	−0.15465	+1.7558	−0.0002	0.905	5.173	0.009	4.911

4.1

(2)	(4)	(5)	(6)	(7)	(8)	(9)
+1.00	+0.0227	+0.36270	+2.2172	0.057	4.529	4.225
+1.02	+0.0237	+0.38229	+2.2995	0.058	4.504	4.177
+1.04	+0.0248	+0.40205	+2.3816	0.059	4.478	4.137
+1.06	+0.0259	+0.42195	+2.4636	0.060	4.451	4.105
+1.08	+0.0270	+0.44194	+2.5454	0.061	4.424	4.077
+1.10	+0.0281	+0.46201	+2.6269	0.062	4.396	4.054
+1.12	+0.0293	+0.48212	+2.7083	0.063	4.369	4.035
+1.14	+0.0305	+0.50225	+2.7894	0.064	4.342	4.019
+1.16	+0.0317	+0.52240	+2.8702	0.065	4.315	4.006
+1.18	+0.0329	+0.54255	+2.9508	0.066	4.289	3.994
+1.20	+0.0341	+0.56269	+3.0311	0.066	4.263	3.985
+1.25	+0.0373	+0.61293	+3.2308	0.068	4.202	3.967
+1.30	+0.0406	+0.66296	+3.4290	0.070	4.147	3.955
+1.35	+0.0440	+0.71275	+3.6257	0.071	4.095	3.947
+1.40	+0.0474	+0.76228	+3.8210	0.072	4.049	3.941
+1.45	+0.0508	+0.81154	+4.0151	0.072	4.006	3.937
+1.50	+0.0543	+0.86056	+4.2080	0.073	3.968	3.935
+1.55	+0.0579	+0.90933	+4.3998	0.073	3.934	3.932
+1.60	+0.0614	+0.95788	+4.5907	0.073	3.904	3.930
+1.65	+0.0650	+1.00623	+4.7806	0.072	3.876	3.929
+1.70	+0.0685	+1.05440	+4.9698	0.072	3.852	3.928
+1.75	+0.0720	+1.10239	+5.1583	0.072	3.830	3.927
+1.80	+0.0756	+1.15022	+5.3462	0.071	3.811	3.927
+1.85	+0.0790	+1.19792	+5.5335	0.070	3.794	3.927
+1.90	+0.0825	+1.24550	+5.7204	0.069	3.780	3.927
+1.95	+0.0859	+1.29297	+5.9068	0.068	3.767	3.928
+2.00	+0.0892	+1.34035	+6.0929	0.067	3.756	3.928
+2.05	+0.0925	+1.38765	+6.2788	0.066	3.747	3.929
+2.10	+0.0958	+1.43488	+6.4643	0.065	3.739	3.930
+2.15	+0.0990	+1.48206	+6.6497	0.064	3.732	3.930
+2.20	+0.1022	+1.52919	+6.8350	0.063	3.727	3.931
+2.25	+0.1053	+1.57628	+7.0201	0.062	3.723	3.932
+2.30	+0.1083	+1.62334	+7.2052	0.061	3.720	3.933
+2.35	+0.1113	+1.67038	+7.3903	0.060	3.717	3.934
+2.40	+0.1143	+1.71741	+7.5753	0.058	3.716	3.935
+2.45	+0.1171	+1.76443	+7.7604	0.057	3.715	3.937
+2.50	+0.1200	+1.81145	+7.9455	0.056	3.715	3.938
+2.60	+0.1255	+1.90551	+8.3160	0.054	3.716	3.940
+2.70	+0.1308	+1.99963	+8.6870	0.052	3.719	3.942
+2.80	+0.1358	+2.09384	+9.0585	0.050	3.724	3.944

4.1 (CONT.)

(2)	(4)	(5)	(6)	(7)	(8)	(9)
+ 2.90	+0.1407	+02.18816	+ 9.4306	0.048	3.730	3.947
+ 3.00	+0.1454	+02.28261	+ 9.8035	0.046	3.736	3.949
+ 3.10	+0.1500	+02.37719	+10.1770	0.044	3.743	3.951
+ 3.20	+0.1543	+02.47192	+10.5514	0.043	3.750	3.953
+ 3.30	+0.1586	+02.56681	+10.9265	0.042	3.757	3.954
+ 3.40	+0.1626	+02.66185	+11.3024	0.040	3.764	3.956
+ 3.50	+0.1666	+02.75704	+11.6791	0.039	3.772	3.958
+ 3.60	+0.1704	+02.85239	+12.0565	0.038	3.779	3.959
+ 3.70	+0.1741	+02.94788	+12.4346	0.036	3.786	3.960
+ 3.80	+0.1777	+03.04352	+12.8135	0.035	3.792	3.962
+ 3.90	+0.1812	+03.13929	+13.1929	0.034	3.798	3.963
+ 4.00	+0.1845	+03.23520	+13.5730	0.033	3.805	3.964
+ 4.10	+0.1878	+03.33123	+13.9538	0.032	3.811	3.965
+ 4.20	+0.1910	+03.42738	+14.3351	0.032	3.816	3.966
+ 4.30	+0.1941	+03.52365	+14.7169	0.031	3.822	3.967
+ 4.40	+0.1972	+03.62003	+15.0993	0.030	3.827	3.968
+ 4.50	+0.2001	+03.71652	+15.4822	0.029	3.831	3.969
+ 4.60	+0.2030	+03.81310	+15.8656	0.028	3.836	3.970
+ 4.70	+0.2058	+03.90978	+16.2494	0.028	3.840	3.970
+ 4.80	+0.2086	+04.00655	+16.6336	0.027	3.845	3.971
+ 4.90	+0.2113	+04.10341	+17.0183	0.027	3.849	3.972
+ 5.00	+0.2140	+04.20034	+17.4033	0.026	3.852	3.972
+ 5.10	+0.2165	+04.29736	+17.7887	0.026	3.856	3.973
+ 5.20	+0.2191	+04.39444	+18.1745	0.025	3.859	3.974
+ 5.30	+0.2215	+04.49160	+18.5605	0.025	3.862	3.974
+ 5.40	+0.2240	+04.58882	+18.9469	0.024	3.866	3.975
+ 5.50	+0.2264	+04.68610	+19.3336	0.024	3.869	3.975
+ 5.60	+0.2287	+04.78345	+19.7206	0.023	3.871	3.976
+ 5.70	+0.2310	+04.88085	+20.1079	0.023	3.874	3.976
+ 5.80	+0.2333	+04.97831	+20.4954	0.022	3.876	3.977
+ 5.90	+0.2355	+05.07581	+20.8832	0.022	3.879	3.977
+ 6.00	+0.2377	+05.17337	+21.2712	0.022	3.881	3.977
+ 6.10	+0.2398	+05.27098	+21.6594	0.021	3.884	3.978
+ 6.20	+0.2419	+05.36863	+22.0478	0.021	3.886	3.978
+ 6.30	+0.2440	+05.46632	+22.4365	0.021	3.888	3.979
+ 6.40	+0.2460	+05.56406	+22.8254	0.020	3.890	3.979
+ 6.50	+0.2480	+05.66184	+23.2144	0.020	3.892	3.979
+ 6.60	+0.2500	+05.75965	+23.6037	0.020	3.893	3.980
+ 6.70	+0.2520	+05.85751	+23.9931	0.019	3.895	3.980
+ 6.80	+0.2539	+05.95539	+24.3827	0.019	3.897	3.980
+ 6.90	+0.2558	+06.05331	+24.7724	0.019	3.898	3.980
+ 7.00	+0.2577	+06.15127	+25.1624	0.019	3.900	3.981
+ 7.10	+0.2595	+06.24925	+25.5524	0.018	3.901	3.981
+ 7.20	+0.2614	+06.34727	+25.9426	0.018	3.903	3.981
+ 7.40	+0.2649	+06.54339	+26.7235	0.018	3.906	3.982
+ 7.60	+0.2684	+06.73962	+27.5049	0.017	3.908	3.982
+ 7.80	+0.2718	+06.93595	+28.2868	0.017	3.911	3.983
+ 8.00	+0.2751	+07.13239	+29.0692	0.016	3.913	3.983
+ 8.20	+0.2783	+07.32892	+29.8520	0.016	3.915	3.984
+ 8.40	+0.2814	+07.52554	+30.6353	0.016	3.917	3.984
+ 8.60	+0.2845	+07.72224	+31.4190	0.015	3.919	3.984
+ 8.80	+0.2875	+07.91902	+32.2031	0.015	3.921	3.985
+ 9.00	+0.2905	+08.11589	+32.9876	0.014	3.923	3.985
+ 9.20	+0.2933	+08.31282	+33.7724	0.014	3.925	3.985
+ 9.40	+0.2962	+08.50982	+34.5576	0.014	3.927	3.986
+ 9.60	+0.2989	+08.70689	+35.3431	0.014	3.928	3.986
+ 9.80	+0.3016	+08.90403	+36.1289	0.013	3.930	3.986
+10.00	+0.3043	+09.10122	+36.9150	0.013	3.931	3.987
+10.20	+0.3068	+09.29847	+37.7013	0.013	3.932	3.987
+10.40	+0.3094	+09.49578	+38.4880	0.013	3.934	3.987
+10.60	+0.3119	+09.69313	+39.2749	0.012	3.935	3.987
+10.80	+0.3144	+09.89055	+40.0621	0.012	3.936	3.987
+11.00	+0.3168	+10.08800	+40.8494	0.012	3.938	3.988
+11.40	+0.3215	+10.48306	+42.4249	0.012	3.940	3.988
+11.80	+0.3260	+10.87828	+44.0012	0.011	3.942	3.989
+12.20	+0.3304	+11.27366	+45.5783	0.011	3.944	3.989

4.2

(2)	(4)	(5)	(6)	(7)	(8)	(9)
+1.80	+0.0817	+1.12519	+ 5.4294	0.092	3.981	4.202
+1.82	+0.0835	+1.14394	+ 5.5078	0.093	3.973	4.153
+1.84	+0.0854	+1.16287	+ 5.5860	0.093	3.963	4.112
+1.86	+0.0872	+1.18193	+ 5.6640	0.094	3.952	4.077
+1.88	+0.0891	+1.20110	+ 5.7419	0.094	3.940	4.049

4.2 (CONT.)

(2)	(4)	(5)	(6)	(7)	(8)	(9)
+1.90	+0.0909	+1.22034	+ 5.8196	0.094	3.928	4.025
+1.92	+0.0928	+1.23964	+ 5.8970	0.094	3.915	4.006
+1.94	+0.0946	+1.25898	+ 5.9743	0.095	3.903	3.989
+1.96	+0.0965	+1.27833	+ 6.0514	0.095	3.890	3.975
+1.98	+0.0984	+1.29770	+ 6.1282	0.094	3.877	3.963
+2.00	+0.1002	+1.31705	+ 6.2048	0.094	3.864	3.954
+2.05	+0.1049	+1.36538	+ 6.3954	0.094	3.833	3.936
+2.10	+0.1096	+1.41356	+ 6.5848	0.094	3.805	3.925
+2.15	+0.1142	+1.46155	+ 6.7729	0.093	3.778	3.917
+2.20	+0.1188	+1.50933	+ 6.9600	0.091	3.755	3.913
+2.25	+0.1233	+1.55692	+ 7.1461	0.090	3.734	3.910
+2.30	+0.1277	+1.60431	+ 7.3313	0.089	3.717	3.909
+2.35	+0.1321	+1.65152	+ 7.5158	0.087	3.701	3.909
+2.40	+0.1364	+1.69858	+ 7.6998	0.086	3.687	3.908
+2.45	+0.1406	+1.74550	+ 7.8832	0.084	3.676	3.909
+2.50	+0.1448	+1.79230	+ 8.0662	0.082	3.667	3.910
+2.55	+0.1488	+1.83900	+ 8.2488	0.080	3.659	3.911
+2.60	+0.1528	+1.88561	+ 8.4311	0.079	3.654	3.912
+2.65	+0.1566	+1.93215	+ 8.6132	0.077	3.649	3.914
+2.70	+0.1604	+1.97864	+ 8.7952	0.075	3.646	3.916
+2.75	+0.1641	+2.02508	+ 8.9771	0.073	3.644	3.917
+2.80	+0.1677	+2.07150	+ 9.1590	0.071	3.643	3.919
+2.90	+0.1747	+2.16429	+ 9.5228	0.068	3.644	3.923
+3.00	+0.1813	+2.25709	+ 9.8870	0.065	3.648	3.926
+3.10	+0.1876	+2.34996	+10.2518	0.061	3.655	3.930
+3.20	+0.1936	+2.44294	+10.6174	0.058	3.663	3.933
+3.30	+0.1993	+2.53608	+10.9838	0.056	3.672	3.936
+3.40	+0.2047	+2.62940	+11.3514	0.053	3.682	3.939
+3.50	+0.2099	+2.72292	+11.7199	0.051	3.692	3.942
+3.60	+0.2149	+2.81666	+12.0896	0.049	3.703	3.945

4.3

(2)	(4)	(5)	(6)	(7)	(8)	(9)
+2.60	+0.1603	+1.85946	+ 8.5112	0.102	3.814	4.194
+2.62	+0.1623	+1.87770	+ 8.5873	0.102	3.811	4.145
+2.64	+0.1644	+1.89613	+ 8.6633	0.102	3.806	4.104
+2.66	+0.1664	+1.91471	+ 8.7392	0.102	3.800	4.069
+2.68	+0.1684	+1.93340	+ 8.8150	0.102	3.794	4.041
+2.70	+0.1705	+1.95217	+ 8.8906	0.101	3.787	4.017
+2.72	+0.1725	+1.97102	+ 8.9661	0.101	3.779	3.998
+2.74	+0.1745	+1.98991	+ 9.0415	0.101	3.770	3.981
+2.76	+0.1765	+2.00883	+ 9.1166	0.100	3.762	3.967
+2.78	+0.1785	+2.02777	+ 9.1917	0.100	3.753	3.955
+2.80	+0.1805	+2.04672	+ 9.2666	0.100	3.745	3.946
+2.85	+0.1855	+2.09408	+ 9.4530	0.098	3.724	3.928
+2.90	+0.1904	+2.14138	+ 9.6385	0.097	3.705	3.917
+2.95	+0.1952	+2.18854	+ 9.8231	0.095	3.688	3.911
+3.00	+0.1999	+2.23557	+10.0069	0.093	3.673	3.907
+3.05	+0.2045	+2.28246	+10.1900	0.091	3.660	3.905
+3.10	+0.2090	+2.32921	+10.3727	0.089	3.649	3.905
+3.15	+0.2134	+2.37583	+10.5546	0.087	3.640	3.905
+3.20	+0.2177	+2.42235	+10.7363	0.085	3.632	3.906
+3.25	+0.2219	+2.46878	+10.9177	0.083	3.627	3.907
+3.30	+0.2260	+2.51513	+11.0988	0.081	3.623	3.909
+3.35	+0.2300	+2.56143	+11.2798	0.079	3.620	3.910
+3.40	+0.2340	+2.60768	+11.4607	0.077	3.619	3.912
+3.45	+0.2378	+2.65390	+11.6416	0.075	3.618	3.914
+3.50	+0.2414	+2.80000	+11.8224	0.073	3.619	3.916
+3.60	+0.2486	+2.79248	+12.1844	0.069	3.623	3.920
+3.70	+0.2553	+2.88492	+12.5469	0.066	3.630	3.924
+3.80	+0.2617	+2.97746	+12.9103	0.062	3.639	3.928
+3.90	+0.2678	+3.07016	+13.2746	0.059	3.649	3.932
+4.00	+0.2735	+3.16304	+13.6400	0.056	3.660	3.935
+4.10	+0.2790	+3.25614	+14.0065	0.054	3.672	3.939
+4.20	+0.2843	+3.34947	+14.3743	0.051	3.684	3.942
+4.30	+0.2893	+3.44304	+14.7432	0.049	3.696	3.945
+4.40	+0.2941	+3.53685	+15.1134	0.047	3.708	3.947

4.4

(2)	(4)	(5)	(6)	(7)	(8)	(9)
+3.40	+0.2412	+2.58160	+11.5399	0.100	3.779	4.194
+3.42	+0.2432	+2.59972	+11.6154	0.100	3.778	4.146
+3.44	+0.2452	+2.61803	+11.6909	0.099	3.775	4.105
+3.46	+0.2472	+2.63648	+11.7664	0.099	3.772	4.072
+3.48	+0.2491	+2.65506	+11.8417	0.099	3.767	4.043
+3.50	+0.2511	+2.67373	+11.9170	0.098	3.761	4.019
+3.52	+0.2531	+2.69247	+11.9921	0.098	3.755	4.000
+3.54	+0.2550	+2.71126	+12.0671	0.098	3.749	3.984
+3.56	+0.2570	+2.73010	+12.1420	0.097	3.742	3.970
+3.58	+0.2589	+2.74895	+12.2168	0.097	3.733	3.958

4.4 (CONT.)

(2)	(4)	(5)	(6)	(7)	(8)	(9)
+3.60	+0.2609	+2.76783	+12.2914	0.096	3.728	3.948
+3.65	+0.2656	+2.81502	+12.4773	0.095	3.710	3.931
+3.70	+0.2704	+2.86217	+12.6624	0.093	3.694	3.920
+3.75	+0.2750	+2.90923	+12.8467	0.092	3.680	3.914
+3.80	+0.2795	+2.95618	+13.0304	0.090	3.668	3.910
+3.85	+0.2840	+3.00301	+13.2134	0.088	3.657	3.908
+3.90	+0.2883	+3.04973	+13.3960	0.086	3.648	3.908
+3.95	+0.2926	+3.09634	+13.5782	0.084	3.640	3.908
+4.00	+0.2967	+3.14287	+13.7600	0.082	3.635	3.909
+4.05	+0.3008	+3.18932	+13.9416	0.080	3.631	3.911
+4.10	+0.3047	+3.23571	+14.1231	0.078	3.627	3.912
+4.15	+0.3086	+3.28205	+14.3044	0.076	3.626	3.914
+4.20	+0.3123	+3.32835	+14.4856	0.074	3.625	3.915
+4.30	+0.3195	+3.42091	+14.8482	0.070	3.628	3.920
+4.40	+0.3264	+3.51346	+15.2112	0.067	3.632	3.923
+4.50	+0.3329	+3.60609	+15.5748	0.063	3.640	3.927
+4.60	+0.3390	+3.69883	+15.9392	0.060	3.649	3.931
+4.70	+0.3449	+3.79174	+16.3045	0.057	3.659	3.934
+4.80	+0.3505	+3.88484	+16.6710	0.054	3.670	3.938
+4.90	+0.3558	+3.97816	+17.0386	0.052	3.682	3.941
+5.00	+0.3609	+4.07170	+17.4073	0.050	3.693	3.944
+5.10	+0.3658	+4.16546	+17.7772	0.048	3.705	3.946
+5.20	+0.3704	+4.25946	+18.1483	0.046	3.716	3.949
+5.30	+0.3749	+4.35369	+18.5205	0.044	3.728	3.951
+5.40	+0.3792	+4.44814	+18.8938	0.042	3.738	3.953
+5.50	+0.3833	+4.54282	+19.2681	0.041	3.748	3.955
+5.60	+0.3873	+4.63770	+19.6435	0.039	3.758	3.957

4.5

(2)	(4)	(5)	(6)	(7)	(8)	(9)
+0.20	+0.0044	-0.42938	- 0.6408	0.036	6.878	4.241
+0.22	+0.0048	-0.40939	- 0.5565	0.038	6.751	4.195
+0.24	+0.0054	-0.38923	- 0.4724	0.041	6.626	4.156
+0.26	+0.0059	-0.36892	- 0.3883	0.043	6.505	4.124
+0.28	+0.0065	-0.34852	- 0.3044	0.046	6.387	4.097
+0.30	+0.0071	-0.32804	- 0.2208	0.048	6.272	4.075
+0.32	+0.0078	-0.30752	- 0.1374	0.051	6.161	4.056
+0.34	+0.0085	-0.28696	- 0.0542	0.054	6.053	4.040
+0.36	+0.0092	-0.26640	+ 0.0288	0.057	5.949	4.027
+0.38	+0.0100	-0.24583	+ 0.1115	0.059	5.850	4.015
+0.40	+0.0109	-0.22527	+ 0.1939	0.062	5.753	4.005
+0.45	+0.0133	-0.17400	+ 0.3988	0.069	5.528	3.986
+0.50	+0.0160	-0.12293	+ 0.6020	0.076	5.324	3.971
+0.55	+0.0191	-0.07215	+ 0.8033	0.083	5.139	3.959
+0.60	+0.0226	-0.02168	+ 1.0028	0.090	4.971	3.949
+0.65	+0.0263	+0.02846	+ 1.2006	0.097	4.819	3.940
+0.70	+0.0304	+0.07826	+ 1.3966	0.103	4.681	3.932
+0.75	+0.0349	+0.12771	+ 1.5908	0.108	4.555	3.924
+0.80	+0.0396	+0.17681	+ 1.7833	0.113	4.440	3.916
+0.85	+0.0447	+0.22558	+ 1.9741	0.118	4.337	3.910
+0.90	+0.0499	+0.27401	+ 2.1633	0.122	4.242	3.903
+0.95	+0.0554	+0.32211	+ 2.3509	0.125	4.155	3.897
+1.00	+0.0611	+0.36990	+ 2.5370	0.127	4.077	3.891
+1.05	+0.0670	+0.41737	+ 2.7216	0.129	4.006	3.886
+1.10	+0.0730	+0.46455	+ 2.9048	0.130	3.942	3.882
+1.15	+0.0790	+0.51145	+ 3.0868	0.130	3.884	3.878
+1.20	+0.0851	+0.55808	+ 3.2676	0.130	3.832	3.875
+1.25	+0.0912	+0.60447	+ 3.4472	0.130	3.785	3.873
+1.30	+0.0974	+0.65062	+ 3.6259	0.128	3.743	3.871
+1.35	+0.1035	+0.69657	+ 3.8037	0.127	3.706	3.870
+1.40	+0.1095	+0.74232	+ 3.9807	0.125	3.674	3.869
+1.45	+0.1155	+0.78789	+ 4.1571	0.123	3.646	3.869
+1.50	+0.1214	+0.83332	+ 4.3328	0.120	3.621	3.870
+1.55	+0.1271	+0.87861	+ 4.5081	0.118	3.600	3.871
+1.60	+0.1328	+0.92379	+ 4.6830	0.115	3.583	3.872
+1.65	+0.1383	+0.96887	+ 4.8576	0.112	3.568	3.874
+1.70	+0.1437	+1.01388	+ 5.0320	0.109	3.556	3.876
+1.75	+0.1490	+1.05883	+ 5.2063	0.106	3.547	3.879
+1.80	+0.1541	+1.10374	+ 5.3805	0.102	3.540	3.881
+1.85	+0.1590	+1.14863	+ 5.5548	0.099	3.535	3.884
+1.90	+0.1639	+1.19351	+ 5.7292	0.096	3.532	3.887
+1.95	+0.1686	+1.23839	+ 5.9037	0.093	3.531	3.890
+2.00	+0.1731	+1.28329	+ 6.0784	0.090	3.531	3.893
+2.05	+0.1775	+1.32821	+ 6.2534	0.087	3.533	3.896
+2.10	+0.1818	+1.37318	+ 6.4286	0.084	3.536	3.899

4.5 (CONT.)

(2)	(.)	(5)	(6)	(7)	(8)	(9)
+2.15	+0.1859	+1.41819	+ 6.6042	0.082	3.540	3.902
+2.20	+0.1899	+1.46326	+ 6.7801	0.079	3.545	3.905
+2.25	+0.1938	+1.50840	+ 6.9565	0.077	3.550	3.908
+2.30	+0.1975	+1.55360	+ 7.1332	0.074	3.557	3.911
+2.35	+0.2011	+1.59889	+ 7.3104	0.072	3.564	3.914
+2.40	+0.2047	+1.64425	+ 7.4880	0.070	3.571	3.917
+2.45	+0.2081	+1.68970	+ 7.6661	0.068	3.579	3.920
+2.50	+0.2114	+1.73524	+ 7.8446	0.066	3.587	3.922
+2.60	+0.2178	+1.82660	+ 8.2032	0.062	3.604	3.927
+2.70	+0.2238	+1.91832	+ 8.5636	0.058	3.621	3.931
+2.80	+0.2294	+2.01042	+ 8.9259	0.055	3.638	3.935
+2.90	+0.2348	+2.10290	+ 9.2900	0.052	3.655	3.940
+3.00	+0.2399	+2.19574	+ 9.6558	0.050	3.671	3.943
+3.10	+0.2448	+2.28892	+10.0234	0.048	3.687	3.946
+3.20	+0.2495	+2.38245	+10.3925	0.046	3.701	3.948

4.6

(2)	(4)	(5)	(6)	(7)	(8)	(9)
+1.00	+0.0695	+0.34430	+ 2.6182	0.166	4.242	4.174
+1.02	+0.0725	+0.36287	+ 2.6952	0.168	4.209	4.120
+1.04	+0.0756	+0.38159	+ 2.7719	0.171	4.175	4.074
+1.06	+0.0788	+0.40043	+ 2.8483	0.173	4.141	4.035
+1.08	+0.0820	+0.41935	+ 2.9243	0.175	4.105	4.001
+1.10	+0.0852	+0.43831	+ 2.9999	0.177	4.071	3.974
+1.12	+0.0885	+0.45730	+ 3.0751	0.178	4.036	3.951
+1.14	+0.0919	+0.47628	+ 3.1499	0.180	4.001	3.930
+1.16	+0.0952	+0.49526	+ 3.2243	0.181	3.968	3.914
+1.18	+0.0986	+0.51421	+ 3.2983	0.182	3.935	3.899
+1.20	+0.1021	+0.53312	+ 3.3720	0.182	3.902	3.886
+1.25	+0.1107	+0.58020	+ 3.5543	0.183	3.827	3.862
+1.30	+0.1194	+0.62691	+ 3.7343	0.183	3.758	3.846
+1.35	+0.1282	+0.67323	+ 3.9122	0.182	3.695	3.834
+1.40	+0.1368	+0.71916	+ 4.0882	0.180	3.639	3.826
+1.45	+0.1454	+0.76470	+ 4.2623	0.177	3.589	3.821
+1.50	+0.1539	+0.80988	+ 4.4349	0.173	3.546	3.818
+1.55	+0.1622	+0.85474	+ 4.6061	0.169	3.510	3.817
+1.60	+0.1703	+0.89929	+ 4.7762	0.164	3.477	3.818
+1.65	+0.1782	+0.94359	+ 4.9453	0.159	3.450	3.819
+1.70	+0.1858	+0.98767	+ 5.1137	0.154	3.428	3.822
+1.75	+0.1932	+1.03156	+ 5.2816	0.148	3.411	3.825
+1.80	+0.2004	+1.07531	+ 5.4489	0.142	3.398	3.829
+1.85	+0.2072	+1.11893	+ 5.6161	0.137	3.388	3.833
+1.90	+0.2138	+1.16247	+ 5.7831	0.131	3.381	3.838
+1.95	+0.2202	+1.20596	+ 5.9500	0.126	3.378	3.843
+2.00	+0.2263	+1.24941	+ 6.1172	0.121	3.378	3.849
+2.05	+0.2321	+1.29286	+ 6.2845	0.115	3.380	3.854
+2.10	+0.2377	+1.33634	+ 6.4522	0.110	3.383	3.859
+2.15	+0.2431	+1.37985	+ 6.6202	0.106	3.389	3.865
+2.20	+0.2482	+1.42341	+ 6.7887	0.101	3.397	3.871
+2.25	+0.2532	+1.46706	+ 6.9578	0.097	3.406	3.876
+2.30	+0.2579	+1.51080	+ 7.1275	0.093	3.416	3.881
+2.35	+0.2624	+1.55464	+ 7.2977	0.089	3.427	3.886
+2.40	+0.2667	+1.59859	+ 7.4686	0.085	3.439	3.891
+2.45	+0.2709	+1.64266	+ 7.6403	0.082	3.451	3.896
+2.50	+0.2749	+1.68687	+ 7.8126	0.079	3.464	3.900
+2.55	+0.2788	+1.73120	+ 7.9856	0.076	3.477	3.904
+2.60	+0.2825	+1.77568	+ 8.1593	0.073	3.491	3.909
+2.70	+0.2895	+1.86506	+ 8.5090	0.068	3.518	3.916
+2.80	+0.2960	+1.95501	+ 8.8616	0.063	3.545	3.923
+2.90	+0.3021	+2.04554	+ 9.2170	0.059	3.572	3.928
+3.00	+0.3078	+2.13663	+ 9.5750	0.056	3.597	3.933
+3.10	+0.3132	+2.22826	+ 9.9356	0.052	3.621	3.938
+3.20	+0.3183	+2.32039	+10.2986	0.050	3.644	3.942
+3.30	+0.3232	+2.41300	+10.6639	0.047	3.665	3.945
+3.40	+0.3278	+2.50606	+11.0312	0.045	3.684	3.948
+3.50	+0.3322	+2.59953	+11.4003	0.043	3.702	3.951

4.7

(2)	(4)	(5)	(6)	(7)	(8)	(9)
+1.80	+0.2151	+1.04432	+ 5.5224	0.187	3.527	4.139
+1.82	+0.2188	+1.06120	+ 5.5918	0.186	3.520	4.086
+1.84	+0.2224	+1.07825	+ 5.6611	0.185	3.512	4.042
+1.86	+0.2261	+1.09545	+ 5.7302	0.183	3.503	4.004
+1.88	+0.2297	+1.11276	+ 5.7993	0.182	3.493	3.973

4.7 (CONT.)

(2)	(4)	(5)	(6)	(7)	(8)	(9)
+1.90	+0.2332	+1.13015	+ 5.8681	0.180	3.484	3.947
+1.92	+0.2368	+1.14761	+ 5.9369	0.178	3.474	3.925
+1.94	+0.2403	+1.16512	+ 6.0054	0.176	3.464	3.907
+1.96	+0.2437	+1.18267	+ 6.0738	0.174	3.454	3.892
+1.98	+0.2472	+1.20024	+ 6.1421	0.172	3.445	3.879
+2.00	+0.2505	+1.21782	+ 6.2102	0.170	3.436	3.869
+2.05	+0.2588	+1.26177	+ 6.3798	0.164	3.414	3.850
+2.10	+0.2668	+1.30568	+ 6.5486	0.158	3.396	3.840
+2.15	+0.2745	+1.34950	+ 6.7168	0.152	3.381	3.835
+2.20	+0.2819	+1.39322	+ 6.8844	0.146	3.370	3.834
+2.25	+0.2890	+1.43685	+ 7.0517	0.140	3.362	3.835
+2.30	+0.2958	+1.48040	+ 7.2188	0.134	3.357	3.838
+2.35	+0.3024	+1.52389	+ 7.3858	0.128	3.355	3.841
+2.40	+0.3086	+1.56735	+ 7.5528	0.123	3.355	3.846
+2.45	+0.3146	+1.61079	+ 7.7200	0.117	3.358	3.852
+2.50	+0.3203	+1.65425	+ 7.8875	0.112	3.364	3.857
+2.55	+0.3258	+1.69773	+ 8.0554	0.107	3.370	3.862
+2.60	+0.3310	+1.74127	+ 8.2236	0.102	3.379	3.868
+2.65	+0.3360	+1.78488	+ 8.3924	0.098	3.389	3.874
+2.70	+0.3408	+1.82857	+ 8.5618	0.094	3.400	3.879
+2.75	+0.3454	+1.87236	+ 8.7318	0.090	3.412	3.885
+2.80	+0.3497	+1.91625	+ 8.9025	0.086	3.425	3.890
+2.85	+0.3539	+1.96029	+ 9.0738	0.082	3.439	3.894
+2.90	+0.3580	+2.00444	+ 9.2459	0.079	3.453	3.899
+3.00	+0.3656	+2.09315	+ 9.5922	0.073	3.481	3.908
+3.10	+0.3726	+2.18243	+ 9.9414	0.068	3.510	3.915
+3.20	+0.3791	+2.27230	+10.2936	0.063	3.539	3.923
+3.30	+0.3852	+2.36276	+10.6488	0.059	3.567	3.928
+3.40	+0.3909	+2.45380	+11.0066	0.055	3.593	3.934
+3.50	+0.3962	+2.54538	+11.3671	0.052	3.618	3.938
+3.60	+0.4013	+2.63749	+11.7300	0.049	3.642	3.942
+3.70	+0.4062	+2.73008	+12.0951	0.047	3.663	3.946
+3.80	+0.4107	+2.82312	+12.4624	0.045	3.683	3.949
+3.90	+0.4151	+2.91659	+12.8316	0.043	3.701	3.951

4.8

(2)	(4)	(5)	(6)	(7)	(8)	(9)
+2.60	+0.3418	+1.71231	+ 8.2964	0.133	3.523	4.169
+2.62	+0.3444	+1.72928	+ 8.3667	0.131	3.526	4.121
+2.64	+0.3470	+1.74645	+ 8.4371	0.130	3.528	4.080
+2.66	+0.3496	+1.76378	+ 8.5075	0.129	3.528	4.046
+2.68	+0.3522	+1.78125	+ 8.5779	0.128	3.527	4.016
+2.70	+0.3547	+1.79883	+ 8.6483	0.126	3.526	3.993
+2.72	+0.3572	+1.81650	+ 8.7187	0.125	3.524	3.972
+2.74	+0.3597	+1.83424	+ 8.7890	0.124	3.522	3.956
+2.76	+0.3622	+1.85204	+ 8.8593	0.122	3.520	3.942
+2.78	+0.3646	+1.86989	+ 8.9295	0.121	3.517	3.930
+2.80	+0.3670	+1.88778	+ 8.9998	0.119	3.515	3.920
+2.85	+0.3729	+1.93260	+ 9.1751	0.116	3.509	3.903
+2.90	+0.3786	+1.97751	+ 9.3501	0.112	3.503	3.894
+2.95	+0.3841	+2.02245	+ 9.5250	0.108	3.499	3.888
+3.00	+0.3894	+2.06740	+ 9.6997	0.105	3.496	3.886
+3.05	+0.3946	+2.11234	+ 9.8743	0.101	3.495	3.886
+3.10	+0.3995	+2.15727	+10.0489	0.098	3.496	3.887
+3.15	+0.4043	+2.20220	+10.2236	0.094	3.498	3.889
+3.20	+0.4090	+2.24714	+10.3985	0.091	3.501	3.892
+3.25	+0.4134	+2.29211	+10.5735	0.088	3.505	3.895
+3.30	+0.4177	+2.33710	+10.7488	0.085	3.511	3.898
+3.35	+0.4219	+2.38213	+10.9244	0.082	3.517	3.901
+3.40	+0.4259	+2.42722	+11.1004	0.079	3.524	3.904
+3.45	+0.4298	+2.47236	+11.2767	0.076	3.532	3.908
+3.50	+0.4336	+2.51757	+11.4535	0.074	3.540	3.911
+3.60	+0.4407	+2.60822	+11.8082	0.069	3.558	3.917
+3.70	+0.4474	+2.69921	+12.1649	0.065	3.577	3.922
+3.80	+0.4537	+2.79056	+12.5234	0.061	3.596	3.927
+3.90	+0.4596	+2.88230	+12.8839	0.058	3.615	3.932
+4.00	+0.4653	+2.97442	+13.2463	0.055	3.634	3.936
+4.10	+0.4706	+3.06692	+13.6106	0.052	3.652	3.940
+4.20	+0.4757	+3.15978	+13.9766	0.049	3.669	3.943
+4.30	+0.4805	+3.25300	+14.3444	0.047	3.686	3.946
+4.40	+0.4851	+3.34657	+14.7138	0.045	3.702	3.949
+4.50	+0.4895	+3.44046	+15.0846	0.043	3.716	3.951
+4.60	+0.4937	+3.53465	+15.4569	0.041	3.730	3.954
+4.70	+0.4977	+3.62912	+15.8305	0.040	3.742	3.956
+4.80	+0.5016	+3.72386	+16.2054	0.038	3.754	3.957
+4.90	+0.5054	+3.81884	+16.5813	0.037	3.765	3.959
+5.00	+0.5090	+3.91404	+16.9583	0.036	3.775	3.961

4.8 (CONT.)

(2)	(4)	(5)	(6)	(7)	(8)	(9)
+5.10	+0.5126	+4.00945	+17.3363	0.035	3.784	3.962
+5.20	+0.5160	+4.10505	+17.7152	0.034	3.793	3.963
+5.30	+0.5193	+4.20084	+18.0948	0.033	3.801	3.965

4.9

(2)	(4)	(5)	(6)	(7)	(8)	(9)
-0.20	+0.0007	-0.82849	- 2.0855	0.013	10.970	4.248
-0.18	+0.0008	-0.80841	- 2.0007	0.014	10.664	4.203
-0.16	+0.0009	-0.78814	- 1.9159	0.015	10.366	4.167
-0.14	+0.0010	-0.76772	- 1.8311	0.017	10.077	4.136
+0.12	+0.0012	-0.74720	- 1.7465	0.018	9.799	4.110
-0.10	+0.0014	-0.72660	- 1.6621	0.020	9.532	4.090
-0.08	+0.0015	-0.70594	- 1.5778	0.022	9.274	4.072
-0.06	+0.0018	-0.68524	- 1.4936	0.024	9.028	4.058
-0.04	+0.0020	-0.66452	- 1.4097	0.026	8.791	4.046
-0.02	+0.0022	-0.64378	- 1.3259	0.028	8.564	4.035
0.00	+0.0025	-0.62305	- 1.2424	0.030	8.348	4.027
+0.05	+0.0034	-0.57127	- 1.0343	0.036	7.845	4.010
+0.10	+0.0045	-0.51963	- 0.8276	0.043	7.397	3.999
+0.15	+0.0058	-0.46818	- 0.6221	0.051	6.996	3.989
+0.20	+0.0074	-0.41696	- 0.4179	0.059	6.637	3.981
+0.25	+0.0094	-0.36597	- 0.2152	0.067	6.314	3.974
+0.30	+0.0118	-0.31525	- 0.0138	0.076	6.025	3.966
+0.35	+0.0145	-0.26479	+ 0.1861	0.086	5.763	3.958
+0.40	+0.0177	-0.21461	+ 0.3845	0.096	5.526	3.950
+0.45	+0.0214	-0.16473	+ 0.5814	0.105	5.311	3.941
+0.50	+0.0255	-0.11515	+ 0.7765	0.115	5.117	3.933
+0.55	+0.0301	-0.06588	+ 0.9700	0.124	4.939	3.923
+0.60	+0.0352	-0.01694	+ 1.1618	0.132	4.777	3.914
+0.65	+0.0407	+0.03166	+ 1.3518	0.140	4.628	3.904
+0.70	+0.0466	+0.07992	+ 1.5400	0.148	4.492	3.894
+0.75	+0.0530	+0.12783	+ 1.7263	0.154	4.368	3.885
+0.80	+0.0597	+0.17538	+ 1.9108	0.160	4.254	3.867
+0.85	+0.0668	+0.22258	+ 2.0935	0.164	4.150	3.867
+0.90	+0.0741	+0.26942	+ 2.2744	0.168	4.055	3.859
+0.95	+0.0816	+0.31591	+ 2.4537	0.170	3.969	3.852
+1.00	+0.0894	+0.36206	+ 2.6313	0.172	3.890	3.845
+1.05	+0.0972	+0.40789	+ 2.8074	0.172	3.819	3.840
+1.10	+0.1051	+0.45340	+ 2.9820	0.172	3.756	3.835
+1.15	+0.1131	+0.49861	+ 3.1553	0.170	3.699	3.832
+1.20	+0.1210	+0.54355	+ 3.3274	0.168	3.648	3.829
+1.25	+0.1289	+0.58823	+ 3.4985	0.165	3.603	3.827
+1.30	+0.1366	+0.63268	+ 3.6686	0.162	3.564	3.827
+1.35	+0.1442	+0.67693	+3.8379	0.158	3.530	3.827
+1.40	+0.1517	+0.72099	+ 4.0066	0.154	3.501	3.828
+1.45	+0.1590	+0.76490	+ 4.1747	0.149	3.477	3.830
+1.50	+0.1661	+0.80868	+ 4.3424	0.144	3.457	3.832
+1.55	+0.1730	+0.85235	+ 4.5099	0.139	3.441	3.836
+1.60	+0.1797	+0.89595	+ 4.6772	0.134	3.429	3.839
+1.65	+0.1861	+0.93948	+ 4.8444	0.130	3.420	3.843
+1.70	+0.1923	+0.98299	+ 5.0117	0.124	3.414	3.848
+1.75	+0.1983	+1.02648	+ 5.1792	0.120	3.411	3.853
+1.80	+0.2041	+1.06998	+ 5.3469	0.115	3.410	3.857
+1.85	+0.2096	+1.11351	+ 5.5149	0.110	3.412	3.862
+1.90	+0.2150	+1.15709	+ 5.6833	0.106	3.415	3.867
+1.95	+0.2201	+1.20072	+ 5.8522	0.102	3.420	3.872
+2.00	+0.2250	+1.24443	+ 6.0215	0.098	3.427	3.877
+2.05	+0.2298	+1.28823	+ 6.1914	0.094	3.435	3.882
+2.10	+0.2343	+1.33213	+ 6.3620	0.090	3.444	3.887
+2.15	+0.2387	+1.37613	+ 6.5331	0.086	3.453	3.891
+2.20	+0.2429	+1.42026	+ 6.7049	0.083	3.464	3.896
+2.25	+0.2470	+1.46450	+ 6.8773	0.080	3.475	3.900
+2.30	+0.2509	+1.50887	+ 7.0505	0.077	3.487	3.904
+2.35	+0.2546	+1.55338	+ 7.2243	0.074	3.499	3.908
+2.40	+0.2582	+1.59802	+ 7.3988	0.071	3.511	3.911
+2.45	+0.2618	+1.64279	+ 7.5740	0.069	3.524	3.915
+2.50	+0.2651	+1.68770	+ 7.7499	0.067	3.536	3.918
+2.55	+0.2684	+1.73276	+ 7.9265	0.064	3.549	3.921
+2.60	+0.2716	+1.77794	+ 8.1038	0.062	3.561	3.924
+2.65	+0.2746	+1.82327	+ 8.2817	0.060	3.573	3.927
+2.70	+0.2776	+1.86873	+ 8.4603	0.058	3.586	3.930
+2.75	+0.2805	+1.91433	+ 8.6395	0.057	3.598	3.932
+2.80	+0.2833	+1.96006	+ 8.8194	0.055	3.609	3.934
+2.85	+0.2860	+2.00591	+ 8.9998	0.054	3.620	3.937
+2.90	+0.2886	+2.05188	+ 9.1809	0.052	3.631	3.939
+2.95	+0.2912	+2.09798	+ 9.3625	0.051	3.642	3.941

4.9 (CONT.)

(2)	(4)	(5)	(6)	(7)	(8)	(9)
+3.00	+0.2937	+2.14420	+ 9.5447	0.049	3.652	3.942
+3.05	+0.2961	+2.19053	+ 9.7274	0.048	3.662	3.944
+3.10	+0.2985	+2.23696	+ 9.9106	0.047	3.672	3.946
+3.15	+0.3008	+2.28351	+10.0942	0.046	3.681	3.948
+3.20	+0.3031	+2.33016	+10.2784	0.045	3.690	3.949
+3.25	+0.3053	+2.37690	+10.4630	0.044	3.699	3.950
+3.30	+0.3074	+2.42374	+10.6481	0.043	3.707	3.952

4.10

(2)	(4)	(5)	(6)	(7)	(8)	(9)
+0.60	+0.0411	-0.04069	+ 1.2456	0.172	4.977	4.186
+0.62	+0.0439	-0.02160	+ 1.3250	0.178	4.911	4.131
+0.64	+0.0468	-0.00236	+ 1.4040	0.184	4.843	4.084
+0.66	+0.0499	+0.01699	+ 1.4826	0.190	4.776	4.044
+0.68	+0.0530	+0.03640	+ 1.5607	0.195	4.709	4.010
+0.70	+0.0563	+0.05584	+ 1.6384	0.200	4.643	3.980
+0.72	+0.0597	+0.07529	+ 1.7156	0.205	4.579	3.955
+0.74	+0.0632	+0.09473	+ 1 7922	0.210	4.516	3.934
+0.76	+0.0668	+0.11413	+ 1.8684	0.215	4.453	3.915
+0.78	+0.0705	+0.13349	+ 1.9440	0.219	4.392	3.897
+0.80	+0.0743	+0.15279	+ 2.0190	0.223	4.333	3.883
+0.85	+0.0842	+0.20073	+ 2.2044	0.232	4.192	3.851
+0.90	+0.0946	+0.24815	+ 2.3864	0.239	4.062	3.827
+0.95	+0.1054	+0.29499	+ 2.5652	0.244	3.943	3.807
+1.00	+0.1165	+0.34125	+ 2.7409	0.247	3.834	3.792
+1.05	+0.1278	+0.38692	+ 2.9138	0.247	3.735	3.778
+1.10	+0.1392	+0.43202	+ 3.0840	0.246	3.647	3.768
+1.15	+0.1506	+0.47659	+ 3.2518	0.243	3.569	3.761
+1.20	+0.1619	+0.52066	+ 3.4173	0.239	3.499	3.755
+1.25	+0.1731	+0.56426	+ 3.5810	0.234	3.439	3.752
+1.30	+0.1840	+0.60745	+ 3.7430	0.227	3.387	3.750
+1.35	+0.1947	+0.65027	+ 3.9036	0.219	3.342	3.751
+1.40	+0.2050	+0.69276	+ 4.0630	0.211	3.305	3.753
+1.45	+0.2150	+0.73499	+ 4.2215	0.202	3.275	3.756
+1.50	+0.2245	+0.77698	+ 4.3794	0.193	3.251	3.761
+1.55	+0.2337	+0.81879	+ 4.5367	0.184	3.233	3.767
+1.60	+0.2424	+0.86046	+ 4.6938	0.175	3.220	3.774
+1.65	+0.2508	+0.90203	+ 4.8509	0.166	3.212	3.782
+1.70	+0.2587	+0.94355	+ 5.0081	0.158	3.209	3.790
+1.75	+0.2663	+0.98504	+ 5.1656	0.149	3.209	3.799
+1.80	+0.2734	+1.02655	+ 5.3234	0.141	3.213	3.808
+1.85	+0.2802	+1.06811	+ 5.4819	0.134	3.220	3.817
+1.90	+0.2866	+1.10975	+ 5.6410	0.126	3.229	3.826
+1.95	+0.2926	+1.15148	+ 5.8008	0.120	3.241	3.835
+2.00	+0.2984	+1.19334	+ 5.9615	0.113	3.255	3.843
+2.05	+0.3038	+1.23535	+ 6.1232	0.107	3.271	3.852
+2.10	+0.3090	+1.27753	+ 6.2858	0.102	3.288	3.860
+2.15	+0.3139	+1.31986	+ 6.4494	0.096	3.306	3.867
+2.20	+0.3186	+1.36239	+ 6.6140	0.092	3.324	3.874
+2.25	+0.3231	+1.40512	+ 6.7797	0.087	3.345	3.881
+2.30	+0.3273	+1.44806	+ 6.9465	0.083	3.364	3.888
+2.35	+0.3313	+1.49121	+ 7.1144	0.079	3.384	3.894
+2.40	+0.3352	+1.53458	+ 7.2834	0.076	3.404	3.900
+2.45	+0.3389	+1.57816	+ 7.4535	0.072	3.424	3.904
+2.50	+0.3424	+1.62196	+ 7.6246	0.069	3.443	3.909
+2.55	+0.3458	+1.66596	+ 7.7967	0.066	3.463	3.914
+2.60	+0.3491	+1.71018	+ 7.9699	0.064	3.482	3.918
+2.65	+0.3522	+1.75461	+ 8.1440	0.062	3.501	3.922
+2.70	+0.3552	+1.79924	+ 8.3192	0.059	3.519	3.925
+2.80	+0.3609	+1.88910	+ 8.6722	0.055	3.554	3.932
+2.90	+0.3663	+1.97971	+ 9.0287	0.052	3.586	3.937
+3.00	+0.3713	+2.07101	+ 9.3884	0.049	3.615	3.942
+3.10	+0.3760	+2.16295	+ 9.7509	0.046	3.642	3.946
+3.20	+0.3805	+2.25547	+10.1162	0.044	3.667	3.949
+3.30	+0.3848	+2.34852	+10.4838	0.042	3.689	3.952
+3.40	+0.3888	+2.44205	+10.8535	0.040	3.709	3.955

4.11

(2)	(4)	(5)	(6)	(7)	(8)	(9)
+1.40	+0.2262	+0.65868	+ 4.1308	0.280	3.405	4.083
+1.42	+0.2315	+0.67481	+ 4.1962	0.278	3.387	4.024
+1.44	+0.2369	+0.69110	+ 4.2613	0.276	3.369	3.976
+1.46	+0.2422	+0.70751	+ 4.3262	0.273	3.351	3.934
+1.48	+0.2474	+0.72401	+ 4.3909	0.270	3.332	3.899

4.11 (CONT.)

(2)	(4)	(5)	(6)	(7)	(8)	(9)
+1.50	+0.2526	+0.74059	+ 4.4552	0.267	3.314	3.870
+1.52	+0.2578	+0.75721	+ 4.5193	0.264	3.296	3.845
+1.54	+0.2629	+0.77386	+ 4.5832	0.260	3.278	3.824
+1.56	+0.2679	+0.79053	+ 4.6468	0.256	3.261	3.807
+1.58	+0.2729	+0.80720	+ 4.7101	0.252	3.245	3.794
+1.60	+0.2778	+0.82386	+ 4.7733	0.248	3.230	3.782
+1.65	+0.2896	+0.86547	+ 4.9301	0.237	3.196	3.762
+1.70	+0.3010	+0.90694	+ 5.0859	0.226	3.167	3.751
+1.75	+0.3118	+0.94826	+ 5.2408	0.214	3.145	3.747
+1.80	+0.3220	+0.98941	+ 5.3950	0.203	3.129	3.749
+1.85	+0.3317	+1.03044	+ 5.5489	0.191	3.118	3.753
+1.90	+0.3409	+1.07136	+ 5.7026	0.180	3.113	3.760
+1.95	+0.3495	+1.11222	+ 5.8564	0.170	3.113	3.769
+2.00	+0.3576	+1.15305	+ 6.0105	0.160	3.116	3.778
+2.05	+0.3653	+1.19389	+ 6.1650	0.150	3.124	3.789
+2.10	+0.3725	+1.23478	+ 6.3201	0.140	3.135	3.799
+2.15	+0.3792	+1.27575	+ 6.4760	0.132	3.148	3.810
+2.20	+0.3856	+1.31683	+ 6.6328	0.124	3.164	3.821
+2.25	+0.3916	+1.35805	+ 6.7905	0.117	3.183	3.832
+2.30	+0.3972	+1.39944	+ 6.9493	0.110	3.203	3.842
+2.35	+0.4025	+1.44102	+ 7.1092	0.104	3.224	3.851
+2.40	+0.4075	+1.48280	+ 7.2703	0.098	3.246	3.860
+2.45	+0.4122	+1.52479	+ 7.4326	0.092	3.270	3.869
+2.50	+0.4167	+1.56702	+ 7.5961	0.087	3.293	3.877
+2.55	+0.4210	+1.60948	+ 7.7608	0.083	3.317	3.884
+2.60	+0.4250	+1.65218	+ 7.9269	0.079	3.341	3.891
+2.65	+0.4288	+1.69513	+ 8.0941	0.075	3.365	3.897
+2.70	+0.4325	+1.73833	+ 8.2626	0.072	3.389	3.903
+2.75	+0.4360	+1.78177	+ 8.4323	0.068	3.412	3.909
+2.80	+0.4393	+1.82546	+ 8.6032	0.065	3.435	3.914
+2.85	+0.4425	+1.86940	+ 8.7752	0.063	3.457	3.918
+2.90	+0.4456	+1.91357	+ 8.9484	0.060	3.478	3.922
+2.95	+0.4485	+1.95797	+ 9.1226	0.058	3.499	3.926
+3.00	+0.4514	+2.00260	+ 9.2979	0.056	3.519	3.929
+3.05	+0.4541	+2.04744	+ 9.4742	0.054	3.539	3.933
+3.10	+0.4568	+2.09249	+ 9.6514	0.052	3.557	3.936
+3.15	+0.4593	+2.13774	+ 9.8296	0.050	3.575	3.938
+3.20	+0.4618	+2.18319	+10.0086	0.049	3.592	3.941
+3.25	+0.4642	+2.22883	+10.1885	0.047	3.608	3.943
+3.30	+0.4665	+2.27464	+10.3692	0.046	3.623	3.945
+3.35	+0.4688	+2.32062	+10.5506	0.044	3.638	3.947
+3.40	+0.4709	+2.36675	+10.7328	0.043	3.652	3.949
+3.45	+0.4731	+2.41304	+10.9156	0.042	3.665	3.951
+3.50	+0.4752	+2.45948	+11.0991	0.041	3.677	3.952
+3.55	+0.4772	+2.50604	+11.2832	0.040	3.689	3.954
+3.60	+0.4792	+2.55274	+11.4678	0.039	3.700	3.955

4.12

(2)	(4)	(5)	(6)	(7)	(8)	(9)
+2.20	+0.4002	+1.28460	+ 6.7008	0.162	3.295	4.142
+2.22	+0.4034	+1.30052	+ 6.7664	0.159	3.301	4.094
+2.24	+0.4066	+1.31665	+ 6.8320	0.156	3.306	4.054
+2.26	+0.4097	+1.33294	+ 6.8978	0.154	3.310	4.020
+2.28	+0.4127	+1.34939	+ 6.9637	0.151	3.313	3.991
+2.30	+0.4157	+1.36597	+ 7.0296	0.149	3.315	3.967
+2.32	+0.4186	+1.38265	+ 7.0956	0.146	3.317	3.947
+2.34	+0.4215	+1.39942	+ 7.1617	0.144	3.319	3.930
+2.36	+0.4243	+1.41628	+ 7.2278	0.141	3.321	3.916
+2.38	+0.4271	+1.43320	+ 7.2939	0.139	3.323	3.905
+2.40	+0.4298	+1.45017	+ 7.3601	0.136	3.324	3.896
+2.45	+0.4365	+1.49280	+ 7.5258	0.130	3.328	3.897
+2.50	+0.4428	+1.53564	+ 7.6918	0.124	3.334	3.871
+2.55	+0.4489	+1.57863	+ 7.8581	0.119	3.340	3.867
+2.60	+0.4547	+1.62175	+ 8.0248	0.114	3.347	3.867
+2.65	+0.4602	+1.66497	+ 8.1920	0.108	3.356	3.869
+2.70	+0.4655	+1.70830	+ 8.3597	0.103	3.366	3.872
+2.75	+0.4706	+1.75173	+ 8.5279	0.099	3.377	3.875
+2.80	+0.4754	+1.79527	+ 8.6968	0.094	3.389	3.880
+2.85	+0.4800	+1.83893	+ 8.8663	0.090	3.402	3.885
+2.90	+0.4844	+1.88272	+ 9.0365	0.086	3.415	3.889
+2.95	+0.4886	+1.92664	+ 9.2074	0.083	3.429	3.894
+3.00	+0.4927	+1.97069	+ 9.3791	0.079	3.444	3.899
+3.05	+0.4966	+2.01489	+ 9.5515	0.076	3.459	3.903
+3.10	+0.5003	+2.05923	+ 9.7246	0.073	3.474	3.907

4.12 (CONT.)

(9)	(2)	(4)	(5)	(6)	(7)	(8)	(9)
3.870	+3.20	+0.5073	+2.14837	+10.0733	0.068	3.504	3.915
3.845	+3.30	+0.5139	+2.23812	+10.4250	0.063	3.534	3.922
3.824	+3.40	+0.5200	+2.32847	+10.7796	0.059	3.562	3.928
3.807	+3.50	+0.5257	+2.41941	+11.1371	0.055	3.590	3.933
3.794	+3.60	+0.5310	+2.51092	+11.4973	0.052	3.615	3.938
3.782	+3.70	+0.5361	+2.60297	+11.8599	0.049	3.639	3.942
3.762	+3.80	+0.5409	+2.69551	+12.2249	0.047	3.661	3.946
3.751	+3.90	+0.5455	+2.78852	+12.5920	0.044	3.682	3.949
3.747	+4.00	+0.5498	+2.88195	+12.9611	0.042	3.700	3.952
3.749	+4.10	+0.5540	+2.97577	+13.3320	0.041	3.718	3.954
3.753	+4.20	+0.5580	+3.06996	+13.7045	0.039	3.733	3.956
3.760	+4.30	+0.5618	+3.16448	+14.0785	0.038	3.747	3.958
3.769	+4.40	+0.5655	+3.25929	+14.4539	0.036	3.760	3.960
3.778	+4.50	+0.5691	+3.35438	+14.8305	0.035	3.772	3.961
3.789	+4.60	+0.5725	+3.44971	+15.2082	0.034	3.782	3.963
3.799	+4.70	+0.5759	+3.54526	+15.5869	0.033	3.792	3.964
3.810	+4.80	+0.5791	+3.64101	+15.9666	0.032	3.801	3.965
3.821	+4.90	+0.5823	+3.73695	+16.3470	0.031	3.809	3.966
3.832	+5.00	+0.5853	+3.83306	+16.7283	0.030	3.816	3.967
3.842	+5.10	+0.5883	+3.92931	+17.1102	0.030	3.823	3.968
3.851	+5.20	+0.5912	+4.02571	+17.4928	0.029	3.829	3.969
3.860	+5.30	+0.5941	+4.12223	+17.8760	0.028	3.834	3.970
3.869	+5.40	+0.5968	+4.21887	+18.2597	0.027	3.840	3.971
3.877	+5.50	+0.5995	+4.31562	+18.6439	0.027	3.845	3.972
3.884	+5.60	+0.6022	+4.41247	+19.0286	0.026	3.849	3.972
3.891	+5.70	+0.6048	+4.50941	+19.4137	0.026	3.853	3.973
3.897	+5.80	+0.6073	+4.60644	+19.7992	0.025	3.857	3.974
3.903	+5.90	+0.6098	+4.70354	+20.1850	0.025	3.861	3.974
3.909	+6.00	+0.6122	+4.80072	+20.5713	0.024	3.864	3.974
3.914	+6.10	+0.6146	+4.89798	+20.9578	0.024	3.867	3.975
3.918	+6.20	+0.6170	+4.99529	+21.3447	0.023	3.870	3.976
3.922	+6.30	+0.6193	+5.09267	+21.7318	0.023	3.873	3.976
3.926	+6.40	+0.6215	+5.19011	+22.1193	0.022	3.876	3.977
3.929	+6.50	+0.6238	+5.28760	+22.5070	0.022	3.878	3.977

4.13

(2)	(4)	(5)	(6)	(7)	(8)	(9)
+3.00	+0.5004	+1.94401	+ 9.4508	0.101	3.597	4.189
+3.02	+0.5025	+1.96128	+ 9.5227	0.101	3.603	4.143
+3.04	+0.5045	+1.97876	+ 9.5947	0.100	3.607	4.103
+3.06	+0.5065	+1.99640	+ 9.6668	0.099	3.610	4.070
+3.08	+0.5084	+2.01420	+ 9.7390	0.098	3.612	4.043
+3.10	+0.5104	+2.03211	+ 9.8112	0.097	3.613	4.019
+3.12	+0.5123	+2.05012	+ 9.8834	0.096	3.613	4.000
+3.14	+0.5142	+2.06821	+ 9.9556	0.096	3.603	3.984
+3.16	+0.5161	+2.08636	+10.0278	0.095	3.612	3.970
+3.18	+0.5180	+2.10457	+10.1000	0.094	3.611	3.959
+3.20	+0.5199	+2.12283	+10.1722	0.093	3.610	3.949
+3.25	+0.5245	+2.16859	+10.3525	0.091	3.607	3.932
+3.30	+0.5290	+2.21448	+10.5327	0.088	3.604	3.923
+3.35	+0.5333	+2.26042	+10.7127	0.086	3.601	3.917
+3.40	+0.5376	+2.30638	+10.8927	0.084	3.599	3.914
+3.45	+0.5417	+2.35235	+11.0726	0.082	3.598	3.912
+3.50	+0.5457	+2.39832	+11.2524	0.079	3.599	3.913
+3.60	+0.5534	+2.49027	+11.6123	0.075	3.601	3.915
+3.70	+0.5607	+2.58226	+11.9726	0.071	3.607	3.918
+3.80	+0.5676	+2.67435	+12.3336	0.067	3.615	3.922
+3.90	+0.5741	+2.76659	+12.6955	0.064	3.625	3.926
+4.00	+0.5803	+2.85901	+13.0586	0.060	3.637	3.930
+4.10	+0.5862	+2.95165	+13.4229	0.057	3.649	3.934
+4.20	+0.5917	+3.04453	+13.7885	0.054	3.663	3.938
+4.30	+0.5970	+3.13767	+14.1553	0.052	3.675	3.941
+4.40	+0.6021	+3.23106	+14.5235	0.050	3.688	3.944
+4.50	+0.6070	+3.32471	+14.8930	0.047	3.701	3.946

4.14

(2)	(4)	(5)	(6)	(7)	(8)	(9)
-0.60	+0.0000	-1.22839	- 3.5349	0.003	21.167	4.250
-0.58	+0.0000	-1.20828	- 3.4499	0.003	20.401	4.205
-0.56	+0.0001	-1.18799	- 3.3649	0.003	19.660	4.169
-0.54	+0.0001	-1.16756	- 3.2801	0.004	18.946	4.139
-0.52	+0.0001	-1.14701	- 3.1953	0.004	18.261	4.114
-0.50	+0.0001	-1.12639	- 3.1107	0.005	17.604	4.094
-0.48	+0.0001	-1.10570	- 3.0262	0.005	16.974	4.077
-0.46	+0.0002	-1.08497	- 2.9418	0.006	16.371	4.063
-0.44	+0.0002	-1.06421	- 2.8576	0.006	15.796	4.052
-0.42	+0.0002	-1.04343	- 2.7735	0.007	15.245	4.042

4.14 (CONT.)

(2)	(4)	(5)	(6)	(7)	(8)	(9)
-0.40	+0.0003	-1.02265	- 2.6896	0.008	14.720	4.034
-0.35	+0.0004	-0.97073	- 2.4805	0.010	13.511	4.020
-0.30	+0.0006	-0.91890	- 2.2724	0.013	12.438	4.011
-0.25	+0.0008	-0.86722	- 2.0652	0.017	11.485	4.005
-0.20	+0.0012	-0.81569	- 1.8590	0.020	10.640	4.001
-0.15	+0.0017	-0.76433	- 1.6536	0.026	9.889	3.997
-0.10	+0.0023	-0.71313	- 1.4490	0.032	9.220	3.993
-0.05	+0.0031	-0.66211	- 1.2454	0.039	8.625	3.990
0.00	+0.0042	-0.61126	- 1.0426	0.047	8.093	3.986
+0.05	+0.0055	-0.56058	- 0.8407	0.056	7.618	3.981
+0.10	+0.0071	-0.51008	- 0.6398	0.065	7.192	3.976
+0.15	+0.0092	-0.45977	- 0.4399	0.076	6.809	3.970
+0.20	+0.0116	-0.40966	- 0.2412	0.088	6.464	3.963
+0.25	+0.0146	-0.35977	- 0.0436	0.100	6.152	3.955
+0.30	+0.0180	-0.31010	+ 0.1525	0.113	5.868	3.945
+0.35	+0.0221	-0.26070	+ 0.3472	0.126	5.610	3.935
+0.40	+0.0267	-0.21157	+ 0.5403	0.139	5.375	3.924
+0.45	+0.0320	-0.16275	+ 0.7316	0.152	5.159	3.913
+0.50	+0.0380	-0.11425	+ 0.9211	0.164	4.962	3.900
+0.55	+0.0445	-0.06610	+ 1.1086	0.176	4.780	3.887
+0.60	+0.0517	-0.01833	+ 1.2940	0.187	4.613	3.874
+0.65	+0.0595	+0.02906	+ 1.4772	0.197	4.459	3.861
+0.70	+0.0678	+0.07603	+ 1.6582	0.206	4.317	3.848
+0.75	+0.0766	+0.12259	+ 1.8371	0.213	4.187	3.835
+0.80	+0.0585	+0.16872	+ 2.0138	0.218	4.068	3.823
+0.85	+0.0954	+0.21443	+ 2.1882	0.222	3.959	3.812
+0.90	+0.1052	+0.25972	+ 2.3607	0.225	3.860	3.802
+0.95	+0.1153	+0.30459	+ 2.5311	0.226	3.769	3.794
+1.00	+0.1255	+0.34906	+ 2.6996	0.225	3.688	3.786
+1.05	+0.1357	+0.39315	+ 2.8664	0.223	3.616	3.780
+1.10	+0.1459	+0.43688	+ 3.0317	0.219	3.551	3.776
+1.15	+0.1560	+0.48028	+ 3.1955	0.215	3.495	3.773
+1.20	+0.1660	+0.52338	+ 3.3581	0.209	3.445	3.772
+1.25	+0.1757	+0.56621	+ 3.5196	0.203	3.403	3.772
+1.30	+0.1852	+0.60880	+ 3.6803	0.196	3.367	3.774
+1.35	+0.1944	+0.65118	+ 3.8403	0.189	3.337	3.777
+1.40	+0.2033	+0.69340	+ 3.9999	0.182	3.313	3.781
+1.45	+0.2118	+0.73548	+ 4.1591	0.174	3.295	3.786
+1.50	+0.2200	+0.77746	+ 4.3181	0.166	3.281	3.791
+1.55	+0.2279	+0.81938	+ 4.4772	0.158	3.272	3.798
+1.60	+0.2354	+0.86126	+ 4.6364	0.151	3.266	3.805
+1.65	+0.2426	+0.90314	+ 4.7959	0.143	3.265	3.812
+1.70	+0.2495	+0.94504	+ 4.9558	0.136	3.267	3.820
+1.75	+0.2560	+0.98699	+ 5.1162	0.130	3.271	3.828
+1.80	+0.2622	+1.02902	+ 5.2772	0.123	3.278	3.835
+1.85	+0.2681	+1.07114	+ 5.4389	0.117	3.287	3.843
+1.90	+0.2737	+1.11338	+ 5.6014	0.111	3.299	3.850
+1.95	+0.2791	+1.15575	+ 5.7647	0.106	3.312	3.858
+2.00	+0.2842	+1.19826	+ 5.9289	0.100	3.326	3.865
+2.05	+0.2890	+1.24095	+ 6.0940	0.096	3.341	3.872
+2.10	+0.2936	+1.28380	+ 6.2600	0.091	3.357	3.878
+2.15	+0.2981	+1.32684	+ 6.4271	0.087	3.374	3.884
+2.20	+0.3023	+1.37006	+ 6.5951	0.083	3.391	3.890
+2.25	+0.3063	+1.41347	+ 6.7641	0.079	3.409	3.896
+2.30	+0.3102	+1.45708	+ 6.9341	0.076	3.427	3.901
+2.35	+0.3139	+1.50088	+ 7.1051	0.073	3.445	3.906
+2.40	+0.3174	+1.54489	+ 7.2770	0.070	3.463	3.910
+2.45	+0.3209	+1.58908	+ 7.4499	0.067	3.480	3.914
+2.50	+0.3242	+1.63348	+ 7.6238	0.065	3.497	3.918
+2.55	+0.3273	+1.67806	+ 7.7986	0.062	3.514	3.922
+2.60	+0.3304	+1.72284	+ 7.9742	0.060	3.531	3.925
+2.65	+0.3333	+1.76779	+ 8.1507	0.058	3.547	3.928
+2.70	+0.3362	+1.81292	+ 8.3281	0.056	3.563	3.931
+2.75	+0.3389	+1.85823	+ 8.5063	0.054	3.578	3.934
+2.80	+0.3416	+1.90370	+ 8.6852	0.053	3.592	3.936
+2.85	+0.3442	+1.94934	+ 8.8649	0.051	3.606	3.939
+2.90	+0.3467	+1.99514	+ 9.0453	0.050	3.620	3.941
+2.95	+0.3492	+2.04108	+ 9.2264	0.048	3.633	3.943
+3.00	+0.3515	+2.08717	+ 9.4082	0.047	3.645	3.945
+3.05	+0.3538	+2.13339	+ 9.5906	0.046	3.657	3.947
+3.10	+0.3561	+2.17975	+ 9.7736	0.045	3.669	3.948
+3.15	+0.3583	+2.22623	+ 9.9572	0.044	3.679	3.949
+3.20	+0.3605	+2.27283	+10.1413	0.042	3.690	3.951
+3.25	+0.3626	+2.31955	+10.3259	0.042	3.699	3.952
+3.30	+0.3646	+2.36638	+10.5110	0.041	3.709	3.954

4.15

(2)	(4)	(5)	(6)	(7)	(8)	(9)
+0.20	+0.0139	−0.43152 − 0.1536		0.113	6.762	4.222
+0.22	+0.0153	−0.41178 − 0.0708		0.121	6.627	4.170
+0.24	+0.0169	−0.39187 + 0.0118		0.128	6.492	4.127
+0.26	+0.0186	−0.37185 + 0.0940		0.136	6.360	4.090
+0.28	+0.0204	−0.35174 + 0.1760		0.144	6.231	4.059
+0.30	+0.0224	−0.33159 + 0.2575		0.152	6.105	4.032
+0.32	+0.0244	−0.31141 + 0.3386		0.160	5.982	4.009
+0.34	+0.0267	−0.29124 + 0.4193		0.168	5.862	3.989
+0.36	+0.0291	−0.27108 + 0.4995		0.177	5.745	3.971
+0.38	+0.0316	−0.25095 + 0.5792		0.186	5.632	3.955
+0.40	+0.0343	−0.23088 + 0.6585		0.194	5.522	3.940
+0.45	+0.0417	−0.18096 + 0.8543		0.214	5.262	3.908
+0.50	+0.0501	−0.13152 + 1.0468		0.235	5.020	3.879
+0.55	+0.0596	−0.08266 + 1.2357		0.254	4.797	3.854
+0.60	+0.0699	−0.03444 + 1.4210		0.271	4.590	3.830
+0.65	+0.0812	+0.01312 + 1.6025		0.287	4.399	3.806
+0.70	+0.0933	+0.06000 + 1.7804		0.300	4.224	3.784
+0.75	+0.1061	+0.10617 + 1.9547		0.310	4.062	3.764
+0.80	+0.1196	+0.15164 + 2.1254		0.317	3.915	3.744
+0.85	+0.1335	+0.19642 + 2.2927		0.322	3.780	3.726
+0.90	+0.1477	+0.24052 + 2.4567		0.323	3.658	3.711
+0.95	+0.1621	+0.28398 + 2.6176		0.322	3.549	3.698
+1.00	+0.1766	+0.32682 + 2.7758		0.317	3.451	3.687
+1.05	+0.1909	+0.36909 + 2.9315		0.311	3.365	3.679
+1.10	+0.2051	+0.41083 + 3.0849		0.302	3.291	3.674
+1.15	+0.2188	+0.45209 + 3.2364		0.291	3.226	3.672
+1.20	+0.2322	+0.49292 + 3.3864		0.279	3.173	3.672
+1.25	+0.2451	+0.53339 + 3.5350		0.266	3.128	3.675
+1.30	+0.2574	+0.57353 + 3.6826		0.253	3.092	3.680
+1.35	+0.2692	+0.61342 + 3.8296		0.239	3.065	3.688
+1.40	+0.2803	+0.65311 + 3.9761		0.225	3.045	3.697
+1.45	+0.2908	+0.69265 + 4.1225		0.211	3.032	3.708
+1.50	+0.3007	+0.73210 + 4.2690		0.198	3.025	3.719
+1.55	+0.3100	+0.77150 + 4.4158		0.185	3.024	3.732
+1.60	+0.3188	+0.81091 + 4.5631		0.173	3.028	3.746
+1.65	+0.3270	+0.85036 + 4.7111		0.162	3.036	3.759
+1.70	+0.3346	+0.88991 + 4.8601		0.151	3.048	3.773
+1.75	+0.3418	+0.92958 + 5.0100		0.141	3.064	3.787
+1.80	+0.3485	+0.96942 + 5.1612		0.132	3.083	3.800
+1.85	+0.3548	+1.00945 + 5.3135		0.123	3.104	3.813
+1.90	+0.3606	+1.04969 + 5.4672		0.115	3.127	3.825
+1.95	+0.3662	+1.09018 + 5.6223		0.108	3.151	3.837
+2.00	+0.3714	+1.13092 + 5.7789		0.102	3.177	3.848
+2.05	+0.3762	+1.17194 + 5.9369		0.095	3.204	3.858
+2.10	+0.3808	+1.21324 + 6.0965		0.090	3.231	3.867
+2.15	+0.3852	+1.25483 + 6.2575		0.085	3.259	3.876
+2.20	+0.3893	+1.29672 + 6.4201		0.080	3.287	3.884
+2.25	+0.3932	+1.33891 + 6.5841		0.076	3.314	3.892
+2.30	+0.3968	+1.38140 + 6.7496		0.072	3.341	3.899
+2.35	+0.4003	+1.42419 + 6.9166		0.069	3.368	3.905
+2.40	+0.4037	+1.46727 + 7.0849		0.066	3.395	3.911
+2.45	+0.4069	+1.51064 + 7.2547		0.063	3.420	3.916
+2.50	+0.4099	+1.55430 + 7.4257		0.060	3.445	3.920
+2.55	+0.4128	+1.59823 + 7.5980		0.057	3.469	3.925
+2.60	+0.4157	+1.64242 + 7.7716		0.055	3.492	3.929
+2.65	+0.4184	+1.68688 + 7.9463		0.053	3.513	3.932
+2.70	+0.4210	+1.73157 + 8.1221		0.051	3.534	3.935
+2.80	+0.4259	+1.82167 + 8.4769		0.048	3.574	3.941
+2.90	+0.4305	+1.91262 + 8.8356		0.045	3.609	3.946
+3.00	+0.4349	+2.00434 + 9.1977		0.042	3.641	3.950
+3.10	+0.4390	+2.09677 + 9.5629		0.040	3.669	3.953
+3.20	+0.4429	+2.18981 + 9.9308		0.038	3.694	3.956
+3.30	+0.4467	+2.28340 +10.3012		0.037	3.717	3.958

4.16

(2)	(4)	(5)	(6)	(7)	(8)	(9)
+1.00	+0.2016	+0.29265 + 2.8407		0.422	3.525	4.023
+1.02	+0.2092	+0.30865 + 2.9045		0.423	3.481	3.954
+1.04	+0.2170	+0.32478 + 2.9678		0.423	3.437	3.896
+1.06	+0.2248	+0.34098 + 3.0305		0.422	3.393	3.846
+1.08	+0.2325	+0.35723 + 3.0926		0.420	3.349	3.802
+1.10	+0.2403	+0.37350 + 3.1542		0.418	3.307	3.765
+1.12	+0.2480	+0.38977 + 3.2151		0.415	3.266	3.734
+1.14	+0.2557	+0.40601 + 3.2756		0.411	3.226	3.707
+1.16	+0.2634	+0.42222 + 3.3355		0.407	3.188	3.684
+1.18	+0.2709	+0.43838 + 3.3948		0.402	3.151	3.665

4.16 (CONT.)

(2)	(4)	(5)	(6)	(7)	(8)	(9)
+1.20	+0.2784	+0.45448 + 3.4537		0.396	3.116	3.648
+1.25	+0.2968	+0.49445 + 3.5987		0.380	3.038	3.619
+1.30	+0.3144	+0.53396 + 3.7413		0.362	2.971	3.601
+1.35	+0.3311	+0.57302 + 3.8818		0.341	2.916	3.593
+1.40	+0.3470	+0.61167 + 4.0206		0.320	2.873	3.592
+1.45	+0.3619	+0.64996 + 4.1582		0.298	2.840	3.597
+1.50	+0.3758	+0.68794 + 4.2950		0.277	2.817	3.607
+1.55	+0.3887	+0.72568 + 4.4314		0.256	2.803	3.621
+1.60	+0.4007	+0.76326 + 4.5678		0.236	2.798	3.638
+1.65	+0.4118	+0.80074 + 4.7044		0.217	2.800	3.656
+1.70	+0.4220	+0.83818 + 4.8417		0.194	2.808	3.675
+1.75	+0.4314	+0.87567 + 4.9798		0.183	2.823	3.696
+1.80	+0.4400	+0.91324 + 5.1191		0.168	2.842	3.716
+1.85	+0.4479	+0.95096 + 5.2597		0.154	2.866	3.737
+1.90	+0.4552	+0.98887 + 5.4017		0.142	2.893	3.756
+1.95	+0.4620	+1.02703 + 5.5454		0.131	2.923	3.775
+2.00	+0.4682	+1.06545 + 5.6908		0.120	2.956	3.794
+2.05	+0.4739	+1.10419 + 5.8381		0.111	2.991	3.810
+2.10	+0.4792	+1.14326 + 5.9873		0.103	3.027	3.826
+2.15	+0.4841	+1.18268 + 6.1384		0.096	3.064	3.841
+2.20	+0.4887	+1.22247 + 6.2915		0.089	3.101	3.854
+2.25	+0.4930	+1.26265 + 6.4466		0.083	3.139	3.866
+2.30	+0.4970	+1.30322 + 6.6037		0.078	3.176	3.877
+2.35	+0.5008	+1.34418 + 6.7626		0.073	3.214	3.887
+2.40	+0.5043	+1.38554 + 6.9236		0.069	3.250	3.895
+2.45	+0.5076	+1.42729 + 7.0864		0.065	3.286	3.903
+2.50	+0.5108	+1.46942 + 7.2510		0.061	3.320	3.910
+2.55	+0.5137	+1.51193 + 7.4173		0.058	3.354	3.917
+2.60	+0.5166	+1.55481 + 7.5854		0.055	3.386	3.922
+2.65	+0.5193	+1.59805 + 7.7551		0.053	3.417	3.927
+2.70	+0.5219	+1.64162 + 7.9263		0.051	3.446	3.932
+2.75	+0.5243	+1.68553 + 8.0990		0.048	3.475	3.936
+2.80	+0.5267	+1.72975 + 8.2731		0.047	3.501	3.939
+2.85	+0.5290	+1.77426 + 8.4485		0.045	3.527	3.943
+2.90	+0.5312	+1.81906 + 8.6252		0.043	3.550	3.945
+2.95	+0.5333	+1.86414 + 8.8031		0.042	3.573	3.948
+3.00	+0.5354	+1.90946 + 8.9821		0.040	3.594	3.950
+3.05	+0.5374	+1.95503 + 9.1621		0.039	3.614	3.952
+3.10	+0.5393	+2.00082 + 9.3431		0.038	3.632	3.954
+3.15	+0.5412	+2.04682 + 9.5250		0.037	3.650	3.956
+3.20	+0.5430	+2.09301 + 9.7078		0.036	3.667	3.958
+3.25	+0.5448	+2.13940 + 9.8914		0.035	3.682	3.959
+3.30	+0.5465	+2.18595 +10.0758		0.034	3.696	3.960
+3.35	+0.5482	+2.23267 +10.2608		0.034	3.709	3.961

4.17

(2)	(4)	(5)	(6)	(7)	(8)	(9)
+1.80	+0.4636	+0.87438	+5.1790	0.223	2.943	4.080
+1.82	+0.4679	+0.88870	+5.2371	0.217	2.951	4.032
+1.84	+0.4722	+0.90321	+5.2953	0.212	2.957	3.991
+1.86	+0.4763	+0.91791	+5.3537	0.206	2.963	3.957
+1.88	+0.4803	+0.93275	+5.4122	0.201	2.969	3.928
+1.90	+0.4842	+0.94774	+5.4709	0.196	2.975	3.905
+1.92	+0.4880	+0.96285	+5.5297	0.190	2.980	3.884
+1.94	+0.4917	+0.97806	+5.5887	0.185	2.986	3.868
+1.96	+0.4954	+0.99338	+5.6478	0.180	2.993	3.855
+1.98	+0.4989	+1.00877	+5.7071	0.175	2.999	3.845
+2.00	+0.5023	+1.02425	+5.7665	0.170	3.005	3.836
+2.05	+0.5104	+1.06323	+5.9158	0.159	3.021	3.823
+2.10	+0.5181	+1.10256	+6.0660	0.148	3.040	3.818
+2.15	+0.5252	+1.14219	+6.2174	0.138	3.060	3.819
+2.20	+0.5318	+1.18211	+6.3699	0.129	3.082	3.823
+2.25	+0.5380	+1.22229	+6.5236	0.121	3.105	3.830
+2.30	+0.5439	+1.26274	+6.6787	0.113	3.131	3.838
+2.35	+0.5493	+1.30344	+6.8351	0.106	3.156	3.847
+2.40	+0.5544	+1.34443	+6.9929	0.099	3.183	3.855
+2.45	+0.5592	+1.38569	+7.1522	0.094	3.211	3.864
+2.50	+0.5638	+1.42723	+7.3129	0.088	3.239	3.872
+2.55	+0.5680	+1.46906	+7.4750	0.083	3.267	3.881
+2.60	+0.5721	+1.51118	+7.6387	0.079	3.295	3.888
+2.65	+0.5759	+1.55360	+7.8037	0.075	3.323	3.895
+2.70	+0.5795	+1.59630	+7.9702	0.071	3.350	3.901
+2.75	+0.5830	+1.63929	+8.1380	0.068	3.377	3.907
+2.80	+0.5863	+1.68257	+8.3072	0.064	3.403	3.913
+2.85	+0.5894	+1.72612	+8.4778	0.062	3.428	3.918
+2.90	+0.5924	+1.76995	+8.6496	0.059	3.453	3.922
+2.95	+0.5953	+1.81404	+8.8226	0.056	3.476	3.926

4.17 (CONT.)

(2)	(4)	(5)	(6)	(7)	(8)	(9)
+3.00	+0.5981	+1.85839	+8.9968	0.054	3.499	3.930
+3.05	+0.6007	+1.90299	+9.1722	0.052	3.521	3.934
+3.10	+0.6033	+1.94782	+9.3486	0.050	3.542	3.937
+3.20	+0.6082	+2.03816	+9.7045	0.047	3.581	3.942
+3.30	+0.6127	+2.12934	+10.0641	0.044	3.615	3.947
+3.40	+0.6170	+2.22126	+10.4270	0.042	3.645	3.951
+3.50	+0.6211	+2.31385	+10.7930	0.040	3.674	3.954
+3.60	+0.6250	+2.40704	+11.1616	0.038	3.699	3.956
+3.70	+0.6287	+2.50076	+11.5324	0.036	3.720	3.959
+3.80	+0.6323	+2.59495	+11.9054	0.035	3.740	3.961
+3.90	+0.6357	+2.68955	+12.2802	0.033	3.756	3.962
+4.00	+0.6390	+2.78451	+12.6566	0.032	3.772	3.964

4.18

(2)	(4)	(5)	(6)	(7)	(8)	(9)
+2.60	+0.5800	+1.48396	+ 7.7059	0.100	3.445	4.186
+2.62	+0.5820	+1.50049	+ 7.7746	0.098	3.456	4.143
+2.64	+0.5840	+1.51724	+ 7.8436	0.097	3.466	4.105
+2.66	+0.5858	+1.53418	+ 7.9129	0.096	3.475	4.073
+2.68	+0.5877	+1.55128	+ 7.9823	0.095	3.483	4.046
+2.70	+0.5896	+1.56853	+ 8.0519	0.093	3.489	4.023
+2.72	+0.5914	+1.58590	+ 8.1216	0.092	3.495	4.003
+2.74	+0.5933	+1.60338	+ 8.1914	0.091	3.500	3.987
+2.76	+0.5951	+1.62095	+ 8.2613	0.090	3.505	3.974
+2.78	+0.5969	+1.63860	+ 8.3314	0.089	3.510	3.963
+2.80	+0.5986	+1.65631	+ 8.4015	0.087	3.514	3.954
+2.85	+0.6029	+1.70084	+ 8.5771	0.085	3.522	3.937
+2.90	+0.6071	+1.74563	+ 8.7532	0.082	3.531	3.927
+2.95	+0.6111	+1.79061	+ 8.9297	0.079	3.538	3.922
+3.00	+0.6150	+1.83574	+ 9.1066	0.077	3.546	3.919
+3.05	+0.6188	+1.88099	+ 9.2839	0.074	3.553	3.917
+3.10	+0.6224	+1.92634	+ 9.4616	0.072	3.561	3.919
+3.15	+0.6260	+1.97178	+ 9.6398	0.070	3.569	3.920
+3.20	+0.6294	+2.01732	+ 9.8183	0.068	3.577	3.922
+3.25	+0.6327	+2.06295	+ 9.9973	0.066	3.586	3.923
+3.30	+0.6359	+2.10867	+10.1767	0.064	3.594	3.926
+3.35	+0.6391	+2.15447	+10.3566	0.062	3.603	3.928
+3.40	+0.6421	+2.20036	+10.5368	0.060	3.612	3.930
+3.45	+0.6451	+2.24634	+10.7176	0.058	3.620	3.932
+3.50	+0.6480	+2.29241	+10.8987	0.057	3.629	3.934
+3.60	+0.6535	+2.38481	+11.2624	0.054	3.646	3.937
+3.70	+0.6587	+2.47756	+11.6278	0.051	3.366	3.941
+3.80	+0.66372	+2.57064	+11.9948	0.049	3.679	3.944
+3.90	+0.6685	+2.66406	+12.3634	0.046	3.694	3.947
+4.00	+0.6730	+2.75780	+12.7335	0.044	3.709	3.950

4.19

(2)	(4)	(5)	(6)	(7)	(8)	(9)
-0.20	+0.0023	-0.82878	- 1.5873	0.041	10.938	4.244
-0.18	+0.0026	-0.80873	- 1.5027	0.044	10.627	4.198
-0.16	+0.0030	-0.78850	- 1.4182	0.049	10.325	4.159
-0.14	+0.0034	-0.76814	- 1.3339	0.053	10.032	4.128
-0.12	+0.0039	-0.74767	- 1.2497	0.058	9.748	4.101
-0.10	+0.0044	-0.72713	- 1.1657	0.064	9.475	4.078
-0.08	+0.0050	-0.70654	- 1.0819	0.069	9.213	4.060
-0.06	+0.0057	-0.68592	- 0.9984	0.075	8.960	4.044
-0.04	+0.0064	-0.66529	- 0.9151	0.082	8.717	4.030
-0.02	+0.0072	-0.64466	- 0.8320	0.088	8.483	4.018
0.00	+0.0081	-0.62404	- 0.7493	0.095	8.259	4.007
+0.05	+0.0108	-0.57260	- 0.5438	0.115	7.736	3.984
+0.10	+0.0142	-0.52141	- 0.3403	0.136	7.262	3.965
+0.15	+0.0185	-0.47055	- 0.1391	0.159	6.832	3.947
+0.20	+0.0236	-0.42008	+ 0.0596	0.184	6.440	3.929
+0.25	+0.0298	-0.37006	+ 0.2557	0.211	6.082	3.909
+0.30	+0.0372	-0.32053	+ 0.4488	0.238	5.752	3.888
+0.35	+0.0457	-0.27153	+ 0.6387	0.266	5.447	3.866
+0.40	+0.0556	-0.22313	+ 0.8253	0.293	5.166	3.841
+0.45	+0.0667	-0.17536	+ 1.0081	0.320	4.904	3.815
+0.50	+0.0791	-0.12827	+ 1.1872	0.344	4.661	3.788
+0.55	+0.0928	-0.08190	+ 1.3622	0.366	4.435	3.760
+0.60	+0.1076	-0.03626	+ 1.5332	0.385	4.226	3.732
+0.65	+0.1235	+0.00860	+ 1.7000	0.400	4.033	3.704
+0.70	+0.1402	+0.05269	+ 1.8627	0.410	3.856	3.678
+0.75	+0.1576	+0.09599	+ 2.0215	0.417	3.693	3.653
+0.80	+0.1755	+0.13853	+ 2.1764	0.418	3.547	3.631
+0.85	+0.1937	+0.18032	+ 2.3277	0.416	3.415	3.612
+0.90	+0.2119	+0.22139	+ 2.4757	0.409	3.298	3.596
+0.95	+0.2300	+0.26179	+ 2.6207	0.398	3.195	3.584

4.19 (CONT.)

(2)	(4)	(5)	(6)	(7)	(8)	(9)
+1.00	+0.2476	+0.30156	+ 2.7631	0.385	3.106	3.576
+1.05	+0.2648	+0.34078	+ 2.9032	0.368	3.030	3.572
+1.10	+0.2814	+0.37948	+ 3.0414	0.350	2.967	3.572
+1.15	+0.2972	+0.41775	+ 3.1782	0.330	2.916	3.576
+1.20	+0.3122	+0.45565	+ 3.3138	0.310	2.875	3.584
+1.25	+0.3263	+0.49325	+ 3.4488	0.289	2.846	3.595
+1.30	+0.3396	+0.53062	+ 3.5834	0.268	2.825	3.608
+1.35	+0.3519	+0.56783	+ 3.7180	0.248	2.814	3.625
+1.40	+0.3634	+0.60495	+ 3.8528	0.229	2.810	3.643
+1.45	+0.3740	+0.64203	+ 3.9883	0.211	2.813	3.662
+1.50	+0.3838	+0.67915	+ 4.1246	0.194	2.822	3.682
+1.55	+0.3928	+0.71636	+ 4.2619	0.179	2.837	3.702
+1.60	+0.4012	+0.75370	+ 4.4006	0.164	2.857	3.722
+1.65	+0.4089	+0.79124	+ 4.5407	0.151	2.881	3.743
+1.70	+0.4160	+0.82900	+ 4.6824	0.139	2.908	3.762
+1.75	+0.4226	+0.86703	+ 4.8258	0.128	2.938	3.780
+1.80	+0.4286	+0.90537	+ 4.9711	0.118	2.970	3.798
+1.85	+0.4343	+0.94403	+ 5.1182	0 110	3.005	3.815
+1.90	+0.4395	+0.98305	+ 5.2674	0.102	3.040	3.830
+1.95	+0.4443	+1.02244	+ 5.4185	0.095	3.077	3.843
+2.00	+0.4489	+1.06221	+ 5.5716	0.088	3.113	3.856
+2.05	+0.4531	+1.10238	+ 5.7267	0.082	3.150	3.868
+2.10	+0.4570	+1.14294	+ 5.8839	0.077	3.188	3.879
+2.15	+0.4608	+1.18391	+ 6.0430	0.073	3.224	3.888
+2.20	+0.4643	+1.22528	+ 6.2040	0.068	3.260	3.897
+2.25	+0.4676	+1.26704	+ 6.3669	0.065	3.295	3.904
+2.30	+0.4707	+1.30919	+ 6.5316	0.061	3.329	3.911
+2.35	+0.4737	+1.35172	+ 6.6981	0.058	3.362	3.917
+2.40	+0.4765	+1.39462	+ 6.8662	0.055	3.393	3.923
+2.45	+0.4791	+1.43788	+ 7.0360	0.053	3.424	3.927
+2.50	+0.4818	+1.48148	+ 7.2074	0.050	3.452	3.932
+2.55	+0.4842	+1.52540	+ 7.3802	0.048	3.480	3.936
+2.60	+0.4866	+1.56964	+ 7.5544	0.047	3.506	3.939
+2.65	+0.4889	+1.61418	+ 7.7299	0.045	3.531	3.942
+2.70	+0.4911	+1.65900	+ 7.9067	0.043	3.554	3.945
+2.75	+0.4932	+1.70409	+ 8.0846	0.042	3.577	3.948
+2.80	+0.4953	+1.74944	+ 8.2637	0.040	3.597	3.950
+2.85	+0.4973	+1.79502	+ 8.4438	0.039	3.617	3.952
+2.90	+0.4992	+1.84082	+ 8.6248	0.038	3.635	3.954
+2.95	+0.5011	+1.88683	+ 8.8068	0.037	3.652	3.956
+3.00	+0.5029	+1.93304	+ 8.9896	0.036	3.668	3.958
+3.05	+0.5047	+1.97943	+ 9.1732	0.035	3.683	3.959
+3.10	+0.5064	+2.02599	+ 9.3576	0.034	3.698	3.960
+3.15	+0.5082	+2.07272	+ 9.5427	0.034	3.711	3.961

4.20

(2)	(4)	(5)	(6)	(7)	(8)	(9)
+0.60	+0.1264	-0.06557	+ 1.6046	0.507	4.330	4.045
+0.62	+0.1347	-0.04840	+ 1.6734	0.520	4.237	3.969
+0.64	+0.1432	-0.03114	+ 1.7413	0.533	4.144	3.901
+0.66	+0.1520	-0.01384	+ 1.8083	0.545	4.052	3.843
+0.68	+0.1611	+0.00346	+ 1.8743	0.556	3.962	3.791
+0.70	+0.1704	+0.02073	+ 1.9394	0.565	3.871	3.745
+0.72	+0.1799	+0.03793	+ 2.0034	0.573	3.784	3.704
+0.74	+0.1896	+0.05504	+ 2.0665	0.580	3.698	3.667
+0.76	+0.1995	+0.07204	+ 2.1285	0.585	3.614	3.634
+0.78	+0.2096	+0.08892	+ 2.1896	0.585	3.533	3.604
+0.80	+0.2198	+0.10567	+ 2.2498	0.592	3.455	3.577
+0.85	+0.2455	+0.14690	+ 2.3960	0.592	3.273	3.519
+0.90	+0.2715	+0.18716	+ 2.5367	0.584	3.110	3.473
+0.95	+0.2973	+0.22645	+ 2.6725	0.569	2.968	3.438
+1.00	+0.3226	+0.26479	+ 2.8038	0.546	2.845	3.413
+1.05	+0.3469	+0.30225	+ 2.9313	0.518	2.741	3.397
+1.10	+0.3701	+0.33891	+ 3.0557	0.487	2.656	3.390
+1.15	+0.3919	+0.37487	+ 3.1776	0.452	2.588	3.390
+1.20	+0.4123	+0.41022	+ 3.2976	0.417	2.535	3.399
+1.25	+0.4311	+0.44508	+ 3.4163	0.381	2.498	3.414
+1.30	+0.4484	+0.47954	+ 3.5343	0.346	2.474	3.434
+1.35	+0.4641	+0.51370	+ 3.6520	0.313	2.461	3.459
+1.40	+0.4783	+0.54767	+ 3.7700	0.282	2.460	3.489
+1.45	+0.4912	+0.58155	+ 3.8887	0.253	2.468	3.520
+1.50	+0.5028	+0.61542	+ 4.0085	0.226	2.485	3.554
+1.55	+0.5132	+0.64936	+ 4.1297	0.203	2.509	3.588
+1.60	+0.5226	+0.68345	+ 4.2526	0.188	2.539	3.622
+1.65	+0.5310	+0.71778	+ 4.3775	0.163	2.575	3.655
+1.70	+0.5386	+0.75239	+ 4.5046	0.146	2.616	3.688
+1.75	+0.5454	+0.78735	+ 4.6340	0.132	2.660	3.718

4.20 (CONT.)

(2)	(4)	(5)	(6)	(7)	(8)	(9)
+1.80	+0.5515	+0.82271	+ 4.7660	0.119	2.708	3.746
+1.85	+0.5570	+0.85851	+ 4.9006	0.107	2.758	3.773
+1.90	+0.5621	+0.89479	+ 5.0380	0.097	2.809	3.797
+1.95	+0.5667	+0.93158	+ 5.1780	0.089	2.861	3.818
+2.00	+0.5709	+0.96890	+ 5.3209	0.081	2.914	3.838
+2.05	+0.5748	+1.00677	+ 5.4666	0.075	2.967	3.855
+2.10	+0.5783	+1.04519	+ 5.6150	0.069	3.019	3.870
+2.15	+0.5816	+1.08417	+ 5.7661	0.164	3.071	3.884
+2.20	+0.5847	+1.12371	+ 5.9199	0.059	3.122	3.896
+2.25	+0.5875	+1.16380	+ 6.0763	0.055	3.171	3.906
+2.30	+0.5908	+1.20443	+ 6.2352	0.052	3.218	3.914
+2.35	+0.5927	+1.24559	+ 6.3964	0.049	3.264	3.922
+2.40	+0.5950	+1.28725	+ 6.5600	0.046	3.307	3.929
+2.45	+0.5973	+1.32942	+ 6.7258	0.044	3.348	3.934
+2.50	+0.5994	+1.37205	+ 6.8937	0.041	3.388	3.940
+2.55	+0.6014	+1.41513	+ 7.0635	0.040	3.425	3.944
+2.60	+0.6033	+1.45864	+ 7.2352	0.038	3.460	3.948
+2.65	+0.6052	+1.50256	+ 7.4086	0.036	3.493	3.951
+2.70	+0.6069	+1.54685	+ 7.5837	0.035	3.524	3.954
+2.75	+0.6086	+1.59150	+ 7.7603	0.034	3.553	3.957
+2.80	+0.6103	+1.63649	+ 7.9384	0.032	3.580	3.959
+2.85	+0.6119	+1.68178	+ 8.1178	0.031	3.605	3.961
+2.90	+0.6134	+1.72737	+ 8.2984	0.030	3.629	3.963
+2.95	+0.6149	+1.77323	+ 8.4802	0.030	3.650	3.964
+3.00	+0.6164	+1.81935	+ 8.6630	0.029	3.670	3.966
+3.05	+0.6178	+1.86569	+ 8.8468	0.028	3.689	3.967
+3.10	+0.6192	+1.91225	+ 9.0315	0.027	3.706	3.968

4.21

(2)	(4)	(5)	(6)	(7)	(8)	(9)
+1.40	+0.5226	+0.49877	+3.8123	0.385	2.487	3.911
+1.42	+0.5298	+0.51109	+3.8602	0.372	2.484	3.859
+1.44	+0.5369	+0.52358	+3.9081	0.359	2.483	3.815
+1.46	+0.5437	+0.53621	+3.9560	0.346	2.483	3.778
+1.48	+0.5503	+0.54898	+4.0041	0.333	2.482	3.747
+1.50	+0.5566	+0.56186	+4.0522	0.321	2.484	3.722
+1.52	+0.5627	+0.57484	+4.1004	0.309	2.485	3.701
+1.54	+0.5686	+0.58792	+4.1487	0.297	2.488	3.686
+1.56	+0.5742	+0.60108	+4.1971	0.285	2.492	3.674
+1.58	+0.5797	+0.61432	+4.2457	0.274	2.496	3.665
+1.60	+0.5849	+0.62763	+4.2944	0.263	2.502	3.659
+1.65	+0.5971	+0.66117	+4.4170	0.237	2.520	3.654
+1.70	+0.6081	+0.69507	+4.5409	0.213	2.544	3.659
+1.75	+0.6180	+0.72931	+4.6664	0.192	2.572	3.672
+1.80	+0.6269	+0.76390	+4.7937	0.172	2.606	3.690
+1.85	+0.6350	+0.79884	+4.9230	0.155	2.644	3.711
+1.90	+0.6423	+0.83416	+5.0545	0.140	2.685	3.733
+1.95	+0.6488	+0.86990	+5.1883	0.127	2.730	3.755
+2.00	+0.6548	+0.90606	+5.3245	0.115	2.776	3.777
+2.05	+0.6602	+0.94269	+5.4632	0.104	2.824	3.797
+2.10	+0.6652	+0.97979	+5.6044	0.095	2.874	3.817
+2.15	+0.6697	+1.01739	+5.7483	0.087	2.924	3.834
+2.20	+0.6739	+1.05551	+5.8948	0.080	2.974	3.851
+2.25	+0.6777	+1.09414	+6.0438	0.074	3.024	3.865
+2.30	+0.6813	+1.13330	+6.1954	0.069	3.073	3.878
+2.35	+0.6846	+1.17299	+6.3496	0.064	3.121	3.890
+2.40	+0.6877	+1.21319	+6.5061	0.060	3.169	3.900
+2.45	+0.6906	+1.25390	+6.6651	0.056	3.214	3.909
+2.50	+0.6933	+1.29512	+6.8264	0.053	3.258	3.917
+2.55	+0.6958	+1.33682	+6.9899	0.050	3.301	3.924
+2.60	+0.6982	+1.37899	+7.1555	0.047	3.341	3.930
+2.65	+0.7005	+1.42162	+7.3231	0.045	3.380	3.935
+2.70	+0.7027	+1.46467	+7.4927	0.042	3.416	3.940
+2.75	+0.7047	+1.50814	+7.6640	0.041	3.451	3.944
+2.80	+0.7067	+1.55200	+7.8371	0.039	3.483	3.947
+2.85	+0.7086	+1.59623	+8.0118	0.037	3.514	3.951
+2.90	+0.7104	+1.64081	+8.1880	0.036	3.542	3.954
+2.95	+0.7122	+1.68572	+8.3656	0.035	3.569	3.956
+3.00	+0.7139	+1.73093	+8.5444	0.034	3.594	3.958
+3.10	+0.7171	+1.82219	+8.9059	0.032	3.639	3.962
+3.20	+0.7202	+1.91445	+9.2715	0.030	3.678	3.965
+3.30	+0.7231	+2.00757	+9.6408	0.029	3.711	3.967
+3.40	+0.7259	+2.10143	+10.0133	0.027	3.740	3.969
+3.50	+0.7286	+2.19591	+10.3883	0.026	3.764	3.970
+3.60	+0.7312	+2.29093	+10.7657	0.025	3.784	3.972

4.21 (CONT.)

(2)	(4)	(5)	(6)	(7)	(8)	(9)
+3.70	+0.7337	+2.38640	+11.1449	0.025	3.802	3.973
+3.80	+0.7361	+2.48225	+11.5258	0.024	3.817	3.973
+3.90	+0.7385	+2.57844	+11.9081	0.023	3.829	3.975
+4.00	+0.7408	+2.67489	+12.2915	0.023	3.840	3.976
+4.10	+0.7430	+2.77159	+12.6760	0.022	3.849	3.977
+4.20	+0.7452	+2.86848	+13.0613	0.022	3.857	3.977
+4.30	+0.7474	+2.96556	+13.4474	0.021	3.864	3.977
+4.40	+0.7495	+3.06278	+13.8341	0.021	3.870	3.978
+4.50	+0.7516	+3.16012	+14.2213	0.021	3.875	3.979
+4.60	+0.7536	+3.25758	+14.6091	0.020	3.880	3.979
+4.70	+0.7556	+3.35513	+14.9972	0.020	3.884	3.979
+4.80	+0.7576	+3.45277	+15.3858	0.020	3.887	3.980
+4.90	+0.7595	+3.55048	+15.7746	0.019	3.890	3.980
+5.00	+0.7614	+3.64826	+16.1638	0.019	3.893	3.980

4.22

(2)	(4)	(5)	(6)	(7)	(8)	(9)
+2.20	+0.6834	+1.02546	+ 5.9563	0.101	3.118	4.173
+2.22	+0.6854	+1.04044	+ 6.0185	0.099	3.139	4.132
+2.24	+0.6873	+1.05566	+ 6.0811	0.097	3.159	4.097
+2.26	+0.6892	+1.07110	+ 6.1441	0.094	3.177	4.067
+2.28	+0.6910	+1.08673	+ 6.2075	0.092	3.195	4.042
+2.30	+0.6929	+1.10254	+ 6.2713	0.090	3.212	4.021
+2.32	+0.6946	+1.11852	+ 6.3354	0.088	3.228	4.003
+2.34	+0.6964	+1.13464	+ 6.3998	0.086	3.243	3.988
+2.36	+0.6981	+1.15090	+ 6.4645	0.084	3.258	3.975
+2.38	+0.6997	+1.16728	+ 6.5295	0.082	3.272	3.965
+2.40	+0.7014	+1.18377	+ 6.5948	0.081	3.286	3.956
+2.45	+0.7053	+1.22544	+ 6.7593	0.077	3.318	3.940
+2.50	+0.7090	+1.26765	+ 6.9254	0.073	3.348	3.931
+2.55	+0.7125	+1.31031	+ 7.0930	0.069	3.376	3.926
+2.60	+0.7159	+1.35335	+ 7.2620	0.066	3.403	3.925
+2.65	+0.7191	+1.39678	+ 7.4324	0.063	3.428	3.925
+2.70	+0.7222	+1.44050	+ 7.6040	0.061	3.452	3.926
+2.75	+0.7252	+1.48452	+ 7.7769	0.058	3.476	3.929
+2.80	+0.7281	+1.52881	+ 7.9510	0.056	3.498	3.931
+2.85	+0.7308	+1.57336	+ 8.1262	0.054	3.519	3.933
+2.90	+0.7335	+1.61815	+ 8.3024	0.052	3.539	3.936
+2.95	+0.7360	+1.66317	+ 8.4796	0.050	3.559	3.938
+3.00	+0.7385	+1.70841	+ 8.6578	0.049	3.577	3.941
+3.05	+0.7409	+1.75385	+ 8.8370	0.047	3.595	3.943
+3.10	+0.7432	+1.79949	+ 9.0170	0.046	3.611	3.945
+3.20	+0.7476	+1.89131	+ 9.3794	0.043	3.642	3.949
+3.30	+0.7518	+1.98380	+ 9.7448	0.041	3.669	3.952
+3.40	+0.7558	+2.07688	+10.1128	0.039	3.694	3.955
+3.50	+0.7596	+2.17049	+10.4831	0.037	3.715	3.958

4.23

(2)	(4)	(5)	(6)	(7)	(8)	(9)
-0.60	+0.0002	-1.22841	- 3.0350	0.008	21.162	4.250
-0.58	+0.0002	-1.20830	- 2.9500	00.009	20.394	4.205
-0.56	+0.0002	-1.18802	- 2.8651	0.010	19.653	4.168
-0.54	+0.0003	-1.16759	- 2.7803	0.011	18.939	4.138
-0.52	+0.0004	-1.14705	- 2.6956	0.013	18.252	4.113
-0.50	+0.0004	-1.12643	- 2.6110	0.014	17.594	4.093
-0.48	+0.0005	-1.10574	- 2.5265	0.016	16.962	4.076
-0.46	+0.0006	-1.08502	- 2.4422	0.018	16.358	4.061
-0.44	+0.0007	-1.06427	- 2.3580	0.020	15.781	4.050
-0.42	+0.0008	-1.04350	- 2.2741	0.022	15.229	4.040
-0.40	+0.0009	-1.02274	- 2.1902	0.025	14.701	4.032
-0.35	+0.0014	-0.97086	- 1.9815	0.032	13.485	4.016
-0.30	+0.0020	-0.91909	- 1.7738	0.042	12.405	4.006
-0.25	+0.0028	-0.86749	- 1.5674	0.053	11.442	3.998
-0.20	+0.0039	-0.81608	- 1.3620	0.066	10.584	3.990
-0.15	+0.0054	-0.76488	- 1.1579	0.082	9.818	3.983
-0.10	+0.0073	-0.71391	- 0.9551	0.101	9.131	3.975
-0.05	+0.0099	-0.66319	- 0.7538	0.123	8.513	3.965
+0.00	+0.0131	-0.61275	- 0.5540	0.148	7.955	3.954
+0.05	+0.0173	-0.56261	- 0.3561	0.175	7.448	3.940
+0.10	+0.0225	-0.51281	- 0.1602	0.206	6.986	3.924
+0.15	+0.0288	-0.46340	+ 0.0332	0.239	6.562	3.905
+0.20	+0.0365	-0.41442	+ 0.2238	0.274	6.171	3.882
+0.25	+0.0456	-0.36596	+ 0.4114	0.310	5.809	3.857
+0.30	+0.0564	-0.31805	+ 0.5955	0.347	5.471	3.828

4.23 (CONT.)

(2)	(4)	(5)	(6)	(7)	(8)	(9)
+0.35	+0.0688	-0.27078	+ 0.7758	0.384	5.156	3.797
+0.40	+0.0830	-0.22421	+ 0.9518	0.419	4.862	3.763
+0.45	+0.0988	-0.17839	+ 1.1234	0.452	4.587	3.727
+0.50	+0.1163	-0.13339	+ 1.2903	0.481	4.330	3.690
+0.55	+0.1353	-0.08926	+ 1.4523	0.505	4.091	3.652
+0.60	+0.1556	-0.04601	+ 1.6094	0.524	3.870	3.615
+0.65	+0.1770	-0.00368	+ 1.7617	0.536	3.667	3.578
+0.70	+0.1993	+0.03773	+ 1.9092	0.542	3.483	3.545
+0.75	+0.2221	+0.07824	+ 2.0522	0.541	3.317	3.515
+0.80	+0.2451	+0.11787	+ 2.1910	0.533	3.169	3.488
+0.35	+0.2680	+0.15668	+ 2.3259	0.519	3.039	3.467
+0.90	+0.2904	+0.19470	+ 2.4574	0.500	2.927	3.452
+0.95	+0.3123	+0.23200	+ 2.5860	0.478	2.843	3.443
+1.00	+0.3332	+0.26866	+ 2.7121	0.449	2.751	3.439
+1.05	+0.3530	+0.30475	+ 2.8363	0.420	2.687	3.442
+1.10	+0.3717	+0.34036	+ 2.9590	0.390	2.637	3.450
+1.15	+0.3892	+0.37558	+ 3.0807	0.359	2.600	3.464
+1.20	+0.4053	+0.41048	+ 3.2020	0.329	2.575	3.482
+1.25	+0.4201	+0.44517	+ 3.3231	0.300	2.561	3.504
+1.30	+0.4337	+0.47971	+ 3.4446	0.272	2.558	3.530
+1.35	+0.4460	+0.51420	+ 3.5668	0.246	2.563	3.557
+1.40	+0.4573	+0.54870	+ 3.6900	0.223	2.576	3.586
+1.45	+0.4675	+0.58330	+ 3.8146	0.201	2.596	3.616
+1.50	+0.4768	+0.61806	+ 3.9408	0.182	2.622	3.646
+1.55	+0.4851	+0.65304	+ 4.0689	0.164	2.654	3.675
+1.60	+0.4927	+0.68830	+ 4.1990	0.148	2.690	3.704
+1.65	+0.4996	+0.72390	+ 4.3313	0.134	2.730	3.731
+1.70	+0.5059	+0.75988	+ 4.4660	0.122	2.772	3.756
+1.75	+0.5116	+0.79627	+ 4.6031	0.111	2.817	3.780
+1.80	+0.5168	+0.83311	+ 4.7428	0.101	2.863	3.802
+1.85	+0.5216	+0.87042	+ 4.8850	0.093	2.911	3.821
+1.90	+0.5260	+0.90824	+ 5.0298	0.085	2.959	3.839
+1.95	+0.5301	+0.94655	+ 5.1773	0.079	3.008	3.855
+2.00	+0.5338	+0.98539	+ 5.3272	0.073	3.056	3.870
+2.05	+0.5373	+1.02474	+ 5.4798	0.068	3.103	3.882
+2.10	+0.5405	+1.06462	+ 5.6348	0.063	3.150	3.893
+2.15	+0.5436	+1.10501	+ 5.7923	0.059	3.195	3.903
+2.20	+0.5464	+1.14591	+ 5.9520	0.056	3.239	3.911
+2.25	+0.5491	+1.18730	+ 6.1141	0.052	3.281	3.919
+2.30	+0.5516	+1.22916	+ 6.2783	0.049	3.322	3.925
+2.35	+0.5540	+1.27149	+ 6.4446	0.047	3.361	3.931
+2.40	+0.5563	+1.31426	+ 6.6128	0.045	3.397	3.936
+2.45	+0.5585	+1.35746	+ 6.7830	0.043	3.432	3.940
+2.50	+0.5606	+1.40106	+ 6.9548	0.041	3.465	3.944
+2.55	+0.5626	+1.44503	+ 7.1284	0.039	3.497	3.948
+2.60	+0.5645	+1.48937	+ 7.3035	0.038	3.526	3.951
+2.65	+0.5663	+1.53404	+ 7.4800	0.036	3.553	3.953
+2.70	+0.5681	+1.57904	+ 7.6580	0.035	3.579	3.956
+2.75	+0.5698	+1.62433	+ 7.8372	0.034	3.603	3.958
+2.80	+0.5715	+1.66990	+ 8.0176	0.033	3.625	3.960
+2.85	+0.5731	+1.71572	+ 8.1991	0.032	3.646	3.962
+2.90	+0.5747	+1.76179	+ 8.3817	0.031	3.665	3.963
+2.95	+0.5762	+1.80809	+ 8.5652	0.030	3.683	3.964
+3.00	+0.5777	+1.85459	+ 8.7495	0.030	3.700	3.966

4.24

(2)	(4)	(5)	(6)	(7)	(8)	(9)
+0.20	+0.0437	-0.43809	+ 0.3069	0.356	6.410	4.157
+0.22	+0.0482	-0.41910	+ 0.3852	0.378	6.247	4.092
+0.24	+0.0532	-0.40000	+ 0.4628	0.402	6.085	4.035
+0.26	+0.0584	-0.38083	+ 0.5396	0.425	5.924	3.984
+0.28	+0.0641	-0.36163	+ 0.6157	0.448	5.764	3.939
+0.30	+0.0702	-0.34246	+ 0.6908	0.472	5.606	3.898
+0.32	+0.0767	-0.32333	+ 0.7650	0.496	5.451	3.861
+0.34	+0.0836	-0.30427	+ 0.8382	0.520	5.298	3.826
+0.36	+0.0910	-0.28532	+ 0.9104	0.543	5.148	3.794
+0.38	+0.0988	-0.26649	+ 0.9816	0.566	5.001	3.762
+0.40	+0.1070	-0.24780	+ 1.0516	0.588	4.857	3.732
+0.45	+0.1293	-0.20177	+ 1.2217	0.641	4.512	3.661
+0.50	+0.1542	-0.15688	+ 1.3845	0.688	4.187	3.593
+0.55	+0.1815	-0.11325	+ 1.5398	0.726	3.887	3.527
+0.60	+0.2108	-0.07093	+ 1.6878	0.754	3.610	3.464
+0.65	+0.2416	-0.02995	+ 1.8284	0.770	3.358	3.403
+0.70	+0.2735	+0.00970	+ 1.9623	0.775	3.132	3.348
+0.75	+0.3060	+0.04806	+ 2.0897	0.766	2.931	3.298
+0.80	+0.3384	+0.08518	+ 2.2114	0.746	2.756	3.256
+0.85	+0.3702	+0.12115	+ 2.3279	0.716	2.606	3.223

4.24 (CONT.)

(2)	(4)	(5)	(6)	(7)	(8)	(9)
+0.90	+0.4010	+0.15607	+ 2.4400	0.677	2.480	3.200
+0.95	+0.4302	+0.19004	+ 2.5484	0.631	2.377	3.186
+1.00	+0.4576	+0.22317	+ 2.6539	0.581	2.294	3.184
+1.05	+0.4830	+0.25559	+ 2.7572	0.529	2.231	3.191
+1.10	+0.5061	+0.28741	+ 2.8590	0.477	2.186	3.208
+1.15	+0.5271	+0.31875	+ 2.9599	0.426	2.157	3.234
+1.20	+0.5459	+0.34974	+ 3.0606	0.378	22.143	3.267
+1.25	+0.5627	+0.38048	+ 3.1616	0.333	2.141	3.306
+1.30	+0.5775	+0.41108	+ 3.2635	0.293	2.151	3.350
+1.35	+0.5906	+0.44165	+ 3.3666	0.256	2.171	3.397
+1.40	+0.6021	+0.47229	+ 3.4715	0.224	2.201	3.446
+1.45	+0.6122	+0.50310	+ 3.5784	0.196	2.238	3.496
+1.50	+0.6211	+0.53414	+ 3.6877	0.171	2.282	3.545
+1.55	+0.6289	+0.56552	+ 3.7997	0.150	2.332	3.592
+1.60	+0.6358	+0.59731	+ 3.9145	0.132	2.386	3.637
+1.65	+0.6418	+0.6296 +	4.0325	0.116	2.445	3.678
+1.70	+0.6472	+0.66234	+ 4.1537	0.103	2.506	3.717
+1.75	+0.6519	+0.69569	+ 4.2783	0.092	2.571	3.752
+1.80	+0.6562	+0.72966	+ 4.4063	0.082	2.636	3.783
+1.85	+0.6600	+0.76429	+ 4.5378	0.073	2.703	3.811
+1.90	+0.6634	+0.79959	+ 4.6728	0.066	2.769	3.836
+1.95	+0.6666	+0.83559	+ 4.8113	0.060	2.836	3.857
+2.00	+0.6694	+0.87230	+ 4.9532	0.055	2.902	3.875
+2.05	+0.6720	+0.90972	+ 5.0986	0.050	2.966	3.891
+2.10	+0.6744	+0.94784	+ 5.2472	0.046	3.028	3.905
+2.15	+0.6766	+0.98666	+ 5.3990	0.043	3.089	3.916
+2.20	+0.6786	+1.02616	+ 5.5538	0.040	3.147	3.926
+2.25	+0.6805	+1.06632	+ 5.7117	0.037	3.203	3.934
+2.30	+0.6823	+1.10712	+ 5.8723	0.035	3.256	3.941
+2.35	+0.6840	+1.14853	+ 6.0356	0.033	3.307	3.947
+2.40	+0.6856	+1.19052	+ 6.2015	0.031	3.354	3.952
+2.45	+0.6871	+1.23307	+ 6.3697	0.030	3.399	3.956
+2.50	+0.6885	+1.27614	+ 6.5402	0.028	3.441	3.959
+2.55	+0.6899	+1.31970	+ 6.7127	0.027	3.481	3.962
+2.60	+0.6912	+1.36372	+ 6.8872	0.026	3.517	3.965
+2.65	+0.6925	+1.40817	+ 7.0635	0.025	3.551	3.967
+2.70	+0.6937	+1.45302	+ 7.2414	0.024	3.582	3.969
+2.75	+0.6949	+1.49824	+ 7.4209	0.023	3.611	3.971
+2.80	+0.6960	+1.54380	+ 7.6019	0.022	3.638	3.972
+2.85	+0.6971	+1.58968	+ 7.7842	0.022	3.663	3.973
+2.90	+0.6982	+1.63585	+ 7.9676	0.021	3.686	3.975
+2.95	+0.6992	+1.68228	+ 8 1522	0.021	3.707	3.976

4.25

(2)	(4)	(5)	(6)	(7)	(8)	(9)
+1.00	+0.5289	+0.16970	+2.6788	0.820	2.202	3.597
+1.02	+0.5437	+0.18088	+2.7186	0.799	2.163	3.517
+1.04	+0.5581	+0.19215	+2.7578	0.776	2.127	3.449
+1.06	+0.5721	+0.20348	+2.7965	0.752	2.093	3.390
+1.08	+0.5857	+0.21486	+2.8348	0.727	2.061	3.340
+1.10	+0.5989	+0.22627	+2.8727	0.701	2.033	3.299
+1.12	+0.6117	+0.23768	+2.9102	0.674	2.006	3.265
+1.14	+0.6240	+0.24911	+2.9473	0.647	1.983	3.237
+1.16	+0.6358	+0.26054	+2.9841	0.620	1.962	3.214
+1.18	+0.6472	+0.27195	+3.0208	0.593	1.944	3.197
+1.20	+0.6581	+0.28335	+3.0572	0.565	1.928	3.185
+1.22	+0.6685	+0.29473	+3.0934	0.538	1.915	3.176
+1.24	+0.6784	+0.30610	+3.1295	0.512	1.905	3.172
+1.26	+0.6878	+0.31744	+3.1655	0.485	1.897	3.172
+1.28	+0.6968	+0.32877	+3.2014	0.460	1.891	3.175
+1.30	+0.7053	+0.34008	+3.2374	0.435	1.888	3.181
+1.35	+0.7247	+0.36829	+3.3274	0.378	1.888	3.206
+1.40	+0.7415	+0.39647	+3.4183	0.326	1.901	3.243
+1.45	+0.7561	+0.42468	+3.5104	0.280	1.925	3.290
+1.50	+0.7686	+0.45301	+3.6043	0.240	1.958	3.342
+1.55	+0.7794	+0.48152	+3.7004	0.205	2.000	3.398
+1.60	+0.7886	+0.51030	+3.7990	0.176	2.050	3.455
+1.65	+0.7966	+0.53943	+3.9005	0.151	2.107	3.512
+1.70	+0.8035	+0.56899	+4.0051	0.130	2.168	3.567
+1.75	+0.8094	+0.59906	+4.1131	0.112	2.235	3.619
+1.80	+0.8146	+0.62968	+4.2247	0.098	2.305	3.667
+1.85	+0.8190	+0.66094	+4.3400	0.085	2.378	3.712
+1.90	+0.8230	+0.69286	+4.4592	0.075	2.452	3.751
+1.95	+0.8264	+0.72551	+4.5822	0.066	2.529	3.787
+2.00	+0.8295	+0.75891	+4.7092	0.058	2.606	3.818

4.25 (CONT.)

(2)	(4)	(5)	(6)	(7)	(8)	(9)
+2.05	+0.8322	+0.79310	+4.8402	0.052	2.682	3.844
+2.10	+0.8347	+0.82808	+4.9751	0.047	2.758	3.867
+2.15	+0.8369	+0.86386	+5.1138	0.042	2.833	3.886
+2.20	+0.8390	+0.90046	+5.2564	0.039	2.906	3.903
+2.25	+0.8408	+0.93786	+5.4026	0.035	2.977	3.916
+2.30	+0.8425	+0.97604	+5.5524	0.032	3.046	3.928
+2.35	+0.8440	+1.01499	+5.7056	0.030	3.111	3.938
+2.40	+0.8455	+1.05469	+5.8621	0.028	3.174	3.945
+2.45	+0.8468	+1.09510	+6.0216	0.026	3.233	3.952
+2.50	+0.8481	+1.13620	+6.1842	0.025	3.289	3.957
+2.55	+0.8493	+1.17794	+6.3495	0.023	3.342	3.962
+2.60	+0.8504	+1.22030	+6.5174	0.022	3.391	3.965
+2.65	+0.8515	+1.26324	+6.6877	0.021	3.438	3.968
+2.70	+0.8525	+1.30671	+6.8603	0.020	3.480	3.971
+2.75	+0.8535	+1.35069	+7.0350	0.019	3.520	3.974
+2.80	+0.8544	+1.39514	+7.2117	0.019	3.557	3.976
+2.85	+0.8553	+1.44003	+7.3901	0.018	3.591	3.977
+2.90	+0.8562	+1.48531	+7.5702	0.017	3.623	3.978
+2.95	+0.8571	+1.53097	+7.7519	0.017	3.651	3.979
+3.00	+0.8579	+1.57696	+7.9349	0.016	3.678	3.980
+3.05	+0.8587	+1.62326	+8.1192	0.016	3.702	3.981
+3.10	+0.8595	+1.66986	+8.3047	0.016	3.724	3.982
+3.15	+0.8603	+1.71671	+8.4913	0.015	3.744	3.982
+3.20	+0.8610	+1.76380	+8.6788	0.015	3.762	3.983
+3.25	+0.8618	+1.81110	+8.8672	0.015	3.779	3.983
+3.30	+0.8625	+1.85860	+9.0565	0.014	3.794	3.984
+3.35	+0.8632	+1.90628	+9.2465	0.014	3.808	3.984
+3.40	+0.8639	+1.95413	+9.4371	0.014	3.820	3.985
+3.45	+0.8646	+2.00212	+9.6283	0.014	3.832	3.985
+3.50	+0.8653	+2.05025	+9.8202	0.014	3.842	3.985
+3.55	+0.8660	+2.09850	+10.0124	0.014	3.852	3.986
+3.60	+0.8666	+2.14686	+10.2052	0.013	3.860	3.986
+3.65	+0.8673	+2.19533	+10.3983	0.013	3.868	3.986
+3.70	+0.8680	+2.24388	+10.5918	0.013	3.875	3.986
+3.75	+0.8686	+2.29251	+10.7857	0.013	3.881	3.986
+3.80	+0.8693	+2.34121	+10.9799	0.013	3.887	3.987
+3.85	+0.8699	+2.38999	+11.1743	0.013	3.892	3.987
+3.90	+0.8706	+2.43882	+11.3690	0.013	3.896	3.987
+3.95	+0.8712	+2.48771	+11.5639	0.012	3.901	3.987
+4.00	+0.8718	+2.53665	+11.7590	0.012	3.904	3.987
+4.10	+0.8730	+2.63465	+12.1498	0.012	3.911	3.987
+4.20	+0.8742	+2.73281	+12.5412	0.012	3.917	3.987
+4.30	+0.8754	+2.83110	+12.9331	0.012	3.922	3.988
+4.40	+0.8766	+2.92948	+13.3254	0.012	3.926	3.988
+4.50	+0.8778	+3.02796	+13.7182	0.012	3.929	3.988
+4.60	+0.8790	+3.12649	+14.1110	0.012	3.931	3.989
+4.70	+0.8801	+3.22509	+14.5043	0.012	3.934	3.989
+4.80	+0.8813	+3.32372	+14.8976	0.011	3.936	3.989
+4.90	+0.8824	+3.42240	+15.2913	0.011	3.937	3.988
+5.00	+0.8835	+3.52114	+15.6851	0.011	3.938	3.989

4.26

(2)	(4)	(5)	(6)	(7)	(8)	(9)
+1.80	+0.8325	+0.58804	+ 4.2764	0.126	2.434	4.102
+1.82	+0.8350	+0.59984	+ 4.3244	0.120	2.465	4.072
+1.84	+0.8373	+0.61189	+ 4.3733	0.115	2.495	4.044
+1.86	+0.8395	+0.62417	+ 4.4228	0.110	2.525	4.020
+1.88	+0.8416	+0.63668	+ 4.4729	0.105	2.555	3.999
+1.90	+0.8436	+0.64940	+ 4.5236	0.100	2.585	3.981
+1.92	+0.8456	+0.66232	+ 4.5750	0.096	2.614	3.967
+1.94	+0.8474	+0.67544	+ 4.6270	0.092	2.643	3.955
+1.96	+0.8492	+0.68875	+ 4.6795	0.088	2.671	3.944
+1.98	+0.8509	+0.70224	+ 4.7327	0.085	2.700	3.936
+2.00	+0.8526	+0.71590	+ 4.7864	0.081	2.728	3.930
+2.05	+0.8566	+0.75077	+ 4.9232	0.074	2.795	3.918
+2.10	+0.8601	+0.78660	+ 5.0635	0.067	2.862	3.914
+2.15	+0.8633	+0.82332	+ 5.2071	0.061	2.927	3.914
+2.20	+0.8662	+0.86086	+ 5.3541	0.056	2.990	3.916
+2.25	+0.8689	+0.89917	+ 5.5042	0.052	3.050	3.920
+2.30	+0.8714	+0.93822	+ 5.6574	0.048	3.108	3.925
+2.35	+0.8738	+0.97796	+ 5.8134	0.045	3.164	3.930
+2.40	+0.8759	+0.01836	+ 5.9723	0.042	3.217	3.935
+2.45	+0.8780	+1.05938	+ 6.1338	0.040	3.267	3.940
+2.50	+0.8799	+1.10099	+ 6.2978	0.037	3.315	3.944
+2.55	+0.8817	+1.14315	+ 6.4642	0.035	3.360	3.948
+2.60	+0.8834	+1.18584	+ 6.6329	0.034	3.403	3.952
+2.65	+0.8850	+1.22903	+ 6.8036	0.032	3.443	3.955
+2.70	+0.8866	+1.27268	+ 6.9763	0.031	3.480	3.958

4.26 CONT.)

(2)	(4)	(5)	(6)	(7)	(8)	(9)
+2.75	+0.8881	+1.31676	+ 7.1509	0.030	3.515	3.961
+2.80	+0.8896	+1.36125	+ 7.3271	0.028	3.547	3.963
+2.85	+0.8910	+1.40612	+ 7.5050	0.027	3.577	3.965
+2.90	+0.8923	+1.45133	+ 7.6843	0.027	3.605	3.967
+2.95	+0.8936	+1.49687	+ 7.8650	0.026	3.631	3.968
+3.00	+0.8949	+1.54271	+ 8.0470	0.025	3.655	3.970
+3.05	+0.8961	+1.58884	+ 8.2301	0.024	3.676	3.971
+3.10	+0.8973	+1.63521	+ 8.4143	0.024	3.697	3.972
+3.15	+0.8985	+1.68183	+ 8.5994	0.023	3.715	3.973
+3.20	+0.8997	+1.72866	+ 8.7855	0.023	3.732	3.974
+3.25	+0.9008	+1.77568	+ 8.9724	0.022	3.748	3.975
+3.30	+0.9019	+1.82289	+ 9.1601	0.022	3.762	3.975
+3.40	+0.9040	+1.91780	+ 9.5374	0.021	3.787	3.976
+3.50	+0.9061	+2.01327	+ 9.9171	0.020	3.809	3.978
+3.60	+0.9081	+2.10922	+10.2988	0.020	3.827	3.979
+3.70	+0.9100	+2.20556	+10.6821	0.019	3.841	3.979
+3.80	+0.9120	+2.30223	+11.0608	0.019	3.854	3.980
+3.90	+0.9138	+2.39918	+11.4527	0.019	3.864	3.980
+4.00	+0.9156	+2.49636	+11.8396	0.018	3.873	3.981
+4.10	+0.9174	+2.59373	+12.2272	0.018	3.880	3.981
+4.20	+0.9192	+2.69126	+12.6155	0.018	3.887	3.982
+4.30	+0.9209	+2.78893	+13.0044	0.017	3.892	3.982
+4.40	+0.9226	+2.88671	+13.3938	0.017	3.896	3.982
+4.50	+0.9243	+2.98460	+13.7836	0.017	3.900	3.982

4.27

(2)	(4)	(5)	(6)	(7)	(8)	(9)
+0.00	+0.0195	-0.63220	- 0.3834	0.232	8.198	4.203
+0.02	+0.0220	-0.61261	- 0.3016	0.251	7.976	4.148
+0.04	+0.0247	-0.59287	- 0.2203	0.271	7.757	4.099
+0.06	+0.0276	-0.57303	- 0.1394	0.292	7.542	4.057
+0.08	+0.0309	-0.55313	- 0.0590	0.314	7.330	4.019
+0.10	+0.0345	-0.53321	+ 0.0207	0.336	7.123	3.986
+0.12	+0.0384	-0.51331	+ 0.0997	0.360	6.919	3.955
+0.14	+0.0427	-0.49343	+ 0.1780	0.384	6.721	3.928
+0.16	+0.0473	-0.47362	+ 0.2556	0.409	6.526	3.901
+0.18	+0.0523	-0.45388	+ 0.3323	0.434	6.336	3.876
+0.20	+0.0578	-0.43424	+ 0.4082	0.460	6.150	3.851
+0.25	+0.0732	-0.38567	+ 0.5938	0.526	5.704	3.791
+0.30	+0.0916	-0.33800	+ 0.7731	0.593	5.283	3.731
+0.35	+0.1128	-0.29140	+ 0.9456	0.659	4.886	3.669
+0.40	+0.1371	-0.24600	+ 1.1107	0.720	4.513	3.604
+0.45	+0.1642	-0.20186	+ 1.2683	0.774	4.164	3.536
+0.50	+0.1941	-0.15910	+ 1.4180	0.818	3.840	3.467
+0.55	+0.2263	-0.11773	+ 1.5600	0.852	3.542	3.398
+0.60	+0.2604	-0.07778	+ 1.6945	0.872	3.271	3.331
+0.65	+0.2958	-0.03923	+ 1.8216	0.878	3.028	3.267
+0.70	+0.3319	-0.00203	+ 1.9421	0.869	2.813	3.209
+0.75	+0.3680	+0.03386	+ 2.0564	0.846	2.626	3.159
+0.80	+0.4035	+0.06855	+ 2.1652	0.810	2.465	3.119
+0.85	+0.4377	+0.10213	+ 2.2694	0.764	2.308	3.089
+0.90	+0.4702	+0.13470	+ 2.3698	0.709	2.221	3.072
+0.95	+0.5006	+0.16640	+ 2.4670	0.650	2.134	3.066
+1.00	+0.5286	+0.19733	+ 2.5619	0.587	2.068	3.072
+1.05	+0.5540	+0.22763	+ 2.6552	0.525	2.021	3.089
+1.10	+0.5768	+0.25742	+ 2.7476	0.465	1.990	3.117
+1.15	+0.5971	+0.28682	+ 2.8398	0.409	1.979	3.155
+1.20	+0.6150	+0.31596	+ 2.9323	0.356	1.975	3.199
+1.25	+0.6307	+0.34494	+ 3.0258	0.309	1.987	3.250
+1.30	+0.6443	+0.37388	+ 3.1206	0.268	2.009	3.304
+1.35	+0.6562	+0.40288	+ 3.2172	0.231	2.041	3.362
+1.40	+0.6665	+0.43203	+ 3.3161	0.199	2.082	3.420
+1.45	+0.6754	+0.46144	+ 3.4176	0.172	2.129	3.478
+1.50	+0.6832	+0.49119	+ 3.5218	0.149	2.183	3.534
+1.55	+0.6899	+0.52136	+ 3.6293	0.129	2.243	3.587
+1.60	+0.6958	+0.55202	+ 3.7400	0.113	2.306	3.637
+1.65	+0.7010	+0.58324	+ 3.8543	0.098	2.374	3.683
+1.70	+0.7055	+0.61508	+ 3.9722	0.086	2.444	3.725
+1.75	+0.7095	+0.64758	+ 4.0939	0.076	2.515	3.762
+1.80	+0.7130	+0.68078	+ 4.2194	0.068	2.589	3.795
+1.85	+0.7162	+0.71473	+ 4.3487	0.060	2.662	3.824
+1.90	+0.7190	+0.74943	+ 4.4819	0.054	2.735	3.849
+1.95	+0.7215	+0.78491	+ 4.6189	0.049	2.808	3.871
+2.00	+0.7238	+0.82118	+ 4.7596	0.045	2.879	3.887
+2.05	+0.7260	+0.85822	+ 4.9039	0.041	2.949	3.904
+2.10	+0.7279	+0.89604	+ 5.0518	0.037	3.017	3.917
+2.15	+0.7297	+0.93462	+ 5.2032	0.035	3.081	3.928

4.27 (CONT.)

(2)	(4)	(5)	(6)	(7)	(8)	(9)
+2.20	+0.7314	+0.97394	+ 5.3578	0.032	3.144	3.937
+2.25	+0.7329	+1.01397	+ 5.5155	0.030	3.203	3.944
+2.30	+0.7344	+1.05468	+ 5.6762	0.028	3.259	3.951
+2.35	+0.7357	+1.09605	+ 5.8398	0.026	3.313	3.956
+2.40	+0.7370	+1.13804	+ 6.0060	0.025	3.363	3.960
+2.45	+0.7382	+1.18062	+ 6.1746	0.024	3.410	3.964
+2.50	+0.7394	+1.22374	+ 6.3457	0.023	3.453	3.967
+2.55	+0.7405	+1.26739	+ 6.5188	0.022	3.494	3.969
+2.60	+0.7416	+1.31151	+ 6.6940	0.021	3.532	3.972
+2.65	+0.7426	+1.35608	+ 6.8711	0.020	3.567	3.974
+2.70	+0.7436	+1.40107	+ 7.0499	0.020	3.599	3.975
+2.70	+0.7445	+1.44644	+ 7.2303	0.019	3.629	3.976
+2.80	+0.7454	+1.49217	+ 7.4122	0.018	3.657	3.978
+2.85	+0.7463	+1.53822	+ 7.5954	0.018	3.682	3.978
+2.90	+0.7472	+1.58457	+ 7.7798	0.017	3.705	3.979

4.28

(2)	(4)	(5)	(6)	(7)	(8)	(9)
+0.80	+0.4775	+0.01824	+ 2.1917	1.146	2.334	3.500
+0.82	+0.4973	+0.02979	+ 2.2315	1.136	2.260	3.394
+0.84	+0.5169	+0.04137	+ 2.2703	1.122	2.190	3.301
+0.86	+0.5364	+0.05296	+ 2.3080	1.104	2.122	3.219
+0.88	+0.5557	+0.06453	+ 2.3449	1.083	2.058	3.147
+0.90	+0.5747	+0.07607	+ 2.3808	1.059	1.998	3.084
+0.92	+0.5933	+0.08755	+ 2.4159	1.032	1.943	3.030
+0.94	+0.6115	+0.09897	+ 2.4502	1.003	1.891	2.982
+0.96	+0.6293	+0.11030	+ 2.4838	0.971	1.843	2.941
+0.98	+0.6465	+0.12156	+ 2.5167	0.937	1.800	2.907
+1.00	+0.6632	+0.13272	+ 2.5490	0.902	1.760	2.878
+1.05	+0.7023	+0.16022	+ 2.6274	0.810	1.677	2.828
+1.10	+0.7375	+0.18716	+ 2.7032	0.714	1.616	2.807
+1.15	+0.7685	+0.21359	+ 2.7774	0.621	1.576	2.811
+1.20	+0.7955	+0.23956	+ 2.8507	0.533	1.554	2.834
+1.25	+0.8188	+0.26520	+ 2.9238	0.453	1.548	2.875
+1.30	+0.8385	+0.29058	+ 2.9974	0.382	1.556	2.929
+1.35	+0.8552	+0.31583	+ 3.0722	0.320	1.577	2.994
+1.40	+0.8692	+0.34105	+ 3.1486	0.267	1.609	3.067
+1.45	+0.8810	+0.36634	+ 3.2272	0.222	1.651	3.144
+1.50	+0.8908	+0.39180	+ 3.3082	0.185	1.702	3.225
+1.55	+0.8990	+0.41753	+ 3.3922	0.154	1.760	3.305
+1.60	+0.9059	+0.44362	+ 3.4795	0.129	1.825	3.384
+1.65	+0.9116	+0.47017	+ 3.5704	0.108	1.896	3.459
+1.70	+0.9165	+0.49725	+ 3.6650	0.091	1.972	3.531
+1.75	+0.9206	+0.52495	+ 3.7638	0.077	2.052	3.596
+1.80	+0.9241	+0.55334	+ 3.8667	0.066	2.135	3.655
+1.85	+0.9271	+0.58247	+ 3.9740	0.056	2.221	3.708
+1.90	+0.9296	+0.61241	+ 4.0857	0.049	2.309	3.755
+1.95	+0.9319	+0.64320	+ 4.2020	0.042	2.398	3.796
+2.00	+0.9338	+0.67488	+ 4.3228	0.037	2.487	3.830
+2.05	+0.9356	+0.70749	+ 4.4482	0.033	2.575	3.860
+2.10	+0.9371	+0.74102	+ 4.5780	0.029	2.663	3.884
+2.15	+0.9385	+0.77550	+ 4.7123	0.026	2.749	3.905
+2.20	+0.9397	+0.81092	+ 4.8509	0.024	2.832	3.921
+2.25	+0.9408	+0.84727	+ 4.9937	0.021	2.913	3.935
+2.30	+0.9418	+0.88454	+ 5.1406	0.020	2.991	3.946
+2.35	+0.9427	+0.92269	+ 5.2913	0.018	3.066	3.955
+2.40	+0.9436	+0.96170	+ 5.4457	0.017	3.136	3.962
+2.45	+0.9444	+1.00153	+ 5.6036	0.016	3.203	3.967
+2.50	+0.9452	+1.04215	+ 5.7648	0.015	3.266	3.971
+2.55	+0.9459	+1.08350	+ 5.9292	0.014	3.326	3.975
+2.60	+0.9465	+1.12556	+ 6.0964	0.013	3.381	3.978
+2.65	+0.9472	+1.16826	+ 6.2663	0.012	3.432	3.980
+2.70	+0.9478	+1.21158	+ 6.4388	0.012	3.480	3.982
+2.75	+0.9483	+1.25545	+ 6.6135	0.011	3.524	3.984
+2.80	+0.9489	+1.29985	+ 6.7904	0.011	3.564	3.985
+2.85	+0.9494	+1.34474	+ 6.9693	0.011	3.601	3.986
+2.90	+0.9499	+1.39006	+ 7.1500	0.010	3.635	3.987
+2.95	+0.9504	+1.43579	+ 7.3323	0.010	3.667	3.988
+3.00	+0.9509	+1.48189	+ 7.5162	0.010	3.695	3.988
+3.05	+0.9514	+1.52833	+ 7.7014	0.009	3.721	3.989
+3.10	+0.9518	+1.57508	+ 7.8879	0.009	3.745	3.989
+3.15	+0.9523	+1.62211	+ 8.0756	0.009	3.766	3.990
+3.20	+0.9527	+1.66940	+ 8.2642	0.009	3.786	3.990
+3.25	+0.9532	+1.71692	+ 8.4539	0.009	3.803	3.990
+3.30	+0.9536	+1.76465	+ 8.6443	0.009	3.819	3.991
+3.35	+0.9540	+1.81257	+ 8.8356	0.008	3.833	3.991
+3.40	+0.9545	+1.86066	+ 9.0275	0.008	3.846	3.991
+3.45	+0.9549	+1.90891	+ 9.2200	0.008	3.858	3.991

4.28 (CONT.)

(2)	(4)	(5)	(6)	(7)	(8)	(9)
+3.50	+0.9553	+1.95729	+ 9.4131	0.008	3.869	3.991
+3.55	+0.9557	+2.00580	+ 9.6067	0.008	3.878	3.991
+3.60	+0.9561	+2.05442	+ 9.8008	0.008	3.887	3.992
+3.65	+0.9565	+2.10315	+ 9.9953	0.008	3.894	3.992
+3.70	+0.9569	+2.15196	+10.1902	0.008	3.901	3.992
+3.75	+0.9573	+2.20086	+10.3853	0.008	3.908	3.992
+3.80	+0.9577	+2.24983	+10.5808	0.008	3.913	3.992
+3.85	+0.9581	+2.29887	+10.7766	0.008	3.919	3.992
+3.90	+0.9584	+2.34798	+10.9726	0.008	3.923	3.992
+3.95	+0.9588	+2.39713	+11.1688	0.008	3.927	3.992
+4.00	+0.9592	+2.44634	+11.3653	0.008	3.931	3.992
+4.10	+0.9600	+2.54487	+11.7587	0.007	3.937	3.992
+4.20	+0.9607	+2.64355	+12.1526	0.007	3.942	3 992
+4.30	+0.9615	+2.74235	+12.5471	0.007	3.946	3.992
+4.40	+0.9622	+2.84124	+12.9419	0.007	3.950	3.993

4.29

(2)	(4)	(5)	(6)	(7)	(8)	(9)
+1.60	+0.9382	+0.39046	+ 3.5168	0.171	1.915	3.955
+1.62	+0.9414	+0.40002	+ 3.5545	0.160	1.945	3.930
+1.64	+0.9444	+0.40979	+ 3.5928	0.151	1.975	3.910
+1.66	+0.9473	+0.41977	+ 3.6317	0.142	2.006	3.893
+1.68	+0.9500	+0.42996	+ 3.6713	0.133	2.037	3.879
+1.70	+0.9525	+0.44034	+ 3.7116	0.125	2.069	3.869
+1.75	+0.9582	+0.46716	+ 3.8151	0.108	2.149	3.851
+1.80	+0.9632	+0.49515	+ 3.9228	0.093	2.231	3.845
+1.85	+0.9675	+0.52426	+ 4.0347	0.081	2.314	3.847
+1.90	+0.9712	+0.55445	+ 4.1510	0.071	2.398	3.854
+1.95	+0.9745	+0.58569	+ 4.2715	0.062	2.481	3.863
+2.00	+0.9774	+0.61794	+ 4.3963	0.055	2.564	3.876
+2.05	+0.9800	+0.65119	+ 4.5253	0.049	2.646	3.888
+2.10	+0.9823	+0.68541	+ 4.6586	0.044	2.727	3.900
+2.15	+0.9844	+0.72056	+ 4.7959	0.040	2.806	3.911
+2.20	+0.9863	+0.75664	+ 4.9372	0.036	2.883	3.921
+2.25	+0.9880	+0.79361	+ 5.0823	0.033	2.957	3.930
+2.30	+0.9896	+0.83144	+ 5.2311	0.030	3.028	3.939
+2.35	+0.9910	+0.87010	+ 5.3835	0.028	3.096	3.946
+2.40	+0.9924	+0.90955	+ 5.5393	0.026	3.161	3.952
+2.45	+0.9936	+0.94976	+ 5.6983	0.024	3.222	3.957
+2.50	+0.9948	+0.99068	+ 5.8603	0.023	3.280	3.961
+2.55	+0.9959	+1.03229	+ 6.0252	0.022	3.334	3.965
+2.60	+0.9970	+1.07453	+ 6.1928	0.021	3.385	3.968
+2.65	+0.9980	+1.11737	+ 6.3628	0.020	3.433	3.971
+2.70	+0.9989	+1.16076	+ 6.5352	0.019	3.477	3.973
+2.75	+0.9998	+1.20468	+ 6.7098	0.018	3.518	3.975
+2.80	+1.0007	+1.24908	+ 6.8863	0.017	3.555	3.977
+2.85	+1.0016	+1.29393	+ 7.0647	0.017	3.590	3.979
+2.90	+1.0024	+1.33918	+ 7.2448	0.016	3.622	3.980
+2.95	+1.0032	+1.38482	+ 7.4264	0.016	3.652	3.981
+3.00	+1.0039	+1.43081	+ 7.6095	0.015	3.679	3.982
+3.05	+1.0047	+1.47711	+ 7.7939	0.015	3.703	3.982
+3.10	+1.0054	+1.52371	+ 7.9795	0.014	3.726	3.983
+3.15	+1.0061	+1.57057	+ 8.1661	0.014	3.746	3.984
+3.20	+1.0068	+1.61768	+ 8.3538	0.014	3.765	3.984
+3.25	+1.0075	+1.66501	+ 8.5424	0.014	3.782	3.985
+3.30	+1.0082	+1.71254	+ 8.7318	0.013	3.797	3.985
+3.35	+1.0088	+1.76025	+ 8.9219	0.013	3.811	3.985
+3.40	+1.0095	+1.80813	+ 9.1128	0.013	3.824	3.986
+3.45	+1.0101	+1.85616	+ 9.3042	0.013	3.836	3.986
+3.50	+1.0108	+1.90432	+ 9.4962	0.013	3.846	3.986
+3.55	+1.0114	+1.95261	+ 9.6887	0.013	3.856	3.986
+3.60	+1.0120	+2.00101	+ 9.8816	0.012	3.864	3.987
+3.65	+1.0126	+2.04951	+10.0750	0.012	3.872	3.987
+3.70	+1.0132	+2.09810	+10.2688	0.012	3.879	3.987
+3.75	+1.0138	+2.14678	+10.4628	0.012	3.886	3.987
+3.80	+1.0144	+2.19553	+10.6572	0.012	3.891	3.988
+3.85	+1.0150	+2.24435	+10.8519	0.012	3.897	3.988
+3.90	+1.0156	+2.29323	+11.0468	0.012	3.901	3.988
+3.95	+1.0162	+2.34216	+11.2420	0.012	3.905	3.988
+4.00	+1.0168	+2.39115	+11.4373	0.012	3.909	3.988
+4.10	+1.0179	+2.48926	+11.8286	0.011	3.916	3.988
+4.20	+1.0191	+2.58751	+12.2204	0.011	3.922	3.988
+4.30	+1.0202	+2.68588	+12.6128	0.011	3.926	3.988
+4.40	+1.0213	+2.78436	+13.0056	0.011	3.930	3.989
+4.50	+1.0224	+2.88292	+13.3987	0.011	3.933	3.989
+4.60	+1.0235	+2.98154	+13.7921	0.011	3.936	3.989
+4.70	+1.0245	+3.08023	+14.1858	0.011	3.938	3.989

4.30

(2)	(4)	(5)	(6)	(7)	(8)	(9)
+0.60	+0.3777	−0.13198	+1.7252	1.389	2.829	3.549
+0.61	+0.3888	−0.12560	+1.7476	1.400	2.767	3.484
+0.62	+0.4002	−0.11923	+1.7696	1.409	2.707	3.422
+0.63	+0.4116	−0.11285	+1.7912	1.417	2.647	3.363
+0.64	+0.4231	−0.10648	+1.8125	1.423	2.588	3.308
+0.65	+0.4347	−0.10012	+1.8334	1.428	2.530	3.254
+0.66	+0.4464	−0.09377	+1.8538	1.433	2.473	3.203
+0.67	+0.4582	−0.08745	+1.8739	1.436	2.418	3.155
+0.68	+0.4701	−0.08115	+1.8937	1.438	2.363	3.109
+0.69	+0.4820	−0.07488	+1.9130	1.438	2.266	3.064
+0.70	+0.4940	−0.06863	+1.9320	1.438	2.258	3.022
+0.71	+0.5060	−0.06242	+1.9507	1.435	2.207	2.983
+0.72	+0.5180	−0.05625	+1.9690	1.432	2.158	2.943
+0.73	+0.5300	−0.05011	+1.9869	1.427	2.110	2.908
+0.74	+0.5421	−0.04401	+2.0046	1.422	2.063	2.873
+0.75	+0.5541	−0.03796	+2.0219	1.415	2.018	2.838
+0.76	+0.5661	−0.03194	+2.0388	1.406	1.974	2.807
+0.77	+0.5780	−0.02597	+2.0555	1.397	1.933	2.777
+0.78	+0.5900	−0.02005	+2.0719	1.386	1.891	2.747
+0.79	+0.6018	−0.01416	+2.0879	1.374	1.851	2.719
+0.80	+0.6136	−0.00833	+2.1037	1.361	1.814	2.694
+0.85	+0.6711	+0.02017	+2.1788	1.281	1.644	2.580
+0.90	+0.7255	+0.04754	+2.2482	1.180	1.508	2.497
+0.95	+0.7756	+0.07385	+2.3132	1.063	1.402	2.441
+1.00	+0.8208	+0.09921	+2.3746	0.938	1.322	2.412
+1.05	+0.8608	+0.12374	+2.4337	0.812	1.266	2.407
+1.10	+0.8954	+0.14756	+2.4912	0.691	1.231	2.425
+1.15	+0.9249	+0.17082	+2.5480	0.579	1.213	2.465
+1.20	+0.9497	+0.19362	+2.6047	0.480	1.212	2.513
+1.25	+0.9702	+0.21611	+2.6621	0.394	1.223	2.589
+1.30	+0.9871	+0.23840	+2.7207	0.320	1.247	2.671
+1.35	+1.0009	+0.26059	+2.7810	0.260	1.281	2.763
+1.40	+1.0121	+0.28280	+2.8435	0.210	1.324	2.861
+1.45	+1.0212	+0.30514	+2.9085	0.169	1.376	2.963
+1.50	+1.0286	+0.32770	+2.9765	0.137	1.436	3.066
+1.55	+1.0346	+0.35057	+3.0478	0.111	1.503	3.168
+1.60	+1.0395	+0.37386	+3.1228	0.090	1.576	3.267
+1.65	+1.0435	+0.39764	+3.2016	0.074	1.654	3.360
+1.70	+1.0468	+0.42201	+3.2846	0.061	1.737	3.448
+1.75	+1.0495	+0.44705	+3.3720	0.050	1.824	3.529
+1.80	+1.0517	+0.47283	+3.4639	0.042	1.916	3.602
+1.85	+1.0536	+0.49941	+3.5606	0.035	2.009	3.668
+1.90	+1.0552	+0.52687	+3.6621	0.030	2.105	3.725
+1.95	+1.0566	+0.55525	+3.7685	0.026	2.203	3.775
+2.00	+1.0578	+0.58460	+3.8800	0.022	2.301	3.816
+2.05	+1.0588	+0.61496	+3.9964	0.019	2.400	3.852
+2.10	+1.0596	+0.64636	+4.1178	0.017	2.497	3.881
+2.15	+1.0604	+0.67880	+4.2441	0.015	2.593	3.905
+2.20	+1.0611	+0.71230	+4.3752	0.013	2.687	3.924
+2.25	+1.0617	+0.74684	+4.5111	0.012	2.779	3.940
+2.30	+1.0623	+0.78242	+4.6515	0.011	2.867	3.952
+2.35	+1.0628	+0.81902	+4.7963	0.010	2.952	3.962
+2.40	+1.0632	+0.85659	+4.9453	0.009	3.033	3.969
+2.45	+1.0637	+0.89511	+5.0983	0.008	3.110	3.975
+2.50	+1.0641	+0.93453	+5.2552	0.008	3.183	3.980
+2.55	+1.0644	+0.97481	+5.4155	0.007	3.251	3.983
+2.60	+1.0648	+1.01590	+5.5792	0.007	3.314	3.986
+2.65	+1.0651	+1.05774	+5.7461	0.006	3.374	3.988
+2.70	+1.0654	+1.10030	+5.9158	0.006	3.429	3.990
+2.75	+1.0657	+1.14351	+6.0882	0.006	3.480	3.991
+2.80	+1.0660	+1.18733	+6.2631	0.005	3.527	3.992
+2.85	+1.0662	+1.23171	+6.4403	0.005	3.570	3.992
+2.90	+1.0665	+1.27661	+6.6196	0.005	3.609	3.993
+2.95	+1.0668	+1.32198	+6.8007	0.005	3.646	3.994
+3.00	+1.0670	+1.36778	+6.9836	0.005	3.678	3.994

4.31

(2)	(4)	(5)	(6)	(7)	(8)	(9)
+1.40	+1.0802	+0.21611	+ 2.8544	0.294	1.320	3.532
+1.42	+1.0857	+0.22338	+ 2.8800	0.271	1.340	3.516
+1.44	+1.0907	+0.23080	+ 2.9060	0.251	1.361	3.504
+1.46	+1.0954	+0.23837	+ 2.9325	0.232	1.384	3.498
+1.48	+1.0997	+0.24609	+ 2.9595	0.214	1.407	3.494
+1.50	+1.1037	+0.25396	+ 2.9870	0.198	1.432	3.494
+1.55	+1.1124	+0.27428	+ 3.0581	0.162	1.498	3.506
+1.60	+1.1196	+0.29551	+ 3.1328	0.133	1.569	3.531
+1.65	+1.1255	+0.31764	+ 3.2112	0.110	1.646	3.564
+1.70	+1.1304	+0.34068	+ 3.2938	0.091	1.728	3.603

4.31 (CONT.)

(2)	(4)	(5)	(6)	(7)	(8)	(9)
+1.75	+1.1345	+0.36466	+ 3.3807	0.076	1.813	3.644
+1.80	+1.1379	+0.38958	+ 3.4721	0.063	1.903	3.686
+1.85	+1.1407	+0.41548	+ 3.5681	0.053	1.995	3.727
+1.90	+1.1431	+0.44238	+ 3.6688	0.045	2.089	3.765
+1.95	+1.1452	+0.47029	+ 3.7744	0.038	2.185	3.800
+2.00	+1.1469	+0.49924	+ 3.8849	0.033	2.281	3.831
+2.05	+1.1485	+0.52925	+ 4.0003	0.029	2.378	3.858
+2.10	+1.1498	+0.56032	+ 4.1205	0.025	2.473	3.882
+2.15	+1.1510	+0.59246	+ 4.2456	0.022	2.568	3.902
+2.20	+1.1520	+0.62566	+ 4.3755	0.020	2.661	3.920
+2.25	+1.1530	+0.65991	+ 4.5100	0.018	2.752	3.934
+2.30	+1.1538	+0.69520	+ 4.6491	0.016	2.839	3.946
+2.35	+1.1545	+0.73150	+ 4.7925	0.014	2.923	3.955
+2.40	+1.1552	+0.76878	+ 4.9401	0.013	3.004	3.963
+2.45	+1.1559	+0.80700	+ 5.0916	0.012	3.081	3.969
+2.50	+1.1565	+0.84612	+ 5.2470	0.011	3.154	3.974
+2.55	+1.1570	+0.88610	+ 5.4059	0.011	3.222	3.977
+2.60	+1.1575	+0.92688	+ 5.5682	0.010	3.286	3.981
+2.65	+1.1580	+0.96843	+ 5.7336	0.009	3.346	3.983
+2.70	+1.1585	+1.01068	+ 5.9020	0.009	3.402	3.985
+2.75	+1.1589	+1.05360	+ 6.0731	0.008	3.454	3.987
+2.80	+1.1593	+1.09714	+ 6.2467	0.008	3.501	3.988
+2.85	+1.1597	+1.14125	+ 6.4226	0.008	3.545	3.989
+2.90	+1.1601	+1.18588	+ 6.6007	0.007	3.586	3.990
+2.95	+1.1604	+1.23100	+ 6.7807	0.007	3.623	3.990
+3.00	+1.1608	+1.27655	+ 6.9625	0.007	3.657	3.991
+3.05	+1.1612	+1.32251	+ 7.1459	0.007	3.687	3.992
+3.10	+1.1615	+1.36884	+ 7.3308	0.007	3.715	3.992
+3.15	+1.1618	+1.41550	+ 7.5171	0.006	3.741	3.992
+3.20	+1.1621	+1.46246	+ 7.7046	0.006	3.764	3.993
+3.25	+1.1624	+1.50971	+ 7.8932	0.006	3.785	3.993
+3.30	+1.1628	+1.55720	+ 8.0829	0.006	3.804	3.993
+3.35	+1.1631	+1.60492	+ 8.2734	0.006	3.821	3.993
+3.40	+1.1634	+1.65284	+ 8.4648	0.006	3.837	3.994
+3.45	+1.1637	+1.70095	+ 8.6570	0.006	3.851	3.993
+3.50	+1.1640	+1.74923	+ 8.8497	0.006	3.863	3.994
+3.55	+1.1642	+1.79765	+ 9.0431	0.006	3.875	3.994
+3.60	+1.1645	+1.84621	+ 9.2371	0.006	3.885	3.994
+3.65	+1.1648	+1.89489	+ 9.4315	0.006	3.894	3.994
+3.70	+1.1651	+1.94368	+ 9.6264	0.006	3.902	3.994
+3.75	+1.1654	+1.99257	+ 9.8216	0.006	3.910	3.994
+3.80	+1.1656	+2.04154	+10.0172	0.006	3.916	3.994
+3.85	+1.1659	+2.09060	+10.2132	0.005	3.922	3.994
+3.90	+1.1662	+2.13972	+10.4094	0.005	3.928	3.994
+3.95	+1.1665	+2.18891	+10.6059	0.005	3.932	3.994
+4.00	+1.1667	+2.23816	+10.8026	0.005	3.937	3.995
+4.05	+1.1670	+2.28745	+10.9995	0.005	3.941	3.995
+4.10	+1.1673	+2.33680	+11.1966	0.005	3.944	3.994
+4.15	+1.1676	+2.38618	+11.3939	0.005	3.947	3.995
+4.20	+1.1678	+2.43560	+11.5913	0.005	3.950	3.995
+4.25	+1.1681	+2.48506	+11.7888	0.005	3.953	3.995
+4.30	+1.1683	+2.54355	+11.9865	0.005	3.955	3.995
+4.35	+1.1686	+2.58406	+12.1843	0.005	3.957	3.995
+4.40	+1.1689	+2.63360	+12.3822	0.005	3.959	3.995

4.32

(2)	(4)	(5)	(6)	(7)	(8)	(9)
+0.44	+0.2768	−0.25649	+1.3382	1.407	3.582	3.687
+0.45	+0.2873	−0.24936	+1.3642	1.429	3.499	3.621
+0.46	+0.2979	−0.24222	+1.3898	1.453	3.417	3.556
+0.47	+0.3088	−0.23508	+1.4149	1.474	3.334	3.495
+0.48	+0.3200	−0.22797	+1.4396	1.496	3.252	3.437
+0.49	+0.3313	−0.22087	+1.4638	1.516	3.171	3.381
+0.50	+0.3429	−0.21380	+1.4875	1.535	3.092	3.327
+0.52	+0.3666	−0.19974	+1.5336	1.571	2.936	3.225
+0.54	+0.3911	−0.18584	+1.5777	1.601	2.785	3.130
+0.56	+0.4163	−0.17213	+1.6200	1.627	2.639	3.040
+0.58	+0.4421	−0.15862	+1.6605	1.648	2.500	2.955
+0.60	+0.4684	−0.14534	+1.6992	1.663	2.367	2.875
+0.62	+0.4952	−0.13230	+1.7362	1.673	2.241	2.799
+0.64	+0.5224	−0.11951	+1.7715	1.678	2.122	2.727
+0.66	+0.5498	−0.10698	+1.8053	1.676	2.010	2.659
+0.68	+0.5774	−0.09470	+1.8375	1.669	1.904	2.594
+0.70	+0.6050	−0.08269	+1.8683	1.655	1.806	2.533
+0.75	+0.6736	−0.05375	+1.9395	1.598	1.589	2.396
+0.80	+0.7402	−0.02633	+2.0036	1.508	1.413	2.283
+0.85	+0.8033	−0.00030	+2.0619	1.391	1.272	2.194

4.32 (CONT.)

(2)	(4)	(5)	(6)	(7)	(8)	(9)
+0.90	+0.8617	+0.02450	+2.1155	1.254	1.163	2.131
+0.95	+0.9144	+0.04821	+2.1656	1.104	1.080	2.092
+1.00	+0.9609	+0.07099	+2.2130	0.952	1.022	2.078
+1.05	+1.0010	+0.09297	+2.2588	0.805	0.984	2.088
+1.10	+1.0349	+0.11431	+2.3036	0.668	0.964	2.120
+1.15	+1.0630	+0.13513	+2.3483	0.546	0.958	2.172
+1.20	+1.0861	+0.15556	+2.3933	0.441	0.966	2.241

4.33

(2)	(4)	(5)	(6)	(7)	(8)	(9)
+1.24	+1.2364	+0.09548	+ 2.4132	0.577	0.856	2.809
+1.25	+1.2418	+0.09837	+ 2.4213	0.553	0.859	2.800
+1.26	+1.2469	+0.10128	+ 2.4294	0.532	0.861	2.787
+1.27	+1.2518	+0.10422	+ 2.4376	0.510	0.864	2.778
+1.28	+1.2566	+0.10719	+ 2.4458	0.488	0.868	2.773
+1.29	+1.2611	+0.11017	+ 2.4541	0.468	0.872	2.765
+1.30	+1.2655	+0.11318	+ 2.4624	0.447	0.876	2.761
+1.32	+1.2736	+0.11927	+ 2.4792	0.410	0.886	2.759
+1.34	+1.2811	+0.12544	+ 2.4962	0.375	0.897	2.760
+1.36	+1.2880	+0.13170	+ 2.5136	0.342	0.910	2.765
+1.38	+1.2943	+0.13805	+ 2.5311	0.312	0.923	2.775
+1.40	+1.3000	+0.14448	+ 2.5490	0.284	0.938	2.788
+1.45	+1.3122	+0.16093	+ 2.5953	0.224	0.982	2.836
+1.50	+1.3218	+0.17792	+ 2.6440	0.177	1.032	2.899
+1.55	+1.3295	+0.19545	+ 2.6954	0.139	1.089	2.974
+1.60	+1.3355	+0.21355	+ 2.7500	0.110	1.153	3.056
+1.65	+1.3403	+0.23226	+ 2.8080	0.087	1.222	3.142
+1.70	+1.3440	+0.25160	+ 2.8696	0.069	1.297	3.230
+1.75	+1.3470	+0.27164	+ 2.9352	0.055	1.377	3.317
+1.80	+1.3495	+0.29241	+ 3.0050	0.044	1.462	3.401
+1.85	+1.3514	+0.31397	+ 3.0792	0.035	1.551	3.481
+1.90	+1.3530	+0.33638	+ 3.1581	0.029	1.645	3.555
+1.95	+1.3543	+0.35967	+ 3.2417	0.024	1.742	3.624
+2.00	+1.3553	+0.38392	+ 3.3303	0.019	1.841	3.685
+2.05	+1.3562	+0.40916	+ 3.4241	0.016	1.943	3.740
+2.10	+1.3569	+0.43543	+ 3.5230	0.014	2.047	3.787
+2.15	+1.3575	+0.46279	+ 3.6272	0.012	2.152	3.828
+2.20	+1.3581	+0.49126	+ 3.7366	0.010	2.256	3.862
+2.25	+1.3585	+0.52086	+ 3.8514	0.009	2.361	3.890
+2.30	+1.3589	+0.55161	+ 3.9714	0.007	2.464	3.914
+2.35	+1.3593	+0.58350	+ 4.0965	0.007	2.565	3.932
+2.40	+1.3596	+0.61655	+ 4.2267	0.006	2.664	3.948
+2.45	+1.3598	+0.65072	+ 4.3618	0.005	2.760	3.960
+2.50	+1.3601	+0.68601	+ 4.5017	0.005	2.853	3.969
+2.55	+1.3603	+0.72237	+ 4.6462	0.004	2.941	3.976
+2.60+	+1.3605	+0.75977	+ 4.7950	0.004	3.026	3.981
+2.65	+1.3607	+0.79816	+ 4.9479	0.004	3.105	3.985
+2.70	+1.3609	+0.83749	+ 5.1047	0.003	3.181	3.989
+2.75	+1.3610	+0.87772	+ 5.2652	0.003	3.251	3.991
+2.80	+1.3612	+0.91879	+ 5.4292	0.003	3.317	3.993
+2.85	+1.3613	+0.96064	+ 5.5963	0.003	3.378	3.994
+2.90	+1.3615	+1.00323	+ 5.7664	0.003	3.434	3.995
+2.95	+1.3616	+1.04649	+ 5.9392	0.003	3.487	3.996
+3.00	+1.3617	+1.09037	+ 6.1146	0.002	3.535	3.996
+3.05	+1.3618	+1.13484	+ 6.2923	0.002	3.579	3.996
+3.10	+1.3620	+1.17982	+ 6.4721	0.002	3.619	3.997
+3.15	+1.3621	+1.22529	+ 6.6538	0.002	3.656	3.997
+3.20	+1.3622	+1.27120	+ 6.8373	0.002	3.689	3.997
+3.25	+1.3623	+1.31751	+ 7.0224	0.002	3.719	3.997
+3.30	+1.3624	+1.36418	+ 7.2090	0.002	3.747	3.998
+3.35	+1.3625	+1.41118	+ 7.3969	0.002	3.772	3.998
+3.40	+1.3626	+1.45847	+ 7.5859	0.002	3.794	3.998
+3.45	+1.3627	+1.50604	+ 7.7761	0.002	3.814	3.998
+3.50	+1.3628	+1.55384	+ 7.9672	0.002	3.833	3.998
+3.55	+1.3629	+1.60187	+ 8.1592	0.002	3.849	3.998
+3.60	+1.3630	+1.65009	+ 8.3520	0.002	3.864	3.998
+3.65	+1.3631	+1.69849	+ 8.5455	0.002	3.877	3.998
+3.70	+1.3632	+1.74705	+ 8.7397	0.002	3.889	3.998
+3.75	+1.3632	+1.79575	+ 8.9344	0.002	3.900	3.998
+3.80	+1.3633	+1.84458	+ 9.1296	0.002	3.910	3.998
+3.85	+1.3634	+1.89352	+ 9.3253	0.002	3.919	3.998
+3.90	+1.3635	+1.94257	+ 9.5214	0.002	3.926	3.998
+3.95	+1.3636	+1.99171	+ 9.7178	0.002	3.933	3.998
+4.00	+1.3637	+1.04093	+ 9.9146	0.002	3.939	3.998
+4.05	+1.3638	+2.09022	+10.1117	0.002	3.945	3.998

4.33 (CONT.)

(2)	(4)	(5)	(6)	(7)	(8)	(9)
+4.10	+1.3639	+2.13958	+10.3090	0.002	3.950	3.998
+4.15	+1.3640	+2.18900	+10.5066	0.002	3.954	3.998
+4.20	+1.3640	+2.23847	+10.7044	0.002	3.958	3.998
+4.25	+1.3641	+2.28799	+10.9024	0.002	3.962	3.998
+4.30	+1.3642	+2.33755	+11.1006	0.002	3.965	3.999
+4.35	+1.3643	+2.38715	+11.2989	0.002	3.968	3.998
+4.40	+1.3644	+2.43679	+11.4974	0.002	3.971	3.998

5.1

(1)	(3)	(5)	(6)	(7)	(8)	(9)
0.00	+0.32576	+0.238100	+0.97584	2.582	1.224	2.500
+0.01	+0.35148	+0.233137	+0.96330	2.563	1.283	2.550
+0.02	+0.37701	+0.228033	+0.95016	2.542	1.346	2.600
+0.03	+0.40231	+0.222783	+0.93638	2.519	1.411	2.650
+0.04	+0.42739	+0.217381	+0.92193	2.496	1.479	2.699
+0.05	+0.45222	+0.211822	+0.90679	2.470	1.550	2.749
+0.06	+0.47679	+0.206100	+0.89092	2.444	1.624	2.798
+0.07	+0.50108	+0.200208	+0.87429	2.415	1.702	2.846
+0.08	+0.52509	+0.194140	+0.85687	2.386	1.782	2.894
+0.09	+0.54880	+0.187890	+0.83863	2.355	1.866	2.942
+0.10	+0.57218	+0.181452	+0.81954	2.322	1.953	2.988
+0.11	+0.59524	+0.174817	+0.79956	2.288	2.044	3.034
+0.12	+0.61794	+0.167978	+0.77865	2.253	2.138	3.079
+0.13	+0.64029	+0.160929	+0.75679	2.216	2.235	3.123
+0.14	+0.66226	+0.153661	+0.73393	2.179	2.337	3.166
+0.15	+0.68384	+0.146165	+0.71005	2.138	2.442	3.207
+0.16	+0.70502	+0.138433	+0.68509	2.097	2.550	3.247
+0.17	+0.72578	+0.130455	+0.65903	2.055	2.663	3.285
+0.18	+0.74611	+0.122220	+0.63182	2.011	2.779	3.322
+0.19	+0.76600	+0.113717	+0.60344	1.967	2.899	3.355
+0.20	+0.78544	+0.104934	+0.57382	1.921	3.024	3.386
+0.21	+0.80441	+0.095855	+0.54295	1.874	3.152	3.414
+0.22	+0.82291	+0.086464	+0.51078	1.826	3.284	3.438
+0.23	+0.84092	+0.076741	+0.47725	1.777	3.421	3.457
+0.24	+0.85844	+0.066663	+0.44234	1.727	3.563	3.471
+0.25	+0.87546	+0.056200	+0.40598	1.676	3.709	3.477
+0.26	+0.89196	+0.045314	+0.36814	1.625	3.860	3.474
+0.27	+0.90795	+0.033957	+0.32875	1.573	4.018	3.460
+0.28	+0.92343	+0.02206	+0.28776	1.522	4.182	3.439
+0.29	+0.93838	+0.00955	+0.24509	1.470	4.353	3.383
+0.30	+0.95282	−0.00372	+0.20066	1.418	4.535	3.311
+0.31	+0.96674	−0.01792	+0.15436	1.366	4.728	3.204
+0.315	+0.97350	−0.02546	+0.13046	1.341	4.830	3.134
+0.320	+0.98015	−0.03335	+0.10605	1.316	4.937	3.052
+0.325	+0.98666	−0.04166	+0.08108	1.291	5.050	2.954
+0.330	+0.99306	−0.05048	+0.05553	1.268	5.171	2.837
+0.335	+0.99934	−0.05993	+0.02936	1.244	5.300	2.699
+0.340	+1.00551	−0.07019	+0.00251	1.222	5.441	2.534

5.2

(1)	(3)	(5)	(6)	(7)	(8)	(9)
0.00	+0.32491	+0.238005	+0.97501	2.583	1.222	2.500
+0.01	+0.35064	+0.233051	+0.96250	2.563	1.281	2.550
+0.02	+0.37617	+0.227956	+0.94938	2.542	1.343	2.600
+0.03	+0.40149	+0.222717	+0.93562	2.520	1.408	2.651
+0.04	+0.42657	+0.217326	+0.92120	2.496	1.476	2.701
+0.05	+0.45141	+0.211780	+0.90608	2.471	1.548	2.750
+0.06	+0.47599	+0.206071	+0.89024	2.444	1.622	2.800
+0.07	+0.50029	+0.200195	+0.87364	2.416	1.699	2.849
+0.08	+0.52431	+0.194144	+0.85626	2.387	1.779	2.897
+0.09	+0.54802	+0.187913	+0.83805	2.356	1.862	2.946
+0.10	+0.57142	+0.181496	+0.81900	2.323	1.950	2.993
+0.11	+0.59448	+0.174885	+0.79905	2.289	2.040	3.040
+0.12	+0.61720	+0.168074	+0.77819	2.254	2.134	3.086
+0.13	+0.63955	+0.161057	+0.75637	2.217	2.231	3.132
+0.14	+0.66153	+0.153825	+0.73356	2.179	2.332	3.176
+0.15	+0.68312	+0.146372	+0.70972	2.139	2.436	3.220
+0.16	+0.70431	+0.138689	+0.68481	2.098	2.545	3.262
+0.17	+0.72508	+0.130769	+0.65881	2.056	2.656	3.304
+0.18	+0.74542	+0.122604	+0.63167	2.012	2.772	3.344
+0.19	+0.76532	+0.114184	+0.60336	1.967	2.892	3.382
+0.20	+0.78476	+0.105501	+0.57383	1.921	3.015	3.419
+0.21	+0.80374	+0.096544	+0.54305	1.874	3.142	3.454
+0.22	+0.82224	+0.087302	+0.51098	1.826	3.273	3.486
+0.23	+0.84025	+0.077763	+0.47758	1.777	3.408	3.516
+0.24	+0.85776	+0.067913	+0.44280	1.726	3.547	3.543
+0.25	+0.87477	+0.057737	+0.40662	1.675	3.690	3.567
+0.26	+0.89127	+0.047215	+0.36899	1.624	3.838	3.586
+0.27	+0.90724	+0.036326	+0.32986	1.571	3.990	3.600
+0.28	+0.92270	+0.025041	+0.28918	1.519	4.146	3.607
+0.29	+0.93762	+0.013324	+0.24691	1.466	4.308	3.606
+0.30	+0.95200	+0.001129	+0.20300	1.412	4.476	3.594
+0.31	+0.96586	−0.011606	+0.15738	1.359	4.650	3.568
+0.32	+0.97918	−0.02497	+0.10997	1.306	4.832	3.524
+0.33	+0.99197	−0.03908	+0.06070	1.253	5.024	3.454
+0.34	+1.00423	−0.05413	+0.00945	1.200	5.228	3.351

5.2 (CONT.)

(1)	(3)	(5)	(6)	(7)	(8)	(9)
+0.35	+1.01598	−0.07040	−0.04392	1.149	5.450	3.202
+0.355	+1.02167	−0.07913	−0.07147	1.125	5.569	3.104
+0.360	+1.02723	−0.08837	−0.09963	1.100	5.696	2.987
+0.365	+1.03267	−0.09825	−0.12845	1.077	5.833	2.848
+0.370	+1.03800	−0.10893	−0.15798	1.054	5.983	2.680
+0.375	+1.04322	−0.12068	−0.18831	1.033	6.150	2.478

5.3

(1)	(3)	(5)	(6)	(7)	(8)	(9)
0.00	+0.32448	+0.237958	+0.97459	2.583	1.220	2.500
+0.01	+0.35022	+0.233008	+0.96209	2.564	1.280	2.550
+0.02	+0.37575	+0.227918	+0.94898	2.543	1.342	2.601
+0.03	+0.40107	+0.222684	+0.93524	2.520	1.407	2.651
+0.04	+0.42616	+0.217299	+0.92083	2.497	1.475	2.701
+0.05	+0.45100	+0.211759	+0.90572	2.472	1.546	2.751
+0.06	+0.47558	+0.206057	+0.88990	2.445	1.620	2.801
+0.07	+0.49989	+0.200188	+0.87331	2.417	1.697	2.850
+0.08	+0.52391	+0.194146	+0.85594	2.387	1.777	2.899
+0.09	+0.54763	+0.187925	+0.83776	2.356	1.861	2.948
+0.10	+0.57103	+0.181518	+0.81872	2.324	1.948	2.996
+0.11	+0.59410	+0.174920	+0.79879	2.290	2.038	3.043
+0.12	+0.61682	+0.168124	+0.77794	2.254	2.132	3.090
+0.13	+0.63918	+0.161122	+0.75615	2.217	2.229	3.136
+0.14	+0.66116	+0.153909	+0.73336	2.179	2.330	3.182
+0.15	+0.68276	+0.146477	+0.70954	2.140	2.434	3.226
+0.16	+0.70395	+0.138820	+0.68467	2.098	2.542	3.270
+0.17	+0.72472	+0.130930	+0.65870	2.056	2.653	3.313
+0.18	+0.74507	+0.122800	+0.63159	2.012	2.769	3.355
+0.19	+0.76497	+0.114423	+0.60331	1.968	2.888	3.396
+0.20	+0.78441	+0.105790	+0.57383	1.921	3.010	3.435
+0.21	+0.80339	+0.096895	+0.54309	1.874	3.137	3.474
+0.22	+0.82189	+0.087728	+0.51108	1.826	3.267	3.511
+0.23	+0.83991	+0.078281	+0.47774	1.776	3.401	3.547
+0.24	+0.85742	+0.068545	+0.44304	1.726	3.539	3.581
+0.25	+0.87443	+0.058511	+0.40695	1.675	3.681	3.613
+0.26	+0.89092	+0.048168	+0.36942	1.623	3.826	3.643
+0.27	+0.90688	+0.037504	+0.33041	1.570	3.975	3.672
+0.28	+0.92232	+0.026508	+0.28990	1.517	4.129	3.697
+0.29	+0.93723	+0.015163	+0.24782	1.464	4.286	3.719
+0.30	+0.95160	+0.003454	+0.20416	1.410	4.448	3.738
+0.31	+0.96542	−0.008642	+0.15886	1.355	4.614	3.752
+0.32	+0.97870	−0.021151	+0.11187	1.301	4.785	3.760
+0.33	+0.99144	−0.034105	+0.06314	1.247	4.961	3.761
+0.34	+1.00364	−0.047550	+0.01263	1.193	5.143	3.751
+0.35	+1.01530	−0.061546	−0.03973	1.139	5.332	3.729
+0.36	+1.02642	−0.07618	−0.09402	1.086	5.528	3.690
+0.37	+1.03702	−0.09156	−0.15034	1.033	5.736	3.626
+0.38	+1.04709	−0.10789	−0.20878	0.982	5.956	3.528
+0.39	+1.05666	−0.12544	−0.26952	0.932	6.196	3.384
+0.395	+1.06126	−0.13482	−0.30082	0.907	6.325	3.288
+0.400	+1.06573	−0.14472	−0.33279	0.883	6.463	3.171
+0.405	+1.07009	−0.15525	−0.36547	0.860	6.612	3.030
+0.410	+1.07434	−0.16661	−0.39894	0.838	6.776	2.858
+0.415	+1.07848	−0.17907	−0.43326	0.817	6.959	2.648
+0.420	+1.08251	−0.19308	−0.46857	0.798	7.171	2.390

5.4

(1)	(3)	(5)	(6)	(7)	(8)	(9)
0.00	+0.32433	+0.237940	+0.97444	2.583	1.220	2.500
+0.01	+0.35007	+0.232992	+0.96195	2.564	1.280	2.550
+0.02	+0.37560	+0.227904	+0.94884	2.543	1.342	2.601
+0.03	+0.40092	+0.222672	+0.93510	2.521	1.407	2.651
+0.04	+0.42601	+0.217289	+0.92070	2.497	1.475	2.701
+0.05	+0.45086	+0.211751	+0.90560	2.472	1.546	2.751
+0.06	+0.47544	+0.206052	+0.88977	2.445	1.620	2.801
+0.07	+0.49975	+0.200186	+0.87320	2.417	1.696	2.851
+0.08	+0.52378	+0.194147	+0.85583	2.387	1.777	2.900
+0.09	+0.54749	+0.187929	+0.83765	2.356	1.860	2.948
+0.10	+0.57090	+0.181526	+0.81862	2.324	1.947	2.997
+0.11	+0.59396	+0.174932	+0.79870	2.290	2.037	3.044
+0.12	+0.61669	+0.168140	+0.77786	2.254	2.131	3.091
+0.13	+0.63905	+0.161145	+0.75607	2.218	2.228	3.138
+0.14	+0.66103	+0.153938	+0.73329	2.179	2.329	3.184

5.4 (CONT.)

(1)	(3)	(5)	(6)	(7)	(8)	(9)
+0.15	+0.68263	+0.146514	+0.70948	2.140	2.433	3.229
+0.16	+0.70382	+0.138866	+0.68462	2.099	2.541	3.273
+0.17	+0.72460	+0.130986	+0.65866	2.056	2.652	3.316
+0.18	+0.74494	+0.122868	+0.63156	2.013	2.767	3.359
+0.19	+0.76485	+0.114505	+0.60330	1.968	2.886	3.400
+0.20	+0.78429	+0.105890	+0.57383	1.922	3.009	3.441
+0.21	+0.80327	+0.097016	+0.54311	1.874	3.135	3.481
+0.22	+0.82177	+0.087874	+0.51111	1.826	3.265	3.519
+0.23	+0.83978	+0.078459	+0.47780	1.776	3.399	3.557
+0.24	+0.85730	+0.068762	+0.44312	1.726	3.536	3.594
+0.25	+0.87430	+0.058776	+0.40706	1.675	3.678	3.629
+0.26	+0.89079	+0.048492	+0.36956	1.623	3.822	3.663
+0.27	+0.90676	+0.037905	+0.33060	1.570	3.971	3.696
+0.28	+0.92220	+0.027004	+0.29014	1.517	4.123	3.728
+0.29	+0.93710	+0.015783	+0.24814	1.463	4.279	3.758
+0.30	+0.95146	+0.004231	+0.20455	1.409	4.438	3.787
+0.31	+0.96527	−0.007660	+0.15936	1.354	4.602	3.815
+0.32	+0.97854	−0.019900	+0.11250	1.300	4.769	3.841
+0.33	+0.99127	−0.032499	+0.06396	1.245	4.940	3.865
+0.34	+1.00345	−0.045471	+0.01368	1.190	5.116	3.887
+0.35	+1.01508	−0.058829	−0.03837	1.136	5.296	3.906
+0.36	+1.02617	−0.072589	−0.09224	1.082	5.480	3.923
+0.37	+1.03672	−0.086771	−0.14798	1.028	5.669	3.937
+0.38	+1.04673	−0.101398	−0.20564	0.975	5.863	3.946
+0.39	+1.05622	−0.116502	−0.26527	0.923	6.064	3.949
+0.40	+1.06519	−0.132123	−0.32693	0.871	6.271	3.945
+0.405	+1.06948	−0.140144	−0.35855	0.846	6.377	3.939
+0.410	+1.07364	−0.148317	−0.39071	0.820	6.486	3.930
+0.415	+1.07768	−0.156652	−0.42341	0.795	6.597	3.917
+0.420	+1.08160	−0.165163	−0.45668	0.771	6.711	3.900
+0.425	+1.08539	−0.173864	−0.49052	0.746	6.827	3.878
+0.430	+1.08906	−0.182776	−0.52496	0.722	6.948	3.849
+0.435	+1.09262	−0.191922	−0.56001	0.699	7.072	3.813
+0.440	+1.09605	−0.201333	−0.59569	0.675	7.201	3.768
+0.445	+1.09937	−0.211048	−0.63202	0.653	7.335	3.711
+0.450	+1.10258	−0.221118	−0.66905	0.630	7.476	3.641
+0.455	+1.10567	−0.231611	−0.70680	0.608	7.626	3.553
+0.460	+1.10866	−0.242617	−0.74533	0.587	7.785	3.444
+0.465	+1.11154	−0.254266	−0.78468	0.566	7.958	3.309
+0.470	+1.11432	−0.26674	−0.82494	0.546	8.148	3.140
+0.475	+1.11701	−0.28034	−0.86620	0.527	8.363	2.928
+0.480	+1.11960	−0.29550	−0.90862	0.510	8.612	2.661
+0.485	+1.12211	−0.31306	−0.95241	0.494	8.916	2.322

5.5

(1)	(3)	(5)	(6)	(7)	(8)	(9)
+0.31	+0.96526	−0.007559	+0.15941	1.354	4.601	3.821
+0.32	+0.97853	−0.019772	+0.11257	1.300	4.768	3.849
+0.33	+0.99125	−0.032336	+0.06404	1.245	4.938	3.875
+0.34	+1.00342	−0.045262	+0.01379	1.190	5.113	3.900
+0.35	+1.01505	−0.058558	−0.03823	1.136	5.292	3.924
+0.36	+1.02614	−0.072234	−0.09206	1.082	5.475	3.947
+0.37	+1.03668	−0.086303	−0.14774	1.028	5.662	3.968
+0.38	+1.04670	−0.100776	−0.20532	0.974	5.854	3.988
+0.39	+1.05618	−0.115668	−0.26484	0.922	6.051	4.006
+0.40	+1.06513	−0.130995	−0.32636	0.870	6.253	4.022
+0.41	+1.07358	−0.146775	−0.38994	0.819	6.462	4.035
+0.42	+1.08152	−0.163030	−0.45562	0.769	6.676	4.046
+0.43	+1.08896	−0.179790	−0.52349	0.720	6.898	4.053
+0.44	+1.09592	−0.197089	−0.59362	0.672	7.129	4.054
+0.445	+1.09922	−0.205955	−0.62956	0.649	7.247	4.052
+0.450	+1.10241	−0.214976	−0.66610	0.626	7.369	4.049
+0.455	+1.10548	−0.224159	−0.70325	0.603	7.493	4.042
+0.460	+1.10844	−0.233515	−0.74103	0.581	7.620	4.033
+0.465	+1.11129	−0.243058	−0.77946	0.559	7.751	4.020
+0.470	+1.11403	−0.252802	−0.81854	0.537	7.886	4.002
+0.475	+1.11666	−0.262768	−0.85832	0.516	8.025	3.979
+0.480	+1.11919	−0.272979	−0.89880	0.495	8.169	3.949
+0.485	+1.12162	−0.283467	−0.94002	0.475	8.319	3.910
+0.490	+1.12394	−0.294270	−0.98200	0.455	8.476	3.861
+0.495	+1.12617	−0.305443	−1.02480	0.436	8.642	3.798
+0.500	+1.12830	−0.317054	−1.06844	0.417	8.818	3.717
+0.505	+1.13034	−0.329202	−1.11300	0.399	9.006	3.615
+0.510	+1.13230	−0.34202	−1.15853	0.381	9.211	3.485
+0.515	+1.13416	−0.35572	−1.20514	0.364	9.438	3.318
+0.520	+1.13594	−0.37060	−1.25296	0.348	9.695	3.103
+0.525	+1.13764	−0.38718	−1.30216	0.333	9.996	2.825
+0.530	+1.13927	−0.40641	−1.35303	0.319	10.37	2.46

5.6

(1)	(3)	(5)	(6)	(7)	(8)	(9)
0.00	+0.32432	+0.237939	+0.97443	2.583	1.220	2.500
+0.01	+0.35006	+0.232991	+0.96193	2.564	1.280	2.550
+0.02	+0.37559	+0.227903	+0.94883	2.543	1.342	2.601
+0.03	+0.40091	+0.222671	+0.93509	2.521	1.407	2.651
+0.04	+0.42600	+0.217288	+0.92068	2.497	1.475	2.701
+0.05	+0.45084	+0.211750	+0.90558	2.472	1.546	2.751
+0.06	+0.47543	+0.206052	+0.88976	2.445	1.620	2.801
+0.07	+0.49974	+0.200186	+0.87318	2.417	1.696	2.851
+0.08	+0.52376	+0.194147	+0.85582	2.387	1.777	2.900
+0.09	+0.54748	+0.187930	+0.83764	2.356	1.860	2.949
+0.10	+0.57088	+0.181528	+0.81860	2.324	1.947	2.997
+0.11	+0.59395	+0.174934	+0.79869	2.290	2.037	3.045
+0.12	+0.61667	+0.168143	+0.77785	2.254	2.131	3.092
+0.13	+0.63903	+0.161148	+0.75606	2.218	2.228	3.138
+0.14	+0.66102	+0.153942	+0.73328	2.179	2.328	3.184
+0.15	+0.68262	+0.146519	+0.70948	2.140	2.433	3.229
+0.16	+0.70381	+0.138872	+0.68462	2.099	2.541	3.273
+0.17	+0.72458	+0.130994	+0.65866	2.056	2.652	3.317
+0.18	+0.74493	+0.122878	+0.63156	2.013	2.767	3.359
+0.19	+0.76483	+0.114517	+0.60330	1.968	2.886	3.401
+0.20	+0.78428	+0.105904	+0.57383	1.922	3.009	3.442
+0.21	+0.80326	+0.097032	+0.54311	1.874	3.135	3.482
+0.22	+0.82176	+0.087894	+0.51112	1.826	3.265	3.521
+0.23	+0.83977	+0.078482	+0.47780	1.776	3.398	3.558
+0.24	+0.85728	+0.068790	+0.44314	1.726	3.536	3.595
+0.25	+0.87429	+0.058810	+0.40707	1.675	3.677	3.631
+0.26	+0.89078	+0.048535	+0.36958	1.623	3.822	3.666
+0.27	+0.90674	+0.037958	+0.33063	1.570	3.970	3.699
+0.28	+0.92218	+0.027070	+0.29017	1.517	4.122	3.732
+0.29	+0.93708	+0.015864	+0.24818	1.463	4.278	3.763
+0.30	+0.95144	+0.004333	+0.20461	1.409	4.437	3.794
+0.31	+0.96525	−0.007531	+0.15942	1.354	4.600	3.823
+0.32	+0.97852	−0.019736	+0.11259	1.300	4.767	3.851
+0.33	+0.99124	−0.032291	+0.06407	1.245	4.938	3.878
+0.34	+1.00342	−0.045204	+0.01382	1.190	5.112	3.904
+0.35	+1.01505	−0.058482	−0.03819	1.136	5.291	3.929
+0.36	+1.02613	−0.072136	−0.09201	1.081	5.474	3.954
+0.37	+1.03668	−0.086174	−0.14768	1.028	5.660	3.977
+0.38	+1.04669	−0.100606	−0.20524	0.974	5.852	4.000
+0.39	+1.05617	−0.115440	−0.26473	0.922	6.048	4.022
+0.40	+1.06512	−0.130687	−0.32621	0.870	6.249	4.043
+0.41	+1.07356	−0.146355	−0.38973	0.819	6.455	4.064
+0.42	+1.08150	−0.162454	−0.45534	0.768	6.667	4.086
+0.43	+1.08894	−0.178992	−0.52309	0.719	6.885	4.109
+0.44	+1.09589	−0.195973	−0.59306	0.672	7.110	4.133
+0.45	+1.10237	−0.213398	−0.66531	0.625	7.341	4.160
+0.46	+1.10839	−0.231261	−0.73991	0.579	7.580	4.193
+0.47	+1.11396	−0.249546	−0.81693	0.535	7.825	4.233

5.7

(1)	(3)	(5)	(6)	(7)	(8)	(9)
0.00	+0.32406	+0.237910	+0.97418	2.584	1.219	2.500
+0.01	+0.34980	+0.232964	+0.96169	2.564	1.279	2.550
+0.02	+0.37534	+0.227879	+0.94859	2.543	1.341	2.601
+0.03	+0.40066	+0.222650	+0.93486	2.521	1.406	2.651
+0.04	+0.42575	+0.217271	+0.92046	2.497	1.474	2.702
+0.05	+0.45060	+0.211737	+0.90537	2.472	1.545	2.752
+0.06	+0.47518	+0.206042	+0.88955	2.445	1.619	2.802
+0.07	+0.49950	+0.200181	+0.87298	2.417	1.696	2.852
+0.08	+0.52352	+0.194148	+0.85563	2.388	1.776	2.901
+0.09	+0.54724	+0.187936	+0.83746	2.357	1.859	2.950
+0.10	+0.57065	+0.181540	+0.81844	2.324	1.946	2.998
+0.11	+0.59372	+0.174954	+0.79853	2.290	2.036	3.046
+0.12	+0.61644	+0.168171	+0.77771	2.255	2.130	3.094
+0.13	+0.63881	+0.161185	+0.75593	2.218	2.226	3.141
+0.14	+0.66080	+0.153990	+0.73316	2.180	2.327	3.187
+0.15	+0.68240	+0.146580	+0.70938	2.140	2.431	3.233
+0.16	+0.70359	+0.138948	+0.68453	2.099	2.539	3.278
+0.17	+0.72437	+0.131087	+0.65859	2.056	2.650	3.322
+0.18	+0.74472	+0.122991	+0.63151	2.013	2.765	3.366
+0.19	+0.76462	+0.114654	+0.60327	1.968	2.884	3.409
+0.20	+0.78407	+0.106071	+0.57382	1.922	3.006	3.452
+0.21	+0.80305	+0.097234	+0.54314	1.874	3.132	3.494
+0.22	+0.82155	+0.088139	+0.51117	1.826	3.262	3.535
+0.23	+0.83957	+0.078780	+0.47789	1.776	3.395	3.576
+0.24	+0.85708	+0.069153	+0.44327	1.726	3.531	3.617

5.7 (CONT.)

(1)	(3)	(5)	(6)	(7)	(8)	(9)
+0.25	+0.87408	+0.059253	+0.40726	1.675	3.671	3.658
+0.26	+0.89057	+0.049078	+0.36983	1.622	3.815	3.699
+0.27	+0.90653	+0.038625	+0.33095	1.570	3.962	3.741
+0.28	+0.92196	+0.027895	+0.29058	1.516	4.112	3.784
+0.29	+0.93685	+0.016890	+0.24870	1.462	4.265	3.828
+0.30	+0.95120	+0.005615	+0.20526	1.408	4.422	3.876
+0.31	+0.96500	−0.005920	+0.16025	1.353	4.581	3.928
+0.32	+0.97825	−0.017702	+0.11364	1.298	4.742	3.986
+0.33	+0.99095	−0.029706	+0.06541	1.242	4.905	4.052

5.8

(1)	(3)	(5)	(6)	(7)	(8)	(9)
−0.01	+0.29470	+0.242306	+0.98267	2.604	1.154	2.449
0.00	+0.32065	+0.237527	+0.97084	2.586	1.211	2.500
+0.01	+0.34642	+0.232616	+0.95844	2.567	1.270	2.551
+0.02	+0.37199	+0.227570	+0.94544	2.546	1.332	2.603
+0.03	+0.39734	+0.222382	+0.93180	2.524	1.396	2.655
+0.04	+0.42246	+0.217049	+0.91750	2.500	1.464	2.706
+0.05	+0.44734	+0.211565	+0.90252	2.475	1.534	2.758
+0.06	+0.47196	+0.205925	+0.88682	2.449	1.607	2.810
+0.07	+0.49631	+0.200124	+0.87037	2.421	1.683	2.862
+0.08	+0.52037	+0.194158	+0.85314	2.391	1.763	2.914
+0.09	+0.54412	+0.188022	+0.83510	2.360	1.846	2.966
+0.10	+0.56757	+0.181711	+0.81622	2.327	1.931	3.018
+0.11	+0.59068	+0.175221	+0.79646	2.294	2.020	3.070
+0.12	+0.61344	+0.168547	+0.77580	2.258	2.113	3.122
+0.13	+0.63584	+0.161686	+0.75419	2.222	2.208	3.175
+0.14	+0.65786	+0.154634	+0.73161	2.183	2.308	3.229
+0.15	+0.67950	+0.147388	+0.70802	2.144	2.410	3.283
+0.16	+0.70073	+0.139948	+0.68339	2.102	2.516	3.338
+0.17	+0.72154	+0.132312	+0.65768	2.060	2.626	3.395
+0.18	+0.74192	+0.124480	+0.63087	2.016	2.738	3.454
+0.19	+0.76186	+0.116457	+0.60291	1.971	2.854	3.515
+0.20	+0.78133	+0.108245	+0.57378	1.924	2.972	3.580
+0.21	+0.80033	+0.099854	+0.54346	1.876	3.094	3.649
+0.22	+0.81885	+0.091293	+0.51190	1.827	3.218	3.724
+0.23	+0.83687	+0.082579	+0.47909	1.777	3.344	3.807
+0.24	+0.85438	+0.073733	+0.44501	1.725	3.473	3.900
+0.25	+0.87138	+0.064782	+0.40964	1.673	3.602	4.006
+0.26	+0.88784	+0.055763	+0.37296	1.619	3.733	4.130
+0.27	+0.90376	+0.046719	+0.33497	1.565	3.864	4.275
+0.28	+0.91913	+0.037705	+0.29568	1.510	3.994	4.449
+0.29	+0.93395	+0.028787	+0.25510	1.453	4.122	4.661
+0.30	+0.94820	+0.020041	+0.21324	1.396	4.248	4.921
+0.31	+0.96187	+0.011554	+0.17016	1.339	4.368	5.245

6.1

(1)	(4)	(5)	(6)	(7)	(8)	(9)
+0.00	−0.4299	+0.2653	+1.0933	2.500	1.460	2.500
+0.02	−0.4794	+0.2535	+1.0627	2.453	1.606	2.698
+0.04	−0.5279	+0.2415	+1.0290	2.396	1.764	2.918
+0.06	−0.5752	+0.2294	+0.9921	2.330	1.931	3.168
+0.08	−0.6211	+0.2172	+0.9517	2.256	2.108	3.453
+0.10	−0.6654	+0.2050	+0.9077	2.174	2.293	3.783
+0.12	−0.7080	+0.1930	+0.8600	2.084	2.483	4.169
+0.14	−0.7487	+0.1812	+0.8083	1.988	2.676	4.627
+0.16	−0.7875	+0.1699	+0.7529	1.886	2.868	5.178
+0.18	−0.8242	+0.1591	+0.6936	1.780	3.055	5.847
+0.20	−0.8587	+0.1490	+0.6308	1.672	3.233	6.669
+0.22	−0.8910	+0.1398	+0.5644	1.562	3.384	7.684
+0.24	−0.9212	+0.1314	+0.4949	1.454	3.546	8.948
+0.26	−0.9492	+0.1239	+0.4227	1.348	3.675	10.52
+0.28	−0.9751	+0.1174	+0.3481	1.246	3.782	12.49
+0.30	−0.9991	+0.1118	+0.2716	1.150	3.866	14.95
+0.32	−1.0212	+0.1070	+0.1936	1.060	3.928	18.02
+0.34	−1.0415	+0.1030	+0.1146	0.978	3.966	21.83
+0.36	−1.0602	+0.0997	+0.0350	0.902	3.986	26.55

6.2

(1)	(4)	(5)	(6)	(7)	(8)	(9)
+0.00	−0.5801	+0.2536	+1.1966	2.306	2.120	2.500
+0.02	−0.6255	+0.2362	+1.1521	2.240	2.340	2.620
+0.04	−0.6690	+0.2179	+1.1029	2.165	2.580	2.743
+0.06	−0.7120	+0.1986	+1.0486	2.080	2.841	2.869
+0.08	−0.7527	+0.1783	+0.9891	1.987	3.122	2.997
+0.10	−0.7914	+0.1569	+0.9237	1.885	3.424	3.129
+0.12	−0.8281	+0.1345	+0.8520	1.776	3.746	3.265
+0.14	−0.8624	+0.1110	+0.7737	1.660	4.087	3.410
+0.16	−0.8944	+0.0866	+0.6884	1.540	4.445	3.567
+0.18	−0.9240	+0.0612	+0.5958	1.415	4.817	3.742
+0.20	−0.9510	+0.0351	+0.4957	1.287	5.198	3.944
+0.22	−0.9755	+0.0086	+0.3878	1.158	5.584	4.189
+0.24	−0.9973	−0.0181	+0.2724	1.030	5.962	4.496
+0.26	−1.0167	−0.0442	+0.1495	0.906	6.322	4.899
+0.28	−1.0336	−0.0694	+0.0197	0.786	6.653	5.449
+0.30	−1.0482	−0.0928	−0.1163	0.674	6.935	6.211
+0.32	−1.0606	−0.1139	−0.2573	0.570	7.152	7.283
+0.34	−1.0711	−0.1319	−0.4019	0.478	7.295	8.810
+0.36	−1.0798	−0.1468	−0.5485	0.397	7.357	10.891
+0.38	−1.0870	−0.1588	−0.6956	0.328	7.343	14.040
+0.40	−1.0930	−0.1679	−0.8418	0.271	7.260	18.319
+0.42	−1.0979	−0.1748	−0.9857	0.224	7.125	24.228

6.3

(1)	(4)	(5)	(6)	(7)	(8)	(9)
+0.00	−0.5883	+0.2528	+1.2016	2.294	2.165	2.500
+0.02	−0.6335	+0.2350	+1.1560	2.226	2.390	2.615
+0.04	−0.6772	+0.2162	+1.1058	2.150	2.636	2.731
+0.06	−0.7194	+0.1964	+1.0505	2.064	2.904	2.848
+0.08	−0.7597	+0.1754	+0.9895	1.970	3.194	2.964
+0.10	−0.7981	+0.1533	+0.9225	1.867	3.506	3.080
+0.12	−0.8344	+0.1299	+0.8491	1.758	3.842	3.197
+0.14	−0.8684	+0.1052	+0.7687	1.642	4.200	3.314
+0.16	−0.8999	+0.0792	+0.6809	1.520	4.580	3.434
+0.18	−0.9291	+0.0518	+0.5854	1.394	4.981	3.557
+0.20	−0.9588	+0.0232	+0.4816	1.266	5.402	3.689
+0.22	−0.9798	−0.0067	+0.3692	1.138	5.841	3.835
+0.24	−1.0013	−0.0377	+0.2479	1.010	6.293	4.006
+0.26	−1.0202	−0.0694	+0.1174	0.884	6.755	4.218
+0.28	−1.0367	−0.1015	−0.0223	0.763	7.215	4.497
+0.30	−1.0508	−0.1333	−0.1710	0.648	7.656	4.882
+0.32	−1.0627	−0.1639	−0.3284	0.540	8.065	5.436
+0.34	−1.0725	−0.1923	−0.4933	0.443	8.410	6.262
+0.36	−1.0805	−0.2173	−0.6641	0.357	8.665	7.503
+0.38	−1.0868	−0.2383	−0.8390	0.283	8.814	9.391
+0.40	−1.0919	−0.2549	−1.0518	0.222	8.845	12.251
+0.42	−1.0958	−0.2673	−1.1923	0.173	8.775	16.557

6.4

(1)	(4)	(5)	(6)	(7)	(8)	(9)
+0.00	−0.5909	+0.2525	+1.2032	2.290	2.180	2.500
+0.02	−0.6361	+0.2346	+1.1574	2.222	2.407	2.613
+0.04	−0.6798	+0.2157	+1.1068	2.144	2.655	2.727
+0.06	−0.7218	+0.1957	+1.0510	2.058	2.926	2.841
+0.08	−0.7620	+0.1745	+0.9896	1.964	3.212	2.953
+0.10	−0.8003	+0.1520	+0.9221	1.861	3.534	3.064
+0.12	−0.8364	+0.1283	+0.8481	1.752	3.874	3.174
+0.14	−0.8703	+0.1032	+0.7670	1.635	4.238	3.281
+0.16	−0.9018	+0.0766	+0.6784	1.514	4.626	3.387
+0.18	−0.9308	+0.0485	+0.5818	1.388	5.038	3.493
+0.20	−0.9573	+0.0189	+0.4767	1.260	5.476	3.599
+0.22	−0.9812	−0.0123	+0.3627	1.132	5.937	3.709
+0.24	−1.0026	−0.0451	+0.2391	1.004	6.422	3.829
+0.26	−1.0214	−0.0794	+0.1056	0.878	6.931	3.965
+0.28	−1.0377	−0.1149	−0.0382	0.756	7.458	4.134
+0.30	−1.0517	−0.1514	−0.1928	0.641	8.000	4.356
+0.32	−1.0634	−0.1881	−0.3582	0.532	8.541	4.671
+0.34	−1.0731	−0.2240	−0.5343	0.433	9.060	5.142
+0.36	−1.0808	−0.2582	−0.7203	0.344	9.528	5.865
+0.38	−1.0869	−0.2887	−0.9148	0.267	9.900	7.031

6.5

(1)	(4)	(5)	(6)	(7)	(8)	(9)
+0.00	-0.5937	+0.2523	+1.2048	2.285	2.195	2.500
+0.02	-0.6387	+0.2342	+1.1586	2.217	2.424	2.612
+0.04	-0.6823	+0.2151	+1.1077	2.140	2.674	2.723
+0.06	-0.7242	+0.1949	+1.0515	2.053	2.946	2.833
+0.08	-0.7643	+0.1735	+0.9897	1.958	3.242	2.942
+0.10	-0.8025	+0.1508	+0.9217	1.855	3.562	3.048
+0.12	-0.8385	+0.1267	+0.8470	1.745	3.906	3.150
+0.14	-0.8722	+0.1015	+0.7652	1.628	4.276	3.248
+0.16	-0.9036	+0.0740	+0.6758	1.507	4.672	3.341
+0.18	-0.9325	+0.0452	+0.5781	1.382	5.097	3.429
+0.20	-0.9588	+0.0145	+0.4717	1.254	5.550	3.509
+0.22	-0.9826	-0.0181	+0.3559	1.126	6.036	3.582
+0.24	-1.0039	-0.0530	+0.2300	0.998	6.560	3.647
+0.26	-1.0226	-0.0902	+0.0933	0.873	7.126	3.703
+0.28	-1.0388	-0.1301	-0.0553	0.752	7.743	3.749
+0.30	-1.0527	-0.1730	-0.2168	0.636	8.427	3.781
+0.32	-1.0643	-0.2194	-0.3929	0.527	9.200	3.799
+0.34	-1.0739	-0.2702	-0.5857	0.427	10.094	3.791

6.6

(1)	(4)	(5)	(6)	(7)	(8)	(9)
+0.00	-0.5964	+0.2520	+1.2064	2.280	2.210	2.500
+0.02	-0.6413	+0.2338	+1.1599	2.212	2.441	2.610
+0.04	-0.6848	+0.2146	+1.1086	2.134	2.693	2.719
+0.06	-0.7266	+0.1941	+1.0520	2.048	2.968	2.827
+0.08	-0.7667	+0.1725	+0.9897	1.952	3.267	2.930
+0.10	-0.8047	+0.1495	+0.9212	1.850	3.590	3.031
+0.12	-0.8406	+0.1251	+0.8459	1.739	3.940	3.126
+0.14	-0.8742	+0.0991	+0.7634	1.622	4.317	3.214
+0.16	-0.9054	+0.0713	+0.6730	1.501	4.722	3.292
+0.18	-0.9342	+0.0416	+0.5743	1.376	5.160	3.360
+0.20	-0.9605	+0.0098	+0.4664	1.248	5.632	3.412
+0.22	-0.9841	-0.0245	+0.3487	1.1195	6.147	3.446
+0.24	-1.0053	-0.0617	+0.2202	0.992	6.714	3.451
+0.26	-1.0239	-0.1026	+0.0797	0.868	7.354	3.417
+0.28	-1.0400	-0.1484	-0.0746	0.748	8.098	3.324
+0.30	-1.0538	-0.2014	-0.2455	0.634	9.020	3.120
+0.31	-1.0599	-0.2319	-0.3385	0.580	9.592	2.955
+0.32	-1.0654	-0.2669	-0.4378	0.529	10.288	2.727

6.7

(1)	(4)	(5)	(6)	(7)	(8)	(9)
+0.00	-0.5991	+0.2517	+1.2079	2.276	2.226	2.500
+0.02	-0.6439	+0.2334	+1.1612	2.207	2.458	2.608
+0.04	-0.6873	+0.2139	+1.1095	2.129	2.712	2.715
+0.06	-0.7290	+0.1934	+1.0525	2.042	2.990	2.819
+0.08	-0.7689	+0.1715	+0.9898	1.946	3.292	2.919
+0.10	-0.8068	+0.1483	+0.9207	1.844	3.619	3.014
+0.12	-0.8426	+0.1234	+0.8448	1.733	3.974	3.101
+0.14	-0.8761	+0.0969	+0.7616	1.616	4.357	3.176
+0.16	-0.9072	+0.0685	+0.6704	1.495	4.770	3.247
+0.18	-0.9359	+0.0379	+0.5705	1.364	5.222	3.291
+0.20	-0.9620	+0.0049	+0.4612	1.242	5.716	3.316
+0.22	-0.9856	-0.0311	+0.3415	1.114	6.262	3.307
+0.24	-1.0066	-0.0712	+0.2102	0.988	6.882	3.256
+0.26	-1.0251	-0.1167	+0.0653	0.864	7.618	3.111
+0.28	-1.0412	-0.1707	-0.0959	0.747	8.548	2.846
+0.29	-1.0484	-0.2029	-0.1844	0.692	9.149	2.637
+0.30	-1.0551	-0.2411	-0.2795	0.640	9.913	2.346
+0.31	-1.0612	-0.2900	-0.3839	0.596	10.997	1.928

7.1

(1)	(3)	(5)	(6)	(7)	(8)	(9)
+0.37	+0.98251	-0.06818	-0.11855	1.194	4.794	4.241
+0.38	+0.99420	-0.079623	-0.16722	1.143	4.941	4.265
+0.39	+1.00538	-0.091351	-0.21738	1.093	5.090	4.287
+0.40	+1.01606	-0.103374	-0.26904	1.043	5.241	4.306
+0.41	+1.02624	-0.115701	-0.32222	0.994	5.394	4.321
+0.42	+1.03594	-0.128347	-0.37694	0.945	5.550	4.332
+0.43	+1.04515	-0.141328	-0.43322	0.897	5.708	4.338
+0.44	+1.05389	-0.154669	-0.49110	0.850	5.869	4.338
+0.45	+1.06216	-0.168397	-0.55061	0.805	6.033	4.330
+0.46	+1.0700	-0.18255	-0.6118	0.760	6.202	4.311

7.1 (CONT.)

(1)	(3)	(5)	(6)	(7)	(8)	(9)
+0.47	+1.0774	-0.19720	-0.6747	0.716	6.376	4.277
+0.48	+1.0843	-0.21240	-0.7393	0.673	6.557	4.225
+0.49	+1.0908	-0.22828	-0.8058	0.633	6.747	4.147
+0.50	+1.0970	-0.24501	-0.8743	0.594	6.950	4.034
+0.51	+1.1027	-0.26286	-0.9449	0.556	7.171	3.870
+0.52	+1.1081	-0.28227	-1.0178	0.520	7.419	3.634
+0.53	+1.1131	-0.30402	-1.0934	0.487	7.712	3.300
+0.54	+1.1178	-0.32983	-1.1724	0.457	8.085	2.81
+0.55	+1.1223	-0.36403	-1.2560	0.433	8.64	2.08

7.2

(1)	(3)	(5)	(6)	(7)	(8)	(9)
+0.37	+0.98249	-0.067946	-0.11841	1.194	4.791	4.263
+0.38	+0.99418	-0.079333	-0.16705	1.143	4.938	4.286
+0.39	+1.00536	-0.090990	-0.21716	1.093	5.086	4.313
+0.40	+1.01603	-0.102920	-0.26877	1.043	5.235	4.338
+0.41	+1.02621	-0.115128	-0.32188	0.993	5.387	4.362
+0.42	+1.03590	-0.127620	-0.37651	0.944	5.540	4.385
+0.43	+1.04510	-0.140401	-0.43269	0.897	5.695	4.405
+0.44	+1.05383	-0.153477	-0.49042	0.850	5.852	4.425
+0.45	+1.06210	-0.166856	-0.54974	0.804	6.011	4.442
+0.46	+1.06991	-0.180545	-0.61065	0.759	6.172	4.457
+0.47	+1.07728	-0.194557	-0.67319	0.715	6.336	4.470
+0.48	+1.08421	-0.208903	-0.73739	0.672	6.503	4.479
+0.49	+1.09072	-0.223601	-0.80326	0.630	6.673	4.485
+0.50	+1.09682	-0.238671	-0.87086	0.590	6.847	4.485
+0.51	+1.10253	-0.254143	-0.94022	0.551	7.025	4.479
+0.52	+1.10785	-0.270053	-1.01138	0.514	7.210	4.465
+0.525	+1.11037	-0.278189	-1.04767	0.496	7.304	4.454
+0.530	+1.11281	-0.286456	-1.08443	0.478	7.401	4.439
+0.535	+1.11515	-0.294864	-1.12168	0.460	7.499	4.420
+0.540	+1.11741	-0.303425	-1.15943	0.443	7.600	4.397
+0.545	+1.11958	-0.312155	-1.19769	0.426	7.704	4.368
+0.550	+1.12168	-0.321071	-1.23648	0.410	7.812	4.332
+0.555	+1.12369	-0.330196	-1.27581	0.394	7.923	4.288
+0.560	+1.12562	-0.339559	-1.31571	0.379	8.039	4.234
+0.565	+1.12747	-0.349195	-1.35621	0.364	8.160	4.168
+0.570	+1.12926	-0.359151	-1.39732	0.349	8.287	4.089
+0.575	+1.13096	-0.369488	-1.43909	0.335	8.423	3.991
+0.580	+1.13260	-0.380286	-1.48156	0.321	8.568	3.872
+0.585	+1.13417	-0.391658	-1.52480	0.307	8.726	3.727
+0.590	+1.13568	-0.403764	-1.56886	0.295	8.901	3.549
+0.595	+1.13712	-0.41684	-1.61384	0.282	9.098	3.330
+0.600	+1.13850	-0.43126	-1.65989	0.271	9.327	3.058
+0.605	+1.13983	-0.44764	-1.70720	0.260	9.604	2.719
+0.610	+1.14111	-0.46714	-1.75607	0.251	9.958	2.293

8.1

(1)	(4)	(5)	(6)	(7)	(8)	(9)
+0.00	+0.99196	-0.232157	-1.83041	2.430	1.707	2.500
+0.01	+0.96842	-0.238901	-1.84742	2.282	1.694	2.542
+0.02	+0.94624	-0.245487	-1.86429	2.156	1.681	2.581
+0.03	+0.92524	-0.251927	-1.88103	2.048	1.667	2.617
+0.04	+0.90523	-0.258228	-1.89763	1.955	1.653	2.652
+0.05	+0.88610	-0.264396	-1.91408	1.873	1.638	2.685
+0.06	+0.86774	-0.270435	-1.93039	1.801	1.623	2.716
+0.07	+0.85006	-0.276349	-1.94654	1.737	1.608	2.748
+0.08	+0.83297	-0.282139	-1.96255	1.681	1.593	2.780
+0.09	+0.81642	-0.287807	-1.97840	1.630	1.577	2.812
+0.10	+0.80035	-0.293352	-1.99409	1.585	1.561	2.846
+0.11	+0.78471	-0.298775	-2.00962	1.544	1.544	2.881
+0.12	+0.76946	-0.304074	-2.02498	1.507	1.528	2.918
+0.13	+0.75456	-0.309248	-2.04017	1.473	1.511	2.956
+0.14	+0.73999	-0.314294	-2.05519	1.442	1.494	2.998
+0.15	+0.72571	-0.319210	-2.07004	1.414	1.476	3.043
+0.16	+0.71169	-0.323995	-2.08472	1.389	1.459	3.092
+0.17	+0.69792	-0.328644	-2.09922	1.365	1.441	3.145
+0.18	+0.68438	-0.333157	-2.11354	1.344	1.423	3.203
+0.19	+0.67104	-0.337528	-2.12767	1.324	1.404	3.266
+0.20	+0.65789	-0.341757	-2.14163	1.306	1.386	3.335
+0.21	+0.64492	-0.345840	-2.15539	1.289	1.367	3.410
+0.22	+0.63210	-0.349775	-2.16897	1.274	1.348	3.492
+0.23	+0.61944	-0.353561	-2.18236	1.259	1.329	3.582
+0.24	+0.60692	-0.357195	-2.19555	1.246	1.310	3.681
+0.25	+0.59452	-0.360677	-2.20855	1.234	1.290	3.789
+0.26	+0.58224	-0.364006	-2.22135	1.222	1.271	3.906

8.2

(1)	(4)	(5)	(6)	(7)	(8)	(9)
+0.00	+1.03570	-0.251648	-1.94168	2.406	1.785	2.500
+0.01	+1.01240	-0.258716	-1.95947	2.260	1.773	2.534
+0.02	+0.99044	-0.265649	-1.97714	2.135	1.761	2.563
+0.03	+0.96964	-0.272460	-1.99468	2.028	1.748	2.588
+0.04	+0.94983	-0.279159	-2.01209	1.935	1.734	2.609
+0.05	+0.93089	-0.285756	-2.02937	1.854	1.721	2.628
+0.06	+0.91271	-0.292257	-2.04651	1.783	1.707	2.644
+0.07	+0.89520	-0.298670	-2.06351	1.720	1.693	2.658
+0.08	+0.87829	-0.304998	-2.08037	1.664	1.679	2.670
+0.09	+0.86190	-0.311247	-2.09708	1.614	1.664	2.680
+0.10	+0.84598	-0.317421	-2.11366	1.569	1.650	2.688
+0.11	+0.83050	-0.323523	-2.13008	1.529	1.635	2.695
+0.12	+0.81539	-0.329555	-2.14636	1.493	1.620	2.701
+0.13	+0.80063	-0.335521	-2.16248	1.460	1.605	2.705
+0.14	+0.78618	-0.341422	-2.17846	1.430	1.590	2.709
+0.15	+0.77202	-0.347261	-2.19428	1.403	1.575	2.712
+0.16	+0.75812	-0.353039	-2.20996	1.378	1.560	2.714
+0.17	+0.74445	-0.358758	-2.22548	1.356	1.544	2.715
+0.18	+0.73101	-0.364417	-2.24084	1.335	1.529	2.715
+0.19	+0.71775	-0.370020	-2.25606	1.317	1.514	2.716
+0.20	+0.70467	-0.375565	-2.27112	1.300	1.498	2.716
+0.21	+0.69176	-0.381054	-2.28602	1.284	1.483	2.715
+0.22	+0.67899	-0.386487	-2.30077	1.270	1.467	2.715
+0.23	+0.66636	-0.391864	-2.31536	1.257	1.452	2.714
+0.24	+0.65385	-0.397184	-2.32980	1.245	1.436	2.714
+0.25	+0.64146	-0.402448	-2.34408	1.234	1.420	2.713
+0.26	+0.62917	-0.407656	-2.35819	1.224	1.405	2.713

8.3

(1)	(4)	(5)	(6)	(7)	(8)	(9)
+0.00	-1.67295	+0.659456	+3.56566	2.493	1.503	2.500
+0.01	-1.69743	+0.653437	+3.55049	2.404	1.532	2.543
+0.02	-1.72106	+0.647404	+3.53503	2.323	1.560	2.583
+0.03	-1.74391	+0.641357	+3.51929	2.249	1.587	2.621
+0.04	-1.76607	+0.635293	+3.50329	2.182	1.613	2.657
+0.05	-1.78758	+0.629212	+3.48702	2.120	1.639	2.691
+0.06	-1.80849	+0.623113	+3.47051	2.064	1.664	2.724
+0.07	-1.82886	+0.616995	+3.45375	2.011	1.688	2.755
+0.08	-1.84873	+0.610858	+3.43674	1.962	1.712	2.785
+0.09	-1.86812	+0.604701	+3.41951	1.917	1.735	2.814
+0.10	-1.88708	+0.598524	+3.40204	1.875	1.758	2.841
+0.11	-1.90562	+0.592326	+3.38435	1.835	1.780	2.868
+0.12	-1.92378	+0.586108	+3.36644	1.797	1.802	2.893
+0.13	-1.94158	+0.579869	+3.34831	1.762	1.824	2.918
+0.14	-1.95903	+0.573609	+3.32996	1.729	1.845	2.942
+0.15	-1.97616	+0.567329	+3.31142	1.698	1.865	2.965
+0.16	-1.99299	+0.561028	+3.29266	1.668	1.886	2.988
+0.17	-2.00952	+0.554707	+3.27370	1.640	1.906	3.010
+0.18	-2.02578	+0.548366	+3.25455	1.612	1.925	3.032
+0.19	-2.04178	+0.542004	+3.23520	1.587	1.945	3.053
+0.20	-2.05752	+0.535624	+3.21565	1.562	1.964	3.074
+0.21	-2.07303	+0.529225	+3.19592	1.539	1.983	3.094
+0.22	-2.08830	+0.522808	+3.17600	1.516	2.001	3.115
+0.23	-2.10335	+0.516374	+3.15589	1.494	2.020	3.135
+0.24	-2.11819	+0.509923	+3.13560	1.474	2.038	3.156
+0.25	-2.13283	+0.503458	+3.11514	1.454	2.056	3.176
+0.26	-2.14727	+0.496979	+3.09449	1.434	2.073	3.197
+0.27	-2.16151	+0.490487	+3.07367	1.416	2.091	3.218
+0.28	-2.17558	+0.483985	+3.05268	1.397	2.108	3.239
+0.29	-2.18946	+0.477474	+3.03152	1.380	2.124	3.261
+0.30	-2.20318	+0.470957	+3.01019	1.363	2.141	3.284
+0.31	-2.21672	+0.464436	+2.98870	1.346	2.157	3.308
+0.32	-2.23011	+0.457914	+2.96704	1.330	2.173	3.333
+0.33	-2.24333	+0.451394	+2.94523	1.315	2.189	3.359
+0.34	-2.25640	+0.444881	+2.92326	1.300	2.205	3.387
+0.35	-2.26932	+0.438378	+2.90114	1.285	2.220	3.417
+0.36	-2.28210	+0.431891	+2.87887	1.270	2.234	3.449
+0.37	-2.29473	+0.425426	+2.85645	1.256	2.249	3.485
+0.38	-2.30722	+0.418987	+2.83390	1.242	2.263	3.523
+0.39	-2.31957	+0.412582	+2.81120	1.228	2.276	3.565
+0.40	-2.33178	+0.406220	+2.78837	1.215	2.289	3.611
+0.41	-2.34386	+0.399908	+2.76542	1.202	2.302	3.663
+0.42	-2.35581	+0.393655	+2.74235	1.188	2.313	3.720
+0.43	-2.36763	+0.387474	+2.71916	1.176	2.325	3.784
+0.44	-2.37932	+0.381374	+2.69586	1.163	2.335	3.857

8.3 (CONT.)

(1)	(4)	(5)	(6)	(7)	(8)	(9)
+0.45	-2.39089	+0.375369	+2.67246	1.150	2.345	3.938
+0.46	-2.40233	+0.369470	+2.64897	1.138	2.353	4.029
+0.47	-2.41364	+0.363692	+2.62539	1.125	2.361	4.133
+0.48	-2.42483	+0.358050	+2.60174	1.113	2.368	4.251
+0.49	-2.43590	+0.352557	+2.57804	1.101	2.374	4.385
+0.50	-2.44684	+0.347228	+2.55428	1.088	2.378	4.537
+0.51	-2.45767	+0.342079	+2.53048	1.076	2.381	4.710
+0.52	-2.46837	+0.337123	+2.50666	1.064	2.383	4.907
+0.53	-2.47895	+0.332372	+2.48283	1.052	2.383	5.132

8.4

(1)	(4)	(5)	(6)	(7)	(8)	(9)
+0.00	-1.67597	+0.660274	+3.57088	2.493	1.506	2.500
+0.01	-1.70044	+0.654245	+3.55568	2.403	1.534	2.542
+0.02	-1.72406	+0.648202	+3.54019	2.322	1.562	2.582
+0.03	-1.74691	+0.642143	+3.52443	2.249	1.590	2.620
+0.04	-1.76905	+0.636066	+3.50840	2.182	1.616	2.656
+0.05	-1.79056	+0.629972	+3.49211	2.120	1.642	2.690
+0.06	-1.81146	+0.623858	+3.47556	2.063	1.667	2.722
+0.07	-1.83183	+0.617724	+3.45877	2.010	1.691	2.752
+0.08	-1.85169	+0.611569	+3.44174	1.962	1.715	2.782
+0.09	-1.87108	+0.605392	+3.42447	1.916	1.738	2.809
+0.10	-1.89002	+0.599194	+3.40698	1.874	1.761	2.836
+0.11	-1.90856	+0.592972	+3.38925	1.834	1.784	2.861
+0.12	-1.92672	+0.586727	+3.37131	1.797	1.806	2.886
+0.13	-1.94451	+0.580458	+3.35314	1.762	1.827	2.909
+0.14	-1.96196	+0.574166	+3.33476	1.728	1.848	2.932
+0.15	-1.97908	+0.567848	+3.31617	1.697	1.869	2.953
+0.16	-1.99590	+0.561506	+3.29738	1.667	1.890	2.974
+0.17	-2.01243	+0.555138	+3.27838	1.639	1.910	2.994
+0.18	-2.02869	+0.548744	+3.25918	1.612	1.930	3.013
+0.19	-2.04468	+0.542325	+3.23977	1.586	1.950	3.031
+0.20	-2.06042	+0.535878	+3.22018	1.562	1.969	3.049
+0.21	-2.07592	+0.529404	+3.20039	1.538	1.989	3.065
+0.22	-2.09119	+0.522903	+3.18041	1.516	2.008	3.081
+0.23	-2.10624	+0.516373	+3.16024	1.494	2.026	3.097
+0.24	-2.12108	+0.509814	+3.13988	1.474	2.045	3.111
+0.25	-2.13572	+0.503225	+3.11933	1.454	2.064	3.125
+0.26	-2.15016	+0.496605	+3.09861	1.435	2.082	3.138
+0.27	-2.16442	+0.489954	+3.07770	1.416	2.100	3.150
+0.28	-2.17849	+0.483270	+3.05660	1.398	2.118	3.161
+0.29	-2.19239	+0.476553	+3.03533	1.381	2.136	3.172
+0.30	-2.20611	+0.469799	+3.01388	1.364	2.154	3.181
+0.31	-2.21967	+0.463009	+2.99225	1.348	2.172	3.189
+0.32	-2.23308	+0.456179	+2.97044	1.332	2.190	3.196
+0.33	-2.24633	+0.449308	+2.94846	1.317	2.207	3.202
+0.34	-2.25942	+0.442393	+2.92630	1.302	2.225	3.207
+0.35	-2.27238	+0.435431	+2.90396	1.288	2.243	3.210
+0.36	-2.28519	+0.428418	+2.88145	1.274	2.260	3.211
+0.37	-2.29786	+0.421350	+2.85875	1.261	2.278	3.210
+0.38	-2.31040	+0.414222	+2.83588	1.248	2.296	3.207
+0.39	-2.32281	+0.407028	+2.81283	1.235	2.314	3.201
+0.40	-2.33510	+0.399761	+2.78960	1.222	2.332	3.192
+0.41	-2.34726	+0.392413	+2.76619	1.210	2.351	3.180
+0.42	-2.35931	+0.384974	+2.74258	1.198	2.370	3.165
+0.43	-2.37124	+0.377433	+2.71879	1.187	2.389	3.144
+0.44	-2.38305	+0.369774	+2.69481	1.176	2.408	3.119
+0.45	-2.39476	+0.361980	+2.67062	1.166	2.429	3.087
+0.46	-2.40636	+0.354031	+2.64623	1.155	2.450	3.049
+0.47	-2.41786	+0.345899	+2.62162	1.145	2.472	3.002
+0.48	-2.42926	+0.337551	+2.59678	1.136	2.495	2.946
+0.49	-2.44058	+0.328945	+2.57171	1.127	2.520	2.879
+0.50	-2.45180	+0.320027	+2.54638	1.118	2.546	2.799
+0.51	-2.46295	+0.310725	+2.52078	1.111	2.575	2.704
+0.52	-2.47402	+0.300943	+2.49488	1.104	2.607	2.591

8.5

(1)	(4)	(5)	(6)	(7)	(8)	(9)
+0.000	-1.009857	+0.4452483	+2.258855	2.511	1.448	2.500
+0.005	-1.022312	+0.4423480	+2.251572	2.472	1.466	2.522
+0.010	-1.034576	+0.4394375	+2.244199	2.434	1.484	2.544
+0.015	-1.046657	+0.4365167	+2.236736	2.398	1.501	2.566
+0.020	-1.058562	+0.4335855	+2.229186	2.364	1.519	2.586
+0.025	-1.070297	+0.4306437	+2.221547	2.331	1.536	2.607
+0.030	-1.081871	+0.4276912	+2.213821	2.299	1.554	2.627
+0.035	-1.093288	+0.4247280	+2.206008	2.268	1.571	2.646
+0.040	-1.104554	+0.4217539	+2.198109	2.239	1.588	2.666
+0.045	-1.115676	+0.4187688	+2.190124	2.210	1.606	2.684
+0.050	-1.126657	+0.4157726	+2.182053	2.183	1.623	2.703
+0.055	-1.137503	+0.4127652	+2.173898	2.156	1.640	2.721
+0.060	-1.148218	+0.4097466	+2.165658	2.130	1.656	2.739
+0.065	-1.158806	+0.4067167	+2.157333	2.105	1.673	2.756
+0.070	-1.169271	+0.4036754	+2.148925	2.081	1.690	2.773
+0.075	-1.179617	+0.4006226	+2.140433	2.058	1.707	2.790
+0.080	-1.189847	+0.3975582	+2.131859	2.035	1.723	2.806
+0.085	-1.199965	+0.3944822	+2.123201	2.013	1.740	2.823
+0.090	-1.209974	+0.3913945	+2.114461	1.991	1.756	2.839
+0.095	-1.219878	+0.3882951	+2.105638	1.970	1.773	2.854
+0.10	-1.229678	+0.3851838	+2.096734	1.950	1.789	2.870
+0.11	-1.248978	+0.3789257	+2.078680	1.911	1.822	2.900
+0.12	-1.267897	+0.3726197	+2.060302	1.873	1.854	2.929
+0.13	-1.286454	+0.3662653	+2.041600	1.838	1.886	2.957
+0.14	-1.304660	+0.3598624	+2.022577	1.804	1.918	2.985
+0.15	-1.322534	+0.3534103	+2.003233	1.771	1.950	3.011
+0.16	-1.340089	+0.3469089	+1.983570	1.740	1.982	3.037
+0.17	-1.357337	+0.3403578	+1.963590	1.710	2.014	3.063
+0.18	-1.374290	+0.3337568	+1.943292	1.681	2.046	3.087
+0.19	-1.390958	+0.3271054	+1.922678	1.653	2.077	3.111
+0.20	-1.407350	+0.3204034	+1.901749	1.626	2.109	3.134
+0.21	-1.423476	+0.3136506	+1.880505	1.600	2.140	3.157
+0.22	-1.439343	+0.3068467	+1.858947	1.574	2.172	3.180
+0.23	-1.454959	+0.2999914	+1.837075	1.549	2.203	3.201
+0.24	-1.470332	+0.2930845	+1.814890	1.525	2.234	3.223
+0.25	-1.485466	+0.2861258	+1.792392	1.502	2.265	3.243
+0.26	-1.500370	+0.2791151	+1.769581	1.479	2.297	3.264
+0.27	-1.515047	+0.2720521	+1.746458	1.457	2.328	3.284
+0.28	-1.529503	+0.2649367	+1.723022	1.435	2.359	3.303
+0.29	-1.543744	+0.2577686	+1.699274	1.413	2.390	3.323
+0.30	-1.557773	+0.2505476	+1.675214	1.392	2.422	3.341
+0.31	-1.571594	+0.2432737	+1.650840	1.372	2.453	3.360
+0.32	-1.585213	+0.2359466	+1.626155	1.352	2.484	3.378
+0.33	-1.598632	+0.2285662	+1.601157	1.332	2.515	3.396
+0.34	-1.611854	+0.2211324	+1.575846	1.313	2.547	3.414
+0.35	-1.624884	+0.2136450	+1.550223	1.293	2.578	3.431
+0.36	-1.637724	+0.2061041	+1.524286	1.275	2.609	3.448
+0.37	-1.650377	+0.1985095	+1.498036	1.256	2.641	3.465
+0.38	-1.662845	+0.1908613	+1.471472	1.238	2.672	3.481
+0.39	-1.675132	+0.1831594	+1.444594	1.220	2.703	3.498
+0.40	-1.687240	+0.1754040	+1.417403	1.202	2.735	3.514
+0.41	-1.699171	+0.1675950	+1.389896	1.184	2.766	3.530
+0.42	-1.710927	+0.1597329	+1.362076	1.167	2.798	3.547
+0.43	-1.722510	+0.1518177	+1.333940	1.150	2.829	3.563
+0.44	-1.733922	+0.1438499	+1.305488	1.133	2.861	3.579
+0.45	-1.745166	+0.1358299	+1.276721	1.116	2.892	3.595
+0.46	-1.756243	+0.1277584	+1.247638	1.099	2.924	3.611
+0.47	-1.767154	+0.1196362	+1.218240	1.083	2.956	3.628
+0.48	-1.777901	+0.1114641	+1.188525	1.067	2.987	3.645
+0.49	-1.788486	+0.1032435	+1.158494	1.050	3.019	3.662
+0.50	-1.798911	+0.0949758	+1.128147	1.034	3.050	3.679
+0.51	-1.809175	+0.0866628	+1.097484	1.019	3.082	3.698
+0.52	-1.819282	+0.0783068	+1.066506	1.003	3.114	3.717
+0.53	-1.829231	+0.0699105	+1.035212	0.987	3.145	3.737
+0.54	-1.839025	+0.0614772	+1.003605	0.972	3.176	3.759
+0.55	-1.84866	+0.053011	+0.97168	0.956	3.208	3.782
+0.56	-1.85815	+0.044516	+0.93945	0.941	3.239	3.807
+0.57	-1.86748	+0.036000	+0.90691	0.926	3.270	3.835
+0.58	-1.87666	+0.027467	+0.87406	0.910	3.300	3.866
+0.59	-1.88569	+0.018928	+0.84091	0.895	3.330	3.900
+0.60	-1.89457	+0.010392	+0.80746	0.880	3.360	3.939
+0.61	-1.90330	+0.001869	+0.77371	0.865	3.389	3.983
+0.62	-1.91188	-0.006624	+0.73968	0.850	3.418	4.033
+0.63	-1.92031	-0.015073	+0.70536	0.836	3.446	4.092
+0.64	-1.92859	-0.023459	+0.67077	0.821	3.472	4.160

8.5 (CONT.)

(1)	(4)	(5)	(6)	(7)	(8)	(9)
+0.65	-1.93673	-0.031760	+0.63592	0.806	3.498	4.240
+0.66	-1.94471	-0.039950	+0.60082	0.791	3.522	4.334
+0.67	-1.95255	-0.048003	+0.56548	0.776	3.544	4.445
+0.68	-1.96023	-0.055887	+0.52994	0.761	3.565	4.577
+0.69	-1.96777	-0.063569	+0.49420	0.746	3.583	4.733
+0.70	-1.97516	-0.071014	+0.45829	0.731	3.598	4.920
+0.71	-1.98240	-0.078184	+0.42224	0.716	3.611	5.143
+0.72	-1.98949	-0.085043	+0.38608	0.701	3.620	5.410
+0.73	-1.99642	-0.091556	+0.34985	0.686	3.626	5.729
+0.74	-2.00321	-0.097691	+0.31358	0.671	3.628	6.109
+0.75	-2.00984	-0.103421	+0.27730	0.656	3.625	6.567

8.6

(1)	(4)	(5)	(6)	(7)	(8)	(9)
+0.000	-1.009866	+0.4452506	+2.258870	2.511	1.448	2.500
+0.005	-1.022322	+0.4423502	+2.251587	2.472	1.466	2.522
+0.010	-1.034581	+0.4394397	+2.244214	2.434	1.484	2.544
+0.015	-1.046661	+0.4365189	+2.236751	2.398	1.501	2.565
+0.020	-1.058566	+0.4335876	+2.229200	2.364	1.519	2.586
+0.025	-1.070302	+0.4306458	+2.221561	2.331	1.536	2.607
+0.030	-1.081876	+0.4276933	+2.213835	2.299	1.554	2.627
+0.035	-1.093293	+0.4247300	+2.206022	2.268	1.571	2.646
+0.040	-1.104560	+0.4217558	+2.198123	2.239	1.588	2.666
+0.045	-1.115681	+0.4187706	+2.190138	2.210	1.606	2.684
+0.050	-1.126662	+0.4157744	+2.182067	2.183	1.623	2.703
+0.055	-1.137508	+0.4127670	+2.173912	2.156	1.640	2.721
+0.060	-1.148223	+0.4097483	+2.165671	2.130	1.656	2.739
+0.065	-1.158811	+0.4067183	+2.157347	2.105	1.673	2.756
+0.070	-1.169276	+0.4036769	+2.148939	2.081	1.690	2.773
+0.075	-1.179623	+0.4006240	+2.140447	2.058	1.707	2.790
+0.080	-1.189853	+0.3975596	+2.131872	2.035	1.723	2.806
+0.085	-1.199971	+0.3944835	+2.123215	2.013	1.740	2.823
+0.090	-1.209981	+0.3913957	+2.114474	1.991	1.756	2.839
+0.095	-1.219884	+0.3882962	+2.105652	1.970	1.773	2.854
+0.10	-1.229684	+0.3851849	+2.096748	1.950	1.789	2.870
+0.11	-1.248985	+0.3789265	+2.078694	1.911	1.822	2.900
+0.12	-1.267904	+0.3726203	+2.060315	1.873	1.854	2.929
+0.13	-1.286459	+0.3662657	+2.041614	1.838	1.886	2.957
+0.14	-1.304666	+0.3598624	+2.022590	1.804	1.918	2.985
+0.15	-1.322540	+0.3534099	+2.003246	1.771	1.950	3.011
+0.16	-1.340095	+0.3469081	+1.983583	1.740	1.982	3.037
+0.17	-1.357344	+0.3403565	+1.963602	1.710	2.014	3.062
+0.18	-1.374296	+0.3337549	+1.943305	1.681	2.046	3.087
+0.19	-1.390964	+0.3271028	+1.922691	1.653	2.077	3.111
+0.20	-1.407357	+0.3204001	+1.901761	1.626	2.109	3.134
+0.21	-1.423483	+0.3136465	+1.880517	1.600	2.140	3.157
+0.22	-1.439350	+0.3068416	+1.858958	1.574	2.172	3.179
+0.23	-1.454967	+0.2999852	+1.837086	1.549	2.203	3.201
+0.24	-1.470339	+0.2930770	+1.814901	1.525	2.234	3.222
+0.25	-1.485474	+0.2861168	+1.792402	1.502	2.266	3.243
+0.26	-1.500378	+0.2791043	+1.769590	1.479	2.297	3.263
+0.27	-1.515056	+0.2720392	+1.746466	1.457	2.328	3.283
+0.28	-1.529512	+0.2649214	+1.723029	1.435	2.359	3.302
+0.29	-1.543754	+0.2577506	+1.699280	1.413	2.391	3.321
+0.30	-1.557783	+0.2505265	+1.675218	1.392	2.422	3.340
+0.31	-1.571605	+0.2432489	+1.650843	1.372	2.453	3.358
+0.32	-1.585224	+0.2359176	+1.626156	1.352	2.484	3.376
+0.33	-1.598643	+0.2285322	+1.601156	1.332	2.516	3.394
+0.34	-1.611866	+0.2210926	+1.575842	1.313	2.547	3.411
+0.35	-1.624896	+0.2135985	+1.550216	1.293	2.578	3.428
+0.36	-1.637737	+0.2060497	+1.524276	1.275	2.610	3.445
+0.37	-1.650390	+0.1984459	+1.498021	1.256	2.641	3.461
+0.38	-1.662860	+0.1907868	+1.471453	1.238	2.673	3.477
+0.39	-1.675148	+0.1830723	+1.444570	1.220	2.704	3.493
+0.40	-1.687257	+0.1753019	+1.417372	1.202	2.736	3.508
+0.41	-1.699189	+0.1674755	+1.389858	1.184	2.767	3.523
+0.42	-1.710946	+0.1595928	+1.362028	1.167	2.799	3.538
+0.43	-1.722532	+0.1516534	+1.333881	1.150	2.831	3.552
+0.44	-1.733946	+0.1436571	+1.305417	1.133	2.862	3.567
+0.45	-1.745193	+0.1356035	+1.276635	1.116	2.894	3.581
+0.46	-1.756272	+0.1274923	+1.247535	1.100	2.926	3.595
+0.47	-1.767187	+0.1193231	+1.218116	1.083	2.958	3.608
+0.48	-1.777938	+0.1110955	+1.188376	1.067	2.990	3.621
+0.49	-1.788527	+0.1028092	+1.158316	1.051	3.022	3.634

8.6 (CONT.)

(1)	(4)	(5)	(6)	(7)	(8)	(9)
+0.50	-1.798957	+0.0944635	+1.127934	1.035	3.054	3.647
+0.51	-1.809228	+0.0860581	+1.097230	1.019	3.087	3.659
+0.52	-1.819341	+0.0775924	+1.066202	1.004	3.119	3.671
+0.53	-1.829298	+0.0690657	+1.034850	0.988	3.151	3.683
+0.54	-1.839102	+0.0604774	+1.003172	0.973	3.184	3.694
+0.55	-1.84875	+0.051827	+0.97117	0.957	3.217	3.705
+0.56	-1.85825	+0.043113	+0.93884	0.942	3.250	3.716
+0.57	-1.86760	+0.034334	+0.90617	0.927	3.283	3.726
+0.58	-1.87680	+0.025490	+0.87318	0.912	3.316	3.735
+0.59	-1.88585	+0.016580	+0.83986	0.898	3.349	3.744
+0.60	-1.89475	+0.007600	+0.80620	0.883	3.383	3.753
+0.61	-1.90350	-0.001450	+0.77220	0.868	3.416	3.760
+0.62	-1.91212	-0.010572	+0.73787	0.854	3.450	3.767
+0.63	-1.92059	-0.019769	+0.70320	0.840	3.484	3.772
+0.64	-1.92891	-0.029046	+0.66818	0.826	3.519	3.777
+0.65	-1.93710	-0.038404	+0.63282	0.812	3.554	3.780
+0.66	-1.94514	-0.047850	+0.59711	0.798	3.589	3.781
+0.67	-1.95305	-0.057389	+0.56104	0.784	3.624	3.780
+0.68	-1.96082	-0.067027	+0.52462	0.770	3.660	3.777
+0.69	-1.96845	-0.076774	+0.48784	0.756	3.697	3.771
+0.70	-1.97595	-0.086641	+0.45068	0.743	3.734	3.761
+0.71	-1.98331	-0.096639	+0.41315	0.730	3.772	3.746
+0.72	-1.99054	-0.106788	+0.37523	0.717	3.812	3.726
+0.73	-1.99764	-0.117107	+0.33691	0.704	3.852	3.700
+0.74	-2.00461	-0.127623	+0.29818	0.691	3.894	3.664
+0.75	-2.01146	-0.138373	+0.25902	0.678	3.938	3.619

8.7

(1)	(4)	(5)	(6)	(7)	(8)	(9)
+0.85	-1.98318	-0.283406	-0.40466	0.492	4.602	4.071
+0.84	-1.97820	-0.272137	-0.35886	0.505	4.556	4.058
+0.83	-1.97308	-0.260948	-0.31353	0.518	4.511	4.046
+0.82	-1.96783	-0.249839	-0.26865	0.532	4.466	4.035
+0.81	-1.96245	-0.238812	-0.22421	0.545	4.421	4.024
+0.80	-1.95693	-0.227867	-0.18022	0.559	4.377	4.014
+0.79	-1.95128	-0.217005	-0.13667	0.572	4.333	4.004
+0.78	-1.94548	-0.206225	-0.09356	0.586	4.290	3.995
+0.77	-1.93956	-0.195528	-0.05088	0.600	4.247	3.985
+0.76	-1.93349	-0.184912	-0.00862	0.614	4.204	3.976
+0.75	-1.92728	-0.174378	+0.03321	0.628	4.162	3.966
+0.74	-1.92093	-0.163924	+0.07461	0.642	4.120	3.957
+0.73	-1.91443	-0.153552	+0.11560	0.656	4.078	3.947
+0.72	-1.90780	-0.143259	+0.15618	0.671	4.037	3.938
+0.71	-1.90101	-0.133045	+0.19635	0.686	3.996	3.928
+0.70	-1.89408	-0.122909	+0.23611	0.700	3.956	3.918
+0.69	-1.88701	-0.112851	+0.27547	0.715	3.916	3.908
+0.68	-1.87979	-0.102870	+0.31442	0.730	3.876	3.898
+0.67	-1.87241	-0.092966	+0.35298	0.745	3.836	3.888
+0.66	-1.86489	-0.083137	+0.39114	0.760	3.796	3.877
+0.65	-1.85722	-0.073383	+0.42891	0.775	3.757	3.867
+0.64	-1.84939	-0.063704	+0.46628	0.790	3.718	3.856
+0.63	-1.84141	-0.054099	+0.50327	0.806	3.679	3.845
+0.62	-1.83327	-0.044568	+0.53987	0.821	3.641	3.834
+0.61	-1.82498	-0.035109	+0.57609	0.837	3.602	3.823
+0.60	-1.81653	-0.025722	+0.61192	0.853	3.564	3.812
+0.59	-1.80792	-0.016407	+0.64737	0.869	3.526	3.800
+0.58	-1.79916	-0.007164	+0.68245	0.885	3.488	3.789
+0.57	-1.79023	+0.002009	+0.71714	0.901	3.451	3.777
+0.56	-1.78114	+0.011112	+0.75147	0.917	3.414	3.765
+0.55	-1.77189	+0.020145	+0.78542	0.933	3.376	3.752
+0.54	-1.76247	+0.029108	+0.81899	0.950	3.339	3.740
+0.53	-1.75289	+0.038003	+0.85220	0.966	3.302	3.727
+0.52	-1.74314	+0.046829	+0.88504	0.983	3.265	3.714
+0.51	-1.73322	+0.055587	+0.91750	1.000	3.229	3.701
+0.50	-1.72314	+0.064277	+0.94961	1.017	3.192	3.687
+0.49	-1.71288	+0.072900	+0.98135	1.034	3.156	3.674
+0.48	-1.70245	+0.081457	+1.01272	1.052	3.119	3.660
+0.47	-1.69184	+0.089947	+1.04373	1.069	3.083	3.646
+0.46	-1.68106	+0.098370	+1.07438	1.087	3.047	3.631
+0.45	-1.67010	+0.106728	+1.10468	1.105	3.011	3.617
+0.44	-1.65897	+0.115021	+1.13461	1.123	2.975	3.602
+0.43	-1.64765	+0.123249	+1.16418	1.141	2.940	3.587
+0.42	-1.63615	+0.131412	+1.19340	1.159	2.904	3.572
+0.41	-1.62447	+0.139511	+1.22226	1.178	2.868	3.556
+0.40	-1.61260	+0.147545	+1.25077	1.196	2.833	3.540
+0.39	-1.60054	+0.155516	+1.27893	1.215	2.798	3.524
+0.38	-1.58830	+0.163424	+1.30673	1.234	2.763	3.508
+0.37	-1.57586	+0.171269	+1.33418	1.254	2.728	3.491
+0.36	-1.56322	+0.179051	+1.36128	1.274	2.692	3.474

8.7 CONT.)

(1)	(4)	(5)	(6)	(7)	(8)	(9)
+0.35	-1.55038	+0.186771	+1.38803	1.293	2.658	3.456
+0.34	-1.53735	+0.194428	+1.41443	1.314	2.623	3.439
+0.33	-1.52411	+0.202024	+1.44048	1.334	2.588	3.421
+0.32	-1.51067	+0.209559	+1.46619	1.355	2.553	3.402
+0.31	-1.49701	+0.217033	+1.49154	1.376	2.518	3.384
+0.30	-1.48314	+0.224446	+1.51656	1.398	2.484	3.364
+0.29	-1.46906	+0.231798	+1.54122	1.420	2.449	3.345
+0.28	-1.45475	+0.239090	+1.56554	1.442	2.415	3.325
+0.27	-1.44022	+0.246323	+1.58952	1.464	2.380	3.305
+0.26	-1.42546	+0.253496	+1.61314	1.488	2.346	3.284
+0.25	-1.41046	+0.260610	+1.63643	1.511	2.311	3.263
+0.24	-1.39523	+0.267665	+1.65937	1.536	2.277	3.241
+0.23	-1.37975	+0.274661	+1.68197	1.560	2.243	3.219
+0.22	-1.36402	+0.281600	+1.70423	1.586	2.208	3.196
+0.21	-1.34803	+0.288480	+1.72614	1.612	2.174	3.173
+0.20	-1.33178	+0.295303	+1.74772	1.639	2.140	3.150
+0.19	-1.31525	+0.302069	+1.76894	1.667	2.106	3.125
+0.18	-1.29844	+0.308778	+1.78983	1.695	2.071	3.100
+0.17	-1.28134	+0.315431	+1.81037	1.725	2.037	3.075
+0.16	-1.26395	+0.322028	+1.83057	1.755	2.003	3.049
+0.15	-1.24624	+0.328569	+1.85043	1.787	1.968	3.022
+0.14	-1.22821	+0.335055	+1.86994	1.820	1.934	2.994
+0.13	-1.20984	+0.341486	+1.88910	1.854	1.899	2.966
+0.12	-1.19113	+0.347862	+1.90792	1.889	1.865	2.937
+0.11	-1.17205	+0.354185	+1.92640	1.927	1.830	2.907
+0.10	-1.15259	+0.360454	+1.94453	1.966	1.795	2.876
+0.09	-1.13273	+0.366670	+1.96231	2.007	1.760	2.844
+0.08	-1.11245	+0.372834	+1.97974	2.050	1.725	2.811
+0.07	-1.09173	+0.378946	+1.99682	2.096	1.690	2.777
+0.06	-1.07053	+0.385006	+2.01354	2.144	1.655	2.742
+0.05	-1.04884	+0.391016	+2.02991	2.195	1.619	2.705
+0.04	-1.02662	+0.396976	+2.04592	2.250	1.583	2.668
+0.03	-1.00382	+0.402887	+2.06157	2.309	1.547	2.628
+0.02	-0.98042	+0.408749	+2.07686	2.372	1.510	2.587
+0.01	-0.95637	+0.414563	+2.09178	2.440	1.474	2.545
0.00	-0.93160	+0.420331	+2.10633	2.514	1.436	2.500

9.1

(1)	(4)	(5)	(6)	(7)	(8)	(9)
0.00	+1.16213	-0.400978	-2.72541	1.000	2.518	3.402
+0.01	+1.15222	-0.408353	-2.75051	0.982	2.502	3.405
+0.02	+1.14248	-0.415676	-2.77546	0.966	2.487	3.408
+0.03	+1.13289	-0.422950	-2.80025	0.952	2.471	3.409
+0.04	+1.12344	-0.430175	-2.82488	0.938	2.456	3.410
+0.05	+1.11413	-0.437351	-2.84936	0.925	2.440	3.411
+0.06	+1.10494	-0.444481	-2.87368	0.913	2.424	3.411
+0.07	+1.09586	-0.451564	-2.89784	0.903	2.408	3.410
+0.08	+1.08688	-0.458601	-2.92183	0.892	2.391	3.409
+0.09	+1.07801	-0.465593	-2.94566	0.883	2.375	3.407
+0.10	+1.06922	-0.472541	-2.96932	0.874	2.358	3.404
+0.11	+1.06052	-0.479445	-2.99282	0.866	2.341	3.401
+0.12	+1.05190	-0.486307	-3.01614	0.859	2.324	3.398
+0.13	+1.04334	-0.493127	-3.03930	0.852	2.307	3.394
+0.14	+1.03485	-0.499905	-3.06229	0.846	2.290	3.389
+0.15	+1.02642	-0.506643	-3.08511	0.840	2.273	3.384
+0.16	+1.01805	-0.513341	-3.10776	0.835	2.256	3.378
+0.17	+1.00972	-0.520000	-3.13023	0.830	2.239	3.371
+0.18	+1.00144	-0.526622	-3.15253	0.826	2.221	3.364
+0.19	+0.99320	-0.533205	-3.17466	0.822	2.204	3.357
+0.20	+0.98499	-0.539753	-3.19661	0.819	2.187	3.348
+0.21	+0.97682	-0.546266	-3.21838	0.816	2.169	3.339
+0.22	+0.96868	-0.552745	-3.23999	0.813	2.152	3.329
+0.23	+0.96056	-0.559191	-3.26141	0.811	2.134	3.319
+0.24	+0.95246	-0.565605	-3.28267	0.809	2.116	3.307
+0.25	+0.94438	-0.571989	-3.30374	0.807	2.099	3.295
+0.26	+0.93631	-0.578345	-3.32464	0.806	2.081	3.282
+0.27	+0.92826	-0.584673	-3.34537	0.805	2.064	3.268
+0.28	+0.92021	-0.590975	-3.36592	0.804	2.046	3.253
+0.29	+0.91217	-0.597255	-3.38629	0.804	2.028	3.237
+0.30	+0.90413	-0.603513	-3.40650	0.804	2.012	3.219
+0.31	+0.89608	-0.609752	-3.42652	0.804	1.994	3.201
+0.32	+0.88804	-0.615974	-3.44638	0.805	1.977	3.181
+0.33	+0.87999	-0.622183	-3.46606	0.806	1.960	3.159
+0.34	+0.87193	-0.628381	-3.48557	0.807	1.943	3.136

9.1 (CONT.)

(1)	(4)	(5)	(6)	(7)	(8)	(9)
+0.35	+0.86386	-0.634572	-3.50492	0.808	1.926	3.111
+0.36	+0.85577	-0.640760	-3.52409	0.810	1.909	3.085
+0.37	+0.84767	-0.646949	-3.54309	0.811	1.892	3.056
+0.38	+0.83954	-0.653145	-3.56193	0.813	1.876	3.025
+0.39	+0.83140	-0.659352	-3.58060	0.816	1.859	2.992
+0.40	+0.82323	-0.665577	-3.59912	0.818	1.843	2.956
+0.41	+0.81503	-0.671827	-3.61747	0.821	1.827	2.916
+0.42	+0.80680	-0.678111	-3.63566	0.824	1.812	2.874
+0.43	+0.79854	-0.684438	-3.65371	0.828	1.797	2.829
+0.44	+0.79025	-0.690817	-3.67160	0.831	1.782	2.779
+0.45	+0.78192	-0.697263	-3.68934	0.835	1.767	2.725
+0.46	+0.77354	-0.703790	-3.70694	0.839	1.753	2.667
+0.47	+0.76513	-0.710415	-3.72440	0.844	1.740	2.604
+0.48	+0.75667	-0.717158	-3.74173	0.849	1.726	2.535

9.2

(1)	(4)	(5)	(6)	(7)	(8)	(9)
0.00	+1.16222	-0.400978	-2.72560	1.000	2.518	3.404
+0.01	+1.15231	-0.408349	-2.75070	0.982	2.502	3.408
+0.02	+1.14257	-0.415667	-2.77564	0.966	2.487	3.410
+0.03	+1.13298	-0.422935	-2.80044	0.952	2.471	3.412
+0.04	+1.12353	-0.430152	-2.82507	0.938	2.456	3.414
+0.05	+1.11422	-0.437320	-2.84955	0.925	2.440	3.415
+0.06	+1.10503	-0.444440	-2.87386	0.913	2.424	3.415
+0.07	+1.09595	-0.451512	-2.89802	0.902	2.407	3.415
+0.08	+1.08698	-0.458536	-2.92201	0.892	2.391	3.415
+0.09	+1.07810	-0.465514	-2.94583	0.883	2.374	3.414
+0.10	+1.06932	-0.472445	-2.96949	0.874	2.358	3.413
+0.11	+1.06062	-0.479330	-2.99298	0.866	2.341	3.411
+0.12	+1.05199	-0.486170	-3.01630	0.859	2.324	3.408
+0.13	+1.04344	-0.492965	-3.03945	0.852	2.307	3.406
+0.14	+1.03495	-0.499715	-3.06243	0.846	2.289	3.403
+0.15	+1.02653	-0.506421	-3.08524	0.840	2.272	3.400
+0.16	+1.01815	-0.513082	-3.10787	0.835	2.255	3.396
+0.17	+1.00983	-0.519700	-3.13033	0.830	2.237	3.392
+0.18	+1.00155	-0.526274	-3.15262	0.826	2.220	3.388
+0.19	+0.99332	-0.532805	-3.17472	0.822	2.202	3.383
+0.20	+0.98512	-0.539292	-3.19666	0.818	2.184	3.378
+0.21	+0.97695	-0.545736	-3.21841	0.815	2.166	3.373
+0.22	+0.96882	-0.552138	-3.23998	0.812	2.149	3.368
+0.23	+0.96070	-0.558496	-3.26138	0.810	2.131	3.362
+0.24	+0.95261	-0.564811	-3.28259	0.808	2.113	3.357
+0.25	+0.94454	-0.571083	-3.30363	0.806	2.095	3.351
+0.26	+0.93648	-0.577313	-3.32448	0.805	2.076	3.345
+0.27	+0.92844	-0.583499	-3.34516	0.804	2.058	3.339
+0.28	+0.92040	-0.589642	-3.36565	0.803	2.040	3.333
+0.29	+0.91238	-0.595741	-3.38596	0.803	2.022	3.327
+0.30	+0.90435	-0.601796	-3.40608	0.802	2.004	3.321
+0.31	+0.89633	-0.607807	-3.42602	0.803	1.985	3.315
+0.32	+0.88830	-0.613774	-3.44578	0.803	1.967	3.309
+0.33	+0.88027	-0.619695	-3.46536	0.803	1.949	3.303
+0.34	+0.87223	-0.625570	-3.48476	0.804	1.930	3.298
+0.35	+0.86419	-0.631399	-3.50396	0.805	1.912	3.293
+0.36	+0.85613	-0.637180	-3.52299	0.806	1.893	3.288
+0.37	+0.84806	-0.642913	-3.54182	0.808	1.875	3.284
+0.38	+0.83998	-0.648597	-3.56048	0.809	1.856	3.280
+0.39	+0.83188	-0.654229	-3.57894	0.811	1.838	3.277
+0.40	+0.82376	-0.659810	-3.59723	0.813	1.819	3.275
+0.41	+0.81562	-0.665337	-3.61532	0.815	1.800	3.273
+0.42	+0.80745	-0.670809	-3.63323.	0.818	1.782	3.273
+0.43	+0.79926	-0.676224	-3.65095	0.820	1.763	3.273
+0.44	+0.79105	-0.681580	-3.66849	0.823	1.744	3.275
+0.45	+0.78281	-0.686876	-3.68584	0.825	1.725	3.278
+0.46	+0.77454	-0.692107	-3.70300	0.828	1.707	3.282
+0.47	+0.76624	-0.697273	-3.71996	0.831	1.688	3.288
+0.48	+0.75791	-0.702370	-3.73675	0.834	1.669	3.296

9.3

(1)	(4)	(5)	(6)	(7)	(8)	(9)
+1.26	-3.04684	-0.357965	-0.07640	0.310	4.182	4.111
+1.25	-3.04372	-0.347804	-0.03466	0.314	4.166	4.104
+1.24	-3.04055	-0.337668	+0.00691	0.319	4.149	4.098
+1.23	-3.03734	-0.327558	+0.04832	0.324	4.133	4.093
+1.22	-3.03408	-0.317476	+0.08957	0.328	4.116	4.088
+1.21	-3.03078	-0.307420	+0.13065	0.333	4.100	4.083

9.3 (CONT.)

(1)	(4)	(5)	(6)	(7)	(8)	(9)
+1.20	-3.02743	-0.297393	+0.17157	0.337	4.084	4.079
+1.19	-3.02403	-0.287395	+0.21233	0.342	4.068	4.075
+1.18	-3.02059	-0.277426	+0.25294	0.346	4.052	4.071
+1.17	-3.01710	-0.267485	+0.29338	0.351	4.037	4.067
+1.16	-3.01357	-0.257574	+0.33367	0.356	4.021	4.063
+1.15	-3.01000	-0.247692	+0.37381	0.360	4.006	4.060
+1.14	-3.00637	-0.237840	+0.41379	0.365	3.990	4.056
+1.13	-3.00270	-0.228016	+0.45362	0.370	3.975	4.052
+1.12	-2.99898	-0.218221	+0.49330	0.374	3.960	4.049
+1.11	-2.99522	-0.208455	+0.53282	0.379	3.945	4.046
+1.10	-2.99140	-0.198718	+0.57220	0.384	3.930	4.042
+1.09	-2.98755	-0.189009	+0.61143	0.388	3.916	4.039
+1.08	-2.98364	-0.179328	+0.65051	0.393	3.901	4.035
+1.07	-2.97969	-0.169676	+0.68944	0.398	3.886	4.032
+1.06	-2.97569	-0.160051	+0.72823	0.402	3.872	4.028
+1.05	-2.97164	-0.150454	+0.76688	0.407	3.857	4.025
+1.04	-2.96754	-0.140885	+0.80538	0.412	3.843	4.022
+1.03	-2.96340	-0.131343	+0.84374	0.417	3.829	4.018
+1.02	-2.95920	-0.121828	+0.88195	0.422	3.814	4.015
+1.01	-2.95496	-0.112340	+0.92002	0.426	3.800	4.011
+1.00	-2.95067	-0.102879	+0.95796	0.431	3.786	4.008
+0.99	-2.94634	-0.093444	+0.99575	0.436	3.772	4.004
+0.98	-2.94195	-0.084036	+1.03341	0.441	3.758	4.000
+0.97	-2.93752	-0.074655	+1.07092	0.446	3.745	3.997
+0.96	-2.93303	-0.065299	+1.10830	0.451	3.731	3.993
+0.95	-2.92850	-0.055969	+1.14554	0.456	3.717	3.990
+0.94	-2.92391	-0.046665	+1.18264	0.461	3.704	3.986
+0.93	-2.91928	-0.037387	+1.21961	0.466	3.690	3.982
+0.92	-2.91460	-0.028134	+1.25644	0.471	3.676	3.979
+0.91	-2.90987	-0.018907	+1.29314	0.476	3.663	3.975
+0.90	-2.90509	-0.009705	+1.32970	0.481	3.650	3.971
+0.89	-2.90026	-0.000528	+1.36613	0.486	3.636	3.968
+0.88	-2.89538	+0.008625	+1.40243	0.491	3.623	3.964
+0.87	-2.89044	+0.017752	+1.43860	0.496	3.610	3.960
+0.86	-2.88546	+0.026855	+1.47463	0.501	3.596	3.956
+0.85	-2.88043	+0.035933	+1.51052	0.506	3.583	3.952
+0.84	-2.87535	+0.044986	+1.54629	0.511	3.570	3.949
+0.83	-2.87022	+0.054016	+1.58193	0.516	3.557	3.945
+0.82	-2.86503	+0.063021	+1.61744	0.521	3.544	3.940
+0.81	-2.85979	+0.072002	+1.65281	0.526	3.531	3.937
+0.80	-2.85451	+0.080959	+1.68806	0.531	3.518	3.933
+0.79	-2.84917	+0.089892	+1.72317	0.536	3.505	3.929
+0.78	-2.84378	+0.098801	+1.75816	0.542	3.492	3.925
+0.77	-2.83834	+0.107686	+1.79301	0.547	3.479	3.921
+0.76	-2.83284	+0.116547	+1.82774	0.552	3.466	3.917
+0.75	-2.82730	+0.125386	+1.86234	0.557	3.454	3.913
+0.74	-2.82170	+0.134200	+1.89681	0.562	3.441	3.908
+0.73	-2.81605	+0.142991	+1.93116	0.568	3.428	3.904
+0.72	-2.81034	+0.151759	+1.96537	0.573	3.415	3.900
+0.71	-2.80459	+0.160503	+1.99946	0.578	3.402	3.896
+0.70	-2.79878	+0.169224	+2.03342	0.584	3.390	3.892
+0.69	-2.79292	+0.177922	+2.06725	0.589	3.377	3.888
+0.68	-2.78700	+0.186597	+2.10096	0.594	3.364	3.883
+0.67	-2.78104	+0.195249	+2.13454	0.599	3.352	3.880
+0.66	-2.77502	+0.203878	+2.16800	0.605	3.339	3.875
+0.65	-2.76894	+0.212485	+2.20132	0.610	3.326	3.870
+0.64	-2.76281	+0.221068	+2.23452	0.616	3.314	3.866
+0.63	-2.75663	+0.229628	+2.26760	0.621	3.301	3.862
+0.62	-2.75040	+0.238166	+2.30055	0.626	3.289	3.857
+0.61	-2.74410	+0.246681	+2.33338	0.632	3.276	3.853
+0.60	-2.73776	+0.255174	+2.36608	0.637	3.264	3.848
+0.59	-2.73136	+0.263644	+2.39865	0.643	3.251	3.843
+0.58	-2.72491	+0.272091	+2.43110	0.648	3.239	3.839
+0.57	-2.71840	+0.280516	+2.46342	0.654	3.226	3.834
+0.56	-2.71184	+0.288918	+2.49562	0.659	3.214	3.830
+0.55	-2.70522	+0.297298	+2.52770	0.665	3.201	3.825
+0.54	-2.69854	+0.305656	+2.55964	0.670	3.189	3.820
+0.53	-2.69182	+0.313991	+2.59147	0.676	3.176	3.816
+0.52	-2.68503	+0.322304	+2.62317	0.681	3.164	3.811
+0.51	-2.67819	+0.330595	+2.65475	0.687	3.151	3.806
+0.50	-2.67129	+0.338864	+2.68620	0.692	3.139	3.801
+0.49	-2.66434	+0.347110	+2.71753	0.698	3.126	3.796
+0.48	-2.65733	+0.355335	+2.74873	0.704	3.114	3.792
+0.47	-2.65026	+0.363537	+2.77981	0.709	3.102	3.787
+0.46	-2.64314	+0.371717	+2.81076	0.715	3.089	3.782
+0.45	-2.63596	+0.379875	+2.84159	0.721	3.077	3.777
+0.44	-2.62873	+0.388011	+2.87230	0.726	3.064	3.772
+0.43	-2.62144	+0.396125	+2.90288	0.732	3.052	3.767
+0.42	-2.61409	+0.404217	+2.93334	0.738	3.040	3.761
+0.41	-2.60668	+0.412287	+2.96368	0.744	3.027	3.756

9.3 (CONT.)

(1)	(4)	(5)	(6)	(7)	(8)	(9)
+0.40	-2.59921	+0.420335	+2.99389	0.749	3.015	3.751
+0.39	-2.59169	+0.428361	+3.02398	0.755	3.002	3.746
+0.38	-2.58411	+0.436366	+3.05394	0.761	2.990	3.741
+0.37	-2.57647	+0.444348	+3.08378	0.767	2.978	3.735
+0.36	-2.56877	+0.452309	+3.11349	0.773	2.965	3.730
+0.35	-2.56101	+0.460248	+3.14308	0.779	2.953	3.725
+0.34	-2.55320	+0.468165	+3.17255	0.784	2.941	3.719
+0.33	-2.54532	+0.476060	+3.20190	0.790	2.928	3.714
+0.32	-2.53739	+0.483933	+3.23112	0.796	2.916	3.708
+0.31	-2.52940	+0.491785	+3.26021	0.802	2.904	3.703
+0.30	-2.52135	+0.499615	+3.28919	0.808	2.891	3.697
+0.29	-2.51323	+0.507423	+3.31804	0.814	2.879	3.692
+0.28	-2.50506	+0.515210	+3.34676	0.820	2.866	3.686
+0.27	-2.49683	+0.522974	+3.37536	0.826	2.854	3.681
+0.26	-2.48854	+0.530718	+3.40384	0.832	2.842	3.675
+0.25	-2.48018	+0.538439	+3.43219	0.838	2.829	3.669
+0.24	-2.47177	+0.546139	+3.46042	0.845	2.817	3.663
+0.23	-2.46329	+0.553817	+3.48852	0.851	2.804	3.657
+0.22	-2.45475	+0.561474	+3.51650	0.857	2.792	3.652
+0.21	-2.44615	+0.569109	+3.54436	0.863	2.780	3.646
+0.20	-2.43749	+0.576722	+3.57209	0.869	2.767	3.640
+0.19	-2.42877	+0.584314	+3.59970	0.876	2.755	3.634
+0.18	-2.41998	+0.591884	+3.62719	0.882	2.742	3.628
+0.17	-2.41114	+0.599432	+3.65455	0.888	2.730	3.621
+0.16	-2.40222	+0.606960	+3.68178	0.894	2.717	3.615
+0.15	-2.39325	+0.614465	+3.70890	0.901	2.705	3.609
+0.14	-2.38421	+0.621949	+3.73588	0.907	2.692	3.603
+0.13	-2.37511	+0.629412	+3.76275	0.913	2.680	3.597
+0.12	-2.36594	+0.636853	+3.78949	0.920	2.668	3.590
+0.11	-2.35671	+0.644272	+3.81610	0.926	2.655	3.584
+0.10	-2.34742	+0.651671	+3.84259	0.933	2.643	3.577
+0.09	-2.33806	+0.659047	+3.86895	0.939	2.630	3.571
+0.08	-2.32863	+0.666402	+3.89519	0.946	2.618	3.564
+0.07	-2.31914	+0.673736	+3.92131	0.952	2.605	3.558
+0.06	-2.30958	+0.681048	+3.94730	0.959	2.593	3.551
+0.05	-2.29996	+0.688339	+3.97316	0.966	2.580	3.544
+0.04	-2.29027	+0.695608	+3.99890	0.972	2.568	3.537
+0.03	-2.28051	+0.702856	+4.02451	0.979	2.555	3.530
+0.02	-2.27068	+0.710082	+4.05000	0.986	2.542	3.524
+0.01	-2.26079	+0.717287	+4.07536	0.993	2.530	3.517
0.00	-2.25082	+0.724471	+4.10060	1.000	2.517	3.510

9.4

(1)	(4)	(5)	(6)	(7)	(8)	(9)
+1.38	-2.93946	-0.548933	-0.95683	0.225	4.657	4.162
+1.37	-2.93719	-0.537767	-0.91039	0.229	4.632	4.156
+1.36	-2.93487	-0.526647	-0.86420	0.234	4.607	4.151
+1.35	-2.93251	-0.515572	-0.81825	0.239	4.583	4.147
+1.34	-2.93010	-0.504544	-0.77254	0.243	4.559	4.143
+1.33	-2.92764	-0.493561	-0.72706	0.248	4.536	4.139
+1.32	-2.92514	-0.482624	-0.68182	0.253	4.513	4.135
+1.31	-2.92259	-0.471733	-0.63681	0.257	4.490	4.131
+1.30	-2.92000	-0.460887	-0.59202	0.262	4.468	4.128
+1.29	-2.91735	-0.450086	-0.54745	0.267	4.446	4.125
+1.28	-2.91466	-0.439330	-0.50310	0.271	4.424	4.121
+1.27	-2.91193	-0.428617	-0.45897	0.276	4.402	4.118
+1.26	-2.90915	-0.417947	-0.41505	0.281	4.381	4.115
+1.25	-2.90632	-0.407320	-0.37134	0.286	4.361	4.112
+1.24	-2.90344	-0.396736	-0.32784	0.290	4.340	4.108
+1.23	-2.90051	-0.386192	-0.28454	0.295	4.320	4.105
+1.22	-2.89753	-0.375690	-0.24144	0.300	4.300	4.102
+1.21	-2.89451	-0.365228	-0.19855	0.305	4.280	4.099
+1.20	-2.89144	-0.354806	-0.15584	0.310	4.260	4.096
+1.19	-2.88832	-0.344424	-0.11334	0.314	4.241	4.092
+1.18	-2.88515	-0.334080	-0.07102	0.319	4.222	4.089
+1.17	-2.88194	-0.323774	-0.02890	0.324	4.203	4.086
+1.16	-2.87867	-0.313507	+0.01304	0.329	4.184	4.083
+1.15	-2.87536	-0.303276	+0.05479	0.334	4.166	4.079
+1.14	-2.87199	-0.293083	+0.09636	0.339	4.148	4.076
+1.13	-2.86858	-0.282926	+0.13774	0.344	4.130	4.073
+1.12	-2.86511	-0.272805	+0.17895	0.349	4.112	4.070
+1.11	-2.86160	-0.262719	+0.21997	0.353	4.094	4.066
+1.10	-2.85803	-0.252669	+0.26082	0.359	4.076	4.063
+1.09	-2.85442	-0.242653	+0.30150	0.364	4.059	4.059
+1.08	-2.85075	-0.232671	+0.34200	0.369	4.042	4.056
+1.07	-2.84704	-0.222724	+0.38233	0.374	4.024	4.053
+1.06	-2.84327	-0.212810	+0.42249	0.379	4.008	4.049

9.4 (CONT.)

(1)	(4)	(5)	(6)	(7)	(8)	(9)
+1.05	-2.83946	-0.202929	+0.46248	0.384	3.991	4.046
+1.04	-2.83559	-0.193081	+0.50231	0.389	3.974	4.042
+1.03	-2.83167	-0.183266	+0.54197	0.394	3.958	4.039
+1.02	-2.82770	-0.173483	+0.58146	0.400	3.941	4.035
+1.01	-2.82368	-0.163732	+0.62079	0.405	3.925	4.031
+1.00	-2.81960	-0.154012	+0.65995	0.410	3.908	4.028
+0.99	-2.81548	-0.144324	+0.69896	0.415	3.892	4.024
+0.98	-2.81130	-0.134667	+0.73780	0.420	3.876	4.021
+0.97	-2.80707	-0.125041	+0.77649	0.426	3.860	4.017
+0.96	-2.80279	-0.115445	+0.81501	0.431	3.845	4.013
+0.95	-2.79845	-0.105880	+0.85338	0.436	3.829	4.009
+0.94	-2.79406	-0.096345	+0.89159	0.441	3.813	4.006
+0.93	-2.78962	-0.086840	+0.92965	0.447	3.798	4.002
+0.92	-2.78513	-0.077364	+0.96755	0.452	3.782	3.998
+0.91	-2.78059	-0.067918	+1.00530	0.457	3.767	3.994
+0.90	-2.77599	-0.058501	+1.04290	0.463	3.752	3.990
+0.89	-2.77134	-0.049112	+1.08034	0.468	3.737	3.986
+0.88	-2.76663	-0.039753	+1.11763	0.473	3.722	3.982
+0.87	-2.76187	-0.030422	+1.15477	0.479	3.707	3.979
+0.86	-2.75706	-0.021120	+1.19176	0.484	3.692	3.975
+0.85	-2.75219	-0.011846	+1.22861	0.489	3.677	3.971
+0.84	-2.74727	-0.002600	+1.26530	0.495	3.662	3.967
+0.83	-2.74229	+0.006618	+1.30184	0.500	3.647	3.962
+0.82	-2.73726	+0.015808	+1.33824	0.506	3.632	3.958
+0.81	-2.73218	+0.024971	+1.37449	0.511	3.618	3.954
+0.80	-2.72704	+0.034106	+1.41060	0.517	3.603	3.950
+0.79	-2.72185	+0.043214	+1.44656	0.522	3.589	3.946
+0.78	-2.71660	+0.052294	+1.48237	0.528	3.574	3.942
+0.77	-2.71129	+0.061348	+1.51804	0.533	3.560	3.938
+0.76	-2.70594	+0.070375	+1.55356	0.539	3.545	3.933
+0.75	-2.70052	+0.079375	+1.58895	0.544	3.531	3.929
+0.74	-2.69505	+0.088348	+1.62418	0.550	3.517	3.925
+0.73	-2.68952	+0.097295	+1.65928	0.555	3.502	3.920
+0.72	-2.68394	+0.106216	+1.69423	0.561	3.488	3.916
+0.71	-2.67830	+0.115110	+1.72904	0.567	3.474	3.912
+0.70	-2.67261	+0.123978	+1.76371	0.572	3.460	3.907
+0.69	-2.66686	+0.132819	+1.79824	0.578	3.446	3.903
+0.68	-2.66105	+0.141635	+1.83262	0.584	3.432	3.898
+0.67	-2.65519	+0.150425	+1.86687	0.589	3.418	3.894
+0.66	-2.64927	+0.159189	+1.90098	0.595	3.404	3.889
+0.65	-2.64330	+0.167928	+1.93494	0.600	3.390	3.885
+0.64	-2.63726	+0.176640	+1.96877	0.606	3.376	3.880
+0.63	-2.63117	+0.185328	+2.00246	0.612	3.362	3.875
+0.62	-2.62502	+0.193989	+2.03600	0.618	3.348	3.871
+0.61	-2.61882	+0.202626	+2.06941	0.623	3.334	3.866
+0.60	-2.61256	+0.211237	+2.10269	0.629	3.320	3.861
+0.59	-2.60624	+0.219823	+2.13582	0.635	3.306	3.857
+0.58	-2.59986	+0.228383	+2.16881	0.641	3.293	3.852
+0.57	-2.59342	+0.236919	+2.20167	0.646	3.279	3.847
+0.56	-2.58693	+0.245430	+2.23439	0.652	3.265	3.842
+0.55	-2.58038	+0.253916	+2.26697	0.658	3.251	3.837
+0.54	-2.57377	+0.262376	+2.29942	0.664	3.238	3.832
+0.53	-2.56710	+0.270812	+2.33173	0.670	3.224	3.827
+0.52	-2.56037	+0.279224	+2.36390	0.676	3.210	3.823
+0.51	-2.55359	+0.287610	+2.39594	0.682	3.197	3.817
+0.50	-2.54674	+0.295972	+2.42784	0.687	3.183	3.812
+0.49	-2.53984	+0.304309	+2.45960	0.693	3.170	3.807
+0.48	-2.53288	+0.312622	+2.49123	0.699	3.156	3.802
+0.47	-2.52586	+0.320911	+2.52272	0.705	3.142	3.797
+0.46	-2.51877	+0.329175	+2.55408	0.711	3.129	3.792
+0.45	-2.51163	+0.337414	+2.58530	0.717	3.115	3.787
+0.44	-2.50443	+0.345629	+2.61639	0.723	3.102	3.781
+0.43	-2.49717	+0.353820	+2.64734	0.729	3.088	3.776
+0.42	-2.48985	+0.361987	+2.67816	0.735	3.075	3.771
+0.41	-2.48247	+0.370129	+2.70884	0.741	3.062	3.765
+0.40	-2.47503	+0.378248	+2.73939	0.747	3.048	3.760
+0.39	-2.46753	+0.386342	+2.76980	0.753	3.035	3.755
+0.38	-2.45997	+0.394412	+2.80008	0.759	3.021	3.749
+0.37	-2.45235	+0.402458	+2.83022	0.765	3.008	3.744
+0.36	-2.44467	+0.410481	+2.86023	0.771	2.994	3.738
+0.35	-2.43692	+0.418479	+2.89011	0.777	2.981	3.733
+0.34	-2.42912	+0.426453	+2.91985	0.784	2.968	3.727
+0.33	-2.42125	+0.434404	+2.94946	0.790	2.954	3.721
+0.32	-2.41332	+0.442331	+2.97893	0.796	2.941	3.716
+0.31	-2.40534	+0.450234	+3.00827	0.802	2.927	3.710
+0.30	-2.39729	+0.458113	+3.03748	0.808	2.914	3.704
+0.29	-2.38918	+0.465968	+3.06656	0.814	2.901	3.698
+0.28	-2.38100	+0.473800	+3.09550	0.820	2.887	3.692
+0.27	-2.37277	+0.481608	+3.12430	0.827	2.874	3.687
+0.26	-2.36447	+0.489392	+3.15298	0.833	2.861	3.681

9.4 (CONT.)

(1)	(4)	(5)	(6)	(7)	(8)	(9)
+0.25	-2.35611	+0.497153	+3.18152	0.839	2.848	3.675
+0.24	-2.34769	+0.504890	+3.20993	0.845	2.834	3.669
+0.23	-2.33921	+0.512604	+3.23820	0.852	2.821	3.663
+0.22	-2.33066	+0.520294	+3.26634	0.858	2.808	3.657
+0.21	-2.32205	+0.527960	+3.29436	0.864	2.794	3.650
+0.20	-2.31338	+0.535604	+3.32223	0.870	2.781	3.644
+0.19	-2.30464	+0.543223	+3.34998	0.877	2.768	3.638
+0.18	-2.29585	+0.550820	+3.37759	0.883	2.755	3.632
+0.17	-2.28699	+0.558393	+3.40507	0.889	2.741	3.626
+0.16	-2.27806	+0.565942	+3.43242	0.896	2.728	3.619
+0.15	-2.26907	+0.573469	+3.45964	0.902	2.714	3.613
+0.14	-2.26002	+0.580972	+3.48672	0.908	2.702	3.606
+0.13	-2.25090	+0.588452	+3.51367	0.915	2.688	3.600
+0.12	-2.24172	+0.595908	+3.54049	0.921	2.675	3.593
+0.11	-2.23248	+0.603342	+3.56718	0.928	2.662	3.587
+0.10	-2.22317	+0.610752	+3.59373	0.934	2.649	3.580
+0.09	-2.21379	+0.618139	+3.62015	0.941	2.636	3.574
+0.08	-2.20435	+0.625503	+3.64644	0.947	2.622	3.567
+0.07	-2.19485	+0.632844	+3.67260	0.954	2.609	3.560
+0.06	-2.18528	+0.640162	+3.69863	0.960	2.596	3.553
+0.05	-2.17564	+0.647457	+3.72452	0.967	2.583	3.546
+0.04	-2.16594	+0.654729	+3.75029	0.973	2.570	3.540
+0.03	-2.15617	+0.661978	+3.77592	0.980	2.557	3.533
+0.02	-2.14634	+0.669203	+3.80142	0.987	2.544	3.526
+0.01	-2.13644	+0.676406	+3.82679	0.993	2.530	3.519
0.00	-2.12647	+0.683586	+3.85203	1.000	2.517	3.512

9.5

(1)	(4)	(5)	(6)	(7)	(8)	(9)
+0.93	-2.60176	-0.058848	+0.95920	0.804	2.690	3.745
+0.92	-2.59370	-0.051657	+0.98606	0.808	2.682	3.729
+0.91	-2.58560	-0.044460	+1.01284	0.811	2.675	3.714
+0.90	-2.57748	-0.037256	+1.03955	0.814	2.667	3.701
+0.89	-2.56932	-0.030049	+1.06618	0.817	2.659	3.689
+0.88	-2.56114	-0.022842	+1.09273	0.820	2.651	3.679
+0.87	-2.55292	-0.015637	+1.11920	0.823	2.643	3.669
+0.86	-2.54468	-0.008435	+1.14559	0.826	2.635	3.660
+0.85	-2.53640	-0.001239	+1.17190	0.829	2.627	3.652
+0.84	-2.52810	+0.005950	+1.19813	0.832	2.619	3.644
+0.83	-2.51976	+0.013132	+1.22428	0.835	2.611	3.637
+0.82	-2.51140	+0.020304	+1.25034	0.837	2.602	3.631
+0.81	-2.50302	+0.027467	+1.27633	0.840	2.594	3.625
+0.80	-2.49460	+0.034619	+1.30223	0.843	2.586	3.619
+0.79	-2.48616	+0.041760	+1.32805	0.845	2.578	3.614
+0.78	-2.47770	+0.048889	+1.35379	0.848	2.570	3.608
+0.77	-2.46920	+0.056005	+1.37946	0.850	2.562	3.603
+0.76	-2.46069	+0.063109	+1.40504	0.853	2.554	3.599
+0.75	-2.45215	+0.070199	+1.43054	0.855	2.546	3.594
+0.74	-2.44358	+0.077277	+1.45596	0.858	2.538	3.590
+0.73	-2.43500	+0.084341	+1.48130	0.860	2.530	3.585
+0.72	-2.42639	+0.091390	+1.50656	0.862	2.522	3.581
+0.71	-2.41775	+0.098427	+1.53174	0.864	2.514	3.577
+0.70	-2.40910	+0.105449	+1.55685	0.866	2.507	3.573
+0.69	-2.40043	+0.112456	+1.58188	0.868	2.499	3.570
+0.68	-2.39173	+0.119450	+1.60683	0.870	2.491	3.566
+0.67	-2.38302	+0.126429	+1.63170	0.872	2.484	3.562
+0.66	-2.37428	+0.133394	+1.65650	0.874	2.476	3.558
+0.65	-2.36553	+0.140345	+1.68122	0.876	2.468	3.555
+0.64	-2.35676	+0.147281	+1.70587	0.878	2.461	3.552
+0.63	-2.34797	+0.154203	+1.73044	0.880	2.454	3.548
+0.62	-2.33917	+0.161111	+1.75494	0.881	2.446	3.545
+0.61	-2.33035	+0.168004	+1.77936	0.883	2.439	3.542
+0.60	-2.32151	+0.174883	+1.80372	0.884	2.432	3.538
+0.59	-2.31266	+0.181747	+1.82799	0.886	2.424	3.535
+0.58	-2.30380	+0.188597	+1.85220	0.887	2.417	3.532
+0.57	-2.29493	+0.195433	+1.87634	0.888	2.410	3.529
+0.56	-2.28604	+0.202255	+1.90040	0.889	2.403	3.526
+0.55	-2.27714	+0.209063	+1.92440	0.890	2.396	3.523
+0.54	-2.26823	+0.215857	+1.94833	0.892	2.389	3.520
+0.53	-2.25931	+0.222637	+1.97218	0.892	2.382	3.518
+0.52	-2.25038	+0.229402	+1.99597	0.893	2.376	3.515
+0.51	-2.24144	+0.236154	+2.01970	0.894	2.369	3.512
+0.50	-2.23250	+0.242893	+2.04336	0.895	2.362	3.510
+0.49	-2.22355	+0.249617	+2.06695	0.895	2.356	3.507
+0.48	-2.21459	+0.256328	+2.09047	0.896	2.350	3.504
+0.47	-2.20563	+0.263026	+2.11394	0.896	2.343	3.502
+0.46	-2.19666	+0.269710	+2.13734	0.897	2.337	3.500

9.5 (CONT.)

(1)	(4)	(5)	(6)	(7)	(8)	(9)
+0.45	-2.18770	+0.276380	+2.16067	0.897	2.331	3.497
+0.44	-2.17873	+0.283038	+2.18395	0.897	2.324	3.495
+0.43	-2.16976	+0.289682	+2.20716	0.897	2.318	3.493
+0.42	-2.16078	+0.296313	+2.23032	0.897	2.312	3.491
+0.41	-2.15181	+0.302931	+2.25341	0.897	2.307	3.489
+0.40	-2.14285	+0.309536	+2.27645	0.897	2.301	3.487
+0.39	-2.13388	+0.316128	+2.29943	0.896	2.295	3.485
+0.38	-2.12492	+0.322708	+2.32235	0.896	2.290	3.483
+0.37	-2.11596	+0.329275	+2.34522	0.895	2.284	3.481
+0.36	-2.10701	+0.335830	+2.36804	0.895	2.279	3.480
+0.35	-2.09807	+0.342372	+2.39080	0.894	2.273	3.478
+0.34	-2.08913	+0.348902	+2.41350	0.893	2.268	3.477
+0.33	-2.08021	+0.355419	+2.43616	0.892	2.263	3.475
+0.32	-2.07129	+0.361925	+2.45876	0.891	2.258	3.474
+0.31	-2.06239	+0.368419	+2.48132	0.890	2.253	3.473
+0.30	-2.05350	+0.374901	+2.50382	0.888	2.248	3.472
+0.29	-2.04462	+0.381371	+2.52628	0.887	2.244	3.471
+0.28	-2.03575	+0.387830	+2.54870	0.886	2.239	3.470
+0.27	-2.02691	+0.394278	+2.57106	0.884	2.234	3.469
+0.26	-2.01808	+0.400714	+2.59339	0.882	2.230	3.468
+0.25	-2.00926	+0.407139	+2.61566	0.880	2.226	3.467
+0.24	-2.00047	+0.413553	+2.63790	0.878	2.222	3.467
+0.23	-1.99170	+0.419956	+2.66010	0.876	2.218	3.466
+0.22	-1.98294	+0.426348	+2.68226	0.874	2.214	3.466
+0.21	-1.97422	+0.432730	+2.70437	0.872	2.210	3.466
+0.20	-1.96551	+0.439101	+2.72646	0.869	2.206	3.466
+0.19	-1.95684	+0.445462	+2.74850	0.866	2.203	3.466
+0.18	-1.94818	+0.451812	+2.77051	0.864	2.199	3.466
+0.17	-1.93956	+0.458153	+2.79249	0.861	2.196	3.466
+0.16	-1.93097	+0.464484	+2.81443	0.858	2.193	3.466
+0.15	-1.92240	+0.470806	+2.83634	0.855	2.190	3.467
+0.14	-1.91387	+0.477117	+2.85823	0.852	2.187	3.467
+0.13	-1.90537	+0.483420	+2.88008	0.848	2.184	3.468
+0.12	-1.89690	+0.489713	+2.90191	0.845	2.181	3.469
+0.11	-1.88847	+0.495997	+2.92371	0.841	2.179	3.470
+0.10	-1.88008	+0.502272	+2.94549	0.838	2.176	3.471
+0.09	-1.87172	+0.508539	+2.96724	0.834	2.174	3.472
+0.08	-1.86340	+0.514797	+2.98897	0.830	2.172	3.473
+0.07	-1.85512	+0.521047	+3.01069	0.826	2.170	3.475
+0.06	-1.84688	+0.527289	+3.03238	0.822	2.168	3.476
+0.05	-1.83868	+0.533523	+3.05406	0.818	2.167	3.478
+0.04	-1.83053	+0.539750	+3.07572	0.813	2.165	3.480
+0.03	-1.82242	+0.545968	+3.09736	0.808	2.164	3.482
+0.02	-1.81436	+0.552180	+3.11901	0.804	2.163	3.484
+0.01	-1.80634	+0.558385	+3.14063	0.799	2.162	3.486
0.00	-1.79837	+0.564583	+3.16224	0.794	2.161	3.488

9.6

(1)	(4)	(5)	(6)	(7)	(8)	(9)
+1.26	-2.17652	-0.605752	-1.65326	0.438	4.056	4.059
+1.25	-2.17210	-0.595774	-1.61281	0.445	4.033	4.049
+1.24	-2.16762	-0.585832	-1.57260	0.452	4.009	4.040
+1.23	-2.16306	-0.575927	-1.53263	0.459	3.986	4.029
+1.22	-2.15844	-0.566061	-1.49289	0.466	3.962	4.024
+1.21	-2.15375	-0.556234	-1.45338	0.473	3.939	4.017
+1.20	-2.14899	-0.546448	-1.41410	0.480	3.916	4.010
+1.19	-2.14416	-0.536703	-1.37506	0.486	3.893	4.004
+1.18	-2.13926	-0.527000	-1.33624	0.493	3.871	3.997
+1.17	-2.13430	-0.517338	-1.29765	0.500	3.848	3.992
+1.16	-2.12926	-0.507719	-1.25928	0.507	3.826	3.986
+1.15	-2.12416	-0.498142	-1.22113	0.514	3.803	3.980
+1.14	-2.11899	-0.488606	-1.18321	0.520	3.781	3.974
+1.13	-2.11375	-0.479113	-1.14551	0.527	3.759	3.969
+1.12	-2.10844	-0.469662	-1.10803	0.534	3.737	3.963
+1.11	-2.10307	-0.460253	-1.07076	0.541	3.716	3.958
+1.10	-2.09762	-0.450885	-1.03372	0.548	3.694	3.952
+1.09	-2.09211	-0.441559	-0.99688	0.554	3.673	3.947
+1.08	-2.08653	-0.432274	-0.96026	0.561	3.651	3.941
+1.07	-2.08089	-0.423030	-0.92385	0.568	3.630	3.936
+1.06	-2.07517	-0.413826	-0.88766	0.575	3.609	3.930
+1.05	-2.06939	-0.404663	-0.85167	0.581	3.588	3.925
+1.04	-2.06354	-0.395540	-0.81588	0.588	3.568	3.920
+1.03	-2.05763	-0.386458	-0.78031	0.595	3.547	3.914
+1.02	-2.05165	-0.377415	-0.74494	0.601	3.527	3.908
+1.01	-2.04560	-0.368411	-0.70978	0.608	3.506	3.903

9.6 (CONT.)

(1)	(4)	(5)	(6)	(7)	(8)	(9)
+1.00	-2.03949	-0.359447	-0.67481	0.615	3.486	3.898
+0.99	-2.03331	-0.350522	-0.64005	0.621	3.466	3.892
+0.98	-2.02707	-0.341636	-0.60549	0.628	3.446	3.887
+0.97	-2.02076	-0.332788	-0.57113	0.634	3.426	3.881
+0.96	-2.01438	-0.323978	-0.53696	0.641	3.407	3.875
+0.95	-2.00795	-0.315207	-0.50300	0.647	3.387	3.870
+0.94	-2.00144	-0.306473	-0.46922	0.653	3.368	3.864
+0.93	-1.99488	-0.297777	-0.43564	0.660	3.348	3.859
+0.92	-1.98825	-0.289118	-0.40226	0.666	3.329	3.853
+0.91	-1.98156	-0.280496	-0.36906	0.672	3.310	3.847
+0.90	-1.97480	-0.271912	-0.33606	0.679	3.291	3.842
+0.89	-1.96798	-0.263364	-0.30325	0.685	3.272	3.836
+0.88	-1.96110	-0.254852	-0.27062	0.691	3.253	3.830
+0.87	-1.95416	-0.246377	-0.23818	0.697	3.234	3.824
+0.86	-1.94716	-0.237937	-0.20593	0.703	3.216	3.819
+0.85	-1.94010	-0.229534	-0.17387	0.709	3.197	3.813
+0.84	-1.93298	-0.221166	-0.14199	0.715	3.179	3.807
+0.83	-1.92580	-0.212833	-0.11029	0.721	3.161	3.801
+0.82	-1.91856	-0.204536	-0.07877	0.727	3.143	3.796
+0.81	-1.91126	-0.196274	-0.04743	0.733	3.125	3.790
+0.80	-1.90391	-0.188047	-0.01628	0.738	3.107	3.784
+0.79	-1.89650	-0.179854	+0.01470	0.744	3.089	3.778
+0.78	-1.88903	-0.171695	+0.04550	0.750	3.071	3.773
+0.77	-1.88151	-0.163571	+0.07613	0.755	3.054	3.767
+0.76	-1.87393	-0.155480	+0.10658	0.761	3.036	3.761
+0.75	-1.86630	-0.147424	+0.13686	0.766	3.019	3.755
+0.74	-1.85862	-0.139401	+0.16696	0.771	3.002	3.749
+0.73	-1.85088	-0.131411	+0.19690	0.776	2.985	3.744
+0.72	-1.84309	-0.123455	+0.22666	0.782	2.968	3.738
+0.71	-1.83525	-0.115531	+0.25626	0.787	2.951	3.732
+0.70	-1.82736	-0.107641	+0.28568	0.792	2.934	3.726
+0.69	-1.81942	-0.099783	+0.31494	0.796	2.918	3.721
+0.68	-1.81143	-0.091957	+0.34404	0.801	2.901	3.715
+0.67	-1.80339	-0.084164	+0.37296	0.806	2.885	3.709
+0.66	-1.79531	-0.076402	+0.40173	0.811	2.869	3.704
+0.65	-1.78718	-0.068673	+0.43034	0.815	2.853	3.698
+0.64	-1.77901	-0.060975	+0.45879	0.820	2.837	3.692
+0.63	-1.77079	-0.053308	+0.48707	0.824	2.821	3.687
+0.62	-1.76253	-0.045673	+0.51520	0.828	2.805	3.681
+0.61	-1.75423	-0.038068	+0.54318	0.832	2.790	3.676
+0.60	-1.74589	-0.030494	+0.57099	0.836	2.774	3.670
+0.59	-1.73750	-0.022951	+0.59866	0.840	2.759	3.665
+0.58	-1.72908	-0.015439	+0.62617	0.844	2.744	3.659
+0.57	-1.72063	-0.007956	+0.65353	0.848	2.729	3.654
+0.56	-1.71213	-0.000504	+0.68074	0.851	2.714	3.648
+0.55	-1.70360	+0.006919	+0.70780	0.855	2.699	3.643
+0.54	-1.69504	+0.014312	+0.73471	0.858	2.684	3.638
+0.53	-1.68644	+0.021676	+0.76148	0.861	2.670	3.633
+0.52	-1.67782	+0.029011	+0.78811	0.864	2.655	3.627
+0.51	-1.66916	+0.036317	+0.81459	0.867	2.641	3.622
+0.50	-1.66048	+0.043594	+0.84093	0.870	2.627	3.617
+0.49	-1.65176	+0.050842	+0.86713	0.873	2.613	3.612
+0.48	-1.64303	+0.058063	+0.89320	0.875	2.600	3.607
+0.47	-1.63426	+0.065255	+0.91912	0.877	2.586	3.602
+0.46	-1.62548	+0.072419	+0.94492	0.880	2.573	3.598
+0.45	-1.61667	+0.079556	+0.97058	0.882	2.559	3.593
+0.44	-1.60784	+0.086665	+0.99610	0.884	2.546	3.588
+0.43	-1.59900	+0.093747	+1.02150	0.886	2.533	3.584
+0.42	-1.59014	+0.100803	+1.04677	0.887	2.520	3.579
+0.41	-1.58126	+0.107832	+1.07191	0.889	2.508	3.575
+0.40	-1.57236	+0.114834	+1.09692	0.890	2.495	3.570
+0.39	-1.56346	+0.121810	+1.12182	0.891	2.483	3.566
+0.38	-1.55454	+0.128760	+1.14659	0.892	2.471	3.562
+0.37	-1.54562	+0.135684	+1.17124	0.893	2.459	3.558
+0.36	-1.53669	+0.142583	+1.19577	0.894	2.447	3.554
+0.35	-1.52775	+0.149456	+1.22019	0.894	2.436	3.550
+0.34	-1.51881	+0.156305	+1.24449	0.894	2.424	3.546
+0.33	-1.50987	+0.163129	+1.26868	0.894	2.413	3.543
+0.32	-1.50092	+0.169928	+1.29275	0.894	2.402	3.539
+0.31	-1.49198	+0.176703	+1.31672	0.894	2.391	3.536
+0.30	-1.48304	+0.183454	+1.34058	0.894	2.381	3.533
+0.29	-1.47411	+0.190182	+1.36434	0.893	2.370	3.530
+0.28	-1.46518	+0.196886	+1.38799	0.892	2.360	3.526
+0.27	-1.45626	+0.203566	+1.41154	0.891	2.350	3.524
+0.26	-1.44735	+0.210224	+1.43499	0.890	2.340	3.521
+0.25	-1.43846	+0.216859	+1.45834	0.889	2.331	3.518
+0.24	-1.42957	+0.223472	+1.48160	0.887	2.321	3.516
+0.23	-1.42071	+0.230063	+1.50476	0.886	2.312	3.514
+0.22	-1.41186	+0.236632	+1.52784	0.884	2.303	3.511
+0.21	-1.40303	+0.243180	+1.55082	0.882	2.294	3.509

9.6 (CONT.)

(1)	(4)	(5)	(6)	(7)	(8)	(9)
+0.20	-1.39423	+0.249706	+1.57372	0.879	2.285	3.507
+0.19	-1.38545	+0.256212	+1.59653	0.877	2.277	3.506
+0.18	-1.37669	+0.262697	+1.61926	0.874	2.269	3.504
+0.17	-1.36796	+0.269161	+1.64190	0.871	2.261	3.503
+0.16	-1.35926	+0.275606	+1.66447	0.868	2.253	3.501
+0.15	-1.35059	+0.282031	+1.68696	0.865	2.246	3.500
+0.14	-1.34196	+0.288436	+1.70938	0.862	2.238	3.499
+0.13	-1.33336	+0.294823	+1.73173	0.858	2.231	3.499
+0.12	-1.32480	+0.301191	+1.75400	0.854	2.224	3.498
+0.11	-1.31627	+0.307540	+1.77622	0.850	2.218	3.498
+0.10	-1.30779	+0.313871	+1.79836	0.846	2.211	3.498
+0.09	-1.29936	+0.320185	+1.82044	0.842	2.205	3.498
+0.08	-1.29096	+0.326481	+1.84246	0.837	2.199	3.498
+0.07	-1.28261	+0.332760	+1.86443	0.833	2.194	3.498
+0.06	-1.27431	+0.339023	+1.88634	0.828	2.198	3.499
+0.05	-1.26606	+0.345269	+1.90820	0.823	2.183	3.499
+0.04	-1.25786	+0.351500	+1.93000	0.817	2.178	3.500
+0.03	-1.24972	+0.357714	+1.95176	0.812	2.173	3.501
+0.02	-1.24163	+0.363914	+1.97346	0.806	2.169	3.503
+0.01	-1.23359	+0.370098	+1.99513	0.800	2.165	3.504
0.00	-1.22562	+0.376268	+2.01676	0.795	2.161	3.506

10.1

(1)	(3)	(5)	(6)	(12)	(7)	(8)	(13)	(9)
-0.70	-2.7686	-0.00062	-0.1927	-2.9620	2.996	0.008	2.986	3.002
-0.68	-2.7087	-0.00068	-0.1929	-2.9023	2.996	0.010	2.984	3.003
-0.66	-2.6488	-0.00074	-0.1931	-2.8426	2.995	0.010	2.982	3.003
-0.64	-2.5889	-0.00082	-0.1933	-2.7830	2.995	0.012	2.980	3.003
-0.62	-2.5290	-0.00090	-0.1936	-2.7234	2.994	0.012	2.979	3.003
-0.60	-2.4691	-0.00098	-0.1938	-2.6638	2.994	0.014	2.977	3.003
-0.58	-2.4092	-0.00108	-0.1941	-2.6043	2.994	0.015	2.974	3.003
-0.56	-2.3494	-0.00118	-0.1944	-2.5448	2.993	0.016	2.972	3.004
-0.54	-2.2895	-0.00129	-0.1947	-2.4854	2.992	0.018	2.970	3.004
-0.52	-2.2297	-0.00142	-0.1951	-2.4261	2.992	0.020	2.966	3.004
-0.50	-2.1698	-0.00155	-0.1955	-2.3668	2.991	0.022	2.964	3.005
-0.48	-2.1100	-0.00170	-0.1960	-2.3075	2.990	0.024	2.960	3.005
-0.46	-2.0502	-0.00187	-0.1965	-2.248*	2.990	0.026	2.957	3.005
-0.44	-1.9904	-0.00205	-0.1970	-2.189?	2.988	0.028	2.952	3.006
-0.42	-1.9307	-0.00224	-0.1976	-2.1303	2.988	0.031	2.948	3.006
-0.40	-1.8709	-0.00246	-0.1982	-2.0714	2.986	0.034	2.942	3.007
-0.38	-1.8112	-0.00270	-0.1990	-2.0126	2.985	0.038	2.937	3.008
-0.36	-1.7515	-0.00296	-0.1997	-1.9539	2.984	0.042	2.931	3.008
-0.34	-1.6919	-0.00324	-0.2006	-1.8954	2.982	0.045	2.924	3.009
-0.32	-1.6322	-0.00355	-0.2015	-1.8369	2.980	0.049	2.917	3.010
-0.30	-1.5727	-0.00389	-0.2026	-1.7787	2.978	0.054	2.910	3.011
-0.28	-1.5131	-0.00427	-0.2037	-1.7206	2.976	0.059	2.900	3.012
-0.26	-1.4536	-0.00468	-0.2049	-1.6626	2.974	0.064	2.892	3.013
-0.24	-1.3941	-0.00513	-0.2063	-1.6049	2.972	0.071	2.881	3.014
-0.22	-1.3347	-0.00562	-0.2078	-1.5474	2.969	0.078	2.870	3.015
-0.20	-1.2754	-0.00616	-0.2094	-1.4901	2.966	0.086	2.857	3.017
-0.18	-1.2161	-0.00676	-0.2112	-1.4331	2.962	0.094	2.844	3.018
-0.16	-1.1569	-0.00740	-0.2131	-1.3764	2.959	0.102	2.829	3.020
-0.14	-1.0977	-0.00812	-0.2153	-1.3200	2.955	0.112	2.812	3.022
-0.12	-1.0387	-0.00889	-0.2176	-1.2639	2.950	0.123	2.795	3.024
-0.10	-0.9797	-0.00974	-0.2202	-1.2082	2.946	0.135	2.776	3.026
-0.08	-0.9209	-0.01068	-0.2230	-1.1529	2.941	0.148	2.755	3.028
-0.06	-0.8621	-0.01170	-0.2261	-1.0980	2.935	0.162	2.732	3.031
-0.04	-0.8034	-0.01282	-0.2295	-1.0436	2.929	0.178	2.707	3.033
-0.02	-0.7449	-0.01405	-0.2332	-0.9897	2.922	0.194	2.680	3.036
-0.00	-0.6866	-0.01539	-0.2373	-0.9364	2.915	0.213	2.650	3.039
+0.02	-0.6283	-0.01686	-0.2418	-0.8837	2.907	0.234	2.618	3.042
+0.04	-0.5703	-0.01846	-0.2467	-0.8317	2.898	0.256	2.584	3.046
+0.06	-0.5124	-0.02022	-0.2520	-0.7804	2.888	0.280	2.546	3.050
+0.08	-0.4548	-0.02215	-0.2579	-0.7299	2.878	0.307	2.504	3.054
+0.10	-0.3973	-0.02425	-0.2643	-0.6802	2.866	0.337	2.460	3.058
+0.12	-0.3401	-0.02656	-0.2714	-0.6315	2.853	0.368	2.412	3.062
+0.14	-0.2832	-0.02907	-0.2791	-0.5838	2.839	0.404	2.360	3.066
+0.16	-0.2266	-0.03183	-0.2875	-0.5371	2.824	0.442	2.304	3.071
+0.18	-0.1703	-0.03484	-0.2968	-0.4917	2.808	0.484	2.244	3.075
+0.20	-0.1143	-0.03813	-0.3069	-0.4474	2.790	0.530	2.179	3.080
+0.22	-0.0587	-0.04172	-0.3180	-0.4045	2.770	0.580	2.110	3.084
+0.24	-0.0035	-0.04565	-0.3301	-0.3631	2.748	0.634	2.036	3.087
+0.26	+0.0512	-0.04995	-0.3434	-0.3232	2.725	0.694	1.956	3.089
+0.28	+0.1055	-0.05465	-0.3579	-0.2849	2.700	0.759	1.872	3.090
+0.30	+0.1592	-0.05979	-0.3738	-0.2483	2.672	0.830	1.784	3.089
+0.32	+0.2123	-0.06541	-0.3911	-0.2136	2.642	0.908	1.690	3.086
+0.34	+0.2649	-0.07156	-0.4101	-0.1808	2.610	0.992	1.590	3.078
+0.36	+0.3167	-0.07832	-0.4309	-0.1500	2.575	1.084	1.488	3.065
+0.38	+0.3678	-0.08574	-0.4535	-0.1213	2.538	1.184	1.380	3.045
+0.40	+0.4182	-0.09391	-0.4783	-0.0948	2.497	1.294	1.269	3.014
+0.41	+0.4430	-0.09832	-0.4916	-0.0824	2.476	1.353	1.212	2.993
+0.42	+0.4677	-0.10296	-0.5054	-0.0705	2.454	1.415	1.154	2.969
+0.43	+0.4921	-0.10786	-0.5199	-0.0593	2.432	1.479	1.096	2.940
+0.44	+0.5163	-0.11303	-0.5350	-0.0486	2.409	1.546	1.038	2.905
+0.45	+0.5403	-0.11852	-0.5508	-0.0385	2.385	1.617	0.979	2.863
+0.46	+0.5640	-0.12434	-0.5673	-0.0290	2.361	1.692	0.919	2.814
+0.47	+0.5875	-0.13056	-0.5846	-0.0202	2.336	1.770	0.860	2.755
+0.48	+0.6107	-0.13722	-0.6027	-0.0118	2.311	1.853	0.800	2.685
+0.49	+0.6337	-0.14439	-0.6217	-0.0041	2.286	1.941	0.741	2.602
+0.50	+0.6564	-0.15218	-0.6415	+0.0030	2.260	2.035	0.682	2.502
+0.51	+0.6789	-0.16071	-0.6624	+0.0095	2.236	2.136	0.622	2.384

(1)	(3)	(5)	(6)	(12)	(7)	(8)	(13)	(9)
−0.70	−2.7743	−0.00059	−0.1984	−2.9733	2.996	0.008	2.986	3.103
−0.68	−2.7144	−0.00065	−0.1986	−2.9136	2.996	0.009	2.984	3.104
−0.66	−2.6545	−0.00071	−0.1988	−2.8539	2.996	0.010	2.983	3.104
−0.64	−2.5946	−0.00078	−0.1990	−2.7943	2.995	0.011	2.982	3.104
−0.62	−2.5347	−0.00085	−0.1992	−2.7347	2.994	0.012	2.980	3.104
−0.60	−2.4748	−0.00094	−0.1994	−2.6751	2.994	0.014	2.978	3.104
−0.58	−2.4149	−0.00103	−0.1997	−2.6156	2.994	0.014	2.976	3.105
−0.56	−2.3550	−0.00112	−0.2000	−2.5561	2.993	0.016	2.974	3.105
−0.54	−2.2952	−0.00123	−0.2004	−2.4967	2.992	0.018	2.970	3.106
−0.52	−2.2354	−0.00135	−0.2007	−2.4373	2.992	0.020	2.968	3.106
−0.50	−2.1755	−0.00148	−0.2011	−2.3780	2.992	0.021	2.965	3.106
−0.48	−2.1157	−0.00162	−0.2016	−2.3187	2.990	0.023	2.961	3.107
−0.46	−2.0559	−0.00178	−0.2020	−2.2595	2.990	0.026	2.958	3.108
−0.44	−1.9961	−0.00195	−0.2026	−2.2004	2.989	0.028	2.954	3.108
−0.42	−1.9363	−0.00214	−0.2032	−2.1414	2.988	0.030	2.949	3.109
−0.40	−1.8766	−0.00235	−0.2038	−2.0824	2.986	0.034	2.944	3.110
−0.38	−1.8169	−0.00257	−0.2045	−2.0236	2.985	0.037	2.939	3.111
−0.36	−1.7572	−0.00282	−0.2053	−1.9649	2.984	0.040	2.933	3.112
−0.34	−1.6975	−0.00309	−0.2061	−1.9063	2.982	0.044	2.926	3.113
−0.32	−1.6379	−0.00339	−0.2070	−1.8478	2.980	0.048	2.920	3.115
−0.30	−1.5783	−0.00371	−0.2081	−1.7895	2.978	0.053	2.912	3.116
−0.28	−1.5188	−0.00407	−0.2092	−1.7314	2.976	0.058	2.903	3.117
−0.26	−1.4593	−0.00446	−0.2104	−1.6734	2.974	0.064	2.894	3.119
−0.24	−1.3998	−0.00488	−0.2117	−1.6156	2.972	0.070	2.884	3.121
−0.22	−1.3404	−0.00535	−0.2132	−1.5581	2.969	0.076	2.873	3.123
−0.20	−1.2811	−0.00587	−0.2148	−1.5007	2.966	0.084	2.861	3.125
−0.18	−1.2218	−0.00643	−0.2165	−1.4436	2.962	0.092	2.848	3.127
−0.16	−1.1626	−0.00705	−0.2185	−1.3868	2.959	0.101	2.833	3.130
−0.14	−1.1034	−0.00773	−0.2206	−1.3303	2.955	0.110	2.817	3.133
−0.12	−1.0444	−0.00847	−0.2229	−1.2742	2.951	0.122	2.800	3.136
−0.10	−0.9854	−0.00928	−0.2254	−1.2183	2.946	0.133	2.782	3.140
−0.08	−0.9265	−0.01016	−0.2282	−1.1629	2.940	0.146	2.760	3.144
−0.06	−0.8678	−0.01113	−0.2313	−1.1079	2.935	0.160	2.738	3.148
−0.04	−0.8091	−0.01220	−0.2346	−1.0534	2.929	0.175	2.714	3.153
−0.02	−0.7506	−0.01336	−0.2383	−0.9994	2.922	0.192	2.688	3.158
0.00	−0.6923	−0.01463	−0.2423	−0.9459	2.914	0.210	2.658	3.163
+0.02	−0.6340	−0.01602	−0.2467	−0.8930	2.906	0.230	2.628	3.169
+0.04	−0.5760	−0.01754	−0.2516	−0.8408	2.898	0.252	2.594	3.176
+0.06	−0.5182	−0.01920	−0.2568	−0.7893	2.888	0.276	2.556	3.183
+0.08	−0.4605	−0.02101	−0.2626	−0.7386	2.877	0.302	2.516	3.191
+0.10	−0.4031	−0.02299	−0.2690	−0.6887	2.865	0.331	2.474	3.200
+0.12	−0.3459	−0.02515	−0.2759	−0.6397	2.852	0.362	2.426	3.209
+0.14	−0.2890	−0.02752	−0.2835	−0.5916	2.838	0.397	2.376	3.219
+0.16	−0.2324	−0.03009	−0.2918	−0.5446	2.823	0.434	2.322	3.230
+0.18	−0.1761	−0.03290	−0.3009	−0.4988	2.806	0.475	2.264	3.242
+0.20	−0.1202	−0.03596	−0.3108	−0.4541	2.788	0.520	2.201	3.255
+0.22	−0.0646	−0.03930	−0.3217	−0.4108	2.768	0.568	2.134	3.269
+0.24	−0.0094	−0.04292	−0.3336	−0.3688	2.746	0.622	2.062	3.284
+0.26	+0.0453	−0.04688	−0.3466	−0.3283	2.723	0.680	1.986	3.299
+0.28	+0.0995	−0.05117	−0.3608	−0.2894	2.698	0.742	1.905	3.316
+0.30	+0.1531	−0.05584	−0.3763	−0.2522	2.670	0.811	1.820	3.335
+0.32	+0.2062	−0.06091	−0.3933	−0.2167	2.639	0.886	1.730	3.354
+0.34	+0.2587	−0.06641	−0.4118	−0.1830	2.606	0.966	1.635	3.373
+0.36	+0.3104	−0.07238	−0.4320	−0.1513	2.570	1.054	1.536	3.394
+0.38	+0.3615	−0.07885	−0.4540	−0.1216	2.532	1.149	1.434	3.414
+0.40	+0.4117	−0.08586	−0.4780	−0.0940	2.490	1.252	1.328	3.434
+0.42	+0.4610	−0.09345	−0.5041	−0.0685	2.445	1.363	1.221	3.452
+0.44	+0.5095	−0.10166	−0.5326	−0.0452	2.397	1.483	1.112	3.468
+0.46	+0.5569	−0.11057	−0.5635	−0.0240	2.345	1.612	1.002	3.481
+0.48	+0.6033	−0.12022	−0.5971	−0.0051	2.290	1.752	0.892	3.486
+0.50	+0.6485	−0.13070	−0.6336	+0.0117	2.232	1.902	0.784	3.481
+0.51	+0.6706	−0.13629	−0.6531	+0.0192	2.201	1.981	0.731	3.473
+0.52	+0.6925	−0.14212	−0.6733	+0.0263	2.170	2.064	0.679	3.461
+0.53	+0.7140	−0.14822	−0.6944	+0.0328	2.137	2.149	0.628	3.443
+0.54	+0.7352	−0.15462	−0.7163	+0.0389	2.104	2.238	0.578	3.419
+0.55	+0.7561	−0.16133	−0.7391	+0.0444	2.071	2.330	0.530	3.387
+0.56	+0.7766	−0.16839	−0.7629	+0.0495	2.036	2.427	0.483	3.345
+0.57	+0.7968	−0.17586	−0.7877	+0.0541	2.002	2.527	0.437	3.292
+0.58	+0.8166	−0.18377	−0.8135	+0.0582	1.966	2.633	0.394	3.225
+0.59	+0.8361	−0.19222	−0.8404	+0.0620	1.931	2.744	0.352	3.141
+0.60	+0.8553	−0.20128	−0.8684	+0.0653	1.895	2.861	0.312	3.036
+0.605	+0.8647	−0.20610	−0.8828	+0.0668	1.877	2.923	0.293	2.975
+0.610	+0.8740	−0.21112	−0.8976	+0.0682	1.860	2.986	0.275	2.906
+0.615	+0.8833	−0.21638	−0.9127	+0.0695	1.842	3.053	0.256	2.830
+0.620	+0.8925	−0.22192	−0.9282	+0.0708	1.825	3.122	0.239	2.745
+0.625	+0.9016	−0.22777	−0.9439	+0.0719	1.808	3.194	0.222	2.651
+0.630	+0.9106	−0.23399	−0.9601	+0.0730	1.792	3.270	0.205	2.546
+0.635	+0.9195	−0.24064	−0.9766	+0.0740	1.776	3.351	0.189	2.429

10.3

(1)	(3)	(5)	(6)	(12)	(7)	(8)	(13)	(9)
+0.04	-0.5768	-0.01742	-0.2522	-0.8421	2.897	0.252	2.595	3.193
+0.06	-0.5189	-0.01907	-0.2575	-0.7906	2.888	0.276	2.558	3.201
+0.08	-0.4613	-0.02087	-0.2633	-0.7398	2.877	0.302	2.518	3.210
+0.10	-0.4039	-0.02283	-0.2696	-0.6898	2.865	0.330	2.476	3.219
+0.12	-0.3467	-0.02498	-0.2765	-0.6408	2.852	0.362	2.428	3.228
+0.14	-0.2898	-0.02732	-0.2841	-0.5927	2.838	0.396	2.378	3.239
+0.16	-0.2332	-0.02987	-0.2924	-0.5457	2.823	0.433	2.324	3.251
+0.18	-0.1769	-0.03266	-0.3014	-0.4998	2.806	0.474	2.266	3.264
+0.20	-0.1209	-0.03569	-0.3113	-0.4550	2.788	0.518	2.204	3.278
+0.22	-0.0654	-0.03899	-0.3222	-0.4116	2.768	0.567	2.137	3.293
+0.24	-0.0102	-0.04258	-0.3340	-0.3696	2.746	0.620	2.066	3.309
+0.26	+0.0445	-0.04649	-0.3470	-0.3290	2.723	0.678	1.990	3.327
+0.28	+0.0987	-0.05074	-0.3611	-0.2900	2.698	0.740	1.910	3.345
+0.30	+0.1524	-0.05535	-0.3766	-0.2526	2.669	0.808	1.824	3.366
+0.32	+0.2054	-0.06036	-0.3935	-0.2171	2.639	0.882	1.734	3.387
+0.34	+0.2579	-0.06579	-0.4119	-0.1833	2.606	0.963	1.640	3.410
+0.36	+0.3097	-0.07167	-0.4321	-0.1515	2.570	1.050	1.542	3.435
+0.38	+0.3607	-0.07803	-0.4540	-0.1216	2.532	1.145	1.440	3.460
+0.40	+0.4109	-0.08491	-0.4779	-0.0939	2.490	1.247	1.336	3.486
+0.42	+0.4602	-0.09235	-0.5040	-0.0682	2.444	1.357	1.229	3.512
+0.44	+0.5087	-0.10038	-0.5323	-0.0447	2.396	1.476	1.120	3.538
+0.46	+0.5561	-0.10905	-0.5631	-0.0234	2.344	1.604	1.011	3.562
+0.48	+0.6024	-0.11841	-0.5965	-0.0043	2.288	1.741	0.902	3.583
+0.50	+0.6476	-0.12851	-0.6328	+0.0127	2.230	1.888	0.796	3.598
+0.52	+0.6916	-0.13943	-0.6721	+0.0275	2.166	2.046	0.692	3.604
+0.54	+0.7342	-0.15126	-0.7147	+0.0404	2.100	2.216	0.592	3.596
+0.56	+0.7756	-0.16412	-0.7608	+0.0512	2.032	2.397	0.498	3.569
+0.58	+0.8155	-0.17819	-0.8107	+0.0603	1.959	2.592	0.410	3.513
+0.60	+0.8539	-0.19375	-0.8646	+0.0677	1.885	2.803	0.330	3.412
+0.61	+0.8726	-0.20222	-0.8932	+0.0708	1.847	2.916	0.293	3.340
+0.62	+0.8908	-0.21125	-0.9229	+0.0736	1.809	3.034	0.258	3.248
+0.63	+0.9087	-0.22095	-0.9539	+0.0760	1.771	3.160	0.226	3.133
+0.64	+0.9262	-0.23149	-0.9862	+0.0781	1.734	3.294	0.195	2.989
+0.645	+0.9349	-0.23714	-1.0028	+0.0791	1.716	3.365	0.181	2.903
+0.650	+0.9434	-0.24309	-1.0198	+0.0799	1.698	3.440	0.167	2.808
+0.655	+0.9519	-0.24941	-1.0372	+0.0807	1.680	3.518	0.154	2.702
+0.660	+0.9602	-0.25614	-1.0550	+0.0815	1.663	3.600	0.141	2.583
+0.665	+0.9685	-0.26338	-1.0732	+0.0821	1.647	3.689	0.128	2.450

10.4

(1)	(3)	(5)	(6)	(12)	(7)	(8)	(13)	(9)
+0.04	-0.5775	-0.01731	-0.2529	-0.8433	2.897	0.251	2.596	3.211
+0.06	-0.5197	-0.01894	-0.2581	-0.7918	2.888	0.275	2.560	3.219
+0.08	-0.4620	-0.02073	-0.2639	-0.7410	2.876	0.301	2.520	3.228
+0.10	-0.4046	-0.02268	-0.2702	-0.6910	2.865	0.330	2.477	3.237
+0.12	-0.3475	-0.02481	-0.2771	-0.6419	2.852	0.361	2.430	3.248
+0.14	-0.2906	-0.02713	-0.2847	-0.5938	2.838	0.395	2.380	3.260
+0.16	-0.2340	-0.02966	-0.2929	-0.5467	2.823	0.432	2.326	3.272
+0.18	-0.1777	-0.03242	-0.3020	-0.5008	2.806	0.473	2.269	3.286
+0.20	-0.1217	-0.03542	-0.3119	-0.4560	2.788	0.518	2.206	3.301
+0.22	-0.0662	-0.03869	-0.3227	-0.4125	2.768	0.566	2.140	3.318
+0.24	-0.0110	-0.04225	-0.3345	-0.3704	2.746	0.618	2.069	3.336
+0.26	+0.0437	-0.04612	-0.3474	-0.3298	2.722	0.676	1.994	3.355
+0.28	+0.0979	-0.05032	-0.3616	-0.2907	2.697	0.738	1.913	3.376
+0.30	+0.1515	-0.05487	-0.3770	-0.2533	2.669	0.806	1.828	3.399
+0.32	+0.2046	-0.05981	-0.3939	-0.2176	2.638	0.880	1.740	3.424
+0.34	+0.2571	-0.06516	-0.4122	-0.1837	2.606	0.960	1.646	3.450
+0.36	+0.3088	-0.07095	-0.4323	-0.1518	2.570	1.047	1.548	3.479
+0.38	+0.3598	-0.07720	-0.4542	-0.1218	2.530	1.140	1.447	3.510
+0.40	+0.4100	-0.08395	-0.4780	-0.0939	2.488	1.242	1.343	3.542
+0.42	+0.4593	-0.09123	-0.5039	-0.0681	2.444	1.350	1.237	3.576
+0.44	+0.5077	-0.09907	-0.5320	-0.0445	2.395	1.468	1.129	3.612
+0.46	+0.5551	-0.10750	-0.5627	-0.0230	2.343	1.594	1.020	3.648
+0.48	+0.6014	-0.11657	-0.5959	-0.0037	2.287	1.730	0.913	3.685
+0.50	+0.6466	-0.12630	-0.6319	+0.0135	2.228	1.874	0.807	3.720
+0.52	+0.6905	-0.13674	-0.6709	+0.0286	2.164	2.029	0.704	3.753
+0.54	+0.7331	-0.14794	-0.7132	+0.0417	2.098	2.193	0.606	3.781
+0.56	+0.7744	-0.15996	-0.7587	+0.0529	2.027	2.368	0.513	3.801
+0.57	+0.7945	-0.16630	-0.7829	+0.0578	1.991	2.459	0.468	3.806
+0.58	+0.8142	-0.17289	-0.8079	+0.0623	1.953	2.553	0.426	3.808
+0.59	+0.8335	-0.17972	-0.8339	+0.0667	1.915	2.650	0.386	3.801
+0.60	+0.8525	-0.18683	-0.8609	+0.0704	1.877	2.750	0.347	3.792
+0.61	+0.8710	-0.19423	-0.8890	+0.0737	1.837	2.853	0.311	3.775
+0.62	+0.8892	-0.20196	-0.9180	+0.0766	1.798	2.959	0.277	3.750
+0.63	+0.9070	-0.21003	-0.9482	+0.0792	1.757	3.069	0.245	3.713
+0.64	+0.9244	-0.21850	-0.9794	+0.0815	1.717	3.183	0.215	3.664

10.4 (CONT.)

(1)	(3)	(5)	(6)	(12)	(7)	(8)	(13)	(9)
+0.65	+0.9413	-0.22743	-1.0118	+0.0835	1.676	3.302	0.188	3.598
+0.66	+0.9579	-0.23689	-1.0455	+0.0853	1.635	3.426	0.163	3.513
+0.67	+0.9740	-0.24698	-1.0804	+0.0868	1.594	3.556	0.140	3.404
+0.68	+0.9898	-0.25784	-1.1166	+0.0881	1.554	3.695	0.119	3.265
+0.69	+1.0051	-0.26970	-1.1543	+0.0892	1.515	3.844	0.100	3.089
+0.70	+1.0201	-0.28288	-1.1936	+0.0901	1.477	4.008	0.082	2.866
+0.705	+1.0274	-0.29011	-1.2138	+0.0905	1.458	4.098	0.074	2.734
+0.710	+1.0347	-0.29791	-1.2346	+0.0909	1.441	4.194	0.067	2.585
+0.715	+1.0418	-0.30639	-1.2558	+0.0912	1.425	4.298	0.060	2.417

10.5

(1)	(3)	(5)	(6)	(12)	(7)	(8)	(13)	(9)
+0.20	-0.1221	-0.03528	-0.3122	-0.4565	2.788	0.516	2.208	3.314
+0.22	-0.0666	-0.03853	-0.3230	-0.4130	2.768	0.565	2.142	3.331
+0.24	-0.0114	-0.04207	-0.3348	-0.3709	2.746	0.618	2.071	3.350
+0.26	+0.0432	-0.04591	-0.3477	-0.3302	2.722	0.675	1.996	3.370
+0.28	+0.0974	-0.05008	-0.3618	-0.2911	2.696	0.737	1.916	3.393
+0.30	+0.1511	-0.05461	-0.3772	-0.2536	2.669	0.805	1.831	3.417
+0.32	+0.2042	-0.05951	-0.3940	-0.2178	2.638	0.878	1.742	3.443
+0.34	+0.2566	-0.06482	-0.4124	-0.1839	2.605	0.958	1.648	3.472
+0.36	+0.3083	-0.07056	-0.4324	-0.1519	2.570	1.044	1.551	3.502
+0.38	+0.3594	-0.07676	-0.4542	-0.1219	2.530	1.138	1.450	3.536
+0.40	+0.4095	-0.08345	-0.4780	-0.0939	2.488	1.239	1.347	3.571
+0.42	+0.4589	-0.09065	-0.5038	-0.0680	2.443	1.348	1.241	3.610
+0.44	+0.5072	-0.09839	-0.5319	-0.0443	2.394	1.464	1.134	3.650
+0.46	+0.5546	-0.10670	-0.5625	-0.0227	2.342	1.590	1.026	3.693
+0.48	+0.6009	-0.11562	-0.5956	-0.0033	2.286	1.724	0.918	3.738
+0.50	+0.6460	-0.12516	-0.6315	+0.0140	2.226	1.868	0.813	3.784
+0.52	+0.6900	-0.13537	-0.6704	+0.0293	2.163	2.020	0.710	3.830
+0.54	+0.7326	-0.14627	-0.7124	+0.0425	2.096	2.182	0.612	3.877
+0.56	+0.7738	-0.15789	-0.7577	+0.0538	2.025	2.354	0.520	3.921
+0.58	+0.8135	-0.17029	-0.8066	+0.0633	1.950	2.534	0.434	3.960
+0.60	+0.8518	-0.18351	-0.8591	+0.0712	1.874	2.724	0.356	3.991
+0.62	+0.8885	-0.19762	-0.9156	+0.0777	1.793	2.924	0.286	4.011
+0.64	+0.9235	-0.21272	-0.9762	+0.0828	1.720	3.135	0.226	4.011
+0.66	+0.9569	-0.22894	-1.0410	+0.0868	1.626	3.356	0.174	3.982
+0.68	+0.9885	-0.24652	-1.1105	+0.0898	1.540	3.590	0.130	3.911
+0.69	+1.0037	-0.25592	-1.1470	+0.0910	1.497	3.712	0.111	3.853
+0.70	+1.0184	-0.26582	-1.1847	+0.0920	1.454	3.839	0.094	3.776
+0.71	+1.0328	-0.27630	-1.2238	+0.0929	1.412	3.973	0.079	3.674
+0.72	+1.0467	-0.28750	-1.2642	+0.0936	1.370	4.113	0.066	3.543
+0.73	+1.0602	-0.29959	-1.3061	+0.0942	1.328	4.263	0.054	3.376
+0.735	+1.0668	-0.30606	-1.3276	+0.0945	1.308	4.344	0.048	3.275
+0.740	+1.0732	-0.31288	-1.3495	+0.0947	1.288	4.426	0.044	3.161
+0.745	+1.0796	-0.32009	-1.3719	+0.0949	1.270	4.516	0.040	3.032
+0.750	+1.0859	-0.32780	-1.3947	+0.0951	1.250	4.610	0.036	2.887
+0.755	+1.0921	-0.33610	-1.4180	+0.0953	1.234	4.712	0.032	2.723
+0.760	+1.0982	-0.34517	-1.4418	+0.0954	1.216	4.824	0.028	2.536
+0.765	+1.1043	-0.35522	-1.4663	+0.0955	1.201	4.949	0.024	2.325

10.6

(1)	(3)	(5)	(6)	(12)	(7)	(8)	(13)	(9)
+0.30	+0.1509	-0.05448	-0.3773	-0.2537	2.668	0.804	1.832	3.425
+0.32	+0.2038	-0.05937	-0.3941	-0.2180	2.638	0.878	1.743	3.453
+0.34	+0.2564	-0.06466	-0.4124	-0.1840	2.604	0.958	1.650	3.482
+0.36	+0.3081	-0.07038	-0.4324	-0.1520	2.569	1.044	1.553	3.514
+0.38	+0.3591	-0.07655	-0.4542	-0.1220	2.530	1.137	1.452	3.549
+0.40	+0.4093	-0.08320	-0.4780	-0.0939	2.488	1.238	1.349	3.586
+0.42	+0.4586	-0.09036	-0.5038	-0.0680	2.443	1.346	1.243	3.626
+0.44	+0.5070	-0.09806	-0.5319	-0.0442	2.394	1.462	1.136	3.670
+0.46	+0.5544	-0.10631	-0.5624	-0.0226	2.342	1.588	1.028	3.715
+0.48	+0.6007	-0.11516	-0.5954	-0.0031	2.286	1.721	0.921	3.764
+0.50	+0.6458	-0.12461	-0.6313	+0.0143	2.226	1.864	0.816	3.815
+0.52	+0.6897	-0.13471	-0.6701	+0.0296	2.162	2.016	0.714	3.869
+0.54	+0.7323	-0.14546	-0.7119	+0.0429	2.096	2.176	0.616	3.922
+0.56	+0.7735	-0.15691	-0.7571	+0.0542	2.024	2.346	0.524	3.978
+0.58	+0.8132	-0.16907	-0.8058	+0.0639	1.950	2.526	0.438	4.032
+0.60	+0.8515	-0.18197	-0.8582	+0.0718	1.872	2.713	0.360	4.085
+0.62	+0.8881	-0.19565	-0.9144	+0.0783	1.792	2.909	0.291	4.132
+0.64	+0.9231	-0.21015	-0.9746	+0.0835	1.708	3.114	0.230	4.171
+0.66	+0.9564	-0.22553	-1.0390	+0.0876	1.622	3.326	0.178	4.198
+0.68	+0.9880	-0.24188	-1.1077	+0.0907	1.536	3.547	0.134	4.205
+0.70	+1.0178	-0.25932	-1.1809	+0.0930	1.448	3.777	0.100	4.183
+0.72	+1.0459	-0.27808	-1.2588	+0.0948	1.360	4.018	0.071	4.118
+0.73	+1.0592	-0.28806	-1.2996	+0.0954	1.316	4.143	0.060	4.063
+0.74	+1.0722	-0.29850	-1.3417	+0.0960	1.272	4.273	0.049	3.988
+0.75	+1.0847	-0.30952	-1.3851	+0.0964	1.229	4.408	0.041	3.889

10.6 (CONT.)

(1)	(3)	(5)	(6)	(12)	(7)	(8)	(13)	(9)
+0.76	+1.0968	-0.32122	-1.4299	+0.0968	1.187	4.550	0.033	3.759
+0.77	+1.1084	-0.33380	-1.4761	+0.0971	1.146	4.701	0.027	3.591
+0.78	+1.1197	-0.34752	-1.5240	+0.0973	1.106	4.866	0.021	3.374
+0.785	+1.1252	-0.35494	-1.5485	+0.0974	1.087	4.956	0.019	3.243
+0.790	+1.1306	-0.36283	-1.5735	+0.0975	1.068	5.051	0.017	3.095
+0.795	+1.1359	-0.37130	-1.5990	+0.0976	1.050	5.154	0.014	2.927
+0.800	+1.1411	-0.38050	-1.6251	+0.0976	1.034	5.267	0.013	2.736
+0.805	+1.1462	-0.39064	-1.6517	+0.0977	1.018	5.393	0.011	2.517
+0.810	+1.1512	-0.40206	-1.6790	+0.0978	1.004	5.537	0.009	2.268

10.7

(1)	(3)	(5)	(6)	(12)	(7)	(8)	(13)	(9)
-0.70	-2.7765	-0.00058	-0.2006	-2.9777	2.996	0.008	2.986	3.144
-0.68	-2.7166	-0.00064	-0.2008	-2.9180	2.996	0.009	2.984	3.144
-0.66	-2.6567	-0.00070	-0.2010	-2.8583	2.995	0.010	2.983	3.144
-0.64	-2.5968	-0.00076	-0.2012	-2.7987	2.995	0.011	2.982	3.144
-0.62	-2.5369	-0.00084	-0.2014	-2.7391	2.994	0.012	2.980	3.145
-0.60	-2.4770	-0.00092	-0.2016	-2.6795	2.994	0.014	2.978	3.145
-0.58	-2.4171	-0.00101	-0.2019	-2.6200	2.994	0.014	2.976	3.145
-0.56	-2.3573	-0.00110	-0.2022	-2.5605	2.993	0.016	2.974	3.146
-0.54	-2.2974	-0.00121	-0.2026	-2.5010	2.992	0.018	2.971	3.146
-0.52	-2.2376	-0.00133	-0.2030	-2.4417	2.992	0.019	2.968	3.147
-0.50	-2.1777	-0.00146	-0.2033	-2.3823	2.992	0.021	2.965	3.147
-0.48	-2.1179	-0.00160	-0.2038	-2.3231	2.990	0.023	2.962	3.148
-0.46	-2.0581	-0.00175	-0.2043	-2.2639	2.990	0.026	2.958	3.149
-0.44	-1.9983	-0.00192	-0.2048	-2.2047	2.988	0.028	2.954	3.149
-0.42	-1.9386	-0.00210	-0.2054	-2.1457	2.988	0.030	2.949	3.150
-0.40	-1.8788	-0.00231	-0.2060	-2.0868	2.986	0.034	2.944	3.151
-0.38	-1.8191	-0.00253	-0.2067	-2.0279	2.985	0.036	2.939	3.153
-0.36	-1.7594	-0.00277	-0.2075	-1.9692	2.984	0.040	2.933	3.154
-0.34	-1.6998	-0.00304	-0.2083	-1.9106	2.982	0.044	2.927	3.155
-0.32	-1.6402	-0.00333	-0.2092	-1.8522	2.980	0.048	2.920	3.157
-0.30	-1.5806	-0.00365	-0.2102	-1.7938	2.978	0.053	2.912	3.158
-0.28	-1.5210	-0.00400	-0.2114	-1.7357	2.976	0.058	2.904	3.160
-0.26	-1.4615	-0.00438	-0.2126	-1.6777	2.974	0.064	2.894	3.162
-0.24	-1.4020	-0.00481	-0.2139	-1.6199	2.972	0.070	2.885	3.164
-0.22	-1.3426	-0.00527	-0.2154	-1.5623	2.969	0.076	2.874	3.166
-0.20	-1.2833	-0.00577	-0.2170	-1.5050	2.966	0.084	2.862	3.169
-0.18	-1.2240	-0.00632	-0.2187	-1.4478	2.962	0.092	2.848	3.172
-0.16	-1.1648	-0.00693	-0.2206	-1.3910	2.958	0.100	2.834	3.175
-0.14	-1.1057	-0.00759	-0.2227	-1.3345	2.955	0.110	2.818	3.178
-0.12	-1.0466	-0.00832	-0.2250	-1.2783	2.950	0.120	2.802	3.182
-0.10	-0.9876	-0.00911	-0.2276	-1.2224	2.946	0.132	2.783	3.186
-0.08	-0.9288	-0.00998	-0.2304	-1.1670	2.940	0.145	2.763	3.191
-0.06	-0.8700	-0.01093	-0.2334	-1.1120	2.934	0.159	2.740	3.196
-0.04	-0.8114	-0.01197	-0.2367	-1.0574	2.928	0.174	2.716	3.201
-0.02	-0.7529	-0.01311	-0.2404	-1.0033	2.922	0.190	2.690	3.207
0.00	-0.6945	-0.01435	-0.2444	-0.9498	2.914	0.209	2.662	3.214
+0.02	-0.6363	-0.01571	-0.2487	-0.8969	2.906	0.229	2.631	3.221
+0.04	-0.5783	-0.01720	-0.2535	-0.8446	2.897	0.250	2.598	3.228
+0.06	-0.5204	-0.01882	-0.2588	-0.7930	2.888	0.274	2.561	3.237
+0.08	-0.4628	-0.02059	-0.2645	-0.7422	2.876	0.300	2.522	3.247
+0.10	-0.4054	-0.02252	-0.2708	-0.6922	2.865	0.329	2.478	3.257
+0.12	-0.3482	-0.02463	-0.2777	-0.6430	2.852	0.360	2.432	3.268
+0.14	-0.2913	-0.02694	-0.2852	-0.5949	2.838	0.394	2.382	3.280
+0.16	-0.2347	-0.02945	-0.2935	-0.5477	2.823	0.431	2.329	3.294
+0.18	-0.1784	-0.03218	-0.3025	-0.5017	2.806	0.472	2.272	3.308
+0.20	-0.1225	-0.03516	-0.3124	-0.4569	2.788	0.516	2.220	3.325
+0.22	-0.0669	-0.03840	-0.3232	-0.4134	2.768	0.564	2.143	3.342
+0.24	-0.0118	-0.04192	-0.3350	-0.3712	2.746	0.617	2.072	3.362
+0.26	+0.0429	-0.04574	-0.3479	-0.3305	2.722	0.674	1.997	3.383
+0.28	+0.0971	-0.04989	-0.3620	-0.2914	2.696	0.736	1.918	3.406
+0.30	+0.1508	-0.05440	-0.3774	-0.2538	2.668	0.804	1.833	3.432
+0.32	+0.2038	-0.05927	-0.3942	-0.2181	2.638	0.878	1.744	3.459
+0.34	+0.2563	-0.06455	-0.4125	-0.1841	2.605	0.957	1.651	3.490
+0.36	+0.3080	-0.07025	-0.4325	-0.1521	2.569	1.043	1.554	3.522
+0.38	+0.3590	-0.07640	-0.4543	-0.1220	2.530	1.136	1.454	3.558
+0.40	+0.4092	-0.08303	-0.4780	-0.0940	2.488	1.236	1.350	3.596
+0.42	+0.4585	-0.09017	-0.5038	-0.0680	2.443	1.345	1.244	3.638
+0.44	+0.5069	-0.09783	-0.5318	-0.0442	2.394	1.462	1.138	3.683
+0.46	+0.5542	-0.10604	-0.5623	-0.0225	2.342	1.586	1.030	3.731
+0.48	+0.6005	-0.11484	-0.5954	-0.0030	2.286	1.720	0.923	3.783
+0.50	+0.6456	-0.12423	-0.6312	+0.0144	2.226	1.862	0.818	3.838
+0.52	+0.6895	-0.13425	-0.6699	+0.0298	2.162	2.013	0.716	3.896
+0.54	+0.7321	-0.14490	-0.7117	+0.0432	2.094	2.173	0.618	3.957
+0.56	+0.7733	-0.15622	-0.7569	+0.0546	2.023	2.342	0.526	4.020
+0.58	+0.8130	-0.16821	-0.8054	+0.0642	1.949	2.519	0.441	4.086

10.7 (CONT.)

(1)	(3)	(5)	(6)	(12)	(7)	(8)	(13)	(9)
+0.60	+0.8512	−0.18088	−0.8577	+0.0723	1.871	2.705	0.363	4.154
+0.62	+0.8878	−0.19426	−0.9137	+0.0788	1.790	2.898	0.294	4.222
+0.64	+0.9228	−0.20834	−0.9737	+0.0841	1.706	3.098	0.233	4.290
+0.66	+0.9560	−0.22315	−1.0377	+0.0882	1.620	3.305	0.181	4.354
+0.68	+0.9875	−0.23870	−1.1059	+0.0914	1.532	3.518	0.138	4.410
+0.70	+1.0173	−0.25499	−1.1784	+0.0938	1.443	3.735	0.103	4.476
+0.72	+1.0452	−0.27206	−1.2553	+0.0956	1.354	3.956	0.075	4.531
+0.74	+1.0714	−0.28994	−1.3367	+0.0968	1.264	4.182	0.053	4.572
+0.76	+1.0958	−0.30866	−1.4226	+0.0977	1.176	4.410	0.037	4.600
+0.77	+1.1074	−0.31837	−1.4673	+0.0981	1.132	4.526	0.015	4.605
+0.78	+1.1185	−0.32832	−1.5131	+0.0983	1.088	4.643	0.012	4.605
+0.79	+1.1291	−0.33854	−1.5602	+0.0986	1.045	4.761	0.010	4.597
+0.80	+1.1394	−0.34905	−1.6084	+0.0987	1.003	4.880	0.008	4.579
+0.81	+1.1492	−0.35987	−1.6578	+0.0989	0.962	5.001	0.007	4.549
+0.82	+1.1586	−0.37105	−1.7084	+0.0990	0.921	5.125	0.005	4.506
+0.83	+1.1676	−0.38264	−1.7602	+0.0991	0.881	5.251	0.004	4.444
+0.84	+1.1762	−0.39471	−1.8134	+0.0992	0.842	5.382	0.003	4.360
+0.85	+1.1845	−0.40737	−1.8679	+0.0992	0.804	5.519	0.002	4.248
+0.86	+1.1923	−0.42076	−1.9238	+0.0993	0.767	5.664	0.002	4.100
+0.87	+1.1998	−0.43509	−1.9812	+0.0993	0.731	5.820	0.001	3.905
+0.875	+1.2034	−0.44271	−2.0105	+0.0993	0.714	5.904	0.001	3.787
+0.880	+1.2070	−0.45071	−2.0403	+0.0993	0.697	5.993	0.001	3.651
+0.885	+1.2104	−0.45916	−2.0705	+0.0993	0.681	6.089	0.000	3.496
+0.890	+1.2138	−0.46817	−2.1012	+0.0993	0.666	6.194	0.000	3.318
+0.895	+1.2171	−0.47788	−2.1324	+0.0994	0.651	6.309	0.000	3.114
+0.900	+1.2203	−0.48851	−2.1643	+0.0994	0.637	6.439	0.000	2.879
+0.905	+1.2234	−0.50038	−2.1969	+0.0994	0.624	6.589	0.000	2.608
+0.910	+1.2265	−0.51401	−2.2302	+0.0994	0.613	6.769	0.000	2.293

10.8

(1)	(3)	(5)	(6)	(12)	(7)	(8)	(9)	(13)
+0.62	+0.8878	−0.19411	−0.9136	+0.0789	1.789	2.897	4.232	0.299
+0.64	+0.9228	−0.20815	−0.9735	+0.0842	1.706	3.097	4.302	0.234
+0.66	+0.9560	−0.22290	−1.0375	+0.0883	1.619	3.303	4.373	0.182
+0.68	+0.9875	−0.23836	−1.1057	+0.0915	1.532	3.515	4.443	0.138
+0.70	+1.0172	−0.25455	−1.1781	+0.0939	1.443	3.731	4.510	0.103
+0.72	+1.0452	−0.27145	−1.2549	+0.0957	1.353	3.950	4.574	0.075
+0.74	+1.0714	−0.28910	−1.3362	+0.0970	1.264	4.173	4.633	0.054
+0.76	+1.0957	−0.30749	−1.4219	+0.0978	1.175	4.398	4.686	0.037
+0.78	+1.1183	−0.32664	−1.5121	+0.0984	1.087	4.624	4.730	0.025
+0.80	+1.1392	−0.34660	−1.6068	+0.0988	1.001	4.851	4.762	0.017
+0.82	+1.1584	−0.36742	−1.7061	+0.0991	0.918	5.080	4.777	0.011
+0.84	+1.1760	−0.38918	−1.8100	+0.0993	0.838	5.311	4.768	0.007
+0.86	+1.1920	−0.41205	−1.9186	+0.0994	0.761	5.547	4.722	0.004
+0.87	+1.1994	−0.42397	−1.9747	+0.0994	0.724	5.667	4.679	0.004
+0.88	+1.2064	−0.43629	−2.0320	+0.0995	0.688	5.791	4.619	0.003
+0.89	+1.2132	−0.44908	−2.0905	+0.0995	0.654	5.919	4.538	0.002
+0.90	+1.2195	−0.46242	−2.1504	+0.0995	0.620	6.053	4.428	0.002
+0.91	+1.2256	−0.47647	−2.2116	+0.0995	0.588	6.195	4.283	0.001
+0.92	+1.2313	−0.49144	−2.2743	+0.0995	0.557	6.350	4.090	0.001
+0.93	+1.2367	−0.50766	−2.3387	+0.0995	0.528	6.522	3.836	0.001
+0.935	+1.2393	−0.51640	−2.3715	+0.0995	0.514	6.618	3.680	0.001
+0.940	+1.2419	−0.52569	−2.4049	+0.0995	0.500	6.723	3.500	0.000
+0.945	+1.2443	−0.53567	−2.4388	+0.0995	0.487	6.839	3.293	0.000
+0.950	+1.2468	−0.54655	−2.4733	+0.0995	0.475	6.971	3.054	0.000
+0.955	+1.2491	−0.55864	−2.5085	+0.0995	0.463	7.124	2.775	0.000
+0.960	+1.2514	−0.57245	−2.5446	+0.0995	0.453	7.309	2.450	0.000

10.9

(1)	(3)	(5)	(6)	(12)	(7)	(8)	(9)	(13)
+0.72	+1.0452	−0.27133	−1.2548	+0.0957	1.353	3.949	4.583	0.075
+0.74	+1.0714	−0.28893	−1.3360	+0.0970	1.263	4.171	4.645	0.054
+0.76	+1.0957	−0.30725	−1.4217	+0.0979	1.174	4.395	4.704	0.037
+0.78	+1.1183	−0.32631	−1.5119	+0.0985	1.087	4.620	4.756	0.025
+0.80	+1.1392	−0.34612	−1.6065	+0.0989	1.001	4.845	4.799	0.017
+0.82	+1.1584	−0.36670	−1.7057	+0.0992	0.918	5.071	4.832	0.011
+0.84	+1.1759	−0.38812	−1.8094	+0.0993	0.837	5.297	4.850	0.007
+0.86	+1.1919	−0.41043	−1.9176	+0.0994	0.760	5.525	4.846	0.004
+0.88	+1.2064	−0.43378	−2.0304	+0.0995	0.687	5.756	4.811	0.002
+0.89	+1.2130	−0.44591	−2.0886	+0.0995	0.652	5.874	4.777	0.002
+0.90	+1.2194	−0.45839	−2.1479	+0.0996	0.618	5.995	4.727	0.002
+0.91	+1.2254	−0.47130	−2.2085	+0.0996	0.585	6.120	4.658	0.001
+0.92	+1.2311	−0.48470	−2.2703	+0.0996	0.554	6.249	4.565	0.001
+0.93	+1.2365	−0.49872	−2.3335	+0.0996	0.523	6.386	4.440	0.001
+0.94	+1.2416	−0.51353	−2.3981	+0.0996	0.494	6.533	4.274	0.001

10.9 (CONT.)

(1)	(3)	(5)	(6)	(12)	(7)	(8)	(9)	(13)
+0.945	+1.2440	-0.52132	-2.4309	+0.0996	0.480	6.612	4.172	0.000
+0.950	+1.2464	-0.52940	-2.4642	+0.0996	0.466	6.695	4.054	0.000
+0.955	+1.2487	-0.53786	-2.4979	+0.0996	0.453	6.785	3.918	0.000
+0.960	+1.2509	-0.54675	-2.5321	+0.0996	0.440	6.881	3.762	0.000
+0.965	+1.2531	-0.55619	-2.5667	+0.0996	0.428	6.987	3.582	0.000
+0.970	+1.2552	-0.56631	-2.6020	+0.0996	0.416	7.104	3.373	0.000
+0.975	+1.2572	-0.57733	-2.6378	+0.0996	0.405	7.237	3.131	0.000
+0.980	+1.2592	-0.58956	-2.6744	+0.0996	0.394	7.393	2.850	0.000
+0.982	+1.2600	-0.59489	-2.6892	+0.0996	0.391	7.463	2.724	0.000
+0.984	+1.2608	-0.60053	-2.7042	+0.0996	0.387	7.539	2.590	0.000
+0.986	+1.2616	-0.60655	-2.7194	+0.0996	0.383	7.623	2.447	0.000

10.10

(1)	(3)	(5)	(6)	(12)	(7)	(8)	(9)	(13)
+0.78	+1.1183	-0.32603	-1.5117	+0.0985	1.086	4.617	4.777	0.025
+0.80	+1.1392	-0.34572	-1.6063	+0.0989	1.001	4.841	4.830	0.017
+0.82	+1.1584	-0.36612	-1.7053	+0.0992	0.917	5.064	4.878	0.011
+0.84	+1.1759	-0.38725	-1.8088	+0.0994	0.837	5.286	4.918	0.007
+0.86	+1.1918	-0.40912	-1.9168	+0.0995	0.759	5.508	4.950	0.004
+0.88	+1.2063	-0.43177	-2.0291	+0.0995	0.686	5.729	4.969	0.003
+0.90	+1.2193	-0.45526	-2.1459	+0.0996	0.617	5.951	4.972	0.001
+0.92	+1.2310	-0.47969	-2.2672	+0.0996	0.551	6.175	4.950	0.001
+0.94	+1.2414	-0.50524	-2.3930	+0.0996	0.491	6.407	4.890	0.000
+0.95	+1.2462	-0.51853	-2.4577	+0.0996	0.462	6.527	4.840	0.000
+0.96	+1.2506	-0.53224	-2.5236	+0.0996	0.435	6.651	4.769	0.000
+0.97	+1.2549	-0.54646	-2.5907	+0.0996	0.408	6.781	4.674	0.000
+0.98	+1.2588	-0.56131	-2.6592	+0.0996	0.383	6.920	4.545	0.000
+0.99	+1.2625	-0.57699	-2.7291	+0.0996	0.359	7.071	4.373	0.000
+1.00	+1.2660	-0.59378	-2.8007	+0.0996	0.337	7.241	4.142	0.000
+1.005	+1.2677	-0.60273	-2.8371	+0.0996	0.326	7.335	3.999	0.000
+1.010	+1.2693	-0.61215	-2.8740	+0.0996	0.315	7.437	3.832	0.000
+1.015	+1.2708	-0.62218	-2.9115	+0.0996	0.305	7.551	3.640	0.000
+1.020	+1.2723	-0.63297	-2.9496	+0.0996	0.296	7.679	3.415	0.000
+1.022	+1.2729	-0.63755	-2.9650	+0.0996	0.292	7.735	3.314	0.000
+1.024	+1.2735	-0.64231	-2.9805	+0.0996	0.289	7.795	3.208	0.000
+1.026	+1.2741	-0.64728	-2.9962	+0.0996	0.285	7.859	3.094	0.000
+1.028	+1.2746	-0.65248	-3.0120	+0.0996	0.282	7.927	2.972	0.000
+1.030	+1.2752	-0.65796	-3.0279	+0.0996	0.279	8.001	2.843	0.000
+1.032	+1.2757	-0.66376	-3.0440	+0.0996	0.275	8.082	2.704	0.000
+1.034	+1.2763	-0.66994	-3.0602	+0.0996	0.273	8.170	2.556	0.000
+1.036	+1.2768	-0.67658	-3.0767	+0.0996	0.270	8.268	2.397	0.000

10.11

(1)	(3)	(5)	(6)	(12)	(7)	(8)	(9)	(13)
+0.86	+1.1918	-0.40873	-1.9165	+0.0995	0.759	5.503	4.980	0.004
+0.87	+1.1992	-0.41987	-1.9721	+0.0995	0.722	5.612	4.999	0.003
+0.88	+1.2063	-0.43119	-2.0288	+0.0995	0.686	5.721	5.016	0.003
+0.89	+1.2130	-0.44268	-2.0865	+0.0996	0.650	5.830	5.031	0.002
+0.90	+1.2193	-0.45436	-2.1454	+0.0996	0.616	5.938	5.045	0.001
+0.91	+1.2253	-0.46623	-2.2053	+0.0996	0.583	6.047	5.056	0.001
+0.92	+1.2310	-0.47828	-2.2663	+0.0996	0.551	6.155	5.064	0.001
+0.93	+1.2363	-0.49054	-2.3284	+0.0996	0.520	6.264	5.069	0.001
+0.94	+1.2414	-0.50300	-2.3916	+0.0996	0.490	6.373	5.071	0.000
+0.95	+1.2461	-0.51568	-2.4558	+0.0996	0.461	6.483	5.068	0.000
+0.96	+1.2506	-0.52860	-2.5212	+0.0996	0.433	6.595	5.059	0.000
+0.97	+1.2548	-0.54176	-2.5877	+0.0996	0.407	6.707	5.043	0.000
+0.98	+1.2587	-0.55521	-2.6554	+0.0996	0.381	6.822	5.018	0.000
+0.99	+1.2624	-0.56897	-2.7242	+0.0996	0.357	6.940	4.982	0.000
+1.00	+1.2659	-0.58309	-2.7942	+0.0996	0.333	7.063	4.930	0.000
+1.01	+1.2691	-0.59764	-2.8655	+0.0996	0.311	7.190	4.859	0.000
+1.02	+1.2721	-0.61272	-2.9380	+0.0996	0.290	7.325	4.762	0.000
+1.03	+1.2749	-0.62846	-3.0120	+0.0996	0.270	7.471	4.630	0.000
+1.04	+1.2775	-0.64508	-3.0875	+0.0996	0.251	7.631	4.452	0.000
+1.045	+1.2787	-0.65380	-3.1259	+0.0996	0.242	7.719	4.340	0.000
+1.050	+1.2799	-0.66288	-3.1647	+0.0996	0.233	7.813	4.210	0.000
+1.055	+1.2811	-0.67239	-3.2040	+0.0996	0.225	7.915	4.059	0.000
+1.060	+1.2822	-0.68242	-3.2439	+0.0996	0.217	8.028	3.881	0.000
+1.065	+1.2832	-0.69313	-3.2843	+0.0996	0.209	8.154	3.674	0.000
+1.070	+1.2843	-0.70470	-3.3255	+0.0996	0.202	8.298	3.430	0.000
+1.072	+1.2847	-0.70964	-3.3421	+0.0996	0.199	8.362	3.320	0.000
+1.074	+1.2851	-0.71478	-3.3589	+0.0996	0.196	8.431	3.203	0.000
+1.076	+1.2855	-0.72018	-3.3759	+0.0996	0.194	8.505	3.078	0.000
+1.078	+1.2859	-0.72585	-3.3930	+0.0996	0.191	8.584	2.943	0.000
+1.080	+1.2862	-0.73186	-3.4102	+0.0996	0.189	8.672	2.799	0.000
+1.082	+1.2866	-0.73827	-3.4276	+0.0996	0.186	8.768	2.644	0.000
+1.084	+1.2870	-0.74516	-3.4453	+0.0996	0.184	8.875	2.478	0.000

10.12

(1)	(3)	(5)	(6)	(12)	(7)	(8)	(9)	(13)
+0.70	+1.0172	-0.25435	-1.1780	+0.0939	1.443	3.729	4.524	0.104
+0.72	+1.0452	-0.27119	-1.2548	+0.0957	1.353	3.948	4.593	0.075
+0.74	+1.0714	-0.28874	-1.3359	+0.0970	1.263	4.170	4.660	0.054
+0.76	+1.0957	-0.30698	-1.4216	+0.0979	1.174	4.392	4.725	0.038
+0.78	+1.1183	-0.32592	-1.5116	+0.0985	1.086	4.616	4.786	0.026
+0.80	+1.1392	-0.34556	-1.6062	+0.0989	1.000	4.839	4.843	0.017
+0.82	+1.1584	-0.36588	-1.7052	+0.0992	0.917	5.061	4.896	0.011
+0.84	+1.1759	-0.38690	-1.8086	+0.0994	0.836	5.282	4.945	0.007
+0.86	+1.1918	-0.40861	-1.9164	+0.0995	0.759	5.501	4.991	0.004

10.13

(1)	(3)	(5)	(6)	(12)	(7)	(8)	(9)	(13)
+0.56	+0.7733	-0.15609	-0.7568	+0.0546	2.023	2.341	4.028	0.527
+0.58	+0.8130	-0.16805	-0.8054	+0.0643	1.949	2.518	4.096	0.442
+0.60	+0.8512	-0.18068	-0.8576	+0.0723	1.870	2.703	4.166	0.364
+0.62	+0.8878	-0.19401	-0.9135	+0.0789	1.789	2.896	4.238	0.294
+0.64	+0.9227	-0.20802	-0.9734	+0.0842	1.705	3.096	4.311	0.234
+0.66	+0.9560	-0.22273	-1.0374	+0.0883	1.619	3.301	4.384	0.182
+0.68	+0.9875	-0.23814	-1.1055	+0.0915	1.532	3.513	4.458	0.139
+0.70	+1.0172	-0.25425	-1.1779	+0.0939	1.442	3.728	4.531	0.104
+0.72	+1.0452	-0.27105	-1.2547	+0.0957	1.353	3.947	4.603	0.076
+0.74	+1.0713	-0.28854	-1.3358	+0.0970	1.263	4.168	4.674	0.054
+0.76	+1.0957	-0.30671	-1.4214	+0.0979	1.174	4.389	4.744	0.038
+0.78	+1.1183	-0.32554	-1.5114	+0.0985	1.086	4.612	4.814	0.026
+0.80	+1.1392	-0.34502	-1.6058	+0.0989	1.000	4.833	4.885	0.017
+0.81	+1.1490	-0.35499	-1.6547	+0.0991	0.958	4.942	4.921	0.014
+0.82	+1.1583	-0.36510	-1.7047	+0.0992	0.916	5.052	4.958	0.011
+0.83	+1.1673	-0.37536	-1.7557	+0.0993	0.876	5.160	4.997	0.009
+0.84	+1.1758	-0.38575	-1.8079	+0.0994	0.836	5.267	5.038	0.007
+0.85	+1.1840	-0.39627	-1.8611	+0.0994	0.796	5.374	5.082	0.005
+0.86	+1.1918	-0.40690	-1.9153	+0.0995	0.758	5.479	5.130	0.004
+0.87	+1.1992	-0.41762	-1.9706	+0.0995	0.721	5.582	5.183	0.003
+0.88	+1.2062	-0.42843	-2.0270	+0.0996	0.684	5.684	5.244	0.003
+0.89	+1.2129	-0.43929	-2.0843	+0.0996	0.649	5.783	5.314	0.002
+0.90	+1.2192	-0.45018	-2.1426	+0.0996	0.614	5.880	5.395	0.002
+0.91	+1.2252	-0.46108	-2.2019	+0.0996	0.581	5.974	5.492	0.001
+0.92	+1.2308	-0.47192	-2.2621	+0.0996	0.548	6.064	5.609	0.001
+0.93	+1.2361	-0.48268	-2.3231	+0.0996	0.517	6.149	5.752	0.001
+0.94	+1.2411	-0.49328	-2.3850	+0.0996	0.486	6.229	5.926	0.001
+0.95	+1.2458	-0.50368	-2.4477	+0.0997	0.457	6.303	6.142	0.001
+0.96	+1.2503	-0.51378	-2.5111	+0.0997	0.429	6.369	6.412	0.000

10.14

(1)	(3)	(5)	(6)	(12)	(7)	(8)	(13)	(9)
+0.36	+0.3079	-0.07018	-0.4325	-0.1521	2.569	1.043	1.555	3.527
+0.38	+0.3589	-0.07632	-0.4543	-0.1220	2.530	1.136	1.454	3.563
+0.40	+0.4091	-0.08294	-0.4780	-0.0940	2.488	1.236	1.351	3.602
+0.42	+0.4584	-0.09006	-0.5038	-0.0680	2.443	1.344	1.245	3.644
+0.44	+0.5068	-0.09770	-0.5318	-0.0442	2.394	1.460	1.138	3.690
+0.46	+0.5541	-0.10589	-0.5623	-0.0225	2.341	1.585	1.031	3.740
+0.48	+0.6004	-0.11466	-0.5953	-0.0029	2.285	1.718	0.924	3.793
+0.50	+0.6455	-0.12402	-0.6310	+0.0145	2.226	1.860	0.819	3.850
+0.52	+0.6894	-0.13399	-0.6697	+0.0299	2.162	2.011	0.717	3.910
+0.54	+0.7320	-0.14460	-0.7115	+0.0432	2.094	2.171	0.620	3.974
+0.56	+0.7732	-0.15584	-0.7566	+0.0547	2.023	2.339	0.528	4.042
+0.58	+0.8129	-0.16774	-0.8052	+0.0644	1.948	2.516	0.442	4.114
+0.60	+0.8511	-0.18030	-0.8573	+0.0725	1.870	2.700	0.365	4.190
+0.62	+0.8877	-0.19352	-0.9132	+0.0791	1.789	2.892	0.296	4.269
+0.64	+0.9226	-0.20740	-0.9730	+0.0844	1.705	3.091	0.235	4.352
+0.66	+0.9559	-0.22193	-1.0369	+0.0885	1.619	3.295	0.183	4.439
+0.68	+0.9874	-0.23709	-1.1048	+0.0917	1.531	3.503	0.140	4.531
+0.70	+1.0171	-0.25284	-1.1770	+0.0942	1.441	3.715	0.105	4.631
+0.72	+1.0450	-0.26915	-1.2534	+0.0960	1.351	3.928	0.077	4.742
+0.74	+1.0711	-0.28594	-1.3341	+0.0973	1.261	4.141	0.055	4.870
+0.76	+1.0955	-0.30312	-1.4190	+0.0982	1.171	4.351	0.039	5.021

(1)	(3)	(5)	(6)	(12)	(7)	(8)	(13)	(9)
-0.70	-2.7798	-0.00056	-0.2039	-2.9843	2.996	0.008	2.986	3.204
-0.68	-2.7199	-0.00062	-0.2040	-2.9246	2.996	0.009	2.985	3.205
-0.66	-2.6600	-0.00068	-0.2042	-2.8649	2.995	0.010	2.983	3.205
-0.64	-2.6001	-0.00075	-0.2044	-2.8052	2.995	0.011	2.982	3.205
-0.62	-2.5402	-0.00082	-0.2047	-2.7456	2.995	0.012	2.980	3.205
-0.60	-2.4803	-0.00090	-0.2049	-2.6860	2.994	0.013	2.978	3.206
-0.58	-2.4204	-0.00098	-0.2052	-2.6265	2.994	0.014	2.976	3.206
-0.56	-2.3606	-0.00108	-0.2055	-2.5670	2.993	0.016	2.974	3.207
-0.54	-2.3007	-0.00118	-0.2058	-2.5075	2.993	0.017	2.971	3.207
-0.52	-2.2409	-0.00130	-0.2062	-2.4481	2.992	0.019	2.968	3.208
-0.50	-2.1810	-0.00142	-0.2066	-2.3888	2.991	0.021	2.965	3.208
-0.48	-2.1212	-0.00156	-0.2070	-2.3295	2.990	0.023	2.962	3.209
-0.46	-2.0614	-0.00171	-0.2075	-2.2703	2.990	0.025	2.958	3.210
-0.44	-2.0016	-0.00187	-0.2080	-2.2112	2.989	0.028	2.954	3.211
-0.42	-1.9419	-0.00205	-0.2086	-2.1522	2.988	0.030	2.950	3.212
-0.40	-1.8821	-0.00225	-0.2092	-2.0932	2.986	0.033	2.945	3.213
-0.38	-1.8224	-0.00246	-0.2099	-2.0344	2.985	0.036	2.940	3.215
-0.36	-1.7627	-0.00270	-0.2107	-1.9756	2.984	0.039	2.934	3.216
-0.34	-1.7031	-0.00296	-0.2116	-1.9170	2.982	0.044	2.927	3.218
-0.32	-1.6435	-0.00324	-0.2125	-1.8585	2.980	0.048	2.921	3.219
-0.30	-1.5839	-0.00356	-0.2135	-1.8002	2.978	0.052	2.913	3.221
-0.28	-1.5243	-0.00390	-0.2146	-1.7420	2.976	0.057	2.905	3.224
-0.26	-1.4648	-0.00427	-0.2158	-1.6840	2.974	0.063	2.896	3.226
-0.24	-1.4054	-0.00468	-0.2171	-1.6261	2.971	0.069	2.886	3.228
-0.22	-1.3460	-0.00513	-0.2185	-1.5685	2.969	0.076	2.875	3.231
-0.20	-1.2866	-0.00562	-0.2201	-1.5112	2.966	0.083	2.863	3.234
-0.18	-1.2273	-0.00616	-0.2218	-1.4540	2.962	0.091	2.850	3.237
-0.16	-1.1681	-0.00675	-0.2238	-1.3971	2.959	0.100	2.836	3.241
-0.14	-1.1090	-0.00739	-0.2258	-1.3406	2.954	0.109	2.821	3.245
-0.12	-1.0499	-0.00809	-0.2281	-1.2843	2.950	0.120	2.804	3.250
-0.10	-0.9910	-0.00887	-0.2306	-1.2284	2.946	0.131	2.786	3.254
-0.08	-0.9321	-0.00971	-0.2334	-1.1729	2.940	0.144	2.766	3.260
-0.06	-0.8733	-0.01063	-0.2364	-1.1178	2.935	0.158	2.744	3.266
-0.04	-0.8147	-0.01164	-0.2397	-1.0631	2.929	0.173	2.720	3.272
-0.02	-0.7562	-0.01275	-0.2433	-1.0090	2.922	0.189	2.694	3.279
-0.00	-0.6978	-0.01395	-0.2473	-0.9554	2.914	0.207	2.666	3.288
+0.02	-0.6396	-0.01527	-0.2516	-0.9023	2.906	0.227	2.636	3.296
+0.04	-0.5816	-0.01671	-0.2564	-0.8500	2.897	0.248	2.603	3.306
+0.06	-0.5237	-0.01828	-0.2616	-0.7982	2.888	0.272	2.567	3.317
+0.08	-0.4661	-0.01999	-0.2673	-0.7473	2.876	0.298	2.528	3.328
+0.10	-0.4087	-0.02186	-0.2735	-0.6972	2.864	0.326	2.486	3.341
+0.12	-0.3515	-0.02390	-0.2804	-0.6479	2.851	0.357	2.440	3.355
+0.14	-0.2946	-0.02612	-0.2878	-0.5996	2.837	0.390	2.391	3.371
+0.16	-0.2380	-0.02854	-0.2960	-0.5523	2.822	0.427	2.338	3.388
+0.18	-0.1818	-0.03117	-0.3050	-0.5061	2.805	0.467	2.282	3.407
+0.20	-0.1258	-0.03403	-0.3147	-0.4610	2.787	0.511	2.221	3.428
+0.22	-0.0703	-0.03713	-0.3254	-0.4173	2.767	0.558	2.156	3.451
+0.24	-0.0152	-0.04050	-0.3371	-0.3748	2.745	0.610	2.087	3.477
+0.26	+0.0395	-0.04416	-0.3498	-0.3338	2.722	0.666	2.013	3.506
+0.28	+0.0937	-0.04811	-0.3638	-0.2944	2.696	0.727	1.935	3.538
+0.30	+0.1473	-0.05239	-0.3790	-0.2565	2.668	0.794	1.852	3.574
+0.32	+0.2004	-0.05700	-0.3955	-0.2203	2.637	0.866	1.765	3.614
+0.34	+0.2528	-0.06198	-0.4136	-0.1859	2.604	0.943	1.674	3.658
+0.36	+0.3045	-0.06732	-0.4333	-0.1534	2.568	1.028	1.579	3.709
+0.38	+0.3554	-0.07306	-0.4548	-0.1228	2.529	1.118	1.481	3.766
+0.40	+0.4056	-0.07921	-0.4781	-0.0942	2.486	1.216	1.380	3.830
+0.42	+0.4549	-0.08576	-0.5034	-0.0676	2.440	1.320	1.277	3.904
+0.44	+0.5032	-0.09273	-0.5309	-0.0431	2.391	1.432	1.173	3.988
+0.46	+0.5505	-0.10012	-0.5608	-0.0207	2.338	1.551	1.069	4.086
+0.48	+0.5967	-0.10790	-0.5935	-0.0004	2.279	1.677	0.963	4.208

11.1

(1)	(4)	(5)	(6)	(7)	(8)	(9)
-0.70	+2.5786	-0.00050	-0.0029	2.993	0.013	5.728
-0.65	+2.4289	-0.00063	-0.0036	2.992	0.017	5.730
-0.60	+2.2794	-0.00080	-0.0046	2.990	0.021	5.733
-0.55	+2.1300	-0.00100	-0.0058	2.987	0.026	5.735
-0.50	+1.9807	-0.00126	-0.0072	2.983	0.033	5.745
-0.45	+1.8316	-0.00159	-0.0091	2.979	0.042	5.752
-0.40	+1.6828	-0.00200	-0.0114	2.974	0.052	5.761
-0.35	+1.5342	-0.00251	-0.0144	2.967	0.066	5.774
-0.30	+1.3861	-0.00315	-0.0181	2.959	0.083	5.790
-0.25	+1.2384	-0.00395	-0.0227	2.949	0.104	5.810
-0.20	+1.0913	-0.00494	-0.0286	2.935	0.130	5.836
-0.15	+0.9449	-0.00619	-0.0358	2.919	0.163	5.872
-0.10	+0.7994	-0.00774	-0.0450	2.899	0.203	5.913
-0.05	+0.6551	-0.00966	-0.0564	2.873	0.254	5.969
0.00	+0.5122	-0.01202	-0.0706	2.842	0.316	6.042
+0.05	+0.3710	-0.01492	-0.0882	2.804	0.393	6.142
+0.10	+0.2320	-0.01844	-0.1101	2.756	0.486	6.273
+0.15	+0.0956	-0.02269	-0.1371	2.698	0.599	6.453
+0.20	-0.0376	-0.02774	-0.1703	2.629	0.733	6.701
+0.25	-0.1670	-0.03363	-0.2109	2.545	0.893	7.058
+0.300	-0.2918	-0.04036	-0.2600	2.446	1.077	7.568
+0.325	-0.3523	-0.04400	-0.2882	2.390	1.178	7.913
+0.350	-0.4113	-0.04779	-0.3190	2.330	1.286	8.335
+0.375	-0.4688	-0.05169	-0.3525	2.266	1.398	8.862
+0.400	-0.5246	-0.05566	-0.3889	2.198	1.514	9.515
+0.425	-0.5787	-0.05962	-0.4283	2.126	1.634	10.34
+0.450	-0.6309	-0.06353	-0.4707	2.051	1.756	11.39
+0.475	-0.6812	-0.06731	-0.5161	1.972	1.877	12.73
+0.500	-0.7295	-0.07088	-0.5645	1.892	1.997	14.46
+0.525	-0.7758	-0.07420	-0.6159	1.809	2.114	16.70
+0.550	-0.8191	-0.07720	-0.6702	1.726	2.224	19.63
+0.575	-0.8621	-0.07986	-0.7271	1.643	2.328	23.48
+0.600	-0.9022	-0.08216	-0.7865	1.562	2.423	28.54
+0.625	-0.9402	-0.08410	-0.8481	1.482	2.508	35.26
+0.650	-0.9763	-0.08572	-0.9118	1.405	2.582	44.19
+0.675	-1.0105	-0.08704	-0.9772	1.332	2.646	56.10
+0.700	-1.0429	-0.08809	-1.0440	1.262	2.698	71.97
+0.725	-1.0736	-0.08893	-1.1120	1.198	2.739	93.17
+0.750	-1.1028	-0.08958	-1.1808	1.138	2.770	121.5
+0.775	-1.1305	-0.09008	-1.2504	1.082	2.790	159.2
+0.800	-1.1570	-0.09046	-1.3203	1.031	2.802	209.4
+0.825	-1.1821	-0.09075	-1.3904	0.984	2.805	276.3
+0.850	-1.2062	-0.09098	-1.4604	0.942	2.800	365.0
+0.875	-1.2293	-0.09114	-1.5303	0.905	2.789	482.2
+0.900	-1.2515	-0.09127	-1.5998	0.871	2.772	636.3
+0.925	-1.2729	-0.09136	-1.6688	0.841	2.749	838.9
+0.950	-1.2935	-0.09143	-1.7372	0.814	2.722	1104.
+0.975	-1.3136	-0.09149	-1.8049	0.791	2.692	1448.
+1.000	-1.3331	-0.09153	-1.8718	0.770	2.658	1895.
+1.025	-1.3521	-0.09156	-1.9378	0.753	2.622	2471.
+1.050	-1.3708	-0.09158	-2.0029	0.738	2.584	3211.

11.2

(1)	(4)	(5)	(6)	(7)	(8)	(9)
-0.70	+2.57849	-0.000602	-0.00288	2.994	0.014	4.742
-0.68	+2.51862	-0.000660	-0.00316	2.993	0.014	4.742
-0.66	+2.45876	-0.000724	-0.00346	2.992	0.016	4.742
-0.64	+2.39892	-0.000795	-0.00379	2.992	0.017	4.742
-0.62	+2.33910	-0.000872	-0.00416	2.991	0.019	4.742
-0.60	+2.27928	-0.000956	-0.00456	2.990	0.021	4.743
-0.58	+2.21949	-0.001049	-0.00500	2.989	0.023	4.743
-0.56	+2.15972	-0.001150	-0.00548	2.988	0.025	4.743
-0.54	+2.09997	-0.001262	-0.00601	2.987	0.028	4.743
-0.52	+2.04024	-0.001384	-0.00659	2.986	0.030	4.743
-0.50	+1.98055	-0.001517	-0.00722	2.984	0.033	4.743
-0.48	+1.92088	-0.001664	-0.00792	2.983	0.036	4.743
-0.46	+1.86124	-0.001825	-0.00868	2.981	0.040	4.743
-0.44	+1.80163	-0.002001	-0.00952	2.979	0.044	4.743
-0.42	+1.74207	-0.002194	-0.01043	2.977	0.048	4.743
-0.40	+1.68254	-0.002405	-0.01143	2.975	0.052	4.743
-0.38	+1.62306	-0.002637	-0.01253	2.973	0.058	4.743
-0.36	+1.56363	-0.002890	-0.01374	2.970	0.063	4.744
-0.34	+1.50425	-0.003168	-0.01506	2.967	0.069	4.744
-0.32	+1.44494	-0.003473	-0.01650	2.964	0.076	4.744

11.2 (CONT.)

(1)	(4)	(5)	(6)	(7)	(8)	(9)
-0.30	+1.38569	-0.003807	-0.01808	2.961	0.083	4.744
-0.28	+1.32651	-0.004172	-0.01982	2.957	0.091	4.744
-0.26	+1.26741	-0.004572	-0.02172	2.953	0.099	4.745
-0.24	+1.20839	-0.005010	-0.02380	2.948	0.109	4.745
-0.22	+1.14947	-0.005490	-0.02607	2.944	0.119	4.745
-0.20	+1.09065	-0.006016	-0.02857	2.938	0.130	4.746
-0.18	+1.03194	-0.006591	-0.03130	2.932	0.143	4.746
-0.16	+0.97335	-0.007221	-0.03429	2.926	0.156	4.746
-0.14	+0.91490	-0.007910	-0.03756	2.919	0.171	4.747
-0.12	+0.85659	-0.008663	-0.04113	2.912	0.187	4.747
-0.10	+0.79844	-0.009488	-0.04505	2.903	0.205	4.748
-0.08	+0.74047	-0.010390	-0.04933	2.894	0.224	4.748
-0.06	+0.68268	-0.011376	-0.05401	2.884	0.245	4.749
-0.04	+0.62510	-0.012454	-0.05913	2.874	0.268	4.750
-0.02	+0.56774	-0.013632	-0.06473	2.862	0.292	4.750
0.00	+0.51063	-0.014918	-0.07084	2.849	0.319	4.751
+0.02	+0.45379	-0.016324	-0.07752	2.835	0.349	4.752
+0.04	+0.39723	-0.017858	-0.08481	2.820	0.381	4.753
+0.06	+0.34099	-0.019532	-0.09276	2.804	0.416	4.755
+0.08	+0.28508	-0.021357	-0.10145	2.786	0.453	4.756
+0.10	+0.22955	-0.023348	-0.11091	2.767	0.494	4.758
+0.12	+0.17442	-0.025516	-0.12123	2.746	0.538	4.760
+0.14	+0.11972	-0.027877	-0.13247	2.724	0.586	4.762
+0.16	+0.06549	-0.030447	-0.14471	2.699	0.638	4.764
+0.18	+0.01177	-0.033241	-0.15803	2.673	0.694	4.767
+0.20	-0.04140	-0.036278	-0.17251	2.645	0.754	4.770
+0.22	-0.0940	-0.03958	-0.1882	2.614	0.820	4.772
+0.24	-0.1460	-0.04315	-0.2053	2.582	0.890	4.777
+0.26	-0.1972	-0.04703	-0.2239	2.546	0.964	4.783
+0.28	-0.2478	-0.05122	-0.2439	2.509	1.045	4.788
+0.30	-0.2976	-0.05576	-0.2657	2.469	1.131	4.794
+0.32	-0.3466	-0.06067	-0.2892	2.426	1.222	4.804
+0.34	-0.3946	-0.06595	-0.3146	2.381	1.320	4.812
+0.36	-0.4418	-0.07164	-0.3420	2.333	1.424	4.825
+0.38	-0.4879	-0.07776	-0.3716	2.282	1.534	4.838
+0.40	-0.5330	-0.08433	-0.4034	2.228	1.650	4.855
+0.42	-0.5770	-0.09136	-0.4376	2.172	1.772	4.875
+0.44	-0.6198	-0.09887	-0.4743	2.112	1.900	4.901
+0.46	-0.6615	-0.10687	-0.5137	2.050	2.034	4.933
+0.48	-0.7018	-0.11537	-0.5557	1.986	2.173	4.974
+0.50	-0.7409	-0.12435	-0.6006	1.918	2.318	5.025
+0.52	-0.7785	-0.13381	-0.6485	1.848	2.468	5.092
+0.54	-0.8148	-0.14373	-0.6994	1.776	2.621	5.177
+0.56	-0.8496	-0.15404	-0.7534	1.702	2.777	5.290
+0.58	-0.8828	-0.16470	-0.8105	1.627	2.934	5.439
+0.60	-0.9146	-0.17559	-0.8708	1.550	3.092	5.639
+0.62	-0.9448	-0.18658	-0.9342	1.471	3.246	5.908
+0.64	-0.9734	-0.19751	-1.0006	1.392	3.396	6.274
+0.66	-1.0005	-0.20816	-1.0699	1.312	3.537	6.777
+0.68	-1.0259	-0.21831	-1.1420	1.232	3.666	7.470
+0.70	-1.0498	-0.22772	-1.2164	1.152	3.780	8.435
+0.72	-1.0720	-0.23617	-1.2930	1.075	3.874	9.778
+0.74	-1.0928	-0.24353	-1.3713	0.999	3.947	11.66
+0.76	-1.1120	-0.24971	-1.4508	0.927	3.997	14.28
+0.78	-1.1298	-0.25475	-1.5310	0.859	4.024	17.93
+0.80	-1.1464	-0.25874	-1.6116	0.796	4.028	22.99
+0.81	-1.1542	-0.26038	-1.6518	0.766	4.023	26.21
+0.82	-1.1617	-0.26181	-1.6920	0.738	4.014	29.98
+0.83	-1.1690	-0.26306	-1.7320	0.711	4.000	34.42
+0.84	-1.1760	-0.26414	-1.7720	0.686	3.982	39.58
+0.85	-1.1827	-0.26508	-1.8117	0.662	3.961	45.65
+0.86	-1.1892	-0.26588	-1.8512	0.639	3.936	52.70
+0.87	-1.1955	-0.26658	-1.8904	0.618	3.909	60.92
+0.88	-1.2016	-0.26717	-1.9293	0.597	3.879	70.48
+0.89	-1.2074	-0.26768	-1.9679	0.578	3.847	81.56
+0.90	-1.2131	-0.26812	-2.0062	0.561	3.813	94.38
+0.91	-1.2187	-0.26849	-2.0442	0.544	3.777	109.2
+0.92	-1.2240	-0.26881	-2.0818	0.528	3.740	126.3
+0.93	-1.2292	-0.26909	-2.1190	0.514	3.701	145.9
+0.94	-1.2343	-0.26932	-2.1558	0.500	3.661	168.5
+0.95	-1.2392	-0.26952	-2.1922	0.488	3.620	194.5
+0.96	-1.2441	-0.26970	-2.2282	0.476	3.579	224.0
+0.97	-1.2488	-0.26984	-2.2638	0.465	3.537	257.8
+0.98	-1.2534	-0.26997	-2.2990	0.455	3.494	296.4
+0.99	-1.2579	-0.27008	-2.3337	0.445	3.451	340.3
+1.00	-1.2623	-0.27018	-2.3680	0.436	3.408	389.9

11.3

(1)	(4)	(5)	(6)	(7)	(8)	(9)
+0.20	-0.04150	-0.036513	-0.17257	2.645	0.755	4.731
+0.22	-0.09410	-0.039841	-0.18832	2.615	0.820	4.732
+0.24	-0.14607	-0.043454	-0.20542	2.582	0.890	4.733
+0.26	-0.19737	-0.047372	-0.22396	2.547	0.966	4.735
+0.28	-0.24794	-0.051618	-0.24407	2.510	1.046	4.736
+0.30	-0.29774	-0.056214	-0.26585	2.470	1.132	4.738
+0.32	-0.34671	-0.061184	-0.28940	2.427	1.224	4.741
+0.34	-0.39480	-0.066553	-0.31486	2.382	1.322	4.744
+0.36	-0.44196	-0.072344	-0.34234	2.334	1.427	4.747
+0.38	-0.48814	-0.078582	-0.37196	2.283	1.537	4.751
+0.40	-0.53326	-0.085293	-0.40386	2.229	1.654	4.756
+0.42	-0.57729	-0.092501	-0.43817	2.173	1.777	4.762
+0.44	-0.62016	-0.100229	-0.47500	2.114	1.907	4.770
+0.46	-0.66182	-0.108501	-0.51450	2.052	2.043	4.780
+0.48	-0.70222	-0.117335	-0.55677	1.988	2.186	4.792
+0.50	-0.74131	-0.126750	-0.60196	1.921	2.334	4.807
+0.52	-0.7790	-0.13676	-0.6502	1.852	2.488	4.827
+0.54	-0.8154	-0.14736	-0.7015	1.780	2.647	4.853
+0.56	-0.8502	-0.15857	-0.7561	1.707	2.811	4.888
+0.58	-0.8836	-0.17036	-0.8140	1.632	2.978	4.933
+0.60	-0.9155	-0.18271	-0.8752	1.556	3.150	4.995
+0.62	-0.9458	-0.19556	-0.9400	1.478	3.322	5.079
+0.64	-0.9746	-0.20884	-1.0081	1.400	3.495	5.194
+0.66	-1.0018	-0.22243	-1.0798	1.321	3.666	5.355
+0.68	-1.0275	-0.23616	-1.1548	1.242	3.834	5.581
+0.70	-1.0515	-0.24982	-1.2330	1.162	3.993	5.901
+0.72	-1.0739	-0.26312	-1.3149	1.082	4.140	6.376
+0.73	-1.0846	-0.26952	-1.3566	1.043	4.208	6.679
+0.74	-1.0948	-0.27570	-1.3990	1.004	4.270	7.045
+0.75	-1.1046	-0.28162	-1.4420	0.966	4.328	7.488
+0.76	-1.1141	-0.28725	-1.4856	0.928	4.379	8.019
+0.77	-1.1232	-0.29253	-1.5296	0.891	4.423	8.659
+0.78	-1.1319	-0.29745	-1.5740	0.854	4.461	9.433
+0.79	-1.1403	-0.30199	-1.6188	0.818	4.490	10.36
+0.80	-1.1483	-0.30612	-1.6638	0.783	4.512	11.49
+0.81	-1.1560	-0.30984	-1.7090	0.750	4.527	12.84
+0.82	-1.1633	-0.31317	-1.7542	0.718	4.534	14.47
+0.83	-1.1703	-0.31612	-1.7996	0.686	4.534	16.43
+0.84	-1.1770	-0.31870	-1.8450	0.656	4.526	18.77
+0.85	-1.1834	-0.32095	-1.8902	0.627	4.512	21.58
+0.86	-1.1896	-0.32289	-1.9352	0.600	4.492	24.94
+0.87	-1.1954	-0.32456	-1.9800	0.574	4.467	28.95
+0.88	-1.2010	-0.32599	-2.0245	0.550	4.436	33.71
+0.89	-1.2064	-0.32720	-2.0687	0.527	4.402	39.34
+0.90	-1.2116	-0.32824	-2.1125	0.506	4.363	46.03
+0.91	-1.2166	-0.32911	-2.1560	0.486	4.322	53.94
+0.92	-1.2213	-0.32985	-2.1990	0.467	4.277	63.25
+0.93	-1.2259	-0.33047	-2.2415	0.450	4.230	74.20
+0.94	-1.2303	-0.33099	-2.2836	0.434	4.181	87.03
+0.95	-1.2346	-0.33143	-2.3251	0.419	4.130	102.0
+0.96	-1.2387	-0.33180	-2.3662	0.405	4.078	119.5
+0.97	-1.2427	-0.33212	-2.4067	0.392	4.025	139.9
+0.98	-1.2465	-0.33238	-2.4466	0.380	3.971	163.6
+0.99	-1.2502	-0.33261	-2.4861	0.368	3.916	190.8
+1.00	-1.2539	-0.33280	-2.5250	0.358	3.861	222.5
+1.01	-1.2574	-0.33296	-2.5633	0.348	3.805	258.8
+1.02	-1.2608	-0.33309	-2.6011	0.340	3.749	300.6

11.4

(1)	(4)	(5)	(6)	(7)	(8)	(9)
+0.50	-0.7415	-0.12770	-0.6025	1.922	2.340	4.724
+0.52	-0.7792	-0.13794	-0.6508	1.853	2.495	4.725
+0.54	-0.8156	-0.14884	-0.7023	1.782	2.657	4.728
+0.56	-0.8505	-0.16043	-0.7572	1.709	2.824	4.732
+0.58	-0.8839	-0.17272	-0.8154	1.634	2.996	4.736
+0.60	-0.9159	-0.18574	-0.8770	1.559	3.174	4.742
+0.62	-0.9463	-0.19950	-0.9423	1.482	3.355	4.750
+0.64	-0.9751	-0.21400	-1.0113	1.404	3.541	4.762
+0.66	-1.0024	-0.22924	-1.0840	1.327	3.730	4.778
+0.68	-1.0282	-0.24522	-1.1605	1.249	3.921	4.801
+0.70	-1.0524	-0.26190	-1.2409	1.171	4.114	4.835
+0.72	-1.0750	-0.27924	-1.3251	1.094	4.308	4.883
+0.73	-1.0858	-0.28813	-1.3686	1.056	4.405	4.916
+0.74	-1.0962	-0.29715	-1.4132	1.018	4.501	4.955
+0.75	-1.1062	-0.30629	-1.4587	0.980	4.597	5.004

11.4 (CONT.)

(1)	(4)	(5)	(6)	(7)	(8)	(9)
+0.76	-1.1158	-0.31552	-1.5051	0.943	4.691	5.063
+0.77	-1.1250	-0.32481	-1.5525	0.906	4.785	5.137
+0.78	-1.1339	-0.33413	-1.6008	0.870	4.876	5.228
+0.79	-1.1424	-0.34344	-1.6500	0.834	4.965	5.342
+0.80	-1.1506	-0.35270	-1.7001	0.798	5.050	5.481
+0.81	-1.1584	-0.36185	-1.7510	0.763	5.132	5.656
+0.82	-1.1659	-0.37083	-1.8027	0.728	5.208	5.873
+0.83	-1.1730	-0.37956	-1.8551	0.694	5.279	6.146
+0.84	-1.1797	-0.38798	-1.9082	0.661	5.342	6.488
+0.85	-1.1862	-0.39600	-1.9620	0.628	5.397	6.916
+0.86	-1.1923	-0.40356	-2.0162	0.596	5.443	7.453
+0.87	-1.1981	-0.41059	-2.0708	0.565	5.479	8.128
+0.88	-1.2036	-0.41703	-2.1257	0.534	5.503	8.973
+0.89	-1.2088	-0.42285	-2.1808	0.505	5.516	10.03
+0.90	-1.2137	-0.42802	-2.2360	0.477	5.517	11.36
+0.91	-1.2183	-0.43257	-2.2911	0.450	5.507	13.01
+0.92	-1.2227	-0.43650	-2.3461	0.424	5.485	15.06
+0.93	-1.2268	-0.43986	-2.4008	0.400	5.454	17.62
+0.94	-1.2307	-0.44271	-2.4551	0.377	5.413	20.78
+0.95	-1.2344	-0.44510	-2.5090	0.356	5.364	24.67
+0.96	-1.2378	-0.44708	-2.5624	0.336	5.308	29.46
+0.97	-1.2411	-0.44872	-2.6152	0.318	5.246	35.33
+0.98	-1.2442	-0.45007	-2.6673	0.301	5.179	42.49
+0.99	-1.2471	-0.45117	-2.7187	0.285	5.109	51.18
+1.00	-1.2499	-0.45208	-2.7694	0.271	5.035	61.71
+1.01	-1.2526	-0.45282	-2.8194	0.258	4.959	74.43
+1.02	-1.2551	-0.45342	-2.8686	0.245	4.881	89.72
+1.03	-1.2575	-0.45391	-2.9170	0.233	4.801	108.0
+1.04	-1.2598	-0.45431	-2.9646	0.224	4.721	129.9
+1.05	-1.2620	-0.45464	-3.0115	0.214	4.641	155.8
+1.06	-1.2640	-0.45491	-3.0575	0.205	4.560	186.6
+1.07	-1.2661	-0.45513	-3.1027	0.198	4.479	222.9
+1.08	-1.2680	-0.45532	-3.1470	0.191	4.399	265.8

11.5

(1)	(4)	(5)	(6)	(7)	(8)	(9)
+0.68	-1.0283	-0.24620	-1.1611	1.249	3.931	4.723
+0.70	-1.0525	-0.26326	-1.2417	1.172	4.128	4.726
+0.72	-1.0752	-0.28115	-1.3263	1.095	4.328	4.731
+0.74	-1.0964	-0.29986	-1.4149	1.020	4.531	4.738
+0.76	-1.1160	-0.31940	-1.5076	0.946	4.736	4.749
+0.78	-1.1342	-0.33975	-1.6043	0.873	4.942	4.765
+0.80	-1.1510	-0.36087	-1.7053	0.803	5.150	4.791
+0.81	-1.1588	-0.37171	-1.7573	0.768	5.254	4.809
+0.82	-1.1663	-0.38272	-1.8104	0.735	5.358	4.831
+0.83	-1.1735	-0.39389	-1.8645	0.701	5.462	4.860
+0.84	-1.1803	-0.40519	-1.9196	0.669	5.566	4.897
+0.85	-1.1869	-0.41661	-1.9758	0.637	5.669	4.943
+0.86	-1.1931	-0.42812	-2.0330	0.605	5.770	5.002
+0.87	-1.1990	-0.43967	-2.0912	0.575	5.870	5.078
+0.88	-1.2046	-0.45122	-2.1504	0.545	5.968	5.177
+0.89	-1.2099	-0.46270	-2.2105	0.516	6.062	5.303
+0.90	-1.2149	-0.47405	-2.2716	0.487	6.151	5.468
+0.91	-1.2196	-0.48517	-2.3335	0.459	6.235	5.681
+0.92	-1.2241	-0.49597	-2.3963	0.432	6.310	5.958
+0.93	-1.2283	-0.50632	-2.4597	0.406	6.377	6.321
+0.94	-1.2322	-0.51610	-2.5238	0.380	6.432	6.795
+0.95	-1.2359	-0.52521	-2.5883	0.356	6.473	7.413
+0.96	-1.2393	-0.53354	-2.6532	0.332	6.499	8.218
+0.97	-1.2425	-0.54101	-2.7182	0.309	6.510	9.268
+0.98	-1.2455	-0.54758	-2.7833	0.288	6.503	10.63
+0.99	-1.2483	-0.55325	-2.8482	0.267	6.480	12.40
+1.00	-1.2509	-0.55804	-2.9129	0.248	6.440	14.69
+1.01	-1.2533	-0.56204	-2.9770	0.230	6.387	17.63
+1.02	-1.2555	-0.56532	-3.0406	0.213	6.321	21.40
+1.03	-1.2575	-0.56798	-3.1034	0.198	6.245	26.22
+1.04	-1.2594	-0.57011	-3.1654	0.184	6.160	32.32
+1.05	-1.2612	-0.57182	-3.2270	0.171	6.068	40.10
+1.06	-1.2629	-0.57316	-3.2872	0.160	5.971	49.80
+1.07	-1.2644	-0.57423	-3.3464	0.149	5.870	61.96
+1.08	-1.2659	-0.57508	-3.4045	0.139	5.767	77.09
+1.09	-1.2672	-0.57574	-3.4617	0.131	5.662	95.84
+1.10	-1.2685	-0.57627	-3.5178	0.123	5.556	118.9

11.6

(1)	(4)	(5)	(6)	(7)	(8)	(9)
+0.82	-1.1664	-0.38406	-1.8112	0.735	5.376	4.726
+0.83	-1.1736	-0.39554	-1.8655	0.702	5.484	4.728
+0.84	-1.1804	-0.40725	-1.9208	0.670	5.593	4.732
+0.85	-1.1870	-0.41918	-1.9773	0.638	5.704	4.737
+0.86	-1.1932	-0.43133	-2.0349	0.607	5.814	4.742
+0.87	-1.1991	-0.44370	-2.0936	0.577	5.927	4.750
+0.88	-1.2047	-0.45629	-2.1534	0.547	6.040	4.760
+0.89	-1.2100	-0.46908	-2.2144	0.518	6.153	4.772
+0.90	-1.2151	-0.48207	-2.2765	0.490	6.268	4.788
+0.91	-1.2198	-0.49525	-2.3398	0.463	6.384	4.810
+0.92	-1.2243	-0.50860	-2.4042	0.437	6.500	4.839
+0.93	-1.2286	-0.52211	-2.4698	0.411	6.617	4.877
+0.94	-1.2326	-0.53573	-2.5365	0.386	6.734	4.927
+0.95	-1.2363	-0.54943	-2.6045	0.362	6.851	4.994
+0.960	-1.2398	-0.56314	-2.6735	0.338	6.964	5.083
+0.965	-1.2415	-0.56998	-2.7085	0.328	7.022	5.140
+0.970	-1.2431	-0.57680	-2.7438	0.316	7.078	5.205
+0.975	-1.2446	-0.58358	-2.7793	0.306	7.132	5.281
+0.980	-1.2461	-0.59030	-2.8151	0.294	7.184	5.368
+0.985	-1.2476	-0.59696	-2.8511	0.284	7.236	5.470
+0.990	-1.2490	-0.60352	-2.8874	0.274	7.286	5.589
+0.995	-1.2503	-0.60998	-2.9240	0.264	7.334	5.729
+1.000	-1.2516	-0.61632	-2.9608	0.254	7.378	5.890
+1.005	-1.2528	-0.62250	-2.9978	0.244	7.418	6.078
+1.010	-1.2540	-0.62852	-3.0349	0.234	7.456	6.298
+1.015	-1.2552	-0.63433	-3.0723	0.224	7.490	6.556
+1.020	-1.2563	-0.63993	-3.1098	0.216	7.520	6.858
+1.025	-1.2573	-0.64529	-3.1475	0.206	7.544	7.209
+1.030	-1.2584	-0.65039	-3.1853	0.198	7.564	7.620
+1.035	-1.2593	-0.65521	-3.2231	0.190	7.578	8.100
+1.040	-1.2602	-0.65974	-3.2610	0.182	7.586	8.658
+1.045	-1.2611	-0.66397	-3.2990	0.174	7.588	9.308
+1.050	-1.2620	-0.66789	-3.3368	0.166	7.584	10.06
+1.055	-1.2628	-0.67151	-3.3747	0.158	7.574	10.94
+1.060	-1.2636	-0.67482	-3.4126	0.150	7.558	11.97
+1.065	-1.2643	-0.67782	-3.4503	0.144	7.536	13.16
+1.070	-1.2650	-0.68054	-3.4879	0.138	7.508	14.54
+1.075	-1.2657	-0.68299	-3.5254	0.130	7.476	16.15
+1.080	-1.2663	-0.68518	-3.5626	0.126	7.438	18.00
+1.085	-1.2669	-0.68713	-3.5998	0.120	7.396	20.14
+1.090	-1.2675	-0.68886	-3.6367	0.114	7.352	22.62
+1.095	-1.2681	-0.69039	-3.6733	0.108	7.302	25.48
+1.100	-1.2686	-0.69173	-3.7097	0.104	7.250	28.75
+1.105	-1.2691	-0.69291	-3.7458	0.098	7.198	32.54
+1.110	-1.2696	-0.69395	-3.7817	0.094	7.138	36.84
+1.115	-1.2701	-0.69486	-3.8172	0.090	7.078	41.78
+1.120	-1.2705	-0.69565	-3.8524	0.086	7.016	47.43
+1.125	-1.2709	-0.69634	-3.8874	0.082	6.954	53.89
+1.130	-1.2713	-0.69694	-3.9220	0.078	6.890	61.24
+1.135	-1.2717	-0.69792	-3.9562	0.074	6.826	69.62
+1.140	-1.2721	-0.69838	-3.9902	0.072	6.768	78.46
+1.145	-1.2724	-0.69879	-4.0239	0.070	6.702	89.17
+1.150	-1.2728	-0.69914	-4.0573	0.066	6.636	101.3
+1.155	-1.2731	-0.69944	-4.0903	0.064	6.570	115.1
+1.160	-1.2734	-0.69971	-4.1230	0.060	6.502	130.6
+1.165	-1.2737	-0.69994	-4.1553	0.058	6.436	148.2
+1.170	-1.2740	-0.70015	-4.1873	0.056	6.372	167.9
+1.175	-1.2742	-0.70032	-4.2190	0.054	6.304	190.1
+1.180	-1.2745	-0.70048	-4.2504	0.052	6.236	215.0

11.7

(1)	(4)	(5)	(6)	(7)	(8)	(9)
+0.90	-1.2151	-0.48293	-2.2770	0.491	6.281	4.721
+0.91	-1.2199	-0.49635	-2.3404	0.463	6.401	4.724
+0.92	-1.2244	-0.51003	-2.4051	0.437	6.523	4.727
+0.93	-1.2286	-0.52395	-2.4709	0.412	6.647	4.731
+0.94	-1.2326	-0.53813	-2.5380	0.387	6.773	4.736
+0.95	-1.2364	-0.55256	-2.6064	0.363	6.902	4.743
+0.96	-1.2399	-0.56724	-2.6761	0.340	7.033	4.751
+0.97	-1.2432	-0.58216	-2.7471	0.318	7.167	4.763
+0.98	-1.2463	-0.59732	-2.8194	0.296	7.304	4.780
+0.99	-1.2491	-0.61272	-2.8932	0.276	7.445	4.804
+1.00	-1.2518	-0.62832	-2.9683	0.256	7.587	4.834
+1.01	-1.2542	-0.64409	-3.0449	0.237	7.733	4.878
+1.02	-1.2565	-0.66000	-3.1230	0.219	7.880	4.939
+1.03	-1.2586	-0.67598	-3.2025	0.202	8.028	5.024
+1.04	-1.2606	-0.69192	-3.2835	0.185	8.175	5.143
+1.05	-1.2623	-0.70771	-3.3660	0.170	8.318	5.312

11.7 (CONT.)

(1)	(4)	(5)	(6)	(7)	(8)	(9)
+1.060	-1.2640	-0.72318	-3.4499	0.155	8.455	5.552
+1.065	-1.2647	-0.73072	-3.4923	0.148	8.520	5.709
+1.070	-1.2654	-0.73809	-3.5351	0.140	8.580	5.895
+1.075	-1.2661	-0.74526	-3.5781	0.134	8.638	6.120
+1.080	-1.2668	-0.75219	-3.6214	0.128	8.690	6.389
+1.085	-1.2674	-0.75885	-3.6650	0.120	8.734	6.708
+1.090	-1.2680	-0.76520	-3.7088	0.114	8.774	7.094
+1.095	-1.2685	-0.77121	-3.7527	0.108	8.806	7.555
+1.100	-1.2691	-0.77685	-3.7968	0.102	8.828	8.107
+1.105	-1.2696	-0.78209	-3.8410	0.096	8.844	8.767
+1.110	-1.2700	-0.78693	-3.8852	0.092	8.850	9.559
+1.115	-1.2705	-0.79135	-3.9295	0.086	8.848	10.50
+1.120	-1.2709	-0.79535	-3.9737	0.082	8.836	11.63
+1.125	-1.2713	-0.79895	-4.0178	0.076	8.816	12.98
+1.130	-1.2717	-0.80215	-4.0618	0.072	8.786	14.58
+1.135	-1.2720	-0.80498	-4.1057	0.068	8.750	16.49
+1.140	-1.2724	-0.80747	-4.1493	0.064	8.706	18.75
+1.145	-1.2727	-0.80963	-4.1927	0.062	8.656	21.44
+1.150	-1.2730	-0.81151	-4.2359	0.056	8.600	24.61
+1.155	-1.2732	-0.81314	-4.2787	0.054	8.538	28.36
+1.160	-1.2735	-0.81453	-4.3212	0.050	8.472	32.79
+1.165	-1.2737	-0.81573	-4.3634	0.048	8.404	37.99
+1.170	-1.2740	-0.81675	-4.4053	0.044	8.332	44.10
+1.175	-1.2742	-0.81763	-4.4467	0.042	8.256	51.25
+1.180	-1.2744	-0.81837	-4.4878	0.040	8.180	59.64
+1.185	-1.2746	-0.81900	-4.5285	0.038	8.102	69.44
+1.190	-1.2748	-0.81954	-4.5688	0.036	8.022	80.85
+1.195	-1.2749	-0.82000	-4.6088	0.034	7.942	94.12
+1.200	-1.2751	-0.82039	-4.6483	0.032	7.862	109.6
+1.205	-1.2753	-0.82072	-4.6874	0.030	7.780	127.4
+1.210	-1.2754	-0.82100	-4.7261	0.028	7.698	148.2
+1.215	-1.2755	-0.82124	-4.7644	0.026	7.616	172.1
+1.220	-1.2757	-0.82145	-4.8022	0.026	7.536	199.7
+1.225	-1.2758	-0.82162	-4.8397	0.024	7.454	231.5
+1.230	-1.2759	-0.82177	-4.8768	0.022	7.374	268.0
+1.235	-1.2760	-0.82190	-4.9135	0.022	7.294	310.1
+1.240	-1.2761	-0.82201	-4.9497	0.020	7.214	358.2
+1.245	-1.2762	-0.82210	-4.9856	0.020	7.134	412.9
+1.250	-1.2763	-0.82218	-5.0211	0.018	7.056	475.7
+1.255	-1.2764	-0.82225	-5.0562	0.018	6.978	547.3
+1.260	-1.2765	-0.82231	-5.0909	0.018	6.900	628.6
+1.265	-1.2766	-0.82236	-5.1252	0.016	6.822	721.0
+1.270	-1.2767	-0.82240	-5.1591	0.016	6.746	825.9

11.8

(1)	(4)	(5)	(6)	(7)	(8)	(9)
-0.70	+2.57848	-0.000611	-0.00288	2.994	0.013	4.714
-0.68	+2.51861	-0.000669	-0.00316	2.993	0.014	"
-0.66	+2.45876	-0.000734	-0.00346	2.992	0.016	"
-0.64	+2.39891	-0.000805	-0.00379	2.992	0.017	"
-0.62	+2.33909	-0.000882	-0.00416	2.991	0.019	"
-0.60	+2.27928	-0.000968	-0.00456	2.990	0.021	4.714
-0.58	+2.21948	-0.001061	-0.00500	2.989	0.023	"
-0.56	+2.15971	-0.001163	-0.00548	2.988	0.025	"
-0.54	+2.09996	-0.001275	-0.00601	2.987	0.028	"
-0.52	+2.04024	-0.001398	-0.00659	2.986	0.030	"
-0.50	+1.98054	-0.001533	-0.00723	2.984	0.033	4.714
-0.48	+1.92086	-0.001680	-0.00792	2.983	0.036	"
-0.46	+1.86122	-0.001842	-0.00868	2.981	0.040	"
-0.44	+1.80162	-0.002019	-0.00952	2.979	0.044	"
-0.42	+1.74205	-0.002214	-0.01043	2.977	0.048	"
-0.40	+1.68253	-0.002426	-0.01144	2.975	0.052	4.714
-0.38	+1.62305	-0.002659	-0.01254	2.973	0.058	"
-0.36	+1.56362	-0.002914	-0.01374	2.970	0.063	"
-0.34	+1.50424	-0.003194	-0.01506	2.967	0.069	"
-0.32	+1.44492	-0.003501	-0.01650	2.964	0.076	"
-0.30	+1.38567	-0.003837	-0.01809	2.961	0.083	4.714
-0.28	+1.32649	-0.004204	-0.01982	2.957	0.091	"
-0.26	+1.26739	-0.004607	-0.02172	2.953	0.099	"
-0.24	+1.20837	-0.005048	-0.02380	2.949	0.109	"
-0.22	+1.14945	-0.005532	-0.02608	2.944	0.119	"
-0.20	+1.09062	-0.006060	-0.02857	2.938	0.130	4.714
-0.18	+1.03191	-0.006640	-0.03130	2.933	0.143	"
-0.16	+0.97332	-0.007274	-0.03429	2.926	0.156	"
-0.14	+0.91487	-0.007968	-0.03756	2.919	0.171	"
-0.12	+0.85656	-0.008727	-0.04114	2.912	0.187	"

11.8 (CONT.)

(1)	(4)	(5)	(6)	(7)	(8)	(9)
-0.10	+0.79841	-0.009558	-0.04506	2.903	0.205	4.714
-0.08	+0.74043	-0.010466	-0.04934	2.894	0.224	"
-0.06	+0.68264	-0.011460	-0.05403	2.884	0.245	"
-0.04	+0.62505	-0.012546	-0.05915	2.874	0.268	"
-0.02	+0.56769	-0.013734	-0.06474	2.862	0.292	"
0.00	+0.51058	-0.015031	-0.07086	2.849	0.320	4.714
+0.02	+0.45373	-0.016448	-0.07754	2.836	0.349	"
+0.04	+0.39716	-0.017995	-0.08484	2.820	0.381	"
+0.06	+0.34092	-0.019684	-0.09280	2.804	0.416	"
+0.08	+0.28501	-0.021526	-0.10148	2.786	0.453	"
+0.10	+0.22947	-0.023536	-0.11095	2.767	0.494	4.714
+0.12	+0.17433	-0.025726	-0.12128	2.746	0.539	"
+0.14	+0.11962	-0.028112	-0.13253	2.724	0.587	"
+0.16	+0.06538	-0.030710	-0.14478	2.700	0.639	"
+0.18	+0.01165	-0.033538	-0.15811	2.674	0.695	"
+0.20	-0.04154	-0.036613	-0.17260	2.645	0.755	4.714
+0.22	-0.09415	-0.039954	-0.18835	2.615	0.820	"
+0.24	-0.14612	-0.043582	-0.20546	2.582	0.891	"
+0.26	-0.19742	-0.047518	-0.22401	2.547	0.966	"
+0.28	-0.24800	-0.051785	-0.24413	2.510	1.047	"
+0.30	-0.29780	-0.056407	-0.26592	2.470	1.133	4.714
+0.32	-0.34678	-0.061407	-0.28949	2.427	1.225	"
+0.34	-0.39488	-0.066810	-0.31496	2.382	1.323	"
+0.36	-0.44205	-0.072644	-0.34247	2.334	1.428	"
+0.38	-0.48823	-0.078935	-0.37212	2.283	1.539	"
+0.40	-0.53336	-0.085710	-0.40406	2.230	1.656	4.714
+0.42	-0.57740	-0.092995	-0.43841	2.174	1.780	"
+0.44	-0.62029	-0.100821	-0.47530	2.115	1.910	"
+0.46	-0.66197	-0.109214	-0.51486	2.053	2.047	"
+0.48	-0.70239	-0.118201	-0.55723	1.989	2.191	"
+0.50	-0.74150	-0.127811	-0.60254	1.922	2.340	4.714
+0.52	-0.77926	-0.138069	-0.65090	1.853	2.496	"
+0.54	-0.81562	-0.149002	-0.70244	1.782	2.658	"
+0.56	-0.85053	-0.160633	-0.75727	1.709	2.826	"
+0.58	-0.88398	-0.172987	-0.81551	1.635	2.999	"
+0.60	-0.91592	-0.186085	-0.87726	1.559	3.177	4.714
+0.62	-0.94634	-0.199949	-0.94262	1.482	3.360	"
+0.64	-0.97522	-0.214598	-1.01167	1.405	3.547	"
+0.66	-1.00254	-0.230048	-1.08451	1.327	3.738	"
+0.68	-1.02832	-0.246315	-1.16120	1.250	3.932	"
+0.70	-1.05254	-0.263416	-1.24182	1.172	4.130	4.714
+0.72	-1.07522	-0.281362	-1.32642	1.096	4.331	"
+0.74	-1.09638	-0.300167	-1.41507	1.020	4.535	"
+0.76	-1.11604	-0.319841	-1.50782	0.946	4.741	"
+0.78	-1.13424	-0.340398	-1.60473	0.874	4.950	"
+0.80	-1.15100	-0.361848	-1.70586	0.804	5.162	4.714
+0.81	-1.15887	-0.372912	-1.75802	0.769	5.270	"
+0.82	-1.16639	-0.384205	-1.81125	0.736	5.378	"
+0.83	-1.17358	-0.395728	-1.86557	0.702	5.487	"
+0.84	-1.18044	-0.407482	-1.92099	0.670	5.597	"
+0.85	-1.18698	-0.419472	-1.97751	0.638	5.708	4.714
+0.86	-1.19321	-0.431697	-2.03514	0.607	5.820	"
+0.87	-1.19913	-0.444162	-2.09391	0.577	5.933	"
+0.88	-1.20475	-0.456870	-2.15381	0.547	6.048	"
+0.89	-1.21008	-0.469822	-2.21488	0.519	6.164	"
+0.90	-1.21512	-0.483024	-2.27711	0.491	6.283	4.714
+0.91	-1.21989	-0.496478	-2.34054	0.464	6.403	"
+0.92	-1.22440	-0.510188	-2.40517	0.437	6.525	"
+0.93	-1.22864	-0.524161	-2.47105	0.412	6.650	"
+0.94	-1.23263	-0.538401	-2.53818	0.387	6.777	"
+0.95	-1.23638	-0.552914	-2.60659	0.363	6.907	4.714
+0.96	-1.23989	-0.567706	-2.67633	0.340	7.040	"
+0.97	-1.24318	-0.582785	-2.74742	0.318	7.177	"
+0.98	-1.24625	-0.598158	-2.81989	0.296	7.318	"
+0.99	-1.24912	-0.613836	-2.89380	0.276	7.464	"
+1.00	-1.25178	-0.629826	-2.96918	0.256	7.614	4.714
+1.01	-1.25424	-0.646140	-3.04609	0.238	7.769	"
+1.02	-1.25653	-0.662791	-3.12459	0.220	7.931	"
+1.03	-1.25864	-0.679792	-3.20473	0.202	8.099	"
+1.04	-1.26058	-0.697156	-3.28659	0.186	8.274	"
+1.05	-1.26237	-0.714901	-3.37025	0.171	8.458	4.714
+1.06	-1.26400	-0.733045	-3.45578	0.156	8.651	"
+1.07	-1.26549	-0.751608	-3.54329	0.142	8.853	"
+1.08	-1.26685	-0.770612	-3.63288	0.129	9.067	"
+1.09	-1.26808	-0.790082	-3.72467	0.117	9.293	"

11.8 (CONT.)

(1)	(4)	(5)	(6)	(7)	(8)	(9)
+1.10	-1.26918	-0.810047	-3.81879	0.105	9.533	4.714
+1.11	-1.27018	-0.830537	-3.91539	0.094	9.789	"
+1.12	-1.27108	-0.851587	-4.01462	0.084	10.062	"
+1.13	-1.27187	-0.873236	-4.11668	0.075	10.354	"
+1.14	-1.27258	-0.895528	-4.22178	0.066	10.668	"
+1.15	-1.27320	-0.918514	-4.33014	0.058	11.008	4.714
+1.16	-1.27374	-0.942250	-4.44203	0.051	11.376	"

11.9

(1)	(4)	(5)	(6)	(7)	(8)	(9)
+0.99	-1.2491	-0.61372	-2.8937	0.276	7.462	4.723
+1.00	-1.2518	-0.62968	-2.9691	0.256	7.611	4.726
+1.01	-1.2542	-0.64593	-3.0460	0.238	7.766	4.731
+1.02	-1.2565	-0.66251	-3.1244	0.220	7.926	4.737
+1.03	-1.2586	-0.67940	-3.2045	0.202	8.092	4.746
+1.04	-1.2606	-0.69661	-3.2863	0.186	8.264	4.758
+1.05	-1.2624	-0.71413	-3.3698	0.171	8.443	4.776
+1.06	-1.2640	-0.73196	-3.4552	0.156	8.629	4.801
+1.07	-1.2655	-0.75007	-3.5424	0.142	8.822	4.837
+1.08	-1.2669	-0.76842	-3.6317	0.129	9.021	4.890
+1.085	-1.2675	-0.77766	-3.6770	0.122	9.124	4.927
+1.090	-1.2681	-0.78693	-3.7229	0.116	9.226	4.969
+1.095	-1.2686	-0.79622	-3.7693	0.110	9.330	5.022
+1.100	-1.2692	-0.80550	-3.8162	0.104	9.434	5.086
+1.105	-1.2697	-0.81476	-3.8636	0.100	9.538	5.165
+1.110	-1.2702	-0.82396	-3.9116	0.094	9.642	5.261
+1.115	-1.2706	-0.83307	-3.9600	0.088	9.742	5.378
+1.120	-1.2711	-0.84206	-4.0090	0.084	9.844	5.524
+1.125	-1.2715	-0.85088	-4.0585	0.078	9.940	5.702
+1.130	-1.2719	-0.85948	-4.1084	0.074	10.030	5.920
+1.135	-1.2722	-0.86780	-4.1587	0.070	10.116	6.192
+1.140	-1.2726	-0.87580	-4.2095	0.066	10.194	6.527
+1.145	-1.2729	-0.88340	-4.2607	0.060	10.264	6.943
+1.150	-1.2732	-0.89056	-4.3121	0.056	10.322	7.456
+1.155	-1.2734	-0.89723	-4.3639	0.052	10.368	8.091
+1.160	-1.2737	-0.90337	-4.4156	0.050	10.400	8.871
+1.165	-1.2739	-0.90895	-4.4677	0.046	10.420	9.840
+1.170	-1.2742	-0.91396	-4.5198	0.042	10.426	11.04
+1.175	-1.2744	-0.91840	-4.5719	0.040	10.418	12.52
+1.180	-1.2746	-0.92229	-4.6240	0.036	10.396	14.34
+1.185	-1.2747	-0.92566	-4.6759	0.034	10.360	16.58
+1.190	-1.2749	-0.92855	-4.7276	0.032	10.314	19.32
+1.195	-1.2750	-0.93101	-4.7790	0.028	10.258	22.68
+1.200	-1.2752	-0.93309	-4.8301	0.026	10.190	26.79
+1.205	-1.2753	-0.93483	-4.8809	0.024	10.118	31.63
+1.210	-1.2754	-0.93629	-4.9313	0.022	10.038	37.91
+1.215	-1.2755	-0.93749	-4.9812	0.022	9.954	45.33

11.10

(1)	(4)	(5)	(6)	(7)	(8)	(9)
+0.860	-1.1932	-0.43158	-2.0351	0.606	5.818	4.724
+0.865	-1.1962	-0.43776	-2.0643	0.592	5.874	4.725
+0.870	-1.1991	-0.44401	-2.0938	0.576	5.930	4.726
+0.875	-1.2020	-0.45031	-2.1236	0.562	5.988	4.728
+0.880	-1.2047	-0.45667	-2.1537	0.546	6.044	4.728
+0.885	-1.2074	-0.46309	-2.1840	0.532	6.102	4.731
+0.890	-1.2100	-0.46957	-2.2147	0.518	6.160	4.733
+0.895	-1.2126	-0.47611	-2.2456	0.504	6.218	4.735
+0.900	-1.2151	-0.48270	-2.2769	0.490	6.278	4.739
+0.905	-1.2175	-0.48936	-2.3084	0.476	6.336	4.742
+0.910	-1.2198	-0.49606	-2.3402	0.462	6.396	4.746
+0.915	-1.2221	-0.50283	-2.3724	0.450	6.456	4.750
+0.920	-1.2243	-0.50966	-2.4048	0.436	6.516	4.755
+0.925	-1.2264	-0.51654	-2.4375	0.424	6.576	4.760
+0.930	-1.2285	-0.52347	-2.4706	0.412	6.638	4.767
+0.935	-1.2306	-0.53046	-2.5039	0.400	6.702	4.776
+0.940	-1.2326	-0.53750	-2.5376	0.386	6.762	4.783
+0.945	-1.2345	-0.54460	-2.5715	0.374	6.824	4.793
+0.950	-1.2363	-0.55174	-2.6058	0.362	6.888	4.805
+0.955	-1.2381	-0.55893	-2.6404	0.352	6.959	4.819
+0.960	-1.2398	-0.56617	-2.6753	0.340	7.014	4.833
+0.965	-1.2415	-0.57344	-2.7105	0.328	7.078	4.852
+0.970	-1.2431	-0.58076	-2.7461	0.318	7.144	4.874

11.10 (CONT.)

(1)	(4)	(5)	(6)	(7)	(8)	(9)
+0.975	-1.2447	-0.58810	-2.7820	0.306	7.208	4.899
+0.980	-1.2462	-0.59547	-2.8182	0.296	7.270	4.925
+0.985	-1.2476	-0.60286	-2.8547	0.286	7.336	4.960
+0.990	-1.2490	-0.61026	-2.8915	0.276	7.402	5.001
+0.995	-1.2504	-0.61766	-2.9287	0.266	7.466	5.047
+1.000	-1.2517	-0.62505	-2.9662	0.256	7.528	5.100
+1.005	-1.2529	-0.63241	-3.0040	0.246	7.592	5.164
+1.010	-1.2541	-0.63974	-3.0421	0.236	7.654	5.239
+1.015	-1.2553	-0.64702	-3.0805	0.228	7.714	5.327
+1.020	-1.2564	-0.65422	-3.1192	0.218	7.774	5.430
+1.025	-1.2575	-0.66132	-3.1583	0.210	7.830	5.552
+1.030	-1.2585	-0.66831	-3.1976	0.200	7.886	5.696
+1.035	-1.2595	-0.67516	-3.2371	0.192	7.936	5.865
+1.040	-1.2604	-0.68184	-3.2769	0.184	7.984	6.065
+1.045	-1.2613	-0.68831	-3.3170	0.176	8.028	6.301
+1.050	-1.2622	-0.69457	-3.3572	0.168	8.068	6.582
+1.055	-1.2630	-0.70056	-3.3976	0.160	8.102	6.913
+1.060	-1.2638	-0.70628	-3.4382	0.152	8.130	7.302
+1.065	-1.2645	-0.71169	-3.4789	0.146	8.152	7.764
+1.070	-1.2652	-0.71677	-3.5197	0.138	8.166	8.309
+1.075	-1.2659	-0.72151	-3.5606	0.132	8.174	8.953
+1.080	-1.2666	-0.72590	-3.6014	0.126	8.174	9.710
+1.085	-1.2672	-0.72993	-3.6423	0.118	8.164	10.60
+1.090	-1.2677	-0.73361	-3.6831	0.112	8.154	11.66
+1.095	-1.2683	-0.73693	-3.7238	0.108	8.132	12.90
+1.100	-1.2688	-0.73992	-3.7644	0.102	8.104	14.35
+1.105	-1.2693	-0.74259	-3.8048	0.096	8.070	16.05
+1.110	-1.2698	-0.74495	-3.8451	0.092	8.030	18.04
+1.115	-1.2702	-0.74704	-3.8851	0.086	7.984	20.38
+1.120	-1.2706	-0.74888	-3.9249	0.082	7.934	23.10
+1.125	-1.2710	-0.75049	-3.9644	0.078	7.880	26.28
+1.130	-1.2714	-0.75189	-4.0037	0.074	7.822	29.97
+1.135	-1.2718	-0.75310	-4.0426	0.070	7.760	34.28
+1.140	-1.2721	-0.75416	-4.0813	0.066	7.696	39.26

12.1

(1)	(4)	(5)	(6)	(7)	(8)	(9)
-0.70	+2.5785	-0.00058	-0.0029	2.994	0.013	5.007
-0.66	+2.4588	-0.00069	-0.0035	2.992	0.016	5.008
-0.62	+2.3391	-0.00083	-0.0042	2.991	0.019	5.010
-0.58	+2.2195	-0.00100	-0.0050	2.989	0.023	5.012
-0.54	+2.1000	-0.00120	-0.0060	2.987	0.028	5.014
-0.50	+1.9806	-0.00144	-0.0072	2.984	0.033	5.017
-0.46	+1.8613	-0.00173	-0.0087	2.981	0.040	5.020
-0.42	+1.7422	-0.00208	-0.0104	2.977	0.048	5.024
-0.38	+1.6232	-0.00250	-0.0125	2.972	0.057	5.029
-0.34	+1.5044	-0.00300	-0.0151	2.967	0.069	5.035
-0.30	+1.3858	-0.00360	-0.0181	2.960	0.083	5.042
-0.26	+1.2676	-0.00432	-0.0217	2.952	0.099	5.051
-0.22	+1.1497	-0.00518	-0.0261	2.943	0.119	5.062
-0.18	+1.0322	-0.00621	-0.0312	2.932	0.143	5.075
-0.14	+0.9152	-0.00744	-0.0375	2.918	0.171	5.090
-0.10	+0.7988	-0.00891	-0.0450	2.902	0.204	5.109
-0.06	+0.6831	-0.01065	-0.0540	2.882	0.244	5.132
-0.02	+0.5682	-0.01273	-0.0646	2.860	0.291	5.160
+0.02	+0.4544	-0.01519	-0.0774	2.832	0.347	5.195
+0.06	+0.3417	-0.01810	-0.0926	2.800	0.413	5.237
+0.10	+0.2304	-0.02153	-0.1106	2.762	0.491	5.290
+0.14	+0.1208	-0.02556	-0.1320	2.718	0.582	5.355
+0.18	+0.0130	-0.03025	-0.1574	2.666	0.687	5.436
+0.22	-0.0924	-0.03570	-0.1872	2.606	0.809	5.539
+0.26	-0.1953	-0.04196	-0.2224	2.537	0.949	5.669
+0.30	-0.2952	-0.04910	-0.2634	2.457	1.108	5.835
+0.32	-0.3439	-0.05301	-0.2865	2.414	1.194	5.936
+0.34	-0.3918	-0.05715	-0.3112	2.367	1.285	6.048
+0.36	-0.4386	-0.06151	-0.3379	2.318	1.380	6.177
+0.38	-0.4844	-0.06608	-0.3665	2.266	1.481	6.326
+0.40	-0.5292	-0.07086	-0.3971	2.211	1.585	6.496
+0.42	-0.5728	-0.07584	-0.4299	2.154	1.693	6.692
+0.44	-0.6153	-0.08098	-0.4649	2.093	1.804	6.917
+0.46	-0.6565	-0.08626	-0.5021	2.030	1.918	7.178
+0.48	-0.6965	-0.09165	-0.5416	1.966	2.033	7.481
+0.50	-0.7351	-0.09711	-0.5834	1.899	2.149	7.833
+0.52	-0.7724	-0.10261	-0.6276	1.831	2.265	8.244
+0.54	-0.8084	-0.10809	-0.6740	1.761	2.380	8.723
+0.56	-0.8428	-0.11350	-0.7227	1.690	2.491	9.283
+0.58	-0.8759	-0.11880	-0.7736	1.619	2.598	9.939

12.1 (CONT.)

(1)	(4)	(5)	(6)	(7)	(8)	(9)
+0.60	-0.9076	-0.12396	-0.8266	1.548	2.702	10.71
+0.62	-0.9379	-0.12890	-0.8816	1.477	2.798	11.61
+0.64	-0.9667	-0.13359	-0.9384	1.408	2.886	12.68
+0.66	-0.9942	-0.13799	-0.9970	1.340	2.966	13.93
+0.68	-1.0203	-0.14210	-1.0570	1.273	3.036	15.40
+0.70	-1.0451	-0.14588	-1.1184	1.209	3.098	17.13
+0.72	-1.0687	-0.14933	-1.1808	1.148	3.148	19.17
+0.74	-1.0910	-0.15245	-1.2442	1.090	3.188	21.55
+0.76	-1.1123	-0.15525	-1.3083	1.034	3.218	24.34
+0.78	-1.1324	-0.15774	-1.3729	0.983	3.238	27.60
+0.80	-1.1516	-0.15995	-1.4377	0.934	3.248	31.39
+0.82	-1.1698	-0.16189	-1.5027	0.890	3.249	35.82
+0.84	-1.1872	-0.16359	-1.5676	0.848	3.242	40.96
+0.86	-1.2038	-0.16506	-1.6324	0.811	3.228	46.88
+0.88	-1.2197	-0.16635	-1.6967	0.776	3.206	53.76
+0.90	-1.2349	-0.16746	-1.7606	0.744	3.180	61.62
+0.92	-1.2495	-0.16842	-1.8239	0.716	3.147	70.66
+0.94	-1.2635	-0.16924	-1.8864	0.690	3.110	80.98
+0.96	-1.2771	-0.16996	-1.9482	0.668	3.070	92.76
+0.98	-1.2903	-0.17057	-2.0092	0.648	3.026	106.1
+1.00	-1.3030	-0.17110	-2.0692	0.629	2.980	121.3
+1.02	-1.3155	-0.17156	-2.1284	0.614	2.931	138.4
+1.04	-1.3276	-0.17195	-2.1865	0.600	2.881	157.6
+1.06	-1.3395	-0.17229	-2.2436	0.588	2.830	179.2
+1.08	-1.3511	-0.17259	-2.2996	0.578	2.778	203.4
+1.10	-1.3626	-0.17284	-2.3547	0.570	2.726	230.3
+1.12	-1.3739	-0.17306	-2.4087	0.563	2.673	260.2
+1.14	-1.3852	-0.17325	-2.4616	0.558	2.620	293.5
+1.16	-1.3963	-0.17342	-2.5135	0.554	2.568	330.2
+1.18	-1.4073	-0.17357	-2.5644	0.552	2.517	370.7
+1.20	-1.4184	-0.17370	-2.6142	0.551	2.466	415.3

12.2

(1)	(4)	(5)	(6)	(7)	(8)	(9)
-0.70	+2.57844	-0.00066	-0.00288	2.994	0.013	4.350
-0.68	+2.51857	-0.00073	-0.00316	2.993	0.015	4.350
-0.66	+2.45872	-0.00080	-0.00346	2.993	0.016	4.351
-0.64	+2.39887	-0.00087	-0.00380	2.992	0.017	4.351
-0.62	+2.33904	-0.00096	-0.00416	2.991	0.019	4.351
-0.60	+2.27923	-0.00105	-0.00456	2.990	0.021	4.351
-0.58	+2.21943	-0.00115	-0.00500	2.989	0.023	4.351
-0.56	+2.15965	-0.00126	-0.00548	2.988	0.025	4.352
-0.54	+2.09990	-0.00138	-0.00601	2.987	0.028	4.353
-0.52	+2.04016	-0.00151	-0.00659	2.986	0.030	4.353
-0.50	+1.98046	-0.00166	-0.00723	2.985	0.033	4.354
-0.48	+1.92078	-0.00182	-0.00792	2.983	0.036	4.354
-0.46	+1.86113	-0.00200	-0.00868	2.982	0.040	4.355
-0.44	+1.80152	-0.00219	-0.00952	2.980	0.044	4.356
-0.42	+1.74194	-0.00240	-0.01044	2.978	0.048	4.356
-0.40	+1.68241	-0.00263	-0.01144	2.976	0.052	4.356
-0.38	+1.62291	-0.00288	-0.01254	2.973	0.058	4.358
-0.36	+1.56347	-0.00315	-0.01374	2.971	0.063	4.359
-0.34	+1.50408	-0.00346	-0.01506	2.968	0.069	4.361
-0.32	+1.44475	-0.00379	-0.01651	2.965	0.076	4.362
-0.30	+1.38548	-0.00415	-0.01810	2.962	0.083	4.362
-0.28	+1.32628	-0.00455	-0.01983	2.958	0.091	4.365
-0.26	+1.26716	-0.00499	-0.02173	2.954	0.100	4.366
-0.24	+1.20812	-0.00546	-0.02382	2.950	0.109	4.369
-0.22	+1.14918	-0.00598	-0.02610	2.945	0.119	4.370
-0.20	+1.09033	-0.00656	-0.02860	2.940	0.131	4.372
-0.18	+1.03160	-0.00718	-0.03133	2.934	0.143	4.374
-0.16	+0.97298	-0.00787	-0.03433	2.928	0.157	4.377
-0.14	+0.91449	-0.00862	-0.03761	2.921	0.171	4.380
-0.12	+0.85615	-0.00944	-0.04120	2.913	0.188	4.382
-0.10	+0.79796	-0.01033	-0.04512	2.905	0.205	4.386
-0.08	+0.73995	-0.01131	-0.04942	2.896	0.225	4.390
-0.06	+0.68212	-0.01238	-0.05412	2.887	0.246	4.394
-0.04	+0.62449	-0.01355	-0.05925	2.876	0.269	4.399
-0.02	+0.56709	-0.01482	-0.06487	2.864	0.294	4.405
0.00	+0.50992	-0.01622	-0.07101	2.852	0.321	4.410
+0.02	+0.45302	-0.01774	-0.07772	2.838	0.350	4.417
+0.04	+0.39640	-0.01940	-0.08505	2.823	0.383	4.423
+0.06	+0.34010	-0.02120	-0.09305	2.807	0.418	4.432
+0.08	+0.28413	-0.02317	-0.10179	2.789	0.456	4.441
+0.10	+0.22853	-0.02532	-0.11132	2.770	0.498	4.450
+0.12	+0.17333	-0.02765	-0.12171	2.750	0.542	4.460
+0.14	+0.11856	-0.03018	-0.13304	2.727	0.591	4.473
+0.16	+0.06426	-0.03294	-0.14538	2.703	0.644	4.486
+0.18	+0.01046	-0.03593	-0.15882	2.677	0.701	4.501

12.2 (CONT.)

(1)	(4)	(5)	(6)	(7)	(8)	(9)
+0.20	-0.04279	-0.03917	-0.17343	2.648	0.762	4.518
+0.22	-0.09545	-0.04268	-0.18933	2.618	0.828	4.538
+0.24	-0.14748	-0.04648	-0.20660	2.585	0.899	4.560
+0.26	-0.19882	-0.05058	-0.22534	2.549	0.976	4.585
+0.28	-0.24943	-0.05500	-0.24567	2.511	1.058	4.612
+0.30	-0.29926	-0.05976	-0.26769	2.471	1.146	4.644
+0.32	-0.34824	-0.06487	-0.29153	2.427	1.239	4.681
+0.34	-0.39632	-0.07035	-0.31730	2.381	1.339	4.723
+0.36	-0.44345	-0.07621	-0.34512	2.332	1.444	4.771
+0.38	-0.48956	-0.08246	-0.37511	2.279	1.556	4.826
+0.40	-0.53460	-0.08911	-0.40740	2.224	1.674	4.889
+0.42	-0.57850	-0.09615	-0.44210	2.166	1.797	4.963
+0.44	-0.62120	-0.10359	-0.47933	2.104	1.927	5.049
+0.46	-0.66264	-0.11141	-0.51920	2.040	2.061	5.150
+0.48	-0.70277	-0.11959	-0.56180	1.973	2.200	5.269
+0.50	-0.74152	-0.12810	-0.60721	1.903	2.342	5.409
+0.52	-0.77886	-0.13689	-0.65550	1.830	2.487	5.574
+0.54	-0.81472	-0.14593	-0.70672	1.756	2.634	5.772
+0.56	-0.84908	-0.15513	-0.76087	1.680	2.781	6.007
+0.58	-0.88189	-0.16442	-0.81795	1.602	2.926	6.288
+0.60	-0.91314	-0.17371	-0.87790	1.523	3.068	6.627
+0.62	-0.94281	-0.18290	-0.94063	1.444	3.204	7.036
+0.64	-0.97089	-0.19189	-1.00601	1.365	3.333	7.529
+0.66	-0.99739	-0.20057	-1.07386	1.286	3.451	8.125
+0.68	-1.0224	-0.20885	-1.1440	1.209	3.558	8.848
+0.70	-1.0458	-0.21663	-1.2161	1.134	3.651	9.724
+0.72	-1.0678	-0.22385	-1.2894	1.062	3.729	10.78
+0.74	-1.0883	-0.23045	-1.3651	0.993	3.791	12.07
+0.76	-1.1075	-0.23641	-1.4414	0.928	3.836	13.62
+0.78	-1.1254	-0.24172	-1.5185	0.866	3.865	15.48
+0.80	-1.1422	-0.14640	-1.5959	0.810	3.878	17.72
+0.82	-1.1579	-0.25049	-1.6735	0.757	3.876	20.41
+0.84	-1.1725	-0.25402	-1.7509	0.709	3.860	23.61
+0.86	-1.1862	-0.25704	-1.8278	0.665	3.831	27.41
+0.88	-1.1991	-0.25962	-1.9040	0.626	3.791	31.90
+0.90	-1.2113	-0.26182	-1.9794	0.590	3.742	37.18
+0.92	-1.2228	-0.26367	-2.0537	0.559	3.685	43.38
+0.94	-1.2337	-0.26523	-2.1267	0.530	3.622	50.58
+0.96	-1.2440	-0.26654	-2.1985	0.506	3.553	58.97
+0.98	-1.2539	-0.26770	-2.2688	0.484	3.480	68.58
+1.00	-1.2634	-0.26863	-2.3377	0.465	3.405	79.73
+1.02	-1.2726	-0.26941	-2.4050	0.448	3.326	92.40
+1.04	-1.2814	-0.27007	-2.4708	0.434	3.247	107.0
+1.06	-1.2900	-0.27063	-2.5349	0.422	3.166	123.2
+1.08	-1.2983	-0.27110	-2.5974	0.412	3.086	141.9
+1.10	-1.3065	-0.27151	-2.6583	0.404	3.006	162.4
+1.12	-1.3145	-0.27185	-2.7177	0.398	2.926	185.8
+1.14	-1.3224	-0.27214	-2.7754	0.393	2.848	211.7
+1.16	-1.3302	-0.27239	-2.8316	0.390	2.771	241.0

12.3

(1)	(4)	(5)	(6)	(7)	(8)	(9)
-0.10	+0.7975	-0.01110	-0.0452	2.907	0.206	4.075
-0.08	+0.7395	-0.01216	-0.0495	2.898	0.226	4.075
-0.06	+0.6816	-0.01331	-0.0542	2.889	0.246	4.076
-0.04	+0.6240	-0.01458	-0.0594	2.878	0.270	4.077
-0.02	+0.5665	-0.01596	-0.0650	2.867	0.295	4.078
0.00	+0.5093	-0.01747	-0.0712	2.855	0.322	4.079
+0.02	+0.4523	-0.01912	-0.0779	2.842	0.352	4.081
+0.04	+0.3956	-0.02092	-0.0853	2.826	0.385	4.082
+0.06	+0.3392	-0.02290	-0.0934	2.810	0.420	4.084
+0.08	+0.2832	-0.02505	-0.1021	2.794	0.459	4.085
+0.10	+0.2275	-0.02740	-0.1117	2.774	0.501	4.087
+0.12	+0.1722	-0.02996	-0.1222	2.754	0.546	4.089
+0.14	+0.1174	-0.03275	-0.1336	2.732	0.596	4.091
+0.16	+0.0630	-0.03579	-0.1460	2.708	0.650	4.094
+0.18	+0.0090	-0.03911	-0.1596	2.682	0.708	4.097
+0.20	-0.0443	-0.04271	-0.1744	2.654	0.771	4.101
+0.22	-0.0971	-0.04664	-0.1905	2.624	0.839	4.104
+0.24	-0.1493	-0.05090	-0.2080	2.592	0.912	4.109
+0.26	-0.2008	-0.05553	-0.2270	2.557	0.992	4.114
+0.28	-0.2516	-0.06055	-0.2477	2.520	1.076	4.119
+0.30	-0.3015	-0.06599	-0.2701	2.479	1.168	4.125
+0.32	-0.3507	-0.07189	-0.2945	2.436	1.267	4.132
+0.34	-0.3990	-0.07826	-0.3208	2.390	1.372	4.141
+0.36	-0.4463	-0.08515	-0.3494	2.341	1.484	4.150
+0.38	-0.4926	-0.09258	-0.3803	2.289	1.604	4.162

12.3 (CONT.)

(1)	(4)	(5)	(6)	(7)	(8)	(9)
+0.40	-0.5379	-0.10058	-0.4136	2.234	1.732	4.174
+0.42	-0.5820	-0.10918	-0.4496	2.176	1.867	4.189
+0.44	-0.6249	-0.11841	-0.4884	2.114	2.010	4.207
+0.46	-0.6665	-0.12830	-0.5301	2.050	2.162	4.228
+0.48	-0.7068	-0.13887	-0.5749	1.982	2.321	4.253
+0.50	-0.7458	-0.15014	-0.6230	1.912	2.488	4.283
+0.52	-0.7833	-0.16211	-0.6745	1.838	2.663	4.318
+0.54	-0.8193	-0.17480	-0.7296	1.762	2.845	4.361
+0.56	-0.8537	-0.18820	-0.7883	1.684	3.034	4.414
+0.58	-0.8866	-0.20228	-0.8509	1.602	3.228	4.478
+0.60	-0.9178	-0.21701	-0.9175	1.520	3.426	4.557
+0.62	-0.9473	-0.23232	-0.9880	1.436	3.628	4.656
+0.64	-0.9752	-0.24814	-1.0626	1.350	3.831	4.779
+0.66	-1.0013	-0.26435	-1.1412	1.264	4.034	4.934
+0.68	-1.0257	-0.28079	-1.2239	1.178	4.232	5.129
+0.70	-1.0484	-0.29728	-1.3105	1.093	4.423	5.378
+0.71	-1.0592	-0.30548	-1.3551	1.050	4.515	5.528
+0.72	-1.0694	-0.31360	-1.4007	1.008	4.603	5.696
+0.73	-1.0793	-0.32163	-1.4472	0.966	4.688	5.888
+0.74	-1.0888	-0.32952	-1.4945	0.925	4.768	6.106
+0.75	-1.0978	-0.33724	-1.5425	0.885	4.842	6.351
+0.76	-1.1065	-0.34476	-1.5913	0.845	4.912	6.631
+0.77	-1.1147	-0.35204	-1.6407	0.806	4.975	6.948
+0.78	-1.1226	-0.35907	-1.6908	0.769	5.031	7.308
+0.79	-1.1301	-0.36580	-1.7413	0.732	5.081	7.717
+0.80	-1.1372	-0.37223	-1.7924	0.697	5.122	8.179
+0.81	-1.1440	-0.37832	-1.8438	0.662	5.156	8.705
+0.82	-1.1505	-0.38407	-1.8955	0.628	5.183	9.300
+0.83	-1.1566	-0.38946	-1.9474	0.596	5.201	9.973
+0.84	-1.1624	-0.39450	-1.9995	0.566	5.211	10.74
+0.85	-1.1679	-0.39917	-2.0516	0.537	5.212	11.59
+0.86	-1.1732	-0.40349	-2.1037	0.509	5.208	12.56
+0.87	-1.1781	-0.40747	-2.1557	0.483	5.195	13.65
+0.88	-1.1828	-0.41111	-2.2076	0.458	5.175	14.87
+0.89	-1.1873	-0.41444	-2.2592	0.434	5.149	16.25
+0.90	-1.1915	-0.41746	-2.3105	0.412	5.117	17.79
+0.91	-1.1955	-0.42020	-2.3615	0.392	5.078	19.50
+0.92	-1.1994	-0.42267	-2.4121	0.373	5.035	21.41
+0.93	-1.2030	-0.42491	-2.4622	0.355	4.988	23.54
+0.94	-1.2065	-0.42692	-2.5118	0.338	4.936	25.91
+0.95	-1.2098	-0.42872	-2.5609	0.322	4.881	28.53
+0.96	-1.2129	-0.43034	-2.6094	0.308	4.822	31.43
+0.97	-1.2159	-0.43179	-2.6573	0.294	4.761	34.63
+0.98	-1.2188	-0.43310	-2.7046	0.282	4.698	38.16
+0.99	-1.2216	-0.43426	-2.7513	0.270	4.633	42.04
+1.00	-1.2242	-0.43530	-2.7973	0.259	4.566	46.27
+1.01	-1.2268	-0.43624	-2.8426	0.249	4.498	50.91
+1.02	-1.2292	-0.43707	-2.8872	0.240	4.429	56.00
+1.03	-1.2316	-0.43782	-2.9312	0.232	4.359	61.54
+1.04	-1.2339	-0.43849	-2.9744	0.224	4.289	67.56
+1.05	-1.2361	-0.43910	-3.0169	0.217	4.219	74.10
+1.06	-1.2382	-0.43964	-3.0588	0.210	4.148	81.19
+1.07	-1.2403	-0.44012	-3.0999	0.204	4.078	88.86
+1.08	-1.2423	-0.44056	-3.1403	0.199	4.007	97.14
+1.09	-1.2443	-0.44095	-3.1800	0.193	3.938	106.0
+1.10	-1.2462	-0.44130	-3.2191	0.189	3.868	115.7

12.4

(1)	(4)	(5)	(6)	(7)	(8)	(9)
+0.20	-0.0446	-0.04337	-0.1746	2.656	0.772	4.031
+0.22	-0.0974	-0.04737	-0.1907	2.626	0.841	4.033
+0.24	-0.1496	-0.05172	-0.2083	2.594	0.915	4.034
+0.26	-0.2011	-0.05645	-0.2273	2.558	0.994	4.035
+0.28	-0.2519	-0.06159	-0.2481	2.521	1.080	4.038
+0.30	-0.3020	-0.06716	-0.2706	2.481	1.172	4.039
+0.32	-0.3512	-0.07321	-0.2950	2.438	1.272	4.040
+0.34	-0.3994	-0.07976	-0.3215	2.392	1.378	4.044
+0.36	-0.4468	-0.08685	-0.3502	2.344	1.492	4.046
+0.38	-0.4932	-0.09452	-0.3812	2.291	1.614	4.051
+0.40	-0.5385	-0.10280	-0.4148	2.236	1.743	4.054
+0.42	-0.5826	-0.11173	-0.4510	2.178	1.881	4.059
+0.44	-0.6256	-0.12135	-0.4901	2.117	2.028	4.064
+0.46	-0.6673	-0.13170	-0.5322	2.052	2.182	4.071
+0.48	-0.7077	-0.14281	-0.5774	1.984	2.347	4.079
+0.50	-0.7467	-0.15472	-0.6261	1.914	2.520	4.088
+0.52	-0.7842	-0.16747	-0.6783	1.840	2.702	4.100
+0.54	-0.8202	-0.18110	-0.7342	1.764	2.893	4.113
+0.56	-0.8548	-0.19562	-0.7941	1.686	3.093	4.130
+0.58	-0.8876	-0.21106	-0.8580	1.604	3.302	4.151

12.4 (CONT.)

(1)	(4)	(5)	(6)	(7)	(8)	(9)
+0.60	−0.9189	−0.22744	−0.9262	1.521	3.519	4.177
+0.62	−0.9485	−0.24475	−0.9988	1.437	3.743	4.209
+0.64	−0.9764	−0.26300	−1.0760	1.351	3.975	4.249
+0.66	−1.0025	−0.28216	−1.1579	1.264	4.214	4.301
+0.68	−1.0269	−0.30217	−1.2446	1.177	4.457	4.367
+0.70	−1.0496	−0.32295	−1.3362	1.090	4.705	4.454
+0.71	−1.0602	−0.33359	−1.3839	1.046	4.829	4.507
+0.72	−1.0705	−0.34437	−1.4328	1.003	4.953	4.567
+0.73	−1.0803	−0.35527	−1.4829	0.960	5.077	4.636
+0.74	−1.0897	−0.36626	−1.5343	0.917	5.199	4.716
+0.75	−1.0986	−0.37731	−1.5869	0.875	5.321	4.809
+0.76	−1.1072	−0.38838	−1.6407	0.833	5.440	4.916
+0.77	−1.1153	−0.39943	−1.6957	0.791	5.556	5.039
+0.78	−1.1230	−0.41041	−1.7518	0.751	5.668	5.182
+0.79	−1.1303	−0.42128	−1.8090	0.711	5.776	5.349
+0.80	−1.1372	−0.43199	−1.8673	0.672	5.878	5.542
+0.81	−1.1438	−0.44248	−1.9266	0.634	5.974	5.768
+0.82	−1.1499	−0.45269	−1.9868	0.597	6.063	6.031
+0.83	−1.1557	−0.46257	−2.0478	0.561	6.142	6.337
+0.84	−1.1612	−0.47206	−2.1096	0.526	6.212	6.694
+0.85	−1.1662	−0.48111	−2.1720	0.493	6.271	7.110
+0.86	−1.1710	−0.48968	−2.2350	0.460	6.320	7.596
+0.87	−1.1754	−0.49774	−2.2984	0.430	6.356	8.160
+0.88	−1.1796	−0.50527	−2.3620	0.400	6.381	8.774
+0.89	−1.1835	−0.51222	−2.4259	0.374	6.393	9.580
+0.90	−1.1871	−0.51861	−2.4899	0.348	6.393	10.46
+0.91	−1.1904	−0.52444	−2.5537	0.324	6.381	11.49
+0.92	−1.1936	−0.52973	−2.6174	0.301	6.358	13.67
+0.93	−1.1965	−0.53449	−2.6809	0.280	6.324	14.04
+0.94	−1.1992	−0.53875	−2.7439	0.260	6.280	15.61
+0.95	−1.2017	−0.54255	−2.8064	0.242	6.226	17.40
+0.96	−1.2040	−0.54592	−2.8684	0.226	6.165	19.45
+0.97	−1.2062	−0.54890	−2.9297	0.210	6.097	21.80
+0.98	−1.2082	−0.55152	−2.9903	0.196	6.022	24.46
+0.99	−1.2101	−0.55384	−3.0502	0.183	5.943	27.49
+1.00	−1.2119	−0.55586	−3.1092	0.172	5.858	30.91
+1.01	−1.2136	−0.55764	−3.1673	0.161	5.771	34.76
+1.02	−1.2151	−0.55919	−3.2246	0.151	5.680	39.09
+1.03	−1.2166	−0.56055	−3.2809	0.142	5.587	43.96
+1.04	−1.2180	−0.56174	−3.3363	0.134	5.492	49.39
+1.05	−1.2193	−0.56278	−3.3907	0.127	5.396	55.46
+1.06	−1.2205	−0.56369	−3.4442	0.120	5.300	62.21
+1.07	−1.2217	−0.56449	−3.4967	0.114	5.202	69.68
+1.08	−1.2228	−0.56519	−3.5483	0.108	5.105	77.95
+1.09	−1.2239	−0.56580	−3.5988	0.103	5.008	87.08
+1.10	−1.2249	−0.56634	−3.6484	0.098	4.912	97.15
+1.11	−1.2259	−0.56682	−3.6971	0.094	4.816	108.2
+1.12	−1.2268	−0.56724	−3.7448	0.090	4.721	120.3
+1.13	−1.2277	−0.56761	−3.7915	0.087	4.627	133.5
+1.14	−1.2285	−0.56793	−3.8373	0.084	4.534	147.9
+1.15	−1.2294	−0.56822	−3.8822	0.081	4.442	163.5
+1.16	−1.2302	−0.56848	−3.9262	0.078	4.351	180.5
+1.17	−1.2309	−0.56871	−3.9692	0.076	4.262	199.0
+1.18	−1.2317	−0.56891	−4.0114	0.073	4.174	218.9
+1.19	−1.2324	−0.56909	−4.0527	0.071	4.088	240.3
+1.20	−1.2331	−0.56925	−4.0932	0.070	4.003	263.4

12.5

(1)	(4)	(5)	(6)	(7)	(8)	(9)
+0.20	−0.0447	−0.04357	−0.1746	2.656	0.773	4.009
+0.22	−0.0975	−0.04759	−0.1908	2.626	0.842	4.010
+0.24	−0.1497	−0.05197	−0.2083	2.594	0.916	4.011
+0.26	−0.2012	−0.05673	−0.2274	2.559	0.996	4.012
+0.28	−0.2520	−0.06190	−0.2482	2.522	1.082	4.013
+0.30	−0.3021	−0.06752	−0.2707	2.482	1.174	4.014
+0.32	−0.3513	−0.07362	−0.2952	2.444	1.273	4.013
+0.34	−0.3996	−0.08022	−0.3217	2.393	1.380	4.014
+0.36	−0.4470	−0.08738	−0.3504	2.344	1.494	4.016
+0.38	−0.4933	−0.09512	−0.3815	2.292	1.616	4.017
+0.40	−0.5386	−0.10348	−0.4151	2.238	1.746	4.019
+0.42	−0.5828	−0.11251	−0.4514	2.179	1.885	4.020
+0.44	−0.6258	−0.12225	−0.4906	2.118	2.032	4.022
+0.46	−0.6675	−0.13274	−0.5328	2.054	2.189	4.024
+0.48	−0.7079	−0.14402	−0.5782	1.986	2.354	4.027

12.5 (CONT.)

(1)	(4)	(5)	(6)	(7)	(8)	(9)
+0.50	−0.7469	−0.15614	−0.6271	1.915	2.530	4.030
+0.52	−0.7844	−0.16914	−0.6795	1.842	2.714	4.034
+0.54	−0.8205	−0.18306	−0.7357	1.766	2.908	4.039
+0.56	−0.8550	−0.19795	−0.7959	1.686	3.112	4.044
+0.58	−0.8879	−0.21385	−0.8602	1.606	3.325	4.052
+0.60	−0.9192	−0.23079	−0.9289	1.523	3.548	4.061
+0.62	−0.9488	−0.24882	−1.0022	1.438	3.782	4.072
+0.64	−0.9767	−0.26795	−1.0803	1.352	4.024	4.086
+0.66	−1.0029	−0.28822	−1.1633	1.265	4.277	4.104
+0.68	−1.0273	−0.30964	−1.2514	1.177	4.540	4.128
+0.70	−1.0500	−0.32220	−1.3449	1.090	4.810	4.159
+0.72	−1.0709	−0.35589	−1.4439	1.002	5.091	4.199
+0.74	−1.0901	−0.38067	−1.5486	0.916	5.380	4.253
+0.76	−1.1076	−0.40645	−1.6592	0.831	5.676	4.327
+0.77	−1.1157	−0.41967	−1.7167	0.789	5.826	4.374
+0.78	−1.1234	−0.43308	−1.7757	0.748	5.976	4.427
+0.79	−1.1306	−0.44666	−1.8362	0.708	6.128	4.492
+0.80	−1.1375	−0.46035	−1.8982	0.668	6.279	4.567
+0.81	−1.1440	−0.47414	−1.9618	0.629	6.429	4.657
+0.82	−1.1501	−0.48795	−2.0268	0.590	6.577	4.762
+0.83	−1.1558	−0.50173	−2.0933	0.553	6.723	4.889
+0.84	−1.1612	−0.51542	−2.1613	0.516	6.864	5.039
+0.85	−1.1661	−0.52895	−2.2306	0.481	7.000	5.219
+0.86	−1.1708	−0.54222	−2.3012	0.447	7.129	5.434
+0.87	−1.1751	−0.55515	−2.3731	0.414	7.248	5.693
+0.88	−1.1791	−0.56765	−2.4462	0.382	7.357	6.003
+0.89	−1.1827	−0.57963	−2.5202	0.352	7.454	6.376
+0.90	−1.1861	−0.59100	−2.5952	0.323	7.536	6.824
+0.91	−1.1892	−0.60170	−2.6709	0.296	7.602	7.361
+0.92	−1.1920	−0.61164	−2.7472	0.271	7.650	8.005
+0.93	−1.1946	−0.62080	−2.8238	0.247	7.681	8.779
+0.94	−1.1970	−0.62913	−2.9007	0.225	7.693	9.705
+0.95	−1.1991	−0.63665	−2.9776	0.204	7.688	10.81
+0.96	−1.2011	−0.64336	−3.0544	0.185	7.664	12.13
+0.97	−1.2028	−0.64930	−3.1309	0.168	7.623	13.69
+0.98	−1.2044	−0.65452	−3.2068	0.153	7.568	15.55
+0.99	−1.2059	−0.65906	−3.2822	0.138	7.498	17.73
+1.00	−1.2072	−0.66300	−3.3568	0.126	7.417	20.30
+1.01	−1.2084	−0.66639	−3.4305	0.114	7.325	23.32
+1.02	−1.2095	−0.66930	−3.5032	0.104	7.225	26.85
+1.03	−1.2105	−0.67179	−3.5750	0.095	7.117	30.94
+1.04	−1.2114	−0.67392	−3.6456	0.086	7.004	35.70
+1.05	−1.2122	−0.67573	−3.7150	0.079	6.886	41.21
+1.06	−1.2130	−0.67728	−3.7833	0.073	6.765	47.54
+1.07	−1.2137	−0.67859	−3.8503	0.067	6.642	54.80
+1.08	−1.2143	−0.67971	−3.9161	0.062	6.517	63.09
+1.09	−1.2149	−0.68067	−3.9807	0.057	6.391	72.54
+1.10	−1.2155	−0.68148	−4.0440	0.053	6.266	83.35
+1.11	−1.2160	−0.68218	−4.1060	0.049	6.140	95.52
+1.12	−1.2165	−0.68277	−4.1668	0.046	6.015	109.3

12.6

(1)	(4)	(5)	(6)	(7)	(8)	(9)
+0.32	−0.3513	−0.07372	−0.2952	2.438	1.274	4.006
+0.34	−0.3996	−0.08034	−0.3218	2.393	1.380	4.008
+0.36	−0.4470	−0.08751	−0.3505	2.344	1.494	4.008
+0.38	−0.4934	−0.09527	−0.3816	2.292	1.617	4.008
+0.40	−0.5387	−0.10366	−0.4153	2.238	1.747	4.009
+0.42	−0.5828	−0.11272	−0.4516	2.179	1.886	4.010
+0.44	−0.6258	−0.12249	−0.4908	2.118	2.034	4.011
+0.46	−0.6675	−0.13301	−0.5330	2.054	2.190	4.012
+0.48	−0.7079	−0.14434	−0.5785	1.986	2.356	4.013
+0.50	−0.7470	−0.15651	−0.6273	1.916	2.532	4.015
+0.52	−0.7845	−0.16958	−0.6798	1.842	2.717	4.017
+0.54	−0.8206	−0.18358	−0.7361	1.766	2.912	4.020
+0.56	−0.8551	−0.19857	−0.7964	1.687	3.116	4.023
+0.58	−0.8880	−0.21458	−0.8608	1.606	3.332	4.026
+0.60	−0.9193	−0.23168	−0.9297	1.523	3.556	4.031
+0.62	−0.9489	−0.24989	−1.0031	1.438	3.792	4.036
+0.64	−0.9768	−0.26927	−1.0814	1.352	4.038	4.043
+0.66	−1.0030	−0.28984	−1.1648	1.265	4.294	4.054
+0.68	−1.0274	−0.31165	−1.2533	1.178	4.562	4.066
+0.70	−1.0501	−0.33473	−1.3473	1.090	4.840	4.082
+0.71	−1.0608	−0.34675	−1.3964	1.046	4.984	4.092
+0.72	−1.0710	−0.35909	−1.4470	1.002	5.130	4.103
+0.73	−1.0808	−0.37176	−1.4990	0.959	5.279	4.115
+0.74	−1.0902	−0.38474	−1.5526	0.916	5.432	4.131
+0.75	−1.0992	−0.39805	−1.6077	0.873	5.587	4.149

12.6 (CONT.)

(1)	(4)	(5)	(6)	(7)	(8)	(9)
+0.76	−1.1077	−0.41168	−1.6644	0.831	5.746	4.170
+0.77	−1.1158	−0.42561	−1.7226	0.789	5.908	4.194
+0.78	−1.1235	−0.43985	−1.7825	0.748	6.072	4.223
+0.79	−1.1308	−0.45437	−1.8441	0.707	6.239	4.256
+0.80	−1.1376	−0.46916	−1.9073	0.667	6.409	4.296
+0.81	−1.1441	−0.48419	−1.9723	0.628	6.581	4.344
+0.82	−1.1502	−0.49945	−2.0389	0.589	6.755	4.402
+0.83	−1.1559	−0.51488	−2.1074	0.552	6.930	4.470
+0.84	−1.1612	−0.53044	−2.1776	0.515	7.106	4.552
+0.85	−1.1662	−0.54608	−2.2495	0.479	7.282	4.652
+0.86	−1.1708	−0.56172	−2.3232	0.444	7.456	4.772
+0.87	−1.1751	−0.57729	−2.3986	0.411	7.627	4.919
+0.88	−1.1790	−0.59270	−2.4757	0.378	7.793	5.097
+0.89	−1.1826	−0.60784	−2.5544	0.347	7.952	5.315
+0.90	−1.1860	−0.62258	−2.6347	0.318	8.101	5.582
+0.91	−1.1890	−0.63682	−2.7164	0.289	8.238	5.910
+0.92	−1.1917	−0.65042	−2.7994	0.263	8.359	6.312
+0.93	−1.1942	−0.66327	−2.8835	0.237	8.463	6.806
+0.94	−1.1965	−0.67526	−2.9686	0.214	8.546	7.413
+0.95	−1.1985	−0.68631	−3.0544	0.192	8.607	8.158
+0.96	−1.2003	−0.69635	−3.1406	0.172	8.644	9.072
+0.97	−1.2020	−0.70536	−3.2272	0.153	8.656	10.19
+0.98	−1.2034	−0.71335	−3.3137	0.137	8.645	11.55
+0.99	−1.2047	−0.72034	−3.4000	0.122	8.611	13.22
+1.00	−1.2058	−0.72640	−3.4858	0.108	8.556	15.23
+1.01	−1.2069	−0.73161	−3.5710	0.096	8.481	17.67
+1.02	−1.2078	−0.73604	−3.6554	0.086	8.391	20.59
+1.03	−1.2086	−0.73978	−3.7388	0.076	8.287	24.10
+1.04	−1.2093	−0.74294	−3.8211	0.068	8.171	28.30
+1.05	−1.2100	−0.74558	−3.9022	0.061	8.045	33.29
+1.06	−1.2106	−0.74780	−3.9820	0.054	7.913	39.19
+1.07	−1.2111	−0.74964	−4.0604	0.049	7.776	46.18
+1.08	−1.2116	−0.75118	−4.1375	0.044	7.634	54.33
+1.09	−1.2120	−0.75246	−4.2131	0.040	7.490	63.91
+1.10	−1.2124	−0.75354	−4.2872	0.036	7.344	75.08
+1.11	−1.2128	−0.75443	−4.3600	0.032	7.198	88.03
+1.12	−1.2131	−0.75518	−4.4312	0.030	7.051	103.0
+1.13	−1.2134	−0.75581	−4.5010	0.027	6.906	120.3
+1.14	−1.2137	−0.75633	−4.5693	0.025	6.761	140.1

12.7

(1)	(4)	(5)	(6)	(7)	(8)	(9)
+0.42	−0.5829	−0.11282	−0.4516	2.180	1.887	4.004
+0.44	−0.6259	−0.12260	−0.4908	2.118	2.034	4.005
+0.46	−0.6676	−0.13315	−0.5331	2.054	2.192	4.006
+0.48	−0.7080	−0.14450	−0.5786	1.986	2.358	4.007
+0.50	−0.7470	−0.15670	−0.6274	1.916	2.533	4.007
+0.52	−0.7845	−0.16980	−0.6799	1.842	2.718	4.008
+0.54	−0.8206	−0.18384	−0.7362	1.766	2.914	4.010
+0.56	−0.8552	−0.19888	−0.7966	1.687	3.119	4.011
+0.58	−0.8881	−0.21496	−0.8611	1.606	3.334	4.013
+0.60	−0.9194	−0.23214	−0.9300	1.523	3.560	4.015
+0.62	−0.9490	−0.25045	−1.0036	1.438	3.797	4.018
+0.64	−0.9769	−0.26995	−1.0820	1.352	4.044	4.022
+0.66	−1.0031	−0.29069	−1.1654	1.266	4.303	4.026
+0.68	−1.0275	−0.31272	−1.2541	1.178	4.574	4.032
+0.70	−1.0502	−0.33608	−1.3484	1.090	4.856	4.040
+0.72	−1.0711	−0.36082	−1.4485	1.003	5.152	4.050
+0.74	−1.0903	−0.38698	−1.5546	0.916	5.461	4.063
+0.76	−1.1078	−0.41459	−1.6670	0.832	5.786	4.082
+0.78	−1.1236	−0.44368	−1.7861	0.748	6.127	4.108
+0.80	−1.1377	−0.47424	−1.9122	0.677	6.486	4.145
+0.81	−1.1442	−0.49007	−1.9780	0.628	6.672	4.168
+0.82	−1.1503	−0.50625	−2.0457	0.589	6.864	4.197
+0.83	−1.1560	−0.52277	−2.1153	0.551	7.060	4.232
+0.84	−1.1613	−0.53960	−2.1869	0.515	7.260	4.273
+0.85	−1.1663	−0.55673	−2.2605	0.479	7.465	4.324
+0.86	−1.1709	−0.57412	−2.3362	0.444	7.674	4.385
+0.87	−1.1752	−0.59171	−2.4140	0.409	7.887	4.461
+0.88	−1.1791	−0.60946	−2.4940	0.377	8.101	4.554
+0.89	−1.1827	−0.62726	−2.5761	0.346	8.317	4.669
+0.90	−1.1860	−0.64504	−2.6603	0.315	8.532	4.812
+0.91	−1.1890	−0.66268	−2.7467	0.287	8.744	4.992
+0.92	−1.1918	−0.68003	−2.8352	0.259	8.949	5.216
+0.93	−1.1942	−0.69694	−2.9256	0.233	9.144	5.497
+0.94	−1.1964	−0.71324	−3.0180	0.208	9.325	5.852
+0.95	−1.1984	−0.72876	−3.1121	0.186	9.487	6.299

12.7 (CONT.)

(1)	(4)	(5)	(6)	(7)	(8)	(9)
+0.96	−1.2001	−0.74331	−3.2077	0.164	9.626	6.865
+0.97	−1.2017	−0.75675	−3.3045	0.145	9.737	7.582
+0.98	−1.2030	−0.76896	−3.4023	0.127	9.817	8.486
+0.99	−1.2042	−0.77987	−3.5007	0.111	9.865	9.626
+1.00	−1.2053	−0.78947	−3.5995	0.096	9.879	11.06
+1.01	−1.2062	−0.79776	−3.6982	0.084	9.861	12.87
+1.02	−1.2070	−0.80482	−3.7966	0.073	9.813	15.12
+1.03	−1.2076	−0.81078	−3.8944	0.063	9.736	17.93
+1.04	−1.2082	−0.81573	−3.9913	0.054	9.637	21.41
+1.05	−1.2087	−0.81982	−4.0870	0.047	9.518	25.70
+1.06	−1.2092	−0.82318	−4.1816	0.041	9.383	30.98
+1.07	−1.2096	−0.82592	−4.2747	0.036	9.236	37.44
+1.08	−1.2099	−0.82814	−4.3662	0.031	9.079	45.28
+1.09	−1.2102	−0.82995	−4.4562	0.027	8.915	54.79
+1.10	−1.2105	−0.83142	−4.5445	0.024	8.748	66.27
+1.11	−1.2107	−0.83261	−4.6312	0.021	8.577	80.01
+1.12	−1.2109	−0.83358	−4.7161	0.018	8.404	96.38
+1.13	−1.2111	−0.83437	−4.7992	0.016	8.231	115.9
+1.14	−1.2113	−0.83501	−4.8807	0.015	8.059	139.0
+1.15	−1.2114	−0.83554	−4.9604	0.013	7.888	166.2
+1.16	−1.2115	−0.83597	−5.0384	0.012	7.718	198.1
+1.17	−1.2116	−0.83632	−5.1148	0.010	7.550	235.4
+1.18	−1.2117	−0.83661	−5.1894	0.009	7.385	278.8
+1.19	−1.2118	−0.83685	−5.2625	0.009	7.222	329.1
+1.20	−1.2119	−0.83705	−5.3339	0.008	7.063	387.2

12.8

(1)	(4)	(5)	(6)	(7)	(8)	(9)
+0.52	−0.7846	−0.16991	−0.6800	1.842	2.720	4.004
+0.54	−0.8207	−0.18398	−0.7363	1.766	2.915	4.005
+0.56	−0.8552	−0.19904	−0.7967	1.688	3.120	4.005
+0.58	−0.8881	−0.21516	−0.8612	1.606	3.336	4.006
+0.60	−0.9194	−0.23237	−0.9302	1.523	3.563	4.008
+0.62	−0.9490	−0.25074	−1.0038	1.438	3.800	4.009
+0.64	−0.9769	−0.27030	−1.0823	1.352	4.048	4.011
+0.66	−1.0031	−0.29113	−1.1658	1.266	4.308	4.013
+0.68	−1.0275	−0.31326	−1.2546	1.178	4.580	4.016
+0.70	−1.0502	−0.33676	−1.3491	1.090	4.864	4.020
+0.72	−1.0712	−0.36168	−1.4493	1.003	5.162	4.025
+0.74	−1.0904	−0.38808	−1.5557	0.916	5.476	4.032
+0.76	−1.1078	−0.41602	−1.6685	0.832	5.806	4.042
+0.78	−1.1236	−0.44555	−1.7880	0.748	6.154	4.055
+0.80	−1.1378	−0.47674	−1.9148	0.667	6.524	4.073
+0.82	−1.1503	−0.50962	−2.0492	0.589	6.918	4.100
+0.84	−1.1614	−0.54422	−2.1917	0.514	7.338	4.139
+0.85	−1.1663	−0.56216	−2.2662	0.478	7.559	4.165
+0.86	−1.1709	−0.58052	−2.3429	0.443	7.789	4.198
+0.87	−1.1752	−0.59928	−2.4219	0.409	8.025	4.237
+0.88	−1.1791	−0.61839	−2.5034	0.377	8.270	4.285
+0.89	−1.1827	−0.63785	−2.5874	0.345	8.523	4.346
+0.90	−1.1860	−0.65759	−2.6739	0.315	8.783	4.423
+0.91	−1.1890	−0.67754	−2.7630	0.285	9.049	4.519
+0.92	−1.1918	−0.69760	−2.8549	0.258	9.318	4.641
+0.93	−1.1942	−0.71764	−2.9494	0.231	9.591	4.798
+0.94	−1.1964	−0.73752	−3.0467	0.206	9.861	4.998
+0.95	−1.1983	−0.75703	−3.1466	0.182	10.124	5.256
+0.96	−1.2000	−0.77596	−3.2491	0.161	10.375	5.590
+0.97	−1.2015	−0.79407	−3.3541	0.141	10.607	6.024
+0.98	−1.2029	−0.81110	−3.4612	0.122	10.813	6.590
+0.99	−1.2040	−0.82681	−3.5702	0.105	10.985	7.330
+1.00	−1.2050	−0.84102	−3.6807	0.090	11.117	8.294
+1.005	−1.2054	−0.84751	−3.7364	0.083	11.166	8.882
+1.010	−1.2058	−0.85359	−3.7924	0.077	11.204	9.553
+1.015	−1.2062	−0.85924	−3.8484	0.071	11.231	10.32
+1.020	−1.2065	−0.86447	−3.9046	0.065	11.246	11.19
+1.025	−1.2068	−0.86930	−3.9609	0.060	11.249	12.19
+1.030	−1.2071	−0.87371	−4.0171	0.055	11.241	13.32
+1.035	−1.2074	−0.87774	−4.0732	0.050	11.223	14.60
+1.040	−1.2076	−0.88140	−4.1293	0.046	11.194	16.06
+1.045	−1.2078	−0.88471	−4.1852	0.042	11.157	17.73
+1.050	−1.2080	−0.88770	−4.2408	0.039	11.110	19.59
+1.055	−1.2082	−0.89039	−4.2962	0.036	11.056	21.72
+1.060	−1.2084	−0.89280	−4.3514	0.033	10.994	24.12
+1.065	−1.2085	−0.89496	−4.4062	0.030	10.926	26.82
+1.070	−1.2087	−0.89688	−4.4606	0.027	10.853	29.86
+1.075	−1.2088	−0.89860	−4.5147	0.025	10.774	33.29
+1.080	−1.2089	−0.90012	−4.5683	0.023	10.692	37.15
+1.085	−1.2090	−0.90148	−4.6216	0.021	10.605	41.49

12.8 (CONT.)

(1)	(4)	(5)	(6)	(7)	(8)	(9)
+1.090	−1.2092	−0.90269	−4.6744	0.019	10.516	46.33
+1.095	−1.2092	−0.90376	−4.7267	0.018	10.423	51.76
+1.100	−1.2093	−0.90471	−4.7786	0.016	10.329	57.80
+1.105	−1.2094	−0.90555	−4.8300	0.015	10.232	64.56
+1.110	−1.2095	−0.90629	−4.8809	0.014	10.134	72.10
+1.115	−1.2096	−0.90696	−4.9314	0.013	10.035	80.48
+1.120	−1.2096	−0.90754	−4.9813	0.012	9.935	89.80
+1.125	−1.2097	−0.90806	−5.0307	0.011	9.834	100.1
+1.130	−1.2097	−0.90853	−5.0796	0.010	9.734	111.6
+1.14	−1.2098	−0.90930	−5.1760	0.009	9.531	138.3
+1.15	−1.2099	−0.90992	−5.2702	0.008	9.329	170.9
+1.16	−1.2100	−0.91040	−5.3625	0.007	9.129	210.4
+1.17	−1.2101	−0.91079	−5.4528	0.006	8.930	258.1
+1.18	−1.2101	−0.91110	−5.5412	0.005	8.734	315.4
+1.19	−1.2102	−0.91135	−5.6275	0.004	8.542	384.0
+1.20	−1.2102	−0.91155	−5.7120	0.004	8.352	465.6
+1.21	−1.2103	−0.91171	−5.7946	0.003	8.165	562.2
+1.22	−1.2103	−0.91184	−5.8753	0.003	7.982	676.3
+1.23	−1.2103	−0.91195	−5.9542	0.003	7.803	810.2
+1.24	−1.2104	−0.91203	−6.0314	0.002	7.628	967.0
+1.25	−1.2104	−0.91210	−6.1068	0.002	7.456	1150.
+1.26	−1.2104	−0.91216	−6.1805	0.002	7.287	1362.
+1.27	−1.2104	−0.91221	−6.2526	0.002	7.122	1606.

12.9

(1)	(4)	(5)	(6)	(7)	(8)	(9)
−0.70	+2.57841	−0.000720	−0.00288	2.994	0.013	4.000
−0.68	+2.51854	−0.000790	−0.00316	2.993	0.015	"
−0.66	+2.45868	−0.000866	−0.00346	2.993	0.016	"
−0.64	+2.39883	−0.000949	−0.00380	2.992	0.017	"
−0.62	+2.33899	−0.001040	−0.00416	2.991	0.019	"
−0.60	+2.27917	−0.001141	−0.00456	2.991	0.021	4.000
−0.58	+2.21937	−0.001251	−0.00500	2.990	0.023	"
−0.56	+2.15959	−0.001371	−0.00548	2.989	0.025	"
−0.54	+2.09983	−0.001503	−0.00601	2.988	0.028	"
−0.52	+2.04009	−0.001648	−0.00659	2.986	0.030	"
−0.50	+1.98037	−0.001807	−0.00723	2.985	0.033	4.000
−0.48	+1.92069	−0.001981	−0.00792	2.984	0.036	"
−0.46	+1.86103	−0.002172	−0.00869	2.982	0.040	"
−0.44	+1.80141	−0.002380	−0.00952	2.980	0.044	"
−0.42	+1.74182	−0.002610	−0.01044	2.978	0.048	"
−0.40	+1.68227	−0.002860	−0.01144	2.976	0.053	4.000
−0.38	+1.62276	−0.003136	−0.01254	2.974	0.058	"
−0.36	+1.56331	−0.003437	−0.01375	2.972	0.063	"
−0.34	+1.50390	−0.003767	−0.01507	2.969	0.069	"
−0.32	+1.44455	−0.004129	−0.01652	2.966	0.076	"
−0.30	+1.38527	−0.004526	−0.01810	2.963	0.083	4.000
−0.28	+1.32605	−0.004961	−0.01984	2.959	0.091	"
−0.26	+1.26690	−0.005437	−0.02175	2.955	0.100	"
−0.24	+1.20785	−0.005959	−0.02384	2.951	0.109	"
−0.22	+1.14888	−0.006530	−0.02612	2.946	0.120	"
−0.20	+1.09000	−0.007156	−0.02862	2.941	0.131	4.000
−0.18	+1.03123	−0.007841	−0.03136	2.936	0.143	"
−0.16	+0.97258	−0.008592	−0.03437	2.930	0.157	"
−0.14	+0.91405	−0.009414	−0.03766	2.923	0.172	"
−0.12	+0.85567	−0.010314	−0.04126	2.916	0.188	"
−0.10	+0.79743	−0.011299	−0.04520	2.908	0.206	4.000
−0.08	+0.73937	−0.012377	−0.04951	2.899	0.225	"
−0.06	+0.68148	−0.013556	−0.05422	2.889	0.247	"
−0.04	+0.62380	−0.014846	−0.05939	2.879	0.270	"
−0.02	+0.56632	−0.016258	−0.06503	2.868	0.295	"
0.00	+0.50909	−0.017801	−0.07120	2.856	0.323	4.000
+0.02	+0.45211	−0.019488	−0.07795	2.842	0.353	"
+0.04	+0.39541	−0.021332	−0.08533	2.828	0.385	"
+0.06	+0.33902	−0.023347	−0.09339	2.812	0.421	"
+0.08	+0.28295	−0.025548	−0.10219	2.794	0.460	"
+0.10	+0.22725	−0.027952	−0.11181	2.776	0.502	4.000
+0.12	+0.17193	−0.030574	−0.12230	2.756	0.548	"
+0.14	+0.11704	−0.033436	−0.13375	2.734	0.598	"
+0.16	+0.06260	−0.036558	−0.14623	2.710	0.652	"
+0.18	+0.00866	−0.039960	−0.15984	2.684	0.710	"
+0.20	−0.04474	−0.043667	−0.17467	2.656	0.773	4.000
+0.22	−0.09757	−0.047703	−0.19081	2.626	0.842	"
+0.24	−0.14978	−0.052095	−0.20838	2.594	0.916	"
+0.26	−0.20131	−0.056872	−0.22749	2.559	0.996	"
+0.28	−0.25212	−0.062064	−0.24826	2.522	1.082	"

12.9 (CONT.)

(1)	(4)	(5)	(6)	(7)	(8)	(9)
+0.30	−0.30216	−0.067702	−0.27081	2.482	1.174	4.000
+0.32	−0.35137	−0.073820	−0.29528	2.439	1.274	"
+0.34	−0.39969	−0.080455	−0.32182	2.393	1.381	"
+0.36	−0.44707	−0.087642	−0.35057	2.344	1.495	"
+0.38	−0.49344	−0.095421	−0.38168	2.292	1.618	"
+0.40	−0.53874	−0.103831	−0.41532	2.238	1.748	4.000
+0.42	−0.58292	−0.112917	−0.45166	2.179	1.887	"
+0.44	−0.62590	−0.122718	−0.49087	2.118	2.035	"
+0.46	−0.66762	−0.133283	−0.53313	2.054	2.192	"
+0.48	−0.70802	−0.144657	−0.57863	1.986	2.359	"
+0.50	−0.74704	−0.156887	−0.62755	1.916	2.535	4.000
+0.52	−0.78462	−0.170020	−0.68008	1.842	2.720	"
+0.54	−0.82071	−0.184108	−0.73643	1.766	2.916	"
+0.56	−0.85524	−0.199199	−0.79680	1.687	3.122	"
+0.58	−0.88818	−0.215346	−0.86138	1.606	3.338	"
+0.60	−0.91948	−0.232600	−0.93040	1.523	3.565	4.000
+0.62	−0.94909	−0.251015	−1.00406	1.438	3.803	"
+0.63	−0.96326	−0.260676	−1.04270	1.395	3.926	"
+0.64	−0.97700	−0.270647	−1.08259	1.352	4.052	"
+0.65	−0.99030	−0.280936	−1.12375	1.309	4.181	"
+0.66	−1.00318	−0.291553	−1.16621	1.265	4.312	4.000
+0.67	−1.01561	−0.302502	−1.21001	1.222	4.447	"
+0.68	−1.02760	−0.313792	−1.25517	1.178	4.586	"
+0.69	−1.03916	−0.325432	−1.30173	1.134	4.727	"
+0.70	−1.05028	−0.337430	−1.34972	1.090	4.872	"
+0.71	−1.06096	−0.349796	−1.39918	1.046	5.021	4.000
+0.72	−1.07121	−0.362536	−1.45015	1.003	5.173	"
+0.73	−1.08102	−0.375664	−1.50266	0.959	5.329	"
+0.74	−1.09040	−0.389187	−1.55675	0.916	5.490	"
+0.75	−1.09934	−0.403118	−1.61247	0.874	5.655	"
+0.76	−1.10787	−0.417468	−1.66987	0.831	5.826	4.000
+0.77	−1.11597	−0.432250	−1.72900	0.789	6.001	"
+0.78	−1.12366	−0.447478	−1.78991	0.748	6.182	"
+0.79	−1.13093	−0.463166	−1.85267	0.707	6.369	"
+0.80	−1.13780	−0.479331	−1.91732	0.667	6.564	"
+0.81	−1.14428	−0.495990	−1.98396	0.628	6.765	4.000
+0.82	−1.15036	−0.513163	−2.05265	0.589	6.975	"
+0.83	−1.15606	−0.530871	−2.12348	0.551	7.193	"
+0.84	−1.16139	−0.549138	−2.19655	0.514	7.422	"
+0.85	−1.16635	−0.567991	−2.27196	0.478	7.662	"
+0.86	−1.17096	−0.587458	−2.34983	0.443	7.914	4.000
+0.87	−1.17522	−0.607574	−2.43030	0.409	8.181	"
+0.88	−1.17914	−0.628375	−2.51350	0.376	8.463	"
+0.89	−1.18275	−0.649903	−2.59961	0.345	8.763	"
+0.90	−1.18605	−0.672207	−2.68883	0.314	9.083	"
+0.91	−1.18904	−0.695340	−2.78136	0.285	9.427	4.000
+0.92	−1.19175	−0.719365	−2.87746	0.257	9.798	"

13.1

(1)	(4)	(6)	(7)	(8)
−0.28	+0.45076	+0.29325	2.535	2.134
−0.26	+0.40193	+0.24912	2.350	2.281
−0.24	+0.35664	+0.20212	2.182	2.417
−0.22	+0.31457	+0.15249	2.028	2.544
−0.20	+0.27543	+0.10045	1.888	2.658
−0.18	+0.23898	+0.04624	1.759	2.761
−0.16	+0.20500	−0.00989	1.641	2.851
−0.14	+0.17328	−0.06772	1.533	2.929
−0.12	+0.14362	−0.12697	1.434	2.995
−0.10	+0.11584	−0.18743	1.344	3.049
−0.08	+0.08980	−0.24886	1.261	3.092
−0.06	+0.06533	−0.31102	1.187	3.124
−0.04	+0.04229	−0.37373	1.118	3.146
−0.02	+0.02055	−0.43678	1.056	3.158
0.00	0.00000	−0.50000	1.000	3.162
+0.01	−0.00987	−0.53162	0.974	3.161
+0.02	−0.01948	−0.56322	0.949	3.159
+0.03	−0.02885	−0.59478	0.925	3.154
+0.04	−0.03800	−0.62629	0.903	3.148
+0.05	−0.04692	−0.65773	0.882	3.140
+0.06	−0.05564	−0.68909	0.862	3.131
+0.07	−0.06415	−0.72034	0.842	3.120
+0.08	−0.07249	−0.75148	0.824	3.108
+0.09	−0.08064	−0.78250	0.807	3.095
+0.10	−0.08863	−0.81337	0.791	3.081

13.1 (CONT.)

(1)	(4)	(6)	(7)	(8)
+0.11	-0.09646	-0.84410	0.775	3.065
+0.12	-0.10414	-0.87468	0.761	3.049
+0.13	-0.11168	-0.90508	0.747	3.032
+0.14	-0.11909	-0.93530	0.734	3.014
+0.16	-0.13351	-0.99520	0.710	2.975
+0.18	-0.14750	-1.05430	0.689	2.934
+0.20	-0.16109	-1.11256	0.670	2.891
+0.22	-0.17433	-1.16989	0.655	2.847
+0.24	-0.18727	-1.22636	0.640	2.807
+0.26	-0.19995	-1.28191	0.628	2.754
+0.28	-0.21241	-1.33652	0.618	2.707
+0.30	-0.22469	-1.39018	0.610	2.659
+0.32	-0.23681	-1.44287	0.603	2.611
+0.34	-0.24882	-1.49462	0.598	2.563
+0.36	-0.26073	-1.54541	0.594	2.516
+0.38	-0.27259	-1.59527	0.592	2.469
+0.40	-0.28441	-1.64419	0.591	2.423
+0.42	-0.29622	-1.69221	0.591	2.378
+0.44	-0.30805	-1.73932	0.592	2.334
+0.46	-0.31992	-1.78556	0.595	2.291
+0.48	-0.33186	-1.83095	0.598	2.248
+0.50	-0.34388	-1.87551	0.603	2.207
+0.52	-0.35600	-1.91926	0.609	2.168
+0.54	-0.36825	-1.96222	0.616	2.129
+0.56	-0.38064	-2.00444	0.624	2.092
+0.58	-0.39320	-2.04593	0.632	2.057
+0.60	-0.40594	-2.08672	0.642	2.023
+0.62	-0.41888	-2.12685	0.652	1.990
+0.64	-0.43203	-2.16633	0.663	1.959
+0.66	-0.44541	-2.20521	0.675	1.929
+0.68	-0.45904	-2.24352	0.688	1.901
+0.70	-0.47292	-2.28128	0.701	1.875
+0.72	-0.48709	-2.31851	0.715	1.850
+0.74	-0.50153	-2.35527	0.730	1.826
+0.76	-0.51628	-2.39157	0.745	1.804
+0.78	-0.53134	-2.42745	0.761	1.784
+0.80	-0.54671	-2.46293	0.777	1.765
+0.82	-0.56242	-2.49805	0.793	1.748
+0.84	-0.57845	-2.53284	0.810	1.732
+0.86	-0.59483	-2.56733	0.828	1.717
+0.88	-0.61156	-2.60154	0.845	1.704
+0.90	-0.62864	-2.63551	0.863	1.693
+0.92	-0.64607	-2.66927	0.880	1.683
+0.94	-0.66385	-2.70284	0.898	1.674
+0.96	-0.68199	-2.73625	0.915	1.667
+0.98	-0.70048	-2.76954	0.933	1.661
+1.00	-0.71932	-2.80272	0.951	1.657
+1.02	-0.73850	-2.83583	0.968	1.654
+1.04	-0.75802	-2.86888	0.984	1.652
+1.06	-0.77787	-2.90192	1.001	1.651

13.2

(1)	(4)	(6)	(7)	(8)
-0.14	+0.20327	-0.06640	2.074	3.441
-0.13	+0.18311	-0.10123	1.958	3.523
-0.12	+0.16408	-0.13683	1.850	3.597
-0.11	+0.14608	-0.17314	1.750	3.664
-0.10	+0.12906	-0.21008	1.656	3.723
-0.09	+0.11295	-0.24758	1.568	3.776
-0.08	+0.09768	-0.28558	1.486	3.822
-0.07	+0.08320	-0.32401	1.410	3.862
-0.06	+0.06946	-0.36280	1.339	3.895
-0.05	+0.05641	-0.40189	1.272	3.923
-0.04	+0.04401	-0.44123	1.210	3.945
-0.03	+0.03220	-0.48077	1.152	3.961
-0.02	+0.02096	-0.52044	1.098	3.972
-0.01	+0.01023	-0.56020	1.047	3.979
0.00	0.00000	-0.60000	1.000	3.981
+0.02	-0.01913	-0.67957	0.915	3.973
+0.04	-0.03666	-0.75883	0.840	3.951
+0.06	-0.05281	-0.83752	0.776	3.916
+0.08	-0.06774	-0.91540	0.719	3.870
+0.10	-0.08162	-0.99228	0.670	3.816
+0.12	-0.09458	-1.06800	0.627	3.755
+0.14	-0.10674	-1.14244	0.590	3.688
+0.16	-0.11821	-1.21548	0.558	3.616
+0.18	-0.12907	-1.28705	0.530	3.541
+0.20	-0.13941	-1.35709	0.505	3.463

13.2 (CONT.)

(1)	(4)	(6)	(7)	(8)
+0.22	-0.14930	-1.42555	0.484	3.383
+0.24	-0.15880	-1.49240	0.466	3.302
+0.26	-0.16798	-1.55763	0.451	3.221
+0.28	-0.17687	-1.62124	0.438	3.140
+0.30	-0.18553	-1.68322	0.428	3.059
+0.32	-0.19399	-1.74354	0.419	2.978
+0.34	-0.20231	-1.80232	0.412	2.899
+0.36	-0.21050	-1.85952	0.407	2.822
+0.38	-0.21861	-1.91519	0.404	2.745
+0.40	-0.22666	-1.96936	0.402	2.671
+0.42	-0.23469	-2.02204	0.401	2.598
+0.44	-0.24278	-2.07330	0.402	2.528
+0.46	-0.25077	-2.12316	0.404	2.459
+0.48	-0.25887	-2.17168	0.407	2.393
+0.50	-0.26705	-2.21888	0.411	2.328
+0.52	-0.27533	-2.26483	0.417	2.266
+0.54	-0.28373	-2.30955	0.423	2.207
+0.56	-0.29227	-2.35311	0.431	2.149
+0.58	-0.30098	-2.39554	0.440	2.094
+0.60	-0.30987	-2.43688	0.450	2.041
+0.62	-0.31898	-2.47720	0.461	1.991
+0.64	-0.32832	-2.51652	0.473	1.942
+0.66	-0.33792	-2.55490	0.487	1.896
+0.68	-0.34779	-2.59239	0.501	1.852
+0.70	-0.35797	-2.62903	0.516	1.811
+0.72	-0.36846	-2.66486	0.533	1.772
+0.74	-0.37929	-2.69992	0.551	1.735
+0.76	-0.39049	-2.73427	0.569	1.700
+0.78	-0.40206	-2.76794	0.589	1.668
+0.80	-0.41405	-2.80098	0.610	1.637
+0.82	-0.42645	-2.83344	0.631	1.609
+0.84	-0.43930	-2.86534	0.654	1.582
+0.86	-0.45260	-2.89674	0.677	1.558
+0.88	-0.46638	-2.92768	0.701	1.536
+0.90	-0.48066	-2.95820	0.726	1.516
+0.92	-0.49544	-2.98833	0.752	1.498
+0.94	-0.51074	-3.01812	0.778	1.482
+0.96	-0.52658	-3.04761	0.805	1.468
+0.98	-0.54295	-3.07683	0.832	1.455
+1.00	-0.55987	-3.10583	0.860	1.445
+1.02	-0.57733	-3.13465	0.887	1.437
+1.04	-0.59535	-3.16331	0.915	1.430
+1.06	-0.61392	-3.19186	0.942	1.425
+1.08	-0.65304	-3.22034	0.970	1.423
+1.10	-0.65271	-3.24877	0.997	1.421
+1.12	-0.67290	-3.27720	1.023	1.422
+1.14	-0.69362	-3.30567	1.049	1.424

13.3

(1)	(4)	(6)	(7)	(8)
-0.10	+0.14861	-0.21548	2.153	4.481
-0.09	+0.12795	-0.26086	1.982	4.593
-0.08	+0.10892	-0.30728	1.827	4.689
-0.07	+0.09137	-0.35459	1.686	4.771
-0.06	+0.07516	-0.40266	1.558	4.840
-0.05	+0.06017	-0.45134	1.442	4.896
-0.04	+0.04629	-0.50053	1.335	4.940
-0.03	+0.03343	-0.55009	1.240	4.973
-0.02	+0.02148	-0.59991	1.152	4.995
-0.01	+0.01036	-0.64991	1.073	5.008
0.00	0.00000	-0.70000	1.000	5.010
+0.02	-0.01869	-0.80013	0.873	4.997
+0.04	-0.03506	-0.89968	0.768	4.955
+0.06	-0.04950	-0.99821	0.680	4.892
+0.08	-0.06233	-1.09529	0.606	4.812
+0.10	-0.07381	-1.19062	0.544	4.719
+0.12	-0.08415	-1.28397	0.492	4.615
+0.14	-0.09354	-1.37517	0.448	4.503
+0.16	-0.10211	-1.46408	0.411	4.386
+0.18	-0.11001	-1.55060	0.380	4.266

13.3 (CONT.)

(1)	(4)	(6)	(7)	(8)
+0.20	-0.11733	-1.63470	0.353	4.143
+0.22	-0.12416	-1.71633	0.331	4.019
+0.24	-0.13058	-1.79548	0.312	3.896
+0.26	-0.13666	-1.87217	0.296	3.773
+0.28	-0.14244	-1.94640	0.283	3.651
+0.30	-0.14797	-2.01823	0.272	3.532
+0.32	-0.15331	-2.08768	0.262	3.414
+0.34	-0.15848	-2.15482	0.255	3.300
+0.36	-0.16352	-2.21970	0.249	3.188
+0.38	-0.16846	-2.28236	0.245	3.079
+0.40	-0.17333	-2.34289	0.242	2.974
+0.42	-0.17815	-2.40135	0.240	2.872
+0.44	-0.18294	-2.45779	0.240	2.773
+0.46	-0.18774	-2.51229	0.240	2.678
+0.48	-0.19255	-2.56491	0.241	2.586
+0.50	-0.19739	-2.61573	0.244	2.497
+0.52	-0.20230	-2.66481	0.247	2.412
+0.54	-0.20728	-2.71221	0.252	2.330
+0.56	-0.21236	-2.75801	0.257	2.251
+0.58	-0.21756	-2.80227	0.263	2.176
+0.60	-0.22290	-2.84506	0.275	2.103
+0.62	-0.22839	-2.88643	0.279	2.034
+0.64	-0.23405	-2.92644	0.288	1.968
+0.66	-0.23992	-2.96517	0.299	1.905
+0.68	-0.24600	-3.00267	0.310	1.845
+0.70	-0.25232	-3.03899	0.323	1.788
+0.72	-0.25891	-3.07420	0.336	1.733
+0.74	-0.26579	-3.10835	0.351	1.682
+0.76	-0.27298	-3.14149	0.368	1.633
+0.78	-0.28051	-3.17368	0.385	1.587
+0.80	-0.28840	-3.20498	0.404	1.543
+0.82	-0.29669	-3.23543	0.425	1.502
+0.84	-0.30539	-3.26508	0.446	1.464
+0.86	-0.31454	-3.29398	0.469	1.427
+0.88	-0.32417	-3.32219	0.494	1.394
+0.90	-0.33431	-3.34975	0.520	1.362
+0.92	-0.34498	-3.37670	0.547	1.333
+0.94	-0.35622	-3.40310	0.576	1.307
+0.96	-0.36804	-3.42899	0.607	1.282
+0.98	-0.38049	-3.45441	0.638	1.260
+1.00	-0.39359	-3.47941	0.671	1.241
+1.02	-0.40736	-3.50404	0.706	1.223
+1.04	-0.42182	-3.52834	0.741	1.207
+1.06	-0.43700	-3.55235	0.777	1.194
+1.08	-0.45292	-3.57611	0.815	1.183
+1.10	-0.46959	-3.59968	0.853	1.174
+1.12	-0.48703	-3.62308	0.891	1.167
+1.14	-0.50524	-3.64636	0.930	1.162
+1.16	-0.52422	-3.66958	0.969	1.159
+1.18	-0.54398	-3.69275	1.008	1.159

13.4

(1)	(4)	(6)	(7)	(8)
-0.04	+0.04936	-0.54987	1.512	6.175
-0.035	+0.04200	-0.58083	1.433	6.209
-0.03	+0.03503	-0.61194	1.359	6.237
-0.025	+0.02841	-0.64319	1.289	6.260
-0.02	+0.02213	-0.67454	1.223	6.279
-0.015	+0.01617	-0.70597	1.162	6.293
-0.01	+0.01051	-0.73746	1.104	6.302
-0.005	+0.00512	-0.76898	1.050	6.308
0.00	0.00000	-0.80000	1.000	6.310
+0.01	-0.00952	-0.86307	0.907	6.303
+0.02	-0.01817	-0.92601	0.824	6.283
+0.03	-0.02603	-0.98870	0.750	6.252
+0.04	-0.03320	-1.05102	0.685	6.212
+0.05	-0.03975	-1.11290	0.627	6.162
+0.06	-0.04576	-1.17425	0.575	6.106
+0.07	-0.05128	-1.23500	0.529	6.043
+0.08	-0.05636	-1.29510	0.488	5.975
+0.09	-0.06105	-1.35450	0.451	5.903
+0.10	-0.06540	-1.41314	0.418	5.826
+0.11	-0.06943	-1.47101	0.389	5.747
+0.12	-0.07318	-1.52807	0.362	5.665
+0.13	-0.07668	-1.58430	0.338	5.581
+0.14	-0.07995	-1.63968	0.317	5.495
+0.15	-0.08302	-1.69419	0.297	5.408
+0.16	-0.08590	-1.74783	0.279	5.320

13.4 (CONT.)

(1)	(4)	(6)	(7)	(8)
+0.18	-0.09117	-1.85246	0.249	5.142
+0.20	-0.09590	-1.95354	0.224	4.965
+0.22	-0.10017	-2.05106	0.204	4.788
+0.24	-0.10406	-2.14508	0.187	4.614
+0.26	-0.10765	-2.23564	0.172	4.443
+0.28	-0.11098	-2.32281	0.161	4.275
+0.30	-0.11409	-2.40668	0.151	4.112
+0.32	-0.11703	-2.48734	0.143	3.954
+0.34	-0.11982	-2.56488	0.137	3.800
+0.36	-0.12250	-2.63939	0.131	3.652
+0.38	-0.12509	-2.71098	0.127	3.508
+0.40	-0.12760	-2.77975	0.124	3.370
+0.42	-0.13005	-2.84580	0.121	3.236
+0.44	-0.13246	-2.90924	0.120	3.108
+0.46	-0.13484	-2.97015	0.119	2.984
+0.48	-0.13722	-3.02864	0.119	2.866
+0.50	-0.13959	-3.08481	0.119	2.752
+0.52	-0.14198	-3.13874	0.120	2.642
+0.54	-0.14440	-3.19053	0.122	2.537
+0.56	-0.14685	-3.24027	0.124	2.437
+0.58	-0.14936	-3.28804	0.127	2.341
+0.60	-0.15192	-3.33392	0.130	2.249
+0.62	-0.15456	-3.37801	0.134	2.161
+0.64	-0.15729	-3.42037	0.139	2.076
+0.66	-0.16001	-3.46108	0.144	1.995
+0.68	-0.16296	-3.50021	0.150	1.918
+0.70	-0.16603	-3.53784	0.157	1.845
+0.72	-0.16924	-3.57404	0.165	1.775
+0.74	-0.17262	-3.60887	0.173	1.709
+0.76	-0.17618	-3.64240	0.183	1.645
+0.78	-0.17993	-3.67469	0.193	1.585
+0.80	-0.18390	-3.70581	0.204	1.527
+0.82	-0.18811	-3.73580	0.217	1.473
+0.84	-0.19258	-3.76473	0.231	1.421
+0.86	-0.19734	-3.79266	0.245	1.372
+0.88	-0.20241	-3.81963	0.262	1.326
+0.90	-0.20782	-3.84570	0.280	1.282
+0.92	-0.21361	-3.87092	0.298	1.241
+0.94	-0.21979	-3.89534	0.320	1.202
+0.96	-0.22641	-3.91900	0.342	1.165
+0.98	-0.23350	-3.94196	0.367	1.131
+1.00	-0.24110	-3.96426	0.393	1.099
+1.02	-0.24924	-3.98594	0.422	1.042
+1.04	-0.25797	-4.00706	0.452	1.070
+1.06	-0.26733	-4.02765	0.484	1.017
+1.08	-0.27736	-4.04775	0.519	0.994
+1.10	-0.28809	-4.06742	0.555	0.973
+1.12	-0.29958	-4.08669	0.594	0.954
+1.14	-0.31186	-4.10560	0.635	0.937
+1.16	-0.32498	-4.12419	0.677	0.923

13.5

(1)	(4)	(6)	(7)	(8)
-0.0150	+0.01667	-0.78100	1.232	7.913
-0.0125	+0.01364	-0.80080	1.190	7.922
-0.0100	+0.01072	-0.82061	1.148	7.930
-0.0075	+0.00790	-0.84044	1.109	7.936
-0.0050	+0.00518	-0.86029	1.071	7.940
-0.0025	+0.00254	-0.88014	1.035	7.942
0.0000	0.00000	-0.90000	1.000	7.943
+0.0025	-0.00246	-0.91986	0.966	7.942
+0.0050	-0.00483	-0.93971	0.934	7.940
+0.0075	-0.00713	-0.95956	0.903	7.936
+0.0100	-0.00935	-0.97939	0.874	7.932
+0.0125	-0.01150	-0.99921	0.845	7.925
+0.0150	-0.01358	-1.01901	0.817	7.917
+0.0175	-0.01559	-1.03880	0.791	7.908
+0.0200	-0.01753	-1.05856	0.766	7.898
+0.025	-0.02124	-1.09799	0.717	7.875
+0.030	-0.02471	-1.13730	0.673	7.847
+0.035	-0.02797	-1.17646	0.632	7.816
+0.040	-0.03104	-1.21545	0.594	7.781
+0.045	-0.03391	-1.25426	0.558	7.743

13.5 (CONT.)

(1)	(4)	(5)	(7)	(8)
+0.050	-0.03662	-1.29287	0.525	7.702
+0.055	-0.03917	-1.33128	0.495	7.659
+0.060	-0.04158	-1.36946	0.467	7.613
+0.065	-0.04384	-1.40741	0.440	7.566
+0.070	-0.04598	-1.44511	0.416	7.516
+0.075	-0.04797	-1.48256	0.393	7.464
+0.080	-0.04988	-1.51975	0.372	7.411
+0.085	-0.05169	-1.55667	0.352	7.357
+0.090	-0.05340	-1.59332	0.334	7.301
+0.100	-0.05657	-1.66577	0.300	7.187
+0.11	-0.05942	-1.73706	0.271	7.070
+0.12	-0.06201	-1.80716	0.246	6.950
+0.13	-0.06435	-1.87606	0.224	6.829
+0.14	-0.06649	-1.94374	0.204	6.706
+0.15	-0.06844	-2.01019	0.187	6.583
+0.16	-0.07023	-2.07541	0.172	6.460
+0.17	-0.07188	-2.13939	0.158	6.337
+0.18	-0.07339	-2.20215	0.146	6.214
+0.19	-0.07480	-2.26368	0.135	6.093
+0.20	-0.07611	-2.32400	0.126	5.972
+0.21	-0.07732	-2.38312	0.117	5.852
+0.22	-0.07846	-2.44105	0.110	5.734
+0.23	-0.07952	-2.49781	0.103	5.617
+0.24	-0.08052	-2.55340	0.097	5.502
+0.25	-0.08146	-2.60786	0.091	5.388
+0.26	-0.08234	-2.66118	0.086	5.277
+0.27	-0.08318	-2.71339	0.082	5.166
+0.28	-0.08398	-2.76451	0.078	5.058
+0.29	-0.08474	-2.81456	0.074	4.952
+0.30	-0.08547	-2.86355	0.071	4.847
+0.31	-0.08617	-2.91150	0.068	4.744
+0.32	-0.08683	-2.95844	0.065	4.643
+0.33	-0.08747	-3.00438	0.063	4.544
+0.34	-0.08809	-3.04933	0.061	4.447
+0.35	-0.08868	-3.09333	0.059	4.352
+0.36	-0.08926	-3.13638	0.057	4.259
+0.37	-0.08982	-3.17850	0.055	4.167
+0.38	-0.09037	-3.21972	0.054	4.077
+0.39	-0.09090	-3.26005	0.052	3.989
+0.40	-0.09142	-3.29952	0.051	3.903
+0.42	-0.09242	-3.37590	0.049	3.736
+0.44	-0.09339	-3.44900	0.048	3.576
+0.46	-0.09432	-3.51898	0.046	3.422
+0.48	-0.09524	-3.58594	0.046	3.275
+0.50	-0.09615	-3.65003	0.045	3.134
+0.52	-0.09705	-3.71135	0.045	3.000
+0.54	-0.09795	-3.77004	0.045	2.870
+0.56	-0.09885	-3.82621	0.045	2.747
+0.58	-0.09976	-3.87996	0.046	2.629
+0.60	-0.10068	-3.93139	0.047	2.516
+0.62	-0.10162	-3.98062	0.048	2.408
+0.64	-0.10258	-4.02774	0.049	2.305
+0.66	-0.10358	-4.07283	0.051	2.206
+0.68	-0.10461	-4.11600	0.052	2.112
+0.70	-0.10568	-4.15732	0.055	2.022
+0.72	-0.10680	-4.19689	0.057	1.936
+0.74	-0.10796	-4.23477	0.060	1.853
+0.76	-0.10919	-4.27105	0.063	1.775
+0.78	-0.11049	-4.30578	0.067	1.700
+0.80	-0.11186	-4.33907	0.071	1.629
+0.82	-0.11332	-4.37096	0.075	1.561
+0.84	-0.11487	-4.40152	0.080	1.496
+0.86	-0.11652	-4.43081	0.086	1.434
+0.88	-0.11830	-4.45890	0.092	1.375
+0.90	-0.12020	-4.48583	0.099	1.319
+0.92	-0.12225	-4.51167	0.106	1.265
+0.94	-0.12446	-4.53647	0.115	1.215
+0.96	-0.12684	-4.56027	0.124	1.166
+0.98	-0.12942	-4.58314	0.134	1.121
+1.00	-0.13221	-4.60571	0.145	1.077
+1.02	-0.13524	-4.62623	0.158	1.036
+1.04	-0.13854	-4.64655	0.172	0.997

13.6

(1)	(4)	(6)	(7)	(8)
+0.0000	0.00000	-1.00000	1.000	10.000
+0.0025	-0.00244	-1.02500	0.955	9.999
+0.0050	-0.00478	-1.04999	0.912	9.995
+0.0075	-0.00701	-1.07497	0.872	9.989
+0.0100	-0.00914	-1.09993	0.834	9.980
+0.0125	-0.01118	-1.12487	0.797	9.970
+0.0150	-0.01313	-1.14978	0.762	9.957
+0.0175	-0.01499	-1.17465	0.729	9.942
+0.0200	-0.01678	-1.19949	0.698	9.926
+0.0250	-0.02012	-1.24903	0.640	9.888
+0.030	-0.02318	-1.29836	0.587	9.844
+0.035	-0.02599	-1.34746	0.539	9.795
+0.040	-0.02858	-1.39630	0.496	9.740
+0.045	-0.03096	-1.44486	0.456	9.682
+0.050	-0.03314	-1.49311	0.420	9.619
+0.055	-0.03516	-1.54105	0.388	9.554
+0.060	-0.03703	-1.58865	0.358	9.485
+0.065	-0.03875	-1.63589	0.331	9.414
+0.070	-0.04034	-1.68278	0.307	9.340
+0.075	-0.04182	-1.72929	0.284	9.265
+0.08	-0.04319	-1.77542	0.264	9.187
+0.09	-0.04564	-1.86651	0.228	9.029
+0.10	-0.04777	-1.95599	0.198	8.867
+0.11	-0.04962	-2.04384	0.172	8.702
+0.12	-0.05123	-2.13003	0.151	8.536
+0.13	-0.05264	-2.21455	0.133	8.368
+0.14	-0.05389	-2.29740	0.117	8.201
+0.15	-0.05499	-2.37858	0.104	8.035
+0.16	-0.05597	-2.45810	0.093	7.870
+0.17	-0.05685	-2.53599	0.083	7.706
+0.18	-0.05763	-2.61224	0.074	7.545
+0.19	-0.05833	-2.68688	0.067	7.385
+0.20	-0.05897	-2.75994	0.060	7.227
+0.21	-0.05954	-2.83144	0.055	7.072
+0.22	-0.06007	-2.90139	0.050	6.919
+0.23	-0.06054	-2.96983	0.046	6.769
+0.24	-0.06098	-3.03679	0.042	6.622
+0.25	-0.06138	-3.10228	0.039	6.477
+0.26	-0.06176	-3.16634	0.036	6.335
+0.27	-0.06210	-3.22899	0.033	6.196
+0.28	-0.06242	-3.29026	0.031	6.059
+0.29	-0.06272	-3.35018	0.029	5.925
+0.30	-0.06299	-3.40878	0.027	5.794
+0.31	-0.06325	-3.46608	0.025	5.666
+0.32	-0.06350	-3.52211	0.024	5.540
+0.33	-0.06373	-3.57689	0.022	5.417
+0.34	-0.06345	-3.63045	0.021	5.296
+0.35	-0.06415	-3.68282	0.020	5.178
+0.36	-0.06435	-3.73401	0.019	5.062
+0.37	-0.06454	-3.78406	0.018	4.949
+0.38	-0.06472	-3.83300	0.018	4.839
+0.39	-0.06489	-3.88085	0.017	4.730
+0.40	-0.06505	-3.92762	0.016	4.624
+0.41	-0.06521	-3.97334	0.016	4.521
+0.42	-0.06536	-4.01805	0.015	4.419
+0.43	-0.06551	-4.06174	0.015	4.320
+0.44	-0.06565	-4.10446	0.014	4.223
+0.45	-0.06579	-4.14622	0.014	4.129
+0.46	-0.06593	-4.18704	0.013	4.036
+0.47	-0.06606	-4.22694	0.013	3.945

13.7

(1)	(4)	(6)	(7)	(8)
0.0000	0.00000	-1.10000	1.000	12.589
+0.0025	-0.00244	-1.13147	0.941	12.588
+0.0050	-0.00472	-1.16293	0.886	12.581
+0.0075	-0.00687	-1.19437	0.834	12.571
+0.0100	-0.00889	-1.22578	0.786	12.557
+0.0125	-0.01080	-1.25716	0.740	12.540
+0.0150	-0.01260	-1.28848	0.698	12.520
+0.0175	-0.01429	-1.31975	0.658	12.496
+0.0200	-0.01589	-1.35096	0.621	12.471
+0.0225	-0.01740	-1.38211	0.586	12.442

13.7 (CONT.)

(1)	(4)	(6)	(7)	(8)
+0.0250	-0.01882	-1.41318	0.553	12.412
+0.0275	-0.02016	-1.44416	0.523	12.378
+0.0300	-0.02144	-1.47507	0.494	12.344
+0.0350	-0.02377	-1.53660	0.441	12.268
+0.0400	-0.02586	-1.59774	0.395	12.186
+0.045	-0.02773	-1.65845	0.354	12.098
+0.050	-0.02940	-1.71872	0.318	12.006
+0.055	-0.03091	-1.77851	0.285	11.910
+0.060	-0.03226	-1.83781	0.257	11.810
+0.065	-0.03348	-1.89661	0.232	11.708
+0.070	-0.03459	-1.95489	0.209	11.603
+0.075	-0.03558	-2.01264	0.189	11.497
+0.080	-0.03648	-2.06985	0.171	11.389
+0.090	-0.03803	-2.18265	0.141	11.170
+0.100	-0.03932	-2.29324	0.117	10.948
+0.11	-0.04030	-2.40160	0.097	10.725
+0.12	-0.04127	-2.50773	0.082	10.502
+0.13	-0.04202	-2.61165	0.069	10.281
+0.14	-0.04265	-2.71335	0.058	10.061
+0.15	-0.04319	-2.81288	0.049	9.844
+0.16	-0.04364	-2.91025	0.042	9.630
+0.17	-0.04404	-3.00550	0.036	9.420
+0.18	-0.04437	-3.09866	0.031	9.212
+0.19	-0.04467	-3.18976	0.027	9.009
+0.20	-0.04492	-3.27885	0.024	8.809
+0.21	-0.04514	-3.36595	0.021	8.613
+0.22	-0.04534	-3.45111	0.018	8.421
+0.23	-0.04551	-3.53437	0.016	8.232
+0.24	-0.04566	-3.61577	0.014	8.048
+0.25	-0.04580	-3.69534	0.013	7.867
+0.26	-0.04592	-3.77312	0.012	7.690
+0.27	-0.04603	-3.84914	0.010	7.517
+0.28	-0.04613	-3.92346	0.009	7.347
+0.29	-0.04622	-3.99610	0.009	7.182
+0.30	-0.04630	-4.06710	0.008	7.019
+0.31	-0.04637	-4.13650	0.007	6.861
+0.32	-0.04644	-4.20433	0.007	6.706
+0.33	-0.04650	-4.27062	0.006	6.554
+0.34	-0.04656	-4.33542	0.006	6.406
+0.35	-0.04661	-4.39874	0.005	6.261
+0.36	-0.04666	-4.46064	0.005	6.119
+0.37	-0.04670	-4.52113	0.004	5.980

13.8

(1)	(4)	(6)	(7)	(8)
+0.0000	0.00000	-1.20000	1.000	15.849
+0.0025	-0.00240	-1.23962	0.924	15.845
+0.0050	-0.00462	-1.27922	0.854	15.835
+0.0075	-0.00668	-1.31879	0.789	15.819
+0.0100	-0.00857	-1.35831	0.730	15.797
+0.0125	-0.01033	-1.39777	0.675	15.770
+0.0150	-0.01195	-1.43716	0.625	15.738
+0.0175	-0.01346	-1.47646	0.579	15.702
+0.0200	-0.01485	-1.51566	0.536	15.662
+0.0225	-0.01614	-1.55476	0.497	15.618
+0.0250	-0.01734	-1.59375	0.461	15.572
+0.0275	-0.01845	-1.63262	0.428	15.522
+0.0300	-0.01948	-1.67136	0.397	15.470
+0.0325	-0.02044	-1.70997	0.369	15.415
+0.0350	-0.02132	-1.74844	0.343	15.358
+0.0375	-0.02215	-1.78676	0.319	15.298
+0.0400	-0.02292	-1.82493	0.296	15.238
+0.0425	-0.02363	-1.86294	0.276	15.175
+0.0450	-0.02430	-1.90080	0.257	15.111
+0.0475	-0.02492	-1.93850	0.239	15.046
+0.0500	-0.02550	-1.97603	0.223	14.980
+0.0525	-0.02604	-2.01340	0.208	14.912
+0.0550	-0.02654	-2.05059	0.194	14.844
+0.0575	-0.02701	-2.08761	0.181	14.774
+0.0600	-0.02745	-2.12446	0.169	14.704
+0.0625	-0.02786	-2.16113	0.158	14.634
+0.0650	-0.02824	-2.19763	0.148	14.562
+0.0675	-0.02859	-2.23394	0.138	14.491
+0.0700	-0.02893	-2.27008	0.129	14.419
+0.0725	-0.02924	-2.30604	0.121	14.346

13.8 (CONT.)

(1)	(4)	(6)	(7)	(8)
+0.0750	-0.02953	-2.34181	0.113	14.274
+0.0775	-0.02981	-2.37741	0.106	14.201
+0.0800	-0.03006	-2.41282	0.099	14.128
+0.0825	-0.03030	-2.44804	0.093	14.054
+0.0850	-0.03053	-2.48309	0.087	13.981
+0.0875	-0.03074	-2.51795	0.082	13.907
+0.0900	-0.03094	-2.55262	0.077	13.834
+0.0925	-0.03110	-2.58712	0.072	13.760
+0.0950	-0.03130	-2.62142	0.068	13.687
+0.0975	-0.03147	-2.65555	0.064	13.613
+0.1000	-0.03162	-2.68949	0.060	13.540
+0.1025	-0.03177	-2.72325	0.056	13.467
+0.1050	-0.03190	-2.75682	0.053	13.394
+0.1075	-0.03203	-2.79022	0.050	13.321
+0.1100	-0.03215	-2.82343	0.047	13.248
+0.1125	-0.03227	-2.85646	0.044	13.176
+0.1150	-0.03238	-2.88931	0.042	13.103
+0.1175	-0.03248	-2.92198	0.040	13.031
+0.1200	-0.03258	-2.95446	0.038	12.959
+0.1225	-0.03267	-2.98677	0.035	12.888
+0.1250	-0.03275	-3.01890	0.033	12.816
+0.1275	-0.03283	-3.05085	0.032	12.745
+0.1300	-0.03291	-3.08262	0.030	12.674
+0.1325	-0.03298	-3.11422	0.028	12.603
+0.1350	-0.03305	-3.14564	0.027	12.533
+0.1375	-0.03312	-3.17688	0.025	12.463
+0.1400	-0.03318	-3.20796	0.024	12.393
+0.1425	-0.03324	-3.23885	0.023	12.324
+0.1450	-0.03329	-3.26957	0.022	12.254
+0.1475	-0.03334	-3.30012	0.020	12.186
+0.1500	-0.03339	-3.33050	0.019	12.117
+0.1525	-0.03344	-3.36071	0.018	12.049
+0.1550	-0.03349	-3.39075	0.018	11.981
+0.1575	-0.03353	-3.42061	0.016	11.913
+0.1600	-0.03357	-3.45031	0.016	11.846
+0.1625	-0.03361	-3.47984	0.015	11.779
+0.1650	-0.03364	-3.50921	0.014	11.712
+0.1675	-0.03368	-3.53841	0.014	11.646
+0.1700	-0.03371	-3.56744	0.013	11.580
+0.1725	-0.03374	-3.59631	0.012	11.514
+0.1750	-0.03377	-3.62501	0.012	11.449
+0.1775	-0.03380	-3.65355	0.011	11.384
+0.1800	-0.03383	-3.68193	0.010	11.320
+0.1825	-0.03385	-3.71015	0.010	11.255
+0.1850	-0.03388	-3.73821	0.010	11.191
+0.1875	-0.03390	-3.76611	0.009	11.128
+0.1900	-0.03392	-3.79385	0.009	11.064
+0.1925	-0.03394	-3.82143	0.008	11.001
+0.1950	-0.03397	-3.84885	0.008	10.939
+0.1975	-0.03398	-3.87612	0.008	10.876
+0.2000	-0.03400	-3.90324	0.007	10.814
+0.2025	-0.03402	-3.93020	0.007	10.753
+0.2050	-0.03404	-3.95700	0.007	10.692
+0.2075	-0.03406	-3.98365	0.006	10.630
+0.2100	-0.03407	-4.01015	0.006	10.570
+0.2125	-0.03409	-4.03650	0.006	10.510
+0.2150	-0.03410	-4.06270	0.006	10.450
+0.2175	-0.03412	-4.08875	0.005	10.390
+0.2200	-0.03413	-4.11465	0.005	10.331
+0.2225	-0.03414	-4.14041	0.005	10.272
+0.2250	-0.03415	-4.16601	0.005	10.213
+0.2275	-0.03417	-4.19147	0.004	10.155
+0.2300	-0.03418	-4.21679	0.004	10.097
+0.2325	-0.03419	-4.24196	0.004	10.039
+0.2350	-0.03420	-4.26698	0.004	9.982
+0.2375	-0.03421	-4.29186	0.004	9.924
+0.2400	-0.03422	-4.31660	0.004	9.868
+0.2425	-0.03423	-4.34120	0.004	9.811
+0.2450	-0.03424	-4.36566	0.004	9.755
+0.2475	-0.03424	-4.38997	0.003	9.700
+0.2500	-0.03425	-4.41415	0.003	9.644
+0.2525	-0.03426	-4.43820	0.003	9.589
+0.2550	-0.03427	-4.46210	0.003	9.534
+0.2575	-0.03428	-4.48586	0.003	9.479
+0.2600	-0.03428	-4.50950	0.003	9.425

13.8 (CONT.)

(1)	(4)	(6)	(7)	(8)
+0.2625	-0.03429	-4.53299	0.003	9.371
+0.2650	-0.03430	-4.55635	0.002	9.318
+0.2675	-0.03430	-4.57958	0.002	9.264
+0.2700	-0.03431	-4.60267	0.002	9.211
+0.2725	-0.03432	-4.62564	0.002	9.158
+0.2750	-0.03432	-4.64847	0.002	9.106
+0.2775	-0.03433	-4.67117	0.002	9.054
+0.2800	-0.03433	-4.69374	0.002	9.002
+0.2825	-0.03434	-4.71618	0.002	8.950
+0.2850	-0.03434	-4.73849	0.002	8.899
+0.2875	-0.03435	-4.76067	0.002	8.848
+0.2900	-0.03435	-4.78273	0.002	8.797
+0.2925	-0.03436	-4.80466	0.002	8.747
+0.2950	-0.03436	-4.82646	0.002	8.697
+0.2975	-0.03436	-4.84814	0.002	8.647
+0.3000	-0.03437	-4.86970	0.002	8.597
+0.3025	-0.03437	-4.89113	0.002	8.548
+0.3050	-0.03438	-4.91244	0.002	8.499
+0.3075	-0.03438	-4.93362	0.002	8.450
+0.3100	-0.03438	-4.95469	0.002	8.402
+0.3125	-0.03439	-4.97563	0.002	8.354
+0.3150	-0.03439	-4.99646	0.002	8.306
+0.3175	-0.03439	-5.01716	0.002	8.258
+0.3200	-0.03440	-5.03775	0.002	8.211
+0.3225	-0.03440	-5.05822	0.002	8.164
+0.3250	-0.03440	-5.07857	0.002	8.117
+0.3275	-0.03440	-5.09881	0.002	8.070
+0.3300	-0.03441	-5.11892	0.002	8.024
+0.3325	-0.03441	-5.13893	0.002	7.978
+0.3300	-0.03441	-5.11892	0.001	8.024
+0.3400	-0.03442	-5.19825	0.001	7.842
+0.3500	-0.03443	-5.27578	0.001	7.664
+0.3600	-0.03444	-5.35154	0.001	7.489
+0.3700	-0.03444	-5.42557	0.001	7.319
+0.3800	-0.03445	-5.49793	0.001	7.152
+0.3900	-0.03446	-5.56863	0.001	6.990
+0.4000	-0.03446	-5.63773	0.001	6.831
+0.4100	-0.03447	-5.70476	0.001	6.675
+0.4200	-0.03447	-5.77075	0.001	6.523
+0.4300	-0.03448	-5.83524	0.000	6.375
+0.4400	-0.03448	-5.89826	0.000	6.230
+0.4500	-0.03449	-5.95985	0.000	6.088
+0.4600	-0.03449	-6.02003	0.000	5.950

13.9

(1)	(4)	(6)	(7)	(8)
+0.0000	0.00000	-1.30000	1.000	19.953
+0.0025	-0.00238	-1.34988	0.902	19.867
+0.0050	-0.00452	-1.39954	0.815	19.930
+0.0075	-0.00646	-1.44933	0.736	19.905
+0.0100	-0.00820	-1.49905	0.665	19.870
+0.0125	-0.00978	-1.54868	0.601	19.828
+0.0150	-0.01121	-1.59819	0.544	19.779
+0.0175	-0.01251	-1.64757	0.492	19.724
+0.0200	-0.01368	-1.69680	0.446	19.664
+0.0225	-0.01474	-1.74588	0.404	19.599
+0.0250	-0.01570	-1.79480	0.367	19.530
+0.0275	-0.01658	-1.84353	0.333	19.457
+0.0300	-0.01737	-1.89208	0.302	19.381
+0.0325	-0.01809	-1.94044	0.275	19.302
+0.0350	-0.01874	-1.98859	0.250	19.220
+0.0375	-0.01934	-2.03653	0.227	19.136
+0.0400	-0.01988	-2.08426	0.207	19.050
+0.0425	-0.02038	-2.13178	0.188	18.961
+0.0450	-0.02083	-2.17907	0.172	18.872
+0.0475	-0.02124	-2.22614	0.157	18.782
+0.0500	-0.02161	-2.27298	0.143	18.690
+0.0525	-0.02195	-2.31959	0.130	18.598
+0.0550	-0.02227	-2.36597	0.119	18.504
+0.0575	-0.02255	-2.41211	0.109	18.410
+0.0600	-0.02281	-2.45801	0.100	18.315
+0.0625	-0.02305	-2.50368	0.091	18.220
+0.0650	-0.02327	-2.54911	0.084	18.125
+0.0675	-0.02347	-2.59431	0.077	18.029
+0.0700	-0.02365	-2.63926	0.070	17.933
+0.0725	-0.02382	-2.68397	0.064	17.837
+0.0750	-0.02398	-2.72844	0.059	17.741
+0.0775	-0.02412	-2.77268	0.054	17.645
+0.0800	-0.02425	-2.81667	0.050	17.549

13.9 (CONT.)

(1)	(4)	(6)	(7)	(8)
+0.0850	-0.02448	-2.90393	0.042	17.357
+0.0900	-0.02468	-2.99024	0.036	17.166
+0.095	-0.02484	-3.07560	0.031	16.976
+0.100	-0.02498	-3.16000	0.026	16.787
+0.110	-0.02520	-3.32601	0.019	16.414
+0.120	-0.02537	-3.48830	0.014	16.046
+0.130	-0.02549	-3.64695	0.010	15.685
+0.140	-0.02558	-3.80203	0.008	15.331
+0.150	-0.02564	-3.95360	0.006	14.985
+0.160	-0.02570	-4.10174	0.005	14.645
+0.170	-0.02574	-4.24653	0.003	14.313
+0.180	-0.02576	-4.38803	0.003	13.988
+0.190	-0.02579	-4.52632	0.002	13.671
+0.200	-0.02581	-4.66136	0.002	13.360
+0.22	-0.02584	-4.82251	0.001	12.760
+0.24	-0.02585	-5.07192	0.001	12.186
+0.26	-0.02587	-5.31011	0.001	11.638
+0.28	-0.02588	-5.53759	0.000	11.114
+0.30	-0.02588	-5.75483	0.000	10.614
+0.32	-0.02589	-5.96230	0.000	10.137
+0.34	-0.02589	-6.16043	0.000	9.680
+0.36	-0.02590	-6.34965	0.000	9.245
+0.38	-0.02590	-6.53035	0.000	8.829
+0.40	-0.02590	-6.70292	0.000	8.431
+0.42	-0.02590	-6.86772	0.000	8.052
+0.44	-0.02590	-7.02511	0.000	7.690
+0.46	-0.02590	-7.17541	0.000	7.344
+0.48	-0.02590	-7.31895	0.000	7.013
+0.50	-0.02590	-7.45603	0.000	6.697
+0.52	-0.02590	-7.58694	0.000	6.396
+0.54	-0.02590	-7.71196	0.000	6.108
+0.56	-0.02590	-7.83135	0.000	5.833

14.1

(14)	(15)	(16)	(17)	(18)	(7)	(8)
0.0	-0.0000	0.678094	0.00000	0.76854	3.000	0.000
0.1	-0.0011	0.677489	0.00023	0.76777	2.998	0.002
0.2	-0.0045	0.675677	0.00180	0.76548	2.996	0.008
0.3	-0.0101	0.672672	0.00607	0.76168	2.990	0.018
0.4	-0.0180	0.668496	0.01434	0.75641	2.983	0.032
0.5	-0.0281	0.663181	0.02788	0.74961	2.973	0.049
0.6	-0.0403	0.656764	0.04789	0.74164	2.962	0.071
0.7	-0.0547	0.649292	0.07554	0.73868	2.948	0.095
0.8	-0.0711	0.640817	0.11187	0.72165	2.933	0.124
0.9	-0.0896	0.631400	0.15787	0.70989	2.916	0.156
1.0	-0.1101	0.621103	0.21443	0.69707	2.896	0.191
1.1	-0.1325	0.609995	0.28234	0.68328	2.876	0.221
1.2	-0.1567	0.598148	0.36226	0.66864	2.853	0.270
1.3	-0.1828	0.585637	0.45477	0.65322	2.829	0.314
1.4	-0.2105	0.572537	0.56034	0.63715	2.806	0.360
1.5	-0.2399	0.558926	0.67931	0.62052	2.777	0.408
1.6	-0.2708	0.544880	0.81192	0.59891	2.749	0.462
1.7	-0.3033	0.530475	0.95831	0.58599	2.720	0.510
1.8	-0.3372	0.515785	0.11853	0.56828	2.699	0.564
1.9	-0.3723	0.500883	1.29251	0.55041	2.658	0.619
2.0	-0.4087	0.485837	1.48010	0.53245	2.626	0.675
2.1	-0.4463	0.470713	1.68109	0.51448	2.593	0.732
2.2	-0.4850	0.455574	1.89516	0.49658	2.560	0.790
2.3	-0.5246	0.440476	2.12195	0.47882	2.526	0.849
2.4	-0.5652	0.425474	2.36104	0.46127	2.491	0.907
2.5	-0.6066	0.410616	2.61193	0.44396	2.456	0.966
2.6	-0.6487	0.395946	2.8741	0.42696	2.421	1.034
2.8	-0.7350	0.367325	3.4302	0.39403	2.351	1.142
3.0	-0.8235	0.339871	4.0244	0.36275	2.280	1.257
3.2	-0.9137	0.313778	4.6520	0.33329	2.210	1.369
3.4	-1.0051	0.289173	5.3080	0.30575	2.141	1.476
3.6	-1.0973	0.266131	5.9876	0.28018	2.074	1.580
3.8	-1.1898	0.244679	6.6862	0.25656	2.008	1.678
4.0	-1.2824	0.224806	7.3995	0.23484	1.944	1.771
4.2	-1.3747	0.206475	8.1237	0.21494	1.883	1.858
4.4	-1.4665	0.189626	8.8553	0.19677	1.824	1.939
4.6	-1.5576	0.174181	9.5912	0.18021	1.768	2.015
4.8	-1.6477	0.160057	10.329	0.16515	1.714	2.085
5.0	-1.7369	0.147164	11.066	0.15147	1.662	2.150
5.2	-1.8248	0.135410	11.800	0.13906	1.614	2.210
5.4	-1.9114	0.124704	12.530	0.12780	1.567	2.264
5.6	-1.9966	0.1149597	13.254	0.11761	1.523	2.313

14.1 (CONT.)

(14)	(15)	(16)	(17)	(18)	(7)	(8)
5.8	−2.0804	0.106092	13.971	0.10833	1.482	2.359
6.0	−2.1627	0.0980228	14.681	0.099935	1.442	2.400
6.2	−2.2435	0.0906785	15.383	0.092316	1.405	2.437
6.4	−2.3228	0.0839915	16.075	0.085396	1.370	2.470
6.6	−2.4005	0.0778996	16.759	0.079108	1.336	2.500
6.8	−2.4767	0.0723459	17.433	0.073389	1.305	2.527
7.0	−2.5513	0.0672787	18.097	0.068180	1.275	2.551
7.5	−2.7312	0.0564431	19.715	0.057080	1.182	2.599
8.0	−2.9019	0.0477516	21.272	0.048206	1.149	2.634
8.5	−3.0638	0.0407299	22.772	0.041060	1·098	2.657
9.0	−3.2173	0.0350139	24.216	0.035258	1.054	2.672
9.5	−3.3629	0.0303251	25.609	0.030508	1.015	2.679
10.0	−3.5012	0.0264495	26.954	0.026588	0.981	2.681
10.5	−3.6326	0.0232221	28.255	0.023330	0.951	2.678
11.0	−3.7576	0.0205152	29.516	0.020599	0.925	2.672
11.5	−3.8767	0.0182292	30.739	0.018296	0.902	2.663
12.0	−3.9902	0.0162858	31.927	0.016338	0.881	2.652
12.5	−4.0985	0.0146234	33.085	0.014665	0.863	2.639
13.0	−4.2020	0.0131928	34.213	0.013238	0.847	2.623
13.5	−4.3011	0.0119549	35.315	0.011983	0.835	2.610
14.0	−4.3959	0.0108778	36.392	0.010901	0.820	2.594
14.5	−4.4868	0.0099361	37.448	0.0099556	0.809	2.577
15.0	−4.5741	0.00910881	38.482	0.0091104	0.799	2.565
15.5	−4.6579	0.00837870	39.498	0.0083925	0.790	2.544
16.0	−4.7386	0.00773163	40.496	0.0077435	0.782	2.527
16.5	−4.8162	0.00715585	41.477	0.0071660	0.775	2.510
17.0	−4.8910	0.00664155	42.444	0.0066506	0.769	2.493
17.5	−4.9631	0.00618050	43.397	0.0061885	0.763	2.477
18.0	−5.0327	0.00576578	44.337	0.0057728	0.758	2.461
18.5	−5.1000	0.00539051	45.266	0.0053977	0.754	2.444
19·0	−5.1650	0.00505270	46.183	0.0050579	0.750	2.428
19.5	−5.2280	0.00474510	47.090	0.0047499	0.747	2.412
20.0	−5.2889	0.00446506	47.987	0.0044693	0.744	2.397
22.0	−5.5148	0.00356353	51.49	0.0035660	0.737	2.339
24.0	−5.7161	0.00291441	54.90	0.0029162	0.734	2.286
26.0	−5.8973	0.00243200	58.22	0.0024335	0.734	2.238
28.0	−6.0616	0.00206378	61.48	0.0020648	0.737	2.195
30.0	−6.2117	0.00177630	64.69	0.0017771	0.741	2.155
32.0	−6.3498	0.00154743	67.88	0.0015479	0.747	2.120
34.0	−6.4774	0.00136213	71.03	0.0013626	0.755	2.089
36.0	−6.5960	0.00120988	74.18	0.0012103	0.764	2.060
38.0	−6.7067	0.00108315	77.31	0.0010835	0.769	2.034
40.0	−6.8104	0.00097645	80.43	0.0009766	0.776	2.011
42.0	−6.9080	0.00088570	83.56	0.0008857	0.785	1.989
44.0	−7.0001	0.00080780	86.68	0.0008078	0.794	1.970
46.0	−7.0873	0.00074037	89.82	0.0007404	0.802	1.952
48.0	−7.1700	0.00068159	92.95	0.0006816	0.811	1.936
50.0	−7.2488	0.00062998	96.10	0.0006300	0.819	1.922
52.0	−7.3239	0.00058440	99.25	0.0005844	0.828	1.909
54.0	−7.3957	0.00054392	102.42	0.0005439	0.836	1·897
56.0	−7.4645	0.00050778	105.60	0.0005078	0.844	1.886
58.0	−7.5305	0.00047536	108.79	0.0004754	0.852	1.876
60.0	−7.5939	0.00044614	111.99	0.0004461	0.860	1.867
65.0	−7.7425	0.00038454	120.1	0.0003845	0.879	1.847
70.0	−7.8788	0.00033555	128.2	0.0003355	0.897	1.832
75.0	−8.0048	0.00029583	136.5	0.0002958	0.914	1.820
80.0	−8.1220	0.00026313	144.9	0.0002631	0.930	1.811
85.0	−8.2315	0.00023582	153·3	0.0002358	0.944	1.804
90.0	−8.3345	0.00021275	161.9	0.0002127	0.958	1.799
95.0	−8.4317	0.00019305	170.6	0.0001930	0.970	1.796
100.0	−8.5237	0.00017608	179.3	0.0001761	0.982	1.793
110.0	−8.6946	0.00014843	197.1	0.0001484	1·002	1.792
120.0	−8.8506	0.00012699	215.2	0.0001270	1.019	1.794
130.0	−8.9943	0.00010999	233.7	0.0001100	1.034	1.798
140.0	−9.1277	0.00009625	252.4	0.0000962	1·046	1.803
150.0	−9.2523	0.00008498	271.4	0.0000850	1.057	1.809
160.0	−9.3693	0.00007559	290.7	0.0000756	1.065	1.817
170.0	−9.4797	0.00006770	310.1	0.0000677	1.072	1.824
180.0	−9·5842	0.00006098	329.8	0.0000610	1.078	1.832
190.0	−9.6834	0.00005522	349.6	0.0000552	1.083	1.840
200.0	−9.7780	0.00005023	369·6	0.0000502	1.087	1·848
210.0	−9.8683	0.00004589	389.8	0.0000459	1.090	1.856

(14)	(15)	(16)	(17)	(18)	(7)	(8)
0.0	+2.0000	2.502458	0.0000	3.69150	3.000	0.000
0.1	+1.9958	2.497052	0.0008	3.68111	3.000	0.006
0.2	+1.9834	2.480916	0.0066	3.65004	2.989	0.022
0.3	+1.9627	2.454288	0.0223	3.59901	2.977	0.051
0.4	+1.9340	2.417561	0.0523	3.52901	2.959	0.089
0.5	+1.8974	2.371270	0.1010	3.44152	2.936	0.139
0.6	+1.8533	2.316080	0.1720	3.33812	2.908	0.199
0.7	+1.8019	2.252771	0.2687	3.22085	2.876	0.268
0.8	+1.7437	2.182215	0.3935	3.09180	2.839	0.347
0·9	+1.5791	2.105359	0.5485	2.95323	2.798	0.434
1.0	+1.6085	2.023203	0.7349	2.80740	2.753	0.530
1.1	+1.5323	1·936776	0.9533	2.65659	2.704	0.632
1.2	+1.4511	1.847114	1.2035	2.50294	2.652	0.740
1.3	+1.3653	1.755239	1.4849	2.34849	2.597	0.854
1.4	+1.2755	1.662139	1.7963	2.19507	2.539	0.971
1.5	+1.1822	1.568750	2.1358	2.04434	2.479	1·093
1.6	+1.0858	1.475938	2.5014	1.89767	2.417	1.216
1.7	+0.9869	1.384492	2.8906	1.75625	2.353	1.340
1·8	+0.8859	1.295108	3.301	1.62098	2.288	1.465
1.9	+0.7833	1.208387	3.729	1.49257	2.223	1.589
2.0	+0.6795	1.124817	4.172	1.37147	2.157	1.711
2.1	+0.5748	1.044831	4.628	1.25798	2.091	1.830
2.2	+0.4697	0.968699	5.093	1·15219	2.025	1.946
2.3	+0.3648	0.896643	5.565	1.05408	1.961	2.058
2.4	+0.2594	0.828790	6.041	0.96349	1.897	2.165
2.6	+0.0509	0.705819	6.996	0.80375	1.773	2.363
2.8	−0.1540	0.599444	7.945	0.67023	1·656	2.538
3.0	−0.3540	0.508584	8.873	0.55964	1.548	2.688
3.2	−0 5481	0.431715	9.773	0.46856	1.447	2.814
3.4	−0.7356	0.367125	10.640	0.39380	1.356	2.917
3.6	−0.9162	0.313085	11.470	0.33251	1.273	3.000
3.8	−1.0896	0.267971	12.263	0.28224	1.199	3.064
4.0	−1.2559	0.230327	13.018	0.24091	1.132	3.111
4.2	−1.4151	0.198886	13.737	0.20674	1.073	3.146
4.4	−1.5675	0.172573	14.422	0.17849	1.019	3.169
4.6	−1.7132	0.150486	15.075	0.15499	0.972	3.182
4.8	−1.8525	0.131883	16.697	0.13534	0.929	3.187
4.0	−1.9858	0.116152	16.291	0.11884	0.891	3.185
5.2	−2.1133	0.102794	16.859	0.10490	0.857	3.177
5.4	−2.2335	0.091401	17.403	0.09306	0.827	3.165
5.6	−2.3521	0.081640	17.926	0.08297	0.800	3.150
5.8	−2.4640	0.073240	18.428	0.07431	0.775	3.132
6.0	−2.5713	0.065979	18.912	0.06685	0.754	3.111
6.2	−2.6743	0.059676	19.378	0.06038	0·734	3.089
6.4	−2.7731	0.054180	19.830	0.05476	0.716	3.065
6.6	−2.8680	0.049368	20.266	0.04985	0.700	3.041
6.8	−2.9592	0.045139	20.690	0.04554	0.686	3.016
7.0	−3.1471	0.041406	21.102	0.04175	0.673	2.990
7.2	−3.1316	0.038100	21.502	0.03839	0.661	2.964
7.4	−3.2130	0.035161	21.892	0.03541	0.651	2.938
7.6	−3.2915	0.032540	22.27	0.03275	0.641	2.912
7.8	−3.3673	0.030194	22.65	0.03037	0.633	2.886
8.0	−3.4404	0.028087	23.01	0.02825	0.625	2.860
8.2	−3.5111	0.026190	23.36	0.02633	0.618	2.834
8.4	−3.5795	0.024477	23.71	0.02460	0.612	2.809
8·6	−3.6456	0.022925	24.05	0.02303	0.606	2.784
8.8	−3.7096	0.021516	24.39	0.02161	0.601	2.760
9.0	−3.7716	0.020233	24.72	0.02031	0.597	2.736
9.5	−3.9185	0.0174876	25.52	0·01755	0.587	2.678
10.0	−4.0549	0.0152719	26.30	0.01532	0.581	2.622
10.5	−4.1819	0.0134600	27.05	0.013496	0.576	2.569
11.0	−4.3006	0.0119609	27.79	0.011990	0.573	2.520
11.5	−4.4118	0.0107072	28·50	0.010730	0.571	2.473
12.0	−4.5163	0.00964865	29.89	0·009667	0.571	2.429
12.5	−4.6148	0.00874590	29.89	0.008762	0.571	2.387
13.0	−4.7078	0.00797253	30.57	0.007985	0.573	2.348
13.5	−4.7958	0.00730261	31.24	0.007313	0.575	2.311
14.0	−4·8793	0.00671910	31.90	0.006800	0.578	2.251
14.5	−4.9587	0.00620767	32.56	0.006216	0.581	2.242
15·0	−5.0343	0.00575680	33.21	0.005764	0.585	2.211
15.5	−5.1064	0.00535720	33.85	0.005363	0.689	2.182
16·0	−5.1753	0.00500127	34.49	0.005007	0.594	2.154
16.5	−5.2412	0.00468278	35.13	0.004687	0.599	2.127
17.0	−5.3044	0.00439654	35.77	0.004400	0.604	2.102
17.5	−5.3650	0.00413827	36.40	0.004142	0.609	2.078
18.0	−5.4233	0.00390434	37.04	0.003908	0.615	2.056
20.0	−5.6359	0.00315773	39.6	0.003160	0.639	1.977
22.0	−5.8213	0.00262392	42.1	0.002625	0.664	1.913
24.0	−5.9854	0.00222707	44.6	0.002228	0.689	1.860

14.2 (CONT.)

(14)	(15)	(16)	(17)	(18)	(7)	(8)
26.0	−6.1325	0.00192263	47.2	0.001923	0.715	1.816
28.0	−6.2658	0.00168293	49.8	0.001683	0.741	1.778
30.0	−6.3875	0.00149010	52.5	0.001490	0.766	1.750
32.0	−6.4997	0.00133212	55.2	0.001332	0.791	1.725
34.0	−6.6036	0.00120065	58.0	0.001201	0.814	1.705
36.0	−6.7006	0.00108976	60.8	0.001090	0.837	1.687
38.0	−6.7915	0.00099513	63.6	0.000995	0.858	1.674
40.0	−6.8770	0.00091354	66.5	0.0009135	0.879	1.663
42.0	−6.9579	0.00084257	69.5	0.0008426	0.899	1.654
44.0	−7.0347	0.00078033	72.5	0.0007803	0.917	1.647
46.0	−7.1078	0.00072535	75.5	0.0007253	0.935	1.641
48.0	−7.1776	0.00067648	78.6	0.0006765	0.952	1.637
50.0	−7.2443	0.00063279	81.7	0.0006328	0.968	1.635
52.0	−7.3084	0.00059352	84.9	0.0005835	0.983	1.633
54.0	−7.3700	0.00055806	88.2	0.0005581	0.997	1.633
56.0	−7.4294	0.00052589	91.4	0.0005259	1.010	1.633
60.0	−7.542	0.00046985	98.1	0.0004698	1.035	1.635
70.0	−7.795	0.00036481	115.	0.0003648	1.083	1.650
80.0	−8.017	0.00029225	134.	0.0002922	1.118	1.672
90.0	−8.216	0.00023964	153.	0.0002396	1.143	1.699
100.0	−8.396	0.00020008	173.	0.0002001	1.159	1.726
110.0	−8.452	0.00016952	193.	0.0001695	1.170	1.754
120.0	−8.715	0.00014536	214.	0.0001454	1.176	1.780

143

(14)	(15)	(16)	(17)	(18)	(7)	(8)
0.0	+3.0000	3.976986	0.0000	6.90248	3.000	0.000
0.1	+2.9934	3.966114	0.0013	6.87617	3.000	0.008
0.2	+2.9736	3.933689	0.0105	6.83718	2.986	0.030
0.3	+2.9408	3.880277	0.0353	6.66986	2.970	0.068
0.4	+2.8953	3.806801	0.0826	6.49512	2.948	0.121
0.5	+2.8376	3.714522	0.1591	6.27818	2.919	0.188
0.6	+2.7683	3.604995	0.2700	6.02430	2.884	0.269
0.7	+2.6878	3.480030	0.4199	5.73945	2.843	0.364
0.8	+2.5971	3.341647	0.6119	5.43003	2.796	0.471
0.9	+2.4969	3.192015	0.8481	5.10262	2.744	0.589
1.0	+2.3880	3.033402	1.1291	4.76374	2.687	0.719
1.1	+2.2714	2.868116	1.4544	4.41964	2.625	0.858
1.2	+2.1479	2.698451	1.8224	4.07608	2.559	1.005
1.3	+2.0186	2.526631	2.2305	3.73752	2.489	1.160
1.4	+1.8843	2.354765	2.6751	3.41048	2.415	1.319
1.5	+1.7459	2.184805	3.1521	3.09651	2.339	1.483
1.6	+1.6044	2.018506	3.657	2.79914	2.261	1.648
1.7	+1.4605	1.857401	4.184	2.52042	2.181	1.814
1.8	+1.3151	1.702784	4.728	2.26167	2.100	1.978
1.9	+1.1688	1.555695	5.286	2.02358	2.118	2.139
2.0	+1.0225	1.416918	5.850	1.80606	1.939	2.293
2.1	+0.0875	1.286996	6.418	1.60885	1.857	2.445
2.2	+0.7316	1.066234	6.984	1.43115	1.778	2.587
2.3	+0.5881	1.054732	7.545	1.38118	1.701	2.505
2.4	+0.4464	0.952400	8.099	1.12983	1.626	2.845
2.6	+0.1700	0.774161	9.172	0.89181	1.483	3.062
2.8	−0.0958	0.628283	10.189	0.70600	1.354	3.238
3.0	−0.0496	0.570489	11.141	0.56187	1.237	3.374
3.2	−0.5908	0.416215	12.026	0.45047	1.134	3.472
3.4	−0.8194	0.341125	12.847	0.36417	1.044	3.539
3.6	−1.0354	0.281399	13.605	0.29710	0.965	3.579
3.8	−1.2394	0.233829	14.307	0.24468	0.897	3.598
4.0	−1.4320	0.195810	14.957	0.20343	0.838	3.599
4.2	−1.6136	0.165275	15.562	0.17070	0.787	3.587
4.4	−1.7851	0.140604	16.125	0.14457	0.743	3.565
4.6	−1.9470	0.120540	16.652	0.12343	0.705	3.535
4.8	−2.1001	0.104110	17.147	0.10627	0.672	3.500
5.0	−2.2449	0.090600	17.613	0.09219	0.643	3.460
5.2	−2.3821	0.0793063	18.053	0.08056	0.618	3.418
5.4	−2.5121	0.0698951	18.472	0.07087	0.596	3.374
5.6	−2.6356	0.0619714	18.870	0.06274	0.577	3.328
5.8	−2.7530	0.0552567	19.250	0.05586	0.560	3.283
6.0	−2.8646	0.0495310	19.614	0.05002	0.545	3.237
6.2	−2.9710	0.0446194	19.963	0.04501	0.533	3.192
6.4	−3.0725	0.0403822	20.300	0.04071	0.521	3.146
6.6	−3.1694	0.0367071	20.625	0.03698	0.512	3.102
6.8	−3.2620	0.0335030	20.940	0.03373	0.503	3.049
7.0	−3.3506	0.0306960	21.245	0.03088	0.494	3.016
7.5	−3.5564	0.0250438	21.863	0.02556	0.481	2.870
8.0	−3.7423	0.0208298	22.457	0.01092	0.471	2.820
8.5	−3.9112	0.0176142	23.308	0.017676	0.464	2.733

14.3 (CONT.)

(14)	(15)	(16)	(17)	(18)	(7)	(8)
9.0	−4.0656	0.0151099	23.932	0.015154	0.460	2.651
9.5	−4.2073	0.0131241	24.534	0.013158	0.459	2.576
10.0	−4.3379	0.0115242	25.118	0.011551	0.459	2.506
10.5	−4.4589	0.0102167	25.687	0.010227	0.460	2.444
11.0	−4.5713	0.00913450	26.245	0.0091508	0.463	2.382
11.5	−4.6761	0.00822860	26.793	0.0082420	0.467	2.326
12.0	−4.7741	0.00746240	27.334	0.0074734	0.472	2.274
12.5	−4.8661	0.00680832	27.868	0.0068178	0.477	2.226
13.0	−4.9527	0.00624522	28.398	0.0062532	0.483	2.182
13.5	−5.0343	0.00575671	28.924	0.0057637	0.490	2.140
14.0	−5.1115	0.00532990	29.447	0.0053359	0.497	2.101
14.5	−5.1847	0.00495461	29.969	0.0049598	0.504	2.065
15.0	−5.2542	0.00462263	30.489	0.0046272	0.512	2.031
15.5	−5.3203	0.00432738	31.009	0.0043314	0.520	1.999
16.0	−5.3833	0.00406344	32.529	0.0040668	0.528	1.969
16.5	−5.4435	0.00382639	32.049	0.0038294	0.536	1.941
17.0	−5.5011	0.00361257	32.571	0.0036151	0.545	1.915
18.0	−5.6092	0.00324284	33.62	0.0032450	0.563	1.866
19.0	−5.7090	0.00293516	34.67	0.0029370	0.581	1.824
20.0	−5.8017	0.00267579	35.74	0.0026773	0.599	1.786
21.0	−5.8880	0.00245465	36.81	0.0024558	0.617	1.752
22.0	−5.9688	0.00226419	37.90	0.0022652	0.636	1.722
23.0	−6.0448	0.00209867	39.01	0.0020995	0.655	1.695
24.0	−6.1165	0.00195366	40.12	0.0019543	0.673	1.671
26.0	−6.2486	0.00171199	42.41	0.0017126	0.710	1.630
28.0	−6.3683	0.00161908	44.75	0.0015196	0.745	1.598
30.0	−6.4776	0.00136181	47.17	0.0013622	0.779	1.572
32.0	−6.5784	0.00123130	49.66	0.0012316	0.812	1.551
34.0	−6.6720	0.00112136	52.21	0.0011217	0.844	1.535
36.0	−6.7594	0.00102754	54.84	0.0010278	0.874	1.523
38.0	−6.8415	0.000946569	57.54	0.0009469	0.903	1.514
40.0	−6.9190	0.000876010	60.31	0.0008762	0.930	1.507
42.0	−6.9924	0.000813992	63.1	0.0008141	0.955	1.503
44.0	−7.0623	0.000759067	66.0	0.0007591	0.979	1.501
46.0	−7.1290	0.000710095	69.0	0.0007101	1.001	1.500
48.0	−7.1929	0.000666169	72.1	0.0006662	1.022	1.501
50.0	−7.2542	0.000626555	75.2	0.0006266	1.042	1.503
52.0	−7.3133	0.000590657	78.3	0.0005907	1.060	1.506
54.0	−7.3702	0.000557984	81.5	0.0005580	1.077	1.510
56.0	−7.4252	0.000528127	84.8	0.0005281	1.093	1.515
58.0	−7.4784	0.000500744	88.2	0.0005007	1.108	1.520
60.0	−7.5301	0.000475548	91.6	0.0004755	1.122	1.526
62.0	−7.5802	0.000452292	95.0	0.0004523	1.134	1.533
64.0	−7.6290	0.000430769	98.5	0.0004308	1.146	1.539
66.0	−7.6765	0.000410797	102.1	0.0004108	1.157	1.547
68.0	−7.7227	0.000392220	105.7	0.0003922	1.167	1.554
70.0	−7.7679	0.000374903	109.3	0.0003749	1.176	1.562

14.4

(14)	(15)	(16)	(17)	(18)	(7)	(8)
0.0	+5.0000	7.83798	0.0000	18.535	3.000	0.000
0.1	+4.9880	7.80940	0.0026	18.433	2.992	0.011
0.2	+4.9480	7.72428	0.0207	18.130	2.982	0.043
0.3	+4.8836	7.58445	0.0692	17.637	2.960	0.099
0.4	+4.7946	7.39289	0.1615	16.971	2.930	0.176
0.5	+4.6822	7.15361	0.3092	16.153	2.891	0.274
0.6	+4.5477	6.87157	0.5218	15.210	2.844	0.393
0.7	+4.3929	6.55241	0.8057	14.171	2.789	0.532
0.8	+4.2195	6.20242	1.1647	13.066	2.727	0.691
0.9	+4.0296	5.82818	1.5994	11.923	2.656	0.869
1.0	+3.8253	5.43651	2.1076	10.773	2.579	1.064
1.1	+3.6088	5.034168	2.6846	9.6398	2.496	1.274
1.2	+3.3823	4.627758	3.323	8.5458	2.406	1.500
1.3	+3.1480	4.223501	4.014	7.5091	2.312	1.737
1.4	+2.9079	3.827126	4.747	6.5433	2.212	1.983
1.5	+2.6642	3.443737	5.510	5.6577	2.109	2.236
1.6	+2.4187	3.077720	6.293	4.8576	2.003	2.492
1.7	+2.1732	2.732670	7.082	4.1446	1.896	2.747
1.8	+1.9291	2.411347	7.869	3.5172	1.787	2.997
1.9	+1.6878	2.115654	8.642	2.9718	1.679	3.238
2.0	+1.4506	1.846660	8.394	2.5021	1.573	3.466

14.4 (CONT.)

(14)	(15)	(16)	(17)	(18)	(7)	(8)
2.1	+1.2184	1.604636	10.117	2.1019	1.469	3.678
2.2	+0.9920	1.389136	10.808	1.7634	1.369	3.870
2.3	+0.7720	1.199101	11.461	1.4790	1.273	4.040
2.4	+0.5588	1.032985	12.076	1.2414	1.182	4.187
2.5	+0.3528	0.888895	12.651	1.0437	1.098	4.310
2.6	+0.1540	0.764728	13.187	0.87955	1.019	4.410
2.7	−0.0374	0.658298	13.686	0.74357	0.947	4.487
2.8	−0.2214	0.567442	14.148	0.63092	0.880	4.544
2.9	−0.3983	0.490103	14.576	0.53753	0.820	4.583
3.0	−0.5681	0.424384	14.973	0.45999	0.765	4.605
3.1	−0.7311	0.368576	15.341	0.39547	0.716	4.612
3.2	−0.8874	0.321175	15.682	0.34164	0.671	4.607
3.3	−1.0375	0.280873	15.999	0.29652	0.631	4.592
3.4	−1.1814	0.246551	16.295	0.25861	0.595	4.569
3.5	−1.3195	0.217257	16.570	0.22663	0.562	4.538
3.6	−1.4520	0.192190	16.827	0.19953	0.533	4.502
3.7	−1.5793	0.170678	17.069	0.17647	0.506	4.462
3.8	−1.7015	0.152159	17.295	0.15676	0.483	4.418
3.9	−1.8189	0.1361630	17.509	0.13985	0.461	4.371
4.0	−1.9318	0.1223004	17.710	0.12528	0.442	4.322
4.1	−2.0404	0.1102448	17.900	0.11266	0.424	4.272
4.2	−2.1448	0.0997245	18.081	0.10170	0.409	4.221
4.3	−2.2453	0.0905122	18.252	0.092153	0.394	4.169
4.4	−2.3423	0.0824177	18.416	0.083770	0.381	4.118
4.5	−2.4357	0.0752817	18.572	0.076410	0.369	4.066
4.6	−2.5258	0.0689699	18.721	0.069917	0.359	4.015
4.7	−2.6127	0.0633692	18.864	0.064169	0.349	3.964
4.8	−2.6967	0.0583841	19.001	0.059062	0.340	3.913
4.9	−2.7777	0.0539333	19.133	0.054512	0.332	3.863
5.0	−2.8561	0.0499480	19.260	0.050445	0.324	3.814
5.2	−3.0052	0.0431468	19.501	0.043518	0.311	3.718
5.4	−3.1449	0.0376041	19.728	0.037886	0.300	3.626
5.6	−3.2760	0.0330412	19.941	0.033259	0.291	3.537
5.8	−3.3995	0.02924939	20.143	0.029419	0.283	3.453
6.0	−3.5158	0.02607072	20.335	0.026206	0.277	3.372
6.2	−3.6256	0.02338429	20.518	0.023493	0.272	3.294
6.4	−3.7294	0.02109665	20.695	0.021186	0.267	3.220
6.6	−3.8278	0.01913483	20.864	0.019208	0.264	3.149
6.8	−3.9212	0.01744133	21.028	0.017502	0.261	3.082
7.0	−4.0099	0.01597049	21.187	0.016021	0.258	3.018
7.5	−4.2134	0.01304423	21.566	0.013078	0.255	2.868
8.0	−4.3946	0.01089192	21.923	0.010915	0.254	2.735
8.5	−4.5570	0.00926491	22.264	0.009281	0.256	2.615
9.0	−4.7036	0.00800572	22.593	0.008019	0.258	2.506
9.5	−4.8367	0.00701117	22.914	0.007021	0.262	2.409
10.0	−4.9581	0.00621156	23.227	0.0062196	0.267	2.320
10.5	−5.0694	0.00555859	23.535	0.0055650	0.273	2.239
11.0	−5.1719	0.00501796	23.840	0.0050233	0.280	2.165
11.5	−5.2668	0.00456485	24.143	0.0046088	0.288	2.107
12.0	−5.3548	0.00418090	24.444	0.0041845	0.296	2.035
12.5	−5.4368	0.00385234	24.745	0.0038553	0.304	1.978
13.0	−5.5134	0.00356869	25.046	0.0035712	0.313	1.925
13.5	−5.5851	0.00332183	25.348	0.0033240	0.322	1.876
14.0	−5.6526	0.00310541	25.652	0.0031074	0.332	1.831
14.5	−5.7161	0.00291441	25.957	0.0029162	0.342	1.789
15.0	−5.7762	0.00274482	26.265	0.0027464	0.353	1.750
16.0	−5.8869	0.00245745	26.888	0.0024587	0.374	1.680
17.0	−5.9868	0.00222382	27.524	0.0022248	0.397	1.618
18.0	−6.0778	0.00203058	28.174	0.0020315	0.420	1.565
19.0	−6.1612	0.00186834	28.840	0.0018690	0.444	1.517
20.0	−6.2379	0.00173037	29.523	0.0017310	0.469	1.475
21.0	−6.3091	0.00161167	30.224	0.0016123	0.494	1.439
22.0	−6.3752	0.00150851	30.945	0.0015090	0.519	1.406
23.0	−6.4371	0.00141806	31.685	0.0014185	0.544	1.377
24.0	−6.4952	0.00133809	32.445	0.0013384	0.570	1.352
25.0	−6.5499	0.00126688	33.227	0.0012672	0.596	1.329
26.0	−6.6016	0.00120305	34.029	0.0012033	0.621	1.309
27.0	−6.6507	0.00114549	34.852	0.0011458	0.647	1.290
28.0	−6.6973	0.00109330	35.699	0.0010936	0.672	1.275
29.0	−6.7418	0.00104574	36.568	0.0010460	0.697	1.261
30.0	−6.7844	0.00100221	37.458	0.0010025	0.722	1.248
31.0	−6.8251	0.00096219	38.372	0.0009624	0.747	1.238
32.0	−6.8643	0.00092527	39.308	0.0009255	0.771	1.228
33.0	−6.9019	0.00089107	40.267	0.0008913	0.795	1.220
34.0	−6.9383	0.00085930	41.248	0.0008595	0.819	1.213

14.4 (CONT.)

(14)	(15)	(16)	(17)	(18)	(7)	(8)
35.0	−6.9733	0.00082969	42.253	0.0008299	0.842	1.207
36.0	−7.0073	0.00080202	43.281	0.0008022	0.865	1.202
37.0	−7.0402	0.00077608	44.332	0.0007762	0.887	1.198
38.0	−7.0721	0.00075171	45.406	0.0007518	0.908	1.195
39.0	−7.1031	0.00072877	46.503	0.0007289	0.940	1.192
40.0	−7.1332	0.00070712	47.943	0.0007072	0.944	1.198

14.5

(14)	(15)	(16)	(17)	(18)	(7)	(8)
0.0	+10.0000	21.34447	0.00000	89.51344	3.000	0.000
0.1	+9.9645	21.23274	0.00709	88.75737	2.994	0.017
0.2	+9.8586	20.90086	0.05621	86.52662	2.975	0.068
0.3	+9.6843	20.35857	0.18674	82.93150	2.943	0.153
0.4	+9.4449	19.62161	0.43304	78.14529	2.900	0.272
0.5	+9.1446	18.71089	0.82235	72.39114	2.844	0.425
0.6	+8.7889	17.65169	1.3732	65.92454	2.776	0.613
0.7	+8.3839	16.47194	2.0946	59.01509	2.697	0.835
0.8	+7.9363	16.20204	2.9855	51.92817	2.607	1.093
0.9	+7.4534	13.87265	4.0354	44.90898	2.506	1.385
1.0	+6.9424	12.51401	5.2252	38.16966	2.395	1.713
1.1	+6.4108	11.15435	6.5284	31.88066	2.275	2.077
1.2	+5.8657	9.82155	7.9134	26.16632	2.145	2.475
1.3	+5.3139	8.53750	9.3450	21.10440	2.007	2.908
1.4	+4.7618	7.32266	10.787	16.72928	1.863	3.373
1.5	+4.2150	6.19338	12.204	13.03749	1.713	3.865
1.6	+3.6795	5.16221	13.564	9.99504	1.559	4.378
1.7	+3.1566	4.23802	14.839	7.54543	1.403	4.903
1.8	+2.6526	3.42591	16.007	5.61772	1.248	5.423
1.9	+2.1692	2.72727	17.055	4.13374	1.097	5.923
2.0	+1.7082	2.13972	17.975	3.01493	0.952	6.379
2.1	+1.2707	1.65721	18.768	2.18703	0.818	6.772
2.2	+0.8570	1.27029	19.440	1.58395	0.696	7.087
2.3	+0.4672	0.96694	20.002	1.14978	0.588	7.314
2.4	+0.1006	0.73372	20.468	0.83949	0.496	7.454
2.5	−0.2438	0.55713	20.852	0.61833	0.417	7.515
2.6	−0.5671	0.424758	21.169	0.46043	0.353	7.511
2.7	−0.8706	0.326033	21.430	0.34709	0.299	7.456
2.8	−1.1555	0.252437	21.647	0.26508	0.256	7.362
2.9	−1.4232	0.197400	21.824	0.20514	0.228	7.243
3.0	−1.6750	0.156000	21.982	0.16084	0.192	7.107
3.1	−1.9121	0.124618	22.111	0.12771	0.168	6.960
3.2	−2.1356	0.100618	22.222	0.10263	0.148	6.808
3.3	−2.3465	0.082089	22.318	0.083430	0.132	6.654
3.4	−2.5457	0.067644	22.402	0.068555	0.119	6.501
3.5	−2.7343	0.0562732	22.475	0.056904	0.107	6.350
3.6	−2.9130	0.0472372	22.540	0.047682	0.098	6.203
3.7	−3.0824	0.0399899	22.598	0.040308	0.090	6.059
3.8	−3.2433	0.0341257	22.650	0.034358	0.083	5.920
3.9	−3.3963	0.0293403	22.697	0.029511	0.077	5.786
4.0	−3.5419	0.0254038	22.740	0.025532	0.071	5.656
4.1	−3.6807	0.0221409	22.779	0.022238	0.067	5.531
4.2	−3.8131	0.0194166	22.814	0.019492	0.063	5.411
4.3	−3.9396	0.0171264	22.847	0.017185	0.060	5.295
4.4	−4.0604	0.0151888	22.878	0.015234	0.017	5.184
4.5	−4.1760	0.0135393	22.906	0.013576	0.054	5.076
5.0	−4.6863	0.00814495	23.024	0.0081580	0.044	4.607
5.5	−5.0158	0.00536054	23.114	0.0053664	0.039	4.198
6.0	−5.4565	0.00377694	23.187	0.0037800	0.035	3.862
6.5	−5.7542	0.00280558	23.252	0.0028074	0.033	3.575
7.0	−6.0101	0.00217285	23.308	0.0021738	0.032	3.198
7.5	−6.2323	0.00174018	23.359	0.0017410	0.031	3.113
8.0	−6.4271	0.00143227	23.406	0.0014329	0.031	2.925
8.5	−6.5994	0.00120573	23.451	0.0012061	0.032	2.758
9.0	−6.7528	0.00103432	23.494	0.0010346	0.032	2.610

(14)	(15)	(16)	(17)	(18)	(7)	(8)
0.00	+20.0000	59.81279	0.00000	484.3789	3.000	0.000
0.05	+19.9751	59.70155	0.00249	482.8904	2.997	0.006
0.10	+19.9005	59.36905	0.01984	478.4516	2.992	0.025
0.15	+19.7768	58.81856	0.06661	471.1412	2.980	0.055
0.20	+19.6048	58.05598	0.15667	460.8100	2.964	0.099
0.25	+19.3856	57.08907	0.30296	448.4664	2.944	0.154
0.30	+19.1206	55.92769	0.51714	433.4930	2.920	0.222
0.35	+18.8116	54.58352	0.80943	416.4188	2.891	0.303
0.40	+18.4605	53.06986	1.1883	397.5232	2.858	0.397
0.45	+18.0596	51.40147	1.6604	376.5926	2.821	0.504
0.50	+17.6414	49.59423	2.2304	355.4813	2.779	0.622
0.55	+17.1784	47.66500	2.9008	332.9664	2.734	0.755
0.60	+16.6834	45.63126	3.6721	309.8775	2.684	0.901
0.65	+16.1593	43.51096	4.5426	286.5214	2.630	1.061
0.70	+15.6092	41.32212	5.5089	263.1891	2.573	1.236
0.75	+15.0361	39.08274	6.5653	240.1505	2.511	1.425
0.80	+14.4431	36.81049	7.7046	217.6500	2.446	1.629
0.85	+13.8333	34.52247	8.9180	195.9031	2.377	1.849
0.90	+13.2098	32.23510	10.195	175.0942	2.305	2.085
0.95	+12.5756	29.96388	11.525	155.3748	2.291	2.340
1.00	+11.9338	27.72331	12.895	136.8640	2.150	2.612
1.05	+11.2870	25.52673	14.293	119.6487	2.067	2.904
1.10	+10.6382	23.38628	15.705	103.7843	1.982	3.217
1.15	+ 9.9899	21.31280	17.118	89.2989	1.894	3.553
1.20	+ 9.3446	19.31584	18.520	76.1935	1.802	3.912
1.25	+ 8.7046	17.40363	19.896	64.4464	1.708	4.298
1.30	+ 8.0720	15.58313	21.235	54.0162	1.612	4.712
1.35	+ 7.4487	13.8601	22.526	44.8444	1.514	5.157
1.40	+ 6.8366	12.2389	23.758	36.8599	1.414	5.635
1.45	+ 6.2371	10.7233	24.922	29.9808	1.311	6.147
1.50	+ 5.6517	9.3155	26.010	24.1188	1.209	6.697
1.55	+ 5.0815	8.0173	27.016	19.1807	1.105	7.285
1.60	+ 4.5275	6.8295	27.935	15.0717	1.001	7.911
1.65	+ 3.9905	5.7523	28.763	11.6970	0.898	8.573
1.70	+ 3.4711	4.7854	29.500	8.9639	0.797	9.264
1.75	+ 2.9698	3.9276	30.147	6.7832	0.698	9.975
1.80	+ 2.4868	3.1772	30.704	5.0705	0.604	10.688
1.85	+ 2.0222	2.53131	31.178	3.7473	0.514	11.384
1.90	+ 1.5758	1.98586	31.573	2.7419	0.431	12.035
1.95	+ 1.1475	1.53490	31.898	1.9905	0.357	12.614
2.00	+ 0.7368	1.17043	32.160	1.4372	0.291	13.095
2.05	+ 0.3433	0.88263	32.369	1.0352	0.235	13.462
2.10	− 0.0336	0.66024	32.534	0.74602	0.188	13.711
2.15	− 0.3947	0.49160	32.662	0.53937	0.150	13.846
2.20	− 0.7405	0.36557	32.763	0.39203	0.119	13.888
2.25	− 1.0718	0.27231	32.841	0.28703	0.094	13.849
2.30	− 1.3895	0.20367	32.902	0.21193	0.075	13.750
2.35	− 1.6941	0.15323	32.950	0.157897	0.060	13.607
2.40	− 1.9863	0.11609	32.988	0.118775	0.049	13.434
2.45	− 2.2670	0.088648	33.018	0.090213	0.040	13.243
2.50	− 2.5366	0.068249	33.042	0.069176	0.032	13.040
2.55	− 2.7958	0.052985	33.061	0.053544	0.027	12.830
2.60	− 3.0452	0.041480	33.076	0.041824	0.022	12.617
2.65	− 3.2853	0.032740	33.089	0.032954	0.018	12.405
2.70	− 3.5166	0.026050	33.100	0.026185	0.016	12.196
2.75	− 3.7395	0.020887	33.108	0.020975	0.013	11.989
2.80	− 3.9545	0.016873	33.116	0.016930	0.011	11.787
2.85	− 4.1620	0.0137285	33.122	0.0137663	0.010	11.590
2.90	− 4.3624	0.0112466	33.127	0.0112721	0.008	11.399
2.95	− 4.5560	0.0092741	33.131	0.0092916	0.007	11.210
3.00	− 4.7432	0.0076957	33.135	0.0077078	0.006	11.028
3.05	− 4.9243	0.0064244	33.138	0.0064327	0.006	10.851
3.10	− 5.0996	0.0053938	33.141	0.0054000	0.005	10.678
3.15	− 5.2693	0.0045534	33.143	0.0045579	0.004	10.511
3.20	− 5.4337	0.0038643	33.146	0.0038674	0.004	10.350
3.25	− 5.5930	0.0032958	33.147	0.0032979	0.003	10.193
3.30	− 5.7476	0.0028244	33.149	0.0028261	0.003	10.039
3.35	− 5.8975	0.0024315	33.150	0.0024330	0.003	9.890
3.40	− 6.0430	0.0021025	33.152	0.0021034	0.002	9.746
3.5	− 6.3216	0.0015915	33.154	0.0015921	0.002	9.469
3.6	− 6.5848	0.0012236	33.156	0.0012239	0.002	9.209
3.7	− 6.8337	0.00095402	33.157	0.00095426	0.001	8.959
3.8	− 7.0695	0.00075365	33.158	0.00075376	0.001	8.725
3.9	− 7.2932	0.00060260	33.159	0.00060267	0.001	8.501
4.0	− 7.5058	0.00048722	33.160	0.00048727	0.001	8.289

14.6 (CONT.)

(14)	(15)	(16)	(17)	(18)	(7)	(8)
4.1	- 7.7080	0.00039805	33.161	0.00039807	0.001	8.088
4.2	- 7.9006	0.00032833	33.162	0.00032835	0.001	7.896
4.3	- 8.0842	0.00027326	33.162	0.00027327	0.001	7.712
4.4	- 8.2595	0.00022933	33.162	0.00022933	0.001	7.537
4.5	- 8.4270	0.00019397	33.163	0.00019397	0.001	7.370
4.6	- 8.5872	0.000165255	33.163	0.000165255	0.000	7.209
4.7	- 8.7406	0.000141756	33.164	0.000141756	0.000	7.056
4.8	- 8.8876	0.000122378	33.164	0.000122378	0.000	6.909
4.9	- 9.0286	0.000106283	33.164	0.000106283	0.000	6.768
5.0	- 9.1639	0.000092829	33.164	0.000092829	0.000	6.633
5.1	- 9.2940	0.000081508	33.165	0.000081508	0.000	6.503
5.2	- 9.4191	0.000071927	33.165	0.000071927	0.000	6.378
5.3	- 9.5394	0.000063772	33.165	0.000063772	0.000	6.258
5.4	- 9.6553	0.000056794	33.165	0.000056794	0.000	6.142
5.5	- 9.7669	0.000050794	33.165	0.000050794	0.000	6.030
5.6	- 9.8746	0.000045609	33.165	0.000045609	0.000	5.922
5.7	- 9.9785	0.000041108	33.165	0.000041108	0.000	5.818
5.8	-10.0788	0.000037184	33.166	0.000037184	0.000	5.718
5.9	-10.1758	0.000033749	33.166	0.000033749	0.000	5.621
6.0	-10.2694	0.000030731	33.166	0.000030731	0.000	5.528
6.1	-10.3601	0.000028069	33.166	0.000028069	0.000	5.437
6.2	-10.4478	0.000025712	33.166	0.000025712	0.000	5.349
6.3	-10.5327	0.000023619	33.166	0.000023619	0.000	5.264
6.4	-10.6149	0.000021754	33.166	0.000021754	0.000	5.182
6.5	-10.6947	0.000020087	33.166	0.000020087	0.000	5.103
6.6	-10.7720	0.000018593	33.166	0.000018593	0.000	5.025
6.7	-10.8470	0.000017249	33.167	0.000017249	0.000	4.950
6.8	-10.9198	0.000016038	33.167	0.000016038	0.000	4.877
6.9	-10.9905	0.000014943	33.167	0.000014943	0.000	4.807
7.0	-11.0591	0.000013952	33.167	0.000013952	0.000	4.738

147

(14)	(15)	(16)	(17)	(18)	(7)	(8)
0.00	+100.0000	666.7489	0.0000	26683	3.000	0.000
0.05	+99.7225	663.9763	0.0277	26499	2.995	0.014
0.10	+98.8943	655.7229	0.2200	25952	2.980	0.056
0.15	+97.5276	642.1793	0.7334	25065	2.955	0.125
0.20	+95.6426	623.6550	1.7084	23872	2.920	0.223
0.25	+93.2668	600.5663	3.2630	22418	2.876	0.350
0.30	+90.4342	573.4207	5.4867	20755	2.822	0.505
0.35	+87.1845	542.7980	8.4373	18942	2.758	0.691
0.40	+83.5621	509.3299	12.1379	17036	2.686	1.091
0.45	+79.6148	473.6785	16.5770	15097	2.604	1.156
0.50	+75.3929	436.5149	21.7096	13175	2.513	1.438
0.55	+70.9482	398.4994	27.4690	11320	2.414	1.758
0.60	+66.3325	360.2631	33.7263	9569.6	2.307	2.116
0.65	+61.5966	322.3925	40.3855	7953.6	2.192	2.518
0.70	+56.7898	285.4172	47.2994	6493.4	2.070	2.970
0.75	+51.9587	249.8010	54.3211	5201.2	1.940	3.478
0.80	+47.1465	215.9356	61.3011	4081.2	1.803	4.054
0.85	+42.3929	184.1389	68.0935	3131.0	1.661	4.711
0.90	+37.7328	154.6549	74.5616	2342.3	1.512	5.470
0.95	+33.1972	127.6575	80.5824	1702.7	1.358	6.359
1.00	+28.8120	103.2553	86.0510	1197.1	1.200	7.423
1.05	+24.5984	81.4994	90.8838	808.42	1.038	8.726
1.10	+20.5733	62.3922	95.0204	519.41	0.874	10.376
1.12	+19.0189	55.4841	96.471	427.83	0.808	11.171
1.14	+17.4972	48.9906	97.804	348.37	0.742	12.065
1.16	+16.0087	42.9079	99.018	280.01	0.676	13.080
1.18	+14.5538	37.2313	100.114	221.75	0.611	14.245
1.20	+13.1328	31.9563	101.092	172.62	0.546	15.595
1.22	+11.7458	27.0784	101.955	131.71	0.482	17.181
1.24	+10.3928	22.5935	102.705	98.142	0.419	19.068
1.26	+9.0739	18.4985	103.346	71.075	0.358	21.347
1.28	+7.7889	14.7917	103 882	49.717	0.299	24.146
1.30	+6.5376	11.4740	104.32	33.316	0.242	27.636
1.31	+5.9245	9.9625	104.50	26.747	0.214	29.711
1.32	+5.3197	8.5508	104.66	21.154	0.188	32.049
1.33	+4.7232	7.2405	104.80	16.448	0.163	34.685
1.34	+4.1348	6.0344	104.92	12.547	0.138	37.654

14.7 (CONT.)

(14)	(15)	(16)	(17)	(18)	(7)	(8)
1.35	+3.5546	4.9355	105.02	9.3694	0.116	40.977
1.36	+2.9824	3.9481	105.10	6.8326	0.094	44.653
1.37	+2.4181	3.07684	105.16	4.8557	0.075	48.640
1.38	+1.8617	2.32660	105.21	3.3577	0.058	52.828
1.39	+1.3131	1.70077	105.25	2.2583	0.043	57.025
1.40	+0.7722	1.19925	105.28	1.47921	0.031	60.967
1.41	+0.2388	0.81595	105.30	0.94654	0.022	64.376
1.42	−0.2871	0.53762	105.31	0.59463	0.015	67.053
1.43	−0.8057	0.34523	105.32	0.36883	0.010	68.938
1.44	−1.3173	0.217707	105.33	0.22712	0.006	70.113
1.45	−1.8217	0.135802	105.33	0.13947	0.004	70.731
1.46	−2.3193	0.084279	105.33	0.085693	0.002	70.956
1.47	−2.8100	0.052253	105.33	0.052799	0.002	70.915
1.48	−3.2942	0.032454	105.33	0.032664	0.001	70.715
1.49	−3.7719	0.020247	105.34	0.020308	0.001	70.483
1.50	−4.2432	0.012664	105.34	0.012696	0.001	70.047
1.51	−4.7082	0.0079689	105.34	0.0079811	0.001	69.652
1.52	−5.1672	0.0050418	105.34	0.0050490	0.000	69.201
1.53	−5.6201	0.0032077	105.34	0.0032098	0.000	68.803
1.54	−6.0672	0.00205231	105.34	0.0020533	0.000	68.368
1.55	−6.5085	0.00132106	105.34	0.0013216	0.000	67.932
1.56	−6.9441	0.00085429	105.34	0.0008546	0.000	67.499
1.57	−7.3742	0.00055574	105.34	0.0005559	0.000	67.074
1.58	−7.7988	0.00036348	105.34	0.0003635	0.000	66.665
1.59	−8.2181	0.00023901	105.34	0.0002390	0.000	66.252

1501

1	4	5	6	7	8
-0.010	+0.00000	-2.03071	-6.07678	0.0000	109.8288
-0.015	+0.00000	-1.85219	-5.63048	0.0001	73.6539
-0.020	+0.00000	-1.72475	-5.31187	0.0002	55.5584
-0.025	+0.00000	-1.62531	-5.06328	0.0003	44.7006
-0.030	+0.00000	-1.54360	-4.85900	0.0003	37.4626
-0.035	+0.00000	-1.47411	-4.68528	0.0004	32.2932
-0.040	+0.00000	-1.41358	-4.53395	0.0005	28.4168
-0.045	+0.00001	-1.35988	-4.39971	0.0006	25.4024
-0.050	+0.00001	-1.31157	-4.27894	0.0007	22.9913
-0.055	+0.00002	-1.26763	-4.16907	0.0008	21.0190
-0.060	+0.00002	-1.22728	-4.06821	0.0009	19.3759
-0.065	+0.00002	-1.18996	-3.97490	0.0010	17.9860
-0.070	+0.00003	-1.15521	-3.88802	0.0011	16.7949
-0.075	+0.00004	-1.12267	-3.80669	0.0012	15.7630
-0.080	+0.00004	-1.09207	-3.73018	0.0013	14.8603
-0.085	+0.00005	-1.06316	-3.65791	0.0014	14.0641
-0.090	+0.00006	-1.03576	-3.58939	0.0015	13.3567
-0.095	+0.00006	-1.00969	-3.52422	0.0015	12.7240
-0.100	+0.00007	-0.98482	-3.46205	0.0016	12.1547
-0.105	+0.00008	-0.96103	-3.40258	0.0017	11.6399
-0.110	+0.00009	-0.93823	-3.34557	0.0018	11.1722
-0.115	+0.00010	-0.91632	-3.29079	0.0019	10.7452
-0.120	+0.00011	-0.89522	-3.23806	0.0019	10.3541
-0.125	+0.00012	-0.87488	-3.18720	0.0020	9.9945
-0.130	+0.00013	-0.85523	-3.13807	0.0021	9.6626
-0.135	+0.00014	-0.83621	-3.09053	0.0021	9.3556
-0.140	+0.00015	-0.81779	-3.04447	0.0022	9.0706
-0.145	+0.00016	-0.79992	-2.99979	0.0023	8.8055
-0.150	+0.00017	-0.78256	-2.95639	0.0023	8.5582
-0.155	+0.00019	-0.76567	-2.91418	0.0024	8.3269
-0.160	+0.00020	-0.74924	-2.87310	0.0024	8.1103
-0.165	+0.00021	-0.73322	-2.83306	0.0025	7.9070
-0.170	+0.00022	-0.71760	-2.79401	0.0025	7.7157
-0.175	+0.00024	-0.70235	-2.75588	0.0026	7.5355
-0.180	+0.00025	-0.68745	-2.71863	0.0026	7.3655
-0.185	+0.00026	-0.67288	-2.68221	0.0027	7.2047
-0.190	+0.00028	-0.65863	-2.64657	0.0027	7.0526
-0.195	+0.00029	-0.64467	-2.61167	0.0028	6.9084
-0.200	+0.00031	-0.63099	-2.57747	0.0028	6.7715
-0.205	+0.00032	-0.61758	-2.54395	0.0028	6.6413
-0.210	+0.00034	-0.60442	-2.51105	0.0029	6.5175
-0.215	+0.00035	-0.59150	-2.47876	0.0029	6.3996
-0.220	+0.00036	-0.57882	-2.44704	0.0029	6.2871
-0.225	+0.00038	-0.56635	-2.41588	0.0029	6.1798
-0.230	+0.00039	-0.55410	-2.38524	0.0030	6.0772
-0.235	+0.00041	-0.54204	-2.35510	0.0030	5.9790
-0.240	+0.00042	-0.53018	-2.32544	0.0030	5.8851
-0.245	+0.00044	-0.51850	-2.29624	0.0030	5.7950
-0.250	+0.00046	-0.50699	-2.26748	0.0030	5.7087
-0.255	+0.00047	-0.49566	-2.23915	0.0031	5.6258
-0.260	+0.00049	-0.48449	-2.21122	0.0031	5.5463
-0.265	+0.00050	-0.47347	-2.18368	0.0031	5.4698
-0.270	+0.00052	-0.46261	-2.15652	0.0031	5.3962
-0.275	+0.00053	-0.45189	-2.12971	0.0031	5.3254
-0.280	+0.00055	-0.44130	-2.10326	0.0031	5.2572
-0.285	+0.00057	-0.43086	-2.07714	0.0031	5.1915
-0.290	+0.00058	-0.42054	-2.05134	0.0031	5.1281
-0.295	+0.00060	-0.41034	-2.02585	0.0031	5.0669
-0.300	+0.00061	-0.40027	-2.00067	0.0031	5.0079
-0.305	+0.00063	-0.39031	-1.97577	0.0031	4.9508
-0.310	+0.00064	-0.38046	-1.95115	0.0031	4.8957
-0.315	+0.00066	-0.37073	-1.92681	0.0031	4.8424
-0.320	+0.00068	-0.36109	-1.90273	0.0031	4.7909
-0.325	+0.00069	-0.35156	-1.87890	0.0031	4.7410
-0.330	+0.00071	-0.34213	-1.85531	0.0031	4.6926
-0.335	+0.00072	-0.33279	-1.83197	0.0031	4.6458
-0.340	+0.00074	-0.32354	-1.80885	0.0031	4.6005
-0.345	+0.00075	-0.31439	-1.78596	0.0031	4.5565
-0.350	+0.00077	-0.30532	-1.76329	0.0031	4.5138
-0.355	+0.00079	-0.29633	-1.74082	0.0031	4.4724
-0.360	+0.00080	-0.28743	-1.71856	0.0030	4.4322
-0.365	+0.00082	-0.27860	-1.69650	0.0030	4.3932
-0.370	+0.00083	-0.26985	-1.67463	0.0030	4.3553
-0.375	+0.00085	-0.26118	-1.65294	0.0030	4.3184
-0.380	+0.00086	-0.25258	-1.63144	0.0030	4.2826
-0.385	+0.00088	-0.24405	-1.61011	0.0030	4.2478
-0.390	+0.00089	-0.23559	-1.58896	0.0030	4.2139
-0.395	+0.00091	-0.22719	-1.56797	0.0029	4.1810
-0.400	+0.00092	-0.21886	-1.54715	0.0029	4.1489
-0.405	+0.00094	-0.21059	-1.52648	0.0029	4.1177
-0.410	+0.00095	-0.20239	-1.50597	0.0029	4.0873
-0.415	+0.00097	-0.19424	-1.48561	0.0029	4.0576
-0.420	+0.00098	-0.18616	-1.46539	0.0028	4.0288
-0.425	+0.00100	-0.17813	-1.44532	0.0028	4.0006
-0.430	+0.00101	-0.17015	-1.42538	0.0028	3.9732
-0.435	+0.00102	-0.16223	-1.40558	0.0028	3.9465
-0.440	+0.00104	-0.15437	-1.38592	0.0028	3.9204
-0.445	+0.00105	-0.14655	-1.36638	0.0027	3.8949
-0.450	+0.00107	-0.13879	-1.34697	0.0027	3.8701
-0.455	+0.00108	-0.13107	-1.32768	0.0027	3.8458
-0.460	+0.00109	-0.12340	-1.30851	0.0027	3.8221
-0.465	+0.00111	-0.11578	-1.28945	0.0027	3.7990
-0.470	+0.00112	-0.10821	-1.27051	0.0026	3.7764
-0.475	+0.00113	-0.10068	-1.25169	0.0026	3.7544
-0.480	+0.00115	-0.09319	-1.23297	0.0026	3.7328
-0.485	+0.00116	-0.08574	-1.21436	0.0026	3.7118
-0.490	+0.00117	-0.07834	-1.19585	0.0025	3.6912
-0.495	+0.00119	-0.07098	-1.17744	0.0025	3.6710
-0.500	+0.00120	-0.06366	-1.15914	0.0025	3.6514
-0.505	+0.00121	-0.05637	-1.14093	0.0025	3.6321
-0.510	+0.00122	-0.04913	-1.12282	0.0024	3.6133
-0.515	+0.00124	-0.04192	-1.10480	0.0024	3.5948
-0.520	+0.00125	-0.03475	-1.08687	0.0024	3.5768
-0.525	+0.00126	-0.02761	-1.06903	0.0024	3.5592
-0.530	+0.00127	-0.02051	-1.05127	0.0024	3.5419
-0.535	+0.00128	-0.01344	-1.03361	0.0023	3.5250
-0.540	+0.00130	-0.00641	-1.01602	0.0023	3.5084
-0.545	+0.00131	+0.00058	-0.99852	0.0023	3.4922
-0.550	+0.00132	+0.00755	-0.98110	0.0023	3.4763
-0.555	+0.00133	+0.01448	-0.96376	0.0022	3.4607
-0.560	+0.00134	+0.02139	-0.94649	0.0022	3.4455
-0.565	+0.00135	+0.02827	-0.92930	0.0022	3.4306
-0.570	+0.00137	+0.03511	-0.91219	0.0022	3.4159
-0.575	+0.00138	+0.04193	-0.89514	0.0021	3.4016
-0.580	+0.00139	+0.04872	-0.87817	0.0021	3.3875
-0.585	+0.00140	+0.05548	-0.86127	0.0021	3.3737
-0.590	+0.00141	+0.06222	-0.84443	0.0021	3.3602
-0.595	+0.00142	+0.06892	-0.82766	0.0020	3.3469
-0.600	+0.00143	+0.07560	-0.81096	0.0020	3.3339
-0.605	+0.00144	+0.08226	-0.79432	0.0020	3.3211

1502

1	4	5	6	7	8
-0.010	+0.00000	-2.03071	-5.77575	0.0001	109.8280
-0.015	+0.00000	-1.85219	-5.32945	0.0003	73.6533
-0.020	+0.00000	-1.72475	-5.01084	0.0004	55.5579
-0.025	+0.00000	-1.62531	-4.76226	0.0006	44.7001
-0.030	+0.00001	-1.54360	-4.55798	0.0007	37.4621
-0.035	+0.00001	-1.47411	-4.38427	0.0009	32.2927
-0.040	+0.00001	-1.41358	-4.23294	0.0011	28.4162
-0.045	+0.00002	-1.35988	-4.09869	0.0013	25.4017
-0.050	+0.00003	-1.31158	-3.97793	0.0015	22.9906
-0.055	+0.00004	-1.26763	-3.86807	0.0017	21.0182
-0.060	+0.00005	-1.22729	-3.76721	0.0019	19.3750
-0.065	+0.00006	-1.18997	-3.67390	0.0020	17.9850
-0.070	+0.00007	-1.15522	-3.58703	0.0022	16.7939
-0.075	+0.00008	-1.12269	-3.50570	0.0024	15.7618
-0.080	+0.00009	-1.09209	-3.42920	0.0026	14.8591
-0.085	+0.00010	-1.06318	-3.35694	0.0028	14.0629
-0.090	+0.00012	-1.03578	-3.28842	0.0030	13.3553
-0.095	+0.00013	-1.00971	-3.22326	0.0031	12.7225
-0.100	+0.00015	-0.98484	-3.16109	0.0033	12.1532
-0.105	+0.00017	-0.96106	-3.10164	0.0035	11.6383
-0.110	+0.00019	-0.93826	-3.04463	0.0036	11.1705
-0.115	+0.00020	-0.91635	-2.98987	0.0038	10.7435
-0.120	+0.00022	-0.89526	-2.93714	0.0039	10.3523
-0.125	+0.00024	-0.87492	-2.88629	0.0041	9.9925
-0.130	+0.00027	-0.85527	-2.83717	0.0042	9.6606
-0.135	+0.00029	-0.83626	-2.78964	0.0043	9.3535
-0.140	+0.00031	-0.81784	-2.74360	0.0045	9.0684
-0.145	+0.00033	-0.79998	-2.69893	0.0046	8.8032
-0.150	+0.00036	-0.78262	-2.65554	0.0047	8.5558
-0.155	+0.00038	-0.76574	-2.61334	0.0048	8.3245
-0.160	+0.00040	-0.74931	-2.57227	0.0049	8.1078
-0.165	+0.00043	-0.73330	-2.53224	0.0050	7.9044
-0.170	+0.00046	-0.71769	-2.49320	0.0051	7.7131
-0.175	+0.00048	-0.70244	-2.45509	0.0052	7.5328
-0.180	+0.00051	-0.68755	-2.41786	0.0053	7.3627
-0.185	+0.00054	-0.67298	-2.38145	0.0054	7.2019
-0.190	+0.00056	-0.65873	-2.34582	0.0055	7.0497
-0.195	+0.00059	-0.64478	-2.31094	0.0056	6.9054
-0.200	+0.00062	-0.63111	-2.27676	0.0056	6.7684
-0.205	+0.00065	-0.61770	-2.24324	0.0057	6.6382

1	4	5	6	7	8
−0.210	+0.00068	−0.60455	−2.21036	0.0058	6.5143
−0.215	+0.00071	−0.59164	−2.17809	0.0058	6.3963
−0.220	+0.00073	−0.57896	−2.14639	0.0059	6.2838
−0.225	+0.00076	−0.56650	−2.11524	0.0059	6.1764
−0.230	+0.00079	−0.55425	−2.08462	0.0060	6.0737
−0.235	+0.00083	−0.54220	−2.05450	0.0060	5.9755
−0.240	+0.00086	−0.53035	−2.02486	0.0061	5.8815
−0.245	+0.00089	−0.51867	−1.99568	0.0061	5.7914
−0.250	+0.00092	−0.50718	−1.96694	0.0061	5.7050
−0.255	+0.00095	−0.49585	−1.93862	0.0062	5.6221
−0.260	+0.00098	−0.48469	−1.91071	0.0062	5.5425
−0.265	+0.00101	−0.47368	−1.88319	0.0062	5.4659
−0.270	+0.00104	−0.46282	−1.85604	0.0062	5.3923
−0.275	+0.00107	−0.45211	−1.82926	0.0062	5.3215
−0.280	+0.00110	−0.44153	−1.80282	0.0063	5.2532
−0.285	+0.00114	−0.43109	−1.77672	0.0063	5.1874
−0.290	+0.00117	−0.42078	−1.75095	0.0063	5.1240
−0.295	+0.00120	−0.41060	−1.72548	0.0063	5.0628
−0.300	+0.00123	−0.40053	−1.70031	0.0063	5.0037
−0.305	+0.00126	−0.39058	−1.67544	0.0063	4.9467
−0.310	+0.00129	−0.38074	−1.65084	0.0063	4.8915
−0.315	+0.00133	−0.37101	−1.62652	0.0063	4.8382
−0.320	+0.00136	−0.36139	−1.60246	0.0063	4.7866
−0.325	+0.00139	−0.35186	−1.57865	0.0063	4.7366
−0.330	+0.00142	−0.34244	−1.55509	0.0062	4.6883
−0.335	+0.00145	−0.33311	−1.53177	0.0062	4.6414
−0.340	+0.00148	−0.32387	−1.50867	0.0062	4.5960
−0.345	+0.00151	−0.31472	−1.48580	0.0062	4.5520
−0.350	+0.00155	−0.30566	−1.46315	0.0062	4.5093
−0.355	+0.00158	−0.29669	−1.44071	0.0062	4.4679
−0.360	+0.00161	−0.28779	−1.41847	0.0061	4.4277
−0.365	+0.00164	−0.27897	−1.39643	0.0061	4.3886
−0.370	+0.00167	−0.27024	−1.37458	0.0061	4.3507
−0.375	+0.00170	−0.26157	−1.35292	0.0061	4.3139
−0.380	+0.00173	−0.25298	−1.33144	0.0060	4.2780
−0.385	+0.00176	−0.24446	−1.31014	0.0060	4.2432
−0.390	+0.00179	−0.23601	−1.28900	0.0060	4.2093
−0.395	+0.00182	−0.22762	−1.26804	0.0059	4.1763
−0.400	+0.00185	−0.21930	−1.24724	0.0059	4.1442
−0.405	+0.00188	−0.21104	−1.22660	0.0059	4.1130
−0.410	+0.00191	−0.20285	−1.20611	0.0058	4.0825
−0.415	+0.00194	−0.19471	−1.18577	0.0058	4.0529
−0.420	+0.00197	−0.18663	−1.16558	0.0057	4.0240
−0.425	+0.00200	−0.17861	−1.14553	0.0057	3.9959
−0.430	+0.00203	−0.17065	−1.12562	0.0057	3.9684
−0.435	+0.00205	−0.16274	−1.10584	0.0056	3.9417
−0.440	+0.00208	−0.15488	−1.08620	0.0056	3.9156
−0.445	+0.00211	−0.14708	−1.06668	0.0055	3.8901
−0.450	+0.00214	−0.13932	−1.04730	0.0055	3.8652
−0.455	+0.00217	−0.13162	−1.02803	0.0055	3.8410
−0.460	+0.00219	−0.12396	−1.00888	0.0054	3.8173
−0.465	+0.00222	−0.11635	−0.98986	0.0054	3.7942
−0.470	+0.00225	−0.10878	−0.97094	0.0053	3.7716
−0.475	+0.00227	−0.10126	−0.95214	0.0053	3.7495
−0.480	+0.00230	−0.09378	−0.93344	0.0052	3.7280
−0.485	+0.00233	−0.08635	−0.91486	0.0052	3.7069
−0.490	+0.00235	−0.07895	−0.89637	0.0051	3.6863
−0.495	+0.00238	−0.07160	−0.87799	0.0051	3.6662
−0.500	+0.00240	−0.06429	−0.85971	0.0050	3.6465
−0.505	+0.00243	−0.05701	−0.84153	0.0050	3.6273
−0.510	+0.00245	−0.04978	−0.82344	0.0049	3.6084
−0.515	+0.00248	−0.04258	−0.80544	0.0049	3.5900
−0.520	+0.00250	−0.03542	−0.78754	0.0049	3.5720
−0.525	+0.00253	−0.02829	−0.76972	0.0048	3.5543
−0.530	+0.00255	−0.02120	−0.75199	0.0048	3.5370
−0.535	+0.00258	−0.01414	−0.73435	0.0047	3.5201
−0.540	+0.00260	−0.00712	−0.71679	0.0047	3.5036
−0.545	+0.00262	−0.00013	−0.69931	0.0046	3.4874
−0.550	+0.00265	+0.00682	−0.68191	0.0046	3.4715
−0.555	+0.00267	+0.01375	−0.66460	0.0045	3.4559
−0.560	+0.00269	+0.02065	−0.64735	0.0045	3.4407
−0.565	+0.00272	+0.02751	−0.63019	0.0044	3.4258
−0.570	+0.00274	+0.03435	−0.61310	0.0044	3.4111
−0.575	+0.00276	+0.04116	−0.59608	0.0043	3.3968
−0.580	+0.00278	+0.04794	−0.57913	0.0043	3.3827
−0.585	+0.00280	+0.05469	−0.56225	0.0042	3.3689
−0.590	+0.00282	+0.06141	−0.54544	0.0042	3.3554
−0.595	+0.00284	+0.06811	−0.52869	0.0041	3.3422
−0.600	+0.00287	+0.07478	−0.51201	0.0041	3.3292
−0.605	+0.00289	+0.08143	−0.49540	0.0040	3.3164

1503

1	4	5	6	7	8
−0.010	+0.00000	−2.03071	−5.59966	0.0002	109.8280
−0.015	+0.00000	−1.85219	−5.15336	0.0004	73.6532
−0.020	+0.00000	−1.72475	−4.83475	0.0006	55.5578
−0.025	+0.00000	−1.62531	−4.58617	0.0009	44.6999
−0.030	+0.00001	−1.54360	−4.38189	0.0011	37.4618
−0.035	+0.00002	−1.47412	−4.20818	0.0014	32.2923
−0.040	+0.00002	−1.41358	−4.05685	0.0017	28.4157
−0.045	+0.00003	−1.35989	−3.92261	0.0020	25.4012
−0.050	+0.00004	−1.31158	−3.80185	0.0022	22.9900
−0.055	+0.00006	−1.26764	−3.69199	0.0025	21.0176
−0.060	+0.00007	−1.22730	−3.59113	0.0028	19.3743
−0.065	+0.00009	−1.18998	−3.49783	0.0031	17.9841
−0.070	+0.00010	−1.15523	−3.41097	0.0034	16.7929
−0.075	+0.00012	−1.12270	−3.32964	0.0037	15.7608
−0.080	+0.00014	−1.09210	−3.25314	0.0039	14.8580
−0.085	+0.00016	−1.06320	−3.18089	0.0042	14.0617
−0.090	+0.00018	−1.03580	−3.11238	0.0045	13.3540
−0.095	+0.00020	−1.00973	−3.04722	0.0047	12.7211
−0.100	+0.00023	−0.98487	−2.98507	0.0050	12.1517
−0.105	+0.00025	−0.96109	−2.92562	0.0052	11.6368
−0.110	+0.00028	−0.93829	−2.86862	0.0054	11.1688
−0.115	+0.00031	−0.91639	−2.81386	0.0057	10.7417
−0.120	+0.00034	−0.89530	−2.76114	0.0059	10.3504
−0.125	+0.00037	−0.87496	−2.71030	0.0061	9.9906
−0.130	+0.00040	−0.85532	−2.66119	0.0063	9.6586
−0.135	+0.00043	−0.83631	−2.61368	0.0065	9.3514
−0.140	+0.00047	−0.81790	−2.56764	0.0067	9.0663
−0.145	+0.00050	−0.80003	−2.52298	0.0069	8.8010
−0.150	+0.00054	−0.78268	−2.47960	0.0071	8.5535
−0.155	+0.00057	−0.76581	−2.43742	0.0073	8.3221
−0.160	+0.00061	−0.74938	−2.39635	0.0074	8.1054
−0.165	+0.00065	−0.73338	−2.35634	0.0076	7.9019
−0.170	+0.00068	−0.71777	−2.31732	0.0077	7.7105
−0.175	+0.00072	−0.70253	−2.27922	0.0079	7.5301
−0.180	+0.00076	−0.68764	−2.24200	0.0080	7.3599
−0.185	+0.00080	−0.67308	−2.20560	0.0081	7.1991
−0.190	+0.00085	−0.65884	−2.16999	0.0083	7.0468
−0.195	+0.00089	−0.64489	−2.13512	0.0084	6.9024
−0.200	+0.00093	−0.63122	−2.10096	0.0085	6.7654
−0.205	+0.00097	−0.61782	−2.06746	0.0086	6.6351
−0.210	+0.00102	−0.60468	−2.03459	0.0087	6.5112
−0.215	+0.00106	−0.59178	−2.00234	0.0088	6.3931
−0.220	+0.00110	−0.57910	−1.97065	0.0089	6.2805
−0.225	+0.00115	−0.56665	−1.93952	0.0089	6.1730
−0.230	+0.00119	−0.55441	−1.90892	0.0090	6.0703
−0.235	+0.00124	−0.54237	−1.87881	0.0091	5.9720
−0.240	+0.00129	−0.53052	−1.84919	0.0091	5.8780
−0.245	+0.00133	−0.51885	−1.82002	0.0092	5.7878
−0.250	+0.00138	−0.50736	−1.79130	0.0092	5.7014
−0.255	+0.00142	−0.49604	−1.76300	0.0093	5.6184
−0.260	+0.00147	−0.48489	−1.73511	0.0093	5.5387
−0.265	+0.00152	−0.47389	−1.70761	0.0093	5.4621
−0.270	+0.00157	−0.46304	−1.68049	0.0094	5.3885
−0.275	+0.00161	−0.45233	−1.65372	0.0094	5.3176
−0.280	+0.00166	−0.44176	−1.62731	0.0094	5.2493
−0.285	+0.00171	−0.43133	−1.60122	0.0094	5.1835
−0.290	+0.00175	−0.42103	−1.57547	0.0094	5.1200
−0.295	+0.00180	−0.41085	−1.55002	0.0094	5.0587
−0.300	+0.00185	−0.40079	−1.52488	0.0095	4.9996
−0.305	+0.00190	−0.39085	−1.50002	0.0095	4.9425
−0.310	+0.00194	−0.38102	−1.47545	0.0094	4.8873
−0.315	+0.00199	−0.37130	−1.45114	0.0094	4.8339
−0.320	+0.00204	−0.36168	−1.42710	0.0094	4.7823
−0.325	+0.00209	−0.35217	−1.40332	0.0094	4.7323
−0.330	+0.00213	−0.34275	−1.37978	0.0094	4.6840
−0.335	+0.00218	−0.33343	−1.35647	0.0094	4.6371
−0.340	+0.00223	−0.32420	−1.33340	0.0093	4.5917
−0.345	+0.00227	−0.31506	−1.31056	0.0093	4.5476
−0.350	+0.00232	−0.30601	−1.28792	0.0093	4.5049
−0.355	+0.00237	−0.29704	−1.26550	0.0093	4.4634
−0.360	+0.00241	−0.28816	−1.24329	0.0092	4.4232
−0.365	+0.00246	−0.27935	−1.22127	0.0092	4.3841
−0.370	+0.00251	−0.27062	−1.19944	0.0091	4.3462
−0.375	+0.00255	−0.26196	−1.17781	0.0091	4.3093
−0.380	+0.00260	−0.25338	−1.15635	0.0091	4.2734
−0.385	+0.00264	−0.24487	−1.13507	0.0090	4.2386
−0.390	+0.00269	−0.23643	−1.11396	0.0090	4.2047
−0.395	+0.00273	−0.22805	−1.09302	0.0089	4.1717
−0.400	+0.00278	−0.21974	−1.07224	0.0089	4.1396
−0.405	+0.00282	−0.21149	−1.05162	0.0088	4.1083

-0.410	+0.00287	-0.20330	-1.03116	0.0088	4.0778
-0.415	+0.00291	-0.19518	-1.01084	0.0087	4.0482
-0.420	+0.00296	-0.18711	-0.99067	0.0086	4.0193
-0.425	+0.00300	-0.17910	-0.97065	0.0086	3.9911
-0.430	+0.00304	-0.17115	-0.95076	0.0085	3.9637
-0.435	+0.00308	-0.16324	-0.93101	0.0085	3.9369
-0.440	+0.00313	-0.15540	-0.91139	0.0084	3.9108
-0.445	+0.00317	-0.14760	-0.89190	0.0083	3.8853
-0.450	+0.00321	-0.13986	-0.87254	0.0083	3.8605
-0.455	+0.00325	-0.13216	-0.85330	0.0082	3.8362
-0.460	+0.00329	-0.12451	-0.83417	0.0081	3.8125
-0.465	+0.00333	-0.11691	-0.81517	0.0081	3.7894
-0.470	+0.00337	-0.10935	-0.79628	0.0080	3.7668
-0.475	+0.00341	-0.10184	-0.77750	0.0079	3.7447
-0.480	+0.00345	-0.09437	-0.75883	0.0079	3.7232
-0.485	+0.00349	-0.08695	-0.74027	0.0078	3.7021
-0.490	+0.00353	-0.07956	-0.72181	0.0077	3.6815
-0.495	+0.00357	-0.07222	-0.70345	0.0077	3.6614
-0.500	+0.00361	-0.06492	-0.68519	0.0076	3.6417
-0.505	+0.00365	-0.05765	-0.66703	0.0075	3.6224
-0.510	+0.00369	-0.05043	-0.64897	0.0075	3.6036
-0.515	+0.00372	-0.04324	-0.63100	0.0074	3.5852
-0.520	+0.00376	-0.03609	-0.61311	0.0073	3.5671
-0.525	+0.00380	-0.02897	-0.59532	0.0072	3.5495
-0.530	+0.00383	-0.02189	-0.57762	0.0072	3.5322
-0.535	+0.00387	-0.01484	-0.56000	0.0071	3.5153
-0.540	+0.00390	-0.00783	-0.54246	0.0070	3.4988
-0.545	+0.00394	-0.00084	-0.52501	0.0069	3.4826
-0.550	+0.00397	+0.00609	-0.50764	0.0069	3.4667
-0.555	+0.00401	+0.01301	-0.49034	0.0068	3.4511
-0.560	+0.00404	+0.01990	-0.47313	0.0067	3.4359
-0.565	+0.00408	+0.02676	-0.45598	0.0067	3.4210
-0.570	+0.00411	+0.03358	-0.43891	0.0066	3.4063
-0.575	+0.00414	+0.04038	-0.42192	0.0065	3.3920
-0.580	+0.00418	+0.04715	-0.40499	0.0064	3.3780
-0.585	+0.00421	+0.05389	-0.38814	0.0064	3.3642
-0.590	+0.00424	+0.06061	-0.37135	0.0063	3.3507
-0.595	+0.00427	+0.06730	-0.35463	0.0062	3.3374
-0.600	+0.00430	+0.07396	-0.33798	0.0061	3.3245
-0.605	+0.00433	+0.08060	-0.32138	0.0061	3.3117

1504

1	4	5	6	7	8
-0.010	+0.00000	-2.03071	-5.37781	0.0004	109.8280
-0.015	+0.00000	-1.85219	-4.93152	0.0007	73.6531
-0.020	+0.00000	-1.72475	-4.61291	0.0011	55.5576
-0.025	+0.00001	-1.62531	-4.36432	0.0015	44.6996
-0.030	+0.00002	-1.54360	-4.16004	0.0019	37.4613
-0.035	+0.00003	-1.47412	-3.98634	0.0024	32.2916
-0.040	+0.00004	-1.41359	-3.83501	0.0028	28.4149
-0.045	+0.00006	-1.35990	-3.70078	0.0033	25.4002
-0.050	+0.00008	-1.31159	-3.58002	0.0038	22.9888
-0.055	+0.00010	-1.26765	-3.47017	0.0042	21.0163
-0.060	+0.00012	-1.22731	-3.36932	0.0047	19.3728
-0.065	+0.00015	-1.19000	-3.27603	0.0052	17.9825
-0.070	+0.00017	-1.15525	-3.18917	0.0057	16.7911
-0.075	+0.00020	-1.12273	-3.10785	0.0061	15.7588
-0.080	+0.00023	-1.09213	-3.03137	0.0066	14.8558
-0.085	+0.00027	-1.06323	-2.95912	0.0070	14.0593
-0.090	+0.00031	-1.03584	-2.89063	0.0075	13.3515
-0.095	+0.00034	-1.00978	-2.82548	0.0079	12.7184
-0.100	+0.00038	-0.98492	-2.76334	0.0083	12.1489
-0.105	+0.00043	-0.96115	-2.70390	0.0087	11.6337
-0.110	+0.00047	-0.93836	-2.64692	0.0091	11.1656
-0.115	+0.00052	-0.91646	-2.59218	0.0095	10.7383
-0.120	+0.00057	-0.89538	-2.53948	0.0099	10.3469
-0.125	+0.00062	-0.87505	-2.48866	0.0102	9.9869
-0.130	+0.00067	-0.85541	-2.43957	0.0106	9.6547
-0.135	+0.00072	-0.83641	-2.39207	0.0109	9.3473
-0.140	+0.00078	-0.81801	-2.34606	0.0112	9.0620
-0.145	+0.00084	-0.80015	-2.30142	0.0116	8.7966
-0.150	+0.00090	-0.78281	-2.25806	0.0119	8.5489
-0.155	+0.00096	-0.76595	-2.21590	0.0121	8.3174
-0.160	+0.00102	-0.74953	-2.17486	0.0124	8.1005
-0.165	+0.00108	-0.73354	-2.13487	0.0127	7.8968
-0.170	+0.00115	-0.71794	-2.09587	0.0129	7.7053
-0.175	+0.00121	-0.70271	-2.05780	0.0132	7.5248
-0.180	+0.00128	-0.68783	-2.02061	0.0134	7.3544
-0.185	+0.00135	-0.67328	-1.98424	0.0136	7.1934
-0.190	+0.00141	-0.65905	-1.94866	0.0138	7.0410
-0.195	+0.00148	-0.64511	-1.91382	0.0140	6.8965
-0.200	+0.00155	-0.63146	-1.87968	0.0142	6.7593
-0.205	+0.00163	-0.61807	-1.84621	0.0144	6.6289

1	4	5	6	7	8
-0.210	+0.00170	-0.60494	-1.81338	0.0145	6.5049
-0.215	+0.00177	-0.59205	-1.78116	0.0147	6.3867
-0.220	+0.00185	-0.57939	-1.74951	0.0148	6.2739
-0.225	+0.00192	-0.56695	-1.71841	0.0149	6.1663
-0.230	+0.00200	-0.55472	-1.68783	0.0150	6.0635
-0.235	+0.00207	-0.54269	-1.65776	0.0152	5.9651
-0.240	+0.00215	-0.53086	-1.62818	0.0153	5.8709
-0.245	+0.00222	-0.51921	-1.59905	0.0153	5.7807
-0.250	+0.00230	-0.50773	-1.57036	0.0154	5.6941
-0.255	+0.00238	-0.49643	-1.54210	0.0155	5.6111
-0.260	+0.00246	-0.48529	-1.51425	0.0156	5.5313
-0.265	+0.00254	-0.47430	-1.48678	0.0156	5.4546
-0.270	+0.00261	-0.46346	-1.45970	0.0157	5.3808
-0.275	+0.00269	-0.45277	-1.43297	0.0157	5.3098
-0.280	+0.00277	-0.44222	-1.40659	0.0157	5.2414
-0.285	+0.00285	-0.43181	-1.38055	0.0158	5.1755
-0.290	+0.00293	-0.42152	-1.35483	0.0158	5.1120
-0.295	+0.00301	-0.41136	-1.32943	0.0158	5.0506
-0.300	+0.00309	-0.40132	-1.30432	0.0158	4.9914
-0.305	+0.00317	-0.39139	-1.27951	0.0158	4.9342
-0.310	+0.00325	-0.38158	-1.25498	0.0158	4.8790
-0.315	+0.00333	-0.37187	-1.23072	0.0158	4.8255
-0.320	+0.00340	-0.36227	-1.20672	0.0158	4.7738
-0.325	+0.00348	-0.35278	-1.18298	0.0157	4.7238
-0.330	+0.00356	-0.34338	-1.15948	0.0157	4.6753
-0.335	+0.00364	-0.33407	-1.13622	0.0157	4.6284
-0.340	+0.00372	-0.32486	-1.11319	0.0156	4.5829
-0.345	+0.00380	-0.31574	-1.09039	0.0156	4.5388
-0.350	+0.00388	-0.30671	-1.06780	0.0155	4.4960
-0.355	+0.00395	-0.29776	-1.04542	0.0155	4.4545
-0.360	+0.00403	-0.28889	-1.02325	0.0154	4.4142
-0.365	+0.00411	-0.28010	-1.00128	0.0154	4.3751
-0.370	+0.00419	-0.27139	-0.97950	0.0153	4.3371
-0.375	+0.00426	-0.26275	-0.95791	0.0152	4.3001
-0.380	+0.00434	-0.25419	-0.93650	0.0152	4.2642
-0.385	+0.00441	-0.24569	-0.91526	0.0151	4.2293
-0.390	+0.00449	-0.23727	-0.89420	0.0150	4.1954
-0.395	+0.00456	-0.22891	-0.87331	0.0149	4.1624
-0.400	+0.00464	-0.22062	-0.85258	0.0148	4.1302
-0.405	+0.00471	-0.21239	-0.83200	0.0147	4.0989
-0.410	+0.00479	-0.20422	-0.81158	0.0147	4.0684
-0.415	+0.00486	-0.19611	-0.79132	0.0146	4.0388
-0.420	+0.00493	-0.18806	-0.77120	0.0145	4.0098
-0.425	+0.00501	-0.18007	-0.75122	0.0144	3.9816
-0.430	+0.00508	-0.17214	-0.73138	0.0143	3.9542
-0.435	+0.00515	-0.16426	-0.71167	0.0142	3.9274
-0.440	+0.00522	-0.15643	-0.69210	0.0141	3.9012
-0.445	+0.00529	-0.14865	-0.67266	0.0140	3.8757
-0.450	+0.00536	-0.14092	-0.65334	0.0138	3.8509
-0.455	+0.00543	-0.13325	-0.63415	0.0137	3.8266
-0.460	+0.00550	-0.12562	-0.61508	0.0136	3.8029
-0.465	+0.00557	-0.11803	-0.59612	0.0135	3.7798
-0.470	+0.00563	-0.11050	-0.57728	0.0134	3.7572
-0.475	+0.00570	-0.10301	-0.55855	0.0133	3.7351
-0.480	+0.00577	-0.09556	-0.53992	0.0132	3.7135
-0.485	+0.00583	-0.08815	-0.52141	0.0131	3.6924
-0.490	+0.00590	-0.08079	-0.50300	0.0129	3.6718
-0.495	+0.00596	-0.07346	-0.48469	0.0128	3.6517
-0.500	+0.00603	-0.06618	-0.46648	0.0127	3.6320
-0.505	+0.00609	-0.05893	-0.44837	0.0126	3.6128
-0.510	+0.00615	-0.05173	-0.43035	0.0125	3.5939
-0.515	+0.00622	-0.04456	-0.41243	0.0123	3.5755
-0.520	+0.00628	-0.03743	-0.39460	0.0122	3.5575
-0.525	+0.00634	-0.03033	-0.37685	0.0121	3.5398
-0.530	+0.00640	-0.02327	-0.35920	0.0120	3.5226
-0.535	+0.00646	-0.01624	-0.34163	0.0119	3.5057
-0.540	+0.00652	-0.00924	-0.32414	0.0117	3.4891
-0.545	+0.00658	-0.00228	-0.30673	0.0116	3.4729
-0.550	+0.00663	+0.00464	-0.28941	0.0115	3.4571
-0.555	+0.00669	+0.01154	-0.27216	0.0114	3.4415
-0.560	+0.00675	+0.01841	-0.25499	0.0113	3.4263
-0.565	+0.00680	+0.02524	-0.23790	0.0111	3.4114
-0.570	+0.00686	+0.03205	-0.22088	0.0110	3.3968
-0.575	+0.00692	+0.03883	-0.20393	0.0109	3.3825
-0.580	+0.00697	+0.04558	-0.18705	0.0108	3.3685
-0.585	+0.00702	+0.05231	-0.17024	0.0107	3.3547
-0.590	+0.00708	+0.05900	-0.15350	0.0105	3.3412
-0.595	+0.00713	+0.06567	-0.13683	0.0104	3.3280
-0.600	+0.00718	+0.07231	-0.12022	0.0103	3.3150
-0.605	+0.00723	+0.07893	-0.10368	0.0102	3.3023

1505

1	4	5	6	7	8
−0.010	+0.00000	−2.03071	−5.20172	0.0006	109.8280
−0.015	+0.00000	−1.85219	−4.75543	0.0011	73.6529
−0.020	+0.00001	−1.72475	−4.43682	0.0016	55.5572
−0.025	+0.00002	−1.62532	−4.18824	0.0023	44.6990
−0.030	+0.00003	−1.54361	−3.98396	0.0029	37.4606
−0.035	+0.00005	−1.47413	−3.81026	0.0036	32.2907
−0.040	+0.00007	−1.41360	−3.65894	0.0043	28.4138
−0.045	+0.00009	−1.35991	−3.52471	0.0050	25.3989
−0.050	+0.00012	−1.31161	−3.40396	0.0057	22.9873
−0.055	+0.00015	−1.26767	−3.29412	0.0064	21.0145
−0.060	+0.00018	−1.22733	−3.19328	0.0071	19.3709
−0.065	+0.00022	−1.19002	−3.09999	0.0078	17.9804
−0.070	+0.00026	−1.15528	−3.01315	0.0085	16.7888
−0.075	+0.00031	−1.12276	−2.93185	0.0092	15.7563
−0.080	+0.00035	−1.09217	−2.85537	0.0099	14.8530
−0.085	+0.00041	−1.06328	−2.78314	0.0106	14.0563
−0.090	+0.00046	−1.03589	−2.71466	0.0112	13.3483
−0.095	+0.00052	−1.00984	−2.64953	0.0119	12.7150
−0.100	+0.00058	−0.98499	−2.58741	0.0125	12.1452
−0.105	+0.00064	−0.96122	−2.52799	0.0131	11.6298
−0.110	+0.00071	−0.93844	−2.47103	0.0137	11.1615
−0.115	+0.00078	−0.91655	−2.41631	0.0143	10.7340
−0.120	+0.00085	−0.89548	−2.36363	0.0148	10.3424
−0.125	+0.00093	−0.87516	−2.31283	0.0154	9.9821
−0.130	+0.00101	−0.85553	−2.26376	0.0159	9.6498
−0.135	+0.00109	−0.83654	−2.21629	0.0164	9.3422
−0.140	+0.00117	−0.81814	−2.17031	0.0169	9.0567
−0.145	+0.00126	−0.80030	−2.12569	0.0174	8.7910
−0.150	+0.00135	−0.78297	−2.08237	0.0178	8.5432
−0.155	+0.00144	−0.76612	−2.04024	0.0182	8.3115
−0.160	+0.00153	−0.74971	−1.99923	0.0187	8.0943
−0.165	+0.00162	−0.73373	−1.95927	0.0191	7.8905
−0.170	+0.00172	−0.71814	−1.92030	0.0194	7.6987
−0.175	+0.00182	−0.70293	−1.88226	0.0198	7.5181
−0.180	+0.00192	−0.68806	−1.84510	0.0201	7.3475
−0.185	+0.00202	−0.67353	−1.80877	0.0205	7.1863
−0.190	+0.00212	−0.65931	−1.77323	0.0208	7.0337
−0.195	+0.00223	−0.64539	−1.73842	0.0210	6.8891
−0.200	+0.00234	−0.63175	−1.70432	0.0213	6.7517
−0.205	+0.00244	−0.61838	−1.67089	0.0216	6.6212
−0.210	+0.00255	−0.60526	−1.63810	0.0218	6.4969
−0.215	+0.00266	−0.59239	−1.60591	0.0220	6.3786
−0.220	+0.00277	−0.57974	−1.57430	0.0222	6.2657
−0.225	+0.00288	−0.56732	−1.54325	0.0224	6.1579
−0.230	+0.00300	−0.55511	−1.51272	0.0226	6.0549
−0.235	+0.00311	−0.54310	−1.48269	0.0228	5.9564
−0.240	+0.00323	−0.53128	−1.45315	0.0229	5.8621
−0.245	+0.00334	−0.51965	−1.42406	0.0231	5.7717
−0.250	+0.00346	−0.50819	−1.39542	0.0232	5.6850
−0.255	+0.00357	−0.49691	−1.36721	0.0233	5.6018
−0.260	+0.00369	−0.48578	−1.33940	0.0234	5.5219
−0.265	+0.00381	−0.47482	−1.31198	0.0235	5.4451
−0.270	+0.00393	−0.46400	−1.28494	0.0236	5.3712
−0.275	+0.00404	−0.45333	−1.25826	0.0236	5.3001
−0.280	+0.00416	−0.44280	−1.23194	0.0237	5.2316
−0.285	+0.00428	−0.43240	−1.20594	0.0237	5.1655
−0.290	+0.00440	−0.42213	−1.18028	0.0237	5.1019
−0.295	+0.00452	−0.41199	−1.15492	0.0238	5.0404
−0.300	+0.00464	−0.40197	−1.12987	0.0238	4.9811
−0.305	+0.00476	−0.39207	−1.10511	0.0238	4.9239
−0.310	+0.00488	−0.38227	−1.08063	0.0237	4.8685
−0.315	+0.00499	−0.37259	−1.05642	0.0237	4.8149
−0.320	+0.00511	−0.36301	−1.03247	0.0237	4.7632
−0.325	+0.00523	−0.35354	−1.00878	0.0237	4.7130
−0.330	+0.00535	−0.34416	−0.98534	0.0236	4.6645
−0.335	+0.00547	−0.33488	−0.96214	0.0236	4.6175
−0.340	+0.00559	−0.32569	−0.93916	0.0235	4.5719
−0.345	+0.00570	−0.31659	−0.91641	0.0234	4.5277
−0.350	+0.00582	−0.30758	−0.89388	0.0234	4.4849
−0.355	+0.00594	−0.29865	−0.87156	0.0233	4.4433
−0.360	+0.00605	−0.28980	−0.84945	0.0232	4.4029
−0.365	+0.00617	−0.28104	−0.82753	0.0231	4.3638
−0.370	+0.00629	−0.27235	−0.80581	0.0230	4.3257
−0.375	+0.00640	−0.26373	−0.78427	0.0229	4.2887
−0.380	+0.00652	−0.25519	−0.76292	0.0228	4.2527
−0.385	+0.00663	−0.24672	−0.74174	0.0227	4.2178
−0.390	+0.00674	−0.23832	−0.72074	0.0226	4.1838
−0.395	+0.00686	−0.22998	−0.69990	0.0224	4.1507
−0.400	+0.00697	−0.22171	−0.67923	0.0223	4.1185
−0.405	+0.00708	−0.21351	−0.65871	0.0222	4.0872
−0.410	+0.00719	−0.20537	−0.63836	0.0220	4.0567
−0.415	+0.00730	−0.19728	−0.61815	0.0219	4.0269
−0.420	+0.00741	−0.18926	−0.59808	0.0218	3.9980
−0.425	+0.00752	−0.18129	−0.57816	0.0216	3.9698
−0.430	+0.00763	−0.17338	−0.55838	0.0215	3.9423
−0.435	+0.00773	−0.16552	−0.53874	0.0213	3.9154
−0.440	+0.00784	−0.15771	−0.51923	0.0212	3.8893
−0.445	+0.00795	−0.14996	−0.49985	0.0210	3.8638
−0.450	+0.00805	−0.14226	−0.48059	0.0208	3.8389
−0.455	+0.00815	−0.13461	−0.46146	0.0207	3.8146
−0.460	+0.00826	−0.12700	−0.44244	0.0205	3.7909
−0.465	+0.00836	−0.11944	−0.42355	0.0203	3.7677
−0.470	+0.00846	−0.11193	−0.40476	0.0202	3.7451
−0.475	+0.00856	−0.10446	−0.38609	0.0200	3.7230
−0.480	+0.00866	−0.09704	−0.36753	0.0198	3.7014
−0.485	+0.00876	−0.08965	−0.34908	0.0196	3.6803
−0.490	+0.00886	−0.08231	−0.33073	0.0195	3.6597
−0.495	+0.00896	−0.07502	−0.31248	0.0193	3.6396
−0.500	+0.00905	−0.06776	−0.29433	0.0191	3.6199
−0.505	+0.00915	−0.06053	−0.27628	0.0189	3.6007
−0.510	+0.00924	−0.05335	−0.25832	0.0188	3.5818
−0.515	+0.00934	−0.04621	−0.24046	0.0186	3.5634
−0.520	+0.00943	−0.03910	−0.22269	0.0184	3.5454
−0.525	+0.00952	−0.03203	−0.20500	0.0182	3.5278
−0.530	+0.00961	−0.02499	−0.18741	0.0180	3.5105
−0.535	+0.00970	−0.01798	−0.16990	0.0178	3.4936
−0.540	+0.00979	−0.01101	−0.15247	0.0177	3.4771
−0.545	+0.00988	−0.00407	−0.13513	0.0175	3.4609
−0.550	+0.00997	+0.00282	−0.11786	0.0173	3.4451
−0.555	+0.01005	+0.00970	−0.10067	0.0171	3.4295
−0.560	+0.01014	+0.01654	−0.08356	0.0169	3.4143
−0.565	+0.01022	+0.02335	−0.06653	0.0168	3.3994
−0.570	+0.01030	+0.03014	−0.04957	0.0166	3.3849
−0.575	+0.01039	+0.03689	−0.03268	0.0164	3.3706
−0.580	+0.01047	+0.04362	−0.01586	0.0162	3.3566
−0.585	+0.01055	+0.05032	+0.00088	0.0160	3.3428
−0.590	+0.01063	+0.05699	+0.01756	0.0158	3.3294
−0.595	+0.01071	+0.06364	+0.03417	0.0157	3.3162
−0.600	+0.01079	+0.07026	+0.05072	0.0155	3.3032
−0.605	+0.01086	+0.07685	+0.06720	0.0153	3.2905

1506

1	4	5	6	7	8
−0.010	+0.00000	−2.03071	−5.07679	0.0008	109.8280
−0.015	+0.00000	−1.85219	−4.63049	0.0015	73.6527
−0.020	+0.00001	−1.72475	−4.31188	0.0022	55.5568
−0.025	+0.00003	−1.62532	−4.06330	0.0030	44.6984
−0.030	+0.00004	−1.54361	−3.85903	0.0039	37.4598
−0.035	+0.00007	−1.47413	−3.68534	0.0048	32.2898
−0.040	+0.00009	−1.41361	−3.53402	0.0057	28.4127
−0.045	+0.00012	−1.35992	−3.39980	0.0066	25.3976
−0.050	+0.00016	−1.31162	−3.27905	0.0076	22.9858
−0.055	+0.00020	−1.26769	−3.16922	0.0085	21.0128
−0.060	+0.00025	−1.22735	−3.06839	0.0095	19.3690
−0.065	+0.00030	−1.19004	−2.97511	0.0104	17.9782
−0.070	+0.00035	−1.15531	−2.88828	0.0114	16.7864
−0.075	+0.00041	−1.12279	−2.80699	0.0123	15.7537
−0.080	+0.00047	−1.09221	−2.73053	0.0132	14.8503
−0.085	+0.00054	−1.06332	−2.65831	0.0141	14.0533
−0.090	+0.00061	−1.03594	−2.58985	0.0150	13.3451
−0.095	+0.00069	−1.00989	−2.52473	0.0158	12.7116
−0.100	+0.00077	−0.98505	−2.46263	0.0167	12.1415
−0.105	+0.00086	−0.96129	−2.40323	0.0175	11.6260
−0.110	+0.00095	−0.93851	−2.34629	0.0183	11.1574
−0.115	+0.00104	−0.91663	−2.29159	0.0191	10.7297
−0.120	+0.00114	−0.89557	−2.23893	0.0198	10.3378
−0.125	+0.00124	−0.87526	−2.18816	0.0205	9.9774
−0.130	+0.00135	−0.85564	−2.13911	0.0212	9.6449
−0.135	+0.00145	−0.83667	−2.09167	0.0219	9.3370
−0.140	+0.00156	−0.81828	−2.04570	0.0226	9.0513
−0.145	+0.00168	−0.80045	−2.00112	0.0232	8.7855
−0.150	+0.00180	−0.78313	−1.95782	0.0238	8.5374
−0.155	+0.00192	−0.76629	−1.91572	0.0244	8.3055
−0.160	+0.00204	−0.74989	−1.87474	0.0249	8.0882
−0.165	+0.00217	−0.73392	−1.83482	0.0254	7.8841
−0.170	+0.00230	−0.71835	−1.79588	0.0259	7.6922
−0.175	+0.00243	−0.70315	−1.75787	0.0264	7.5114
0.180	+0.00256	−0.68830	−1.72075	0.0269	7.3407
−0.185	+0.00270	−0.67378	−1.68445	0.0273	7.1793
−0.190	+0.00283	−0.65957	−1.64894	0.0277	7.0265
−0.195	+0.00297	−0.64567	−1.61417	0.0281	6.8816
−0.200	+0.00312	−0.63204	−1.58011	0.0285	6.7441
−0.205	+0.00326	−0.61869	−1.54672	0.0288	6.6134

1	4	5	6	7	8
-0.210	+0.00340	-0.60559	-1.51397	0.0291	6.4890
-0.215	+0.00355	-0.59273	-1.48182	0.0294	6.3705
-0.220	+0.00370	-0.58010	-1.45025	0.0297	6.2575
-0.225	+0.00385	-0.56769	-1.41924	0.0300	6.1495
-0.230	+0.00400	-0.55550	-1.38875	0.0302	6.0464
-0.235	+0.00415	-0.54350	-1.35877	0.0304	5.9477
-0.240	+0.00430	-0.53170	-1.32926	0.0306	5.8533
-0.245	+0.00446	-0.52009	-1.30023	0.0308	5.7627
-0.250	+0.00461	-0.50865	-1.27163	0.0310	5.6759
-0.255	+0.00477	-0.49738	-1.24346	0.0311	5.5926
-0.260	+0.00492	-0.48628	-1.21570	0.0312	5.5125
-0.265	+0.00508	-0.47533	-1.18833	0.0314	5.4356
-0.270	+0.00524	-0.46453	-1.16134	0.0315	5.3616
-0.275	+0.00540	-0.45388	-1.13471	0.0315	5.2903
-0.280	+0.00555	-0.44337	-1.10843	0.0316	5.2217
-0.285	+0.00571	-0.43299	-1.08249	0.0317	5.1556
-0.290	+0.00587	-0.42275	-1.05687	0.0317	5.0918
-0.295	+0.00603	-0.41262	-1.03157	0.0317	5.0303
-0.300	+0.00619	-0.40262	-1.00656	0.0317	4.9709
-0.305	+0.00635	-0.39274	-0.98185	0.0317	4.9135
-0.310	+0.00651	-0.38297	-0.95742	0.0317	4.8580
-0.315	+0.00667	-0.37331	-0.93327	0.0317	4.8044
-0.320	+0.00682	-0.36375	-0.90938	0.0317	4.7525
-0.325	+0.00698	-0.35430	-0.88574	0.0316	4.7023
-0.330	+0.00714	-0.34494	-0.86235	0.0316	4.6537
-0.335	+0.00730	-0.33568	-0.83920	0.0315	4.6066
-0.340	+0.00746	-0.32651	-0.81628	0.0314	4.5609
-0.345	+0.00761	-0.31743	-0.79359	0.0313	4.5167
-0.350	+0.00777	-0.30844	-0.77111	0.0312	4.4737
-0.355	+0.00793	-0.29954	-0.74885	0.0311	4.4321
-0.360	+0.00808	-0.29072	-0.72679	0.0310	4.3917
-0.365	+0.00824	-0.28197	-0.70493	0.0309	4.3524
-0.370	+0.00839	-0.27330	-0.68326	0.0307	4.3143
-0.375	+0.00854	-0.26471	-0.66179	0.0306	4.2772
-0.380	+0.00870	-0.25619	-0.64049	0.0305	4.2412
-0.385	+0.00885	-0.24775	-0.61937	0.0303	4.2062
-0.390	+0.00900	-0.23937	-0.59843	0.0301	4.1722
-0.395	+0.00915	-0.23106	-0.57765	0.0300	4.1391
-0.400	+0.00930	-0.22281	-0.55703	0.0298	4.1068
-0.405	+0.00945	-0.21463	-0.53658	0.0296	4.0754
-0.410	+0.00960	-0.20651	-0.51628	0.0295	4.0449
-0.415	+0.00974	-0.19845	-0.49613	0.0293	4.0151
-0.420	+0.00989	-0.19045	-0.47612	0.0291	3.9861
-0.425	+0.01004	-0.18250	-0.45626	0.0289	3.9579
-0.430	+0.01018	-0.17462	-0.43654	0.0287	3.9303
-0.435	+0.01032	-0.16678	-0.41696	0.0285	3.9035
-0.440	+0.01047	-0.15900	-0.39751	0.0283	3.8773
-0.445	+0.01061	-0.15127	-0.37818	0.0281	3.8518
-0.450	+0.01075	-0.14359	-0.35899	0.0278	3.8269
-0.455	+0.01088	-0.13596	-0.33991	0.0276	3.8025
-0.460	+0.01102	-0.12838	-0.32096	0.0274	3.7788
-0.465	+0.01116	-0.12085	-0.30212	0.0272	3.7556
-0.470	+0.01129	-0.11336	-0.28340	0.0269	3.7330
-0.475	+0.01143	-0.10592	-0.26479	0.0267	3.7109
-0.480	+0.01156	-0.09852	-0.24629	0.0265	3.6893
-0.485	+0.01169	-0.09116	-0.22790	0.0263	3.6682
-0.490	+0.01183	-0.08384	-0.20961	0.0260	3.6476
-0.495	+0.01196	-0.07657	-0.19142	0.0258	3.6275
-0.500	+0.01208	-0.06933	-0.17333	0.0255	3.6078
-0.505	+0.01221	-0.06214	-0.15534	0.0253	3.5885
-0.510	+0.01234	-0.05498	-0.13745	0.0251	3.5697
-0.515	+0.01246	-0.04786	-0.11964	0.0248	3.5513
-0.520	+0.01259	-0.04077	-0.10193	0.0246	3.5333
-0.525	+0.01271	-0.03372	-0.08431	0.0243	3.5157
-0.530	+0.01283	-0.02671	-0.06677	0.0241	3.4984
-0.535	+0.01295	-0.01973	-0.04932	0.0238	3.4815
-0.540	+0.01307	-0.01278	-0.03196	0.0236	3.4650
-0.545	+0.01319	-0.00587	-0.01467	0.0234	3.4489
-0.550	+0.01330	+0.00100	+0.00252	0.0231	3.4330
-0.555	+0.01342	+0.00785	+0.01965	0.0229	3.4175
-0.560	+0.01353	+0.01467	+0.03670	0.0226	3.4023
-0.565	+0.01364	+0.02146	+0.05367	0.0224	3.3875
-0.570	+0.01376	+0.02822	+0.07057	0.0221	3.3729
-0.575	+0.01387	+0.03496	+0.08740	0.0219	3.3586
-0.580	+0.01398	+0.04166	+0.10416	0.0217	3.3446
-0.585	+0.01408	+0.04834	+0.12085	0.0214	3.3309
-0.590	+0.01419	+0.05498	+0.13747	0.0212	3.3175
-0.595	+0.01430	+0.06161	+0.15403	0.0209	3.3043
-0.600	+0.01440	+0.06820	+0.17052	0.0207	3.2914
-0.605	+0.01450	+0.07477	+0.18694	0.0204	3.2788

1	4	5	6	7	8
-0.010	+0.00000	-2.03071	-4.90069	0.0012	109.8272
-0.015	+0.00001	-1.85219	-4.45440	0.0022	73.6519
-0.020	+0.00002	-1.72475	-4.13580	0.0033	55.5557
-0.025	+0.00004	-1.62532	-3.88723	0.0046	44.6971
-0.030	+0.00007	-1.54362	-3.68296	0.0058	37.4582
-0.035	+0.00010	-1.47414	-3.50928	0.0072	32.2878
-0.040	+0.00014	-1.41362	-3.35797	0.0086	28.4104
-0.045	+0.00019	-1.35994	-3.22376	0.0100	25.3949
-0.050	+0.00024	-1.31164	-3.10303	0.0114	22.9827
-0.055	+0.00030	-1.26772	-2.99321	0.0128	21.0093
-0.060	+0.00037	-1.22739	-2.89240	0.0143	19.3650
-0.065	+0.00045	-1.19009	-2.79915	0.0157	17.9739
-0.070	+0.00053	-1.15536	-2.71233	0.0171	16.7816
-0.075	+0.00062	-1.12286	-2.63107	0.0185	15.7485
-0.080	+0.00071	-1.09229	-2.55464	0.0198	14.8446
-0.085	+0.00082	-1.06341	-2.48245	0.0212	14.0473
-0.090	+0.00093	-1.03604	-2.41402	0.0225	13.3386
-0.095	+0.00104	-1.01001	-2.34894	0.0238	12.7046
-0.100	+0.00116	-0.98518	-2.28687	0.0250	12.1342
-0.105	+0.00129	-0.96143	-2.22751	0.0263	11.6182
-0.110	+0.00143	-0.93867	-2.17061	0.0275	11.1492
-0.115	+0.00157	-0.91681	-2.11595	0.0286	10.7211
-0.120	+0.00171	-0.89576	-2.06334	0.0297	10.3288
-0.125	+0.00186	-0.87547	-2.01261	0.0308	9.9679
-0.130	+0.00202	-0.85587	-1.96361	0.0319	9.6349
-0.135	+0.00218	-0.83692	-1.91622	0.0329	9.3267
-0.140	+0.00235	-0.81855	-1.87031	0.0339	9.0406
-0.145	+0.00252	-0.80074	-1.82578	0.0348	8.7743
-0.150	+0.00270	-0.78344	-1.78253	0.0357	8.5259
-0.155	+0.00288	-0.76663	-1.74049	0.0366	8.2936
-0.160	+0.00307	-0.75026	-1.69957	0.0374	8.0759
-0.165	+0.00326	-0.73431	-1.65971	0.0382	7.8714
-0.170	+0.00345	-0.71877	-1.62084	0.0390	7.6791
-0.175	+0.00365	-0.70359	-1.58290	0.0397	7.4979
-0.180	+0.00385	-0.68877	-1.54584	0.0404	7.3268
-0.185	+0.00405	-0.67428	-1.50962	0.0410	7.1651
-0.190	+0.00426	-0.66010	-1.47418	0.0417	7.0120
-0.195	+0.00447	-0.64622	-1.43948	0.0422	6.8668
-0.200	+0.00468	-0.63263	-1.40550	0.0428	6.7289
-0.205	+0.00490	-0.61930	-1.37218	0.0433	6.5979
-0.210	+0.00511	-0.60623	-1.33951	0.0438	6.4731
-0.215	+0.00533	-0.59341	-1.30744	0.0442	6.3543
-0.220	+0.00556	-0.58081	-1.27595	0.0447	6.2409
-0.225	+0.00578	-0.56844	-1.24502	0.0451	6.1327
-0.230	+0.00601	-0.55628	-1.21462	0.0454	6.0293
-0.235	+0.00624	-0.54432	-1.18472	0.0457	5.9303
-0.240	+0.00647	-0.53255	-1.15531	0.0461	5.8356
-0.245	+0.00670	-0.52097	-1.12636	0.0463	5.7448
-0.250	+0.00693	-0.50957	-1.09785	0.0466	5.6577
-0.255	+0.00716	-0.49834	-1.06978	0.0468	5.5741
-0.260	+0.00740	-0.48727	-1.04211	0.0470	5.4938
-0.265	+0.00763	-0.47636	-1.01483	0.0472	5.4166
-0.270	+0.00787	-0.46560	-0.98794	0.0473	5.3423
-0.275	+0.00811	-0.45499	-0.96140	0.0475	5.2708
-0.280	+0.00834	-0.44452	-0.93522	0.0476	5.2020
-0.285	+0.00858	-0.43418	-0.90938	0.0476	5.1356
-0.290	+0.00882	-0.42397	-0.88386	0.0477	5.0716
-0.295	+0.00906	-0.41389	-0.85866	0.0477	5.0099
-0.300	+0.00930	-0.40393	-0.83376	0.0478	4.9503
-0.305	+0.00954	-0.39409	-0.80915	0.0478	4.8927
-0.310	+0.00978	-0.38436	-0.78483	0.0477	4.8370
-0.315	+0.01002	-0.37474	-0.76078	0.0477	4.7832
-0.320	+0.01026	-0.36523	-0.73699	0.0476	4.7311
-0.325	+0.01049	-0.35581	-0.71346	0.0476	4.6808
-0.330	+0.01073	-0.34650	-0.69018	0.0475	4.6320
-0.335	+0.01097	-0.33729	-0.66714	0.0474	4.5847
-0.340	+0.01121	-0.32816	-0.64433	0.0473	4.5389
-0.345	+0.01144	-0.31913	-0.62175	0.0471	4.4945
-0.350	+0.01168	-0.31018	-0.59939	0.0470	4.4514
-0.355	+0.01191	-0.30132	-0.57723	0.0468	4.4097
-0.360	+0.01215	-0.29254	-0.55529	0.0467	4.3691
-0.365	+0.01238	-0.28384	-0.53354	0.0465	4.3297
-0.370	+0.01261	-0.27522	-0.51199	0.0463	4.2915
-0.375	+0.01284	-0.26668	-0.49062	0.0461	4.2543
-0.380	+0.01307	-0.25821	-0.46944	0.0459	4.2182
-0.385	+0.01330	-0.24980	-0.44844	0.0456	4.1831
-0.390	+0.01353	-0.24147	-0.42761	0.0454	4.1489
-0.395	+0.01376	-0.23321	-0.40695	0.0451	4.1157
-0.400	+0.01398	-0.22501	-0.38645	0.0449	4.0834
-0.405	+0.01421	-0.21687	-0.36611	0.0446	4.0519

−0.410	+0.01443	−0.20880	−0.34593	0.0443	4.0213
−0.415	+0.01465	−0.20079	−0.32590	0.0441	3.9915
−0.420	+0.01487	−0.19283	−0.30601	0.0438	3.9624
−0.425	+0.01509	−0.18494	−0.28627	0.0435	3.9341
−0.430	+0.01530	−0.17710	−0.26667	0.0432	3.9065
−0.435	+0.01552	−0.16931	−0.24720	0.0429	3.8796
−0.440	+0.01573	−0.16158	−0.22787	0.0426	3.8533
−0.445	+0.01595	−0.15390	−0.20867	0.0422	3.8278
−0.450	+0.01616	−0.14627	−0.18959	0.0419	3.8028
−0.455	+0.01637	−0.13868	−0.17064	0.0416	3.7784
−0.460	+0.01657	−0.13115	−0.15181	0.0412	3.7547
−0.465	+0.01678	−0.12367	−0.13309	0.0409	3.7315
−0.470	+0.01698	−0.11622	−0.11449	0.0406	3.7088
−0.475	+0.01718	−0.10883	−0.09600	0.0402	3.6867
−0.480	+0.01738	−0.10148	−0.07762	0.0399	3.6651
−0.485	+0.01758	−0.09417	−0.05935	0.0395	3.6440
−0.490	+0.01778	−0.08690	−0.04118	0.0392	3.6234
−0.495	+0.01798	−0.07967	−0.02311	0.0388	3.6032
−0.500	+0.01817	−0.07249	−0.00515	0.0385	3.5835
−0.505	+0.01836	−0.06534	+0.01271	0.0381	3.5643
−0.510	+0.01855	−0.05823	+0.03049	0.0377	3.5455
−0.515	+0.01874	−0.05116	+0.04817	0.0374	3.5271
−0.520	+0.01892	−0.04412	+0.06576	0.0370	3.5090
−0.525	+0.01911	−0.03712	+0.08326	0.0366	3.4914
−0.530	+0.01929	−0.03015	+0.10067	0.0363	3.4742
−0.535	+0.01947	−0.02322	+0.11800	0.0359	3.4574
−0.540	+0.01965	−0.01633	+0.13525	0.0355	3.4409
−0.545	+0.01983	−0.00946	+0.15241	0.0352	3.4247
−0.550	+0.02000	−0.00263	+0.16950	0.0348	3.4089
−0.555	+0.02018	+0.00417	+0.18650	0.0344	3.3934
−0.560	+0.02035	+0.01094	+0.20343	0.0341	3.3783
−0.565	+0.02052	+0.01768	+0.22029	0.0337	3.3634
−0.570	+0.02069	+0.02439	+0.23707	0.0333	3.3489
−0.575	+0.02085	+0.03108	+0.25378	0.0330	3.3347
−0.580	+0.02102	+0.03773	+0.27041	0.0326	3.3207
−0.585	+0.02118	+0.04436	+0.28698	0.0322	3.3071
−0.590	+0.02134	+0.05096	+0.30349	0.0319	3.2937
−0.595	+0.02150	+0.05753	+0.31992	0.0315	3.2806
−0.600	+0.02165	+0.06408	+0.33629	0.0311	3.2677
−0.605	+0.02181	+0.07061	+0.35260	0.0308	3.2551

1508

1	4	5	6	7	8
−0.010	+0.00000	−2.03071	−4.77576	0.0016	109.8272
−0.015	+0.00001	−1.85220	−4.32947	0.0030	73.6515
−0.020	+0.00003	−1.72476	−4.01087	0.0045	55.5550
−0.025	+0.00006	−1.62533	−3.76230	0.0061	44.6961
−0.030	+0.00009	−1.54362	−3.55804	0.0078	37.4568
−0.035	+0.00014	−1.47415	−3.38436	0.0096	32.2861
−0.040	+0.00019	−1.41364	−3.23307	0.0115	28.4082
−0.045	+0.00025	−1.35996	−3.09887	0.0133	25.3923
−0.050	+0.00032	−1.31167	−2.97815	0.0152	22.9797
−0.055	+0.00041	−1.26775	−2.86835	0.0171	21.0059
−0.060	+0.00050	−1.22743	−2.76755	0.0190	19.3612
−0.065	+0.00060	−1.19014	−2.67432	0.0209	17.9697
−0.070	+0.00071	−1.15542	−2.58753	0.0228	16.7770
−0.075	+0.00082	−1.12292	−2.50629	0.0246	15.7434
−0.080	+0.00095	−1.09236	−2.42988	0.0265	14.8391
−0.085	+0.00109	−1.06350	−2.35772	0.0283	14.0413
−0.090	+0.00124	−1.03614	−2.28932	0.0300	13.3322
−0.095	+0.00139	−1.01012	−2.22428	0.0317	12.6978
−0.100	+0.00155	−0.98530	−2.16224	0.0334	12.1269
−0.105	+0.00172	−0.96158	−2.10292	0.0351	11.6105
−0.110	+0.00190	−0.93883	−2.04606	0.0367	11.1410
−0.115	+0.00209	−0.91698	−1.99144	0.0382	10.7125
−0.120	+0.00229	−0.89596	−1.93887	0.0397	10.3198
−0.125	+0.00249	−0.87568	−1.88819	0.0412	9.9585
−0.130	+0.00270	−0.85611	−1.83924	0.0426	9.6251
−0.135	+0.00292	−0.83717	−1.79190	0.0439	9.3165
−0.140	+0.00314	−0.81883	−1.74604	0.0452	9.0299
−0.145	+0.00337	−0.80104	−1.70157	0.0465	8.7632
−0.150	+0.00360	−0.78376	−1.65838	0.0477	8.5144
−0.155	+0.00385	−0.76697	−1.61640	0.0489	8.2817
−0.160	+0.00409	−0.75062	−1.57554	0.0500	8.0636
−0.165	+0.00435	−0.73470	−1.53574	0.0510	7.8588
−0.170	+0.00460	−0.71918	−1.49693	0.0521	7.6661
−0.175	+0.00487	−0.70403	−1.45906	0.0530	7.4845
−0.180	+0.00513	−0.68924	−1.42207	0.0539	7.3130

1	4	5	6	7	8
−0.185	+0.00541	−0.67477	−1.38591	0.0548	7.1509
−0.190	+0.00568	−0.66063	−1.35054	0.0556	6.9975
−0.195	+0.00596	−0.64678	−1.31592	0.0564	6.8519
−0.200	+0.00625	−0.63321	−1.28201	0.0572	6.7137
−0.205	+0.00654	−0.61992	−1.24877	0.0579	6.5823
−0.210	+0.00683	−0.60688	−1.21618	0.0585	6.4573
−0.215	+0.00712	−0.59408	−1.18419	0.0591	6.3381
−0.220	+0.00742	−0.58152	−1.15279	0.0597	6.2245
−0.225	+0.00772	−0.56918	−1.12194	0.0602	6.1159
−0.230	+0.00802	−0.55706	−1.09162	0.0607	6.0122
−0.235	+0.00833	−0.54513	−1.06181	0.0611	5.9129
−0.240	+0.00863	−0.53340	−1.03248	0.0615	5.8179
−0.245	+0.00894	−0.52186	−1.00362	0.0619	5.7268
−0.250	+0.00925	−0.51049	−0.97521	0.0623	5.6394
−0.255	+0.00956	−0.49930	−0.94722	0.0626	5.5556
−0.260	+0.00988	−0.48827	−0.91965	0.0628	5.4750
−0.265	+0.01019	−0.47739	−0.89247	0.0631	5.3976
−0.270	+0.01051	−0.46667	−0.86567	0.0633	5.3231
−0.275	+0.01083	−0.45610	−0.83923	0.0634	5.2513
−0.280	+0.01114	−0.44567	−0.81315	0.0636	5.1823
−0.285	+0.01146	−0.43537	−0.78740	0.0637	5.1157
−0.290	+0.01178	−0.42520	−0.76199	0.0638	5.0515
−0.295	+0.01210	−0.41516	−0.73688	0.0638	4.9895
−0.300	+0.01242	−0.40524	−0.71209	0.0639	4.9297
−0.305	+0.01274	−0.39544	−0.68758	0.0639	4.8719
−0.310	+0.01306	−0.38575	−0.66336	0.0638	4.8160
−0.315	+0.01338	−0.37618	−0.63942	0.0638	4.7620
−0.320	+0.01370	−0.36670	−0.61574	0.0637	4.7098
−0.325	+0.01402	−0.35734	−0.59232	0.0636	4.6592
−0.330	+0.01433	−0.34807	−0.56915	0.0635	4.6103
−0.335	+0.01465	−0.33889	−0.54621	0.0634	4.5629
−0.340	+0.01497	−0.32981	−0.52351	0.0632	4.5169
−0.345	+0.01528	−0.32082	−0.50104	0.0631	4.4723
−0.350	+0.01560	−0.31192	−0.47879	0.0629	4.4291
−0.355	+0.01591	−0.30311	−0.45675	0.0627	4.3872
−0.360	+0.01623	−0.29437	−0.43491	0.0624	4.3465
−0.365	+0.01654	−0.28572	−0.41328	0.0622	4.3070
−0.370	+0.01685	−0.27714	−0.39184	0.0619	4.2686
−0.375	+0.01716	−0.26864	−0.37059	0.0616	4.2314
−0.380	+0.01747	−0.26022	−0.34952	0.0613	4.1951
−0.385	+0.01777	−0.25186	−0.32864	0.0610	4.1599
−0.390	+0.01808	−0.24358	−0.30792	0.0607	4.1257
−0.395	+0.01838	−0.23536	−0.28738	0.0604	4.0924
−0.400	+0.01868	−0.22721	−0.26700	0.0601	4.0600
−0.405	+0.01898	−0.21912	−0.24678	0.0597	4.0284
−0.410	+0.01928	−0.21109	−0.22671	0.0593	3.9977
−0.415	+0.01957	−0.20313	−0.20680	0.0590	3.9678
−0.420	+0.01987	−0.19522	−0.18703	0.0586	3.9386
−0.425	+0.02016	−0.18737	−0.16741	0.0582	3.9103
−0.430	+0.02045	−0.17958	−0.14793	0.0578	3.8826
−0.435	+0.02074	−0.17184	−0.12858	0.0574	3.8556
−0.440	+0.02103	−0.16416	−0.10937	0.0569	3.8294
−0.445	+0.02131	−0.15652	−0.09029	0.0565	3.8037
−0.450	+0.02159	−0.14894	−0.07133	0.0561	3.7787
−0.455	+0.02187	−0.14141	−0.05250	0.0556	3.7543
−0.460	+0.02215	−0.13392	−0.03379	0.0552	3.7305
−0.465	+0.02242	−0.12648	−0.01519	0.0547	3.7073
−0.470	+0.02270	−0.11909	+0.00328	0.0543	3.6846
−0.475	+0.02297	−0.11175	+0.02165	0.0538	3.6625
−0.480	+0.02323	−0.10444	+0.03990	0.0534	3.6408
−0.485	+0.02350	−0.09718	+0.05806	0.0529	3.6197
−0.490	+0.02376	−0.08996	+0.07610	0.0524	3.5991
−0.495	+0.02402	−0.08278	+0.09405	0.0519	3.5789
−0.500	+0.02428	−0.07565	+0.11189	0.0515	3.5592
−0.505	+0.02454	−0.06855	+0.12964	0.0510	3.5400
−0.510	+0.02479	−0.06149	+0.14729	0.0505	3.5212
−0.515	+0.02505	−0.05446	+0.16485	0.0500	3.5028
−0.520	+0.02529	−0.04747	+0.18232	0.0495	3.4848
−0.525	+0.02554	−0.04052	+0.19970	0.0490	3.4672
−0.530	+0.02578	−0.03361	+0.21700	0.0485	3.4500
−0.535	+0.02603	−0.02672	+0.23420	0.0480	3.4331
−0.540	+0.02627	−0.01987	+0.25133	0.0475	3.4167
−0.545	+0.02650	−0.01306	+0.26837	0.0470	3.4005
−0.550	+0.02674	−0.00627	+0.28533	0.0465	3.3848
−0.555	+0.02697	+0.00047	+0.30222	0.0461	3.3693
−0.560	+0.02720	+0.00720	+0.31903	0.0456	3.3542
−0.565	+0.02742	+0.01389	+0.33576	0.0451	3.3394
−0.570	+0.02765	+0.02056	+0.35242	0.0446	3.3249
−0.575	+0.02787	+0.02719	+0.36901	0.0441	3.3107
−0.580	+0.02809	+0.03380	+0.38553	0.0436	3.2968
−0.585	+0.02831	+0.04038	+0.40198	0.0431	3.2832
−0.590	+0.02852	+0.04693	+0.41836	0.0426	3.2699
−0.595	+0.02873	+0.05346	+0.43468	0.0421	3.2568
−0.600	+0.02894	+0.05996	+0.45093	0.0416	3.2440
−0.605	+0.02915	+0.06644	+0.46712	0.0411	3.2315

1509

1	4	5	6	7	8
-0.010	+0.00001	-2.03071	-4.59967	0.0025	109.8264
-0.015	+0.00002	-1.85220	-4.15338	0.0045	73.6503
-0.020	+0.00005	-1.72476	-3.83479	0.0067	55.5533
-0.025	+0.00009	-1.62534	-3.58623	0.0092	44.6937
-0.030	+0.00014	-1.54364	-3.38199	0.0117	37.4537
-0.035	+0.00021	-1.47417	-3.20833	0.0144	32.2823
-0.040	+0.00029	-1.41366	-3.05705	0.0172	28.4037
-0.045	+0.00038	-1.35999	-2.92288	0.0200	25.3870
-0.050	+0.00049	-1.31172	-2.80219	0.0229	22.9737
-0.055	+0.00061	-1.26781	-2.69242	0.0257	20.9990
-0.060	+0.00075	-1.22751	-2.59166	0.0286	19.3535
-0.065	+0.00090	-1.19023	-2.49847	0.0314	17.9611
-0.070	+0.00106	-1.15553	-2.41172	0.0342	16.7675
-0.075	+0.00124	-1.12306	-2.33053	0.0370	15.7331
-0.080	+0.00143	-1.09251	-2.25418	0.0397	14.8280
-0.085	+0.00164	-1.06367	-2.18208	0.0424	14.0293
-0.090	+0.00186	-1.03634	-2.11374	0.0451	13.3193
-0.095	+0.00209	-1.01035	-2.04876	0.0477	12.6840
-0.100	+0.00233	-0.98556	-1.98680	0.0502	12.1123
-0.105	+0.00259	-0.96186	-1.92755	0.0527	11.5950
-0.110	+0.00286	-0.93915	-1.87077	0.0551	11.1247
-0.115	+0.00314	-0.91734	-1.81623	0.0574	10.6953
-0.120	+0.00343	-0.89635	-1.76376	0.0597	10.3017
-0.125	+0.00374	-0.87611	-1.71317	0.0618	9.9396
-0.130	+0.00405	-0.85657	-1.66431	0.0640	9.6053
-0.135	+0.00438	-0.83767	-1.61707	0.0660	9.2958
-0.140	+0.00471	-0.81937	-1.57132	0.0680	9.0085
-0.145	+0.00506	-0.80162	-1.52695	0.0699	8.7410
-0.150	+0.00541	-0.78439	-1.48388	0.0717	8.4914
-0.155	+0.00578	-0.76765	-1.44201	0.0735	8.2579
-0.160	+0.00615	-0.75135	-1.40128	0.0752	8.0390
-0.165	+0.00653	-0.73548	-1.36160	0.0768	7.8334
-0.170	+0.00692	-0.72001	-1.32292	0.0783	7.6400
-0.175	+0.00731	-0.70492	-1.28518	0.0798	7.4576
-0.180	+0.00771	-0.69017	-1.24833	0.0812	7.2854
-0.185	+0.00812	-0.67577	-1.21231	0.0825	7.1226
-0.190	+0.00854	-0.66168	-1.17709	0.0837	6.9684
-0.195	+0.00896	-0.64789	-1.14261	0.0849	6.8222
-0.200	+0.00939	-0.63438	-1.10885	0.0860	6.6833
-0.205	+0.00982	-0.62115	-1.07577	0.0871	6.5512
-0.210	+0.01026	-0.60817	-1.04333	0.0881	6.4255
-0.215	+0.01070	-0.59544	-1.01150	0.0890	6.3057
-0.220	+0.01115	-0.58295	-0.98026	0.0899	6.1914
-0.225	+0.01160	-0.57067	-0.94958	0.0907	6.0823
-0.230	+0.01206	-0.55861	-0.91943	0.0914	5.9779
-0.235	+0.01252	-0.54676	-0.88979	0.0921	5.8781
-0.240	+0.01298	-0.53510	-0.86064	0.0927	5.7825
-0.245	+0.01344	-0.52363	-0.83196	0.0933	5.6908
-0.250	+0.01391	-0.51233	-0.80373	0.0938	5.6029
-0.255	+0.01438	-0.50121	-0.77593	0.0943	5.5185
-0.260	+0.01486	-0.49026	-0.74854	0.0947	5.4375
-0.265	+0.01533	-0.47946	-0.72155	0.0951	5.3595
-0.270	+0.01581	-0.46882	-0.69494	0.0954	5.2845
-0.275	+0.01629	-0.45832	-0.66870	0.0957	5.2123
-0.280	+0.01676	-0.44797	-0.64281	0.0959	5.1428
-0.285	+0.01724	-0.43775	-0.61726	0.0961	5.0757
-0.290	+0.01773	-0.42766	-0.59205	0.0962	5.0111
-0.295	+0.01821	-0.41770	-0.56715	0.0963	4.9487
-0.300	+0.01869	-0.40786	-0.54256	0.0963	4.8884
-0.305	+0.01917	-0.39815	-0.51826	0.0963	4.8303
-0.310	+0.01965	-0.38854	-0.49425	0.0963	4.7740
-0.315	+0.02013	-0.37905	-0.47052	0.0963	4.7196
-0.320	+0.02062	-0.36966	-0.44705	0.0962	4.6670
-0.325	+0.02110	-0.36038	-0.42384	0.0960	4.6161
-0.330	+0.02158	-0.35120	-0.40089	0.0959	4.5668
-0.335	+0.02206	-0.34211	-0.37817	0.0957	4.5191
-0.340	+0.02253	-0.33312	-0.35569	0.0954	4.4728
-0.345	+0.02301	-0.32422	-0.33344	0.0952	4.4279
-0.350	+0.02349	-0.31541	-0.31141	0.0949	4.3844
-0.355	+0.02396	-0.30668	-0.28959	0.0946	4.3422
-0.360	+0.02443	-0.29804	-0.26799	0.0942	4.3013
-0.365	+0.02490	-0.28947	-0.24658	0.0939	4.2615
-0.370	+0.02537	-0.28099	-0.22537	0.0935	4.2229
-0.375	+0.02584	-0.27258	-0.20435	0.0931	4.1854
-0.380	+0.02630	-0.26425	-0.18351	0.0926	4.1489
-0.385	+0.02676	-0.25598	-0.16286	0.0922	4.1135
-0.390	+0.02722	-0.24779	-0.14237	0.0917	4.0791
-0.395	+0.02768	-0.23967	-0.12206	0.0912	4.0456
-0.400	+0.02814	-0.23161	-0.10192	0.0907	4.0130
-0.405	+0.02859	-0.22361	-0.08193	0.0902	3.9812
-0.410	+0.02904	-0.21568	-0.06210	0.0896	3.9504
-0.415	+0.02949	-0.20781	-0.04243	0.0891	3.9203
-0.420	+0.02993	-0.20000	-0.02290	0.0885	3.8910
-0.425	+0.03037	-0.19225	-0.00351	0.0879	3.8625
-0.430	+0.03081	-0.18455	+0.01572	0.0873	3.8347
-0.435	+0.03124	-0.17691	+0.03482	0.0866	3.8076
-0.440	+0.03168	-0.16932	+0.05380	0.0860	3.7812
-0.445	+0.03211	-0.16178	+0.07264	0.0854	3.7555
-0.450	+0.03253	-0.15430	+0.09135	0.0847	3.7304
-0.455	+0.03295	-0.14686	+0.10994	0.0840	3.7060
-0.460	+0.03337	-0.13947	+0.12841	0.0834	3.6821
-0.465	+0.03379	-0.13213	+0.14677	0.0827	3.6588
-0.470	+0.03420	-0.12484	+0.16500	0.0820	3.6360
-0.475	+0.03461	-0.11759	+0.18313	0.0813	3.6139
-0.480	+0.03501	-0.11038	+0.20114	0.0806	3.5922
-0.485	+0.03541	-0.10322	+0.21905	0.0799	3.5710
-0.490	+0.03581	-0.09609	+0.23686	0.0792	3.5504
-0.495	+0.03621	-0.08901	+0.25456	0.0784	3.5302
-0.500	+0.03660	-0.08197	+0.27216	0.0777	3.5105
-0.505	+0.03698	-0.07497	+0.28966	0.0770	3.4913
-0.510	+0.03737	-0.06801	+0.30707	0.0762	3.4724
-0.515	+0.03775	-0.06108	+0.32439	0.0755	3.4540
-0.520	+0.03812	-0.05419	+0.34161	0.0748	3.4361
-0.525	+0.03849	-0.04734	+0.35875	0.0740	3.4185
-0.530	+0.03886	-0.04052	+0.37580	0.0733	3.4013
-0.535	+0.03923	-0.03373	+0.39276	0.0725	3.3845
-0.540	+0.03959	-0.02698	+0.40965	0.0718	3.3681
-0.545	+0.03995	-0.02026	+0.42645	0.0710	3.3520
-0.550	+0.04030	-0.01357	+0.44317	0.0703	3.3363
-0.555	+0.04065	-0.00691	+0.45981	0.0695	3.3209
-0.560	+0.04099	-0.00029	+0.47638	0.0688	3.3059
-0.565	+0.04134	+0.00630	+0.49287	0.0680	3.2911
-0.570	+0.04168	+0.01287	+0.50929	0.0673	3.2767
-0.575	+0.04201	+0.01941	+0.52564	0.0665	3.2626
-0.580	+0.04234	+0.02592	+0.54192	0.0658	3.2488
-0.585	+0.04267	+0.03240	+0.55813	0.0650	3.2353
-0.590	+0.04299	+0.03886	+0.57427	0.0643	3.2220
-0.595	+0.04331	+0.04529	+0.59035	0.0635	3.2091
-0.600	+0.04363	+0.05170	+0.60636	0.0628	3.1964
-0.605	+0.04394	+0.05808	+0.62231	0.0621	3.1839

1510

1	4	5	6	7	8
-0.010	+0.00001	-2.03071	-4.47473	0.0033	109.8264
-0.015	+0.00003	-1.85220	-4.02845	0.0060	73.6495
-0.020	+0.00007	-1.72477	-3.70986	0.0090	55.5518
-0.025	+0.00012	-1.62535	-3.46131	0.0122	44.6916
-0.030	+0.00019	-1.54365	-3.25708	0.0157	37.4509
-0.035	+0.00028	-1.47420	-3.08343	0.0193	32.2787
-0.040	+0.00039	-1.41369	-2.93218	0.0230	28.3994
-0.045	+0.00051	-1.36003	-2.79803	0.0267	25.3819
-0.050	+0.00065	-1.31177	-2.67737	0.0305	22.9677
-0.055	+0.00082	-1.26787	-2.56763	0.0343	20.9923
-0.060	+0.00100	-1.22759	-2.46691	0.0381	19.3459
-0.065	+0.00120	-1.19032	-2.37376	0.0419	17.9526
-0.070	+0.00142	-1.15564	-2.28706	0.0457	16.7582
-0.075	+0.00165	-1.12319	-2.20591	0.0494	15.7229
-0.080	+0.00191	-1.09267	-2.12961	0.0530	14.8169
-0.085	+0.00218	-1.06385	-2.05757	0.0566	14.0173
-0.090	+0.00248	-1.03654	-1.98929	0.0602	13.3064
-0.095	+0.00279	-1.01057	-1.92438	0.0636	12.6703
-0.100	+0.00311	-0.98582	-1.86249	0.0670	12.0977
-0.105	+0.00346	-0.96215	-1.80331	0.0703	11.5795
-0.110	+0.00382	-0.93947	-1.74661	0.0735	11.1083
-0.115	+0.00419	-0.91769	-1.69216	0.0766	10.6781
-0.120	+0.00458	-0.89673	-1.63977	0.0797	10.2836
-0.125	+0.00499	-0.87653	-1.58927	0.0826	9.9207
-0.130	+0.00541	-0.85703	-1.54052	0.0854	9.5856
-0.135	+0.00584	-0.83817	-1.49338	0.0882	9.2753
-0.140	+0.00629	-0.81991	-1.44773	0.0908	8.9871
-0.145	+0.00675	-0.80221	-1.40347	0.0934	8.7188
-0.150	+0.00723	-0.78503	-1.36051	0.0958	8.4684
-0.155	+0.00771	-0.76833	-1.31876	0.0982	8.2341
-0.160	+0.00821	-0.75208	-1.27815	0.1004	8.0144
-0.165	+0.00872	-0.73626	-1.23860	0.1026	7.8080
-0.170	+0.00924	-0.72084	-1.20005	0.1047	7.6138
-0.175	+0.00976	-0.70580	-1.16244	0.1066	7.4307
-0.180	+0.01030	-0.69111	-1.12572	0.1085	7.2578
-0.185	+0.01085	-0.67676	-1.08984	0.1103	7.0943
-0.190	+0.01141	-0.66273	-1.05476	0.1120	6.9394
-0.195	+0.01197	-0.64900	-1.02044	0.1136	6.7924
-0.200	+0.01254	-0.63555	-0.98683	0.1151	6.6529
-0.205	+0.01312	-0.62238	-0.95390	0.1165	6.5202

1	4	5	6	7	8
−0.210	+0.01371	−0.60947	−0.92161	0.1179	6.3938
−0.215	+0.01430	−0.59680	−0.88995	0.1191	6.2734
−0.220	+0.01490	−0.58437	−0.85887	0.1203	6.1584
−0.225	+0.01550	−0.57217	−0.82836	0.1214	6.0487
−0.230	+0.01611	−0.56017	−0.79838	0.1224	5.9437
−0.235	+0.01673	−0.54839	−0.76891	0.1233	5.8433
−0.240	+0.01735	−0.53680	−0.73994	0.1242	5.7471
−0.245	+0.01797	−0.52540	−0.71143	0.1250	5.6549
−0.250	+0.01860	−0.51418	−0.68338	0.1257	5.5664
−0.255	+0.01923	−0.50313	−0.65576	0.1263	5.4815
−0.260	+0.01986	−0.49225	−0.62856	0.1269	5.3999
−0.265	+0.02050	−0.48153	−0.60176	0.1274	5.3214
−0.270	+0.02113	−0.47096	−0.57534	0.1278	5.2459
−0.275	+0.02177	−0.46054	−0.54929	0.1282	5.1732
−0.280	+0.02242	−0.45026	−0.52360	0.1285	5.1032
−0.285	+0.02306	−0.44013	−0.49826	0.1288	5.0357
−0.290	+0.02370	−0.43012	−0.47324	0.1289	4.9706
−0.295	+0.02435	−0.42024	−0.44855	0.1291	4.9078
−0.300	+0.02500	−0.41049	−0.42416	0.1292	4.8472
−0.305	+0.02564	−0.40085	−0.40007	0.1292	4.7886
−0.310	+0.02629	−0.39133	−0.37627	0.1292	4.7319
−0.315	+0.02693	−0.38192	−0.35275	0.1291	4.6772
−0.320	+0.02758	−0.37262	−0.32949	0.1290	4.6242
−0.325	+0.02822	−0.36342	−0.30650	0.1288	4.5729
−0.330	+0.02887	−0.35433	−0.28376	0.1286	4.5233
−0.335	+0.02951	−0.34533	−0.26127	0.1284	4.4752
−0.340	+0.03015	−0.33643	−0.23901	0.1281	4.4286
−0.345	+0.03079	−0.32761	−0.21698	0.1277	4.3835
−0.350	+0.03143	−0.31889	−0.19517	0.1273	4.3397
−0.355	+0.03207	−0.31025	−0.17358	0.1269	4.2972
−0.360	+0.03270	−0.30170	−0.15219	0.1265	4.2560
−0.365	+0.03333	−0.29323	−0.13102	0.1260	4.2159
−0.370	+0.03396	−0.28484	−0.11003	0.1255	4.1771
−0.375	+0.03459	−0.27652	−0.08924	0.1249	4.1393
−0.380	+0.03521	−0.26828	−0.06864	0.1244	4.1026
−0.385	+0.03583	−0.26011	−0.04821	0.1238	4.0670
−0.390	+0.03645	−0.25201	−0.02797	0.1231	4.0323
−0.395	+0.03706	−0.24398	−0.00789	0.1225	3.9986
−0.400	+0.03767	−0.23601	+0.01201	0.1218	3.9659
−0.405	+0.03828	−0.22811	+0.03176	0.1211	3.9340
−0.410	+0.03888	−0.22028	+0.05135	0.1203	3.9029
−0.415	+0.03948	−0.21250	+0.07079	0.1196	3.8727
−0.420	+0.04008	−0.20479	+0.09008	0.1188	3.8433
−0.425	+0.04067	−0.19713	+0.10923	0.1180	3.8146
−0.430	+0.04126	−0.18953	+0.12823	0.1172	3.7867
−0.435	+0.04184	−0.18198	+0.14710	0.1163	3.7595
−0.440	+0.04242	−0.17449	+0.16583	0.1155	3.7330
−0.445	+0.04300	−0.16705	+0.18443	0.1146	3.7072
−0.450	+0.04357	−0.15966	+0.20290	0.1138	3.6820
−0.455	+0.04414	−0.15232	+0.22125	0.1129	3.6574
−0.460	+0.04470	−0.14503	+0.23948	0.1120	3.6335
−0.465	+0.04526	−0.13778	+0.25759	0.1110	3.6101
−0.470	+0.04581	−0.13059	+0.27558	0.1101	3.5873
−0.475	+0.04636	−0.12344	+0.29346	0.1092	3.5651
−0.480	+0.04690	−0.11633	+0.31123	0.1082	3.5434
−0.485	+0.04744	−0.10926	+0.32890	0.1073	3.5222
−0.490	+0.04798	−0.10224	+0.34646	0.1063	3.5015
−0.495	+0.04851	−0.09525	+0.36391	0.1053	3.4813
−0.500	+0.04903	−0.08831	+0.38127	0.1043	3.4616
−0.505	+0.04955	−0.08141	+0.39853	0.1033	3.4423
−0.510	+0.05006	−0.07454	+0.41569	0.1024	3.4235
−0.515	+0.05057	−0.06771	+0.43277	0.1014	3.4051
−0.520	+0.05108	−0.06092	+0.44975	0.1004	3.3872
−0.525	+0.05158	−0.05416	+0.46664	0.0994	3.3696
−0.530	+0.05207	−0.04744	+0.48344	0.0983	3.3525
−0.535	+0.05256	−0.04075	+0.50016	0.0973	3.3357
−0.540	+0.05305	−0.03410	+0.51680	0.0963	3.3193
−0.545	+0.05352	−0.02748	+0.53336	0.0953	3.3033
−0.550	+0.05400	−0.02089	+0.54984	0.0943	3.2876
−0.555	+0.05447	−0.01433	+0.56624	0.0933	3.2723
−0.560	+0.05493	−0.00780	+0.58256	0.0923	3.2573
−0.565	+0.05539	−0.00130	+0.59881	0.0913	3.2426
−0.570	+0.05585	+0.00517	+0.61499	0.0902	3.2283
−0.575	+0.05629	+0.01161	+0.63109	0.0892	3.2143
−0.580	+0.05674	+0.01802	+0.64713	0.0882	3.2005
−0.585	+0.05718	+0.02441	+0.66310	0.0872	3.1871
−0.590	+0.05761	+0.03077	+0.67900	0.0862	3.1740
−0.595	+0.05804	+0.03711	+0.69484	0.0852	3.1611
−0.600	+0.05846	+0.04342	+0.71062	0.0842	3.1485
−0.605	+0.05888	+0.04970	+0.72633	0.0832	3.1362

1511

1	4	5	6	7	8
−0.010	+0.00001	−2.03072	−4.37783	0.0041	109.8256
−0.015	+0.00004	−1.85220	−3.93155	0.0075	73.6483
−0.020	+0.00009	−1.72477	−3.61297	0.0112	55.5501
−0.025	+0.00015	−1.62536	−3.36443	0.0153	44.6892
−0.030	+0.00024	−1.54367	−3.16021	0.0196	37.4479
−0.035	+0.00035	−1.47422	−2.98658	0.0241	32.2750
−0.040	+0.00048	−1.41372	−2.83535	0.0287	28.3949
−0.045	+0.00064	−1.36007	−2.70122	0.0334	25.3766
−0.050	+0.00082	−1.31182	−2.58059	0.0381	22.9617
−0.055	+0.00102	−1.26794	−2.47088	0.0429	20.9854
−0.060	+0.00125	−1.22766	−2.37019	0.0477	19.3382
−0.065	+0.00150	−1.19042	−2.27708	0.0524	17.9441
−0.070	+0.00177	−1.15576	−2.19043	0.0571	16.7488
−0.075	+0.00207	−1.12332	−2.10933	0.0618	15.7126
−0.080	+0.00239	−1.09282	−2.03309	0.0663	14.8057
−0.085	+0.00273	−1.06403	−1.96110	0.0709	14.0053
−0.090	+0.00310	−1.03674	−1.89289	0.0753	13.2936
−0.095	+0.00349	−1.01080	−1.82804	0.0796	12.6566
−0.100	+0.00390	−0.98607	−1.76622	0.0838	12.0831
−0.105	+0.00433	−0.96244	−1.70712	0.0880	11.5640
−0.110	+0.00478	−0.93979	−1.65050	0.0920	11.0920
−0.115	+0.00525	−0.91804	−1.59613	0.0959	10.6609
−0.120	+0.00574	−0.89712	−1.54383	0.0997	10.2656
−0.125	+0.00624	−0.87696	−1.49343	0.1034	9.9017
−0.130	+0.00677	−0.85749	−1.44477	0.1070	9.5658
−0.135	+0.00731	−0.83868	−1.39773	0.1104	9.2547
−0.140	+0.00788	−0.82046	−1.35218	0.1138	8.9657
−0.145	+0.00845	−0.80280	−1.30804	0.1170	8.6966
−0.150	+0.00904	−0.78566	−1.26519	0.1200	8.4453
−0.155	+0.00965	−0.76901	−1.22356	0.1230	8.2102
−0.160	+0.01028	−0.75281	−1.18306	0.1259	7.9898
−0.165	+0.01091	−0.73704	−1.14364	0.1286	7.7827
−0.170	+0.01156	−0.72167	−1.10522	0.1312	7.5877
−0.175	+0.01222	−0.70668	−1.06774	0.1337	7.4038
−0.180	+0.01290	−0.69205	−1.03116	0.1360	7.2302
−0.185	+0.01358	−0.67776	−0.99542	0.1383	7.0659
−0.190	+0.01428	−0.66378	−0.96049	0.1404	6.9103
−0.195	+0.01499	−0.65011	−0.92631	0.1424	6.7627
−0.200	+0.01571	−0.63673	−0.89285	0.1444	6.6224
−0.205	+0.01643	−0.62362	−0.86007	0.1462	6.4890
−0.210	+0.01717	−0.61077	−0.82794	0.1479	6.3620
−0.215	+0.01791	−0.59816	−0.79644	0.1494	6.2409
−0.220	+0.01866	−0.58580	−0.76553	0.1509	6.1254
−0.225	+0.01942	−0.57366	−0.73518	0.1523	6.0150
−0.230	+0.02019	−0.56173	−0.70537	0.1536	5.9094
−0.235	+0.02096	−0.55002	−0.67607	0.1548	5.8084
−0.240	+0.02173	−0.53850	−0.64728	0.1559	5.7116
−0.245	+0.02252	−0.52717	−0.61895	0.1569	5.6189
−0.250	+0.02330	−0.51602	−0.59108	0.1578	5.5298
−0.255	+0.02410	−0.50505	−0.56365	0.1586	5.4444
−0.260	+0.02489	−0.49424	−0.53663	0.1594	5.3622
−0.265	+0.02569	−0.48359	−0.51002	0.1600	5.2833
−0.270	+0.02649	−0.47310	−0.48379	0.1606	5.2073
−0.275	+0.02730	−0.46276	−0.45794	0.1611	5.1341
−0.280	+0.02810	−0.45257	−0.43245	0.1615	5.0636
−0.285	+0.02891	−0.44251	−0.40730	0.1618	4.9957
−0.290	+0.02972	−0.43258	−0.38249	0.1621	4.9301
−0.295	+0.03053	−0.42279	−0.35799	0.1623	4.8669
−0.300	+0.03134	−0.41311	−0.33381	0.1624	4.8058
−0.305	+0.03216	−0.40356	−0.30993	0.1624	4.7468
−0.310	+0.03297	−0.39412	−0.28634	0.1624	4.6898
−0.315	+0.03378	−0.38480	−0.26303	0.1623	4.6346
−0.320	+0.03459	−0.37558	−0.23999	0.1622	4.5813
−0.325	+0.03540	−0.36647	−0.21722	0.1620	4.5297
−0.330	+0.03621	−0.35746	−0.19469	0.1618	4.4797
−0.335	+0.03702	−0.34855	−0.17242	0.1614	4.4313
−0.340	+0.03783	−0.33974	−0.15038	0.1611	4.3844
−0.345	+0.03863	−0.33102	−0.12857	0.1607	4.3389
−0.350	+0.03943	−0.32238	−0.10698	0.1602	4.2948
−0.355	+0.04023	−0.31383	−0.08562	0.1597	4.2520
−0.360	+0.04103	−0.30537	−0.06446	0.1592	4.2105
−0.365	+0.04183	−0.29699	−0.04351	0.1586	4.1702
−0.370	+0.04262	−0.28869	−0.02276	0.1579	4.1311
−0.375	+0.04341	−0.28047	−0.00220	0.1572	4.0931
−0.380	+0.04419	−0.27232	+0.01817	0.1565	4.0562
−0.385	+0.04497	−0.26424	+0.03836	0.1558	4.0204
−0.390	+0.04575	−0.25623	+0.05837	0.1550	3.9855
−0.395	+0.04652	−0.24830	+0.07821	0.1541	3.9516
−0.400	+0.04729	−0.24043	+0.09789	0.1533	3.9186
−0.405	+0.04805	−0.23262	+0.11740	0.1524	3.8865

-0.410	+0.04881	−0.22488	+0.13676	0.1515	3.8553
-0.415	+0.04957	−0.21720	+0.15596	0.1505	3.8250
-0.420	+0.05032	−0.20958	+0.17501	0.1495	3.7954
-0.425	+0.05107	−0.20202	+0.19391	0.1485	3.7666
-0.430	+0.05181	−0.19451	+0.21268	0.1475	3.7385
-0.435	+0.05254	−0.18706	+0.23130	0.1465	3.7112
-0.440	+0.05327	−0.17967	+0.24979	0.1454	3.6846
-0.445	+0.05400	−0.17232	+0.26815	0.1443	3.6587
-0.450	+0.05472	−0.16503	+0.28638	0.1432	3.6334
-0.455	+0.05543	−0.15779	+0.30448	0.1421	3.6087
-0.460	+0.05614	−0.15060	+0.32247	0.1409	3.5847
-0.465	+0.05684	−0.14345	+0.34033	0.1398	3.5613
-0.470	+0.05754	−0.13635	+0.35808	0.1386	3.5384
-0.475	+0.05823	−0.12930	+0.37572	0.1374	3.5161
-0.480	+0.05891	−0.12229	+0.39324	0.1362	3.4944
-0.485	+0.05959	−0.11532	+0.41066	0.1350	3.4732
-0.490	+0.06026	−0.10839	+0.42798	0.1338	3.4524
-0.495	+0.06093	−0.10151	+0.44519	0.1326	3.4322
-0.500	+0.06159	−0.09466	+0.46230	0.1313	3.4125
-0.505	+0.06224	−0.08786	+0.47932	0.1301	3.3932
-0.510	+0.06289	−0.08109	+0.49623	0.1288	3.3744
-0.515	+0.06353	−0.07436	+0.51306	0.1276	3.3560
-0.520	+0.06416	−0.06767	+0.52980	0.1263	3.3381
-0.525	+0.06479	−0.06101	+0.54644	0.1251	3.3205
-0.530	+0.06542	−0.05438	+0.56300	0.1238	3.3034
-0.535	+0.06603	−0.04779	+0.57948	0.1225	3.2867
-0.540	+0.06664	−0.04124	+0.59587	0.1212	3.2703
-0.545	+0.06724	−0.03471	+0.61218	0.1199	3.2543
-0.550	+0.06784	−0.02822	+0.62841	0.1187	3.2387
-0.555	+0.06843	−0.02176	+0.64457	0.1174	3.2234
-0.560	+0.06902	−0.01532	+0.66065	0.1161	3.2085
-0.565	+0.06959	−0.00892	+0.67666	0.1148	3.1939
-0.570	+0.07016	−0.00255	+0.69259	0.1135	3.1796
-0.575	+0.07073	+0.00379	+0.70845	0.1123	3.1657
-0.580	+0.07129	+0.01011	+0.72425	0.1110	3.1520
-0.585	+0.07184	+0.01640	+0.73997	0.1097	3.1387
-0.590	+0.07238	+0.02266	+0.75564	0.1084	3.1256
-0.595	+0.07292	+0.02890	+0.77123	0.1072	3.1129
-0.600	+0.07346	+0.03511	+0.78677	0.1059	3.1004
-0.605	+0.07398	+0.04130	+0.80224	0.1046	3.0882

1512

1	4	5	6	7	8
-0.010	+0.00002	−2.03072	−4.29865	0.0050	109.8248
-0.015	+0.00005	−1.85221	−3.85237	0.0090	73.6471
-0.020	+0.00011	−1.72478	−3.53380	0.0135	55.5483
-0.025	+0.00019	−1.62537	−3.28527	0.0184	44.6868
-0.030	+0.00029	−1.54368	−3.08107	0.0236	37.4448
-0.035	+0.00042	−1.47424	−2.90745	0.0289	32.2712
-0.040	+0.00058	−1.41375	−2.75624	0.0345	28.3904
-0.045	+0.00077	−1.36011	−2.62214	0.0401	25.3714
-0.050	+0.00098	−1.31187	−2.50154	0.0458	22.9556
-0.055	+0.00123	−1.26800	−2.39186	0.0515	20.9785
-0.060	+0.00150	−1.22774	−2.29121	0.0572	19.3305
-0.065	+0.00180	−1.19051	−2.19814	0.0629	17.9355
-0.070	+0.00213	−1.15587	−2.11153	0.0686	16.7394
-0.075	+0.00249	−1.12345	−2.03049	0.0742	15.7023
-0.080	+0.00287	−1.09297	−1.95429	0.0797	14.7946
-0.085	+0.00328	−1.06420	−1.88236	0.0851	13.9933
-0.090	+0.00372	−1.03694	−1.81421	0.0904	13.2807
-0.095	+0.00419	−1.01103	−1.74943	0.0956	12.6428
-0.100	+0.00468	−0.98633	−1.68768	0.1007	12.0684
-0.105	+0.00519	−0.96272	−1.62866	0.1057	11.5485
-0.110	+0.00574	−0.94011	−1.57212	0.1105	11.0756
-0.115	+0.00630	−0.91839	−1.51784	0.1153	10.6436
-0.120	+0.00689	−0.89751	−1.46562	0.1198	10.2475
-0.125	+0.00750	−0.87738	−1.41531	0.1243	9.8828
-0.130	+0.00813	−0.85796	−1.36675	0.1286	9.5460
-0.135	+0.00879	−0.83918	−1.31981	0.1327	9.2341
-0.140	+0.00946	−0.82101	−1.27437	0.1368	8.9443
-0.145	+0.01015	−0.80339	−1.23033	0.1406	8.6743
-0.150	+0.01087	−0.78630	−1.18760	0.1444	8.4223
-0.155	+0.01160	−0.76969	−1.14608	0.1479	8.1864
-0.160	+0.01235	−0.75354	−1.10571	0.1514	7.9651
-0.165	+0.01311	−0.73782	−1.06641	0.1547	7.7572
-0.170	+0.01389	−0.72250	−1.02812	0.1578	7.5615
-0.175	+0.01469	−0.70757	−0.99078	0.1608	7.3769
-0.180	+0.01550	−0.69299	−0.95433	0.1637	7.2025
-0.185	+0.01633	−0.67875	−0.91873	0.1664	7.0375
-0.190	+0.01717	−0.66483	−0.88394	0.1690	6.8812
-0.195	+0.01802	−0.65122	−0.84991	0.1715	6.7329
-0.200	+0.01888	−0.63790	−0.81660	0.1738	6.5919
-0.205	+0.01976	−0.62485	−0.78398	0.1760	6.4579

1	4	5	6	7	8
−0.210	+0.02064	−0.61206	−0.75201	0.1781	6.3302
−0.215	+0.02154	−0.59952	−0.72067	0.1800	6.2085
−0.220	+0.02244	−0.58722	−0.68992	0.1818	6.0923
−0.225	+0.02335	−0.57515	−0.65973	0.1835	5.9813
−0.230	+0.02428	−0.56330	−0.63009	0.1851	5.8751
−0.235	+0.02521	−0.55165	−0.60097	0.1865	5.7735
−0.240	+0.02614	−0.54020	−0.57235	0.1879	5.6761
−0.245	+0.02708	−0.52894	−0.54421	0.1891	5.5828
−0.250	+0.02803	−0.51786	−0.51652	0.1902	5.4932
−0.255	+0.02899	−0.50696	−0.48927	0.1912	5.4072
−0.260	+0.02995	−0.49623	−0.46244	0.1921	5.3245
−0.265	+0.03091	−0.48566	−0.43602	0.1930	5.2451
−0.270	+0.03188	−0.47525	−0.40998	0.1937	5.1686
−0.275	+0.03285	−0.46499	−0.38433	0.1943	5.0949
−0.280	+0.03382	−0.45487	−0.35903	0.1948	5.0240
−0.285	+0.03479	−0.44489	−0.33408	0.1952	4.9555
−0.290	+0.03577	−0.43505	−0.30947	0.1955	4.8896
−0.295	+0.03675	−0.42533	−0.28518	0.1958	4.8259
−0.300	+0.03773	−0.41574	−0.26121	0.1960	4.7644
−0.305	+0.03871	−0.40627	−0.23753	0.1960	4.7050
−0.310	+0.03969	−0.39692	−0.21415	0.1960	4.6475
−0.315	+0.04067	−0.38768	−0.19106	0.1960	4.5920
−0.320	+0.04165	−0.37855	−0.16823	0.1958	4.5383
−0.325	+0.04263	−0.36952	−0.14567	0.1956	4.4863
−0.330	+0.04361	−0.36060	−0.12336	0.1953	4.4360
−0.335	+0.04458	−0.35178	−0.10131	0.1950	4.3872
−0.340	+0.04556	−0.34305	−0.07949	0.1945	4.3400
−0.345	+0.04653	−0.33442	−0.05790	0.1941	4.2942
−0.350	+0.04750	−0.32587	−0.03654	0.1935	4.2498
−0.355	+0.04846	−0.31742	−0.01540	0.1929	4.2068
−0.360	+0.04943	−0.30905	+0.00552	0.1923	4.1650
−0.365	+0.05039	−0.30076	+0.02624	0.1916	4.1244
−0.370	+0.05134	−0.29255	+0.04676	0.1908	4.0851
−0.375	+0.05230	−0.28442	+0.06709	0.1900	4.0468
−0.380	+0.05324	−0.27636	+0.08723	0.1891	4.0097
−0.385	+0.05419	−0.26838	+0.10719	0.1882	3.9736
−0.390	+0.05513	−0.26046	+0.12697	0.1873	3.9385
−0.395	+0.05606	−0.25262	+0.14658	0.1863	3.9044
−0.400	+0.05699	−0.24485	+0.16602	0.1852	3.8712
−0.405	+0.05791	−0.23714	+0.18529	0.1842	3.8390
−0.410	+0.05883	−0.22949	+0.20441	0.1831	3.8076
−0.415	+0.05974	−0.22190	+0.22337	0.1819	3.7771
−0.420	+0.06065	−0.21438	+0.24218	0.1808	3.7473
−0.425	+0.06155	−0.20691	+0.26085	0.1796	3.7184
−0.430	+0.06245	−0.19951	+0.27937	0.1783	3.6902
−0.435	+0.06334	−0.19215	+0.29775	0.1771	3.6628
−0.440	+0.06422	−0.18485	+0.31600	0.1758	3.6360
−0.445	+0.06509	−0.17761	+0.33411	0.1745	3.6100
−0.450	+0.06596	−0.17041	+0.35210	0.1731	3.5846
−0.455	+0.06683	−0.16327	+0.36996	0.1718	3.5599
−0.460	+0.06768	−0.15617	+0.38770	0.1704	3.5358
−0.465	+0.06853	−0.14913	+0.40532	0.1690	3.5123
−0.470	+0.06937	−0.14212	+0.42282	0.1676	3.4894
−0.475	+0.07021	−0.13517	+0.44022	0.1661	3.4670
−0.480	+0.07103	−0.12826	+0.45750	0.1647	3.4452
−0.485	+0.07185	−0.12139	+0.47467	0.1632	3.4239
−0.490	+0.07267	−0.11456	+0.49174	0.1617	3.4032
−0.495	+0.07347	−0.10777	+0.50870	0.1603	3.3829
−0.500	+0.07427	−0.10103	+0.52557	0.1588	3.3632
−0.505	+0.07506	−0.09432	+0.54233	0.1573	3.3439
−0.510	+0.07584	−0.08765	+0.55901	0.1557	3.3251
−0.515	+0.07662	−0.08102	+0.57559	0.1542	3.3067
−0.520	+0.07739	−0.07442	+0.59208	0.1527	3.2888
−0.525	+0.07815	−0.06786	+0.60848	0.1511	3.2712
−0.530	+0.07890	−0.06134	+0.62479	0.1496	3.2541
−0.535	+0.07964	−0.05485	+0.64102	0.1480	3.2374
−0.540	+0.08038	−0.04839	+0.65716	0.1465	3.2211
−0.545	+0.08111	−0.04196	+0.67323	0.1449	3.2051
−0.550	+0.08183	−0.03557	+0.68922	0.1434	3.1896
−0.555	+0.08254	−0.02920	+0.70513	0.1418	3.1743
−0.560	+0.08325	−0.02287	+0.72096	0.1403	3.1595
−0.565	+0.08394	−0.01656	+0.73672	0.1387	3.1449
−0.570	+0.08463	−0.01029	+0.75241	0.1371	3.1307
−0.575	+0.08532	−0.00404	+0.76803	0.1356	3.1169
−0.580	+0.08599	+0.00217	+0.78358	0.1340	3.1033
−0.585	+0.08666	+0.00836	+0.79906	0.1325	3.0900
−0.590	+0.08732	+0.01453	+0.81448	0.1310	3.0771
−0.595	+0.08797	+0.02067	+0.82984	0.1294	3.0644
−0.600	+0.08861	+0.02679	+0.84513	0.1279	3.0520
−0.605	+0.08925	+0.03288	+0.86036	0.1263	3.0399

1513

1	4	5	6	7	8
−0.010	+0.00002	−2.03072	−4.23170	0.0058	109.8240
−0.015	+0.00006	−1.85221	−3.78543	0.0105	73.6458
−0.020	+0.00013	−1.72478	−3.46687	0.0157	55.5465
−0.025	+0.00022	−1.62538	−3.21835	0.0214	44.6844
−0.030	+0.00034	−1.54370	−3.01416	0.0275	37.4418
−0.035	+0.00049	−1.47426	−2.84056	0.0338	32.2675
−0.040	+0.00068	−1.41378	−2.68937	0.0402	28.3859
−0.045	+0.00090	−1.36015	−2.55529	0.0468	25.3661
−0.050	+0.00115	−1.31192	−2.43472	0.0535	22.9495
−0.055	+0.00143	−1.26807	−2.32508	0.0601	20.9716
−0.060	+0.00175	−1.22782	−2.22446	0.0668	19.3227
−0.065	+0.00210	−1.19061	−2.13143	0.0734	17.9269
−0.070	+0.00249	−1.15598	−2.04487	0.0800	16.7299
−0.075	+0.00290	−1.12358	−1.96387	0.0866	15.6921
−0.080	+0.00335	−1.09313	−1.88773	0.0930	14.7834
−0.085	+0.00383	−1.06438	−1.81586	0.0993	13.9812
−0.090	+0.00435	−1.03714	−1.74778	0.1056	13.2678
−0.095	+0.00489	−1.01126	−1.68306	0.1117	12.6290
−0.100	+0.00546	−0.98659	−1.62138	0.1176	12.0538
−0.105	+0.00606	−0.96301	−1.56244	0.1234	11.5330
−0.110	+0.00670	−0.94042	−1.50597	0.1291	11.0592
−0.115	+0.00736	−0.91874	−1.45178	0.1346	10.6264
−0.120	+0.00804	−0.89789	−1.39965	0.1400	10.2294
−0.125	+0.00876	−0.87781	−1.34943	0.1452	9.8638
−0.130	+0.00950	−0.85842	−1.30097	0.1502	9.5262
−0.135	+0.01026	−0.83968	−1.25413	0.1551	9.2134
−0.140	+0.01105	−0.82155	−1.20879	0.1598	8.9228
−0.145	+0.01186	−0.80398	−1.16486	0.1644	8.6520
−0.150	+0.01269	−0.78693	−1.12224	0.1688	8.3992
−0.155	+0.01355	−0.77037	−1.08085	0.1730	8.1625
−0.160	+0.01442	−0.75427	−1.04059	0.1770	7.9405
−0.165	+0.01532	−0.73860	−1.00142	0.1809	7.7318
−0.170	+0.01623	−0.72334	−0.96326	0.1846	7.5353
−0.175	+0.01716	−0.70845	−0.92605	0.1881	7.3500
−0.180	+0.01811	−0.69393	−0.88974	0.1915	7.1749
−0.185	+0.01908	−0.67975	−0.85428	0.1947	7.0091
−0.190	+0.02006	−0.66589	−0.81963	0.1978	6.8521
−0.195	+0.02106	−0.65233	−0.78575	0.2007	6.7031
−0.200	+0.02207	−0.63907	−0.75259	0.2034	6.5614
−0.205	+0.02309	−0.62608	−0.72012	0.2060	6.4267
−0.210	+0.02413	−0.61336	−0.68831	0.2085	6.2984
−0.215	+0.02518	−0.60088	−0.65713	0.2108	6.1760
−0.220	+0.02624	−0.58865	−0.62654	0.2129	6.0591
−0.225	+0.02731	−0.57664	−0.59653	0.2149	5.9475
−0.230	+0.02838	−0.56486	−0.56706	0.2168	5.8407
−0.235	+0.02947	−0.55328	−0.53811	0.2185	5.7385
−0.240	+0.03057	−0.54190	−0.50967	0.2201	5.6406
−0.245	+0.03168	−0.53071	−0.48170	0.2216	5.5467
−0.250	+0.03279	−0.51971	−0.45419	0.2230	5.4566
−0.255	+0.03391	−0.50888	−0.42713	0.2242	5.3700
−0.260	+0.03503	−0.49823	−0.40049	0.2253	5.2868
−0.265	+0.03616	−0.48773	−0.37425	0.2262	5.2068
−0.270	+0.03729	−0.47740	−0.34841	0.2271	5.1298
−0.275	+0.03843	−0.46721	−0.32295	0.2278	5.0557
−0.280	+0.03957	−0.45717	−0.29785	0.2285	4.9842
−0.285	+0.04071	−0.44727	−0.27310	0.2290	4.9154
−0.290	+0.04186	−0.43751	−0.24869	0.2294	4.8489
−0.295	+0.04301	−0.42788	−0.22461	0.2297	4.7848
−0.300	+0.04416	−0.41837	−0.20084	0.2299	4.7229
−0.305	+0.04531	−0.40898	−0.17738	0.2301	4.6631
−0.310	+0.04646	−0.39972	−0.15421	0.2301	4.6052
−0.315	+0.04761	−0.39056	−0.13132	0.2300	4.5493
−0.320	+0.04876	−0.38152	−0.10871	0.2299	4.4952
−0.325	+0.04991	−0.37258	−0.08636	0.2296	4.4429
−0.330	+0.05106	−0.36374	−0.06428	0.2293	4.3922
−0.335	+0.05220	−0.35501	−0.04244	0.2289	4.3431
−0.340	+0.05335	−0.34637	−0.02084	0.2284	4.2956
−0.345	+0.05449	−0.33783	+0.00051	0.2279	4.2495
−0.350	+0.05562	−0.32937	+0.02164	0.2273	4.2048
−0.355	+0.05676	−0.32101	+0.04256	0.2266	4.1614
−0.360	+0.05789	−0.31272	+0.06326	0.2258	4.1193
−0.365	+0.05902	−0.30453	+0.08376	0.2250	4.0785
−0.370	+0.06014	−0.29641	+0.10405	0.2241	4.0389
−0.375	+0.06126	−0.28837	+0.12415	0.2232	4.0004
−0.380	+0.06237	−0.28041	+0.14405	0.2222	3.9630
−0.385	+0.06348	−0.27252	+0.16378	0.2212	3.9267
−0.390	+0.06459	−0.26470	+0.18332	0.2201	3.8914
−0.395	+0.06568	−0.25695	+0.20270	0.2189	3.8571
−0.400	+0.06678	−0.24927	+0.22190	0.2177	3.8237
−0.405	+0.06786	−0.24165	+0.24093	0.2165	3.7913
−0.410	+0.06894	−0.23410	+0.25981	0.2152	3.7597
−0.415	+0.07001	−0.22662	+0.27853	0.2138	3.7290
−0.420	+0.07108	−0.21919	+0.29710	0.2125	3.6991
−0.425	+0.07214	−0.21182	+0.31553	0.2111	3.6701
−0.430	+0.07319	−0.20451	+0.33381	0.2096	3.6417
−0.435	+0.07423	−0.19725	+0.35195	0.2081	3.6142
−0.440	+0.07527	−0.19005	+0.36995	0.2066	3.5873
−0.445	+0.07630	−0.18290	+0.38782	0.2051	3.5612
−0.450	+0.07732	−0.17580	+0.40556	0.2035	3.5357
−0.455	+0.07834	−0.16876	+0.42318	0.2019	3.5109
−0.460	+0.07934	−0.16176	+0.44067	0.2003	3.4867
−0.465	+0.08034	−0.15481	+0.45805	0.1987	3.4631
−0.470	+0.08133	−0.14791	+0.47531	0.1970	3.4401
−0.475	+0.08231	−0.14105	+0.49245	0.1953	3.4177
−0.480	+0.08328	−0.13424	+0.50948	0.1936	3.3958
−0.485	+0.08425	−0.12746	+0.52641	0.1919	3.3745
−0.490	+0.08520	−0.12074	+0.54323	0.1901	3.3537
−0.495	+0.08615	−0.11405	+0.55995	0.1884	3.3334
−0.500	+0.08709	−0.10740	+0.57657	0.1866	3.3137
−0.505	+0.08802	−0.10079	+0.59309	0.1848	3.2944
−0.510	+0.08894	−0.09422	+0.60951	0.1830	3.2755
−0.515	+0.08985	−0.08769	+0.62584	0.1812	3.2571
−0.520	+0.09075	−0.08120	+0.64208	0.1794	3.2392
−0.525	+0.09164	−0.07473	+0.65824	0.1776	3.2217
−0.530	+0.09253	−0.06831	+0.67430	0.1758	3.2046
−0.535	+0.09340	−0.06192	+0.69028	0.1740	3.1879
−0.540	+0.09427	−0.05556	+0.70618	0.1721	3.1716
−0.545	+0.09512	−0.04923	+0.72200	0.1703	3.1557
−0.550	+0.09597	−0.04293	+0.73774	0.1685	3.1402
−0.555	+0.09681	−0.03667	+0.75340	0.1666	3.1250
−0.560	+0.09764	−0.03043	+0.76899	0.1648	3.1102
−0.565	+0.09846	−0.02423	+0.78451	0.1630	3.0957
−0.570	+0.09927	−0.01805	+0.79995	0.1611	3.0816
−0.575	+0.10007	−0.01190	+0.81532	0.1593	3.0678
−0.580	+0.10086	−0.00578	+0.83063	0.1574	3.0543
−0.585	+0.10164	+0.00031	+0.84587	0.1556	3.0411
−0.590	+0.10242	+0.00638	+0.86104	0.1538	3.0282
−0.595	+0.10318	+0.01242	+0.87615	0.1520	3.0156
−0.600	+0.10394	+0.01844	+0.89120	0.1502	3.0033
−0.605	+0.10468	+0.02444	+0.90618	0.1484	2.9913

1514

1	4	5	6	7	8
−0.010	+0.00002	−2.03072	−4.17371	0.0067	109.8241
−0.015	+0.00007	−1.85221	−3.72744	0.0120	73.6452
−0.020	+0.00014	−1.72479	−3.40889	0.0180	55.5452
−0.025	+0.00025	−1.62539	−3.16038	0.0245	44.6824
−0.030	+0.00039	−1.54371	−2.95620	0.0314	37.4390
−0.035	+0.00057	−1.47428	−2.78262	0.0386	32.2639
−0.040	+0.00078	−1.41381	−2.63144	0.0460	28.3816
−0.045	+0.00103	−1.36019	−2.49739	0.0535	25.3610
−0.050	+0.00131	−1.31197	−2.37684	0.0611	22.9436
−0.055	+0.00164	−1.26813	−2.26723	0.0687	20.9649
−0.060	+0.00200	−1.22790	−2.16666	0.0764	19.3151
−0.065	+0.00240	−1.19070	−2.07367	0.0840	17.9185
−0.070	+0.00284	−1.15609	−1.98714	0.0915	16.7206
−0.075	+0.00332	−1.12372	−1.90620	0.0990	15.6819
−0.080	+0.00383	−1.09328	−1.83011	0.1064	14.7724
−0.085	+0.00438	−1.06456	−1.75830	0.1136	13.9693
−0.090	+0.00497	−1.03735	−1.69027	0.1207	13.2549
−0.095	+0.00559	−1.01149	−1.62563	0.1277	12.6153
−0.100	+0.00625	−0.98684	−1.56401	0.1346	12.0392
−0.105	+0.00694	−0.96329	−1.50514	0.1412	11.5175
−0.110	+0.00766	−0.94074	−1.44876	0.1477	11.0429
−0.115	+0.00841	−0.91910	−1.39465	0.1541	10.6092
−0.120	+0.00920	−0.89828	−1.34261	0.1602	10.2113
−0.125	+0.01002	−0.87823	−1.29248	0.1662	9.8450
−0.130	+0.01086	−0.85888	−1.24411	0.1720	9.5065
−0.135	+0.01174	−0.84019	−1.19738	0.1776	9.1929
−0.140	+0.01264	−0.82210	−1.15215	0.1830	8.9014
−0.145	+0.01357	−0.80457	−1.10833	0.1882	8.6298
−0.150	+0.01452	−0.78757	−1.06582	0.1933	8.3762
−0.155	+0.01550	−0.77105	−1.02454	0.1981	8.1387
−0.160	+0.01650	−0.75500	−0.98441	0.2028	7.9159
−0.165	+0.01753	−0.73938	−0.94536	0.2072	7.7064
−0.170	+0.01857	−0.72417	−0.90732	0.2115	7.5092
−0.175	+0.01964	−0.70934	−0.87025	0.2156	7.3231
−0.180	+0.02073	−0.69487	−0.83408	0.2195	7.1472
−0.185	+0.02184	−0.68074	−0.79876	0.2232	6.9808
−0.190	+0.02296	−0.66694	−0.76425	0.2268	6.8230
−0.195	+0.02411	−0.65344	−0.73052	0.2301	6.6733
−0.200	+0.02526	−0.64024	−0.69751	0.2333	6.5309
−0.205	+0.02644	−0.62732	−0.66519	0.2363	6.3955

1	4	5	6	7	8
-0.210	+0.02763	-0.61465	-0.63354	0.2391	6.2665
-0.215	+0.02883	-0.60225	-0.60252	0.2418	6.1435
-0.220	+0.03005	-0.59008	-0.57210	0.2443	6.0260
-0.225	+0.03127	-0.57814	-0.54225	0.2466	5.9138
-0.230	+0.03251	-0.56642	-0.51295	0.2488	5.8064
-0.235	+0.03376	-0.55491	-0.48418	0.2508	5.7036
-0.240	+0.03502	-0.54360	-0.45591	0.2527	5.6050
-0.245	+0.03629	-0.53249	-0.42812	0.2544	5.5106
-0.250	+0.03757	-0.52156	-0.40080	0.2560	5.4199
-0.255	+0.03885	-0.51080	-0.37392	0.2574	5.3328
-0.260	+0.04014	-0.50022	-0.34746	0.2587	5.2491
-0.265	+0.04144	-0.48981	-0.32142	0.2599	5.1685
-0.270	+0.04274	-0.47955	-0.29577	0.2609	5.0910
-0.275	+0.04405	-0.46944	-0.27050	0.2618	5.0164
-0.280	+0.04536	-0.45948	-0.24560	0.2625	4.9445
-0.285	+0.04667	-0.44966	-0.22105	0.2631	4.8751
-0.290	+0.04799	-0.43998	-0.19685	0.2637	4.8082
-0.295	+0.04931	-0.43043	-0.17297	0.2641	4.7437
-0.300	+0.05063	-0.42100	-0.14941	0.2643	4.6813
-0.305	+0.05195	-0.41170	-0.12615	0.2645	4.6211
-0.310	+0.05327	-0.40252	-0.10319	0.2646	4.5629
-0.315	+0.05460	-0.39345	-0.08052	0.2645	4.5066
-0.320	+0.05592	-0.38449	-0.05812	0.2644	4.4521
-0.325	+0.05724	-0.37564	-0.03599	0.2641	4.3994
-0.330	+0.05856	-0.36689	-0.01412	0.2638	4.3483
-0.335	+0.05988	-0.35824	+0.00748	0.2634	4.2989
-0.340	+0.06120	-0.34969	+0.02886	0.2628	4.2510
-0.345	+0.06251	-0.34124	+0.05000	0.2622	4.2046
-0.350	+0.06382	-0.33287	+0.07091	0.2615	4.1596
-0.355	+0.06512	-0.32460	+0.09159	0.2608	4.1159
-0.360	+0.06643	-0.31641	+0.11207	0.2599	4.0736
-0.365	+0.06772	-0.30830	+0.13233	0.2590	4.0325
-0.370	+0.06902	-0.30028	+0.15240	0.2580	3.9926
-0.375	+0.07030	-0.29233	+0.17226	0.2569	3.9539
-0.380	+0.07159	-0.28446	+0.19194	0.2558	3.9163
-0.385	+0.07286	-0.27666	+0.21143	0.2546	3.8797
-0.390	+0.07413	-0.26894	+0.23074	0.2534	3.8442
-0.395	+0.07540	-0.26129	+0.24987	0.2520	3.8097
-0.400	+0.07665	-0.25370	+0.26883	0.2507	3.7761
-0.405	+0.07790	-0.24618	+0.28763	0.2493	3.7435
-0.410	+0.07915	-0.23873	+0.30627	0.2478	3.7117
-0.415	+0.08038	-0.23133	+0.32475	0.2463	3.6809
-0.420	+0.08161	-0.22400	+0.34308	0.2447	3.6508
-0.425	+0.08283	-0.21673	+0.36126	0.2431	3.6216
-0.430	+0.08404	-0.20952	+0.37930	0.2414	3.5931
-0.435	+0.08524	-0.20236	+0.39720	0.2397	3.5654
-0.440	+0.08644	-0.19525	+0.41495	0.2380	3.5384
-0.445	+0.08762	-0.18820	+0.43258	0.2362	3.5122
-0.450	+0.08880	-0.18120	+0.45008	0.2344	3.4866
-0.455	+0.08997	-0.17426	+0.46745	0.2326	3.4616
-0.460	+0.09113	-0.16736	+0.48470	0.2307	3.4374
-0.465	+0.09228	-0.16051	+0.50182	0.2288	3.4137
-0.470	+0.09342	-0.15370	+0.51883	0.2269	3.3906
-0.475	+0.09455	-0.14694	+0.53573	0.2250	3.3682
-0.480	+0.09567	-0.14023	+0.55252	0.2230	3.3462
-0.485	+0.09678	-0.13356	+0.56920	0.2210	3.3249
-0.490	+0.09788	-0.12693	+0.58577	0.2190	3.3040
-0.495	+0.09897	-0.12034	+0.60224	0.2170	3.2837
-0.500	+0.10005	-0.11379	+0.61861	0.2150	3.2639
-0.505	+0.10112	-0.10728	+0.63488	0.2129	3.2446
-0.510	+0.10218	-0.10081	+0.65105	0.2108	3.2258
-0.515	+0.10323	-0.09438	+0.66714	0.2088	3.2074
-0.520	+0.10427	-0.08798	+0.68313	0.2067	3.1894
-0.525	+0.10529	-0.08162	+0.69903	0.2046	3.1719
-0.530	+0.10631	-0.07530	+0.71485	0.2025	3.1549
-0.535	+0.10732	-0.06900	+0.73058	0.2004	3.1382
-0.540	+0.10832	-0.06274	+0.74623	0.1982	3.1219
-0.545	+0.10930	-0.05652	+0.76180	0.1961	3.1060
-0.550	+0.11028	-0.05032	+0.77729	0.1940	3.0905
-0.555	+0.11124	-0.04415	+0.79271	0.1919	3.0754
-0.560	+0.11220	-0.03802	+0.80805	0.1897	3.0607
-0.565	+0.11314	-0.03191	+0.82332	0.1876	3.0462
-0.570	+0.11407	-0.02583	+0.83851	0.1855	3.0322
-0.575	+0.11500	-0.01978	+0.85364	0.1834	3.0184
-0.580	+0.11591	-0.01376	+0.86870	0.1812	3.0050
-0.585	+0.11681	-0.00776	+0.88369	0.1791	2.9919
-0.590	+0.11770	-0.00179	+0.89862	0.1770	2.9791
-0.595	+0.11858	+0.00415	+0.91348	0.1749	2.9666
-0.600	+0.11945	+0.01007	+0.92828	0.1728	2.9544
-0.605	+0.12031	+0.01596	+0.94303	0.1707	2.9425

1	4	5	6	7	8
-0.010	+0.00003	-2.03072	-4.12256	0.0075	109.8234
-0.015	+0.00008	-1.85221	-3.67630	0.0135	73.6439
-0.020	+0.00016	-1.72479	-3.35775	0.0202	55.5434
-0.025	+0.00028	-1.62539	-3.10925	0.0276	44.6800
-0.030	+0.00044	-1.54373	-2.90508	0.0354	37.4359
-0.035	+0.00064	-1.47430	-2.73152	0.0434	32.2601
-0.040	+0.00087	-1.41384	-2.58037	0.0518	28.3770
-0.045	+0.00115	-1.36023	-2.44634	0.0602	25.3557
-0.050	+0.00148	-1.31202	-2.32582	0.0688	22.9375
-0.055	+0.00184	-1.26819	-2.21624	0.0774	20.9579
-0.060	+0.00225	-1.22798	-2.11570	0.0860	19.3074
-0.065	+0.00270	-1.19080	-2.02275	0.0945	17.9099
-0.070	+0.00320	-1.15620	-1.93628	0.1030	16.7112
-0.075	+0.00373	-1.12385	-1.85538	0.1114	15.6716
-0.080	+0.00431	-1.09343	-1.77935	0.1197	14.7612
-0.085	+0.00493	-1.06473	-1.70759	0.1279	13.9572
-0.090	+0.00559	-1.03755	-1.63963	0.1359	13.2420
-0.095	+0.00629	-1.01171	-1.57505	0.1438	12.6015
-0.100	+0.00703	-0.98710	-1.51351	0.1515	12.0245
-0.105	+0.00781	-0.96358	-1.45471	0.1591	11.5020
-0.110	+0.00862	-0.94106	-1.39841	0.1664	11.0265
-0.115	+0.00947	-0.91945	-1.34438	0.1735	10.5919
-0.120	+0.01036	-0.89867	-1.29243	0.1805	10.1932
-0.125	+0.01128	-0.87865	-1.24240	0.1872	9.8260
-0.130	+0.01223	-0.85934	-1.19413	0.1938	9.4867
-0.135	+0.01321	-0.84069	-1.14749	0.2001	9.1722
-0.140	+0.01423	-0.82264	-1.10237	0.2063	8.8799
-0.145	+0.01528	-0.80516	-1.05866	0.2122	8.6075
-0.150	+0.01635	-0.78820	-1.01626	0.2179	8.3531
-0.155	+0.01746	-0.77173	-0.97510	0.2234	8.1148
-0.160	+0.01859	-0.75573	-0.93509	0.2286	7.8912
-0.165	+0.01974	-0.74016	-0.89617	0.2337	7.6810
-0.170	+0.02092	-0.72500	-0.85826	0.2385	7.4830
-0.175	+0.02213	-0.71022	-0.82132	0.2432	7.2961
-0.180	+0.02336	-0.69581	-0.78528	0.2476	7.1195
-0.185	+0.02460	-0.68174	-0.75011	0.2519	6.9523
-0.190	+0.02587	-0.66799	-0.71574	0.2559	6.7938
-0.195	+0.02716	-0.65456	-0.68215	0.2597	6.6434
-0.200	+0.02847	-0.64141	-0.64930	0.2633	6.5004
-0.205	+0.02980	-0.62855	-0.61714	0.2668	6.3643
-0.210	+0.03114	-0.61595	-0.58564	0.2700	6.2346
-0.215	+0.03250	-0.60361	-0.55478	0.2731	6.1109
-0.220	+0.03387	-0.59150	-0.52452	0.2759	5.9928
-0.225	+0.03526	-0.57963	-0.49484	0.2786	5.8799
-0.230	+0.03666	-0.56798	-0.46572	0.2811	5.7719
-0.235	+0.03807	-0.55654	-0.43712	0.2834	5.6685
-0.240	+0.03949	-0.54530	-0.40902	0.2856	5.5694
-0.245	+0.04092	-0.53426	-0.38142	0.2875	5.4744
-0.250	+0.04237	-0.52340	-0.35427	0.2894	5.3831
-0.255	+0.04382	-0.51273	-0.32758	0.2910	5.2955
-0.260	+0.04528	-0.50222	-0.30131	0.2925	5.2112
-0.265	+0.04674	-0.49188	-0.27546	0.2938	5.1302
-0.270	+0.04821	-0.48170	-0.25000	0.2950	5.0522
-0.275	+0.04969	-0.47167	-0.22493	0.2960	4.9770
-0.280	+0.05118	-0.46179	-0.20023	0.2969	4.9046
-0.285	+0.05266	-0.45205	-0.17588	0.2977	4.8348
-0.290	+0.05415	-0.44244	-0.15188	0.2983	4.7675
-0.295	+0.05565	-0.43298	-0.12820	0.2988	4.7025
-0.300	+0.05714	-0.42363	-0.10485	0.2991	4.6397
-0.305	+0.05864	-0.41441	-0.08180	0.2994	4.5790
-0.310	+0.06013	-0.40532	-0.05905	0.2995	4.5204
-0.315	+0.06163	-0.39633	-0.03659	0.2994	4.4637
-0.320	+0.06313	-0.38746	-0.01441	0.2993	4.4089
-0.325	+0.06463	-0.37869	+0.00749	0.2991	4.3558
-0.330	+0.06612	-0.37003	+0.02914	0.2987	4.3044
-0.335	+0.06761	-0.36148	+0.05053	0.2982	4.2546
-0.340	+0.06910	-0.35302	+0.07169	0.2977	4.2064
-0.345	+0.07059	-0.34465	+0.09260	0.2970	4.1596
-0.350	+0.07207	-0.33638	+0.11329	0.2963	4.1143
-0.355	+0.07355	-0.32819	+0.13375	0.2954	4.0704
-0.360	+0.07503	-0.32009	+0.15399	0.2945	4.0277
-0.365	+0.07650	-0.31208	+0.17403	0.2935	3.9864
-0.370	+0.07796	-0.30415	+0.19386	0.2924	3.9462
-0.375	+0.07942	-0.29629	+0.21349	0.2912	3.9072
-0.380	+0.08087	-0.28852	+0.23293	0.2899	3.8693
-0.385	+0.08232	-0.28082	+0.25219	0.2886	3.8326
-0.390	+0.08376	-0.27319	+0.27126	0.2872	3.7968
-0.395	+0.08519	-0.26563	+0.29016	0.2857	3.7621
-0.400	+0.08662	-0.25814	+0.30888	0.2842	3.7283
-0.405	+0.08804	-0.25071	+0.32744	0.2826	3.6955

−0.410	+0.08944	−0.24335	+0.34584	0.2809	3.6636
−0.415	+0.09085	−0.23606	+0.36408	0.2792	3.6325
−0.420	+0.09224	−0.22882	+0.38217	0.2774	3.6023
−0.425	+0.09362	−0.22165	+0.40011	0.2756	3.5729
−0.430	+0.09499	−0.21453	+0.41790	0.2738	3.5443
−0.435	+0.09636	−0.20747	+0.43555	0.2718	3.5165
−0.440	+0.09771	−0.20046	+0.45307	0.2699	3.4894
−0.445	+0.09906	−0.19351	+0.47045	0.2679	3.4630
−0.450	+0.10039	−0.18661	+0.48770	0.2658	3.4373
−0.455	+0.10172	−0.17976	+0.50482	0.2638	3.4122
−0.460	+0.10303	−0.17296	+0.52182	0.2617	3.3879
−0.465	+0.10433	−0.16621	+0.53870	0.2595	3.3641
−0.470	+0.10563	−0.15950	+0.55546	0.2574	3.3410
−0.475	+0.10691	−0.15285	+0.57211	0.2551	3.3184
−0.480	+0.10818	−0.14623	+0.58865	0.2529	3.2965
−0.485	+0.10944	−0.13966	+0.60508	0.2507	3.2750
−0.490	+0.11068	−0.13313	+0.62140	0.2484	3.2542
−0.495	+0.11192	−0.12664	+0.63762	0.2461	3.2338
−0.500	+0.11315	−0.12019	+0.65374	0.2438	3.2140
−0.505	+0.11436	−0.11379	+0.66976	0.2415	3.1946
−0.510	+0.11556	−0.10742	+0.68569	0.2391	3.1758
−0.515	+0.11675	−0.10108	+0.70152	0.2367	3.1574
−0.520	+0.11793	−0.09479	+0.71726	0.2344	3.1394
−0.525	+0.11910	−0.08852	+0.73292	0.2320	3.1219
−0.530	+0.12025	−0.08230	+0.74848	0.2296	3.1049
−0.535	+0.12139	−0.07610	+0.76397	0.2272	3.0882
−0.540	+0.12252	−0.06994	+0.77937	0.2248	3.0720
−0.545	+0.12364	−0.06382	+0.79469	0.2224	3.0561
−0.550	+0.12475	−0.05772	+0.80993	0.2199	3.0407
−0.555	+0.12584	−0.05165	+0.82509	0.2175	3.0256
−0.560	+0.12692	−0.04562	+0.84019	0.2151	3.0108
−0.565	+0.12799	−0.03961	+0.85520	0.2127	2.9965
−0.570	+0.12905	−0.03363	+0.87015	0.2103	2.9825
−0.575	+0.13009	−0.02768	+0.88503	0.2078	2.9688
−0.580	+0.13113	−0.02175	+0.89984	0.2054	2.9554
−0.585	+0.13215	−0.01586	+0.91458	0.2030	2.9424
−0.590	+0.13316	−0.00998	+0.92926	0.2006	2.9297
−0.595	+0.13416	−0.00414	+0.94388	0.1982	2.9173
−0.600	+0.13514	+0.00168	+0.95844	0.1958	2.9051
−0.605	+0.13611	+0.00747	+0.97293	0.1934	2.8933

1516

1	4	5	6	7	8
−0.010	+0.00003	−2.03072	−4.07681	0.0083	109.8224
−0.015	+0.00009	−1.85222	−3.63055	0.0150	73.6426
−0.020	+0.00018	−1.72480	−3.31201	0.0225	55.5416
−0.025	+0.00031	−1.62540	−3.06352	0.0307	44.6776
−0.030	+0.00049	−1.54374	−2.85936	0.0393	37.4329
−0.035	+0.00071	−1.47432	−2.68582	0.0483	32.2564
−0.040	+0.00097	−1.41387	−2.53469	0.0575	28.3726
−0.045	+0.00128	−1.36027	−2.40068	0.0669	25.3504
−0.050	+0.00164	−1.31207	−2.28019	0.0764	22.9314
−0.055	+0.00205	−1.26826	−2.17065	0.0860	20.9511
−0.060	+0.00250	−1.22805	−2.07014	0.0955	19.2997
−0.065	+0.00301	−1.19089	−1.97723	0.1051	17.9013
−0.070	+0.00355	−1.15632	−1.89080	0.1145	16.7018
−0.075	+0.00415	−1.12398	−1.80995	0.1239	15.6613
−0.080	+0.00479	−1.09359	−1.73398	0.1331	14.7500
−0.085	+0.00548	−1.06491	−1.66228	0.1422	13.9452
−0.090	+0.00622	−1.03775	−1.59438	0.1512	13.2291
−0.095	+0.00699	−1.01194	−1.52986	0.1599	12.5877
−0.100	+0.00782	−0.98736	−1.46840	0.1685	12.0099
−0.105	+0.00868	−0.96387	−1.40968	0.1769	11.4865
−0.110	+0.00959	−0.94138	−1.35345	0.1851	11.0101
−0.115	+0.01053	−0.91980	−1.29951	0.1931	10.5747
−0.120	+0.01152	−0.89906	−1.24765	0.2008	10.1751
−0.125	+0.01254	−0.87908	−1.19770	0.2084	9.8070
−0.130	+0.01360	−0.85981	−1.14953	0.2157	9.4669
−0.135	+0.01470	−0.84120	−1.10299	0.2227	9.1516
−0.140	+0.01583	−0.82319	−1.05798	0.2296	8.8585
−0.145	+0.01699	−0.80575	−1.01438	0.2362	8.5853
−0.150	+0.01819	−0.78884	−0.97209	0.2426	8.3300
−0.155	+0.01942	−0.77242	−0.93105	0.2487	8.0909
−0.160	+0.02068	−0.75646	−0.89116	0.2546	7.8665
−0.165	+0.02196	−0.74094	−0.85236	0.2603	7.6555
−0.170	+0.02328	−0.72583	−0.81459	0.2657	7.4567
−0.175	+0.02462	−0.71111	−0.77777	0.2709	7.2691
−0.180	+0.02599	−0.69675	−0.74188	0.2759	7.0918
−0.185	+0.02738	−0.68273	−0.70684	0.2807	6.9239
−0.190	+0.02880	−0.66905	−0.67262	0.2852	6.7647
−0.195	+0.03023	−0.65567	−0.63918	0.2895	6.6135
−0.200	+0.03169	−0.64259	−0.60647	0.2936	6.4698
−0.205	+0.03317	−0.62979	−0.57447	0.2975	6.3330

1	4	5	6	7	8
−0.210	+0.03467	−0.61725	−0.54313	0.3011	6.2027
−0.215	+0.03618	−0.60497	−0.51243	0.3045	6.0784
−0.220	+0.03771	−0.59293	−0.48234	0.3078	5.9596
−0.225	+0.03926	−0.58113	−0.45283	0.3108	5.8461
−0.230	+0.04082	−0.56955	−0.42387	0.3136	5.7375
−0.235	+0.04240	−0.55818	−0.39544	0.3163	5.6335
−0.240	+0.04398	−0.54701	−0.36753	0.3187	5.5338
−0.245	+0.04558	−0.53604	−0.34010	0.3210	5.4381
−0.250	+0.04719	−0.52525	−0.31314	0.3230	5.3463
−0.255	+0.04881	−0.51465	−0.28663	0.3249	5.2581
−0.260	+0.05044	−0.50422	−0.26055	0.3266	5.1734
−0.265	+0.05208	−0.49395	−0.23489	0.3282	5.0918
−0.270	+0.05372	−0.48385	−0.20963	0.3295	5.0133
−0.275	+0.05538	−0.47390	−0.18475	0.3307	4.9376
−0.280	+0.05703	−0.46410	−0.16025	0.3318	4.8648
−0.285	+0.05869	−0.45444	−0.13610	0.3326	4.7945
−0.290	+0.06036	−0.44492	−0.11230	0.3334	4.7267
−0.295	+0.06203	−0.43553	−0.08883	0.3339	4.6612
−0.300	+0.06370	−0.42627	−0.06568	0.3344	4.5980
−0.305	+0.06537	−0.41714	−0.04285	0.3347	4.5369
−0.310	+0.06704	−0.40812	−0.02031	0.3348	4.4779
−0.315	+0.06872	−0.39922	+0.00193	0.3348	4.4208
−0.320	+0.07039	−0.39044	+0.02389	0.3347	4.3655
−0.325	+0.07207	−0.38176	+0.04559	0.3345	4.3121
−0.330	+0.07374	−0.37319	+0.06702	0.3341	4.2603
−0.335	+0.07541	−0.36472	+0.08819	0.3336	4.2102
−0.340	+0.07708	−0.35635	+0.10912	0.3330	4.1616
−0.345	+0.07874	−0.34807	+0.12981	0.3323	4.1146
−0.350	+0.08040	−0.33989	+0.15027	0.3315	4.0689
−0.355	+0.08205	−0.33179	+0.17050	0.3306	4.0247
−0.360	+0.08370	−0.32379	+0.19052	0.3296	3.9818
−0.365	+0.08535	−0.31586	+0.21032	0.3285	3.9401
−0.370	+0.08699	−0.30802	+0.22992	0.3273	3.8997
−0.375	+0.08862	−0.30026	+0.24932	0.3260	3.8604
−0.380	+0.09025	−0.29258	+0.26853	0.3246	3.8223
−0.385	+0.09187	−0.28497	+0.28755	0.3231	3.7853
−0.390	+0.09348	−0.27744	+0.30639	0.3216	3.7493
−0.395	+0.09509	−0.26998	+0.32504	0.3199	3.7144
−0.400	+0.09668	−0.26258	+0.34353	0.3182	3.6804
−0.405	+0.09827	−0.25525	+0.36185	0.3165	3.6474
−0.410	+0.09985	−0.24799	+0.38001	0.3146	3.6153
−0.415	+0.10141	−0.24079	+0.39800	0.3127	3.5840
−0.420	+0.10297	−0.23365	+0.41585	0.3108	3.5537
−0.425	+0.10452	−0.22658	+0.43354	0.3087	3.5241
−0.430	+0.10606	−0.21956	+0.45109	0.3067	3.4953
−0.435	+0.10759	−0.21259	+0.46850	0.3045	3.4674
−0.440	+0.10911	−0.20569	+0.48577	0.3023	3.4401
−0.445	+0.11061	−0.19883	+0.50290	0.3001	3.4136
−0.450	+0.11211	−0.19203	+0.51990	0.2978	3.3878
−0.455	+0.11359	−0.18528	+0.53678	0.2955	3.3627
−0.460	+0.11506	−0.17858	+0.55353	0.2932	3.3382
−0.465	+0.11652	−0.17193	+0.57016	0.2908	3.3143
−0.470	+0.11797	−0.16532	+0.58668	0.2883	3.2911
−0.475	+0.11941	−0.15876	+0.60308	0.2859	3.2685
−0.480	+0.12083	−0.15225	+0.61936	0.2834	3.2465
−0.485	+0.12224	−0.14578	+0.63554	0.2809	3.2250
−0.490	+0.12364	−0.13935	+0.65162	0.2783	3.2041
−0.495	+0.12503	−0.13296	+0.66758	0.2757	3.1837
−0.500	+0.12640	−0.12661	+0.68345	0.2732	3.1638
−0.505	+0.12776	−0.12030	+0.69922	0.2705	3.1444
−0.510	+0.12910	−0.11403	+0.71490	0.2679	3.1255
−0.515	+0.13044	−0.10780	+0.73048	0.2652	3.1071
−0.520	+0.13176	−0.10161	+0.74597	0.2626	3.0892
−0.525	+0.13306	−0.09544	+0.76137	0.2599	3.0717
−0.530	+0.13436	−0.08932	+0.77669	0.2572	3.0546
−0.535	+0.13564	−0.08323	+0.79192	0.2545	3.0380
−0.540	+0.13690	−0.07717	+0.80707	0.2518	3.0217
−0.545	+0.13816	−0.07114	+0.82214	0.2491	3.0059
−0.550	+0.13939	−0.06514	+0.83713	0.2464	2.9905
−0.555	+0.14062	−0.05918	+0.85204	0.2437	2.9754
−0.560	+0.14183	−0.05324	+0.86689	0.2409	2.9607
−0.565	+0.14303	−0.04733	+0.88165	0.2382	2.9464
−0.570	+0.14421	−0.04145	+0.89635	0.2355	2.9325
−0.575	+0.14538	−0.03560	+0.91098	0.2327	2.9188
−0.580	+0.14654	−0.02978	+0.92554	0.2300	2.9056
−0.585	+0.14769	−0.02398	+0.94004	0.2273	2.8926
−0.590	+0.14882	−0.01821	+0.95447	0.2246	2.8799
−0.595	+0.14993	−0.01246	+0.96884	0.2219	2.8676
−0.600	+0.15103	−0.00674	+0.98314	0.2192	2.8556
−0.605	+0.15212	−0.00104	+0.99739	0.2165	2.8438

1517

1	4	5	6	7	8
-0.010	+0.00003	-2.03072	-4.03542	0.0092	109.8216
-0.015	+0.00010	-1.85222	-3.58916	0.0165	73.6414
-0.020	+0.00020	-1.72480	-3.27063	0.0247	55.5398
-0.025	+0.00035	-1.62541	-3.02215	0.0337	44.6752
-0.030	+0.00054	-1.54376	-2.81801	0.0432	37.4298
-0.035	+0.00078	-1.47435	-2.64448	0.0531	32.2526
-0.040	+0.00107	-1.41390	-2.49337	0.0633	28.3680
-0.045	+0.00141	-1.36031	-2.35939	0.0736	25.3451
-0.050	+0.00181	-1.31212	-2.23893	0.0841	22.9253
-0.055	+0.00225	-1.26832	-2.12942	0.0946	20.9441
-0.060	+0.00275	-1.22813	-2.02895	0.1051	19.2919
-0.065	+0.00331	-1.19098	-1.93608	0.1156	17.8927
-0.070	+0.00391	-1.15643	-1.84970	0.1260	16.6923
-0.075	+0.00457	-1.12411	-1.76890	0.1363	15.6510
-0.080	+0.00527	-1.09374	-1.69297	0.1465	14.7388
-0.085	+0.00603	-1.06508	-1.62133	0.1565	13.9332
-0.090	+0.00684	-1.03795	-1.55349	0.1664	13.2162
-0.095	+0.00770	-1.01217	-1.48905	0.1761	12.5739
-0.100	+0.00860	-0.98761	-1.42765	0.1855	11.9952
-0.105	+0.00955	-0.96415	-1.36901	0.1948	11.4709
-0.110	+0.01055	-0.94170	-1.31286	0.2038	10.9937
-0.115	+0.01159	-0.92015	-1.25900	0.2126	10.5574
-0.120	+0.01268	-0.89944	-1.20723	0.2212	10.1570
-0.125	+0.01380	-0.87950	-1.15738	0.2295	9.7880
-0.130	+0.01497	-0.86027	-1.10930	0.2376	9.4471
-0.135	+0.01618	-0.84170	-1.06287	0.2454	9.1309
-0.140	+0.01743	-0.82373	-1.01796	0.2530	8.8370
-0.145	+0.01871	-0.80634	-0.97446	0.2603	8.5629
-0.150	+0.02003	-0.78947	-0.93230	0.2674	8.3069
-0.155	+0.02138	-0.77310	-0.89137	0.2742	8.0670
-0.160	+0.02277	-0.75719	-0.85160	0.2807	7.8418
-0.165	+0.02419	-0.74172	-0.81293	0.2870	7.6300
-0.170	+0.02564	-0.72666	-0.77528	0.2931	7.4305
-0.175	+0.02712	-0.71199	-0.73860	0.2988	7.2421
-0.180	+0.02863	-0.69769	-0.70284	0.3044	7.0640
-0.185	+0.03017	-0.68373	-0.66795	0.3097	6.8954
-0.190	+0.03173	-0.67010	-0.63387	0.3147	6.7355
-0.195	+0.03331	-0.65678	-0.60058	0.3195	6.5836
-0.200	+0.03492	-0.64376	-0.56803	0.3240	6.4392
-0.205	+0.03655	-0.63102	-0.53618	0.3283	6.3018
-0.210	+0.03821	-0.61855	-0.50500	0.3324	6.1708
-0.215	+0.03988	-0.60633	-0.47446	0.3363	6.0458
-0.220	+0.04157	-0.59436	-0.44453	0.3399	5.9264
-0.225	+0.04328	-0.58262	-0.41518	0.3433	5.8122
-0.230	+0.04500	-0.57111	-0.38640	0.3465	5.7030
-0.235	+0.04674	-0.55981	-0.35815	0.3494	5.5984
-0.240	+0.04850	-0.54871	-0.33041	0.3522	5.4981
-0.245	+0.05026	-0.53781	-0.30316	0.3547	5.4019
-0.250	+0.05204	-0.52710	-0.27638	0.3570	5.3095
-0.255	+0.05383	-0.51657	-0.25006	0.3592	5.2208
-0.260	+0.05563	-0.50622	-0.22417	0.3611	5.1354
-0.265	+0.05744	-0.49603	-0.19870	0.3628	5.0533
-0.270	+0.05926	-0.48600	-0.17363	0.3644	4.9743
-0.275	+0.06109	-0.47613	-0.14895	0.3658	4.8982
-0.280	+0.06292	-0.46641	-0.12464	0.3670	4.8248
-0.285	+0.06476	-0.45683	-0.10070	0.3680	4.7540
-0.290	+0.06660	-0.44739	-0.07710	0.3688	4.6858
-0.295	+0.06845	-0.43808	-0.05383	0.3695	4.6199
-0.300	+0.07030	-0.42891	-0.03089	0.3700	4.5562
-0.305	+0.07215	-0.41986	-0.00827	0.3704	4.4947
-0.310	+0.07400	-0.41093	+0.01405	0.3706	4.4353
-0.315	+0.07585	-0.40211	+0.03608	0.3707	4.3778
-0.320	+0.07771	-0.39341	+0.05783	0.3706	4.3221
-0.325	+0.07956	-0.38482	+0.07930	0.3704	4.2683
-0.330	+0.08141	-0.37634	+0.10051	0.3700	4.2162
-0.335	+0.08326	-0.36796	+0.12147	0.3695	4.1657
-0.340	+0.08511	-0.35967	+0.14217	0.3689	4.1168
-0.345	+0.08695	-0.35149	+0.16264	0.3682	4.0694
-0.350	+0.08879	-0.34340	+0.18287	0.3673	4.0235
-0.355	+0.09062	-0.33539	+0.20288	0.3663	3.9789
-0.360	+0.09245	-0.32748	+0.22266	0.3652	3.9357
-0.365	+0.09428	-0.31965	+0.24224	0.3640	3.8937
-0.370	+0.09609	-0.31190	+0.26160	0.3627	3.8530
-0.375	+0.09790	-0.30424	+0.28077	0.3613	3.8135
-0.380	+0.09971	-0.29665	+0.29974	0.3598	3.7752
-0.385	+0.10150	-0.28914	+0.31852	0.3582	3.7379
-0.390	+0.10329	-0.28170	+0.33712	0.3565	3.7017
-0.395	+0.10507	-0.27433	+0.35554	0.3547	3.6665
-0.400	+0.10684	-0.26703	+0.37379	0.3529	3.6323
-0.405	+0.10860	-0.25980	+0.39187	0.3509	3.5991
-0.410	+0.11035	-0.25263	+0.40978	0.3489	3.5668
-0.415	+0.11209	-0.24553	+0.42754	0.3468	3.5354
-0.420	+0.11381	-0.23849	+0.44514	0.3447	3.5048
-0.425	+0.11553	-0.23151	+0.46259	0.3424	3.4751
-0.430	+0.11724	-0.22459	+0.47989	0.3401	3.4462
-0.435	+0.11893	-0.21772	+0.49705	0.3378	3.4181
-0.440	+0.12062	-0.21091	+0.51407	0.3354	3.3907
-0.445	+0.12229	-0.20416	+0.53096	0.3329	3.3641
-0.450	+0.12395	-0.19746	+0.54772	0.3304	3.3381
-0.455	+0.12559	-0.19081	+0.56434	0.3279	3.3129
-0.460	+0.12723	-0.18421	+0.58085	0.3253	3.2883
-0.465	+0.12885	-0.17765	+0.59723	0.3226	3.2644
-0.470	+0.13045	-0.17115	+0.61349	0.3199	3.2411
-0.475	+0.13205	-0.16469	+0.62964	0.3172	3.2184
-0.480	+0.13363	-0.15827	+0.64568	0.3144	3.1962
-0.485	+0.13519	-0.15190	+0.66160	0.3116	3.1747
-0.490	+0.13674	-0.14557	+0.67743	0.3088	3.1537
-0.495	+0.13828	-0.13929	+0.69314	0.3060	3.1333
-0.500	+0.13980	-0.13304	+0.70876	0.3031	3.1134
-0.505	+0.14131	-0.12683	+0.72428	0.3002	3.0940
-0.510	+0.14280	-0.12066	+0.73970	0.2972	3.0750
-0.515	+0.14428	-0.11453	+0.75503	0.2943	3.0566
-0.520	+0.14575	-0.10844	+0.77027	0.2913	3.0387
-0.525	+0.14720	-0.10238	+0.78542	0.2884	3.0211
-0.530	+0.14863	-0.09635	+0.80048	0.2854	3.0041
-0.535	+0.15005	-0.09036	+0.81546	0.2824	2.9874
-0.540	+0.15146	-0.08440	+0.83036	0.2794	2.9712
-0.545	+0.15285	-0.07847	+0.84517	0.2763	2.9554
-0.550	+0.15422	-0.07258	+0.85991	0.2733	2.9400
-0.555	+0.15558	-0.06671	+0.87457	0.2703	2.9250
-0.560	+0.15692	-0.06088	+0.88916	0.2672	2.9104
-0.565	+0.15825	-0.05507	+0.90368	0.2642	2.8961
-0.570	+0.15957	-0.04929	+0.91812	0.2612	2.8822
-0.575	+0.16086	-0.04354	+0.93250	0.2581	2.8686
-0.580	+0.16215	-0.03782	+0.94681	0.2551	2.8554
-0.585	+0.16342	-0.03212	+0.96106	0.2521	2.8425
-0.590	+0.16467	-0.02645	+0.97524	0.2490	2.8299
-0.595	+0.16591	-0.02080	+0.98936	0.2460	2.8176
-0.600	+0.16713	-0.01518	+1.00341	0.2430	2.8057
-0.605	+0.16834	-0.00958	+1.01741	0.2400	2.7940

1518

1	4	5	6	7	8
-0.010	+0.00004	-2.03072	-3.99763	0.0100	109.8206
-0.015	+0.00011	-1.85222	-3.55138	0.0180	73.6401
-0.020	+0.00022	-1.72481	-3.23286	0.0270	55.5380
-0.025	+0.00038	-1.62542	-2.98439	0.0368	44.6728
-0.030	+0.00059	-1.54377	-2.78026	0.0472	37.4268
-0.035	+0.00085	-1.47437	-2.60675	0.0580	32.2489
-0.040	+0.00117	-1.41393	-2.45566	0.0690	28.3635
-0.045	+0.00154	-1.36035	-2.32170	0.0803	25.3398
-0.050	+0.00197	-1.31218	-2.20127	0.0918	22.9193
-0.055	+0.00246	-1.26838	-2.09179	0.1032	20.9373
-0.060	+0.00301	-1.22821	-1.99136	0.1147	19.2842
-0.065	+0.00361	-1.19108	-1.89853	0.1262	17.8842
-0.070	+0.00427	-1.15654	-1.81219	0.1376	16.6829
-0.075	+0.00498	-1.12424	-1.73144	0.1488	15.6407
-0.080	+0.00576	-1.09390	-1.65557	0.1599	14.7277
-0.085	+0.00658	-1.06526	-1.58399	0.1709	13.9211
-0.090	+0.00747	-1.03815	-1.51621	0.1817	13.2033
-0.095	+0.00840	-1.01240	-1.45183	0.1922	12.5602
-0.100	+0.00939	-0.98787	-1.39051	0.2026	11.9805
-0.105	+0.01043	-0.96444	-1.33194	0.2127	11.4554
-0.110	+0.01152	-0.94202	-1.27587	0.2226	10.9773
-0.115	+0.01265	-0.92051	-1.22210	0.2323	10.5402
-0.120	+0.01384	-0.89983	-1.17041	0.2416	10.1388
-0.125	+0.01507	-0.87993	-1.12066	0.2508	9.7691
-0.130	+0.01635	-0.86074	-1.07268	0.2596	9.4273
-0.135	+0.01767	-0.84220	-1.02634	0.2682	9.1103
-0.140	+0.01903	-0.82428	-0.98154	0.2765	8.8155
-0.145	+0.02043	-0.80693	-0.93815	0.2845	8.5407
-0.150	+0.02187	-0.79011	-0.89610	0.2923	8.2838
-0.155	+0.02335	-0.77378	-0.85529	0.2998	8.0431
-0.160	+0.02487	-0.75792	-0.81564	0.3070	7.8171
-0.165	+0.02642	-0.74250	-0.77710	0.3139	7.6046
-0.170	+0.02801	-0.72750	-0.73958	0.3205	7.4043
-0.175	+0.02963	-0.71288	-0.70303	0.3269	7.2151
-0.180	+0.03128	-0.69863	-0.66741	0.3330	7.0363
-0.185	+0.03296	-0.68473	-0.63265	0.3388	6.8669
-0.190	+0.03467	-0.67116	-0.59873	0.3444	6.7063
-0.195	+0.03640	-0.65790	-0.56558	0.3497	6.5537
-0.200	+0.03817	-0.64494	-0.53318	0.3547	6.4086
-0.205	+0.03995	-0.63226	-0.50148	0.3595	6.2705

1	4	5	6	7	8
−0.210	+0.04176	−0.61985	−0.47046	0.3640	6.1388
−0.215	+0.04359	−0.60770	−0.44008	0.3683	6.0131
−0.220	+0.04544	−0.59579	−0.41032	0.3723	5.8931
−0.225	+0.04731	−0.58412	−0.38114	0.3760	5.7783
−0.230	+0.04920	−0.57268	−0.35253	0.3796	5.6685
−0.235	+0.05111	−0.56144	−0.32445	0.3829	5.5633
−0.240	+0.05303	−0.55042	−0.29689	0.3859	5.4624
−0.245	+0.05497	−0.53959	−0.26982	0.3888	5.3656
−0.250	+0.05692	−0.52895	−0.24322	0.3914	5.2726
−0.255	+0.05888	−0.51850	−0.21708	0.3938	5.1833
−0.260	+0.06086	−0.50822	−0.19138	0.3960	5.0975
−0.265	+0.06284	−0.49811	−0.16610	0.3979	5.0148
−0.270	+0.06484	−0.48816	−0.14123	0.3997	4.9353
−0.275	+0.06684	−0.47836	−0.11675	0.4012	4.8587
−0.280	+0.06885	−0.46872	−0.09264	0.4026	4.7848
−0.285	+0.07087	−0.45922	−0.06889	0.4038	4.7136
−0.290	+0.07289	−0.44986	−0.04550	0.4048	4.6448
−0.295	+0.07491	−0.44064	−0.02244	0.4056	4.5785
−0.300	+0.07694	−0.43155	+0.00028	0.4062	4.5144
−0.305	+0.07898	−0.42258	+0.02270	0.4066	4.4524
−0.310	+0.08101	−0.41374	+0.04481	0.4069	4.3926
−0.315	+0.08305	−0.40501	+0.06663	0.4070	4.3347
−0.320	+0.08508	−0.39640	+0.08816	0.4070	4.2787
−0.325	+0.08712	−0.38789	+0.10942	0.4068	4.2245
−0.330	+0.08915	−0.37950	+0.13041	0.4065	4.1720
−0.335	+0.09118	−0.37120	+0.15114	0.4060	4.1211
−0.340	+0.09321	−0.36301	+0.17162	0.4053	4.0719
−0.345	+0.09523	−0.35492	+0.19186	0.4046	4.0241
−0.350	+0.09726	−0.34691	+0.21187	0.4036	3.9779
−0.355	+0.09927	−0.33900	+0.23164	0.4026	3.9330
−0.360	+0.10128	−0.33118	+0.25120	0.4014	3.8895
−0.365	+0.10329	−0.32344	+0.27054	0.4002	3.8473
−0.370	+0.10528	−0.31579	+0.28967	0.3988	3.8063
−0.375	+0.10727	−0.30822	+0.30861	0.3972	3.7665
−0.380	+0.10926	−0.30072	+0.32734	0.3956	3.7279
−0.385	+0.11123	−0.29331	+0.34589	0.3939	3.6903
−0.390	+0.11320	−0.28596	+0.36425	0.3921	3.6539
−0.395	+0.11515	−0.27869	+0.38243	0.3901	3.6185
−0.400	+0.11710	−0.27149	+0.40043	0.3881	3.5841
−0.405	+0.11903	−0.26435	+0.41827	0.3860	3.5507
−0.410	+0.12096	−0.25728	+0.43594	0.3838	3.5182
−0.415	+0.12287	−0.25028	+0.45345	0.3816	3.4866
−0.420	+0.12477	−0.24334	+0.47081	0.3792	3.4558
−0.425	+0.12666	−0.23645	+0.48802	0.3768	3.4260
−0.430	+0.12854	−0.22963	+0.50507	0.3743	3.3969
−0.435	+0.13041	−0.22287	+0.52199	0.3717	3.3686
−0.440	+0.13226	−0.21616	+0.53876	0.3691	3.3411
−0.445	+0.13410	−0.20950	+0.55540	0.3664	3.3143
−0.450	+0.13592	−0.20290	+0.57190	0.3637	3.2883
−0.455	+0.13774	−0.19635	+0.58828	0.3608	3.2629
−0.460	+0.13953	−0.18985	+0.60454	0.3580	3.2382
−0.465	+0.14132	−0.18339	+0.62067	0.3551	3.2142
−0.470	+0.14308	−0.17699	+0.63668	0.3521	3.1908
−0.475	+0.14484	−0.17063	+0.65258	0.3491	3.1680
−0.480	+0.14658	−0.16432	+0.66836	0.3461	3.1458
−0.485	+0.14830	−0.15805	+0.68403	0.3430	3.1242
−0.490	+0.15001	−0.15182	+0.69960	0.3399	3.1031
−0.495	+0.15170	−0.14563	+0.71507	0.3368	3.0827
−0.500	+0.15338	−0.13949	+0.73043	0.3336	3.0627
−0.505	+0.15504	−0.13338	+0.74570	0.3304	3.0432
−0.510	+0.15668	−0.12731	+0.76086	0.3272	3.0243
−0.515	+0.15831	−0.12128	+0.77594	0.3240	3.0058
−0.520	+0.15992	−0.11529	+0.79092	0.3207	2.9879
−0.525	+0.16152	−0.10933	+0.80582	0.3174	2.9703
−0.530	+0.16309	−0.10341	+0.82063	0.3141	2.9533
−0.535	+0.16466	−0.09752	+0.83535	0.3108	2.9366
−0.540	+0.16620	−0.09166	+0.85000	0.3075	2.9204
−0.545	+0.16773	−0.08584	+0.86456	0.3041	2.9047
−0.550	+0.16925	−0.08004	+0.87904	0.3008	2.8893
−0.555	+0.17074	−0.07428	+0.89345	0.2975	2.8743
−0.560	+0.17222	−0.06854	+0.90779	0.2941	2.8597
−0.565	+0.17368	−0.06284	+0.92205	0.2907	2.8454
−0.570	+0.17513	−0.05716	+0.93624	0.2874	2.8316
−0.575	+0.17656	−0.05151	+0.95037	0.2840	2.8180
−0.580	+0.17797	−0.04589	+0.96442	0.2807	2.8049
−0.585	+0.17936	−0.04029	+0.97842	0.2773	2.7920
−0.590	+0.18074	−0.03472	+0.99235	0.2740	2.7795
−0.595	+0.18210	−0.02917	+1.00621	0.2707	2.7673
−0.600	+0.18345	−0.02365	+1.02002	0.2673	2.7554
−0.605	+0.18478	−0.01815	+1.03377	0.2640	2.7439

1519

1	4	5	6	7	8
−0.010	+0.00004	−2.03072	−3.96287	0.0109	109.8207
−0.015	+0.00011	−1.85222	−3.51663	0.0195	73.6394
−0.020	+0.00024	−1.72482	−3.19810	0.0293	55.5366
−0.025	+0.00041	−1.62543	−2.94964	0.0399	44.6707
−0.030	+0.00064	−1.54379	−2.74553	0.0511	37.4239
−0.035	+0.00092	−1.47439	−2.57204	0.0628	32.2453
−0.040	+0.00127	−1.41396	−2.42096	0.0748	28.3592
−0.045	+0.00167	−1.36039	−2.28703	0.0871	25.3347
−0.050	+0.00214	−1.31223	−2.16663	0.0994	22.9133
−0.055	+0.00267	−1.26845	−2.05718	0.1119	20.9305
−0.060	+0.00326	−1.22829	−1.95678	0.1243	19.2766
−0.065	+0.00391	−1.19117	−1.86400	0.1368	17.8757
−0.070	+0.00463	−1.15665	−1.77770	0.1491	16.6736
−0.075	+0.00540	−1.12437	−1.69700	0.1613	15.6305
−0.080	+0.00624	−1.09405	−1.62118	0.1734	14.7166
−0.085	+0.00714	−1.06544	−1.54966	0.1853	13.9092
−0.090	+0.00809	−1.03835	−1.48194	0.1970	13.1904
−0.095	+0.00911	−1.01263	−1.41763	0.2085	12.5464
−0.100	+0.01018	−0.98812	−1.35637	0.2197	11.9659
−0.105	+0.01130	−0.96473	−1.29788	0.2307	11.4399
−0.110	+0.01248	−0.94233	−1.24190	0.2415	10.9610
−0.115	+0.01372	−0.92086	−1.18820	0.2519	10.5229
−0.120	+0.01500	−0.90022	−1.13661	0.2621	10.1208
−0.125	+0.01634	−0.88035	−1.08694	0.2721	9.7502
−0.130	+0.01772	−0.86120	−1.03906	0.2817	9.4075
−0.135	+0.01916	−0.84271	−0.99283	0.2910	9.0897
−0.140	+0.02063	−0.82483	−0.94813	0.3001	8.7941
−0.145	+0.02216	−0.80752	−0.90485	0.3089	8.5184
−0.150	+0.02372	−0.79074	−0.86291	0.3173	8.2607
−0.155	+0.02533	−0.77446	−0.82222	0.3255	8.0192
−0.160	+0.02698	−0.75865	−0.78270	0.3333	7.7924
−0.165	+0.02866	−0.74328	−0.74427	0.3409	7.5791
−0.170	+0.03039	−0.72833	−0.70688	0.3482	7.3780
−0.175	+0.03215	−0.71376	−0.67047	0.3551	7.1881
−0.180	+0.03394	−0.69957	−0.63499	0.3618	7.0086
−0.185	+0.03576	−0.68572	−0.60037	0.3682	6.8385
−0.190	+0.03762	−0.67221	−0.56659	0.3743	6.6771
−0.195	+0.03951	−0.65901	−0.53359	0.3801	6.5238
−0.200	+0.04142	−0.64611	−0.50133	0.3856	6.3780
−0.205	+0.04336	−0.63349	−0.46979	0.3908	6.2392
−0.210	+0.04533	−0.62115	−0.43893	0.3958	6.1068
−0.215	+0.04732	−0.60906	−0.40872	0.4005	5.9805
−0.220	+0.04933	−0.59722	−0.37912	0.4049	5.8598
−0.225	+0.05137	−0.58562	−0.35011	0.4091	5.7444
−0.230	+0.05343	−0.57424	−0.32166	0.4130	5.6339
−0.235	+0.05550	−0.56308	−0.29376	0.4166	5.5281
−0.240	+0.05759	−0.55213	−0.26638	0.4200	5.4266
−0.245	+0.05970	−0.54137	−0.23949	0.4232	5.3293
−0.250	+0.06182	−0.53081	−0.21308	0.4261	5.2357
−0.255	+0.06396	−0.52042	−0.18712	0.4288	5.1459
−0.260	+0.06611	−0.51022	−0.16161	0.4312	5.0595
−0.265	+0.06827	−0.50018	−0.13652	0.4334	4.9763
−0.270	+0.07045	−0.49031	−0.11184	0.4354	4.8962
−0.275	+0.07263	−0.48060	−0.08756	0.4371	4.8191
−0.280	+0.07482	−0.47103	−0.06365	0.4387	4.7447
−0.285	+0.07701	−0.46162	−0.04010	0.4400	4.6730
−0.290	+0.07922	−0.45234	−0.01691	0.4412	4.6038
−0.295	+0.08143	−0.44320	+0.00593	0.4421	4.5370
−0.300	+0.08364	−0.43419	+0.02845	0.4428	4.4725
−0.305	+0.08586	−0.42531	+0.05066	0.4434	4.4101
−0.310	+0.08807	−0.41655	+0.07256	0.4438	4.3498
−0.315	+0.09029	−0.40791	+0.09416	0.4439	4.2915
−0.320	+0.09251	−0.39938	+0.11548	0.4440	4.2351
−0.325	+0.09473	−0.39097	+0.13651	0.4438	4.1805
−0.330	+0.09695	−0.38266	+0.15728	0.4435	4.1276
−0.335	+0.09917	−0.37445	+0.17779	0.4430	4.0764
−0.340	+0.10138	−0.36635	+0.19805	0.4423	4.0268
−0.345	+0.10359	−0.35835	+0.21807	0.4415	3.9788
−0.350	+0.10580	−0.35043	+0.23784	0.4406	3.9322
−0.355	+0.10800	−0.34262	+0.25739	0.4395	3.8870
−0.360	+0.11019	−0.33489	+0.27672	0.4383	3.8432
−0.365	+0.11238	−0.32724	+0.29582	0.4369	3.8006
−0.370	+0.11456	−0.31968	+0.31472	0.4354	3.7594
−0.375	+0.11674	−0.31220	+0.33342	0.4338	3.7193
−0.380	+0.11890	−0.30480	+0.35192	0.4321	3.6804
−0.385	+0.12106	−0.29748	+0.37023	0.4303	3.6427
−0.390	+0.12320	−0.29023	+0.38835	0.4283	3.6060
−0.395	+0.12534	−0.28306	+0.40629	0.4262	3.5703
−0.400	+0.12747	−0.27595	+0.42405	0.4241	3.5357
−0.405	+0.12958	−0.26891	+0.44165	0.4218	3.5021

-0.410	+0.13168	−0.26194	+0.45908	0.4194	3.4694
-0.415	+0.13378	−0.25503	+0.47634	0.4170	3.4376
-0.420	+0.13585	−0.24819	+0.49345	0.4144	3.4067
-0.425	+0.13792	−0.24141	+0.51041	0.4118	3.3766
-0.430	+0.13997	−0.23468	+0.52722	0.4091	3.3474
-0.435	+0.14201	−0.22802	+0.54389	0.4063	3.3189
-0.440	+0.14404	−0.22141	+0.56041	0.4035	3.2913
-0.445	+0.14605	−0.21485	+0.57680	0.4006	3.2644
-0.450	+0.14804	−0.20835	+0.59306	0.3976	3.2382
-0.455	+0.15002	−0.20190	+0.60919	0.3945	3.2127
-0.460	+0.15199	−0.19550	+0.62519	0.3914	−3.1879
-0.465	+0.15394	−0.18915	+0.64107	0.3882	3.1637
-0.470	+0.15587	−0.18284	+0.65683	0.3850	3.1402
-0.475	+0.15779	−0.17658	+0.67247	0.3818	3.1174
-0.480	+0.15969	−0.17037	+0.68800	0.3785	3.0951
-0.485	+0.16157	−0.16420	+0.70342	0.3751	3.0734
-0.490	+0.16344	−0.15808	+0.71874	0.3717	3.0523
-0.495	+0.16529	−0.15199	+0.73395	0.3683	3.0318
-0.500	+0.16712	−0.14595	+0.74906	0.3648	3.0117
-0.505	+0.16894	−0.13995	+0.76407	0.3613	2.9923
-0.510	+0.17074	−0.13398	+0.77898	0.3578	2.9733
-0.515	+0.17252	−0.12805	+0.79380	0.3543	2.9548
-0.520	+0.17428	−0.12216	+0.80853	0.3507	2.9368
-0.525	+0.17603	−0.11630	+0.82317	0.3471	2.9193
-0.530	+0.17775	−0.11048	+0.83772	0.3435	2.9022
-0.535	+0.17946	−0.10469	+0.85219	0.3399	2.8855
-0.540	+0.18115	−0.09894	+0.86658	0.3362	2.8693
-0.545	+0.18282	−0.09322	+0.88089	0.3326	2.8536
-0.550	+0.18448	−0.08753	+0.89512	0.3289	2.8382
-0.555	+0.18611	−0.08186	+0.90927	0.3252	2.8232
-0.560	+0.18773	−0.07623	+0.92335	0.3216	2.8086
-0.565	+0.18933	−0.07063	+0.93736	0.3179	2.7944
-0.570	+0.19091	−0.06505	+0.95129	0.3142	2.7806
-0.575	+0.19247	−0.05951	+0.96516	0.3105	2.7671
-0.580	+0.19401	−0.05398	+0.97897	0.3068	2.7540
-0.585	+0.19554	−0.04849	+0.99271	0.3032	2.7412
-0.590	+0.19705	−0.04302	+1.00638	0.2995	2.7288
-0.595	+0.19854	−0.03757	+1.01999	0.2958	2.7166
-0.600	+0.20001	−0.03215	+1.03355	0.2922	2.7048
-0.605	+0.20146	−0.02675	+1.04704	0.2885	2.6933

1520

1	4	5	6	7	8
-0.010	+0.00004	−2.03072	−3.93069	0.0117	109.8197
-0.015	+0.00012	−1.85223	−3.48445	0.0210	73.6381
-0.020	+0.00026	−1.72482	−3.16593	0.0315	55.5348
-0.025	+0.00044	−1.62544	−2.91748	0.0429	44.6683
-0.030	+0.00069	−1.54380	−2.71338	0.0550	37.4209
-0.035	+0.00099	−1.47441	−2.53991	0.0676	32.2416
-0.040	+0.00136	−1.41399	−2.38886	0.0806	28.3547
-0.045	+0.00180	−1.36043	−2.25495	0.0938	25.3294
-0.050	+0.00230	−1.31228	−2.13457	0.1071	22.9073
-0.055	+0.00287	−1.26851	−2.02516	0.1205	20.9236
-0.060	+0.00351	−1.22837	−1.92480	0.1339	19.2689
-0.065	+0.00421	−1.19127	−1.83205	0.1473	17.8671
-0.070	+0.00498	−1.15677	−1.74580	0.1606	16.6641
-0.075	+0.00582	−1.12451	−1.66515	0.1738	15.6202
-0.080	+0.00672	−1.09420	−1.58938	0.1868	14.7055
-0.085	+0.00769	−1.06562	−1.51792	0.1997	13.8972
-0.090	+0.00872	−1.03856	−1.45026	0.2123	13.1775
-0.095	+0.00981	−1.01286	−1.38602	0.2247	12.5327
-0.100	+0.01097	−0.98830	−1.32483	0.2368	11.9513
-0.105	+0.01218	−0.96502	−1.26641	0.2487	11.4244
-0.110	+0.01345	−0.94265	−1.21051	0.2603	10.9446
-0.115	+0.01478	−0.92121	−1.15690	0.2717	10.5057
-0.120	+0.01617	−0.90061	−1.10539	0.2827	10.1027
-0.125	+0.01761	−0.88078	−1.05582	0.2934	9.7312
-0.130	+0.01910	−0.86166	−1.00804	0.3039	9.3877
-0.135	+0.02065	−0.84321	−0.96190	0.3140	9.0690
-0.140	+0.02224	−0.82537	−0.91731	0.3238	8.7726
-0.145	+0.02389	−0.80811	−0.87415	0.3333	8.4961
-0.150	+0.02558	−0.79138	−0.83232	0.3424	8.2375
-0.155	+0.02731	−0.77515	−0.79174	0.3513	7.9953
-0.160	+0.02909	−0.75939	−0.75234	0.3598	7.7677
-0.165	+0.03091	−0.74407	−0.71404	0.3680	7.5536
-0.170	+0.03277	−0.72916	−0.67678	0.3759	7.3518
-0.175	+0.03467	−0.71465	−0.64051	0.3835	7.1611
-0.180	+0.03660	−0.70051	−0.60516	0.3908	6.9808
-0.185	+0.03858	−0.68672	−0.57068	0.3977	6.8099
-0.190	+0.04058	−0.67327	−0.53704	0.4043	6.6479
-0.195	+0.04262	−0.66013	−0.50419	0.4107	6.4939
-0.200	+0.04469	−0.64729	−0.47209	0.4167	6.3474
-0.205	+0.04679	−0.63473	−0.44070	0.4224	6.2079

1	4	5	6	7	8
−0.210	+0.04891	−0.62245	−0.41000	0.4279	6.0748
−0.215	+0.05106	−0.61043	−0.37995	0.4330	5.9478
−0.220	+0.05324	−0.59865	−0.35051	0.4379	5.8265
−0.225	+0.05544	−0.58712	−0.32167	0.4424	5.7105
−0.230	+0.05767	−0.57581	−0.29340	0.4467	5.5994
−0.235	+0.05991	−0.56472	−0.26567	0.4507	5.4929
−0.240	+0.06217	−0.55383	−0.23846	0.4545	5.3908
−0.245	+0.06446	−0.54315	−0.21175	0.4579	5.2929
−0.250	+0.06675	−0.53266	−0.18553	0.4612	5.1988
−0.255	+0.06907	−0.52235	−0.15976	0.4641	5.1084
−0.260	+0.07139	−0.51222	−0.13444	0.4668	5.0214
−0.265	+0.07374	−0.50227	−0.10954	0.4693	4.9377
−0.270	+0.07609	−0.49247	−0.08505	0.4715	4.8571
−0.275	+0.07845	−0.48284	−0.06096	0.4735	4.7795
−0.280	+0.08082	−0.47335	−0.03725	0.4752	4.7046
−0.285	+0.08320	−0.46401	−0.01391	0.4767	4.6324
−0.290	+0.08559	−0.45482	+0.00906	0.4780	4.5627
−0.295	+0.08798	−0.44576	+0.03171	0.4791	4.4955
−0.300	+0.09038	−0.43684	+0.05402	0.4800	4.4305
−0.305	+0.09278	−0.42804	+0.07602	0.4806	4.3677
−0.310	+0.09519	−0.41936	+0.09770	0.4811	4.3070
−0.315	+0.09759	−0.41081	+0.11909	0.4814	4.2483
−0.320	+0.10000	−0.40237	+0.14019	0.4814	4.1914
−0.325	+0.10241	−0.39404	+0.16101	0.4813	4.1365
−0.330	+0.10481	−0.38582	+0.18156	0.4810	4.0832
−0.335	+0.10722	−0.37771	+0.20185	0.4806	4.0317
−0.340	+0.10962	−0.36969	+0.22188	0.4799	3.9817
−0.345	+0.11202	−0.36178	+0.24167	0.4791	3.9333
−0.350	+0.11441	−0.35396	+0.26121	0.4781	3.8864
−0.355	+0.11680	−0.34623	+0.28053	0.4770	3.8409
−0.360	+0.11918	−0.33860	+0.29963	0.4757	3.7967
−0.365	+0.12156	−0.33105	+0.31850	0.4743	3.7539
−0.370	+0.12392	−0.32358	+0.33717	0.4728	3.7123
−0.375	+0.12628	−0.31619	+0.35563	0.4711	3.6720
−0.380	+0.12864	−0.30889	+0.37389	0.4692	3.6329
−0.385	+0.13098	−0.30166	+0.39196	0.4673	3.5948
−0.390	+0.13331	−0.29451	+0.40984	0.4652	3.5579
−0.395	+0.13563	−0.28743	+0.42754	0.4630	3.5220
−0.400	+0.13794	−0.28042	+0.44506	0.4607	3.4872
−0.405	+0.14024	−0.27348	+0.46241	0.4582	3.4533
−0.410	+0.14252	−0.26661	+0.47960	0.4557	3.4204
−0.415	+0.14479	−0.25980	+0.49662	0.4531	3.3884
−0.420	+0.14705	−0.25305	+0.51348	0.4504	3.3573
−0.425	+0.14930	−0.24637	+0.53019	0.4475	3.3271
−0.430	+0.15153	−0.23974	+0.54676	0.4446	3.2977
−0.435	+0.15374	−0.23318	+0.56317	0.4416	3.2691
−0.440	+0.15595	−0.22667	+0.57945	0.4386	3.2413
−0.445	+0.15813	−0.22021	+0.59559	0.4354	3.2142
−0.450	+0.16030	−0.21381	+0.61159	0.4322	3.1879
−0.455	+0.16245	−0.20746	+0.62747	0.4289	3.1623
−0.460	+0.16459	−0.20116	+0.64322	0.4255	3.1373
−0.465	+0.16671	−0.19491	+0.65884	0.4221	3.1131
−0.470	+0.16881	−0.18871	+0.67435	0.4186	3.0895
−0.475	+0.17089	−0.18255	+0.68974	0.4151	3.0665
−0.480	+0.17296	−0.17644	+0.70502	0.4115	3.0442
−0.485	+0.17501	−0.17037	+0.72018	0.4079	3.0224
−0.490	+0.17704	−0.16435	+0.73524	0.4042	3.0012
−0.495	+0.17905	−0.15837	+0.75020	0.4005	2.9806
−0.500	+0.18105	−0.15243	+0.76505	0.3967	2.9605
−0.505	+0.18302	−0.14652	+0.77980	0.3929	2.9410
−0.510	+0.18498	−0.14066	+0.79446	0.3891	2.9220
−0.515	+0.18691	−0.13484	+0.80902	0.3852	2.9035
−0.520	+0.18883	−0.12905	+0.82350	0.3814	2.8854
−0.525	+0.19073	−0.12329	+0.83788	0.3774	2.8679
−0.530	+0.19260	−0.11758	+0.85218	0.3735	2.8508
−0.535	+0.19446	−0.11189	+0.86639	0.3696	2.8341
−0.540	+0.19630	−0.10624	+0.88052	0.3656	2.8179
−0.545	+0.19812	−0.10062	+0.89457	0.3616	2.8022
−0.550	+0.19992	−0.09503	+0.90854	0.3576	2.7868
−0.555	+0.20169	−0.08947	+0.92244	0.3536	2.7718
−0.560	+0.20345	−0.08394	+0.93626	0.3496	2.7573
−0.565	+0.20519	−0.07844	+0.95001	0.3456	2.7431
−0.570	+0.20691	−0.07297	+0.96369	0.3416	2.7293
−0.575	+0.20861	−0.06752	+0.97731	0.3376	2.7159
−0.580	+0.21029	−0.06210	+0.99085	0.3336	2.7028
−0.585	+0.21194	−0.05671	+1.00434	0.3296	2.6900
−0.590	+0.21358	−0.05134	+1.01775	0.3256	2.6776
−0.595	+0.21520	−0.04600	+1.03111	0.3216	2.6656
−0.600	+0.21680	−0.04068	+1.04441	0.3176	2.6538
−0.605	+0.21838	−0.03539	+1.05765	0.3136	2.6424

1521

1	4	5	6	7	8
−0.010	+0.00005	−2.03073	−3.90073	0.0125	109.8189
−0.015	+0.00013	−1.85223	−3.45449	0.0225	73.6369
−0.020	+0.00027	−1.72483	−3.13599	0.0338	55.5331
−0.025	+0.00047	−1.62545	−2.88755	0.0460	44.6659
−0.030	+0.00074	−1.54382	−2.68346	0.0590	37.4178
−0.035	+0.00107	−1.47443	−2.51000	0.0725	32.2378
−0.040	+0.00146	−1.41402	−2.35897	0.0864	28.3502
−0.045	+0.00193	−1.36047	−2.22509	0.1005	25.3242
−0.050	+0.00247	−1.31233	−2.10474	0.1148	22.9012
−0.055	+0.00308	−1.26857	−1.99535	0.1292	20.9167
−0.060	+0.00376	−1.22845	−1.89503	0.1436	19.2611
−0.065	+0.00451	−1.19136	−1.80233	0.1579	17.8585
−0.070	+0.00534	−1.15688	−1.71612	0.1722	16.6547
−0.075	+0.00624	−1.12464	−1.63552	0.1863	15.6099
−0.080	+0.00720	−1.09436	−1.55981	0.2003	14.6943
−0.085	+0.00824	−1.06579	−1.48840	0.2141	13.8851
−0.090	+0.00934	−1.03876	−1.42081	0.2276	13.1646
−0.095	+0.01052	−1.01308	−1.35663	0.2409	12.5189
−0.100	+0.01175	−0.98864	−1.29552	0.2540	11.9366
−0.105	+0.01306	−0.96530	−1.23717	0.2668	11.4089
−0.110	+0.01442	−0.94297	−1.18135	0.2792	10.9282
−0.115	+0.01585	−0.92156	−1.12782	0.2914	10.4884
−0.120	+0.01734	−0.90099	−1.07641	0.3033	10.0845
−0.125	+0.01888	−0.88120	−1.02693	0.3148	9.7122
−0.130	+0.02048	−0.86213	−0.97924	0.3261	9.3678
−0.135	+0.02214	−0.84371	−0.93321	0.3370	9.0483
−0.140	+0.02385	−0.82592	−0.88872	0.3475	8.7511
−0.145	+0.02562	−0.80870	−0.84566	0.3578	8.4737
−0.150	+0.02743	−0.79201	−0.80395	0.3677	8.2144
−0.155	+0.02929	−0.77583	−0.76349	0.3772	7.9713
−0.160	+0.03120	−0.76012	−0.72421	0.3864	7.7430
−0.165	+0.03316	−0.74485	−0.68604	0.3953	7.5281
−0.170	+0.03516	−0.73000	−0.64891	0.4038	7.3255
−0.175	+0.03720	−0.71554	−0.61276	0.4120	7.1341
−0.180	+0.03928	−0.70145	−0.57755	0.4199	6.9530
−0.185	+0.04140	−0.68772	−0.54322	0.4274	6.7814
−0.190	+0.04355	−0.67432	−0.50972	0.4346	6.6186
−0.195	+0.04574	−0.66124	−0.47702	0.4415	6.4639
−0.200	+0.04797	−0.64846	−0.44507	0.4480	6.3167
−0.205	+0.05022	−0.63597	−0.41384	0.4543	6.1765
−0.210	+0.05251	−0.62375	−0.38329	0.4602	6.0428
−0.215	+0.05482	−0.61179	−0.35340	0.4658	5.9151
−0.220	+0.05717	−0.60009	−0.32413	0.4711	5.7931
−0.225	+0.05953	−0.58862	−0.29546	0.4760	5.6765
−0.230	+0.06193	−0.57738	−0.26736	0.4807	5.5647
−0.235	+0.06434	−0.56635	−0.23981	0.4851	5.4577
−0.240	+0.06678	−0.55554	−0.21278	0.4892	5.3550
−0.245	+0.06923	−0.54493	−0.18625	0.4930	5.2564
−0.250	+0.07171	−0.53451	−0.16020	0.4966	5.1618
−0.255	+0.07420	−0.52428	−0.13462	0.4998	5.0708
−0.260	+0.07671	−0.51423	−0.10949	0.5028	4.9833
−0.265	+0.07923	−0.50435	−0.08479	0.5055	4.8991
−0.270	+0.08176	−0.49463	−0.06049	0.5080	4.8179
−0.275	+0.08431	−0.48507	−0.03660	0.5102	4.7398
−0.280	+0.08686	−0.47567	−0.01309	0.5122	4.6644
−0.285	+0.08943	−0.46641	+0.01004	0.5139	4.5917
−0.290	+0.09200	−0.45730	+0.03282	0.5153	4.5216
−0.295	+0.09458	−0.44832	+0.05526	0.5166	4.4538
−0.300	+0.09717	−0.43948	+0.07736	0.5176	4.3884
−0.305	+0.09976	−0.43077	+0.09915	0.5184	4.3252
−0.310	+0.10235	−0.42218	+0.12062	0.5190	4.2640
−0.315	+0.10495	−0.41371	+0.14179	0.5193	4.2049
−0.320	+0.10755	−0.40536	+0.16267	0.5195	4.1477
−0.325	+0.11014	−0.39712	+0.18327	0.5194	4.0923
−0.330	+0.11274	−0.38899	+0.20360	0.5192	4.0387
−0.335	+0.11534	−0.38096	+0.22366	0.5187	3.9868
−0.340	+0.11793	−0.37304	+0.24347	0.5181	3.9365
−0.345	+0.12052	−0.36522	+0.26303	0.5173	3.8877
−0.350	+0.12310	−0.35749	+0.28235	0.5163	3.8404
−0.355	+0.12568	−0.34985	+0.30144	0.5152	3.7946
−0.360	+0.12825	−0.34231	+0.32030	0.5138	3.7501
−0.365	+0.13082	−0.33485	+0.33894	0.5124	3.7070
−0.370	+0.13338	−0.32748	+0.35737	0.5107	3.6652
−0.375	+0.13593	−0.32019	+0.37560	0.5090	3.6246
−0.380	+0.13847	−0.31298	+0.39362	0.5070	3.5851
−0.385	+0.14100	−0.30585	+0.41145	0.5050	3.5469
−0.390	+0.14352	−0.29879	+0.42909	0.5028	3.5097
−0.395	+0.14603	−0.29181	+0.44655	0.5004	3.4736
−0.400	+0.14852	−0.28490	+0.46383	0.4980	3.4385
−0.405	+0.15101	−0.27805	+0.48093	0.4954	3.4044
−0.410	+0.15348	−0.27128	+0.49787	0.4927	3.3713
−0.415	+0.15593	−0.26457	+0.51465	0.4899	3.3391
−0.420	+0.15838	−0.25792	+0.53127	0.4870	3.3078
−0.425	+0.16080	−0.25134	+0.54773	0.4840	3.2774
−0.430	+0.16322	−0.24481	+0.56404	0.4809	3.2478
−0.435	+0.16561	−0.23834	+0.58021	0.4777	3.2190
−0.440	+0.16799	−0.23193	+0.59623	0.4744	3.1910
−0.445	+0.17036	−0.22558	+0.61212	0.4710	3.1638
−0.450	+0.17270	−0.21928	+0.62787	0.4675	3.1374
−0.455	+0.17503	−0.21303	+0.64350	0.4640	3.1116
−0.460	+0.17734	−0.20683	+0.65899	0.4604	3.0866
−0.465	+0.17964	−0.20068	+0.67436	0.4567	3.0622
−0.470	+0.18191	−0.19458	+0.68962	0.4530	3.0385
−0.475	+0.18417	−0.18853	+0.70475	0.4492	3.0154
−0.480	+0.18640	−0.18252	+0.71977	0.4453	2.9930
−0.485	+0.18862	−0.17655	+0.73468	0.4414	2.9712
−0.490	+0.19082	−0.17063	+0.74949	0.4374	2.9499
−0.495	+0.19300	−0.16475	+0.76418	0.4334	2.9292
−0.500	+0.19515	−0.15892	+0.77878	0.4294	2.9091
−0.505	+0.19729	−0.15312	+0.79328	0.4253	2.8895
−0.510	+0.19941	−0.14736	+0.80767	0.4211	2.8704
−0.515	+0.20150	−0.14164	+0.82198	0.4169	2.8518
−0.520	+0.20358	−0.13595	+0.83619	0.4127	2.8338
−0.525	+0.20563	−0.13030	+0.85032	0.4085	2.8162
−0.530	+0.20766	−0.12468	+0.86436	0.4043	2.7991
−0.535	+0.20967	−0.11910	+0.87831	0.4000	2.7824
−0.540	+0.21166	−0.11355	+0.89218	0.3957	2.7662
−0.545	+0.21363	−0.10804	+0.90597	0.3914	2.7504
−0.550	+0.21558	−0.10255	+0.91969	0.3871	2.7351
−0.555	+0.21750	−0.09710	+0.93333	0.3827	2.7201
−0.560	+0.21940	−0.09167	+0.94689	0.3784	2.7056
−0.565	+0.22128	−0.08627	+0.96038	0.3740	2.6914
−0.570	+0.22314	−0.08091	+0.97381	0.3697	2.6776
−0.575	+0.22498	−0.07556	+0.98716	0.3653	2.6642
−0.580	+0.22680	−0.07025	+1.00045	0.3610	2.6512
−0.585	+0.22859	−0.06496	+1.01367	0.3566	2.6385
−0.590	+0.23036	−0.05969	+1.02684	0.3522	2.6262
−0.595	+0.23211	−0.05445	+1.03994	0.3479	2.6141
−0.600	+0.23384	−0.04924	+1.05298	0.3436	2.6025
−0.605	+0.23555	−0.04404	+1.06596	0.3392	2.5911

1522

1	4	5	6	7	8
−0.010	+0.00005	−2.03073	−3.87270	0.0134	109.8182
−0.015	+0.00014	−1.85223	−3.42647	0.0240	73.6356
−0.020	+0.00029	−1.72483	−3.10797	0.0360	55.5313
−0.025	+0.00051	−1.62546	−2.85954	0.0491	44.6635
−0.030	+0.00079	−1.54383	−2.65547	0.0629	37.4148
−0.035	+0.00114	−1.47445	−2.48203	0.0773	32.2340
−0.040	+0.00156	−1.41405	−2.33102	0.0921	28.3457
−0.045	+0.00206	−1.36051	−2.19716	0.1072	25.3188
−0.050	+0.00263	−1.31238	−2.07684	0.1225	22.8951
−0.055	+0.00328	−1.26864	−1.96749	0.1378	20.9098
−0.060	+0.00401	−1.22852	−1.86720	0.1532	19.2534
−0.065	+0.00482	−1.19146	−1.77454	0.1685	17.8499
−0.070	+0.00570	−1.15699	−1.68838	0.1837	16.6453
−0.075	+0.00665	−1.12477	−1.60782	0.1988	15.5996
−0.080	+0.00769	−1.09451	−1.53217	0.2138	14.6831
−0.085	+0.00879	−1.06597	−1.46082	0.2285	13.8730
−0.090	+0.00997	−1.03896	−1.39329	0.2430	13.1517
−0.095	+0.01122	−1.01331	−1.32918	0.2572	12.5051
−0.100	+0.01254	−0.98889	−1.26813	0.2712	11.9219
−0.105	+0.01393	−0.96559	−1.20987	0.2848	11.3933
−0.110	+0.01539	−0.94329	−1.15412	0.2982	10.9117
−0.115	+0.01692	−0.92191	−1.10068	0.3112	10.4711
−0.120	+0.01850	−0.90138	−1.04935	0.3239	10.0664
−0.125	+0.02015	−0.88163	−0.99997	0.3363	9.6932
−0.130	+0.02187	−0.86259	−0.95237	0.3484	9.3480
−0.135	+0.02364	−0.84422	−0.90645	0.3600	9.0276
−0.140	+0.02547	−0.82646	−0.86206	0.3714	8.7295
−0.145	+0.02735	−0.80929	−0.81912	0.3824	8.4514
−0.150	+0.02929	−0.79265	−0.77752	0.3930	8.1913
−0.155	+0.03128	−0.77651	−0.73718	0.4032	7.9474
−0.160	+0.03332	−0.76085	−0.69802	0.4131	7.7182
−0.165	+0.03541	−0.74563	−0.65997	0.4227	7.5024
−0.170	+0.03755	−0.73083	−0.62297	0.4319	7.2992
−0.175	+0.03973	−0.71642	−0.58696	0.4407	7.1070
−0.180	+0.04196	−0.70239	−0.55188	0.4492	6.9252
−0.185	+0.04422	−0.68872	−0.51769	0.4573	6.7528
−0.190	+0.04653	−0.67538	−0.48434	0.4651	6.5893
−0.195	+0.04887	−0.66235	−0.45179	0.4725	6.4339
−0.200	+0.05125	−0.64963	−0.41999	0.4796	6.2860
−0.205	+0.05367	−0.63720	−0.38891	0.4863	6.1451

1	4	5	6	7	8
-0.210	+0.05612	−0.62505	−0.35853	0.4927	6.0107
-0.215	+0.05860	−0.61316	−0.32880	0.4988	5.8824
-0.220	+0.06111	−0.60152	−0.29969	0.5045	5.7598
-0.225	+0.06364	−0.59011	−0.27119	0.5100	5.6424
-0.230	+0.06621	−0.57894	−0.24326	0.5150	5.5301
-0.235	+0.06879	−0.56799	−0.21588	0.5198	5.4224
-0.240	+0.07140	−0.55725	−0.18903	0.5243	5.3191
-0.245	+0.07404	−0.54671	−0.16268	0.5285	5.2200
-0.250	+0.07669	−0.53637	−0.13682	0.5323	5.1247
-0.255	+0.07936	−0.52621	−0.11143	0.5359	5.0332
-0.260	+0.08205	−0.51623	−0.08648	0.5392	4.9451
-0.265	+0.08475	−0.50643	−0.06197	0.5422	4.8604
-0.270	+0.08747	−0.49679	−0.03787	0.5449	4.7787
-0.275	+0.09020	−0.48731	−0.01418	0.5474	4.7000
-0.280	+0.09294	−0.47799	+0.00912	0.5496	4.6242
-0.285	+0.09570	−0.46881	+0.03206	0.5515	4.5510
-0.290	+0.09846	−0.45978	+0.05464	0.5532	4.4804
-0.295	+0.10123	−0.45089	+0.07687	0.5546	4.4122
-0.300	+0.10400	−0.44213	+0.09876	0.5557	4.3463
-0.305	+0.10679	−0.43350	+0.12033	0.5567	4.2826
-0.310	+0.10957	−0.42500	+0.14159	0.5574	4.2210
-0.315	+0.11236	−0.41662	+0.16255	0.5578	4.1615
-0.320	+0.11515	−0.40835	+0.18321	0.5581	4.1039
-0.325	+0.11794	−0.40020	+0.20359	0.5581	4.0481
-0.330	+0.12073	−0.39216	+0.22369	0.5579	3.9941
-0.335	+0.12352	−0.38422	+0.24353	0.5575	3.9418
-0.340	+0.12631	−0.37639	+0.26311	0.5569	3.8911
-0.345	+0.12909	−0.36865	+0.28245	0.5561	3.8420
-0.350	+0.13187	−0.36102	+0.30154	0.5551	3.7944
-0.355	+0.13464	−0.35348	+0.32039	0.5540	3.7482
-0.360	+0.13741	−0.34602	+0.33902	0.5526	3.7035
-0.365	+0.14017	−0.33866	+0.35743	0.5511	3.6600
-0.370	+0.14292	−0.33138	+0.37563	0.5494	3.6179
-0.375	+0.14566	−0.32419	+0.39361	0.5476	3.5770
-0.380	+0.14839	−0.31707	+0.41140	0.5456	3.5373
-0.385	+0.15112	−0.31004	+0.42899	0.5434	3.4987
-0.390	+0.15383	−0.30308	+0.44639	0.5411	3.4613
-0.395	+0.15653	−0.29619	+0.46360	0.5386	3.4250
-0.400	+0.15922	−0.28938	+0.48064	0.5361	3.3896
-0.405	+0.16189	−0.28263	+0.49750	0.5333	3.3553
-0.410	+0.16455	−0.27596	+0.51419	0.5305	3.3220
-0.415	+0.16719	−0.26934	+0.53072	0.5275	3.2896
-0.420	+0.16982	−0.26280	+0.54709	0.5244	3.2581
-0.425	+0.17244	−0.25631	+0.56331	0.5212	3.2275
-0.430	+0.17504	−0.24989	+0.57937	0.5179	3.1977
-0.435	+0.17762	−0.24352	+0.59529	0.5145	3.1688
-0.440	+0.18018	−0.23721	+0.61106	0.5110	3.1406
-0.445	+0.18273	−0.23096	+0.62669	0.5074	3.1133
-0.450	+0.18526	−0.22476	+0.64219	0.5037	3.0867
-0.455	+0.18777	−0.21861	+0.65756	0.4999	3.0608
-0.460	+0.19026	−0.21251	+0.67280	0.4961	3.0356
-0.465	+0.19273	−0.20647	+0.68792	0.4921	3.0111
-0.470	+0.19518	−0.20047	+0.70292	0.4881	2.9873
-0.475	+0.19761	−0.19452	+0.71779	0.4840	2.9641
-0.480	+0.20002	−0.18861	+0.73256	0.4799	2.9416
-0.485	+0.20241	−0.18275	+0.74721	0.4757	2.9196
-0.490	+0.20478	−0.17693	+0.76176	0.4714	2.8983
-0.495	+0.20712	−0.17115	+0.77620	0.4671	2.8775
-0.500	+0.20945	−0.16542	+0.79053	0.4628	2.8573
-0.505	+0.21175	−0.15972	+0.80477	0.4584	2.8377
-0.510	+0.21403	−0.15407	+0.81891	0.4539	2.8185
-0.515	+0.21629	−0.14845	+0.83296	0.4494	2.7999
-0.520	+0.21853	−0.14287	+0.84691	0.4449	2.7818
-0.525	+0.22074	−0.13732	+0.86078	0.4404	2.7642
-0.530	+0.22293	−0.13181	+0.87456	0.4358	2.7471
-0.535	+0.22510	−0.12633	+0.88825	0.4312	2.7304
-0.540	+0.22724	−0.12089	+0.90186	0.4265	2.7142
-0.545	+0.22936	−0.11548	+0.91539	0.4219	2.6984
-0.550	+0.23146	−0.11009	+0.92884	0.4172	2.6830
-0.555	+0.23354	−0.10474	+0.94222	0.4125	2.6681
-0.560	+0.23559	−0.09942	+0.95553	0.4078	2.6535
-0.565	+0.23762	−0.09413	+0.96876	0.4031	2.6394
-0.570	+0.23962	−0.08886	+0.98192	0.3984	2.6256
-0.575	+0.24160	−0.08363	+0.99502	0.3937	2.6122
-0.580	+0.24356	−0.07841	+1.00805	0.3890	2.5992
-0.585	+0.24549	−0.07323	+1.02101	0.3843	2.5866
-0.590	+0.24740	−0.06807	+1.03391	0.3796	2.5743
-0.595	+0.24929	−0.06293	+1.04675	0.3749	2.5623
-0.600	+0.25115	−0.05782	+1.05954	0.3702	2.5507
-0.605	+0.25299	−0.05273	+1.07226	0.3655	2.5394

1523

1	4	5	6	7	8
−0.010	+0.00006	−2.03073	−3.82156	0.0151	109.8178
−0.015	+0.00016	−1.85224	−3.37533	0.0270	73.6339
−0.020	+0.00033	−1.72484	−3.05684	0.0405	55.5282
−0.025	+0.00057	−1.62548	−2.80843	0.0552	44.6591
−0.030	+0.00088	−1.54386	−2.60438	0.0708	37.4090
−0.035	+0.00128	−1.47449	−2.43097	0.0870	32.2267
−0.040	+0.00176	−1.41411	−2.28000	0.1037	28.3369
−0.045	+0.00232	−1.36058	−2.14619	0.1207	25.3085
−0.050	+0.00296	−1.31248	−2.02593	0.1378	22.8831
−0.055	+0.00370	−1.26876	−1.91664	0.1551	20.8962
−0.060	+0.00452	−1.22868	−1.81643	0.1724	19.2381
−0.065	+0.00542	−1.19164	−1.72385	0.1897	17.8329
−0.070	+0.00641	−1.15721	−1.63777	0.2069	16.6265
−0.075	+0.00749	−1.12503	−1.55732	0.2239	15.5791
−0.080	+0.00865	−1.09481	−1.48177	0.2408	14.6609
−0.085	+0.00990	−1.06632	−1.41053	0.2574	13.8491
−0.090	+0.01123	−1.03936	−1.34313	0.2738	13.1259
−0.095	+0.01264	−1.01377	−1.27915	0.2899	12.4775
−0.100	+0.01413	−0.98941	−1.21825	0.3056	11.8927
−0.105	+0.01569	−0.96616	−1.16013	0.3211	11.3623
−0.110	+0.01734	−0.94393	−1.10455	0.3362	10.8790
−0.115	+0.01906	−0.92262	−1.05128	0.3510	10.4366
−0.120	+0.02085	−0.90216	−1.00012	0.3654	10.0301
−0.125	+0.02271	−0.88247	−0.95092	0.3795	9.6553
−0.130	+0.02464	−0.86352	−0.90353	0.3932	9.3083
−0.135	+0.02664	−0.84522	−0.85780	0.4065	8.9863
−0.140	+0.02871	−0.82756	−0.81362	0.4194	8.6866
−0.145	+0.03083	−0.81047	−0.77090	0.4319	8.4068
−0.150	+0.03303	−0.79392	−0.72953	0.4440	8.1450
−0.155	+0.03527	−0.77787	−0.68942	0.4557	7.8995
−0.160	+0.03758	−0.76231	−0.65051	0.4670	7.6688
−0.165	+0.03994	−0.74719	−0.61271	0.4779	7.4515
−0.170	+0.04236	−0.73249	−0.57597	0.4885	7.2465
−0.175	+0.04483	−0.71820	−0.54023	0.4986	7.0529
−0.180	+0.04735	−0.70428	−0.50543	0.5083	6.8695
−0.185	+0.04991	−0.69071	−0.47152	0.5177	6.6957
−0.190	+0.05252	−0.67749	−0.43845	0.5266	6.5307
−0.195	+0.05518	−0.66458	−0.40620	0.5352	6.3739
−0.200	+0.05788	−0.65199	−0.37470	0.5434	6.2245
−0.205	+0.06061	−0.63968	−0.34394	0.5512	6.0823
−0.210	+0.06339	−0.62765	−0.31387	0.5586	5.9465
−0.215	+0.06620	−0.61589	−0.28446	0.5657	5.8169
−0.220	+0.06905	−0.60438	−0.25569	0.5724	5.6929
−0.225	+0.07192	−0.59311	−0.22752	0.5787	5.5743
−0.230	+0.07483	−0.58208	−0.19994	0.5847	5.4607
−0.235	+0.07777	−0.57127	−0.17291	0.5903	5.3517
−0.240	+0.08074	−0.56067	−0.14641	0.5956	5.2472
−0.245	+0.08373	−0.55028	−0.12043	0.6005	5.1469
−0.250	+0.08674	−0.54008	−0.09494	0.6051	5.0505
−0.255	+0.08978	−0.53007	−0.06992	0.6094	4.9578
−0.260	+0.09284	−0.52025	−0.04535	0.6133	4.8686
−0.265	+0.09591	−0.51060	−0.02122	0.6170	4.7828
−0.270	+0.09900	−0.50111	+0.00247	0.6203	4.7001
−0.275	+0.10211	−0.49179	+0.02577	0.6232	4.6204
−0.280	+0.10524	−0.48263	+0.04868	0.6259	4.5435
−0.285	+0.10837	−0.47362	+0.07121	0.6283	4.4693
−0.290	+0.11152	−0.46475	+0.09338	0.6304	4.3977
−0.295	+0.11468	−0.45602	+0.11519	0.6322	4.3286
−0.300	+0.11784	−0.44743	+0.13667	0.6338	4.2617
−0.305	+0.12102	−0.43898	+0.15781	0.6350	4.1972
−0.310	+0.12419	−0.43064	+0.17864	0.6360	4.1347
−0.315	+0.12738	−0.42244	+0.19917	0.6367	4.0743
−0.320	+0.13056	−0.41435	+0.21939	0.6372	4.0159
−0.325	+0.13375	−0.40637	+0.23933	0.6374	3.9593
−0.330	+0.13693	−0.39851	+0.25899	0.6374	3.9045
−0.335	+0.14012	−0.39075	+0.27838	0.6371	3.8515
−0.340	+0.14331	−0.38310	+0.29750	0.6366	3.8000
−0.345	+0.14649	−0.37555	+0.31638	0.6359	3.7502
−0.350	+0.14967	−0.36810	+0.33501	0.6350	3.7019
−0.355	+0.15284	−0.36074	+0.35340	0.6338	3.6551
−0.360	+0.15600	−0.35348	+0.37156	0.6324	3.6097
−0.365	+0.15916	−0.34630	+0.38950	0.6309	3.5656
−0.370	+0.16231	−0.33921	+0.40722	0.6291	3.5229
−0.375	+0.16545	−0.33221	+0.42473	0.6272	3.4814
−0.380	+0.16858	−0.32529	+0.44204	0.6250	3.4411
−0.385	+0.17170	−0.31844	+0.45915	0.6227	3.4020
−0.390	+0.17481	−0.31168	+0.47606	0.6202	3.3640
−0.395	+0.17791	−0.30499	+0.49279	0.6175	3.3272
−0.400	+0.18099	−0.29837	+0.50933	0.6147	3.2914
−0.405	+0.18405	−0.29182	+0.52570	0.6117	3.2566

−0.410	+0.18710	−0.28534	+0.54190	0.6086	3.2228
−0.415	+0.19014	−0.27893	+0.55793	0.6053	3.1899
−0.420	+0.19316	−0.27258	+0.57380	0.6019	3.1580
−0.425	+0.19616	−0.26629	+0.58952	0.5983	3.1270
−0.430	+0.19914	−0.26007	+0.60508	0.5947	3.0969
−0.435	+0.20211	−0.25391	+0.62049	0.5908	3.0676
−0.440	+0.20505	−0.24780	+0.63575	0.5869	3.0391
−0.445	+0.20798	−0.24175	+0.65088	0.5829	3.0114
−0.450	+0.21088	−0.23575	+0.66587	0.5787	2.9845
−0.455	+0.21376	−0.22981	+0.68073	0.5745	2.9583
−0.460	+0.21662	−0.22392	+0.69545	0.5701	2.9328
−0.465	+0.21946	−0.21808	+0.71006	0.5657	2.9081
−0.470	+0.22228	−0.21229	+0.72454	0.5612	2.8840
−0.475	+0.22508	−0.20654	+0.73890	0.5565	2.8606
−0.480	+0.22785	−0.20084	+0.75314	0.5518	2.8379
−0.485	+0.23060	−0.19519	+0.76728	0.5471	2.8157
−0.490	+0.23332	−0.18958	+0.78130	0.5422	2.7942
−0.495	+0.23602	−0.18401	+0.79522	0.5373	2.7732
−0.500	+0.23869	−0.17849	+0.80904	0.5323	2.7529
−0.505	+0.24134	−0.17300	+0.82275	0.5273	2.7331
−0.510	+0.24397	−0.16755	+0.83637	0.5222	2.7138
−0.515	+0.24656	−0.16214	+0.84989	0.5171	2.6951
−0.520	+0.24914	−0.15677	+0.86332	0.5119	2.6769
−0.525	+0.25168	−0.15144	+0.87666	0.5067	2.6592
−0.530	+0.25420	−0.14614	+0.88991	0.5014	2.6419
−0.535	+0.25670	−0.14087	+0.90308	0.4962	2.6252
−0.540	+0.25917	−0.13563	+0.91617	0.4908	2.6089
−0.545	+0.26161	−0.13043	+0.92917	0.4855	2.5931
−0.550	+0.26402	−0.12526	+0.94210	0.4801	2.5777
−0.555	+0.26641	−0.12012	+0.95495	0.4747	2.5627
−0.560	+0.26877	−0.11501	+0.96773	0.4693	2.5482
−0.565	+0.27110	−0.10993	+0.98043	0.4639	2.5341
−0.570	+0.27341	−0.10487	+0.99307	0.4585	2.5203
−0.575	+0.27569	−0.09985	+1.00564	0.4530	2.5070
−0.580	+0.27794	−0.09484	+1.01814	0.4476	2.4940
−0.585	+0.28016	−0.08987	+1.03058	0.4422	2.4814
−0.590	+0.28236	−0.08492	+1.04296	0.4367	2.4692
−0.595	+0.28453	−0.07999	+1.05527	0.4313	2.4573
−0.600	+0.28668	−0.07509	+1.06753	0.4259	2.4457
−0.605	+0.28879	−0.07021	+1.07973	0.4204	2.4345

1524

1	4	5	6	7	8
−0.010	+0.00006	−2.03073	−3.77580	0.0167	109.8161
−0.015	+0.00018	−1.85224	−3.32959	0.0300	73.6314
−0.020	+0.00037	−1.72485	−3.01112	0.0450	55.5246
−0.025	+0.00063	−1.62550	−2.76273	0.0614	44.6543
−0.030	+0.00098	−1.54389	−2.55871	0.0787	37.4028
−0.035	+0.00142	−1.47454	−2.38533	0.0967	32.2192
−0.040	+0.00195	−1.41417	−2.23440	0.1152	28.3278
−0.045	+0.00258	−1.36066	−2.10064	0.1341	25.2979
−0.050	+0.00329	−1.31258	−1.98043	0.1532	22.8709
−0.055	+0.00411	−1.26889	−1.87121	0.1725	20.8823
−0.060	+0.00502	−1.22883	−1.77107	0.1917	19.2226
−0.065	+0.00603	−1.19183	−1.67857	0.2110	17.8158
−0.070	+0.00713	−1.15744	−1.59258	0.2301	16.6076
−0.075	+0.00833	−1.12530	−1.51223	0.2491	15.5585
−0.080	+0.00962	−1.09512	−1.43679	0.2678	14.6385
−0.085	+0.01101	−1.06667	−1.36567	0.2864	13.8250
−0.090	+0.01248	−1.03976	−1.29839	0.3046	13.1001
−0.095	+0.01405	−1.01422	−1.23454	0.3226	12.4499
−0.100	+0.01571	−0.98992	−1.17379	0.3402	11.8633
−0.105	+0.01746	−0.96673	−1.11582	0.3575	11.3312
−0.110	+0.01929	−0.94456	−1.06040	0.3745	10.8461
−0.115	+0.02120	−0.92332	−1.00729	0.3910	10.4020
−0.120	+0.02320	−0.90293	−0.95632	0.4072	9.9938
−0.125	+0.02527	−0.88332	−0.90730	0.4229	9.6172
−0.130	+0.02742	−0.86444	−0.86010	0.4383	9.2686
−0.135	+0.02965	−0.84623	−0.81457	0.4532	8.9449
−0.140	+0.03196	−0.82865	−0.77061	0.4677	8.6435
−0.145	+0.03433	−0.81165	−0.72811	0.4818	8.3620
−0.150	+0.03677	−0.79519	−0.68696	0.4954	8.0986
−0.155	+0.03928	−0.77924	−0.64709	0.5086	7.8515
−0.160	+0.04186	−0.76377	−0.60842	0.5214	7.6192
−0.165	+0.04450	−0.74875	−0.57088	0.5338	7.4004
−0.170	+0.04720	−0.73416	−0.53440	0.5457	7.1938
−0.175	+0.04996	−0.71997	−0.49892	0.5572	6.9986
−0.180	+0.05277	−0.70616	−0.46439	0.5682	6.8138
−0.185	+0.05564	−0.69271	−0.43077	0.5788	6.6385
−0.190	+0.05856	−0.67960	−0.39799	0.5890	6.4720
−0.195	+0.06153	−0.66682	−0.36603	0.5988	6.3137
−0.200	+0.06454	−0.65434	−0.33484	0.6082	6.1630
−0.205	+0.06761	−0.64216	−0.30439	0.6171	6.0193

1	4	5	6	7	8
−0.210	+0.07072	−0.63026	−0.27464	0.6256	5.8822
−0.215	+0.07386	−0.61863	−0.24556	0.6337	5.7512
−0.220	+0.07705	−0.60725	−0.21712	0.6414	5.6259
−0.225	+0.08028	−0.59612	−0.18929	0.6488	5.5060
−0.230	+0.08354	−0.58522	−0.16205	0.6557	5.3911
−0.235	+0.08684	−0.57455	−0.13537	0.6622	5.2809
−0.240	+0.09016	−0.56410	−0.10923	0.6683	5.1752
−0.245	+0.09352	−0.55385	−0.08361	0.6741	5.0737
−0.250	+0.09690	−0.54380	−0.05849	0.6795	4.9761
−0.255	+0.10031	−0.53394	−0.03384	0.6845	4.8823
−0.260	+0.10375	−0.52427	−0.00966	0.6892	4.7920
−0.265	+0.10721	−0.51477	+0.01407	0.6935	4.7050
−0.270	+0.11068	−0.50544	+0.03739	0.6974	4.6212
−0.275	+0.11418	−0.49628	+0.06029	0.7010	4.5404
−0.280	+0.11769	−0.48728	+0.08280	0.7043	4.4625
−0.285	+0.12122	−0.47843	+0.10492	0.7072	4.3874
−0.290	+0.12477	−0.46973	+0.12668	0.7098	4.3148
−0.295	+0.12832	−0.46117	+0.14807	0.7121	4.2447
−0.300	+0.13189	−0.45275	+0.16913	0.7141	4.1769
−0.305	+0.13546	−0.44446	+0.18985	0.7157	4.1114
−0.310	+0.13904	−0.43630	+0.21025	0.7171	4.0481
−0.315	+0.14263	−0.42827	+0.23033	0.7181	3.9868
−0.320	+0.14623	−0.42035	+0.25012	0.7189	3.9275
−0.325	+0.14982	−0.41255	+0.26961	0.7194	3.8701
−0.330	+0.15342	−0.40487	+0.28882	0.7196	3.8146
−0.335	+0.15702	−0.39729	+0.30776	0.7195	3.7607
−0.340	+0.16061	−0.38983	+0.32643	0.7192	3.7085
−0.345	+0.16421	−0.38246	+0.34485	0.7186	3.6580
−0.350	+0.16780	−0.37519	+0.36302	0.7178	3.6090
−0.355	+0.17139	−0.36802	+0.38094	0.7167	3.5615
−0.360	+0.17497	−0.36095	+0.39863	0.7154	3.5154
−0.365	+0.17854	−0.35396	+0.41610	0.7138	3.4706
−0.370	+0.18211	−0.34706	+0.43334	0.7120	3.4273
−0.375	+0.18566	−0.34025	+0.45037	0.7100	3.3852
−0.380	+0.18921	−0.33352	+0.46720	0.7078	3.3443
−0.385	+0.19274	−0.32687	+0.48382	0.7054	3.3046
−0.390	+0.19626	−0.32030	+0.50024	0.7027	3.2661
−0.395	+0.19977	−0.31381	+0.51648	0.6999	3.2287
−0.400	+0.20326	−0.30738	+0.53253	0.6969	3.1924
−0.405	+0.20674	−0.30103	+0.54841	0.6937	3.1571
−0.410	+0.21020	−0.29476	+0.56411	0.6903	3.1228
−0.415	+0.21364	−0.28854	+0.57964	0.6868	3.0895
−0.420	+0.21706	−0.28240	+0.59501	0.6830	3.0572
−0.425	+0.22047	−0.27631	+0.61021	0.6792	3.0258
−0.430	+0.22386	−0.27029	+0.62526	0.6751	2.9952
−0.435	+0.22722	−0.26433	+0.64017	0.6710	2.9655
−0.440	+0.23057	−0.25843	+0.65492	0.6667	2.9367
−0.445	+0.23389	−0.25258	+0.66953	0.6622	2.9086
−0.450	+0.23719	−0.24679	+0.68401	0.6576	2.8814
−0.455	+0.24047	−0.24106	+0.69835	0.6529	2.8549
−0.460	+0.24372	−0.23537	+0.71256	0.6481	2.8291
−0.465	+0.24695	−0.22974	+0.72664	0.6431	2.8040
−0.470	+0.25015	−0.22416	+0.74060	0.6381	2.7797
−0.475	+0.25333	−0.21862	+0.75444	0.6330	2.7560
−0.480	+0.25648	−0.21313	+0.76816	0.6277	2.7330
−0.485	+0.25961	−0.20769	+0.78177	0.6224	2.7107
−0.490	+0.26270	−0.20229	+0.79527	0.6169	2.6889
−0.495	+0.26578	−0.19693	+0.80866	0.6114	2.6678
−0.500	+0.26882	−0.19162	+0.82195	0.6059	2.6472
−0.505	+0.27183	−0.18634	+0.83514	0.6002	2.6272
−0.510	+0.27482	−0.18111	+0.84822	0.5945	2.6078
−0.515	+0.27778	−0.17591	+0.86122	0.5887	2.5889
−0.520	+0.28071	−0.17075	+0.87412	0.5828	2.5706
−0.525	+0.28361	−0.16563	+0.88692	0.5770	2.5528
−0.530	+0.28648	−0.16054	+0.89964	0.5710	2.5354
−0.535	+0.28932	−0.15549	+0.91228	0.5650	2.5186
−0.540	+0.29213	−0.15046	+0.92483	0.5590	2.5022
−0.545	+0.29491	−0.14548	+0.93730	0.5529	2.4863
−0.550	+0.29766	−0.14052	+0.94970	0.5468	2.4709
−0.555	+0.30038	−0.13559	+0.96201	0.5407	2.4559
−0.560	+0.30307	−0.13070	+0.97426	0.5346	2.4413
−0.565	+0.30572	−0.12583	+0.98643	0.5284	2.4271
−0.570	+0.30835	−0.12099	+0.99853	0.5222	2.4134
−0.575	+0.31095	−0.11617	+1.01056	0.5160	2.4000
−0.580	+0.31351	−0.11139	+1.02253	0.5098	2.3871
−0.585	+0.31605	−0.10662	+1.03443	0.5036	2.3745
−0.590	+0.31855	−0.10189	+1.04628	0.4974	2.3623
−0.595	+0.32102	−0.09717	+1.05806	0.4912	2.3504
−0.600	+0.32346	−0.09248	+1.06978	0.4849	2.3389
−0.605	+0.32587	−0.08782	+1.08145	0.4787	2.3278

1525

1	4	5	6	7	8
-0.010	+0.00007	-2.03073	-3.73442	0.0184	109.8151
-0.015	+0.00020	-1.85225	-3.28821	0.0330	73.6294
-0.020	+0.00040	-1.72487	-2.96975	0.0496	55.5215
-0.025	+0.00070	-1.62552	-2.72138	0.0675	44.6499
-0.030	+0.00108	-1.54392	-2.51738	0.0866	37.3970
-0.035	+0.00157	-1.47458	-2.34404	0.1064	32.2119
-0.040	+0.00215	-1.41423	-2.19315	0.1268	28.3191
-0.045	+0.00283	-1.36074	-2.05944	0.1476	25.2876
-0.050	+0.00363	-1.31268	-1.93929	0.1686	22.8589
-0.055	+0.00452	-1.26902	-1.83013	0.1898	20.8687
-0.060	+0.00552	-1.22899	-1.73006	0.2110	19.2073
-0.065	+0.00663	-1.19202	-1.63764	0.2322	17.7987
-0.070	+0.00785	-1.15767	-1.55174	0.2533	16.5889
-0.075	+0.00917	-1.12556	-1.47149	0.2743	15.5380
-0.080	+0.01059	-1.09543	-1.39615	0.2950	14.6163
-0.085	+0.01212	-1.06703	-1.32515	0.3154	13.8010
-0.090	+0.01374	-1.04017	-1.25799	0.3356	13.0743
-0.095	+0.01547	-1.01468	-1.19428	0.3555	12.4224
-0.100	+0.01730	-0.99043	-1.13366	0.3750	11.8340
-0.105	+0.01922	-0.96731	-1.07585	0.3941	11.3002
-0.110	+0.02124	-0.94520	-1.02059	0.4129	10.8133
-0.115	+0.02335	-0.92403	-0.96765	0.4312	10.3675
-0.120	+0.02555	-0.90371	-0.91685	0.4491	9.9576
-0.125	+0.02784	-0.88418	-0.86802	0.4666	9.5793
-0.130	+0.03022	-0.86537	-0.82101	0.4837	9.2290
-0.135	+0.03268	-0.84724	-0.77569	0.5003	8.9036
-0.140	+0.03522	-0.82974	-0.73194	0.5164	8.6004
-0.145	+0.03784	-0.81283	-0.68965	0.5321	8.3173
-0.150	+0.04054	-0.79646	-0.64873	0.5473	8.0523
-0.155	+0.04332	-0.78061	-0.60910	0.5621	7.8035
-0.160	+0.04616	-0.76524	-0.57067	0.5764	7.5696
-0.165	+0.04908	-0.75032	-0.53338	0.5902	7.3492
-0.170	+0.05206	-0.73583	-0.49716	0.6035	7.1411
-0.175	+0.05511	-0.72175	-0.46195	0.6164	6.9444
-0.180	+0.05823	-0.70805	-0.42770	0.6288	6.7580
-0.185	+0.06140	-0.69471	-0.39436	0.6408	6.5812
-0.190	+0.06464	-0.68172	-0.36187	0.6523	6.4133
-0.195	+0.06792	-0.66905	-0.33021	0.6633	6.2535
-0.200	+0.07127	-0.65670	-0.29932	0.6739	6.1014
-0.205	+0.07466	-0.64464	-0.26918	0.6841	5.9563
-0.210	+0.07811	-0.63287	-0.23975	0.6937	5.8178
-0.215	+0.08160	-0.62137	-0.21099	0.7030	5.6854
-0.220	+0.08514	-0.61012	-0.18289	0.7118	5.5588
-0.225	+0.08872	-0.59913	-0.15540	0.7201	5.4376
-0.230	+0.09234	-0.58837	-0.12850	0.7281	5.3214
-0.235	+0.09600	-0.57784	-0.10218	0.7356	5.2100
-0.240	+0.09970	-0.56753	-0.07639	0.7427	5.1030
-0.245	+0.10343	-0.55742	-0.05114	0.7494	5.0003
-0.250	+0.10719	-0.54752	-0.02638	0.7556	4.9015
-0.255	+0.11098	-0.53782	-0.00212	0.7615	4.8065
-0.260	+0.11480	-0.52829	+0.02168	0.7669	4.7151
-0.265	+0.11865	-0.51895	+0.04503	0.7720	4.6270
-0.270	+0.12252	-0.50978	+0.06795	0.7767	4.5421
-0.275	+0.12642	-0.50078	+0.09046	0.7810	4.4603
-0.280	+0.13033	-0.49194	+0.11256	0.7849	4.3813
-0.285	+0.13427	-0.48325	+0.13428	0.7885	4.3051
-0.290	+0.13822	-0.47472	+0.15562	0.7917	4.2315
-0.295	+0.14218	-0.46633	+0.17660	0.7945	4.1604
-0.300	+0.14616	-0.45808	+0.19722	0.7970	4.0917
-0.305	+0.15015	-0.44996	+0.21752	0.7991	4.0253
-0.310	+0.15415	-0.44197	+0.23748	0.8009	3.9611
-0.315	+0.15816	-0.43411	+0.25713	0.8024	3.8989
-0.320	+0.16218	-0.42638	+0.27648	0.8036	3.8388
-0.325	+0.16620	-0.41876	+0.29552	0.8044	3.7805
-0.330	+0.17022	-0.41125	+0.31428	0.8049	3.7241
-0.335	+0.17425	-0.40386	+0.33277	0.8051	3.6695
-0.340	+0.17827	-0.39657	+0.35098	0.8050	3.6165
-0.345	+0.18230	-0.38939	+0.36894	0.8047	3.5652
-0.350	+0.18632	-0.38231	+0.38664	0.8040	3.5155
-0.355	+0.19034	-0.37533	+0.40409	0.8031	3.4672
-0.360	+0.19435	-0.36844	+0.42131	0.8018	3.4205
-0.365	+0.19836	-0.36164	+0.43830	0.8004	3.3751
-0.370	+0.20235	-0.35494	+0.45507	0.7986	3.3310
-0.375	+0.20634	-0.34832	+0.47161	0.7966	3.2883
-0.380	+0.21032	-0.34178	+0.48795	0.7944	3.2468
-0.385	+0.21429	-0.33533	+0.50408	0.7919	3.2066
-0.390	+0.21824	-0.32896	+0.52002	0.7892	3.1675
-0.395	+0.22218	-0.32266	+0.53576	0.7863	3.1295
-0.400	+0.22610	-0.31644	+0.55132	0.7831	3.0926
-0.405	+0.23001	-0.31029	+0.56669	0.7798	3.0568
-0.410	+0.23390	-0.30421	+0.58189	0.7762	3.0221
-0.415	+0.23777	-0.29820	+0.59691	0.7725	2.9883
-0.420	+0.24163	-0.29226	+0.61177	0.7685	2.9555
-0.425	+0.24546	-0.28638	+0.62647	0.7643	2.9236
-0.430	+0.24927	-0.28056	+0.64101	0.7600	2.8926
-0.435	+0.25306	-0.27481	+0.65540	0.7555	2.8625
-0.440	+0.25683	-0.26911	+0.66964	0.7509	2.8332
-0.445	+0.26057	-0.26347	+0.68373	0.7460	2.8048
-0.450	+0.26429	-0.25789	+0.69769	0.7410	2.7771
-0.455	+0.26798	-0.25236	+0.71150	0.7359	2.7503
-0.460	+0.27165	-0.24689	+0.72519	0.7306	2.7242
-0.465	+0.27529	-0.24147	+0.73875	0.7252	2.6988
-0.470	+0.27890	-0.23609	+0.75218	0.7197	2.6742
-0.475	+0.28248	-0.23077	+0.76549	0.7140	2.6502
-0.480	+0.28604	-0.22549	+0.77868	0.7083	2.6269
-0.485	+0.28957	-0.22026	+0.79176	0.7024	2.6043
-0.490	+0.29306	-0.21507	+0.80473	0.6964	2.5823
-0.495	+0.29653	-0.20993	+0.81759	0.6903	2.5609
-0.500	+0.29997	-0.20483	+0.83034	0.6841	2.5401
-0.505	+0.30337	-0.19977	+0.84299	0.6778	2.5199
-0.510	+0.30674	-0.19475	+0.85554	0.6715	2.5003
-0.515	+0.31009	-0.18977	+0.86799	0.6650	2.4813
-0.520	+0.31339	-0.18482	+0.88035	0.6585	2.4628
-0.525	+0.31667	-0.17992	+0.89262	0.6519	2.4448
-0.530	+0.31991	-0.17504	+0.90480	0.6453	2.4273
-0.535	+0.32312	-0.17021	+0.91690	0.6386	2.4103
-0.540	+0.32630	-0.16540	+0.92891	0.6318	2.3938
-0.545	+0.32944	-0.16063	+0.94084	0.6250	2.3778
-0.550	+0.33255	-0.15589	+0.95269	0.6182	2.3623
-0.555	+0.33562	-0.15118	+0.96446	0.6113	2.3472
-0.560	+0.33866	-0.14650	+0.97616	0.6044	2.3325
-0.565	+0.34167	-0.14185	+0.98779	0.5974	2.3183
-0.570	+0.34464	-0.13723	+0.99934	0.5905	2.3045
-0.575	+0.34757	-0.13263	+1.01083	0.5835	2.2911
-0.580	+0.35047	-0.12806	+1.02226	0.5765	2.2781
-0.585	+0.35334	-0.12352	+1.03362	0.5694	2.2655
-0.590	+0.35617	-0.11900	+1.04491	0.5624	2.2533
-0.595	+0.35896	-0.11451	+1.05615	0.5554	2.2415
-0.600	+0.36172	-0.11003	+1.06733	0.5484	2.2300
-0.605	+0.36445	-0.10559	+1.07845	0.5413	2.2189

1526

1	4	5	6	7	8
-0.010	+0.00008	-2.03073	-3.69663	0.0201	109.8134
-0.015	+0.00022	-1.85225	-3.25043	0.0360	73.6269
-0.020	+0.00044	-1.72488	-2.93199	0.0541	55.5179
-0.025	+0.00076	-1.62554	-2.68364	0.0737	44.6451
-0.030	+0.00118	-1.54395	-2.47967	0.0945	37.3909
-0.035	+0.00171	-1.47463	-2.30636	0.1161	32.2044
-0.040	+0.00234	-1.41429	-2.15552	0.1383	28.3100
-0.045	+0.00309	-1.36082	-2.02185	0.1610	25.2770
-0.050	+0.00396	-1.31278	-1.90176	0.1840	22.8468
-0.055	+0.00493	-1.26915	-1.79266	0.2072	20.8549
-0.060	+0.00603	-1.22915	-1.69267	0.2304	19.1918
-0.065	+0.00724	-1.19221	-1.60033	0.2535	17.7816
-0.070	+0.00856	-1.15789	-1.51452	0.2766	16.5700
-0.075	+0.01001	-1.12583	-1.43437	0.2995	15.5174
-0.080	+0.01156	-1.09574	-1.35914	0.3222	14.5939
-0.085	+0.01323	-1.06738	-1.28825	0.3446	13.7769
-0.090	+0.01501	-1.04057	-1.22122	0.3667	13.0485
-0.095	+0.01689	-1.01514	-1.15764	0.3885	12.3948
-0.100	+0.01889	-0.99095	-1.09717	0.4098	11.8047
-0.105	+0.02099	-0.96788	-1.03951	0.4308	11.2690
-0.110	+0.02320	-0.94584	-0.98440	0.4514	10.7805
-0.115	+0.02551	-0.92473	-0.93163	0.4716	10.3329
-0.120	+0.02791	-0.90448	-0.88101	0.4913	9.9212
-0.125	+0.03042	-0.88503	-0.83237	0.5106	9.5412
-0.130	+0.03302	-0.86630	-0.78555	0.5293	9.1892
-0.135	+0.03571	-0.84825	-0.74043	0.5476	8.8621
-0.140	+0.03850	-0.83084	-0.69689	0.5655	8.5573
-0.145	+0.04137	-0.81401	-0.65483	0.5828	8.2726
-0.150	+0.04432	-0.79774	-0.61414	0.5996	8.0058
-0.155	+0.04736	-0.78198	-0.57474	0.6160	7.7555
-0.160	+0.05048	-0.76670	-0.53656	0.6318	7.5200
-0.165	+0.05368	-0.75189	-0.49952	0.6472	7.2980
-0.170	+0.05696	-0.73750	-0.46356	0.6620	7.0883
-0.175	+0.06030	-0.72353	-0.42862	0.6764	6.8900
-0.180	+0.06372	-0.70994	-0.39464	0.6902	6.7021
-0.185	+0.06720	-0.69671	-0.36158	0.7036	6.5238
-0.190	+0.07075	-0.68383	-0.32939	0.7164	6.3544
-0.195	+0.07437	-0.67129	-0.29802	0.7288	6.1932
-0.200	+0.07804	-0.65906	-0.26744	0.7407	6.0396
-0.205	+0.08177	-0.64712	-0.23761	0.7521	5.8931

1	4	5	6	7	8
−0.210	+0.08556	−0.63548	−0.20850	0.7630	5.7532
−0.215	+0.08940	−0.62411	−0.18007	0.7734	5.6195
−0.220	+0.09330	−0.61300	−0.15229	0.7834	5.4916
−0.225	+0.09724	−0.60214	−0.12514	0.7929	5.3690
−0.230	+0.10122	−0.59152	−0.09860	0.8019	5.2515
−0.235	+0.10526	−0.58113	−0.07262	0.8105	5.1389
−0.240	+0.10933	−0.57096	−0.04720	0.8186	5.0306
−0.245	+0.11344	−0.56100	−0.02231	0.8263	4.9267
−0.250	+0.11759	−0.55125	+0.00207	0.8335	4.8267
−0.255	+0.12178	−0.54169	+0.02596	0.8403	4.7305
−0.260	+0.12599	−0.53232	+0.04938	0.8466	4.6379
−0.265	+0.13024	−0.52314	+0.07234	0.8525	4.5487
−0.270	+0.13452	−0.51413	+0.09487	0.8580	4.4627
−0.275	+0.13882	−0.50529	+0.11698	0.8631	4.3798
−0.280	+0.14315	−0.49661	+0.13867	0.8678	4.2998
−0.285	+0.14750	−0.48808	+0.15998	0.8721	4.2226
−0.290	+0.15187	−0.47971	+0.18090	0.8759	4.1480
−0.295	+0.15626	−0.47149	+0.20146	0.8794	4.0759
−0.300	+0.16067	−0.46341	+0.22167	0.8825	4.0062
−0.305	+0.16509	−0.45546	+0.24153	0.8853	3.9389
−0.310	+0.16952	−0.44765	+0.26106	0.8876	3.8737
−0.315	+0.17396	−0.43997	+0.28027	0.8896	3.8106
−0.320	+0.17841	−0.43241	+0.29917	0.8912	3.7496
−0.325	+0.18287	−0.42497	+0.31777	0.8925	3.6905
−0.330	+0.18734	−0.41764	+0.33608	0.8934	3.6333
−0.335	+0.19181	−0.41043	+0.35411	0.8940	3.5778
−0.340	+0.19628	−0.40333	+0.37186	0.8943	3.5241
−0.345	+0.20075	−0.39633	+0.38935	0.8942	3.4720
−0.350	+0.20522	−0.38944	+0.40658	0.8938	3.4215
−0.355	+0.20969	−0.38265	+0.42357	0.8931	3.3725
−0.360	+0.21415	−0.37595	+0.44031	0.8921	3.3250
−0.365	+0.21861	−0.36935	+0.45682	0.8908	3.2789
−0.370	+0.22306	−0.36283	+0.47310	0.8892	3.2342
−0.375	+0.22750	−0.35641	+0.48917	0.8873	3.1908
−0.380	+0.23193	−0.35007	+0.50501	0.8851	3.1487
−0.385	+0.23635	−0.34381	+0.52066	0.8827	3.1078
−0.390	+0.24076	−0.33764	+0.53609	0.8800	3.0681
−0.395	+0.24515	−0.33154	+0.55134	0.8770	3.0296
−0.400	+0.24953	−0.32552	+0.56639	0.8738	2.9921
−0.405	+0.25389	−0.31957	+0.58126	0.8704	2.9558
−0.410	+0.25823	−0.31369	+0.59595	0.8667	2.9205
−0.415	+0.26256	−0.30789	+0.61047	0.8628	2.8862
−0.420	+0.26686	−0.30215	+0.62482	0.8586	2.8528
−0.425	+0.27114	−0.29648	+0.63900	0.8543	2.8205
−0.430	+0.27540	−0.29087	+0.65302	0.8497	2.7890
−0.435	+0.27964	−0.28532	+0.66689	0.8450	2.7585
−0.440	+0.28385	−0.27983	+0.68061	0.8400	2.7288
−0.445	+0.28804	−0.27440	+0.69418	0.8349	2.6999
−0.450	+0.29220	−0.26903	+0.70761	0.8295	2.6719
−0.455	+0.29634	−0.26371	+0.72090	0.8240	2.6446
−0.460	+0.30044	−0.25845	+0.73406	0.8184	2.6182
−0.465	+0.30452	−0.25324	+0.74709	0.8125	2.5924
−0.470	+0.30857	−0.24808	+0.75999	0.8065	2.5675
−0.475	+0.31259	−0.24297	+0.77276	0.8004	2.5432
−0.480	+0.31657	−0.23791	+0.78542	0.7941	2.5196
−0.485	+0.32053	−0.23289	+0.79796	0.7877	2.4966
−0.490	+0.32445	−0.22792	+0.81039	0.7812	2.4743
−0.495	+0.32834	−0.22299	+0.82270	0.7745	2.4527
−0.500	+0.33220	−0.21811	+0.83491	0.7677	2.4317
−0.505	+0.33602	−0.21327	+0.84702	0.7608	2.4112
−0.510	+0.33980	−0.20846	+0.85903	0.7538	2.3914
−0.515	+0.34356	−0.20370	+0.87094	0.7468	2.3721
−0.520	+0.34727	−0.19897	+0.88275	0.7396	2.3534
−0.525	+0.35095	−0.19429	+0.89447	0.7323	2.3352
−0.530	+0.35460	−0.18963	+0.90610	0.7250	2.3175
−0.535	+0.35820	−0.18502	+0.91765	0.7175	2.3004
−0.540	+0.36177	−0.18043	+0.92911	0.7101	2.2837
−0.545	+0.36530	−0.17588	+0.94049	0.7025	2.2676
−0.550	+0.36880	−0.17136	+0.95179	0.6949	2.2519
−0.555	+0.37225	−0.16687	+0.96301	0.6873	2.2367
−0.560	+0.37567	−0.16241	+0.97415	0.6795	2.2219
−0.565	+0.37905	−0.15798	+0.98523	0.6718	2.2076
−0.570	+0.38239	−0.15358	+0.99623	0.6640	2.1937
−0.575	+0.38569	−0.14921	+1.00717	0.6562	2.1803
−0.580	+0.38895	−0.14486	+1.01804	0.6484	2.1672
−0.585	+0.39217	−0.14054	+1.02884	0.6405	2.1545
−0.590	+0.39536	−0.13624	+1.03958	0.6326	2.1423
−0.595	+0.39850	−0.13197	+1.05026	0.6248	2.1304
−0.600	+0.40161	−0.12772	+1.06089	0.6169	2.1189
−0.605	+0.40467	−0.12349	+1.07145	0.6090	2.1077

1527

1	4	5	6	7	8
−0.010	+0.00008	−2.03074	−3.66188	0.0218	109.8127
−0.015	+0.00023	−1.85226	−3.21568	0.0390	73.6249
−0.020	+0.00048	−1.72489	−2.89725	0.0586	55.5147
−0.025	+0.00082	−1.62556	−2.64892	0.0798	44.6406
−0.030	+0.00128	−1.54398	−2.44498	0.1023	37.3850
−0.035	+0.00185	−1.47467	−2.27170	0.1258	32.1971
−0.040	+0.00254	−1.41435	−2.12090	0.1499	28.3012
−0.045	+0.00335	−1.36090	−1.98728	0.1745	25.2666
−0.050	+0.00429	−1.31288	−1.86724	0.1994	22.8347
−0.055	+0.00535	−1.26927	−1.75821	0.2246	20.8412
−0.060	+0.00653	−1.22930	−1.65829	0.2497	19.1765
−0.065	+0.00784	−1.19240	−1.56603	0.2749	17.7645
−0.070	+0.00928	−1.15811	−1.48032	0.2999	16.5512
−0.075	+0.01084	−1.12609	−1.40026	0.3248	15.4969
−0.080	+0.01253	−1.09604	−1.32514	0.3494	14.5717
−0.085	+0.01434	−1.06773	−1.25437	0.3738	13.7528
−0.090	+0.01627	−1.04097	−1.18746	0.3979	13.0227
−0.095	+0.01832	−1.01559	−1.12401	0.4215	12.3672
−0.100	+0.02048	−0.99146	−1.06368	0.4449	11.7753
−0.105	+0.02277	−0.96846	−1.00617	0.4677	11.2379
−0.110	+0.02516	−0.94648	−0.95123	0.4902	10.7476
−0.115	+0.02767	−0.92544	−0.89863	0.5122	10.2983
−0.120	+0.03028	−0.90526	−0.84818	0.5337	9.8849
−0.125	+0.03301	−0.88588	−0.79972	0.5548	9.5032
−0.130	+0.03583	−0.86723	−0.75310	0.5753	9.1494
−0.135	+0.03876	−0.84926	−0.70819	0.5954	8.8207
−0.140	+0.04178	−0.83193	−0.66486	0.6149	8.5142
−0.145	+0.04491	−0.81519	−0.62301	0.6340	8.2278
−0.150	+0.04812	−0.79901	−0.58255	0.6525	7.9594
−0.155	+0.05143	−0.78334	−0.54339	0.6704	7.7074
−0.160	+0.05483	−0.76817	−0.50545	0.6879	7.4703
−0.165	+0.05831	−0.75345	−0.46867	0.7048	7.2467
−0.170	+0.06188	−0.73917	−0.43297	0.7212	7.0355
−0.175	+0.06552	−0.72530	−0.39829	0.7371	6.8356
−0.180	+0.06925	−0.71182	−0.36459	0.7524	6.6462
−0.185	+0.07305	−0.69871	−0.33181	0.7672	6.4664
−0.190	+0.07692	−0.68595	−0.29991	0.7815	6.2955
−0.195	+0.08086	−0.67352	−0.26884	0.7953	6.1328
−0.200	+0.08487	−0.66141	−0.23857	0.8085	5.9778
−0.205	+0.08895	−0.64961	−0.20905	0.8213	5.8299
−0.210	+0.09308	−0.63809	−0.18026	0.8335	5.6886
−0.215	+0.09728	−0.62685	−0.15216	0.8452	5.5535
−0.220	+0.10153	−0.61587	−0.12472	0.8564	5.4242
−0.225	+0.10584	−0.60515	−0.09791	0.8671	5.3003
−0.230	+0.11020	−0.59467	−0.07170	0.8773	5.1815
−0.235	+0.11462	−0.58442	−0.04608	0.8870	5.0676
−0.240	+0.11907	−0.57439	−0.02102	0.8963	4.9581
−0.245	+0.12358	−0.56458	+0.00350	0.9050	4.8529
−0.250	+0.12812	−0.55498	+0.02751	0.9133	4.7517
−0.255	+0.13271	−0.54557	+0.05102	0.9211	4.6544
−0.260	+0.13734	−0.53636	+0.07406	0.9284	4.5606
−0.265	+0.14199	−0.52733	+0.09663	0.9353	4.4702
−0.270	+0.14669	−0.51848	+0.11876	0.9417	4.3831
−0.275	+0.15141	−0.50980	+0.14047	0.9477	4.2991
−0.280	+0.15616	−0.50128	+0.16176	0.9532	4.2180
−0.285	+0.16094	−0.49292	+0.18265	0.9583	4.1397
−0.290	+0.16575	−0.48472	+0.20316	0.9630	4.0641
−0.295	+0.17057	−0.47666	+0.22330	0.9672	3.9910
−0.300	+0.17542	−0.46875	+0.24308	0.9711	3.9204
−0.305	+0.18028	−0.46098	+0.26251	0.9745	3.8520
−0.310	+0.18516	−0.45334	+0.28160	0.9775	3.7859
−0.315	+0.19006	−0.44583	+0.30037	0.9801	3.7219
−0.320	+0.19496	−0.43845	+0.31883	0.9823	3.6600
−0.325	+0.19988	−0.43119	+0.33698	0.9841	3.6000
−0.330	+0.20481	−0.42405	+0.35483	0.9856	3.5419
−0.335	+0.20974	−0.41702	+0.37240	0.9866	3.4856
−0.340	+0.21467	−0.41011	+0.38969	0.9873	3.4311
−0.345	+0.21961	−0.40330	+0.40671	0.9877	3.3782
−0.350	+0.22455	−0.39659	+0.42347	0.9877	3.3269
−0.355	+0.22949	−0.38999	+0.43998	0.9873	3.2772
−0.360	+0.23442	−0.38348	+0.45625	0.9866	3.2289
−0.365	+0.23935	−0.37707	+0.47228	0.9856	3.1821
−0.370	+0.24428	−0.37075	+0.48807	0.9842	3.1367
−0.375	+0.24919	−0.36452	+0.50365	0.9826	3.0926
−0.380	+0.25410	−0.35838	+0.51900	0.9806	3.0498
−0.385	+0.25900	−0.35232	+0.53415	0.9783	3.0083
−0.390	+0.26389	−0.34635	+0.54909	0.9757	2.9679
−0.395	+0.26876	−0.34045	+0.56383	0.9728	2.9288
−0.400	+0.27361	−0.33463	+0.57838	0.9696	2.8908
−0.405	+0.27845	−0.32889	+0.59274	0.9662	2.8538

-0.410	+0.28328	−0.32322	+0.60692	0.9625	2.8179
-0.415	+0.28808	−0.31762	+0.62092	0.9585	2.7831
-0.420	+0.29286	−0.31208	+0.63475	0.9543	2.7492
-0.425	+0.29762	−0.30662	+0.64841	0.9498	2.7164
-0.430	+0.30236	−0.30122	+0.66192	0.9451	2.6844
-0.435	+0.30707	−0.29588	+0.67526	0.9402	2.6534
-0.440	+0.31176	−0.29060	+0.68845	0.9350	2.6232
-0.445	+0.31642	−0.28539	+0.70149	0.9296	2.5939
-0.450	+0.32106	−0.28023	+0.71439	0.9240	2.5654
-0.455	+0.32566	−0.27512	+0.72715	0.9182	2.5378
-0.460	+0.33024	−0.27007	+0.73977	0.9122	2.5109
-0.465	+0.33479	−0.26508	+0.75226	0.9060	2.4848
-0.470	+0.33930	−0.26013	+0.76462	0.8996	2.4594
-0.475	+0.34378	−0.25524	+0.77686	0.8930	2.4347
-0.480	+0.34823	−0.25040	+0.78897	0.8863	2.4108
-0.485	+0.35264	−0.24560	+0.80097	0.8794	2.3875
-0.490	+0.35702	−0.24084	+0.81285	0.8724	2.3649
-0.495	+0.36137	−0.23614	+0.82462	0.8652	2.3429
-0.500	+0.36568	−0.23147	+0.83628	0.8579	2.3216
-0.505	+0.36995	−0.22685	+0.84783	0.8504	2.3009
-0.510	+0.37418	−0.22227	+0.85929	0.8428	2.2807
-0.515	+0.37838	−0.21773	+0.87064	0.8351	2.2612
-0.520	+0.38253	−0.21322	+0.88190	0.8273	2.2422
-0.525	+0.38665	−0.20876	+0.89307	0.8193	2.2238
-0.530	+0.39073	−0.20433	+0.90414	0.8113	2.2059
-0.535	+0.39476	−0.19993	+0.91513	0.8032	2.1886
-0.540	+0.39876	−0.19557	+0.92603	0.7950	2.1717
-0.545	+0.40271	−0.19125	+0.93685	0.7867	2.1554
-0.550	+0.40662	−0.18695	+0.94758	0.7783	2.1395
-0.555	+0.41050	−0.18269	+0.95824	0.7699	2.1241
-0.560	+0.41432	−0.17845	+0.96882	0.7614	2.1092
-0.565	+0.41811	−0.17425	+0.97933	0.7528	2.0947
-0.570	+0.42185	−0.17007	+0.98977	0.7442	2.0807
-0.575	+0.42555	−0.16593	+1.00014	0.7355	2.0671
-0.580	+0.42921	−0.16180	+1.01045	0.7268	2.0539
-0.585	+0.43282	−0.15771	+1.02068	0.7181	2.0412
-0.590	+0.43639	−0.15364	+1.03086	0.7094	2.0288
-0.595	+0.43992	−0.14959	+1.04097	0.7006	2.0168
-0.600	+0.44340	−0.14557	+1.05103	0.6918	2.0052
-0.605	+0.44683	−0.14157	+1.06103	0.6830	1.9940

1528

1	4	5	6	7	8
-0.010	+0.00009	−2.03074	−3.62970	0.0235	109.8110
-0.015	+0.00025	−1.85227	−3.18352	0.0420	73.6224
-0.020	+0.00052	−1.72490	−2.86510	0.0631	55.5111
-0.025	+0.00089	−1.62557	−2.61679	0.0860	44.6358
-0.030	+0.00138	−1.54401	−2.41287	0.1102	37.3789
-0.035	+0.00199	−1.47471	−2.23963	0.1355	32.1895
-0.040	+0.00274	−1.41440	−2.08887	0.1615	28.2921
-0.045	+0.00361	−1.36098	−1.95530	0.1880	25.2560
-0.050	+0.00462	−1.31298	−1.83532	0.2149	22.8226
-0.055	+0.00576	−1.26940	−1.72635	0.2419	20.8274
-0.060	+0.00704	−1.22946	−1.62650	0.2691	19.1610
-0.065	+0.00845	−1.19259	−1.53433	0.2962	17.7473
-0.070	+0.01000	−1.15834	−1.44870	0.3233	16.5323
-0.075	+0.01168	−1.12635	−1.36874	0.3501	15.4762
-0.080	+0.01350	−1.09635	−1.29373	0.3768	14.5493
-0.085	+0.01545	−1.06809	−1.22307	0.4031	13.7287
-0.090	+0.01753	−1.04137	−1.15629	0.4291	12.9968
-0.095	+0.01974	−1.01605	−1.09298	0.4547	12.3396
-0.100	+0.02208	−0.99197	−1.03279	0.4800	11.7460
-0.105	+0.02454	−0.96903	−0.97543	0.5048	11.2068
-0.110	+0.02713	−0.94712	−0.92065	0.5291	10.7147
-0.115	+0.02983	−0.92614	−0.86822	0.5530	10.2637
-0.120	+0.03266	−0.90604	−0.81795	0.5764	9.8486
-0.125	+0.03560	−0.88673	−0.76968	0.5993	9.4651
-0.130	+0.03865	−0.86816	−0.72325	0.6216	9.1096
-0.135	+0.04181	−0.85027	−0.67854	0.6435	8.7792
-0.140	+0.04509	−0.83303	−0.63542	0.6648	8.4710
-0.145	+0.04846	−0.81637	−0.59379	0.6855	8.1829
-0.150	+0.05194	−0.80028	−0.55356	0.7057	7.9129
-0.155	+0.05552	−0.78471	−0.51464	0.7254	7.6593
-0.160	+0.05919	−0.76963	−0.47694	0.7445	7.4205
-0.165	+0.06296	−0.75502	−0.44041	0.7630	7.1954
-0.170	+0.06682	−0.74084	−0.40497	0.7810	6.9826
-0.175	+0.07077	−0.72708	−0.37056	0.7985	6.7812
-0.180	+0.07481	−0.71371	−0.33714	0.8154	6.5902
-0.185	+0.07893	−0.70071	−0.30465	0.8317	6.4089
-0.190	+0.08313	−0.68807	−0.27304	0.8475	6.2365
-0.195	+0.08740	−0.67576	−0.24227	0.8627	6.0723
-0.200	+0.09175	−0.66378	−0.21230	0.8774	5.9159
-0.205	+0.09618	−0.65209	−0.18310	0.8916	5.7665

1	4	5	6	7	8
-0.210	+0.10067	−0.64071	−0.15462	0.9052	5.6238
-0.215	+0.10523	−0.62960	−0.12685	0.9182	5.4873
-0.220	+0.10985	−0.61875	−0.09974	0.9308	5.3567
-0.225	+0.11453	−0.60816	−0.07327	0.9428	5.2315
-0.230	+0.11928	−0.59782	−0.04742	0.9543	5.1114
-0.235	+0.12408	−0.58772	−0.02215	0.9652	4.9961
-0.240	+0.12893	−0.57783	+0.00254	0.9757	4.8854
-0.245	+0.13383	−0.56817	+0.02670	0.9856	4.7789
-0.250	+0.13878	−0.55872	+0.05034	0.9950	4.6765
-0.255	+0.14378	−0.54946	+0.07348	1.0040	4.5780
-0.260	+0.14882	−0.54040	+0.09613	1.0124	4.4830
-0.265	+0.15391	−0.53153	+0.11831	1.0203	4.3915
-0.270	+0.15903	−0.52283	+0.14005	1.0278	4.3033
-0.275	+0.16418	−0.51431	+0.16135	1.0348	4.2181
-0.280	+0.16937	−0.50596	+0.18223	1.0413	4.1360
-0.285	+0.17460	−0.49777	+0.20271	1.0473	4.0566
-0.290	+0.17985	−0.48973	+0.22281	1.0529	3.9799
-0.295	+0.18512	−0.48184	+0.24252	1.0580	3.9058
-0.300	+0.19043	−0.47410	+0.26187	1.0627	3.8342
-0.305	+0.19575	−0.46651	+0.28086	1.0669	3.7648
-0.310	+0.20110	−0.45904	+0.29952	1.0707	3.6978
-0.315	+0.20646	−0.45171	+0.31785	1.0740	3.6329
-0.320	+0.21184	−0.44451	+0.33585	1.0769	3.5700
-0.325	+0.21723	−0.43743	+0.35355	1.0794	3.5091
-0.330	+0.22263	−0.43047	+0.37095	1.0815	3.4501
-0.335	+0.22804	−0.42363	+0.38805	1.0832	3.3930
-0.340	+0.23346	−0.41690	+0.40488	1.0845	3.3376
-0.345	+0.23889	−0.41028	+0.42143	1.0854	3.2838
-0.350	+0.24432	−0.40376	+0.43772	1.0859	3.2318
-0.355	+0.24975	−0.39735	+0.45375	1.0860	3.1812
-0.360	+0.25518	−0.39104	+0.46954	1.0858	3.1322
-0.365	+0.26060	−0.38482	+0.48508	1.0852	3.0847
-0.370	+0.26603	−0.37870	+0.50039	1.0842	3.0385
-0.375	+0.27145	−0.37266	+0.51547	1.0829	2.9937
-0.380	+0.27686	−0.36672	+0.53033	1.0812	2.9502
-0.385	+0.28226	−0.36086	+0.54497	1.0792	2.9080
-0.390	+0.28765	−0.35509	+0.55941	1.0768	2.8670
-0.395	+0.29303	−0.34939	+0.57364	1.0741	2.8272
-0.400	+0.29839	−0.34378	+0.58768	1.0711	2.7886
-0.405	+0.30374	−0.33824	+0.60153	1.0678	2.7510
-0.410	+0.30907	−0.33277	+0.61520	1.0642	2.7145
-0.415	+0.31438	−0.32738	+0.62868	1.0603	2.6791
-0.420	+0.31967	−0.32206	+0.64199	1.0561	2.6447
-0.425	+0.32494	−0.31680	+0.65513	1.0516	2.6113
-0.430	+0.33019	−0.31161	+0.66810	1.0469	2.5788
-0.435	+0.33541	−0.30648	+0.68092	1.0418	2.5472
-0.440	+0.34061	−0.30142	+0.69358	1.0366	2.5165
-0.445	+0.34577	−0.29642	+0.70609	1.0310	2.4867
-0.450	+0.35092	−0.29147	+0.71845	1.0252	2.4578
-0.455	+0.35603	−0.28658	+0.73067	1.0192	2.4297
-0.460	+0.36111	−0.28175	+0.74275	1.0130	2.4023
-0.465	+0.36616	−0.27697	+0.75469	1.0065	2.3758
-0.470	+0.37117	−0.27225	+0.76651	0.9998	2.3500
-0.475	+0.37616	−0.26757	+0.77819	0.9929	2.3249
-0.480	+0.38110	−0.26295	+0.78976	0.9858	2.3006
-0.485	+0.38601	−0.25837	+0.80120	0.9785	2.2769
-0.490	+0.39089	−0.25384	+0.81253	0.9711	2.2539
-0.495	+0.39572	−0.24935	+0.82374	0.9634	2.2316
-0.500	+0.40052	−0.24491	+0.83484	0.9556	2.2099
-0.505	+0.40528	−0.24051	+0.84584	0.9476	2.1889
-0.510	+0.41000	−0.23616	+0.85674	0.9395	2.1684
-0.515	+0.41468	−0.23184	+0.86753	0.9312	2.1486
-0.520	+0.41931	−0.22756	+0.87822	0.9228	2.1293
-0.525	+0.42390	−0.22332	+0.88882	0.9142	2.1106
-0.530	+0.42845	−0.21912	+0.89933	0.9055	2.0924
-0.535	+0.43296	−0.21495	+0.90975	0.8967	2.0748
-0.540	+0.43742	−0.21082	+0.92008	0.8878	2.0577
-0.545	+0.44184	−0.20672	+0.93033	0.8788	2.0411
-0.550	+0.44621	−0.20265	+0.94049	0.8696	2.0250
-0.555	+0.45053	−0.19862	+0.95058	0.8604	2.0094
-0.560	+0.45481	−0.19462	+0.96059	0.8511	1.9943
-0.565	+0.45905	−0.19064	+0.97052	0.8418	1.9796
-0.570	+0.46323	−0.18670	+0.98038	0.8323	1.9654
-0.575	+0.46737	−0.18278	+0.99018	0.8228	1.9516
-0.580	+0.47146	−0.17889	+0.99990	0.8133	1.9383
-0.585	+0.47550	−0.17503	+1.00956	0.8037	1.9254
-0.590	+0.47950	−0.17119	+1.01916	0.7940	1.9128
-0.595	+0.48344	−0.16737	+1.02869	0.7843	1.9007
-0.600	+0.48734	−0.16358	+1.03817	0.7746	1.8890
-0.605	+0.49119	−0.15982	+1.04758	0.7649	1.8776

1529

1	4	5	6	7	8
−0.010	+0.00010	−2.03074	−3.59974	0.0251	109.8106
−0.015	+0.00027	−1.85227	−3.15356	0.0450	73.6207
−0.020	+0.00055	−1.72491	−2.83516	0.0676	55.5081
−0.025	+0.00095	−1.62559	−2.58687	0.0921	44.6314
−0.030	+0.00148	−1.54404	−2.38298	0.1181	37.3731
−0.035	+0.00214	−1.47475	−2.20977	0.1452	32.1823
−0.040	+0.00293	−1.41446	−2.05904	0.1731	28.2834
−0.045	+0.00387	−1.36105	−1.92552	0.2015	25.2456
−0.050	+0.00495	−1.31308	−1.80560	0.2303	22.8106
−0.055	+0.00617	−1.26952	−1.69670	0.2594	20.8138
−0.060	+0.00754	−1.22961	−1.59692	0.2885	19.1456
−0.065	+0.00906	−1.19278	−1.50482	0.3177	17.7303
−0.070	+0.01072	−1.15856	−1.41929	0.3467	16.5136
−0.075	+0.01253	−1.12662	−1.33943	0.3755	15.4557
−0.080	+0.01448	−1.09665	−1.26452	0.4042	14.5270
−0.085	+0.01657	−1.06844	−1.19398	0.4325	13.7047
−0.090	+0.01880	−1.04178	−1.12732	0.4605	12.9710
−0.095	+0.02117	−1.01650	−1.06415	0.4881	12.3121
−0.100	+0.02368	−0.99249	−1.00410	0.5153	11.7166
−0.105	+0.02633	−0.96960	−0.94689	0.5420	11.1757
−0.110	+0.02910	−0.94775	−0.89226	0.5683	10.6819
−0.115	+0.03201	−0.92685	−0.84000	0.5941	10.2291
−0.120	+0.03504	−0.90681	−0.78991	0.6193	9.8122
−0.125	+0.03820	−0.88758	−0.74183	0.6441	9.4270
−0.130	+0.04148	−0.86908	−0.69560	0.6683	9.0699
−0.135	+0.04488	−0.85128	−0.65109	0.6919	8.7377
−0.140	+0.04840	−0.83412	−0.60818	0.7150	8.4278
−0.145	+0.05203	−0.81756	−0.56677	0.7376	8.1381
−0.150	+0.05578	−0.80155	−0.52677	0.7595	7.8664
−0.155	+0.05963	−0.78608	−0.48808	0.7809	7.6111
−0.160	+0.06359	−0.77110	−0.45063	0.8017	7.3708
−0.165	+0.06765	−0.75659	−0.41435	0.8220	7.1440
−0.170	+0.07181	−0.74252	−0.37917	0.8416	6.9296
−0.175	+0.07606	−0.72886	−0.34504	0.8607	6.7266
−0.180	+0.08041	−0.71560	−0.31189	0.8792	6.5341
−0.185	+0.08485	−0.70272	−0.27968	0.8972	6.3513
−0.190	+0.08938	−0.69019	−0.24836	0.9145	6.1774
−0.195	+0.09400	−0.67800	−0.21789	0.9313	6.0118
−0.200	+0.09870	−0.66614	−0.18823	0.9475	5.8538
−0.205	+0.10347	−0.65458	−0.15934	0.9632	5.7030
−0.210	+0.10833	−0.64332	−0.13119	0.9782	5.5589
−0.215	+0.11326	−0.63234	−0.10374	0.9928	5.4211
−0.220	+0.11825	−0.62163	−0.07697	1.0067	5.2890
−0.225	+0.12332	−0.61118	−0.05084	1.0201	5.1625
−0.230	+0.12846	−0.60098	−0.02533	1.0330	5.0411
−0.235	+0.13365	−0.59102	−0.00042	1.0453	4.9245
−0.240	+0.13891	−0.58128	+0.02391	1.0570	4.8125
−0.245	+0.14422	−0.57176	+0.04770	1.0683	4.7048
−0.250	+0.14959	−0.56246	+0.07096	1.0790	4.6011
−0.255	+0.15501	−0.55336	+0.09372	1.0891	4.5013
−0.260	+0.16048	−0.54445	+0.11598	1.0988	4.4052
−0.265	+0.16600	−0.53573	+0.13778	1.1079	4.3125
−0.270	+0.17156	−0.52720	+0.15912	1.1165	4.2231
−0.275	+0.17716	−0.51884	+0.18001	1.1246	4.1369
−0.280	+0.18281	−0.51065	+0.20049	1.1322	4.0536
−0.285	+0.18849	−0.50262	+0.22056	1.1394	3.9731
−0.290	+0.19420	−0.49475	+0.24023	1.1460	3.8954
−0.295	+0.19994	−0.48704	+0.25951	1.1521	3.8202
−0.300	+0.20572	−0.47947	+0.27843	1.1578	3.7475
−0.305	+0.21152	−0.47205	+0.29699	1.1629	3.6772
−0.310	+0.21735	−0.46476	+0.31521	1.1677	3.6092
−0.315	+0.22320	−0.45761	+0.33309	1.1719	3.5433
−0.320	+0.22907	−0.45058	+0.35065	1.1757	3.4795
−0.325	+0.23496	−0.44369	+0.36789	1.1790	3.4177
−0.330	+0.24086	−0.43691	+0.38483	1.1819	3.3578
−0.335	+0.24677	−0.43026	+0.40147	1.1844	3.2997
−0.340	+0.25270	−0.42371	+0.41783	1.1864	3.2434
−0.345	+0.25864	−0.41728	+0.43391	1.1880	3.1889
−0.350	+0.26458	−0.41096	+0.44972	1.1892	3.1359
−0.355	+0.27053	−0.40474	+0.46527	1.1900	3.0846
−0.360	+0.27648	−0.39862	+0.48057	1.1903	3.0348
−0.365	+0.28243	−0.39259	+0.49562	1.1903	2.9865
−0.370	+0.28838	−0.38667	+0.51043	1.1898	2.9395
−0.375	+0.29433	−0.38084	+0.52502	1.1890	2.8940
−0.380	+0.30027	−0.37509	+0.53938	1.1878	2.8498
−0.385	+0.30621	−0.36944	+0.55352	1.1862	2.8069
−0.390	+0.31214	−0.36386	+0.56745	1.1843	2.7652
−0.395	+0.31805	−0.35837	+0.58117	1.1819	2.7247
−0.400	+0.32395	−0.35296	+0.59470	1.1793	2.6854
−0.405	+0.32984	−0.34763	+0.60803	1.1763	2.6472
−0.410	+0.33572	−0.34237	+0.62117	1.1729	2.6101
−0.415	+0.34157	−0.33719	+0.63413	1.1692	2.5740
−0.420	+0.34741	−0.33208	+0.64691	1.1652	2.5390
−0.425	+0.35323	−0.32703	+0.65952	1.1609	2.5050
−0.430	+0.35902	−0.32206	+0.67197	1.1562	2.4719
−0.435	+0.36479	−0.31715	+0.68424	1.1513	2.4398
−0.440	+0.37053	−0.31230	+0.69637	1.1460	2.4086
−0.445	+0.37625	−0.30751	+0.70833	1.1405	2.3782
−0.450	+0.38194	−0.30278	+0.72015	1.1347	2.3488
−0.455	+0.38759	−0.29811	+0.73182	1.1286	2.3201
−0.460	+0.39322	−0.29350	+0.74335	1.1222	2.2923
−0.465	+0.39882	−0.28894	+0.75475	1.1156	2.2653
−0.470	+0.40438	−0.28444	+0.76601	1.1087	2.2390
−0.475	+0.40990	−0.27999	+0.77714	1.1016	2.2135
−0.480	+0.41539	−0.27559	+0.78814	1.0943	2.1887
−0.485	+0.42085	−0.27123	+0.79903	1.0867	2.1646
−0.490	+0.42626	−0.26693	+0.80979	1.0789	2.1412
−0.495	+0.43163	−0.26267	+0.82044	1.0709	2.1185
−0.500	+0.43697	−0.25845	+0.83098	1.0627	2.0964
−0.505	+0.44226	−0.25428	+0.84141	1.0542	2.0750
−0.510	+0.44751	−0.25015	+0.85173	1.0457	2.0541
−0.515	+0.45272	−0.24606	+0.86195	1.0369	2.0339
−0.520	+0.45788	−0.24202	+0.87207	1.0279	2.0143
−0.525	+0.46300	−0.23801	+0.88209	1.0188	1.9953
−0.530	+0.46807	−0.23403	+0.89202	1.0095	1.9768
−0.535	+0.47309	−0.23010	+0.90186	1.0001	1.9588
−0.540	+0.47807	−0.22620	+0.91161	0.9905	1.9414
−0.545	+0.48300	−0.22233	+0.92128	0.9809	1.9245
−0.550	+0.48788	−0.21850	+0.93086	0.9710	1.9081
−0.555	+0.49271	−0.21470	+0.94036	0.9611	1.8923
−0.560	+0.49749	−0.21093	+0.94978	0.9510	1.8768
−0.565	+0.50222	−0.20719	+0.95913	0.9409	1.8619
−0.570	+0.50690	−0.20348	+0.96840	0.9306	1.8474
−0.575	+0.51153	−0.19980	+0.97761	0.9203	1.8334
−0.580	+0.51610	−0.19615	+0.98674	0.9099	1.8198
−0.585	+0.52063	−0.19252	+0.99581	0.8994	1.8067
−0.590	+0.52510	−0.18892	+1.00481	0.8888	1.7940
−0.595	+0.52952	−0.18534	+1.01375	0.8782	1.7816
−0.600	+0.53388	−0.18179	+1.02263	0.8675	1.7697
−0.605	+0.53819	−0.17827	+1.03144	0.8568	1.7582

1530

1	4	5	6	7	8
−0.010	+0.00010	−2.03074	−3.57171	0.0268	109.8088
−0.015	+0.00029	−1.85228	−3.12555	0.0480	73.6181
−0.020	+0.00059	−1.72492	−2.80716	0.0721	55.5045
−0.025	+0.00102	−1.62561	−2.55889	0.0983	44.6266
−0.030	+0.00158	−1.54407	−2.35503	0.1260	37.3670
−0.035	+0.00228	−1.47480	−2.18185	0.1549	32.1747
−0.040	+0.00313	−1.41452	−2.03117	0.1847	28.2743
−0.045	+0.00413	−1.36113	−1.89770	0.2150	25.2350
−0.050	+0.00528	−1.31319	−1.77783	0.2458	22.7984
−0.055	+0.00659	−1.26965	−1.66899	0.2768	20.8000
−0.060	+0.00805	−1.22977	−1.56929	0.3079	19.1302
−0.065	+0.00967	−1.19296	−1.47727	0.3391	17.7131
−0.070	+0.01144	−1.15879	−1.39183	0.3701	16.4947
−0.075	+0.01337	−1.12688	−1.31207	0.4010	15.4351
−0.080	+0.01545	−1.09696	−1.23727	0.4316	14.5047
−0.085	+0.01769	−1.06879	−1.16684	0.4619	13.6806
−0.090	+0.02007	−1.04218	−1.10031	0.4919	12.9451
−0.095	+0.02261	−1.01696	−1.03727	0.5215	12.2844
−0.100	+0.02529	−0.99300	−0.97736	0.5507	11.6872
−0.105	+0.02811	−0.97018	−0.92031	0.5794	11.1445
−0.110	+0.03108	−0.94839	−0.86584	0.6076	10.6490
−0.115	+0.03419	−0.92755	−0.81375	0.6353	10.1944
−0.120	+0.03743	−0.90759	−0.76384	0.6625	9.7758
−0.125	+0.04081	−0.88843	−0.71594	0.6891	9.3889
−0.130	+0.04432	−0.87001	−0.66990	0.7152	9.0300
−0.135	+0.04796	−0.85229	−0.62559	0.7407	8.6961
−0.140	+0.05173	−0.83521	−0.58290	0.7656	8.3846
−0.145	+0.05562	−0.81874	−0.54171	0.7900	8.0932
−0.150	+0.05963	−0.80283	−0.50194	0.8138	7.8198
−0.155	+0.06376	−0.78745	−0.46349	0.8369	7.5629
−0.160	+0.06800	−0.77257	−0.42628	0.8595	7.3209
−0.165	+0.07235	−0.75816	−0.39026	0.8815	7.0925
−0.170	+0.07681	−0.74419	−0.35534	0.9029	6.8766
−0.175	+0.08138	−0.73064	−0.32147	0.9237	6.6720
−0.180	+0.08605	−0.71749	−0.28860	0.9439	6.4780
−0.185	+0.09082	−0.70472	−0.25667	0.9635	6.2936
−0.190	+0.09568	−0.69231	−0.22565	0.9825	6.1182
−0.195	+0.10064	−0.68024	−0.19548	1.0009	5.9511
−0.200	+0.10569	−0.66850	−0.16612	1.0187	5.7917
−0.205	+0.11083	−0.65707	−0.13755	1.0360	5.6395

1	4	5	6	7	8
-0.210	+0.11605	−0.64594	−0.10972	1.0526	5.4939
-0.215	+0.12136	−0.63509	−0.08260	1.0686	5.3547
-0.220	+0.12674	−0.62452	−0.05616	1.0841	5.2213
-0.225	+0.13220	−0.61420	−0.03038	1.0990	5.0933
-0.230	+0.13773	−0.60414	−0.00522	1.1134	4.9706
-0.235	+0.14333	−0.59432	+0.01933	1.1271	4.8527
-0.240	+0.14900	−0.58473	+0.04331	1.1403	4.7394
-0.245	+0.15473	−0.57536	+0.06673	1.1530	4.6304
-0.250	+0.16053	−0.56620	+0.08962	1.1651	4.5255
-0.255	+0.16638	−0.55725	+0.11199	1.1766	4.4245
-0.260	+0.17229	−0.54850	+0.13387	1.1876	4.3272
-0.265	+0.17826	−0.53994	+0.15527	1.1980	4.2333
-0.270	+0.18427	−0.53157	+0.17621	1.2079	4.1427
-0.275	+0.19034	−0.52337	+0.19670	1.2173	4.0553
-0.280	+0.19645	−0.51534	+0.21677	1.2262	3.9709
-0.285	+0.20260	−0.50748	+0.23642	1.2345	3.8894
-0.290	+0.20879	−0.49978	+0.25567	1.2423	3.8105
-0.295	+0.21502	−0.49224	+0.27453	1.2496	3.7343
-0.300	+0.22129	−0.48484	+0.29301	1.2564	3.6606
-0.305	+0.22759	−0.47759	+0.31114	1.2627	3.5892
-0.310	+0.23391	−0.47048	+0.32891	1.2686	3.5202
-0.315	+0.24027	−0.46351	+0.34634	1.2739	3.4533
-0.320	+0.24665	−0.45667	+0.36345	1.2787	3.3885
-0.325	+0.25306	−0.44996	+0.38023	1.2831	3.3258
-0.330	+0.25948	−0.44337	+0.39671	1.2869	3.2649
-0.335	+0.26593	−0.43689	+0.41289	1.2903	3.2060
-0.340	+0.27239	−0.43054	+0.42877	1.2933	3.1488
-0.345	+0.27886	−0.42430	+0.44438	1.2958	3.0934
-0.350	+0.28534	−0.41817	+0.45971	1.2978	3.0396
-0.355	+0.29184	−0.41214	+0.47478	1.2994	2.9874
-0.360	+0.29834	−0.40621	+0.48959	1.3006	2.9368
-0.365	+0.30484	−0.40039	+0.50415	1.3013	2.8876
-0.370	+0.31135	−0.39466	+0.51847	1.3016	2.8399
-0.375	+0.31786	−0.38903	+0.53255	1.3015	2.7936
-0.380	+0.32437	−0.38349	+0.54640	1.3009	2.7486
-0.385	+0.33087	−0.37803	+0.56004	1.3000	2.7049
-0.390	+0.33737	−0.37267	+0.57346	1.2986	2.6625
-0.395	+0.34385	−0.36738	+0.58667	1.2969	2.6213
-0.400	+0.35033	−0.36218	+0.59967	1.2947	2.5813
-0.405	+0.35680	−0.35706	+0.61248	1.2922	2.5424
-0.410	+0.36326	−0.35201	+0.62510	1.2893	2.5046
-0.415	+0.36969	−0.34704	+0.63753	1.2861	2.4679
-0.420	+0.37612	−0.34214	+0.64978	1.2824	2.4323
-0.425	+0.38252	−0.33731	+0.66185	1.2784	2.3976
-0.430	+0.38890	−0.33255	+0.67376	1.2741	2.3639
-0.435	+0.39526	−0.32785	+0.68550	1.2694	2.3312
-0.440	+0.40159	−0.32322	+0.69707	1.2644	2.2994
-0.445	+0.40790	−0.31865	+0.70849	1.2591	2.2685
-0.450	+0.41419	−0.31415	+0.71976	1.2534	2.2385
-0.455	+0.42044	−0.30970	+0.73088	1.2474	2.2093
-0.460	+0.42666	−0.30531	+0.74185	1.2411	2.1809
-0.465	+0.43285	−0.30097	+0.75269	1.2346	2.1533
-0.470	+0.43901	−0.29669	+0.76339	1.2277	2.1266
-0.475	+0.44513	−0.29247	+0.77396	1.2205	2.1005
-0.480	+0.45121	−0.28829	+0.78440	1.2131	2.0752
-0.485	+0.45726	−0.28416	+0.79471	1.2054	2.0507
-0.490	+0.46326	−0.28009	+0.80490	1.1974	2.0268
-0.495	+0.46923	−0.27606	+0.81498	1.1892	2.0036
-0.500	+0.47516	−0.27207	+0.82494	1.1808	1.9811
-0.505	+0.48104	−0.26813	+0.83479	1.1721	1.9592
-0.510	+0.48688	−0.26423	+0.84454	1.1632	1.9380
-0.515	+0.49267	−0.26038	+0.85417	1.1540	1.9173
-0.520	+0.49842	−0.25656	+0.86371	1.1447	1.8973
-0.525	+0.50412	−0.25279	+0.87315	1.1351	1.8778
-0.530	+0.50977	−0.24905	+0.88249	1.1254	1.8590
-0.535	+0.51537	−0.24535	+0.89174	1.1155	1.8406
-0.540	+0.52093	−0.24169	+0.90090	1.1054	1.8229
-0.545	+0.52643	−0.23806	+0.90997	1.0951	1.8056
-0.550	+0.53188	−0.23447	+0.91896	1.0847	1.7889
-0.555	+0.53727	−0.23091	+0.92786	1.0741	1.7726
-0.560	+0.54262	−0.22738	+0.93668	1.0633	1.7569
-0.565	+0.54791	−0.22388	+0.94543	1.0525	1.7416
-0.570	+0.55314	−0.22041	+0.95410	1.0415	1.7268
-0.575	+0.55832	−0.21697	+0.96270	1.0303	1.7125
-0.580	+0.56345	−0.21356	+0.97123	1.0191	1.6986
-0.585	+0.56851	−0.21017	+0.97969	1.0078	1.6852
-0.590	+0.57352	−0.20682	+0.98808	0.9964	1.6722
-0.595	+0.57848	−0.20348	+0.99641	0.9848	1.6596
-0.600	+0.58337	−0.20018	+1.00468	0.9732	1.6474
-0.605	+0.58821	−0.19689	+1.01288	0.9616	1.6356

1531

1	4	5	6	7	8
−0.010	+0.00011	−2.03074	−3.54539	0.0285	109.8079
−0.015	+0.00031	−1.85228	−3.09923	0.0510	73.6161
−0.020	+0.00063	−1.72493	−2.78085	0.0766	55.5013
−0.025	+0.00108	−1.62563	−2.53260	0.1044	44.6222
−0.030	+0.00168	−1.54410	−2.32877	0.1339	37.3611
−0.035	+0.00242	−1.47484	−2.15562	0.1646	32.1674
−0.040	+0.00333	−1.41458	−2.00498	0.1963	28.2655
−0.045	+0.00439	−1.36121	−1.87156	0.2285	25.2246
−0.050	+0.00561	−1.31329	−1.75175	0.2613	22.7864
−0.055	+0.00700	−1.26978	−1.64297	0.2943	20.7863
−0.060	+0.00856	−1.22993	−1.54334	0.3274	19.1148
−0.065	+0.01028	−1.19315	−1.45141	0.3605	17.6961
−0.070	+0.01216	−1.15901	−1.36605	0.3936	16.4759
−0.075	+0.01421	−1.12715	−1.28639	0.4265	15.4146
−0.080	+0.01643	−1.09727	−1.21170	0.4592	14.4824
−0.085	+0.01880	−1.06915	−1.14139	0.4915	13.6565
−0.090	+0.02134	−1.04258	−1.07498	0.5235	12.9193
−0.095	+0.02404	−1.01742	−1.01207	0.5551	12.2568
−0.100	+0.02689	−0.99351	−0.95231	0.5862	11.6579
−0.105	+0.02990	−0.97075	−0.89540	0.6169	11.1134
−0.110	+0.03306	−0.94903	−0.84110	0.6471	10.6161
−0.115	+0.03637	−0.92826	−0.78917	0.6768	10.1598
−0.120	+0.03983	−0.90837	−0.73944	0.7059	9.7395
−0.125	+0.04343	−0.88928	−0.69173	0.7344	9.3508
−0.130	+0.04717	−0.87094	−0.64588	0.7624	8.9902
−0.135	+0.05106	−0.85330	−0.60178	0.7899	8.6546
−0.140	+0.05507	−0.83631	−0.55930	0.8167	8.3414
−0.145	+0.05922	−0.81992	−0.51834	0.8429	8.0482
−0.150	+0.06350	−0.80411	−0.47879	0.8686	7.7733
−0.155	+0.06791	−0.78882	−0.44057	0.8936	7.5147
−0.160	+0.07244	−0.77404	−0.40362	0.9180	7.2711
−0.165	+0.07709	−0.75973	−0.36784	0.9418	7.0411
−0.170	+0.08185	−0.74586	−0.33318	0.9650	6.8235
−0.175	+0.08674	−0.73243	−0.29959	0.9875	6.6174
−0.180	+0.09173	−0.71939	−0.26699	1.0095	6.4218
−0.185	+0.09683	−0.70673	−0.23535	1.0308	6.2359
−0.190	+0.10204	−0.69444	−0.20462	1.0516	6.0590
−0.195	+0.10735	−0.68249	−0.17475	1.0717	5.8904
−0.200	+0.11275	−0.67087	−0.14570	1.0912	5.7295
−0.205	+0.11826	−0.65957	−0.11744	1.1101	5.5758
−0.210	+0.12385	−0.64856	−0.08993	1.1284	5.4288
−0.215	+0.12954	−0.63785	−0.06314	1.1461	5.2881
−0.220	+0.13531	−0.62741	−0.03704	1.1632	5.1533
−0.225	+0.14117	−0.61723	−0.01160	1.1798	5.0240
−0.230	+0.14711	−0.60731	+0.01320	1.1957	4.8999
−0.235	+0.15313	−0.59763	+0.03740	1.2110	4.7807
−0.240	+0.15922	−0.58818	+0.06101	1.2258	4.6661
−0.245	+0.16539	−0.57896	+0.08407	1.2400	4.5558
−0.250	+0.17162	−0.56995	+0.10658	1.2536	4.4497
−0.255	+0.17792	−0.56116	+0.12857	1.2666	4.3474
−0.260	+0.18429	−0.55256	+0.15006	1.2791	4.2488
−0.265	+0.19071	−0.54416	+0.17107	1.2910	4.1538
−0.270	+0.19720	−0.53594	+0.19161	1.3024	4.0620
−0.275	+0.20374	−0.52791	+0.21169	1.3132	3.9735
−0.280	+0.21033	−0.52005	+0.23135	1.3235	3.8879
−0.285	+0.21697	−0.51236	+0.25058	1.3332	3.8052
−0.290	+0.22366	−0.50483	+0.26940	1.3424	3.7253
−0.295	+0.23039	−0.49745	+0.28784	1.3511	3.6480
−0.300	+0.23717	−0.49023	+0.30589	1.3592	3.5732
−0.305	+0.24399	−0.48316	+0.32357	1.3668	3.5008
−0.310	+0.25084	−0.47623	+0.34090	1.3739	3.4307
−0.315	+0.25773	−0.46943	+0.35788	1.3805	3.3628
−0.320	+0.26464	−0.46277	+0.37453	1.3866	3.2970
−0.325	+0.27159	−0.45624	+0.39086	1.3922	3.2333
−0.330	+0.27857	−0.44984	+0.40687	1.3972	3.1715
−0.335	+0.28556	−0.44356	+0.42258	1.4018	3.1116
−0.340	+0.29258	−0.43739	+0.43799	1.4059	3.0535
−0.345	+0.29962	−0.43134	+0.45311	1.4095	2.9972
−0.350	+0.30668	−0.42540	+0.46796	1.4127	2.9425
−0.355	+0.31375	−0.41957	+0.48254	1.4153	2.8894
−0.360	+0.32083	−0.41384	+0.49686	1.4175	2.8379
−0.365	+0.32792	−0.40822	+0.51093	1.4193	2.7880
−0.370	+0.33502	−0.40269	+0.52474	1.4205	2.7394
−0.375	+0.34213	−0.39726	+0.53832	1.4214	2.6923
−0.380	+0.34924	−0.39192	+0.55167	1.4218	2.6465
−0.385	+0.35635	−0.38667	+0.56479	1.4217	2.6021
−0.390	+0.36345	−0.38151	+0.57769	1.4212	2.5589
−0.395	+0.37056	−0.37643	+0.59038	1.4203	2.5169
−0.400	+0.37766	−0.37144	+0.60286	1.4189	2.4762
−0.405	+0.38475	−0.36653	+0.61515	1.4172	2.4365

−0.410	+0.39183	−0.36169	+0.62723	1.4150	2.3980
−0.415	+0.39890	−0.35694	+0.63913	1.4124	2.3606
−0.420	+0.40595	−0.35225	+0.65084	1.4094	2.3243
−0.425	+0.41299	−0.34764	+0.66237	1.4061	2.2890
−0.430	+0.42001	−0.34309	+0.67373	1.4023	2.2546
−0.435	+0.42701	−0.33862	+0.68492	1.3981	2.2212
−0.440	+0.43399	−0.33421	+0.69595	1.3936	2.1888
−0.445	+0.44095	−0.32986	+0.70681	1.3887	2.1573
−0.450	+0.44788	−0.32558	+0.71752	1.3835	2.1266
−0.455	+0.45479	−0.32136	+0.72808	1.3779	2.0968
−0.460	+0.46166	−0.31719	+0.73849	1.3720	2.0679
−0.465	+0.46850	−0.31308	+0.74876	1.3657	2.0397
−0.470	+0.47532	−0.30903	+0.75889	1.3591	2.0124
−0.475	+0.48210	−0.30503	+0.76889	1.3521	1.9858
−0.480	+0.48884	−0.30109	+0.77875	1.3448	1.9599
−0.485	+0.49554	−0.29719	+0.78849	1.3373	1.9348
−0.490	+0.50221	−0.29335	+0.79810	1.3294	1.9104
−0.495	+0.50884	−0.28955	+0.80759	1.3212	1.8867
−0.500	+0.51542	−0.28580	+0.81697	1.3128	1.8637
−0.505	+0.52197	−0.28210	+0.82623	1.3040	1.8413
−0.510	+0.52846	−0.27843	+0.83538	1.2950	1.8195
−0.515	+0.53492	−0.27482	+0.84443	1.2858	1.7984
−0.520	+0.54132	−0.27124	+0.85337	1.2762	1.7779
−0.525	+0.54768	−0.26770	+0.86221	1.2664	1.7580
−0.530	+0.55399	−0.26421	+0.87095	1.2564	1.7386
−0.535	+0.56024	−0.26075	+0.87960	1.2462	1.7199
−0.540	+0.56645	−0.25733	+0.88815	1.2357	1.7016
−0.545	+0.57260	−0.25394	+0.89661	1.2250	1.6840
−0.550	+0.57870	−0.25059	+0.90499	1.2142	1.6668
−0.555	+0.58474	−0.24727	+0.91328	1.2031	1.6501
−0.560	+0.59073	−0.24399	+0.92149	1.1918	1.6340
−0.565	+0.59666	−0.24074	+0.92962	1.1804	1.6183
−0.570	+0.60253	−0.23752	+0.93768	1.1688	1.6031
−0.575	+0.60835	−0.23432	+0.94566	1.1570	1.5884
−0.580	+0.61410	−0.23116	+0.95356	1.1450	1.5742
−0.585	+0.61980	−0.22803	+0.96140	1.1330	1.5603
−0.590	+0.62543	−0.22492	+0.96917	1.1208	1.5469
−0.595	+0.63101	−0.22184	+0.97687	1.1084	1.5340
−0.600	+0.63652	−0.21878	+0.98451	1.0960	1.5214
−0.605	+0.64197	−0.21575	+0.99208	1.0834	1.5093

1532

1	4	5	6	7	8
−0.010	+0.00012	−2.03075	−3.52057	0.0302	109.8064
−0.015	+0.00033	−1.85229	−3.07442	0.0540	73.6137
−0.020	+0.00066	−1.72494	−2.75606	0.0811	55.4977
−0.025	+0.00114	−1.62565	−2.50783	0.1106	44.6174
−0.030	+0.00177	−1.54412	−2.30402	0.1418	37.3550
−0.035	+0.00257	−1.47488	−2.13091	0.1743	32.1598
−0.040	+0.00352	−1.41464	−1.98031	0.2078	28.2565
−0.045	+0.00465	−1.36129	−1.84694	0.2421	25.2140
−0.050	+0.00594	−1.31339	−1.72718	0.2767	22.7742
−0.055	+0.00741	−1.26991	−1.61848	0.3117	20.7725
−0.060	+0.00906	−1.23008	−1.51892	0.3469	19.0993
−0.065	+0.01088	−1.19334	−1.42707	0.3820	17.6789
−0.070	+0.01288	−1.15924	−1.34180	0.4171	16.4570
−0.075	+0.01506	−1.12741	−1.26223	0.4520	15.3939
−0.080	+0.01740	−1.09757	−1.18765	0.4867	14.4600
−0.085	+0.01992	−1.06950	−1.11746	0.5211	13.6324
−0.090	+0.02261	−1.04299	−1.05118	0.5551	12.8934
−0.095	+0.02547	−1.01787	−0.98840	0.5887	12.2292
−0.100	+0.02850	−0.99403	−0.92878	0.6219	11.6284
−0.105	+0.03169	−0.97132	−0.87203	0.6546	11.0822
−0.110	+0.03505	−0.94967	−0.81788	0.6868	10.5832
−0.115	+0.03856	−0.92896	−0.76613	0.7184	10.1251
−0.120	+0.04223	−0.90914	−0.71657	0.7495	9.7030
−0.125	+0.04606	−0.89013	−0.66904	0.7800	9.3126
−0.130	+0.05003	−0.87187	−0.62340	0.8100	8.9503
−0.135	+0.05416	−0.85431	−0.57950	0.8394	8.6130
−0.140	+0.05842	−0.83741	−0.53723	0.8681	8.2981
−0.145	+0.06284	−0.82111	−0.49648	0.8963	8.0033
−0.150	+0.06739	−0.80538	−0.45717	0.9238	7.7266
−0.155	+0.07207	−0.79019	−0.41919	0.9507	7.4664
−0.160	+0.07689	−0.77550	−0.38248	0.9770	7.2211
−0.165	+0.08184	−0.76130	−0.34696	1.0027	6.9895
−0.170	+0.08692	−0.74754	−0.31256	1.0277	6.7704
−0.175	+0.09212	−0.7342[illegible]	−0.27923	1.0521	6.5627
−0.180	+0.09744	−0.72128	−0.24692	1.0759	6.3655
−0.185	+0.10288	−0.70874	−0.21556	1.0991	6.1781
−0.190	+0.10843	−0.69656	−0.18512	1.1216	5.9996
−0.195	+0.11410	−0.68473	−0.15555	1.1436	5.8295
−0.200	+0.11987	−0.67324	−0.12681	1.1649	5.6672
−0.205	+0.12574	−0.66206	−0.09887	1.1856	5.5120

1	4	5	6	7	8
−0.210	+0.13172	−0.65118	−0.07168	1.2056	5.3636
−0.215	+0.13780	−0.64060	−0.04522	1.2251	5.2215
−0.220	+0.14397	−0.63029	−0.01945	1.2439	5.0853
−0.225	+0.15024	−0.62026	+0.00563	1.2622	4.9546
−0.230	+0.15659	−0.61047	+0.03009	1.2798	4.8292
−0.235	+0.16304	−0.60093	+0.05393	1.2969	4.7086
−0.240	+0.16956	−0.59163	+0.07719	1.3133	4.5927
−0.245	+0.17617	−0.58256	+0.09987	1.3292	4.4811
−0.250	+0.18285	−0.57371	+0.12200	1.3445	4.3737
−0.255	+0.18961	−0.56506	+0.14361	1.3592	4.2702
−0.260	+0.19645	−0.55662	+0.16471	1.3733	4.1703
−0.265	+0.20335	−0.54838	+0.18532	1.3869	4.0740
−0.270	+0.21031	−0.54032	+0.20546	1.3999	3.9811
−0.275	+0.21735	−0.53245	+0.22514	1.4123	3.8914
−0.280	+0.22444	−0.52476	+0.24438	1.4242	3.8046
−0.285	+0.23159	−0.51723	+0.26319	1.4355	3.7208
−0.290	+0.23879	−0.50987	+0.28159	1.4463	3.6398
−0.295	+0.24605	−0.50267	+0.29959	1.4565	3.5613
−0.300	+0.25336	−0.49562	+0.31721	1.4662	3.4855
−0.305	+0.26071	−0.48873	+0.33445	1.4753	3.4120
−0.310	+0.26811	−0.48197	+0.35133	1.4839	3.3409
−0.315	+0.27555	−0.47536	+0.36786	1.4920	3.2719
−0.320	+0.28303	−0.46889	+0.38406	1.4996	3.2051
−0.325	+0.29055	−0.46254	+0.39992	1.5066	3.1404
−0.330	+0.29810	−0.45632	+0.41546	1.5131	3.0776
−0.335	+0.30568	−0.45023	+0.43070	1.5192	3.0168
−0.340	+0.31329	−0.44425	+0.44564	1.5247	2.9577
−0.345	+0.32092	−0.43840	+0.46028	1.5297	2.9004
−0.350	+0.32858	−0.43265	+0.47464	1.5342	2.8448
−0.355	+0.33627	−0.42701	+0.48873	1.5382	2.7909
−0.360	+0.34397	−0.42149	+0.50256	1.5417	2.7385
−0.365	+0.35168	−0.41606	+0.51612	1.5448	2.6876
−0.370	+0.35941	−0.41073	+0.52943	1.5473	2.6382
−0.375	+0.36716	−0.40551	+0.54251	1.5494	2.5902
−0.380	+0.37491	−0.40037	+0.55534	1.5510	2.5436
−0.385	+0.38266	−0.39533	+0.56794	1.5522	2.4984
−0.390	+0.39043	−0.39038	+0.58033	1.5529	2.4544
−0.395	+0.39819	−0.38551	+0.59249	1.5531	2.4116
−0.400	+0.40596	−0.38073	+0.60444	1.5529	2.3701
−0.405	+0.41372	−0.37603	+0.61619	1.5522	2.3297
−0.410	+0.42148	−0.37141	+0.62774	1.5511	2.2904
−0.415	+0.42923	−0.36687	+0.63910	1.5495	2.2523
−0.420	+0.43698	−0.36240	+0.65027	1.5475	2.2152
−0.425	+0.44471	−0.35801	+0.66126	1.5451	2.1791
−0.430	+0.45243	−0.35368	+0.67206	1.5423	2.1441
−0.435	+0.46013	−0.34943	+0.68270	1.5391	2.1100
−0.440	+0.46782	−0.34524	+0.69317	1.5354	2.0769
−0.445	+0.47548	−0.34112	+0.70347	1.5313	2.0447
−0.450	+0.48313	−0.33706	+0.71361	1.5269	2.0134
−0.455	+0.49075	−0.33307	+0.72360	1.5220	1.9829
−0.460	+0.49835	−0.32913	+0.73344	1.5168	1.9533
−0.465	+0.50592	−0.32525	+0.74314	1.5112	1.9245
−0.470	+0.51346	−0.32143	+0.75269	1.5052	1.8965
−0.475	+0.52097	−0.31766	+0.76211	1.4988	1.8693
−0.480	+0.52845	−0.31395	+0.77139	1.4921	1.8429
−0.485	+0.53589	−0.31029	+0.78054	1.4850	1.8171
−0.490	+0.54330	−0.30668	+0.78956	1.4775	1.7921
−0.495	+0.55067	−0.30312	+0.79846	1.4698	1.7678
−0.500	+0.55800	−0.29961	+0.80724	1.4617	1.7442
−0.505	+0.56529	−0.29615	+0.81590	1.4532	1.7213
−0.510	+0.57253	−0.29273	+0.82445	1.4445	1.6990
−0.515	+0.57973	−0.28935	+0.83289	1.4354	1.6773
−0.520	+0.58688	−0.28602	+0.84123	1.4260	1.6562
−0.525	+0.59399	−0.28272	+0.84946	1.4163	1.6358
−0.530	+0.60105	−0.27947	+0.85759	1.4064	1.6159
−0.535	+0.60805	−0.27626	+0.86562	1.3961	1.5966
−0.540	+0.61501	−0.27309	+0.87355	1.3856	1.5778
−0.545	+0.62191	−0.26995	+0.88140	1.3748	1.5596
−0.550	+0.62876	−0.26685	+0.88915	1.3638	1.5420
−0.555	+0.63555	−0.26378	+0.89682	1.3525	1.5248
−0.560	+0.64228	−0.26075	+0.90440	1.3410	1.5082
−0.565	+0.64896	−0.25775	+0.91190	1.3292	1.4920
−0.570	+0.65558	−0.25478	+0.91932	1.3173	1.4763
−0.575	+0.66213	−0.25184	+0.92667	1.3051	1.4611
−0.580	+0.66863	−0.24893	+0.93394	1.2927	1.4464
−0.585	+0.67506	−0.24605	+0.94113	1.2801	1.4321
−0.590	+0.68143	−0.24320	+0.94826	1.2673	1.4183
−0.595	+0.68773	−0.24038	+0.95532	1.2544	1.4049
−0.600	+0.69397	−0.23758	+0.96231	1.2412	1.3919
−0.605	+0.70014	−0.23481	+0.96924	1.2280	1.3793

1533

1	4	5	6	7	8
-0.010	+0.00012	-2.03075	-3.49709	0.0319	109.8055
-0.015	+0.00035	-1.85229	-3.05095	0.0571	73.6117
-0.020	+0.00070	-1.72495	-2.73260	0.0857	55.4946
-0.025	+0.00121	-1.62567	-2.48439	0.1168	44.6129
-0.030	+0.00187	-1.54415	-2.28061	0.1497	37.3491
-0.035	+0.00271	-1.47492	-2.10753	0.1841	32.1525
-0.040	+0.00372	-1.41470	-1.95697	0.2195	28.2476
-0.045	+0.00491	-1.36137	-1.82365	0.2556	25.2036
-0.050	+0.00628	-1.31349	-1.70395	0.2922	22.7622
-0.055	+0.00783	-1.27003	-1.59530	0.3292	20.7588
-0.060	+0.00957	-1.23024	-1.49582	0.3664	19.0840
-0.065	+0.01149	-1.19353	-1.40405	0.4036	17.6618
-0.070	+0.01361	-1.15946	-1.31887	0.4407	16.4382
-0.075	+0.01590	-1.12767	-1.23940	0.4777	15.3734
-0.080	+0.01838	-1.09788	-1.16493	0.5144	14.4377
-0.085	+0.02105	-1.06985	-1.09485	0.5508	13.6083
-0.090	+0.02389	-1.04339	-1.02870	0.5869	12.8676
-0.095	+0.02691	-1.01833	-0.96605	0.6225	12.2016
-0.100	+0.03012	-0.99454	-0.90657	0.6577	11.5991
-0.105	+0.03349	-0.97190	-0.84997	0.6925	11.0511
-0.110	+0.03704	-0.95031	-0.79599	0.7267	10.5503
-0.115	+0.04076	-0.92967	-0.74440	0.7603	10.0905
-0.120	+0.04464	-0.90992	-0.69502	0.7935	9.6666
-0.125	+0.04869	-0.89098	-0.64768	0.8260	9.2745
-0.130	+0.05290	-0.87280	-0.60223	0.8579	8.9104
-0.135	+0.05727	-0.85533	-0.55853	0.8893	8.5714
-0.140	+0.06180	-0.83850	-0.51648	0.9200	8.2548
-0.145	+0.06647	-0.82229	-0.47595	0.9502	7.9583
-0.150	+0.07130	-0.80666	-0.43687	0.9797	7.6799
-0.155	+0.07627	-0.79156	-0.39913	1.0085	7.4181
-0.160	+0.08138	-0.77697	-0.36266	1.0368	7.1712
-0.165	+0.08664	-0.76287	-0.32739	1.0644	6.9379
-0.170	+0.09203	-0.74921	-0.29326	1.0914	6.7172
-0.175	+0.09755	-0.73599	-0.26020	1.1177	6.5079
-0.180	+0.10320	-0.72318	-0.22816	1.1434	6.3092
-0.185	+0.10898	-0.71075	-0.19709	1.1685	6.1202
-0.190	+0.11489	-0.69869	-0.16694	1.1929	5.9402
-0.195	+0.12091	-0.68698	-0.13768	1.2168	5.7686
-0.200	+0.12705	-0.67561	-0.10925	1.2400	5.6047
-0.205	+0.13331	-0.66456	-0.08162	1.2625	5.4481
-0.210	+0.13968	-0.65381	-0.05475	1.2845	5.2982
-0.215	+0.14615	-0.64336	-0.02862	1.3058	5.1547
-0.220	+0.15274	-0.63319	-0.00320	1.3265	5.0171
-0.225	+0.15942	-0.62329	+0.02155	1.3466	4.8850
-0.230	+0.16620	-0.61365	+0.04565	1.3662	4.7582
-0.235	+0.17308	-0.60425	+0.06914	1.3851	4.6363
-0.240	+0.18005	-0.59510	+0.09202	1.4034	4.5190
-0.245	+0.18711	-0.58617	+0.11434	1.4211	4.4061
-0.250	+0.19426	-0.57747	+0.13609	1.4382	4.2974
-0.255	+0.20150	-0.56898	+0.15732	1.4548	4.1926
-0.260	+0.20881	-0.56070	+0.17803	1.4707	4.0915
-0.265	+0.21620	-0.55261	+0.19824	1.4861	3.9940
-0.270	+0.22367	-0.54472	+0.21797	1.5009	3.8998
-0.275	+0.23121	-0.53701	+0.23724	1.5152	3.8089
-0.280	+0.23882	-0.52948	+0.25607	1.5289	3.7210
-0.285	+0.24650	-0.52212	+0.27446	1.5420	3.6360
-0.290	+0.25424	-0.51494	+0.29243	1.5546	3.5538
-0.295	+0.26204	-0.50791	+0.31000	1.5666	3.4742
-0.300	+0.26991	-0.50104	+0.32718	1.5781	3.3972
-0.305	+0.27782	-0.49432	+0.34398	1.5890	3.3227
-0.310	+0.28580	-0.48774	+0.36041	1.5994	3.2504
-0.315	+0.29382	-0.48131	+0.37648	1.6092	3.1805
-0.320	+0.30189	-0.47502	+0.39222	1.6186	3.1126
-0.325	+0.31000	-0.46886	+0.40761	1.6274	3.0469
-0.330	+0.31816	-0.46283	+0.42269	1.6356	2.9831
-0.335	+0.32636	-0.45693	+0.43745	1.6434	2.9212
-0.340	+0.33459	-0.45115	+0.45190	1.6506	2.8612
-0.345	+0.34287	-0.44548	+0.46606	1.6573	2.8029
-0.350	+0.35117	-0.43993	+0.47994	1.6636	2.7464
-0.355	+0.35950	-0.43449	+0.49353	1.6693	2.6915
-0.360	+0.36786	-0.42917	+0.50685	1.6745	2.6381
-0.365	+0.37625	-0.42394	+0.51992	1.6792	2.5864
-0.370	+0.38465	-0.41882	+0.53272	1.6834	2.5361
-0.375	+0.39308	-0.41380	+0.54528	1.6872	2.4872
-0.380	+0.40152	-0.40887	+0.55760	1.6904	2.4397
-0.385	+0.40998	-0.40404	+0.56968	1.6932	2.3936
-0.390	+0.41845	-0.39929	+0.58153	1.6955	2.3487
-0.395	+0.42694	-0.39464	+0.59317	1.6973	2.3051
-0.400	+0.43543	-0.39007	+0.60459	1.6986	2.2627
-0.405	+0.44392	-0.38559	+0.61580	1.6995	2.2215
-0.410	+0.45242	-0.38119	+0.62681	1.6999	2.1815
-0.415	+0.46092	-0.37686	+0.63762	1.6998	2.1425
-0.420	+0.46942	-0.37261	+0.64823	1.6993	2.1047
-0.425	+0.47791	-0.36844	+0.65866	1.6983	2.0678
-0.430	+0.48640	-0.36434	+0.66891	1.6969	2.0320
-0.435	+0.49488	-0.36031	+0.67899	1.6951	1.9972
-0.440	+0.50335	-0.35635	+0.68889	1.6928	1.9633
-0.445	+0.51181	-0.35246	+0.69862	1.6900	1.9304
-0.450	+0.52025	-0.34863	+0.70819	1.6869	1.8983
-0.455	+0.52868	-0.34486	+0.71761	1.6833	1.8671
-0.460	+0.53709	-0.34116	+0.72687	1.6792	1.8368
-0.465	+0.54547	-0.33752	+0.73598	1.6748	1.8073
-0.470	+0.55383	-0.33393	+0.74494	1.6700	1.7786
-0.475	+0.56217	-0.33040	+0.75376	1.6647	1.7507
-0.480	+0.57048	-0.32693	+0.76245	1.6591	1.7236
-0.485	+0.57876	-0.32351	+0.77100	1.6530	1.6972
-0.490	+0.58701	-0.32014	+0.77942	1.6465	1.6715
-0.495	+0.59523	-0.31682	+0.78772	1.6397	1.6466
-0.500	+0.60341	-0.31355	+0.79589	1.6325	1.6223
-0.505	+0.61155	-0.31033	+0.80394	1.6249	1.5987
-0.510	+0.61966	-0.30716	+0.81188	1.6169	1.5757
-0.515	+0.62772	-0.30403	+0.81970	1.6086	1.5534
-0.520	+0.63574	-0.30094	+0.82742	1.5999	1.5317
-0.525	+0.64372	-0.29790	+0.83502	1.5909	1.5107
-0.530	+0.65165	-0.29490	+0.84252	1.5815	1.4902
-0.535	+0.65953	-0.29194	+0.84992	1.5718	1.4702
-0.540	+0.66737	-0.28902	+0.85723	1.5618	1.4509
-0.545	+0.67515	-0.28613	+0.86444	1.5514	1.4321
-0.550	+0.68288	-0.28329	+0.87155	1.5407	1.4138
-0.555	+0.69056	-0.28048	+0.87857	1.5297	1.3961
-0.560	+0.69818	-0.27770	+0.88551	1.5184	1.3788
-0.565	+0.70574	-0.27496	+0.89236	1.5069	1.3621
-0.570	+0.71325	-0.27225	+0.89913	1.4950	1.3458
-0.575	+0.72069	-0.26958	+0.90582	1.4828	1.3301
-0.580	+0.72808	-0.26693	+0.91244	1.4704	1.3147
-0.585	+0.73540	-0.26432	+0.91897	1.4578	1.2999
-0.590	+0.74266	-0.26173	+0.92544	1.4449	1.2855
-0.595	+0.74985	-0.25918	+0.93183	1.4317	1.2715
-0.600	+0.75697	-0.25665	+0.93815	1.4183	1.2579
-0.605	+0.76403	-0.25414	+0.94441	1.4047	1.2448

1534

1	4	5	6	7	8
-0.010	+0.00013	-2.03075	-3.47482	0.0335	109.8037
-0.015	+0.00036	-1.85230	-3.02869	0.0601	73.6092
-0.020	+0.00074	-1.72496	-2.71036	0.0902	55.4910
-0.025	+0.00127	-1.62569	-2.46217	0.1229	44.6081
-0.030	+0.00197	-1.54419	-2.25841	0.1576	37.3431
-0.035	+0.00285	-1.47497	-2.08537	0.1938	32.1450
-0.040	+0.00391	-1.41476	-1.93485	0.2311	28.2386
-0.045	+0.00516	-1.36145	-1.80157	0.2691	25.1931
-0.050	+0.00661	-1.31359	-1.68193	0.3078	22.7500
-0.055	+0.00824	-1.27016	-1.57335	0.3467	20.7450
-0.060	+0.01008	-1.23040	-1.47394	0.3859	19.0685
-0.065	+0.01210	-1.19372	-1.38225	0.4251	17.6447
-0.070	+0.01433	-1.15969	-1.29717	0.4643	16.4193
-0.075	+0.01675	-1.12794	-1.21780	0.5033	15.3528
-0.080	+0.01936	-1.09819	-1.14342	0.5421	14.4153
-0.085	+0.02217	-1.07021	-1.07347	0.5806	13.5842
-0.090	+0.02517	-1.04379	-1.00744	0.6187	12.8417
-0.095	+0.02836	-1.01879	-0.94493	0.6564	12.1739
-0.100	+0.03173	-0.99506	-0.88559	0.6937	11.5697
-0.105	+0.03529	-0.97247	-0.82914	0.7305	11.0199
-0.110	+0.03904	-0.95095	-0.77531	0.7667	10.5173
-0.115	+0.04296	-0.93038	-0.72390	0.8025	10.0557
-0.120	+0.04706	-0.91070	-0.67470	0.8376	9.6302
-0.125	+0.05134	-0.89184	-0.62754	0.8722	9.2363
-0.130	+0.05578	-0.87373	-0.58229	0.9062	8.8705
-0.135	+0.06040	-0.85634	-0.53880	0.9396	8.5297
-0.140	+0.06518	-0.83960	-0.49695	0.9723	8.2114
-0.145	+0.07012	-0.82348	-0.45665	1.0045	7.9132
-0.150	+0.07522	-0.80793	-0.41779	1.0360	7.6332
-0.155	+0.08048	-0.79293	-0.38029	1.0669	7.3697
-0.160	+0.08589	-0.77845	-0.34407	1.0971	7.1212
-0.165	+0.09145	-0.76444	-0.30905	1.1267	6.8863
-0.170	+0.09716	-0.75089	-0.27518	1.1557	6.6639
-0.175	+0.10301	-0.73778	-0.24239	1.1841	6.4530
-0.180	+0.10900	-0.72507	-0.21063	1.2118	6.2527
-0.185	+0.11512	-0.71276	-0.17985	1.2389	6.0622
-0.190	+0.12139	-0.70082	-0.15000	1.2653	5.8807
-0.195	+0.12778	-0.68923	-0.12103	1.2911	5.7075
-0.200	+0.13430	-0.67798	-0.09291	1.3163	5.5422
-0.205	+0.14094	-0.66706	-0.06559	1.3409	5.3841

1	4	5	6	7	8
−0.210	+0.14770	−0.65644	−0.03905	1.3648	5.2328
−0.215	+0.15459	−0.64612	−0.01326	1.3882	5.0878
−0.220	+0.16159	−0.63609	+0.01182	1.4109	4.9487
−0.225	+0.16870	−0.62632	+0.03623	1.4330	4.8153
−0.230	+0.17592	−0.61682	+0.05999	1.4545	4.6870
−0.235	+0.18324	−0.60757	+0.08311	1.4754	4.5638
−0.240	+0.19067	−0.59856	+0.10563	1.4958	4.4452
−0.245	+0.19820	−0.58979	+0.12757	1.5155	4.3309
−0.250	+0.20582	−0.58124	+0.14895	1.5346	4.2209
−0.255	+0.21354	−0.57290	+0.16979	1.5532	4.1148
−0.260	+0.22136	−0.56477	+0.19010	1.5712	4.0125
−0.265	+0.22926	−0.55685	+0.20992	1.5886	3.9137
−0.270	+0.23724	−0.54912	+0.22925	1.6055	3.8183
−0.275	+0.24531	−0.54157	+0.24811	1.6218	3.7261
−0.280	+0.25346	−0.53421	+0.26651	1.6375	3.6370
−0.285	+0.26168	−0.52702	+0.28448	1.6527	3.5508
−0.290	+0.26999	−0.52000	+0.30203	1.6673	3.4675
−0.295	+0.27836	−0.51315	+0.31916	1.6814	3.3868
−0.300	+0.28680	−0.50646	+0.33590	1.6949	3.3086
−0.305	+0.29531	−0.49991	+0.35225	1.7079	3.2330
−0.310	+0.30388	−0.49352	+0.36823	1.7204	3.1596
−0.315	+0.31251	−0.48727	+0.38385	1.7324	3.0886
−0.320	+0.32120	−0.48117	+0.39912	1.7438	3.0196
−0.325	+0.32995	−0.47519	+0.41405	1.7547	2.9528
−0.330	+0.33875	−0.46935	+0.42865	1.7650	2.8880
−0.335	+0.34760	−0.46364	+0.44294	1.7749	2.8251
−0.340	+0.35650	−0.45805	+0.45691	1.7843	2.7640
−0.345	+0.36544	−0.45258	+0.47058	1.7931	2.7048
−0.350	+0.37443	−0.44723	+0.48396	1.8014	2.6472
−0.355	+0.38345	−0.44199	+0.49706	1.8093	2.5914
−0.360	+0.39252	−0.43686	+0.50988	1.8166	2.5371
−0.365	+0.40162	−0.43184	+0.52243	1.8235	2.4843
−0.370	+0.41075	−0.42693	+0.53472	1.8298	2.4331
−0.375	+0.41992	−0.42211	+0.54676	1.8357	2.3833
−0.380	+0.42911	−0.41739	+0.55856	1.8410	2.3349
−0.385	+0.43833	−0.41277	+0.57012	1.8459	2.2879
−0.390	+0.44757	−0.40824	+0.58144	1.8503	2.2421
−0.395	+0.45683	−0.40380	+0.59254	1.8543	2.1976
−0.400	+0.46611	−0.39945	+0.60342	1.8577	2.1544
−0.405	+0.47541	−0.39518	+0.61409	1.8607	2.1123
−0.410	+0.48472	−0.39100	+0.62455	1.8632	2.0714
−0.415	+0.49404	−0.38689	+0.63480	1.8653	2.0316
−0.420	+0.50337	−0.38287	+0.64486	1.8668	1.9929
−0.425	+0.51271	−0.37892	+0.65473	1.8680	1.9552
−0.430	+0.52205	−0.37505	+0.66442	1.8686	1.9186
−0.435	+0.53139	−0.37125	+0.67392	1.8688	1.8830
−0.440	+0.54074	−0.36751	+0.68325	1.8686	1.8483
−0.445	+0.55008	−0.36385	+0.69241	1.8678	1.8145
−0.450	+0.55942	−0.36026	+0.70140	1.8667	1.7817
−0.455	+0.56875	−0.35672	+0.71023	1.8651	1.7497
−0.460	+0.57807	−0.35326	+0.71890	1.8630	1.7186
−0.465	+0.58738	−0.34985	+0.72741	1.8605	1.6883
−0.470	+0.59667	−0.34650	+0.73578	1.8576	1.6589
−0.475	+0.60595	−0.34321	+0.74400	1.8543	1.6302
−0.480	+0.61521	−0.33998	+0.75209	1.8505	1.6023
−0.485	+0.62446	−0.33680	+0.76003	1.8463	1.5752
−0.490	+0.63368	−0.33368	+0.76784	1.8416	1.5488
−0.495	+0.64287	−0.33061	+0.77552	1.8365	1.5231
−0.500	+0.65204	−0.32759	+0.78307	1.8311	1.4981
−0.505	+0.66118	−0.32461	+0.79050	1.8252	1.4737
−0.510	+0.67029	−0.32169	+0.79781	1.8188	1.4500
−0.515	+0.67937	−0.31881	+0.80500	1.8121	1.4270
−0.520	+0.68841	−0.31598	+0.81208	1.8050	1.4046
−0.525	+0.69742	−0.31319	+0.81905	1.7975	1.3828
−0.530	+0.70639	−0.31045	+0.82591	1.7896	1.3616
−0.535	+0.71532	−0.30775	+0.83267	1.7813	1.3410
−0.540	+0.72420	−0.30509	+0.83932	1.7726	1.3209
−0.545	+0.73304	−0.30246	+0.84588	1.7635	1.3014
−0.550	+0.74184	−0.29988	+0.85234	1.7541	1.2824
−0.555	+0.75058	−0.29733	+0.85870	1.7443	1.2640
−0.560	+0.75928	−0.29482	+0.86498	1.7341	1.2460
−0.565	+0.76792	−0.29235	+0.87116	1.7236	1.2286
−0.570	+0.77652	−0.28991	+0.87727	1.7127	1.2116
−0.575	+0.78505	−0.28750	+0.88328	1.7015	1.1952
−0.580	+0.79353	−0.28513	+0.88922	1.6900	1.1792
−0.585	+0.80195	−0.28278	+0.89508	1.6781	1.1636
−0.590	+0.81031	−0.28047	+0.90086	1.6659	1.1485
−0.595	+0.81861	−0.27819	+0.90656	1.6533	1.1339
−0.600	+0.82685	−0.27594	+0.91220	1.6405	1.1196
−0.605	+0.83502	−0.27371	+0.91776	1.6274	1.1058

1535

1	4	5	6	7	8
−0.010	+0.00014	−2.03075	−3.45364	0.0352	109.8023
−0.015	+0.00038	−1.85230	−3.00752	0.0631	73.6068
−0.020	+0.00078	−1.72497	−2.68920	0.0947	55.4876
−0.025	+0.00134	−1.62571	−2.44103	0.1291	44.6034
−0.030	+0.00207	−1.54421	−2.23730	0.1655	37.3370
−0.035	+0.00300	−1.47501	−2.06429	0.2035	32.1376
−0.040	+0.00411	−1.41482	−1.91381	0.2427	28.2297
−0.045	+0.00542	−1.36153	−1.78058	0.2827	25.1826
−0.050	+0.00694	−1.31369	−1.66099	0.3233	22.7379
−0.055	+0.00866	−1.27029	−1.55248	0.3643	20.7313
−0.060	+0.01058	−1.23055	−1.45314	0.4055	19.0531
−0.065	+0.01271	−1.19391	−1.36153	0.4467	17.6275
−0.070	+0.01505	−1.15991	−1.27654	0.4880	16.4004
−0.075	+0.01759	−1.12820	−1.19727	0.5290	15.3322
−0.080	+0.02034	−1.09850	−1.12300	0.5699	14.3930
−0.085	+0.02329	−1.07056	−1.05316	0.6105	13.5601
−0.090	+0.02645	−1.04420	−0.98726	0.6507	12.8158
−0.095	+0.02980	−1.01925	−0.92488	0.6905	12.1463
−0.100	+0.03335	−0.99557	−0.86569	0.7298	11.5402
−0.105	+0.03710	−0.97305	−0.80939	0.7687	10.9887
−0.110	+0.04104	−0.95158	−0.75572	0.8070	10.4843
−0.115	+0.04517	−0.93108	−0.70448	0.8448	10.0210
−0.120	+0.04949	−0.91147	−0.65545	0.8820	9.5937
−0.125	+0.05399	−0.89269	−0.60849	0.9187	9.1980
−0.130	+0.05867	−0.87466	−0.56343	0.9548	8.8305
−0.135	+0.06354	−0.85735	−0.52014	0.9902	8.4881
−0.140	+0.06857	−0.84070	−0.47851	1.0251	8.1680
−0.145	+0.07379	−0.82466	−0.43842	1.0593	7.8682
−0.150	+0.07917	−0.80921	−0.39979	1.0929	7.5865
−0.155	+0.08471	−0.79431	−0.36253	1.1258	7.3213
−0.160	+0.09042	−0.77992	−0.32656	1.1582	7.0711
−0.165	+0.09630	−0.76601	−0.29180	1.1899	6.8346
−0.170	+0.10232	−0.75257	−0.25819	1.2209	6.6106
−0.175	+0.10850	−0.73956	−0.22567	1.2514	6.3981
−0.180	+0.11484	−0.72697	−0.19419	1.2812	6.1962
−0.185	+0.12132	−0.71477	−0.16369	1.3103	6.0041
−0.190	+0.12794	−0.70295	−0.13413	1.3389	5.8211
−0.195	+0.13470	−0.69148	−0.10547	1.3668	5.6464
−0.200	+0.14161	−0.68036	−0.07766	1.3941	5.4795
−0.205	+0.14864	−0.66956	−0.05066	1.4208	5.3199
−0.210	+0.15581	−0.65907	−0.02444	1.4469	5.1672
−0.215	+0.16311	−0.64888	+0.00101	1.4723	5.0207
−0.220	+0.17054	−0.63898	+0.02576	1.4972	4.8802
−0.225	+0.17808	−0.62936	+0.04983	1.5215	4.7454
−0.230	+0.18575	−0.62000	+0.07323	1.5452	4.6157
−0.235	+0.19354	−0.61089	+0.09599	1.5683	4.4911
−0.240	+0.20143	−0.60203	+0.11815	1.5908	4.3711
−0.245	+0.20944	−0.59340	+0.13971	1.6127	4.2555
−0.250	+0.21756	−0.58501	+0.16071	1.6341	4.1442
−0.255	+0.22578	−0.57682	+0.18116	1.6549	4.0368
−0.260	+0.23411	−0.56886	+0.20108	1.6751	3.9331
−0.265	+0.24253	−0.56109	+0.22050	1.6948	3.8331
−0.270	+0.25106	−0.55352	+0.23942	1.7139	3.7364
−0.275	+0.25967	−0.54614	+0.25787	1.7325	3.6430
−0.280	+0.26838	−0.53895	+0.27586	1.7506	3.5527
−0.285	+0.27718	−0.53193	+0.29340	1.7681	3.4653
−0.290	+0.28606	−0.52508	+0.31051	1.7851	3.3808
−0.295	+0.29503	−0.51840	+0.32721	1.8016	3.2989
−0.300	+0.30408	−0.51189	+0.34351	1.8175	3.2196
−0.305	+0.31320	−0.50552	+0.35941	1.8329	3.1428
−0.310	+0.32241	−0.49931	+0.37494	1.8478	3.0683
−0.315	+0.33168	−0.49325	+0.39010	1.8622	2.9961
−0.320	+0.34103	−0.48733	+0.40491	1.8761	2.9261
−0.325	+0.35044	−0.48154	+0.41937	1.8895	2.8582
−0.330	+0.35992	−0.47589	+0.43349	1.9024	2.7923
−0.335	+0.36947	−0.47037	+0.44729	1.9148	2.7283
−0.340	+0.37907	−0.46498	+0.46078	1.9268	2.6662
−0.345	+0.38873	−0.45971	+0.47396	1.9382	2.6059
−0.350	+0.39845	−0.45455	+0.48684	1.9492	2.5474
−0.355	+0.40823	−0.44951	+0.49943	1.9596	2.4905
−0.360	+0.41805	−0.44459	+0.51175	1.9696	2.4352
−0.365	+0.42792	−0.43977	+0.52379	1.9792	2.3814
−0.370	+0.43784	−0.43506	+0.53557	1.9882	2.3292
−0.375	+0.44780	−0.43045	+0.54708	1.9968	2.2785
−0.380	+0.45781	−0.42595	+0.55835	2.0050	2.2291
−0.385	+0.46785	−0.42154	+0.56938	2.0127	2.1811
−0.390	+0.47794	−0.41722	+0.58017	2.0199	2.1344
−0.395	+0.48805	−0.41300	+0.59073	2.0266	2.0890
−0.400	+0.49820	−0.40886	+0.60106	2.0330	2.0448
−0.405	+0.50838	−0.40482	+0.61118	2.0388	2.0018

-0.410	+0.51859	−0.40086	+0.62108	2.0442	1.9600
-0.415	+0.52882	−0.39698	+0.63078	2.0492	1.9193
-0.420	+0.53908	−0.39318	+0.64028	2.0537	1.8797
-0.425	+0.54936	−0.38946	+0.64958	2.0578	1.8411
-0.430	+0.55966	−0.38581	+0.65869	2.0614	1.8036
-0.435	+0.56997	−0.38224	+0.66762	2.0646	1.7671
-0.440	+0.58030	−0.37874	+0.67636	2.0673	1.7315
-0.445	+0.59065	−0.37532	+0.68493	2.0697	1.6969
-0.450	+0.60100	−0.37196	+0.69333	2.0715	1.6632
-0.455	+0.61136	−0.36866	+0.70157	2.0730	1.6304
-0.460	+0.62173	−0.36543	+0.70964	2.0740	1.5984
-0.465	+0.63210	−0.36227	+0.71755	2.0745	1.5673
-0.470	+0.64248	−0.35916	+0.72531	2.0747	1.5370
-0.475	+0.65285	−0.35612	+0.73292	2.0744	1.5075
-0.480	+0.66322	−0.35313	+0.74039	2.0737	1.4788
-0.485	+0.67358	−0.35020	+0.74771	2.0725	1.4508
-0.490	+0.68394	−0.34733	+0.75490	2.0710	1.4235
-0.495	+0.69429	−0.34451	+0.76195	2.0690	1.3970
-0.500	+0.70463	−0.34174	+0.76887	2.0666	1.3712
-0.505	+0.71496	−0.33902	+0.77566	2.0637	1.3460
-0.510	+0.72527	−0.33635	+0.78233	2.0604	1.3215
-0.515	+0.73556	−0.33374	+0.78888	2.0568	1.2976
-0.520	+0.74584	−0.33116	+0.79531	2.0526	1.2744
-0.525	+0.75609	−0.32864	+0.80163	2.0481	1.2518
-0.530	+0.76632	−0.32616	+0.80783	2.0432	1.2298
-0.535	+0.77652	−0.32372	+0.81392	2.0378	1.2083
-0.540	+0.78670	−0.32132	+0.81991	2.0321	1.1874
-0.545	+0.79684	−0.31897	+0.82580	2.0259	1.1671
-0.550	+0.80696	−0.31665	+0.83159	2.0193	1.1473
-0.555	+0.81704	−0.31438	+0.83727	2.0123	1.1280
-0.560	+0.82708	−0.31214	+0.84287	2.0049	1.1093
-0.565	+0.83708	−0.30994	+0.84837	1.9971	1.0910
-0.570	+0.84705	−0.30778	+0.85378	1.9889	1.0733
-0.575	+0.85697	−0.30565	+0.85910	1.9803	1.0560
-0.580	+0.86685	−0.30355	+0.86434	1.9713	1.0391
-0.585	+0.87669	−0.30149	+0.86950	1.9619	1.0228
-0.590	+0.88647	−0.29946	+0.87457	1.9521	1.0069
-0.595	+0.89621	−0.29746	+0.87957	1.9419	0.9914
-0.600	+0.90589	−0.29549	+0.88448	1.9314	0.9763
-0.605	+0.91552	−0.29356	+0.88933	1.9205	0.9616

1536

1	4	5	6	7	8
-0.010	+0.00014	−2.03075	−3.43344	0.0369	109.8016
-0.015	+0.00040	−1.85231	−2.98732	0.0661	73.6049
-0.020	+0.00081	−1.72498	−2.66902	0.0992	55.4844
-0.025	+0.00140	−1.62572	−2.42087	0.1352	44.5989
-0.030	+0.00217	−1.54424	−2.21716	0.1734	37.3311
-0.035	+0.00314	−1.47505	−2.04418	0.2133	32.1302
-0.040	+0.00431	−1.41488	−1.89375	0.2543	28.2208
-0.045	+0.00568	−1.36160	−1.76057	0.2962	25.1722
-0.050	+0.00727	−1.31379	−1.64104	0.3388	22.7259
-0.055	+0.00907	−1.27041	−1.53259	0.3818	20.7176
-0.060	+0.01109	−1.23071	−1.43332	0.4250	19.0377
-0.065	+0.01332	−1.19410	−1.34179	0.4684	17.6104
-0.070	+0.01577	−1.16013	−1.25689	0.5117	16.3816
-0.075	+0.01844	−1.12846	−1.17772	0.5548	15.3116
-0.080	+0.02132	−1.09880	−1.10356	0.5978	14.3706
-0.085	+0.02442	−1.07091	−1.03383	0.6404	13.5360
-0.090	+0.02773	−1.04460	−0.96805	0.6827	12.7900
-0.095	+0.03125	−1.01970	−0.90581	0.7246	12.1186
-0.100	+0.03497	−0.99608	−0.84676	0.7661	11.5108
-0.105	+0.03891	−0.97362	−0.79061	0.8070	10.9575
-0.110	+0.04304	−0.95222	−0.73711	0.8475	10.4514
-0.115	+0.04738	−0.93179	−0.68603	0.8874	9.9863
-0.120	+0.05192	−0.91225	−0.63719	0.9268	9.5572
-0.125	+0.05665	−0.89354	−0.59040	0.9655	9.1598
-0.130	+0.06157	−0.87559	−0.54554	1.0037	8.7906
-0.135	+0.06669	−0.85836	−0.50246	1.0413	8.4464
-0.140	+0.07199	−0.84179	−0.46104	1.0783	8.1246
-0.145	+0.07747	−0.82585	−0.42118	1.1146	7.8231
-0.150	+0.08313	−0.81049	−0.38278	1.1503	7.5397
-0.155	+0.08897	−0.79568	−0.34575	1.1855	7.2728
-0.160	+0.09499	−0.78139	−0.31002	1.2199	7.0210
-0.165	+0.10117	−0.76758	−0.27552	1.2538	6.7828
-0.170	+0.10752	−0.75425	−0.24217	1.2870	6.5572
-0.175	+0.11404	−0.74135	−0.20993	1.3196	6.3431
-0.180	+0.12072	−0.72887	−0.17872	1.3516	6.1397
-0.185	+0.12756	−0.71678	−0.14851	1.3830	5.9460
-0.190	+0.13455	−0.70508	−0.11925	1.4137	5.7614
-0.195	+0.14169	−0.69373	−0.09089	1.4439	5.5851
-0.200	+0.14899	−0.68273	−0.06338	1.4734	5.4168
-0.205	+0.15643	−0.67206	−0.03671	1.5024	5.2557

1	4	5	6	7	8
−0.210	+0.16401	−0.66170	−0.01082	1.5307	5.1014
−0.215	+0.17173	−0.65165	+0.01431	1.5585	4.9535
−0.220	+0.17959	−0.64189	+0.03872	1.5856	4.8116
−0.225	+0.18759	−0.63240	+0.06244	1.6122	4.6753
−0.230	+0.19572	−0.62318	+0.08548	1.6383	4.5442
−0.235	+0.20397	−0.61422	+0.10789	1.6637	4.4182
−0.240	+0.21235	−0.60550	+0.12967	1.6886	4.2968
−0.245	+0.22086	−0.59703	+0.15086	1.7130	4.1799
−0.250	+0.22948	−0.58878	+0.17148	1.7368	4.0672
−0.255	+0.23822	−0.58076	+0.19154	1.7601	3.9585
−0.260	+0.24708	−0.57295	+0.21107	1.7828	3.8535
−0.265	+0.25605	−0.56534	+0.23008	1.8050	3.7522
−0.270	+0.26513	−0.55793	+0.24860	1.8267	3.6542
−0.275	+0.27432	−0.55072	+0.26663	1.8479	3.5596
−0.280	+0.28361	−0.54369	+0.28420	1.8686	3.4680
−0.285	+0.29300	−0.53685	+0.30132	1.8887	3.3794
−0.290	+0.30250	−0.53017	+0.31800	1.9084	3.2936
−0.295	+0.31209	−0.52367	+0.33426	1.9276	3.2105
−0.300	+0.32177	−0.51733	+0.35011	1.9463	3.1300
−0.305	+0.33155	−0.51115	+0.36556	1.9646	3.0520
−0.310	+0.34142	−0.50512	+0.38063	1.9823	2.9764
−0.315	+0.35137	−0.49924	+0.39533	1.9996	2.9031
−0.320	+0.36142	−0.49351	+0.40967	2.0165	2.8319
−0.325	+0.37154	−0.48791	+0.42365	2.0329	2.7629
−0.330	+0.38174	−0.48245	+0.43730	2.0488	2.6959
−0.335	+0.39203	−0.47713	+0.45062	2.0643	2.6308
−0.340	+0.40239	−0.47193	+0.46361	2.0794	2.5676
−0.345	+0.41282	−0.46685	+0.47630	2.0940	2.5063
−0.350	+0.42333	−0.46190	+0.48868	2.1082	2.4466
−0.355	+0.43390	−0.45707	+0.50077	2.1220	2.3887
−0.360	+0.44455	−0.45235	+0.51257	2.1353	2.3323
−0.365	+0.45526	−0.44774	+0.52409	2.1483	2.2776
−0.370	+0.46603	−0.44323	+0.53535	2.1608	2.2243
−0.375	+0.47686	−0.43884	+0.54634	2.1729	2.1725
−0.380	+0.48776	−0.43454	+0.55708	2.1846	2.1221
−0.385	+0.49871	−0.43035	+0.56756	2.1960	2.0731
−0.390	+0.50972	−0.42625	+0.57781	2.2069	2.0255
−0.395	+0.52078	−0.42224	+0.58782	2.2174	1.9790
−0.400	+0.53189	−0.41833	+0.59760	2.2276	1.9339
−0.405	+0.54305	−0.41451	+0.60716	2.2373	1.8899
−0.410	+0.55426	−0.41077	+0.61650	2.2467	1.8471
−0.415	+0.56552	−0.40712	+0.62564	2.2557	1.8055
−0.420	+0.57682	−0.40355	+0.63456	2.2643	1.7649
−0.425	+0.58816	−0.40006	+0.64329	2.2726	1.7254
−0.430	+0.59955	−0.39665	+0.65182	2.2804	1.6869
−0.435	+0.61097	−0.39331	+0.66016	2.2879	1.6494
−0.440	+0.62243	−0.39005	+0.66831	2.2950	1.6129
−0.445	+0.63392	−0.38686	+0.67629	2.3018	1.5773
−0.450	+0.64544	−0.38374	+0.68409	2.3082	1.5427
−0.455	+0.65700	−0.38069	+0.69172	2.3142	1.5089
−0.460	+0.66859	−0.37770	+0.69918	2.3199	1.4760
−0.465	+0.68020	−0.37478	+0.70648	2.3252	1.4440
−0.470	+0.69184	−0.37192	+0.71362	2.3302	1.4128
−0.475	+0.70350	−0.36913	+0.72061	2.3348	1.3823
−0.480	+0.71519	−0.36639	+0.72745	2.3390	1.3527
−0.485	+0.72689	−0.36372	+0.73414	2.3429	1.3238
−0.490	+0.73861	−0.36110	+0.74069	2.3464	1.2956
−0.495	+0.75036	−0.35853	+0.74710	2.3496	1.2681
−0.500	+0.76211	−0.35603	+0.75337	2.3524	1.2414
−0.505	+0.77388	−0.35357	+0.75951	2.3549	1.2153
−0.510	+0.78566	−0.35116	+0.76552	2.3570	1.1898
−0.515	+0.79745	−0.34881	+0.77141	2.3587	1.1650
−0.520	+0.80925	−0.34650	+0.77718	2.3601	1.1409
−0.525	+0.82105	−0.34424	+0.78282	2.3611	1.1173
−0.530	+0.83286	−0.34203	+0.78835	2.3618	1.0943
−0.535	+0.84467	−0.33987	+0.79377	2.3621	1.0720
−0.540	+0.85648	−0.33774	+0.79907	2.3621	1.0501
−0.545	+0.86829	−0.33567	+0.80427	2.3617	1.0289
−0.550	+0.88010	−0.33363	+0.80936	2.3610	1.0081
−0.555	+0.89190	−0.33163	+0.81435	2.3599	0.9879
−0.560	+0.90369	−0.32968	+0.81924	2.3584	0.9682
−0.565	+0.91548	−0.32776	+0.82403	2.3566	0.9490
−0.570	+0.92726	−0.32588	+0.82873	2.3544	0.9302
−0.575	+0.93903	−0.32404	+0.83334	2.3518	0.9120
−0.580	+0.95078	−0.32223	+0.83785	2.3489	0.8942
−0.585	+0.96252	−0.32046	+0.84228	2.3456	0.8768
−0.590	+0.97423	−0.31872	+0.84662	2.3420	0.8599
−0.595	+0.98594	−0.31702	+0.85088	2.3380	0.8435
−0.600	+0.99761	−0.31535	+0.85506	2.3336	0.8274
−0.605	+1.00927	−0.31371	+0.85916	2.3289	0.8117

1	4	5	6	7	8
−0.010	+0.00015	−2.03076	−3.41414	0.0386	109.7999
−0.015	+0.00042	−1.85231	−2.96803	0.0691	73.6024
−0.020	+0.00085	−1.72500	−2.64974	0.1037	55.4809
−0.025	+0.00146	−1.62574	−2.40161	0.1414	44.5942
−0.030	+0.00227	−1.54427	−2.19793	0.1813	37.3251
−0.035	+0.00328	−1.47510	−2.02499	0.2230	32.1227
−0.040	+0.00450	−1.41494	−1.87459	0.2659	28.2118
−0.045	+0.00594	−1.36168	−1.74146	0.3098	25.1616
−0.050	+0.00760	−1.31389	−1.62199	0.3544	22.7137
−0.055	+0.00949	−1.27054	−1.51361	0.3994	20.7038
−0.060	+0.01160	−1.23086	−1.41441	0.4446	19.0222
−0.065	+0.01394	−1.19429	−1.32297	0.4900	17.5933
−0.070	+0.01650	−1.16036	−1.23815	0.5354	16.3627
−0.075	+0.01929	−1.12873	−1.15908	0.5806	15.2910
−0.080	+0.02231	−1.09911	−1.08503	0.6257	14.3483
−0.085	+0.02555	−1.07127	−1.01542	0.6704	13.5119
−0.090	+0.02901	−1.04500	−0.94976	0.7149	12.7641
−0.095	+0.03270	−1.02016	−0.88765	0.7589	12.0909
−0.100	+0.03660	−0.99660	−0.82875	0.8025	11.4814
−0.105	+0.04072	−0.97420	−0.77275	0.8456	10.9263
−0.110	+0.04506	−0.95286	−0.71941	0.8882	10.4184
−0.115	+0.04960	−0.93250	−0.66850	0.9302	9.9516
−0.120	+0.05436	−0.91303	−0.61983	0.9717	9.5207
−0.125	+0.05932	−0.89439	−0.57324	1.0126	9.1216
−0.130	+0.06448	−0.87653	−0.52857	1.0530	8.7506
−0.135	+0.06985	−0.85937	−0.48569	1.0927	8.4047
−0.140	+0.07541	−0.84289	−0.44448	1.1319	8.0812
−0.145	+0.08117	−0.82704	−0.40484	1.1704	7.7779
−0.150	+0.08711	−0.81177	−0.36667	1.2084	7.4929
−0.155	+0.09325	−0.79705	−0.32989	1.2457	7.2243
−0.160	+0.09957	−0.78286	−0.29441	1.2824	6.9708
−0.165	+0.10607	−0.76916	−0.26016	1.3185	6.7310
−0.170	+0.11276	−0.75593	−0.22707	1.3539	6.5038
−0.175	+0.11961	−0.74314	−0.19510	1.3888	6.2881
−0.180	+0.12664	−0.73077	−0.16418	1.4231	6.0830
−0.185	+0.13384	−0.71880	−0.13425	1.4567	5.8878
−0.190	+0.14121	−0.70721	−0.10528	1.4898	5.7016
−0.195	+0.14874	−0.69599	−0.07722	1.5223	5.5238
−0.200	+0.15643	−0.68511	−0.05003	1.5542	5.3539
−0.205	+0.16428	−0.67457	−0.02367	1.5855	5.1913
−0.210	+0.17229	−0.66434	+0.00188	1.6163	5.0355
−0.215	+0.18044	−0.65442	+0.02669	1.6465	4.8862
−0.220	+0.18875	−0.64479	+0.05076	1.6761	4.7428
−0.225	+0.19720	−0.63544	+0.07412	1.7052	4.6050
−0.230	+0.20580	−0.62637	+0.09682	1.7338	4.4726
−0.235	+0.21454	−0.61755	+0.11886	1.7618	4.3451
−0.240	+0.22342	−0.60898	+0.14028	1.7893	4.2224
−0.245	+0.23243	−0.60066	+0.16109	1.8163	4.1041
−0.250	+0.24158	−0.59256	+0.18132	1.8428	3.9900
−0.255	+0.25086	−0.58469	+0.20100	1.8688	3.8799
−0.260	+0.26027	−0.57704	+0.22013	1.8943	3.7737
−0.265	+0.26980	−0.56960	+0.23874	1.9193	3.6710
−0.270	+0.27946	−0.56235	+0.25685	1.9439	3.5718
−0.275	+0.28924	−0.55531	+0.27446	1.9680	3.4758
−0.280	+0.29914	−0.54845	+0.29161	1.9916	3.3830
−0.285	+0.30916	−0.54177	+0.30830	2.0148	3.2931
−0.290	+0.31929	−0.53527	+0.32455	2.0376	3.2061
−0.295	+0.32953	−0.52895	+0.34037	2.0599	3.1218
−0.300	+0.33989	−0.52278	+0.35577	2.0818	3.0401
−0.305	+0.35035	−0.51678	+0.37077	2.1034	2.9609
−0.310	+0.36092	−0.51094	+0.38538	2.1245	2.8841
−0.315	+0.37160	−0.50525	+0.39962	2.1452	2.8096
−0.320	+0.38237	−0.49970	+0.41348	2.1655	2.7373
−0.325	+0.39325	−0.49430	+0.42699	2.1855	2.6671
−0.330	+0.40423	−0.48903	+0.44016	2.2051	2.5989
−0.335	+0.41530	−0.48390	+0.45299	2.2243	2.5327
−0.340	+0.42647	−0.47890	+0.46549	2.2432	2.4684
−0.345	+0.43773	−0.47402	+0.47767	2.2617	2.4059
−0.350	+0.44909	−0.46927	+0.48955	2.2799	2.3452
−0.355	+0.46053	−0.46464	+0.50113	2.2978	2.2861
−0.360	+0.47207	−0.46013	+0.51242	2.3153	2.2287
−0.365	+0.48369	−0.45573	+0.52342	2.3326	2.1728
−0.370	+0.49539	−0.45143	+0.53415	2.3495	2.1185
−0.375	+0.50718	−0.44725	+0.54461	2.3662	2.0656
−0.380	+0.51905	−0.44317	+0.55481	2.3825	2.0142
−0.385	+0.53101	−0.43919	+0.56475	2.3986	1.9641
−0.390	+0.54304	−0.43531	+0.57445	2.4144	1.9154
−0.395	+0.55515	−0.43153	+0.58391	2.4299	1.8679
−0.400	+0.56734	−0.42784	+0.59313	2.4452	1.8217
−0.405	+0.57960	−0.42424	+0.60213	2.4602	1.7767

1	4	5	6	7	8
−0.410	+0.59194	−0.42073	+0.61090	2.4750	1.7329
−0.415	+0.60435	−0.41731	+0.61946	2.4896	1.6902
−0.420	+0.61684	−0.41397	+0.62781	2.5039	1.6486
−0.425	+0.62939	−0.41071	+0.63595	2.5180	1.6081
−0.430	+0.64202	−0.40754	+0.64389	2.5319	1.5686
−0.435	+0.65471	−0.40444	+0.65164	2.5456	1.5301
−0.440	+0.66748	−0.40142	+0.65919	2.5591	1.4925
−0.445	+0.68030	−0.39847	+0.66656	2.5724	1.4559
−0.450	+0.69320	−0.39559	+0.67375	2.5855	1.4203
−0.455	+0.70616	−0.39279	+0.68077	2.5985	1.3855
−0.460	+0.71918	−0.39005	+0.68761	2.6113	1.3516
−0.465	+0.73227	−0.38738	+0.69429	2.6239	1.3185
−0.470	+0.74542	−0.38477	+0.70080	2.6363	1.2863
−0.475	+0.75864	−0.38223	+0.70715	2.6487	1.2548
−0.480	+0.77191	−0.37975	+0.71335	2.6608	1.2241
−0.485	+0.78524	−0.37734	+0.71939	2.6729	1.1942
−0.490	+0.79864	−0.37498	+0.72529	2.6848	1.1650
−0.495	+0.81209	−0.37267	+0.73104	2.6966	1.1365
−0.500	+0.82561	−0.37043	+0.73666	2.7083	1.1087
−0.505	+0.83918	−0.36824	+0.74213	2.7199	1.0815
−0.510	+0.85281	−0.36610	+0.74747	2.7314	1.0551
−0.515	+0.86649	−0.36402	+0.75269	2.7428	1.0292
−0.520	+0.88023	−0.36199	+0.75777	2.7542	1.0040
−0.525	+0.89403	−0.36000	+0.76273	2.7655	0.9794
−0.530	+0.90789	−0.35807	+0.76756	2.7767	0.9553
−0.535	+0.92180	−0.35618	+0.77228	2.7878	0.9319
−0.540	+0.93577	−0.35434	+0.77688	2.7990	0.9090
−0.545	+0.94979	−0.35254	+0.78137	2.8100	0.8866
−0.550	+0.96387	−0.35079	+0.78575	2.8211	0.8648
−0.555	+0.97800	−0.34908	+0.79002	2.8321	0.8434
−0.560	+0.99219	−0.34742	+0.79419	2.8432	0.8226
−0.565	+1.00643	−0.34579	+0.79825	2.8542	0.8023
−0.570	+1.02073	−0.34421	+0.80221	2.8652	0.7824
−0.575	+1.03509	−0.34266	+0.80607	2.8763	0.7630
−0.580	+1.04950	−0.34116	+0.80984	2.8874	0.7441
−0.585	+1.06396	−0.33969	+0.81352	2.8985	0.7256
−0.590	+1.07848	−0.33825	+0.81710	2.9096	0.7075
−0.595	+1.09306	−0.33686	+0.82059	2.9209	0.6899
−0.600	+1.10769	−0.33549	+0.82400	2.9322	0.6728
−0.605	+1.12238	−0.33416	+0.82732	2.9436	0.6558

AN ANALYSIS OF THE MAGNETIC VARIABLE α^2 CANUM VENATICORUM*

G. R. BURBIDGE AND E. MARGARET BURBIDGE
Cambridge, England
Received October 19, 1954; revised December 6, 1954

ABSTRACT

A detailed spectrophotometric study of α^2 CVn through its magnetic period has been made, based on 9 coudé spectrograms obtained at the McDonald Observatory. A table of about 1200 lines and their equivalent widths through the period is given. The original grouping of the lines into those which show maxima or minima or remain constant has been revised and extended. In addition to *Cr* II and *Fe* II, *Mg* II, *Si* II, *Cr* I, and *Fe* I reach a maximum at mid-phase. No correlations between the amplification factor (defined as W_{max}/W_{min}) and excitation potential or Zeeman splitting have been found, although there is possibly some correlation with the mean equivalent widths for the lines of *Ti* II and *Cr* II. A study of the profiles of $H\gamma$ and $H\delta$ has given a value for the electron pressure of about 70 dynes. The reasons for this rather low value are discussed.

A curve of growth for *Ti* II, *V* II, *Cr* II, *Fe* I, and *Fe* II has been constructed by using γ Gem, analyzed by Buscombe, as a standard star. The points have been fitted to a theoretical curve given by Wrubel. The excitation temperature of α^2 CVn is 8000°, and the ionization temperature is 1000° higher than that of γ Gem. By using solar equivalent widths, a curve of growth for the elements *Zr* II, *La* II, and the rare earths has been plotted. Abundances of *Mg*, *Al*, *Si*, *Ca*, *Sc*, *Ti*, *V*, *Cr*, *Mn*, *Fe*, *Ni*, and *Sr* relative to γ Gem and of *Y*, *Zr*, *Ba*, *La*, *Ce*, *Pr*, *Nd*, *Sm*, *Eu*, *Gd*, and *Dy* relative to the sun have been determined. *Si* and *Sr* are overabundant by factors of the order of 10; *Mg* and *Ca* are underabundant by factors of about 2.5 and 50, respectively. The metallic group all tend to be slightly overabundant, the factor for *Cr* being 5. *Y* and *Zr* are overabundant relative to the sun by factors of the order of 20; and *La* and the rare earths are very overabundant, the mean ratio relative to the sun being 830. *Ba* apparently has a normal abundance. A search for deuterium, *Tc*, *Sn*, *Pb*, *Th*, and *U* has been made. Deuterium is possibly present, and *Pb* is almost certainly present, in which case it is overabundant by a factor of ~1500. For the other elements the evidence is either negative or uncertain. A discussion of the possible reasons for the abundance differences is given, and it is concluded that they are, for the most part, probably real.

For the elements *Ti*, *Cr*, and *Fe*, the apparent abundance variations through the period have been studied, and it has been concluded that some of these variations can be accounted for by stratification and motions of layers through the magnetic period. The relationship of the apparent velocities determined from the curve of growth (~4 km/sec) and magnetic intensification is discussed, and it is concluded that this effect is not important in explaining the anomalous abundances or the variations through the period. The results have been considered in terms of a magnetic oscillator model discussed by Cowling. The "mean" atmosphere has many of the characteristics of a normal stellar atmosphere of type A0, although the effective and ionization temperatures are more nearly those of a B8 star.

The possible ways in which anomalous abundances might arise are considered, and it is concluded that nuclear reactions on the stellar surface are probable. A brief discussion of the Swann mechanism for accelerating ions in stellar spots is given.

It is shown that there is good correlation between the nuclei which are excessively stable, particularly those having closed shells of neutrons and/or protons, and those which are overabundant, especially for *Si*, *Cr*, *Sr*, *Y*, *Zr*, *La*, some of the rare earths, and *Pb*. A qualitative discussion of possible nuclear reactions is given. Small fluxes of high-energy protons and α-particles, continuously acting over long time scales (~10^{16} sec), will give rise to neutrons. These will be captured by heavy elements, giving peaks about the magic-number nuclei. Deuterium may also be formed. Nuclear reactions involving heavy accelerated ions are discussed.

I. INTRODUCTION

The star α^2 Canum Venaticorum (A0p) has for a long time been known as a classical example of the spectrum variable stars of type A. Early spectroscopic observations, notably by Belopolsky (1913*a*, *b*; 1927), showed that the spectrum lines belonged to three groups; two (characterized originally by a group of unidentified lines and by *Cr* II) varied oppositely in phase in a period of approximately $5\frac{1}{2}$ days, and one remained

* *Contributions from the McDonald Observatory, University of Texas*, No. 248.

constant. After Baxandall (1913) had identified the strongest unknown lines with *Eu* II, it was clear that this element was abnormally strong in the spectrum. Miss Farnsworth (1932) obtained an accurate period for the spectral variations given by:

$$\text{Maximum intensity of } Eu \text{ II} = \text{JD}2419869.720 + 5.46939E\,.$$

Morgan (1935) made a further contribution when he discussed the spectrum of this star as part of a study of the peculiar A stars; a later discussion was given by Struve (1942). The most comprehensive study of the spectrum was made by Struve and Swings (1943), who identified and listed about 3000 lines in the photographic and ultraviolet region of the spectrum and gave further details of the variation of the lines through the cycle. Radial-velocity-curves were obtained for a large number of elements. This was a major contribution, since they were able to use recent laboratory material on the rare-earth and other spectra to identify a large number of lines.

Parallel with observations of the spectrum, the light-variations have been studied by various workers. Guthnick and Prager (1914) found brightness variations of 0.051 mag., with a period of 5.54 days, and later authors found a similar, but slightly smaller, amplitude. The most recent investigation was made by Provin (1953), who found an amplitude of 0.050 mag. and a color change of 0.02 mag., much smaller than the color change found earlier by Nikonov and Brodskaya (1950). Maximum light occurs at maximum *Eu* II intensity, and the star is bluest at minimum light.

The last major contribution to our knowledge of this star was made by Babcock and Miss Burd (1952), who discovered that it had a magnetic field with a period of variation the same as that of the spectrum variations, with a range of $+5000$ to -4000 gauss.

In 1953, when the authors began a program of spectrophotometry of magnetic stars, α^2 CVn was chosen because it has a period of convenient length from the observer's point of view and also because the extensive spectrum identifications by Struve and Swings obviated a great amount of preliminary work before large-scale measurement of equivalent widths could be made. A previous spectrophotometric study of α^2 CVn was made by Tai (1940), and it will be convenient to discuss his work in the next section, when a comparison can be made with our own.

II. OBSERVATIONS AND MEASUREMENTS

In April and May, 1953, nine spectrograms were obtained with the A camera of the coudé grating spectrograph of the 82-inch telescope at the McDonald Observatory. The linear dispersion of these plates is 4.8 A/mm, and the region covered is approximately λλ 4950–3600. Eastman Kodak IIa-O plates were used; calibration over the whole spectral range was done by means of the grating calibration spectrograph described in a previous paper (Burbidge and Burbidge 1954), and the method used was the same. Tracings of the spectra and calibrations were made with the Beals microphotometer at the Yerkes Observatory. In order to reduce the labor of reduction in this very rich spectrum, all but the strongest lines were treated as triangles in obtaining their areas (a preliminary investigation showed that errors due to this method were small).

The spectrograms were obtained during three successive periods. The phases, measured from zero at time of maximum *Eu* II, were as follows: 0.055, 0.141, 0.227, 0.445, 0.534, 0.702, 0.773, 0.819, 0.969. The equivalent widths measured on all plates are listed under the separate elements in Table 1, in order of increasing atomic weight. This table is intended to be used in conjunction with the identification list by Struve and Swings (1943), who give in detail the contributors to blends. We have merely indicated the degree of blending by a letter at the end of the nine equivalent-width measures; "a" denotes blending which is probably unimportant, "b" denotes more serious blending but the line is still usable, "c" denotes serious blending such that the line should probably not be used in plotting curves of growth. However, the values of log η_0 given in this

TABLE 1

EQUIVALENT WIDTHS AND LOG η_0

λ	0.055	0.141	0.227	0.445	0.534	0.702	0.773	0.819	0.969	E.P.	log W/b	log η_0
He I												
4026.19	21						16		12	20.87	−0.41	−0.35
Mg II												
4384.64				20	15			26		9.95	− .34	−0.26
4428.00		21	30			28		30	24 c	9.95	− .21	−0.08
4436.48									39 c	11.52	− .06	+0.14
4481.23	218	221	207	249	255	253	265	231	186 a	8.83	+ .71	+2.08
Al I												
3944.01	50		30						a	0.00	− .11	+0.06
Al II												
4026.50	27			38		29	32	29		13.59	− .11	+0.06
4159.4							26	26	19 c	15.24	− .24	−0.13
4159.8	18					16	19			15.24	− .36	−0.28
4240.75	24								b	14.98	− .25	−0.14
4640.4	27	16	20							15.24	− .35	−0.27
4650.6	40	21				20			c	15.24	− .24	−0.13
Si II												
3856.02	217	249	210	264	268	207	238	225	172	6.83	+ .75	+2.22
3862.59	162	161	166	201	232	189	181	199	158 a	6.83	+ .72	+2.12
4075.45			79	124	113				a		+ .41	+1.30
4076.78	82	103	87	122	132	104	120	81	66 c		+ .37	+1.14
4128.05	210	239	230	274	286	231	267	240	181	9.79	+ .75	+2.22
4130.88	250	234	253	285	281	232	259	234	185	9.80	+ .76	+2.26
4190.74	44	61	85			47			b		+ .15	+0.54
4198.17	55	94	71	92	70				b		+ .27	+0.82
4683.02							41		a		− .06	+0.14
P II												
4288.53		55	49	64	82		77	62	c	13.38	+ .19	+0.62
4475.27		13							a	13.03	− .54	−0.50
4565.22							16	23	9 a	13.64	− .46	−0.41
4601.97		13							a	12.80	− .55	−0.51
4658.12	40	38	28				34	21	36 c	12.80	− .15	0.00
A I												
4158.59						24	26	20	30 a	11.50	− .35	−0.27
4266.29				33			30		38 b	11.57	− .23	−0.11
4510.73					22			20		11.78	− .46	−0.41
Ca I												
4226.73	29	22	11					22	22 b	0.00	− .58	−0.55
4455.89		19		27	18	18	26	19	22 c	1.89	− .46	−0.41
4585.85					37			17	47 c	2.51	− .26	−0.16
Ca II												
3933.66	202	157	121	162	151	132	152	171	198 a	0.00	+ .63	+2.08
Sc II												
4415.56				10		15			23	0.59	− .44	−0.39
Ti I												
3998.64			37			18			a	0.05	− .27	−0.17
4060.26		16			25				23	1.05	− .41	−0.35
4186.12	25					14			12 b	1.50	− .51	−0.47
4261.61						18		14	20 c	2.30	− .52	−0.48
4263.13				28			36	25	c	1.88	− .27	−0.17
4272.44							7		a	0.82	− .90	−0.90
4274.58	32	50	23							0.81	− .21	−0.08
4281.37	32	31	14			14	22	20	27	0.81	− .43	−0.37
4289.07		7	8	12	20		19		20 a	0.81	− .61	−0.58
4295.75		27	16	20	14				a	0.81	− .47	−0.42
4301.09	31	25	25	27					a	0.83	− .32	−0.24
4404.28						12				2.24	− .68	−0.66
4450.90		19				42			26 b	1.87	− .31	−0.22
4453.31	31						29		22 b	1.42	− .34	−0.26
4457.43		15		12					a	1.45	− .64	−0.62
4474.85		27								1.44	− .34	−0.26
4479.72		19	17						a	1.73	−0.51	−0.47

TABLE 1—*Continued*

λ	0.055	0.141	0.227	0.445	0.534	0.702	0.773	0.819	0.969	E.P.	log W/b	log η_0
Ti I—*Cont.*												
4482.69	.....	13	16	.....	.....	20	.....	.....	.....	1.45	−0.57	−0.54
4512.73	24	.....	.....	.....	.....	.....	22	.....	a	0.83	− .41	−0.35
4518.02	38	.....	.....	.....	.....	30	26	42	.....	0.82	− .24	−0.13
4533.24	.....	44	38	.....	38	26	47	.....	43 b	0.84	− .19	−0.16
4535.57	.....	25	25	.....	47	44	.....	46	38 a	0.82	− .20	−0.07
4555.49	12	.....	.....	.....	.....	.....	.....	26	33 a	0.84	− .40	−0.34
4639.37	.....	24	14	.....	14	22	.....	.....	10 a	1.73	− .56	−0.53
4639.94	.....	.....	12	.....	.....	.....	.....	.....	23	1.73	− .55	−0.51
4645.19	.....	.....	.....	.....	.....	.....	.....	.....	7 a	1.73	− .94	−0.94
4650.02	.....	21	.....	.....	.....	.....	.....	12	a	1.73	− .58	−0.55
4656.47	37	31	22	.....	13	.....	25	.....	.....	0.00	− .41	−0.35
4667.59	43	.....	.....	.....	.....	.....	.....	.....	c	0.02	− .16	−0.01
Ti II												
3913.46 p	76	79	67	84	.....	65	92	84	86 b	1.11	+ .42	+1.35
3932.01 p	70	.....	50	58	54	43	52	87	84 a	1.13	+ .31	+0.94
4025.14 p	.....	51	.....	.....	33	32	48	52	45 a	0.60	+ .13	+0.49
4028.33 p	80	85	58	44	68	.....	60	70	71 a	1.88	+ .32	+0.97
4053.81	71	.....	.....	.....	60	.....	.....	.....	76 b	1.88	+ .34	+1.03
4064.35	.....	32	21	.....	.....	18	.....	.....	15	2.59	− .16	−0.01
4163.64 p	.....	76	68	44	49	43	53	61	75 a	2.58	+ .28	+0.85
4171.90	90	90	99	116	123	97	129	102	91 c	2.59	+ .52	+1.84
4174.09	55	46	39	44	36	.....	.....	34	a	2.59	+ .11	+0.45
4181.17	.....	.....	13	.....	.....	.....	.....	.....	.....	2.04	− .40	−0.34
4252.05	.....	.....	.....	.....	.....	21	.....	.....	.....	2.04	− .20	−0.07
4287.89 p	48	51	39	40	37	48	43	49	.....	1.08	+ .12	+0.47
4294.10	78	72	41	61	68	55	72	49	a	1.08	+ .27	+0.82
4300.05	86	90	50	43	.....	.....	.....	106	103 b	1.18	+ .35	+1.07
4301.93 p	115	96	45	67	68	58	90	70	b	1.16	+ .41	+1.30
4312.86 p	100	94	59	103	110	91	112	100	85 b	1.18	+ .47	+1.61
4314.98	70	77	60	81	95	79	84	78	79 a	1.16	+ .37	+1.14
4316.81 p	.....	.....	29	.....	.....	.....	43	.....	a	2.04	+ .03	+0.29
4367.66	.....	63	.....	.....	.....	39	48	.....	b	2.58	+ .17	+0.58
4374.82	.....	94	54	.....	74	.....	46	.....	c	2.05	+ .30	+0.90
4386.86	116	98	.....	86	70	.....	72	88	100 b	2.59	+ .43	+1.40
4394.06 p	.....	48	31	43	48	.....	32	32	38 a	1.22	+ .06	+0.34
4395.03	126	127	64	87	101	71	98	84	89 a	1.08	+ .44	+1.45
4395.85	76	71	56	64	.....	64	.....	65	78 c	1.24	+ .30	+0.90
4398.31	64	51	.....	.....	29	34	.....	42	69 a	1.22	+ .16	+0.56
4399.77 p	84	64	27	.....	67	50	59	.....	74	1.23	+ .23	+0.71
4407.68	67	38	39	52	53	.....	47	.....	a	1.22	+ .16	+0.56
4409.22 p	44	.....	.....	.....	.....	.....	.....	.....	26 a	1.24	+ .01	+0.26
4411.08 p	63	51	28	.....	32	28	.....	.....	46 a	3.08	+ .07	+0.37
4411.94 p	33	26	.....	.....	.....	24	.....	.....	42 a	1.22	− .09	+0.09
4417.72 p	73	58	42	61	54	44	58	46	55 a	1.16	+ .20	+0.64
4418.34 p	46	33	24	33	25	26	39	30	33 a	1.23	.00	+0.24
4421.95 p	58	48	22	.....	.....	22	38	.....	41 a	2.05	+ .02	+0.27
4423.22	.....	.....	.....	.....	.....	11	.....	.....	.....	1.23	− .50	−0.46
4441.73 p	.....	.....	14	.....	35	.....	31	.....	.....	1.18	− .11	+0.06
4443.80	.....	.....	48	62	57	50	62	63	b	1.08	+ .22	+0.69
4450.49	72	60	42	.....	69	43	.....	.....	59 a	1.08	+ .22	+0.69
4456.65	49	38	.....	.....	27	22	41	46	56 b	3.11	+ .03	+0.29
4464.46	72	56	32	56	.....	29	51	43	73 b	1.16	+ .19	+0.62
4468.49	98	79	67	79	84	58	77	86	a	1.13	+ .35	+1.07
4469.16	34	24	.....	30	24	20	33	31	a	1.08	− .09	+0.09
4470.86 p	53	33	.....	36	24	19	30	.....	a	1.16	+ .03	+0.29
4488.32	36	38	.....	38	.....	51	60	60	b	3.11	+ .17	+0.58
4495.46	.....	25	.....	.....	.....	.....	34	.....	b	1.18	− .06	+0.14
4501.27 p	108	98	.....	96	90	68	99	81	74 b	1.11	+ .41	+1.30
4524.73	.....	.....	.....	.....	.....	.....	44	36	b	1.23	+ .05	+0.32
4529.46 p	47	45	41	44	49	39	47	64	51 a	1.56	+ .13	+0.49
4544.01	56	35	15	.....	.....	21	.....	43	41 b	1.24	− .03	+0.19
4545.14	62	41	.....	.....	.....	42	40	40	c	1.13	+0.11	+0.45

TABLE 1—*Continue*

λ	0.055	0.141	0.227	0.445	0.534	0.702	0.773	0.819	0.969	E.P.	log W/b	log η_0
Ti II—*Cont.*												
4563.76 p					42		58	67	87 a	1.22	+0.26	+0.80
4568.31							13		b	1.22	− .44	−0.38
4571.97 p	134	95	69		89	66	90	93	100	1.56	+ .45	+1.50
4580.46	30	24							36	1.23	− .07	+0.12
4655.75					7	15	27	22		1.16	− .30	−0.21
4708.66	44	29	29			19	41	31		1.23	− .07	+0.12
4719.52	60	38						38	40	1.24	+ .08	+0.39
V II												
3997.13			26						b	1.47	− .18	−0.04
4002.94	50								c	1.42	+ .11	+0.45
4005.71 p	36	39			19	36		22	27 a	1.81	− .13	+0.03
4023.29 p	45	28	19		21	18	15	16	33 b	1.80	− .14	+0.01
4036.78 p		12							9	1.47	− .56	−0.53
4183.44 p	40	31	35		55	30		34		2.04	− .03	+0.19
4528.51	58	52			37	36	37	29	39 b	2.27	− .04	+0.17
4564.59									11	2.26	− .61	−0.58
4600.19		23						17	b	2.26	− .35	−0.27
Cr I												
4001.44		37	20		22		25		12 c	3.87	− .39	−0.32
4126.52	40	36	29		33	38	40	40	30 c	2.53	− .21	−0.08
4191.75			13						c	2.53	− .66	−0.64
4197.23				27	18				c	3.83	− .42	−0.36
4198.52	46								c	3.83	− .11	+0.06
4203.59	34	28				28	24	40	c	2.53	− .28	−0.18
4254.35	50	85	64	83	74	80	81	64	a	0.00	+ .07	+0.37
4274.80	19	18			40	42	38	36	23 a	0.00	− .30	−0.21
4289.72	15		25						b	0.00	− .48	−0.43
4299.72			25						c	2.89	− .38	−0.31
4530.74						22	37	19	c	2.53	− .40	−0.34
4544.62		12						19	b	2.53	− .62	−0.59
4545.96		8								0.94	− .91	−0.91
4600.75		11					31		c	1.00	− .47	−0.42
4616.14		20	21				24		15 c	0.98	− .51	−0.47
4646.17					18	23			25 c	1.03	− .47	−0.42
4651.28	23	22							c	0.98	− .48	−0.43
4652.16	57				38				c	1.00	− .14	+0.01
4697.06						18	22	26	c	2.70	− .48	−0.43
4708.04	42	35						22	38 c	3.15	+ .29	+0.20
4718.43	41	19						51	16 c	3.18	+ .31	+0.22
4729.72		10				37		25	c	3.08	− .44	−0.38
Cr II												
3856.93				45	37	30	43	41	34 a		.00	+0.24
3859.38	48	27	19	43	28				38 b		− .05	+0.16
3865.59	80	82	69		112	110	118	133	78 a	5.30	+ .41	+1.30
3866.01	56	48	23				39	34	27 b	4.90	.00	+0.24
3866.54	31	32	28			42	47	56	37 b	4.92	+ .01	+0.26
3867.80	25	16				17	31	32	24 b		− .20	−0.07
3868.32	68	51	38		53	44	46	51	57 b		+ .13	+0.49
3869.62	66								b		+ .24	+0.74
3911.4	52			70	85	72	75	72	46	4.92	+ .23	+0.71
3930.88					26	19				4.92	− .24	−0.13
3936.95	43	39	22	31	26	21			62 b	4.92	− .04	+0.17
3937.61	36	39	35			22			30 b		− .07	+0.12
3945.11	32	51	59	85	73			30	37 c	4.92	+ .16	+0.56
4003.33	59	68	59	57	61	57	55	57		6.46	+ .18	+0.60
4006.75	26	47	30			22		35	29 b		− .08	+0.10
4007.56		25				19		29	b		− .21	−0.08
4012.50	129	127	115	124	148		162	154	129 b	5.64	+ .56	+2.04
4017.96	35	40	33	39	32	30	28		21 a	5.31	− .08	+0.10
4022.36	82	70	54		69	61	71	58	53 c	5.65	+ .22	+0.69
4030.68	40	30	25		20		21		b		− .17	−0.03
4038.03		82	92		100	94	109		a	6.46	+0.38	+1.18

TABLE 1—*Continued*

λ	0.055	0.141	0.227	0.445	0.534	0.702	0.773	0.819	0.969	E.P.	log W/b	log η_0
Cr II—*Cont.*												
4048.02								41	c	5.65	+0.01	+0.26
4049.14			78							6.46	+ .29	+0.88
4051.97 p	39	61	60		61	61	65	62	a	3.09	+ .17	+0.58
4053.45	38					31			a	3.09	− .07	+0.12
4054.11		96	68		59		79		c	3.09	+ .22	+0.69
4056.07		52			42	41	46	38	a	5.64	+ .04	+0.31
4064.14		14			13				a		− .47	−0.42
4070.90			73	66	61	56	73	55	39 a	6.46	+ .18	+0.60
4072.56	49			104	88	61	68		b	3.70	+ .22	+0.69
4075.97				44					b		+ .04	+0.31
4082.30			41						a	5.30	+ .01	+0.26
4127.08	42	54	48	61		68	64	69	b	5.65	+ .16	+0.56
4132.41			54		49				a	3.74	+ .11	+0.45
4135.77						19	13	14	a	5.30	− .43	−0.37
4145.77	50	71	58			76	85	82	35 b	5.30	+ .20	+0.64
4146.45									14 a		− .46	−0.41
4151.00	73	69	47	60	55	49	67	51	49 b	5.31	+ .15	+0.54
4170.86	82					63	65	63	74 b	5.64	+ .23	+0.71
4172.60		47	35	41	38	40	40	37		3.09	− .01	+0.22
4179.43	76	82	62	82	66	84	98	86	a	3.81	+ .29	+0.88
4185.50	23								18 a	5.31	− .31	−0.22
4195.41	55	80	66	60	53	69	72	57	a	5.30	+ .20	+0.64
4204.66				30			18			4.92	− .23	−0.11
4207.35	31	54	43	65	44	49			a	3.81	+ .07	+0.37
4209.02	50	45			29		53	51	56 b	5.30	+ .06	+0.34
4209.84	19					32	30	33		5.65	− .16	−0.01
4217.0			30							3.09	− .13	+0.03
4222.00	34	21	29		28					5.64	− .17	−0.03
4224.85	41	48	53		40	52	64		a	5.31	+ .08	+0.39
4239.31				25							− .22	−0.10
4242.38	83		97	109	101	61	124	85	b	3.85	+ .35	+1.07
4250.51	84	74							c		+ .28	+0.85
4252.62 p	68	70	72	99	93	94	74	76	61 a	3.84	+ .30	+0.90
4256.16						66	52	72	68 a	6.46	+ .19	+0.62
4261.92 p	93	119	102	112	111	140	140	135	67 a	3.85	+ .42	+1.35
4268.93	46	38	25	51					b	6.46	− .02	+0.20
4269.28 p		63	62	55	84	87	99	69	47	3.84	+ .25	+0.77
4275.57 p	55	72	56		96	70	100	76	32 a	3.84	+ .21	+0.67
4283.02		16	12						8 a		− .54	−0.50
4284.21 p	55	55	57	74	97	92	107	83	52 a	3.84	+ .28	+0.85
4302.58	28			25		13	20		10 a		− .34	−0.26
4306.95		73	52		76	69	73	65	63		+ .23	+0.71
4309.75		42	36	41		36	49	46	a		.00	+0.24
4318.77			13							3.87	− .51	−0.47
4362.93	43		68			40	65		31 a	5.64	+ .06	+0.34
4382.53			67		39		55	42	b		+ .08	+0.39
4456.84		46			27	42	52		c	3.09	− .02	+0.20
4465.78		48	32			50	56	38	a	6.46	+ .01	+0.26
4539.62	75								c	4.02	+ .23	+0.71
4555.02 p	61	74	82	84	78	80	95	77	40 a	4.05	+ .17	+0.58
4558.66 p	130	117	118	142	160	149	178	158	105	4.06	+ .50	+1.76
4564.27							30	29	13		− .27	−0.17
4565.78 p	76	82	67	83	81	75	81	88	52 a	4.02	+ .23	+0.71
4588.22 p	104	120			123		136	106	80 a	4.05	+ .39	+1.22
4589.89		89			66		75	82	63 c	4.05	+ .23	+0.71
4592.09 p	94	88			110		100	80	68	4.06	+ .30	+0.90
4616.64 p		75	71		82	121	117	79	58	4.05	+ .30	+0.90
4618.83		53	97		119	120	138	119	b	4.06	+ .38	+1.18
4621.41							26		61 c	3.70	− .01	+0.22
4624.58		12					18	32			− .33	−0.25
4634.11 p	94	81	100		102	92	98	88		4.05	+ .32	+0.97
4671.36	36		31		34	24	24	36	b	5.64	−0.17	−0.03

TABLE 1—*Continued*

λ	0.055	0.141	0.227	0.445	0.534	0.702	0.773	0.819	0.969	E.P.	log W/b	log η_0
Cr II—*Cont.*												
4697.62	20	20	34			63	55	32	32	5.65	−0.03	+0.19
4715.12	84	79	68			81	73	69	66 c	5.64	+ .21	+0.67
Mn I												
4034.49	27				45	12				0.00	− .28	−0.18
4041.36	55	53				24	34	35	42	2.11	− .16	−0.02
4235.29	57	48	49	66	51			40	b	2.88	− .03	+0.19
4239.72	22	43		43	34	17			27 a	2.93	− .26	−0.16
4265.92	28	33					29		12 a	2.93	− .34	−0.26
4381.70	38	34	30								− .23	−0.11
4472.79	57								c	2.94	− .01	+0.22
4502.22	34	18	13			24		28	19 a	2.91	− .41	−0.35
4605.36		40			47	46	59	53	35		− .11	+0.06
4642.81		38	27			20	41	33	30 c		− .28	−0.18
4739.11	50	43				38		40			− .17	−0.03
Mn II												
4000.06	51	37			32				b		.00	+0.24
4010.84	25	29			31				25 a		− .15	0.00
4125.86		32					20	17	a		− .26	−0.16
4136.91	54			44	35	47	62	64	b		+ .11	+0.45
4200.25					14				a		− .47	−0.42
4206.38	68	54	25		20	47			57 b	5.37	− .01	+0.22
4244.26		32					33			5.35	− .11	+0.06
4253.02	35	35							a	5.36	− .09	+0.09
4259.20	56			75		69		65	71 c	5.37	+ .20	+0.64
4283.77		19	24						13 a	5.35	− .35	−0.27
4730.36		29								5.35	− .21	−0.08
4738.29						42		31	a	5.36	− .12	+0.05
Fe I												
3856.37 p									36	0.05	− .17	−0.03
3859.91 p		60	60	77	62	68	64	76		0.00	+ .10	+0.43
3867.22	45	26	36			42	31	49	44 c	3.00	− .14	+0.01
3910.84	30	28	17		23		22	29	c	2.75	− .37	−0.30
3916.73							18		c	3.22	− .47	−0.42
3917.18	29				24				c	0.99	− .30	−0.21
3920.26	57	56	43	40	34	45		44	69 c	0.12	− .05	+0.16
3922.91	28	27		74	47				c	0.05	− .09	+0.09
3925.95	20	10		35	22	15	21	23	15 c	2.85	− .43	−0.37
3927.92	65		38		36	28			c	0.11	− .11	+0.06
3932.63			36		37	36		30	c	2.72	− .19	−0.06
3937.33	8				11		9		c	2.68	− .78	−0.77
3940.88		30							c	0.95	− .26	−0.16
3942.44									51 c	2.83	− .03	+0.19
3947.00					25				c	3.20	− .34	−0.26
3949.96		24							24 c	2.17	− .36	−0.28
3997.40			28				50	43	c	2.72	− .14	+0.01
4001.67			17					23	c	2.17	− .44	−0.38
4005.25 p	36	46			33	32		34	41	1.55	− .17	−0.03
4006.32	24		24		8				c	3.25	− .46	−0.41
4007.27	35					22			27 c	2.75	− .29	−0.20
4009.72	29	18							c	2.21	− .37	−0.30
4014.53							14	34	c	3.56	− .36	−0.28
4017.15							21		c	3.03	− .42	−0.36
4021.87	38	33	16		25	28	22	33	32 b	2.75	− .31	−0.22
4030.49	67	85	73		70	69	70	66	c	3.20	+ .10	+0.43
4044.61	30						14	18	18 c	2.82	− .45	−0.39
4045.82 p	90	92	83		83	74	87	68		1.48	+ .17	+0.58
4058.23	50			31	38				48 c	3.20	− .13	+0.03
4058.76							25		c	2.41	− .35	−0.27
4062.44	42								c	2.83	− .13	+0.03
4063.60 p			81	86	92	81	68	69	a	1.55	+ .15	+0.54
4067.98		25							b	3.20	− .35	−0.27
4071.74 p	38	46	54	51	66	70	54	48	47 a	1.60	−0.01	+0.22

TABLE 1—*Continued*

λ	0.055	0.141	0.227	0.445	0.534	0.702	0.773	0.819	0.969	E.P.	log W/b	log η_0
Fe I—*Cont.*												
4074.79					25	29		12	c	3.03	−0.41	−0.35
4079.84	34	22	23	38	42		59	47	c	2.85	− .17	−0.03
4126.19	30						40	40	c	3.32	− .18	−0.04
4132.06 p							28		a	1.60	− .31	−0.22
4134.68		30					30	22	22 b	2.82	− .34	−0.26
4143.42					54		24	31	52 c	3.03	− .16	−0.01
4143.87 p	53	45			38	36	42	31	38 a	1.55	− .16	−0.01
4147.67	17		18		9					1.48	− .58	−0.55
4150.26					37		23	18	c	3.42	− .35	−0.27
4154.6	34	44		56		42	43	48	50 b	2.82	− .11	+0.06
4156.80	30	21			40	27	40	22	24 c	2.82	− .28	−0.18
4158.80						25	38	35	c	3.42	− .24	−0.13
4175.64		54		61		32	45		c	2.83	− .08	+0.10
4176.57	18								b	3.35	− .50	−0.46
4181.76	28								18 b	2.82	− .40	−0.34
4184.90	25	30		30	36	29	27	32	22 c	2.82	− .30	−0.21
4187.04	59	57			74	53	68	76	b	2.44	+ .05	+0.32
4187.80		49			56	59	65	72	36 b	2.41	− .05	+0.16
4191.44					26	26	48	48	b	2.46	− .19	−0.06
4196.21	55		40		38	38	63		c	3.38	− .09	+0.09
4199.10	43				33		36	38	a	3.03	− .18	−0.04
4202.03 p	38	50		54	52		43	43	19	1.48	− .20	−0.07
4203.99	31	32				20	25	34	30 a	2.83	− .36	−0.28
4206.70		26	21		32				c	0.05	− .35	−0.27
4207.13			21						c	2.82	− .44	−0.38
4208.61	31								c	3.38	− .27	−0.17
4210.35	27	31			40	26	48	42	b	2.47	− .20	−0.07
4213.65		22							49 c	2.83	− .21	−0.08
4216.19					10	11			c	0.00	− .77	−0.76
4217.56	23								c	3.42	− .40	−0.34
4220.35		15				22		24	c	3.06	− .47	−0.42
4222.22 p							18		17	2.44	− .51	−0.47
4227.43 p			52			40			a	3.32	− .10	+0.08
4235.94 p	59	75		37	43				a	2.41	− .04	+0.17
4245.26								17	28 c	2.85	− .41	−0.35
4246.09	29	51							c	3.63	− .17	−0.03
4247.43 p	49	56				28			a	3.35	− .12	+0.05
4248.23 p	28							14	24	3.06	− .43	−0.37
4260.48 p	35	47	48		53	51	53	44		2.39	− .11	+0.06
4266.97	39	40					23		c	2.72	− .24	−0.13
4271.16 p			43	41	46					2.44	− .14	+0.01
4271.76 p		50	60	71	65	62	65	54	41 a	1.48	− .03	+0.19
4282.41	90	89	42	62		54			c	2.17	+ .07	+0.37
4285.44				51			36		c	3.22	− .13	+0.03
4291.47	52	39				27	58	44	40 b	0.05	− .14	+0.01
4298.04						21		29	c	3.03	− .37	−0.30
4299.24 p		25	18		26	34			31 a	2.41	− .34	−0.26
4305.46	22							59	33 c	3.00	− .19	−0.06
4309.38							14		c	2.94	− .62	−0.59
4315.09	48	44	19						b	2.19	− .20	−0.07
4367.91		56							c	1.60	− .03	+0.19
4373.57					38	39	36	37	c	2.55	− .20	−0.07
4375.93	20	25			28		33		14 c	0.00	− .40	−0.34
4383.55 p	50	68	75	88	90	69	66	72	69 a	1.48	+ .07	+0.37
4404.75 p	132	106	86	100	106	122			102	1.55	+ .25	+0.77
4415.12 p		27	33	22						1.60	− .35	−0.27
4427.31								20	22 c	0.05	− .46	−0.41
4433.22					23				c	3.64	− .42	−0.36
4442.34 p			13		28					2.19	− .47	−0.42
4443.20 p	44			22	28	38	62	63	74 b	2.85	− .10	+0.08
4454.38 p	13	12	12						a	2.82	− .71	−0.69
4459.12 p			14						a	2.17	−0.64	−0.62

TABLE 1—*Continued*

λ	0.055	0.141	0.227	0.445	0.534	0.702	0.773	0.819	0.969	E.P.	log W/b	log η_0
Fe I—*Cont.*												
4461.65	.....	.....	85	92	87	80	94	88	c	0.09	+0.15	+0.54
4466.55	64	49	27	.....	50	40	53	52	68 c	2.82	− .16	−0.01
4469.38	19	.....	22	.....	26	21	.....	.....	c	3.64	− .45	−0.39
4476.02 p	30	27	37	.....	39	54	44	50	.....	2.83	− .17	−0.03
4482.17	.....	25	22	.....	.....	48	43	41	c	0.11	− .18	−0.04
4485.68	.....	.....	.....	.....	.....	28	20	.....	c	3.67	− .41	−0.35
4489.74	42	10	15	32	28	.....	14	28	25 c	0.12	− .41	−0.35
4490.76	35	16	.....	.....	.....	.....	.....	.....	32 c	3.93	− .34	−0.26
4494.57 p	.....	36	.....	.....	.....	.....	.....	.....	.....	2.19	− .24	−0.13
4525.14	.....	.....	.....	.....	.....	.....	32	39	c	3.59	− .24	−0.13
4528.62 p	.....	.....	.....	.....	22	.....	.....	.....	.....	2.17	− .45	−0.39
4531.15	38	.....	.....	.....	.....	6	.....	.....	c	1.48	− .45	−0.39
4547.85	.....	.....	.....	.....	20	.....	.....	.....	c	3.53	− .50	−0.46
4556.12	36	.....	.....	.....	.....	.....	.....	29	c	2.94	− .29	−0.20
4574.72	44	.....	.....	.....	.....	.....	.....	.....	c	2.27	− .16	−0.01
4581.52	.....	.....	.....	.....	.....	30	30	32	32 c	3.23	− .31	−0.22
4592.66	.....	21	.....	.....	.....	.....	.....	13	12	1.55	− .62	−0.59
4607.65	.....	34	.....	.....	.....	.....	48	51	36 c	3.25	− .18	−0.04
4611.29	63	27	.....	.....	.....	.....	.....	.....	c	3.64	− .15	0.00
4613.22	.....	.....	.....	.....	.....	.....	.....	14	c	3.28	− .65	−0.63
4625.06	73	65	.....	.....	.....	.....	90	71	c	3.23	+ .02	+0.27
4630.13	.....	.....	.....	.....	.....	28	36	48	48 c	2.27	− .21	−0.08
4637.52	.....	20	.....	.....	.....	.....	.....	.....	.....	3.27	− .51	−0.47
4638.02	53	52	68	.....	63	.....	61	47	32 c	3.59	− .08	+0.10
4647.44	.....	.....	.....	.....	33	41	.....	32	c	2.94	− .26	−0.16
4668.14	.....	.....	.....	.....	25	36	.....	46	c	3.25	− .25	−0.14
4673.17	.....	.....	.....	.....	.....	.....	15	.....	15	3.64	− .63	−0.60
4678.85	.....	.....	.....	.....	.....	.....	33	28	25 c	3.59	− .35	−0.27
4691.41	56	.....	.....	.....	.....	.....	34	45	56 c	2.98	− .13	+0.03
4708.96	53	.....	.....	.....	.....	28	.....	19	c	3.62	− .29	−0.20
4736.78	35	.....	33	.....	.....	.....	.....	.....	.....	3.20	− .28	−0.18
Fe II												
3863.41	.....	69	46	.....	57	.....	42	.....	b	4.71	+ .11	+0.45
3863.95	53	64	65	.....	94	74	71	74	66 b	4.48	+ .25	+0.77
3914.48	46	49	.....	57	82	61	41	57	a	1.66	+ .14	+0.51
3935.94	.....	70	68	72	79	90	96	98	95 b	5.54	+ .30	+0.90
3938.29	105	101	73	94	94	76	89	75	83 c	1.66	+ .32	+0.97
3938.97	105	80	92	66	90	68	63	75	b	5.89	+ .28	+0.85
4002.07 p	.....	46	51	.....	32	43	48	53	53 a	2.77	+ .03	+0.29
4002.55	49	52	.....	77	88	78	.....	78	60 b	5.93	+ .20	+0.64
4007.72	.....	.....	.....	.....	.....	27	21	32	34 a	5.89	− .18	−0.04
4024.55	86	81	91	84	105	79	86	76	78 a	4.48	+ .30	+0.90
4031.46	62	42	58	.....	51	48	63	55	b	4.71	+ .09	+0.41
4032.95	.....	102	92	.....	77	78	81	62	52 c	4.48	+ .25	+0.77
4035.54	22	.....	.....	.....	24	.....	22	.....	a	2.53	− .28	−0.18
4044.01 p	34	49	46	.....	51	.....	54	40	29	5.55	+ .01	+0.26
4048.83	.....	.....	.....	.....	.....	113	.....	.....	81 c	5.54	+ .35	+1.07
4057.46 p	80	84	60	80	76	69	74	56	68 a	7.24	+ .22	+0.69
4061.79	87	86	79	72	116	59	98	91	97 c	5.93	+ .30	+0.90
4069.88	.....	.....	.....	68	.....	.....	.....	.....	c	5.89	+ .19	+0.62
4074.41	.....	.....	.....	.....	.....	.....	.....	.....	15 a	.....	− .46	−0.41
4122.64	82	104	122	.....	122	110	113	120	82 a	2.57	+ .37	+1.14
4128.74 p	.....	68	72	.....	.....	.....	90	.....	32 b	2.57	+ .17	+0.58
4138.21	48	68	67	66	56	54	51	54	38	4.71	+ .10	+0.43
4168.66	28	21	.....	.....	.....	.....	11	.....	a	2.63	− .35	−0.27
4173.45 p	94	131	133	153	134	112	122	108	105 a	2.57	+ .44	+1.45
4178.86 p	73	78	91	117	129	97	.....	91	a	2.57	+ .34	+1.03
4233.17 p	138	167	173	214	233	185	156	177	140 b	2.57	+ .60	+2.28
4258.16 p	121	100	94	114	141	124	109	70	83 b	2.69	+ .38	+1.18
4263.90	42	50	63	62	56	56	66	43	a	.....	+ .07	+0.37
4273.32 p	86	84	98	103	126	92	87	76	41	2.69	+ .25	+0.77
4278.13	58	53	58	70	78	75	76	66	52 b	2.68	+0.17	+0.58

TABLE 1—*Continued*

λ	0.055	0.141	0.227	0.445	0.534	0.702	0.773	0.819	0.969	E.P.	log W/b	log η_0
Fe II—*Cont.*												
4286.31	.....	54	54	64	70	53	46	48	42 b	.....	+0.08	+0.39
4296.57 p	78	.....	103	116	137	103	.....	97	a	2.69	+ .36	+1.10
4303.17 p	99	104	94	110	140	124	130	130	77	2.69	+ .38	+1.18
4314.29	68	44	51	89	85	70	77	63	55 a	2.66	+ .19	+0.62
4318.22	.....	.....	23	.....	.....	35	31	28	.....	7.85	− .21	−0.08
4319.72	56	.....	54	.....	.....	.....	.....	.....	a	7.81	+ .07	+0.37
4361.25	.....	.....	73	88	90	79	.....	.....	b	6.11	+ .24	+0.74
4366.16	.....	36	31	.....	36	.....	.....	24	38 b	7.67	− .09	+0.09
4368.26	14	.....	.....	.....	28	.....	.....	.....	30 b	.....	− .26	−0.16
4369.40	85	84	78	87	98	81	90	119	88 c	2.77	+ .28	+0.85
4385.38 p	119	124	113	126	134	134	140	126	81 a	2.77	+ .41	+1.30
4389.40	32	27	.....	.....	.....	25	.....	22	a	.....	− .26	−0.16
4402.88	55	51	58	.....	65	71	54	52	.....	.....	+ .12	+0.47
4413.60 p	66	39	56	74	71	59	.....	54	46 a	2.66	+ .10	+0.43
4416.82 p	94	82	96	122	123	102	126	114	86 a	2.77	+ .35	+1.07
4431.63	.....	40	42	52	46	47	67	44	43	7.91	.00	+0.24
4446.25	.....	.....	37	39	49	43	.....	46	34 a	5.93	− .07	+0.12
4449.66	66	.....	.....	.....	.....	60	76	73	61 c	7.89	+ .15	+0.54
4451.54 p	86	54	62	84	72	76	83	81	57 b	.....	+ .18	+0.60
4455.26	69	51	50	67	73	66	70	66	54 a	.....	+ .12	+0.47
4472.92 p	60	57	58	100	114	.....	.....	.....	b	2.83	+ .25	+0.77
4474.19	.....	14	.....	.....	44	30	.....	.....	a	5.55	− .22	−0.10
4489.18 p	61	71	90	114	132	112	127	87	73	2.82	+ .30	+0.90
4491.40 p	80	74	85	84	91	76	66	70	75 b	2.84	+ .21	+0.67
4493.58	91	68	57	98	75	65	68	88	77 b	7.89	+ .20	+0.64
4499.71	.....	34	45	66	52	52	58	41	37 a	.....	− .02	+0.20
4508.28	126	87	84	149	118	106	123	126	79	2.84	+ .37	+1.14
4515.34 p	116	114	118	148	145	148	124	124	117	2.83	+ .44	+1.45
4520.24 p	93	99	72	90	124	119	104	114	75 a	2.79	+ .33	+1.00
4522.63 p	98	119	95	110	142	128	148	128	101 a	2.83	+ .39	+1.22
4526.58	.....	.....	.....	.....	.....	48	48	48	a	5.54	− .01	+0.22
4534.17	157	141	136	129	157	133	.....	133	99 c	2.84	+ .44	+1.45
4541.52 p	76	57	77	108	114	104	97	101	74	2.84	+ .23	+0.71
4549.4	240	164	209	256	263	229	251	238	176 a	2.82	+ .64	+2.56
4555.89 p	75	96	109	127	139	86	119	98	55	2.82	+ .29	+0.88
4576.33 p	86	78	71	95	108	85	92	87	a	2.83	+ .25	+0.77
4579.52	63	68	.....	.....	75	49	55	72	35 b	.....	+ .09	+0.41
4580.05	52	34	.....	.....	68	41	52	44	31 a	2.57	− .03	+0.19
4582.84 p	56	96	89	.....	88	72	80	71	73	2.83	+ .20	+0.64
4583.83 p	124	128	131	.....	178	150	174	164	124	2.79	+ .48	+1.66
4595.68	.....	26	.....	.....	.....	.....	.....	.....	.....	2.84	− .28	−0.18
4598.53	53	68	.....	.....	66	.....	59	66	.....	7.77	+ .10	+0.43
4601.34	50	43	.....	.....	.....	.....	38	.....	35 b	2.88	− .07	+0.12
4620.51 p	.....	76	59	.....	78	70	81	80	63 a	2.82	+ .16	+0.56
4625.90	.....	46	50	.....	55	48	73	45	.....	5.93	+ .03	+0.29
4626.78	.....	.....	16	.....	.....	.....	.....	.....	a	5.54	− .49	−0.45
4629.34 p	103	88	94	.....	94	94	107	84	.....	2.79	+ .28	+0.86
4631.90	64	41	48	.....	59	60	67	63	.....	7.83	+ .06	+0.34
4635.33 p	89	73	72	.....	102	76	87	85	56	5.93	+ .21	+0.67
4640.84	42	65	49	.....	42	63	72	84	66 b	.....	+ .08	+0.39
4648.93	34	.....	25	.....	.....	24	.....	26	.....	2.57	− .27	−0.17
4656.97	94	88	84	.....	80	89	99	84	77 c	2.88	+ .24	+0.74
4663.70	46	48	45	.....	47	67	55	50	b	2.88	+ .01	+0.26
4664.23	.....	9	.....	.....	.....	.....	.....	.....	a	.....	− .75	−0.74
4666.75 p	77	90	82	.....	96	83	104	70	a	2.82	+ .23	+0.71
4670.17	64	76	71	.....	.....	.....	.....	.....	c	2.57	+ .15	+0.54
4697.32	.....	.....	.....	.....	.....	.....	25	26	.....	.....	− .29	−0.20
4731.44	78	58	89	.....	.....	110	116	88	62	2.88	+ .25	+0.77
4734.89	.....	.....	.....	.....	.....	32	.....	24	a	.....	− .25	−0.14
Ni I												
4401.55	90	41	.....	22	36	26	58	54	80 b	3.18	− .01	+0.22
4648.66	47	.....	.....	.....	.....	14	.....	.....	b	3.40	−0.31	−0.22

TABLE 1—*Continued*

λ	0.055	0.141	0.227	0.445	0.534	0.702	0.773	0.819	0.969	E.P.	log W/b	log η_0
Ni II												
4015.50							30	36	a	4.01	−0.09	+0.09
4244.80		34							b	4.01	− .10	+0.08
Sr II												
4077.71	88		87						a	0.00	+ .33	+1.00
4161.80	65	44			44	31	41	52	c	2.93	+ .10	+0.43
4215.52	119	112	101	77	93	95	88	92	88 b	0.00	+ .36	+1.10
Y II												
4398.02	34				13				32 a	0.13	− .38	−0.31
Zr II												
3915.94	26	17		24	24	30	22	22	21 b	0.52	− .38	−0.31
3934.14		56	24				13		c	0.32	− .25	−0.14
3998.98 p	60				32	37	53		59 a	0.56	− .09	+0.09
4018.38	48	44	22		31	24	23		31 b	0.96	− .22	−0.10
4149.22	54				25				49 a	0.80	− .19	−0.06
4156.24	88	72			35	38	50	54	53 c	0.71	+ .01	+0.26
4210.62 p	24				25					1.66	− .39	−0.32
4277.37	47	45		36	40	34	37	34	32 c	0.80	− .20	−0.07
4317.32 p	29						36			0.71	− .27	−0.17
4379.78 p	66	53	47		16		48	59	53 b	1.53	− .19	−0.06
4388.50						16	46	28	c	2.48	− .32	−0.24
4440.45	51	31	21			13	25		43	1.20	− .36	−0.28
4461.22	47	55								1.01	− .09	+0.09
4496.96 p		20			29	20		27	a	0.71	− .43	−0.37
4553.96	24							22	b	2.41	− .44	−0.38
4574.49 p	32	32								2.42	− .30	−0.21
La II												
3864.49	32	14				6	13	25		3.53	+ .08	+0.39
3921.54 p					27					0.23	+ .16	+0.56
3929.22 p	65						16		71 b	0.17	+ .43	+1.40
3936.22	26	22	12	13	5	11	28	32	b	0.13	+ .11	+0.45
3995.74 p	39		29				27	23	a	0.17	+ .20	+0.64
4123.23 p			38		42		58		b	0.32	+ .37	+1.14
4152.78			33	52	14				a	1.75	+ .22	+0.69
4192.35							22		26	1.77	+ .08	+0.39
4194.36						12	18			3.98	− .12	+0.05
4238.38 p		31				14	17		a	0.40	+ .02	+0.27
4249.99		31								1.94	+ .18	+0.60
4286.97		16		31	33	32	18	16	11 b	1.94	+ .03	+0.29
4429.90 p	30	22	24			24	46		24 a	0.23	+ .12	+0.47
4432.95		15							c	0.24	− .15	0.00
4498.76									13 b	2.25	− .22	−0.10
4526.12	39					14	24			0.77	+ .07	+0.37
4538.87	56	27				36	41	44	41	3.64	+ .22	+0.69
4540.71		40	24	28				29	c	1.95	+ .14	+0.51
4559.28						13	27	22	26	0.77	+ .00	+0.24
4574.87 p	27							14	b	0.17	− .03	+0.19
4636.42		13	15			21		22	23 b	2.33	− .07	+0.12
4655.49	42								c	1.94	+ .27	+0.82
4662.51 p		22	22		18		26		b	0.00	− .01	+0.22
4668.91	30									1.77	+ .13	+0.49
4688.65	54		34		43	38	55	52	a	2.12	+ .31	+0.94
4691.17	23								c	0.17	+ .01	+0.26
4692.50							8	18		1.75	− .24	−0.13
4699.62	86	82	34		48	55	42	55	66 c	0.40	+ .43	+1.40
4703.27	34						27		a	1.94	+ .13	+0.49
4719.93			22				36	21	a	1.95	+ .06	+0.34
4728.41	46					42			b	0.17	+ .29	+0.88
4739.80	46	22						27	c	0.92	+ .15	+0.54
4740.27	56	36							42	0.13	+ .29	+0.88
Ce II												
3909.31							56	64	c	0.44	+ .03	+0.29
3912.42 p						37		50		0.29	−0.05	+0.16

TABLE 1—*Continued*

λ	0.055	0.141	0.227	0.445	0.534	0.702	0.773	0.819	0.969	E.P.	log W/b	log η_0
Ce II—*Cont.*												
3921.73	64	68	....	58	45	....	....	....	c	0.71	+0.03	+0.29
3924.64 p	....	....	....	....	9	....	....	....	18 a	0.56	− .59	−0.56
3931.09	....	....	29	24	21	31	45	52	62 b	0.17	− .16	−0.01
3940.34 p	....	37	....	....	17	....	27	32	a	0.32	− .31	−0.22
3942.75 p	....	41	26	....	....	....	40	33	b	0.85	− .20	−0.07
3943.89	45	....	30	....	42	41	44	38	51 b	0.79	− .13	+0.03
3993.82 p	....	37	....	....	....	43	....	....	38 a	0.43	− .16	−0.01
3999.24 p	....	57	....	....	45	....	....	....	a	0.29	− .04	+0.17
4003.77	....	31	....	29	23	23	39	24	b	0.93	− .30	−0.21
4014.90 p	32	36	....	....	....	....	....	....	a	0.53	− .22	−0.10
4015.88 p	....	....	....	....	....	....	25	33	b	1.04	− .29	−0.20
4040.76	64	55	30	....	34	28	43	45	49 a	0.44	− .13	+0.03
4042.58 p	43	53	37	....	45	41	48	57	44 a	0.49	− .09	+0.09
4046.34	80	71	54	....	53	46	65	66	76	0.55	+ .01	+0.26
4054.99	....	....	....	....	....	....	46	....	52 b	0.32	− .07	+0.12
4067.28	21	....	....	....	33	38	41	29	b	0.58	− .25	−0.14
4068.84 p	18	21	19	....	24	....	27	21	a	0.70	− .42	−0.36
4080.44	....	....	14	....	....	....	....	....	....	0.36	− .61	−0.58
4081.22	....	....	35	....	....	....	....	....	b	0.00	− .22	−0.10
4123.87 p	25	....	....	....	34	44	50	....	a	0.85	− .19	−0.06
4133.80	....	....	....	....	54	48	47	41	a	0.04	− .09	+0.09
4137.65 p	....	....	40	....	37	....	52	42	....	0.04	− .13	+0.03
4142.40	31	34	....	....	....	....	....	34	15 a	0.22	− .25	−0.14
4148.90 p	23	....	37	....	30	....	....	....	....	0.61	− .29	−0.20
4149.94	....	....	....	....	....	....	....	....	24 b	0.72	− .39	−0.32
4151.97	....	27	....	....	37	....	31	32	b	0.20	− .26	−0.16
4159.03	27	....	....	....	....	25	....	....	b	1.02	− .36	−0.28
4161.18	62	....	....	56	....	59	65	56	c	0.48	+ .01	+0.26
4165.61 p	....	....	....	31	30	....	....	39	30 a	0.43	− .25	−0.14
4167.80	....	25	....	32	....	....	....	....	16	0.64	− .39	−0.32
4169.72	29	....	....	46	53	36	....	....	b	0.72	− .16	−0.01
4185.33	27	....	....	....	....	....	18	....	b	0.42	− .42	−0.36
4186.60	59	....	....	....	47	51	52	44	62 a	0.38	− .05	+0.16
4193.85	....	....	....	....	....	18	41	42	52 b	0.55	− .19	−0.16
4198.7	....	....	34	....	....	....	....	....	....	0.04	− .24	−0.13
4202.94 p	58	49	....	....	44	53	57	50	b	0.56	− .06	+0.14
4209.41	....	30	....	....	....	....	....	....	22	0.20	− .36	−0.28
4213.04	....	....	....	....	10	14	....	10	a	0.67	− .73	−0.72
4214.04	....	17	24	....	21	19	22	....	20 a	0.61	− .45	−0.39
4222.60 p	....	....	....	....	....	....	....	....	25 a	0.12	− .38	−0.31
4231.74	....	29	....	36	....	....	....	....	27 c	....	− .29	−0.20
4239.91	29	....	....	....	....	31	....	24	a	0.00	− .33	−0.25
4246.71	40	49	....	....	....	....	....	....	c	0.46	− .14	+0.01
4248.68	54	40	....	....	34	13	21	33	28 a	0.20	− .27	−0.17
4255.78	....	....	....	....	....	....	50	41	38 c	0.70	− .15	0.00
4257.12 p	....	....	....	....	....	8	....	....	a	0.46	− .87	−0.87
4261.16	....	....	....	....	....	12	31	29	33 a	0.61	− .37	−0.30
4264.37	40	34	....	....	....	....	....	....	....	0.90	− .21	−0.08
4268.16	32	....	16	....	26	17	....	17	21 a	....	− .43	−0.37
4270.72	56	....	....	....	....	....	....	....	c	0.48	− .03	+0.19
4280.14	32	....	....	....	....	....	....	....	b	0.73	− .27	−0.17
4289.45	27	....	....	....	....	....	....	....	....	0.44	− .35	−0.27
4289.94	154	136	50	82	86	70	137	138	154 b	0.33	+ .28	+0.85
4300.33	....	....	....	16	....	25	....	27	b	0.44	− .42	−0.36
4364.66 p	14	....	....	....	28	....	36	....	a	0.49	− .37	−0.30
4388.01	74	60	33	....	31	36	36	48	57 c	0.38	− .09	+0.09
4391.66 p	70	56	56	....	66	48	55	....	b	0.32	− .02	+0.20
4407.28 p	....	16	....	....	....	....	....	....	a	0.70	− .59	−0.56
4410.64 p	....	19	....	....	....	....	....	....	....	0.87	− .52	−0.48
4418.78	92	46	40	56	82	63	83	76	67 c	0.38	+ .03	+0.29
4423.68 p	....	....	....	....	....	....	....	13	....	0.58	− .69	−0.67
4437.61	16	18	....	....	....	....	....	....	....	0.82	−0.57	−0.54

TABLE 1—*Continued*

λ	0.055	0.141	0.227	0.445	0.534	0.702	0.773	0.819	0.969	E.P.	log W/b	log η_0
Ce II—*Cont.*												
4440.88		11					31			0.80	−0.48	−0.43
4444.39	101	98	65	84	82	70	85	85	95 c	0.44	+ .13	+0.49
4449.34 p	55	75			12	17	34	43	48 a	0.61	− .20	−0.07
4460.21	35	33	20		26	37	25	28	23	0.00	− .35	−0.27
4461.14	68		26			39	46	64	60 b	0.43	− .23	−0.11
4463.41			17			20		20	19 a	0.48	− .52	−0.48
4469.85	30	14	19						c	0.74	− .48	−0.43
4479.4	44	13	25			35	51	39	37 b	0.42	− .26	−0.16
4483.90 p	30			38		30	32	39	22 b	0.38	− .30	−0.21
4486.91 p	43			55	44	33	48	44		0.29	− .16	−0.01
4491.10 p		7	14			16		22	17	0.61	− .63	−0.60
4497.85 p		14			32			21	a	0.48	− .46	−0.41
4527.35	48	28	27	16		25	40	47	49 a	0.32	− .30	−0.21
4539.76	86			74	83	92	118	114	113 c	0.33	+ .18	+0.60
4551.30	38					27			c	0.74	− .30	−0.21
4560.28 p	51						42	39	33	0.43	− .20	−0.07
4560.96 p	61			33	30	16	19	27	42 a	0.20	− .23	−0.11
4593.93 p	66	74			45		70	48	44 b	0.22	− .05	+0.16
4606.40 p	62	27				29	45	40	30 b	0.43	− .22	−0.10
4628.16 p	82	66	26		36	40	51	60	55 a	0.04	− .09	+0.09
4654.29	111	78	50		38	52	61	73		0.52	+ .03	+0.29
4680.13	50	42				27			45	0.58	− .21	−0.08
4684.61	85	70			48	62	76	64	b	0.90	.00	+0.24
4737.28	58					54	55		a		− .07	+0.12
Pr II												
3858.26		16				30		35	34 b		− .28	−0.18
3867.55	6	13									− .77	−0.76
3909.62							37	36	c		− .18	−0.04
3912.90	76				19			39	c	0.20	− .11	+0.06
3924.14	25	20	25		22				27		− .36	−0.28
3927.45	22					35		41	a	0.22	− .22	−0.10
3929.26						30	38		b		− .21	−0.08
3940.15					9		24	19	a		− .52	−0.48
3947.63	28				22		33	35	a	0.20	− .27	−0.17
3949.44 p	43	25		34	18	31	43	27	27 a	0.20	− .26	−0.16
3994.83 p			46		37		47	42	a	0.05	− .12	+0.05
4016.75							31	31			− .26	−0.16
4022.74			8						a		− .85	−0.85
4025.55		62	58	77	76	69	71	62	41 c		+ .06	+0.34
4026.84	19				14	17	26	22	14		− .45	−0.39
4033.86	70	48			11	35	32		38 b	0.37	− .17	−0.03
4044.82	29				23	26	30	32	29	0.00	− .31	−0.22
4052.58						32	47	42	38 c		− .16	−0.01
4056.54		29	33		42	45	51	34	36	0.63	− .18	−0.04
4062.82	42	71	37			40			b	0.42	− .08	+0.10
4081.90			23						b		− .40	−0.34
4164.19	16		28		19		41		a	0.20	− .36	−0.28
4172.27									28	0.20	− .32	−0.24
4189.52		32					33	35	b	0.37	− .25	−0.14
4219.65	18	25							b		− .44	−0.38
4243.53								6		0.22	−1.00	−1.00
4249.08		38					22		15		− .38	−0.31
4249.48					17					0.37	− .55	−0.51
4272.27						26	30		b	0.37	− .33	−0.25
4293.14	76			34	32	45	62	68	83 c		− .02	+0.20
4293.58	18						7	14			− .67	−0.65
4294.70	45	9	17			20	44	32	38 b		− .32	−0.24
4297.76	17	13	14						a	0.00	− .60	−0.57
4298.92			17		26						− .44	−0.38
4306.08		26	12				24		b		− .46	−0.41
4370.80	53	64		47			32	25	44 c		− .15	0.00
4371.61									61 c		0.00	+0.24

TABLE 1—*Continued*

λ	0.055	0.141	0.227	0.445	0.534	0.702	0.773	0.819	0.969	E.P.	log W/b	log η_0
Pr II—*Cont.*												
4384.14	123	112	82	111	117	80	95	90	c	.....	+0.21	+0.67
4403.60	.....	.....	21	18	....	9	.....	.....	.....	0.63	− .59	−0.56
4405.85	.....	31	.....	.....	63	49	.....	.....	c	0.55	− .11	+0.06
4408.84 p	44	20	21	.....	.....	.....	53	55	.....	0.00	− .20	−0.07
4419.67	67	57	48	50	60	52	64	59	64 c	.....	− .04	+0.17
4429.24 p	63	25	23	41	30	47	54	77	46 a	0.00	− .18	−0.04
4432.34	.....	11	.....	26	.....	.....	.....	.....	a	.....	− .53	−0.49
4445.87	.....	.....	.....	.....	.....	.....	.....	.....	39 c	.....	− .21	−0.08
4446.98	.....	.....	9	.....	.....	16	19	.....	21 a	.....	− .60	−0.57
4458.34	.....	23	12	.....	.....	.....	26	39	a	0.55	− .40	−0.34
4465.98	.....	.....	17	.....	.....	.....	.....	.....	a	.....	− .57	−0.54
4477.26 p	.....	.....	17	.....	21	22	20	22	a	0.20	− .50	−0.46
4488.0	.....	.....	.....	32	.....	.....	.....	.....	.....	0.05	− .29	−0.20
4492.43	.....	.....	.....	14	.....	20	12	.....	a	0.42	− .62	−0.59
4494.19	70	.....	.....	.....	31	28	55	49	64 c	.....	− .16	−0.01
4496.43	.....	.....	.....	.....	29	.....	44	37	b	0.05	− .23	−0.11
4510.16	.....	42	.....	.....	.....	42	67	64	61 c	0.42	− .08	+0.10
4520.78	.....	26	.....	.....	26	24	.....	.....	19 c	.....	− .43	−0.37
4529.93	53	22	.....	.....	.....	.....	.....	.....	22 c	.....	− .30	−0.21
4548.54	.....	16	13	10	9	11	18	14	10 a	.....	− .71	−0.69
4561.46	53	.....	.....	21	19	12	27	31	27 c	0.22	− .38	−0.31
4563.13	.....	41	.....	22	22	28	34	44	54 c	.....	− .23	−0.11
4570.56	.....	36	.....	.....	18	.....	39	31	.....	.....	− .32	−0.24
4578.14	.....	22	.....	.....	43	.....	25	18	c	0.37	− .38	−0.31
4612.07	.....	.....	.....	.....	.....	30	.....	45	c	0.00	− .23	−0.11
4628.75	.....	33	26	.....	33	45	52	55	67 b	0.05	− .18	−0.04
4651.52 p	53	.....	.....	.....	.....	.....	54	50	a	0.20	− .10	+0.08
4672.08	.....	19	.....	.....	.....	.....	22	.....	.....	0.22	− .51	−0.47
4707.54	.....	.....	.....	.....	.....	23	.....	24	14 c	0.20	− .52	−0.48
Nd II												
3866.80	38	23	20	.....	.....	.....	.....	.....	.....	.....	− .31	−0.22
3912.23	.....	.....	.....	.....	.....	29	.....	48	b	.....	− .16	−0.01
3920.96	.....	.....	23	.....	25	.....	.....	.....	.....	.....	− .36	−0.28
3948.32	40	.....	.....	.....	41	.....	33	.....	b	.....	− .17	−0.03
3951.15	.....	.....	.....	.....	.....	.....	44	43	a	0.18	− .11	+0.06
3995.24	60	43	50	.....	28	22	45	44	53 b	.....	− .15	0.00
4004.01	.....	24	.....	30	18	19	24	28	35 b	.....	− .34	−0.26
4013.22	.....	.....	.....	.....	.....	.....	19	20	.....	.....	− .46	−0.41
4018.83	7	.....	23	.....	.....	.....	.....	.....	.....	0.06	− .57	−0.54
4020.87	49	.....	46	47	.....	43	50	52	41 b	0.32	− .08	+0.10
4021.33 p	24	.....	.....	.....	.....	.....	.....	.....	.....	0.32	− .37	−0.30
4023.00	.....	17	.....	.....	18	10	15	.....	a	.....	− .58	−0.55
4031.81	24	24	20	.....	.....	15	.....	11	14 a	.....	− .50	−0.46
4043.60	29	17	.....	.....	.....	.....	15	13	a	0.32	− .49	−0.45
4051.14	35	30	.....	.....	.....	.....	.....	.....	b	0.38	− .25	−0.14
4056.84	.....	28	35	.....	.....	32	.....	.....	c	.....	− .25	−0.14
4059.96 p	33	29	.....	.....	.....	.....	33	.....	36 b	0.20	− .24	−0.13
4061.08	21	24	15	.....	.....	32	34	32	.....	0.47	− .35	−0.27
4069.27 p	.....	.....	.....	.....	18	12	.....	22	a	0.06	− .53	−0.49
4080.23	.....	.....	7	.....	.....	.....	.....	.....	.....	0.06	− .91	−0.91
4135.32	.....	41	38	.....	.....	36	47	35	31 b	.....	− .19	−0.06
4136.23	38	47	47	.....	25	24	46	.....	c	.....	− .24	−0.13
4157.58	46	.....	.....	.....	.....	32	42	28	c	.....	− .20	−0.07
4165.04	33	24	.....	.....	.....	.....	.....	.....	c	.....	− .32	−0.24
4177.32 p	.....	.....	.....	.....	.....	.....	.....	.....	38 a	0.06	− .19	−0.06
4178.64	.....	.....	.....	20	11	14	.....	16	b	.....	− .59	−0.56
4182.29	35	.....	.....	.....	.....	.....	.....	.....	28 c	.....	− .26	−0.16
4195.03	.....	.....	.....	.....	15	.....	.....	.....	.....	.....	− .59	−0.56
4205.60	.....	.....	.....	83	74	68	75	79	81 c	0.63	+ .12	+0.47
4212.75	22	.....	.....	.....	10	.....	.....	.....	14	.....	− .59	−0.56
4228.4	44	.....	.....	.....	23	.....	27	36	48	0.47	− .22	−0.10
4228.84	.....	.....	.....	.....	.....	.....	.....	.....	6	.....	−1.00	−1.00
4256.82	.....	25	14	.....	.....	.....	.....	.....	.....	.....	−0.49	−0.45

TABLE 1—*Continued*

λ	0.055	0.141	0.227	0.445	0.534	0.702	0.773	0.819	0.969	E.P.	log W/b	log η_0
Nd II—*Cont.*												
4277.28	10		7							0.18	−0.85	−0.85
4284.52 p	37	46							b	0.63	− .22	−0.10
4290.96	46	27		23	36	28	36	37	34 c		− .26	−0.16
4310.51	25								c	0.20	− .38	−0.31
4368.63				14	14				7	0.06	− .71	−0.69
4372.73	36						27	30	c		− .30	−0.21
4381.29		25					28	23	35	0.20	− .34	−0.26
4390.66	68	70	45	55	41		31	42	52 c		− .09	+0.09
4400.83 p	38				39			32	28	0.06	− .26	−0.16
4410.25					26		27		c		− .37	−0.30
4412.26	39	14							b	0.06	− .37	−0.30
4439.00	29					23	19	24	19 a		− .44	−0.38
4447.99	80						40	37	48 c		− .09	+0.09
4451.98					22	11				0.00	− .58	−0.55
4462.41			17			13			14 a	0.20	− .62	−0.59
4462.98 p						9		19	a	0.56	− .65	−0.63
4485.95							21			0.38	− .48	−0.43
4487.62		28	34		43	42	43	37	c		− .22	−0.10
4501.81	16	11								0.20	− .67	−0.65
4505.75	12					19	27	19	6 b	0.00	− .57	−0.54
4513.33	29										− .34	−0.26
4516.35	28			50	43		50		c		− .17	−0.03
4516.64	28	26							c		− .37	−0.30
4523.57					16	28	29	22			− .43	−0.37
4541.27								30	26 c	0.38	− .37	−0.30
4542.60	23				14	18			a		− .55	−0.51
4556.74									14 a	0.18	− .66	−0.64
4567.61					34		31	34	17 b	0.20	− .35	−0.27
4579.31	37					16	21	28	15 a		− .45	−0.39
4584.04	51								c		− .10	+0.08
4594.45					7		13			0.20	− .81	−0.81
4602.24							28		c	0.47	− .36	−0.28
4609.15		24					34	27	23 c	0.18	− .36	−0.28
4629.90	30				13	7	11	13			− .63	−0.60
4632.69	41	21			10			10	c	0.20	− .51	−0.47
4664.45			31						c		− .33	−0.25
4680.73	34	17							16	0.06	− .48	−0.43
4706.54 p							33	30		0.00	− .33	−0.25
4709.71						20		22	a	0.18	− .50	−0.46
Sm II												
3862.05	21	34	33				29			0.10	− .28	−0.18
3922.40	13							7	a	0.38	− .74	−0.73
3935.76							6			0.28	− .97	−0.97
3943.24					36			33	a	0.10	− .22	−0.10
3948.0	44				21		28	30	a	0.11	− .26	−0.16
4019.98	26	17				21	23	27	30 c	0.18	− .37	−0.30
4035.11 p	25	24					17		20 a	0.33	− .46	−0.41
4041.68						27	33	25	31	0.19	− .30	−0.21
4047.16		10	9						19 a	0.18	− .65	−0.63
4064.58 p		21		12					22 a	0.25	− .53	−0.49
4066.74									16 a	0.28	− .56	−0.53
4068.33 p	31	28					21		b	0.43	− .33	−0.25
4129.23		54							38 c	0.25	− .11	+0.06
4155.22							31			0.10	− .28	−0.18
4169.48	18						18		a	0.25	− .51	−0.47
4183.76	27								b	0.04	− .34	−0.26
4188.13		16	15		10				a	0.54	− .62	−0.59
4206.13								43	c	0.38	− .14	+0.01
4225.33		45	34						b	0.19	− .18	−0.04
4229.70	60					25			b	0.04	− .16	−0.01
4234.57				20		15	11		a	0.43	− .60	−0.57
4237.66	27	15		15	9	12		13	22 a	0.10	−0.52	−0.48

TABLE 1—*Continued*

λ	0.055	0.141	0.227	0.445	0.534	0.702	0.773	0.819	0.969	E.P.	log W/b	log η_0
Sm II—*Cont.*												
4244.70	41								38 c	0.28	−0.18	−0.04
4256.39 p		29							a	0.38	− .32	−0.24
4262.68 p				27		15	16			0.38	− .50	−0.46
4265.08						14	8	9	10 b	0.18	− .78	−0.77
4279.68	15									0.28	− .60	−0.57
4281.01		39	18			25	17		c		− .38	−0.31
4286.64									12 a	0.43	− .70	−0.68
4292.18					30		46		b	0.33	− .20	−0.07
4309.01		27	14						a	0.18	− .47	−0.42
4362.04			26	30	27	20			b	0.48	− .38	−0.31
4378.24	45	48					39	31	29 c	0.66	− .21	−0.08
4403.36		27	19			20			27 a	0.19	− .43	−0.37
4420.53 p						11			30 a	0.33	− .50	−0.46
4424.34	62	46				40		63	56 b	0.48	− .12	+0.05
4433.88									40 b	0.43	− .20	−0.07
4434.32	100	44		44	64	51	71	80	79 c	0.38	+ .05	+0.32
4452.73 p	41	53			8		30	30	33	0.28	− .32	−0.24
4454.63	52	33	8							0.54	− .31	−0.22
4458.52			9		21				a	0.10	− .62	−0.59
4511.83					53	65	65		c	0.18	− .01	+0.22
4519.63 p	45	21	16	14		19	30	25	29 a	0.54	− .39	−0.32
4537.95	67	18			26				c	0.48	− .24	−0.13
4552.66	17		43			21	32		15 b	0.25	− .40	−0.34
4591.82								15	a	0.18	− .63	−0.60
4595.29		19					28	20	28 a	0.48	− .43	−0.37
4615.44					29	31	42	34	c	0.54	− .28	−0.18
4615.69 p						13				0.19	− .70	−0.68
4642.24 p						23	24	31		0.38	− .40	−0.34
4648.16						29		48	c	0.00	− .24	−0.13
4669.5	60						39		b	0.10	− .12	+0.05
4674.60	61	42					30	58	37 b	0.18	− .16	−0.01
4676.91	78	42					35	45	42 c	0.04	− .14	+0.01
4704.40	20								20 a	0.00	− .52	−0.48
Eu II												
3861.18	48		19		29				26 a		− .26	−0.16
3865.29	47	16	23				15	26			− .33	−0.25
3907.10 p	102	103			31	28	60	74	107	0.21	+ .08	+0.39
3913.72	71						45		60 c		+ .07	+0.37
3917.29	66	72		39	36	30	30	36	55 a	1.37	− .06	+0.14
3917.70					22	26	39	40		1.23	− .26	−0.16
3919.09	32								59 b		− .08	+0.10
3929.91				22		15	22	27	b	3.00	− .41	−0.35
3930.50 p	150	136				71	136	127	201	0.21	+ .37	+1.14
3942.21	48	58	45		44	42	51	60	43 b	1.25	− .06	+0.14
3943.0								19	a	2.93	− .48	−0.43
3945.67					21		10		a		− .56	−0.53
4004.59	29								b	1.25	− .29	−0.20
4011.69	24	13	22	34	26			34	24	3.00	− .35	−0.27
4012.82			24						b		− .37	−0.30
4017.58	31	36	20		17	21	26	35	30 a	1.31	− .38	−0.31
4042.02	43	29			17	14	16	14	b	1.27	− .42	−0.36
4062.15	29			22	28				a		− .35	−0.27
4066.05					35				c		− .22	−0.10
4071.38					11	11	10	10			− .74	−0.73
4124.54									49 c	2.09	− .07	+0.12
4129.73 p	170	127	53	41	50	49	68	87	123	0.00	+ .25	+0.77
4133.10					18	24	37	34	42 b		− .31	−0.22
4136.59									26		− .36	−0.28
4139.67	39		35		31	21	24	25	26		− .31	−0.22
4140.02	14								11 a		− .68	−0.66
4141.02	42	41							b		− .15	0.00
4145.23	77	53	56	62	57	55	71	69	73 c		+0.04	+0.31

TABLE 1—*Continued*

λ	0.055	0.141	0.227	0.445	0.534	0.702	0.773	0.819	0.969	E.P.	log W/b	log η_0
Eu II—*Cont.*												
4147.22	98	54	40	.....	37	33	.....	54	63	.....	+0.02	+0.27
4148.40	.....	42	31	.....	18	.....	.....	.....	a	.....	− .29	−0.20
4160.48	80	.....	61	76	75	69	65	72	65 b	.....	+ .08	+0.39
4162.14	.....	.....	.....	.....	.....	18	.....	.....	.....	.....	− .51	−0.47
4172.80	.....	.....	21	.....	.....	.....	.....	.....	28 a	.....	− .39	−0.32
4175.16	.....	.....	.....	33	.....	31	.....	.....	a	.....	− .26	−0.16
4179.88	35	21	.....	36	10	9	13	12	19 a	.....	− .49	−0.45
4205.05 p	202	176	.....	53	60	64	89	124	203 a	0.00	+ .34	+1.03
4211.28	.....	.....	.....	.....	.....	.....	32	49	32 a	.....	− .19	−0.06
4213.48	.....	40	.....	.....	39	32	.....	.....	c	.....	− .20	−0.07
4217.75	.....	.....	.....	.....	.....	47	40	44	40	.....	− .14	+0.01
4218.45	.....	.....	.....	.....	.....	.....	9	17	a	.....	− .66	−0.64
4219.03	30	27	27	.....	.....	8	11	.....	23	.....	− .54	−0.50
4221.08	.....	19	.....	.....	24	.....	17	34	a	.....	− .41	−0.35
4223.88	40	.....	.....	.....	.....	.....	.....	.....	a	.....	− .18	−0.04
4225.68	.....	.....	16	.....	.....	.....	.....	.....	a	.....	− .58	−0.55
4229.33	19	.....	.....	.....	.....	9	.....	9	.....	1.31	− .70	−0.68
4230.63	29	20	16	.....	.....	.....	.....	.....	a	.....	− .44	−0.38
4236.22	.....	.....	35	38	48	44	50	56	37 b	.....	− .16	−0.01
4240.21	22	28	.....	34	31	42	26	28	18 c	.....	− .30	−0.21
4241.60	10	.....	18	.....	14	17	14	9	.....	.....	− .63	−0.60
4244.41	18	.....	.....	.....	.....	33	.....	.....	23	.....	− .38	−0.31
4245.46	41	39	21	.....	.....	.....	.....	.....	29	.....	− .27	−0.17
4245.85	24	.....	.....	.....	.....	25	.....	22	c	.....	− .40	−0.34
4247.06	.....	.....	.....	.....	.....	.....	.....	.....	46	.....	− .12	+0.05
4247.88	.....	.....	.....	.....	.....	20	.....	.....	b	.....	− .48	−0.43
4253.80	.....	.....	.....	.....	.....	.....	13	14	a	.....	− .65	−0.63
4264.91	29	28	22	.....	.....	18	19	18	22 c	.....	− .44	−0.38
4270.24	.....	.....	.....	.....	.....	26	23	25	18 a	.....	− .42	−0.36
4270.50	74	70	21	.....	.....	.....	38	41	64 c	.....	− .18	−0.04
4272.76	.....	.....	.....	.....	.....	16	.....	.....	b	.....	− .58	−0.55
4276.20	18	16	21	17	12	.....	.....	16	22 a	.....	− .55	−0.51
4281.92	.....	.....	14	31	.....	26	.....	.....	.....	.....	− .40	−0.34
4311.28	34	22	.....	.....	.....	.....	.....	.....	22 c	.....	− .37	−0.30
4313.85	.....	27	.....	14	8	20	33	35	37 a	.....	− .50	−0.46
4317.67	42	.....	17	.....	31	.....	44	.....	b	.....	− .26	−0.16
4362.43	.....	.....	21	.....	.....	.....	.....	.....	b	.....	− .47	−0.42
4365.18	19	.....	.....	.....	.....	.....	.....	.....	b	.....	− .51	−0.47
4369.47	45	.....	.....	.....	.....	.....	.....	.....	.....	.....	− .14	+0.01
4370.34	.....	.....	.....	.....	.....	.....	30	35	.....	.....	− .28	−0.18
4376.42	43	41	39	46	.....	19	31	.....	31 c	.....	− .23	−0.11
4399.32	42	29	.....	.....	26	25	32	26	29 b	.....	− .32	−0.24
4402.26	15	.....	14	.....	.....	10	17	.....	b	.....	− .64	−0.62
4405.27	39	.....	.....	.....	.....	.....	.....	.....	.....	2.09	− .20	−0.07
4412.98	24	11	.....	.....	.....	.....	.....	.....	b	.....	− .55	−0.51
4414.64	77	59	24	28	.....	26	.....	56	86 b	.....	− .09	+0.09
4426.42	.....	.....	.....	.....	.....	.....	11	.....	a	.....	− .76	−0.75
4434.81	.....	.....	.....	.....	11	.....	.....	16	.....	3.36	− .67	−0.65
4435.58	137	67	41	.....	23	38	88	90	115 a	0.21	+ .07	+0.37
4437.96	.....	.....	.....	.....	.....	28	.....	.....	c	.....	− .35	−0.27
4441.47	36	28	21	.....	9	11	30	30	38	.....	− .54	−0.50
4442.42	29	.....	.....	.....	.....	.....	.....	.....	27 b	.....	− .35	−0.27
4462.14	.....	17	10	.....	.....	.....	.....	.....	a	1.25	− .67	−0.65
4464.97	.....	24	21	.....	.....	39	.....	.....	42 b	3.36	− .29	−0.20
4469.64	.....	.....	19	.....	23	11	30	29	a	.....	− .45	−0.39
4471.64	.....	.....	19	.....	.....	.....	47	35	c	.....	− .27	−0.17
4472.34	.....	.....	25	.....	.....	.....	17	.....	.....	.....	− .48	−0.43
4476.89	.....	.....	.....	.....	.....	.....	27	18	c	.....	− .45	−0.39
4489.26	39	.....	.....	.....	.....	.....	.....	.....	c	.....	− .21	−0.08
4495.98	.....	.....	.....	.....	.....	28	42	34	c	.....	− .26	−0.16
4500.27	.....	.....	.....	.....	.....	36	.....	.....	a	.....	− .24	−0.13
4504.52	.....	.....	.....	.....	.....	.....	18	.....	b	.....	− .54	−0.50
4505.98	.....	.....	.....	73	81	.....	.....	41	c	.....	+0.01	+0.26

TABLE 1—*Continued*

λ	0.055	0.141	0.227	0.445	0.534	0.702	0.773	0.819	0.969	E.P.	log W/b	log η_0
Eu II—*Cont.*												
4522.57	34								a	0.21	−0.28	−0.18
4533.63						24			c		− .43	−0.37
4545.45		18							c	2.12	− .55	−0.51
4547.22		16			29	21		23	14 b		− .49	−0.45
4552.14							15		23 a		− .53	−0.49
4573.66	25						25	22	b		− .43	−0.37
4576.93		8				17			7	1.31	− .77	−0.76
4612.43		21						21	b		− .49	−0.45
4614.63	35	20	21		34	26	38	33	21	2.12	− .36	−0.28
4633.07	22	10	12		6				11 a	1.23	− .74	−0.73
4652.44					16		29	32	b		− .41	−0.35
4658.63	67				33		36	41	b	2.11	− .18	−0.04
4695.35	55		35			32	39	53	c	2.10	− .24	−0.13
Eu III												
4422.2	82	62	15				33		82		− .15	0.00
Gd II												
3863.05	56								70		+ .06	+0.34
3910.26	35	37	15		16	15	22	40	33 c		− .36	−0.28
3916.51	78	69		54	56	56	58	73	65 a	0.60	+ .07	+0.37
3918.24		96							c	0.60	+ .24	+0.74
3923.25	99	65		16	18	20	71		a	0.55	+ .01	+0.26
3932.98	31		16		14			41	b		− .33	−0.25
3934.82	44	48	42	19		29	31	35	47 a	0.03	− .23	−0.11
3994.16		40							a	0.52	− .15	0.00
3996.32	53		48	44	39	30	46		b		− .12	+0.05
3997.76			46				33	47	b	1.06	− .13	+0.03
4001.26							30		a	0.52	− .27	−0.17
4004.94					26	24		40	46 a		− .22	−0.10
4008.91	52	49	46		21	52	61	72	a		− .08	+0.10
4009.22	46	28	31								− .21	−0.08
4013.80	24						28	36	32 a		− .27	−0.17
4037.33	74	45				43	60	68	50 a	0.66	.00	+0.24
4039.6	57	41							44 a		− .09	+0.09
4046.84			30		25	49	54		b		− .16	−0.01
4047.81		40	21					28			− .28	−0.18
4048.60						19					− .48	−0.43
4049.43			23							0.66	− .40	−0.34
4049.86			24		37	39	46	42	a		− .18	−0.04
4053.29	77	75			47	49	55	54	69 b		+ .03	+0.29
4059.37	20	18		13		18	26	22	b	1.72	− .45	−0.39
4061.30					20						− .46	−0.41
4063.39						36	33				− .23	−0.11
4065.61					21				c		− .44	−0.38
4070.3	83								93 b	0.42	+ .18	+0.60
4073.20	97								90 c	0.43	+ .21	+0.67
4073.76	40				34				b	0.82	− .19	−0.06
4078.44	48			59	65	61	68	56	67 b	0.60	+ .03	+0.29
4130.37 p							45			0.60	− .09	+0.09
4132.28	143					125	127	116	152 c	0.60	+ .35	+1.07
4140.45						28	28	38		0.55	− .28	−0.18
4150.61			28						c		− .32	−0.24
4151.63	17	14			20		21	10	15 a		− .57	−0.54
4153.51 p						26	28		a	1.58	− .34	−0.26
4162.73			22	22		26	37	36	28 a	0.49	− .32	−0.24
4167.16							40		c	0.42	− .17	−0.03
4170.11	18								21 a	0.43	− .48	−0.43
4184.25	79	79		77	67	75	81	80	66 b	0.49	+ .11	+0.45
4191.07 p	68	48				56			77 a	0.43	+ .02	+0.27
4193.15	28	39			28	16	43	40	b		− .26	−0.16
4197.07	25	21							28 b	1.59	− .37	−0.30
4197.68	60					23	36	45	a		− .16	−0.01
4202.52	80	70			42				63 c		+0.04	+0.31

TABLE 1—*Continued*

λ	0.055	0.141	0.227	0.445	0.534	0.702	0.773	0.819	0.969	E.P.	log W/b	log η_0
Gd II—*Cont.*												
4208.37						37		52	c		−0.13	+0.03
4212.00	53	53		34	34	31	58	77	76	0.42	− .03	+0.19
4215.02	44	36	25	21	14	28	38	56	52	0.43	− .21	−0.08
4217.20	52		28	21	25	35	52	66	68 a	0.66	− .11	+0.06
4223.02					59	43	58	57	c	2.34	− .05	+0.16
4229.80				37					c	1.61	− .21	−0.08
4232.47			19						a		− .50	−0.46
4235.07			13								− .67	−0.65
4238.78	79	70	38	64	43	53	46	43	b		− .05	+0.16
4241.28	59	40	25	37	22	34	48	42	52 a	1.61	− .16	−0.01
4243.84	69	46		21	12		26	31	60		− .18	−0.04
4246.57					43	39	54	55	b	1.13	− .12	+0.05
4251.73 p			34	35	39	47	63	73	79 a	0.38	− .02	+0.20
4253.37 p	59	52			29	33		48	56 a	0.55	− .14	+0.01
4280.49 p							46		a	0.35	− .12	+0.05
4292.75					27				b	2.22	− .35	−0.27
4296.08					15		46	39	a	0.50	− .26	−0.16
4297.17	34	19	12	16	10		29		23 a		− .45	−0.39
4298.43	24	16	10						21		− .48	−0.43
4303.47		50							35 c		− .16	−0.01
4304.09	47	22					20		b	2.21	− .30	−0.21
4304.90	67							52	53		− .02	+0.20
4308.23	53								33 c	0.52	− .15	0.00
4310.98							24	25	20 a	0.49	− .42	−0.36
4316.2 p					28	28	39	33	a	0.66	− .28	−0.18
4364.14	54				21		22		39 b	0.43	− .26	−0.16
4380.64		45				38		41	36 a	1.15	− .19	−0.06
4382.06	22				20	26	27	25	21 b	0.55	− .42	−0.36
4383.12					31		21	22	b	1.17	− .39	−0.32
4387.67		21			28	11	27	24	22 a	0.42	− .45	−0.39
4388.98	47	43	22		25		10		33 c		− .38	−0.31
4390.95	87	59			28	37	62	60	70 b	0.43	− .04	+0.17
4397.51	20				15	17					− .56	−0.53
4400.18			27						c	1.15	− .36	−0.28
4406.67		62								1.42	.00	+0.24
4408.25	63	40							a	0.55	− .07	+0.12
4421.24	50	25							b	1.31	− .22	−0.10
4426.15							14		a	0.38	− .65	−0.63
4427.03						15		20	32 b		− .46	−0.41
4427.61									12	1.15	− .72	−0.71
4433.64					25	25	39	27		1.31	− .34	−0.26
4436.22	43		24		19	22	41	35	35	1.72	− .31	−0.22
4437.45	14								b		− .65	−0.63
4438.26		30							a	0.66	− .32	−0.24
4446.49				35					a	0.49	− .26	−0.16
4453.93	62	32	11	15	8	15	39		44 a	1.06	− .25	−0.14
4463.25		29	22	34					30	1.25	− .34	−0.26
4467.23	63	37		47		19	43	65	b	1.33	− .14	+0.01
4471.29	71	59			29	48	60	56	b	1.28	− .10	+0.08
4478.80 p	68		25		19	30		29	53 b	0.60	− .19	−0.06
4483.33	95	43		35		30	62	57	73 c	1.06	− .02	+0.20
4484.47	26										− .39	−0.32
4486.35						16	18	21		2.30	− .54	−0.50
4488.40	50	29							c	1.35	− .20	−0.07
4494.85		13					19	18	22 a	0.42	− .54	−0.50
4498.28 p	53						24	30	33	0.43	− .26	−0.16
4500.64			33			21	52		62 c		− .18	−0.04
4506.33	41					25		21	22	0.50	− .37	−0.30
4506.93	59	52	43			45			c	0.42	− .10	+0.08
4509.08	27	18		21	31	20	31	33	13 a	1.25	− .42	−0.36
4514.50		26				65	37			1.37	− .17	−0.03
4517.30		53			33		38		c	2.30	−0.19	−0.16

TABLE 1—*Continued*

λ	0.055	0.141	0.227	0.445	0.534	0.702	0.773	0.819	0.969	E.P.	log W/b	log τ_0
Gd II—*Cont.*												
4521.94			15	20	15	20	33	25	29	2.31	−0.47	−0.42
4525.61							17				− .58	−0.55
4530.65	53	26	21	31	12	13	21	22	30 b		− .33	−0.25
4536.56		27						32	c		− .33	−0.25
4550.05								30	14 c		− .47	−0.42
4550.95 p	34	23			23	22		36	24 a	0.73	− .38	−0.31
4551.46	43				24		42		50 b	1.10	− .21	−0.08
4558.08	64	68		31			22	33	50 a	0.50	− .19	−0.06
4570.98		22	16						b	1.28	− .53	−0.49
4581.09	28	22			21	19	26	25	18 a	0.66	− .45	−0.39
4582.5 p	76				30	35	47	57	82 a	1.06	− .06	+0.14
4596.98	45	25			17				41 a	0.52	− .30	−0.21
4610.94								24	c		− .43	−0.37
4619.63	46	25	20			29	38	36	c		− .33	−0.25
4622.63	26								c		− .40	−0.34
4639.00	63	24	20					21	41 a	1.06	− .29	−0.20
4654.99					17	14	16	24	31	1.06	− .52	−0.48
4675.27							16	28	c		− .48	−0.43
4675.78	42	37							27 c		− .28	−0.18
4681.85									23 c		− .46	−0.41
4711.98	39	28					17	19	a	1.10	− .41	−0.35
4712.80	43	29				20	14		a		− .41	−0.35
4719.04	64	51							54	0.55	− .07	+0.12
4723.73		23					39		14		− .42	−0.36
4725.78		23				43	50	62	36 b		− .19	−0.06
4728.47	26					33			40 a	1.10	− .30	−0.21
4732.60	56	25					24	23	28	1.10	− .33	−0.25
4735.76	64	41				26	36	45	57 c		− .24	−0.13
Tb II												
3924.81			58		66	48	53	50	43 c		− .02	+0.20
3925.45	25	41	46		50	47	42	55	30 b		− .14	+0.01
3935.25	25					21	24	28	a		− .35	−0.27
3939.60	26	18	22	30	13		11	20	16 a		− .46	−0.41
3946.87	59	34	32	44	21	31	46	37	45 b		− .13	+0.03
4009.54							10				− .75	−0.74
4016.34		47					34	34	c		− .17	−0.03
4019.14	18		17			13	15				− .55	−0.51
4020.47	16					13			a		− .58	−0.55
4051.52	26								c		− .35	−0.27
4052.43	27	39							23 c		− .28	−0.18
4052.87	35	31	20						a		− .30	−0.21
4125.25	25	16	28	40	14	26	20	25	15		− .41	−0.35
4144.47							34	28	b		− .28	−0.18
4188.53							31	21	c		− .36	−0.28
4276.75	15	18		10		13	15	9	a		− .67	−0.65
4278.54	23			32		22	26	16	a		− .40	−0.34
4312.09	24	26	22	39			42	26	c		− .27	−0.17
4378.73		22	32		22				c		− .39	−0.32
4386.09		30									− .31	−0.22
4416.28	38			28	19	19			40		− .33	−0.25
4503.58	34	23				18	30	21	c		− .40	−0.34
4512.97					29		26	14			− .44	−0.38
4531.83			29	37	32	54	49	35	24 c		− .24	−0.13
4562.25	54	27	26	23		24	43	39	44 b		− .28	−0.18
4571.42						18		24	c		− .49	−0.45
4578.62	30	16						18	16 a		− .51	−0.47
4584.62	27	18							c		− .46	−0.41
4604.08		18			37		26	43	29 c		− .32	−0.24
Dy II												
3914.88	59	54				33		49	b		− .05	+0.16
3915.60	70	42		36		28	34	54	58 b		− .06	+0.14
3932.23	23										−0.38	−0.31

TABLE 1—*Continued*

λ	0.055	0.141	0.227	0.445	0.534	0.702	0.773	0.819	0.969	E.P.	log W/b	log η_0
Dy II—*Cont.*												
3944.69	83	71	36			33	62	53	73		−0.02	+0.20
3950.40		81			39				93 c		+ .10	+0.43
3996.70 p	45					22	27		a	...	− .26	−0.16
4000.45	85	57			16	41	51	60	90 a		− .02	+0.20
4010.08	33	27							c		− .27	−0.17
4011.30	48	46	40					24	34 b		− .17	−0.03
4019.48	26	29							c		− .30	−0.21
4027.79	60	51			30			60	59		− .10	+0.08
4032.48			16			32	34	38	a		− .28	−0.18
4036.34	97	74	37		45	41			84 c		+ .05	+0.32
4038.53	36	28							37 b		− .23	−0.11
4050.58	96	70			21				76 c		+ .06	+0.34
4055.16									39 a		− .17	−0.03
4060.58		29	23	32	32	23		26	29 b		− .31	−0.22
4074.02							21	13	10		− .58	−0.55
4143.10		62	44		31	45	63	70	61 b		− .09	+0.09
4152.43		34							c		− .24	−0.13
4154.22	16						9		b		− .67	−0.65
4182.42	40			30			15		39 a		− .28	−0.18
4238.04				33	15	16	17	28	c		− .44	−0.38
4294.94	37	43	12		12	19	26	29	32 b		− .40	−0.34
4308.62	46	33		39	46			52	35 b		− .16	−0.01
4375.33					16		50		a		− .27	−0.17
4409.38	75	73		57	66	63	77		67 b		− .04	+0.17
4431.00	51	35	18	29		39		43	48		− .24	−0.13
4448.23	25	68	37		44	40	47	43	36 c		− .18	−0.04
4468.0 p			30	22			32		a		− .35	−0.27
4518.54	43								24 a		− .27	−0.17
4527.78	33	17					17	10	21		− .51	−0.47
4538.76	41	18							16 a		− .41	−0.35
4541.70	26	30									− .36	−0.28
4556.46					23						− .45	−0.39
4573.87	32	24						22	27		− .40	−0.34
4617.27	29	18	11		22	17	23	18	21 b		− .51	−0.47
4664.68		17			14				a		− .63	−0.60
4689.77 p	52	24			31		22	33	34		− .30	−0.21
4698.69	64	44				22	36	40	37 a		− .22	−0.10
4727.13	52	47					34	43	30 a		− .21	−0.08
4731.85	32	23									− .37	−0.30
Dy III												
3919.4	61	68		49		46	44	56	79		+ .03	+0.29
4034.2	57	55				50	46				− .04	+0.17
4138.9		32				24	38	35			− .26	−0.16
4164.6	46	39	30	28	21	23	33	30			− .25	−0.14
4176.8	26			37		21	43	40	32		− .25	−0.14
4189.0					31		43	43			− .18	−0.04
4194.1	51										− .06	+0.14
4199.4	37	44				59	54				− .09	+0.09
4212.6							7	14			− .77	−0.76
4259.5	35										− .24	−0.13
4377.1	60	41						59	37		− .10	+0.08
4393.1	43	29	26		22				29		− .31	−0.22
4393.6		31	24		22		28	24	43		− .33	−0.25
4410.0	94	76	22						102		+ .02	+0.27
4445.2		31	25		26	37	31		24		− .34	−0.26
4487.4		28	34		43	42	43	37			− .22	−0.10
4499.2						19	30	26	30		− .39	−0.32
4511.6		37							45		− .19	−0.06
4514.1	144	113	83	96	126		121	120	114		+ .29	+0.88
4526.3	44	49						18			− .24	−0.13
4534.9	58	36	35		42	30	38	37	28		− .23	−0.11
4540.4				33					46		−0.21	−0.08

TABLE 1—*Continued*

λ	0.055	0.141	0.227	0.445	0.534	0.702	0.773	0.819	0.969	E.P.	log W/b	log η_0
Dy III—*Cont.*												
4569.3	63	.....	30	.....	28	.....	46	39	.....	.....	−0.16	−0.01
4573.0	97	56	20	.....	27	31	50	73	65	.....	− .08	+0.10
4575.5	97	57	23	.....	22	26	43	62	83	.....	− .07	+0.12
4604.4	68	52	.....	.....	44	.....	41	40	52	.....	− .11	+0.06
4610.5	62	37	.....	.....	34	.....	.....	.....	46	.....	− .16	−0.01
4618.2	23	14	17	.....	14	19	26	17	.....	.....	− .53	−0.49
4618.7	.....	61	.....	.....	.....	.....	.....	.....	.....	.....	− .02	+0.20
4660.7	80	51	47	.....	57	54	65	72	73	.....	− .02	+0.20
4665.5	44	32	.....	.....	13	.....	31	29	37	.....	− .39	−0.32
4685.9	58	46	.....	.....	.....	20	26	30	41	.....	− .26	−0.16
4713.7	91	66	61	.....	.....	112	103	93	68	.....	+ .11	+0.45
Ho II												
3861.68	19	.....	18	.....	.....	.....	27	.....	25	.....	− .40	−0.34
3940.55	.....	.....	.....	.....	.....	.....	20	34	.....	.....	− .32	−0.24
4014.18	.....	.....	.....	.....	.....	.....	21	.....	.....	.....	− .43	−0.37
4045.43	29	24	23	.....	16	31	.....	.....	a	.....	− .36	−0.28
4065.10	48	.....	24	25	33	.....	30	29	30 b	.....	− .31	−0.22
Er II												
4007.97	32	.....	29	.....	.....	26	21	24	16	.....	− .35	−0.27
4526.92	37	.....	.....	.....	.....	.....	.....	.....	.....	.....	− .24	−0.13
Yb II												
4180.83	60	46	23	.....	.....	28	.....	.....	49 b	.....	− .15	0.00
4726.08	62	.....	.....	.....	.....	.....	.....	.....	b	.....	−0.03	+0.19

SOME WELL-DEFINED UNIDENTIFIED LINES

λ	0.055	0.141	0.227	0.445	0.534	0.702	0.773	0.819	0.969	log W/λ
3857.7	.....	.....	.....	54	40	38	46	55	53	−4.91
3920.6	40	50	74	63	94	78	64	59	52	−4.76
3923.9	.....	.....	29	35	17	30	34	.....	.....	−5.13
3926.7	.....	25	.....	45	32	.....	.....	25	11	−5.14
3948.7	71	52	66	.....	24	51	44	.....	56	−4.94
3996.9	.....	.....	29	.....	.....	22	19	27	16	−5.24
4023.8	62	69	24	.....	41	26	42	48	66	−4.93
4029.6	101	58	24	.....	26	53	42	61	.....	−4.82
4134.2	42	34	30	.....	17	.....	.....	26	.....	−5.16
4153.8	69	39	35	.....	24	39	24	.....	50	−4.99
4166.7	84	84	.....	.....	.....	25	43	47	80	−4.85
4177.7	56	97	89	108	98	92	.....	115	78	−4.66
4190.1	.....	.....	42	50	36	41	64	52	.....	−4.94
4207.8	110	72	.....	.....	40	32	.....	57	104	−4.77
4216.5	.....	.....	14	8	14	9	14	.....	12	−5.54
4224.3	82	45	23	31	.....	37	56	59	74	−4.92
4233.9	70	.....	.....	47	.....	.....	38	42	56	−4.92
4273.9	16	18	.....	17	14	17	13	14	18	−5.43
4363.4	110	73	31	47	46	47	61	.....	100	−4.76
4366.9	39	37	26	27	12	16	29	.....	21	−5.23
4420.8	49	30	.....	.....	.....	38	44	40	.....	−5.05
4430.4	71	56	20	39	.....	40	51	39	67	−4.95
4447.5	121	109	30	.....	41	.....	40	70	92	−4.78
4459.6	.....	.....	25	.....	18	24	18	24	30	−5.29
4546.6	116	55	26	.....	40	34	66	54	85	−4.82
4596.0	71	54	.....	.....	76	.....	91	90	.....	−4.76
4599.3	24	26	.....	.....	16	.....	.....	20	14	−5.36
4602.7	49	25	.....	.....	19	.....	39	34	40	−5.18
4621.6	.....	.....	.....	.....	148	136	111	108	.....	−4.56
4631.2	24	14	14	.....	21	.....	18	.....	.....	−5.41
4649.5	41	21	.....	.....	.....	16	.....	43	28	−5.16
4673.3	91	70	103	.....	145	108	116	89	55	−4.67
4693.3	53	49	53	.....	58	49	61	52	.....	−4.94
4693.9	.....	16	30	.....	.....	20	20	16	.....	−5.37
4694.4	.....	21	20	.....	.....	.....	17	20	30	−5.33
4703.8	63	49	.....	.....	.....	22	35	28	53	−5.10
4705.2	38	30	.....	.....	.....	.....	37	37	42	−5.10
4711.3	50	40	36	.....	.....	35	48	54	.....	−5.03
4718.0	26	20	23	.....	.....	.....	.....	15	23	−5.35
4722.9	91	63	31	.....	.....	.....	27	48	68	−4.99

case may be usable in plotting curves for other magnetic stars with similar spectral type, and hence similar blending of lines. When full lists of laboratory wave lengths of doubly ionized rare earths become available, some of these lines may turn out to be principally due to these. In the first column, after the wave length of the line, "p" denotes that the line was plotted on the curves of growth described in Sections V and VIII.

The equivalent-width measures are given in milliangstroms and are listed in the second to tenth columns in order of increasing phase. In the eleventh column are listed the excitation potentials of the lower levels of the lines (taken from the *Revised Multiplet Table*, Moore 1945, or from references given therein); in the twelfth column are listed values of log W/b derived from the "mean" equivalent widths (see Sec. V); in the last column are given values of log η_0 read off the curves of growth. Where lines are blends of two lines of the same element, wave lengths are given to one decimal, and the lower excitation potential is quoted. Lines in the wings of the broad hydrogen lines were not measured, with the exception of a few at the extreme edges. The wave-length range measured was λλ 4750–3860; to the ultraviolet of *H*9 the hydrogen lines certainly overlap, and on the long-wave-length side of λ 4750 the plate densities are usually below the optimum range. The plate at phase 0.445 was slightly underexposed, and the range measured here extended only to λ 4580.

Very few changes were made in the line identifications by Struve and Swings. The chief ones are as follows:

λ 4076.8 is listed by us with *Si* II as major and *Cr* II as minor contributor. λλ 4186.1, 4301.4, and 4656.3 are listed by us as *Ti* I instead of *Fe* I and *V* II. λ 4166.7 and λ 4546.6 were listed as *Fe* II and *Cr* II, but they are strong lines with a variation similar to that of *Eu* II and are probably due to doubly ionized rare earths. We have listed them as unidentified. A number of weaker lines originally attributed to various elements also come into this category but have not been listed. λ 4363.4, a strong line varying like *Eu* II, was listed as *Mo* II; yet other lines from the same multiplet, which should be equally strong, are weak. The line is thus listed as unidentified.

The possible identification of certain elements not considered by Struve and Swings, in particular deuterium and *Pb*, will be discussed in Section IX.

In Table 1 we have given one line attributed to *Eu* III and thirty-three lines attributed to *Dy* III. The identifications of *Eu* III and two of the *Dy* III lines were given by Swings (1944). For the remainder we are indebted to Dr. Swings for supplying us with an unpublished list of possible identifications by himself and Dr. A. S. King from spark spectra. These identifications should still be regarded as provisional. The best observed unidentified lines are given at the end of Table 1. The variations of many of these show that they also probably belong to the doubly ionized rare earths.

We have compared our values with those of Tai (1940) for those lines which are common to both lists and found that Tai's equivalent widths are systematically larger than ours. This is presumably the well-known effect due to the different dispersions, recently discussed by Deutsch (1954). He has shown that it can be explained by the relatively greater ratio of microphotometer analyzing slit-width to line-width in the case of low-dispersion plates. Struve and Swings (1942) have also noted that in the few cases where they measured equivalent widths, these were systematically smaller than those of Tai. The effect may also be due partly to unresolved blends on lower-dispersion plates. The equivalent width of $H\gamma$ measured by Petrie and Maunsell (1951) was 9.1 A, and the mean value obtained by us (see Sec. IV) is 9.8 A.

III. PRELIMINARY DISCUSSION OF LINE-INTENSITY VARIATIONS

Table 2 gives the type of variation shown in the line strengths. Here A, B, and C denote lines which have maximum or minimum intensity near zero phase or are constant, respectively. A dash signifies that no classification could be made. This table was compiled by studying those lines in Table 1 for which five or more measures were made

(approximately 500 from about 1200 lines), although in many cases the type of variation was apparent from fewer measures. Most of the elements showing maxima or minima also have lines which appear to remain constant, and the reason for this is not fully clear, although blending may be partly the cause. Also, blending which is present during part only of the period, due to differing radial-velocity variations between elements, sometimes causes scatter in the measures and makes it difficult to determine the true variation of a line. Some examples of line variations are shown in Figure 1.

For those elements which Tai also classified, the agreement is good, except that he assigned *Cr* I and *Fe* I to group C (and Struve and Swings thought that both were probably group A).

For all the lines in Table 2 which show distinct variation, the equivalent widths were plotted against phase, and smooth curves were drawn. From these the maximum and minimum values were estimated, also the phases at which they occur (mean phases

TABLE 2

THE VARIATIONS OF THE ELEMENTS

Element	Group	Phase of		No.	Element	Group	Phase of		No.
		Maximum	Minimum				Maximum	Minimum	
Mg II	B	0.63	0.97	1	*Sr* II	C:	.....	.....	1
Al II	C	.....	.....	1	*Zr* II	A	0.05	0.49	5
Si II	B	.52	.98	5	*La* II	A	.99	.47	5
P II	B:	.6	.2	1	*Ce* II	A	.05	.50	14
Ca I	.....	.....	.....	.....	*Pr* II	A	.01	.50	9
Ca II	A	.03	.57	1	*Nd* II	A	.03	.58	6
Ti I	A:	.05	.48	2	*Sm* II	A	.02	.46	6
Ti II	A	.03	.50	19	*Eu* II	A	.00	.52	19
V II	C	.....	.....	2	*Eu* III	A	.01	.....	1
Cr I	B	.62	.05	2	*Gd* II	A	.01	.51	31
Cr II	B	.62	.01	19	*Tb* II	A:	.04	.46	4
Mn I	C:	.....	.....	5	*Dy* II	A	.02	.49	11
Mn II	A:	.97	.46	2	*Dy* III	A	.02	0.50	11
Fe I	B	.56	.02	9	*Ho* II	C:	.....	.....	2
Fe II	B	.54	.04	32	*Er* II	C:	.....	.....	1
Ni I	A:	0.05	0.44	1	*Yb* II	A:	0.04	.....	1

being shown in Table 2). The last column in this table gives the number of good lines with more than 5 measures, used in determining the phases of maximum and minimum. It should be emphasized that the phases are rather uncertain and probably depend to some extent on the phases of the plotted points. The weighted means for groups A and B are, respectively, phase of maximum = 0.02, phase of minimum = 0.50, and phase of maximum = 0.57, phase of minimum = 0.02.

The ratios of maximum to minimum equivalent width (amplification factors F) have also been obtained. The mean values of F for *Ti* II, *Cr* II, *Fe* I, and *Fe* II are 2.4, 2.1, 1.9, and 1.7, respectively. The scatter for these elements is fairly small (cf. Fig. 2). For the rare-earth group the scatter is much larger, lying in the range 1.5–10, and we consider that mean values have no significance here. The largest values are uncertain because of the smallness of minimum equivalent widths and consequent errors of measurement. The values of F for *Mg* II, *Si* II, and *Ca* II (based on few lines) are 1.4, 1.5, and 1.5, respectively.

We looked for correlations between F and (1) excitation potential, (2) Zeeman

splitting, (3) "mean" equivalent width (the straight mean of the maximum and minimum values). No simple correlations were found for (1) and (2) for any of the elements. There appears to be some correlation in (3) for the elements *Ti* II and *Cr* II alone, the weaker lines being amplified most. This is shown in Figure 2. This effect may be partly or wholly due to selection, since in weak lines having small values of F the variation may tend to be missed and the lines classed as constant.

IV. THE HYDROGEN LINES

In Table 3 are given the equivalent widths (in angstroms) and central intensities (as percentages of the continuum) of $H\gamma$ and $H\delta$ through the period of variation. These lines were chosen as being the best for profile measurement. Though there is clearly a

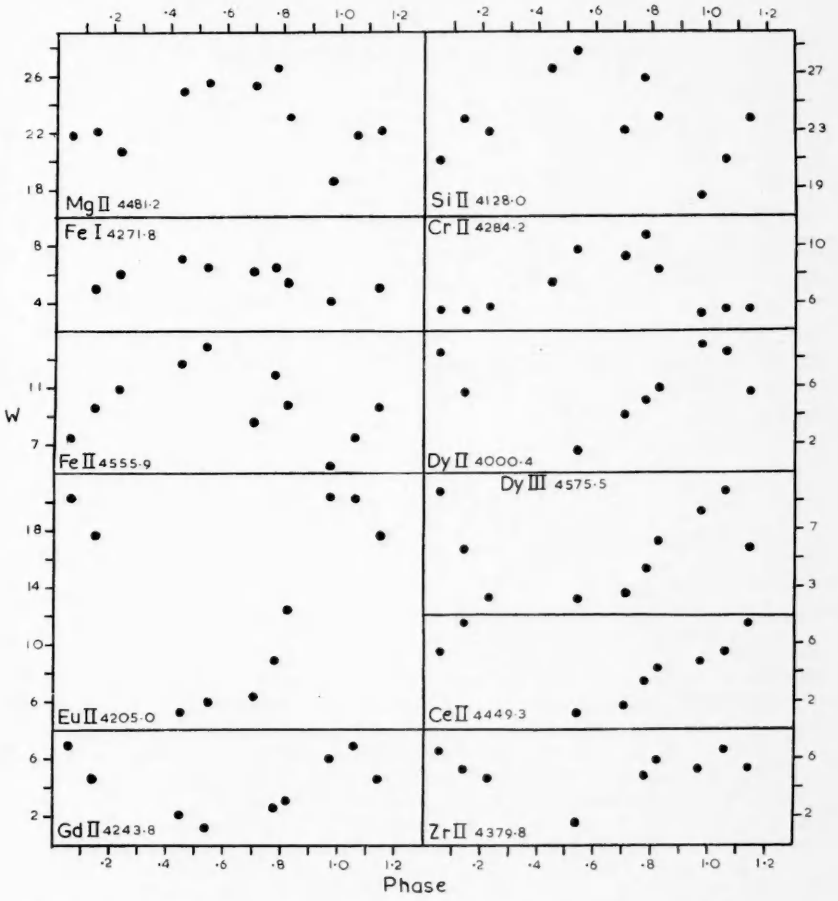

FIG. 1.—Intensity variations shown by some lines (*abscissae:* phase; *ordinates:* equivalent widths in units of 10 milliangstroms).

small maximum for $H\delta$ ($F = 1.1$), the points for $H\gamma$ are more scattered. This may be due to observational errors, but this is not certain. In Figure 3 the mean profiles from phases 0.055, 0.141, 0.227, 0.969, taken together, those from phases 0.445, 0.702, 0.773, 0.819, and that from phase 0.534 are shown for both lines (the grouping was determined by the grouping of the equivalent widths of $H\delta$).

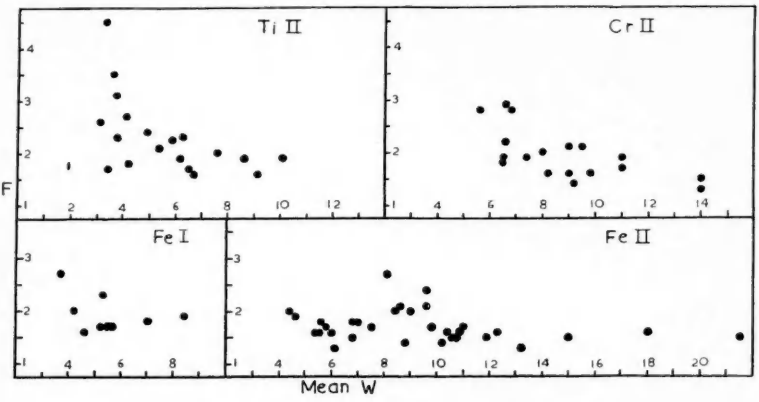

FIG. 2.—Plot of amplification factor F ($= W_{max}/W_{min}$) against mean equivalent width W ($= [W_{max} + W_{min}]/2$) in units of 10 milliangstroms, for *Ti* II, *Cr* II, *Fe* I, and *Fe* II.

TABLE 3

EQUIVALENT WIDTHS AND CENTRAL INTENSITIES OF $H\gamma$ AND $H\delta$

PHASE	$H\gamma$		$H\delta$		PHASE	$H\gamma$		$H\delta$	
	E.W.	Central Intensity	E.W.	Central Intensity		E.W.	Central Intensity	E.W.	Central Intensity
0.055.....	10.09	13.4	9.63	16.4	0.702.....	9.42	20.5	10.18	20.2
.141.....	9.48	17.5	9.65	19.1	.773.....	10.08	15.9	10.24	17.4
.227.....	9.44	20.6	9.60	23.2	.819.....	8.98	17.5	9.91	17.7
.445.....	9.93	20.4	10.07	20.4	0.969.....	9.27	20.7	9.42	19.7
0.534.....	11.18	16.8	10.94	14.0					

It is well known that the hydrogen lines are a good coarse indicator of conditions in a stellar atmosphere. Their use in the choice of a standard star will be mentioned in Section V. Here we shall use mean profiles through the period to obtain a value of the electron pressure. The formula given by Unsöld (1938) for the Stark profile based on the Milne-Eddington model for the atmosphere leads to

$$p_e = A\,(\Delta\lambda)\,(\Delta\lambda)^{5/2}\left\{1 + 4\left(\frac{\kappa}{\bar{\kappa}}\right)(1 - e^{h\nu/kT})\left(\frac{h\nu}{kT}\right)^{-1}\right\}\frac{k_{2n}T}{640C}, \qquad (1)$$

where $C = 4.42 \times 10^{-17}$ ($H\gamma$) and 3.09×10^{-17} ($H\delta$). Values of $(\kappa/\bar{\kappa})$ were taken from the work of Chandrasekhar and Münch (1946), and the line-absorption coefficients k_{2n}

have been computed. The mean values of the widths of the lines are 49.8 A ($H\gamma$) and 50.2 A ($H\delta$). By tabulating the values of $A(\Delta\lambda)(\Delta\lambda)^{5/2}$, it was found that this expression is reasonably constant, and hence the simple Stark theory can be applied in the region in the wings 10.8–20.3 A ($H\gamma$) and 10.8–20.5 A ($H\delta$) measured from the center. From equation (1) the means of five measures for each line give $p_e = 67$ and 76 dynes from $H\gamma$ and $H\delta$, respectively. The mean error is of the order of 10 per cent.

Another estimate of the electron pressure can be obtained from the number of the last observable hydrogen line by using the Inglis-Teller formula: $\log n_e = 23.26 - 7.5 \log n$. For this star $n = 19$, so that $p_e = n_e kT = 60$ dynes.

Thus the results obtained by these two methods are in good agreement. However, the electron pressure is low when compared with the value of at least 100 dynes which we

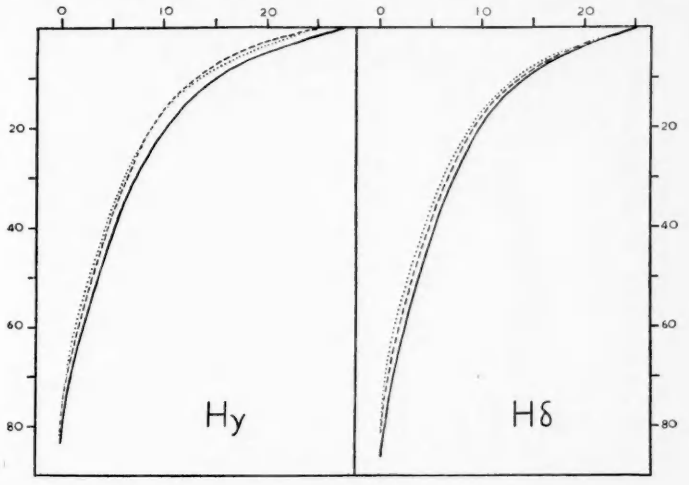

FIG. 3.—Mean profiles of $H\gamma$ and $H\delta$. Dotted lines represent mean profiles for phases 0.055, 0.141, 0.227, 0.969; dashed lines represent mean profiles for phases 0.445, 0.702, 0.773, 0.819; full lines represent the profiles for phase 0.534 (abscissae in angstroms; ordinates in percentage absorption).

expect for a star of this spectral type. For main-sequence early A stars Aller (1953*a*) gives $p_e \sim 160$ dynes. That this method for normal stars gives a low value has been previously mentioned by Aller (1942). In that case there are several possible explanations.[1] One possibility is that the assumption of complete hydrostatic equilibrium, which is implicit in the method, is incorrect. Even in normal stars Aller has suggested that departures from hydrostatic equilibrium may explain the discrepancy. In magnetic stars where the magnetic forces must be very powerful, it is almost certain that this equilibrium condition is not applicable. For γ Gem, Aller obtained $p_e \sim 100$ dynes by the same method. We shall return to this point in Section XII.

V. EXCITATION TEMPERATURE AND CURVE OF GROWTH FOR METALS

This star is classified as A0p from its spectrum, but the color, as is the case for other peculiar A stars, agrees with that for a B8 dwarf (Deutsch 1947; Provin 1953). Provin

[1] We are indebted to the referee for pointing out to us that recent work carried out under Professors L. H. Aller and O. Laporte at the University of Michigan on the broadening of hydrogen lines in shock-tube experiments may lead to considerable changes in the Inglis-Teller formula and the profiles given by the Holtsmark theory (cf. *A.J.*, **59**, 349, 1954).

(1954) estimates that the measured change in color during the period represents a temperature change of about 500° K, the star being hottest when the rare-earth lines are at minimum intensity.

As was pointed out by Struve and Swings (1942), Tai's suggested explanation of the line-intensity variations as ionization effects due to the changing temperature is not satisfactory. This is emphasized, since the temperature variation suggested by Provin is smaller than that used by Tai. The demonstration by Swings (1944) that lines due to the doubly ionized rare earths vary in phase with those due to singly ionized rare earths further rules out this explanation. He showed that it also rules out the attempt to explain the anomalous strengths of the rare-earth lines and weakness of the *Ca* II K line in terms of selective radiation effects in the Lyman region.

To determine effective ionization and excitation temperatures and abundances, curve-of-growth studies have been made. Greenstein (1948) has shown that if values of the abscissae of the curve of growth (log η_0) can be taken from those already determined for a star of similar spectral type, the scatter in plotting the curve is much less than when a standard star of different spectral type is used. Aller (1942) constructed curves of growth for the normal A stars γ Gem and α CMi, and Buscombe (1951) carried out a similar analysis of γ Gem and α Cyg. Of these three stars, γ Gem, classified as A0 IV (Morgan), is the most similar to α^2 CVn, as far as the hydrogen lines are concerned (Petrie and Maunsell 1951), and this star was therefore chosen as the standard. It has been convenient to use the study by Buscombe, since he tabulated values of log η_0.

We used the same theoretical curve of growth as that used by Buscombe for the photographic region of γ Gem, i.e., the curve for a Milne-Eddington model atmosphere (Wrubel 1949) with $B_0/B_1 = \frac{1}{3}$ and log $a = -3.0$. The ordinate was log $W/b' = \log (W/\lambda)(c/v')$, where v' is the most probable thermal velocity. Thermal velocities corresponding to $T = 10{,}000°$ have been used throughout, since the correct temperature cannot be uniquely determined and the corresponding errors in v' are small.

For the lines having constant equivalent widths, through the period, straight means of all the measures have been taken. This has also been done for lines with too few measures to determine the type of variation; these latter have to be used, since we are limited to those lines for which log η_0 has been given by Buscombe. For the variable lines, the means of the maximum and minimum values read off the curves have been used. Preliminary curves of growth of *Ti* II, *Cr* II, and *Fe* II showed that the constant lines agreed well with the mean values for the variable lines. Consequently, in the following analysis, unless otherwise stated, mean values for both constant and variable lines have been used together.

To determine the excitation temperature, the curve of growth for *Fe* I was plotted, using the laboratory *gf*-values (King and King 1938; Carter 1949). Owing to the weakness of the lines of *Fe* I and their consequent tendency to be badly affected by blends, great care was taken in choosing them. The best fit to the theoretical curve was obtained for $T_{exc} = 8000°$. The curve of growth for *Fe* I was also plotted with the values of log η_0 for γ Gem. However, the scatter was greater in this case, so that it was not possible by this means to determine a difference in T_{exc} between α^2 CVn and γ Gem. There is considerable uncertainty in the excitation temperature of γ Gem, since Aller (1942) obtained 6000°, while Buscombe used 10,080°.

Preliminary plots were made for *Fe* II, where the lines arise from a fairly large range of excitation potentials, for a series of values of $\Delta\theta$. By this method it was found that $0 < \Delta\theta < 0.1$, so that $8000° > T_{exc}$ (γ Gem) $> 7000°$. Consideration of the high-excitation lines of *Mg* II and *Si* II (Sec. VII) shows that $\Delta\theta$ is probably smaller than 0.1 (unless a unique value is inapplicable to lines with widely different excitation potentials). The curve of growth was finally plotted for the various elements with unchanged values of log η_0 (γ Gem). This might affect the values of the abundances of the elements relative to those in γ Gem, but the factor will be small for all except *Si* and *Mg*.

The theoretical curve of growth and the plots for *Ti* II, *V* II, *Cr* I, *Cr* II, *Fe* I, and *Fe* II are shown in Figure 4. The number of lines used for each element, the mean excitation potential, and the horizontal and vertical shifts, $\Delta \log \eta_0$ and $\log (v/v')$, necessary to bring them onto the curve are shown in Table 4, together with the value of v, the total

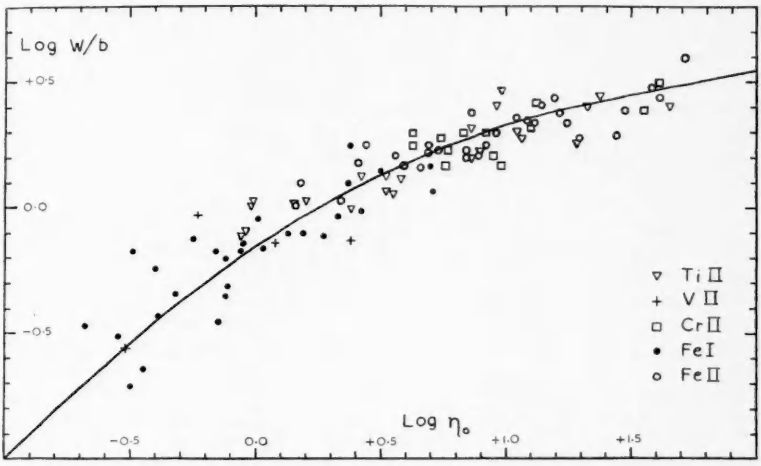

FIG. 4.—Curve of growth for *Ti* II, *V* II, *Cr* II, *Fe* I, and *Fe* II. The theoretical curve for $B_0/B_1 = \frac{1}{3}$ and $\log a = -3.0$ is plotted.

TABLE 4

RESULTS FROM THE METALS

	No. of Lines	Mean E.P. (Ev)	$\Delta \log \eta_0$ (α^2 CVn − γ Gem)	$\log (v/v')$	v (Km/Sec)
Ti II	23	1.43	+0.36	+0.10	2
V II	4	1.78	+ .10	+ .22	3
Cr I	2	0.00	− .20	.....	.....
Cr II	13	3.90	+ .72	+ .22	3
Fe I	28	1.96	− .40	+ .38	4
Fe II	30	3.25	+0.46	+0.27	3

effective velocity. *Fe* I was adjusted to the same horizontal scale. There were only two unblended lines of *Cr* I which could be used. For this element the vertical shift was set equal to the value determined from *Fe* I. It is well known that

$$\log \eta_0 = C + \log N_r - \log \kappa_\lambda - \log v - \log g_0 + \log gf\lambda - \chi\theta\,, \tag{2}$$

so that, between two stars,

$$\Delta \log \eta_0 = \Delta \log N_r - \Delta \log \kappa_\lambda - \Delta \log v - \chi \Delta\theta\,. \tag{3}$$

Since the values of $\Delta \log \eta_0$ are not the same for all ions, it is clear that they cannot be accounted for by differences in opacity alone. Also in both stars the opacity is due mainly

to the continuous absorption of neutral hydrogen, and it has already been pointed out that the stars are quite similar as far as the hydrogen lines are concerned. The maximum difference allowable is $\Delta \log \kappa_\lambda \sim 0.1$, as can be seen from the tables given by Ueno (1954). The differences between the velocities in Table 4 and in γ Gem are small, so that $\Delta \log v$ can be neglected. Differences in excitation temperature have been shown to be small. Systematic differences in equivalent-width measurement cannot be ruled out. However, we do not believe that they can account for more than a small part of the observed differences.

VI. ELECTRON PRESSURE AND IONIZATION TEMPERATURE

From the hydrogen-line analysis it was concluded that the electron pressure in α^2 CVn was slightly less than that in γ Gem. Model atmosphere calculations (Aller 1953*a*) have shown that $\log p_e = 2.2$ or 2.3 is the appropriate value for an A0 star near the main sequence. In his original discussion of γ Gem and α CMi Aller used values of $\log p_e = 2.0$ and 2.4 and found that both values led to an ionization temperature of 8700°. These values are considerably less than that used by Buscombe, i.e., $\log p_e = 3.7$ for γ Gem, with a corresponding ionization temperature of 10,080°. We believe that the values given by Aller are preferable and have accordingly taken $\log p_e = 2.0$ and 2.2 for α^2 CVn and γ Gem, respectively.

In considering the ratios *Fe* II/*Fe* I, etc., differences in opacity and velocity cancel out. Using the abundances of *Cr* I, *Cr* II, *Fe* I, and *Fe* II obtained by Buscombe for γ Gem, we have derived the ionization temperatures for the two stars as follows: From *Cr*, $T_{\text{ion}} = 7100°$ (γ Gem) and 8000° (α^2 CVn), and from *Fe*, $T_{\text{ion}} = 7500°$ (γ Gem) and 8400° (α^2 CVn). More weight should be attached to results from *Fe*. Also, Buscombe's determination of the abundances in γ Gem depends on the value of T_{exc} used by him. This might account for the difference between Aller's value of T_{ion} for γ Gem and that deduced from Buscombe's abundances by using the same value of $\log p_e$.

We conclude that, although there is some uncertainty in the absolute values, the ionization temperature of α^2 CVn is about 1000° higher than that of γ Gem. The result also shows that there is no significant difference between the ionization and excitation temperatures in α^2 CVn and that both are considerably less than the effective temperature derived from the color, since 12,800° is given by Keenan and Morgan (1951) for a B8 star.

VII. ABUNDANCES OF ELEMENTS RELATIVE TO γ GEM

By using the ionization equation and assuming $\Delta \log v - \Delta \log \kappa_\lambda - \chi \Delta\theta$ to be negligible, the relative abundances of the ions appearing on the curve of growth have been converted to relative abundances of the elements. These are given in Table 5 (Sec. VIII). The table also contains estimated abundances of *Mg*, *Al*, *Si*, *Ca*, *Sc*, *Mn*, *Ni*, and *Sr*, which have only one or two lines common to both stars and hence cannot be plotted as curves of growth. For these it was assumed that the velocities v for neutral and singly ionized atoms were the same as those obtained for *Fe* I and *Fe* II, respectively. Where values from two lines are available, both are given, and the relative abundance has been obtained from the mean. The following points should be noted:

a) Where the relative abundance has been derived from $\Delta \log N_0$, the result depends critically on the difference ΔT_{ion} between the two stars, and the results have lower weight than those derived from $\Delta \log N_1$.

b) For the strong lines of *Mg* II, *Si* II, and *Ca* II, the result depends on the assumed value of $\log a$. Buscombe used $\log a = -1.8$ (classical damping) for *Ca* II, and $\log a = -1.4$ for *Mg* II. These values have also been used by us. For *Si* II in α^2 CVn, we have taken $\log a = -1.4$ also, while in γ Gem the lines were so much weaker that it was not necessary to choose a value of $\log a$. The large abundance ratio determined for *Si* II would be still further increased if a smaller damping constant were used.

c) Because of the high excitation potentials of the *Si* II lines, the large overabundance of *Si* could be removed if it were assumed that $\Delta\theta_{\text{exc}} = 0.1$. However, in this case the apparent underabundance of *Mg* would be much increased, because the excitation potentials of the *Mg* II lines are even larger. θ_{exc} cannot be adjusted to remove both abundance anomalies together.

d) The low relative abundance of *Ca* and the high value for *Sr* were determined from resonance lines and hence are unaffected by changes in θ_{exc}. It is interesting that the single available *Ca* I line, λ 4227, also gives a low relative abundance, although by a much smaller factor than that given by *Ca* II. This line is blended with lines of *Al* II and *Eu* II, and these may dominate in the observed line, which is weak and could not be observed in mid-cycle.

It is of interest to consider the abundance of *O*. On one grating plate covering the infrared region, taken by us, a line due to *O* I λλ 7772–7775 is just visible, but we have not been able to determine an effective abundance from it. The excitation potential is 9.11 ev, similar to that of *Si* II and *Mg* II, and the ionization potential is almost exactly the same as that of hydrogen. Slettebak (1951) has observed the *O* I lines in the infrared in a number of peculiar A stars, including α^2 CVn. In general, they were weak or absent, in comparison with normal stars, and he gave the intensity estimate of λ 7774 in α^2 CVn as zero. We conclude that neutral *O* is apparently underabundant, and shall discuss possible reasons for this in Sections XII and XIV.

VIII. ABUNDANCES OF *V*, *Zr*, *Ba*, *La*, AND THE RARE EARTHS RELATIVE TO THE SUN

The most striking difference between the spectrum of α^2 CVn and a normal A star is found in the abnormally strong rare-earth lines and, to a lesser extent, lines of *Zr* II and *La* II, which are present in α^2 CVn and are extremely weak or nonexistent in normal A stars. About 600 of the 1200 lines in Table 1 are attributed to the singly ionized rare earths. A few equivalent-width measures of rare-earth lines were made by Greenstein (1948) in some F stars, but only in the solar spectrum are there sufficient rare-earth lines available to make relative abundance determinations possible.

The only solar abundance determination for the rare earths was made by Russell (1929) in his classical investigation. A chromospheric abundance determination was made by Menzel (1931). Relatively few rare-earth lines common to both α^2 CVn and the sun are given in the *Revised Rowland Table*, but later authors have published lists of identifications for *Sm* II (Albertson 1936), *Eu* II (King 1939), *Gd* II (King 1943), and *Dy* II (King and Moore 1943). We have made further identifications and are very grateful to Mrs. C. E. Moore-Sitterly for checking and correcting our list. The equivalent-width measures were obtained either from the lists of Allen (1934, 1938) or from the new lists by Minnaert and his collaborators (1955).[2] The remainder were measured by us from the Utrecht *Atlas*, using the method described by Allen. The lines used are indicated in Table 1.

From the solar curve of growth for *V*, *Ti*, and *Fe* given by Goldberg and Pierce (Aller 1953*b*), values of log η_0 (sun) were obtained from the equivalent widths of the rare-earth lines. The zero-point shift of the horizontal co-ordinate in the curves for the sun and α^2 CVn, which represents the differences in opacity and effective velocity, was obtained empirically by using Allen's equivalent-width measures of 15 *Fe* I lines common to both stars and judged to be free of blending. The following mean value was found:

$$\log \eta_0 \text{ (sun)} - \log \eta_0 (\alpha^2 \text{ CVn}) + \chi[\theta \text{ (sun)} - \theta (\alpha^2 \text{ CVn})] = 2.66 \pm 0.09 .$$

Here excitation temperatures of 8000° and 4770° (Aller 1953*c*) were taken. For the sun, values of log p_e and θ as a function of τ were taken from the photospheric model given by Minnaert (1954*a*). Log $(N_0 + N_1)/N_0$ was plotted against τ; this quantity was found

[2] We are indebted to Dr. M. Minnaert for permission to use these measures prior to publication.

to change by a factor of less than 2 in the range $0.056 < \tau < 0.294$, and the value of 0.8, corresponding to $\tau = 0.15$, was taken. The zero-point correction was then 0.44, so that, for the rare earths,

$$\log \eta_0 (\alpha^2 \text{ CVn}) = \log \eta_0 (\text{sun}) + 0.43\chi - 0.44 .$$

The values of $\log \eta_0$ thus obtained were plotted against $\log (W/b')$. For *Dy*, there is no published spectrum analysis, but we are indebted to Dr. J. M. Blank for sending us the results of his preliminary analysis. From his diagram showing the probable placing of

TABLE 5

RELATIVE ABUNDANCES OF THE ELEMENTS IN α^2 CVn

Element	$\Delta \log N_0$ (α^2 CVn − Standard)	$\Delta \log N_1$	Abundance Ratio (α^2 CVn/Standard)
			Relative to γ Gem
Mg		−0.42 −0.42	0.4
Al	−0.69		1.1
Si		+1.01	10
Ca	−1.18	−2.02	0.02
Sc		−0.21	0.7
Ti		+0.36	2.6
V		+0.10	1.3
Cr	−0.20	+0.72	5.2
Mn	+0.41 +0.25		16
Fe	−0.40	+0.46	2.9
Ni		+0.32 +0.64	3.0
Sr		+0.66	14
			Relative to the Sun
Y		+1.09	20:
Zr		+1.46	30
Ba		−0.89	≤0.9:
La		+2.40	1020:
Ce		+2.04	400
Pr		+2.46	1070
Nd		+1.82	250
Sm		+2.00	410
Eu		+2.58	1910
Gd		+2.34	810
Dy		+2.44	760

some of the levels, we have estimated excitation potentials for the three lines of *Dy* II which we have used. Since the potentials are low for all the rare-earth lines, we hope that no great error has been introduced. The horizontal shifts necessary to fit the points onto the theoretical curve of growth of Wrubel, used previously, then give the abundances of the ions relative to the sun. Implicit in this step is the assumption that the absolute abundances of *Fe* in α^2 CVn and the sun are the same. If *Fe* is actually overabundant in α^2 CVn, then the rare-earth abundances should be correspondingly increased. The curve of growth for these elements is shown in Figure 5. Owing to the scatter of the points, both horizontal and vertical shifts together are determinate only in the case of *Ce* II and, less accurately, *Zr* II, *La* II, and *Eu* II. Since *Ce* II and *Eu* II both give a vertical shift of $\log (v/v') = +0.60$, the vertical shifts of the other rare earths have all been set equal to this, which gives a total velocity v equal to 4.2 km/sec for *Ce* II, in good agree-

ment with that obtained for the elements considered in Section V. The values of v for *Zr* II and *La* II are 4.3 and 1.5 km/sec, respectively. The small value for *La* II is surprising, and $\Delta \log N_1$ is poorly determined for this element.

Finally, the relative abundances of the elements were obtained by applying the ionization formula. This last step is very insensitive as far as the optical depth assumed in the sun is concerned. However, the second ionization potentials are not known for *Ce*, *Pr*, *Nd*, *Gd*, *Dy*. The rest have closely grouped values, and we have therefore taken 11.5 ev for *Ce*, *Pr*, *Nd*, *Gd*, and 11.8 ev for *Dy*. The partition functions B_0 and B_1 have been computed by Claas (1951) for *La* and *Yb*, and, for these, log $(2B_1/B_0)$ is near to $+0.5$ in the range $1.0 > \theta > 0.6$. We have taken the value $+0.5$ for all the rare earths. Log $(2B_2/B_1)$ is needed in considering α^2 CVn. The values for *Y* and *Zr* given by Aller (1953*d*)

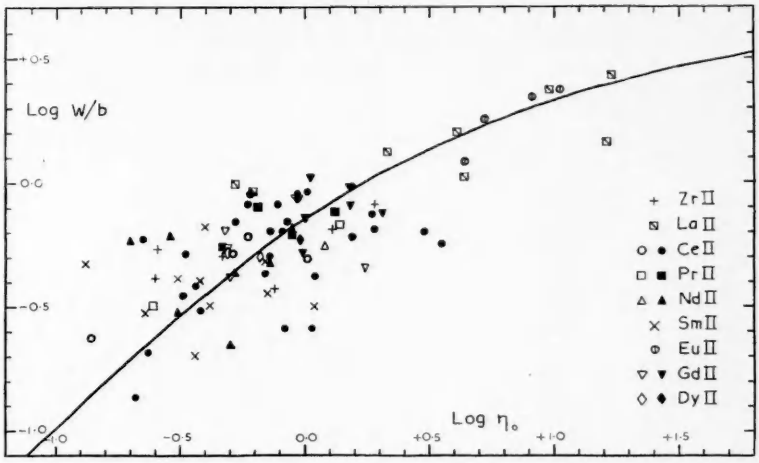

FIG. 5.—Curve of growth for *Zr* II, *La* II, *Ce* II, *Pr* II, *Nd* II, *Sm* II, *Eu* II, *Gd* II, and *Dy* II. Where two symbols are given for an element, the open symbol represents doubtful solar identifications. The theoretical curve for $B_0/B_1 = \frac{1}{3}$ and $\log a = -3.0$ is plotted.

are -0.11 and -0.04. We have taken this quantity to be zero for *La* and all the rare earths. This approximation may have introduced an error not greater than 2 in the final abundances.

The value for *Y* depends on one line only and was obtained by setting the vertical shift equal to that for *Zr*. The value for *Ba* is only an upper limit. The ultimate line of *Ba* II, λ 4554.03, is probably present, blended with a line of *Zr* II, and an estimate of the maximum possible abundance was obtained by supposing that this line is wholly due to *Ba* II.

The results for all the elements together are given in Table 5. We have preferred to list the elements in this way rather than to use Buscombe's table of abundances in γ Gem to correct for differences which can be seen when comparison is made with Claas's solar abundances. We are, in fact, assuming that, since the sun and γ Gem are both normal stars, they have similar abundance ratios (cf. the tables by Kuiper [1952] and Urey [1952]), thus avoiding the inclusion of any possible errors arising in the less-well-determined results for γ Gem.

In view of the uncertainties involved in the determination, the results are satisfactory. For the elements *La*, *Ce*, *Pr*, *Nd*, *Sm*, *Eu*, *Gd*, and *Dy*, the mean value of the overabun-

dance ratio is 830. The remaining rare-earth elements cannot be considered because of lack of laboratory data or lack of available lines. The normal abundance of *Ba* is puzzling from a theoretical standpoint (see Sec. XIV), but it does provide some check on the observational method.

IX. SEARCH FOR DEUTERIUM, *Tc*, *Sn*, *Pb*, *Th*, AND *U*

For reasons which are discussed in Section XIV, we have made a careful search for the elements listed, *D*, *Tc*, *Sn*, *Pb*, *Th*, and *U*. The results are given in some detail, since some of the elements have never been positively identified in stellar spectra.

a) DEUTERIUM

In Table 6 are given the wave lengths of the four strongest *D* Balmer lines in the region observed by Struve and Swings (1943), together with lines observed by them close to these wave lengths and their original identifications. Our conclusions are as follows:

λ *4339.29.*—The contribution by *Cr* I is negligible (from the weakness of the few strong *Cr* I lines present). The multiplet containing *Ce* II 4339.32 has only one other line, λ 4062.22 (60). There is a weak line at this wave length, but the major contributor has been listed as *Eu* II. *Ce* II probably contributes to the line at λ 4339.3, but it may not be sufficient to account for the whole line, and *D* could also contribute.

TABLE 6

POSSIBLE IDENTIFICATIONS OF DEUTERIUM

λ_{lab}	Observed λ (Struve and Swings)	Identifications (Struve and Swings)
Dγ 4339.29	.23 (0), .35 (0)	*Ce* II .32 (30) (*Cr* I .45 [300])
Dδ 4100.62	.66 (0n), .64 (1)	*Fe* I .74 (80) *Pr* II .75 (150)
Dε 3969.00	.00 (0)	*Fe* I .26 (600) (*Gd* II .29 [300])
*D*8 3887.99	.06 (0)	*Nd* II .87 (30)

λ *4100.62.*—*Fe* I 4100.74 must be too weak to be an appreciable contributor to this line. *Pr* II 4100.75 is a member of a multiplet, of which two lines are listed as the sole contributors to observed lines. *Pr* II undoubtedly contributes to the observed line, which, however, appears to be stronger than the other three lines and *Dδ* could be present.

λ *3969.00.*—*Fe* I 3969.26 should be visible in the spectrum, and this line could be wholly due to that.

λ *3887.99.*—*Nd* II 3887.87 is a member of a multiplet with two other lines, one of which, λ 3811.77, is the sole identification for an observed line and one is an unimportant contributor to a strong line of *Cr* II. Both λ 3887.87 and λ 3811.77 have rather large wave-length differences from the observed lines, in the opposite sense to that expected from the *Nd* II velocity-curve. *Nd* II may contribute to λ 3888.06, but the line could easily be mainly due to *D*.

The mean difference for the four lines between the measured wave lengths and those of the tabulated *D* lines is 0.04 A, and this is much smaller than the difference for the majority of the identifications. We conclude that the presence of *D* cannot definitely be established or ruled out. In two cases, *Dγ* and *D*8, it is quite possible that an identification can be made, but there is uncertainty for *Dδ* and *Dε* and consequently for all the lines.

The positions of the lines only about 1 A from the centers of the corresponding hydrogen lines make the measurement of equivalent widths totally uncertain. The smallest equivalent width of a distinguishable line is ~0.005 A. If we suppose that the line at

λ 4339.3 is wholly due to $D\gamma$ and that it has $W = 0.005$ A, we find from the curve of growth, using the same parameters as for other elements and the known f-value and allowing for the increased opacity in the wing of $H\gamma$, that $\log N_D = 19.2$. Now if hydrogen has the same abundance relative to that of *Fe* in the sun and in γ Gem, then $A_D/A_H = 3 \times 10^{-6}$ in α^2 CVn.

b) Tc AND *Sn*

No positive identifications for these elements have been made.

c) Pb

In Table 7 are given the laboratory wave lengths of the only three lines of *Pb* I in the observed wave-length region and the two strongest lines of *Pb* II. The third column gives the wave lengths and intensities of near-by lines observed by Struve and Swings; the fourth column gives their original identifications; the fifth column gives our mean equivalent widths, with the number of measures in parentheses. The next strongest lines of *Pb* II (intensity 10) did not provide any identifications.

TABLE 7

IDENTIFICATIONS OF *Pb*

λ_{lab} (Int)	E.P. (Ev)	Observed λ (Struve and Swings)	Identifications (Struve and Swings)	Mean E.W. (mA) and No. of Measures
Pb I 3639.57 (500)	0.97	.60 (0), .70 (1), .84 (1)	None	.....
3683.47 (1000)	0.97	.44 (1), .49 (1)	None	.....
		.44 (1n), .65(1n)		
4057.81 (1000)	1.31	.01 (0), .78 (0)	*La* II .08 (5) *Pb* I .81	11 (7)
Pb II 4245.1 (20)	8.55	.26 (1), .20 (1)	*Fe* I .26 (80) *Cr* II .08 (1)	22 (2)
4386.4 (20)	8.64	.53 (1n), .53 (1n)	None	22 (3)
		.27 (0), .24 (1), .30 (1)		

In our opinion, *La* II 4058.08 is too weak to be a satisfactory identification. *Cr* II 4245.08 probably contributes to the adjacent observed line at λ 4245.0, while *Fe* I 4245.26, from our experience with this spectrum, is too weak to be an appreciable contributor. We conclude, therefore, that *Pb* is present in α^2 CVn.

Pb I λ 4058, λ 3683 have been identified in the solar spectrum; λ 3640 is masked; λ 4058 occurs in the wing of a strong line in the solar spectrum; but we have measured λ 3683 from the Utrecht *Atlas*. Assuming that λ 4058, which has the same laboratory intensity and nearly the same E.P., has the same equivalent width as λ 3683, then from the curve of growth we find that $A_{\alpha^2 CVn}/A_{sun} = 1500$, using the same method as that for the rare earths. Thus the abundance is increased by a factor of the same order as that for the rare earths.

d) Th

The stellar line near the wave length of the ultimate line of *Th* II, λ 4019.14, has an apparently satisfactory identification as *Tb* II. There are observed lines near most of the other listed lines of *Th* II, but almost all have satisfactory identifications. We conclude that there is no evidence for or against the presence of *Th*.

e) U

Laboratory analyses of *U* I and *U* II have been made by Kiess *et al.* (1946) and Schuurmans *et al.* (1947), respectively. No identifications of lines of *U* I or of the two

sensitive *U* II lines, λ 4543.63 and λ 4472.34, have been made in the sun.[3] In the spectrum of α^2 CVn no identifications with *U* I have been made. However, *U* is an element of rare-earth type in its electron configuration, and neutral lines would not be expected. There are coincidences with the two sensitive lines of *U* II, i.e., a weak unidentified line at λ 4543.77 and a line at λ 4472.26 identified by Struve and Swings as *Eu* II (6). In addition, between thirty and forty other low-level lines fall near weak unidentified or unsatisfactorily identified lines in α^2 CVn. In view of the very rich spectrum of *U* II and of the large number of lines in α^2 CVn, a fair number of chance coincidences is to be expected.

Thus the evidence for the presence of *U* is not conclusive, although the number of coincidences makes it desirable to investigate both the probability of chance coincidences and also the possibility of its presence in other stars of this group.

X. VARIATIONS IN EFFECTIVE ABUNDANCES THROUGH THE PERIOD

For the ions *Ti* II, *Cr* II, and *Fe* II there are sufficient observations of variable lines for curves of growth to be plotted separately for maxima and minima. Since the number of

TABLE 8

CURVE-OF-GROWTH VARIATIONS THROUGH THE PERIOD

	Phase	Δ log η_0 (α^2 CVn − γ Gem)	v (Km/Sec)	Abundance Ratios [α^2 CVn(0.0)/ α^2 CVn(0.5)]
Ti II	0.0 (Max.)	+0.44	2.9	*Ti*=2.6
	.5	− .04	2.3	
Cr II	.0	+ .68	2.2	*Cr*=0.6
	.5 (Max.)	+ .90	3.6	
Fe II	.0	+ .42	2.9	*Fe*=0.7
	0.5 (Max.)	+0.56	3.8	

lines which can be used is only about half the number available for the mean curves, these latter curves are not so well defined. The results are shown in Table 8. The abundance ratios in the last column are the ratios of the apparent abundances at phases 0.0 and 0.5. These were obtained by using $T_{\text{ion}} = 8150°$ and 8650° at phases 0.0 and 0.5, corresponding to a variation of 500°, suggested by Provin's color measures, about a mean of 8400°. However, the ratios are very insensitive to a variation of 500° in this temperature range. The differences in the total velocity v between phases 0.0 and 0.5, if real, act in the wrong sense to explain the differences in Δ log η_0. The occurrence of a maximum instead of a minimum in the lines of *Fe* I and *Cr* I at mid-period suggests that the ionization temperature change may actually be smaller than 500°, since the neutral lines are more sensitive to temperature change than are lines from the ionized elements.

For *Zr*, *La*, and the rare earths there are few lines which can be treated in this way. Some estimates show that the ratios of the apparent abundances at phases 0.0 and 0.5 lie between 4.5 and 8, except for *Eu*, where the ratio could lie in the range 5–30, owing to the position of the *Eu* II lines on the flat part of the curve of growth. These latter results are very uncertain.

XI. MAGNETIC INTENSIFICATION

H. W. Babcock (1949) has shown that the equivalent width of a spectrum line produced in a region having a strong magnetic field may be increased several fold, owing to

[3] Private communication from Mrs. Sitterly.

Zeeman splitting of the atomic levels. Later he concluded that the effect, while it undoubtedly occurs in magnetic stars, is probably of minor importance (Babcock and Cowling 1953).

Magnetic intensification will occur only for a line which was saturated in the absence of a magnetic field, so that it acts like an increased turbulent velocity in extending the 45° slope of the curve of growth. The values of v may therefore include, or be wholly due to, magnetic intensification. We have in no case found v greater than about 4 km/sec, and this value is in agreement with that found for γ Gem by Buscombe. Yet it might be argued that (*a*) most studies of dwarf stars have shown that the turbulent velocity is very little in excess of the thermal velocity, and Aller found no appreciable turbulence in γ Gem; (*b*) in a magnetic star having a sufficient strong field, the magnetic forces may severely damp the turbulent eddies in some regions, but in others hydromagnetic turbulence may be important (cf. the recent solar observations by Babcock and Babcock [1954] and their possible interpretation).

In the case of the rare earths, the vertical shift necessary to fit the points to the curve of growth was determined only for *Ce* II and (less certainly) for *Eu* II. The rest of the elements were arbitrarily shifted by the same amount, such that $v/v' = 4$. If the degree of magnetic intensification is different for the different elements, then their apparent abundances might be expected to be correlated with the degree of intensification (in the sense that too large abundances will have been derived for elements which have, on the average, large intensification factors). No significant correlation has been found, but it is very difficult to estimate the amount of intensification to be expected for lines with complex Zeeman patterns.

In the previous section the velocity v for the metallic lines was found to differ between maximum and minimum intensity. The ratio v(max.)/v(min.) was about 1.4; if this were due to changing magnetic intensification, it would imply that at maximum these elements (which may be stratified) lie in regions of larger magnetic field. On the other hand, the motions shown by the radial-velocity measures (cf. Sec. XII) might lead to actual changes in turbulent velocity; and it should be remembered that the separate curves of growth for lines at maximum and minimum intensity were not very well determined, so that the ratio 1.4 may not be significantly different from unity.

We conclude that we have not yet sufficient data to say to what extent magnetic intensification may affect the equivalent widths. It may well be detectable in the rare-earth lines, but the bad scatter around the curve, which is due chiefly to the comparison with weak solar lines, means that it cannot be detected in α^2 CVn. Studies in other magnetic stars with different fields, using our values of log η_0 for the rare-earth lines and comparing lines with different Zeeman patterns, may settle the question.

It is clear that the magnetic intensification effect is not important in explaining the apparent mean anomalous abundances. In particular, it is negligible when considering the large overabundance ratios of the rare earths. The variations also are hard to explain by this means, since the magnetic field changes from positive to negative, crossing the zero axis twice during the period. For *Ti* II, *Cr* II, and *Fe* II, where the curve of growth is well determined, the effect could contribute only to the parameter v, not to the abundances.

XII. THEORIES CONCERNING MAGNETIC STARS AND THEIR BEARING ON OBSERVATIONAL RESULTS

The unsatisfactory state of theoretical knowledge concerning magnetic stars is well known, and a summary of the situation has been given by Babcock and Cowling (1953). The magnetic oscillator theory has met with difficulties of a fundamental nature (Schwarzschild 1949; Gjellestad 1950, 1952; Cowling 1952), especially concerning the period and the explanation of the reversal of the field; but in our opinion it is still the most physically plausible theory, particularly as far as the atmospheric motions are concerned.

A simple formula for the period, showing how it varies as a function of the magnetic energy, has been derived by Chandrasekhar and Limber (1954).

On the other hand, the oblique rotator theory (Babcock 1951; Deutsch 1952; Runcorn 1955) can explain in a simple manner the change in polarity of the field. The observations by Deutsch, with good correlation for some stars between the line widths and the period of rotation, lend considerable support to this theory. However, it also has a fundamental difficulty, which is that it needs to concentrate the elements into two groups in regions of opposite polarity, the grouping being reversed in α^2 CVn relative to that in HD 125248 (Babcock 1951), a similar magnetic variable. Also, no model of a star with the main magnetic axis making a large angle with the axis of rotation has yet been studied in detail, but it might be that, even if this situation prevailed in the early part of the star's evolutionary path, the star would later evolve so that the axes were nearly coincident.

We shall discuss our results in terms of the magnetic oscillator theory. In using the curve-of-growth method, comparison has been made with a standard star having an atmosphere in hydrostatic equilibrium. Thus the results, particularly concerning the abundances, apply to an atmospheric level which is some kind of a mean through the periodic motions, and which may be different for different elements. It is therefore convenient to divide the discussion into three parts.

a) VARIATIONS THROUGH THE MAGNETIC PERIOD

We have numerically integrated the radial-velocity-curves for some elements given by Babcock and Burd (1952), to give the total distance traveled in the line of sight by the various ions. The results, in units of 10^{10} cm, are: *Eu* II, +15, −15; *Gd* II, +12, −12; *Sr* II, +8, −8; *Cr* II, +5, −3, +6, −8; *Ti* II, +4, −4, +3, −3; *Fe* I, +5, −5; *Fe* II, +5, −5. These distances are measured from arbitrary levels of about −2 km/sec, which appear to be the mean velocities. The amplitudes of *Eu* II and *Gd* II, on the one hand, and *Cr* II, *Ti* II, *Fe* I, and *Fe* II are sensibly different. *Cr* II and *Ti* II have well-marked double waves, which are only slightly apparent in *Fe* I and *Fe* II. For *Eu* II, the total displacement in each direction is about one stellar radius. These results and the differing line-intensity variations for different elements can be explained in a qualitative way by supposing that there is some stratification between the elements. In a model making nonradial oscillations, such as has been discussed by Cowling (1952), we should expect rapid horizontal motions. Thus the atmospheric gas would tend to stream from the polar regions toward the equator and back again, the total distance moved in the line of sight being roughly proportional in this picture to the numbers given earlier. The distribution of the elements measured outward from the stellar surface would be in the sense (*Mg*, *Si*, *Ca*); (*Fe*, *Ti*, *Cr*); (*Sr*, *Gd*, *Eu*). H. W. Babcock[4] has pointed out that although there are no appreciable radial-velocity variations for *Si* II, *Ca* II, and *Mg* II, there are definite line-intensity variations. We have confirmed this, although the intensity variations are relatively small (cf. Sec. III). For the groups (*Mg*, *Si*, *Ca*), (*Ti*, *Cr*, *Fe*), and the rare-earth group, the amplification factors vary in step with the velocity variations, but *Ca* and *Ti* both vary in the opposite sense to the other members of their groups. A simple picture of the relationship between the radial-velocity-curves and the line variations for the rare earths may be given in the following way. The lines reach minimum strength when the layers containing the rare earths lie thickest in the equatorial zone, the polar axis lying along the line of sight, so that limb darkening will be effective in weakening the lines. At this phase (0.5) the radial velocity is zero and is changing from a velocity of recession to one of approach. The velocity of approach now reaches a maximum and decreases, becoming zero again when the lines have reached maximum strength, and at this point the layers containing the rare earths lie thickest in the polar regions. The situation must actually be very complex, since the presence of

[4] Private communication.

a double wave in the velocity-curves for some elements indicates the presence of higher harmonics in any oscillation.

The variations in apparent abundance discussed in Section X do not enable us to determine definite separations between the different elements so that they can be compared with the stratification effects shown earlier, because of the uncertainties described there. It is certain, however, that there is no *unique* apparent abundance ratio between maximum and minimum.

In his study of HD 125248, Babcock has discussed the motions of ions in crossed electric and magnetic fields, using Schwarzschild's model. His discussion might be adapted to α^2 CVn. Qualitatively, the model attempts to explain the separation of the elements into zones, the tendency being for the heavier ions to be located in the polar regions and the lighter ones in an equatorial belt.

There is one further point concerning possible stratification effects. Menzel (1931) in his study of the solar chromosphere, using a simplified theory and lacking laboratory data on the spectra, found that the abundances of the rare earths were apparently about twenty times greater than those in the photosphere determined by Russell (1929). It is very important that this question should be re-examined, now that laboratory data are available, so that the reality of this abundance anomaly can be checked.

Despite the qualitative evidence for some form of stratification with the heavier elements lying above the lighter ones, the implausibility of such a *steady state* ever being achieved and maintained is evident. Though the mass spectrograph effects discussed by Babcock are possible in localized regions, the building-up of such effects over a large part of the stellar surface is difficult. Babcock has suggested some form of resonance between the period of magnetic oscillation and the travel time between atmospheric zones for ions having different ratios of e/m. However, localized spot fields, unipolar fields such as have been observed on the sun, and other irregularities superimposed on the main-field variations will tend to disturb any equilibrium oscillation condition.

b) CONDITIONS IN THE "MEAN" ATMOSPHERE

An important result is that our comparison with a normal star has shown that the gross behavior of a magnetic star's atmosphere is much the same as that of a normal star. The hydrogen lines and electron pressure are similar; the metal abundances may be slightly increased in the magnetic star, but no great anomalies in these are present. The effective level of formation of the lines is probably similar. However, the effective temperature and the ionization temperature are greater by about 1000° than those expected for a normal A0 star, so that in these respects the star corresponds to a late B-type star. It may be, therefore, that if the gross effects of the magnetic field could be imagined to be removed, the star would have the spectral characteristics of a B8 star. Thus the departures from thermodynamic equilibrium may be greater than in a normal star's atmosphere. The general tendency for abundance ratios larger than unity for the metals could be due partly to a slightly lower effective opacity in α^2 CVn. Since hydrogen is the main cause of the opacity, this might be a consequence of the stratification suggested earlier, if we consider H, although predominant throughout the atmosphere, as being relatively slightly more abundant in the lower levels, where Si and Mg tend to be grouped.

The mean magnetic pressure exerted in the atmosphere at the levels at which the lines are produced, since currents are flowing, is of the order of 10^5 dynes, while the total gas pressure in a normal atmosphere of this type is about 10^3 dynes. Thus we might expect that the magnetic field would control the atmospheric structure, and the assumption of hydrostatic equilibrium would not apply. However, if the motions are entirely horizontal, so that no vertical currents flow, as we might expect in a nonradial oscillation, this difficulty may be resolvable.[5] In sunspot regions Michard (1953) and Minnaert (1954*b*)

[5] We are indebted to Dr. V. C. A. Ferraro for a discussion of this point.

have shown that the different conditions inside and immediately outside a spot are due mainly to the different absorption coefficients and are caused only indirectly by the magnetic field. If such conditions between localized regions having different field strengths in a magnetic star were assumed, then there might be pseudo-stratification due to the effect of different absorption coefficients in the adjacent regions. However, to explain any of the stratification effects in this way, grouping of the different elements in the separate regions would have to be postulated.

Another important problem is that of the interaction between the dynamical and the magnetic forces. We have already described how the velocities v may be velocities associated with the small eddies of the hydromagnetic turbulence spectrum. The line broadening associated by Deutsch with rotation may be due partly to large-scale hydromagnetic turbulent elements. In the atmospheres of normal A stars, convection zones are probably present (Rosa 1948; Unsöld 1948; Vitense 1951). The presence of a sufficiently strong magnetic field will tend to inhibit the onset of convection (Chandrasekhar 1952, 1954*b*), and, since the star probably has a small rotation, the combination of rotation and magnetic field will make the consequent behavior of the convective zone exceedingly complex (Chandrasekhar 1954*a*). In a later paper we hope to investigate some of these phenomena.

c) THE ABUNDANCE ANOMALIES

Although the details of the atmospheric structure are not yet clear, the results given in Table 5 for the apparent anomalous abundances do appear to be significant. Stratification effects may account for a small part of these anomalies and for a large part of the variations through the period, but the large mean factors—$\sim$1000 for *Pb* and the rare earths, $\sim$20 for the *Sr*, *Y*, *Zr* group and *Si*—and the underabundance of *Ca* are suggestive of real abundance differences. In particular, we have shown that *Ba* has no apparent overabundance, but in any stratification process *Ba* would be expected to be closely allied with the rare earths.

Mechanisms of the type suggested by Greenstein (1949) to account for the apparent *underabundances* of elements with second ionization potentials between 12 and 16 ev in τ UMa cannot be important here. *Ti* (second I.P. = 13.57 ev) is not underabundant, and *Zr* (second I.P. = 14.03 ev) is overabundant. The first I.P. of *O* is 13.61 ev, and this is closer to that of *H* (13.60) than are the I.P.'s of the other elements (Moore 1949), so that if the resonance for the charge-transfer reaction suggested by Greenstein were sufficiently narrow, it is possible that the weakness of *O* might be explained in this way. However, in general, the width of the resonance is several electron volts, and there is no reason to supposed that in this atmosphere the conditions for this process would be very different. Consequently, the underabundance of *O* is probably real.

In the remainder of this paper we shall consider the possible ways in which real surface abundance differences can arise. There are the following possibilities: (1) there have been accretion processes affecting particular elements, so that abnormal surface abundances have been produced from the interstellar gas; (2) the star condensed from material containing abnormal (relative to the cosmical) element abundances; (3) there has been preferential mixing from the stellar interior or preferential reactions in the interior, followed by mixing; (4) the abundance anomalies have been produced by nuclear processes at work on the stellar surface.

It is highly probable that possibilities 1 and 2 can be ruled out, since, apart from the negligible rate of accretion in most cases (McCrea 1953), both would demand clouds having these abundance anomalies. Selective mixing processes also seem very improbable. Appreciable mixing during the lifetime of a normal star is well known to be unlikely, though until a stellar model having a magnetic field has been constructed, no final answer can be given. A magnetic field inhibits the onset of convection, and this may make any mixing process more difficult than in a nonmagnetic star.

Of the four alternatives, No. 4 seems to be the most plausible. In order that nuclear

reactions can take place on the stellar surface, it is necessary that fluxes of sufficiently highly energetic ions should be produced. A mechanism for doing this will be discussed in the following section.

XIII. ACCELERATION OF IONS IN STELLAR SPOT FIELDS

A mechanism for accelerating ions in a magnetic star is that originally proposed by Swann (1933) for the acceleration of highly energetic cosmic-ray particles in sunspots. The basic suggestion is that of betatron acceleration processes in trochoidal orbits in the varying magnetic fields in stellar spots. We shall use results due to Riddiford and Butler (1952). The important parameters which govern the energy attainable by ions accelerated in this way, in the ideal case, are the time of injection of the ion in the growing spot, and the injection velocity. It is assumed that the rate of change of the magnetic field is uniform, so that

$$H = a_0 t\,. \tag{4}$$

The departure from homogeneity in the actual field has not been considered important. We can put a lower limit on a_0 by supposing that spot fields in magnetic stars change more rapidly than the total observed change of field through the period. For α^2 CVn this gives $a_0 \geq 6 \times 10^{-13}$ e.s.u. The magnetic curve for α^2 CVn published by Babcock indicates more rapid fluctuations of the observed field within the period of variation. If we use these as indications that spot regions are present, then a very rough estimate suggests that H might vary locally by perhaps 2000 gauss in 6 hours, giving $a_0 \sim 4 \times 10^{-12}$ e.s.u. This is comparable to values given for sunspots.

If we write

$$\omega = \frac{a_0 e t}{m},$$

and let ω_0 be the value of ω at the injection time t_0, Riddiford and Butler have shown that the velocity v is given approximately by

$$v\,(t) = \frac{\omega}{\omega_0}\left(\frac{t_0}{t}\right)^{1/2}\left[\left(u_0+\frac{r_0}{2t_0}\right)^2+u_0^2\right]^{1/2}, \tag{5}$$

where u_0 is the injection velocity of the ion and r_0 is the radius of the spot. We then find that

$$\text{For } u_0 \gg \frac{r_0}{2t_0}, \qquad v = \sqrt{2}\,u_0\left(\frac{t}{t_0}\right)^{1/2}, \tag{5a}$$

$$\text{And for } u_0 \ll \frac{r_0}{2t_0}, \qquad v = \frac{r_0}{2t_0}\left(\frac{t}{t_0}\right)^{1/2}. \tag{5b}$$

If we use the representative values $a_0 = 4 \times 10^{-12}$, $t = 2 \times 10^4$ sec, $r_0 = 5 \times 10^9$ cm, $u_0 = 10^6$ cm/sec, we find from equation (5*b*) that particles will gain most energy if they are injected in the early stages of the spot's growth (within the first 40 minutes for the values taken above). Some representative energies attained by various ions for different injection times are shown in Table 9. The mechanism is very sensitive to the injection time, and the table clearly gives only a general indication of the final energies which may be reached. It is sufficient to show that a whole range of energies can be achieved by this mechanism. If the time of variation of the magnetic field is several days instead of several hours, the same energies will result for ions injected at proportionately later times. The final result does not depend strongly on the place of injection in the spot region. Only a very small proportion of the stellar surface (perhaps 0.1 per cent) will be an efficient generator of ions; but it may be supposed that a very large number of magnetic cycles

of the star have taken place ($\sim 10^{10}$, not taking into account secular variations of the period). A small number of ions sufficiently energetic for nuclear reactions to be possible may have been available over a long period, of the order of the lifetime of the star. The form of the energy spectrum is

$$f(E) \propto E^{-5/3}$$

for ions injected near the edge of the spot. We conclude that in spot regions there will be fluxes of ions, mainly protons and α-particles, having an energy spectrum which will give a mean energy considerably greater than that due to a Maxwellian distribution at stellar core temperatures.

One possible objection to this theory should be pointed out. Only a small proportion of the ions can be accelerated, otherwise large currents will be set up, looping the spot so that the betatron is effectively short-circuited and the field ceases to grow (cf. Alfvén 1950). Arguments which are confined to single-particle orbits do not consider this, al-

TABLE 9

SOME ENERGIES ATTAINED BY ACCELERATED IONS

	KINETIC ENERGY (MEV)			KINETIC ENERGY (MEV)	
	Injection Time $t_0 = 10$ Sec.	Injection Time $t_0 = 100$ Sec		Injection Time $t_0 = 10$ Sec	Injection Time $t_0 = 100$ Sec
p	74	0.065	Fe^+	4100	3.6
α	290	0.26	Zr^+	6700	5.9
O^+	1170	1.0	Gd^+	11,500	10.2
Si^+	2060	1.8			

though Riddiford and Butler have shown that it is possible for this difficulty to be avoided.

We have discussed only one idealized mechanism here, but, in general, in a magnetically active star some acceleration processes are almost certainly at work. The occurrence of fluxes of ions will mean that in some small localized regions excessive ionization will be produced by the low-energy components of these streams.

XIV. NUCLEAR REACTIONS, NUCLEAR STABILITY, AND ANOMALOUS ABUNDANCES

In the previous section we have shown that nuclear reactions will be energetically possible on the stellar surface. The relative probabilities of the large numbers of possible reactions can be obtained only if the distribution of the energetic ions and the cross-sections for the reactions are known. The kinetic-energy distribution is, however, quite unknown, and many of the likely reactions, particularly those involving heavy ions, have not yet been produced in the laboratory. Consequently, only a general discussion is possible.

The elements may be grouped in the following way: *O*, *Mg*, *Si*, *Ca*; *Ti*, *V*, *Cr*, *Mn*, *Fe*, *Ni*; *Sr*, *Y*, *Zr*; *Ba*, *La*, and the rare-earth group; *Pb*.

a) NUCLEAR STRUCTURE

One of the most significant pieces of circumstantial evidence suggesting that nuclear processes have been continuously taking place on the stellar surface is seen by considering the nuclear stability of the elements showing abundance anomalies. It has been pointed out by Maria Mayer (1948) that nuclei with closed shells of protons or neutrons (the magic-number nuclei) are, in general, more stable than other nuclei surrounding

them in the periodic table, particularly for the heavier elements. This stability is often reflected in the cosmical abundances of these elements. The magic numbers are 2, 8, 14, 20, 28, 50, 82, and 126, and the evidence tends to be stronger for neutron magic numbers. A comparison of anomalies and magic numbers gives the following results:

O^{16} has 8 protons and 8 neutrons and is underabundant. However, anomalies in the abundances of the light elements *C*, *N*, and *O* are often found in peculiar stars, and magic number or stability does not have great significance. Reactions involving neutrons may be important here.

Si^{28} with 14 protons and 14 neutrons is overabundant. From the factor given in Table 5 and from the cosmical abundances given by H. Brown (1949), the abundance of *Si* in α^2 CVn per 10,000 atoms of *Fe* (the cosmical abundance), is 54,600.

Ca^{40} has 20 protons and 20 neutrons but is underabundant. The reasons for this are obscure, though there seems to be a general tendency for the underabundance of the lighter elements, with the exception of *Si*. Again reactions with neutrons may be responsible. The relative abundance of *Ca* in the units given above is 7.

In the metallic group, the relative abundances of isotopes with 28 neutrons are Ti^{50} (5.3 per cent), V^{51} (99.8 per cent), Cr^{52} (83.8 per cent), and Fe^{54} (5.8 per cent) (Hollander *et al.* 1953). It is well known that in this group the magic number is not the best indication of stability, the cosmical abundances being in the order *Fe*, *Cr*, *Ti*, *V*. It may, however, be significant that Cr^{52} has the greatest overabundance ratio of this group in Table 5.

The correlation between the magic number of 50 neutrons and the overabundance of the *Sr*, *Y*, *Zr* group is very good. The isotopic abundances of these elements with 50 neutrons are Sr^{88} (82.6 per cent), Y^{89} (100 per cent), and Zr^{90} (51.5 per cent). The relative abundances of these elements in α^2 CVn, in the units given above, are 3, 1, and 25, respectively.

The rare-earth group is concentrated among the nuclei with a closed shell of 82 neutrons. The isotopic abundances of those members of the group with 82 neutrons are Ba^{138} (71.7 per cent), La^{139} (99.9 per cent), Ce^{140} (88.5 per cent), Pr^{141} (100 per cent), Nd^{142} (27.1 per cent), and Sm^{144} (3.2 per cent). The remainder of the group, *Eu*, *Gd*, *Tb*, and *Dy*, have excesses of between 6 and 16 neutrons over the closed shell. We have not been able to determine the abundance of Tb^{159} (excess of 12 neutrons), although it is probably overabundant by a similar factor. *Ho*, *Er*, and *Yb* all have few lines identified, and nothing can be said about the abundances. No positive identifications of *Tm* and *Lu* have been made. The relative abundances of *La*, *Ce*, *Pr*, *Nd*, *Sm*, *Eu*, *Gd*, and *Dy*, in the units given above, are 11, 5, 6, 5, 3, 3, 8, 8, respectively. The cosmical abundances of the rare-earth elements (from the meteoritic analyses [Brown 1949]) are fairly homogeneous, though *Eu*, *Tb*, and *Ho* are lower than the rest. In α^2 CVn the outstanding exception is *Ba*, which is 10^2–10^3 times less abundant than the others of the group, but whose normal cosmical abundance is homogeneous with them. In terms of the nuclear structure of *Ba*, this is a surprising result.

Pb is overabundant, and the isotopic abundance of the doubly magic Pb^{208} (126 neutrons, 82 protons) is 52.3 per cent. In the units given above, the abundance in α^2 CVn is $\sim$200.

It may be significant that, within the errors involved in the determination, the abundances of *Ca*, *Sr*, *Y*, *Zr*, *La*, and the rare earths are approximately the same in this star.

b) REACTIONS INVOLVING NEUTRONS

The continuous injection of a small admixture of fast protons and α-particles over a time scale $\sim 10^{16}$ sec into a gas having normal cosmical abundances is discussed more fully elsewhere (Burbidge, Burbidge, and Fowler 1955), where a brief study of the apparent anomalous abundances of the peculiar A and F stars, the *Ba* II, and the S stars is made. The interaction of high-energy protons with thermal protons or very light nuclei will

not be important in altering the abundance ratios, since the important reactions will be elastic and inelastic scattering and radiative capture. From our point of view the (p, n) or (α, n) reactions will be the most important, and the threshold for these is very large for the light nuclei and the lighter of the intermediate nuclei, e.g., $-Q_{pn} = 6.6$ Mev for Cl^{35}. Above these thresholds the emission of a neutron is the most probable reaction (cf. Blatt and Weisskopf 1952). Thus a beam of protons having energies $\sim$100 Mev will produce a smaller (perhaps 1 per cent) flux of neutrons. These will very rapidly be slowed to thermal energies (1.3 ev) and will be captured or decay. Calculations of the relative probability of these processes, given elsewhere, suggest that at photospheric levels in the atmosphere these two rates are of the same order, so that an appreciable fraction of the neutrons will be captured before decay.

Some of the results of the appearance of neutrons will be as follows:

1. The production of deuterium, which will be stable in a thermal atmosphere at $\sim$10,000° so that its abundance will grow.

2. Complex reactions involving the light nuclei, which may tend to deplete particular elements.

3. The capture of thermal neutrons by the heavier nuclei. A detailed discussion shows that nuclei having closed shells of neutrons will tend to be built because, in general, the thermal-neutron-capture cross-sections reach minima for the closed shells. The qualitative agreement of this result with the overabundances discussed earlier is spoiled, because of the great overabundance of *Eu*, *Gd*, and *Dy*, which do not have closed shells and have large resonant capture cross-sections in the thermal region (AEC 1952), so that on this picture they would be rapidly destroyed. However, there is the possibility that isotopes in which this does not occur are more abundant than the terrestrially abundant isotopes.

4. The buildup process may lead to an excess of fissionable nuclei. Fission processes will then tend to produce excesses of nuclei lying near the peaks of the fission fragment-curve, i.e., the *Sr*, *Y*, *Zr* group and the early members of the *Ba*, *La*, rare-earth group. The possible presence of *U* in this star is very important in this connection. More complete analyses of other magnetic stars and a search for the transuranic elements are very desirable.

At sufficiently high energies such that the Coulomb barrier is not important, direct capture of fast protons by heavy elements may also be important.

c) OTHER NUCLEAR REACTIONS

Though neutron processes will probably be the most important reactions, others, sometimes involving accelerated heavy ions, may be expected. The abundances of the heavy ions are much lower than those of *H* and *He*, but there may be processes which make their acceleration more efficient. Some reactions which might have significance are the following:

(i) $O^{16} + O^{16} \rightarrow S^{32*} \rightarrow Si^{28} + \alpha + 11$ Mev (Salpeter 1953).

(ii) Spallation reactions; a few of these, initiated by the bombardment of heavy nuclei by protons, α-particles, or deuterons, have been studied in the laboratory. In such reactions, sizes of fragments vary continuously from nucleons and α-particles through the light nuclei up to the sizes of fission fragments (Spence and Ford 1953). This type of reaction is related to fission reactions initiated by charged ions. A typical reaction which has been studied is

$$Cu^{63} + p \rightarrow Cl^{38} + p + n + 6\alpha \text{ (threshold 110 Mev)}.$$

The rate of this reaction has been compared with that of

$$Cu^{63} + p \rightarrow Cl^{38} + Al^{25} + n \text{ (threshold 50 Mev)}.$$

Since there is an abundance peak at *Fe*, we might suggest, by analogy, reactions of the form

$$Fe^{56} + Cr^{52} \rightarrow Sr^{88} + 4\alpha + 4p$$

or

$$Fe^{56} + Fe^{56} \rightarrow Zr^{90} + 5\alpha + 2p\,.$$

Although such collisions are rare, *Fe* will not be depleted by other processes, as, for example, *O* may be by neutron reactions, thus slowing down reaction (i). No laboratory data are yet available about these heavy-ion reactions, but it is probable that, if large fragments are emitted, they will cluster about the stable sizes.

(iii) Deuterium can be produced by the inverse deuteron-stripping reaction, of which the following is an example:

$$p + Be^9 \rightarrow Be^8 + D\,.$$

This process may be important for the heavier elements. At sufficiently high proton energies (above the meson production threshold) deuterium may also be produced by the reaction

$$p + p \rightarrow D + \pi^+\,.$$

Recently Cameron (1954, 1955) has attempted to explain the apparent anomalous abundances in the S stars by supposing that neutron-capture processes are taking place in the stellar core. If this theory were applied to this star, it would be an alternative explanation corresponding to possibility 3 discussed in Section XII(*c*). However, the Cameron process demands both an appreciable helium core in which C^{12} is being produced and considerable mixing between the core and the envelope, and we do not currently believe that either of these conditions is fulfilled in this star. In particular, the peculiar A stars as a group lie very close to the normal A and B stars on the main sequence.

XV. CONCLUSION

We have described this analysis in detail, in order that similar studies of other magnetic stars, in particular β CrB and HD 133029, and the peculiar A star ϵ UMa, which are under way at the present time, may be more briefly treated and in order that the limitations of our method may be understood. It is very important that a theoretical study of a stellar atmosphere containing a large magnetic field be made. Notwithstanding the difficulties underlying the theory of variable magnetic stars, knowledge of the behavior of the *atmosphere alone* will enable much more interpretation to be made of the observational results concerning the motions and the effective abundance changes through the period. Apart from the magnetic field, the abundance anomalies are the most striking feature of this star. Their confirmation in other peculiar A stars and in stars of other types showing apparent abundance anomalies, if forthcoming, may enable us to relate these seemingly different groups.

This study forms part of a program of spectrophotometry of magnetic and variable stars begun by the authors at the Yerkes and McDonald Observatories in 1953. We are indebted to many colleagues for discussing various aspects of this work. In particular, we are deeply grateful to Dr. H. W. Babcock for suggestions and very helpful correspondence; to Dr. W. A. Fowler for many stimulating discussions and suggestions concerning Sections XII, XIII, and XIV. We are also indebted to Mrs. C. M. Sitterly, Dr. P. Swings, and Dr. M. Minnaert, and Dr. J. M. Blank for help and unpublished material concerning different aspects of the heavy-element spectra, and to Dr. S. S. Provin for information on the color variations of α^2 CVn.

REFERENCES

AEC. 1952, Neutron Cross Sections, No. AECU-2040.
Albertson, W. 1936, *Ap. J.*, **84,** 26.
Alfvén, H. 1950, *Cosmical Electrodynamics* (Oxford University Press), p. 230.
Allen, C. W. 1934, *Mem. Commonwealth Solar Obs. Canberra*, Part 5.
———. 1938, *ibid.*, Part 6.
Aller, L. H. 1942, *Ap. J.*, **96,** 321.
———. 1953*a*, *Astrophysics* (New York: Ronald Press), pp. 225, 226.
———. 1953*b*, *ibid.*, p. 292.
———. 1953*c*, *ibid.*, p. 302.
———. 1953*d*, *ibid.*, p. 78.
Babcock, H. D., and Babcock, H. W. 1954, paper read at the meeting of the A.A.S. at Ann Arbor, June.
Babcock, H. W. 1949, *Ap. J.*, **110,** 126.
———. 1951, *ibid.*, **114,** 1.
Babcock, H. W., and Burd, S. 1952, *Ap. J.*, **116,** 7.
Babcock, H. W., and Cowling, T. G. 1953, *M.N.*, **113,** 357.
Baxandall, F. E. 1913, *Observatory*, **36,** 440.
Belopolsky. 1913*a*, *A.N.*, **196,** 6.
———. 1913*b*, *Bull. Acad. Imp. Sci. St. Petersburg*, **7,** 689.
———. 1927, *Bull. Obs. Pulkovo*, No. 101.
Blatt, J. M., and Weisskopf, V. F. 1952, *Theoretical Nuclear Physics* (New York: John Wiley & Sons), chap. 9.
Brown, H. 1949, *Rev. Mod. Phys.*, **21,** 625.
Burbidge, G. R., and Burbidge, E. M. 1954, *Ap. J.*, **120,** 76.
Burbidge, G. R., Burbidge, E. M., and Fowler, W. A. 1955 (in preparation).
Buscombe, W. 1951, *Ap. J.*, **114,** 73.
Cameron, A. G. W. 1954, *Phys. Rev.*, **93,** 932.
———. 1955, *Ap. J.*, **121,** 144.
Carter, W. W. 1949, *Phys. Rev.*, **76,** 972.
Chandrasekhar, S. 1952, *Phil. Mag.*, **43,** 501.
———. 1954*a*, *Proc. R. Soc. London*, *A*, **225,** 173.
———. 1954*b*, *Phil. Mag.*, **45,** 1177.
Chandrasekhar, S., and Limber, D. N. 1954, *Ap. J.*, **119,** 10.
Chandrasekhar, S., and Münch, G. 1946, *Ap. J.*, **104,** 446.
Claas, W. 1951, *Rech. Astr. Obs. Utrecht*, Vol. **12,** Part 1.
Cowling, T. G. 1952, *M.N.*, **112,** 527.
Deutsch, A. J. 1947, *Ap. J.*, **105,** 283.
———. 1952, *Trans. I.A.U.*, **8,** 801.
———. 1954, *J. Opt. Soc. Amer.*, **44,** 492.
Farnsworth, G. 1932, *Ap. J.*, **76,** 313.
Gjellestad, G. 1950, *Rept. No. 1, Inst. Theoret. Ap., Oslo.*
———. 1952, *Ann. d'ap.*, **15,** 276.
Greenstein, J. L. 1948, *Ap. J.*, **107,** 151.
———. 1949, *ibid.*, **109,** 121.
Guthnick, P., and Prager, R. 1914, *Veröff. Berlin-Babelsberg*, **1,** 44.
Hollander, J. M., Perlman, I., and Seaborg, G. T. 1953, *Rev. Mod. Phys.*, **25,** 469.
Keenan, P. C., and Morgan, W. W. 1951, *Astrophysics*, ed. J. A. Hynek (New York: McGraw-Hill Book Co.), p. 23.
Kiess, C. C., Humphreys, C. J., and Laun, D. D. 1946, *J. Res. Nat. Bur. Standards*, **37,** 57.
King, A. S. 1939, *Ap. J.*, **89,** 377.
———. 1943, *ibid.*, **97,** 323.
King, A. S., and Moore, C. E. 1943, *Ap. J.*, **98,** 33.
King, R. B., and King, A. S. 1938, *Ap. J.*, **87,** 24.
Kuiper, G. P. 1952, *The Atmospheres of the Earth and Planets* (Chicago: University of Chicago Press), p. 329.
McCrea, W. H. 1953, *M.N.*, **113,** 162.
Mayer, M. G. 1948, *Phys. Rev.*, **74,** 235.
Menzel, D. H. 1931, *Pub. Lick Obs.*, Vol. **17,** Part I.
Michard, R. 1953, *Ann. d'ap.*, **16,** 217.
Minnaert, M. 1954*a*, *The Sun*, ed. G. P. Kuiper (Chicago: University of Chicago Press), p. 127.
———. 1954*b*, *ibid.*, p. 722.
———. 1955, *Revised Rowland Table, New Edition* (in preparation).
Moore, C. E. 1945, *Contr. Princeton U. Obs.*, No. 20.
———. 1949, *Atomic Energy Levels* (N.B.S. Circ. No. 467).
Morgan, W. W. 1935, *Pub. Yerkes Obs.*, Vol. **7,** Part 3.

Nikonov and Brodskaya. 1950, *Bull. Abastumani Ap. Obs.*, **11**, 7.
Petrie, R. M., and Maunsell, C. D. 1951, *Pub. Dom. Ap. Obs. Victoria*, **8**, 253.
Provin, S. S. 1953, *Ap. J.*, **118**, 489.
———. 1954, private communication.
Riddiford, L., and Butler, S. T. 1952, *Phil. Mag.*, **43**, 447.
Rosa, A. 1948, *Zs. f. Ap.*, **25**, 1.
Runcorn, S. K. 1955, *Vistas in Astronomy* (London: Pergamon Press).
Russell, H. N. 1929, *Ap. J.*, **70**, 11.
Salpeter, E. E. 1953, "Cyclostyled Notes: Symposium on Astrophysics, University of Michigan" (discussed for stellar interiors).
Schuurmans, P., van den Bosch, J. C., and Dijkwal, N. 1947, *Physica*, **13**, 117.
Schwarzschild, M. 1949, *Ann. d'ap.*, **12**, 148.
Slettebak, A. 1951, *Ap. J.*, **113**, 437.
Spence, R. W., and Ford, G. P. 1953, *Ann. Rev. Nuclear Sci.*, **2**, 399.
Struve, O. 1942, *Proc. Amer. Phil. Soc.*, **85**, 349.
Struve, O., and Swings, P. 1942, *Observatory*, **64**, 291.
———. 1943, *Ap. J.*, **98**, 361.
Swann, W. F. G. 1933, *Phys. Rev.*, **43**, 217.
Swings, P. 1944, *Ap. J.*, **100**, 132.
Tai, W. S. 1940, *M.N.*, **100**, 94.
Ueno, S. 1954, *Contr. Inst. Ap. U. Kyoto*, No. 42.
Unsöld, A. 1938, *Physik der Sternatmosphären* (Berlin: Springer), p. 241.
———. 1948, *Zs. f. Ap.*, **25**, 11.
Urey, H. C. 1952, *The Planets* (New Haven: Yale University Press), p. 189.
Vitense, E. 1951, *Zs. f. Ap.*, **28**, 81.
Wrubel, M. 1949, *Ap. J.*, **109**, 66.

THE THERMODYNAMIC STATE OF THE OUTER SOLAR ATMOSPHERE III. THE ANALYSIS OF THE BALMER DECREMENT OBSERVED AT THE 1932 AND 1952 ECLIPSES

SATOSHI MATSUSHIMA
University of Utah and High Altitude Observatory*
Received August 25, 1954

ABSTRACT

The preliminary analysis, made by Thomas, of the Balmer decrement at the 1932 eclipse in terms of self-absorption is extended. An attempt to obtain a significant nonequilibrium term for the higher levels appears unsuccessful because of the scatter in the data. The height gradient of the population of the Balmer ground state falls below that of the higher levels rather than exceeds them, as found in Thomas' analysis, thus implying a significant gradient in the nonequilibrium term for the second level. The same analysis applied to the 1952 observations yields more precise results. A nonequilibrium term appears present in the higher levels, but no accurate height gradient of this term can be stated. The gradient of the Balmer ground state again exceeds that of the higher levels; further, the 1952 gradient exceeds that of 1932.

I. INTRODUCTION

The first paper of this series[1] (Thomas 1950) discussed the possibility of interpreting the Balmer decrement in the solar flash spectrum in terms of a significant self-absorption. The importance of such self-absorption is well recognized for the earlier members of the Balmer series; but for the lines later than $H10$—which are those discussed by the paper—the self-absorption had hitherto been considered negligible. If the self-absorption were actually significant for these higher lines and could be determined, the fact that it depends only upon the population of the second quantum level provides a method for inferring an "absolute" density from a measure of relative line intensities only.

The discussion in Paper I, based on the 1932 eclipse data (Cillié and Menzel 1935), was inadequate from a self-consistency standpoint in two respects. First, the influence of any departure from thermodynamic equilibrium was explicitly neglected in the quantitative analysis of the self-absorption effect. The neglect was necessitated by a lack of knowledge as to the behavior of this nonequilibrium effect—unless the temperature and density structure of the chromosphere were to be prejudged—but did provide a lower limit on the self-absorption present. Second, only one pair of lines at each height was used in the analysis—the minimum necessary to obtain the self-absorption and the occupation number of the second quantum level.

It was clear that these two weak points should be strengthened. Further, it was clear that the method should be exploited at a future eclipse, making attempts to increase the height resolution of the observations. Thus a complete reanalysis of the 1932 data was undertaken, using all observations, both because of its intrinsic interest and as preparation for the 1952 eclipse. Precisely the same analysis was then made of the 1952 data. These analyses have been performed on the basic assumption that a self-absorption effect does exist and on certain specific assumptions as to the possibility of separating it from effects of nonequilibrium occupation numbers. On the basis of the results, certain conclusions regarding the self-absorption effect and the method of our analysis follow. It becomes clear that this analysis is not the definitive one.

* Now at Haverford College.

[1] Hereafter called "Paper I."

II. THE METHOD OF ANALYSIS

The eclipse data to be analyzed are the rates of emission, E_{n2}, from a strip of chromosphere 1 cm wide, extending out above the moon's edge, h. Thus

$$E_{n2}=\frac{A_{n2}h\nu_{n2}}{4\pi}\int_0^\infty \frac{\alpha_{2n,\,\nu}}{\alpha_{2n}}\int_{-\infty}^{\infty}\int_h^\infty n_n(x,\,y)\exp\left[-\int_y^\infty n_2\alpha_{2n,\,\nu}dy\right]dx\,dy\,d\nu\,, \tag{1}$$

where

$$\alpha_{2n}=\int_0^\infty \alpha_{2n,\,\nu}d\nu\,, \tag{2}$$

so that the emission-coefficient profile is assumed to be that of the absorption coefficient. For the latter, we assume a pure Doppler profile. Finally, we assume the occupation number of each energy level to decrease exponentially with height, with the same exponent for all levels, viz.,

$$n_n = n_n(0)e^{-\beta h} \tag{3}$$

(β is thus the density gradient of hydrogen). These were the assumptions underlying the expressions used in Paper I. Thus we obtain the expression for E_{n2} of the earlier papers (Thomas 1949):

$$E_{n2}=\sqrt{(2\pi R_\odot)}\,\frac{A_{n2}h\nu_{n2}}{4\pi}\,\beta^{-3/2}n_n(h)\,(\text{Abs.})\,, \tag{4}$$

where

$$(\text{Abs.})=\sum_{m=0}^{\infty}\left\{(-1)^m(N_2a_n)^m[2^m m!\,(1+m)^{3/2}]^{-1}\sum_{j=0}^{m/2}\frac{m!}{(2j)!\,(m-2j)!}I_{2j}\right\}, \tag{5}$$

$$N_2=n_2(h)\,\beta^{-1/2}\sqrt{(2\pi R_\odot)}\,, \tag{6}$$

$$a_n=\frac{\pi\epsilon^2}{mc}f_{2n}\frac{c}{\nu}\left(\frac{m_H}{2\pi kT_e}\right)^{1/2}, \tag{7}$$

$$I_{2j}=\frac{2}{\sqrt{\pi}}\int_0^\infty e^{-2t^2}\left[\frac{2}{\sqrt{\pi}}\int_0^t e^{-s^2}ds\right]^{2j}dt\,. \tag{8}$$

Here (Abs.) is the self-absorption term, and a_n is the absorption coefficient at the line center. Also we have the nonequilibrium form of the Boltzmann-Saha relation,

$$n_n=\left(\frac{h^2}{2\pi m_e k}\right)^{3/2}n_e n_p T_e^{-3/2}\,\frac{\varpi_n}{2}\exp\left[\frac{\mathrm{X}_n}{kT_e}\right]b_n\,. \tag{9}$$

Then the Balmer decrement is

$$\Delta_n\log E_{n2}=\Delta_n\log(A_{n2}\nu_{n2}\varpi_n)+\Delta_n\log\,b_n+\Delta_n\log(\text{Abs.})+\Delta_n\frac{\mathrm{X}}{2.3kT_e}\,. \tag{10}$$

For the higher Balmer lines, the excitation term, χ_n, is so small as to be relatively insensitive to T_e. Thus the problem is to interpret the difference between the observed Balmer decrement and that coming from the factor $(A_{n2}\nu_{n2}\varpi_n)$. This factor characterizes a thin atmosphere in thermodynamic equilibrium. We seek to interpret the difference in terms of the b_n and (Abs.). Earlier work (Cillié and Menzel 1935) considered only the b_n to be relevant. Thomas (1950) suggested that the self-absorption was important for the higher lines. Ignoring either b_n or (Abs.), one may determine the other from equation (10). Dealing thus with the line emission alone, we obtain only relative values of the b_n, but absolute values of N_2a_n. The problem is to treat both effects together.

In Paper I, data from the 1932 eclipse were used to evaluate N_2a_n from equation (10), ignoring the b_n and X_n terms and thus presumably placing a lower limit on the derived absorption. Only one pair of lines was used at each height—the pair differing with the height. As a first step in the analysis, I have therefore recomputed the self-absorption, with the same neglect of b_n and X_n, using the same pairs of lines but at all heights included in the 1932 data. Table 1 contains the results, converted to values of N_2a_{30} for the purpose of intercomparison.

TABLE 1

VALUES OF N_2a_{30} (1932)

$n-n+k$	h (Km)				$n-n+k$	h (Km)			
	670	1500	2330	3170		670	1500	2330	3170
25–30	0.94	.....	.....	.....	10–15	0.25	0.19	0.08	.....
20–25	.65	.....	.....	.....	10–13	0.32	0.25	0.12	0.05
15–20	0.30	0.17	.....	.....					

The computation has been considerably facilitated by noting that the I_{2j} used by Thomas, defined in equation (8), can be explicitly evaluated:

$$I_{2j} = \frac{2}{\sqrt{\pi}} \int_0^\infty e^{-2t^2} \left[\frac{2}{\sqrt{\pi}} \int_0^t e^{-s^2} ds \right]^{2j} dt$$

$$= \int_0^\infty \frac{dg(t)}{dt} [g(t)]^{2j} dt = \frac{1}{2j+1}, \tag{11}$$

while

$$\sum_{j=0}^{m/2} \frac{m!}{(2j)!(m-2j)!} I_{2j} = \sum_{j=0}^{m/2} \frac{m!}{(2j)!(m-2j)!} \frac{1}{2j+1} = \frac{2^m}{m+1}. \tag{12}$$

Thus equation (5) becomes

$$(\text{Abs.}) = \sum_{m=0}^{\infty} (-1)^m (N_2a_n)^m [m!(1+m)^{5/2}]^{-1}. \tag{13}$$

Figure 1 exhibits Abs. (N_2a) in the range $N_2a \leq 10$. For larger N_2a, series (13) converges so slowly as to make the evaluation of (Abs.) prohibitively slow in terms of the significance of the results. Such high self-absorption places the point of "effective" emission so far out along the tangential line through the atmosphere as to raise considerable doubt regarding the validity of the simplifying assumptions made thus far. Further, since $a \propto T_e^{-1/2}$ from equation (7), we have tacitly assumed a slowly varying T_e. The approximation

$$\log (\text{Abs.}) = -0.076(N_2a)^{3/4}, \tag{14}$$

which represents the precise relation in Figure 1 within an accuracy of ± 0.01 in log (Abs.), over the same range, also suffices when useful. Data do not exist for the blank entries in Table 1, except for the second row, third column, where we would have log (Abs.) $= +0.01$, implying a negative self-absorption and thus providing an estimate of the scatter in the data.

It is tempting to regard the scatter in values at a given height in Table 1 as purely observational, but we also note what appears to be a systematic effect in the values from the lower heights. We note that, if $b_n > 1$,

$$\log \frac{b_{n'}}{b_{n'+k}} > \log \frac{b_n}{b_{n+k}} \qquad (n' < n)\,, \quad (15)$$

and thus our neglect of the b_n in obtaining the results of Table 1 from equation (10) may induce such an effect as that observed. That is, the underestimation in the inferred self-absorption due to the neglect of b_n becomes greater as n decreases. The N_2a value from

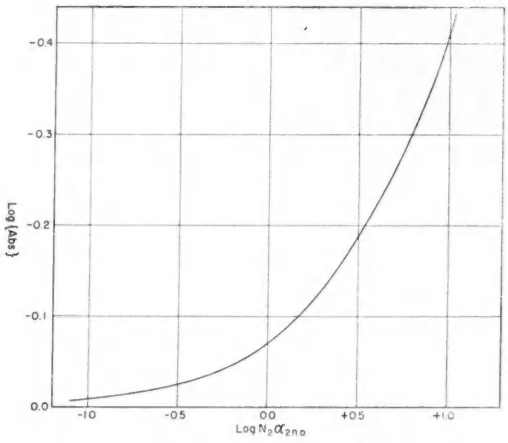

FIG. 1.—Log (self-absorption) versus log $N_2a_{2n,0}$

the higher n should then be the more realistic. Thus we hoped that the data might yield an estimate, at least, of the b_n trend—and we considered an analysis leading to both b_n and self-absorption, by a process of differential correction.

Define

$$\phi_n = \log\,(E_{n2} - C_1)_0 - \log\,[A_{n2}(n^2 - 4)] - \log\,(\text{Abs.})_0\,, \quad (16)$$

where C_1 is that part of equation (4) independent of n (but, of course, depending upon h) and where $(\text{Abs.})_0$ is a value of equation (13) computed from some trial value of N_2a—say the top entry in each of the columns of Table 1. Thus, comparing equations (4) and (16), we obtain

$$\phi_n = \log\, b_n + \frac{\Delta \log\,(\text{Abs.})}{\Delta\,(N_2a_n)}\,\Delta\,(N_2a_n) + \frac{X_n}{2.3kT_e} + \Delta C_1\,; \quad (17)$$

and we propose to determine the quantities in equation (17) by a least-squares fit of the ϕ_n. The dependence of all quantities in equation (17) upon n are known, save for b_n. We note that $b_n \to 1$ asymptotically for large n, regardless of whether our conjecture that $b_n > 1$ is valid or not. Further, we consider only data for large n (≥ 10). Thus we assume

$$\log\, b_n = p + \frac{q}{n}\,. \quad (18)$$

Since $X_n = X_1/n^2$, including a term in n^{-2} in equation (18) does not improve the representation. Further, equation (18) appears quite satisfactory in representing the theoretical computations of b_n which we have available from our own computations. Thus we investigate

$$\phi_n = (\Delta C_1 + p) + \frac{q}{n} + \frac{(X_1/2.3kT_e)}{n^2} + \left[\frac{\Delta \log (\text{Abs.})}{\Delta (N_2 a_n)}\right]\Delta (N_2 a_n) \tag{19}$$

at each height, in an attempt to use all the data to obtain the best $N_2a(h)$ and $b_n(h)$. The process must, of course, be one of successive approximation to obtain a consistent (Abs.) term. The coefficient of $\Delta(N_2a)$ in equation (19) follows from equation (13).

III. THE 1932 OBSERVATIONS

We use the eclipse results tabulated by Cillié and Menzel (1935), which provide data up to $H31$ at $h = 670$ km; $H9$–$H30$ at 1500 km; $H10$–$H17$ at 2330 km; $H8$–$H13$ at 3170 km. Our primary interest lies in n greater than about 10. Several preliminary calculations showed that the precision of the representation was not altered by including or neglecting the term in n^{-2} in equation (19). Thus the excitation term is smaller than the probable errors in the present data, and we have omitted it.

The process of successive approximation to a consistent value for N_2a proved not so satisfactory for the 1932 data. The process seems reasonably convergent for the lowest height, 670 km. For $h = 1500$ km, the run of the ϕ_n values are such that a series of differential corrections on N_2a fixes a range of possible values for it essentially by the sign of the correction, rather than a reliable numerical value. For the greater heights, the results are quite unreliable. Thus we obtain the values in the accompanying tabulation.

h	N_2a_{30}	q
670	0.95 ± 0.05	$\sim +4$
1500	$0.25 < N_2a_{30} < 0.5$	$\sim +1$

Remarking briefly on q, which measures the relative b_n values, we note only that $q > 0$. Thus b_n asymptotically approaches 1 from above; hence $b_n > 1$, in harmony with the earlier arguments in these papers.

From these results, we obtain

$$-\frac{d \ln n_2}{dh} \sim 0.8 - 1.6 \times 10^{-8} \text{ cm}^{-1}, \tag{20}$$

which is smaller than $(-d \ln n_\infty/dh)$ inferred from the emission gradient corrected for the self-absorption just found, numerically $\sim 1.7 \times 10^{-8}$. This result is the reverse of that found in Paper I, where a value $\sim 1.9 \times 10^{-8}$ replaced that of relation (20). From equation (9), we obtain

$$\begin{aligned} -\frac{d \ln n_2}{dh} &= -\frac{d \ln (n_e n_p T_e^{-3/2})}{dh} - \frac{d \ln b_2}{dh} + \frac{X_2}{kT_e}\frac{d \ln T_e}{dh} \\ &= -\frac{d \ln n_\infty}{dh} - \frac{d \ln b_2}{dh} + \frac{X_2}{kT_e}\frac{d \ln T_e}{dh}. \end{aligned} \tag{21}$$

In Paper I, the b_2 term was explicitly ignored, and these results were used to infer $d \ln T_e/dh$. With the present values, this procedure would lead to $d \ln T_e/dh < 0$. It would then appear that the $d \ln b_2/dh$ term is the larger, numerically, of the last two

terms in equation (21). Thus some further attempt to increase the amount and reliability of the information from these 1932 data seemed warranted.

Combining equations (14) and (10), we have

$$\Delta_n \log E_{n2} - \Delta_n \log [A_{n2}(n^2-4)] - \Delta_n \frac{X_n}{2.3kT_e} - \Delta_n \log b_n = -0.076\Delta_n (N_2 a_n)^{3/4}. \tag{22}$$

Given the last two terms on the left, both of which are presumably small, we can compute $(N_2 a_{30})$ from any pair of lines. Because various estimates on conditions in the chromosphere have given, approximately,

$$6000^\circ < T_e < 35{,}000^\circ, \tag{23}$$

we solve equation (22) for the three cases: (i) $T_e = 6000^\circ$, $b_n = 1$; (ii) $T_e = 35{,}000^\circ$, $b_n = 1$; (iii) $T_e = 35{,}000^\circ$, $b_n =$ the values computed by Thomas (1949) as an *upper* limit on b_n for this T_e and $n_e = 2 \times 10^{11}$. This set formed the only values available for our region of interest, $n > 10$; but, because they are an upper limit, they should certainly cover the range of b_n values likely to be of interest. The $b_n = 1$ for case i are consistent with physical expectation and the empirical result of q in the least-squares solution. We restrict our data to $n > 10$; and evaluate N_2 from equation (22) for all combinations of lines with $\Delta n = 3$ and 5. Table 2 contains the results.

It is of considerable interest to note that the range in N_2 across the rather extreme range in T_e is a factor of only 2.5, 90 per cent of which comes from the $T_e^{1/2}$ factor in a_n. That is, $N_2 a_{30}$ is well determined, quite apart from any uncertainty in b_n. And, of course, the uniform results in $d \ln n_2/dh$ $(\equiv d \ln N_2/dh)$ come just from this fact. Moreover, the data do not appear to show much variation with height for this quantity. Thus $0.9 < N_2 \times 10^{16} < 2.2$ at 670 km and

$$\frac{d \ln n_2}{dh} \sim 0.85 \times 10^{-8} \text{ cm}^{-1}. \tag{24}$$

Unfortunately, not much can be inferred from the results as to which of cases i–iii is the more likely one. The 1952 eclipse expedition from the High Altitude Observatory was planned to take somewhat better advantage of this self-absorption effect; so, before discussing the significance of the foregoing results, we treat the 1952 data.

IV. THE 1952 OBSERVATIONS

We use the data presented by Athay, Billings, Evans, and Roberts (1954), which contain observations up through $H31$, at intervals of 110 km, from 530 to 2400 km, and through $H12$ up to 3720 km, at somewhat greater intervals of height. Since the 1932 observations had a height interval of 830 km and results through $H30$ at only two heights, the 1952 data should permit considerably greater accuracy.

We have already noted that the 1932 data do not appear to require including a b_n effect. We obtain a quick pictorial view of both 1932 and 1952 data by considering the quantity

$$R_n = \log E_{n2} \text{ (observed)} - \log E_{n2} \text{ (thin-atmosphere, thermodynamic equilibrium)}$$

$$= \log E_{n2} \text{ (obs.)} - \log A_{n2}(n^2-4) - \frac{X_n}{kT_e} - \text{Const.} \tag{25}$$

$$= \log b_n + \log \text{ (Abs.)}.$$

TABLE 2

$N_2 \times 10^{-16}$

Height (km)	$T_e = 6000°$, Incl. exp X_n				$T_e = 35{,}000°$, Incl. b_n exp X_n				$T_e = 35{,}000°$ No b_n Incl. exp X_n			
	670	1500	2330	3170	670	1500	2330	3170	670	1500	2330	3170
25–30	1.20	13.70*	.....	.....	3.14	35.7*	.....	.....	2.53	33.1*	.....	.....
24–29	1.04	3.48*	.....	.....	2.72	9.15*	.....	.....	2.51	8.40*	.....	.....
23–28	0.64	0.37	.....	.....	1.65	0.95	.....	.....	1.49	0.86	.....	.....
22–27	1.54	†	.....	.....	4.11	†	.....	.....	3.74	†	.....	.....
21–26	0.47	†	.....	.....	1.23	†	.....	.....	1.03	†	.....	.....
20–25	0.94	†	.....	.....	2.49	†	.....	.....	1.79	†	.....	.....
19–24	0.39	†	.....	.....	1.03	†	.....	.....	0.94	†	.....	.....
18–23	1.50	0.14	.....	.....	3.91	0.36	.....	.....	3.41	0.31	.....	.....
17–22	0.27	0.15	.....	.....	0.72	0.39	.....	.....	0.63	0.33	.....	.....
16–21	0.84	0.85	.....	.....	2.26	2.30	.....	.....	1.90	1.93	.....	.....
15–20	0.31	0.22	.....	.....	0.85	0.62	.....	.....	0.72	0.46	.....	.....
14–19	0.41	0.29	.....	.....	1.13	0.79	.....	.....	0.88	0.63	.....	.....
13–18	0.09*	0.23	.....	.....	0.26*	0.67	.....	.....	0.22*	0.51	.....	.....
12–17	0.33	0.25	0.46*	.....	0.93	0.75	1.00*	.....	0.69	0.54	0.75*	.....
11–16	0.39	0.26	0.46*	.....	1.12	0.75	0.98*	.....	0.76	0.52	0.70*	.....
10–15	0.35	0.29	0.18	.....	1.02	0.88	0.37	.....	0.71	0.52	0.25	.....
27–30	1.18	†	.....	.....	2.91	†	.....	.....	2.83	†	.....	.....
26–29	†	1.98*	.....	.....	†	4.60*	.....	.....	†	4.47*	.....	.....
25–28	2.04	4.63*	.....	.....	5.22	11.03*	.....	.....	4.92	10.40*	.....	.....
24–27	1.75	2.56*	.....	.....	4.48	6.11*	.....	.....	4.23	5.77*	.....	.....
23–26	0.56	†	.....	.....	1.44	†	.....	.....	1.36	†	.....	.....
22–25	1.69	†	.....	.....	4.33	†	.....	.....	4.08	†	.....	.....
21–24	†	†	.....	.....	†	†	.....	.....	†	†	.....	.....
20–23	1.75	0.90	.....	.....	4.48	2.14	.....	.....	4.23	2.02	.....	.....
19–22	5.23*	1.04	.....	.....	13.86*	2.56	.....	.....	12.60*	2.33	.....	.....
18–21	2.11	0.40	.....	.....	5.41	0.97	.....	.....	4.92	0.88	.....	.....
17–20	0.30	†	.....	.....	0.76	†	.....	.....	0.69	†	.....	.....
16–19	0.50	0.79	.....	.....	1.28	1.97	.....	.....	1.13	1.74	.....	.....
15–18	0.24	0.57	.....	.....	0.63	1.38	.....	.....	0.56	1.22	.....	.....
14–17	0.20*	0.29	0.21	.....	0.53*	0.71	0.53	.....	0.45*	0.61	0.45	.....
13–16	0.10*	†	0.33	.....	0.27*	†	0.81	.....	0.23*	†	0.69	.....
12–15	0.24	0.12	0.09	.....	0.65	0.30	0.22	.....	0.54	0.25	0.18	.....
11–14	0.40	0.38	0.43	.....	1.07	0.94	1.07	.....	0.86	0.76	0.86	.....
10–13	0.47	0.47	0.19	0.08	1.28	1.20	0.48	0.19	0.97	0.91	0.36	0.14
15–17	.....	.....	1.33*	.....	.....	.....	3.28*	.....	.....	.....	3.11*	.....
14–16	.....	.....	0.07	.....	.....	.....	0.19	.....	.....	.....	0.17	.....
13–15	.....	.....	†	.....	.....	.....	†	.....	.....	.....	†	.....
12–14	.....	.....	0.45*	.....	.....	.....	1.18*	.....	.....	.....	1.03*	.....
11–13	.....	.....	0.34	0.13	.....	.....	0.79	0.35	.....	.....	0.67	0.29
10–12	.....	.....	0.14	0.11	.....	.....	0.37	0.30	.....	.....	0.30	0.24
Mean...	0.852	0.422	0.221	0.107	2.223	1.086	0.537	0.280	1.966	0.912	0.437	0.223
$d \ln N_2^0/dh$	0.85	0.78	0.86		0.86	0.65	0.78		0.92	0.91	0.80	

* These entries show abnormally large departures from the mean and were not included in the average value of N_2.

† The data for these entries gave negative values of N_2.

Figure 2 exhibits R_n versus n. The horizontal line represents, in each case, the mean of R_n and serves only as a reference axis. The difference in trend of R_n versus n as h increases is marked in the 1952 data. If we regard this effect as the combination of a decrease in self-absorption with height and of the $b_n > 1$, the trend is understood.

We then repeat the least-squares analysis of Section III, with one change, using

$$\log b_n = s + tn \tag{26}$$

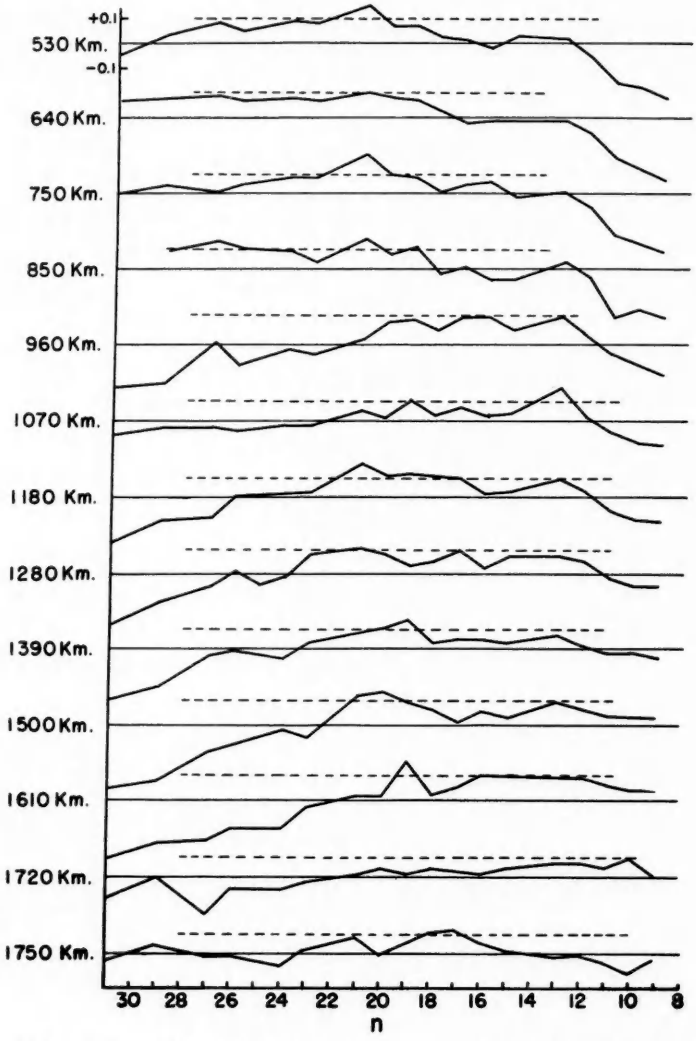

FIG. 2*a*.—Relative amount of log b_n (Abs.) for heights between 530 and 1750 km, using 1952 data

rather than relation (18). Although equation (18) is more precise, actual computation gives little difference. The solution proceeds by successive approximations, stopping when the probable errors in $\Delta(N_2\alpha_{30})$ and t become comparable with the differential correction. As in the analysis of the 1932 data, the significance of adding a term in n^{-2} to account for the Boltzmann factor was tested, and the term was judged negligible. Further, those lines recognized as strong blends have been omitted from the analysis, viz.: *H*8, *H*14, *H*25, *H*28, *H*30. The lowest line included in the solution appears in brackets after the height in Table 3, which contains the results of the solution. (This limit on the lowest line to be included is placed by the self-absorption expansion.)

As discussed in the analysis of the 1932 data, determining N_2 from the $N_2\alpha_{30}$ values

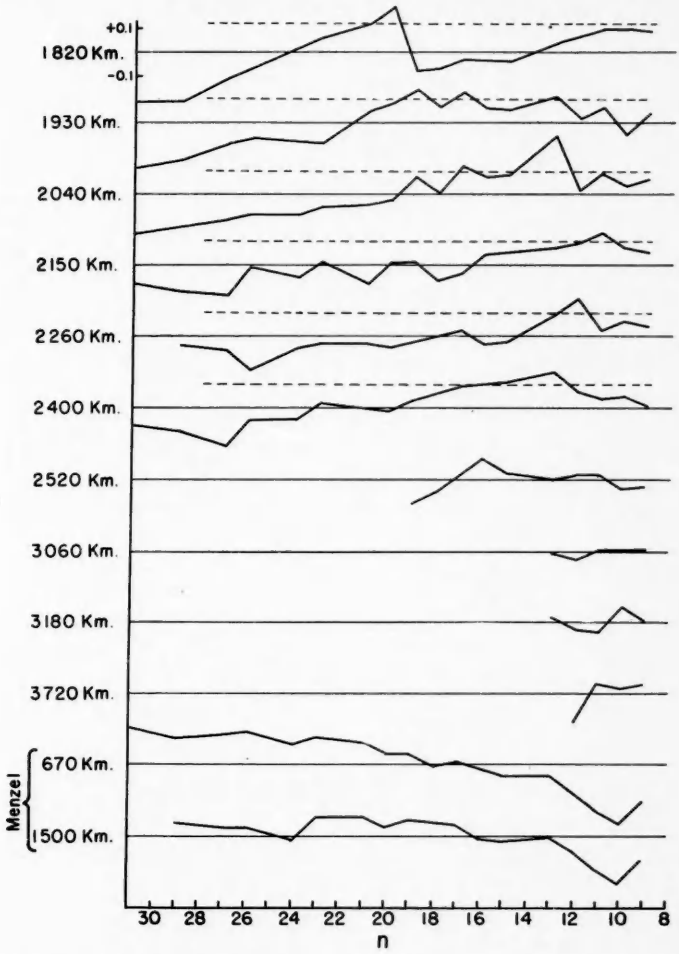

FIG. 2*b*.—Relative amount of log b_n (Abs.) for heights between 1820 and 3720 km, using 1952 data, and for heights of 670 and 1500 km, using 1932 data.

requires a knowledge of T_e, since $\alpha \propto T_e^{-1/2}$, but $d \ln n_2/dh$ is independent of this factor. Thus Figure 3 exhibits N_2 for $T_e = 35{,}000°$, from Table 3, and all points should simply be displaced by 0.38 in log N_2 to obtain the results for $T_e = 6000°$. All points save those plotted as X appear well represented by a straight line—and the solid lines represent this relation for 35,000° and 6000°. It is hard to justify excluding the X-values, on other grounds than numerical consistency, but we have done so, since the scatter introduced by them does not seem systematic. Indeed, we note that it is these four points that show the greatest scatter in the values of t, again not in any systematic manner. Thus we ignore them. The remaining values of t appear as constant with height as their accuracy allows inference, with a value of $t \sim -0.022$. We summarize the results thus:

$$\log N_2 = 16.37 + \tfrac{1}{2} \log \left(\frac{T_e}{5040} \right) - 0.58 \times 10^{-8} h \,, \tag{27}$$

$$\log b_n - \log b_{n+k} = 0.022 k \,. \tag{28}$$

TABLE 3

LEAST-SQUARES ANALYSIS OF THE 1952 DATA

h	$N_{2\alpha 30} \pm \epsilon$		$t \pm \epsilon$		h	$N_{2\alpha 30} \pm \epsilon$		$t \pm \epsilon$	
530 (*H*15)	1.19	0.10	−0.021	0.015	1930 (*H*9)	0.16	0.01	−0.027	0.007
750 (*H*13)	0.83	.47	+ .024	.11	2040 (*H*9)	.12	.01	− .019	.006
960 (*H*12)	0.54	.04	− .028	.010	2150 (*H*9)	.06	.01	− .008	.004
1180 (*H*11)	0.41	.05	− .023	.014	2260 (*H*9)	.06	.01	− .006	.006
1390 (*H*11)	0.45	.04	− .029	.011	2400 (*H*9)	.09	.01	− .014	.006
1610 (*H*10)	0.22	.02	− .023	.009	3060 (*H*9)	.04	.01	− .013	.007
1820 (*H*9)	0.19	0.04	−0.023	0.018	3180 (*H*9)	0.04	0.01	−0.032	0.018

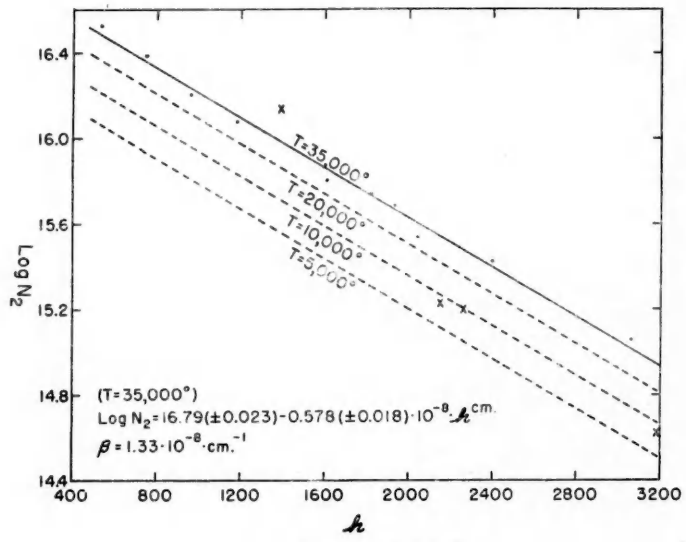

FIG. 3.—Log N_2 versus height

Simply for comparison, because they are the only results available on b_n for these high n's, in Figure 4 we plot Thomas' upper limit on b_n for $T_e = 35{,}000°$. Plotted points represent the computed b_n, and the solid curve represents the best fit of equation (26) to them. The dotted curve represents equation (28), with, of course, an arbitrary constant displacement permitted in the ordinate.

V. DISCUSSION

Our purpose has been to investigate the Balmer decrement observed at the 1932 and 1952 eclipses, aiming to separate the effects of self-absorption and non-Boltzmann distribution for the occupation numbers. Our analysis would give at best an absolute measure of the self-absorption and relative values of the non-Boltzmann term, b_n. While

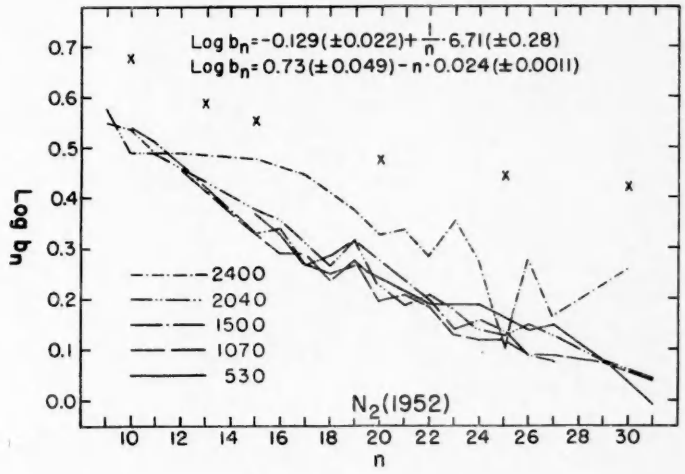

FIG. 4.—Log b_n versus n

neither self-absorption nor relative b_n gives a direct measure of T_e, we had hoped that some indirect measure of T_e might result from each and also from a combination of these results on emission lines with those from the continuum. This combination of line and continuum measures will be treated in a following paper. Consider a brief comment on the first, indirect, measure of T_e.

The apparent invariance of the relation $b_n(n)$ as h changes would appear to indicate that T_e changes fairly slowly in the region under investigation (530 km $\leq h \leq$ 3000 km). The greater slope of the empirical relation than that of the computed b_n in Figure 4 would, at first sight, appear to indicate that T_e actually exceeds the 35,000° figure for which the computations were performed, since the slope should increase with T_e. We note, however, an inconsistency in our analysis, which casts doubt upon too detailed an analysis of this behavior of b_n. We have assumed the same constant logarithmic height gradient for all occupation numbers (eq. [3]). Yet, while the gradient of the higher lines indicates $\beta \sim 1.7 \times 10^{-8}$ cm^{-1} in 1932 and $\sim 2.2 \times 10^{-8}$ cm^{-1} in 1952, the results in N_2 suggest $\beta_2 \sim 0.85 \times 10^{-8}$ cm^{-1} in 1932 and $\sim 1.35 \times 10^{-8}$ cm^{-1} in 1952. This result causes complications only in the expression for the self-absorption, where β_2/β_n enters as a parameter. Our adopted expression (5) rests on the assumption $\beta_2/\beta_n = 1$. Thus our

results are not completely self-consistent, and any extended discussion of them must await our evaluation of the effect of this $\beta_2/\beta_n \neq 1$. Thomas (unpublished) has suggested a method of investigating the effect of $\beta_2 \neq \beta_n$, working with the observed β_n (which are much better determined from the 1952 data than from the 1932) rather than the E_{n2}. A following paper by Athay and Thomas treats the problem. Thus we believe we have established $\beta_2 < \beta_\infty$, and advanced strong evidence that not only is $d \ln b_2/dh > 0$, but the numerical magnitude is of the order of 1×10^{-8} cm^{-1}. This result provides a strong boundary condition for any model of the chromosphere.

Finally, we recognize that, while the $N_2\alpha_{30}$ inferred from the analysis may change with the explicit form of (Abs.), the present analysis can leave little question as to its presence, contrary to the doubt expressed by van de Hulst (1953). Thus the procedure of inferring empirical b_n from a combination of continuum and line measures, ignoring the effects of self-absorption, as suggested originally by Menzel and Cillié (1935) and reiterated by van de Hulst (1953), can hardly be accepted.

This work was supported by the Office of Naval Research and carried out in co-operation with the Naval Research Laboratory. The author is further indebted to the University of Utah for a research fellowship; to the High Altitude Observatory and Dr. W. O. Roberts for research fellowships and the opportunity to work there; and to Harvard College Observatory and Dr. D. H. Menzel for the opportunity to work there. He is indebted to Dr. R. G. Athay, Dr. J-C. Pecker, and Dr. Max Krook for discussions of the problems considered here; and particularly to Dr. R. N. Thomas, with whom the author has carried out his study.

REFERENCES

Athay, R. G., Billings, D. E., Evans, J. W., and Roberts, W. O. 1954, *Ap. J.*, **120**, 94.
Cillié, G. C., and Menzel, D. H. 1935, *Harvard Obs. Circ.*, No. 410.
Hulst, H. C. van de. 1953, *The Sun*, ed. G. P. Kuiper (Chicago: University of Chicago Press), p. 207.
Thomas, R. N. 1949, *Ap. J.*, **109**, 480.
———. 1950, *ibid.*, **111**, 165.

THE THERMODYNAMIC STATE OF THE OUTER SOLAR ATMOSPHERE IV. SELF-ABSORPTION AND THE POPULATION OF THE SECOND QUANTUM LEVEL

R. G. Athay and R. N. Thomas
High Altitude Observatory and Harvard College Observatory
Received August 30, 1954

ABSTRACT

The quantitative dependence of the observed logarithmic emission gradient, β_n, of the Balmer lines upon quantum number provides a direct substantiation of the influence of self-absorption on the higher lines (n greater than about 10). An analysis assuming that the (β, n) dependence arises *only* from self-absorption permits a direct determination of the population of the second quantum level, n_2, as a function of height, leading to a scale height of ~2000 km for n_2 by contrast with ~500 km for the highest quantum levels. The scale height for the non-Boltzmann term, b_2, is thus ~600 km. The derived self-absorption is so large that at $H11$ only some 7 per cent of the (slitless spectrograph) emission at $h = 1000$ km escapes from the chromosphere. The analysis is self-consistent, provided that T_e is sufficiently low that b_{10} is less than about 2; a discrepancy arises because the line emission is relatively too great for that of the continuum, leading to excessive empirical b_n. The question of a nonuniform chromosphere arises and is deferred, together with a general model, pending the analysis of the continuum.

I. INTRODUCTION

The first two papers in this series (Thomas 1950*a*, *b*) discussed an empirical approach to the problem of the thermodynamic state of hydrogen in the solar chromosphere. In essence, the approach centered on three points: (1) an interpretation of the observed Balmer decrement for the higher lines, n greater than about 10; (2) a comparison of the line emission with that in the Balmer continuum; and (3) a further comparison of the emission in the Balmer continuum with that in greater wave lengths. The discussion of the Balmer decrement contrasts the observed decrement with that expected from a thin atmosphere in thermodynamic equilibrium. We interpret the difference as a measure of the self-absorption and the departures from thermodynamic equilibrium. Absolute values of self-absorption and relative values of nonequilibrium effects result. These relative values may be converted to absolute values by combining data from the free-bound Balmer continuum with the line data. The combination of the two continua, in and outside the Balmer free-bound region, should provide values for electron temperature and density, T_e and n_e, respectively.

The preliminary analysis in Paper I treated only a portion of the 1932 data discussed by Menzel and Cillié (1935), but it became evident that the amount of data was not sufficient—in view of their uncertainty—to obtain all the desired information. Thus the need for two kinds of extension of the work became evident. First, more of the same kind of data should be obtained at a future eclipse, with greatly increased resolution in chromospheric height and also including the Paschen region. Second, a more detailed analysis of the 1932 data should be made, using all the available observations. This first objective has been largely accomplished, and the results of preliminary reduction and analysis of the data are reported elsewhere (Athay, Billings, Evans, and Roberts 1954). The second objective, a more detailed treatment of the 1932 data, has been attempted by Matsushima. He also applied the same analysis to the 1952 data, and the two analyses appear in the preceding paper in this series (Matsushima 1954).

This analysis by Matsushima represents a straightforward attempt to apply the concepts developed in the first paper of this series to all the available data. In essence, the procedure assumes that the major differences between the observed Balmer decrement

and that for a thin atmosphere in thermodynamic equilibrium, for the Balmer lines of n greater than about 10, comes from a self-absorption effect, with the nonequilibrium contribution forming a small perturbation. It is somewhat difficult to infer the validity of the assumption from the results. While the last part of this analysis was in progress, van de Hulst presented (1953) a summary of the physical state of the chromosphere, in which he argued against the necessity to include these self-absorption effects in the higher Balmer lines, n greater than about 10, and interpreted the Balmer decrement in terms of $b_n < 1$. The principal objective of our 1952 efforts was to provide sufficient data in unambiguous form for the validity of the conclusions based on the 1932 data to be checked in detail. Because of the greatly increased height resolution of the 1952 data, we find it possible to argue somewhat more directly toward ascertaining those physical parameters required in any interpretive theory of the Balmer lines. Unfortunately, the plates were underexposed in the Paschen region, so we lack the possibility of applying the important check which would be furnished by the Paschen series. In this paper, therefore, we restrict our discussion to a simple attempt to establish the validity of the self-absorption effect in the higher lines, together with its magnitude, and to establish the direction of the inequality $b_n \gtrless 1$.

II. OBSERVATIONAL FEATURES OF THE BALMER LINES IN THE CHROMOSPHERE

In the following, we refer to eclipse observations made with a slitless system. The observations thus imply an integration through the solar atmosphere along the line of sight and above the moon's limb. From a purely empirical basis, three aspects of the hydrogen emission seem well established in the literature of eclipse observations:

(0–1): There exists some height, above which the logarithm of the emission in each hydrogen line decreases linearly with height, to the accuracy of the existing observational data.

(0–2): The slope of the straight-line portion in (0–1) shows a numerical decrease with (principal) quantum number of the line. An alternative statement is that the Balmer decrement increases with height. (The Paschen decrement has been insufficiently observed for comment.)

(0–3): The slopes differ from one eclipse to another; and localized regions of the solar atmosphere may show large departure from the mean at a given eclipse.

A concise statement of the van de Hulst approach and our own lies in the observation that he ignores (0–2) and (0–3), whereas our analysis rests upon the assumption that these observations represent physical effects. We interpret (0–2) in terms of self-absorption and departures from a Boltzmann distribution. In the first approximation to the structure we explicitly neglect (0–3). In essence, the problem is the difference between an observed emission gradient and an actual density gradient.

Although other data exist, we restrict our discussion here to the 1952 data. The primary advantage of these data over those from 1932, for our immediate purpose, lies in the greater height resolution. Thus the 1932 observations provided values of E_{n2} at four heights for five lines, and at but two heights for most of the lines. From the 1952 data, we have observations at eighteen heights for all lines, $H8$–$H31$, and at twenty-one heights for five lines, $H12$–$H8$. Thus, for the 1952 data, we may work directly with the slopes, having strong confidence in their reliability from a detailed numerical standpoint, while for the 1932 data we were able to rely only on a trend.

a) THE CHARACTER OF THE EMISSION HEIGHT GRADIENT

The observed total emission from line H_n is

$$E_{n2} = \int_0^\infty \int_{-\infty}^{\infty} \int_h^\infty \frac{n_n A_{n2} \nu_{n2} h_p}{4\pi} f(\nu)\, d\nu\, e^{-\tau_n} dy\, dx\,, \tag{1}$$

with x measured along a solar radius and y orthogonal to it, toward the observer. Here n_n represents the volume density of the population of energy state n (ignoring fine structure, n is the principal quantum number), and h is the position of the moon's limb; $f(\nu)d\nu$ represents the line contour, which we assume is Doppler; h_p is Planck's constant. The optical depth, τ_n, is

$$\tau_n = \int_y^\infty \alpha_{2n\nu} n_2 \left[1 - \frac{B_{n2}}{B_{2n}} \frac{n_n}{n_2}\right] dy \,, \tag{2}$$

with the same factor $f(\nu)$ appearing in $\alpha_{2n\nu}$. The A's and B's are the Einstein coefficients.

Consider the empirical result (0–1) that log E_{n2} is linear in h and varies monotonically with n, above a certain height h. Throughout the discussion, we assume a homogeneous

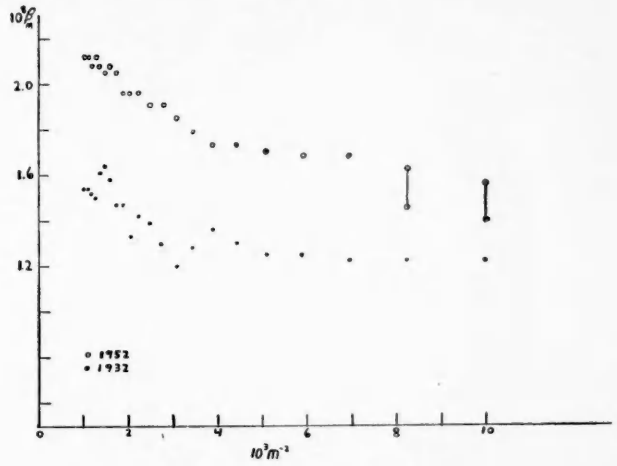

FIG. 1.—A plot of β_n versus n^{-2} showing a nonlinear relationship

atmosphere. (We plan to exhaust its possibilities before turning to the nonuniform case.) Then the empirical relation,

$$E_{n2} = \text{Const. } e^{-\beta_n h} \,, \tag{3}$$

applied rigorously to equation (1) requires

$$n_n e^{-\tau_n} = \text{Const. } e^{-\beta_n h} \tag{4}$$

(all the constants may depend upon n, through atomic constants).

For negligible self-absorption, equation (4) implies an exponential variation of n_n with h, and the dependence of β_n upon n must come, then, wholly through that of n_n upon n. The modified Boltzmann-Saha relation gives

$$n_n = \left(\frac{h_p^2}{2\pi k m}\right)^{3/2} n_e n_p T_e^{-3/2} e^{\chi_n/kT_e} b_n n^2 \,. \tag{5}$$

If $\beta(n)$ results from the excitation term χ_n, it should be proportional to n^{-2} (and, incidentally, from the direction of the variation, would require T_e to decrease outward). Figure 1 contains the data from the 1932 (Cillié and Menzel 1935) and 1952 (Athay *et al.*

1954) eclipses. We plot β_n versus n^{-2}. The (β, n^{-2}) relation is hardly linear. Thus an explanation of the $\beta(n)$ relation mainly in terms of an excitation effect through X_n must be discarded.

The other n-dependent term in equation (5), which may vary with height in the chromosphere, is b_n. For the $\beta(n)$ dependence to arise mainly from $d \ln b_n/dh$, this last quantity must, in the vicinity of $n = 10$, have a value near $+0.6 \times 10^{-8}$ cm^{-1} and be larger, the lower the height in the atmosphere. This numerical value is implausible on the basis on what computations of b_n exist and for reasonable assumptions of T_e in this height range. The direction of change of the numerical value is even less plausible—it would appear to require T_e considerably exceeding $10^{4\circ}$ K near 100 km in the chromosphere, and *dT_e/dh decreasing* outward. We conclude, then, that at least a part of the dependence of β_n on n results from something other than the gradient of n_n, i.e., from self-absorption.

For nonnegligible self-absorption, the inference of an exponential variation of n_n with h from equation (4) fails. The obvious suggestion is that the self-absorption becomes negligible at such heights that equation (3) is precisely true. For those (low) heights where β_n varies with height, the self-absorption would then enter. We note, however, that a small or slowly varying self-absorption, coupled with a reasonable amount of observational scatter, may introduce the observed relation (3), in the case that n_n is exponential with height, viz.,

$$n_n = \text{Const. } e^{-\gamma_n h} . \tag{6}$$

For equation (1) then integrates directly to

$$E_{n2}(h) = \sqrt{(2\pi R_\odot)} \frac{A_{n2} h_p \nu_{n2}}{4\pi} \gamma_n^{-3/2} n_n(h) \sum_{m=0}^{\infty} c_m (N_2 \alpha_{2n})^m , \tag{7}$$

where

$$N_2 = n_2(h) \gamma_2^{-1/2} \sqrt{(2\pi R_\odot)} , \tag{8}$$

where $R_\odot$ is the solar radius, α_{2n} the absorption coefficient at the line center, and

$$c_m = (-1)^m [2^m m! (1 + m k^{-1}) (1 + m)^{1/2}]^{-1} \sum_{j=0}^{m/2} \frac{m!}{(2j)!(m - 2j)!} I_{k, 2j} ,$$

$$k = \frac{\gamma_2}{\gamma_n} , \tag{9}$$

$$I_{k, l} = 2\sqrt{\frac{k}{\pi}} \int_0^\infty e^{-k^2 t^2} \left[\frac{2}{\sqrt{\pi}} \int_0 e^{-s^2} d_s \right]^l dt .$$

The sum in equation (7) represents the self-absorption. Thus

$$-\beta_n = \frac{d \ln E_{n2}}{dh} = -\gamma_n + \gamma_2 (N_2 \alpha_n) c_1 \left[1 - \sum_1^\infty d_s (N_2 \alpha_n)^s \right] , \tag{10}$$

with the last term, which is self-absorption, being of the form

$$a z e^{-z} + \sum_{j=3}^{\infty} a_j z^j \qquad (a_j \text{ small}) , \tag{11}$$

and this function varies slowly near $z = 1$. Thus for small self-absorption, the second term in equation (10) is small; and for reasonable variation in $N_2\alpha$ (with height, say), the variation in β_n will be small. For $N_2\alpha$ larger, corresponding to z near 1, β_n will again show

small variation. Figure 2 demonstrates the feasibility of the suggestion, containing a plot of β_n versus f_{2n} (f_{2n} is the oscillator strength, thus proportional to a_{2n}).

A quantitative evaluation of the contribution of self-absorption to the β_n may be accomplished from two directions. First, the Balmer decrement provides values of the differential self-absorption. Second, we note that the free-bound emission at the head of the Balmer continuum may be written as follows:

$$E_{3647}d\nu = \frac{Kh_p}{8}\frac{\sqrt{(2\pi R_\odot)}}{4\pi}\gamma_\infty^{-3/2}(n_e n_p T_e^{-3/2})_{h=0}e^{-\gamma_\infty h}d\nu\,, \tag{12}$$

under the assumption

$$n_e n_p T_e^{-3/2} = \text{Const. } e^{-\gamma_\infty h} \tag{13}$$

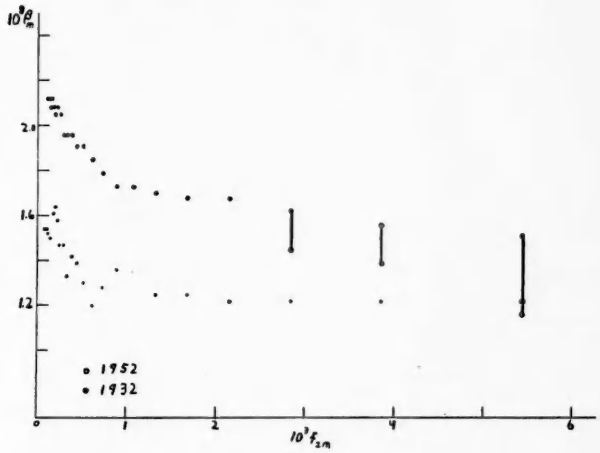

FIG. 2.—A plot of β_n versus f_{2n}

(eq. [13] corresponds to eq. [6] for large n). Using equation (6) and

$$X_n = \frac{\chi_n}{kT_e},$$

equations (7) and (12) then give

$$[b_n(\text{Abs.})\ e^{X_n}] = \frac{E_{n2}}{E_{3647}}\left(\frac{\gamma_n}{\gamma_\infty}\right)^{3/2}(A_{n2}n^2\nu_{n2})^{-1}\frac{K}{8}\left(\frac{2\pi k m}{h_p^2}\right)^{3/2}, \tag{14}$$

providing a measure for b_n and self-absorption. Note that the early discussion by Cillié and Menzel, echoed by van de Hulst, ignores all terms on the left of equation (14) but b_n. Further, the discussion implicitly sets $\gamma_n = \gamma_\infty$ in the numerical computations. We have already remarked that $\gamma_n = \gamma_\infty$ requires the whole dependence of β_n upon n to come from self-absorption, whose effect van de Hulst dismisses. We consider the two approaches in the following two sections.

b) SELF-ABSORPTION FROM THE DEPENDENCE OF β_n UPON n

If γ_n varies significantly with n, a discussion based only on equation (10) and the observed β_n provides no information on self-absorption. We have already considered—

and rejected—the case that self-absorption can be completely neglected and the whole $\beta(n)$ dependence ascribed to $d \ln n_n/dh$ through b_n and the excitation term. Consider the other extreme assumption, that γ_n does not depend upon n, for $n \geq 10$.

From equation (10), with constant γ_n, β_n depends upon n through a_{2n}—hence through f_{2n}—except for the dependence of the d_s upon $(\gamma_n/\gamma_2) = k$. Setting

$$w = N_2 a ,$$

we use equation (9) to evaluate equation (10) for $k = 1, 2, 3, 4, 5$. Because of the requirement of constant γ_n, $n \geq 10$, and the physical requirement that the higher Balmer lines merge smoothly into the continuum, we impose the added condition (from observations on the Balmer continuum):

$$\gamma_n = \gamma_\infty = 2.2 \times 10^{-8} \text{ cm}^{-1} . \tag{15}$$

Then we reduce the resulting expression to a power series in z, defining z from the series expansion so that it may be taken directly over to the form (11). Table 1 contains the

TABLE 1

β_n REPRESENTATIONS ($n > 10$)

EMPIRICAL ($f' = 10^3 f$)

Exp. about $f' = 0$ $\beta_n = 2.17 - 1.59z[1 - z + 0.363z^2 - 0.021z^3]$ $z = 0.405f'$
Exp. about $f' = 2$ $\beta_n = 2.23 - 1.48z[1 - z + 0.438z^2 - 0.067z^3]$ $z = 0.662f'$

THEORETICAL

$k=\gamma_n/\gamma_2$	γ_2		
1.....	2.20	$\beta_n=2.20-2.09z[1-z+0.676z^2-0.240z^3+0.0555z^4\ldots]$	$z=0.186w$
2.....	1.10	$\beta_n=2.20-1.90z[1-z+0.579z^2-0.157z^3\ldots]$	$z=0.137w$
3.....	0.71	$\beta_n=2.20-1.65z[1-z+0.531z^2+0.024z^3-0.267z^4\ldots]$	$z=0.114w$
4.....	0.55	$\beta_n=2.20-1.54z[1-z+0.447z^2+0.119z^3-0.274z^4\ldots]$	$z=0.101w$
5.....	0.44	$\beta_n=2.20-1.41z[1-z+0.361z^2+0.189z^3\ldots]$	$z=0.092w$

results. Using the 1952 data—the 1932 are clearly inadequate because of the small number of heights at which observations were made for each line—an empirical representation as a power series in the f_{2n} was made by least squares. The two empirical representations in Table 1 refer to expansions about $f_{2n} = 0$ and $f_{2n} = 2 \times 10^{-3}$. Clearly, the former weights the large values of f_{2n} disproportionately in the determination of the coefficients of the higher powers of f_{2n}, so we prefer the results from the expansion about $f_{2n} = 2 \times 10^{-3}$. Representations out to the third, fourth, and fifth powers of f_{2n} were attempted, and the residuals indicated that the representation out to f_{2n}^4 should be used for our discussion.

Comparing the empirical representations with the theoretical expressions for the self-absorption, we find good agreement for k between 3.5 and 4.5 in the first two coefficients of the absorption expression. The check between γ_∞ and γ from the empirical solution is quite good. The third coefficient of the absorption expression differs considerably from that of the theoretical expressions. We note, however, that the first two coefficients in the empirical absorption expression refer to that part of the curve where z is small, and should thus be reasonably well determined. On the other hand, when z nears 1, a large number of terms in the theoretical expressions becomes necessary (compare the run of the coefficients), and the third empirical coefficient (in the self-absorption expression) represents a "mean" effect over the range of empirical data used. (But a very bad fit for extrapolation!) Thus this comparison of empirical fit with theoretical expression for self-absorption

would indicate that the self-absorption with

$$10^8\gamma_n(n \geq 10) \sim 2.2 \pm 1 \text{ per cent}, \qquad 10^8\gamma_2 \sim \tfrac{1}{4}\gamma_n \sim 0.55 \pm 15 \text{ per cent},$$
$$N_2a_{2n} \sim 6.6f'_{2n} \pm 50 \text{ per cent}, \tag{16}$$

is capable, by itself, of providing the variation with n of the β_n values from the 1952 eclipse. Several comments arise.

First, because β_n, $n \geq 12$, is constant with height to the accuracy of estimation from the data, the precise height at which the foregoing value of N_2a applies is dubious. But, because γ_2 is so small, corresponding to a scale height of 2000 km while the data cover the interval 500–2500 km, the problem is not serious in view of the accuracy given in relations (16). That is, using a self-absorption corresponding to $N_2a_n \sim 6.6f'_{2n}$ somewhere in the range 1000–2000 km (the range used by Athay in his determination of the β_n values used here), we obtain a reasonable representation of the data. For example, we integrate the empirical expression with $f' = 2$ in Table 1, using $\gamma_2 = 0.55 \times 10^{-8}$, to obtain

$$\ln E_{n2} = \text{Const. } (n) - 2.20 \times 10^{-8}h - 2.70z\,[1 - 0.5z + 0.146z^2 - 0.0168z^3]\,. \tag{17}$$

Adjusting the constant to agree with observation at 1500 km and choosing the N_2a value to apply here, viz.,

$$z = 0.662f'_{2n} \exp\,[-0.55(h - 1500 \text{ km})10^{-8} \text{ cm}^{-1}]\,, \tag{18}$$

we obtain the solid curve in Figures 3*a*, 3*b*, 3*c*, and 3*d*. Clearly, the agreement is as good as the scatter in observational data permits. We have of course not *proved* that the whole β_n dependence on n comes through self-absorption, or even that the value of N_2a chosen is the correct one. We have only demonstrated that the self-absorption coupled with a constant height gradient for $\ln n_n$ can reproduce $E_n(h)$ very satisfactorily.

Second, the small value of γ_2 requires a large positive value of $d \ln (b_2e^{X_2})/dh$. If this results from the X_2 terms, T_e must *decrease outward* at such a rate as to be physically impossible in view of the whole body of observations on the chromosphere. Thus we conclude that

$$\frac{d \ln b_2}{dh} \geq 1.6 \times 10^{-8} \text{ cm}^{-1}. \tag{19}$$

Such a result may seem startling at first sight, in view of our neglect of $d \ln b_n/dh$, $n \geq 10$. A rough set of computations is given in Table 2. These computations are particularly uncertain for the high values of n_e at low T_e, for the optical depth in the Lyman continuum enters exponentially as a direct factor in b_1 (Thomas 1952). Thus we expect a greater effect of n_e on b_1 and b_2 than Table 2 implies. Particularly, the effect should be of interest in the range $T_e < 10^4$, which has been omitted here not from lack of interest but because the problem—with a proper inclusion of the Lyman continuum—has not been solved. Nonetheless, these rough computations illustrate the possibility of extremely rapid variation of b_2 with only small effect in b_n, $n > 10$, at least until very high temperatures appear. Thus the result on $d \ln b_2/dh$ does not contradict the assumption on $d \ln b_n/dh$, $n \geq 10$, in the sense that there appears to be a range of values of (n_e, T_e) within which the result and assumption would be compatible.

Finally, the value of the constant which must be adopted in equation (17) provides a comment on the consistency of the approach. From equations (8) and (6), that part of the constant dependent upon n should be $[A_{n2}(n^2 - 4)b_ne^{X_n}]$. Thus

$$\Delta_n \log [\text{constant from (17)}] - \Delta_n \log [A_{n2}(n^2 - 4)] = \Delta_n \log (b_ne^{X_n})\,, \tag{20}$$

and we have the values given in Table 3. We note that $\log e^{X_n} = (11.4/n^2)(6000°/T_e)$,

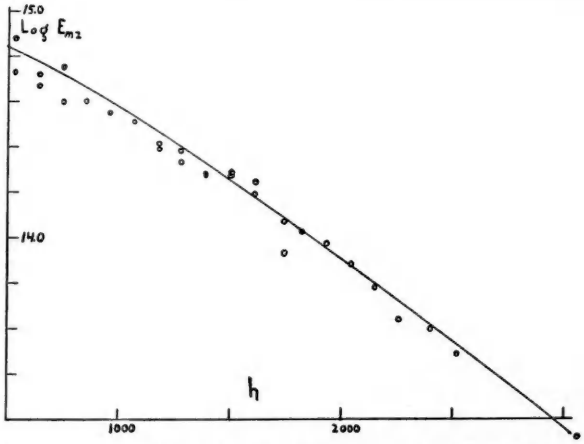

FIG. 3*a*.—A plot of log E versus height for $H11$, demonstrating the possibility of explaining the observed β_n in terms of self-absorption effects.

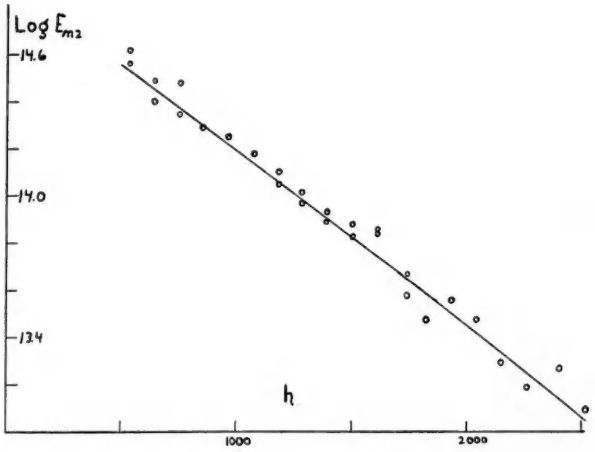

FIG. 3*b*.—A plot of log E versus height for $H15$, demonstrating the possibility of explaining the observed β_n in terms of self-absorption effects.

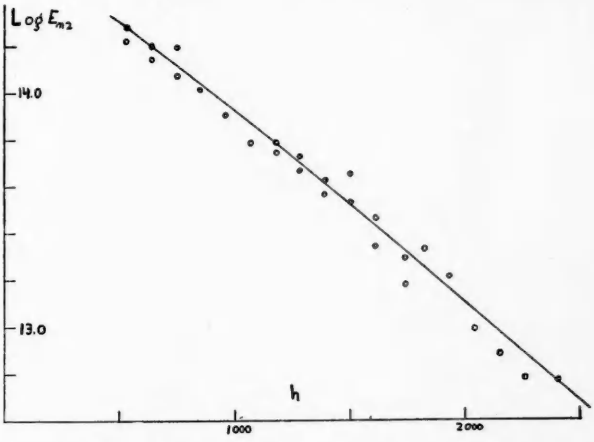

FIG. 3*c*.—A plot of log E versus height for $H20$, demonstrating the possibility of explaining the observed β_n in terms of self-absorption effects.

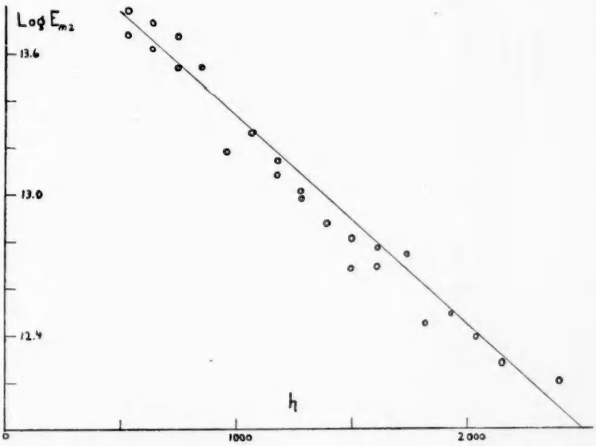

FIG. 3*d*.—A plot of log E versus height for $H29$, demonstrating the possibility of explaining the observed β_n in terms of self-absorption effects.

so the contribution to the last column from e^{X_n} is small compared to the value tabulated there. Thus, since we expect b_n to be near unity for $H29$, the last column should be very close to log b_n for the smaller n. The fact that equation (17), with the one empirical constant, fits the data so well (Fig. 3) indicates that the assumption of negligible $d \ln b_n/dh$ is satisfied. Clearly, however, the b_n's resulting from Table 3 are too large to be consistent with our comments based on the values in Table 2. Since a consideration of the empirical b_n obtained from a combination of free-bound continuum and line emission leads to a result similar to that from Table 3, we consider these empirical b_n's before discussing the foregoing results.

TABLE 2

T_e	n_e	b_1	b_2	b_5	b_{10}
10^4	10^{12}	2.1×10^2	84	1.1	1
	10^{10}	1.3×10^4	86	1.1	1
$2\cdot10^4$	10^{12}	3.4×10^3	1.0×10^3	3.0	1.4
	10^{10}	2.4×10^5	1.0×10^3	2.4	1.3
$3.5\cdot10^4$	10^{11}	5×10^4	1×10^4	15	4.5

TABLE 3

$n_i - n_j$	Δ_n log Const.	Δ_n log $[A_{n2}(n^2-4)]$	Δ_n log $(b_n e^{X_n})$
11–29	2.27	1.26	1.01
15–29	1.42	0.86	0.56
20–29	0.82	0.48	0.34

c) EMPIRICAL b_n VALUES

From equation (14) and the observed data we obtain log $[b_n e^{X_n}(\text{Abs.})]$, *if* we know γ_n/γ_∞. Two extreme values exist:

$$a)\quad \frac{\gamma_n}{\gamma_\infty} = 1 \rightarrow \text{self-absorption provides the whole } \beta\,(n) \text{ effect}\,, \qquad (21)$$

$$b)\quad \frac{\gamma_n}{\gamma_\infty} = \frac{\beta_n}{\beta_\infty} \rightarrow \text{no self-absorption}\,.$$

The entries in Table 4 correspond to case *a*. The second column contains the correction $\frac{3}{2}\log \beta_n/\beta_\infty$, which, applied to each row, gives case *b*. The strong blends at $H28$ and $H30$ and the weaker blends at $H12$, $H13$, $H14$, and $H20$ stand out in the low chromosphere. The change in β_n with h for $H9$–$H11$ makes the interpretation in terms of no self-absorption difficult, as already discussed in Section I. Using Table 4, case *a*, and the self-absorption computed for Figure 3, we obtain for $T_e = 6000°$ (in order to give as strong weight as possible to the e^{X_n} term) the b_n values in Table 5. The results are essentially the same as those obtained in the last section.

Consider precisely what our analysis has thus far produced. Clearly, using equation (3) and the observed values of $E_n(h)$, we may, in principle, determine a set $n_n(h)$ for *each assumed* function $n_2(h)$. The problem consists of the choice of the "correct" function $n_2(h)$; this choice can be accomplished only by introducing other considerations than the $E_n(h)$ data alone. With the failure of our infrared observations at the 1952 eclipse, we lost

the most extensive additional data, the Paschen series. Our "additional considerations" have then been only the Balmer free-bound emission and the requirement that the higher Balmer lines grade asymptotically into it.

Because both the line emisson and the free-bound emission exhibit a constant logarithmic height gradient, our "additional considerations" suggest that we investigate functions $n_2(h)$ that give a constant logarithmic height gradient for the occupation number of each energy state. In general, not all functions $n_2(h)$ lead to exponential $n_n(h)$, even with the observed result that $E_{n2}(h) \rightarrow E_\infty(h)$, because of the term $b_n e^{x_n}$. We have considered the two simplest cases: one, where the absence of self-absorption forces n_n to

TABLE 4

LOG ($b_n e^{x_n}$ ABS.)

n	$\frac{3}{2}\log \beta_\infty/\beta_n$	h (KM)									
		530	750	960	1180	1390	1610	1820	2040	2260	2400
8	0.55–0.30	−0.19	−0.19	−0.05	+0.06	+0.23	+0.29	+0.37	+0.38	+0.46	+0.78
9	.41– .24	− .30	− .30	− .20	− .01	+ .10	+ .16	+ .16	+ .19	+ .15	+ .32
10	.30– .22	− .27	− .27	− .16	+ .01	+ .13	+ .16	+ .18	+ .16	+ .17	+ .36
11	.27– .20	− .25	− .22	− .12	+ .03	+ .13	+ .18	+ .17	+ .01	+ .13	+ .35
12	.17	− .14	− .13	− .05	+ .10	+ .14	+ .20	+ .14	+ .14	+ .26	+ .38
13	.17	− .05	− .06	+ .03	+ .16	+ .19	+ .21	+ .11	+ .37	+ .19	+ .46
14	.16	− .02	+ .02	+ .06	+ .17	+ .23	+ .25	+ .09	+ .34	+ .26	+ .47
15	.15	− .06	− .08	− .02	+ .11	+ .16	+ .21	+ .03	+ .21	+ .08	+ .42
16	.15	− .06	− .02	+ .04	+ .16	+ .17	+ .21	+ .03	+ .20	+ .06	.....
17	.13	− .08	− .03	+ .03	+ .16	+ .18	+ .18	+ .04	+ .24	+ .12	+ .40
18	.11	− .07	− .06	− .02	+ .17	+ .15	+ .10	.00	+ .13	+ .10	+ .23
19	.09	− .02	.00	+ .02	+ .18	+ .25	+ .27	− .01	+ .19	+ .08	+ .34
20	.09	− .02	+ .01	+ .01	+ .17	+ .22	+ .05	+ .26	+ .10	+ .05	+ .30
21	.07	+ .06	+ .08	− .06	+ .22	+ .20	+ .14	+ .19	+ .07	+ .07	+ .31
22	.07	− .03	− .01	− .09	+ .18	+ .15	+ .09	+ .23	+ .09	+ .03	+ .26
23	.07	− .01	.00	− .12	+ .11	+ .16	+ .09	+ .13	+ .07	+ .07	+ .33
24	.04	.00	− .01	− .10	+ .10	+ .10	+ .01	+ .09	+ .03	+ .05	+ .26
25	.03	+ .08	+ .03	− .14	+ .12	+ .12	.00	− .01	+ .02	+ .03	+ .09
26	.04	− .03	− .02	− .16	+ .09	+ .13	+ .02	.00	+ .04	− .04	+ .26
27	.03	− .01	− .05	− .07	+ .02	+ .12	− .03	− .04	+ .02	+ .04	+ .15
28	.02	+ .11	+ .02	− .11	+ .01	+ .11	− .01	.00	− .02	+ .01	+ .33
29	.03	− .06	− .04	− .23	.00	− .01	− .05	− .14	− .02	+ .06	+ .21
30	.02	+ .32	+ .21	− .04	+ .11	+ .14	+ .09	− .02	+ .09	+0.15	+ .33
31	0.02	−0.14	−0.07	−0.25	−0.08	+0.07	−0.11	−0.14	−0.06	.....	+0.24

TABLE 5

LOG b_n ESTIMATES FROM FREE-BOUND EMISSION AND LINES INCLUDING SELF-ABSORPTION

n	h (KM)							
	500	1000	1200	1400	1600	1800	2000	2500
11	1.04	1.01	1.03	1.10	1.10	1.04	1.05	0.98
15	0.73	0.74	0.73	0.73	0.76	0.69	0.70	0.69
20	0.44	0.40	0.49	0.50	0.45	0.48	0.43	.....
29	0.12	0.13	0.11	0.10	.....	.....	0.11	.....

the desired behavior, with the variation of β_n coming from $(b_n e^{X_n})$; the other, where we assume n_n to be exponential in h and compute the required self-absorption to give $\beta(n)$, ignoring the variation of $(b_n e^{X_n})$. We rejected the first alternative; and the second appears to give too large b_n, which implies an overestimate of the self-absorption effect. Thus it would appear that some attempt to introduce a $d \ln b_n/dh > 0$ is necessary to reconcile all types of data.

A consideration of a "smoothed" version of Table 5—which results from the direct observations in both lines and continuum—illustrates some of the points just mentioned. Taking values from a smooth curve drawn through line and continuum observations in the (log E, h) plane, we obtain Table 6, where we consider just the four lines used earlier for reference. The first entry, case b of equation (21), demonstrates the impossibility of this case. For, whether $b_n \gtrless 1$, it must approach 1 monotonically, at least for these values of n; and the values do not do so. In a similar way, the simple alternative, essentially adopted in Paper I, of using negative entries in Table 4 to provide minimum values of

TABLE 6

SMOOTHED VALUES OF LOG $(b_n e^{X_n}$ ABS.)

n	h (KM)									
	530	750	960	1180	1390	1610	1820	2040	2260	2400
11	−0.45	−0.36	−0.29	−0.21	−0.13	−0.03	+0.01	+0.08	+0.14	+0.17
	− .20	− .11	− .04	+ .04	+ .09	+ .18	+ .21	+ .26	+ .32	+ .35
15	− .21	− .16	− .11	− .07	− .02	+ .02	+ .07	+ .12	+ .16	+ .19
	− .06	− .01	+ .04	+ .08	+ .13	+ .17	+ .22	+ .27	+ .31	+ .34
20	− .07	− .02	+ .01	+ .04	+ .06	+ .09	+ .11	+ .14	+ .17	+ .18
	+ .02	+ .07	+ .10	+ .13	+ .15	+ .18	+ .20	+ .23	+ .26	+ .27
29	− .02	− .01	.00	+ .02	+ .03	+ .04	+ .05	+ .07	+ .09	+ .09
	+0.01	+0.02	+0.03	+0.05	+0.06	+0.07	+0.08	+0.10	+0.12	+0.12

self-absorption fails for the same reason. (Note particularly the run of values in the interval 1000–2000 km.)

Finally, the entries in Table 6 near 2000–2500 km suggest one result that is independent of the uncertainty as to the amount of self-absorption: viz., a comparison of these entries with those in Table 2 would suggest that we require T_e greater than about 2×10^4 at these heights. Preliminary measures in the continuum do not indicate such large values of T_e. Thus, in essence, our anomaly remains the same—too great emission in the lines.

On the basis of the present discussion, there would appear to be three sources of resolution. First, if the self-absorption is indeed as great as our analysis of $\beta(n)$ would indicate, the emission from the lower lines and that from the continuum come from considerably different regions of the atmosphere. Table 7 illustrates this point. The second column contains $N_2 a$, the optical thickness of the chromosphere, in the center of the line, at the height h of the moon's limb. The following columns contain the actual height, h_1, to which corresponds $\tau = 1$, measured along the line of sight *from* the earth. These columns correspond to different positions from the line center, assuming a Doppler emission profile, $\exp(-p^2)$. Blank entries indicate that the optical half-thickness of the chromosphere at this position is less than unity. By contrast, the optical thickness at the head of the Balmer continuum is 0.032. Although our analysis formally compares values extrapolated to the mid-point of the atmosphere, along the line of sight, the values in Table 7

make it clear that a more detailed analysis, based on some preliminary distribution of (T_e, n_e), must be carried through to ascertain the effect of a large increase in b_n only in the region above, say, the 2500-km height, which represents the maximum h considered here.

Second, the presence of *such* large self-absorption as that above might make us abandon our reservations on the b_n behavior and simply interpret the entries in Tables 5 and 6 as b_n with a minimum self-absorption correction. Unfortunately, this requires the relatively large b_n and $d \ln b_n/dh$ of Tables 5 and 6, which ultimately imply a large gradient in b_2, hence a small gradient in n_2. Unless the value of n_2 at 500 km can be radically decreased, this procedure does not aid us. We return to this point when we discuss the continuum, to re-estimate this quantity there.

Third, if the structure of the atmosphere is appreciably nonuniform even at these lower heights, the relative emission in line and continuum can be appreciably affected.

TABLE 7

EFFECTIVE EMISSION REGION AT VARIOUS PARTS OF THE LINE IN THE CHROMOSPHERE

h	$N_{2\alpha}$	$p=0$	$p=1$	$p=\sqrt{2}$	$N_{2\alpha}$	$p=0$	$p=1$	$p=\sqrt{2}$
	*H*11				*H*15			
500	32.6	3680	2240	1020	12.3	2270	1040	.....
1500	18.8	3880	2500	1570	7.1	2560	1580	.....
2500	10.8	4100	2910	.....	4.1	2940	.....	.....
	*H*20				*H*29			
500	5.1	1150	.....	.....	1.6	.....	.....	.....
1500	2.9	1650	.....	.....	1.0	.....	.....	.....
2500	1.7	.....	.....	.....	0.5	.....	.....	.....

And also, of course, the $\beta(n)$ dependence may be considerably altered. For example, the structure might consist of the two-temperature columnar structure suggested by Giovanelli (1949), possibly in the form of cool spicules in a warm atmosphere, as discussed by one of us (Thomas 1948) in quite another connection.

The appearance of the chromospheric lines for h greater than about 5500 km is a point of special interest here. At these heights, all the visible chromospheric lines on our spectrograms (*Hα*, *Hβ*, *Hγ*, *Hδ*; *H*, *K*, λλ 8662, 8542, 8498 of Ca^+; λ 4471 and λ 5875 of *He*) show a nonuniform structure of columnar type; indeed, all these lines appear to be a series of spicules at these heights (Athay and Roberts 1954). For h less than about 5000 km, a spicule structure is not evident in any of the chromospheric lines. On our spectrograms *Hα* persists to ~8000 km. Yet there is strong evidence that coronal-line emission begins near these same heights, where the (relatively) low-excitation emission becomes concentrated into spicules (Athay and Roberts 1954). Thus we apparently have "cold" spicules in a "hot" medium at these heights. In the earlier discussion of such a model (Thomas 1948) in connection with the heating of the chromosphere, the total mass in the spicule system increased with height relative to that in the chromosphere. The interest there lay in an increased energy transfer per unit mass of chromospheric material; it would appear now that the development of a columnar structure is at least as significant as the heating. Thus it is important to settle the question of the

heights at which a columnar structure becomes important in terms of emission and of mechanical structure. We defer further discussion until the analysis of the data from the continuum.

Finally, we note that in the detailed computation of the self-absorption we used a Doppler profile for emission and absorption coefficient. For the higher lines, Stark effect should be included, and some change in the amount of absorption will result. It seems doubtful that this effect will alter the situation near $H11$–$H15$, where our primary difficulty arises.

This work was supported by the Office of Naval Research and carried out in co-operation with the Naval Research Laboratory. We are indebted to Dr. J-C. Pecker for discussions on the problems considered in the paper.

REFERENCES

Athay, R. G., Billings, D. E., Evans, J. W., and Roberts, W. O. 1954, *Ap. J.*, **120**, 94.
Cillié, G. C., and Menzel, D. H. 1935, *Harvard Obs. Circ.*, No. 410.
Giovanelli, R. G. 1949, *M.N.*, **109**, 298.
Hulst, H. C. van de. 1953, *The Sun*, ed. G. P. Kuiper (Chicago: University of Chicago Press), p. 207.
Matsushima, S. 1955, this supplement, p. 479.
Thomas, R. N. 1948, *Ap. J.*, **108**, 142.
———. 1950*a*, *ibid.*, **111**, 165.
———. 1950*b*, *ibid.*, **112**, 337.
———. 1952, *ibid.*, **115**, 550.

THE THERMODYNAMIC STATE OF THE OUTER SOLAR ATMOSPHERE. V. A MODEL OF THE CHROMOSPHERE FROM THE CONTINUUM EMISSION

R. G. Athay, D. H. Menzel, J-C. Pecker, and R. N. Thomas
High Altitude Observatory and Harvard College Observatory
Received August 30, 1954; revised January 28, 1955

ABSTRACT

Four semi-independent analyses of 1952 eclipse data contribute to a determination of n_e and T_e in the solar chromosphere in the height range from -120 km to 6000 km: (1) The intensity of the continuous emission at λ 4700 indicates that T_e increases with height from about 4800° at -65 km. (2) The emission, per cubic centimeter, in the Balmer continuum attains a maximum near 500 km, which indicates that here the free electrons begin to come mainly from H rather than from metals, and thus places the limits: $5000° < T_e < 7000°$, $4 \times 10^{11} < n_e < 5 \times 10^{11}$ at this height. (3) The intensities of the continuum at λ 4700 and λ 3640 require values of T_e as follows: 5000° at 500 km, 6100° at 1000 km, and 6700° at 3000 km. In the interval 1000–3000 km the ionization of H increases from about 3 to about 80 per cent. (4) Above 3000 km no data on the Balmer free-bound continuum exist, and an extension of the results of 3 to greater heights requires the use of the height gradient of the Balmer lines to replace that of the continuum. Such a technique fixes T_e only within certain limits, which, at 6000 km, are: $2 \times 10^4 < T_e < 1.2 \times 10^4$. The chief uncertainty of the analysis lies in the use of the assumption of a continuous distribution of material in the atmosphere. The results of the analysis suggest the validity of such assumption below about 2500 km, and its breakdown above about 3000 km. An estimate of optical depth in the continuum, from the present analysis, at a height of 500 km produces a value agreeing well with an estimate based on the analysis of the lines.

I. INTRODUCTION

The primary handicap in an attempt to develop a model of the solar chromosphere from observations of the continuous spectrum alone has been the poor height resolution of existing data. In an attempt to improve upon the 700-km interval of the 1932 data (Cillié and Menzel 1935) used in our earlier discussion (Thomas 1950), during the 1952 eclipse we employed high-speed photography (Athay, Billings, Evans, and Roberts 1954) that gave observation every 100 km, between 500 and 2500 km in altitude. Below 500 km, we have several observations which cover the height range down to -120 km. With this height resolution, we have hoped to obtain a careful separation between emission from Balmer free-bound, electron-scattering, and H^--emission sources. Such a separation requires values for the absolute, as well as relative, intensity in different spectral regions and at different heights in the chromosphere.

On the other hand, an analysis of the combined Balmer decrement and Balmer continuum requires a knowledge only of relative spectral intensities at the same height. The two preceding papers (Matsushima 1955; Athay and Thomas 1955) contain such an analysis of the 1952 data. From these results it appears that self-absorption in even the higher lines ($n > 10$) is so great as to make quite uncertain a determination of (n_e, T_e) from the lines and free-bound continuum alone. Thus, rather than combine results from the analysis of the lines, as we did at first, with this present analysis of the continuum it seems preferable to treat the continuum entirely independently and seek a distribution of (n_e, T_e) with height from the continuum data. We may then introduce the results of the line analysis, seeking to test the consistency of our model and to clarify several uncertainties in our discussions of the lines. An analysis in progress of the helium and the metallic lines should provide further correlative information. Observations (Athay and Roberts 1955) showing coronal-line emission below 10,000 km and spicule-type irregularities in the chromosphere above 5000 km set further limitations on the final model.

The following discussion rests on the assumption of a uniform chromosphere and represents only an attempt to exhaust the simplest possibilities before turning to the more complex.

The data used in the following analysis consist of the emission in the Balmer continuum at λ 3640 and the continuous emission at λ 4700, measured from flash spectra secured with objective-grating spectrographs. Employ a rectangular co-ordinate system, with x directed along the solar radius, y along the line of sight, and z tangential to the moon's

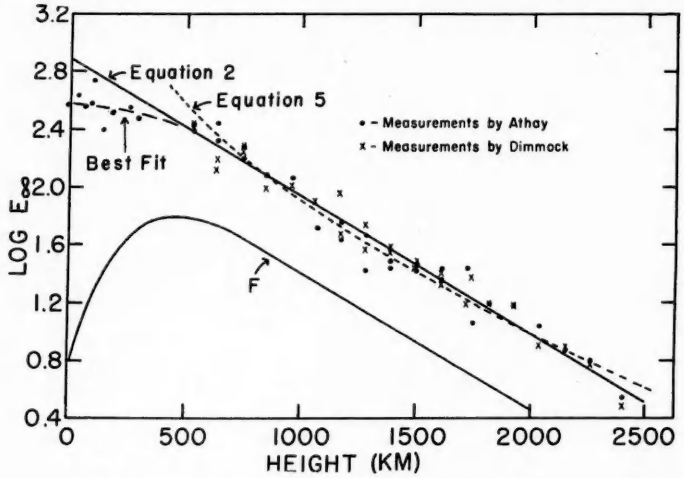

FIG. 1.—Balmer free-bound emission

limb. Then the total emission from a slab 1 cm in width along z and bounded by the moon's limb at $x = h$ is

$$E = \int_h^\infty \int_{-\infty}^{\infty} \mathfrak{E}\, e^{-\tau} dy\, dx\,, \tag{1}$$

where $\mathfrak{E}$ is the emission per unit volume and τ is the optical depth to the observer from the emitting volume. In most of the following, unless otherwise specified, we shall ignore the self-absorption term. This term is small except in the lowest chromosphere, and we discuss its value in Section III*c*.

II. REDUCTION OF DATA

a) FREE-BOUND EMISSION AT λ 3640

The free-bound data have been published (Athay *et al.* 1954). Subsequent independent measures by Dimmock (1953) gave excellent agreement with these published data, which contained only one observation at heights below 530 km. Recent measurements at two other neighboring points gave, because of irregularities in the lunar profile, data at several heights below 530 km. Figure 1 exhibits the combined data. A single exponential term, fitted by least squares, gives a good representation in the range 500 km $< h <$ 2400 km (we denote the emission at the head of the Balmer continuum by subscript ∞, denoting the limiting quantum number):

$$E_\infty = 780 \exp\left[-2.19 \times 10^{-8}\, h\ (\text{cm})\right]. \tag{2}$$

The continuum at λ 3640 is too weak to measure above 2400 km. However, we have Balmer-line data extending to 6400 km. Observationally, we note that the decrement in the continuum exceeds that in the line, in agreement with theoretical expectation (Athay *et al.* 1954). Thus

$$\beta_\infty \equiv -\frac{d \ln E_\infty}{dh} > -\frac{d \ln E_n}{dh} \equiv \beta_n . \tag{3}$$

Observations on the lines give

$$\beta_6 = 1.7 \times 10^{-8} \text{ cm}^{-1} \text{ for } 4000 \text{ km} < h < 6000 \text{ km} ; \tag{4}$$

and this value may be used as a lower limit on β_∞ over the extended height range up to 6400 km.

The expression

$$E_\infty = 3000 e^{-5\times10^{-8}h} + 360 e^{-1.8\times10^{-8}h} \tag{5}$$

agrees with equation (2) at 2000 km, does not diverge seriously from the observed data until h is less than about 800 km, and flattens above 2500 km to a height gradient slightly larger than the lower limit set by β_6. We shall use equation (5) in Section III to illustrate the effect on our results of an actual decrease in β_∞ above the height range in which observations exist.

The data in Figure 1 show a marked decrease of β_∞ below ~500 km and a slight decrease near the upper limits of the heights. The decrease for the greater heights becomes of marginal significance when investigated by a least-squares analysis. The higher lines show the same trend, again marginal, in statistical significance. Because of this low weight of any curvature term, we do not consider it further, simply remarking on its possible presence. We discuss the decrease in β_∞ near 500 km in Section III*a*. Here we note only that this behavior implies a maximum in $\mathfrak{E}_\infty$ near 500 km. The surface brightness of an optically thin chromosphere is

$$F = -\frac{dE}{dh} = \int_{-\infty}^{\infty} \mathfrak{E} dy . \tag{6}$$

The insert in Figure 1 exhibits log F_∞ versus h, as derived from the curve designated by "best fit" in Figure 1. Although the differentiation process inevitably magnifies small errors in the initial curve, we consider that the maximum in log F_∞ near 500 km cannot be avoided, and consequently a maximum in $\mathfrak{E}_\infty$ occurs near the same height.

b) THE CONTINUUM AT λ 4700

At each point of a slitless spectrogram the continuous intensity results from the contribution of all the overlapping monochromatic images. Each such image is a ring of light, of which the moon's limb fixes the inner boundaries, and the radial extent of the corona the outer boundary. Thus each point on the spectrogram represents the superposition of a solar image from each height above the moon's limb and from both east and west limbs. The different solar images correspond to different wave lengths, with the scale set by the observed size of the solar image on the spectrum. Thus we may express the total continuum intensity at λ 4700 as follows:

$$E_T = \int_h^\infty \int_{-\infty}^{\infty} \mathfrak{E}_E dy dx\,(\lambda) + \int_{h'}^\infty \int_{-\infty}^{\infty} \mathfrak{E}_W dy dx'\,(\lambda) , \tag{7}$$

where subscripts E and W refer to the east and west limbs of the sun. In practice, we may introduce some simplifications. Certainly points more than a solar diameter above the limb contribute little. Hence the overlap in wave length will not exceed 200 A, over which range neither $\mathfrak{E}_\lambda$ nor E_λ will vary significantly at λ 4700. We choose λ 4700 because

this region is relatively free from intense chromospheric lines, thus giving a well-defined continuum.

In order to reduce errors arising from local film irregularities, the continuum intensities were also measured at λ 4400 and λ 4100 and were corrected by a constant factor to give best agreement with the intensities at λ 4700. The three sets of data were accordant at all heights, and the averages of the three intensities at each height were taken as the final data.

To use the continuum data at λ 4700, we must separate the contributions from the two limbs of the sun. The telluric absorption bands in the infrared regions of the spectrum furnish a straightforward means for accomplishing such separation. These bands, which appear as absorption rings, affect the emission from only one side of the sun at a given point on the spectrum. Figure 2, *a*, represents a microdensitometer tracing through the

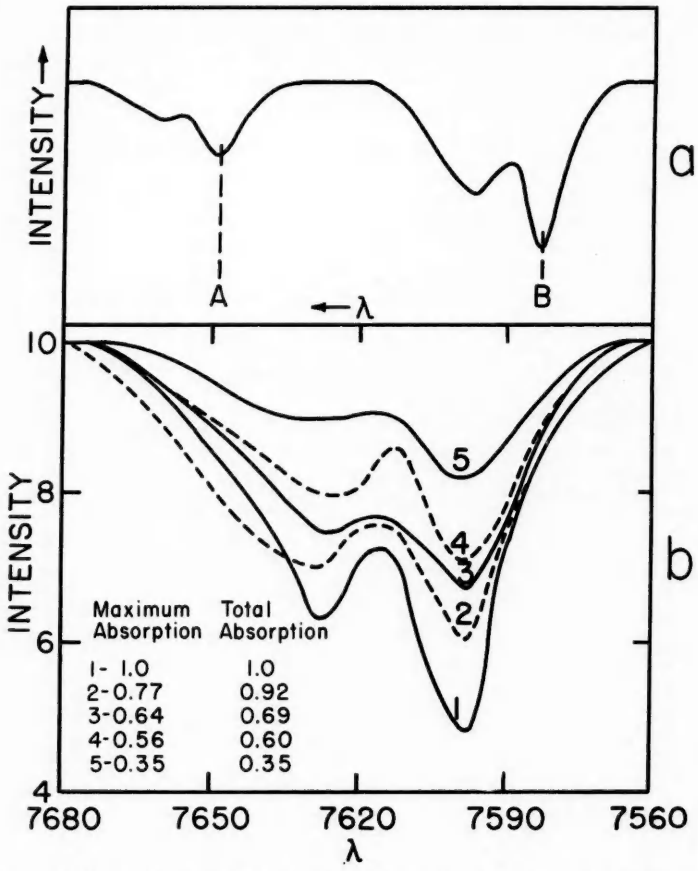

FIG. 2.—*a*, Profile of telluric absorption band, showing east and west limb absorptions. *b*, Profile of absorption band for five heights of the moon on the east limb. Relative values of total absorption and maximum absorption are tabulated.

O_2 band at λ 7596. The intensities in this band are measurable over the height range from about 3000 to 48,000 km relative to one limb of the sun. At these heights, electron scattering is the source of the continuum (cf. Sec. IV). In consequence, E_E/E_W is independent of wave length, and a value of E_E/E_W determined at λ 7596 may be used at λ 4700 without danger of systematic error. In theory, these observations require corrections for lack of resolving power, for incomplete absorption away from the band head, and for finite width of the coronal source. However, determinations of band profiles at five heights between 3000 and 46,000, as shown in Figure 2, *b*, showed good agreement between maximum absorption and integrated absorption, which latter is independent of these disturbing factors.

At each wave length in the band let k be the percentage of terrestrial atmospheric absorption. Now, if we replot a tracing of the continuum on a scale such that the maximum is equal to unity, on both sides of the absorption bands, we have the equations

$$kE_W + E_E = E_a\,, \tag{8a}$$

$$E_W + kE_E = E_b\,, \tag{8b}$$

$$E_W + E_E = 1\,, \tag{8c}$$

which yield the solution

$$\frac{E_E}{E_W} = \frac{1-E_b}{1-E_a}. \tag{9}$$

Since k is a function of λ, we can check this expression for each wave length or for the integrated equivalent width of the absorption band. In our discussion, we have actually used the absorption at the band head. To check our procedure we have determined band profiles for one limb of the sun at five heights between 3000 and 46,000 km. Figure 2, *b*, exhibits such profiles at several heights. At four of these heights, including the two extremes, the band profiles showed the same ratio between absorption at the band head and integrated absorption. The one exception showed an obvious defect in one side of the band that accounted for the discrepancy and lay in the opposite sense from that expected from the effect of a change in resolving power. We then conclude that for our purposes the absorption at the band head is proportional to the integrated absorption.

We thus separate the contribution from the two limbs of the sun, to give the data in Table 1 and Figure 3, which represent the integral equation (1). To solve the equation, we have arbitrarily fitted the data to a series of exponential terms. Relatively small changes in the form of E_{4700} produce considerably larger changes in the derivative of this function, which represents $\mathfrak{E}_{4700}$. Our final objective of determining n_e and T_e as functions of height follows from a combination of obsrvations at λ 4700 and λ 3640. Uncertainties resulting from the various representations of E_{4700} and of E_{3640} above ~2500 km will produce a range of possible solutions for T_e and n_e.

We list in Table 2 the coefficients A_i and γ_i used in six alternative representations:

$$E_{4700} = \sum_i A_i\, e^{-\gamma_i h}\,. \tag{10}$$

The data scarcely justify our using as many terms as given for representation (*f*), which we reached by trial and error, seeking the smoothest possible run of final values for (T_e, n_e). We note that the first two terms represent the data below ~2000 km, the last two those at the greatest heights, and the intermediate two provide a continuous transition. In further discussion, we refer to representation (*f*).

III. ANALYSIS OF DATA

The emissions at λ 3640 and λ 4700 depend, in different ways, upon n_e and T_e. Given the functional form of this dependence, we can express the observational data from

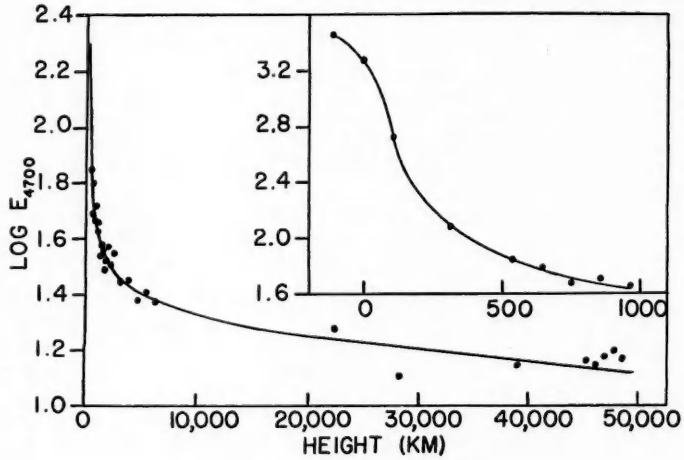

FIG. 3.—Continuous emission at λ 4700

TABLE 1

CONTINUUM INTENSITIES* AT λ 4700

Height (Km)	log (E_E+E_W)	E_E/E_W	log E_E	Height (Km)	log (E_E+E_W)	E_E/E_W	log E_E
− 120	3.44	.....	3.44	1980	1.69	.....	1.57
− 10	3.28	.....	3.28	2250	1.64	.....	1.51
+ 100	2.72	.....	2.72	2520	1.68	.....	1.55
+ 310	2.12	.....	2.09	3060	1.58	2.60	1.43
+ 530	1.91	.....	1.85	3870	1.61	2.47	1.46
+ 640	1.87	.....	1.80	4680	1.55	.....	1.38
+ 750	1.76	.....	1.69	5400	1.58	1.90	1.40
+ 850	1.80	.....	1.72	6300	1.58	1.59	1.37
+ 960	1.76	.....	1.67	22,500	1.54	1.03	1.25
+1070	1.75	.....	1.66	28,400	1.40	0.92	1.08
+1180	1.73	.....	1.63	39,100	1.48	0.80	1.13
+1280	1.65	.....	1.54	45,300	1.48	0.83	1.14
+1390	1.69	.....	1.58	46,100	1.51	0.72	1.13
+1500	1.67	.....	1.56	46,900	1.56	0.63	1.15
+1610	1.61	.....	1.49	47,700	1.60	0.64	1.19
+1750	1.64	.....	1.52	48,500	1.60	0.61	1.18

* Intensities are in ergs sec^{-1} $freq^{-1}$ from a slice of chromosphere and corona 1 cm wide.

Section II in terms of two equations, each involving n_e and T_e for a particular height. We solve these equations to obtain n_e and T_e at each height, subject to the uncertainties already discussed.

a) THE EQUATIONS FOR THE EMISSION

Our analysis has provided values for the part of the emission at λ 3640 which comes from free-bound transitions at the Balmer limit (Menzel 1932),

$$\mathfrak{E}_\infty = 2.63 \times 10^{-33} n_p n_e T_e^{-3/2}, \tag{11}$$

where n_p and n_e are the numbers of protons and electrons per cubic centimeter and T_e is the electron temperature. Combining equation (11) with equations (1) and (2), we obtain

$$n_p n_e T_e^{-3/2} = 1.45 \times 10^{18} e^{-2.19\times10^{-8}h}. \tag{12}$$

TABLE 2

COEFFICIENTS IN VARIOUS REPRESENTATIONS OF FORM (10)

Representation	A_1	$10^8\gamma_1$	A_2	$10^8\gamma_2$	A_3	$10^9\gamma_3$	A_4	$10^9\gamma_4$	A_5	$10^{10}\gamma_5$	A_6	$10^{11}\gamma_6$
(*a*)	83	1.7	.....	.....	.....	.....	15.0	1.0	.....	.....	17.4	5
(*b*)	156	3.4	.....	.....	24.3	5.5	.....	.....	10.0	7	17.4	5
(*c*)	351	7.0	63.6	2.5	24.3	5.5	.....	.....	10.0	7	17.4	5
(*d*)	155	3.3	25.0	1.1	.....	.....	15.0	1.0	.....	.....	17.4	5
(*e*)	166	3.3	17.3	1.1	.....	.....	19.0	1.4	.....	.....	16.2	2
(*f*)	385	7.0	67.5	2.2	10.0	6.0	12.1	4.0	8.5	7	17.4	5

The continuum at λ 4700 comes mainly from electron scattering and H^- emission. The contribution from electron scattering is

$$\mathfrak{E}_e = \frac{4\pi I_p n_e \sigma_e}{2} = 9.4 \times 10^{-24} n_e, \tag{13}$$

where

$$\sigma_e = \frac{8\pi}{3}\left(\frac{\epsilon^2}{m c^2}\right)^2 \tag{14}$$

is the cross-section for Thomson scattering by a free electron. We have represented the photospheric radiation field by an isotropic field, I_p, over the outgoing hemisphere, and zero field over the ingoing. I_p is the observed intensity of the photospheric continuum for the integrated disk (Nicolet 1951). Let $\alpha_\nu(T_e)$ = the absorption coefficient of H^- tabulated by Chandrasekhar and Breen (1946); B_ν = the Planck function; and n_H = the density of neutral hydrogen atoms.

If the lower chromosphere is in local thermodynamic equilibrium, for the dissociation of H^- the emission from H^- becomes

$$\mathfrak{E}_- = 4\pi k n_e n_H B_\nu(T_e)\alpha_\nu(T_e)T_e. \tag{15}$$

Now, substituting for n_H from the ionization equation, which is

$$n_H = 4.14 \times 10^{-16} n_p n_e T_e^{-3/2} 10^{6.82\times10^4/T_e}, \tag{16}$$

we obtain, for equation (15),

$$\mathfrak{E}_- = 2.72 \times 10^{-33} n_p n_e^2 \alpha_\nu(T_e) T_e^{-1/2} 10^{5.49\times10^4/T_e}. \tag{17}$$

For $T_e = 5000°$ and $n_p = n_e = 10^{11}$, $\mathfrak{E}_- \sim 10^{-28} n_e$, and H^- emission assumes equal importance with electron scattering. The importance of the H^- term decreases rapidly as n_e decreases and T_e increases; hence it will be important only in the very low chromosphere, where the assumption of local thermodynamic equilibrium is more likely to be valid.

The maximum possible contribution from the Paschen continuum, for $n_p = 10^{11}$, is $4 \times 10^{-30} n_e$, which is negligible in comparison with electron scattering. Free-free emission is even smaller; free-bound continua from metals are also negligible.

From equations (1) and (10) and representation (*f*) in Table 2, we obtain $\mathfrak{E}_e + \mathfrak{E}_-$ as a function of height. When this solution is combined with equations (13) and (17), we obtain

$$n_e + 2.9 \times 10^{-5}\, n_p n_e^2 \mathfrak{a}_\nu(T_e) T_e^{-1/2} 10^{5.49\times10^4/T_e} = 1.14 \times 10^{14}\, e^{-7\times10^{-8}h} + 3.5 \times 10^{12}\, e^{-2.2\times10^{-8}h} + 7.4 \times 10^{10}\, e^{-6\times10^{-9}h} + 4.9 \times 10^{10}\, e^{-4\times10^{-9}h} + 2.5 \times 10^{9}\, e^{-7\times10^{-10}h} + 9.8 \times 10^{7}\, e^{-5\times10^{-11}h}. \quad (18)$$

Equations (12) and (18) provide the two relations between n_e and T_e, as functions of h, which we mentioned earlier. As previously noted, they are strictly applicable only when we can neglect self-absorption. The equations contain one further unknown, n_p. If most of the free electrons come from hydrogen, $n_e \sim n_p$; otherwise, we shall have to know the ratio of hydrogen to metals. Self-absorption is more likely to be serious in the lower chromosphere, where the intensity is greatest. The uncertainties of the source of electrons are also greatest in this region, where hydrogen may not yet be appreciably ionized. Hence we shall consider this region of the atmosphere first.

b) THE CHROMOSPHERE FOR $h < 500$ KM

Consider the data at λ 4700 (Fig. 3), which extend down to $h = -120$ km. If we may make the assumption of local thermodynamic equilibrium at this wave length, we may rewrite equation (1) in the form

$$E_{4700}(h) = \int_h^\infty \int_0^{\tau(h,\,\lambda)} B_{4700}[T_e(h)]\; e^{-\tau} d\tau dx, \quad (19)$$

where we explicitly include the self-absorption at these low heights. The flux per square centimeter column then becomes

$$F_{4700} = -\frac{dE_{4700}}{dh} = \int_0^{\tau(\lambda,\,h)} B_{4700}[T_e(h)]\; e^{-\tau} d\tau \sim \bar{B}_{4700}(1 - e^{-\tau}), \quad (20)$$

where $\bar{B}_{4700}$ is the mean value of the Planck source function along the line of sight, weighted by the self-absorption term. If the lower chromosphere were isothermal, dF/dh would be constant or negative, since τ decreases with increasing height. From Figure 3 we see that F_{4700} actually increases with height in the lowest region observed. Accordingly, T_e must increase with increasing height. To evaluate T_e, we require a knowledge of τ.

We note the usual remark that $\tau \sim 1$ at the base of the chromosphere, $h = 0$. For an isothermal chromosphere and an exponential dependence of τ on h, we see from equation (20) that the minimum in dF/dh would occur at $\tau = 1$. Call this point h_1 on our scale of heights. This minimum in dF/dh would correspond to the point of greatest upward curvature in $E(h)$, thus to a point of decreasing slope. Our zero height has been defined (Athay *et al.* 1954) as the point at which the *increase* of slope of $E(h)$ is a maximum. Thus, from Figure 3, $h_1 > 0$, and $\tau(h = 0) > \tau(h = h_1)$. While the conditions under which $\tau(h = h_1) = 1$ are not fulfilled, the departure from τ near 1 cannot be large.

From the observed values of E_{4700} we set an upper limit on T_e, using equation (19) with $\tau_{4700} \gg 1$. We obtain the following values:

$$\begin{aligned} \Delta h &\sim -120 \text{ to } -10 \text{ km}, \qquad T_e \geq 4850^\circ ; \\ \Delta h &\sim -10 \text{ to } 100 \text{ km}, \qquad T_e \geq 5200^\circ . \end{aligned} \tag{21}$$

For greater heights, we attribute the observed decrease of F to increasing transparency of the chromosphere, which tends to mask further increase in temperature at higher levels. By assuming the constant value of $T_e = 5200^\circ$, from relations (21), throughout the region $h > 100$ km, we set an *upper limit* on τ_{4700} of 0.01 at 500 km.

In summary, the measures at λ 4700 over the range -120 km $< h <$ 500 km lead us to conclude that

$$T_e(\sim -65 \text{ km}) \geq 4850^\circ, \qquad \frac{dT_e}{dh}(h > -65 \text{ km}) > 0,$$

$$\tau_{4700}(h = 500 \text{ km}) < 0.01 .$$

Consider, now, the free-bound emisson. The data of Figure 1 indicate a maximum in F_∞ at about 500 km, which also requires a maximum in $\mathfrak{E}_\infty$. From equation (12), this rise to a maximum in $\mathfrak{E}_\infty$ requires that $n_p n_e T_e^{-3/2}$ increase with increasing height for h less than about 500 km. Such an effect requires that n_p increase with height, in view of our conclusion that T_e increases with height. Thus above 500 km the supply of free electrons must come more from hydrogen than from the metals. Adopting 10^4 as a reasonable value for the hydrogen-to-metal ratio (the exact value is not critical) and noting that n_e must exceed 10^{10} as an extreme lower limit at h less than about 500 km, we find

$$5000^\circ < T_e < 7000^\circ \text{ at } 500 \text{ km} .$$

If equation (2) is valid at 500 km, these limits on T_e further restrict n_e to the range

$$4 \times 10^{11} < n_e < 5.5 \times 10^{11} .$$

Above the height of the maximum in $\mathfrak{E}_\infty$, $h \sim 500$ km, we have $n_e \sim n_p$.

c) THE REGION ABOVE 500 KM

Section *b* indicates that we may safely neglect self-absorption for $h > 500$ km and set $n_e \sim n_p$. As a further check on the validity of this last assumption, we may set

$$n_e = n_p + n_i , \tag{22}$$

where n_i is the number of ions other than hydrogen. Rosa (1948) has computed tables giving the total gas pressure as a function of n_e and T_e for the solar abundances of the elements. Equations (12), (18), and (22) can be solved by iteration, using Rosa's tables. The solutions give $n_p = n_e$ at all heights above 500 km. Therefore, we may replace n_p by n_e in the foregoing equations and solve for n_e and T_e directly. The second and third columns of Table 3 contain the results.

As we mentioned in Section II*a*, the data on which equation (2) rests extend only to 2500 km. We have also remarked that the data on the lines extend considerably higher and may be used to set a limit on the behavior of the free-bound emission at λ 3640. The use of equation (2) at heights up to 6000 km places one limit. Equation (5) places another limit, and its use, rather than equation (2), in all the foregoing development involving the free-bound emission provides the results given in the fourth and fifth columns of Table 3. For the greater heights, the emission at λ 4700 comes from electron scattering; so n_e is determined independently of T_e.

The two models in Table 3 show good agreement for $h < 3000$ km, but they diverge considerably at higher levels. Here the divergence arises from the two limits on β_∞. The empirical representations of E_{4700} given in Table 2 demonstrate that the $\mathfrak{E}_{4700}$ inferred from the observed E_{4700} may vary by a factor of 2. The influence of such variation is more serious in the high chromosphere than in the low. Figure 4 demonstrates the limits on the solution, resulting from these uncertainties in the $\mathfrak{E}$ inferred from the E. At 6000 km the range in solution for T_e is $2 \times 10^4 < T_e < 1.2 \times 10^5$.

Another possible source of errors in the results contained in Table 3 lies in the absolute-intensity calibration of the spectrograms. If we arbitrarily change all absolute intensities by a factor of 2, T_e changes by about 50° at 500 and 1000 km because of the predominance of H^- emission. However, at greater heights, where H^- emission is negligible, the same change in absolute intensities produces a factor of 1.6 change in T_e. This differential effect on T_e at the high and low heights, resulting from change in the absolute

TABLE 3

n_e AND T_e*

Height (Km)	Equation (2)		Equation (5)	
	log n_e	T_e	log n_e	T_e
500	11.66	5750	.....	.....
1000	11.44	6100	11.44	6100
2000	10.95	6400	10.95	6400
3000	10.53	7000	10.53	6400
	(10.52)	(6800)	(10.55)	(6700)
4000	10.28	13,600	10.28	10,000
5000	10.08	31,600	10.08	17,800
6000	9.91	79,000	9.91	34,700
10,000	9.38	.....	.....	.....
20,000	8.86	.....	.....	.....
30,000	8.59	.....	.....	.....
40,000	8.36	.....	.....	.....
50,000	8.19	.....	.....	.....

* The values given in parentheses are discussed in Sec. III*d*.

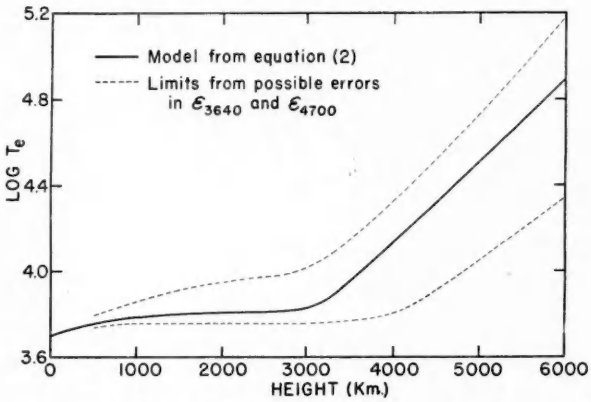

FIG. 4.—T_e versus height, showing limits resulting from various sources of errors

intensities, provides a means of checking the internal consistency of our absolute-intensity scale. For $h > 2000$ km, H^- emission is small compared with electron scattering. Thus equation (18) fixes $d \log n_e/dh$. From equation (12) we have

$$\frac{d \log T_e}{dh} = \frac{2}{3}\left[2 \frac{d \log n_e}{dh} + 0.95 \times 10^{-8}\right]. \tag{23}$$

Thus $d \log T_e/dh$ is well determined for $h > 2000$ km. Hence, if we plot $\log T_e$ against h and arbitrarily change the absolute-intensity scale, we displace the entire curve for $h > 2000$ km parallel to the $\log T_e$ axis. On the other hand, the values of $\log T_e$ at 500 and 1000 km remain practically constant. If we attempt to decrease the absolute intensities by a factor greater than 1.5, we find values of T_e at 3000 km considerably smaller than those at 1000 km. Since it is very unlikely that T_e goes through two minima, one being below 500 km, we do not believe that we can permit a significant decrease in the absolute-intensity scale. Unfortunately, we cannot exclude the possibility of a significant increase in the absolute intensities, which would increase all values of T_e. However, since the independent calibrations of the ultraviolet and visible spectrograms in the overlapping spectral range differed by less than a factor of 1.25, serious errors in the absolute intensities appear somewhat unlikely.

TABLE 4

n_e AND T_e FROM EQUATION (18)

T_e	4500	5000	5500	6000	7000
$\log n_e$	8.5	10.0	11.1	11.9	12.4

That T_e in the low chromosphere is essentially independent of the model follows from the strong temperature dependence of the H^- emission. This can be demonstrated in the following way. From equations (11), (12), (13), and (14), we obtain

$$\frac{\mathfrak{E}_\infty}{\mathfrak{E}_{4700}} = \frac{4.06 \times 10^{13}\, e^{-2.19\times10^{-8}h}}{n_e\,[1 + 4.2 \times 10^{13} a_\nu(T_e)\, T_e 10^{5.49\times10^4/T_e} e^{-2.19\times10^{-8}h}]}. \tag{24}$$

If we use either equation (2) or (5), together with equations (1) and (10) and representation (*f*) in Table 2, we obtain $(\mathfrak{E}_\infty/\mathfrak{E}_{4700}) \sim 3$ at 500 km and $\mathfrak{E}_\infty/\mathfrak{E}_{4700} \sim 10$ at 1000 km. The values of n_e and T_e necessary to produce a ratio of 3 are given in Table 4. If we adopt $n_e \sim 10^{11}$, as many independent chromospheric observations indicate, T_e is limited to a narrow range. As an illustration of this point, consider the chromospheric models proposed by Woolley and Allen (1950), van de Hulst (1953), and Piddington (1954). These models all give $(\mathfrak{E}_\infty/\mathfrak{E}_{4700}) \sim 0.1$ for most of the low chromosphere, a result clearly inconsistent with the relatively strong Balmer continuum in this height range.

We may use the results from Table 3 in conjunction with those from section *b* to improve our estimate of the optical depth at λ 4700. We assume $\tau_{4700} \gg 1$ at the lowest observed level in relations (21), thus reaching $T_e = 4850°$ as the true value at -65 km. We further assume that T_e increases linearly from this low height to the value at 500 km given in Table 3, 5750°. Then equation (20) permits an evaluation of τ_{4700}. Table 5 contains the results. The value of T_e in the third column falls below the lower limit given in relations (21). This result demonstrates the uncertainty of the results in Table 5, with the uncertainty arising from the assumed linear variation of T_e with h and from observational errors in $\Delta E/\Delta h$. If we assume further that τ varies exponentially with h, the fourth and fifth columns of Table 5 give

$$\tau_{4700} \sim 1.7\, e^{-1.2\times10^{-7}h}, \tag{25}$$

leading to $\tau_{4700} = 1$ at 45 km.

In our discussion of the Balmer-line intensities (Athay and Thomas 1955), we evaluated $N_2 a_{2n}$, the optical depth at the line center. Here N_2 is the total number of atoms in the Balmer ground state per square centimeter column tangential to the solar limb for given h. Hence

$$N_2 a_{2n} = 6.6 \times 10^3 f_{2n} \exp\left[-0.55 \times 10^{-8} (h - 1.5 \times 10^8)\right], \tag{26}$$

$$N_2 = n_2 \gamma_2^{-1/2} (2\pi R_\odot)^{1/2}, \tag{27}$$

where γ_2 is the logarithmic height gradient of n_2. We expressed concern that we might have overestimated N_2. We may use relations (25) and (26) to estimate the opacity in

TABLE 5

τ_{4700} FOR $h < 500$ KM

h (Km)	−120 to −10	−10 to 100	100–310	310–530
T_e	4850	5000	5250	5600
ΔE	850	1385	402	52
τ_{4700}	.....	.....	0.14	0.011

both free-bound and H^-. Again we use subscript ∞ to denote the head of the Balmer continuum, λ 3640. Thus

$$N_2 a_\infty = N_2 a_{2n} \frac{a_\infty}{a_{2n}} = 0.32 \left(\frac{T_e}{6000}\right)^{1/2} \quad \text{at} \quad h = 500 \text{ km}; \tag{28}$$

$$N_{H^-} a_{H^-} = \frac{N_{H^-}}{N_2} \frac{a_{H^-}}{a_\infty} N_2 a_\infty = \frac{n_H}{n_2} \left(\frac{\gamma_2}{\gamma_{H^-}}\right)^{1/2} [4.1 \times 10^{-16} n_e T_e^{-3/2} \exp(\chi_{H^-}/kT_e)] \frac{a_{H^-}}{a_\infty} N_2 a_\infty = 0.0072 \left(\frac{\gamma_2}{\gamma_{H^-}}\right)^{1/2} \quad \text{at} \quad h = 500 \text{ km}, \; T_e = 5750, \; n_e = 5 \times 10^{11}. \tag{29}$$

We recognize that $(\gamma_2/\gamma_{H^-})^{1/2} < 1$; equations (26) and (25) yield 0.21, so that $N_{H^-} a_{H^-} = 0.0016$, a value less by a factor 3 than that given in our discussion of the continuum in Table 5 and equation (25). In view of the simplifying assumptions underlying equation (25) and the few available data, the disagreement is hardly serious. We conclude only that two methods set the two tangential optical depths in the range 0.001–0.01 at 500 km.

From equation (25), the radial optical depth becomes 0.016 at −65 km, where we have taken $T_e - 4850°$. The data from the lines suggest $\tau \sim 0.006$. A great variety of recent work (Pecker 1951; de Jager 1952; von Regemorter 1953; Henriksen 1954) indicates a solar boundary temperature near 4000°. One of our main interests has been the relation of our results to these recent investigations on the boundary temperature. Relations (26) and (25) suggest that, at the time of the 1952 eclipse, T_e exceeded the boundary temperature and had a positive outward derivative at $\tau_{\text{rad}} \sim 0.006 - 0.016$.

d) THE HIGH CHROMOSPHERE

If T_e were to increase with height at the rate indicated by Table 3, it would attain values in the high chromosphere sufficiently large to excite the coronal lines. Measurements of the intensities of the *Fe* XI line at λ 7892 (Athay and Roberts 1954) on the Khartoum eclipse spectrograms, at the point where the continuum measurements were made and at one other point on the opposite side of the sun, showed that the maximum emission, per cubic centimeter, occurred definitely below 10,000 km, and probably as low as 8000 km, to which level *Hα* emission extends. These measured regions appear to be representative of the undisturbed regions of the chromosphere and corona. They strongly suggest coexistence or overlapping of upper chromosphere and lower corona. Thus the rapid rise in T_e shown by the models in Table 2 is consistent with the coronal-line emission.

At previous eclipses *Hα* has been observed to heights that are 4000–6000 km above the maximum height observed at Khartoum. Furthermore, Cillié and Menzel (1935) obtained $\beta_n \sim 1.5 \times 10^{-8}$ for large n, whereas our data show much larger β_n for the same n. These differences suggest that the increase in T_e in the high chromosphere may have been more abrupt in 1952 than in 1932. A later paper will discuss the evidence for periodic change in chromospheric structure, as inferred from existing eclipse data.

IV. DISCUSSION OF MODELS

T_e DISTRIBUTION

The models given in Table 3 resulted directly from the analysis of the data. As we have pointed out and exhibited in Figure 4, the values of T_e are subject to considerable error. Some improvement in the models results if we also impose the requirement that the total mass density decrease smoothly with increasing height. The total density is proportional to $n_H + n_e$, since $n_p = n_e$, and n_H follows from the models and equation (13). The values of $n_H + n_e$ obtained in this way showed small, abrupt changes in the vicinity of the temperature plateaus. Of special interest is the internal energy per gram of the chromospheric gases. This internal energy is the sum of kinetic, ionization, and excitation energies. As before, small, abrupt changes occur in the vicinity of the plateaus. Small alterations in the models enable us to obtain smooth changes of both density and internal energy with height, as given in parentheses in Table 3. When these changes are made, the internal energy per gram increases with height. The most rapid rate of increase still comes in the region of the plateau.

A recomputation of the models, employing the data of Table 5, still gives a plateau in the curves of T_e versus height. We note in particular that the percentage ionization of hydrogen increases from ~3 to ~80 per cent on this plateau. Thus the plateau suggests that the chromosphere may depend on a supply of mechanical energy, as opposed to mere momentum, from the lower regions. In other words, the state of the chromosphere depends on more than a simple velocity field that does not couple directly with the internal degrees of freedom of the gas. In the regions above and below the plateau, the energy supplied goes mainly into kinetic energy. In the plateau, however, the energy goes to ionize the hydrogen. In most of the other chromospheric models thus far proposed (cf. Woolley and Allen 1950; van de Hulst 1953; Piddington 1954) the principal ionization occurs where T_e rises most rapidly. All such models require a sharp increase in the internal energy per gram at heights where $n_H/n_e \sim 3$ and require a considerably different type of energy source than that implied by our model.

Our discussion rests on an assumed homogeneous chromosphere. Elsewhere (Athay and Roberts 1955) we have pointed out that the chromosphere above ~5500 km is distinctly nonuniform or spicular in structure. On spectrograms taken at heights below ~5500 km, this nonuniform structure does not appear. Does this apparent uniformity

result from lack of optical resolution, or is it real? A consideration of the mechanical structure provides some insight into the problem.

If the chromosphere is in hydrostatic equilibrium, we may write

$$\frac{d_p}{d_h} = -(n_e + n_H)\, m_H g\,, \tag{30}$$

where m_H is the mass of the hydrogen atom and

$$p = (2n_e + n_H)kT_e\,. \tag{31}$$

Set

$$\eta = \frac{n_e}{n_e + n_H}\,. \tag{32}$$

Equations (30)–(32) give

$$g = \frac{(\eta+1)\,kT_e}{0.434\,m_H}\left[\frac{1}{\eta+1}\,\frac{d\log\eta}{dh} - \frac{d\log T_e}{dh} - \frac{d\log n_e}{dh}\right]. \tag{33}$$

To evaluate the quantities appearing in equation (33), we use the final model in Table 3—the values in parentheses in the second and third columns. Table 6 contains in the first six

TABLE 6

CHECK ON HYDROSTATIC EQUILIBRIUM

	HEIGHT						
	500	1000	2000	3000	4000	5000	6000
$10^8\, d\log n_e/dh$	−0.40	−0.46	−0.46	−0.35	−0.21	−0.18	−0.16
$10^8\, d\log T_e/dh$	0.10	0.02	0.02	0.16	0.34	0.40	0.42
$\log n_H$	14.15	12.97	11.46	9.93	3.95	0.19	−2.04
η	0.003	0.03	0.2	0.8	1	1	1
$10^8\, d\log \eta/dh$	3.3	0.97	0.78	0.87	0	0	0
g_e/g	1.4	0.6	0.6	0.6	−0.2	−1.0	−3.0

rows the quantities entering the right side of equation (33). The seventh row contains the ratio of g computed from equation (33), which we call g_e, to the true value of the solar g. In the computations we neglect departures from thermodynamic equilibrium.

For h less than about 2000–3000 km, $g_e \sim g$, and the conditions of hydrostatic equilibrium are very nearly satisfied. Slight changes in the model can bring $g_e = g$. However, for h greater than about 3000 km, the conditions of hydrostatic equilibrium cannot be satisfied.

The failure of hydrostatic equilibrium above 3000 km suggests two possible implications. On the one hand, our assumption of a uniform continuous structure for the emitting material may break down. The observations of the spicules in the upper chromosphere, which we have already discussed, suggest such a structure. In this case we cannot accept the values of n_e and T_e from Table 3 as actually characterizing the chromosphere above 3000 km. The values represent some kind of a mean, but the actual structure is not clear. On the other hand, the failure of hydrostatic equilibrium may imply some kind of dynamic support for the chromosphere. When investigated in detail, such a situation actually differs very little from the first alternative.

We defer discussion of these structural problems to a later paper. We note only that all observations suggest that a treatment of the 1952 chromosphere as a uniform,

quiescent medium for $h < 2500$ km is a fair representation of the actual situation. And as one progresses upward in height, the nonuniformity in emitting material increases, however such nonuniformity arises.

This work was supported in part by the Office of Naval Research, carried out in cooperation with the Naval Research Laboratory, and in part by the Air Force Cambridge Research Center, Geophysics Research Directorate, through Contract AF19(604)-146 with Harvard University.

REFERENCES

Athay, R. G., Billings, D. E., Evans, J. W., and Roberts, W. O. 1954, *Ap. J.*, **120**, 94.
Athay, R. G., and Roberts, W. O. 1954, *Ap. J.*, **121**, 231.
Athay, R. G., and Thomas, R. N. 1954, this supplement, p. 491.
Chandrasekhar, S., and Breen, F. H. 1946, *Ap. J.*, **104**, 430.
Cillié, C. G., and Menzel, D. H. 1935, *Harvard Obs. Circ.*, No. 410.
Dimmock, D. 1953, unpublished.
Henriksen, S. W. 1954, *Ap. J.*, **120**, 521.
Hulst, H. C. van de. 1953, *The Sun*, ed. G. P. Kuiper (Chicago: University of Chicago Press).
Jager, C. de. 1952, *Rech. Astr. Obs. Utrecht*, **13**, 1.
Matsushima, S. 1954, this supplement, p. 479.
Menzel, D. H. 1932, *M.N.*, **92**, 820.
Nicolet, M. 1951, *Ann. d'ap.*, **14**, 249.
Pecker, J-C. 1951, *Ann. astr.*, **14**, 152.
Piddington, J. H. 1954, *Ap. J.*, **119**, 531.
Regemorter, H. van. 1953, *C.R.*, **236**, 1536.
Rosa, H. 1948, *Zs. f. Ap.*, **25**, 1.
Thomas, R. N. 1950, *Ap. J.*, **112**, 337.
Woolley, R. v. d. R., and Allen, C. W. 1950, *M.N.*, **110**, 358.